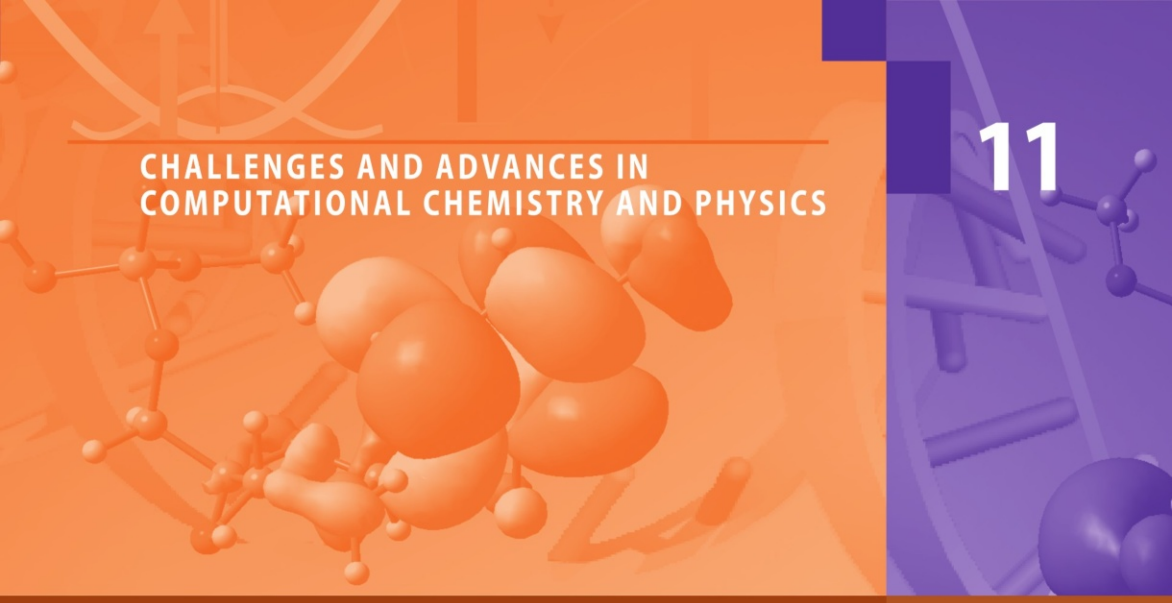

CHALLENGES AND ADVANCES IN COMPUTATIONAL CHEMISTRY AND PHYSICS

11

Series Editor J. Leszczynski

Volume Editors P. Čársky · J. Paldus · J. Pittner

Recent Progress in Coupled Cluster Methods

Theory and Applications

Springer

Recent Progress in Coupled Cluster Methods

CHALLENGES AND ADVANCES IN COMPUTATIONAL CHEMISTRY AND PHYSICS

Volume 11

Series Editor:

JERZY LESZCZYNSKI
Department of Chemistry, Jackson State University, U.S.A.

For further volumes:
http://www.springer.com/series/6918

Recent Progress in Coupled Cluster Methods

Theory and Applications

Edited by

Petr Čársky
J. Heyrovský Institute of Physical Chemistry v.v.i., Prague, Czech Republic

Josef Paldus
University of Waterloo, ON, Canada

and

Jiří Pittner
J. Heyrovský Institute of Physical Chemistry v.v.i., Prague, Czech Republic

Springer

Editors
Prof. Dr. Petr Čársky
ASCR Praha
J. Heyrovský Inst. Physical Chemistry
Dolejškova 3
182 23 Praha 8
Czech Republic
petr.carsky@jh-inst.cas.cz

Prof. Josef Paldus
University of Waterloo
Fac. Mathematics
Dept. Applied Mathematics
200 University Avenue W.
Waterloo ON N2L 3G1
Canada
paldus@scienide2.uwaterloo.ca

Dr. Jiří Pittner
ASCR Praha
J. Heyrovský Inst. Physical Chemistry
Dolejškova 3
182 23 Praha 8
Czech Republic
jiri.pittner@jh-inst.cas.cz

ISBN 978-90-481-2884-6 e-ISBN 978-90-481-2885-3
DOI 10.1007/978-90-481-2885-3
Springer Dordrecht Heidelberg London New York

Library of Congress Control Number: 2010926693

FOREWORD

I feel very honored that I have been asked to write a Foreword to this book. The subject of the book – "Coupled cluster theory" – has been around for about half a century. The basic theory and explicit equations for closed-shell ground states were formulated before 1970. At the beginning of the seventies the first ab initio calculation were carried out. At that time speed and memory of computers were very limited compared to today's standards. Moreover, the size of one-electron bases employed was small, so that it was only possible to achieve an orientation in methodical aspects rather than to generate new significant results. Extensive use of the coupled-cluster method started at the beginning of the eighties. With the help of more powerful computers the results of coupled-cluster approaches started to yield more and more interesting results of relevance to the interpretation of experimental data. New ideas in methodology kept appearing and computer codes became more and more efficient. This exciting situation continues to this very day. Remarkably enough, even the required equations can now be generated by a computer with the help of symbolic languages. The size of this monograph and the rich variety of articles it contains attests to the usefulness and viability of the couple-cluster formalism for the handling of many-electron correlation effects. This represents a vivid testimony of a tremendous work that has been accomplished in coupled-cluster methodology and its exploitation.

Jiří Čížek

PREFACE

Coupled-cluster approaches to the many-electron correlation problem that are based on the exponential Ansatz for the wave operator represent nowadays widely used techniques in molecular electronic structure calculations thanks to their accuracy and reliability. Moreover, the linear scaling of the coupled-cluster energy with the electron number, the so-called size-extensivity, represents an important aspect in handling of dissociative or associative phenomena and is absolutely essential in a description of extended systems, such as polymers and solids. It was precisely this size-extensive nature of the exponential cluster Ansatz, first realized by nuclear physicists, that led to a widespread exploitation of the coupled-cluster formalism in the modeling of many-electron systems, as witnessed by a plethora of various coupled-cluster methods and a number of standard approaches that are available in most quantum-chemistry software packages. Applications range from small molecular systems involving 4–20 electrons, in which case large basis sets enable one to generate highly accurate results, to relatively large systems, such as benzene dimers, naphthyne diradicals, nucleic acid bases or DNA base pairs, and the like. Likewise, the range of both the energetic and non-energetic properties that are accessible via coupled-cluster approaches is steadily expanding.

In particular the so-called CCSD(T) method (coupled clusters with singles and doubles perturbatively corrected for triples) that enjoys a very extensive usage by both theoretical and experimental chemists and physicists, thanks to its universality and a favorable accuracy-to-cost ratio, is often refered to as the "gold standard" of quantum chemistry. Yet, it is well known that its applicability is restricted to non-degenerate states, thus preventing its exploitation in situations involving highly-stretched genuine chemical bonds and open-shell systems in general. Even in applications where the use of CCSD(T) is justified, the cost of calculations prohibitively increases with the size of the molecular system considered, so that the requirements of many problems of contemporary chemistry and physics cannot be satisfied. Hence, the efforts to improve the accuracy and to reduce the cost of the coupled-cluster-based software continue to represent a very topical subject of current research activities, many of them focusing on multi-reference-type approaches.

In recent years a number of novel approaches that exploit the exponential cluster Ansatz has been proposed and tested. These developments are often highly technical and thus difficult to evaluate and to exploit by a casual user, or even by quantum

chemists working in other areas of the field. Although a number of excellent reviews on the subject of coupled-cluster methodology is available in the literature (for recent ones, see, e.g., [1–12], for a quasi-historical account see [13, 14] and authoritative monograph by Shavitt and Bartlett [15]), there is a definite need for a synoptic account of the most recent developments in the field, last time brought about by the volume "Recent Advances in Coupled-Cluster Methods" [16] more than a decade ago. This is precisely the goal of this volume whose 22 chapters written by the experts who substantially contributed to recent developments of the coupled-cluster theory and its applications represent a contemporary stage in the development of the theory and its exploitation, outline several "hot" topics in this field, and point out to future developments. We thus believe that this monograph will prove to be helpful in this regard and will become a useful source of information not only for those scientists who actively participate in the development of quantum chemical computational methods, but also for all kind of actual users of quantum chemical software of computational chemistry and physics, material science, nanotechnology, and drug design.

Prague, Czech Republic — Petr Čársky
Waterloo, ON — Josef Paldus
Prague, Czech Republic — Jiří Pittner

REFERENCES

1. J. Paldus, in *Methods in Computational Molecular Physics*, *NATO ASI Series B: Physics*, vol. 293, Eds. S. Wilson, G. H. F. Diercksen (Plenum, New York, 1992), pp. 99–194
2. R. J. Bartlett, J. F. Stanton, in *Reviews in Computational Chemistry*, vol. 5, Eds. K. B. Lipkowitz, D. B. Boyd (VCH Publishers, New York, 1994), pp. 65–169
3. J. Paldus, in *Relativistic and Correlation Effects in Molecules and Solids*, *NATO ASI Series B: Physics*, vol. 318, Ed. G. L. Malli (Plenum, New York, 1994), pp. 207–282
4. R. J. Bartlett, in *Modern Electronic Structure Theory*, Ed. D. R. Yarkony (World Scientific, Singapore, 1995), pp. 1047–1131
5. J. Gauss, in *The Encyclopedia of Computational Chemistry*, Eds. by P. v. R. Schleyer, N. L. Allinger, T. Clark, J. Gasteiger, P. A. Kollman, H. F. Schaefer III, P. R. Scheiner (Wiley, Chichester, 1998), pp. 615–636
6. J. Paldus, X. Li, Adv. Chem. Phys. **110**, 1 (1999)
7. J. Paldus, in *Handbook of Molecular Physics and Quantum Chemistry*, vol. 2, Ed. S. Wilson (Wiley, Chichester, 2003), pp. 272–313
8. T. D. Crawford, H. F. Schaefer III, in *Reviews in Computational Chemistry*, vol. 14, Eds. K. B. Lipkowitz, D. B. Boyd (Wiley, Ney York, 2000), pp. 33–136
9. J. F. Stanton, J. Gauss, Int. Rev. Phys. Chem. **19**, 61 (2000)
10. P. Piecuch, K. Kowalski, I. S. O. Pimienta, M. J. McGuire, Int. Rev. Phys. Chem. **21**, 527 (2002)
11. P. Piecuch, K. Kowalski, I. S. O. Pimienta, P.-D. Fan, M. Lodriguito, M. J. McGuire, S. A. Kucharski, T. Kuś, M. Musiał, Theor. Chem. Acc. **112**, 349 (2004)
12. R. J. Bartlett, M. Musial, Rev. Mod. Phys. **79**, 291 (2007)

13. J. Paldus, in *Theory and Applications of Computational Chemistry: The First Forty Years*, Eds. C. E. Dykstra, G. Frenking, K. S. Kim, G. E. Scuseria (Elsevier, Amsterdam, 2005), pp. 115–147
14. R. J. Bartlett, in *Theory and Applications of Computational Chemistry: The First Forty Years*, Eds. C. E. Dykstra, G. Frenking, K. S. Kim, G. E. Scuseria (Elsevier, Amsterdam, 2005), pp. 1191–1221
15. I. Shavitt, R. J. Bartlett, *Many-Body Methods in Chemistry and Physics: MBPT and Coupled-Cluster Theory* (Cambridge University Press, Cambridge, 2009)
16. R. J. Bartlett, Ed., *Recent Advances in Coupled Cluster Methods* (World Scientific, Singapore, 1997), 130 pages

CONTENTS

CHAPTER 1

THE YEARN TO BE HERMITIAN

RODNEY J. BARTLETT[1], MONIKA MUSIAŁ[1,2], VICTOR LOTRICH[1], AND TOMASZ KUŚ[1]

[1] *Quantum Theory Project, Departments of Chemistry and Physics, University of Florida, Gainesville, FL 32611-8435, USA, e-mail: bartlett@qtp.ufl.edu; lotrich @qtp.ufl.edu;kus@qtp.ufl.edu*
[2] *Institute of Chemistry, University of Silesia, Szkolna 9, 40-006 Katowice, Poland, e-mail: musial@qtp.ufl.edu*

Abstract: In this work we analyze hermitian aspects of methods which can offer improved numerical approximations, simpler computational evaluations or other benefits. There is a route toward approximations to the correlation problem that is neither purely perturbative, nor infinite order as is Coupled Cluster (CC), and this has certain hermitian aspects that are of interest. As perturbation theory (PT) is hermitian, we consider CCPT. The CCPT approach might be offered as an alternative to the infinite order CC approach for the reference state correlation problem itself with some advantages like, potentially, e.g., a more rapid convergence to a satisfactory answer in low order. The CCPT methods up to fifth order with the inclusion of the connected quadruple excitations have been formulated and implemented. We illustrate its results by comparison with several full configuration interaction values. For comparison purposes we also compare our new results with results obtained using the standard CC and MBPT variants like: CCSD, CCSD(T), CCSDT, CCSDTQ, MBPT2, MBPT3, MBPT4, MBPT5 and MBPT6.

Keywords: Hermitian coupled cluster, Coupled cluster perturbation theory, Hermitian theories

1.1. INTRODUCTION

Before coupled-cluster (CC) theory virtually all methods in quantum chemistry were built upon hermitian forms. As we know, operators have to be hermitian to ensure real eigenvalues. Expectation values, $\langle O\rangle$, were given by the symmetric forms, $\langle\Psi|O|\Psi\rangle/\langle\Psi|\Psi\rangle$, and for the energy in particular, $\langle H\rangle \geq E_{\text{exact}}$. The best possible many-particle wave function was the complete CI, and in a basis set, the full CI, $|\Psi_{FCI}\rangle = (1 + \widehat{C})|0\rangle$, with $|0\rangle$ a Fermi vacuum defined from some independent particle reference function. Hence,

$$E = \langle 0|(1 + \widehat{C}^{\dagger})H(1 + \widehat{C})|0\rangle/\langle 0|(1 + \widehat{C}^{\dagger})(1 + \widehat{C})|0\rangle \geq E_{\text{exact}} \quad (1\text{-}1)$$

$$= \langle 0|H(1 + \widehat{C})|0\rangle \quad (1\text{-}2)$$

P. Čársky et al. (eds.), Recent Progress in Coupled Cluster Methods, 1–36.
DOI 10.1007/978-90-481-2885-3_1,

The prevalence of symmetric, hermitian forms have dramatically colored the field. However, now it is well-known that any CI truncation of $\widehat{C}$ in such a wave function fails to give an *extensive* result for the energy [1], which means it cannot be used for infinite systems like the electron gas, or for crystalline solids, or even to provide a table of pre-computed energies to employ in freshman chemistry evaluations of heats of reactions from computed heats of formation. The latter is a manifestation that without extensivity even the relative energies along a potential energy surface will not be accurate, which is as fundamental as chemistry itself. However to satisfy the property of size-extensivity usually prohibits the variational bound in Eq. (1-1) until the FCI is reached. For quantum chemists of the previous generation, such a variational bound was *de rigor*, and it was felt it should never be compromised. Besides, it was exceedingly useful as a tool to develop approximate wave functions. Yet, a bound on the total energy means little as the quantities of interest in chemistry like structures, excitation energies, dissociation energies, activation barriers, vibrational frequencies, etc, do not correspond to bounded quantities anyway. Except maybe for potential energy surfaces, an upper bound on the total energy is really only useful if there is a corresponding lower bound. So *many-body* methods that ensure extensivity like coupled-cluster theory, but compromise some of the hermitian aspects discussed above, have emerged as offering the best approximations for the largest number of problems in the field [2].

However, there are also situations where hermitian forms would be useful in CC theory instead of contending with unsymmetric expressions for the energy, density matrices and first-order properties. In particular for second-order properties two expressions can be derived and each have their justification, but they are not numerically equal [3]. In a hermitian theory this could not happen [4]. In this chapter we raise the question of whether hermitian forms in CC theory can offer improved numerical approximations, simpler computational evaluations, or other benefits in addition to the essential extensivity properties built into many-body methods.

1.2. COUPLED-CLUSTER METHODS

Coupled-cluster theory [1, 5, 6] built upon the wave function,

$$\begin{aligned} |\Psi_{CC}\rangle &= \exp(T)|0\rangle \\ T &= T_1 + T_2 + T_3 + ... \\ T_m &= \frac{1}{m!} \sum_{i,j,...a,b,...} t_{ij...}^{ab...} \{a^\dagger b^\dagger ... ji\} \end{aligned} \tag{1-3}$$

with $|0\rangle$ the Fermi vacuum, provides the best, ab initio results for the largest number of problems in quantum chemistry [2]. Much of this success stems from the similarity transformed Hamiltonian in the Schrödinger equation,

$$\exp(-T)H\exp(T)|0\rangle = E|0\rangle$$
$$\overline{H}|0\rangle = E|0\rangle \tag{1-4}$$

where in normal-ordered form,

$$H = \langle 0|H|0\rangle + \sum_{p,q} f_{pq}\{p^\dagger q\} + \frac{1}{4}\sum_{p,q,r,s}\langle pq||rs\rangle\{p^\dagger q^\dagger sr\} \tag{1-5}$$

The transformed Hamiltonian

$$\overline{H} = H + [H,T] + \frac{1}{2}[[H,T]T] + \frac{1}{3!}[[[H,T]T]T] + \frac{1}{4!}[[[[H,T]T]T]T] \tag{1-6}$$

naturally terminates after four T operators, giving the energy and amplitude equations in closed form,

$$EP = P\overline{H}P = \langle 0|H|0\rangle + \Delta E \tag{1-7}$$

$$Q\overline{H}P = 0 \tag{1-8}$$

$$Q = 1 - P = \sum(|_i^a\rangle\langle_i^a| + |_{ij}^{ab}\rangle\langle_{ij}^{ab}| + ...) \tag{1-9}$$
$$= Q_1 + Q_2 + Q_3 + ...$$

Obviously, *i,j,k*. . . indicate spin orbitals occupied in $|0\rangle$ and *a,b,c*. . . those unoccupied; *p,q,r,*... are unspecified. Q consists of all excited (spin-orbital) determinants with the same S_z value. Obviously E is linked and T is connected. Properly handled, all related quantities of interest, like density matrices, analytical gradients, and excited states are also evaluated from closed form equations.

That is, for an atomic displacement, dX_α,

$$\partial E/\partial X_\alpha = \langle 0|(1+\Lambda)\exp(-T)\partial H/\partial X_\alpha \exp(T)|0\rangle \tag{1-10}$$

where

$$\Lambda = P\overline{H}Q(\Delta E - \overline{H})^{-1}Q$$
$$= P\overline{H}\overline{R} \tag{1-11}$$

For density matrices,

$$\gamma_{pq} = \langle 0|(1+\Lambda)\exp(-T)p^\dagger q\exp(T)|0\rangle \tag{1-12}$$

For excited states the ansatz,

$$\Psi_k = R_k \Psi_{CC} \tag{1-13}$$

$$[R_k, T] = 0$$

provides the EOM-CC equations [7],

$$[\overline{H}, R_k]|0\rangle = \omega_k R_k|0\rangle \tag{1-14}$$

$$\langle 0|L_k \overline{H} = \langle 0|L_k \omega_k \tag{1-15}$$

$$\langle 0|L_k R_l|0\rangle = \delta_{kl} \tag{1-16}$$

where the L_k is the left-hand eigenfunction of $\overline{H}$, and the transition density matrices,

$$\gamma_{pq}^{kl} = \langle 0|L_k \exp(-T) p^\dagger q \exp(T) R_l|0\rangle \tag{1-17}$$

For the ground (or reference state), $L_0 = (1 + \Lambda)$ and $R_0 = 1$, while for excited states, these are naturally generalized to L_k and R_k respectively.

1.3. ORIGIN OF THE CC FUNCTIONAL

The CC functional most obviously arises from the simple expedient of considering properties in addition to the energy in CC theory. The energy and amplitudes are obtained in one-CC calculation, yet for N atoms, we require ~3N derivatives, $\partial T/\partial X_\alpha$. A straight-forward approach would thus necessitate doing ~3N calculations for ~3N displacements. Without solving this problem, CC theory would never have been anything but a curiosity in quantum chemistry, since "chemistry" requires moving atoms in molecules.

The solution is rather straight-forward once the right question is asked. Since

$$EP = P\overline{H}P \tag{1-18}$$

$$E^\alpha P = \partial E/\partial X_\alpha P = P \partial \overline{H}/\partial X_\alpha P \tag{1-19}$$

Separating the $\overline{H}$ derivative,

$$\partial \overline{H}/\partial X_\alpha = e^{-T}\{[\overline{H}, \partial T/\partial X_\alpha] + \partial H/\partial X_\alpha]\}e^T \tag{1-20}$$

$$= [(\overline{H}T^\alpha)_C + \overline{H}^\alpha] \tag{1-21}$$

It helps to realize that the first-order perturbed wave function in CC theory is

$$|\Psi^\alpha\rangle = T^\alpha e^T|0\rangle \tag{1-22}$$

Hence, inserting it into the usual inhomogeneous equations of perturbation theory,

$$(E - H)|\Psi^{\alpha}\rangle = (H^{\alpha} - E^{\alpha})|\Psi_{CC}\rangle \tag{1-23}$$

after left-multiplication by e^{-T} and Q,

$$Q(E - \overline{H})T^{\alpha}|0\rangle = Q(\overline{H}^{\alpha} - E^{\alpha})|0\rangle \tag{1-24}$$

In terms of the resolvent operator, we have the expression

$$T^{\alpha}|0\rangle = \overline{R}(\overline{H}^{\alpha} - E^{\alpha})|0\rangle \tag{1-25}$$

$$\overline{R} = (E - \overline{H})^{-1}Q \tag{1-26}$$

Hence, once again using the expression for E^{α},we have from Eq. (1-19)

$$E^{\alpha}P = P\overline{H}^{\alpha}P + P\overline{HRH}^{\alpha}P \tag{1-27}$$

Introducing the perturbation independent quantity,

$$\Lambda = P\overline{HR} \tag{1-28}$$

$$E^{\alpha} = \langle 0|(1 + \Lambda)\overline{H}^{\alpha}|0\rangle \tag{1-29}$$

This provides all ~3N derivatives at the cost of solving the Λ equations in addition to the CC ones. By natural extension, we also have the density matrices as in Eq. (1-12) for *any approximation to CC,* regardless of whether it corresponds to a wave function or not. In fact, since most CC densities obtained from a wave function would require a non-terminating form like $e^{T^{\dagger}}e^{T}$, such a quantity does not suit the treatment of properties in CC theory. Instead, the concept of a "response" density was introduced [8] along with its generalization to a "relaxed" form by allowing the orbitals in the reference determinant to change to accommodate the perturbation [9]. These new concepts for density matrices are another critical part of the fabric of CC theory.

Integration of Eq. (1-29) obviously provides the CC functional

$$E = \langle 0|(1 + \Lambda)\overline{H}|0\rangle \tag{1-30}$$

whose stationarity with respect to Λ provides the CC equations, Eq. (1-8), and stationarity to T provides the Λ equations, Eq. (1-11).

Obviously, if we were able to maintain Hermitian symmetry in CC theory we would have no need for Λ. This de-excitation CI-like operator,

$$\Lambda = \Lambda_1 + \Lambda_2 + ... \tag{1-31}$$

$$\Lambda_1 = \sum_{i,a} \lambda_i^a \{\widehat{i}^\dagger \widehat{a}\} \tag{1-32}$$

$$\Lambda_2 = \frac{1}{4} \sum_{i,j,a,b} \lambda_{ij}^{ab} \{\widehat{i}^\dagger \, \widehat{a} \widehat{j}^\dagger \, \widehat{b}\} \tag{1-33}$$

$$... \tag{1-34}$$

which is not connected in Λ_2 and higher terms, arises from the requirement that $Q\overline{H}P \neq P\overline{H}Q$.This causes Λ to have a residual role in any analysis of properties, but not necessarily for energies. As such, Λ is a step toward an hermitian theory, and we will see some of its consequences later. One worth mentioning in passing is that Eq. (1-30) is CI from the left and CC from the right. In the limit, either will give the exact result, while the former is bounded from below but not extensive. Hence, the functional is a kind of geometric mean of the two methods.

1.4. HERMITIAN THEORIES

If we actually had an hermitian CC theory, the most satisfactory realization would probably be a unitary form where $\tau = T - T^\dagger$, and $\mathrm{t}_{ijk...}^{abc...} = (t_{ijk...}^{abc...})^*$,

$$|\Psi_{UCC}\rangle = \exp(\tau)|0\rangle \tag{1-35}$$

$$\tau = \tau_1 + \tau_2 + \tau_3 + ... \tag{1-36}$$

$$\tau_1 = \sum_{a,i} (\langle a|\tau|i\rangle [\{a^\dagger i\} - \{i^\dagger a\}] \tag{1-37}$$

$$\tau_2 = \sum_{i,j,a,b} (\langle ab|\tau|ij\rangle_A [\{a^\dagger i b^\dagger j\} - \{i^\dagger a j^\dagger b\}] \tag{1-38}$$

$$... \tag{1-39}$$

Then from the ansatz, we immediately have

$$\widetilde{H} = e^{-\tau} H e^{\tau} = e^{\tau^\dagger} H e^{\tau} = (He^{\tau})_C \tag{1-40}$$

$$\widetilde{H}|0\rangle = E|0\rangle \tag{1-41}$$

$$\langle 0|\widetilde{H}|0\rangle = E \geq E_{\text{exact}} \tag{1-42}$$

$$\gamma_{pq} = \langle 0|e^{-\tau} p^\dagger q e^{\tau}|0\rangle = \langle 0|(p^\dagger q e^{\tau})_C|0\rangle \tag{1-43}$$

The equations for the amplitudes would follow from the variational principle, but once optimum, it follows that the projected condition has to hold,

$$Q\widetilde{H}P = 0 \tag{1-44}$$

All properties would be just as we would want them to be, except for the lack of termination of $\widetilde{H}$. This, of course, is the overwhelming problem of UCC. Because it fails to terminate, we are forced to truncate. The obvious methods to do so have to exploit some form of perturbation theory [10] or equivalently orders in H or T [11]. Such truncations through UCC(5) have been implemented and explored, even including analytical gradients [10, 12]. More recently, MR-UCC truncations have been considered [13]. Once truncation is enforced, however, much of the infinite-order power of CC might be compromised.

Perhaps the most important aspect of UCC for single-reference cases, if it could be done with truncation, would be to at least maintain some quasi-variational bound related to the above. This would tend to eliminate any "turnover" of the sort that occurs for molecules as they dissociate, when trying to use an incorrectly separating RHF reference function in CC calculations. Frequently the problem can be alleviated at separation, though not completely eliminated in the spin-recoupling region of the curve, by using an unrestricted reference function [2]. However, note the poor behavior of CCSD(T) for F_2 when using an RHF reference function in Figure 1-1 [14].

However, it is much improved once $\Lambda CCSD(T)$ is used [15].This method simply replaces $T^{\dagger}$ which is used in CCSD(T) with the CI-like Λ that was first introduced in CC gradient theory [8, 9, 16]. The method is still perturbative and has the same computational scaling but requires Λ in addition to T, adding a factor of two to

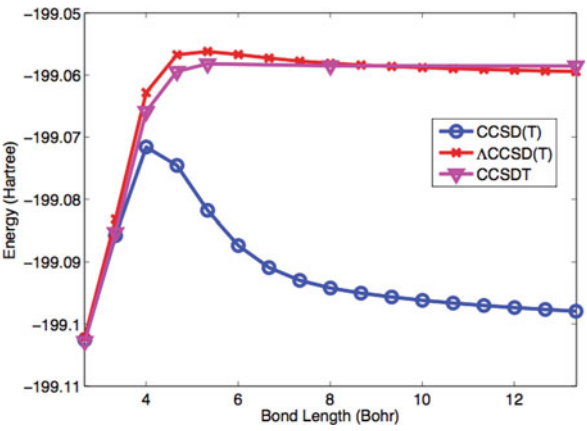

Figure 1-1. Potential energy curves for the F_2 molecule using CCSD(T), ΛCCSD(T) and CCSDT methods

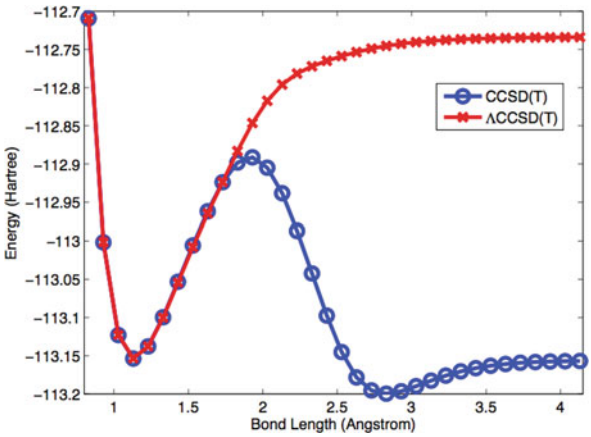

Figure 1-2. Potential energy curves for the CO molecule using CCSD(T) and ΛCCSD(T) methods

the computation. The improved curve for CO in Figure 1-2 is even more impressive, though more detailed analysis shows it is not correctly separating to the right limit [14]. Even though there is no bound on these energies, it appears that the CC functional with its natural mix of CC and CI, benefits from better behavior. For N_2 however, it will still fail [14].

In other cases some benefit can accrue due to other choices of reference single determinants, like the Brueckner determinant that has maximum overlap with the exact wave function [14]. We have also explored the first natural determinant as a reference, and the Kohn-Sham determinant [17] which is supposed to provide the exact correlated density.

The results for $\Lambda CCSD(T)$ tend to suggest that moving toward a hermitian theory, even with approximations might pay dividends. But we insist that any such approach be extensive.

A second equally important condition on suitable CC approximations is that they also be invariant to rotations among the occupied and unoccupied orbitals. This is a common failure of many approximations including CEPA [18], which also do not correspond to an exponential wave function and hence, do not satisfy extensivity. In fact, the proof that extensivity is satisfied, $\Psi_{AB} = \exp(T_A + T_B)|AB\rangle = \exp(T_A)|A\rangle \exp(T_B)|B\rangle$ for A and B far apart, follows from the evaluation of only linked diagrams which, because they are individually invariant to orbital localization, transparently proves the theorem in the non-interacting limit.

However, beyond potential bounding properties, such hermitized methods might well offer a superior rate of convergence to the exact solution than the normal,

$$\text{CCD} < \text{CCSD} < \text{CCSD(T)} < \text{CCSDT} < \text{CCSDT(Q)} < \text{CCSDTQ}$$

sequence of improving approximations.

For example, we know that properties and density matrices can be obtained from $\gamma_{pq} = \langle 0|e^{T^\dagger} p^\dagger q e^T|0\rangle_C$ [19, 20]. In fact, this kind of an expression leads to very rapid convergence for a one-electron property. However, since it does not terminate, it is not suited to analytical gradients where the exact critical point has to be identified, like the unsymmetric Λ based expressions above. Can the same apply for the energy? In other words, what if we arrange to enforce more hermitian symmetry? Can we identify a sequence that shows better convergence to the ultimate answer than the normal CC one? Such a sequence might be expected to include the adjoints of any diagrams that occur in a given order, for example, unlike CC theory. Also any such approach that makes $T^\dagger = T$ will eliminate the need to determine both Λ and T.

1.5. THE ALTERNATIVE OF GENERALIZED CC PERTURBATION THEORY

Perturbation theory begins with the separation of a Hamiltonian, H, into an unperturbed part, H_0, preferably easy to solve, and a perturbation, V, that will ultimately dictate the effort and order required to obtain satisfactory solutions. Once this separation is made, the linked diagram theorem of many-body perturbation theory (MBPT) provides the energy and wave function via the familiar, intermediately normalized formulae,

$$E = \langle 0|H + \sum_{k=1}^{\infty} H(R_0 H)^k|0\rangle_L \tag{1-45}$$

$$\Psi = |0\rangle + \sum_{k=1}^{\infty} (R_0 H)^k|0\rangle_L \tag{1-46}$$

$$= |0\rangle + \psi^{(1)} + \psi^{(2)} + \ldots \tag{1-47}$$

$$E = \langle 0|H|\Psi\rangle_L \tag{1-48}$$

At any order, the MBPT equations are Hermitian and provide the usual $2m + 1$ and $2m$ rules,

$$E^{(2m+1)} = \langle \psi^{(m)}|V|\psi^{(m)}\rangle_L \tag{1-49}$$

$$E^{(2m)} = \langle \psi^{(m)}|E_0 - H_0|\psi^{(m)}\rangle_L \tag{1-50}$$

We limit ourselves to non-degenerate problems for n electrons, with n + N functions. The L indicates the limitation to linked diagrams, $|0\rangle$, is a Fermi vacuum that corresponds to some single determinant, Φ_0, like that of Kohn-Sham (KS), Hartree-Fock (HF), Brueckner (B), the natural determinant (N) etc. and the resolvent operator,

$$R_0 = Q(E_0 - H_0)^{-1} Q \tag{1-51}$$

$$Q = 1 - P = 1 - |0\rangle\langle 0| \tag{1-52}$$

Subject to

$$H_0 = \sum_i h^{\text{eff}}(i) \tag{1-53}$$

$$h^{\text{eff}}(1)\phi_p(1) = \varepsilon_p \phi_p(1) \tag{1-54}$$

$$E_0 = \sum_i^n \varepsilon_i \tag{1-55}$$

$$R_0|_{ij\ldots}^{ab\ldots}\rangle = (\varepsilon_i + \varepsilon_j + \ldots - \varepsilon_a - \varepsilon_b \ldots)^{-1}|_{ij\ldots}^{ab\ldots}\rangle \tag{1-56}$$

$$R_0 = R_S^0 + R_D^0 + R_T^0 + \ldots = R_1^0 + R_2^0 + R_3^0 + \ldots \tag{1-57}$$

The last form of the resolvent indicates its single, double, triple, etc excitation components. For a diagonal (or block diagonal) resolvent, this separation pertains.

Hence, basing PT upon a mean-field single determinant approximation lends itself to a straightforward MBPT expansion for each order in V

$$E = E_0 + E^{(1)} + E^{(2)} + \ldots \tag{1-58}$$

$$\Psi = \Phi_0 + \psi^{(1)} + \psi^{(2)} + \ldots. \tag{1-59}$$

$$E^{(m+1)} = \langle 0|V(R_0 V)^m|0\rangle_L \tag{1-60}$$

$$\psi^{(m)} = (R_0 V)^m|0\rangle_L \tag{1-61}$$

which has been extensively pursued for the correlation problem in atoms [21] and for molecules [22, 23] for about 40 years. Note the lack of the familiar Rayleigh-Schrödinger renormalization terms in the energy and wave function of each order. This leads to MBPTm [22], frequently also called MPm when based upon a HF mean-field [24]. The formal development of the latter avoided the elegant simplicity of a second-quantized based MBPT in favor of a tedious Slater rule treatment based upon determinantal matrix elements. Of course, once the latter is accomplished, and the simplifications that are readily apparent in the second-quantized based treatment but hidden in the determinantal approach are identified, which becomes difficult in fourth-order [25]; the actual computational formulae are the same for the HF case.

The difficulties with straight-forward PT based on a mean-field single determinant are well known. From the inception of MBPT, it was apparent that order-by-order PT will frequently diverge for some cases like the high-density electron gas [26], the hard-sphere potential then used for nuclei [26] , and, more recently, such divergence has been demonstrated for molecular problems [27]. However, in the latter case, virtually any resummation of the diverging terms such as the use of Pade' approximants easily provides the correct answer [28], so the divergence is not fundamental. The most attractive and powerful resummation technique is offered by coupled-cluster theory [1, 2, 5, 6].

Coupled-cluster theory begins with the recognition that the linked MBPT wave function can be written to all orders as in Eq. (1-3) in terms of a connected T operator that ensures that exp(T)|0⟩ is "linked" [2]. Instead of PT, the "connected" CC approximations are defined to be *infinite-order* in categories of T_p, as CCSD means include all contributions from T_1 and T_2 into the wave function, $|\Psi\rangle_{\mathrm{CCSD}} = \exp(T_1 + T_2)|0\rangle$ CCSDT adds T_3. But because it is more expensive, scaling as $\sim n^3N^5$, instead of $\sim n^2N^4$ as does CCSD; *perturbative* corrections for T_3 like CCSD(T) [29] and ΛCCSD(T) [14, 15], that scale only as $\sim n^3N^4$ are very popular in practice [2].

There is another route toward such approximations to the correlation problem that is neither purely perturbative, nor infinite order as is CC theory. This is CC perturbation theory [30]. CCPT is often used in treating properties in CC theory [8, 9], where $H_0 = \overline{H}$, $E_0 = E_{\mathrm{CC}}$, would correspond to the CC solution and V would be a perturbing electric [31], or magnetic field [32], or other combinations as in NMR coupling constants [33]. This is also true for analytical derivatives where the perturbations are the atomic displacements in a molecule, and basis function changes are required to be in the equations [8, 9, 16]. Essentially everything one wants to compute can be obtained from the theory with these perturbative additions.

However, the CCPT approach can also be offered as an alternative to the infinite-order CC approach for the reference state correlation problem itself, and this has some potential advantages in computational strategies, including, perhaps, a more rapid convergence to a satisfactory answer in low order. It also might offer some new insights into the relationship between various T_p operators.

The following treatment of CCPT will be tied to the convenient mean-field starting point, but the particular choice of H_0 will result in the first-order solution for the double excitation wave function being that for linearized CCD, Ψ_{LinCCD}, (also known as LCCD, CEPA0 and D-MBPT(∞))

$$E_{\mathrm{LinCCD}} = \langle 0|H|0\rangle + \langle 0|H|\Psi_{\mathrm{LinCCD}}\rangle = E_0 + E^{(1)} + \Delta E_D^{(2)} \tag{1-62}$$

$$\Delta E_D^{(2)} = \frac{1}{4}\sum_{i,j,a,b}\langle ij||ab\rangle t_{ij}^{ab(1)} \tag{1-63}$$

whose energy, defined to be second-order in CCPT, is already correct through third-order compared to orders of conventional MBPT, and will have certain terms summed to infinite-order. Its solution is given by the linear equation,

$$\mathbf{M}_{22}\mathbf{t}_2^{(1)} = \mathbf{v}_2^{(1)} \tag{1-64}$$

$$\mathbf{M}_{22} = \langle \mathbf{2}|H - E_0|\mathbf{2}\rangle \tag{1-65}$$

$$\mathbf{v}_2 = \langle \mathbf{2}|H|0\rangle \tag{1-66}$$

where $|\mathbf{2}\rangle$ represents the vector of *all* distinct double excitations. $E_0 = \sum_i \varepsilon_i$, and $(\mathbf{M}_{22})^{-1} = -\mathbf{R}_2^{(0)}$, is the double excitation component of the resolvent matrix for CCPT. LinCC methods result in symmetric Hamiltonian matrices, ensuring that all Hermitian adjoints of terms are included along with their counterparts. The

Hermitian property also makes LinCC analytical gradients easy to evaluate, since the left-hand eigenvector, Λ, introduced in CC analytical gradient theory [9] corresponds to $T^{\dagger}$. When **M** is singular, LinCCD will immediately fail, unless some kind of singular value decomposition (generalized inverse) is used to overcome the problem [34]. This will typically happen when quasidegeneracies are encountered due to open shell complications or bond breaking. Such studies have been made by Paldus and co-workers [35].

To introduce CCPT, consider the usual normal-ordered Hamiltonian $H=\{H\}+\langle 0|H|0\rangle$ of Eq. (1-4). We have already exploited the fact that if our choice of orbitals has the off-diagonal f_{ij} and f_{ab} non-vanishing (like KS orbitals), we subject them to a semi-canonical transformation that makes $f_{ij} = f_{ii}\delta_{ij}$,and $f_{ab} = f_{aa}\delta_{ab}$.This degree of freedom cannot change any results, since any proper correlated method is invariant to transformations among just the occupied or unoccupied orbitals. Of course, f_{ai} remains in the perturbation, V.

From observation of the exceptional results often obtained by LinCCD (Tables 1-1 and 1-2) [34, 36] we choose to separate the full one-particle and two-particle Hamiltonian into terms that correspond to a zero excitation level and the others that will change the excitation by one or two [36, 37].

Table 1-1. Total energies (Hartree) for some small molecules at their equilibrium geometry[a] and cc-pVQZ basis set

Molecule	MBPT2	CCSD	CCSD(T)	CCPT2SD≡ LinCCD
HF	−100.396686	−100.397200	−100.405232	−100.400475
H_2O	−76.378126	−76.381861	−76.391086	−76.386615
NH_3	−56.504675	−56.515257	−56.524215	−56.521021
CH_4	−40.454994	−40.473974	−40.481152	−40.479531
N_2	−109.446817	−109.443011	−109.463748	−109.454037
CO	−113.225769	−113.227116	−113.246075	−113.235350
HCN	−93.337852	−93.340065	−93.360033	−93.351033
CO_2	−188.454966	−188.443290	−188.475063	−188.453231
C_2H_2	−77.238538	−77.249087	−77.267427	−77.260313
CH_2O	−114.402262	−114.410145	−114.428973	−114.419642
HNO	−130.373121	−130.375951	−130.398427	−130.389709
N_2H_2	−110.541198	−110.550317	−110.571755	−110.564223
O_3	−225.278459	−225.241996	−225.292632	−225.270213
C_2H_4	−78.481161	−48.503769	−78.520651	−78.515746
F_2	−199.399105	−199.399679	−199.421743	−199.414999
HOF	−175.429226	−175.431803	−175.452997	−175.443345
H_2O_2	−151.444435	−151.448191	−151.469785	−151.460277
HCl	−460.343089	−460.361297	−460.369653	−460.368439
CH_4O	−40.427655	−40.448457	−40.454938	−40.453756
C_2H_6	−79.384824	−79.412422	−79.428623	−79.424028
SiH_4O	−291.463161	−291.493110	−291.498026	−291.497647

[a] The equilibrium geometries were determined at the CCPT2SD level except for HCl, CH_4O, C_2H_6, and SiH_4O where the experimental equilibium geometries were used.

Table 1-2. Deviations of calculated equilibrium geometries (pm) from experiment for molecules from Table 1-1

Method	$\bar{\Delta}$	$\bar{\Delta}_{\text{abs}}$	Δ_{std}	Δ_{max}
MBPT2	−0.26	0.54	0.67	1.67
MBPT3	−1.30	1.30	1.04	4.24
MBPT4	0.24	0.41	0.54	1.48
CCSD	−0.89	0.89	0.79	3.07
CCSD(T)	−0.19	0.22	0.30	1.20
CISD	−1.80	1.80	1.48	5.72
CCPT2SD	−0.39	0.52	0.61	1.92

This procedure, which underlies our easily applied diagrammatic approach [2, 25], offers a natural dichotomy that in principle, provides a much better unperturbed Hamiltonian than the usual sum of one-particle operators. The diagrammatic expressions are more transparent and shown in Figures 1-3, 1-4, 1-5, 1-6, 1-7, 1-8, 1-9, and 1-10. We also present the algebraic treatment below along with the discussion that pertains to either.

Hence we separate the Hamiltonian into the following parts:

$$\{H\} = \{F^{[0]}\} + \{W^{[0]}\} + \{F^{[\pm 1]}\} + \{W^{[\pm 1]}\} + \{W^{[\pm 2]}\} \tag{1-67}$$

$$\{H^{[0]}\} = \{F^{[0]}\} + \{W^{[0]}\} \tag{1-68}$$

$$\{V\} = \{F^{[\pm 1]}\} + \{W^{[\pm 1]}\} + \{W^{[\pm 2]}\} \tag{1-69}$$

where the [±k] superscript specifies what effect the operator has in terms of particle number. [0] means it does not change the particle number, up or down, while [+1] means it introduces an excitation while [− 1] is a de-excitation, while [±2] means the operator causes a net of two excitations or deexcitations. These operators are shown in Figure 1-3. Orders, however, are still specified by order in the combined perturbation, V. That is, $T_2^{(1)}$ means the first-order in V correction to T_2. Clearly we could further separate the perturbation into just excitations or deexcitations, or single versus double excitations, or rings, or ladders, or could isolate different kinds of spin contributions, and even separate coulomb terms from exchange terms; if any of those separations aid us in arranging for the best zeroth-order approximation to a problem (We might add the last would have the advantage that the largest perturbation, the Coulomb perturbation, might be selectively summed to high orders *before* introducing the exchange, whose effect might then correspond to a smaller and shorter range perturbation). This is further discussed in the Summary. However, we insist that the choice made still makes the results invariant to occupied–occupied and virtual–virtual orbital rotations, which requires full diagrams. Hence, a choice that would separate MBPT diagrams into diagonal and off-diagonal terms, like the

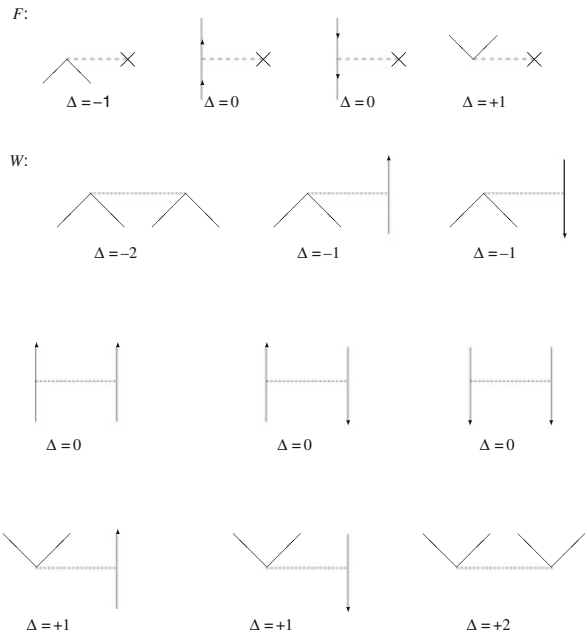

Figure 1-3. Diagrammatic form of the F and W operators

well-known Epstein-Nesbet choice [38], does not satisfy orbital invariance and is not recommended.

To relate to the usual perturbation, $\{F^{[0]}\}$ would define the unperturbed problem, following the semi-canonical transformation. This is the choice made in generalized MBPT (GMBPT) [39] which means it is applicable to any single determinant reference function unlike the usual Hartree-Fock based method. Here, however, we prefer to augment the choice of $\{F^{[0]}\}$,which is a one-particle operator with $\{W^{[0]}\}$,which are the most important parts of the two-particle operator.

The specific algebraic definition of the second-quantized operators then become,

$$\{H_0\} = \{F^{[0]}\} + \{W^{[0]}\} \tag{1-70}$$

$$= \sum_p f_{pp}\{p^\dagger p\} + \frac{1}{4}\sum_{a,b,c,d}\langle ab||cd\rangle\{a^\dagger b^\dagger dc\} + \frac{1}{4}\sum_{i,j,k,l}\langle ij||kl\rangle\{i^\dagger j^\dagger lk\} \tag{1-71}$$

$$+ \sum_{a,b,i,j}\langle aj||bi\rangle\{a^\dagger j^\dagger ib\} \tag{1-72}$$

which consist of the particle–particle ladder term, the hole–hole ladder, and the hole–particle (ring) interaction. As each corresponds to full diagrams, any of the three could define another suitable $\{H_0\}$ if useful. Then the perturbation,

$$\{V\} = \{F^{[\pm 1]}\} + \{W^{[\pm 1]}\} + \{W^{[\pm 2]}\} \tag{1-73}$$

$$\{F^{[\pm 1]}\} = \sum_{i,a} f_{ia}\{a^\dagger i + i^\dagger a\} \tag{1-74}$$

$$\{W^{[\pm 1]}\} = +\frac{1}{2}\sum_{a,b,c,i} [\langle ab||ic\rangle\{a^\dagger b^\dagger ci\} + \langle ia||cb\rangle\{i^\dagger a^\dagger bc\} \tag{1-75}$$

$$\langle ak||ij\rangle\{a^\dagger k^\dagger ji\} + \langle kj||ai\rangle\{k^\dagger j^\dagger ia\}] \tag{1-76}$$

$$\{W^{[\pm 2]}\} = +\frac{1}{4}\sum_{i,j,a,b} \langle ab||ij\rangle\{a^\dagger b^\dagger ji\} + \frac{1}{4}\sum_{i,j,a,b} \langle ij||ab\rangle\{i^\dagger j^\dagger ba\} \tag{1-77}$$

All terms are presented diagrammatically in Figure 1-3. Undirected lines are used in short-hand notation when there is no confusion.

It then follows that the general form of the CCPT equations for first order in V (all products connected) are

$$1st\ Order \tag{1-78}$$

$$0 = \langle {}^a_i|(F^{[0]} + W^{[0]})T_1^{(1)} + F^{[+1]}|0\rangle_C \tag{1-79}$$

$$0 = \langle {}^{ab}_{ij}|(F^{[0]} + W^{[0]})T_2^{(1)} + W^{[+2]}|0\rangle_C \tag{1-80}$$

In perturbation theory form,

$$\mathbf{t}_1^{(1)} = \langle \mathbf{1}|T_1^{(1)}|0\rangle = \mathbf{R}_1^{(0)}\langle \mathbf{1}|F^{[+1]}|0\rangle = \mathbf{R}_1^{(0)}\mathbf{v}_1^{(1)} \tag{1-81}$$

$$\mathbf{t}_2^{(1)} = \langle \mathbf{2}|T_2^{(1)}|0\rangle = \mathbf{R}_2^{(0)}\langle \mathbf{2}|W^{[+2]}|0\rangle = \mathbf{R}_2^{(0)}\mathbf{v}_2^{(1)} \tag{1-82}$$

where $(\mathbf{R}_1^{(0)})^{-1} = \langle \mathbf{1}|(E_0 - H_0)|\mathbf{1}\rangle = -\langle \mathbf{1}|(F^{[0]} + W^{[0]})|\mathbf{1}\rangle$,with $|\mathbf{1}\rangle$ meaning the vector of all single excitations, and the same for $(\mathbf{R}_2^{(0)})^{-1} = -\langle \mathbf{2}|(F^{[0]} + W^{[0]})|\mathbf{2}\rangle$, where $|\mathbf{2}\rangle$ means double excitations. The operator form for R= $|\mathbf{1}\rangle\mathbf{R}_1^{(0)}\langle \mathbf{1}| + |\mathbf{2}\rangle\mathbf{R}_2^{(0)}\langle \mathbf{2}|$, and will be extended to any level of excitation as required, later. The form using $\mathbf{v}$, above, recognizes that out of all the terms that constitute the perturbation V, only very specific ones have non-vanishing contributions to the matrix element. See the diagrams in Figure 1-4.

The first-order singles equation, $T_1^{(1)}$, is identically zero when HF orbitals are used, since $F^{[+1]}$ would vanish for that case, but to allow for any choice of orbitals it will be retained in all (algebraic) equations. The first-order $T_2^{(1)}$gives the LinCCD solution, as discussed in Eq. (1-80) above. That is, it typically requires an

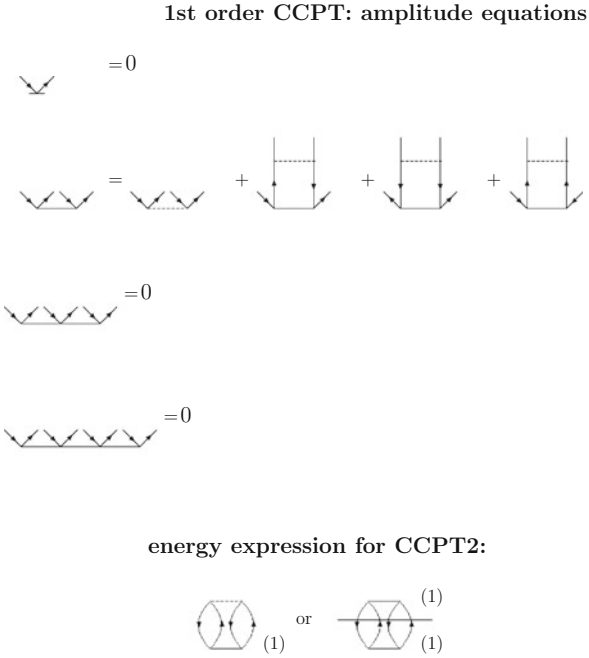

Figure 1-4. Diagrammatic form (in the antisymmetrized formalism) of the CCPT2 model

iterative solution of the linear equation since the $(\mathbf{M}_{22})^{-1} = -\mathbf{R}_2^{(0)}$ matrix has rank, ~n^2N^2,and is *non-diagonal*, unlike that in ordinary MBPT.

The non-HF single-excitation equation for $T_1^{(1)}$ is also linear, and is decoupled from the equation for the $T_2^{(1)}$. Notice that despite the semi-canonical transformation that $\mathbf{R}_1^{(0)}$ is not diagonal as single excitations couple across $W^{[0]}$.

The second-order energy is

$$\Delta E^{(2)} = \frac{1}{4}\sum_{i,j,a,b}\langle ij||ab\rangle t_{ij}^{ab(1)} + \sum_{i,a} f_{ia}t_{ia}^{(1)} \tag{1-83}$$

$$\Delta E^{(2)} = \langle 0|V|\psi^{(1)}\rangle = \langle 0|V(Q_1R_1^{(0)} + Q_2R_2^{(0)})V|0\rangle_L \tag{1-84}$$

$$= \langle \psi_S^{(1)}|(R_1^{(0)})^{-1}|\psi_S^{(1)}\rangle_L + \langle \psi_D^{(1)}|(R_2^{(0)})^{-1}|\psi_D^{(1)}\rangle_L \tag{1-85}$$

$$= \Delta E_D^{(2)} + \Delta E_S^{(2)} \tag{1-86}$$

and in the HF case reduces to just LinCCD. The resolvent operator $R_2^{(0)} = |\mathbf{2}\rangle\langle\mathbf{2}|E_0 - H_0|\mathbf{2}\rangle^{-1}\langle\mathbf{2}|$ which is $-Q_2\{H_0\}^{-1}Q_2 = -Q_2\{F^{(0)} + W^{[0]}\}Q_2$. The computational role for $W^{[0]}$ will arise from the non-diagonal part of the resolvent operator.

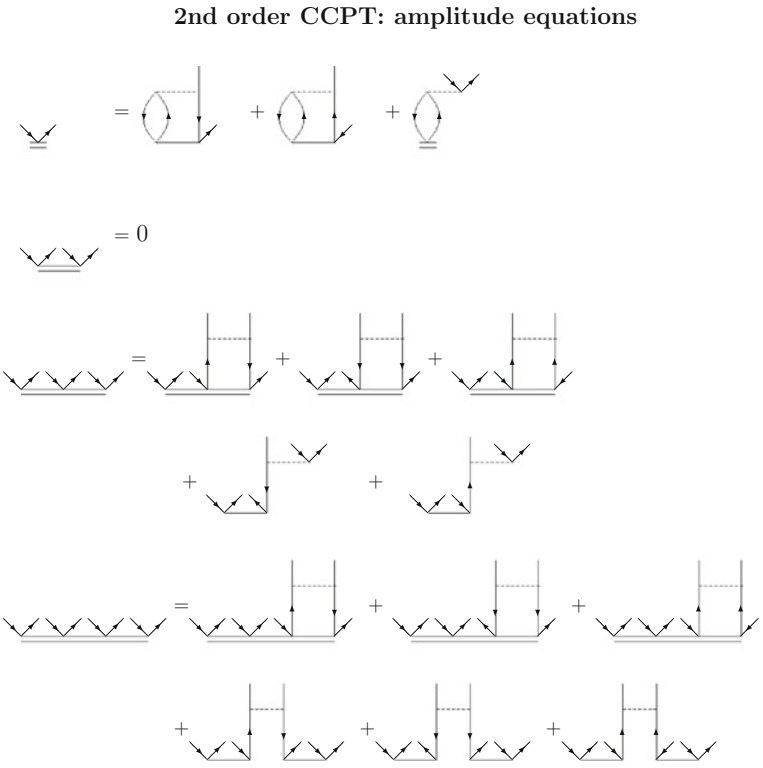

Figure 1-5. Diagrammatic form (in the antisymmetrized formalism) of the CCPT3 model

Continuing to the second-order wave function (the diagrams drawn are limited to HF orbitals in Figure 1-5),

$$2nd\ Order \tag{1-87}$$

$$0 = \langle_i^a|(F^{[0]} + W^{[0]})T_1^{(2)} + (V^{[-1]})T_2^{(1)}|0\rangle_C \tag{1-88}$$

$$0 = \langle_{ij}^{ab}|(F^{[0]} + W^{[0]})(T_2^{(2)} + T_1^{(1)^2}/2) + W^{[+1]}T_1^{(1)}|0\rangle_C \tag{1-89}$$

$$0 = \langle_{ijk}^{abc}|(F^{[0]} + W^{[0]})(T_3^{(2)} + T_1^{(1)}T_2^{(1)}) + W^{[+1]}T_2^{(1)}|0\rangle_C \tag{1-90}$$

$$0 = \langle_{ijkl}^{abcd}|(F^{[0]} + W^{[0]})(T_4^{(2)} + T_2^{(1)^2}/2)|0\rangle_C \tag{1-91}$$

The equations now couple the single and double excitation parts of the equations. With a Hartree-Fock reference, $T_1^{(1)} = 0$, eliminating several terms. For that choice, $T_2^{(2)} = 0$, while $T_1^{(2)}$ will be the first non-vanishing contribution to T_1. For non-HF

cases to avoid the inversion we would return to the linear equation to obtain the $T_2^{(2)}$ increment, which is

$$Q_2 T_2^{(2)}|0\rangle_C = Q_2 R_2^{(0)}[(W^{[0]})(T_3^{(2)} + T_1^{(1)2}/2) + (V^{[1]}T_1^{(1)})]|0\rangle_C \tag{1-92}$$

The third-order energy in CCPT is

$$\Delta E^{(3)} = \frac{1}{4}\sum_{i,j,a,b}[\langle ij||ab\rangle(t_{ij}^{ab(2)} + t_i^{a(1)}t_j^{b(1)} - t_j^{a(1)}t_i^{b(1)})] + \sum_{i,a} f_{ia}t_{ia}^{(2)} \tag{1-93}$$

$$\Delta E^{(3)} = \langle 0|V|\psi^{(2)}\rangle_C = \langle 0|V|\mathbf{1}\rangle \mathbf{T}_1^{(2)} + \langle 0|V|\mathbf{2}\rangle \mathbf{C}_2^{(2)} \tag{1-94}$$

where $C_2^{(2)} = T_2^{(2)} + T_1^{(1)}T_1^{(1)}/2$. For the HF case, $T_2^{(2)} = 0$, $T_1^{(1)} = 0$, and $F^{[\pm 1]} = 0$, so $\Delta E^{(3)} = 0$. Hence, $\Delta E_D^{(2)} = \Delta E_{\text{LinCCD}}$, is obviously correct through third-order in the HF case. For non-HF, $\Delta E^{(3)}$ consists of the usual non-HF third-order single-excitation terms.

Note the incremental nature of these equations. For non-HF cases, the determination of $T_2^{(2)}$ depends upon its increment relative to ${T_1^{(1)}}^2/2$. Also, $T_3^{(2)}$ is the increment relative to $T_1^{(1)}T_2^{(1)}$and $T_4^{(2)}$that relative to ${T_2^{(1)}}^2/2$.

This incremental property is a characteristic of the CCPT equations, as all $T_p^{(m)}$will be increments relative to a fixed, known combination of T-products, suggesting that for some value of m and p, the increment should eventually become vanishingly small. At that point the equations will decouple, which would then impose the condition that the right side would vanish. Once that happens, there will be relationships between different cluster operators that might be useful in devising additional approximations.

The triple excitation terms first appear in the second-order wave function, just as in ordinary MBPT. Also since $T_3^{(2)}$has no effect on $T_2^{(2)}$ or $T_1^{(2)}$and all energy corrections have to come through updated T_2 and T_1 operators, the actual effects of triples will first occur in the fourth-order energy. The most notable new element is that the straight-forward evaluation of triples would require the $W^{[0]}T_3^{(2)}$ term, which is computationally ~n^4N^4, compared to the $W^{[+1]}T_2^{(1)}$ term, which is ~n^3N^4. Including this term in a low-order of perturbation theory might seem to be a step in the wrong direction. but the CCPT theory suggests that perhaps the combination of this term with the latter is actually a better measure of the correct inclusion of triple excitations.

There are also alternative approaches that might improve upon the solution of these very-high rank linear equations, like a Cholesky decomposition of the negative definite resolvent operator. Finally, considering the underlying MBPT which would make the $W^{[0]}T_3^{[2]}$ term fifth-order while the $W^{[+1]}T_2^{(1)}$ is fourth could be invoked in approximations. Limiting the $W^{[0]}$ operator to just diagonal terms would make these computations very easy, as that would simply correspond to a denominator shift, but

that is an Epstein-Nesbet choice which can violate orbital invariance. In this first study we prefer not to make such approximations as we want to assess the full effect of $W^{[0]}$ in the CCPT equations.

Paying attention to the resolvent operator,

$$\begin{aligned} R_p &= -Q_p(\{F^{(0)}\} + \{W^{(0)}\})^{-1} \\ &= -Q_p[\{F^{(0)}\}^{-1} - \{F^{(0)}\}^{-1}\{W^{[0]}\}]R_p \qquad (1\text{-}95) \\ &= -R_p^{(0)} + R_p^{(0)}\{W^{[0]}\}R_p \qquad (1\text{-}96) \end{aligned}$$

we have

$$R_p^{(0)}\{W^{[0]}\} = (R_p + R_p^{(0)})R_p^{-1}$$

Hence, using the non-diagonal form of the resolvent, R_p, the above equations can be expressed as

$$T_1^{(2)}|0\rangle = R_1 V^{[-1]} T_2^{(1)}|0\rangle_C \qquad (1\text{-}97)$$

$$T_2^{(2)}|0\rangle = R_2[W^{[0]}T_1^{(1)^2}/2 + W^{[+1]}T_1^{(1)}]|0\rangle_C \qquad (1\text{-}98)$$

$$T_3^{(2)}|0\rangle = R_3[W^{[0]}T_1^{(1)}T_2^{(1)} + W^{[+1]}T_2^{(1)}]|0\rangle_C \qquad (1\text{-}99)$$

$$T_4^{(2)}|0\rangle = R_4[W^{[0]}T_2^{(1)^2}/2|0\rangle_C \qquad (1\text{-}100)$$

This form emphasizes that the usual diagrammatic expressions for T amplitudes can be regained with most of the effect of $W^{[0]}$ being relegated to the resolvent. This exploits the fact that the choice of $\{H_0\}$ does not change particle number.

Continuing on to the third-order wave function,

3rd Order (1-101)

$$\begin{aligned} 0 = \langle_i^a|(F^{[0]} + W^{[0]})T_1^{(3)} + (F^{[-1]} + W^{[-1]})(T_2^{(2)} + T_1^{(1)}T_1^{(1)}/2) \\ + W^{[-2]}(T_1^{(1)}T_2^{(1)} + T_3^{(2)})|0\rangle_C \qquad (1\text{-}102) \end{aligned}$$

$$\begin{aligned} 0 = \langle_{ij}^{ab}|(F^{[0]} + W^{[0]})T_2^{(3)} + W^{[0]}T_1^{(2)}T_1^{(1)} + W^{[+1]}T_1^{(2)} + (F^{[-1]} + W^{[-1]})\times \\ (T_1^{(1)}T_2^{(1)} + T_3^{(2)}) + W^{[-2]}(T_2^{(1)}T_2^{(1)}/2 + T_4^{(2)})|0\rangle_C \qquad (1\text{-}103) \end{aligned}$$

$$\begin{aligned} 0 = \langle_{ijk}^{abc}|(F^{[0]} + W^{[0]})T_3^{(3)} + W^{[0]}(T_1^{(2)}T_2^{(1)} + T_1^{(1)}T_2^{(2)}) + W^{[+1]}T_2^{(2)} \\ + W^{[-1]}(T_2^{(1)^2}/2 + T_4^{(2)}) + F^{[-1]}T_4^{(2)}|0\rangle_C \qquad (1\text{-}104) \end{aligned}$$

$$0 = \langle_{ijkl}^{abcd}|(F^{[0]} + W^{[0]})T_4^{(3)} + W^{[0]}(T_2^{(1)}T_2^{(2)} + T_1^{(1)^2}T_2^{(1)}/2 + T_1^{(1)}T_3^{(2)}) + W^{[+1]}T_3^{(2)}|0\rangle_C \tag{1-105}$$

$$0 = \langle_{ijklm}^{abcde}|(F^{[0]} + W^{[0]})T_5^{(3)} + W^{[0]}(T_2^{(1)}T_3^{(2)} + T_2^{(2)}T_3^{(1)} + T_1^{(1)}T_4^{(2)}) + W^{[+1]}T_4^{(2)}|0\rangle_C \tag{1-106}$$

$$0 = \langle_{ijklmn}^{abcdef}|(F^{[0]} + W^{[0]})T_6^{(3)} + W^{[0]}(T_2^{(1)}T_4^{(2)})|0\rangle_C \tag{1-107}$$

The third-order, $T_2^{(3)}$, $T_1^{(3)}$, $T_3^{(3)}$, $T_4^{(3)}$, $T_5^{(3)}$, $T_6^{(3)}$ all depend upon quantities that are already known at this point. Such a boot-strap approach is customary in perturbation theory, avoiding any need for a direct, infinite-order solution of the non-linear CC equations. Because of the quantities being known from prior orders, the equations for the new amplitudes are all *linear*, and this will continue to any order. We now have a need for $T_3^{(2)}$ to obtain updated $T_1^{(3)}$and $T_2^{(3)}$amplitudes, and they will then introduce an energy correction from $T_3^{(2)}$. We also have the effect of $T_4^{(2)}$now contributing to $T_2^{(3)}$and consequently the energy. Neither $T_4^{(3)}$or $T_3^{(3)}$ have any effect on the energy yet.

The diagrams for the 3rd order wave function through quadruple excitations and HF orbitals are shown in Figures 1-6 and 1-7.

The fourth-order CCPT energy is

$$\Delta E^{(4)} = \frac{1}{4}\sum_{i,j,a,b}[\langle ij||ab\rangle[t_{ij}^{ab(3)} + 2(t_i^{a(2)}t_j^{b(1)} - t_j^{a(2)}t_i^{b(1)})] + \sum_{i,a} f_{ia}t_{ia}^{(3)} \tag{1-108}$$

$$\Delta E^{(4)} = \langle 0|V|\psi^{(3)}\rangle_C = \langle 0|V|\mathbf{1}\rangle\mathbf{T}_1^{(3)} + \langle 0|V|\mathbf{2}\rangle\mathbf{C}_2^{(3)} \tag{1-109}$$

$C_2^{(3)} = T_2^{(3)} + T_1^{(1)}T_1^{(2)}$. The energy is composed of contributions from the C-type grouping of single, double, triple, and quadruple excitations. For the first term, we have

$$\Delta E_a^{(4)} = \langle 0|F^{[-1]}R_1^{(0)}[W^{[0]}T_1^{(3)} + V^{[-1]}C_2^{(3)} + W^{[-2]}C_3^{(3)}]|0\rangle \tag{1-110}$$

The second term is

$$\Delta E_b^{(4)} = \langle 0|W^{[-2]}R_2^{(0)}[W^{[0]}T_2^{(3)} + W^{[0]}T_1^{(2)}T_1^{(1)} + W^{[+1]}C_1^{(2)} + V^{[-1]}C_3^{(2)} + W^{[-2]}C_4^{(2)}]|0\rangle \tag{1-111}$$

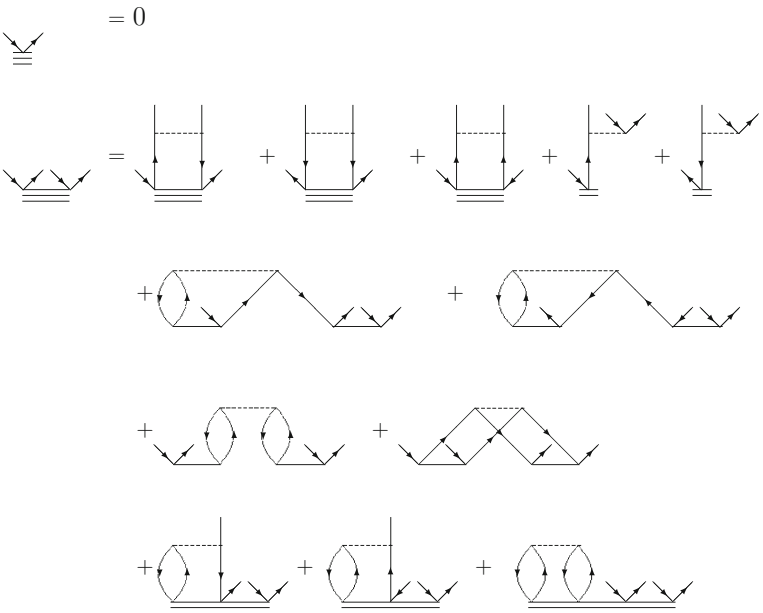

Figure 1-6. Diagrammatic form (in the antisymmetrized formalism) of the CCPT4 model (T_1 and T_2 amplitudes)

Isolating the individual contributions from different categories of excitations,

$$\Delta E_S^{(4)} = \langle 0|W^{[-2]}R_2^{(0)}W^{[+1]}C_1^{(2)}|0\rangle_C + \langle 0|F^{[-1]}R_1^{(0)}[W^{[0]}T_1^{(2)}]|0\rangle_C \tag{1-112}$$

$$\Delta E_D^{(4)} = \langle 0|W^{[-2]}R_2^{(0)}[W^{[0]}C_2^{(3)}]|0\rangle_C + \langle 0|F^{[-1]}R_1^{(0)}[V^{[-1]}C_2^{(2)}]|0\rangle_C \tag{1-113}$$

$$\Delta E_T^{(4)} = \langle 0|W^{[-2]}R_2^{(0)}[V^{[-1]}C_3^{(2)}]|0\rangle_C + \langle 0|F^{[-1]}R_1^{(0)}[W^{[-2]}C_3^{(2)}]|0\rangle_C \tag{1-114}$$

$$\Delta E_Q^{(4)} = \langle 0|W^{[-2]}R_2^{(0)}W^{[-2]}C_4^{(2)}]|0\rangle_C \tag{1-115}$$

These are similar to the usual terms in MBPT4, except in every case the $W^{[0]}C_p$ term has a role, as shown explicitly in the singles and doubles equations, and implicitly in $C_3^{(2)}$ and $C_4^{(2)}$.

As discussed in Eqs. (1-95) and (1-96), the third-order amplitudes can be defined relative to the combined, non-diagonal resolvents, R_p instead of $R_p^{(0)}$. In this form, it is readily apparent that the vertices in the $\Delta E^{(4)}$ expressions such as $\langle 0|W^{[-2]}R_2^{(0)}$ become $\langle 0|W^{[-2]}R_2$, which emphasize that the L in CCD effects are incorporated into

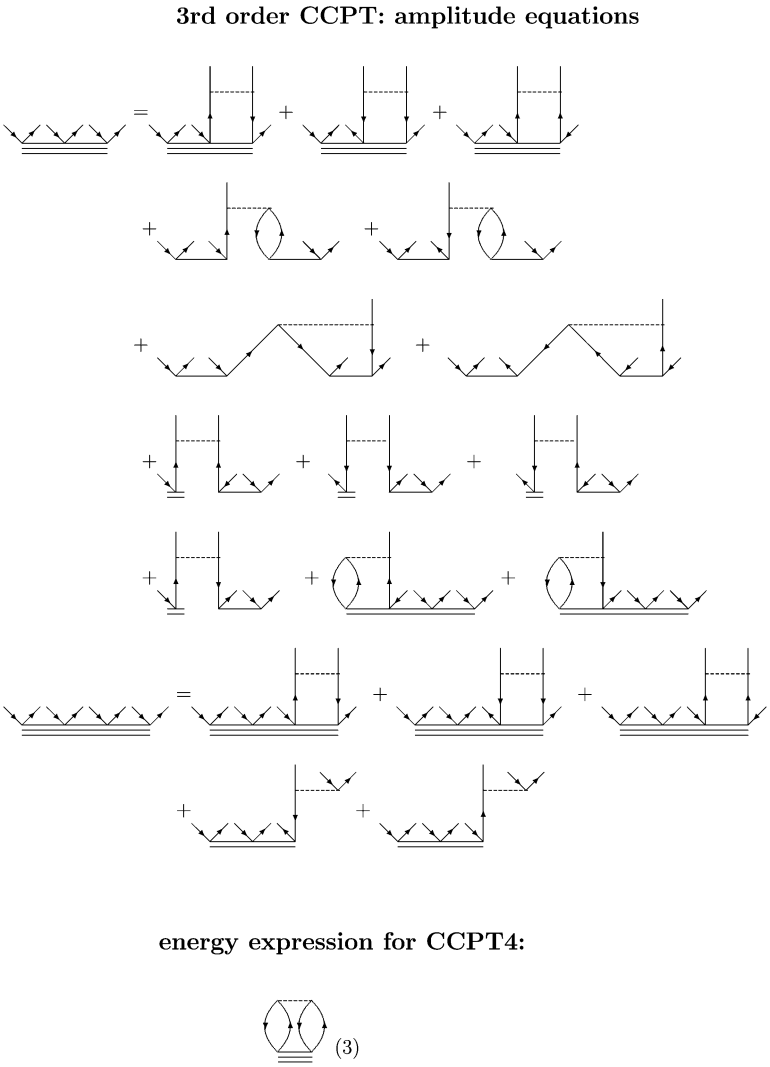

Figure 1-7. Diagrammatic form (in the antisymmetrized formalism) of the CCPT4 model (T_3 and T_4 amplitudes along with the fourth-order energy expression)

them, as well as in all intermediate R_p's hidden in the other amplitudes. However, these expressions are numerically the same. They just differ, conceptually, in how the solution was obtained using the standard CC approach or from a direct solution of the linear equation. The former has $R_p^{(0)} W^{[0]} T_p$ terms in its expression instead of their elimination from the *energy* (and amplitude) expressions in favor of R_p.

As an illustration, the energy change $\Delta E_T^{(4)}$ from Eq. (1-114) can be written

$$\Delta E_T^{(4)} = \langle 0|T_1^{(1)\dagger}\{W^{[-2]}R_3^{(0)}[W^{[0]}(T_3^{(2)} + T_1^{(2)}T_1^{(1)}) + W^{[+1]}T_2^{(2)}]\}|0\rangle_C \quad (1\text{-}116)$$

$$+ \langle 0|T_2^{(1)\dagger}\{V^{[-1]}R_3^{(0)}[W^{[0]}(T_3^{(2)} + T_1^{(2)}T_1^{(1)}) + W^{[+1]}T_2^{(2)}]|0\rangle_C \quad (1\text{-}117)$$

where the complex conjugate was introduced in both expressions. Temporarily disregarding the $W^{[0]}$ term, the $\langle 0|T_1^{(1)\dagger}W^{[-2]}R_3^{(0)}$ is a disconnected triple de-excitation amplitude, and $\langle 0|T_2^{(1)\dagger}V^{[-1]}R_3^{(0)}$ is connected for $W^{[-1]}$ and disconnected for $F^{[-1]}$. The term

$$\langle 0|T_2^{(1)\dagger}W^{[-1]}R_3^{(0)}W^{[+1]}T_2^{(2)}]|0\rangle_C = \langle 0|T_3^{(2)\dagger}R_3^{(0)}T_3^{(2)}]|0\rangle_C \quad (1\text{-}118)$$

is the usual fourth-order MBPT term that arises from $W^{[+1]}T_2^{(1)}$, except that $T_2^{(1)}$ now comes from LinCCD. This makes it a linear doubles approximation instead of CCSD to T(CCSD)=[T] [40], $T_1^{(1)}$ and $F^{[\pm 1]}$ will not appear for HF cases but would for non-HF examples. The terms, $\langle 0|T_1^{(1)\dagger}W^{[-2]}R_3^{(0)}W^{[+1]}T_2^{(2)})]|0\rangle_C$, and $\langle 0|T_2^{(1)\dagger}F^{[-1]}R_3^{(0)}W^{[+1]}T_2^{(2)})]|0\rangle_C$ then give the other two diagrams for the generalized (T) [2]. The new term

$$\langle 0|T_3^{(2)\dagger}R_3^{(0)}[W^{[0]}(T_3^{(0)} + T_1^{(2)}T_1^{(1)})]|0\rangle_C \quad (1\text{-}119)$$

has to be computed in this version of CCPT. The quadratic term disappears for HF cases. Changing R_3^0 to R_3 would have the effect of also eliminating the $W^{[0]}T_3^{(0)}$ in this expression as the effect is in the R_3 resolvent.

Following the same simplification as in the triples case, for quadruple excitation energy contributions we obtain

$$\Delta E_Q^{(4)} = \langle 0|(T_2^{(1)})^\dagger\{W^{[-2]}R_4^{(0)}[W^{[0]}(T_4^{(2)} + T_2^{(1)^2}/2) + T_2^{(1)^2}/2]\}|0\rangle_C \quad (1\text{-}120)$$

The last term accounts for all the normal linked quadruple excitation diagrams in fourth-order, but now modified to include the infinite-order effects of LCCD through $T_2^{(1)}$.

The new terms arise from $T_4^{(2)}$ and $T_2^{(1)2}/2$. The latter has a particularly interesting form. Expanding notation a bit, $[R_4^{(0)}]^{-1} \Longrightarrow (\varepsilon_i + \varepsilon_j + \varepsilon_k + \varepsilon_l - \varepsilon_a - \varepsilon_b - \varepsilon_c - \varepsilon_d) = [R_2^{(0)}]^{-1}(ijab) + [R_2^{(0)'}]^{-1}(klcd)$, is an eight index denominator that is characteristic of quadruple excitations, and typically leads to an ~n^4N^6 computational procedure. Using the ' to indicate the two different $R_2^{(0)}$'s and $W^{[-2]} = T_2^{(1)'}[R_2^{(0)'}]^{-1}$, it follows that this term becomes

$$= \langle 0|(T_2^{(1)})^\dagger(T_2^{(1)'})^\dagger[R_2^{(0)\prime}]^{-1}R_4^{(0)}W^{[0]}T_2^{(1)^2}/2|0\rangle \quad (1\text{-}121)$$

Without restriction we can simply relabel this term with the opposite choice of the (ie indices) and take one half of the equivalent expressions, to give

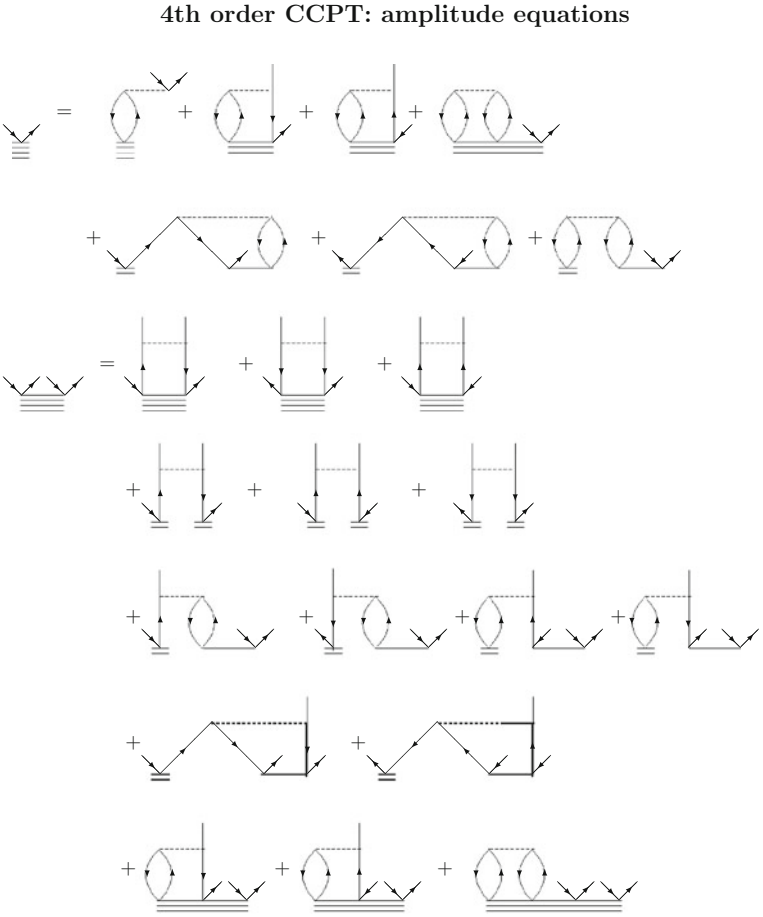

Figure 1-8. Diagrammatic form (in the antisymmetrized formalism) of the CCPT5 model (T_1 and T_2 amplitudes)

$$\frac{1}{2}\langle 0|(T_2^{(1)})^\dagger (T_2^{(1)'})^\dagger W^{[0]} T_2^{(1)^2}/2|0\rangle \tag{1-122}$$

This eliminates the eight index denominator in favor of the product of two, four index ones. The resulting computation is reduced to ~N^6 or alternatively, ~n^2N^5, an enormous savings [41]. This kind of factorization is not customary in CC theory, since all connected T_p should not be further reduced. However, we see here that a characteristic of this more general factorization is that half of the diagram arises from disconnected terms. The same situation will pertain to other occurrences of this structure.

The last term contributing to fourth-order quadruples is

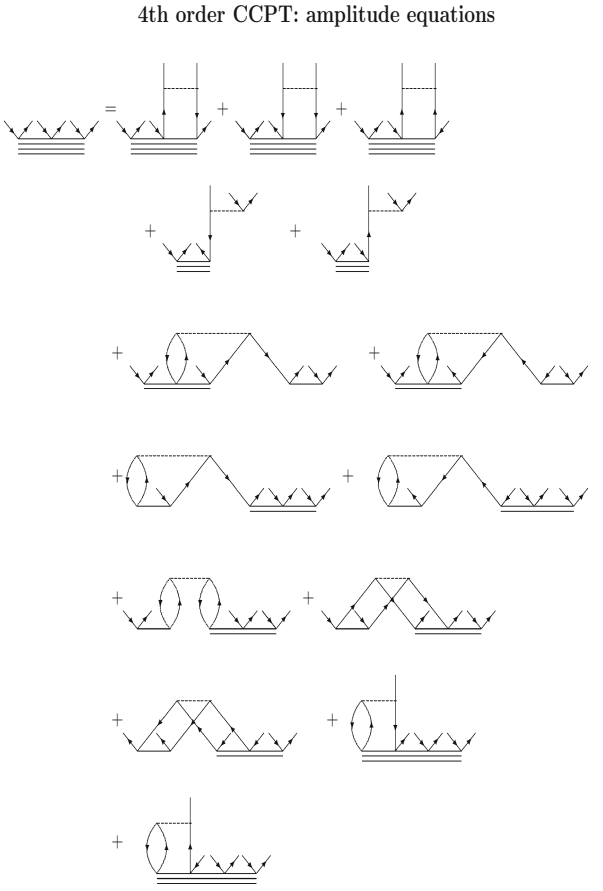

Figure 1-9. Diagrammatic form (in the antisymmetrized formalism) of the CCPT5 model(T_3 amplitude)

$$\langle 0|(T_2^{(1)})^\dagger (T_2^{(1)\prime})^\dagger [R_2^{(0)\prime}]^{-1} R_4^{(0)} [W^{[0]}(T_4^{(2)})]|0\rangle_C \tag{1-123}$$

Allowing for the same factorization trick, we obtain

$$\frac{1}{2}\langle 0|(T_2^{(1)})^\dagger (T_2^{(1)\prime})^\dagger [W^{[0]}(T_4^{(2)})]|0\rangle_C \tag{1-124}$$

Here, however, though the last $R_4^{(0)}$ is removed, there are still equivalent computational demands because of the requirement of computing $W^{[0]}T_4^{(2)}$. The only way to remove this term is to replace the $R_4^{(0)}$ by its full analog, R_4.

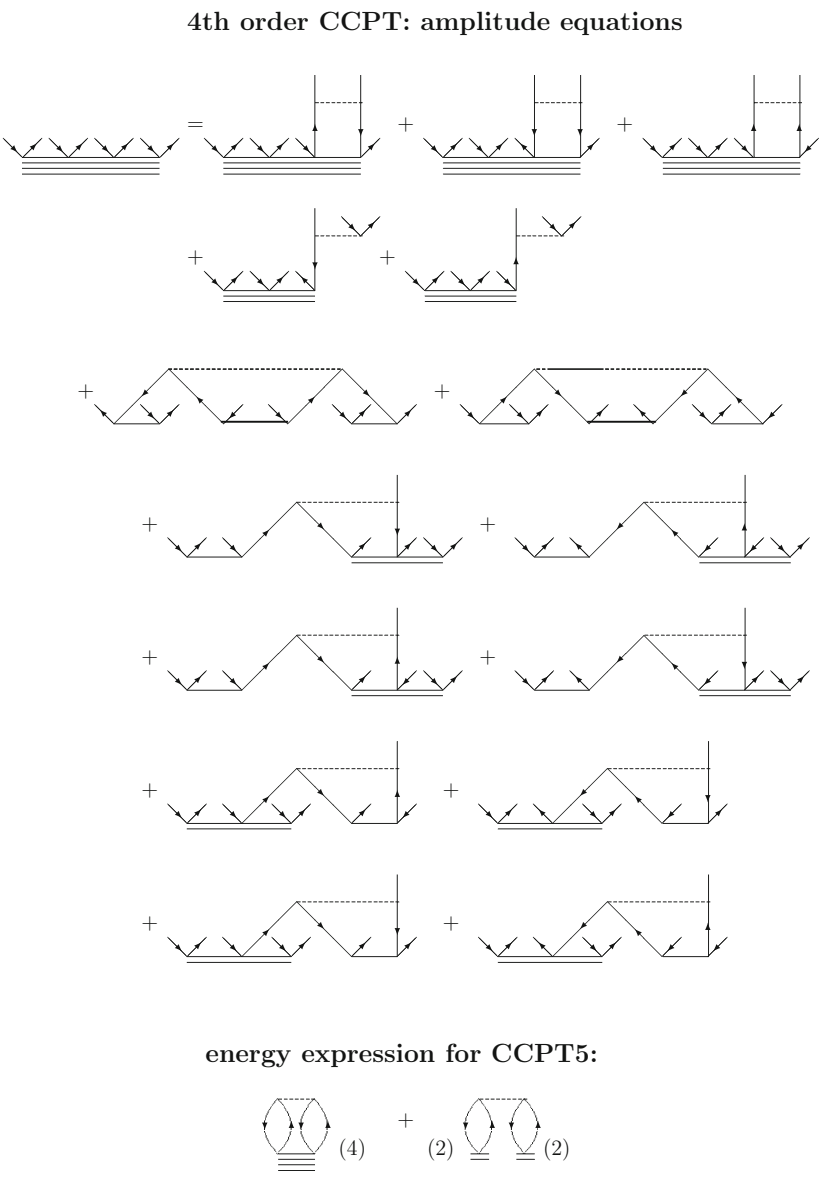

Figure 1-10. Diagrammatic form (in the antisymmetrized formalism) of the CCPT5 model (T_4 amplitude along with the fifth-order energy expression)

It is worth noting that the removal of the "long" denominator is a necessary but not sufficient condition for obtaining an efficient computational scheme. The latter can be obtained if – additionally – the terms contributing to T_4 contain amplitudes of the lower cluster rank, e.g. T_2 or T_3. Having a T_4 to T_4 component (see first three contributions to T_4 in Figure 1-5) prevents us from benefiting from the factorization theorem.

Although we report results through fifth-order, at this point we depend upon the diagrams rather than any further algebraic discussion. The diagrams for the fourth-order wave function through quadruple excitations and HF orbitals are shown in Figures 1-8, 1-9, and 1-10 along with the fifth-order energy expressions.

1.6. RESULTS AND DISCUSSION

The results obtained with the variants introduced in the previous section are collected in Tables 1-3,1-4,1-5, and 1-6

All calculations are done using the ACES II [42] program system supplemented with the CCPT methods. The main goal of computational tests is to compare the correlation corrections obtained with new methods with reference data provided by the full configuration interaction (FCI) scheme. We selected five systems: the molecules HF, H_2O and SiH_2 in the DZP basis set, H_2O in the DZ basis set, and N_2 in the cc-pVDZ basis set for which the FCI values are available [43–46].

Adopting the same geometry we are able to assess the performance of the newly constructed approximations. For some systems we considered also the geometry with stretched bonds to test the sensitivity of the method with respect to the increased multiconfigurational character of the reference function.

In Table 1-3 we list standard CC models with full inclusion of the relevant clusters, i.e., CCSD, CCSDT and CCSDTQ and compare their results with those obtained by the respective CCPT schemes. The comparison shows that the new SD scheme which is simply LinCCD provides better agreement with the exact data than does the standard CCSD approach. However, the incorporation of the higher clusters T_3 and T_4 generally works better for standard CC than for the CCPT ones. The notable exception is the water molecule in both basis sets for which the CCPT4SDT method shows lower deviations from the exact values than does the CCSDT. At the quadruple level the standard scheme is significantly better than the new one. We also quote the results obtained with the approximate scheme, CCSD(T), which is known to provide values comparable in accuracy with the full CCSDT scheme. For the cases studied in this paper this is more or less true except for the SiH_2 system for which the CCSD(T) scheme is worse by more than an order of magnitude. However, in an absolute error sense, the approximate CCPT4SDT model performs noticeably better than the noniterative CCSD(T) approach but the appearance of several negative values point to future difficulties.

Table 1-3. Correlation corrections with various CC and CCPT methods relative to FCI[a] values (mHartree)

		CC[b]				CCPT		
		SD	SDT	SDTQ	SD(T)	2SD	4SDT	5SDTQ
HF(DZP)	R_e	3.006	0.266	0.018	0.360	2.041	−0.359	0.106
	$1.5R_e$	5.099	0.646	0.041	1.069	3.208	−0.692	0.089
	$2.0R_e$	10.181	1.125	0.062	2.745	4.026	−5.325	−2.229
H_2O(DZ)	R_e	1.790	0.434	0.015	0.574	2.422	0.028	0.036
	$1.5R_e$	5.590	1.473	0.141	1.465	2.899	−0.285	0.412
H_2O(DZP)	R_e	4.122	0.531	0.023	0.766	1.819	0.001	0.044
	$1.5R_e$	10.158	1.784	0.139	2.861	0.997	0.147	0.821
SiH_2(DZP)	R_e	2.843	0.100	0.002	1.234	−0.950	−0.075	0.070
	$1.5R_e$	6.685	0.058	−0.015	3.175	−0.299	−1.680	−0.436
N_2(pVDZ)	R_e	13.465	1.626	0.192	1.235	6.694	−1.079	

[a] References [43–46].
[b] References [15, 47, 48].

In Table 1-4 we compare the correlation corrections obtained with the various MBPTn schemes up to $n = 6$. The superiority of the CCPT schemes is evident, in particular for the cases in which we have multiconfigurational character. We see that even the crudest approximation, i.e. CCPT2SD is better than, e.g., the MBPT5. The failure of the standard single reference MBPT methods for multireference problems is well known, but it is worth noticing that the CCPT scheme treats such cases better due to the infinite summation of certain classes of diagrams.

As we have shown in the previous sections the assumed strategy of generating the CCPT methods allows for a number of variants. In Table 1-5 we study the

Table 1-4. Correlation corrections with various MBPT and CCPT variants relative to FCI[a] values (mHartree)

		MBPT[b]					CCPT		
		(2)	(3)	(4)	(5)	(6)	2SD	4SDT	5SDTQ
HF(DZP)	R_e	7.804	5.438	−0.264	0.859	−0.229	2.041	−0.359	0.106
	$1.5R_e$	10.639	11.852	0.768	2.797	−0.407	3.208	−0.692	0.089
	$2.0R_e$	24.045	26.959	4.840	8.103	−1.132	4.026	−5.325	−2.229
H_2O(DZ)	R_e	8.550	7.159	0.990	0.810	0.087	2.422	0.028	0.036
	$1.5R_e$	19.945	25.130	6.126	4.750	1.910	2.899	−0.285	0.412
H_2O(DZP)	R_e	12.964	7.222	0.919	0.703	0.077	1.819	0.001	0.044
	$1.5R_e$	23.310	26.361	5.764	4.984	1.816	0.997	0.147	0.821
SiH_2(DZP)	R_e	29.423	9.701	3.658	1.617		−0.950	−0.075	0.070
	$1.5R_e$	48.582	23.353	11.033	5.456		−0.299	−1.680	−0.436
N_2(pVDZ)	R_e	16.687	20.726	−1.450			6.694	−1.079	

[a] References [43–46].
[b] References [49, 50].

Table 1-5. Correlation corrections with various CCPT variants relative to FCI[a] values (mHartree)

		CCPT											
		2SD	4SD	4SDn	5SD	5SDn	4SDT	4SDTn	5SDT	5SDTn	4SDTQ	5SDTQ	5SDTQn
HF(DZP)	R_e	2.041	2.689	4.974	3.092	5.377	−0.359	1.927	0.288	2.858	−0.935	0.106	0.390
	$1.5R_e$	3.208	4.513	7.173	5.319	7.979	−0.692	1.967	0.586	3.678	−1.875	0.089	0.521
	$2.0R_e$	4.026	7.906	9.474	8.336	9.905	−5.325	−3.756	−1.874	0.428	−7.303	−2.229	−1.495
H_2O(DZ)	R_e	2.422	1.612	4.078	1.885	4.351	0.028	2.494	0.453	3.118	−0.628	0.036	0.235
	$1.5R_e$	2.899	5.949	9.430	6.504	9.984	−0.285	3.195	1.423	4.712	−2.415	0.412	0.211
H_2O(DZP)	R_e	1.819	4.061	6.538	4.291	6.767	0.001	2.477	0.527	3.045	−0.878	0.044	0.086
	$1.5R_e$	0.997	12.223	14.666	12.759	15.202	0.147	2.590	2.104	4.176	−2.582	0.821	0.451
SiH_2(DZP)	R_e	−0.950	3.310	3.200	3.404	3.293	−0.075	−0.185	0.136	−0.359	−0.269	0.070	−0.046
	$1.5R_e$	−0.299	6.962	5.904	7.911	6.853	−1.680	−2.737	−0.573	−1.970	−1.945	−0.436	−0.776
N_2(pVDZ)	R_e	6.694	13.582	16.833	14.537	17.788	−1.079	2.172	1.319	3.126			

[a] References [43–46].

Table 1-6. Correlation corrections with various CCPT4SDT and CCPT5SDT variants relative to FCI[a] values (mHartree)

			CCPT4SDT+(T)				CCPT5SDT+(T)		
		CCPT4SDT	$T_2^{[1]}W^{[+1]}$	$T_2^{(1)}W^{[+1]}$	$T_3^{(3)}(const.)$	CCPT5SDT	$T_2^{[1]}W^{[+1]}$	$T_2^{(1)}W^{[+1]}$	$T_3^{(4)}(const.)$
HF(DZP)	R_e	−0.359	−0.102	−0.115	−0.359	0.288	0.336	0.338	0.287
	$1.5R_e$	−0.692	−0.213	−0.220	−0.692	0.586	0.736	0.763	0.585
	$2.0R_e$	−5.325	−2.913	−2.305	−5.720	−1.874	−1.375	−1.192	−1.879
H_2O(DZ)	R_e	0.028	0.181	0.180	0.029	0.453	0.470	0.473	0.452
	$1.5R_e$	−0.285	0.635	0.868	−0.293	1.423	1.660	1.860	1.420
H_2O(DZP)	R_e	0.001	0.301	0.297	0.074	0.527	0.601	0.610	0.490
	$1.5R_e$	0.147	1.330	1.568	0.151	2.104	2.671	3.284	2.077
SiH_2(DZP)	R_e	−0.075	0.009	0.043	−0.070	0.136	0.231	0.344	0.130
	$1.5R_e$	−1.680	−1.549	−1.522	−1.666	−0.573	−0.255	0.022	−0.587
N_2(pVDZ)	R_e	−1.079	0.428	0.363	−1.062	1.319	1.873	1.973	1.312

[a] References [43–46].

performance of some of them. The columns headed with the 2SD, 4SD and 5SD acronyms represent the SD model at various levels of sophistication of the T_2 equation, see Figures 1-4, 1-5, 1-6, 1-7, 1-8, 1-9, and 1-10. Note that these models neglect the T_3 and T_4 clusters.The general conclusion is that the simplest model works best which means that making the T_2 equation more complex generates some misbalance when ignoring higher clusters. The same is generally true for the models which include the T_3 operator, see columns with 4SDT and 5SDT. The only exception is the SDTQ model where the best results are obtained for the 5SDTQ model.

In Table 1-5 we also include variants based on the *nCC* approach [51, 52], see the columns with headers SDn, SDTn and SDTQn. The detailed analysis of this class of approximations is given elsewhere [51, 52]. Here we compare only the respective values. A general feature of *nCC* models is their more stable character with respect to multireference situations albeit with less work. The deviations from the exact values are larger, however, but less affected by the distorted geometry of the molecules investigated.

In Table 1-6 we investigate the sub-models of the CCPTSDT scheme based on the noniterative inclusion of the T_3 operator. Each noniterative T_3 contribution is obtained in a different manner depending upon the energy expression involving the T_3 operator. The energy expression is obtained by "closing" the T_3 operator with the product of $T_2W^{[+1]}$ taken in such a way that it generates triple excitation (in fact it will be used in the deexcitation form). Contrary to our usual notation, here $T_2^{[1]}$ represents the pure first MBPT order, while $T_2^{(1)}$ is the amplitude obtained by solving the first order CCPT T_2 equation (ie LCCD). Finally, the $T_3^{(3)}(const.)$ represents the T_3 operator obtained with the T_3 amplitude which neglects the T_3 to T_3 contribution (see Figures 1-7 and 1-9 for amplitude equations). The small change due to the latter approximation suggests that the computationally involved step can often be eliminated, though it is an essential part of the theory as presented in this first study.

Surprisingly some of the noniterative schemes give quite good results. E.g. the approaches denoted as $T_2^{[1]}W^{[+1]}$ and $T_2^{(1)}W^{[+1]}$ give values which are close to each other and in some cases better than the parent model. In particular the HF results are significantly improved with the error reduced nearly 3 times. The same is true for SiH_2 and N_2 systems, where the mentioned noniterative scheme works better than the parent scheme.

1.7. SUMMARY

The problem with CC theory and symmetry is that all correlation information is summed into the amplitude equations from the bottom. This leads to beautiful, connected equations and very powerful, *infinite-order* summation methods. But its weakness is that a truncation of the latter to CCSD, eg., will miss terms that are hermitian conjugates that only arise from higher connected cluster operators like T_4. The Kucharski-Bartlett [2, 15, 41] factorized inclusion of T_4 in fifth-order MBPT,

which arises in 4th order here,

$$E_Q^{(4)} = \langle 0|[T_2^{(1)\dagger}]^2 W^{[0]} T_4^{(2)}|0\rangle = \frac{1}{2}\langle 0|[T_2^{(1)\dagger}]^2 W^{[0]}[T_2^{(1)^2}]|0\rangle, \tag{1-125}$$

is an illustration. First, it arises from T_4 in standard CC theory. Yet aided by denominator factorization it becomes a symmetric expression that reduces an otherwise, ~n^4N^5 computation if the 8 index denominator in $T_4^{(2)}$ had to be included, to ~n^2 N^5 while only requiring consideration of T_2 operators. Such terms naturally arise in symmetric formulations of PT [53] based upon the expectation value, $\langle 0|\exp(T^\dagger)H\exp(T)|0\rangle_L$, while only retaining T_2 operators This is part of the driving force for finding more symmetric, or hermitian forms for the equations. However, it has been discussed that using such symmetric formulations, whether UCC, XCC, SXCC and even the proposed SC-XCC, all have their weaknesses, too [54].

Here we show that such quadruple diagrams arise in CCPT but not until after simplification as in Eqs. (1-121) and (1-122), due to their symmetry, that tells us only T_2 is required in the computation. That is because CCPT is still built upon "connected" terms just as is CC theory itself. To achieve the full benefit of symmetric forms "connected" has to be relaxed to "linked" as that will enable the symmetric $2m$ formulae to be used routinely to derive expansions. This extension will be presented elsewhere. However, the first useful step toward this goal is the CCPT presented here, with the understanding that the fully symmetric route to approximations [54] still will be more hermitian than CCPT.

The nice thing about perturbation theory is that it is innately hermitian, albeit at the cost of being limited to finite order instead of the infinite-order analogs offered by CC theory. So the potential compromise is that we sum much more into the perturbation theory by defining a new H_0, but still retain the underlying hermitian aspects and whatever benefits might accrue.

In CCPT we pursue the full CI solution order-by-order in terms of a generalized PT. MBPT would formally accomplish the same thing but with the standard choice of $H_0 = F^{[0]}$. Rather than pursuing the standard MBPT route, we introduce an alternative choice of H_0 that includes infinite-order sums of selected double excitation operators from the beginning. This is a hermitian choice and it provides the LinCCD result in even the lowest order wave function, at the cost of using a non-diagonal resolvent. We also know that barring singularities, that approximation is really quite good [34, 36]. The latter, however, remains computationally attractive, as it only requires the solution to a linear equation, analogous to how EOM-CC second-order properties are evaluated [31] and lends itself to convenient massively parallel evaluation, which is important to ACES III [55]. Further simplifications should be possible by subjecting such high-rank linear equations to procedures that provide an effective lower rank, like that due to Cholesky [56] or singular value decomposition [57], to enable to be able to solve these equations efficiently, if the accuracy obtained warrants it.

CCPT could be viewed as simply an alternative iterative solution of the CC equations starting from the LinCCD approximation, long used as a first approximation to solve CC equations [6]. However, here, it intentionally differs from an iterative solution of the CC equations because we want to have the PT symmetry. Furthermore, we want to have *all* contributions of a given excitation level in the particular order. In other words, what really distinguishes MBPT from CI perturbation theory is the insistence on including all excitations for a given order. In that way, all unlinked diagrams disappear. The linked diagram theorem cancels them from the beginning, leading to linked and eventually to the connected equations of CC, but the fact they can also be removed from CI by this expedient, tells us that a hermitian formulation can be recovered in finite order.

Another potential advantage of this approach is what it might tell us about the role of triple, quadruple, and higher excitations. Relationships that relate different cluster operators might be obtained, somewhat similar to the Kucharski-Bartlett expression, once a threshold is reached toward convergence, e.g. We would hope that by putting more infinite-order correlation into the unperturbed H_0, that we can obtain a more rapidly converging sequence of approximations for molecular applications. We also want the flexibility to hide some kinds of correlation effects into correlated orbitals [58], thereby potentially alleviating the need to have to consider those effects elsewhere in the calculations. In particular, the implementation of such higher excitation methods demand a much more severe scaling than that of CCSD. As the equations show, in terms of the new orders of CCPT, their appearance occurs in higher-order, and has the interesting feature of PT in that their first appearance in the wave function does not actually change the energy until the next order.

The numerical results are limited so far, but as one would expect, CCPT has to offer superior convergence to ordinary MBPT, unless we encounter singularities that are not removed by higher-order terms. For those situations, the singularity free variant [34] would be preferred. However, the latter mostly fixes LinCCSD so that it becomes virtually CCSD, which is not always the optimum approach. Further work will address what hermitian methods can offer beyond the simple examples illustrated here.

One other hermitian model is worthy of mention as an illustration of symmetric expressions and limiting H_0 to only Coulomb terms. This is the ancient one of the sum of just the ring diagrams for the correlation without any exchange. It is known that it is exact for the high-density electron gas [26], unlike the finite sum of MBPT diagrams. Any such infinite summation of ring diagrams can be extracted from CC theory by simplifying the CCD equations in such a way that only the repeated pair bubbles are produced, with no "ladder" type interactions anywhere in the analysis. Such ring CCD (r-CCD) methods have become of interest in DFT circles because of the viewpoint that exchange is put elsewhere in DFT and the only other term of interest is the Coulomb part of the correlation [59]. This pertains to the so-called GW theory [60], and in the recent work on van der Waals' interactions in DFT [61, 62]. The sum of ring diagrams can be written in terms of a Coulomb only $\mathbf{T}_2$ set of amplitudes, assuming Goldstone diagrams, by the expression

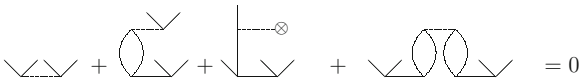

which can be written in matrix form as ([61]):

$$\mathbf{B} + \mathbf{A}\mathbf{T}_2 + \mathbf{T}_2\mathbf{A} + \mathbf{T}_2\mathbf{B}\mathbf{T}_2 = \mathbf{0} \tag{1-126}$$

where the **A** and **B** matrices are the usual ones familiar from TDHF or RPA. **A** is also the matrix that accounts for CIS' approximations to excited states, while **B** introduces the single de-excitation term. It has been shown [61] that the solution of this equation may also be obtained from the RPA equations

$$\begin{pmatrix} \mathbf{A} & \mathbf{B} \\ -\mathbf{B} & -\mathbf{A} \end{pmatrix} \begin{pmatrix} \mathbf{X} \\ \mathbf{Y} \end{pmatrix} = \begin{pmatrix} \mathbf{X} \\ \mathbf{Y} \end{pmatrix} \begin{pmatrix} \omega_1 & & \mathbf{0} \\ & \ddots & \\ \mathbf{0} & & \omega_n \end{pmatrix} \tag{1-127}$$

and constructing $\mathbf{T}_2$ as $\mathbf{T} = \mathbf{Y}\mathbf{X}^{-1}$. See [25, 63] for a derivation of the RPA equations with exchange from the expectation value of $\exp(T_1)$. With or without exchange this equation is obviously hermitian, making $T_2^\dagger = T_2$. So it could be used as another choice to define a hermitian H_0.

A calculation of the r-CCD correlation energy without exchange for five small systems (N_2, F_2, C_2, O_3, and HF) around their equilibrium geometries gives 0.031 H of average differences with the CCSD correlation energy, compared to a CCD value of -0.007 H. If we use Brueckner orbitals taken from CCSD in such a ring approximation, we obtain 0.036 H. This work will be published elsewhere [64].

ACKNOWLEDGMENTS

This work has been supported by the U.S. Air Force Office of Scientific Research, under grant No. FA9550-07-1-0070.

REFERENCES

1. R. J. Bartlett, G. D. Purvis III, Int. J. Quantum Chem. **14**, 561 (1978)
2. R. J. Bartlett, M. Musial, Rev. Mod. Phys. **79**, 291 (2007)
3. H. Sekino, R. J. Bartlett, Adv. Quantum Chem. **35**, 149 (1999)
4. A. Taube, R. J. Bartlett, Int. J. Quantum Chem. **106**, 3393, (2006)
5. J. Čížek, J. Chem. Phys. **45**, 4256, (1966)
6. J. Paldus, J. Čížek, I. Shavitt, Phys. Rev. A **5**, 50 (1972)
7. J. F. Stanton, R. J. Bartlett, J. Chem. Phys. **98**, 7029 (1993)
8. R. J. Bartlett, 'Analytical evaluation of gradients in coupled-cluster and many-body perturbation theory' in *Geometrical Derivatives of Energy Surfaces and Molecular Properties*, Eds. P. Jørgensen, J. Simons (Reidel, Dordrecht, The Netherlands, 1986), pp. 35–61

9. E. A. Salter, G. W. Trucks, R. J. Bartlett, J. Chem. Phys. **90**, 1752 (1989)
10. R. J. Bartlett, S. A. Kucharski, J. Noga, Chem. Phys. Lett. **155**, 133 (1989)
11. W. Kutzelnigg, in *Methods of Electronic Structure Theory*, Ed. H. F. Schaefer III (Plenum, New York, 1977), p. 129
12. J. D. Watts, G. W. Trucks, R. J. Bartlett, Chem. Phys. Lett. **164**, 502 (1989)
13. T. Yanai, G. K.-L. Chan, J. Chem. Phys. **124**, 194106 (2006)
14. A. Taube, R. J. Bartlett, J. Chem. Phys. **128**, 044110 (2008)
15. S. A. Kucharski, R. J. Bartlett, J. Chem. Phys., 108, 5243 (1998)
16. L. Adamowicz, W. D. Laidig, R. J. Bartlett, Int. J. Quantum Chem. Symp. **18**, 245–254 (1984)
17. S. Villaume, C Daniel, A. Strich, A. Perera, R. J. Bartlett, J. Chem. Phys. **122**, 044313 (2005)
18. W. Meyer, J. Chem. Phys. **5**8, 10 (1973)
19. J. Noga, M. Urban, Theor. Chim. Acta **73**, 291 (1988)
20. E. A. Salter, H. Sekino, R. J. Bartlett, Chem. Phys. **87**, 502 (1987)
21. H. P. Kelly, Adv. Chem. Phys. **14**, 129 (1969)
22. R. J. Bartlett, D. M. Silver, Phys. Rev. A **10**, 1927 (1974)
23. R. J. Bartlett, D. M. Silver, Chem. Phys. Lett. **29**, 199 (1974)
24. J. A. Pople, J. S. Binkley, R. Seeger, Int. J. Quantum Chem. Sym. **10**, 1 (1976)
25. I. Shavitt, R. J. Bartlett, *Many-Body Methods in Quantum Chemistry: Many-Body Perturbation Theory and Coupled-Cluster Theory* (Cambridge Press, Cambridge, 2009)
26. A. L. Fetter, J. D. Walecka, *Quantum Theory of Many-Body Systems* (McGraw-Hill, New York, 1971)
27. J. Olsen, O. Christiansen, H. Koch, P. Joergensen, J. Chem. Phys. **105**, 5082 (1996)
28. S. Hirata, R. J. Bartlett, Chem. Phys. Lett. **321**, 216 (2000)
29. K. Ragavachari, G. W. Trucks, J. A. Pople, M. Head-Gordon, Chem. Phys. Lett. **157**, 479 (1989)
30. T. Helgaker, P. Jörgensen, J. Olsen, in *Molecular Electronic Structure Theory* (Wiley, Chichester, 2000).
31. J. F. Stanton, R. J. Bartlett, J. Chem. Phys. **99**, 5178 (1993)
32. J. F. Gauss, J. F. Stanton, J. Chem. Phys. **103**, 3561 (1995)
33. S. A. Perera, R. J. Bartlett, J. Am. Chem. Soc. **122**, 1231 (2000)
34. A. Taube, R. J. Bartlett, J. Chem. Phys. **130**, 144112 (2009)
35. J. Paldus, P. E. S. Wormer, F. Visser, A. van der Avoird, J. Chem. Phys. **76**, 2458 (1982)
36. V. Lotrich, R. J. Bartlett, unpublished
37. I. Grabowski, V. Lotrich, R. J. Bartlett, J. Chem. Phys. **127**, 154111 (2007)
38. P. S. Epstein, Phys. Rev. **28**, 695 (1926)
39. R. J. Bartlett, in *Modern Electronic Structure Theory*, vol. 2, Ed. D. R. Yarkony (World Scientific, Singapore, 1995), pp. 1047–1131
40. M. Urban, J. Noga, S. J. Cole, R. J. Bartlett, J. Chem. Phys. **83**, 4041 (1985)
41. S. A. Kucharski, R. J. Bartlett, J. Chem. Phys. **108**, 9221 (1998)
42. ACES II program is a product of the Quantum Theory Project, University of Florida Authors: J. F. Stanton, J. Gauss, J. D. Watts, M. Nooijen, N. Oliphant, S. A. Perera, P. G. Szalay, W. J. Lauderdale, S. A. Kucharski, S. R. Gwaltney, S. Beck, A. Balková, M. Musial, D. E. Bernholdt, K.-K. Baeck, H. Sekino, P. Rozyczko, C. Huber, R. J. Bartlett, Integral packages included are VMOL (J. Almlöf, P. Taylor); VPROPS (P. R. Taylor); A modified version of ABACUS integral derivative package (T. U. Helgaker, H. J. Aa. Jensen, J. Olsen, P. Jørgensen, P. R. Taylor)
43. C. W. Bauschlicher Jr., S. R. Langhoff, P. R. Taylor, N. C. Handy, P. J. Knowles, J. Chem. Phys. **85**, 1469 (1986)
44. C. W. Bauschlicher Jr., P. R. Taylor, J. Chem. Phys. **85**, 2779 (1986)
45. C. W. Bauschlicher Jr., P. R. Taylor, J. Chem. Phys. **86**, 1420 (1987)
46. O. Christiansen, H. Koch, P. Jörgensen, J. Olsen, Chem. Phys. Lett. **256**, 185 (1996)

47. S. A. Kucharski, R. J. Bartlett, J. Chem. Phys. **97**, 4282 (1992)
48. M. Musiał, S. A. Kucharski, R. J. Bartlett, J. Chem. Phys. **116**, 4382 (2002)
49. S. A. Kucharski, R. J. Bartlett, Chem. Phys. Lett. **237**, 264 (1995)
50. S. A. Kucharski, J. Noga, R. J. Bartlett, J. Chem. Phys. **90**, 7282 (1989)
51. R. J. Bartlett, M. Musiał, J. Chem. Phys. **125**, 204105 (2006)
52. M. Musiał, R. J. Bartlett, J. Chem. Phys. **127**, 024106 (2007)
53. R. J. Bartlett, S. A. Kucharski, J. Noga, J. D. Watts, G. W. Trucks, in *Some Consideration of Alternative Ansatz in Coupled-Cluster Theory*, Lecture Notes in Chemistry, vol. 52, Ed. U. Kaldor (Springer-Verlag, Heidelberg, 1989), pp. 125–149
54. P. G. Szalay, M. Nooijen, R. J. Bartlett, J. Chem. Phys. **103**, 281 (1994)
55. V. Lotrich, N. Flocke, M. Ponton, A. D. Yau, A. Perera, E. Deumens, R. J. Bartlett, J. Chem. Phys. **128**, 194104 (2008)
56. N. H. F. Beebe, J. Linderberg, Int. J. Quantum Chem. **12**, 683 (1977)
57. T. Kinoshita, O. Hino, R. J. Bartlett, J. Chem. Phys. **119**, 7756 (2003)
58. R. J. Bartlett, Chem. Phys. Lett. **484**, 1 (2009)
59. F. Furche, Phys. Rev. B **64**, 195120 (2001)
60. J. Harl, G. Kresse, Phys. Rev. B **77**, 045136 (2008)
61. G. E. Scuseria, T. M. Henderson, D. C. Sorensen, J. Chem. Phys. **129**, 231101 (2008)
62. B. G. Janesko, T. M. Henderson, G. E. Scuseria, J. Chem. Phys. **130**, 081105 (2009)
63. X. Li, J. Paldus, in *Recent Advances in Coupled-Cluster Methods*, Ed. R. J. Bartlett (World Scientific, Singapore, 1997), pp. 183–219
64. T. Kuś, R. J. Bartlett, unpublished.

CHAPTER 2

REDUCED-SCALING COUPLED-CLUSTER THEORY FOR RESPONSE PROPERTIES OF LARGE MOLECULES

T. DANIEL CRAWFORD

Department of Chemistry, Virginia Tech, Blacksburg, VA, USA, e-mail: crawdad@vt.edu

Abstract: The current state of locally correlated coupled cluster theory is reviewed, with an emphasis on recent developments applicable to response properties. The "correlation domain" selection schemes that have yielded great success for computations of ground-state energies are found to be inadequate for field-response properties, including polarizabilities, excitation energies, and transition probabilities. Alternative approaches for expanding the venerated Boughton–Pulay orbital domains are considered, including the use of the first-order orbital response via the coupled-perturbed Hartree–Fock equations. Applications of these selection schemes to frequency-dependent dipole-polarizabilities and optical rotation in chiral species demonstrate that local correlation methods have great promise for such properties for large molecules.

Keywords: Response properties, Locally correlated coupled cluster, Large molecules

2.1. INTRODUCTION

One of the great triumphs of modern quantum chemistry is its ability to provide reliable predictions of a wide variety of molecular properties [1], including those associated with the response of a molecule to external electromagnetic fields via scattering, refraction, and absorption [2–4]. Quantum chemical models are now routinely employed to compute absorption properties such as excitation energies [5–8], oscillator strengths [9, 10], and circular dichroism rotational strengths [11–17], as well as non-absorption properties such as static and frequency-dependent dipole (hyper)polarizabilities and magnetizabilities [18–23], and mixed-field perturbations, such as those related to chiroptical response [11, 13–17].

Among the wide array of electronic structure models used to compute response properties is coupled cluster theory [24–26], often referred to in the chemical literature as the "gold standard" of quantum chemistry for its exceptional accuracy compared to experiment for common properties such as molecular structure and thermodynamic constants [27, 28]. The first extension of coupled cluster theory to response properties was reported in 1977 by Monkhorst [29], who demonstrated that

P. Čársky et al. (eds.), Recent Progress in Coupled Cluster Methods, 37–55.
DOI 10.1007/978-90-481-2885-3_2,

the use of an exponential *Ansatz* for both the perturbed and unperturbed wave functions leads to expressions for second- and higher-order properties that are at least quadratic in the perturbed amplitudes. Two years later, Mukherjee and Mukherjee [30] presented the theory behind computation of transition energies using the coupled cluster approach, including equations for the necessary matrix elements. The first chemical tests of coupled cluster response methods appeared in 1984 with the work of Sekino and Bartlett [5], who also considered orbital relaxation effects and reported excitation energies of ethylene. In 1990, Koch and Jørgensen presented an alternative derivation of coupled cluster response theory based on a time-dependent Lagrangian formalism [31], including application to excitation energies [6]. A few years later, Stanton and Bartlett [7] discussed the application of the closely related equation-of-motion coupled cluster (EOM-CC) method to excitation energies, transition probabilities, and other properties. The Lagrangian approach to CC response properties pioneered by the Danish and Norwegian groups has continued to flourish with the efficient implementation of linear response functions for excitation energies [32, 33], frequency-dependent dipole-polarizabilities [21, 34], and transition probabilities [10], as well as the development of a hierarchical series of methods, including CC2 [35] as an approximation to CCSD (coupled cluster singles and double), and CC3 [34, 36–38] as an approximation to CCSDT (coupled cluster singles, doubles, and triples). More recently, several groups have reported the application of CC response theory to chiroptical properties, including optical rotation and circular dichroism spectra, with the ultimate goal of producing computational tools for the identification of absolute stereochemical configurations of chiral molecules [12, 39–46].

The Achilles' heel of conventional coupled cluster theory is its high-order scaling with molecular size – $\mathcal{O}(N^6)$ or worse. This so-called "polynomial scaling wall" prevents the routine application of coupled cluster methods to larger, more chemically significant molecules. While many implementations of coupled cluster response theory on high-performance computing hardware are known for their efficiency (including NWChem [47], CFOUR [48], ACESIII [49], DALTON [50], and PSI [51]), they still require substantial resources – both in terms of computing time and memory/disk storage – and are typically limited to response computations on molecules containing 10–12 non-hydrogen atoms (in the absence of symmetry). To overcome this deficiency, a number of research groups have recently pursued the development of reduced-scaling coupled cluster models based on the local correlation approach first suggested by Pulay and Saebø in the 1980s [52–63]. The central assumption of this idea is that, by adopting well-localized forms of the MOs which are used to construct the determinantal expansion of the wave function, the parameters associated with interactions of electrons in spatially distant MOs should be negligible and may therefore be ignored. This approach has been utilized extensively for ground-state energies by Werner, Schütz, and co-workers, who have demonstrated that it is possible to obtain CC ground-state energies (including perturbative triple excitations) for chains of up to 16 glycine molecules in a matter of hours using desktop workstations [61, 62].

The extension of the local correlation concept to response properties, however, has been more difficult than for ground-state energies for several reasons. First, even in a well-localized orbital basis, the sparsity of the perturbed wave functions is reduced relative to their unperturbed counterparts, resulting in cross-over points between canonical and localized algorithms at larger molecules for response properties than for energies. Second, the construction of the most effective scheme for partitioning the wave function in the localized orbital basis (i.e. the construction of reliable orbital domains) for different types of external-field perturbations is much more involved for perturbed wave functions and response functions. Third, while the implementation of efficient locally correlated CC energies is a significantly more complicated task than canonical-orbital energies, the level of complexity of the code increases further for response properties, thus impeding the development of new software.

This chapter will review the current state of reduced-scaling coupled cluster methods for molecular response properties. We will begin with an overview of the relevant theoretical methods, including EOM-CC and response formalisms, before focusing on the various factors that arise when extending the Pulay–Sæbø local-correlation approach to response properties. Finally, we will consider possible future developments that may allow computations of molecules containing dozens of atoms using some of the most reliable quantum chemical models.

2.2. LOCAL COUPLED CLUSTER THEORY

The coupled cluster energy functional is given by [24]

$$E_{\mathrm{CC}} = \langle 0|\,(1+\Lambda)\,e^{-T}H_0e^{T}\,|0\rangle = \langle 0|\,(1+\Lambda)\,\bar{H}_0|0\rangle = E^{(0)}, \tag{2-1}$$

where $|0\rangle$ is a single-determinant reference wave function (typically a Hartree–Fock wave function), and H_0 is the electronic Hamiltonian. The cluster excitation, T, and de-excitation, Λ, operators are determined, respectively, from the stationary conditions [64]

$$\left(\frac{\partial E_{\mathrm{CC}}}{\partial \Lambda_\phi}\right)_T = \langle \phi|\bar{H}_0|0\rangle = 0 \tag{2-2}$$

and

$$\left(\frac{\partial E_{\mathrm{CC}}}{\partial T_\phi}\right)_\Lambda = \langle 0|(1+\Lambda)\big(\bar{H}_0 - E^{(0)}\big)|\phi\rangle = 0, \tag{2-3}$$

where $|\phi\rangle$ represents the set of excited determinants generated by T from $|0\rangle$ [e.g., for the coupled cluster singles and doubles (CCSD) [65] model, $T = T_1 + T_2$].

Unfortunately, the computational scaling of the coupled cluster model – both in terms of storage and CPU time – is high-degree polynomial. For the CCSD method,

the T_2 amplitudes require nominally $\mathcal{O}(N^4)$ storage and (iterative) $\mathcal{O}(N^6)$ CPU, where N is a measure of the size of the molecule (i.e. a function of the number of occupied and virtual molecular orbitals). Triples may be included using non-iterative (CCSD(T) [66, 67]) or iterative (CCSDT-n [68] or CC3 [36]) algorithms with $\mathcal{O}(N^7)$ scaling that avoid explicit storage of the $\mathcal{O}(N^6)$ T_3 amplitudes and the $\mathcal{O}(N^8)$ scaling of the full CCSDT approach. In practical terms, these scalings imply that doubling the size of the molecule of interest leads to a factor of 32–64 increase is amplitude storage and a factor of 64–128 (or worse) increase in the CPU time. Clearly such costs are prohibitive for applications involving molecules beyond a dozen or so non-hydrogen atoms (depending on the molecular symmetry).

The underlying reason for this polynomial scaling is the use of canonical molecular orbitals (MOs), which, although mathematically convenient, tend to yield little sparsity and large numbers of non-negligible determinantal wave function contributions. There exist a number of schemes under active development for reducing the scaling of the coupled cluster method, including atomic-orbital [69] and projected-orbital [70] basis techniques, fragment-molecular-orbital methods [71], transferable-amplitude concepts [72], and more [73, 74]. The fundamental concept underlying all of these approaches is the idea that the electronic wave function may be partitioned in some a priori manner that allows the systematic neglect of vast numbers of small (or, ideally, vanishing) contributions. In the reduced-scaling approach pioneered by Pulay and Sæbø in the 1980s [52–56], this partitioning hinges on the localization of the molecular orbitals that underlie the determinantal expansion of the wave function.

In most applications of the Pulay–Sæbø scheme, the occupied orbitals are first subjected to a localization criterion such as the minimization of the orbital spatial-extent used by Boys [75, 76] or the charge localization approach of Pipek and Mezey [77]. The unoccupied/virtual orbitals, however, are typically much more difficult to localize directly, and are thus taken to be the virtual-space projection of the atomic-orbital basis set. This maintains the necessary orthogonality between the occupied and unoccupied orbital subspaces, at the expense of the introduction of redundancy (linear dependence) in the virtual space and the loss of orthogonality among the virtual orbitals themselves. Next, for each localized occupied orbital, ϕ_i, a subset of the virtual orbitals is identified as a single-excitation "domain", denoted $[i]$, into which determinantal substitutions will be allowed in the correlated wave function. If the atomic-orbital basis functions are atom-centered, which is by far the most common choice, the projected atomic orbitals (PAOs) that comprise the virtual orbitals will likewise be atom-centered. Thus, the correlation domain of a given occupied orbital consists of all PAOs associated with a given set of atoms.

The selection of the orbital domains is pivotal to the success or failure of the Pulay–Sæbø approach, and much effort has been expended on their construction for various applications [63]. For ground-state wave functions, the most common choice for the single-excitation domains is based on the Boughton-Pulay "completeness" criterion:

$$f_i(C') = \min\left\{\int (\phi_i - \phi')^2 d\tau\right\} = 1 - \sum_{\mu\in[i]}\sum_{\nu} C'^{i}_{\mu} S_{\mu\nu} C^{i}_{\nu}, \tag{2-4}$$

where ϕ' is the approximation to occupied molecular orbital ϕ_i for the chosen set of atomic orbitals, with associated coefficients C'^{i}_{μ} and C^{i}_{μ}, respectively. The overlap matrix in the atomic orbital basis is given by $S_{\mu\nu}$. To compute the completeness function for a given occupied orbital, the atoms are first organized into decreasing order of importance (often based on contributions to the orbital's total population, for example). The first atom (or group of symmetry equivalent atoms) and its associated PAOs is selected for the domain, and the value of the completeness function f_i is computed. If the value falls below a chosen cutoff, the domain for the orbital is sufficiently complete; if not, the set of PAOs on subsequent atoms in the list is added to the domain until the cutoff is reached. A typical value of the completeness criterion for ground-state local-MP2 and local-CCSD computations is 0.02, which preserves bonded atoms in well-localized systems and yields domains that are compact – typically consisting only of bonded atoms, lone pairs, etc.

Once the single-excitation domains have been selected, double- and higher-excitation domains must also be considered. The single-excitation domain structure described above yields linear scaling of the number of T_1 cluster amplitudes with the size of the molecular system, and such scaling is sought for the doubles and higher amplitudes, as well. However, if one were to choose the simple union of the single-excitation domains, $[i] \cup [j]$, for the two occupied orbitals, ϕ_i and ϕ_j, involved in a given double excitation, this would result in quadratic scaling in the number of T_2 amplitudes. On the other hand, limiting the pair-excitation domain to disjoint excitations such that excitations from ϕ_i are limited to the domain $[i]$ and those from ϕ_j to $[j]$ ignores essential correlation contributions (including dispersion). For these reasons, Pulay and Sæbø suggested partitioning the doubles amplitudes based on the distance between the corresponding occupied-orbital pair: strong, weak, and distant pairs. The strong pairs are treated with no approximation, while weak pairs may be treated at a lower level of theory (e.g. local-MP2), and distant pairs may be neglected entirely. The number of strong and weak pairs increases linearly with the size of the molecule, as desired, and the loss of accuracy in energies is typically small [57].

Numerous applications of the local-CC method for ground-state energetics have been presented, with Werner, Schütz, and co-workers providing the most impressive results to date. For example, upon coupling their local-CC methodology to emerging density-fitting (DF) techniques for rapid evaluation of important two-electron integrals, Schütz and Manby reported local-CCSD computations on chains containing up to 16 glycine molecules and well over 1,000 basis functions that required only a few hours of CPU time (whereas canonical-orbital CCSD algorithms would require years to complete). Such new technology has enabled applications of coupled cluster theory to realistic chemical systems, including the reaction barriers in enzymes [78].

2.3. LOCAL COUPLED CLUSTER FOR GROUND-STATE MOLECULAR RESPONSE PROPERTIES

In the development of a local-correlation approach to molecular response properties, there are a number of desirable characteristics of the canonical approach we should try to retain in the reduced-scaling formulation:

1. The approach should be applicable to both static and dynamic response functions. A method that is not extensible to frequency-dependent properties is limited in value.
2. Localization criteria – including the selection of orbital domains – must be identical for both perturbed and unperturbed wave functions. If this condition is not met, e.g. if one chose to use smaller orbital domains for the ground-state wave function for efficiency and then to expand those domains when computing the perturbed wave functions and response function, the resulting property would not be equivalent to that obtained via a finite-field computation, for example.
3. The localization approach should not change the pole structure of the response function. In most applications of CC response property computations, orbital relaxation is not explicitly included, in part because the resulting dispersion curves would exhibit an artifactual pole structure – second-order poles arising from orbital Hessian singularities, and first order poles arising from the correlated wave functions. The exclusion of orbital relaxation contributions yields the correct, first-order pole structure, and thus they should also be excluded in the locally correlated model.
4. For the balanced treatment of excited states, all states of interest should be treated using the same overall domain structure, including the ground state. If, for example, one were to solve the ground-state CC amplitude equations with one choice of domains, but then modify them for the construction of the similarity-transformed Hamiltonian, this would change the ground-state energy, which is implicitly the lowest eigenvalue of this matrix.
5. The canonical-MO coupled cluster equations are invariant to the choice of factorization used to reduce the overall computational cost of their solution. Many such factorizations exist [79–82], and their respective efficiencies depend somewhat on the molecule in question and the computer architecture employed. Thus, the local-CC scheme employed should be similarly invariant, for both practical and philosophical reasons.

Keeping the above issues in mind, our first step in the development of a locally correlated coupled cluster method to molecular properties is the choice of formulation.

2.3.1. The Equation-of-Motion and Response Theory Formulations

The two most widely used approaches for determining the molecular response to a (presumably) small perturbation, V are coupled cluster response (CCR) theory

[29, 30, 83, 84] and equation-of-motion coupled cluster (EOM-CC) theory, which are distinguished primarily by their choice of parametrization of the perturbed wave functions. In the EOM-CC approach, the Hamiltonian is partitioned using its similarity-transformed representation, viz.

$$\bar{H} = e^{-T} H e^{T} = e^{-T} H_0 e^{T} + e^{-T} V e^{T} = \bar{H}_0 + \bar{V}, \tag{2-5}$$

and the perturbed wave functions are expanded in a linear, CI-like ansatz through the cluster operators:

$$|\psi_{\mathrm{EOM-CC}}\rangle = \left(1 + T^{(1)} + T^{(2)} + \ldots\right)|0\rangle, \tag{2-6}$$

where the superscripts indicate the order of the perturbation and the cluster operators, $T^{(n)}$, produce the same set of determinants from the reference determinant $|0\rangle$ as the unperturbed cluster operator $T \equiv T^{(0)}$. As a result, the natural choice for the EOM-CC zeroth-order right- and left-hand wave functions are

$$|\psi^{(0)}\rangle = |0\rangle, \tag{2-7}$$

and

$$\langle\psi^{(0)}| = \langle 0|\,(1 + \Lambda)\,, \tag{2-8}$$

respectively, while the right-hand nth-order perturbed wave functions may be written simply as

$$|\psi^{(n)}\rangle = T^{(n)}|0\rangle. \tag{2-9}$$

In the CCR approach, the Hamiltonian is partitioned in its untransformed representation,

$$H = H_0 + V, \tag{2-10}$$

and the perturbed wave function is expressed in terms of an exponential parametrization,

$$|\psi_{\mathrm{CCR}}\rangle = e^{T^{(0)} + T^{(1)} + T^{(2)} + \cdots}|0\rangle. \tag{2-11}$$

In this case, the CC right- and left-hand zeroth-order wave functions are naturally chosen to be

$$|\psi^{(0)}\rangle = e^{T}|0\rangle, \tag{2-12}$$

and

$$\langle\psi^{(0)}| = \langle 0|\,(1 + \Lambda)\,e^{-T}, \tag{2-13}$$

respectively, and the right-hand first- and second-order wave functions may be written as

$$|\psi^{(1)}\rangle = e^T T^{(1)}|0\rangle, \tag{2-14}$$

and

$$|\psi^{(2)}\rangle = e^T \left[\frac{1}{2}\left(T^{(1)}\right)^2 + T^{(2)}\right]|0\rangle. \tag{2-15}$$

In order to determine molecular properties by these approaches, we employ Rayleigh–Schrödinger perturbation theory. In this formalism, the Schrödinger equation in first, second, and third order, becomes, respectively,

$$\left(E^{(0)} - H_0\right)|\psi^{(1)}\rangle = \left(V - E^{(1)}\right)|\psi^{(0)}\rangle, \tag{2-16}$$

$$E^{(2)}|\psi^{(0)}\rangle = \left(V - E^{(1)}\right)|\psi^{(1)}\rangle + \left(H_0 - E^{(0)}\right)|\psi^{(2)}\rangle, \tag{2-17}$$

and

$$E^{(3)}|\psi^{(0)}\rangle = \left(V - E^{(1)}\right)|\psi^{(2)}\rangle + \left(H_0 - E^{(0)}\right)|\psi^{(3)}\rangle - E^{(2)}|\psi^{(1)}\rangle. \tag{2-18}$$

By inserting the definition of the partitioned Hamiltonian and perturbed wave functions into the above expressions, followed by projection onto the corresponding zeroth-order wave function, we may obtain expressions for the perturbed energies within the EOM-CC and CCR models. In first-order, both approaches yield the same result:

$$E^{(1)} = \langle 0|e^{-T} V e^T|0\rangle = \langle 0|\bar{V}|0\rangle, \tag{2-19}$$

which is identical to that obtained by the derivative formulation. In second-order, however, the two approaches differ. In EOM-CC, we obtain

$$\begin{aligned} E^{(2)}_{\text{EOM-CC}} &= \langle\psi^{(0)}|\left(\bar{V} - E^{(1)}\right)|\psi^{(1)}\rangle - \langle\psi^{(0)}|\left(E^{(0)} - \bar{H}_0\right)|\psi^{(2)}\rangle \\ &= \langle 0|\,(1+\Lambda)\left(\bar{V} - E^{(1)}\right)T^{(1)}|0\rangle - \langle 0|\,(1+\Lambda)\left(E^{(0)} - \bar{H}_0\right)T^{(2)}|0\rangle \\ &= \langle 0|\,(1+\Lambda)\left(\bar{V} - E^{(1)}\right)T^{(1)}|0\rangle, \end{aligned} \tag{2-20}$$

where we have recognized that $T^{(2)}$ can generate only those determinants in the same space as T, and thus the stationary conditions for Λ in Eq. (2-3) eliminate the second term on the right-hand side. The first-order cluster operators required for the above equation may be determined by projecting the first-order EOM-CC

Schrödinger equation onto the set of determinants generated by $T|0\rangle$, resulting in a set of linear equations:

$$\langle\phi|\left(E^{(0)}-\bar{H}_0\right)T^{(1)}|0\rangle=\langle\phi|\bar{V}|0\rangle. \tag{2-21}$$

Although the form of Eq. (2-20) is appealing in its simplicity, it is not size-extensive unless the perturbed and unperturbed cluster operators include all possible excitations.

The CCR second-order Rayleigh–Schrödinger equation projected onto the zeroth-order left-hand wave function gives a somewhat different result:

$$\begin{aligned}
E^{(2)}_{\mathrm{CCR}} &= \langle\psi^{(0)}|\left(V-E^{(1)}\right)|\psi^{(1)}\rangle-\langle\psi^{(0)}|\left(E^{(0)}-H_0\right)|\psi^{(2)}\rangle \\
&= \langle 0|\left(1+\Lambda\right)e^{-T}\left(V-E^{(1)}\right)e^{T}T^{(1)}|0\rangle- \\
&\quad \langle 0|\left(1+\Lambda\right)e^{-T}\left(E^{(0)}-H_0\right)e^{T}\left[\frac{1}{2}\left(T^{(1)}\right)^2+T^{(2)}\right]|0\rangle \\
&= \langle 0|\left(1+\Lambda\right)\left(\bar{V}-E^{(1)}\right)T^{(1)}|0\rangle- \\
&\quad \langle 0|\left(1+\Lambda\right)\left(E^{(0)}-\bar{H}_0\right)\left[\frac{1}{2}\left(T^{(1)}\right)^2\right]|0\rangle.
\end{aligned} \tag{2-22}$$

The first term on the right-hand side above is identical to its EOM-CC counterpart, but the second term is unique to CCR. As before, the term containing $T^{(2)}$ in the above equation is zero because Eq. (2-3) is satisfied in the space of determinants generated by $T|0\rangle$. However, $\left(T^{(1)}\right)^2$ generates higher determinants, and thus may yield non-zero contributions. It may be shown [85] that the unlinked diagrams generated by the first term on the right-hand side of Eq. (2-22) are exactly canceled by corresponding terms arising from the second, quadratic term. Thus, Eq. (2-22) may be written in its more common form as [86]

$$E^{(2)}=\langle 0|\left(1+\Lambda\right)\left(\left[\bar{V},T^{(1)}\right]+\frac{1}{2}\left[\left[\bar{H}_0,T^{(1)}\right],T^{(1)}\right]\right)|0\rangle. \tag{2-23}$$

The appearance of commutators between $T^{(1)}$ and both $\bar{V}$ and $\bar{H}_0$ in this expression emphasizes the size-extensive/intensive nature of CCR properties. However, the quadratic terms also increase the computational expense of the CCR approach relative to EOM-CC, and modifications of the EOM-CC approach that result in size-extensive properties have been considered [85, 87].

The corresponding EOM-CC and CCR equations for the time-/frequency-dependent case may be derived in multiple ways, but the practical changes to the above time-independent formulas are relatively small, with the external field frequency appearing both in the perturbed wave functionequations and in the expression for

the perturbed energies. However, since the frequency-dependent expressions are not essential to our present discussion of local correlation, we will avoid presenting them explicitly here and merely direct the reader to the relevant references [3, 29–31, 85].

2.3.2. Localized Orbital Domains and Response Properties

The first complication in formulating a local-CC approach within either the CCR or EOM-CC frameworks is that the sparsity of the perturbed wave functions determined using Eq. (2-21) is reduced relative to that of the unperturbed wave functions in Eq. (2-2), even when expressed in a localized-orbital basis. For example, Figure 2-1 plots the distribution of double-excitation amplitudes in *n*-octane at the CCSD/6-31G* level of theory. The perturbed amplitudes in this case correspond to the solution of Eq. (2-21) for a static electric field polarized along the long axis of the molecule; the occupied space corresponds to the Pipek–Mezey [77] orbitals, while the virtual space is the projected atomic-orbital basis of Pulay and Sæbø. Both distributions appear to be statistically normal, but with different peak positions. While the unperturbed amplitudes exhibit a maximum at around 10^{-6}, the perturbed amplitude distribution is shifted up by nearly two orders of magnitude, just above 10^{-4}. Hence, the wave function's response to the external field leads to reduced sparsity, which

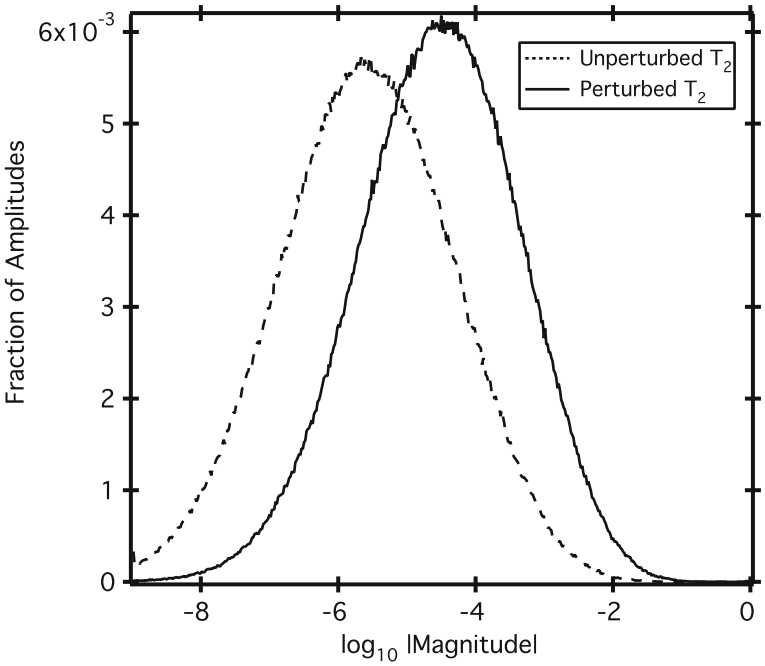

Figure 2-1. Statistical distribution of CCSD/6-31G* double-excitation amplitudes for *n*-octane in a localized orbital basis. The perturbed T_2 amplitudes correspond to the solution to Eq. (2-21) for a static electric field perturbation along the *A* axis of the molecule

means that the orbital domains used for the ground state will be inadequate for the perturbed state, for which more computational effort will be required. (It should be noted, however, that the sparsity reduction is in the *perturbed* wave function; the wave function computed in the presence of a weak external field should have similar sparsity to the field-free wave function.) The question then arises as to how to predict this sparsity a priori, i.e., what changes to the Pulay–Sæbø orbital domain structure would be effective for the locally correlated response?

The first application of local-CC theory to response properties was published in 2004 by Korona et al. [88], who reported benchmark computations using a pilot local-CCSD program for dipole moments and static dipole polarizabilities. They found that, indeed, the usual Boughton–Pulay domains are not sufficient for molecular property calculations, and proposed to expand them based on bond-connectivity criteria, where bonds between atoms were assumed to depend on the covalent radii of the atoms in question. They found that the effect of orbital relaxation on the computed properties was larger for the local-CC case than for canonical-MO CC, and they were able to reduce the localization errors on polarizabilities, for example, to less than 1% when such orbital response was included.

In our own work in this area, we sought a different approach to the domain-selection scheme that avoided problems associated with orbital relaxation effects. In the spirit of the Boughton–Pulay completeness approach, in which the ground-state orbitals themselves provide information on the correlated wave function sparsity, we have formulated a domain-selection scheme that utilizes the *response* of the ground-state orbitals to external perturbations [89, 90]. Within Hartree–Fock theory, a single component of the dipole-polarizability tensor may be written as

$$\alpha_{xy} = \sum_{i}^{\text{occ}} \sum_{a}^{\text{vir}} U_{ai}^{x} \mu_{ai}^{y}, \tag{2-24}$$

where a and i denote virtual and occupied MOs, respectively, the μ_{ai}^{y} are electric-dipole integrals in the MO basis, and the U_{ai}^{x} are solutions to the electric-dipole coupled-perturbed Hartree–Fock (CPHF) equations, i.e. the first-order response of the MOs to the external electric field. The summation over virtual orbitals may be converted to a summation over atomic orbitals (identified by Greek indices) to give

$$\alpha_{xy} = \sum_{i}^{\text{occ}} \sum_{\rho}^{\text{AO}} U_{\rho i}^{x} \mu_{\rho i}^{y}. \tag{2-25}$$

If the AOs are grouped by atom, then the two summations may be decomposed – the sum over i into (localized) atomic orbitals and the sum over μ into atoms to obtain

$$\alpha_{xy}^{iA} = \sum_{\rho \in A}^{\text{AO}} U_{\rho i}^{x} \mu_{\rho i}^{y}, \tag{2-26}$$

where the notation $\rho \in A$ indicates that only those basis function on center A are included in the summation. To account for the varying signs associated with individual contributions to this "pseudo-polarizability," we use the above equation to define a new completeness check:

$$\varepsilon_{xy}^{i} = \sum_{\rho}^{\mathrm{AO}} \left| U_{\rho i}^{x} \mu_{\rho i}^{y} \right| - \sum_{\rho \in [i]}^{\mathrm{AO}} \left| U_{\rho i}^{x} \mu_{\rho i}^{y} \right|, \tag{2-27}$$

where the notation $\rho \in [i]$ indicates that the summation includes only those AOs on atoms within the current guess at the domain associated with occupied orbital, i. This provides a simple algorithm for extending the domains based on the magnitudes of the polarizability completeness cutoff, ε_{xy}^{i}: starting from the Boughton– Pulay domains for the unperturbed orbitals, additional groups of PAOs are added to the domain for a given occupied orbital, i, until the value of ε_{xy}^{i} falls below a chosen threshold: the smaller the threshold, the larger the domains.

Using a pilot local-CCR implementation applied to a number of benchmark systems – including He-atom chains, linear alkanes, and non-saturated molecules up to *N*-acetylglycine – we found that we could reproduce canonical-MO CCSD dipole polarizabilities to within 1% using the CPHF domain-selection scheme above and without the need to include orbital relaxation effects [89]. Given that our CPHF-based scheme is readily applicable to both static and frequency-dependent response properties, the avoidance of explicit inclusion of orbital relaxation effects is important because, as noted in desiderata 1–3 above, this localization approach avoids corruption of the pole structure of the frequency-dependent response function. The primary drawback to the expansion of the orbital domains, of course, is that the cost of the computation increases significantly. While the Boughton–Pulay domains yield compact CCSD wave functions, the CPHF-based domains are significantly larger. Of course, even with larger domains, the number of strong-pair double-excitation amplitudes will scale linearly with the size of the system, as long as appropriate weak-pair treatments are used to avoid significant loss of accuracy.

In a more recent application of the CPHF-based domain selection scheme, we considered the frequency-dependent mixed electric-dipole/magnetic-dipole polarizability tensor that is related to optical rotation and circular dichroism spectra in chiral molecules [90]. In this case, we found it necessary to include both electric-field and magnetic-field contributions in the CPHF scheme, leading to an additional completeness check, viz.

$$\varepsilon_{xy}^{i} = \sum_{\rho}^{\mathrm{AO}} \left| M_{\rho i}^{x} m_{\rho i}^{y} \right| - \sum_{\rho \in [i]}^{\mathrm{AO}} \left| M_{\rho i}^{x} m_{\rho i}^{y} \right|, \tag{2-28}$$

where the $M_{\rho i}^{x}$ are the solutions to the magnetic-field CPHF equations and the $m_{\rho i}^{y}$ are the corresponding magnetic dipole integrals. Thus, the orbital domains would

naturally expand, based on the proposed CPHF cutoffs, to accommodate both relevant perturbations. We found that the chiroptical response is much more sensitive to the structure of the orbital domains than dipole polarizabilities, and that smaller cutoffs for the CPHF completeness check were necessary to achieve similar accuracy as compared to canonical-MO computations. Although the resulting local-CCSD wave functions (perturbed and unperturbed) were reasonably compact for linear molecules (e.g., H_2 polymers, fluoroalkanes, and triangulanes [91]), the more three-dimensional the molecular structure (e.g. norbornenones) the larger the domains and the further out the cross-over point between the local-CC and canonical-CC algorithms.

2.4. LOCAL COUPLED CLUSTER THEORY AND ELECTRONICALLY EXCITED STATES

The high accuracy of CC theory for electronically excited states is well documented. For states dominated by a single excitation relative to the ground-state, the CCSD approximation typically yields transition energies accurate to within 0.2 eV [7]; for higher excitations, at least triple excitations are necessary in the excited-state wave function parametrization [92–94]. The determination of electronic excitation energies in coupled cluster theory involves the computation of eigenvalues of the matrix on the left-hand side of Eq. (2-21), namely the similarity-transformed Hamiltonian. This task is normally accomplished via the Davidson approach [95] and its generalization to non-symmetric matrices by Hirao and Nakatsuji [96]. From a local-correlation perspective, the key step in the Davidson algorithm is the formation of the so-called σ vector, viz.

$$\sigma_m \equiv \bar{H} B_m, \tag{2-29}$$

where B_m is an approximation to the true m-th eigenvector of $\bar{H}$. In the CC method, the guess eigenvectors are represented as a CI-like (linear) expansion of excited determinants involving a set of cluster operators analogous to the T_n operators of the ground-state wave function. Thus, for the CCSD method, for which the computation of σ for a given state scaled nominally as $\mathcal{O}(N^6)$, the introduction of a local-correlation approach involves truncation of the cluster expansion using similar orbital-domain arguments as those described above for perturbed wave functions. However, the difficulty in designing an effective local-CC approach to excited states rests in the inherently delocalized nature of many states, such as that arising from strong Rydberg character or perhaps charge-transfer.

In the first published approach to locally correlated excited-states in CC theory [97], we examined a series of organic molecules ranging from ethanal to glycine using a pilot local-EOM-CCSD program and compared canonical-MO CCSD excitation energies to those computed using simple Boughton–Pulay orbital domains for both the ground and excited states. We found that these domains – when used in

conjunction with reasonable basis sets, including molecule-centered Rydberg functions – were sufficient for some localized valence transitions, but too small for many other types of excitations. In addition, we developed a weak-pair correction analogous to that developed by Werner and co-workers for ground-state energies based on local-MP2 theory. Specifically, we considered the well-known (D) correction of Head-Gordon and co-workers [98–100] for excited states within the configuration interactions singles (CIS) approximation, which takes the form

$$\omega_{(D)} = \frac{1}{4}\sum_{ijab} b_{ij}^{ab}\langle_{ij}^{ab}|\left(\bar{H}^{[1]}\hat{U}_1\right)_C|0\rangle + \sum_{ia} b_i^a\langle_i^a|\left(\bar{H}^{[2]}\hat{U}_1\right)_C|0\rangle, \tag{2-30}$$

where b_i^a is an excited state amplitude which parameterizes the CIS excitation operator $\hat{U}_1$ and $\bar{H}^{[n]}$ is the n-order contribution to the CCSD $\bar{H}$. In our approach, the corresponding excited-state weak-pair correction involves only the first term of Eq. (2-30), and the summation is limited only to the weak-pair components. In the localized-orbital basis, the requisite double-excitation amplitudes are computed iteratively, much like the first-order wave function amplitudes in LMP2:

$$b_{ij}^{ab}\omega = \langle_{ij}^{ab}|\left(\bar{H}^{[1]}\hat{U}_1\right)_C|0\rangle + f_{ac}b_{ij}^{cb} + f_{cb}b_{ij}^{ac} - f_{ki}b_{kj}^{ab} - f_{kj}b_{ik}^{ab}, \tag{2-31}$$

where the intermediate $\langle_{ij}^{ab}|\left(\bar{H}^{[1]}\hat{U}_1\right)_C|0\rangle$ depends on the CIS excited state wavefunction amplitudes b_i^a and is given by

$$\langle_{ij}^{ab}|\left(\bar{H}^{[1]}\hat{U}_1\right)_C|0\rangle = \langle ab||cj\rangle b_i^c - \langle ab||ci\rangle b_j^c + \langle ka||ij\rangle b_k^b - \langle kb||ij\rangle b_k^a. \tag{2-32}$$

Although the weak-pair (D) correction yielded some reduction in the localization errors, it could not overcome the lack of flexibility in the Boughton–Pulay domains for certain excited states.

Korona and Werner [101] implemented an alternative approach whereby the orbital domain structure for a given excited state is based on the weights of the corresponding CIS wave function, thus defining the localization structure independently for each excited state. Using a pilot local-EOM-CCSD programs, they were able to obtain much smaller localization errors – on average less than 0.1 eV – than the fixed-domain scheme. This domain-selection approach has also been utilized by Kats et al. [102] more recently for the first production-level implementation of excitation energies at the CC2 level of theory in conjunction with DF methods. By choosing to limit only the pair domains and leave the singles untruncated, the resulting program performed well – yielding localization errors of less than 0.05 eV – and highly efficient, as demonstrated on benchmark computations on molecules containing up to several dozen non-hydrogen atoms. One drawback of this CIS domain-selection approach is that the ground-state T amplitudes are solved in a different domain than that used to construct $\bar{H}$for the subsequent eigenvalue computation.

Thus, the ground-state energy (defined as the lowest eigenvalue of $\bar{H}$) implicitly shifts for each excited state, and, although reasonable excitation energies result, it remains unclear whether the corresponding excited-state wave function will yield accurate transition probabilities or excited-state properties. Indeed, Kats et al. [103] reported the need to enlarge the CIS-based excited-state domains using a CPHF-based scheme with some similarities to that described above for polarizabilities and optical rotation.

2.5. CONCLUSIONS AND FUTURE DIRECTIONS

The application of local-correlation idea pioneered by Pulay and Sæbø to coupled cluster theory has yielded much fruit for high-accuracy computations of ground-state energetics of large molecules. The use of compact orbital domain structures for partitioning the correlated wave function into more tractable components has enabled truly impressive production-level CC computations on molecules containing dozens of atoms and thousands of basis functions [62]. However, for molecular response properties, the sparsity of the perturbed wave function is significantly reduced relative to the unperturbed wave function. Thus, the usual orbital-domain selection schemes are not sufficient, and new approaches must be devised.

For electric- and magnetic-field perturbations, we have found that a domain-selection approach based on the CPHF equations provides reasonably robust results for static and dynamic dipole polarizabilities and optical rotation, especially for strongly linear molecular structures. For cage-like structures, however, the orbital domains must be expanded significantly, leading to much less ideal cross-over points between the canonical-MO and local-MO algorithms. For excited states, the simple ground-state orbital domains have been found to be inadequate to retain the accuracy of the local-EOM-CC method, but domain selection based on CIS states, while yielding robust excitation energies, are not apparently sufficient to provide correspondingly robust transition probabilities and excited-state properties.

Within the confines of the Pulay–Sæbø local-correlation approach, there is much work remaining before the coupled cluster method will be routinely applicable to response properties of large molecules. Some of this work involves the development of efficient production-level programs that take every technological advantage, from integral pre-screening and density fitting, to implementation on parallel computing architectures. Other aspects will involve new scientific advances, including the development of reduced-scaling methods that are applicable extended systems such as polyenes or surfaces with much more complicated electronic structure characteristics than simple, isolated organic molecules. Success in both areas – artful programming and clever science – will be necessary to achieve the final goal of reliable quantum chemical computations on large molecules.

ACKNOWLEDGEMENTS

This work was supported by a grant from the US National Science Foundation (CHE-0715185) and a subcontract from Oak Ridge National Laboratory by the Scientific Discovery through Advanced Computing (SciDAC) program of the US Department of Energy, the division of Basic Energy Science, Office of Science, under contract number DE-AC05-00OR22725.

REFERENCES

1. T. Helgaker, T. A. Ruden, P. Jørgensen, J. Olsen, W. Klopper, J. Phys. Org. Chem **17**(11), 913 (2004)
2. J. Olsen, P. Jørgensen, in *Modern Electronic Structure Theory*, *Advanced Series in Physical Chemistry*, vol. 2, Ed. D. Yarkony (World Scientific, Singapore, 1995), chap. 13, pp. 857–990
3. O. Christiansen, P. Jørgensen, C. Hättig, Int. J. Quantum Chem. **68**, 1 (1998)
4. F. Jensen, *Introduction to Computational Chemistry* (Wiley, New York, 1999)
5. H. Sekino, R. J. Bartlett, Int. J. Quantum Chem. Symp. **18**, 255 (1984)
6. H. Koch, H. J. Aa. Jensen, P. Jørgensen, T. Helgaker, J. Chem. Phys. **93**(5), 3345 (1990)
7. J. F. Stanton, R. J. Bartlett, J. Chem. Phys. **98**(9), 7029 (1993)
8. O. Christiansen, H. Koch, A. Halkier, P. Jørgensen, T. Helgaker, A. S. de Merás, J. Chem. Phys. **105**(16), 6921 (1996)
9. R. S. Mulliken, C. A. Rieke, Rep. Prog. Phys. **8**, 231 (1941)
10. T. B. Pedersen, H. Koch, Chem. Phys. Lett. **293**, 251 (1998)
11. L. D. Barron, *Molecular Light Scattering and Optical Activity*, second edition (Cambridge University Press, Camridge, 2004)
12. T. B. Pedersen, H. Koch, K. Ruud, J. Chem. Phys. **110**(6), 2883 (1999)
13. P. L. Polavarapu, A. Petrovic, F. Wang, Chirality **15**, S143 (2003)
14. P. J. Stephens, D. M. McCann, J. R. Cheeseman, M. J. Frisch, Chirality **17**, S52 (2005)
15. M. Pecul, K. Ruud, Adv. Quantum Chem. **50**, 185 (2005)
16. T. D. Crawford, Theor. Chem. Acc. **115**, 227 (2006)
17. P. L. Polavarapu, Chem. Rec. **7**, 125 (2007)
18. J. F. Stanton, R. J. Bartlett, J. Chem. Phys. **99**, 5178 (1993)
19. P. B. Rozyczko, S. A. Perera, M. Nooijen, R. J. Bartlett, J. Chem. Phys. **107**(17), 6736 (1997)
20. P. Rozyczko, R. J. Bartlett, J. Chem. Phys. **107**(24), 10823 (1997)
21. O. Christiansen, C. Hättig, J. Gauss, J. Chem. Phys. **109**(12), 4745 (1998)
22. J. Gauss, O. Christiansen, J. F. Stanton, Chem. Phys. Lett. **296**, 117 (1998)
23. K. Ruud, T. Helgaker, K. L. Bak, P. Jørgensen, H. J. Aa. Jensen, J. Chem. Phys. **99**(5), 3847 (1999)
24. R. J. Bartlett, M. Musial, Rev. Mod. Phys. **79**, 291 (2007)
25. J. Gauss, in *Encyclopedia of Computational Chemistry*, Ed. P. Schleyer, N. L. Allinger, T. Clark, J. Gasteiger, P. A. Kollman, H. F. Schaefer III, P. R. Schreiner (John Wiley and Sons, Chichester, 1998), pp. 615–636
26. T. D. Crawford, H. F. Schaefer, in *Reviews in Computational Chemistry*, vol. 14, Ed. K. B. Lipkowitz, D. B. Boyd (VCH Publishers, New York, 2000), chap. 2, pp. 33–136
27. T. J. Lee, G. E. Scuseria, in *Quantum Mechanical Electronic Structure Calculations with Chemical Accuracy*, Ed. S. R. Langhoff (Kluwer Academic Publishers, Dordrecht, 1995), pp. 47–108
28. T. H. Dunning, J. Phys. Chem. A **104**(40), 9062 (2000)
29. H. J. Monkhorst, Int. J. Quantum Chem. Symp. **11**, 421 (1977)

30. D. Mukherjee, P. K. Mukherjee, Chem. Phys. **39**, 325 (1979)
31. H. Koch, P. Jørgensen, J. Chem. Phys. **93**(5), 3333 (1990)
32. O. Christiansen, A. Halkier, H. Koch, P. Jørgensen, T. Helgaker, J. Chem. Phys. **108**(7), 2801 (1998)
33. K. Hald, P. Jørgensen, O. Christiansen, H. Koch, J. Chem. Phys. **116**(14), 5963 (2002)
34. K. Hald, P. Jørgensen, C. Hättig, J. Chem. Phys. **118**(3), 1292 (2003)
35. O. Christiansen, H. Koch, P. Jørgensen, Chem. Phys. Lett. **243**, 409 (1995)
36. H. Koch, O. Christiansen, P. Jørgensen, A. M. S. deMerás, T. Helgaker, J. Chem. Phys. **106**(5), 1808 (1997)
37. O. Christiansen, H. Koch, P. Jørgensen, J. Chem. Phys. **103**(17), 7429 (1995)
38. K. Hald, P. Jørgensen, Phys. Chem. Chem. Phys. **4**, 5221 (2002)
39. T. B. Pedersen, H. Koch, J. Chem. Phys. **112**(5), 2139 (2000)
40. K. Ruud, T. Helgaker, Chem. Phys. Lett. **352**, 533 (2002)
41. K. Ruud, P. J. Stephens, F. J. Devlin, P. R. Taylor, J. R. Cheeseman, M. J. Frisch, Chem. Phys. Lett. **373**, 606 (2003)
42. M. C. Tam, N. J. Russ, T. D. Crawford, J. Chem. Phys. **121**, 3550 (2004)
43. T. B. Pedersen, H. Koch, L. Boman, A. M. J. S. de Meras, Chem. Phys. Lett. **393**(4–6), 319 (2004)
44. J. Kongsted, T. B. Pedersen, M. Strange, A. Osted, A. E. Hansen, K. V. Mikkelsen, F. Pawlowski, P. Jørgensen, C. Hättig, Chem. Phys. Lett. **401**, 385 (2005)
45. J. Kongsted, T. B. Pedersen, L. Jensen, A. E. Hansen, K. V. Mikkelsen, J. Am. Chem. Soc. **128**(3), 976 (2006)
46. T. D. Crawford, M. C. Tam, M. L. Abrams, J. Phys. Chem. A **111**, 12057 (2007)
47. R. A. Kendall, E. Apra, D. E. Bernholdt, E. J. Bylaska, M. Dupuis, G. I. Fann, R. J. Harrison, J. Ju, J. A. Nichols, J. Nieplocha, T. P. Straatsma, T. L. Windus, A. T. Wong, Comp. Phys. Comm. **128**, 260 (2000)
48. CFOUR, a quantum chemical program package, written by J. F. Stanton, J. Gauss, M. E. Harding, P. G. Szalay with contributions from A. A. Auer, R. J. Bartlett, U. Benedikt, C. Berger, D. E. Bernholdt, Y. J. Bomble, O. Christiansen, M. Heckert, O. Heun, C. Huber, T.-C. Jagau, D. Jonsson, J. Jusélius, K. Klein, W. J. Lauderdale, D. A. Matthews, T. Metzroth, D. P. O'Neill, D. R. Price, E. Prochnow, K. Ruud, F. Schiffmann, S. Stopkowicz, M. E. Varner, J. Vázquez, F. Wang, J. D. Watts and the integral packages MOLECULE (J. Almlöf and P. R. Taylor), PROPS (P. R. Taylor), ABACUS (T. Helgaker, H. J. Aa. Jensen, P. Jørgensen J. Olsen), and ECP routines by A. V. Mitin and C. van Wüllen (2009)
49. V. Lotrich, N. Flocke, M. Ponton, A. D. Yau, A. Perera, E. Deumens, R. J. Bartlett, J. Chem. Phys. **128**, 194104 (2008)
50. Dalton, a molecular electronic structure program, Release 2.0 (2005), written by T. Helgaker, H. J. Aa. Jensen, P. Jørgensen, J. Olsen, K. Ruud, H. Agren, A. A. Auer, K. L. Bak, V. Bakken, O. Christiansen, S. Coriani, P. Dahle, E. K. Dalskov, T. Enevoldsen, B. Fernandez, C. Hättig, K. Hald, A. Halkier, H. Heiberg, H. Hettema, D. Jonsson, S. Kirpekar, R. Kobayashi, H. Koch, K. V. Mikkelsen, P. Norman, M. J. Packer, T. B. Pedersen, T. A. Ruden, A. Sanchez, T. Saue, S. P. A. Sauer, B. Schimmelpfennig, K. O. Sylvester-Hvid, P. R. Taylor, O. Vahtras
51. T. D. Crawford, C. D. Sherrill, E. F. Valeev, J. T. Fermann, R. A. King, M. L. Leininger, S. T. Brown, C. L. Janssen, E. T. Seidl, J. P. Kenny, W. D. Allen, J. Comp. Chem. **28**, 1610 (2007)
52. P. Pulay, Chem. Phys. Lett. **100**, 151 (1983)
53. S. Sæbø, P. Pulay, Chem. Phys. Lett. **113**, 13 (1985)
54. S. Sæbø, P. Pulay, J. Chem. Phys. **86**(2), 914 (1987)
55. S. Sæbø, P. Pulay, J. Chem. Phys. **88**, 1884 (1988)
56. S. Sæbø, P. Pulay, Ann. Rev. Phys. Chem. **44**, 213 (1993)

57. C. Hampel, H. J. Werner, J. Chem. Phys. **104**(16), 6286 (1996)
58. M. Schütz, H. J. Werner, Chem. Phys. Lett. **318**(4–5), 370 (2000)
59. M. Schütz, H. J. Werner, J. Chem. Phys. **114**(2), 661 (2001)
60. M. Schütz, J. Chem. Phys. **116**(20), 8772 (2002)
61. M. Schütz, Phys. Chem. Chem. Phys. **4**(16), 3941 (2002)
62. M. Schütz, F. R. Manby, Phys. Chem. Chem. Phys. **5**(16), 3349 (2003)
63. H. J. Werner, K. Pflüger, Ann. Rep. Comp. Chem. **2**, 53 (2006)
64. P. G. Szalay, M. Nooijen, R. J. Bartlett, J. Chem. Phys. **103**(1), 281 (1995)
65. G. D. Purvis, R. J. Bartlett, J. Chem. Phys. **76**, 1910 (1982)
66. K. Raghavachari, G. W. Trucks, J. A. Pople, M. Head-Gordon, Chem. Phys. Lett. **157**, 479 (1989)
67. R. J. Bartlett, J. D. Watts, S. A. Kucharski, J. Noga, Chem. Phys. Lett. **165**, 513 (1990); Erratum: **167**, 609 (1990).
68. J. Noga, R. J. Bartlett, M. Urban, Chem. Phys. Lett. **134**, 126 (1987)
69. G. E. Scuseria, P. Y. Ayala, J. Chem. Phys. **111**(18), 8330 (1999)
70. P. E. Maslen, M. S. Lee, M. Head-Gordon, Chem. Phys. Lett. **319**(3–4), 205 (2000)
71. D. G. Fedorov, K. Kitaura, J. Chem. Phys. **123**, 134103 (2005)
72. N. Flocke, R. J. Bartlett, Chem. Phys. Lett. **367**(1–2), 80 (2003)
73. S. Li, J. Shen, W. Li, Y. Jiang, J. Chem. Phys. **125**, 074109 (2006)
74. W. Li, P. Piecuch, J. R. Gour, in *Theory and Applications of Computational Chemistry*, *AIP Conference Proceedings*, vol. 1102, Ed. D. Q. Wei, X. J. Wang (American Institute of Physics, Melville, NY, 2009), pp. 68–113
75. S. F. Boys, Rev. Mod. Phys. **32**, 296–299 (1960)
76. J. M. Foster, S. F. Boys, Rev. Mod. Phys. **32**, 300 (1960)
77. J. Pipek, P. G. Mezey, J. Chem. Phys. **90**(9), 4916 (1989)
78. F. Claeyssens, J. N. Harvey, F. R. Manby, R. A. Mata, A. J. Mulholland, K. E. Ranaghan, M. Schütz, S. Thiel, W. Thiel, H. J. Werner, Angew. Chem. Int. Ed. Engl. **45**, 6856 (2006)
79. T. J. Lee, J. E. Rice, Chem. Phys. Lett. **150**, 406 (1988)
80. G. E. Scuseria, C. L. Janssen, H. F. Schaefer, J. Chem. Phys. **89**, 7382 (1988)
81. J. F. Stanton, J. Gauss, J. D. Watts, R. J. Bartlett, J. Chem. Phys. **94**(6), 4334 (1991). URL http://dx.doi.org/10.1063/1.460620
82. S. A. Kucharski, R. J. Bartlett, Theor. Chem. Acc. **80**(4, 5), 387 (1991)
83. E. Dalgaard, H. J. Monkhorst, Phys. Rev. A **28**(3), 1217 (1983)
84. A. E. Kondo, P. Piecuch, J. Paldus, J. Chem. Phys. **102**(16), 6511 (1995)
85. H. Sekino, R. J. Bartlett, Adv. Quantum Chem. **35**, 149 (1999)
86. R. Kobayashi, H. Koch, P. Jørgensen, Chem. Phys. Lett. **219**, 30 (1994)
87. T. D. Crawford, H. Sekino, Prog. Theor. Chem. Phys. **19**, 225 (2009)
88. T. Korona, K. Pflüger, H. J. Werner, Phys. Chem. Chem. Phys **6**, 2059 (2004)
89. N. J. Russ, T. D. Crawford, Chem. Phys. Lett. **400**, 104 (2004)
90. N. J. Russ, T. D. Crawford, Phys. Chem. Chem. Phys. **10**, 3345 (2008)
91. T. D. Crawford, L. S. Owens, M. C. Tam, P. R. Schreiner, H. Koch, J. Am. Chem. Soc. **127**, 1368 (2005)
92. J. D. Watts, S. R. Gwaltney, R. J. Bartlett, J. Chem. Phys. **105**(16), 6979 (1996)
93. J. D. Watts, R. J. Bartlett, Chem. Phys. Lett. **258**(5, 6), 581 (1996)
94. C. E. Smith, R. A. King, T. D. Crawford, J. Chem. Phys. **122**(05), 054110 (2005)
95. E. R. Davidson, J. Comput. Phys. **17**, 87 (1975)
96. K. Hirao, H. Nakatsuji, J. Comput. Phys. **45**, 246 (1982)
97. T. D. Crawford, R. A. King, Chem. Phys. Lett. **366**, 611 (2002)

98. M. Head-Gordon, R. J. Rico, M. Oumi, T. J. Lee, Chem. Phys. Lett. **219**, 21 (1994)
99. J. F. Stanton, J. Gauss, N. Ishikawa, M. Head-Gordon, J. Chem. Phys. **103**(10), 4160 (1995)
100. M. Head-Gordon, T. J. Lee, in *Recent Advances in Coupled-Cluster Methods*, Ed. R. J. Bartlett (World Scientific Publishing, Singapore, 1997), pp. 221–253
101. T. Korona, H. J. Werner, J. Chem. Phys. **118**(7), 3006 (2003)
102. D. Kats, T. Korona, M. Schütz, J. Chem. Phys. **125**, 104106 (2006)
103. D. Kats, T. Korona, M. Schütz, J. Chem. Phys. **127**, 064107 (2007)

CHAPTER 3

DEVELOPMENT AND APPLICATIONS OF NON-PERTURBATIVE APPROXIMANTS TO THE STATE-SPECIFIC MULTI-REFERENCE COUPLED CLUSTER THEORY: THE TWO DISTINCT VARIANTS

SANGHAMITRA DAS[1], SHUBHRODEEP PATHAK[2], RAHUL MAITRA[3], AND DEBASHIS MUKHERJEE[3]

[1]*Department of Physical Chemistry and Materials Science, Budapest University of Technology and Economics, Budapest 1111, Hungary, e-mail: das.sangha@gmail.com*
[2]*Department of Physical Chemistry, Indian Association for the Cultivation of Science, Calcutta 700 032, India, e-mail: pathak.shubhro@gmail.com*
[3]*Raman Center for Atomic, Molecular and Optical Sciences, Indian Association for the Cultivation of Science, Calcutta 700 032, India, e-mail: maitra.rah@gmail.com; pcdm@iacs.res.in*

Abstract: In this chapter, two useful non-perturbative approximants to the state specific multi-reference coupled cluster theory (SS-MRCC) of Mukherjee et al. are developed and pilot numerical applications are presented. The parent formulation is rigorously size-extensive and the use of a complete active space leads to a size-consistent theory as well when localized orbitals are used. The redundancy of cluster amplitudes, which is customary when the Jeziorski-Monkhorst wave-operator is used in a state-specific theory is bypassed by employing strict requirements of size-extensivity of energy and the avoidance of intruders, thus rendering the parent SS-MRCC theory rigorously size-extensive as well as intruder-free when the desired state is well separated from virtual functions. In the working equations, the cluster amplitudes for the operators acting on the different model functions are coupled. In addition, the state-specific nature of the formalism leads to a lot of redundant cluster amplitudes. The equations are thus rather complex with both coupling terms and requiring sufficiency conditions to eliminate redundancy. The two approximants discussed in this chapter are designed to reduce the complexity of the working equations mentioned above via well-defined non-perturbative approximations in two different ways. In the first variant, to be called the uncoupled state-specific MRCC(UC-SS-MRCC), we use an analogue of the anonymous parentage approximation in the coupling term, which leads to considerable simplification of the working equations, yet with very little deterioration of the quality of the computed energy. In the second one, named internally contracted inactive excitations in SS-MRCC(ICI-SS-MRCC), the cluster amplitudes for all the inactive double excitations are regarded as independent of the model functions. Since the all-inactive double excitation amplitudes are the most numerous, this variant leads to a dramatic reduction in the total number of cluster amplitudes. The ICI-SS-MRCC, unlike analogous theories, such as IC-MRCISD or CASPT2, uses relaxed coefficients for the model functions and

P. Čársky et al. (eds.), Recent Progress in Coupled Cluster Methods, 57–77.
DOI 10.1007/978-90-481-2885-3_3,

at the same time employs projection manifolds for the virtuals obtained from inactive *n* hole-*n* particle (nh-np) excitations on the relaxed multi-reference combinations. Our pilot numerical applications on a few important test cases indicate that the ICI-SS-MRCC performs remarkably well, closely paralleling the performance of the full-blown SS-MRCC.

Keywords: Multireference coupled cluster, State-specific, Uncoupled approximation, Anonymous parentage, Jeziorski – Monkhorst ansatz

3.1. INTRODUCTION

The coupled cluster approach for treating electron correlation for studying small to medium sized molecules has become the standard tool in quantum chemistry, in particular when the reference function is a single determinant [1–9]. Inspired by this success, multi-reference generalizations has been attempted to encompass situations which warrants a multi-reference (MR) starting description. The generalization of SR exponential ansatz to MR case has resulted in several different formulations which emphasize different aspects of electron correlation which are special to the MR case. For example, there are two distinct Effective Hamiltonian Formulations viz. valence universal MRCC (VU-MRCC) [10, 11] and state-universal MRCC (SU-MRCC) [12, 13] theories. They differ in the forms of the wave operators used to generate the CC wave function and have been widely used over the last two decades for treating strong dynamical as well as non-dynamical electron correlation effects in a group of states which are quasi-degenerate in energy.

Effective hamiltonian methodology [14] works within the relevant subspace, spanned by the corresponding quasi-degenerate model functions $\{\phi_\mu\}$. It proceeds through projections of some exact wave functions into the model space, and folds via the Bloch Equation [15] the effects of the virtual functions onto the effective hamiltonian (H_{eff}).

Just as in the SRCC method, which unlike the SR-CI, preserves size-extensivity, the various effective hamiltonian based MRCC methods also guarantee size-extensivity, provided a CAS is used.

Although formally elegant,the Effective Hamiltonian methods based on CAS suffer from some serious limitations:

1. they often suffer from the ubiquitous intruder state problems [16]. In a CAS based strategy, involving well-spread out valence orbitals, some virtual space determinants are almost always close in energy to some model space determinants, resulting in a strong mixing of such virtual space determinants (intruder states) with the model space determinants leading to the divergence in the perturbation series for H_{eff} or ill-conditioning of the MRCC equations;
2. the need to calculate more states than possibly desired simultaneously for both VU and SU case as there are more unknown parameters than can be fixed by projection onto elements of P and Q, greatly complicate a practical and useful exploitation of these methods;

3. the multiplicity of the solutions and in the VU case, their genealogy, greatly complicate a practical and useful exploitation of these methods;
4. the SU/VU MRCC methods that use only one- and two-body cluster amplitudes often provide rather unsatisfactory results than the SRCC method in the regions of non-degeneracy. For the states at fixed geometries, the problem of intruder can be avoided using a judicious choice of incomplete active space (IAS) [17–19]. But to generate the PES over the wide range of geometries, this approach is not satisfactory, since there is no unique and also natural choice of an IAS to avoid the intruders at all points [19].

One way-out to avoid intruders suggested long ago was to exclude the offending model function in the active space, so that intruders are avoided. Ways to guarantee size-extensivity in such choices of active space has been suggested by Mukherjee [17, 18], Kutzelnigg et al. [20] and Lindgren [21]. Though this strategy works for states at limited geometries, this usually doesn't work for computing potential energy surfaces (PES), since this requires different IAS in the different regions of PES.

Another approach, first introduced by Kirtman [22], and later considerably expanded in its scope by Malrieu et al. [23], Mukherjee et al. [24, 25] and Kaldor et al. [26] abandoned the idea of using an effective hamiltonian altogether and concentrated on fewer roots M for diagonalization of an N-dimensional effective operator ($M < N$). This relaxation of having to generate N eigenvalues for an effective operator can be exploited to bypass intruders. Maintenance of size-extensivity is considerably more difficult to guarantee in such formalisms.

As an extreme example of the intermediate hamiltonian formalism, one may envision a targeting just one-root of interest for the target function, though one works with an N-dimensional effective operator in a model space. Such "state-specific" formulations will automatically eliminate intruders as long as the target state energy remains well separated from the energies of the virtual space functions. These *state-specific* formulations have become promising methods of choice over the last decade or so. Methods of immediate relevance in this context are the dressed MR-CISD formulation of Malrieu et al. [27–29], the single-root multi-reference Brillouin Wigner CC theory (sr-MRBWCC) of Hubač, Pittner and Čársky [30–32], the state-specific MRCC(SS-MRCC) theories of Mukherjee et al. [33–35] and the allied methodologies of Evangelista et al. [36, 37], the MRexp(T) theory of Hanrath [38], and the state-specific equation of motion method of Nooijen et al. [39].

In this chapter, we will focus on the development and preliminary molecular applications of certain non-perturbative approximants to the parent SS-MRCC methods of Mukherjee et al. [40–42].

The chapter is organized as follows:

(a) in Section 3.2, we will motivate towards the development of non-perturbative approximants by a succinct summary of the parent SS-MRCC
(b) Section 3.3 discusses the development of the Uncoupled SS-MRCC (UC-SS-MRCC) where simplification of the so-called coupling terms of working equations of the parent theory leads to their simpler structure

(c) in Section 3.4, we introduce another non-perturbative approximant, where an entire combination $\Psi_0 = \sum_\mu \phi_\mu C_\mu$ of the model functions $\{\phi_\mu\}$ is used to generate composite virtual functions $|\chi_l\rangle = Y_l^\dagger|\Psi_0\rangle$, which involves various nh-np inactive excitations on Ψ_0.This approach is thus the non-perturbative analogue of the internally contracted MR-CI [43–45] or similar perturbative versions, such as CASPT2 [46, 47] or MRMP2 [48]. There is an important difference, however. In the internal contraction of the inactive excitations in SS-MRCC (ICI-SS-MRCC) scheme, the coefficients C_μ of ϕ_μ in Ψ_0 are *relaxed* as they should be in the exact function Ψ and *not* frozen at some predetermined values, as e.g. obtained from CAS-CI calculation. Thus ICI-SS-MRCC entails relaxation of the coefficients C_μ in presence of dynamical correlations, although the virtual functions $\{\chi_l\}$ for the inactive excitations are generated by the action of various nh-np excitations $\left\{Y_l^\dagger\right\}$ acting on a relaxed Ψ_0

(d) in Section 3.5, molecular application to four prototypical systems with strong quasi-degeneracy are presented. The encouraging results for both the formalisms prove their efficacy.

3.2. A BRIEF RESUME OF THE PARENT SS-MRCC THEORY

3.2.1. Structure of the Working Equations

In the parent SS-MRCC theory [33–35], the wave function is represented as a superposition of exponential excitation operators $\exp(T^\mu)$ acting on the respective model functions ϕ_μ. The model functions are assumed to span a CAS. The exact wave-function ψ thus is written as

$$\psi = \sum_\mu \exp(T^\mu)\phi_\mu c_\mu \tag{3-1}$$

Following the traditional nomenclature of the multi-reference formalisms, we will call the doubly occupied orbitals common to all the model functions as inactive holes, the empty orbitals in the model functions as inactive particles, and partially occupied orbitals as active. The cluster operators T^μ's acting on the respective model space determinants ϕ_μ, generate the various virtual functions $\{\chi_l\}$ by exciting the electrons in orbitals occupied in ϕ_μ to another set which are unoccupied in ϕ_μ. T^μ's have the property that at least one orbital involved in it must be inactive, thus none of the T^μ operators can produce excitations within the model space. Since each χ_l can be reached from the different ϕ_μ's, there is a *redundancy* in the number of cluster amplitudes. This flexibility was exploited in the SS-MRCC formalism to achieve the two desirable objectives: (a) to bypass intruders naturally and (b) to guarantee size-extensivity rigorously. Without going into the details of derivation, we present below the working equations of the formalism:

$$\underset{(termI)}{\langle\chi_l|\overline{H}_\mu|\phi_\mu\rangle c_\mu} + \underset{(termII)}{\sum_\nu \langle\chi_l|\exp(-T^\mu)\exp(T^\nu)|\phi_\mu\rangle\tilde{H}_{\mu\nu}c_\nu} = 0\forall l,\mu \tag{3-2}$$

where

$$\bar{H}_\mu = \exp(-T^\mu) H \exp(T^\mu) \tag{3-3}$$

and

$$\tilde{H}_{\mu\nu} = \langle \phi_\mu | \bar{H}_\nu | \phi_\nu \rangle \tag{3-4}$$

In SS-MRCC theory, we have the flexibility of either using certain frozen combining coefficients $\{c_\mu\}$ determined from a CI or CAS-SCF calculation (the unrelaxed description), or of updating the coefficients to the values they should have in the presence of the virtual functions (the relaxed description). In what follows, we will consider only the latter, since it is more general. The unrelaxed formalism follows trivially if we freeze the coefficients to some preassigned values.

In the relaxed description, the coefficients and the energy of the target state are obtained by diagonalizing the matrix $\tilde{H}_{\mu\nu}$ defined in CMS:

$$\sum_\nu \tilde{H}_{\mu\nu} c_\nu = E c_\mu \tag{3-5}$$

with E as the desired eigenvalue.

Equation (3-2) are coupled non-linear equations involving the cluster amplitudes of various T^μ's and the c_μ's. The first term in Eq. (3-2), the "direct" one (term I) just looks like that of the SRCC equation, except that, for each model function,ϕ_μ there is a separate matrix-element involving $\bar{H}_\mu$. This term for each ϕ_μ contains only the operator T^μ. The second term (Term II), the "coupling" one, couples the amplitudes of various other model functions ϕ_ν's. Apart from the couplings appearing via $\tilde{H}_{\mu\nu}$, there is the factor $\langle \chi_l | e^{-T_\mu} e^{T_\nu} | \phi_\mu \rangle$,where $T_\nu s$, defined as excitations from ϕ_ν, acts on ϕ_μ in this term. In the term $\tilde{H}_{\mu\nu}$, however T_ν acts on ϕ_ν. Thus there is a strong coupling of T's in the second term.

Proving the size-extensivity of both cluster amplitudes and the energy E is a rather involved exercise, and we refer to the original papers for details [33–35]. The SS-MRCC theory is invariant with respect to separate unitary transformation among inactive holes and particle orbitals separately. It is not invariant with respect to transformation among the active orbitals. However, using localized inactive and active orbitals, the theory is rigorously size-consistent with respect to fragmentation.

At this point, we want to emphasize the important aspects of arriving at the proof of size-extensivity of Eq. (3-2). This will serve two purposes:

(a) to emphasize the importance of the coupling term, and
(b) to underline our non-perturbative approximants

to the SS-MRCC (vide-infra) will require a similar analysis to ensure extensivity Since the first term (the "direct" term) involving T^μ and H of Eq. (3-2) has manifestly connected expression via the multi-commutator expansion if T^μ is connected, *it is enough to show* that the second term produces disconnected terms $Y_{\mu\nu}\ \tilde{H}_{\mu\nu}$ is

manifestly connected and it is enough to establish that $Y_{\mu\nu}\tilde{H}_{\mu\nu}$ is connected, where $Y_{\mu\nu}$=$\langle\chi_l|\left[\exp(-T^{\mu})\exp(T^{\nu})\right]|\phi_\mu\rangle$. The first factor, $Y_{\mu\nu}$, unlike the analogous one in the SUMRCC [12, 13], has an interesting simpler structure. Since $\exp(T^{\nu})$ acts on ϕ_μ, only that subset of T^{ν}s gives non-zero contributions on their action on ϕ_μ which have the same excitation structure as those of T^{μ}. Let us denote these set from T^{ν} as $T^{\nu\prime}$. T^{ν} thus can involve those orbitals which are common to both ϕ_ν and ϕ_μ. Thus $T^{\nu\prime}$ also commutes with T^{μ}. The expression for $Y_{\mu\nu}$ can thus be simplified as

$$Y_{\mu\nu} = \langle\chi_l|\exp -[T^{\mu} - T^{\nu\prime}]|\phi_\mu\rangle \tag{3-6}$$

where both T^{μ} and $T^{\nu\prime}$ are included in the single exponential using their commutativity.

The proof of the connectivity of $Y_{\mu\nu}\tilde{H}_{\mu\nu}$ follows from the two following important properties:

(a) $\tilde{H}_{\mu\nu}$ has explicit functional dependence on all the active orbitals which distinguish ϕ_μ and ϕ_ν,
(b) the difference $(T^{\mu} - T^{\nu\prime})$ is implicitly dependent functionally on some or all the active orbitals distinguishing ϕ_μ and ϕ_ν.

The property (b) arises because T^{μ} and $T^{\nu\prime}$ have the same implicit functional dependence on the respective set of orbitals occupied in ϕ_μ and ϕ_ν. Since T^{μ} and $T^{\nu\prime}$ have the same set of orbitals occupied in ϕ_μ and ϕ_ν, the *difference* between them can only depend on all or some of the active orbitals which distinguish ϕ_μ and ϕ_ν. Hence $\langle\chi_l|\exp\left(-T^{\mu} + T^{\nu\prime}\right)|\phi_\mu\rangle\tilde{H}_{\mu\nu}$ is a connected entity. In the UC-SS-MRCC to be discussed in Section 3.3, we will invoke suitable uncoupling approximations to the coupling term II. The insight gleaned above in (a) and (b) will be used to satisfy size-extensivity.

3.3. THE UNCOUPLED STATE-SPECIFIC MRCC THEORY

3.3.1. Discussion of the Simplification Leading to UC-SS-MRCC

In the uncoupled state-specific MRCC (UC-SS-MRCC) [40, 41] theory we use Jeziorski-Monkhorst Ansatz: $\Omega = \sum_\mu \exp(T^{\mu})|\phi_\mu\rangle\langle\phi_\mu|$ involving a different cluster operator $\exp(T^{\mu})$ acting on its corresponding model function ϕ_μ as in SS-MRCC theory and we replace the rigorous coupling term of SS-MRCC by a modified form where T^{ν}'s does not appear at all in the factor $Y_{\mu\nu}$. Only the cluster amplitudes of T^{μ} enter in the coupling term.

To arrive at the uncoupled approximant to the parent SS-MRCC theory, we replace the explicit coupling term $Y_{\mu\nu} = \langle\chi_l|\exp(-T^{\mu} + T^{\nu\prime}|\phi_\mu\rangle$ by a simpler expression containing T^{μ} only:

$$Y_{\mu\nu} \rightarrow Y^{UC}_{\mu\nu} = \langle\chi_l|\exp(-T^{\mu} + T^{\mu\prime}(\nu)|\phi_\mu\rangle \tag{3-7}$$

where $T^{\mu\prime}(\nu)$s denote the subset of T^{μ} which have the same excitation structure of $T^{\nu\prime}$. These terms are characterized by explicit appearance of creation-annihilation of either holes or particles and/or of those active orbitals which are occupied or unoccupied in both ϕ_μ and ϕ_ν. They thus contain *all* orbitals common in ϕ_μ and ϕ_ν. In this case then, the difference $[-T^{\mu}+T^{\mu\prime}(\nu)] \equiv [-\overline{T}^{\mu}(\nu)]$ contain only those excitations which contain active orbitals distinguishing ϕ_μ and ϕ_ν. Hence $Y^{UC}_{\mu\nu}\tilde{H}_{\mu\nu}$ will still be a connected entity. With this small but significant change, the UC-SS-MRCC equations take the form

$$\langle\chi_l|\overline{H}_\mu|\phi_\mu\rangle c_\mu + \sum_{\nu\neq\mu}\langle\chi_l|\exp(-\overline{T}^{\mu}(\nu)|\phi_\mu\rangle\tilde{H}_{\mu\nu}c_\mu = 0 \tag{3-8}$$

This can be simplified further to yield

$$\langle\chi_l|\overline{H}_\mu|\phi_\mu\rangle c_\mu + \sum_{\nu\neq\mu}\langle\chi_l|\Big[-\overline{T}^{\mu}(\nu)+\frac{1}{2}\overline{T}^{\mu 2}(\nu)\Big]|\phi_\mu\rangle\tilde{H}_{\mu\nu}c_\mu = 0 \tag{3-9}$$

for the truncation of T_μ up to doubles.

It may be instructive to emphasize here that, since $\overline{T}^{\mu}(\nu)$ is labeled by active orbitals distinguishing ϕ_μ and ϕ_ν, $\overline{T}^{\mu}(\nu)$ annihilate all $|\phi_\nu\rangle$ for $\nu \neq \mu$:

$$\overline{T}^{\mu}(\nu)|\phi_\nu\rangle = 0 \tag{3-10}$$

For the SD truncation scheme, Eq. (3-8) can be written as

$$\langle\chi_{l1}|[\overline{H}_\mu]_1|\phi_\mu\rangle c_\mu + \sum_{\nu\neq\mu}\langle\chi_{l1}|-\overline{T}^{\mu}_1(\nu)|\phi_\mu\rangle\tilde{H}_{\mu\nu}c_\nu = 0 \tag{3-11}$$

for the single excitation projections on to $\langle\chi_{l1}|$. $[\bar{H}_\mu]_1$ are the one body excitations of $\bar{H}_\mu$. Likewise, for the doubles excitations, projections onto the double excited states $\langle\chi_{l2}|$ reached from ϕ_μ lead us to

$$\langle\chi_{l2}|[\overline{H}_\mu]_2|\phi_\mu\rangle c_\mu + \sum_{\nu\neq\mu}\langle\chi_{l2}|\Big[-\overline{T}^{\mu}_2(\nu)+\frac{1}{2}\overline{T}^{\mu 2}_1(\nu)\Big]|\phi_\mu\rangle\tilde{H}_{\mu\nu}c_\nu = 0 \tag{3-12}$$

The Eqs. (3-11) and (3-12) are the working equations for uncoupled state-specific MRCC (UC-SS-MRCC) theory. They are simpler in structure as compared to the rigorously size-extensive SS-MRCC theory containing genuine coupling term. Though by this modification the scaling with respect to the orbitals is not altered, we get a simpler coupling term. The main purpose for suggesting this uncoupling approximation is *not* to counterpose this approximate version against the rigorous SSMRCC formulation, but to establish that an essential simplification of the coupling term is possible which, as the results discussed in Section 3.5 would indicate, does not lead

to deterioration of the quality of computed energies as the result of the uncoupling approximation.

3.3.2. Relation Between sr-MRBWCCSD and UC-SS-MRCC

The Hubač – Čársky – Pittner single root (sr) multi-reference Brillouin – Wigner coupled cluster [30–32] theory (sr-MRBWCC) is also an intruder free state-specific theory where the coupling term is simpler than in the SS-MRCC. The coupling appears indirectly via the energy E, the only problem being its manifest size-inextensivity. Though both SS-MRCC and sr-MRBWCC theory use the Jeziorski – Monkhorst cluster Ansatz [10] in the wave-function, they are built on different sufficiency conditions. Each corresponds to a projection on to a virtual function χ_l reached from a model function ϕ_μ as equal to zero. As has been discussed in Section 3.2, in SS-MRCC there are two sets of terms in the working equations. The first set, the "direct" term contains only powers of T^μ for the excitations from ϕ_μ.The second set, the "coupling" term, where other T^νs ($\mu \neq \nu$) also figure in the term. The coupling term is crucial for the twin desirable goals of the formulation, viz. (1) avoidance of intruders and (2) maintenance of rigorous size-extensivity. We replace the operators $T^{\nu'}$ in the coupling term in the UC-SS-MRCC theory by $T^{\mu'}$, thereby empirically eliminating the couplings. In contrast, in the sr-MRBWCC theory the "direct" term is rather analogous to the one in SS-MR theory, while in place of the "coupling" term there is a simpler looking expression containing the target energy E itself multiplied by certain expressions containing just the amplitudes of the same T^μ for each ϕ_μ. The working equations look like

$$\langle \chi_l | H \exp T^\mu | \phi_\mu \rangle = \langle \chi_l | \exp T^\mu | \phi_\mu \rangle E \; \forall l, \mu \tag{3-13}$$

Unfortunately, despite the simpler structure of the sr-MRBWCC theory, it is not manifestly size-extensive. Attempts have been made [32, 49] by reverting to a Rayleigh-Schrödinger like expansion of E, but this runs into the danger of entailing intruders. The UC-SS-MRCC, in contrast, is manifestly size-extensive, though here the simplification of the coupling term is achieved by an empirical replacement of $T^{\nu'}$ by $T^{\mu'}$. In sr-MRBWCC, the coupling of the various T^μs with different ϕ_μs is thus *implicit*, appearing via E, since E involves all the cluster operators with different T^νs. Due to the absence of explicit couplings of the various T^μs, the working equation in sr-MRBWCC is simpler in structure as compared to that of SS-MRCC and this is why we could characterize sr-MRBWCC as an uncoupled MRCC approach.

We also want to emphasize that the UC-SS-MRCC is not only completely size extensive, but also – as will be exemplified by numerical results presented in Section 3.5 – capable of providing potential energy surface with almost no deterioration of the quality of the computed energies vis-a-vis the parent SS-MRCC.

To summarize, we have developed in this section a formalism which emerges from the rigorous SSMRCC formulation of Mukherjee et al., where the coupling term of

the parent formalism is simplified in a way that for excitations from a model function ϕ_μ to a virtual function χ_l, only T^μs appear. Since the simplifying approximations in UC-SS-MRCC consists in replacing the nontrivial $T^{\nu'}$ operators appearing in the coupling term $Y_{\mu\nu} = \langle\chi_l|\exp\left(-T^\mu + T^{\nu'}\right)|\phi_\mu\rangle$ by the corresponding $T^{\mu'}$ operators, this is somewhat like invoking an *anonymous parentage approximation* while evaluating the coupling terms. When ϕ_μ and ϕ_ν are widely separated in energy, it is not immediately obvious that the use of anonymous parentage approximation will be a good one. As will be illustrated with numerical applications in Section 3.5, the excellent performance of the UC-SS-MRCC as compared to that from sr-MRBWCC implies that maintenance of size-extensivity may very well compensate for the error due to the anonymous parentage approximation. Some insight into this assertion can be gleaned by looking at the PES of Li_2 presented in Section 3.5, where the UC-SS-MRCC performs as well as the SSMRCC at large internuclear distance (where the model functions are practically degenerate), while the performance of the sr-MRBWCC gets increasingly inferior at large internuclear separation. Formulation and discussion of the merits of UC-SS-MRCC is not meant to advocate replacement of the parent SSMRCC with the UC-SS-MRCC generally, since one does not gain much improvement in scaling behavior with respect to orbital basis. Rather it is meant to throw light on the role of maintaining size-extensivity in the simplified treatment of the coupling term. The UC-SS-MRCC is likely to turn out to be computationally useful in SSMRCEPA like approximations, where an eigenvalue equation like structure can emerge with diagonal dressing of the MR-CISD matrix in the UC-SS-MRCC. (Pathak et al. to be published)

3.4. DEVELOPMENT OF SIZE-EXTENSIVE APPROXIMANT TO THE SS-MRCC WITH MODEL-SPACE INDEPENDENT INACTIVE EXCITATIONS

3.4.1. Motivations and Insights for an Internally Contracted Inactive Excitation Scheme (ICI-SS-MRCC)

We are going to present in this section in the same spirit as in the internally contracted MRCI (IC-MRCI) method [43–45], a size-extensive state-specific MRCC method, where for the inactive excitations are taken to be independent of the model space function ϕ_μ they act upon. To motivate towards this formulation, we adduce simple perturbative arguments to see why and where the inactive excitations can be taken to be independent of μ. An analogous exercise was done for the contracted MR-CI scheme too, long time ago [43, 44]. In particular, the inactive double excitation of the type ij$\rightarrow$ ab are the most numerous, and there will be dramatic simplification if these cluster amplitudes have really weak dependence on μ. In a contracted MR-CI, the multi-configurational reference function $\psi_0 = \sum_\mu \phi_\mu c_\mu$, is treated as a single contracted reference configuration, and excited configurations are generated by the application of inactive excitation operators $\{Y_I^\dagger\}$ to this contracted function. Each excited configuration is then a linear combination of many ordinary configuration

state functions, with the linear coefficients fixed by the reference wave function. As a result, the number of independently varied coefficients is similar to the number of terms in a SR calculation. For given number of orbitals and electrons, the length of an uncontracted MRCISD expansion is approximately proportional to the number of reference configurations. Therefore, internal contraction can provide a *drastic reduction* in the length of the CI vector and allow the use of substantially larger reference spaces than would be practical in uncontracted calculation, making the use of CMS more affordable. At the same time it should be noted that the reduction in the computational effort is not as drastic as in the length of the CI vector, since the Hamiltonian matrix in contracted CI is not near as sparse as for the uncontracted expansions. Multi-reference perturbation theories using the concept of IC configurations have also been appeared in the literature [46].

In the same spirit as in the contracted MR-CI, we develop the corresponding contracted version of the SS-MRCC method, where the inactive excitations are independent of μ. We propose the ICI-SS-MRCC Ansatz as:

$$\psi = \exp(T_i) \sum_{\mu} \exp(T^{\mu}) |\phi_{\mu}\rangle c_{\mu} \tag{3-14}$$

in which only the cluster operators T_i causing pure inactive excitations from the reference functions $\psi_0 = \sum_{\mu} |\phi_{\mu}\rangle c_{\mu}$, are independent of model space determinants. Thus, the reduction of the cluster amplitudes is obvious from our proposed theory.

In the development stage of ICI-SS-MRCC, we have tried two different variants of ICI-SS-MRCC formalism. One is ICI-SS-MRCC(1), where only the pure two-body inactive excitations were made model function independent and the other is ICI-SS-MRCC(2), where both the one- and two-body pure inactive excitations were made reference determinant independent. We have presented applications of these two variants in Section 3.5.

From an estimate of the cluster amplitudes from the first order perturbation theory we know that cluster amplitudes causing double excitation, involve the two-body portion of H in the numerator depending only on the orbitals involved in the excitation. The denominator is roughly of the order of the energy differences of the doubly occupied and the virtual orbitals and a shift which could be weakly dependent on ϕ_{μ}.

$$t_{ij}^{ab}(\mu) \simeq \frac{V_{ij}^{ab}}{\Delta E_{\text{shift}}^{\mu} + \varepsilon_i + \varepsilon_j - \varepsilon_a - \varepsilon_b} \tag{3-15}$$

The two-body cluster inactive amplitudes can thus be assumed to be ϕ_{μ} independent without any significant loss of accuracy.

On the other hand, the cluster amplitudes causing single excitations from a given ϕ_{μ} involve Fock-operator f_{μ} in the numerator which is strongly μ-dependent and hence it does not appear to be a good approximation at all to make the one-body cluster amplitudes μ-independent. In what follows, we will develop the ICI-SS-

MRCC formalism in a way that allows some inactive excitations to be μ-dependent, if we so wish. The version ICI-SS-MRCC(1) involves only T_{2i}s which are μ-independent, while the version ICI-SS-MRCC(2) involves both T_{1i}s and T_{2i}s which are μ-independent. Since the assumption of T_{1i} may not be a good one, the version (2) is not expected to perform as well as the other version. This is shown to be the case, as exemplified in Section 3.5.

3.4.2. Development of the General ICI-SS-MRCC Formalism

We now describe the theoretical development of our ICI-SS-MRCC approximation. The μ-independent excitations containing inactive orbitals only are generally denoted from now on as T_i. The rest, μ-dependent excitations are denoted by T_μ We posit on the exact state $|\psi\rangle$, spanning the target space, the following Ansatz:

$$\psi = \exp(T_i) \sum_\mu \exp(T^\mu)|\phi_\mu\rangle c_\mu \tag{3-16}$$

As discussed in Section 3.4.1, such type of Ansatz reduces the number of inactive cluster amplitudes enormously. The cluster operator T_i is taken to be independent of μ will finally be restricted to purely inactive double excitations, but for the general development, we will not necessarily assume this to be the case. The excitations induced by the other set of cluster operator T^μ involve the complements of all possible excitations left out by T_i. Again, in our applications we will advocate inclusion of single excitations of all types and the double excitations involving at least one active orbital in the set $\{T^\mu\}$ for all μ.

We will denote the space functions reached by T_i on ψ_0 as Q_i, while the complementary projector spanned by the space of functions reached by the set $\{T^\mu\}$ on ϕ_μ's will be denoted by Q_a. The union $Q_i + Q_a$ for all distinct functions is denoted by the projector Q. The projector for the model space is denoted by P.

To derive the working equations, for ICI-SS-MRCC, we use the Ansatz Eq. (3-16), in the Schrödinger Equation, and invoke certain sufficiency conditions using the projection on virtual functions reached by T_i and T^μ.

To arrive at these equations, it is convenient to introduce the following composites:

$$\overline{H} = \exp(-T) H \exp(T) \tag{3-17}$$

$$\overline{\overline{H}}_\nu = \overline{\overline{H} \exp(T^\nu)} \tag{3-18}$$

Using the composite $\overline{H}$ as defined in Eq. (3-17), write the Schrödinger Equation as:

$$H \exp(T) \sum_\mu \exp(T^\mu)|\phi_\mu\rangle c_\mu = E \exp(T) \sum_\mu \exp(T^\mu)|\phi_\mu\rangle c_\mu \tag{3-19}$$

and obtain

$$\overline{H}\sum_{\mu}\exp(T^{\mu})|\phi_{\mu}\rangle c_{\mu} = E\sum_{\mu}\exp(T^{\mu})|\phi_{\mu}\rangle c_{\mu} \tag{3-20}$$

using the definition of Eq. (3-18), we can simplify Eq. (3-20) even further:

$$\sum_{\mu}\exp(T^{\mu})\overline{\overline{H}}_{\mu}|\phi_{\mu}\rangle c_{\mu} = E\sum_{\mu}\exp(T^{\mu})|\phi_{\mu}\rangle c_{\mu} \tag{3-21}$$

Using the resolution of identity, $I = P + Q$, we have

$$\sum_{\mu}\exp(T^{\mu})(P+Q)\overline{\overline{H}}_{\mu}|\phi_{\mu}\rangle c_{\mu} = E\sum_{\mu}\exp(T^{\mu})|\phi_{\mu}\rangle c_{\mu} \tag{3-22}$$

We now introduce the subscripts i and a for an operator X, viz. X_i and X_a to denote excitations of the type induced by T_i's and T_μ's respectively. We also denote X_{ex}, the general excitations components of X, leading to the Q space.

Using the expressions for Q and P and using $Q = Q_i + Q_a$, we get

$$\begin{aligned}\sum_{\mu}\exp(T^{\mu})\overline{\overline{H}}_{\mu\,ex}|\phi_{\mu}\rangle c_{\mu} \;&+\sum_{\mu\nu}\exp(T^{\mu})|\phi_{\nu}\rangle\langle\phi_{\nu}|\overline{\overline{H}}_{\mu}|\phi_{\mu}\rangle c_{\mu}\\ &= E\sum_{\mu}\exp(T^{\mu})|\phi_{\mu}\rangle c_{\mu}\end{aligned} \tag{3-23}$$

Inspired by the manipulations leading to the parent SS-MRCC [33–35] theory, we interchange μ and ν in Eq. (3-23) on the second term on its left hand side and obtain:

$$\begin{aligned}\sum_{\mu}\exp(T^{\mu})\overline{\overline{H}}_{\mu\,ex}|\phi_{\mu}\rangle c_{\mu} \;&+\sum_{\mu\nu}\exp(T^{\nu})|\phi_{\mu}\rangle\tilde{\tilde{H}}_{\mu\nu}c_{\nu}\\ &= E\sum_{\mu}\exp(T^{\mu})|\phi_{\mu}\rangle c_{\mu}\end{aligned} \tag{3-24}$$

where,

$$\tilde{\tilde{H}}_{\mu\nu} = \langle\phi_{\mu}|\overline{\overline{H}}_{\nu}|\phi_{\nu}\rangle \tag{3-25}$$

We now separate the "i" and "a" components of the entire space of excitation component.

$$\begin{aligned}\sum_{\mu}\exp(T^{\mu})\overline{\overline{H}}_{\mu\,i}|\phi_{\mu}\rangle c_{\mu} \;&+\sum_{\mu}\exp(T^{\mu})\overline{\overline{H}}_{\mu\,a}|\phi_{\mu}\rangle c_{\mu} + \sum_{\mu\nu}\exp(T^{\nu})|\phi_{\mu}\rangle\tilde{\tilde{H}}_{\mu\nu}c_{\nu}\\ &= E\sum_{\mu}\exp(T^{\mu})|\phi_{\mu}\rangle c_{\mu}\end{aligned} \tag{3-26}$$

Following the ideas introduced in the parent MRCC theory, we write the resolution of identity in the following manner:

$$\begin{aligned} I &= exp(T^{\mu})(P + Q_i + Q_a)exp(-T^{\mu}) \\ &= P_{\mu} + Q_{\mu i} + Q_{\mu a} \end{aligned} \tag{3-27}$$

Equation (3-26) can then be rewritten as

$$\begin{aligned} &\sum_{\mu} \exp(T^{\mu}) Q_i \overline{\overline{H}}_{\mu\, i} |\phi_{\mu}\rangle c_{\mu} + \sum_{\mu} \exp(T^{\mu}) Q_a \overline{\overline{H}}_{\mu\, a} |\phi_{\mu}\rangle c_{\mu} \\ &\quad + \sum_{\mu\nu} \exp(T^{\mu})(Q_i + Q_a) \exp(-T^{\mu}) \exp(T^{\nu}) |\phi_{\mu}\rangle \widetilde{\widetilde{H}}_{\mu\nu} c_{\nu} = 0 \end{aligned} \tag{3-28}$$

where we made use of the relations

$$Q_a X_i = Q_i X_a = 0 \tag{3-29}$$

and

$$(Q_{\mu i} + Q_{\mu a}) \exp(T^{\mu}) |\phi_{\mu}\rangle = \exp(T^{\mu})(Q_i + Q_a) |\phi_{\mu}\rangle = 0 \tag{3-30}$$

We now use two different kinds of projection manifolds for the virtual functions to arrive at the equations for the cluster amplitudes. For the inactive excitations involving internally contracted functions, we introduce $Q_i = \sum_{l_i} |\chi_{l_i}\rangle\langle\chi_{l_i}|$ with $|\chi_{l_i}\rangle = Y_{l_i}|\Psi_0\rangle$ and use projections $Q_{\mu i} = exp(T^{\mu})Q_i exp(-T^{\mu})$ obtained therefrom. For every excitation $T_{l_i} = t_{l_i} Y_{l_i}^{\dagger}, T_{l_i} \in T_i$, there is always a projection coming from $exp(T^{\mu})|\chi_{l_i}\rangle\langle\chi_{l_i}|exp(-T^{\mu})$. From Eq. (3-28), for every χ_{l_i} we get a set of equations

$$\begin{aligned} &\sum_{\mu} \langle\chi_{l_i}| \exp(T^{\mu}) Q_i \overline{\overline{H}}_{\mu\, i} |\phi_{\mu}\rangle c_{\mu} = 0 \forall l_i \in Q_i \\ \text{or} \quad &\sum_{\mu\lambda} C_{\lambda} \langle\phi_{\lambda}| Y_l^{\dagger} \exp(T^{\mu}) \overline{\overline{H}}_{\mu\, i} |\phi_{\mu}\rangle c_{\mu} = 0 \forall l_i \in Q_i \end{aligned} \tag{3-31}$$

These equations are the ones determining the cluster amplitudes of $T_i = \sum_{l_i} T_{l_i} = \sum_{l_i} t_{l_i} Y_{l_i}^{\dagger}$. They consist of connected terms only, though it may not be immediately obvious. We do not have the space to discuss the proof here, which will form the subject of a forthcoming, comprehensive communication [42]. Here we merely sketch the essentials.

For every μ, we can rewrite Eq. (3-31) as

$$\sum_{\mu} {c_{\mu}}^2 \sum_{\lambda} \frac{C_{\lambda}}{c_{\mu}} \langle\phi_{\lambda}| Y_l^{\dagger} \exp(T^{\mu}) \overline{\overline{H}}_{\mu\, i} |\phi_{\mu}\rangle c_{\mu} = 0 \tag{3-32}$$

The ratio $\frac{C_\lambda}{c_\mu}$ can be expressed in terms of a cluster expansion from $\langle\phi_\mu|$ with a de-excitation operator $\sigma_\mu^\dagger$ involving de-excitations with active orbitals only.

$$\frac{C_\lambda}{c_\mu} = \langle\phi_\mu|\exp(\sigma_\mu^\dagger)|\phi_\lambda\rangle \tag{3-33}$$

For a CAS, $\sigma_\mu^\dagger$ is a connected operator. Using Eq. (3-33), Eq. (3-32) can be cast in the form

$$\sum_\mu {c_\mu}^2 \sum_\lambda \langle\phi_\mu|[\exp(\sigma_\mu^\dagger)]_\mu^\lambda Y_l^\dagger \exp(T^\mu)\overline{\overline{H}}_{\mu\, i}|\phi_\mu\rangle = 0 \tag{3-34}$$

Since $Y_l^\dagger$ has only de-excitations with inactive labels and $\overline{\overline{H}}_{\mu\, i}$ has excitations involving inactive labels, they must connect among themselves for a non-zero contribution of $\langle\phi_\mu|\cdots|\phi_\mu\rangle$. Also since $\sigma_\mu^\dagger$ has active de-excitations, they must contract with active excitations stemming from $\exp(T^\mu)$. Thus some inactive lines of $Y_l^\dagger$ are connected to some inactive lines of $\exp(T^\mu)$, and the remaining active must be joined between those in $\left[\exp\left(\sigma_\mu^\dagger\right)\right]_\mu^\lambda$ and $\exp(T^\mu)$. For the T^μ operators, we use the sufficiency conditions of the same type as invoked in the parent theory to arrive at

$$\langle\chi_l|\overline{\overline{H}}_\mu|\phi_\mu\rangle c_\mu + \sum_\nu \langle\chi_l|\exp(-T^\mu)\exp(T^\nu)|\phi_\mu\rangle \widetilde{\widetilde{H}}_{\mu\nu} C_\nu = 0 \tag{3-35}$$

which can be shown to be manifestly size-extensive. The energy is obtained from

$$\sum_\nu \widetilde{\widetilde{H}}_{\mu\nu} C_\nu = E c_\mu \tag{3-36}$$

Equations (3-34), (3-35), and (3-36) are all coupled and they are solved by a nested macro- and micro-iteration with the $\{c_\mu\}$ computed from Eq. (3-36) in the macro-loop and T_{l_i} and T_μ^l solved in the micro-loop.

The use of Eq. (3-34) equivalently of Eq. (3-31) is the most crucial, since it demonstrates clearly the dramatic reduction of the number of the cluster-amplitudes for inactive excitations. In our preliminary applications, we shall use two schemes:

a. in one, to be called ICI-SS-MRCC(1), we take the inactive T_2's to be μ-independent, and
b. in the other, to be called ICI-SS-MRCC(2), we take both T_1 and T_2 for the inactive excitations to be μ-independent.

It turns out that the latter is a poorer approximation compared to the former.

3.5. RESULTS AND DISCUSSION

In this section we present application of both the UC-SS-MRCC and ICI-SS-MRCC theory to four prototypical systems. Since we wanted to work with spin-adapted formulations as far as feasible, we deliberately choose only those molecular electronic states which are described well in their model representation in terms of closed-shell determinants only. The spin-adaptation of the working equations both for the parent SS-MRCC, and the approximants we are considering in this article becomes a straightforward exercise in this situation. We simply replace, exactly as is done in the SRCC theory, the spin-orbital indices with the orbital indices, and assign a factor 2 for each loop. This stratagem has been followed in all of our applications.

For our system studies, we have looked at the full potential energy surface (PES) of the ground state of BeH_2 model system, Li_2, and the single point energy on lowest singlet state of CH_2, and O_3 at their equilibrium geometry.

All the states considered, encounter severe intruder problems if treated in the effective hamiltonian formalism, but our applications in the state-specific context do not display presence of intruders at all. For systems such as BeH_2, the highest lying valence orbitals cross each other, demanding a state-specific theory where all model functions are treated on the same footing. The performance of our method has been assessed against the corresponding FCI values and we have also shown results from the rigorous SS-MRCC [33–35] formalism.

All the systems studied by us are described well by two determinant model spaces whose model functions are described generically by the closed-shell functions ϕ_1=[core]a^2 and ϕ_2=[core]b^2 with two active orbital "a" and "b" belonging to different symmetries. The model space used in our applications is thus complete. In all our calculations we have used (2,2) CASSCF orbitals. The CASSCF and FCI calculations were performed using the US-GAMESS electronic package of 2007.

In this section we have also presented results from another version of ICI-SS-MRCC theory where in addition to $2h-2p$ type pure inactive excitation, $1h-1p$ type pure inactive excitations have also made independent of reference determinants. Results corresponding to this theory is referred to as results from ICI-SS-MRCC(2), whereas results corresponding to ICI-SS-MRCC with T=T_2 is referred to as results from ICI-SS-MRCC(1).

3.5.1. PES of Perpendicular Insertion of Be into H_2

As the first system, we present here C_{2v} insertion reaction of Be to H_2 to form the BeH_2 molecule. Since, in the Be atom, the 2s and 2p orbitals are quasi-degenerate, and its insertion into the H_2 molecule requires breaking of the H_2 bond, it makes both the $1\sigma_g^2$ and $1\sigma_u^2$ configurations equally important. In the CI description of the composite system at the bond-breaking geometry, both configurations are equally important. Thus the PES studies of the insertion reaction warrants a two-configuration reference description.

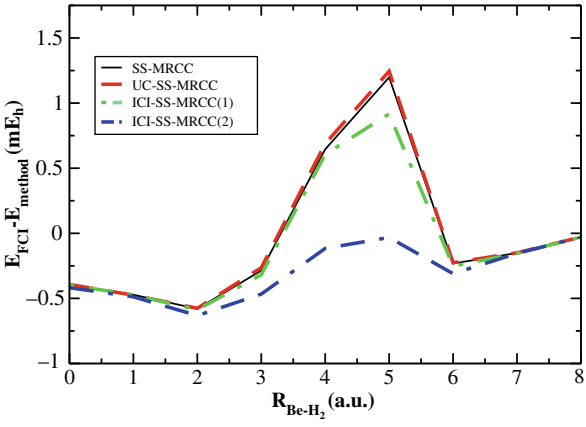

Figure 3-1. Difference energy curve for the perpendicular insertion of Be into H_2 of SS-MRCC, UC-SS-MRCC, ICI-SS-MRCC(1), ICI-SS-MRCC(2) with respect to FCI

The insertion path displays avoided crossings as the distance of approach R, of Be atom to the two hydrogen atoms in H_2 is varied. The system has been widely studied both at the geometries where the two configurations are equally important [50] and for the reaction path at other geometries as well [50, 51]. We have followed exactly the same points of the sample path as studied by Purvis et al. [50]. The arrangements of Be and the two H atoms for the various H-H distances and R for all sample points are shown in Fig. 1 of Ref. [35].

Beyond the sample point E, the dominant configuration is $1a_1^2 2a_1^2 3a_1^2$, which in our study has been taken as ϕ_2. However, for sample points A, B, C, and D, the determinant $1a_1^2 2a_1^2 1b_2^2$ is seen to have a lower energy, we have considered this configuration as ϕ_1. Corresponding to the sample point E both these configurations are seen to be equally weighted. We have used the lowest root of (2, 2)CAS and have used the CASSCF natural orbitals from GAMESS(US)-2007 electronic package. The success of UC-SS-MRCC and ICI-SS-MRCC(1) like SS-MRCC [34] over the entire range of R is a stringent test of the formulations. A comparison with the FCI results indicates a very good global behavior for our UC-SS-MRCC as well as ICI-SS-MRCC(1) theory as is evident from Table 3-1 and Figure 3-1.

3.5.2. Ground State PES of Li_2 Molecule

The second system we present here is the study on ground state of Li_2 molecule, which has also been studied by many workers in great details [34, 52–54]. A very detailed calculation involving the first nine excited states of this system has already been carried out by Kaldor [52], using a rather large basis involving 74 Gaussian type orbitals using the VU-MRCC theory in an incomplete model space(IMS). Figure 1

Table 3-1. Absolute energy (E_h) from various MRCC based methods and FCI for ground state of BeH_2. (Basis and geometry: Second entry of Ref. [59]; configuration for $\phi_1 : 1a_1^2 2a_1^2 1b_2^2$)

Geometry	Coordinates (y,R)(a.u.)	SS-MR CC	UC-SS-MR CC	ICI-SS-MR(1) CC	ICI-SS-MR(2) CC	FCI
A	2.540,0.000	−15.778776	−15.778779	−15.778775	−15.778754	−15.779172
B	2.080,1.000	−15.736753	−15.736750	−15.736752	−15.736737	−15.737225
C	1.620,2.000	−15.674238	−15.674242	−15.674232	−15.674186	−15.674818
D	1.390,2.500	−15.622598	−15.622620	−15.622566	−15.622416	−15.622884
E	1.275,2.750	−15.603564	−15.603607	−15.603525	−15.602803	−15.602919
F	1.160,3.000	−15.626162	−15.626210	−15.625882	−15.624932	−15.624964
G	0.930,3.500	−15.692963	−15.692969	−15.692942	−15.692885	−15.693195
H	0.700,4.000	−15.736537	−15.736538	−15.736534	−15.736534	−15.736688
I	0.700,6.000	−15.760849	−15.760850	−15.760849	−15.760848	−15.760878

in Ref. [52] makes it clear that Li_2 has a wealth of low-lying excited functions, which mix strongly with the model space functions, especially at the equilibrium geometry [52] and also around $R = 8.5$ a.u. Hence it is a good choice for testing the efficacy of any theory designed to bypass intruders.

In our calculation the determinants $\phi_1 = 1\sigma_g^2 1\sigma_u^2 2\sigma_g^2$ and $\phi_2 = 1\sigma_g^2 1\sigma_u^2 2\sigma_u^2$ comprise the two reference determinants that make up our active space. We have used basis cc-pVDZ from http://www.emsl.pnl.gov/forms/basisform.html and D_{2h} point group in our calculation. The orbitals used are CAS-SCF orbitals for the lowest root of the (2, 2)CAS.

In Table 3-2, we present absolute energies in E_h for the ground state of the Li_2 molecule obtained from SS-MRCC, UC-SS-MRCC, ICI-SS-MRCC(1), ICI-SS-MRCC(2) and FCI.

Analyzing Figure 3-2 as well as Table 3-2 ,we conclude that UC-SS-MRCC and ICI-SS-MRCC(1) shows a very good global behavior. In low internuclear distances ICI-SS-MRCC(2) deviates more from FCI.

3.5.3. The Lowest $^1A_1$ State of CH_2 at Equilibrium Geometry

The lowest $^1A_1$ state of CH_2 at equilibrium geometry has already been studied systematically by many workers [33, 34, 55–57] as a typical system which, even at equilibrium geometry, possesses pronounced MR character. Hence for a qualitative description, both the model space functions $\phi_1 = 1a_1^2\, 2a_1^2\, 1b_2^2\, 3a_1^2$ and $\phi_2 = 1a_1^2\, 2a_1^2\, 1b_2^2\, 1b_1^2$ are required.

In our computations we have used standard Huzinaga – Dunning triple-ζ basis (from GAMESS BASIS SET LIBRARY) augmented with a set of six-d type polarization functions on carbon [α_d=1.50] and one set of p-polarization function on each hydrogen [α_p(H)=1.50]. We have kept 1*s* orbital of C and the highest virtual

Table 3-2. Absolute energies (E_h) from different MRCC based methods and FCI for the ground state of the Li_2 molecule at various internuclear distances(a.u.) using cc-pVDZ basis

R	SS-MRCC	UC-SS-MRCC	ICI-SS-MRCC(1)	ICI-SS-MRCC(2)	FCI
4.50	−14.900697	−14.900698	−14.900696	−14.900680	−14.900797
5.00	−14.903945	−14.903946	−14.903945	−14.903929	−14.904022
5.1696	−14.903929	−14.903930	−14.903928	−14.903913	−14.904000
5.50	−14.902785	−14.902786	−14.902785	−14.902770	−14.902848
6.00	−14.899192	−14.899193	−14.899192	−14.899178	−14.899245
6.50	−14.894439	−14.894440	−14.894439	−14.894426	−14.894486
7.00	−14.889368	−14.889369	−14.889368	−14.889356	−14.889411
7.50	−14.884535	−14.884535	−14.884535	−14.884523	−14.884576
8.00	−14.880276	−14.880277	−14.880276	−14.880266	−14.880317
8.50	−14.876755	−14.876756	−14.876755	−14.876746	−14.876796
9.00	−14.873995	−14.873996	−14.873995	−14.873987	−14.874038
9.50	−14.871926	−14.871927	−14.871926	−14.871920	−14.871970
10.00	−14.870429	−14.870429	−14.870429	−14.870424	−14.870474
10.50	−14.869372	−14.869372	−14.869372	−14.869368	−14.869418
11.00	−14.868637	−14.868637	−14.868637	−14.868634	−14.868685
12.00	−14.867780	−14.867780	−14.867780	−14.867778	−14.867828
14.00	−14.867160	−14.867160	−14.867160	−14.867159	−14.867208

orbital frozen. The equilibrium geometry has been taken from the work done by Sherrill et al. [57].

In Table 3-3, we have presented deviations of the various MRCC approaches (SS-MRCC, UC-SS-MRCC, ICI-SS-MRCC(1), ICI-SS-MRCC(2)) with respect to the FCI. The deviation of the result in ICI-SS-MRCC(2) with respect to FCI is large,

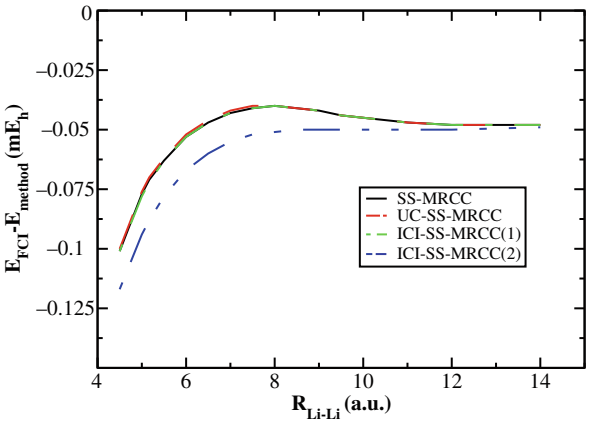

Figure 3-2. Difference Energy plot for the Ground State of Li_2 of SS-MRCC, UC-SS-MRCC, ICI-SS-MRCC(1), ICI-SS-MRCC(2) w.r.t. FCI

Table 3-3. Total energies (E_h) of 1^1A_1 state of the CH_2 at equilibrium geometry

Methods	Energies
SS-MRCC	−39.011598
UC-SS-MRCC	−39.011708
ICI(1)-SS-MRCC	−39.011501
ICI(2)-SS-MRCC	−39.011006
FCI	−39.013938

while that in UC-SS-MRCC and ICI-SS-MRCC(1) is comparable with the rigorous SSMRCC value.

3.5.4. Ground State of O_3 at Equilibrium Geometry

At last we are going to present state energy calculation of O_3 ground state at minimum energy(equilibrium) geometry, which like lowest $^1A_1$ state of CH_2, also possess a pronounced MR character due to considerable mixing between the [core....]$4b_2^2 6a_1^2 1a_2^2$ and [core....]$4b_2^2 6a_1^2 2b_1^2$ configurations [58]. We thus have taken these two configurations in our model space.

In our calculation we have used DZP(Dunning) basis set from "http://www.emsl.pnl.gov/forms/basisform.html" which have been contracted with a set of six-d type polarization functions on oxygen[α_d=1.211]. The minimum energy geometry is taken from experimental result [58].

In Table 3-4, we have presented state energies with various MRCC approaches (SSMRCC, UC-SS-MRCC, ICI-SS-MRCC(1), ICI-SS-MRCC(2)) at minimum energy geometry of O_3 molecule. From the table we could conclude that ICI-SS-MRCC(1) seems to be comparable with SS-MRCC whereas ICI-SS-MRCC(2) is deviated more from SS-MRCC.

Table 3-4. Total molecular energies (E_h) of O_3 with various MRCCSD theory at minimum energy geometry

Methods	Energies
SS-MRCC	–224.923955
UC-SS-MRCC	–224.925052
ICI(1)-SS-MRCC	–224.923758
ICI(2)-SS-MRCC	–224.919734

3.6. CONCLUSION

In this chapter, we have presented developments and pilot numerical applications of two outcomes of the search for viable size-extensive methods which are computationally tractable and stable over a wide range of nuclear geometries, including quasi-degeneracies leading to avoided crossings process. These are non-perturbative approximants UC-SS-MRCC and ICI-SS-MRCC of rigorously size-extensive SS-MRCC theory [33–35]. Our discussions and numerical applications clearly show that though there is considerable simplification of the working equations, as in the case of UC and drastic reduction in the number of cluster amplitudes, as in the case of ICI, there has been no significant compromise as far as accuracy is concerned.

ACKNOWLEDGMENTS

The authors are indebted to the editors for their extraordinary patience with them. SD acknowledges the CSIR and DST for research fellowships. SP and RM are grateful to the DST for research fellowships. DM acknowledges DST for the J.C. Bose Fellowship. The authors gratefully acknowledge the Indo-Hungarian and Indo-Swedish Bilateral Project.

REFERENCES

1. F. Coester, Nucl. Phys. **7**, 421 (1958)
2. H. Kummel, Nucl. Phys. **17**, 477 (1960)
3. J. Čížek, J. Chem. Phys. **45**, 4256 (1966)
4. R. J. Bartlett, G. D. Purvis III, Int. J. Quantum Chem. **14**, 561 (1978)
5. J. Paldus, J. Čížek, I. Shavitt, Phys. Rev. A **5**, 50 (1972)
6. R. J. Bartlett, Annu. Rev. Phys. Chem. **32**, 359 (1981)
7. R. J. Bartlett, in *Modern Electronic Structure Theory*, Ed. D. R. Yarkony (World Scientific, Singapore, 1995), pp. 1047–1131
8. J. Paldus, X. Li, Adv. Chem. Phys. **110**, 1 (1999)
9. J. Čížek, Adv. Chem. Phys. **9**, 105 (1975)
10. D. Mukherjee, R. K. Moitra, A. Mukhopadhyay, Mol. Phys. **30**, 1861 (1975), Mol. Phys. **33**, 955 (1977)
11. I. Lindgren, Int. J. Quantum. Chem. **S12**, 33 (1978)
12. B. Jeziorski, H. J. Monkhorst, Phys. Rev. A **24**, 1668 (1981)
13. B. Jeziorski, J. Paldus, J. Chem. Phys. **88**, 5673 (1988)
14. P. Durand, J. P. Malrieu, Adv. Chem. Phys. **67**, 321 (1987)
15. C. Bloch, Nucl. Phys. **6**, 329 (1958)
16. T. H. Schucan, H. A. Weidenmuller, Ann. Phys. **73**, 108 (1972)
17. D. Mukherjee, Chem. Phys. Lett. **125**, 207 (1986); Int. J. Quantum. Chem **S20**, 409 (1986)
18. D. Mukhopadhyay, D. Mukherjee, Chem. Phys. Lett. **163**, 171 (1989), Chem. Phys. Lett. **177**, 441 (1991)
19. U. Kaldor, Theor. Chim. Acta, **80**, 427 (1991) and references therein
20. W. Kutzelnigg, J. Chem. Phys. **77**, 3081 (1982); W. Kutzelnigg, S. Koch, J. Chem. Phys. **79**, 4315 (1983)

21. I. Lindgren, J. Phys. B **7**, 2441 (1974)
22. B. Kirtman, J. Chem. Phys. **75**, 798 (1981)
23. J. P. Malrieu, Ph. Durand, J. P. Daudey, J. Phys. A Math. Gen. **18**, 809 (1985); J. L. Heully, J. P. Daudey, J. Chem. Phys. **88**, 1046 (1988)
24. D. Mukhopadhyay, B. Datta, D. Mukherjee, Chem. Phys. Lett. **197**, 236 (1992)
25. B. Datta, D. Mukherjee, J. Mol. Struct. THEOCHEM **361**, 21 (1996)
26. A. Landau, E. Eliav, Y. Ishikawa, U. Kaldor, J. Chem. Phys. **113**, 9905 (2000)
27. J. Meller, J. P. Malrieu, R. Caballol, J. Chem. Phys. **104**, 4068 (1996)
28. I. Nebot-Gil, J. Sanchez-Marin, J. P. Malrieu, J. L. Heully, D. Maynau, J. Chem. Phys. **103**, 2576 (1995)
29. J. P. Malrieu, J. P. Daudey, R. Caballol, J. Chem. Phys. **101**, 8908 (1994)
30. J. Mášik, I. Hubač, in *Quantum Systems in Chemistry and Physics: Trends in Methods and Applications*, Ed. R. McWeeny et al. (KA, Dordrecht, 1997)
31. J. Mášik, I. Hubač, P. Mach, J. Chem. Phys. **108**, 6571 (1998)
32. J. Pittner, J. Chem. Phys. **118**, 10876 (2003)
33. U. S. Mahapatra, B. Datta, B. Bandyopadhyay, D. Mukherjee, Adv. Quantum Chem. **30**, 163 (1998)
34. U. S. Mahapatra, B. Datta, D. Mukherjee, Mol. Phys. **94**, 157 (1998)
35. U. S. Mahapatra, B. Datta, D. Mukherjee, J. Chem. Phys. **110**, 6171 (1999)
36. F. A. Evangelista, W. D. Allen, H. F. Schaefer III, J. Chem. Phys. **125**, 154113 (2006)
37. F. A. Evangelista, W. D. Allen, H. F. Schaefer III, J. Chem. Phys. **127**, 024102 (2007)
38. M. Hanrath, J. Chem. Phys. **123**, 084102 (2005)
39. M. Nooijen, R. J. Bartlett, J. Chem. Phys. **106**, 6441 (1997)
40. S. Das, N. Bera, S. Ghosh, D. Mukherjee, THEOCHEM **79**, 771 (2006)
41. S. Das, D. Datta, R. Maitra, D. Mukherjee, Chem. Phys. **349**, 115 (2008)
42. S. Das, S. Pathak, R. Maitra, D. Mukherjee, *under preparation* Approximants to SS-MRCC 23
43. W. Meyer, in *Methods of Electronic Structure Theory*, Ed. H. F. Schaefer III (Plenum, New York, 1977)
44. H. J. Werner, E. A. Reinsch, J. Chem. Phys. **76**, 3144 (1982)
45. H. J. Werner, P. J. Knowles, J Chem. Phys. **89**, 5803 (1988)
46. B. O. Roos, Adv. Chem. Phys. **69**, 399 (1987)
47. K. Andersson, P. A. Malmqvist, B. O. Roos, A. J. Sadlej, K. Wolinski, J. Phys. Chem. **94**, 5483 (1990), J. Chem. Phys. **96**, 1218 (1992)
48. K. Hirao, Chem. Phys. Lett. **190**, 374 (1992); Int. J. Quantum. Chem. **S26**, 517; R. B. Murphy, R. P. Messmer, J. Chem. Phys. **97**, 4170 (1992); Y. K. Choe, Y. Nakano, K. Hirao, J. Chem. Phys. **115**, 621 (2001)
49. I. Hubač, J. Pittner, P. Čársky, J. Chem. Phys. **112**, 8779 (2000)
50. G. D. Purvis, R. Sheppard, F. B. Brown, R. J. Bartlett., Int. J. Quantum Chem. **23**, 835 (1983)
51. A. Banerjee, J. Simons, Chem. Phys. **87**, 215 (1984)
52. U. Kaldor, Chem. Phys. **140**, 1 (1990)
53. U. Kaldor, Theor. Chim. Acta **80**, 427 (1991)
54. I. Garcia-Cuesta, J. Sanchez-Marin, A. Sanchez de Meras, N. B. Amor, J. Chem. Phys. **107**, 6306 (1997)
55. D. Pahari, S. Chattopadhyay, A. Deb, D. Mukherjee, Chem. Phys. Lett. **386**, 307–312 (2004)
56. S. Chattopadhyay, D. Pahari, D. Mukherjee, U. S. Mahapatra, J. Chem. Phys. **120**, 5968 (2004)
57. C. D. Sherril, L. M. Leininger, T. J. Van Huis, H. F. Shaefer III, J. Chem. Phys. **108**, 1040 (1998)
58. J. F. Stanton, W. N. Lipscomb, D. Magers, J. Bartlett, J. Chem. Phys. **90**, 1077 (1989)
59. K. Jankowski, J. Paldus, Int. J. Quantum Chem. **18**, 1243 (1980) and references therein; S. Wilson, K. Jankowski, J. Paldus, Int. J. Quantum Chem. **23**, 1781 (1983)

CHAPTER 4

DEVELOPMENT OF SAC-CI GENERAL-*R* METHOD FOR THEORETICAL FINE SPECTROSCOPY

MASAHIRO EHARA[1,3] AND HIROSHI NAKATSUJI[2,3]

[1] *Institute for Molecular Science, 38 Nishigo-Naka, Myodaiji, Okazaki 444-8585, Japan, e-mail: ehara@ims.ac.jp*

[2] *Quantum Chemistry Research Institute, Kyodai Katsura Venture Plaza 106, Kyoto 615-8245, Japan, e-mail: h.nakatsuji@qcri.or.jp*

[3] *JST, CREST, Sanboncho-5, Chiyoda-ku, Tokyo 102-0075, Japan*

Abstract: The SAC-CI general-*R* method has enabled the accurate theoretical spectroscopy of the multi-electron processes. In this article, we review the development and some recent applications of the SAC-CI general-*R* method. We first explain the theoretical background of the general-*R* method and its analytical energy gradients. We overview some recent applications of the method to the molecular spectroscopies where the multi-electronic processes play an essential role. The inner-valence ionization spectra and doubly excited states of butadiene, acrolein, and glyoxal are introduced. Theoretical studies of the excited-state geometries and adiabatic properties of the multi-electron processes are shown for CH^+, NH^+, acetylene and N_3. The high precision calculations of the core-electron processes, the g-u splitting of the main line and the vibrational spectra of the shake-up satellites of N_2 are reviewed. The relativistic effect of the *K*-shell ionization of second-row atoms is also described.

Keywords: SAC-CI, General-R SAC-CI, SAC-CI analytic gradients, Theoretical spectroscopy

4.1. INTRODUCTION

Development of the accurate state-of-the-art theoretical methods has made us possible to obtain the precise knowledge of the excited and ionized states of molecules. Theoretical information on these states is indispensable to interpret the recent high-resolution molecular spectroscopy. Theory can predict the fine details of the excitation and ionization processes and even support to design the new experiment. Thus, the interplay between theory and experiment has become standard in the modern excited-state chemistry so that the predicting ability of theory is an essential issue.

The SAC[1]/SAC-CI(symmetry-adapted cluster configuration interaction) method [1–6] was developed in the dawn of the theoretical chemistry for the molecular excited states in 1978 by Nakatsuji. Theory was formulated as the

P. Čársky et al. (eds.), Recent Progress in Coupled Cluster Methods, 79–112.
DOI 10.1007/978-90-481-2885-3_4,

general expansion for the excited, ionized, and electron-attached states in any spin multiplicity. The method was first implemented at the SD level where the excitation operators in the expansion are included up to singles and doubles. This method is useful for the ordinary single-electron processes and has been established as the reliable methodology in many successful applications [5–8] of wide varieties of the excited-state chemistry like molecular spectroscopy [8–16], biological chemistry [17–23], and surface chemistry [24–26]. The multi-reference SAC theory [27] and exponentially generated CI (EGCI) theory [28–30] were proposed and implemented for investigating the multi-electronic processes and the quasi-degenerate systems in 1985. The method was shown to be useful for the multiply excited states and bond dissociation.

In 1991, the SAC-CI general-*R* method [31] was proposed and implemented for accurately investigating the multi-electron processes. The potential usefulness and applicability of the method were demonstrated by the applications to the excited and ionized states of C_2, CO and N_2 [31, 32]. The exponential generation algorithm was shown to be useful for generating the higher-order operators. It was also shown that the general-*R* method is useful for the excited states of open-shell systems, since they are often described by the two-electron processes from the closed-shell SAC state [33].

We have applied the general-*R* method to wide varieties of the theoretical spectroscopy of the multi-electronic processes [7, 33]. In one of such applications we have investigated the inner-valence ionization spectra where the many shake-up satellites appear. Since large number of states should be calculated for the ionization spectra, the general-*R* method has an advantage: the computational dimension of the general-*R* method is much smaller than the ordinary CI approaches. We have demonstrated the accuracy and efficiency of the method by the applications to the spectra of N_2 and CO by comparison with the full CI calculations [32]. We investigated the inner-valence ionization spectra of HCl [34], ethylene [35], CO_2 [36], $XONO_2$(X=F, Cl, Br, I) [37], H_2X(X=O, S, Se) [38], H_3X(X=N, P, As) [39], cyclopentadiene [40], pyridine [41], furan, thiophene, pyrrole [42], N_2O, HN_3 [43], Cl_2O, ClOOCl, F_2O [44], CS_2, OCS [45], butadiene, acrolein, glyoxal, and methylenecyclopropene [46] and of other species. We have also investigated some doubly excited states of butadiene, acrolein, glyoxal [47], and trans stilbene [48] etc.

The general-*R* method is also useful for the inner-shell electronic processes. For the core-electronic processes, theory should describe both the orbital relaxation and electron correlations. We have investigated various kinds of core-electronic processes using the general-*R* method [49–62], like the core-electron binding energies [50], inner-shell shake-up satellite spectra [50, 51, 54–56], vibrational spectra and geometry relaxation of satellites [52, 54, 56], g-u splitting [54, 62], valence-Rydberg coupling [58, 60] and its vibration-induced suppression [63]. We also examined the relativistic effect of the *K*-shell ionization energy using the scalar relativistic SAC-CI method based on DK2 Hamiltonian [61]. These series of studies clarified the essence of the core-electron processes.

The geometry optimization of the excited states is also an important issue in the theoretical chemistry of molecular excited states. The analytical energy gradient of the SAC-CI method has been formulated and implemented at the SD level in 1997 [64, 65]. The method was extended to the SAC-CI general-*R* method [33, 66, 67] and also to the SAC-CI method for the high-spin multiplicity [68]. In order to perform stable geometry optimization, the Minimum Orbital-Deformation (MOD) method has also been developed [69, 70]. The analytical energy gradient of the general-*R* method has provided a useful tool for the accurate calculations of the spectroscopic properties such as geometry, vibrational frequency, and adiabatic excitation energies of the multi-electron processes in the excited, ionized, and electron-attached states. The method has been applied to the spectroscopy of the molecular excited states of CH^+, OH, C_2, N_2, acetylene, CNC, N_3 and other species [67].

As the theory for the molecular excited states based on the cluster expansion, coupled cluster linear response theory (CC-LRT) was also formulated by Monkhorst et al. [71, 72] and Mukherjee et al. [73]. Later, the CC-LRT theory was reformulated [74, 75] and the equation-of-motion coupled-cluster (EOM-CC) method was proposed [76–79]. The CC-LRT and EOM-CC methods are theoretically identical to the SAC-CI method. These three methodologies have been utilized for investigating the molecular excited states and established as the standard. This shows the SAC-CI method developed in 1978 has already achieved the essence for the theory of the molecular excited states. The general-*R* method which is the extension to include the higher-order operators is also related to the higher approximations of the EOM-CCSDT [80]/SDTQ [81, 82] or response theory CC3 [83].

For investigating the quasi-degenerate system and bond dissociation region, varieties of multi-reference cluster expansion theories have been developed [27, 84–93] from the work of Jeziorski and Monkhorst [84]. Theoretical studies of the excited states are possible with these methods, for example, MR-SAC by Nakatsuji [27], state-specific multi-reference couple cluster (SS-MRCC) by Mukherjee and coworkers [87, 88], Reduced MRCC by Li and Paldus [89, 90], and MR Brillouin-Wigner CC by Hubač, Pittner, Čársky and co-workers [91–93].

Recently, we have implemented the active-space method in the framework of the SAC-CI method [94, 95]. The method has originally developed by Piecuch, Adamowicz and their coworkers [96–103]. In this method, the higher operators are restricted to only those including the active-space MOs. The method was shown to be accurate and efficient for the multiply excited states even in the bond dissociation region. We have demonstrated that the active-space method describes the potential energy curves of the multi-electron processes accurately for OH and CH^+ [94]. We also have investigated the excited-state geometries and adiabatic properties of CNC, C_2N, NCO, and N_3 with the active-space method [95].

In this article, we briefly introduce the SAC/SAC-CI method [2–4] and in particular, we focus on the development of the SAC-CI general-*R* method [31, 32] and its analytical energy gradients [66, 67] in Section 4.2. In Section 4.3, we review some recent applications of the general-*R* method to the theoretical fine spectroscopy.

First, we explain the inner-valence ionization spectra of 4π-electronic molecules, butadiene, acrolein, and glyoxal, examining the low-lying shake-up satellites [46]. We also show the doubly excited states of butadiene and glyoxal [47]. Then, we introduce the geometry optimization of the multi-electronic processes for the diatomic molecules, CH^+ and NH^+, and also for the polyatomic molecules, acetylene and N_3 [67]. Finally, we show some of our recent progresses in the study of the inner-shell electronic processes; g-u splitting [54], vibrational spectra of the inner-shell satellites of N_2 [54], and relativistic effect for K-shell ionization [62]. Section 4.4 summarizes the development and applications of the SAC-CI general-R method.

4.2. THEORY

4.2.1. SAC/SAC-CI Theory

First, we explain the SAC/SAC-CI theory. The SAC wave function describes the ground state and is defined as,

$$\Psi_g^{SAC} = \exp\left(\sum_I C_I S_I^\dagger\right)|0\rangle \tag{4-1}$$

where $|0\rangle$ is the Hartree-Fock and $S_I^\dagger$ is the spin-symmetry and space-symmetry adapted excitation operator. The SAC expansion can also be defined for the higher-symmetries [1].

In the SAC method, the unknown variables C_I are associated to the excitation operator $S_I^\dagger$ so that for solving C_I we require that the Schrödinger equation is satisfied within the configuration space of $\left\{|0\rangle, S_I^\dagger|0\rangle\right\}$ as,

$$\langle 0|H - E_g\left|\Psi_g^{SAC}\right\rangle = 0 \tag{4-2}$$

$$\langle 0|S_I(H - E_g)\left|\Psi_g^{SAC}\right\rangle = 0. \tag{4-3}$$

This SAC equation is called as non-variational method.

The variational method is also possible in the SAC method by applying the variational principle to the SAC wave function and we obtain,

$$\left\langle\Psi_g^{SAC}|H - E_g|\Psi_g^{SAC}\right\rangle = 0 \tag{4-4}$$

$$\left\langle\Psi_g^{SAC}|S_I(H - E_g)|\Psi_g^{SAC}\right\rangle = 0. \tag{4-5}$$

The variational solution is more difficult than the non-variational one, since it includes the integrals between product terms and the integrals do not terminate even

if $S_I^\dagger$ is approximated as singles and doubles. Variational CCD solution was investigated by Voorhis et al. [104] and shown to behave properly even up to dissociation limit.

The SAC theory defines not only the SAC wave function for the ground state, but also the excited functions which span the basis for the excited states [2–4]. Using the correlated ground-state SAC wave function, we define the excited functions $\{\Phi_K\}$ as

$$\Phi_K = PS_K^\dagger \left|\Psi_g^{\mathrm{SAC}}\right\rangle \tag{4-6}$$

where P is an projector which projects out the ground state,

$$P = 1 - \left|\Psi_g^{SAC}\right\rangle\left\langle\Psi_g^{\mathrm{SAC}}\right|. \tag{4-7}$$

These functions $\{\Phi_K\}$ satisfy the orthogonality and Hamiltonian orthogonality relations to the ground-state SAC wave function as,

$$\left\langle\Phi_K \mid \Psi_g^{\mathrm{SAC}}\right\rangle = 0 \tag{4-8}$$

$$\left\langle\Phi_K\right|H\left|\Psi_g^{\mathrm{SAC}}\right\rangle = 0 \tag{4-9}$$

which means that the functions $\{\Phi_K\}$ constitute a basis for excited state. Therefore, we describe the excited state by a linear combination of these functions as,

$$\Psi_e^{\text{SAC-CI}} = \sum_K d_K \Phi_K \tag{4-10}$$

which is the SAC-CI expansion.

Applying the variational principle for solving the SAC-CI wave function, we obtain,

$$\left\langle\Phi_K\right| H\left|\Psi_e^{\text{SAC-CI}}\right\rangle = 0. \tag{4-11}$$

The SAC-CI wave function automatically satisfies the orthogonality and Hamiltonian orthogonality with the ground state and with different excited states.

The SAC-CI wave function can also be defined for the excited states having different symmetries and also for the ionized and electron-attached states. We generalize Eq. (4-6) as

$$\Phi_K = PR_K^\dagger \left|\Psi_g^{\mathrm{SAC}}\right\rangle \tag{4-12}$$

where $\left\{R_K^\dagger\right\}$ represents a set of the excitation, ionization and electron-attachment operators.

The non-variational SAC-CI solution is obtained by projecting the Schrödinger equation to the $\left\{R_K^\dagger |0\rangle\right\}$ configuration spaces,

$$\langle 0| R_K (H - E_e) \left|\Psi_e^{\text{SAC-CI}}\right\rangle = 0. \tag{4-13}$$

In the case of the totally symmetric singlet excited states, the non-variational SAC-CI formulation including the SAC solution is written as,

$$\begin{pmatrix} \langle 0| (H - E_e) e^S |0\rangle & \langle 0| (H - E_e) R_K^\dagger e^S |0\rangle \\ \langle 0| R_K (H - E_e) e^S |0\rangle & \langle 0| R_K (H - E_e) R_K^\dagger e^S |0\rangle \end{pmatrix} = 0. \tag{4-14}$$

The SAC-CI theory utilizes the transferability of correlations between ground and excited states. This can be understood by writing the SAC-CI wave function as,

$$\Psi_e^{\text{SAC-CI}} = \Re \Psi_g^{\text{SAC}} \tag{4-15}$$

where the excitation operator $\Re$ is defined as,

$$\Re = \sum_K d_K R_K^\dagger. \tag{4-16}$$

For totally symmetric states, we may include identity operator within $\left\{R_K^\dagger\right\}$ to ensure the orthogonality of the excited states to the ground state. The electron correlation of the ground state is well described by the SAC wave function and the excitation operator describes a modification of the electron correlation by excitation: this is much faster than calculating all the correlations of the excited states from the beginning.

For evaluating the one-electron properties of the ground and excited states and the transition properties among them, the density matrix and transition density matrix between the SAC-CI states are calculated. The method for calculating these matrices has already been formulated [105]. Another useful method is also possible as follows.

Let Q be a spin-independent one-electron operator,

$$Q = \sum_\nu q(\nu). \tag{4-17}$$

Neglecting some less important product terms, density matrix and transition density matrix between the SAC-CI states are calculated by the similar expression to the SAC-CI energy,

$$\langle Q\rangle^{pq} = \langle \psi^{L(p)}_{\text{SAC-CI}} | Q | \psi^{R(q)}_{\text{SAC-CI}} \rangle$$
$$= \sum_M \sum_N d^{L(p)}_M d^{R(q)}_N \left(Q_{MN} + \sum_I C_I Q_{M,NI} \right) \tag{4-18}$$

where Q_{MN} and $Q_{M,NI}$ are the density matrices defined by $\langle 0| R_M Q R^\dagger_N |0\rangle$ and $\langle 0| R_M Q R^\dagger_N S^\dagger_I |0\rangle$, respectively, $d^{L(p)}_M$ and $d^{R(q)}_N$ are the SAC-CI left- and right-vectors of p-th and q-th solutions, and C_I is the SAC coefficients. The density matrix and transition density matrix are given by $p = q$ and $p \neq q$, respectively. Note that this expression avoids the calculations between the product terms like $\langle 0| S_I R_M Q R^\dagger_N S^\dagger_J |0\rangle$. Then, the dipole strength is calculated by

$$\langle D\rangle^{pq} = \langle Q\rangle^{pq} \langle Q\rangle^{qp} . \tag{4-19}$$

The formula of the approximate SAC-CI-V is given by replacing $d^{L(p)}_M = d^{(p)}_M$ and $d^{R(q)}_N = d^{(q)}_N$ in Eq. (4-18).

4.2.2. SAC-CI General-*R* Method

There are two standards in the SAC-CI method with respect to the *R* operators. The SAC-CI SD-*R* method is to include single and double excitation operators within the *R* operators, for example, the SD-*R* wave function for the singlet excited states is given by,

$$\Psi^{\text{SAC-CI}}_{\text{SD-R}} = \left(\sum_{ia} d^a_i R^a_i + \sum_{ijab} d^{ab}_{ij} R^{ab}_{ij} \right) \exp\left(\sum_I C_I S_I \right) |0\rangle . \tag{4-20}$$

This method is accurate and efficient for the one-electron processes of the excitations and ionizations. The method has been established through the successful applications to molecular spectroscopy, biological chemistry, and surface chemistry.

The other choice is to include not only single and double excitation operators, but also triple- and quadruple- and higher-excitation operators within the *R* operators. This method is called as SAC-CI general-*R* method and is necessary for investigating the multi-electron processes in the excitation and ionization phenomena. The general-*R* wave function is written as,

$$\Psi^{\text{general-R}} = \left(\sum_{ia} d^a_i R^a_i + \sum_{ijab} d^{ab}_{ij} R^{ab}_{ij} + \sum_{ijkabc} d^{abc}_{ijk} R^{abc}_{ijk} + \sum_{ijklabcd} d^{abcd}_{ijkl} R^{abcd}_{ijkl} + \cdots \right)$$
$$\times \exp\left(\sum_I C_I S_I \right) |0\rangle \tag{4-21}$$

For generating the triple-, quadruple- and higher-excitation operators in the general-*R* method, the exponential generation algorithm [28–30] is useful for high

performance. This generation algorithm combined with the perturbation selection is accurate and efficient. The algorithm to generate all the triples and quadruple operators followed by the perturbation selection is also possible for small systems. In the present program system, both of these algorithms are possible and this general-*R* method can be applied to various electronic states, singlet and triplet excited states, double ionized and electron-attached states, and high-spin states from quartet to septet states. The possible *R* operators in the present program system are summarized in Table 4-1 [33, 67].

The SAC-CI general-*R* method has the following feature.

1. The method is applicable to the various electronic states of the multi-electron processes of singlet to septet spin multiplicity as shown in Table 4-1.
2. It is applicable to solve the large number of the excited and ionized states simultaneously up to higher energy region.
3. It is useful to calculate the excited states of open-shell systems since their excited states are often described by the two-electron processes from the closed-shell SAC state.
4. It is applicable to investigate the excited-state chemical reaction and relaxation processes since the multi-electron processes may appear in those processes.

On the other hand, the general-*R* method is based on the SAC method and therefore, it may fail in the bond dissociation region. In such cases, the multi-reference SAC/SAC-CI and EGCI methods are useful.

The general-*R* method can also be applied to the inner-shell electronic processes [49, 50]. In this case, the higher-order *R* operators such as triples and quadruples are necessary for describing both orbital relaxation and electron correlations of the core-electronic processes. Although the SD-*R* method is accurate for the one-electron processes of the valence excitations and ionizations, higher-order operators are indispensable for the core-electronic processes. For example, for calculating the core-electron binding energy, *R* operators up to triples are necessary and for the shake-up satellite states, the SDTQ-*R* calculations are required [50]. One-rank higher operator is necessary for describing large orbital relaxation in the calculation of the core-electronic processes. Thus, this method is simple and accurate, but, its computational cost is relatively high since it usually includes higher operators for the accurate calculations. Nonetheless, this method is useful since it can be applied to the general core-electronic processes like the g-u splitting in the molecules with equivalent atoms.

The other approach for studying the core-electronic processes is the open-shell reference (OR) SAC-CI method [106], in which the core-ionized ROHF is used for the reference;

$$\Psi^{\text{OR-SAC-CI}} = \left(\sum_{ia} d_i^a R_i^a + \sum_{ijab} d_{ij}^{ab} R_{ij}^{ab}\right) \Psi^{OR-SAC} \tag{4-22}$$

Table 4-1. R operator for each spin multiplicity in the present SAC-CI program system. Subscripts i, j, k, l, m, n and a, b, c, d, e, f denote occupied and unoccupied orbitals, respectively, in the reference configuration $|0\rangle$

	Single	Double	Triple	Quadruple	Quintuple	Sextuple
Singlet	${}^1R_i^a = \left(a^+_{a\alpha}a_{i\alpha} + a^+_{a\beta}a_{i\beta}\right)\Big/\sqrt{2}$	${}^1R_{ij}^{ab}$	${}^1R_{ijk}^{abc}$	${}^1R_{ijkl}^{abcd}$	$({}^1R_{ijklm}^{abcde})^{\mathrm{a}}$	$({}^1R_{ijklmn}^{abcdef})^{\mathrm{a}}$
Doublet (Ionized)	${}^2R_i = a_{i\beta}$	${}^2R_{ij}^{b}$	${}^2R_{ijk}^{ab}$	${}^2R_{ijkl}^{abc}$	$({}^2R_{ijklm}^{abcd})^{\mathrm{a}}$	$({}^2R_{ijklmn}^{abcde})^{\mathrm{a}}$
Doublet (Anionized)	${}^2R^a = a^+_{a\alpha}$	${}^2R_{j}^{ab}$	${}^2R_{ij}^{abc}$	${}^2R_{ijk}^{abcd}$	$({}^2R_{ijkl}^{abcde})^{\mathrm{a}}$	$({}^2R_{ijklm}^{abcdef})^{\mathrm{a}}$
Triplet	${}^3R_i^a = a^+_{a\alpha}a_{i\beta}$	${}^3R_{ij}^{ab}$	${}^3R_{ijk}^{abc}$	${}^3R_{ijkl}^{abcd}$	$({}^3R_{ijklm}^{abcde})^{\mathrm{a}}$	$({}^3R_{ijklmn}^{abcdef})^{\mathrm{a}}$
Quartet (Ionized)		${}^4R_{ij}^{a} = a^{\dagger}_{a\alpha}a_{i\beta}a_{j\beta}$	${}^4R_{ijk}^{ab}$	${}^4R_{ijkl}^{abc}$	$({}^4R_{ijklm}^{abcd})^{\mathrm{a}}$	$({}^4R_{ijklmn}^{abcde})^{\mathrm{a}}$
Quintet		${}^5R_{ij}^{ab} = a^{\dagger}_{a\alpha}a^{\dagger}_{b\alpha}a_{i\beta}a_{j\beta}$	${}^5R_{ijk}^{abc}$	${}^5R_{ijkl}^{abcd}$	$({}^5R_{ijklm}^{abcde})^{\mathrm{a}}$	$({}^5R_{ijklmn}^{abcdef})^{\mathrm{a}}$
Sextet (Ionized)			${}^6R_{ijk}^{ab} = a^{\dagger}_{a\alpha}a^{\dagger}_{b\alpha}a_{i\beta}a_{j\beta}a_{k\beta}$	${}^6R_{ijkl}^{abc}$	$({}^6R_{ijklm}^{abcd})^{\mathrm{a}}$	$({}^6R_{ijklmn}^{abcde})^{\mathrm{a}}$
Septet			${}^7R_{ijk}^{abc} = a^{\dagger}_{a\alpha}a^{\dagger}_{b\alpha}a^{\dagger}_{c\alpha}a_{i\beta}a_{j\beta}a_{k\beta}$	${}^7R_{ijkl}^{abcd}$	$({}^7R_{ijklm}^{abcde})^{\mathrm{a}}$	$({}^7R_{ijklmn}^{abcdef})^{\mathrm{a}}$

[a] The wave functions adopting operators in the parentheses are not available for the present SAC-CI energy gradient program system.

$$\Psi^{\text{OR-SAC}} = \exp\left(\sum_I C_I S_I\right) \exp\left(\sum_J C_J' S_J'\right) O_K |0\rangle \tag{4-23}$$

where $O_K |0\rangle$ represents the core-hole ROHF. The S and S' operators are the excitation and de-excitation operators, respectively. Since the OR-SAC-CI method starts from the core-hole state, the SD-R method is sufficient for describing the core-hole state. However, it introduces the complex expansion due to the de-excitation operators. For applying the g-u splitting of the molecules with equivalent atoms, the accurate calculations including higher-order product terms are necessary since it starts from the different reference functions for g- and u- states.

4.2.3. Analytical Energy Gradients of SAC/SAC-CI

The analytical energy gradients for the SAC/SAC-CI method was formulated by Nakajima and Nakatsuji in 1997 [64, 65] and implemented in the SAC/SAC-CI program system. Later, the method was implemented in the Gaussian03 suite of programs [107]. We briefly review the analytical energy gradients of the SAC/SAC-CI method in particular its extension to the general-R method [66, 67].

4.2.3.1. Analytical Energy Gradients of SAC

The SAC Eqs. (4-2) and (4-3) can be rewritten as

$$\Delta E_{\text{SAC}} = \sum_I C_I H_{0I}, \tag{4-24}$$

and

$$H_{K0} + \sum_I C_I \left(H_{KI} - \Delta E_{\text{SAC}} S_{KI}\right) + \frac{1}{2} \sum_I \sum_J C_I C_J H_{K,IJ} = 0 \tag{4-25}$$

where $\Delta E_{\text{SAC}} = E_{\text{SAC}} - E_{HF}$ and S_{IJ} represents the overlap matrix, $\langle 0| S_I S_j^+ |0\rangle$. H_{0I}, H_{IJ} and $H_{I,JK}$ are the Hamiltonian matrices defined by $\langle 0| HS_I^+ |0\rangle$, $\langle 0| S_I H S_J^+ |0\rangle$ and $\langle 0| S_I H S_J^+ S_K^+ |0\rangle$, respectively.

The first derivative of the SAC correlation energy with respect to the external parameter a is given as [64, 65],

$$\frac{\partial \Delta E_{\text{SAC}}}{\partial a} = \sum_I \left[\left\{1 + \left(\sum_K \sum_J Z_K^{\text{SAC}} C_J S_{KJ}\right)\right\} C_I - Z_I^{SAC}\right] \frac{\partial H_{0I}}{\partial a}$$

$$- \sum_K \sum_I Z_K^{\text{SAC}} C_I \frac{\partial H_{KI}}{\partial a} - \frac{1}{2} \sum_K \sum_I \sum_J Z_K^{\text{SAC}} C_I C_J \frac{\partial H_{K,IJ}}{\partial a} \tag{4-26}$$

where Z_K^{SAC} is a component of the SAC Z-vector and is calculated from the following simultaneous linear equation [65],

$$\sum_K \left\{ H_{KI} - \left(\sum_J C_J S_{KJ} \right) H_{0I} - \Delta E_{SAC} S_{KI} + \sum_J C_J H_{K,IJ} \right\} Z_K^{SAC} = H_{0I} \tag{4-27}$$

Explicit calculation of the first derivatives of the SAC coefficients $\partial C_I / \partial a$ is circumvented by using the interchange technique [108] or the so-called Z-vector method [109].

In Eq. (4-26), the first derivatives of the Hamiltonian matrix element are expressed in terms of one- and two-electron coupling constants as

$$\frac{\partial H_{XY}}{\partial a} = \sum_{ij}^{MO} \gamma_{ij}^{XY} \frac{\partial f_{ij}}{\partial a} + \sum_{ijkl}^{MO} \Gamma_{ijkl}^{XY} \frac{\partial \, (ij \,|kl\,)}{\partial a} \tag{4-28}$$

where the i, j, k, l refer to the orbitals, and f_{ij} and $(ij\,|kl\,)$ denote Fock matrix element and two-electron MO integral, respectively. The matrix elements γ_{ij}^{XY} and Γ_{ijkl}^{XY} are the one- and two-electron coupling constants between configuration functions Φ_X and Φ_Y and are independent of the parameter a, where X and Y correspond to I, J for the SAC wave function and to M, N for the SAC-CI wave function.

Using Eq. (4-28), we can rewrite Eq. (4-26) in an MO representation in terms of effective density matrices (EDMs) for the SAC wave function as,

$$\frac{\partial \Delta E_{\mathrm{SAC}}}{\partial a} = \sum_{ij}^{MO} \gamma_{ij}^{\mathrm{SAC}} \frac{\partial f_{ij}}{\partial a} + \sum_{ijkl}^{MO} \Gamma_{ijkl}^{SAC} \frac{\partial \, (ij|kl)}{\partial a}. \tag{4-29}$$

The matrix elements $\gamma_{ij}^{\mathrm{SAC}}$ and $\Gamma_{ijkl}^{\mathrm{SAC}}$ of the EDMs are given by

$$\begin{aligned} \gamma_{ij}^{\mathrm{SAC}} \equiv & \sum_I \left[\left\{ 1 + \left(\sum_K \sum_J Z_K^{\mathrm{SAC}} C_J S_{KJ} \right) \right\} C_I - Z_I^{\mathrm{SAC}} \right] \gamma_{ij}^{0I} \\ & - \sum_K \sum_I Z_K^{\mathrm{SAC}} C_I \gamma_{ij}^{KI} - \frac{1}{2} \sum_K \sum_I \sum_J Z_K^{\mathrm{SAC}} C_I C_J \gamma_{ij}^{K,IJ} \end{aligned} \tag{4-30}$$

and

$$\begin{aligned} \Gamma_{ijkl}^{\mathrm{SAC}} \equiv & \sum_I \left[\left\{ 1 + \left(\sum_K \sum_J Z_K^{\mathrm{SAC}} C_J S_{KJ} \right) \right\} C_I - Z_I^{\mathrm{SAC}} \right] \Gamma_{ijkl}^{0I} \\ & - \sum_K \sum_I Z_K^{\mathrm{SAC}} C_I \Gamma_{ijkl}^{KI} - \frac{1}{2} \sum_K \sum_I \sum_J Z_K^{\mathrm{SAC}} C_I C_J \Gamma_{ijkl}^{K,IJ}, \end{aligned} \tag{4-31}$$

respectively [64, 65]. Thus, the first derivative of the SAC energy is evaluated from Eqs. (4-27), (4-29), (4-30), and (4-31).

4.2.3.2. Analytical Energy Gradients of SAC-CI

Next, we summarize the analytical energy gradient of the SAC-CI method, which were first formulated and implemented at the SD-*R* method [64, 65] and then extended to the general-*R* method [66, 67].

The SAC-CI wave function is generated from the correlated SAC ground state as,

$$\Psi^p_{\text{SAC-CI}} = \sum_K d^p_K R^\dagger_K \Psi_{\text{SAC}} \tag{4-32}$$

where $\{R^+_K\}$ represents a set of excitation, ionization and/or electron-attachment operators, and $\{d^p_K\}$ is its coefficients for the p-th excited state.

By using the non-variational SAC-CI equation (4-13) and neglecting some less important unlinked integrals, the SAC-CI energy relative to the HF energy, $\Delta E^p_{\text{SAC-CI}}$, is derived as

$$\Delta E^p_{SAC-CI} = \sum_M \sum_N d^{L(p)}_M d^{R(p)}_N \left(H_{MN} + \sum_I C_I H_{M,NI} \right) \tag{4-33}$$

where $\Delta E^p_{\text{SAC-CI}} = E^p_{\text{SAC-CI}} - E_{HF}$, H_{MN} and $H_{M,NI}$ are the Hamiltonian matrices defined by $\langle 0|R_M H R^+_N|0\rangle$ and $\langle 0|R_M H R^+_N S^+_I|0\rangle$, respectively, d^L_M and d^R_N are the SAC-CI left- and right-vectors.

The first derivative of the SAC-CI correlation energy is given in the Hamiltonian matrix form as [65],

$$\begin{aligned}\frac{\partial \Delta E_{\text{SAC-CI}}}{\partial a} &= \sum_I \left\{ \sum_K Z^{\text{SAC-CI}}_K \left(\sum_J C_J S_{KJ} \right) C_I - Z^{\text{SAC-CI}}_I \right\} \frac{\partial H_{0I}}{\partial a} \\ &+ \sum_M \sum_N d^L_M d^R_N \frac{\partial H_{MN}}{\partial a} - \sum_K \sum_I Z^{\text{SAC-CI}}_K C_I \frac{\partial H_{KI}}{\partial a} \\ &+ \sum_M \sum_N \sum_I d^L_M d^R_N C_I \frac{\partial H_{M,NI}}{\partial a} - \frac{1}{2} \sum_K \sum_I \sum_J Z^{\text{SAC-CI}}_K C_I C_J \frac{\partial H_{K,IJ}}{\partial a}\end{aligned} \tag{4-34}$$

where $Z^{\text{SAC-CI}}_K$ is a component of the SAC-CI Z-vector and is calculated from the SAC-CI Z-vector equation [65],

$$\sum_K \left\{ H_{KI} - \left(\sum_J C_J S_{KJ} \right) H_{0I} - \Delta E_{\mathrm{SAC}} S_{KI} + \sum_J C_J H_{K,IJ} \right\} Z_K^{\mathrm{SAC\text{-}CI}} = \sum_M \sum_N d_M^L d_N^R H_{M,NI}. \tag{4-35}$$

By using Eq. (4-28), Eq. (4-34) is rewritten in an MO representation in term of EDMs for the SAC-CI wave function,

$$\frac{\partial \Delta E_{\mathrm{SAC\text{-}CI}}}{\partial a} = \sum_{ij}^{MO} \gamma_{ij}^{\mathrm{SAC\text{-}CI}} \frac{\partial f_{ij}}{\partial a} + \sum_{ijkl}^{MO} \Gamma_{ijkl}^{\mathrm{SAC\text{-}CI}} \frac{\partial \, (ij \,|kl)}{\partial a}. \tag{4-36}$$

The matrix elements of the EDMs $\gamma_{ij}^{\mathrm{SAC\text{-}CI}}$ and $\Gamma_{ijkl}^{\mathrm{SAC\text{-}CI}}$ are represented as

$$\begin{aligned} \gamma_{ij}^{\mathrm{SAC\text{-}CI}} \equiv & \sum_I \left\{ \sum_K Z_K^{\mathrm{SAC\text{-}CI}} \left(\sum_J C_J S_{KJ} \right) C_I - Z_I^{\mathrm{SAC\text{-}CI}} \right\} \gamma_{ij}^{0I} \\ & + \sum_M \sum_N d_M^L d_N^R \gamma_{ij}^{MN} - \sum_K \sum_I Z_K^{\mathrm{SAC\text{-}CI}} C_I \gamma_{ij}^{KI} \\ & + \sum_M \sum_N \sum_I d_M^L d_N^R C_I \gamma_{ij}^{M,NI} - \frac{1}{2} \sum_K \sum_I \sum_J Z_K^{\mathrm{SAC\text{-}CI}} C_I C_J \gamma_{ij}^{K,IJ} \end{aligned} \tag{4-37}$$

and

$$\begin{aligned} \Gamma_{ijkl}^{\mathrm{SAC\text{-}CI}} \equiv & \sum_I \left\{ \sum_K Z_K^{\mathrm{SAC\text{-}CI}} \left(\sum_J C_J S_{KJ} \right) C_I - Z_I^{\mathrm{SAC\text{-}CI}} \right\} \Gamma_{ijkl}^{0I} \\ & + \sum_M \sum_N d_M^L d_N^R \Gamma_{ijkl}^{MN} - \sum_K \sum_I Z_K^{\mathrm{SAC\text{-}CI}} C_I \Gamma_{ijkl}^{KI} \\ & + \sum_M \sum_N \sum_I d_M^L d_N^R C_I \Gamma_{ijkl}^{M,NI} - \frac{1}{2} \sum_K \sum_I \sum_J Z_K^{\mathrm{SAC\text{-}CI}} C_I C_J \Gamma_{ijkl}^{K,IJ} \end{aligned} \tag{4-38}$$

respectively [64, 65].

In the SAC-CI general-*R* method, the analytical energy gradient is calculated by Eq. (4-36) using the SAC-CI Z-vector equation (4-35) and the EDMs of Eqs. (4-37) and (4-38) for the general-*R* wave function. In the implementation, the unlinked terms that are redundant with the linked terms are neglected in Eqs. (4-35), (4-37) and (4-38). The SAC-CI general-*R* energy gradient code was implemented in the GAUSSIAN03 suite of programs [107] and the algorithm is summarized as follows [66, 67]:

1. The SCF calculation is performed and the derivatives of the one- and two-electron AO integrals are calculated.

2. The SAC and SAC-CI general-*R* calculations are carried out.
3. The CPSAC Z-vector equations (4-27) or (4-35) are solved using Pulay's direct inversion in the iterative subspace (DIIS) method [110]. In the SAC-CI general-*R* calculations, the right term of Eq. (4-28) are evaluated not only for the single and double *R* operators but also for the triple, quadruple, and higher *R* operators.
4. The MO EDMs for the SAC-CI general-*R* wave function given by Eqs. (4-37) and (4-38) are constructed and stored.
5. The first derivatives of energy are evaluated by summing up the products between the AO integral derivatives and the corresponding coefficients which are obtained via back-transformation of the EDMs [65] and solving linear equations for CPHF, as usual [111–116]. In addition, the CPMOD equations are solved in GAUSSIAN03 if the MOD method is used for calculation [69, 70]. In evaluation of the forces on *N* atoms, explicit determination of the 3*N* sets of the first derivatives of MO coefficients are circumvented by the interchange technique [108, 109], as well as the SAC coefficient derivatives.

4.3. APPLICATIONS OF SAC-CI GENERAL-*R* METHOD

We have applied the SAC-CI general-*R* method to wide varieties of the theoretical spectroscopy of the multi-electronic processes such as inner-valence ionization spectra, doubly excited states of π-conjugated molecules, excited-state geometry and adiabatic properties of the multiply excited states, and the core-electron processes, etc.

4.3.1. Inner-Valence Ionization Spectra and Doubly Excited States

We have investigated the inner-valence ionization spectra where many shake-up satellite states appear as mentioned in Section 4.1. In the present section, we show the general-*R* results for the valence ionization spectra of butadiene, acrolein, glyoxal, methylenecyclopropene, and methylenecyclopropane [46]. We also briefly note the doubly excited states of butadiene, acrolein, and glyoxal [47].

4.3.1.1. Butadiene, Acrolein, and Glyoxal

Satellite states reflect the electron correlations of molecules [117, 118]. Low-lying satellites of π-conjugated molecules are attributed to the two-electron processes accompanied by the $\pi\pi^*$ transition. *Trans*-butadiene constitutes a fundamental linear π-conjugation unit and its valence ionization spectrum has been extensively investigated [46, 119]. Another possibility for the low-lying satellites can be found in systems with lone pair electrons in π-conjugation. The $n\pi^*$ transition is usually as low as $\pi\pi^*$ transition and therefore, low-lying $n^{-1}\pi^{-1}\pi^*$ and $n^{-2}\pi^*$ shake-up states may appear. Acrolein and glyoxal are isoelectronic system to butadiene and have

oxygen atoms in π-conjugation and therefore, their ionization spectra are candidates for the low-lying satellites.

First, we explain the valence ionization spectrum of butadiene. The valence orbital sequence of trans butadiene is,

$$(\text{core})^8(3b_u)^2(3a_g)^2(4a_g)^2(4b_u)^2(5b_u)^2(5a_g)^2(6a_g)^2(6b_u)^2(7a_g)^2(1a_u)^2(1b_g)^2,$$

where $1a_u$ and $1b_g$ MOs are π orbitals and $4b_u$ to $7a_g$ MOs describe the C-H and CC σ-bonding. The $3b_u$, $3a_g$, and $4a_g$ MOs correspond to 2s orbitals and the ionizations from these orbitals appear in the inner-valence region. In Figure 4-1, the SAC-CI general-*R* spectrum was compared with the He I photoelectron spectra (PES) [120] and X-ray photoelectron spectra (XPS) [121]. Theory reproduced the experimental spectra satisfactorily and gave the detailed assignments.

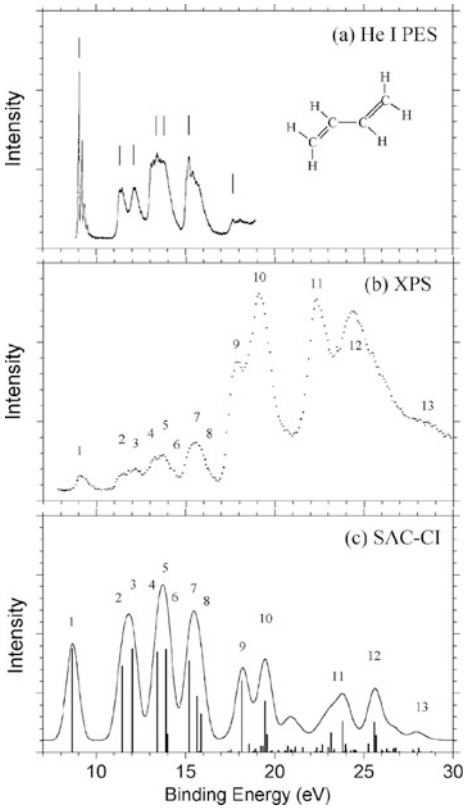

Figure 4-1. Valence ionization spectra of 1, 3-*trans* butadiene by He I PES [120], (**b**) XPS [121] and (**c**) SAC-CI general-*R* method [46]

The thirteen peaks were measured by XPS. In the energy region up to ∼14 eV, the peaks are in the order of Koopmans' states and the lowest shake-up state, $\pi^{-2}\pi^*$ ($1b_g^{-2}1a_u$), was calculated at 13.98 eV with the pole strength of 0.16. The intensity is distributed by the interaction with the ionization from next-HOMO. In XPS [121], peak 6 was observed as the shoulder of the higher energy side of peak 5; this shake-up state is one candidate of this shoulder.

Peaks 7 and 8 were observed as the continuous asymmetric band. These peaks correspond to the ionizations from $5a_g$ and $5b_u$ MOs. In the SAC-CI results, the $5b_u$ state splits into two peaks by the interaction with the $\sigma^{-1}\pi^{-1}\pi^*$ shake-up state; this splitting explains the asymmetric shape of the observed band. Peaks 9 and 10 are the ionizations from the $4b_u$ and $4a_g$ MOs. Many shake-up states appear from this energy region. In particular, the intensity due to $4a_g$ component distributes to many shake-up states through final-ionic-state interaction. In the higher-energy region of these two peaks, the shake-up states whose intensities are due to $4a_g$ MOs continue up to ∼ 25 eV. These shake-up states are dominantly characterized as $\sigma^{-1}\pi^{-1}\pi^*$ states. The orbital picture is not valid for peaks 11 and 12 and many shake-up states exist that are characterized as the ionizations from $3a_g$ or $3b_u$ MOs accompanied by the $\pi\pi^*$ transition.

Next, we show the ionization spectra of *s-trans* acrolein and *s-trans* glyoxal. These molecules have the lone pairs of O atom, and therefore, their ionization spectra may have the low-lying satellites accompanied by the $n\pi^*$ transition. Figures 4-2 and 4-3 compare the SAC-CI theoretical spectra with the experimental photoelectron spectra [120, 122] for acrolein and glyoxal, respectively. Theory reproduced the experimental spectra satisfactorily and gave the quantitative assignments. In this article, we explain only the low-energy region of these molecules.

The Hartree-Fock orbital sequence of *s-trans* acrolein is,

$$(\text{core})^8(5a')^2(6a')^2(7a')^2(8a')^2(9a')^2(10a')^2(11a')^2(12a')^2(1a'')^2(13a')^2(2a'')^2,$$

where two a″ orbitals are π MOs and 13a′ MO is due to the lone pairs of O atom. The 5a′ to 7a′ MOs correspond to 2s orbitals of C and other MOs represent CH, CC, and CO σ-bonding. In the valence ionization spectrum of acrolein, the low-lying peaks up to ∼15 eV can be regarded as main peaks. The first two peaks observed at 10.10 and 10.92 eV [120] are 13a′ and 2a″ states, respectively. Koopmans' ordering reverses for these peaks. In the ionized states, the effect of electron correlation originating from the *n* orbital is larger than from the π orbital. This feature was also found in other π-conjugated systems including lone pair electrons like *p*-benzoquinone [123]. For the next overlapping peaks 3 and 4 at 13.7 eV, the 1a″ and 12a′ states were assigned, respectively. At the foot of 12a′ state, the lowest shake-up state was calculated at 13.74 eV, however, the intensity was very small as 0.02 [46]. This state is characterized as $n^{-1}\pi^{-1}\pi^*$ ($13a'^{-1}3a''2a''^{-1}$). The neutral acrolein has the $n\pi^*$

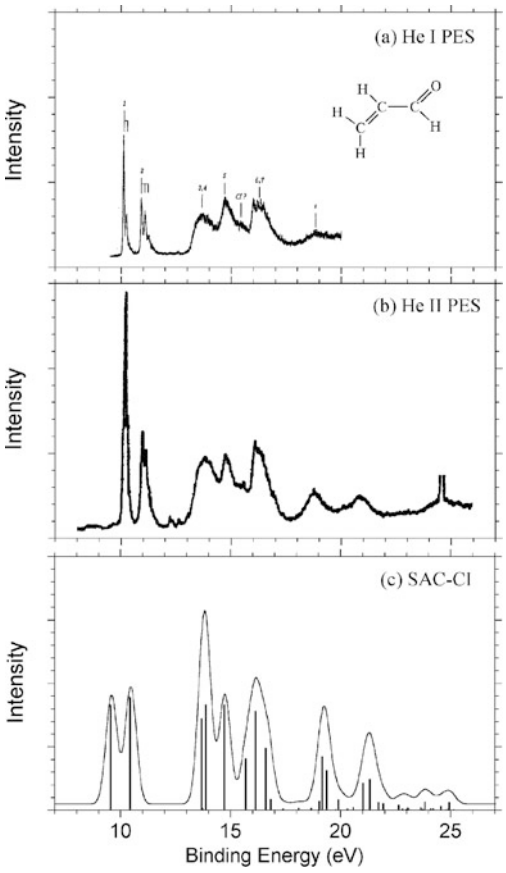

Figure 4-2. Valence ionization spectra of *s-trans* acrolein by He I PES [120], (**b**) He II PES [122] and (**c**) SAC-CI general-*R* method [46]

excited state at 3.29 eV. The $11a'$ state was obtained at 14.71 eV in accordance with peak 5 observed at 14.60 eV [120].

The *s-trans* glyoxal has two O atoms in π conjugation and its Hartree-Fock orbital sequence is written as,

$$(\text{core})^8(3a_g)^2(3b_u)^2(4a_g)^2(4b_u)^2(5a_g)^2(5b_u)^2(6a_g)^2(1a_u)^2(6b_u)^2(1b_g)^2(7a_g)^2,$$

where $1b_g$ and $1a_u$ orbitals are π MOs, $7a_g$ and $6b_u$ orbitals correspond to the lone pairs of O atoms. The peaks in the outer-valence region up to $\sim$17 eV of glyoxal are main peaks. The electron correlations of the ionized states due to *n* orbitals were also calculated to be large as in acrolein; Koopmans' ordering reversed between

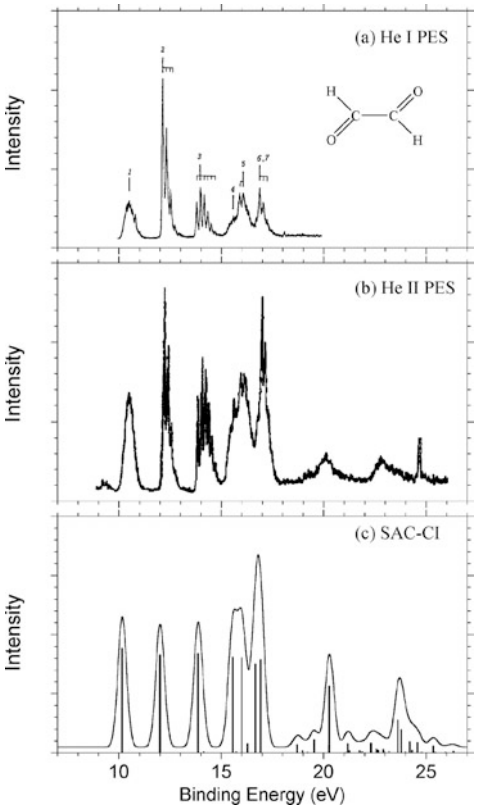

Figure 4-3. Valence ionization spectra of *s-trans* acrolein by (**a**) He I PES [120], (**b**) He II PES [122] and (**c**) SAC-CI general-*R* method [46]

$6b_u$ and $1b_g$ states. The first two peaks were ionizations from n orbitals, $7a_g$ and $6b_u$ states. The π orbitals exist in higher energy region compared with butadiene and acrolein. The vibrational structure is remarkable in the observed peaks 2 and 3; the structure relaxation of these states is characteristic. The overlapping bands were observed at ~16.9 eV are assigned to the $5a_g$ and $5b_u$ states. Some shake-up states were calculated in the energy region of 13 ~ 17 eV, though their intensities were small. The lowest shake-up state was calculated at 12.91 eV and was characterized as $n^{-2}\pi^*$ [46]. On the other hand, the lowest $n^{-1}\pi^{-1}\pi^*$ and $\pi^{-2}\pi^*$ shake-up states were obtained at 14.14 and 17.96 eV, respectively [46].

4.3.1.2. Outermost Shake-Up Satellites

The position and intensity of the low-lying shake-up states of 4π-electron molecules, butadiene, acrolein, and glyoxal are of interest, since they have characteristic

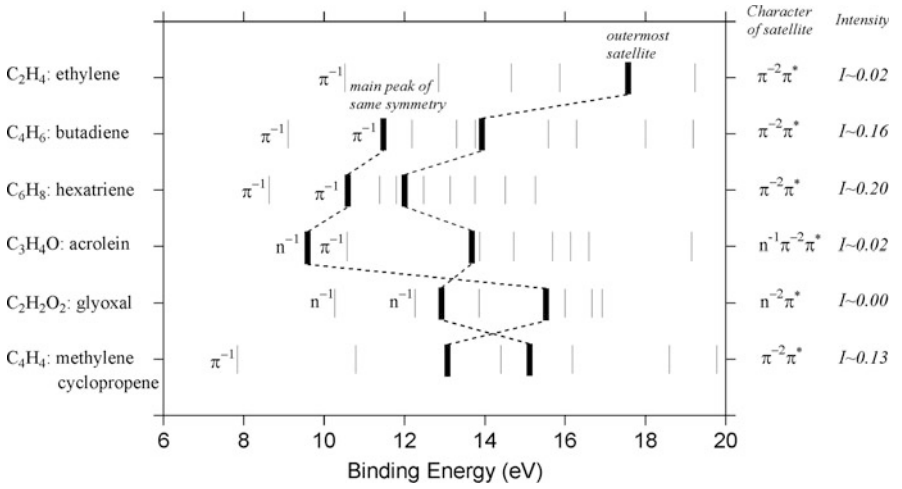

Figure 4-4. Comparison of the main peaks and outermost satellites of the π-conjugated molecules

π-conjugation. In Figure 4-4, the calculated IPs of the valence ionized states of these molecules are compared; main peaks and outermost satellites are shown [46].

In Figure 4-4, we can see the effect of the pattern of π-conjugation and the nπ* transitions on the position and intensity of the satellite peaks. First, as the π-conjugation becomes longer, the IP of the outermost satellite peak becomes lower. The calculated IPs of the outermost satellites were 17.55, 13.98, and 11.92 eV, for ethylene, 1,3 trans butadiene, and 1,3,5-trans hexatriene, respectively. The intensity of these satellites is dominantly due to the final-ionic-state interaction with the next-HOMO for butadiene and hexatriene. The intensity of these satellites becomes larger as the π-conjugation becomes longer; monopole intensities were calculated as 0.01, 0.16, and 0.20, respectively [46].

The nπ* transition is usually as low as $\pi\pi$* transition in the excitation spectra of molecules, and therefore, lower satellites accompanied by the nπ* transitions are expected for the π-conjugated molecules with lone-pair electrons. The outermost satellites of acrolein and glyoxal were lower than butadiene, 13.76 and 12.91 eV, respectively. However, the intensities of these states were very small such as 0.02 and 0.00. This is because these shake-up states do not effectively interact with the main peaks. The outermost satellite of glyoxal is A_u state at 12.91 eV and the main peak of A_u symmetry exists at 15.54 eV.

4.3.1.3. $2A_g$ State

The doubly excited state, so called 2^1A_g state of butadiene, acrolein, and glyoxal were investigated by the general-*R* method [47]. The energy spectra of the excited states of these molecules are compared in Figure 4-5. For butadiene, vertical excitation of the 2^1A_g state has been studied by some theoretical works [124–126]. The

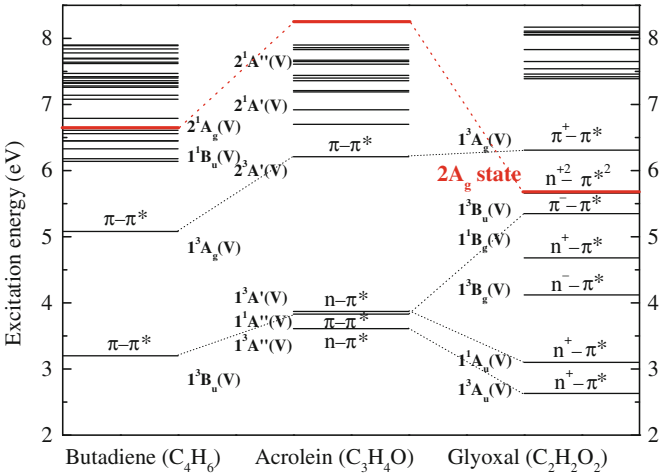

Figure 4-5. Calculated energy levels of the excited states of butadiene, acrolein, and glyoxal [47]

general-*R* method calculated the vertical transition energy of 6.56 eV [47], in agreement with other theoretical calculations. It is important to include up to quadruple excitation operators in the general-*R* calculation. For acrolein, this state was located in the higher energy region at 8.16 eV. The 2^1A_g states of butadiene and acrolein

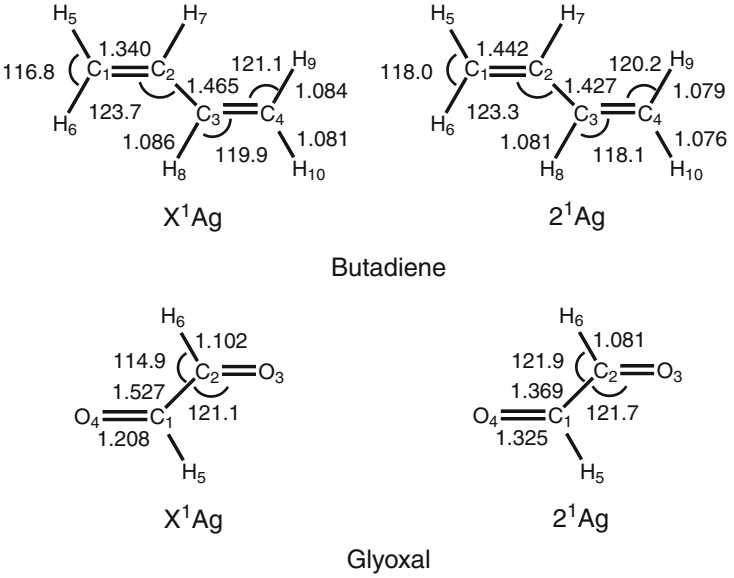

Figure 4-6. Geometry of the ground (X^1A_g) and doubly excited (2^1A_g) states of butadiene and glyoxal

were characterized as the $\pi\pi^*$ transition with moderate contributions by doubles whose SAC-CI coefficients are ~0.3. On the other hand, the 2^1A_g state of glyoxal is characterized as pure (n_{O+},$n_{O+} \rightarrow \pi^*$,π^*) double excitation [47]. This is because there is no singly excited state interacting with this state in the same energy region. This 2^1A_g state of glyoxal was predicted to be very low at 5.66 eV, which is reasonable if we consider the 1^3A_u state, $n_{O+} \rightarrow \pi^*$, exist at 2.63 eV.

The equilibrium structures of these 2^1A_g states for butadiene and glyoxal were obtained by the general-*R* geometry optimization [47]. The geometries are displayed in Figure 4-6. For butadiene, the CC bond length of the 2^1A_g state increases by 0.102 Å, which is much larger than other singlet states. The same is true for the CO bond length of glyoxal: the CO bond elongation was calculated to be 0.117 Å, while the CC bond length of this state shrinks by 0.156 Å. The relaxation energies of these states were calculated to be very large, 1.18 and 1.77 eV for butadiene and glyoxal, respectively, which are much larger than other singly excited states [47].

4.3.2. Excited-State Geometry of Two-Electron Processes

The analytical energy gradient of the SAC-CI general-*R* method enables the accurate investigation of the molecular structures, spectroscopic constants, chemical reactions, and energy relaxation in particular for the multi-electron processes. It is also useful for the excited states of open-shell systems. The method has been applied to some diatomic molecules, CH^+, NH^+, C_2, CO^+, NO, N_2^+, N_2, and also to polyatomic molecules as acetylene, CNC, and N_3 [66, 67].

4.3.2.1. Singlet and Triplet States of CH^+ and Doublet States of NH^+

First, we show the SAC-CI general-*R* applications to the singlet and triplet excited states of CH^+ and to the doublet states of NH^+ [67]. Both the SD-*R* and general-*R* methods were performed without doing perturbation selection using the cc-pVTZ [127, 128] without f function for C and N and without d function for H, (10*s*5*p*2*d*/5*s*2*p*)/[4*s*3*p*2*d*/3*s*2*p*]. In the general-*R* calculations, systematic calculations were performed using SDT and SDTQ *R* operators in order to examine the effect of the *R* operators in different orders. Table 4-2 shows the SAC-CI results of r_e, ω_e, and T_e, compared with the experiments [129]. The excitation level denotes the number of electrons involved in the excitation process. The values of ω_e were numerically calculated using the analytical first derivatives.

The low-lying $A^1\Pi$ state of CH^+ is described essentially by the one-electron excitation from the ground state, while the $b^3\Sigma^-$ and $B^1\Delta$ states are described by the two-electron excitations from the ground state. For the ground state of CH^+, the experimental r_e was well reproduced by the SAC method. For the one-electron process, the SD-*R* and general-*R* methods gave very similar results in agreement with experiments, but for the two-electron processes, the general-*R* method gave considerably better results than the SD-*R* method, especially for T_e; the average deviations of the general-*R*(SDTQ) result from the experimental values were 0.004 Å, 53 cm^{-1},

Table 4-2. Spectroscopic constants for the singlet and triplet states of CH^+ and the doublet states of NH^+

State	Method	Excitation level	r_e (Å)	ω_e (cm^{-1})	T_e (eV)
CH^+					
$X^1\Sigma^+$	SAC	0	1.128	2,848	–
	Exptl.[a]		1.131	2,740	–
$A^1\Pi$	SD-*R*	1	1.238	1,818	3.101
	SDT-*R*	1	1.249	1,729	2.998
	SDTQ-*R*	1	1.251	1,715	2.988
	Exptl.[a]		1.234	1,865	2.989
$b^3\Sigma^-$	SD-*R*	2	1.211	2,273	5.952
	SDT-*R*	2	1.246	2,034	4.754
	SDTQ-*R*	2	1.250	2,013	4.696
	Exptl.[a]		1.245	1,939	4.736
$B^1\Delta$	SD-*R*	2	1.210	2,224	7.780
	SDT-*R*	2	1.232	2,070	6.700
	SDTQ-*R*	2	1.236	2,044	6.641
	Exptl.[a]		1.233	2,076	6.513
NH^+					
$X^2\Pi$	SD-*R*	1	1.064	3,122	–
	SDT-*R*	1	1.070	3,041	–
	SDTQ-*R*	1	1.070	3,029	–
	Exptl.[a]		1.070	2,922	–
$A^2\Sigma^-$	SD-*R*	2	1.123	2,574	6.564
	SDT-*R*	2	1.232	1,811	2.948
	SDTQ-*R*	2+3	1.261	1,627	2.746
	Exptl.[a]		1.251	1,585	2.752
$B^2\Delta$	SD-*R*	2	1.073	2,921	5.673
	SDT-*R*	2	1.128	2,422	3.053
	SDTQ-*R*	2	1.136	2,331	3.004
	Exptl.[a]		(1.152)	2,280	2.889
$C^2\Sigma^+$	SD-*R*	2	1.092	2,743	6.623
	SDT-*R*	2	1.148	2,285	4.555
	SDTQ-*R*	2	1.152	2,239	4.506
	Exptl.[a]		1.163	2,151	4.339

[a] Reference [129].

and 0.08 eV for r_e, ω_e, and T_e, respectively. The effect of including up to quadruples amounts up to c.a. 1.2 eV for T_e. Thus, for the two-electron processes, we should use the general-*R* method for obtaining quantitatively reliable results.

The ground state of NH^+ is described by the one-electron process, while the other excited states, $A^2\Sigma^-$, $B^2\Delta$, and $C^2\Sigma^+$, are represented by the two-electron

processes. For the ground state, both SD-*R* and general-*R* methods gave good bond distance and the ω_e was improved by 93 cm^{-1} with the general-*R* method. For the other states, the general-*R* method greatly improves the results of the SD-*R* method, especially for T_e. The effects of including triples in the *R* operators are as large as 0.06–0.11 Å, 500–760 cm^{-1}, and 2.1–3.6 eV for r_e, ω_e, and T_e, respectively. The effect of including up to quadruples is prominent for the $A^2\Sigma^-$ state and the results are improved by 0.03 Å (r_e), 180 cm^{-1} (ω_e), and 0.20 eV (T_e). This is because the three-electron processes such as $(3\sigma^{-3}1\pi^2)$ considerably mix to this state. The agreements of the general-*R* results with the experimental values were satisfactory regardless of the excitation levels of the states.

4.3.2.2. Trans-Bent Structures in Excited States of Acetylene

Acetylene has trans-bent structure in the excited states. The lowest excited (A^1A_u) state of acetylene has been extensively studied both experimentally and theoretically. The EOM-CCSD calculation [130] has investigated the trans-bent structure in the A^1A_u state and reproduced the experimental structure. In 1992, the trans-bent structure in the C'^1A_g state of C_2H_2 has been measured by Lundberg et al. [131]. The A^1A_u state is described by the one-electron process, while the C'^1A_g state is described by the two-electron process. Therefore, the spectroscopic constants of these excited states are of interest in particular for the C'^1A_g state. Table 4-3 summarizes the SD-*R* and general-*R* results for the ground and excited states of C_2H_2, in comparison with the experiments [131–133]. The SAC method for the ground state well reproduced the experimental geometries [132]. For the A^1A_u state, both SD-*R* and general-*R* methods gave the results of the same quality. For the C'^1A_g state, the general-*R* method drastically improves the results of the SD-*R* method, especially for

Table 4-3. Spectroscopic constants of ground and excited states of acetylene

State	Method	Excitation level	R_{CH} (Å)	R_{CC} (Å)	θ_{CCH} (degree)	T_e (eV)
X^1A_g	SAC	–	1.068	1.219	180	–
(linear)	Exptl.[a]		1.063	1.203	180	–
A^1A_u	SD-*R*	1	1.098	1.377	122.6	5.485
(trans)	General-*R*	1	1.097	1.385	121.7	5.329
	Exptl.[b]		1.097	1.375	122.5	5.232
C'^1A_g	SD-*R*	2	1.105	1.634	103.8	10.098
(trans)	General-*R*	2	1.111	1.643	103.0	7.844
	Exptl.[c]		1.14	1.65	103	7.723

[a] Reference [132].
[b] Reference [133].
[c] Reference [131].

Table 4-4. Spectroscopic constants of the ground and excited states of N_3

State	Method	Excitation level	R_{NN} (Å)	θ (degree)	T_e (eV)
$X^2\Pi_g$	SD-*R*	1	1.191	180	-
($D_{\infty h}$)	General-*R*	1	1.188	180	-
	CASCI[b]		1.170	180	-
	UMP2[b]		1.185	180	-
	Exptl.[a]		1.182	180	-
$^4B_1$	SAC-CI DT-*R*	2	1.273	118.3	2.108
(C_{2v})	SAC-CI DTQ-*R*	2	1.275	118.0	1.754
	CASCI[b]		1.265	118.9	1.76
	UMP2[b]		1.258	118.5	2.45
$a^4\Pi_u$	SAC-CI DT-*R*	2	1.271	180	4.013
($D_{\infty h}$)	SAC-CI DTQ-*R*	2	1.275	180	3.705
	CASCI[b]		1.259	180	3.85
	UMP2[b]		1.257	180	4.58

[a] Reference [134].
[b] Reference [135].

T_e. The optimized geometries are in excellent agreement with experimental values; the deviations are within 0.02 Å and 0.03°. The A^1A_u and C'^1A_g states are described as $1a_u^{-1}4a_g$ and $1a_u^{-2}4a_g^2$, respectively, in which $1a_u$ orbital corresponds to valence $1\pi_u$ orbital for the liner structure. Thus, trans-bent structures become stable in these excited states by the single or double excitation from $1\pi_u$ orbital.

4.3.2.3. Lowest Doublet and Quartet States of N_3 Radical

The azide free radical N_3 has been extensively studied experimentally as well as theoretically. The ground state of N_3 has been recognized as the doublet state, $X^2\Pi_g$, in the linear structure which has been spectroscopically determined by Douglas et al. [134]. Though there are no experimental data for the quartet states, the lowest quartet state has been theoretically studied using the CASCI, UMP2 [135] and MRD-CI [136] methods: the former work predicted that the bent $^4B_1$ state is more stable than linear $a^4\Pi_u$ state. We calculated these doublet and quartet states of N_3 by the SAC-CI general-*R* energy gradient method. For the quartet state, both linear and bent structures were examined. The doublet and quartet states of N_3 were obtained by the ionization from the closed-shell N_3^-. Table 4-4 summarizes the optimized geometries, adiabatic excitation energies for the lowest doublet and quartet states of N_3, compared with experimental [134] and other theoretical results [135].

The ground state, $X^2\Pi_g$, is described by the one-electron process from the closed-shell state. Both SD-*R* and general-*R* (SDT) methods gave excellent results in com-

parison with the experiment within 0.008 Å for R_{NN}. For the lowest quartet state, the SAC-CI results are close to those of the CASCI method and show that the bent $^4B_1$ state is energetically stable relative to the linear $a^4\Pi_u$ state. For T_e, the DTQ-*R* method improves the values by including quadruple *R* operators: the difference between the DT-*R* and DTQ-*R* results are 0.004 Å, 0.3° and 0.33 eV for R_{NN}, θ and T_e, respectively.

4.3.3. Inner-Shell Electronic Processes

We have applied the general-*R* method to wide varieties of the core-electron processes; the core-electron binding energies [50], the inner-shell ionization satellite spectra of CH_4, NH_3 [50], H_2O [55], formaldehyde [51], and the vibrational spectrum of the core-hole state of H_2O [49]. The g-u splitting of homonuclear molecules like N_2 [54, 63], C_2H_2, C_2H_4, and C_2H_6 [50] was well predicted. The overlapping vibrational spectra of the low-lying $\pi\pi^*/\sigma\pi^*$ shake-up satellite states of CO [52, 56] and N_2 [54] were also successfully interpreted by the present method. Geometry relaxation in the core-excited and ionized states were examined for CH_4, NH_3, H_2O, HF, N_2O, and CO_2 [53, 57, 59, 61]. The unusual vibrational progression observed in the O1s excitations of N_2O was analyzed in terms of the valence-Rydberg coupling [58]. The vibration-induced suppression of the intensity in the nsσ excitations of N_2O was also clarified [60]. We also examined the relativistic effect of the *K*-shell ionization energy using based on DK2 Hamiltonian [62]. In this section, we introduce the g-u splitting of N_2, vibrational spectra of $\pi\pi^*/\sigma\pi^*$ shake-up satellites of N_2 [54] and the relativistic effect of the *K*-shell ionizations of the second-row atoms [62].

4.3.3.1. g-u Splitting

In the molecules with two equivalent atoms, each of the main line and satellite states splits into closely-separated gerade and ungerade states. The energy separation between the mainline gerade and ungerade states is only 100 meV but still one can experimentally separate these states. So far, the g-u splitting have been observed in acetylene and N_2 molecules. Hergenhahn et al. [137] noted that different Franck-Condon (FC) factors were necessary for the two different states of N_2.

Figure 4-7 compares the N 1*s* photoelectron spectrum and the calculated SAC-CI spectrum [54]. Experimentally, the FC ratio $I(v' = 1)/I(v' = 0)$ for the gerade and ungerade states were estimated as 0.146(8) and 0.079(5), respectively. From the SAC-CI SDT-*R* potential energy curves, the geometry relaxation is larger in the $1\sigma_u$ state than the $1\sigma_g$ state. The FC factors were calculated from the vibrational wave functions based on ab initio potential curves and the SAC-CI $I(v' = 1)/I(v' = 0)$ ratios were 0.168 and 0.122 for the for $1\sigma_u$ and $1\sigma_g$ states, respectively, in good agreement with the experimental values [54].

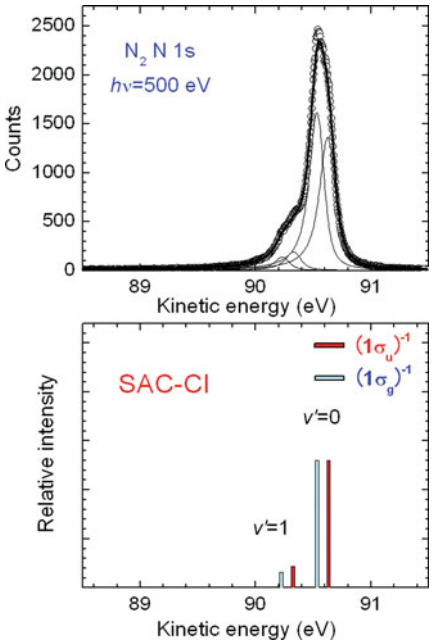

Figure 4-7. Vibrational spectra of the $1\sigma_g$ and $1\sigma_u$ ionized states of N_2. Upper and lower panels are experimental and SAC-CI spectra, respectively [54]

4.3.3.2. Vibrational Spectra of Inner-Shell Satellites

The geometry relaxation and vibrational spectra can be observed for the inner-shell shake-up satellite states. Those of $\pi\pi^*$ and $\sigma\pi^*$ shake-up satellites are analyzed in details for CO [52, 56] and N_2 [54] by the experiment and theory. The low-lying shake-up satellite states of N_2 have electron configurations $1\sigma_u^{-1}1\pi_u^{-1}1\pi_g(^2\Sigma_g^+)$, $1\sigma_g^{-1}1\pi_u^{-1}1\pi_g(^2\Sigma_u^+)$, $1\sigma_g^{-1}3\sigma_g^{-1}1\pi_g(^2\Pi_g)$, and $1\sigma_u^{-1}3\sigma_g^{-1}1\pi_g(^2\Pi_u)$. The correlation satellites [117, 118] can be classified into two groups phenomenologically [138]. The first group includes satellites whose excitation cross sections relative to the single-hole ionization cross section stay constant, while the second group includes those whose excitation cross sections sharply decrease with an increase in energy. These two different types of energy dependence have been attributed to the two lowest-order correlation terms, often called the direct and conjugate shake-up terms [139]. In the case of low-lying $\pi\pi^*$ and $\sigma\pi^*$ shake-up states of N_2, the transitions leading to the $^2\Sigma_g^+$ and $^2\Sigma_u^+$ states are dominated by the direct shake-up term and the transitions leading to the $^2\Pi_g$ and $^2\Pi_u$ states are dominated by the conjugate shake-up contribution.

The SAC-CI potential energy curves of the N 1*s* shake-up states in the energy region of $\pi\pi^*$ and $\sigma\pi^*$ satellites are shown in Figure 4-8 [54]. The potential curves of the counterpart ungerade states, almost overlap with the corresponding gerade

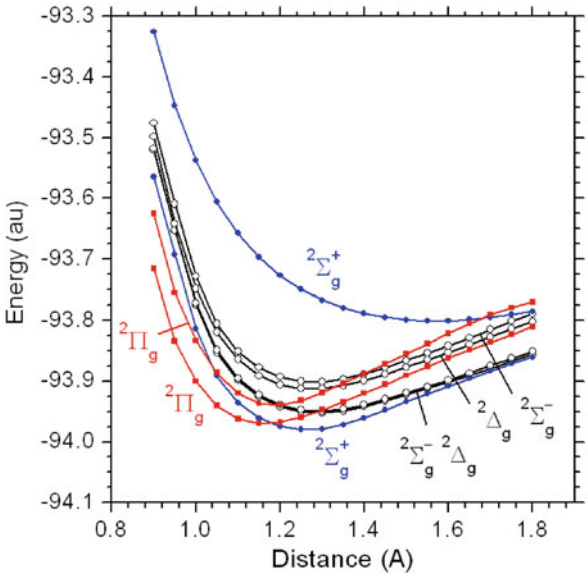

Figure 4-8. Calculated potential energy *curves* of the N1s shake-up satellite $^2\Sigma_g^+$, $^2\Pi_g$, $^2\Sigma_g^-$, and Δ_g states of N_2

states. The geometry relaxation by the shake-up ionization of N_2 is large for the $^2\Sigma_g^+$ state, and the calculated value of r_e is 1.259 Å, 0.164 Å longer than that of the ground state. Since the gerade state $^2\Sigma_g^+$ has a hole in the $1\sigma_u$ orbital, it is located slightly lower in energy than the ungerade state $^2\Sigma_u^+$. The calculated g-u splitting for these satellites is ~40 meV, much smaller than that of the single-hole state of 101 meV. The geometry relaxation for the $^2\Pi_{g,u}$ states is much smaller than for the $^2\Sigma_{g,u}^+$ states: the equilibrium distances of the lower and higher $^2\Pi_g$ states are $r_e = 1.161$ and 1.186 Å, respectively. The geometry change of these states, 0.066 and 0.091 Å are larger than the corresponding changes for CO of 0.042 and 0.068 Å [56]. This is because the $^2\Pi_{g,u}$ states of N_2 have the character of $\sigma\pi^*$ transitions and the $^2\Pi$ states of CO are $n\pi^*$ transitions.

The SAC-CI theoretical spectra for the $^2\Sigma_g^+$ and $^2\Sigma_u^+$ states are compared with the experimental photoelectron satellite spectra in Figure 4-9 [54]. The theoretical spectrum for $^2\Sigma_{g,u}^+$ has a maximum intensity at $v' = 6$, reproducing the shape of the experimental spectrum. The activation of the high vibrational states is due to the large geometry relaxation. Figure 4-10 compares the SAC-CI spectra for the $^2\Pi_{g,u}$ states with the experimental spectra, where the 90° spectrum dominantly represents the Π component [54]. For the lower $^2\Pi_g$ band, the vibrational levels of $v' = 0$ and $v' = 1$ have almost the same intensity and the higher levels are populated in the gerade state. In the higher Π band, $v' = 2$ has the maximum intensity. Since the $^2\Pi_g$ state has a hole in the $1\sigma_g$ orbital, the geometry relaxation of the $^2\Pi_g$ state is larger than that of the $^2\Pi_u$ state and the theoretical spectra reflect this difference

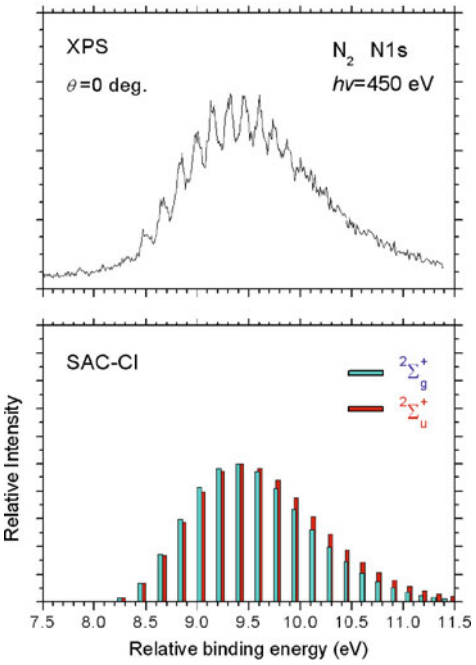

Figure 4-9. Experimental and SAC-CI vibrationally resolved spectra of the N1s satellite bands of N_2 in Σ symmetry [54]

of geometry change. The higher vibrational levels are more strongly populated than for CO, since the satellites of N_2 are populated by $\sigma\pi^*$ transitions, as noted above. The higher $^2\Sigma^+_{g,u}$ states (singlet satellites) are repulsive in the FC region and have shallow minimum at about 1.57 $\sim$ 1.59 Å; no vibrational structure is expected for these states.

4.3.3.3. Relativistic Effect in K-Shell IPs of Second-Row Atoms

The relativistic effect of the *K*-shell IPs of molecules containing second-row atoms, SiH_4, PH_3, H_2S, OCS, and CH_3Cl was investigated [62]. The Si, P, S, and Cl 1s IPs are presented in Table 4-5 along with the experimental values [140–143]. The non-relativistic SAC-CI calculations underestimated the core-electron binding energies (CEBE) compared with the experimental values; the deviations are large about 3–6 eV. The relativistic SAC-CI calculations improved the CEBEs but slightly overestimated the values. The relativistic effect amounted to 4–9 eV for the CEBEs of these molecules. For example, the S 1s CEBE of H_2S was measured as 2,478.5 eV [142] and our theoretical values were 2,479.51 and 2,472.98 eV with and without relativistic effect, respectively. The deviations from the experimental values were about 1 eV for the molecules containing Si, P, and S. These errors amount to 0.03–0.06%

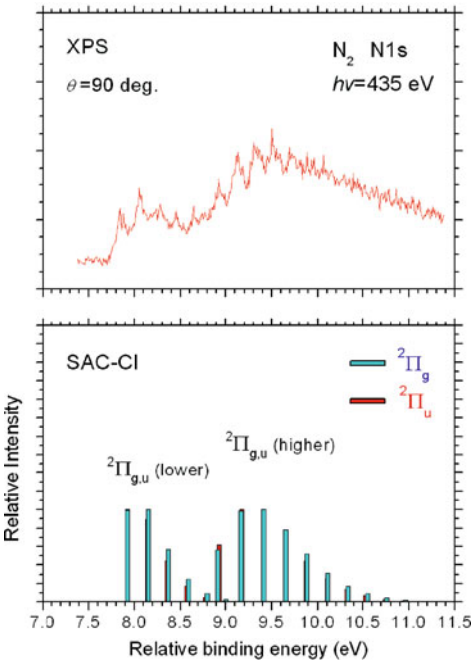

Figure 4-10. Experimental and SAC-CI vibrationally resolved spectra of the N1s satellite bands of N_2 in Π symmetry [54]

of the absolute values of the CEBEs. The CASPT2 calculations also gave the same order of deviations [144]; the errors were large for the inner-shell ionizations of the heavy elements. These errors may be attributed to the crudeness of the basis sets, the higher-order relativistic effects, and/or insufficiency of describing orbital relaxation. Kotsis and Staemmler [145] discussed the difficulty of the basis set selection for

Table 4-5. Calculated and observed Si, P, S, and Cl 1s core-electron binding energies (eV)

		Relativistic	Non-relativistic	Relativistic effect (eV)	
Molecule	Exptl.	SAC-CI	SAC-CI	SAC-CI [e]	Koopmans' theorem
$\underline{Si}H_4$	1,847.1[a]	1,848.24	1,843.96	4.28	3.97
$\underline{P}H_3$	2,150.5[b]	2,151.25	2,146.32	4.93	5.30
$H_2\underline{S}$	2,478.5[c]	2,479.51	2,472.98	6.53	6.94
O$\underline{C}$S	2,480.3[a]	2,481.84	2,475.06	6.78	6.93
$CH_3\underline{Cl}$	2,829.4[d]	2,832.15	2,823.35	8.80	8.95

[a] Reference [141].
[b] Reference [140].
[c] Reference [142].
[d] Reference [143].
[e] ΔE = E(Non-Relativistic SAC-CI)-E(Relativistic SAC-CI).

the balanced description of the core and valence electron correlations. The effect of electron correlations is very small compared with the relativistic effect in those molecules containing the second-row atoms.

4.4. SUMMARY

Theoretical fine spectroscopy of the multi-electron processes has been achieved by the SAC-CI general-*R* method. In this article, we review the development and some recent applications of the general-*R* method.

First, we explained the theoretical background of the SAC-CI method, in particular the general-*R* method. Some advantages and features of the general-*R* method as well as the possible *R* operators in the present program were described. Theory and computational algorithm of the analytical energy gradient of the SAC-CI method were also briefly reviewed.

We also introduced some recent applications of the general-*R* method to the molecular spectroscopies where the multi-electronic processes play an essential role. Theoretical spectroscopy of the inner-valence ionization spectra was explained for the applications to 4π-electron molecules, butadiene, acrolein and glyoxal and the low-lying shake-up satellites were discussed. The doubly excited states of these molecules were also compared. Theoretical study of the excited-state geometries and adiabatic properties of the multi-electron processes and open-shell systems by the analytical energy gradient of the general-*R* method were shown for the diatomic molecules CH^+ and NH^+, and also for the polyatomic molecules, acetylene and N_3. The accuracy of the methods was examined with the systematic calculations of including the higher-order *R* operators for the diatomic molecules. The high precision calculations of the inner-shell electronic processes, the g-u splitting of the main line and the geometry relaxation of the inner-shell shake-up satellites of N_2 appearing in the vibrational spectra were reviewed. The relativistic effect of the *K*-shell ionization of the second-row atoms was also described.

ACKNOWLEDGEMENTS

The authors are grateful to Drs. T. Nakajima, M. Ishida, and K. Toyota for the works on the SAC-CI general-*R* analytical energy gradients, to Prof. K. Ueda for the works on the inner-shell electronic processes, to Drs. B. Saha and M. Nakata for the work of doubly excited states and ionization spectra of 4π-electron molecules. This study was supported by JST, CREST and a Grant-in-Aid for Scientific Research in Priority Areas "Molecular Theory for Real Systems" from the Ministry of Education, Culture, Sports, Science and Technology of Japan.

REFERENCES

1. H. Nakatsuji, K. Hirao, J. Chem. Phys. **68**, 2053 (1978)

2. H. Nakatsuji, Chem. Phys. Lett. **59**, 362 (1978)
3. H. Nakatsuji, Chem. Phys. Lett. **67**, 329 (1979)
4. H. Nakatsuji, Chem. Phys. Lett. **67**, 334 (1979)
5. H. Nakatsuji, Acta Chim. Hungarica, Models in Chemistry **129**, 719 (1992)
6. H. Nakatsuji, in *Computational Chemistry – Reviews of Current Trends*, Ed. J. Leszczynski (World Scientific, Singapore, 1997)
7. M. Ehara, J. Hasegawa, H. Nakatsuji, *SAC-CI Method Applied to Molecular Spectroscopy, in Theory and Applications of Computational Chemistry: The First 40 Years, A Volume of Technical and Historical Perspectives* (Elsevier, Amsterdam, 2005)
8. H. Nakatsuji, Chem. Phys. **75**, 425 (1983)
9. H. Nakatsuji, Chem. Phys. **76**, 283 (1983)
10. H. Nakatsuji, O. Kitao, T. Yonezawa, J. Chem. Phys. **83**, 723 (1985)
11. O. Kitao, H. Nakatsuji, J. Chem. Phys. **87**, 1169 (1987)
12. H. Nakatsuji, M. Ehara, M. H. Palmer, M. F. Guest, J. Chem. Phys. **97**, 2561 (1992)
13. H. Nakatsuji, M. Ehara, J. Chem. Phys. **98**, 7179 (1993)
14. H. Nakatsuji, M. Ehara, T. Momose, J. Chem. Phys. **100**, 5821 (1994)
15. H. Nakatsuji, M. Ehara, J. Chem. Phys. **101**, 7658 (1994)
16. M. Ehara, H. Nakatsuji, J. Chem. Phys. **102**, 6822 (1995)
17. H. Nakatsuji, J. Hasegawa, M. Hada, J. Chem. Phys. **104**, 2321 (1996)
18. H. Nakatsuji, J. Hasegawa, K. Ohkawa, Chem. Phys. Lett. **296**, 499 (1998)
19. J. Hasegawa, K. Ohkawa, H. Nakatsuji, J. Phys. Chem. B **102**, 10410 (1998)
20. J. Hasegawa, H. Nakatsuji, J. Phys. Chem. B **102**, 10420 (1998)
21. K. Fujimoto, J. Hasegawa, S. Hayashi, S. Kato, H. Nakatsuji, Chem. Phys. Lett. **414**, 239 (2005)
22. J. Hasegawa, K. Fujimoto, B. Swerts, T. Miyahara, H. Nakatsuji, J. Comp. Chem. **189**, 205 (2007)
23. N. Nakatani, J. Hasegawa, H. Nakatsuji, J. Am. Chem. Soc. **129**, 8756 (2007)
24. H. Nakatsuji, H. Nakai, Chem. Phys. Lett. **174**, 283 (1990)
25. H. Nakatsuji, H. Nakai, J. Chem. Phys. **98**, 2423 (1993)
26. H. Nakatsuji, R. Kuwano, H. Morita, H. Nakai, J. Mol. Catalysis **82**, 211 (1993)
27. H. Nakatsuji, J. Chem. Phys. **83**, 713 (1985)
28. H. Nakatsuji, J. Chem. Phys. **83**, 5743 (1985)
29. H. Nakatsuji, J. Chem. Phys. **94**, 6716 (1991)
30. H. Nakatsuji, J. Chem. Phys. **95**, 4296 (1991)
31. H. Nakatsuji, Chem. Phys. Lett. **177**, 331 (1991)
32. M. Ehara, H. Nakatsuji, Chem. Phys. Lett. **282**, 347 (1998)
33. M. Ehara, M. Ishida, K. Toyota, H. Nakatsuji, in *Reviews in Modern Quantum Chemistry* Ed. K. D. Sen (World Scientific, Singapore, 2002) pp. 293–319.
34. M. Ehara, P. Tomasello, J. Hasegawa, H. Nakatsuji, Theor. Chem. Acta. **102**, 161 (1999)
35. J. Hasegawa, M. Ehara, H. Nakatsuji, Chem. Phys. **230**, 23 (1998)
36. M. Ehara, H. Nakatsuji, Spectrochim. Acta. **A55**, 487 (1998)
37. M. Ehara, Y. Ohtsuka, H. Nakatsuji, Chem. Phys. **226**, 113 (1998)
38. M. Ehara, M. Ishida, H. Nakatsuji, J. Chem. Phys. **114**, 8282 (2001)
39. M. Ishida, M. Ehara, H. Nakatsuji, J. Chem. Phys. **116**, 1934 (2002)
40. J. Wan, M. Ehara, M. Hada, H. Nakatsuji, J. Chem. Phys. **113**, 5245 (2000)
41. J. Wan, M. Hada, M. Ehara, H. Nakatsuji, J. Chem. Phys. **114**, 5117 (2001)
42. M. Ehara, Y. Ohtsuka, H. Nakatsuji, M. Takahashi, Y. Udagawa, J. Chem. Phys. **122**, 234219 (2005)
43. M. Ehara, S. Yasuda, H. Nakatsuji, Z. Phys. Chem. **217**, 161 (2003)
44. P. Tomasello, M. Ehara, H. Nakatsuji, J. Chem. Phys. **118**, 5811 (2003)

45. M. Ehara, M. Ishida, H. Nakatsuji, J. Chem. Phys. **117**, 3248 (2002)
46. M. Ehara, M. Nakata, H. Nakatsuji, Mol. Phys. **104**, 971 (2006)
47. B. Saha, M. Ehara, H. Nakatsuji, J. Chem. Phys. **125**, 014316 (2006)
48. B. Saha, M. Ehara, H. Nakatsuji, J. Phys. Chem. A **111**, 5473 (2007)
49. R. Sankari, M. Ehara, H. Nakatsuji, Y. Senba, K. Hosokawa, H. Yoshida, A. D. Fanis, Y. Tamenori, S. Aksela, K. Ueda, Chem. Phys. Lett. **380**, 647 (2003)
50. K. Kuramoto, M. Ehara, H. Nakatsuji, J. Chem. Phys. **122**, 014304 (2005)
51. K. Kuramoto, M. Ehara, H. Nakatsuji, M. Kitajima, H. Tanaka, A. D. Fanis, Y. Tamenori, K. Ueda, J. Electron Spectrosc. Relat. Phenom. **142**, 253 (2005)
52. K. Ueda, M. Hoshino, T. Tanaka, M. Kitajima, H. Tanaka, A. D. Fanis, Y. Tamenori, M. Ehara, F. Oyagi, K. Kuramoto, H. Nakatsuji, Phys. Rev. Lett. **94**, 243004 (2005)
53. M. Matsumoto, K. Ueda, E. Kukk, H. Yohisda, T. Tahara, M. Kitajima, H. Tanaka, Y. Tamenori, K. Kuramoto, M. Ehara, H. Nakatsuji, Chem. Phys. Lett. **417**, 89 (2006)
54. M. Ehara, H. Nakatsuji, M. Matsumoto, T. Hatamoto, X.-J. Liu, T. Lischke, G. Pruemper, T. Tanaka, C. Makochekanwa, M. Hoshino, H. Tanaka, J. R. Harries, Y. Tamenori, K. Ueda, J. Chem. Phys. **124**, 124311 (2006)
55. R. Sankari, M. Ehara, H. Nakatsuji, A. D. Fanis, H. Aksela, S. L. Sorensen, M. N. Piancastelli, E. Kukk, K. Ueda, Chem. Phys. Lett. **422**, 51 (2006)
56. M. Ehara, K. Kuramoto, H. Nakatsuji, M. Hoshino, T. Tanaka, M. Kitajima, H. Tanaka, Y. Tamenori, A. D. Fanis, K. Ueda, J. Chem. Phys. **125**, 114304 (2006)
57. T. Hatamoto, M. Matsumoto, X.-J. Liu, K. Ueda, M. Hoshino, K. Nakagawa, T. Tahara, H. Tanaka, K. Kuramoto, M. Ehara, R. Tamaki, H. Nakatsuji, J. Electron Spectrosc. Relat. Phenom. **155**, 54 (2007)
58. T. Tanaka, K. Ueda, R. Feifel, L. Karlsson, H. Tanaka, M. Hoshino, M. Kitajima, M. Ehara, R. Fukuda, R. Tamaki, H. Nakatsuji, Chem. Phys. Lett. **435**, 182 (2007)
59. M. Ehara, R. Tamaki, H. Nakatsuji, R. R. Lucchese, J. Soderstrom, T. Tanaka, M. Hoshino, M. Kitajima, H. Tanaka, A. D. Fanis, K. Ueda, Chem. Phys. Lett. **438**, 14 (2007)
60. M. Ehara, H. Nakatsuji, Coll. Czech Chem. Commun. **73**, 771 (2008)
61. M. Ehara, K. Kuramoto, H. Nakatsuji, Chem. Phys. **356**, 195 (2008)
62. K. Ueda, R. Puttner, N. A. Cherepkov, F. Gel'mukhanov, M. Ehara, Eur. Phys. J. **169**, 95 (2009)
63. T. Tanaka, M. Hoshino, H. Kato, M. Ehara, N. Yamada, R. Fukuda, H. Nakatsuji, Y. Tamenori, J. R. Harries, G. Pruemper, H. Tanaka, K. Ueda, Phys. Rev. A. **77**, 012709 (2008)
64. T. Nakajima, H. Nakatsuji, Chem. Phys. Lett. **280**, 79 (1997)
65. T. Nakajima, H. Nakatsuji, Chem. Phys. **242**, 177 (1999)
66. M. Ishida, K. Toyoda, M. Ehara, H. Nakatsuji, Chem. Phys. Lett. **347**, 493 (2001)
67. M. Ishida, K. Toyoda, M. Ehara, M. J. Frisch, H. Nakatsuji, J. Chem. Phys. **120**, 2593 (2004)
68. M. Ishida, K. Toyoda, M. Ehara, H. Nakatsuji, Chem. Phys. Lett. **350**, 351 (2001)
69. K. Toyota, M. Ehara, H. Nakatsuji, Chem. Phys. Lett. **356**, 1 (2002)
70. K. Toyota, M. Ishida, M. Ehara, M. J. Frisch, H. Nakatsuji, Chem. Phys. Lett. **367**, 730 (2003)
71. H. Monkhorst, Int. J. Quantum Chem. Symp. **11**, 421 (1977)
72. E. Dalgaard, H. Monkhorst, Phys. Rev. A **28**, 1217 (1983)
73. D. Mukherjee, P. K. Mukherjee, Chem. Phys. **39**, 325 (1979)
74. H. Koch, P. Jorgensen, J. Chem. Phys. **93**, 3333 (1990)
75. H. Koch, H. J. A. Jensen, T. Helgaker, P. Jorgensen, J. Chem. Phys. **93**, 3345 (1990)
76. J. Geertsen, M. Rittby, R. J. Bartlett, Chem. Phys. Lett. **164**, 57 (1989)
77. J. F. Stanton, R. J. Bartlett, J. Chem. Phys. **98**, 7029 (1993)
78. J. F. Stanton, J. Gauss, J. Chem. Phys. **101**, 8938 (1994)
79. J. F. Stanton, R. J. Bartlett, J. Chem. Phys. **102**, 3629 (1995)
80. D. J. Wadt, R. J. Bartlett, J. Chem. Phys. **101**, 3073 (1994)

81. S. Hirata, J. Chem. Phys. **121**, 51 (2004)
82. M. Kallay, J. Gauss, J. Chem. Phys. **121**, 9257 (2004)
83. O. Christiansen, H. Koch, P. Jorgensen, Chem. Phys. Lett. **243**, 409 (1999)
84. B. Jeziorski, H. J. Monkhorst, Phys. Rev. A. **24**, 1668 (1981)
85. I. Lindgren, D. Mukherjee, Phys. Rep. **151**, 93 (1987)
86. D. Mukherjee, S. Pal, Adv. Quantum. Chem. **20**, 291 (1989)
87. U. S. Mahapatra, B. Datta, B. Bandyopadhyay, D. Mukherjee, Adv. Quantum. Chem. **30**, 163 (1998)
88. U. S. Mahapatra, B. Datta, D. Mukherjee, J. Chem. Phys. **110**, 6171 (1999)
89. X. Li, J. Paldus, J. Chem. Phys. **107**, 6257 (1997)
90. X. Li, J. Paldus, J. Chem. Phys. **128**, 144118 (2008)
91. I. Hubač, P. Neogrady, Phys. Rev. A **50**, 4558 (1994)
92. J. Pittner, P. Nachtigall, P. Čársky, J. Mášik, I. Hubač, J. Chem. Phys. **110**, 10275 (1999)
93. I. Hubač, J. Pittner, P. Čársky, J. Chem. Phys. **112**, 8779 (2000)
94. Y. Ohtsuka, P. Piecuch, J. R. Gour, M. Ehara, H. Nakatsuji, J. Chem. Phys. **126**, 164111 (2007)
95. M. Ehara, J. R. Gour, P. Piecuch, Mol. Phys. **107**, 871 (2009)
96. J. R. Gour, P. Piecuch, M. Wloch, J. Chem. Phys. **123**, 134113 (2005)
97. J. R. Gour, P. Piecuch, M. Wloch, Int. J. Quantum Chem. **106**, 2854 (2006)
98. J. R. Gour, P. Piecuch, J. Chem. Phys. **125**, 234107 (2006)
99. N. Oliphant, L. Adamowicz, J. Chem. Phys. **94**, 1229 (1991)
100. P. Piecuch, N. Oliphant, L. Adamowicz, J. Chem. Phys. **99**, 1875 (1993)
101. P. Piecuch, S. A. Kucharski, R. J. Bartlett, J. Chem. Phys. **110**, 6103 (1999)
102. K. Kowalski, P. Piecuch, J. Chem. Phys. **115**, 643 (2001)
103. K. Kowalski, P. Piecuch, Chem. Phys. Lett. **347**, 237 (2001)
104. T. V. Voohis, M. Head-Gordon, P. Jorgensen, J. Chem. Phys. **113**, 8873 (1999)
105. H. Nakatsuji, K. Hirao, Intern. J. Quantum Chem. **20**, 1301 (1981)
106. Y. Ohtsuka, H. Nakatsuji, J. Chem. Phys. **124**, 054110 (2006)
107. M. J. Frisch, G. W. Trucks, H. B. Schlegel, G. E. Scuseria, M. A. Robb, J. R. Cheeseman, J. J. A. Montgomery, T. Vreven, K. N. Kudin, J. C. Burant, J. M. Millam, S. S. Iyengar, J. Tomasi, V. Barone, B. Mennucci, M. Cossi, G. Scalmani, N. Rega, G. A. Petersson, H. Nakatsuji, M. Hada, M. Ehara, K. Toyota, R. Fukuda, J. Hasegawa, M. Ishida, T. Nakajima, Y. Honda, O. Kitao, H. Nakai, M. Klene, X. Li, J. E. Knox, H. P. Hratchian, J. B. Cross, C. Adamo, J. Jaramillo, R. Gomperts, R. E. Stratmann, O. Yazyev, R. Cammi, C. Pomelli, J. Ochterski, P. Y. Ayala, K. Morokuma, W. L. Hase, G. Voth, P. Salvador, J. J. Dannenberg, V. G. Zakrzewski, S. Dapprich, A. D. Daniels, M. C. Strain, O. Farkas, D. K. Malick, A. D. Rabuck, K. Raghavachari, J. B. Foresman, J. V. Ortiz, Q. Cui, A. G. Baboul, S. Clifford, J. Cioslowski, B. B. Stefanov, G. Liu, A. Liashenko, P. Piskorz, I. Komaromi, R. L. Martin, D. J. Fox, T. Keith, M. A. Al-Laham, C. Y. Peng, A. Nanayakkara, M. Challacombe, P. M. W. Gill, B. Johnson, W. Chen, M. W. Wong, C. Gonzalez, J. A. Pople, *Gaussian Development Version*, Revision A.03 (Gaussian, Inc., Pittsburgh PA, 2003)
108. A. Dalgarno, A. L. Stewart, Proc. R. Soc. Lond. Ser. A **247**, 245 (1968)
109. N. C. Handy, H. F. Schaefer_III, J. Chem. Phys. **81**, 5031 (1984)
110. P. Pulay, Chem. Phys. Lett. **73**, 393 (1980)
111. Y. Yamaguchi, Y. Osamura, J. D. Goddard, H. F. Schaefer III, *A New Dimension to Quantum Chemistry: Analytic Derivative Methods in Ab Initio Molecular Electronic Structure Theory* (Oxford University Press, New York, 1994)
112. P. Jorgensen, J. Simons, *Geometrical Derivatives of Energy Surfaces and Molecular Properties* (Reidel, Dordrecht, 1986)
113. J. Gerratt, I. M. Mills, J. Chem. Phys. **49**, 1719 (1968)
114. P. Pulay, J. Chem. Phys. **78**, 5043 (1983).

115. J. A. Pople, R. Krishan, H. B. Schlegel, J. S. Binkley, Int. J. Quantum. Chem. Symp. **13**, 225 (1979)
116. N. C. Handy, R. D. Amos, J. F. Gaw, J. E. Rice, E. D. Simandiras, Chem. Phys. Lett. **120**, 151 (1985)
117. L. S. Cederbaum, W. Domcke, J. Schirmer, W. von Niessen, Adv. Chem. Phys. **65**, 115 (1986)
118. A. D. O. Bawagan, E. R. Davidson, Adv. Chem. Phys. **110**, 215 (1999)
119. M. S. Deleuze, L. S. Cederbaum, Adv. Quantum Chem. **35**, 77 (1999)
120. K. Kimura, S. Katsumata, Y. Achiba, T. Yamazaki, S. Iwata, *Handbook of He I Photoelectron Spectra of Fundamental Organic Molecules* (Japan Scientific, Tokyo, 1981)
121. M. P. Kaene, A. N. d. Brito, N. Correia, S. Svensson, L. Karlsson, B. Wannberg, U. Gelius, S. Lunell, W. R. Salaneck, M. Logdlund, D. B. Swanson, A. G. MacDiarmid, Phys. Rev. B **45**, 6390 (1992)
122. W. von Niessen, G. Bieri, L. Asbrink, J. Electron Spectrosc. Relat. Phenom. **21**, 175 (1980)
123. Y. Honda, M. Hada, M. Ehara, H. Nakatsuji, J. Phys. Chem. **106**, 3838 (2002)
124. L. Serrano-Andres, J. Sanchez-Mann, I. Nebot-Gil, J. Chem. Phys. **97**, 7499 (1992)
125. J. Lappe, R. J. Cave, J. Phys. Chem. A **104**, 2294 (2000)
126. M. Dallos, H. Lischka, Theor. Chem. Acc. **112**, 16 (2004)
127. T. H. Dunning Jr, J. Chem. Phys. **90**, 1007 (1989)
128. D. E. Woon, T. H. Dunning Jr., J. Chem. Phys. **98**, 1358 (1993)
129. K. P. Huber, G. Herzberg, *Molecular Spectra and Molecular Structure, IV. Constants of Diatomic Molecules* (Van Nostrand, New York, 1979)
130. J. F. Stanton, C. M. Huang, P. G. Szalay, J. Chem. Phys. **101**, 356 (1994)
131. J.-K. Lundberg, Y. Chen, J.-P. Pique, R. W. Field, J. Mol. Spectrosc. **156**, 104 (1992)
132. R. J. Berry, M. D. Harmony, Struct. Chem. **1**, 49 (1990)
133. T. R. Huet, M. Godefroid, M. Herman, J. Mol. Spectrosc. **144**, 32 (1990)
134. A. E. Douglas, W. J. Jones, Can. J. Phys. **43**, 2216 (1965)
135. J. Wasilewski, J. Chem. Phys. **105**, 10969 (1996)
136. C. Petrongolo, J. Mol. Struct. **175**, 215 (1988)
137. U. Hergenhahn, O. Kugeler, A. Rueel, E. E. Rennie, A. M. Bradshaw, J. Phys. Chem. A **105**, 5704 (2001)
138. U. Becker, D. A. Shirley, Phys. Scr. **T31**, 56 (1990)
139. L. Ungier, T. D. Thomas, Phys. Rev. Lett. **53**, 435 (1984)
140. A. A. Bakke, A. W. Chen, W. L. Jolly, J. Electron Spectrosc. Relat. Phenom. **20**, 333 (1980)
141. A. A. Potts, H. F. Fhadil, J. M. Benson, I. H. Hiller, Chem. Phys. Lett. **230**, 543 (1994)
142. O. Keski-Rahkonen, M. O. Krause, J. Electron Spectrosc. Relat. Phenom. **9**, 371 (1976)
143. A. W. Potts, H. F. Fhadil, J. M. Benson, I. H. Hiller, A. A. MacDowell, S. Jones, J. Phys. B **27**, 473 (1994)
144. M. Barysz, J. Leszcynski, J. Chem. Phys. **126**, 154106 (2007)
145. K. Kotsis, V. Staemmler, Phys. Chem. Chem. Phys. **8**, 1490 (2006)

CHAPTER 5

RELATIVISTIC FOUR-COMPONENT MULTIREFERENCE COUPLED CLUSTER METHODS: TOWARDS A COVARIANT APPROACH

EPHRAIM ELIAV AND UZI KALDOR
School of Chemistry, Tel Aviv University, 69978 Tel Aviv, Israel,
e-mail: ephraim@tau.ac.il; kaldor@tau.ac.il

Abstract: Four-component relativistic all-order methods are the most accurate available for heavy atoms and molecules, and are used extensively in benchmark calculations of these systems. Their current status and perspectives for further development are reviewed, and representative applications are shown. Benchmarking requires continued improvement of the relativistic Hamiltonian towards the goal of a fully covariant description, as well as the development of sophisticated all-order correlation methods suitable for general open shell systems. One of the best relativistic many-body approaches available for the purpose is the multiroot, multireference Fock space coupled cluster (FSCC) method. It is size extensive, and usually gives the most accurate results within the 4-component no-virtual-pair approximation (NVPA). The relativistic FSCC method and its recent applications are described. Relativistic effects beyond NVPA may be studied using quantum electrodynamics (QED). We discuss the challenges of introducing covariant many-body QED methods suitable for use in quantum chemical calculations of general open shell systems. The mathematical and physical foundations for merging the infinite order multireference many-body approach with an all-order QED treatment are presented. A promising technique is the double-Fock-space CC scheme, based on Lindgren's covariant evolution operator method, implemented within a generalized Fock space scheme with variable numbers of electrons and uncontracted virtual photons. A brief description of this scheme, a covariant multireference multiroot many-body QED approach, concludes this chapter.

Keywords: Relativistic coupled cluster, Four-component coupled cluster, Multireference coupled cluster, Fock space coupled cluster, Intermediate Hamiltonian, Quantum electrodynamics

5.1. INTRODUCTION

The chapter starts with a description of the relativistic four-component methodology based on the QED many-body Hamiltonian (Section 5.1.2) and its no-virtual pair approximation (Section 5.1.3). We then proceed to describe the relativistic Fock-space coupled cluster (Section 5.2.1) and intermediate Hamiltonian

P. Čársky et al. (eds.), Recent Progress in Coupled Cluster Methods, 113–144.
DOI 10.1007/978-90-481-2885-3_5,

(Section 5.2.2) approaches, followed by applications to heavy (Section 5.3) and superheavy (Section 5.4) atoms. The methods described have also been used to study heavy molecules such as UO_2 (Section 5.3), nuclear quadrupole moments (Section 5.3.3) and emission spectra of the superheavy elements No ($Z = 102$) and Lr ($Z = 103$) (Section 5.4.4). Because of space limitations, only a brief description of applications is given; the interested reader is referred to our recent review [1] and to the original publications. The last part (Section 5.5) delineates directions under development which promise, in our opinion, exciting progress in the foreseeable future.

5.1.1. Relativistic Many-Body Theory and QED

A relativistically covariant (Lorentz invariant) quantum description of many-body micro-world phenomena is possible only if matter (electrons), the radiation field (photons) and their interactions are described on equal footing. Fundaments of the theory based on these principles were introduced by Feynman, Dyson, Schwinger, Tomonaga and others in the late 1940s [2–5]. The theory is commonly called quantum electrodynamics (QED), a relativistically consistent quantum description of all electromagnetic processes, neglecting the other fundamental interactions (weak, strong and gravitational). QED is probably the most successful fundamental physical theory developed to date. It can describe almost all observed microscopic events of size greater than 10^{-13} cm, and may thus be regarded as a natural basis for the development of relativistic quantum chemistry. The use of properly formulated covariant many-body-QED methods can be very important for the study of the chemistry and physics of heavy and super-heavy elements, in particular their highly charged ions. However, the impact of QED on the development of quantum chemistry has been rather limited. This is due to the high cost of applying QED, which involves four-component electronic wave functions and photonic degrees of freedom; in addition, the very physical interpretation of wave functions described by relativistic equations and, consequently, the methodology of solving these equations in QED, are substantially different from the many-body techniques used in quantum chemistry. QED is, in principle, an infinite-body theory; it describes systems with infinite numbers of degrees of freedom, namely fields, which are relativistically and gauge invariant. In order to cover the methodological gap between the two approaches, quantum field theory, a system of mathematical tools developed especially for solving QED and other gauge theory problems, must be properly adapted to the objects of quantum chemistry, which are finite size atomic and molecular systems in stationary states. This adaptation, which is still far from complete, should be regarded as a necessary step in a consistent merging of the special theory of relativity and quantum chemistry. The next subsection gives a very brief presentation of the QED Hamiltonian in a form suitable for developing a covariant many-body procedure, with the aim of applying this procedure later in molecular electronic structure calculations.

5.1.2. The QED Hamiltonian

The starting point for QED field theory is the covariant Lagrangian formalism, which allows the correct identification of conjugate momenta appearing in the Hamiltonian [6]. Below we present a very brief introduction of the QED Lagrangian and Hamiltonian formalisms. The covariant (Lorentz invariant) Lagrangian density for interacting electromagnetic and fermionic fields has the form

$$\mathcal{L}_{\text{QED}} = \mathcal{L}_{\text{rad}} + \mathcal{L}_{\text{mat}} + \mathcal{L}_{\text{int}}\,. \tag{5-1}$$

The first term describes the electromagnetic degrees of freedom,

$$\mathcal{L}_{\text{rad}} = -\frac{1}{16\pi} F^{\mu\nu} F_{\mu\nu}, \tag{5-2}$$

where $F^{\mu\nu} = \partial^{\mu} A^{\nu} - \partial^{\nu} A^{\mu}$ is the antisymmetric electromagnetic field tensor, and $A^{\mu} = (\mathbf{A}, \frac{i}{c}\phi)$ is the 4-potential. The scalar ϕ and vector $\mathbf{A}$ potentials define the electric ($\mathbf{E}$) and magnetic ($\mathbf{B}$) fields by the Maxwell equations. The second term $\mathcal{L}_{\text{mat}}$ is the Dirac 4-spinor matter (fermionic) field ψ,

$$\mathcal{L}_{\text{mat}} = \overline{\psi}\left(i\gamma_{\mu}\partial^{\mu} - mc\right)\psi, \tag{5-3}$$

where γ_{μ} are related to the Dirac α and β matrices, $\gamma_{\mu} = \beta\,(\alpha\,, iI_4)$, and the four-gradient ∂^{μ} is $\left(\boldsymbol{\nabla}, -\frac{i}{c}\frac{\partial}{\partial t}\right)$. $\overline{\psi} = \psi^{+}\gamma_0 = \left(\psi_1^*, \psi_2^*, -\psi_3^*, -\psi_4^*\right)$ is the adjoint 4-component spinor. The last term $\mathcal{L}_{\text{int}}$ describes the interaction between the fermionic and electromagnetic fields as the product of the 4-current $j_{\mu} = (\mathbf{j}, ic\rho)$ and the 4-potential A_{μ}, $\mathcal{L}_{\text{int}} = j_{\mu}A^{\mu}$. This term was first proposed by Schwarzschild [7] to satisfy Lorentz covariance and the local gauge invariance. The 4-current j_{μ} is defined by

$$j_{\mu} = -ec\psi^{\dagger}\beta\gamma_{\mu}\psi; \quad \rho = -e\psi^{\dagger}I_4\psi; \quad \mathbf{j} = -ec\psi^{\dagger}\boldsymbol{\alpha}\psi. \tag{5-4}$$

The Lagrangian $\mathcal{L}_{\text{QED}}$ describes both the electromagnetic and fermionic degrees of freedom, as well as interactions between them, simultaneously and on equal footing as dynamic variables. The Lagrangian has all the necessary symmetry properties for correctly formulated Abelian one dimensional U(1) gauge invariant and Lorentz covariant theory. The least action principle, $\delta S = \delta \int d^4x\, \mathcal{L}_{\text{QED}} = 0$ under arbitrary infinitesimal variations of the dynamic field variables A_{μ} and ψ, yields the coupled equations of motion

$$\begin{aligned} \partial_{\mu}F^{\mu\nu} &= 4\pi j^{\nu} \\ \left(i\gamma_{\mu}\partial^{\mu} - mc\right)\psi &= e\gamma_{\mu}A^{\mu}\psi. \end{aligned} \tag{5-5}$$

The first of these equations is the most general covariant form of the inhomogeneous Maxwell equations. It implies directly the continuity equation $\partial_\mu j^\mu = 0$. The second equation in (5-5) is the covariant Dirac equation in the presence of an external electromagnetic field. A more familiar form of the Dirac equation is obtained upon multiplication by βc from the left,

$$\left(\hat{h}_{D;A_\mu} - i\frac{\partial}{\partial t}\right)\psi = 0, \quad \hat{h}_{D;A\mu} = \beta mc^2 + \boldsymbol{\alpha}\cdot(-i\boldsymbol{\nabla} - e\mathbf{A}) - e\phi\,, \tag{5-6}$$

where $\hat{h}_{D;A\mu}$ is the Dirac Hamiltonian of a single electron in an external field. Dirac's α matrices have been introduced here for convenience, $\alpha = \gamma^0\gamma$. Note that the Dirac equation has been derived here from the least action principle, and is thus interpreted as an Euler-Lagrange equation for the spinor field ψ rather than a quantum mechanical wave equation for a single electron. Detailed accounts of the mathematical properties and physical interpretation of the Dirac equation, important for quantum chemistry, may be found in several recently published books [8–14], and will not be repeated here; some pertinent points will be addressed below. The operators appearing in the Dirac equation (5-6) are 4×4 matrix operators, and the corresponding wave function is therefore a 4-component vector function ψ. The upper and lower two components are generally referred to as the large and small components, respectively. The four degrees of freedom reflect the fact that the Dirac equation describes both electrons and positrons and explicitly includes spin. For a given external potential and the chosen charge $q = -e$, both the positive energy and negative energy solutions correspond to *electronic* states. For the same potential, the negative energy branch of the spectrum gives the positronic solutions indirectly, either by charge conjugation of the electronic solutions (see, e.g., [14, 15]) or, following the original idea of Dirac, by filling all negative energy continuum states with electrons using the Pauli principle (Dirac's filled sea) and then regarding the positrons as hole states in this electron-filled continuum.

In molecular electronic structure theory we employ $\hat{h}_{D;V}$, the Dirac operator in the nuclear field. It corresponds to the introduction of the 4-potential

$$\phi(\mathbf{r}_i) = \sum_A \frac{Z_A e}{|\mathbf{r}_i - \mathbf{R}_A|}; \quad \mathbf{A}(\mathbf{r}_i) = 0, \tag{5-7}$$

where $Z_A e$ and $\mathbf{R}_A$ are the charge and position of nucleus A. The nuclei are treated as sources of external scalar potentials, and nuclear spins are ignored. This "clamped nucleus" approximation is essentially the Born and Oppenheimer picture [16] in non-relativistic theory, in which the main assumption is that electrons follow the slower movements of nuclei adiabatically.

Our next step is the transition of the QED theory from Lagrangian to Hamiltonian formulation, using the Legendre transformation. This step requires the definition of the conjugate momenta

$$\pi = \frac{\partial \mathcal{L}_{\mathrm{QED}}}{\partial \dot{\psi}} = i\psi, \qquad \Pi_\mu = \frac{\partial \mathcal{L}_{\mathrm{QED}}}{\partial \dot{A^\mu}} = \frac{1}{4c} F_{\mu 0}. \tag{5-8}$$

After some tedious mathematical manipulations, the final QED Hamiltonian density is given by

$$\begin{aligned} \Re_{\mathrm{QED}} &= \Pi_\mu \dot{A^\mu} + \pi \dot{\psi} - \mathcal{L}_{\mathrm{QED}} = \\ &\frac{1}{8}(\mathbf{E}^2 + \mathbf{B}^2) + \frac{1}{4}\mathbf{E} \cdot \nabla\varphi - \overline{\psi}(i\gamma_\mu \partial^\mu - mc)\psi - e\overline{\psi}\gamma^\mu \psi A_\mu. \end{aligned} \tag{5-9}$$

This expression for the Hamiltonian density is no longer manifestly Lorentz or gauge invariant. However, all physical observables, including energies, field gradients, transition amplitudes, etc., which may be deduced from this Hamiltonian density, are Lorentz and gauge invariant. After integration over all space, using partial integration in the second term of (5-9) and the Gauss law, the QED Hamiltonian is obtained,

$$\begin{aligned} H_{\mathrm{QED}} &= \int dr^3 \Re_{\mathrm{QED}} = \\ &\int dr^3 \left\{ \frac{1}{8}(\mathbf{E}^2 + \mathbf{B}^2) + \psi^+ [\boldsymbol{\alpha} \cdot (-i\nabla - e\mathbf{A}) + \beta mc - e\varphi]\psi \right\}. \end{aligned} \tag{5-10}$$

Expression (5-10) is the Hamiltonian of the U(1) gauge field theory of interacting dynamic electromagnetic and fermionic fields, written in a particular gauge independent form. In the second quantized form of (5-10) all fields have been upgraded to field operators, acting on occupation number vectors in an appropriate Fock space with variable numbers of electrons/positrons and photons. One of the options in this canonical formalism is to express all physical observables by particle-antiparticle creation/destruction operators arranged in normal order, renormalizing the vacuum energy to zero. The problem of negative energy states is completely removed, since both electrons and positrons have positive energies due to normal ordering.

Unfortunately the expression (5-10), where the photonic degrees of freedom are involved explicitly, does not lead to analytical closed form electron–electron potential. Standard QED methods, such as Green's functions and S-matrix, use time-dependent Feynman diagram techniques to integrate over the photonic degrees of freedom and express the electron–photon exchange in a perturbation series. The main drawback of existing QED methods from the point of view of quantum chemistry is their ability to calculate just the first order energy correction, but not wave function corrections. Another important point is that most QED methods (with some exceptions, see [17, 18]) cannot treat degenerate or quasi-degenerate configurations, which are common in open shell heavy species. In quantum chemistry, the derivation of the Hamiltonian is distinct from solving for its eigenvalues; in contrast, the same QED approach is used both for deriving the potential (integrating over photonic degrees of freedom) and calculating the energy shift it causes. A novel powerful QED

method, with structure resembling that of stationary many-body approaches, has been developed recently by Lindgren and coworkers [18–23]. It offers the possibility of being merged with quantum chemical machinery based on the Bloch equation to provide a unified tool suitable for application to general quasidegenerate atomic and molecular configurations. This so-called covariant evolution operator (CEO) method is free of the computational drawbacks discussed above; it is described briefly in Section 5.5.1. The total number of particles in QED is not conserved, and electron–positron pair creation processes should be included in calculations. The number of photons is also variable, depending on the particular process. The CEO method has a particularly simple form when formulated in generalized Fock space with variable numbers of fermions and so-called uncontracted virtual photons. This is why we consider it a natural framework for implementing Fock-space many-body quantum chemical approaches, capable of describing systems with a variable number of particles. In particular, the relativistic Fock-space coupled cluster (FSCC) approach, which is an all-order, size extensive, multiroot, multireference method (for a recent review see [24]), is an ideal candidate for merging with CEO. We shall see below (Section 5.5) that the FSCC method may be used to derive the potential energy terms from a fully covariant relativistic many-body QED approach *and* solve this potential in an efficient and accurate manner. The relativistic FSCC method and its recent applications in the effective and intermediate Hamiltonian formulations are described in Sections 5.2, 5.3, and 5.4. In the last Section we present briefly an efficient way of simultaneously including the most important correlation and QED effects in all-order and size-extensive fashion, using summation of the many electron and photon contributions in a double (electronic and photonic) Fock space coupled cluster procedure based on the CEO method.

5.1.3. The No-Virtual-Pair Approximation

The very philosophy and structure of existing relativistic quantum chemistry methods, mostly adapted from the non-relativistic realm, are different from those of QED. Atomic and molecular systems are described in chemistry as systems with a finite number of particles interacting via instantaneous, energy independent two-body potentials. This picture, based on relativistic and quantum description of electrons and approximate (e.g. semi-classical) consideration of electromagnetic fields, ignores partially or fully some fundamental phenomena, such as the existence of the negative energy state continuum, radiative effects and retardation of the interparticle interactions, which are important for a fully covariant description. Fortunately, many of these QED corrections are numerically small for real atomic and molecular systems, explaining the relative success of rather simple semiclassical approximations of photonic fields. The most straightforward derivation of relativistic many-body Hamiltonians from the generic H_{QED} (5-10) ignores the multiphotonic quantum effects of radiation and electron–positron pair creation and adopts instead the so called zero frequency single photon exchange approximation for the electromagnetic

field, leading to interparticle two-body "classical" instantaneous potentials. The most advanced such 4-component time- (or energy-) independent Hamiltonian is the projected Dirac-Coulomb-Breit (DCB) electronic Hamiltonian

$$\hat{H}^{+}_{\mathrm{DCB}} = \sum_{i} \hat{h}_{D;V}(i) + \frac{1}{2} \sum_{i \neq j} \Lambda^{+}_{i} \{ \hat{g}^{\mathrm{Coulomb}}(i,j) + \hat{g}^{\mathrm{Breit}}(i,j) \} \Lambda^{+}_{j} \tag{5-11}$$

$$\Lambda^{+}_{i} = \sum_{n}^{+} \psi^{+}_{n}(x_i) \psi_{n}(x_i), \tag{5-12}$$

where $\hat{h}_{D;V}(i)$ are the one-electron 4-component Dirac operators in the molecular field. The interelectronic potential consists of two parts, the electrostatic Coulomb term $\hat{g}^{\mathrm{Coulomb}}(i,j) = e^2/r_{ij}$ and the Breit interaction, which includes leading magnetostatic and retardation effects [25],

$$\hat{g}^{\mathrm{Breit}}(1,2) = -\frac{e^2}{2c^2 r_{12}} \left[(c\alpha_1 \cdot c\alpha_2) + \frac{1}{r^2_{12}} (c\alpha_1 \cdot \mathbf{r}_{12})(c\alpha_2 \cdot \mathbf{r}_{12}) \right]. \tag{5-13}$$

The Breit term may be derived as the low-frequency limit of the single virtual photon exchange interaction in the Coulomb gauge ($\nabla \mathbf{A} = \mathbf{0}$) as described by QED (see Section 5.5.1). The projection operators onto the positive energy spectrum, Λ^{+}, are used to exclude the so-called "continuum dissolution determinants", which include electron–positron pairs, from the correlation part of the wave-function [26]. H^{+}_{DCB} gives the no virtual pair approximation (NVPA). The H^{+}_{DCB} Hamiltonian is not unique, since the distinction between electron and positron creation and annihilation operators, as well as the operators Λ^{+}, depend on the orbital set in which the field operators are expanded. The most popular choice is the solutions of the Dirac equation in the molecular bare nucleus or SCF field (5-7), leading to the Furry picture [27].

H^{+}_{DCB} is correct to second order in the fine-structure constant α, but is not covariant. Properly designed 4-component many-electron NVPA methods are currently the most accurate approaches for neutral and weakly-ionized atoms and molecules [28], and are used for benchmark calculations. Most of the many-body approaches implemented were adapted from the non-relativistic realm by using relativistically invariant double point groups, as well as Kramers (time-reversal) symmetry when applicable. In the atomic case, the high symmetry allows the separation of radial and angular degrees of freedom. The angular part may be solved analytically with the help of Racah algebra [29], whereas the radial equations may be solved by finite difference methods. In molecular calculations one has to resort to the *algebraic approximation*, the use of finite basis set expansions. This approximation is often used for atoms too.

The coupled cluster (CC) approach is the most powerful and accurate of electron correlation methods. This has been shown in many benchmark applications

of 4-component relativistic CC methods to atoms [30–36] and molecules [37–43]. The CC method is an all-order, size-extensive and systematic many-body approach. Multireference variants of relativistic 4-component CC methods capable of handling quasidegeneracies, which are important for open-shell heavy atomic and molecular systems, have been developed in recent years [34–37, 39, 43]. In particular, the multireference FSCC scheme is applicable to systems with a variable number of particles [44, 45], and is an ideal candidate for merging with QED theory to create an infinite-order size-extensive covariant many-body method applicable to systems with variable numbers of paricles and photons.

5.2. THE NVPA MULTIROOT MULTIREFERENCE FOCK-SPACE COUPLED CLUSTER METHOD

Here we describe the FSCC method, followed by the more recent and powerful intermediate Hamiltonian approach. The latter is illustrated by representative applications demonstrating its capabilities.

5.2.1. Basic FSCC Method

The NVPA Dirac-Coulomb-Breit Hamiltonian H^+_{DCB} may be rewritten in second-quantized form [46, 47] in terms of normal-ordered products of spinor creation and annihilation operators $\{a_r^+ a_s\}$ and $\{a_r^+ a_s^+ a_u a_t\}$, corresponding to the Furry picture,

$$H = H^+_{\mathrm{DCB}} - \langle 0|H^+_{\mathrm{DCB}}|0\rangle = \sum_{rs} f_{rs}\{a_r^+ a_s\} + \frac{1}{4}\sum_{rstu}\langle rs||tu\rangle\{a_r^+ a_s^+ a_u a_t\}. \qquad (5\text{-}14)$$

Here f_{rs} and $\langle rs||tu\rangle$ are, respectively, elements of the one-electron Dirac-Fock-Breit and antisymmetrized two-electron Coulomb-Breit interaction matrices over Dirac four-component spinors. The effect of the projection operators Λ^+ is now taken over by normal ordering, denoted by the curly braces in (5-14), which requires annihilation operators to be moved to the right of creation operators as if all anticommutation relations vanish. The Fermi level is set at the top of the highest occupied positive energy state, and the negative energy states are ignored.

The development of a general multiroot multireference scheme for treating electron correlation effects usually starts from consideration of the Schrödinger equation for a number (d) of target states,

$$H\Psi^\alpha = E^\alpha \Psi^\alpha \quad , \alpha = 1, ..., d. \qquad (5\text{-}15)$$

The physical Hamiltonian is divided into two parts, $H = H_0 + V$, so that V is a small perturbation to the zero-order Hamiltonian H_0, which has known eigenvalues and eigenvectors, $H_0|\mu\rangle = E_0^\mu|\mu\rangle$.

The case of exact or quasi-degeneracy, occurring in many open shell heavy compound systems, involves the equality or near equality of some energy values E_0^α. By adopting the NVPA approximation, a natural and straightforward extension of the nonrelativistic open-shell CC theory emerges. The multireference valence-universal Fock-space coupled-cluster approach is presented here briefly; a fuller description may be found in [44, 45]. FSCC defines and calculates an effective Hamiltonian in a d-dimensional model space $P = \sum |\mu\rangle \langle\mu|$, $\mu = 1, .., d$, comprising the most strongly interacting zero order many electron wave functions. All other functions are in the complementary Q-space, so that $P+Q = 1$. All d eigenvalues of H_{eff} coincide with the relevant eigenvalues of the physical Hamiltonian,

$$H_{\text{eff}}\Psi_0^\alpha = E^\alpha \Psi_0^\alpha \ , \alpha = 1, ..., d. \tag{5-16}$$

There is no summation over the index α, and $\Psi_0^\alpha = C_\mu^a |\mu\rangle$, $\alpha = 1, ..., d$ describes the projection $P\Psi^\alpha$, which constitutes the major part of Ψ^α. The effective Hamiltonian has the form [30, 48]

$$H_{\text{eff}} = PH\Omega P \ , \ H_{\text{eff}} = H_0 + V_{\text{eff}}. \tag{5-17}$$

Ω is the normal-ordered wave operator, mapping the eigenfunctions of the effective Hamiltonian onto the exact ones, $\Omega\Psi_0^\alpha = \Psi^\alpha$, $\alpha = 1, ..., d$. It satisfies intermediate normalization, $P\Omega P = P$. The effective Hamiltonian and wave operator are connected by the generalized Bloch equation, which for a complete model space P may be written in the compact linked form [48]

$$Q[\Omega, H_0]P = Q(V\Omega - \Omega H_{\text{eff}})_{\text{linked}} P. \tag{5-18}$$

Ω is parameterized exponentially in the coupled cluster method. A particularly compact form is obtained with the normal ordered form $\Omega = \{\exp(S)\}$.

The Fock-space approach starts from a reference state (closed-shell in our applications, but other single-determinant functions may also be used), correlates it, then adds and/or removes electrons one at a time, recorrelating the whole system at each stage. The sector (m, n) of the Fock space includes all states obtained from the reference determinant by removing m electrons from designated occupied orbitals, called valence holes, and adding n electrons in designated virtual orbitals, called valence particles. The practical limit is $m + n \leq 2$, although higher sectors have also been tried [49]. The excitation operator S, defined by the exponential parameterization of Ω, is partitioned into sector operators $S = \sum_{m\geq 0} \sum_{n\geq 0} S^{(m,n)}$. This partitioning allows for partial decoupling of the open-shell CC equations according to the so called subsystem embedding condition [44]. The equations for the (m, n) sector involve only S elements from sectors (k, l) with $k \leq m$ and $l \leq n$, so that the very large system of coupled nonlinear equations is separated into smaller subsystems, which are solved consecutively: first, the equations for $S^{(0,0)}$ are iterated to convergence; the $S^{(1,0)}$ (or $S^{(0,1)}$) equations are then solved using the known $S^{(0,0)}$, and so on.

This separation, which is exact, reduces the computational effort significantly. The effective Hamiltonian (5-17) is also partitioned by sectors. An important advantage of the method is the simultaneous calculation of a large number of states.

Each sector excitation operator is, in the usual way, a sum of virtual excitations of one, two, ..., electrons, normally truncated at some point. The level of truncation reflects the quality of the approximation, i.e., the extent to which the complementary Q space is taken into account in the evaluation of the effective Hamiltonian. The applications described below are truncated at the CCSD level, and involve the fully self-consistent, iterative calculation of all one- and two-body virtual excitation amplitudes, with all relevant diagrams summed to infinite order. The FSCC equations for a particular (m, n) sector of the Fock space are derived by inserting the normal-ordered wave operator into the Bloch equation (5-18). The final form of the FSCC equation for a complete model space includes only *connected* terms [30, 48],

$$Q[S_l^{(m,n)}, H_0]P = Q\{(V\Omega - \Omega H_{\text{eff}})_l^{(m,n)}\}_{\text{conn}}P, \tag{5-19}$$

$$H_{\text{eff}}^{(m,n)} = P(H\Omega)_{\text{conn}}^{(m,n)}P\,. \tag{5-20}$$

As negative energy states are excluded from the Q space, the diagrammatic summations in the CC equations are carried out only within the subspace of the positive energy branch of the DF spectrum. After converging the FSCC equation (5-19), the effective Hamiltonian (5-20) is diagonalized, yielding directly transition energies. The effective Hamiltonian in the FSCC approach has "diagonal" structure with respect to the different Fock-space sectors. From (5-20) it follows that two Fock space sectors belonging to a common Hilbert space (with the same number of particles) do not mix even if they have strongly interacting states. This means that important nondynamic correlation effects are approximated. The mixed-sector CC presented below avoids this problem.

The FSCC equation (5-19) is solved iteratively, usually by the Jacobi algorithm. As in other CC approaches, denominators of the form $(E_0^P - E_0^Q)$ appear, originating in the left-hand side of the equation. The well-known intruder state problem, appearing when some Q states are close to and strongly interacting with P states, may lead to divergence of the CC iterations. The intermediate Hamiltonian method avoids this problem in many cases and allows much larger and more flexible P spaces.

5.2.2. The Intermediate Hamiltonian CC Method

5.2.2.1. Need and Formulation

The accuracy and convergence of the Fock-space coupled cluster method depend on an appropriate partitioning of the function space into P and Q subspaces. Ideally, the P space should include all functions important to the states considered, since the effective Hamiltonian is diagonalized in P, whereas Q-space contributions are included approximately. On the other hand, convergence of the coupled cluster

iterations is enhanced by maximal separation and minimal interaction between P and Q. These requirements are not always easy to reconcile. Relatively high P functions have often strong interaction with or are energetically close to Q states, making convergence slow or impossible. The offending functions are usually included in P because of their significant contribution to the lower P states, and we may not be particularly interested in the correlated states generated from them by the wave operator; however, the FSCC is an all-or-nothing method, and lack of convergence means that no states at all are obtained. The intermediate Hamiltonian coupled cluster method developed recently [50] addresses this problem, making possible larger and more flexible P spaces, thereby extending the scope of the coupled cluster method and increasing its accuracy.

An additional advantage of the ability to use extended model spaces may be reducing the need for including high excitation levels in the formalism. The need for high excitations (triple and higher) is usually limited to a small group of virtual orbitals. If such orbitals are brought into P, all excitations involving them are included to infinite order by diagonalizing the effective Hamiltonian, avoiding the need for the (usually expensive) treatment of their contribution to dynamical correlation.

The intermediate Hamiltonian method has been proposed by Malrieu [51] in the framework of degenerate perturbation theory. The P space is partitioned into the main P_m subspace, which includes all the states of interest, and the intermediate P_i subspace, serving as a buffer between P_m and the rest of the functional space Q. The corresponding operators satisfy the equations

$$P_m + P_i = P\,, \qquad P + Q = 1\,. \tag{5-21}$$

The rationale for this partitioning is the following: the relatively high states in P contribute significantly to the states of interest, which evolve from the lower P states, but couple strongly with intruders from Q and spoil the convergence of the iterations; they should therefore be treated differently from the lower states. This goal is achieved by partitioning P and allowing more approximate treatment of P_i states. The intermediate Hamiltonian H_I is constructed in P according to the same rules as the effective Hamiltonian,

$$H_I = PH\Omega P\,, \tag{5-22}$$

but only $|\Psi_m\rangle$ states with their largest part in P_m are required to have energies E_m closely approximating those of the physical Hamiltonian,

$$H_I P|\Psi_m\rangle = E_m P|\Psi_m\rangle\,. \tag{5-23}$$

The other eigenvalues, which correspond to states $|\Psi_i\rangle$ with the largest components in P_i, may be more or less accurate. This leads to some freedom in defining the relevant eigenfunctions and eigenvalues, and, therefore, in the evaluation of problematic QSP_i

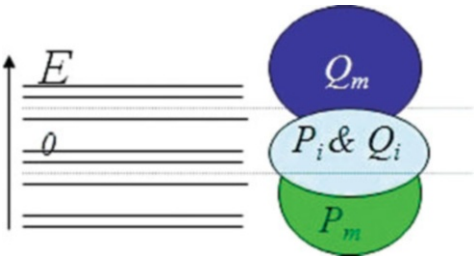

Figure 5-1. Model spaces in the modified intermediate Hamiltonian method

matrix elements. To limit this freedom and make the approach more general and flexible, we also use the partitioning

$$Q = Q_i + Q_m. \tag{5-24}$$

This additional partitioning narrows the overlap of the P and Q energies, which becomes limited to P_i and Q_i subspaces (see Figure 5-1), reducing the number of problematic amplitudes, now $Q_i S P_i$.

Partitioning the P and Q projectors of the FSCC equation (5-19) into the main and intermediate parts by formulas (5-21, 5-24) yields four coupled CC equations,

$$Q_m[S, H_0]P_m = Q_m\{V\Omega - \Omega H_{\text{eff}}\}_{\text{conn}}P_m \tag{5-25}$$
$$Q_i[S, H_0]P_m = Q_i\{V\Omega - \Omega H_{\text{eff}}\}_{\text{conn}}P_m \tag{5-26}$$
$$Q_m[S, H_0]P_i = Q_m\{V\Omega - \Omega H_{\text{eff}}\}_{\text{conn}}P_i \tag{5-27}$$
$$Q_i[S, H_0]P_i = Q_i\{V\Omega - \Omega H_{\text{eff}}\}_{\text{conn}}P_i. \tag{5-28}$$

Only the last of these can cause convergence problems. Successful replacement of this equation by another, based on physical considerations, is the central point of the IH method. The new equation to be used instead of (5-28) will be called the *IH condition* (IHC). Ideally, it should satisfy the following demands:

- be free of convergence problems;
- have minimal impact on the other coupled equations (5-25), (5-26), and (5-27).

Subject to these demands, the IHC should be as close to (5-28) as possible.

Several IH FSCC methods have been developed and applied recently, based on different IH conditions. The first such approach [50], denoted IH1, uses the condition

$$Q_i \Omega P_m H \Omega P_i = Q_i H \Omega P_i, \tag{5-29}$$

which is similar to the equation proposed by Malrieu and applied up to the 3rd order of degenerate perturbation theory [51]. While Malrieu's scheme could not go

beyond 3rd order because terms with small denominators appear, the IH CC variants developed in our group are all-order and may be used in the framework of any multireference CC formulation.

The next IH FSCC scheme (IH2) is based on the perturbation expansion of the problematic Q_iSP_i amplitudes. In the lowest order we simply take

$$Q_iSP_i = 0. \tag{5-30}$$

This type of IH condition has also been used for developing a new type of hybrid multireference coupled cluster schemes, including the mixed sector CC presented below.

Another IH condition leads to the most flexible and useful scheme, the extrapolated IH (XIH) [52, 53], which can yield correct solutions both for P_m and P_i, thus recovering the whole effective Hamiltonian spectrum in the extended model space P. This can be accomplished even when the standard FSCC approach using the same model space P has intruder states leading to divergence. The IH condition for the XIH approach has the form

$$Q_i[S, H_0 + P_i\Delta P_i]P_i = Q_i\{\beta\Delta S + V\Omega - \Omega H_{\text{eff}}\}_{\text{conn}}P_i. \tag{5-31}$$

Δ is an energy shift parameter, correcting small energy denominators for the problematic intruder states. A compensation term with the multiplicative parameter β ($\beta \leq 1$) is added on the right-hand side. For $\beta = 1$, the $P_i\Delta P_i$ term on the left-hand side is fully compensated, so that (5-31) is equivalent to (5-28). Proper choice of the two parameters makes it possible to reach convergence in (5-31) and thus in the non-problematic equations (5-25), (5-26), and (5-27). Several calculations with different values of the parameters allow extrapolation of both P_m and P_i level energies to the limit $\Delta \to 0$ or $\beta \to 1$. This extrapolation was found to be robust, in most cases linear for P_m states and quadratic for states in P_i. In the extrapolation limit the IH method transforms into the effective Hamiltonian approach. The XIH approach is asymptotically size extensive and in many cases size consistent, even for incomplete P_m, requiring only that the entire model space P is complete. A somewhat similar IH FSCC scheme has been proposed by Mukhopadhyay et al. [54], but to the best of our knowledge has never been implemented.

The intermediate Hamiltonian approaches presented here may be applied within any multiroot multireference infinite order method. Recently [55] we implemented the XIH scheme to another all-order relativistic multiroot multireference approach, the Hilbert space or state universal CC, which is the main alternative to and competitor of Fock-space CC. The HSCC is based on the Jeziorski-Monkhorst parameterization of the wave operator [56], which in the normal ordered form is

$$\Omega = \sum_{\mu=1}^{d}\Omega_\mu = \sum_{\mu=1}^{d}\{\exp(S^\mu)\}P^\mu;\ P^\mu = |\mu\rangle\langle\mu|. \tag{5-32}$$

Here every determinant μ belonging to the P space serves as a reference state (Fermi vacuum), and the excitation operators S^μ are vacuum dependent. The nature of the determinants in the model space may be general; the only requirement is that all determinants belong to the same Hilbert space. The most useful scheme is probably the HSCC approach with a model space built of general MCSCF solutions. This will make the HSCC method suitable for global potential surface calculations. The XIH-HSCC equation in the case of complete model space P is

$$\begin{aligned}
&[S^\mu, H_0 + P_i \Delta P_i] P^\mu = \\
&\{\beta \Delta S^\mu P_i P^\mu + V\{\exp(S^\mu)\} P^\mu - \{\exp(S^\nu)\} P^\nu H_{\text{eff}} P^\mu\}_{\text{conn}} \\
&P^\nu H_{\text{eff}} P^\mu = P^\nu (H\{\exp(S^\mu)\})_{\text{conn}} P^\mu .
\end{aligned} \tag{5-33}$$

The HSCC effective Hamiltonian (5-33), unlike the FSCC effective Hamiltonian, has non-diagonal structure, coupling different Fock-space sectors belonging to the same Hilbert space. This leads to better treatment of nondynamic correlation. A *mixed sector coupled cluster* (MSCC), which may be regarded as a hybrid approach combining the advantages of FSCC and HSCC, has recently been derived [57] within the IH2 method based on IHC (5-30). The MSCC exponential parameterization of the wave operator Ω and the working equation are formally similar to those of FSCC (5-19), but the subsystem embedding condition is now relaxed and several sectors of Fock space belonging to the same Hilbert space mix and are diagonalized together. MSCC may thus yield the most balanced inclusion of dynamic and nondynamic correlation effects. Implementation of the XIH method to higher sectors (up to six valence electrons/holes [49]) of the Fock space is also in progress [58]. All the multireference multiroot CC methods described above may be used for the challenging task of benchmark calculations for heavy quasidegenerate systems with more than two electrons/holes in the valence open shell.

Summing up, we conclude that the IH method is an efficient and universal tool, applicable to all multiroot multireference methods. It avoids intruder states, while at the same time allowing the use of large, complete model spaces, improving significantly the accuracy of the calculation.

5.2.2.2. Demonstrating the Power of IH Methods

A major advantage of the intermediate Hamiltonian approach is the flexibility in selecting the model space. This has been a major problem in applying the Fock-space scheme, as noted at the beginning of this section. While in the Fock-space coupled cluster method one may consider oneself lucky to find any partitioning of the function space into P and Q with convergent CC iterations, the intermediate Hamiltonian method makes it possible for the first time to vary the model space systematically and study the effect upon calculated properties. An example is provided by the calculation of the electron affinity of alkali atoms by the IH1 method [59]. The P_m and P_i spaces were increased until the EAs converged to 1 meV, giving agreement of 5 meV or better with experimental values [60].

Another benefit of the IH approach is its increased scope of applicability in terms of states amenable to calculation, determined primarily by the model space selected. Two examples demonstrate this point:

- Excited states of Ba and Ra were calculated by FSCC, starting from the M^{2+} reference and adding two electrons [61]. The only model space giving convergence for Ba included all states with two electrons in the $5d$, $6s$ and $6p$ orbitals, excluding the $6p^2$ states. The IH method made possible larger model spaces, giving many more states as well as higher accuracy [62]. All states used in FSCC, plus $6p^2$, were put in P_m; P_i was defined by adding states with occupied $7s$–$10s$, $7p$–$10p$, $6d$–$9d$, and $4f$–$6f$ orbitals, yielding a very large P ($= P_m + P_i$) space. The mean absolute error in states accessible to both methods was reduced by a factor of 5, from 742 cm^{-1} (relative error 3.11%) for FSCC to 139 cm^{-1} (relative error 0.69%) for IH. In addition, many more states, including those belonging to the $6p^2$ term, were obtained [62]. Similar results were obtained for Ra.
- In the rare gases Xe and Ar, the neutral closed-shell atoms provide a natural choice for reference state, and the excited states are therefore in the 1-hole 1-particle sector. The excitation energies are relatively high and not too far apart, and we could not find *any* partitioning leading to convergence of the Fock-space coupled cluster iterations. The improved convergence properties of the intermediate Hamiltonian approach solved this problem [63]. Over 20 excitation energies of each atom were obtained, with an average error of 0.06 eV (0.6%). The original publication may be consulted for details.

5.3. APPLICATIONS: HEAVY ELEMENTS

Quantitative description of heavy atoms requires high-level inclusion of both relativity and correlation. These two effects are non-additive, as demonstrated in our early work on the gold atom [34]. The reasons are obvious: the spatial distribution of the relativistic orbitals differs significantly from that of non-relativistic counterparts (s and p orbitals undergo contraction, whereas d and f orbitals expand), leading to correlation energy changes.

Representative applications of the NVPA Fock-space CC method to heavy atoms are listed below. These are just a small fraction of the many calculations carried out over the last 15 years, addressing various atomic systems with dozens of transition energies calculated per atom. Most results agreed with experiment within a few hundredths of an eV. A fuller description may be found in the original publications and in our recent review [1].

The spherical symmetry of atoms, which leads to angular decomposition of the wave function and coupled cluster equations, is used at both the Dirac-Fock-Breit [46] and CC [34, 64] stages of the calculation. The energy integrals and CC amplitudes, which appear in the Goldstone-type diagrams defining the CC equations, are decomposed in terms of vector coupling coefficients, expressed by angular

momentum diagrams, and reduced Coulomb-Breit or S matrix elements, respectively. The reduced equations for single and double excitation amplitudes are derived using the Jucys-Levinson-Vanagas theorem [30] and solved iteratively. This technique makes possible the use of large basis sets with high l values, as a basis orbital gives rise to two functions at most, with $j = l \pm 1/2$, whereas in Cartesian coordinates the number of functions increases rapidly with l. Typically we go up to h ($l = 5$) or i ($l = 6$) orbitals, but higher orbitals (up to $l = 8$) have been used. To account for core-polarization effects, which may be important for many systems, we correlate at least the two outer shells, usually 20–50 electrons, but as many as 119 electrons were correlated for the anion of element 118 (Section 5.4.3). Finally, uncontracted Gaussians are used, since contraction leads to problems in satisfying kinetic balance and correctly representing the small components. On the other hand, it has been found that high-energy virtual orbitals have little effect on the transition energies we calculate, since these orbitals have nodes in the inner regions of the atom and correlate mostly the inner-shell electrons, which we do not correlate anyway. These virtual orbitals, with energies above 80 or 100 hartree, are therefore eliminated from the CC calculation, constituting in effect a post-SCF contraction.

The Fock-space coupled cluster and its intermediate Hamiltonian extension have been incorporated into the DIRAC package [65], opening the way to molecular applications. The heavy species NpO_2^+, NpO_2^{2+}, and PuO_2^{2+} were calculated, giving access to the ground and many excited states and leading to reassignment of some of the observed spectroscopic peaks [41]. A later application addressed UO_2 and UO_2^+ [42], with less conclusive results, due to the highly complicated open-shell character of these species.

Most of the applications involved heavy atomic systems, and proved the power of the method. A few examples are described in the current section. These successes make the FSCC and IH approaches a useful tool for predicting properties of superheavy elements, not easy to access experimentally. Applications to these elements may be found in Section 5.4.

5.3.1. Ionization Potentials and Electron Affinities of Alkali Atoms: 1 meV Accuracy

Alkali atoms are basically one-valence-electron systems, and correlation would therefore not be expected to play a major role in the determination of properties such as ionization potentials. Nevertheless, a Hartree-Fock (or, for the heavier alkali atoms, Dirac-Fock) calculation gives sizable errors for this property. If accuracy below the 1% level is desired, as would be needed, for example, in studies of parity nonconservation effects [66], high-level treatment of correlation is essential. The Fock-space CC method was applied to all alkali atom IPs [64] using extensive, converged basis sets. The results, with 0.02–0.11% deviation from experiment, were better than any previous calculation. Further improvement was given by the XIH method, which gave agreement of 1 meV for all alkali atoms [53]. Similar accuracy was obtained for the electron affinities of the alkali atoms [52] and for transition energies of alkaline earth atoms [67].

5.3.2. The f^2 Levels of Pr^{3+}: Dynamic Correlation

Lanthanides and actinides possess open f shells, which give rise to large manifolds of closely spaced states. As an example of these systems we discuss the energy levels of the Pr^{3+} ion, which has an f^2 ground state configuration. The spectrum is well characterized experimentally [68] and provides a good test for high-accuracy methods incorporating relativity and correlation. The system has been studied by both MCDF and Fock-space CC, and comparison between these methods can therefore be made.

The MCDF calculations [69] involved between 354 and 1,708 CSFs for the different J states. The number of CSFs was much larger in the CC calculations [70], since all excitations from the $4spdf5sp$ orbitals to virtual orbitals with energies up to 100 hartree, as well as excitations from $4spd5sp$ to the partially filled $4f$, were included. Thus, a much larger part of dynamic correlation was accounted for. The Pr^{5+} closed shell state served as reference, and two electrons were added in the $4f$ shell to obtain the levels of interest. Three basis sets were used, with l going up to 4, 5 and 6, giving mean absolute errors of 394, 245 and 222 cm^{-1}, respectively. This may be compared with the 853 cm^{-1} MAE of the MCDF calculation.

5.3.3. Properties: Nuclear Quadrupole Moments

Nuclear quadrupole moments (NQM) are of considerable interest in chemical spectroscopy. They are also required in nuclear physics for testing nuclear models. One of the best ways to determine the nuclear quadrupole moment Q is by combining the experimental nuclear quadrupole coupling constant B, also known as the electric quadrupole hyperfine interaction constant, with accurate calculations of the electric field gradient (EFG) at the nucleus, q. The nuclear quadrupole coupling constant is given by the relation $B = -eqQ/h$, where e is the absolute value of the electron charge and h is Planck's constant.

Atomic and molecular properties, such as the nuclear quadrupole moment, are usually observed via the energy shifts generated by coupling to an external field. The desired property is the derivative of the energy with respect to the external field. We used the finite field method [71] to calculate the EFG at the relevant nuclei. The interaction with an arbitrary NQM Q is added to the Hamiltonian $\hat{H}_0$, giving $\hat{H}(Q) = \hat{H}_0 - eqQ/h$. The Dirac-Coulomb Hamiltonian for the atom served as $\hat{H}_0$. The energy, which is the expectation value of $\hat{H}(Q)$, may be expanded as a power series in Q, and the EFG is obtained by

$$\left.\frac{dE(Q)}{dQ}\right|_{Q=0} = -\frac{e}{h}\langle\Psi_0|\hat{q}_{zz}|\Psi_0\rangle. \tag{5-34}$$

Conflicting considerations determine the value of Q used in practice. The energy change must be large enough not to disappear in the precision of the calculations, but too large a perturbation may go beyond the linear regime and introduce errors in the derivative. Linearity is therefore monitored throughout the application.

The calculations were carried out using the DIRAC relativistic ab initio electronic structure program [65]. Nuclei were described by the Gaussian finite nucleus model, and the uncontracted well tempered basis set of Huzinaga and Klobukowski [72] was employed; it was systematically extended until the calculated EFG converged to 0.1%. The Hamiltonian used includes the external field from the start, so that the Dirac-Hartree-Fock orbitals already see it. Previous attempts of adding the field at the perturbative (coupled cluster) step were less satisfactory.

The first application addressed the halogen atoms Cl, Br and I [73]. The electric field splits the $P_{3/2}$ atomic levels into two sublevels separated by $2B$, and the size of the splitting as function of Q gives the required derivative, from which the electric field gradient is calculated. Using the splitting rather than the energy shift of individual levels has the advantage that the second-derivative term in the series expansion of $E(Q)$ cancels out, and deviation from linearity starts with the cubic term. An additional advantage is that the splitting vanishes identically for $Q = 0$. The effect of the Gaunt term, the major part of the Breit interaction, is obtained at the Dirac-Hartree-Fock level by taking the expectation value of the relevant operator. The total size of the effect is small, well below 1%, and the neglect of interaction between Gaunt and correlation contributions is not significant.

Using the calculated EFG values and the experimental B values [74–76], the following NQM values are obtained: $Q(^{35}\mathrm{Cl}) = -81.1(1.2)$ mb, $Q(^{79}\mathrm{Br}) = 302(5)$ mb, and $Q(^{127}\mathrm{I}) = -680(10)$ mb. The Q of Cl agrees with the previous reference value of $-81.65(80)$ mb [77], while that of Br differs somewhat from the accepted 313(3) mb. Iodine shows the largest correction to the previous $-710(10)$ mb, in line with the $-696(12)$ mb obtained from molecular calculations [78]. A more detailed discussion may be found in [73].

An even more interesting case is that of ^{179}Au, where the long accepted muonic value of 547(16) mb [77] had been challenged [79]. Gold presents a particularly tough case, possibly because of relatively small EFG at its nucleus. Experimentally, the EFG is highly sensitive to the molecular environment, as shown by the large NQCC differences between AuCl (9.6 MHz) and its noble gas complexes (-259.8 for Ar-AuCl, -349.9 MHz for Kr-AuCl) [80]. Computationally, very strong dependence on the gold-containing molecule and the particular method used has been observed [81], with the EFG varying between -0.374 and $+0.746$ a.u. for the AuX molecules (X=F,Cl,Br,I) calculated with the Dirac-Coulomb and Douglas-Kroll Hamiltonians at the CCSD(T) level, yielding NQM values from -1.51 to $+0.65$ b. A recent molecular calculation [82] obtained 510(15) mb.

We applied the finite-field FSCC method [83] using both the well-tempered [72] and universal [84] basis sets. An intrinsic check is provided by the availability of two independent sets of quadrupole coupling constants for the $^2D_{5/2}$ and $^2D_{3/2}$ states [85]. The difference between NQMs calculated for the two states was $\sim$1% for medium size basis sets, going down to 0.1% for the largest sets. Our final result is $Q(^{197}\mathrm{Au}) = 521(7)$ mb, in good agreement with the molecular 510(15) mb [82].

More recently, the NQMs of Ga and In were calculated [86].

5.4. APPLICATIONS: SUPER-HEAVY ELEMENTS

As may be expected, the effect of relativity increases when we go to super-heavy elements. This term is usually applied to elements with atomic number above 100 (trans-fermium elements). The chemistry of some of these elements has been studied [87, 88]. An important relativistic effect involves changes in the level ordering, leading sometimes to a ground state configuration which differs from that of lighter atoms in the same group and, consequently, to different chemistry.

5.4.1. Ground States of Rutherfordium and Roentgenium

The ground state configuration of an element is the main determining factor of its chemistry. The deviation of superheavy elements from the ground state of the lighter homologues is therefore a most interesting question. Here we briefly discuss this problem in two cases, Rf (element 104) and Rg (element 111).

The nature of the rutherfordium ground state has been a subject of interest for a long time. Rutherfordium is the first atom after the actinide series, and in analogy with the lighter group-4 elements it should have the ground-state configuration $[\mathrm{Rn}]5f^{14}6d^27s^2$. Keller [89] suggested that the relativistic stabilization of the $7p_{1/2}$ orbital would yield a $7s^27p_{1/2}^2$ ground state. MCDF calculations [90, 91] found that the $7p^2$ state was rather high; they indicated a $6d7s^27p$ ground state, with the lowest state of the $6d^27s^2$ configuration higher by 0.5 [90] or 0.24 eV [91]. The two calculations are similar, using numerical MCDF [92] in a space including all possible distributions of the four external electrons in the $6d$, $7s$ and $7p$ orbitals, and the difference may be due to the different programs used or to minor computational details. These MCDF calculations take into account nondynamic correlation only, which is due to near-degeneracy effects and can be included by using a small number of configurations. A similar approach by Desclaux and Fricke [93] gave errors of 0.4–0.5 eV for the energy differences between $(n-1)d$ and np configurations of Y, La and Lu, with the calculated np energy being too low. Desclaux and Fricke corrected the corresponding energy difference in Lr by a similar amount [93]. A similar shift in the MCDF results for Rf would reverse the order of the two lowest states. A careful study of electron correlation has therefore been undertaken, increasing gradually the number of correlated electrons and the space of virtual orbitals [94]. It was found that including correlation at the level adopted by the MCDF calculations leads, indeed, to a $6d7p$ ground state. However, improving the correlation treatment by increasing the number of correlated electrons and/or the space of virtual orbitals favors the $6d^2$ configuration, and the converged result showed it was 0.3 eV lower than the $6d7p$. The final basis included $34s24p19d13f8g5h4i$ G-spinors, and the external 36 electrons were correlated. The details may be found in the original publication [94].

This example shows the intricate interplay of relativity and correlation. It is well known that relativity stabilizes p vs. d orbitals, and correlation has the opposite effect. When both effects are important and the result not obvious a priori, one

must apply methods, such as relativistic CC, which treat relativity and correlation simultaneously to high order.

A simpler case is that of Rg. The electron configuration of the coinage metals Cu, Ag and Au is $(n-1)d^{10}ns^1$. It was suspected that the strong stabilization of s vs. d orbitals may lead to a $(n-1)d^9ns^2$ ground state for Rg. This stabilization leads to a substantial reduction of the $(n-1)d \rightarrow ns$ transition energy in Au relative to what is expected by extrapolating the corresponding energies in Cu and Ag, a reduction responsible for many of the interesting properties of gold. Our first application of FSCC to superheavy elements was aimed therefore at Rg [95]. It was indeed found that the ground state of Rg was $6d^97s^2$, which lies 3 eV below $6d^{10}7s^1$.

5.4.2. Electronic Spectrum of Nobelium (Z = 102) and Lawrencium (Z = 103)

The spectroscopic study of super-heavy atoms presents a severe challenge to the experimentalist. While certain chemical properties of these elements may be elucidated in single-atom experiments [87, 88], spectra can be measured only in sizable samples. The first such study of a superheavy atom [96] used 2.7×10^{10} atoms of ^{255}Fm with a half life of 20.1 h, and was accompanied and guided by MCDF predictions of spectral energies. No and Lr have shorter lifetimes, on the order of seconds, and spectroscopic measurements for them were undertaken by a collaboration based at GSI [97]. The low production rates of the atoms and their short lifetimes necessitate reliable prediction of the position of transition lines, to avoid the need for broad wavelength scans. Theoretical studies are also crucial for line identification. Four-component FSCC calculations were carried out for No [98] and Lr [99]. The accuracy of the predicted spectra for these elements was estimated by applying the same method to ytterbium [98] and lutetium [99], their lighter homologues, where experimental transition energies are available. Large, converged basis sets ($37s31p26d21f16g11h6i$) and P spaces (up to $8s6p6d4f2g1h$) were used in the framework of the IH-FSCC method. Many electrons (42 for No, 43 for Lr) were correlated, so that any core polarizations effects were included. The mean absolute error for the 20 lowest excitation energies was 0.04 eV for Yb, 0.05 eV for Lu. The calculated IP of No was 6.632 eV, in agreement with the semiempirically extrapolated value of 6.65(7) eV [100]. The simulated spectra of the two atoms may be seen in Refs. [98, 99]. The salient feature of the No spectrum is a strong line at $30{,}100 \pm 800\,\mathrm{cm}^{-1}$, with an amplitude $A = 5 \times 10^8 \mathrm{s}^{-1}$. Other lines have amplitudes at least one order of magnitude lower. Lr is predicted to have two strong lines in the prime observation range ($20{,}000$–$30{,}000\,\mathrm{cm}^{-1}$), at $20{,}100$ and $28{,}100\,\mathrm{cm}^{-1}$.

5.4.3. Can a Rare Gas Atom Bind an Electron?

One of the most dramatic effects of relativity is the contraction and concomitant stabilization of s orbitals. An intriguing question is whether the $8s$ orbital of element 118, the next rare gas, would be stabilized sufficiently to give the atom a positive

electron affinity. Using the neutral atom Dirac-Fock orbitals as a starting point raises a problem, since the 8*s* orbital has positive energy and tends to "escape" to the most diffuse basis functions. This may be avoided by calculating the unoccupied orbitals in an artificial field, obtained by assigning partial charges to some of the occupied shells. The nonphysical fields are compensated by including an appropriate correction in the perturbation operator. A series of calculations with a variety of fields gave electron affinities differing by a few wave numbers [101], from which an electron affinity of 0.056(10) eV was deduced. More recently, the issue of possible quantum electrodynamic effects on this quantity was raised. The impetus was a calculation of QED effects on the ionization potential of E119, which was estimated at 0.0173 eV [102], of the same order as the calculated EA of 118. Thus, QED effects could change the EA significantly, and their treatment was undertaken [103].

An improved basis set with 36*s*32*p*24*d*22*f*10*g*7*h*6*i* uncontracted Gaussian-type orbitals was used and all 119 electrons were correlated, leading to a better estimate of the electron affinity within the Dirac-Coulomb-Breit Hamiltonian, 0.064(2) eV [103]. Since the method for calculating the QED corrections [102] is based on the one-electron orbital picture, the 8*s* orbital of E118 was extracted by projecting the 119-electron CC correlated function of the anion onto the 118-e correlated function of the neutral species. Using the resulting orbital and the total electron density, the self-energy and vacuum polarization terms were calculated, giving a total QED effect of 0.0059(5) eV, thereby reducing the electron affinity by 9% (for details see Ref. [103]). This is the largest QED effect found so far for neutral or weakly ionized species, confirming the importance of QED corrections for superheavy elements.

It should be noted that correlated nonrelativistic or relativistic uncorrelated calculations yield no electron affinity for element 118. The Rn atom does not show a bound state of the anion even at the relativistic CC level.

5.4.4. Adsorption of Super-Heavy Atoms on Surfaces – Identifying and Characterizing New Elements

One of the exciting fields in nuclear physics is the production of new super-heavy elements. The newly produced atoms coming out of the accelerator must be separated from other reaction products and identified to establish their atomic number. Identification is relatively easy if the nucleus decays by a series of α emissions. However, many of the neutron-rich isotopes, which have relatively long lifetimes and may therefore be amenable to chemical studies, decay by spontaneous fission to unknown products. This is the case for the recently produced $^{283}112$ ($t_{1/2} = 3.8\,s$), $^{287}114$ ($t_{1/2} = 0.5\,s$), and $^{288}114$ ($t_{1/2} = 0.5\,s$) [104] , as well as $^{284}113$ ($t_{1/2} = 0.48\,s$) [105]. Elements 112 and higher are expected to be volatile, and their adsorption behavior can be used in gas-phase chromatography, whereby atoms are deposited on detectors located along a chromatography column according to their volatility. The deposition temperatures are measured and associated with the adsorption enthalpies ΔH_{ads}. Transition metals, mainly gold, are generally used as detector surfaces, since they stay clean of oxide layers.

The volatility of element 112 relative to that of Hg was studied by this technique [106]. The two elements showed similar behavior on gold-covered detectors. The adsorption behavior of element 114 relative to Pb is currently being studied, and similar experiments may be expected for element 113 and others. Prediction of the adsorption behavior of these elements and their lighter homologues on different surfaces is important in designing the experiments, choosing appropriate adsorption surfaces, etc. Calculations pertaining to elements 112–114 and 118 have recently been carried out [107–109]. Required atomic properties, in particular polarizabilities, were calculated by the finite field method (see Section 5.3.3). Adding a static uniform electric field **F** to the Hamiltonian gives the energy as a power series in **F**, where the first derivative is the atomic dipole moment, which vanishes. For a uniform field $F = F_z$ in the z direction, the second derivative gives the polarizability α.

We calculated the polarizabilities of Hg, Pb, Rn, and elements 112, 114 and 118 [107–109]. Experimental values are available for Hg and Pb [110, 111]. The calculated α for Hg was 34.15 a.u., close to the experimental 33.91 a.u., and similar agreement was obtained for Pb (46.96 and 45.89 a.u., respectively). The calculated values were used in a physisorption model to obtain adsorption enthalpies. It was found that the ΔH_{ads} values of Hg and 112 on inert surfaces (quartz, ice, Teflon) were too close ($\sim$2 kJ/mol differences) to distinguish between the two elements experimentally. The differences between Pb and 114 are somewhat larger, 7 kJ/mol on quartz and ice, 3 kJ/mol on Teflon. Element 118 is also problematic, giving adsorption enthalpies very close to those of Rn both on noble metals and inert surfaces. A possible candidate for separating these two elements is charcoal; further studies are needed to explore this possibility.

5.5. DIRECTIONS FOR FUTURE DEVELOPMENT

The methods and applications described above show that much progress has taken place in the field. Still, there are many open problems, and we are far from being able to apply relativistic quantum chemistry routinely to systems with significant QED effects. Recent developments by Lindgren and coworkers [18–23] show great promise for overcoming at least some of these problems. These developments are described briefly in the current section; the full details may be found in the original publications. Based on these novel schemes, we propose in Section 5.5.2 a new double Fock-space formalism, with variable numbers of electrons and photons.

5.5.1. Beyond NVPA: QED Many-Body Description and the Covariant Evolution Operator Approach

The QED description is fully covariant and, in principle, time dependent. To make connection between stationary infinite order many-body NVPA and QED, let us consider a time dependent perturbation theory approach, which provides a convenient

way to get rid of time dependence in a rigorous and elegant manner, following [18–23].

The QED Hamiltonian may be written as $\widehat{H}_{\mathrm{QED}} = \widehat{H_0} + \widehat{V}$. Here $\widehat{H}_0$ includes the sum of the noninteracting quantized electronic and photonic field densities,

$$\widehat{H}_0 = \frac{1}{8}(\mathbf{E}^2 + \mathbf{B}^2) - \overline{\psi}(i\gamma_\mu \partial^\mu - mc)\psi, \tag{5-35}$$

and the perturbation

$$\widehat{V} = -e\overline{\psi}\gamma^\mu A_\mu \psi \tag{5-36}$$

represents the electron interaction with the electromagnetic field A_μ.

The basic tool in time-dependent perturbation theory is the time-evolution operator, which in the interaction picture defines the evolution of the field operators,

$$|\Psi(t)\rangle = \widehat{U}(t, t_0)\,|\Psi(t_0)\rangle\,, \quad (t > t_0). \tag{5-37}$$

Perturbative description of the evolution operator $\widehat{U}(t, t_0)$ leads to the expansion

$$\widehat{U}(t, t_0) = \sum_{n=0}^{\infty} \frac{(-i)^n}{n!} \int_{t_0}^{t} dx_1 \ldots \int_{t_0}^{t} dx_n T[\widehat{V}(x_1)\ldots\widehat{V}(x_n)]. \tag{5-38}$$

T is the time-ordering operator. The contraction of two $\widehat{V}$ interactions using Wick's theorem [112] corresponds to the exchange of a single retarded photon. The operator (5-38) is non-covariant, since only positive energy states are involved, and time moves only in the positive direction (Figure 5-2, left). It can be made covariant by inserting electron propagators S_F on the in- and outgoing lines. By definition, operators act to the right on unperturbed model states, which implies that with adiabatic damping we can set the initial time $t_0 = -\infty$, so that no propagators on incoming lines are needed. Time can then flow in both directions on outgoing lines,

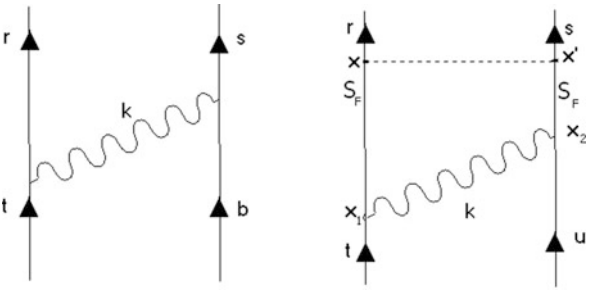

Figure 5-2. The non-covariant and covariant evolution operators for single-photon exchange

and both positive and negative energy states are accounted for (Figure 5-2, right). The covariant evolution operator for single-photon exchange is now expressed by

$$\widehat{U}_{\mathrm{Cov}}(t,-\infty) = -\int\int d^3x d^3x' \widehat{\psi}^{\dagger}(x)\widehat{\psi}^{\dagger}(x') \times \int\int d^4x_1 d^4x_2 S_F(x;x_1) S_F(x';x_2) V_{\mathrm{sp}}(x_1;x_2)\widehat{\psi}(x_1)\widehat{\psi}(x_2). \tag{5-39}$$

The energy-dependent single photon potential V_{sp} is given in the Fourier transform by

$$\langle rs|V_{\mathrm{sp}}(E)|tu\rangle = \langle rs|\int_0^{\infty} dk f(k)\Big(\frac{1}{E-\varepsilon_t-\varepsilon_u-\mathrm{sgn}(\varepsilon_t)(k-i\gamma)} + \frac{1}{E-\varepsilon_s-\varepsilon_r-\mathrm{sgn}(\varepsilon_s)(k-i\gamma)}\Big)|tu\rangle, \tag{5-40}$$

where E is the total energy and ε is the orbital energy. Orbitals are generated by the Dirac equation in the nuclear field or by the SCF procedure (Furry picture). k is the photon momentum, and $f(k)$ is a known gauge-dependent function [18]. The expression for the interaction potential V_{sp} is valid even when energy is not conserved between initial and final states. This feature is needed for treating quasidegeneracy with the extended model space technique, based on the effective or intermediate Hamiltonians described in Sections 5.2.1 and 5.2.2.

The covariant evolution operator is generally singular, due to intermediate model space states. Eliminating the singularities leads to the *Green's operator* $\widehat{G}$ [20]. Green's operator is closely related to the field theoretical Green's function, used extensively in QED (see e.g. [17]). The Green's function is just the zero-body term in the second-quantized representation of the Green's operator.

The Green's operator is separated into open and closed parts, $\widehat{G} = 1 + Q\widehat{G}_{\mathrm{op}}P + P\widehat{G}_{\mathrm{cl}}P$, where $\widehat{G}_{\mathrm{op}}$ operates outside and $\widehat{G}_{\mathrm{cl}}$ inside the model space, as indicated explicitly by the projection operators P and Q. $\widehat{G}_{\mathrm{op}}$ is essentially the wave operator, used in the many-body approaches in quantum chemistry and presented in Section 5.2.1, and $\widehat{G}_{\mathrm{cl}}$ yields the effective Hamiltonian [18, 20]

$$\Omega = P + Q\widehat{G}_{\mathrm{op}}P \tag{5-41}$$

$$\widehat{V}_{\mathrm{eff}} = P\Big(i\frac{\partial}{\partial t}\widehat{G}_{\mathrm{cl}}(t)\Big)_{t=0}P. \tag{5-42}$$

The Green's operator can be applied also to energy–dependent interactions of the QED type and forms therefore a link between many-body electronic structure and quantum field theory. Eliminating the singularity from the covariant evolution operator leaves some finite residuals [18–20],

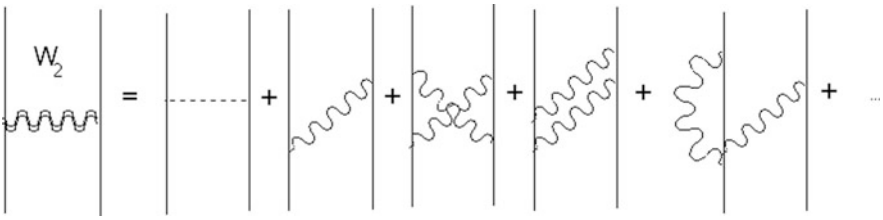

Figure 5-3. The two-body part of the effective potential $\widehat{W}$ in the Bethe-Salpeter-Bloch equation (5-46) contains all irreducible two-body potential diagrams, including the Coulomb interaction as well as all retardation and radiative effects

$$\widehat{G}(t) = \widehat{G}_0(t) + \sum \frac{\delta^n \widehat{G}_0(t)}{\delta E^n} (\widehat{V}_{\text{eff}})^n, \tag{5-43}$$

where $\widehat{G}_0(t)$ represents the Green's operator without any intermediate model-space states,

$$\widehat{G}_0 = 1 + \mathbb{R}_Q \widehat{W} + \mathbb{R}_Q \widehat{W} \mathbb{R}_Q \widehat{W} + ...; \quad \mathbb{R}_Q = \frac{Q}{E_0 - H_0}. \tag{5-44}$$

$\widehat{W}$ is the sum of all irreducible multiphoton interactions (Figure 5-3), and $\mathbb{R}_Q$ is the zero order resolvent operator. The difference ratios transform into derivatives in the case of complete degeneracy. These terms represent the model-space contributions and are analogous to the folded diagrams of open-shell FSCC (see Section 5.2.1), but also contain energy derivatives (difference ratios) of the energy-dependent interaction. Summing the contributions to all orders gives the generalized Bethe-Salpeter (BS) equation in the form of the Schrödinger equation with energy dependent potential,

$$\left(E - \widehat{H}_0\right) |\Psi\rangle = \widehat{W}(E) |\Psi\rangle . \tag{5-45}$$

A similar covariant equation has been derived in 1951 by Bethe and Salpeter for the complete solution of the two-body relativistic problem [113]. The BS equation may be solved self-consistently, using, e.g., the Brillouin-Wigner perturbation theory. In order to maintain the size-extensivity [48], important to heavy multielectronic systems, we prefer to work with the Rayleigh-Schrödinger theory and the linked-diagram representation. This may be achieved by transforming the BS equation to the corresponding Bloch equation (5-18)

$$\left(E_0 - \widehat{H}_0\right) \widehat{\Omega} P = (\widehat{W}(E)\widehat{\Omega} - \widehat{\Omega}\widehat{W}_{\text{eff}}(E))_{\text{linked}} P, \quad \widehat{W}_{\text{eff}} = P\widehat{W}\widehat{\Omega}P, \tag{5-46}$$

referred to as the generalized Bethe-Salpeter-Bloch (BSB) equation. The Bloch equation (5-46) may be used to generate a perturbative expansion of the wave operator for energy–dependent interactions. The difficulty here is in evaluating the

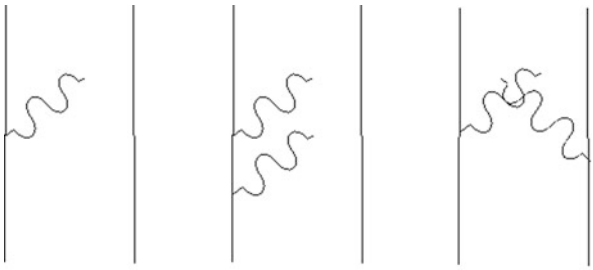

Figure 5-4. The wave function with uncontracted photons lies in an extended Fock space

energy derivatives of the (multiphoton) perturbation $\widehat{W}(E)$, which is itself calculated numerically. This difficulty can be overcome by developing efficient all-order (CC-like) methods in the extended Fock space with variable numbers of so called uncontracted virtual photons (Figure 5-4). These photons may be described by Feynman diagrams corresponding to the time after they have been radiated by one electron but not yet absorbed by another (or the same) electron. Matrix elements describing these diagrams are derived using CEO. These matrix elements are energy independent [18], and the standard many-body machinery may therefore be used. If the virtual photon is absorbed by the same electron it has been radiated from, we get radiative effects, which should be properly renormalized [18].

The photonic Fock space treatment may be combined with consideration of electron (and positron) processes and interactions, using the fermionic Fock space formalism presented in Section 5.2.1. A generalized ("double") Fock space CC approach, which treats the electronic and photonic degrees of freedom on equal footing, thereby ensuring covariance, is presented below.

5.5.2. Generalized Fock Space: Double Fock-Space CC

With the uncontracted interactions (5-36), the wave function lies in an extended Fock space with a variable number of (virtual) photons or photonic Fock-space sectors (Figure 5-4). The Bloch equation (5-18) will have a particularly simple structure,

$$[\widehat{\Omega}, H_0]P = (\widehat{V}\widehat{\Omega} - \widehat{\Omega}\widehat{V}_{\text{eff}})_{\text{linked}}P, \quad \widehat{V}_{\text{eff}} = P\widehat{V}\widehat{\Omega}P. \tag{5-47}$$

$\widehat{V}$ is the energy-independent perturbation (5-36), which may be divided according to the number of uncontracted virtual photons,

$$\widehat{V} = \sum_{\mu \geq 0} {}^{(\mu)}\widehat{V}(k_1 l_1, ..., k_\mu l_\mu). \tag{5-48}$$

(μ) is the number of retarded uncontracted photons, k_ν and l_ν stand for the energy and momentum of photon ν. Expressions for ${}^{(\mu)}\widehat{V}(k_1 l_1, ..., k_\mu l_\mu)$ are derived using CEO [18], and are not shown here.

We consider here explicitly for the first time the exponential form of the wave operator $\widehat{\Omega} = \{\exp(\widehat{S})\}$ in the generalized Fock space with a variable number of uncontracted virtual photons and electrons/positrons. This parametrization leads to the double Fock-space CC method, presented below. The double Fock-space excitation amplitudes have the structure

$$\widehat{S} = \sum_{m\geq 0}\sum_{n\geq 0}\sum_{\mu\geq 0} {}^{(\mu)}\widehat{S}^{(m,n)}(k_1 l_1, ..., k_\mu l_\mu), \tag{5-49}$$

where (m, n) is the electronic valence sector, and (μ) is the number of retarded uncontracted photons (photonic sectors). The double FSCC equation is

$$Q[{}^{(\mu)}S_l^{(m,n)}, H_0]P = Q\{{}^{(\mu)}(V\Omega - \Omega V_{\text{eff}})_l^{(m,n)}\}_{\text{conn}}P. \tag{5-50}$$

The Fock-space excitation operator ${}^{(\mu)}S_l^{(m,n)}$ and resolvent ${}^{(\mu)}R_Q$ are divided into components acting in subspaces with $\mu = 0, 1, \cdots$ uncontracted photons. The generalized double FSCC equation (for $\mu = 0$, 1, 2) may then be separated into

$$\begin{aligned}
{}^{(0)}S_l^{(m,n)} &= {}^{(0)}R_{l,Q}^{(m,n)}\{{}^{(0)}V^{(0)}\Omega + \overbrace{{}^{(1)}V^{(1)}\Omega} + \overbrace{\overbrace{{}^{(2)}V^{(2)}\Omega}} - {}^{(0)}\Omega V_{\text{eff}})_l^{(m,n)}\}_{\text{conn}}P,\\
{}^{(1)}S_l^{(m,n)} &= \\
&{}^{(1)}R_{l,Q}^{(m,n)}\{{}^{(1)}V^{(0)}\Omega + {}^{(0)}V^{(1)}\Omega + \overbrace{{}^{(2)}V^{(1)}\Omega} + \overbrace{{}^{(1)}V^{(2)}\Omega} - {}^{(1)}\Omega V_{\text{eff}})_l^{(m,n)}\}_{\text{conn}}P,\\
{}^{(2)}S_l^{(m,n)} &= \\
&{}^{(2)}R_{l,Q}^{(m,n)}\{{}^{(2)}V^{(0)}\Omega + {}^{(0)}V^{(2)}\Omega + {}^{(1)}V^{(1)}\Omega + \overbrace{{}^{(2)}V^{(2)}\Omega} - {}^{(2)}\Omega V_{\text{eff}})_l^{(m,n)}\}_{\text{conn}}P.
\end{aligned} \tag{5-51}$$

The upper curly brackets stand for numerical integration over the photonic energy k and momentum l. Thus, multiphotonic retarded energy–dependent interactions are evaluated numerically in the generalized Fock-space by contraction of the photonic uncontracted lines of ${}^{(\mu)}\widehat{V}$ with those of ${}^{(\mu)}\widehat{S}^{(m,n)}$ in all possible ways. Note that an exponential form of $\widehat{\Omega}$ will introduce powers of $\widehat{S}$ in (5-51); the integration (unlike the more familiar contraction) is carried out over V and the first S in the term. Multiphotonic terms describing the interelectronic potential are evaluated by an efficient all-order CC procedure. The effective potential derived by iterative solution of the FSCC equations in the photonic sectors is used in the equation for the electronic sectors. The energy dependence is introduced either by the energy denominators or by the folded diagrams with a double energy denominator. After reaching convergence in the double FSCC equations (5-51), the effective (or intermediate) Hamiltonian in

the pure electronic valence sectors, $H_{\text{eff}} = H_0 + V_{\text{eff}}$, is diagonalized to yield directly electronic transition energies.

The double Fock-space CC approach presented here is under development. More details and applications will be reported in a future publication [114].

5.6. SUMMARY AND CONCLUSION

The no-virtual-pair Dirac-Coulomb-Breit Hamiltonian, correct to second order in the fine-structure constant α, provides the framework for four-component methods, the most accurate approximations in electronic structure calculations. The status, features and perspectives for further development of benchmark NVPA multireference CC methods have been reviewed. When applied within the effective or intermediate Hamiltonian technique, these methods give remarkably high-quality results for the most complicated cases of dense quasidegenerate open shell levels in heavy atomic and molecular systems. The IH Fock-space coupled cluster method has structure and features highly suitable for benchmark calculation within NVPA, as well as for extrapolations transcending NVPA towards proper merging with QED theory. Representative calculations included in this review demonstrate the power and reliability of the NVPA-FSCC method.

While NVPA correlated four-component methods provide excellent results where applicable, they are less accurate for highly ionized heavy and super-heavy systems, due to large QED effects. Most current QED approaches can only be applied in single-particle approximations, and cannot incorporate electron correlation and quasidegeneracy effects to high order. The recently developed covariant evolution operator method of Lindgren [18] is free of these drawbacks, and opens new perspectives for deriving truly covariant many-body schemes. As an example of such approaches, we presented a double Fock-space CC method, which couples electronic and photonic degrees of freedom in rigorous manner. QED four-component benchmark calculations for carefully selected systems will be necessary to test the approaches under development.

ACKNOWLEDGMENTS

Many of the atomic results reported here were obtained in collaboration with Yasuyuki Ishikawa of the University of Puerto Rico. Molecular FSCC calculations have been done in collaboration with Lucas Visscher of the Free University in Amsterdam. The authors are grateful to Ingvar Lindgren and Trond Saue for many stimulating discussions. We had fruitful collaboration with Bernd Hess, Valeria Pershina, Pekka Pyykkö, Peter Schwerdtfeger, and with our past and present graduate students Arik Landau, Tal Koren, Nastya Borschevsky and Hani Yakobi; we thank all of them. Financial support has been provided by the Israel Science Foundation and the US-Israel Binational Science Foundation.

REFERENCES

1. E. Eliav, U. Kaldor, in *Relativistic Methods for Chemists* M. Barysz and Y. Ishikawa, Eds. (Springer, 2010), Chap. 7
2. J. Schwinger, Phys. Rev. **75**, 1912 (1949); Phys. Rev. **75**, 651 (1949)
3. R. Feynman, Phys. Rev. **76**, 749 (1949); Phys. Rev. **76**, 769 (1949)
4. S. Tomonaga, Phys. Rev. **74**, 224 (1948)
5. F. Dyson, Phys. Rev. **75**, 486 (1949); Phys. Rev. **75**, 1736 (1949)
6. D. P. Craig, T. Thirunamachandran, *Molecular quantum electrodynamics* (Dover, New York, 1998)
7. K. Schwarzschild, Gött. Nach. Math.-Phys. Kl. 26 (1903)
8. P. Schwerdtfeger (Ed.), *Relativistic Electronic Structure Theory. Part 1. Fundamentals* (Elsevier, Amsterdam, 2002)
9. P. Schwerdtfeger (Ed.), *Relativistic Electronic Structure Theory. Part 2. Applications* (Elsevier, Amsterdam, 2004)
10. B. A. Hess (Ed.), *Relativistic Effects in Heavy-Element Chemistry and Physics* (Wiley, Chichester, 2002)
11. U. Kaldor, S.Wilson (Eds.), *Theoretical Chemistry and Physics of Heavy and Super-Heavy Elements* Ed. U. Kaldor, S. Wilson (Kluwer, Amsterdam, 2003)
12. I. P. Grant, *Relativistic Quantum Theory of Atoms and Molecules. Theory and computation* (Springer, New York, 2007)
13. K. Hirao, Y. Ishikawa (Eds.), *Recent Advances in Relativistic Molecular Theory* (World Scientific Publishing, Singapore, 2004)
14. K. G. Dyall, K. Faegri Jr., *Introduction to Relativistic Quantum Chemistry* (Oxford University Press, New York, 2007)
15. T. Saue, L. Visscher, in *Theoretical Chemistry and Physics of Heavy and Super-Heavy Elements*, Eds. U. Kaldor, S. Wilson (Kluwer, Amsterdam, 2003), p. 211 ff
16. M. Born, J. R. Oppenheimer, Ann. Phys. **84**, 457 (1927)
17. V. M. Shabaev, Phys. Rep. **356**, 119 (2002)
18. I. Lindgren, S. Salomonson, B. Åsén, Phys. Rep. **389**, 161 (2004)
19. I. Lindgren, S. Salomonson, D. Hedendahl, Can. J. Phys. **83**, 183 (2005)
20. I. Lindgren, S. Salomonson, D. Hedendahl, Phys. Rev. A **73**, 062502 (2006)
21. I. Lindgren, S. Salomonson, D. Hedendahl, Int. J. Mod. Phys. E **16**, 1221 (2007)
22. I. Lindgren, S. Salomonson, D. Hedendahl, Int. J. Quantum Chem. **12**, 2272 (2008)
23. I. Lindgren, http://fy.chalmers.se/∼f3ail/Publications/Corfu.pdf
24. U. Kaldor, E. Eliav, A. Landau, in *Fundamental World of Quantum Chemistry*, vol. III, Eds. E. J. Brandas, E. S. Kryachko (Kluwer, New York, 2004), p. 365
25. G. Breit, Phys. Rev. **34**, 553 (1929), Phys. Rev. **36**, 383 (1930), Phys. Rev. **39**, 616 (1932)
26. G. E. Brown, D. G. Ravenhall, Proc. R. Soc. Lond. A **208**, 552 (1951)
27. W. H. Furry, Phys. Rev. **81**, 115 (1951)
28. I. Lindgren, in *Many-Body Methods in Quantum Chemistry*, Lecture Notes in Chemistry, vol. 52, Ed. U. Kaldor (Springer-Verlag, Heidelberg, 1989) p. 293; Nucl. Instrum. Methods **B31**, 102 (1988)
29. I. P. Grant, Proc. R. Soc. Lond. A **262**, 555 (1961)
30. S. Salomonson, I. Lindgren, A.-M. Mårtensson, Phys. Scr. **21**, 351 (1980)
31. S. A. Blundell, W. R. Johnson, Z. W. Liu, J. Sapirstein, Phys. Rev. A **39**, 3768 (1989), Phys. Rev. A **40**, 2233 (1989); S. A. Blundell, W. R. Johnson, J. Sapirstein, Phys. Rev. Lett. **65**, 1411 (1990), Phys. Rev. A **43**, 3407 (1991)
32. Z. W. Liu, H. P. Kelly, Phys. Rev. A **43**, 3305 (1991)
33. S. Salomonson, P. Öster, Phys. Rev. A **40**, 5548 (1989)

34. E. Eliav, U. Kaldor, Y. Ishikawa, Phys. Rev. A **49**, 1724 (1994)
35. U. Kaldor, E. Eliav, Adv. Quantum Chem. **31**, 313 (1998)
36. B. P. Das, K. V. P. Latha, B. K. Sahoo, C. Sur, R. K. Chaudhuri, D. Mukherjee, J. Theor. Comp. Chem. **1**, 1 (2005)
37. E. Eliav, U. Kaldor, Chem. Phys. Lett. **248**, 405 (1996)
38. L. Visscher, T. J. Lee, K. G. Dyall, J. Chem. Phys. **105**, 8769 (1996)
39. L. Visscher, E. Eliav, U. Kaldor, J. Chem. Phys. **115**, 759 (2001)
40. E. Eliav, U. Kaldor, B. A. Heß, J. Chem. Phys. **108**, 3409 (1998)
41. I. Infante, A. S. P. Gomes, L. Visscher, J. Chem. Phys. **125**, 074301 (2006)
42. I. Infante, E. Eliav, L. Visscher, U. Kaldor, J. Chem. Phys. **127**, 124308 (2007)
43. T. Fleig, L. K. Sorensen, J. Olsen, Theor. Chem. Acc. **118**, 347 (2007)
44. S. Pal, D. Mukherjee, Adv. Quantum Chem. **20**, 292 (1989)
45. U. Kaldor, Theor. Chim. Acta **80**, 427 (1991)
46. Y. Ishikawa, R. C. Binning, H. Sekino, Chem. Phys. Lett. **160**, 206 (1989); Y. Ishikawa, Phys. Rev. A **42**, 1142 (1990), Chem. Phys. Lett. **166**, 321 (1990); Y. Ishikawa, H. M. Quiney, Phys. Rev. A **47**, 1732 (1993); Y. Ishikawa, K. Koc, Phys. Rev. A **50**, 4733 (1994)
47. J. Sucher, Phys. Scr. **36**, 271 (1987)
48. I. Lindgren, J. Morrison, *Atomic Many-Body Theory*, second edition (Springer-Verlag, Berlin, 1986)
49. S. R. Hughes, U. Kaldor, Chem. Phys. Lett. **194**, 99 (1992), **204**, 339 (1993), Phys. Rev. A **47**, 4705 (1993), J. Chem. Phys. **99**, 6773 (1993), Intern. J. Quantum Chem. **55**, 127 (1995)
50. A. Landau, E. Eliav, U. Kaldor, Chem. Phys. Lett. **313**, 399 (1999), Adv. Quantum Chem. **39**, 172 (2001)
51. J.-P. Malrieu, Ph. Durand, J.-P. Daudey, J. Phys. A **18**, 809 (1985)
52. E. Eliav, M. J. Vilkas, Y. Ishikawa, U. Kaldor, J. Chem. Phys. **122**, 224113 (2005)
53. E. Eliav, M. J. Vilkas, Y. Ishikawa, U. Kaldor, Chem. Phys. **311**, 163 (2005)
54. D. Mukhopadhyay, B. Datta, D. Mukherjee, Chem. Phys. Lett. **197**, 236 (1992)
55. E. Eliav, A. Borschevsky, R. K. Shamasundar, S. Pal, U. Kaldor, Int. J. Quantum Chem. **109**, 2909 (2009)
56. B. Jeziorski, H. J. Monkhorst, Phys. Rev. A **24**, 1668 (1981)
57. A. Landau, E. Eliav, Y. Ishikawa, U. Kaldor, J. Chem. Phys. **121**, 6634 (2004)
58. E. Eliav, N. Borschevsky, H. Yakobi, U. Kaldor, unpublished
59. A. Landau, E. Eliav, Y. Ishikawa, U. Kaldor, J. Chem. Phys. **115**, 2389 (2001)
60. H. Hotop, W. C. Lineberger, J. Phys. Chem. Ref. Data **4**, 539 (1975), J. Phys. Chem. Ref. Data **14**, 731 (1985)
61. E. Eliav, U. Kaldor, Y. Ishikawa, Phys. Rev. A **53**, 3050 (1996)
62. A. Landau, E. Eliav, Y. Ishikawa, U. Kaldor, J. Chem. Phys. **113**, 9905 (2000)
63. A. Landau, E. Eliav, Y. Ishikawa, U. Kaldor, J. Chem. Phys. **115**, 6862 (2001)
64. E. Eliav, U. Kaldor, Y. Ishikawa, Phys. Rev. A **50**, 1121 (1994)
65. DIRAC, a relativistic ab initio electronic structure program, Release DIRAC04.0 (2004), written by H. J. Aa. Jensen, T. Saue, L. Visscher with contributions from V. Bakken, E. Eliav, T. Enevoldsen, T. Fleig, O. Fossgaard, T. Helgaker, J. Laerdahl, C. V. Larsen, P. Norman, J. Olsen, M. Pernpointner, J. K. Pedersen, K. Ruud, P. Salek, J. N. P. van Stralen, J. Thyssen, O. Visser, T. Winther (http://dirac.chem.sdu.dk)
66. A.-M. Mårtensson-Pendrill, in *Methods in Computational Chemistry*, vol. 5, Ed. S. Wilson (Plenum Press, New York, 1992) p. 99
67. T. Koren, E. Eliav, Y. Ishikawa, U. Kaldor, J. Mol. Struct. (Theochem) **768**, 127 (2006)
68. W. C. Martin, R. Zalubas, L. Hagan, *Atomic Energy Levels—The Rare-Earth Elements*, Natl. Bur. Stand. Ref. Data Series, NBS Circ. No. 60 (US GPO, Washington, DC, 1978)

69. Z. Cai, V. Meiser Umar, C. Froese Fischer, Phys. Rev. Lett. **68**, 297 (1992)
70. E. Eliav, U. Kaldor, Y. Ishikawa, Phys. Rev. A **51**, 225 (1995)
71. D. Kunik, U. Kaldor, J. Chem. Phys. **55**, 4127 (1971); H. J. Monkhorst, Int. J. Quantum Chem. **11**, 421 (1977)
72. S. Huzinaga, M. Klobukowski, Chem. Phys. Lett. **212**, 260 (1993)
73. H. Yakobi, E. Eliav, L. Visscher, U. Kaldor, J. Chem. Phys. **120**, 054301 (2007)
74. L. Davis, B. T. Feld, C. W. Zabel, J. R. Zacharias, Phys. Rev. **76**, 1076 (1949); V. Jaccarino, J. G. King, Phys. Rev. **83**, 471 (1951)
75. J. G. King, V. Jaccarino, Phys. Rev. **94**, 1610 (1954)
76. V. Jaccarino, J. G. King, R. A. Satten, H. H. Stroke, Phys. Rev. **94**, 1798 (1954)
77. P. Pyykkö, Mol. Phys. **99**, 1617 (2001)
78. J. N. P. van Stralen, L. Visscher, Mol. Phys. **101**, 2115 (2003)
79. D. Sundholm, J. Olsen, Phys. Rev. Lett. **68**, 927 (1992)
80. C. J. Evans, A. Lesarri, M. C. L. Gerry, J. Am. Chem. Soc. **122**, 6100 (2000)
81. P. Schwerdtfeger, R. Bast, M. C. L. Gerry, C. R. Jacob, M. Jansen, V. Kellö, A. V. Mudring, A. J. Sadlej, T. Söhnel, F. E. Wagner, J. Chem. Phys. **122**, 124317 (2005)
82. L. Belpassi, F. Tarantelli, A. Sgamelloti, H. M. Quiney, J. N. P. van Stralen, L. Visscher, J. Chem. Phys. **126**, 064314 (2007)
83. H. Yakobi, E. Eliav, U. Kaldor, J. Chem. Phys. **126**, 184305 (2007)
84. G. L. Malli, A. B. F. Da Silva, Y. Ishikawa, Phys. Rev. A, **47**, 143 (1993)
85. W. G. Childs, L. S. Goodman, Phys. Rev. **141**, 176 (1966); A. G. Blachman, D. A. Landman, A. Lurio, Phys. Rev. **161**, 60 (1967)
86. H. Yakobi, E. Eliav, U. Kaldor, Can. J. Chem. **87**, 802 (2009)
87. V. Pershina, D. C. Hoffman, in *Theoretical Chemistry and Physics of Heavy and Superheavy Elements* (Kluwer Academic Publishers, Dordrecht, 2003), p. 55
88. M. Schädel (Ed.), *The Chemistry of Superheavy Elements* (Kluwer Academic Publishers, Dordrecht, 2003)
89. O. L. Keller, Radiochim. Acta **37**, 169 (1984); See also J. B. Mann, quoted by B. Fricke, J. T. Waber, Actinides Rev. **1**, 433 (1971)
90. V. A. Glebov, L. Kasztura, V. S. Nefedov, B. L. Zhuikov, Radiochim. Acta **46**, 117 (1989)
91. E. Johnson, B. Fricke, O. L. Keller, C. W. Nestor Jr., T. C. Tucker, J. Chem. Phys. **93**, 8041 (1990)
92. I. P. Grant, Adv. Phys. **19**, 747 (1970); I. P. Grant, H. M. Quiney, Adv. At. Mol. Phys. **23**, 37 (1988)
93. J.-P. Desclaux, B. Fricke, J. Phys. **41**, 943 (1980)
94. E. Eliav, U. Kaldor, Y. Ishikawa, Phys. Rev. Lett. **74**, 1079 (1995)
95. E. Eliav, U. Kaldor, P. Schwerdtfeger, B. A. Hess, Y. Ishikawa, Phys. Rev. Lett. **73**, 3203 (1994)
96. M. Sewtz, H. Backe, A. Dretzke, G. Kube, W. Lauth, P. Schwamb, K. Eberhardt, C. Grüning, P. Thörle, N. Trautmann, P. Kunz, J. Lassen, G. Passler, C. Z. Dong, S. Fritzsche, R. G. Haire, Phys. Rev. Lett. **90**, 163002 (2003)
97. H. Backe et al., Eur. Phys. J. D **45**, 99 (2007)
98. A. Borschevsky, E. Eliav, M. J. Vilkas, Y. Ishikawa, U. Kaldor, Phys. Rev. A **75**, 042514 (2007)
99. A. Borschevsky, E. Eliav, M. J. Vilkas, Y. Ishikawa, U. Kaldor, Eur. Phys. J. D **45**, 115 (2007)
100. J. Sugar, J. Chem. Phys. **60**, 4103 (1974)
101. E. Eliav, U. Kaldor, Y. Ishikawa, P. Pyykkö, Phys. Rev. Lett. **77**, 5350 (1996)
102. P. Pyykkö, M. Tokman, L. Labzowsky, Phys. Rev. A **57**, R689 (1998); L. Labzowsky, I. Goidenko, M. Tokman, P. Pyykkö, Phys. Rev. A **59**, 2707 (1999)
103. I. Goidenko, L. Labzowsky, E. Eliav, U. Kaldor, P. Pyykkö, Phys. Rev. A **67**, 020101(R) (2003)
104. Yu. Ts. Oganessian et al., Phys. Rev. C **74**, 044602 (2006)

105. Yu. Ts. Oganessian, J. Phys. G, Nucl. Part. Phys. **34**, R165 (2007)
106. R. Eichler et al., Nature **447**, 72 (2007)
107. V. Pershina, A. Borschevsky, E. Eliav, U. Kaldor, J. Chem. Phys. **128**, 024707 (2008)
108. V. Pershina, A. Borschevsky, E. Eliav, U. Kaldor, J. Phys. Chem. **112**, 13712 (2008)
109. V. Pershina, A. Borschevsky, E. Eliav, U. Kaldor, J. Chem. Phys. **129**, 144106 (2008)
110. D. R. Lide (Ed.), *Handbook of Chemistry and Physics*, seventy fourth edition (CRC Press, Boca Raton FL, 1993)
111. D. Goebel, U. Hohm, J. Phys. Chem. **100**, 7710 (1996)
112. G. C. Wick, Phys. Rev. **80**, 268 (1950)
113. E. E. Salpeter, H. A. Bethe, Phys. Rev. **84**, 1232 (1951)
114. E. Eliav, unpublished

CHAPTER 6

BLOCK CORRELATED COUPLED CLUSTER THEORY WITH A COMPLETE ACTIVE-SPACE SELF-CONSISTENT-FIELD REFERENCE FUNCTION: THE GENERAL FORMALISM AND APPLICATIONS

TAO FANG, JUN SHEN, AND SHUHUA LI

Key Laboratory of Mesoscopic Chemistry of Ministry of Education, School of Chemistry and Chemical Engineering, Institute of Theoretical and Computational Chemistry, Nanjing University, Nanjing, 210093, P. R. China, e-mail: ftao@qcri.or.jp; sj@itcc.nju.edu.cn; shuhua@nju.edu.cn

Abstract: We have presented in this chapter the general formalism of block correlated coupled cluster method with a CASSCF reference function (CAS-BCCC in short) and a number of its applications for electronic structure calculations of molecules with multireference character. The CAS-BCCC method has the following features: (1) free of the intruder states; (2) invariant with respect to orbital rotations within separated orbital subspaces (occupied, active, and virtual); (3) cost-effective; (4) core-extensive, but not size-extensive with respect to the total number of electrons. With the cluster operator truncated up to the four-block correlation level, the approximate CAS-BCCC method is named as CAS-BCCC4. The CAS-BCCC4 method is applied to investigate a number of chemical problems such as bond breaking potential energy surfaces, singlet-triplet gaps of diradicals, reaction barriers, spectroscopic constants of diatomic molecules, and low-lying excited states. Comparisons between results from CAS-BCCC4 and those from FCI or other theoretical methods demonstrate that the CAS-BCCC4 approach provides very accurate descriptions for all problems under study. The overall performance of CAS-BCCC4 is illustrated to be better than that of CASPT2 and MR-CISD methods.

Keywords: Block correlated coupled cluster, CAS reference

6.1. INTRODUCTION

The coupled cluster singles and doubles (CCSD) [1–3], and CCSD(T) [4] (with perturbative triples), have become the standard theoretical methods for computing ground-state electronic structures of molecules at their equilibrium structures. However, the accuracy of CCSD or CCSD(T) deteriorates for molecules with significantly stretched bonds or radical character, since the Hartree-Fock (HF) reference determinant is not a good zeroth-order wave function. In such cases, frontier orbitals are

P. Čársky et al. (eds.), Recent Progress in Coupled Cluster Methods, 145–174.
DOI 10.1007/978-90-481-2885-3_6,

usually degenerate or quasi-degenerate so that a number of determinants may be as important as the HF determinant. Thus, a multiconfigurational function (a linear combination of several determinants) is required to provide a qualitatively correct description.

Within the single reference CC framework, a number of approaches have been suggested to treat electronic states with strong multiconfigurational character. The most straightforward one is to improve the CCSD scheme with full triples (CCSDT) [5–7] or with full triples and quadruples (CCSDTQ) [8, 9]. Such schemes can indeed deal with some problems with multiconfigurational character [10] (such as some bond-breaking processes). Nevertheless, they are all computationally very expensive, and have not been used very much. Another simple approach is to use CCSD or CCSD(T) based on the unrestricted HF (UHF) reference function [11]. The UHF-based CCSD and CCSD(T) methods [12] can usually provide quite good descriptions for certain problems (such as bond breaking potential energy surfaces). However, it has been found that these methods can not provide balanced descriptions for different regions of potential energy surfaces, due to the spin contamination of the UHF reference function [13, 14]. Besides these two approaches, other effective approaches have also been proposed, which include: the reduced multireference CCSD [15–24], the spin-flip method [25–32], the orbital-optimized CC approach [33–40], the completely renormalize CC approaches [41–49], active-space CC approaches [50–63], and tailored coupled cluster approach [64], etc. The common feature of most of these approaches is to include higher-than-double excitations through some approximate or perturbative ways. It should be mentioned that the reduced multireference CCSD [15–24] may be considered as an elegant combination of the CCSD method with the multireference configuration interaction singles and doubles (MR-CISD) method. In this approach, the important triple and quadruple amplitudes are obtained by the cluster analysis of the corresponding MR CISD wave function, and then the correlation energy is obtained by solving the externally corrected CCSD equations. This approach and other approaches have been demonstrated to provide accurate descriptions on quasidegenerate electronic states in many cases. Nevertheless, when the dominant configuration changes dramatically in some regions of potential energy surfaces, the accuracy of these approaches may decrease significantly.

Another direction for treating quasidegenerate electronic states is to develop the multireference coupled cluster (MRCC) methods [65–103] based on a genuine multiconfigurational reference function. However, the development of MRCC methods is neither straightforward nor unique. Based on the effective Hamiltonian spanned by the reference determinants (the model space), a number of MRCC methods have been established, which consists of three broad types: valence-universal (VU) approach [65–74], the Hilbert-space or state-universal (SU) approach [75–86], and the state-specific, state-selective (SS) approach [87–103]. In the VU approach, one universal wave operator is employed for all sectors of Fock space. This method can provide direct predictions for energy differences of spectroscopic interest in a single computation [65–74]. In the SU approach, the wave operator is described by a set of

exponential operators, each of which acts on a specific determinant in the reference space. This method is designed to treat a set of electronic states within a single computation [75–86]. However, both VU- and SU-MRCC methods suffer from the intruder state problem [104, 105], and thus their application are still limited. To avoid the intruder states, the SS-MRCC approach [87–103], which treats one state at a time with a state-specific wave operator, has been developed. Existing SS-MRCC methods include, for example, Mk-CCSD [78–95], single-root MR BWCCSD [96–101], and MRexpT [102, 103]. These methods have been shown to give quite accurate descriptions for electronic structures of molecules with strong multireference character. It should be mentioned that the computational cost of these methods roughly scales as the number of determinants in the model space times the cost of one single-reference CCSD calculation.

Besides SS-MRCC methods mentioned above, some state-specific MRCC methods [106–110] are based on the following exponential ansatz for the wave function,

$$|\Psi\rangle = e^{S}\Phi_0. \tag{6-1}$$

where Φ_0 is a multiconfigurational reference function and the cluster operator S is defined with respect to the entire function Φ_0. Φ_0 is usually chosen to be a complete active-space self-consistent-field (CASSCF) function so that nondynamical correlation is incorporated. The exponential operator e^S is designed to take care of the remaining dynamical correlation. The main difficulty faced by MRCC methods based on the ansatz (6-1) is that the excitation operators included in the cluster operator do not always commute with each other [110], unlike in the single reference CC case (in which Φ_0 is a single determinant). Thus, simplifications should be made to avoid this problem. In the approach proposed by Banerjee and Simons [106, 107], only valence excitations (from valence orbitals to virtual orbitals) are included in the cluster operator. Clearly, this approximation is not justified in many cases. Later, in the MR linearized coupled cluster method (MR-LCCM) advocated by Bartlett and coworkers [108, 109], all excitations (excluding internal excitations) are included, but their contributions are all treated at the linearized level (i.e., the Baker-Campbell-Hausdorff expansion truncated at the first commutator). The MR-LCCM results were found to be very similar to the traditional MR-CISD results [109]. In some related approaches based on the ansatz (1), an anti-Hermitian cluster operator S is employed, and different ways of determining the excitation amplitudes have been suggested. These approaches include the unitary coupled cluster method by Hoffmann and Simons [111] and the canonical transformation method by Chan and Yanai [112, 113]. In addition, Mukherjee and coworkers proposed a normal order exponential ansatz [87, 88] built on a CASSCF reference function, which is supposed to be size-extensive and devoid of the intruder state problem. As the cluster operators within the normal products commutate with each other, various types of excitations can be included. With the extended Wick's theorem [114, 115], a practical procedure for solving the amplitudes has been suggested, but no implementation of this method has been reported.

Another type of MR CC approach (called as CASCCSD) proposed by Adamowicz and his co-workers [116–122] employs the following exponential ansatz for the wave function,

$$|\Psi\rangle = e^{S(\text{ext})}(1 + C^{(\text{int})})|0\rangle, \tag{6-2}$$

where $|0\rangle$ is a formal reference determinant, and a CI-like operator $(1 + \mathrm{C}^{(\text{int})})$ acting on $|0\rangle$ produces the CASSCF function, and the CC operator $S(\text{ext})$ includes external and semiexternal excitations from the Fermi vacuum determinant. Test applications have showed a very good performance of this approach in describing ground and excited electronic states with strong multireference character [120–122]. However, this approach computationally scales as the seventh power of the system size, and thus applications may be limited to quite small systems.

In 2004, we have developed an alternative MR CC approach, called block-correlated coupled cluster (BCCC) [123], to deal with near-degenerate electronic states. Assume that orthonormal orbitals in a system can be divided into a set of blocks containing several near-degenerate orbitals, it is well known that a good reference function of this system could be expressed as the tensor product of the most important state in each block. Such block-based reference functions include the separated electron pair wave function [124], the generalized valence bond-perfect pairing (GVB in short) wave function [125], and even the complete active-space self-consistent-field (CASSCF) function (as a special case), depending on the definition of blocks. These reference functions can provide a qualitatively correct description for single-bond bond breaking processes or electronic structures of diradical systems, and offer a natural way to incorporate intra-block correlation (or nondynamic correlation). Apparently, the single reference CC method cannot be generalized in a straightforward manner to deal with these reference functions. To include remaining dynamic correlation among blocks, which is essential for quantitative descriptions, we have suggested an exponential ansatz with the cluster operators defined in terms of block states (a spin orbital may be considered as a single-orbital block) [123]. Depending on the definition of blocks, the BCCC formalism may return back to single reference CC (each block is a spin orbital), GVB-based BCCC (each block is an electron pair), and CAS-BCCC, which employs the CASSCF wave function as a reference.

Very recently, we have developed the general formalism of CAS-BCCC for generate active spaces [126, 127], and reported its efficient implementation for ground-state and excited-state calculations [126–133]. In the CAS-BCCC method, a multi-orbital block is defined to contain all active orbitals in the active space, and all other blocks involve just a single spin orbital (occupied or virtual). When the cluster operators are truncated up to the four-block correlation level, the approximate CAS-BCCC approach is named as the CAS-BCCC4 scheme. The CAS-BCCC approach employs the same ansatz as shown in Eq. (6-1) for the wave function, but the definitions of the cluster operators in CAS-BCCC are very different from those adopted in other

methods. The inherent relationship between CAS-BCCC and other related methods will be analyzed later in the next section. The CAS-BCCC4 method has been applied to study a number of chemical problems [126–133], including the bond breaking potential energy surfaces (PESs), the singlet-triplet gaps for diradicals, activation barriers, spectroscopic constants for diatomic molecules, and low-lying excitation energies. Comparisons between CAS-BCCC4 results and those from full configuration interaction (FCI) or other multireference approaches have demonstrated that the CAS-BCCC4 approach provides highly accurate descriptions for chemical problems under study.

In this review, we will first introduce the general formalism of CAS-BCCC, and its implementation details in Section 6.2. The strengths and drawbacks of this method, and its relationship with other related methods will also be discussed in this section. Then, in Section 6.3 CAS-BCCC4 will be applied to study a number of chemical problems, and its performance will be assessed with the results from FCI or other multireference approaches. In Section 6.4, we will give a brief summary and some perspectives on the CAS-BCCC approach.

6.2. CAS-BCCC METHOD

6.2.1. The CAS-BCCC Wave Function

The wave function in the CAS-BCCC framework is formulated as [126]:

$$|\Psi\rangle = e^{T}|\Phi_0\rangle, \tag{6-3}$$

where the CASSCF reference function $|\Phi_0\rangle$ can be expressed in the second-quantized form below,

$$|\Phi_0\rangle = A_0{}^{+} i^{+} j^{+} \cdots |0\rangle. \tag{6-4}$$

Here A_0^+ represents the creation operator for the reference state of block A, which contains all active orbitals in the active space, and i^+ stands for the creation operator in the i th occupied spin orbital. Hereafter, we will use $i, j, k, \cdots$, for occupied orbitals (always occupied in the reference function), $a, b, c, \cdots$, for virtual orbitals (always unoccupied in the reference function), and $r, s, t, \cdots$, for active orbitals (partially occupied in the reference function). The multi-orbital block A has a one-to-one correspondence to the active space, which can be signified as (N_0, M) (N_0 electrons in M spatial orbitals). Once a CASSCF(N_0, M) calculation is done, the reference state of block A is automatically defined, which corresponds to the lowest energy state in the N_0-electron subspace, if the ground state is the target state. On the other hand, distributing N_0 electrons into M spatial orbitals will lead to many N_0-electron determinants (the total number of determinants in this subspace is denoted by P), and a full CI within this N_0-electron subspace (in the Coulomb field of all doubly

occupied electrons) will yield the reference state and (P − 1) other N_0-electron block states. These (P − 1) block states (orthogonal to the reference state) and the block states within various Fock spaces (with different numbers of electrons), will also be included in the definition of the cluster operators, and they together are called as "excited" block states for convenience [126]. Except for block A, each of the other blocks is defined to be a spin orbital (occupied or virtual), and a single spin orbital is also called as a block for convenience in some cases. It is worth pointing out that a spin orbital has only two states, occupied or vacuum. Thus, the CASSCF reference function can also be considered as the tensor product of the most important state of all block states. All orbitals defined for all blocks in CAS-BCCC are from a CASSCF calculation.

Now we turn to the cluster operators. Here the cluster operators are defined in terms of both block states (of block A) and spin orbitals. Depending on how many blocks are involved (here a spin orbital is also called as a block), the cluster operators may be called n-block correlation operators. For example, all cluster operators up to the four-block correlation level can be explicitly expressed as below [126],

$$T_1 = \sum_{U}^{N_0} T_1(U) = \sum_{U}^{N_0} A_U^+ A_0^- t_1(U) \tag{6-5}$$

$$T_2 = T_{2A} + T_{2B} + T_{2C} \tag{6-6}$$

$$T_{2A} = \sum_{U}^{N_0-1} \sum_{a}^{\text{vir}} T_{2A}(U,a) = \sum_{U}^{N_0-1} \sum_{a}^{\text{vir}} A_U^+ A_0{}^- a^+ t_{2A}(U,a) \tag{6-7}$$

$$T_{2B} = \sum_{U}^{N_0+1} \sum_{i}^{\text{occ}} A_U^+ A_0{}^- i^- t_{2B}(U,i) \tag{6-8}$$

$$T_{2C} = \sum_{i}^{\text{occ}} \sum_{a}^{\text{vir}} a^+ i^- t_{2C}(i,a) \tag{6-9}$$

$$T_3 = T_{3A} + T_{3B} + T_{3C} \tag{6-10}$$

$$T_{3A} = \frac{1}{2} \sum_{U}^{N_0-2} \sum_{a,b}^{\text{vir}} A_U^+ A_0{}^- a^+ b^+ t_{3A}(U,a,b) \tag{6-11}$$

$$T_{3B} = \frac{1}{2} \sum_{U}^{N_0+2} \sum_{i,j}^{\text{occ}} A_U^+ A_0{}^- i^- j^- t_{3B}(U,i,j) \tag{6-12}$$

$$T_{3C} = \sum_{U}^{N_0} \sum_{i}^{\text{occ}} \sum_{a}^{\text{vir}} A_U^+ A_0^- a^+ i^- t_{3C}\,(U,i,a) \tag{6-13}$$

$$\mathrm{T}_4 = T_{4A} + T_{4B} + T_{4C} + T_{4D} + T_{4E} \tag{6-14}$$

$$T_{4A} = \frac{1}{2} \sum_{U}^{N_0-1} \sum_{a,b}^{\text{vir}} \sum_{i}^{\text{occ}} A_U^+ A_0{}^- i^- a^+ b^+ t_{4A}\,(U,i,a,b) \tag{6-15}$$

$$T_{4B} = \frac{1}{2} \sum_{U}^{N_0+1} \sum_{i,j}^{\text{occ}} \sum_{a}^{\text{vir}} A_U^+ A_0{}^- a^+ i^- j^- t_{4B}\,(U,a,i,j) \tag{6-16}$$

$$T_{4C} = \frac{1}{4} \sum_{i,j}^{\text{occ}} \sum_{a,b}^{\text{vir}} a^+ b^+ i^- j^- t_{4C}\,(i,j,a,b) \tag{6-17}$$

$$T_{4D} = \frac{1}{3!} \sum_{U}^{N_0-3} \sum_{a,b,c}^{\text{vir}} A_U^+ A_0{}^- a^+ b^+ c^+ t_{4D}\,(U,a,b,c) \tag{6-18}$$

$$T_{4E} = \frac{1}{3!} \sum_{U}^{N_0+3} \sum_{i,j,k}^{\text{occ}} A_U^+ A_0{}^- i^- j^- k^- t_{4E}\,(U,i,j,k). \tag{6-19}$$

Here the capital letter U represents various block states of block A, which may belong to Fock subspaces with different numbers of electrons. For example, the summation over U in Eq. (6-7) runs over only the subspace with (N_0-1) electrons. $A_U^+ A_0^-$ denotes a replacement operator that replaces the reference state of block A with the U-th "excited" state of block A when acting on the CASSCF reference function, $t_1(U)$, $t_{2A}(U,a)$ (and so on) are the excitation amplitudes to be determined in CAS-BCCC calculations. In general, the n-block correlation operators can be divided into three types. The first type describes core excitations (from doubly occupied orbitals to virtual orbitals), such as T_{2C} and T_{4C}. In fact, T_{2C} and T_{4C} are just the single and double excitation operators, respectively, in the single-reference CC methods. The second type includes only T_1, which involves active orbitals only. This operator is responsible for internal excitations (or the relaxation effect), which allow the relative weights of different determinants in the CASSCF function to be relaxed. The third type contains the remaining operators, which describes semi-internal excitations between block A and spin orbitals (occupied or virtual, or both). Let us take one of the semi-internal excitation type, T_{3A}, to illustrate its qualitative electron correlation picture. When acting on the CASSCF reference function, this operator will transfer two electrons from block A to two virtual spin orbitals, producing "excited" configuration

functions, in which block A is in the ionized states with ($N_0 - 2$) electrons and two virtual spin orbital are occupied.

Similarly, one can write down explicit expressions for higher n-block correlation operators ($n > 4$). However, to make computations feasible, we need to truncate the cluster operator T to a certain level. The first reasonable approximation is to truncate T up to the four-block correlation level, i.e.,

$$T \approx T_1 + T_2 + T_3 + T_4, \tag{6-20}$$

the resulting approximate CAS-BCCC method is abbreviated as CAS-BCCC4. This approximation is reasonable, because "excited" configuration functions produced by higher T_n ($n \geq 5$) operators will not interact with Φ_0 directly (e.g., $\langle \Phi_0 | H | T_n \Phi_0 \rangle = 0$ ($n \geq 5$)). In more accurate CAS-BCCCn methods (beyond CAS-BCCC4), these T_n ($n \geq 5$) operators will make indirect contributions.

6.2.2. CAS-BCCC4 Equations

To determine the excitation amplitudes, one can project the corresponding Schrödinger equation onto the reference function (Φ_0) and all excited configuration functions to obtain a set of coupled nonlinear equations [126] listed below,

$$\langle \Phi_0 | H | \Psi_{BCCC} \rangle = E_{BCCC} \langle \Phi_0 \mid \Psi_{BCCC} \rangle = E_{BCCC}, \tag{6-21}$$

$$\langle \Phi^V | H | \Psi_{BCCC} \rangle = E_{BCCC} \langle \Phi^V \mid \Psi_{BCCC} \rangle, \tag{6-22}$$

$$\langle \Phi^{V,a} | H | \Psi_{BCCC} \rangle = E_{BCCC} \langle \Phi^{V,a} \mid \Psi_{BCCC} \rangle, \tag{6-23}$$

.....

Here $\Phi^V = A_V^+ A_0^- \Phi_0$, $\Phi^{V,a} = A_V^+ A_0^- a^+ \Phi_0$, etc, are excited configuration functions. Substituting Eq. (6-21) into Eqs. (6-22), (6-23) (and so on) will lead to equations involving only excitation amplitudes. Since the number of unknown amplitudes is equal to the number of equations, the amplitudes can be unambiguously determined in an iterative way. With the amplitudes, the CAS-BCCC energy is computed from Eq. (6-21).

It is very challenging to derive the working equations for various excitation amplitudes. A computer program has been written for this purpose. The details have been described previously [126–130]. It should be noted that in substituting the CAS-BCCC4 wave function into the left-hand side of Eqs. (6-22), (6-23) (and so on), the exponential expansion will terminate after several terms, due to the rule that the Hamiltonian matrix element between any two configuration functions vanishes when these two functions differ by more than four block indices [123]. In addition, we want to point out that the products of any operators involving block A two (or more times) are not allowed by their definitions described above, since the reference state of block

A can not be annihilated twice (or more). For instance, $T_{2A}T_{3C} = 0$, $T_{2A}T_{4A} = 0$, etc. We will discuss this issue in more details later in this section.

The non-linear equations for excitation amplitudes can be solved in the iterative manner with the updated equation proposed by Hirata and Bartlett [134],

$$t(u)^{k+1} = t(u)^k - \frac{\langle \Phi(u)| H |\Psi_{BCCC}\rangle - E_{BCCC} \langle \Phi(u) \mid \Psi_{BCCC}\rangle}{\Delta E_{shift} + \langle \Phi(u)| H |\Phi(u)\rangle - E_{BCCC}}. \tag{6-24}$$

Here a compound index u is used for simplicity to represent a set of indices that define a particular excitation amplitude. Correspondingly, $\Phi(u)$ is a shorthand notation for a given "excited" configuration function. A positive value, ΔE_{shift}, is added in the denominator to improve the convergence (in some cases). For the ground state, the converged amplitudes can always be obtained, since the energy difference in the denominator (excluding ΔE_{shift}) of Eq. (6-24) is always a positive value, due to the variational nature of the CASSCF function. Thus, the CAS-BCCC approach is devoid of the intruder state problem for the ground state.

6.2.3. Implementation Details

To implement the CAS-BCCC4 method efficiently, we have to transform the spin orbital formulations into the spatial orbital formulations, then rewrite all formulations with a number of intermediate arrays, and transform very complicated equations to an efficient computer program. Fortunately, a computer program can be devised to achieve all these processes automatically. Some details for implementation have been discussed in our previous work [126–128]. It is worthwhile to mention the computational cost of CAS-BCCC4 calculations. One can get a rough idea about the computational scaling of CAS-BCCC4 by analyzing the number of amplitudes. In fact, for relatively large systems with small active spaces (say, no more than (6,6)), the number of t_{4C} amplitudes in CAS-BCCC4 is much larger than other type of amplitudes, being similar to that in the corresponding CCSD. While in most MRCC methods the total number of amplitudes is the number of the reference determinants in the active space times the number of amplitudes in the corresponding CCSD. As a result, the computational cost of CAS-BCCC4 should be much less expensive than that of most genuine MRCC methods. For large molecules with small active spaces, the CAS-BCCC4 approach shares the same computational scaling as the traditional CCSD method. Nevertheless, for small systems, CAS-BCCC4 is usually computationally more demanding than the single reference CCSD, since the dominant amplitudes may be not t_{4C} amplitudes. A somewhat detailed analysis on the computational scaling of CAS-BCCC4 has been reported elsewhere [127]. From discussions above, one can conclude that for small active spaces CAS-BCCC4 calculations are affordable for medium-sized molecules with moderate basis sets.

As shown by equations from (6-5) to (6-19), all electronic states of block A within a certain Fock subspace are included in the definition of a certain type of the cluster operator. The unique definitions of these cluster operators and the variational nature

of the CASSCF reference function ensure that the CAS-BCCC4 wave function is invariant with respect to the orbital rotations in occupied, active, and virtual subspaces, respectively. Thus, any orbitals (canonical, natural, or localized) from CASSCF calculations can be employed for CAS-BCCC4 calculations.

6.2.4. Excited States

In all discussions above, the CAS-BCCC4 method is assumed to treat the electronic state of the ground state. However, the exponential ansatz, Eq. (6-3), is also a good approximation to some low-lying excited states, if the CASSCF reference function is a good zeroth-order wave function for the excited state of interest. If the target state is an excited state, the reference state of block A corresponds to the CASSCF wave function for the corresponding excited state. Obviously, some "excited" states within the N_0-electron subspace may have lower energies than the reference block state defined above.

In defining the CAS-BCCC4 equations for an excited state, we need to slightly modify the definition of the T_1 operator, which allows the CASSCF reference function to mix with all "excited" block states within the N_0-electron subspace. The key point is to remove some components of the T_1 operator, which correspond to those "excited" block states that are lower in energy than the reference block state. By doing so, the denominator in the updated equation, Eq. (6-24), will be ensured to be positive, thus the iteration procedure for retained $t_1(U)$ amplitudes will lead to converged results. The neglect of these "excited" block states will have a minor effect on the low-lying excited states, since the number of block states excluded is relatively small, compared to the total number of block states within the N_0-electron subspace. On the other hand, the CASSCF function itself is optimized for the excited state under study so that the relaxation effect of the CASSCF function is usually small. Thus, with this simple strategy the CAS-BCCC4 method can also be applied to treat some low-lying excited states [129]. The accuracy of the CAS-BCCC4 approach for excited states significantly depends on the quality of the CASSCF reference function. If orbitals are fully optimized from single-state CASSCF calculations, the CAS-BCCC4 approach usually provides quite accurate excitation energies. However, if state-averaged orbitals have to be used, the weight of the state of interest in the CASSCF calculation should be as large as possible. It should be noted that a more general method for treating excited states within the CAS-BCCC framework is to develop a linear response [91, 135–138], SAC-CI [139–142] or equation-of-motion [143–146] type approach based on the ground-state CAS-BCCC wave function.

6.2.5. Comparison with Related MRCC Methods

As described earlier, the CAS-BCCC4 method employs the same exponential ansatz as other MRCC methods such as MR-LCCM [108–109] and that proposed by Banerjee and Simons [106, 107]. Clearly, these methods mainly differ from each other in

the definition of the cluster operators. In Section 6.2.1, we mention that the products of the cluster operators involving block A are prohibited, since the reference state of block A can not be annihilated twice (or more). With this restriction, the CAS-BCCC4 wave function can be reformulated into another identical form,

$$|\Psi\rangle = (1 + T_1 + \bar{T}_2 + T_3 + \bar{T}_4)e^{T_{2C}+T_{4C}}|\Phi_0\rangle, \tag{6-25}$$

with

$$\bar{T}_2 = T_2 - T_{2C} = T_{2A} + T_{2B}, \tag{6-26}$$

$$\bar{T}_4 = T_4 - T_{4C} = T_{4A} + T_{4B} + T_{4D} + T_{4E}. \tag{6-27}$$

Thus, one can see that the core excitations (T_{2C}, T_{4C}) (from occupied orbitals to virtual orbitals) are described with an exponential expansion structure, while the internal excitations and semi-internal excitations are described with a linear combination of the corresponding operators, as in an ordinary CI. Thus, in some sense, the CAS-BCCC4 approach may be considered as a combined CC/CI approach. It should be noticed that the internal excitations are fully incorporated here by using the T_1 operator, since all "excited" block states within the N_0-electron subspace are included in the definition of the T_1 operator for the ground state (or almost all for an excited state). Nevertheless, a linear CI-like expansion for describing semi-internal excitations constitutes an approximation. This strategy works well for small active spaces, but will become less effective with increasing the size of the active space. The above analysis shows that among three types of excitations (internal, semi-internal, and core), core and internal excitations are fully incorporated in the CAS-BCCC4 wave function, but semi-internal excitations are approximately taken into account via a CI-like expansion. In the MRCC method of Banerjee and Simons [106, 107], internal and core excitations are totally ignored, and only part of semi-internal excitations (from active orbitals to virtual orbitals) are fully considered. While in the MR-LCCM approach [108–109], only semi-internal and core excitations are included, and their contributions are considered at the linear level. Hence, these two methods are expected to be less accurate than the CAS-BCCC4 method.

As revealed from the discussions above, the CAS-BCCC4 method is not size extensive, but it is core-extensive [110], like the state specific equation-of-motion coupled cluster method [147]. Clearly, the size-extensivity error of CAS-BCCC4 originates from the CI-like expansion for semi-internal excitations [129]. If a supermolecule consists of two separated fragments, one single reference fragment and another multireference fragment (which contains block A), then the CAS-BCCC4 energy is size-extensive. But if a molecule dissociates into two fragments by breaking one (or more) chemical bond, and the active space (or block A) is across two fragments, the CAS-BCCC4 energy will not be size-extensive. Due to the core-extensivity, the size-extensivity error of CAS-BCCC4 does not increase with increasing the total number of core (or doubly occupied) electrons, but mainly depends on the size of the active space.

6.3. SOME APPLICATION EXAMPLES

6.3.1. Ground-State Bond Breaking Potential Energy Surfaces

The potential energy surfaces (PESs) for bond breaking processes provide stringent tests for various electronic structure methods. The CAS-BCCC4 method has been applied to investigate the potential energy surfaces for single-bond and multi-bond dissociation processes in a series of molecules including HF, BH, F_2, C_2, N_2, CH_4, H_2O, C_2H_4, etc. [126, 127, 133] In the CAS-BCCC4 calculation, a minimum active space is usually chosen according to the nature of the broken bond. The corresponding CASSCF calculation is carried out with the GAMESS package [148]. Then, with the CASSCF orbitals and integrals from the GAMESS package, our program is employed to perform subsequent CAS-BCCC4 calculations. In most cases, the results from FCI are used to validate the performance of CAS-BCCC4, as well as the internally contracted MR-CISD [149–152], and the CASSCF second-order perturbation theory (CASPT2) [153, 154]. The MOLPRO package [155] is employed for carrying out MR-CISD and CASPT2 calculations. For approximate theoretical methods, the maximum absolute error (MAE) with respect to the FCI value, and the nonparallelity error (NPE) (the difference of the maximum deviation and the minimum deviation along the whole PES) will be used to describe the deviation of their PESs with respect to the FCI PES.

In the following, we will only show the results of various theoretical methods for two typical molecules, F_2 and H_2O. For F_2, its bond-breaking PES has been studied extensively [14, 23, 27, 90, 119, 156]. In CAS-BCCC4 calculations, a double-zeta (DZ) basis set [157, 158] is employed, and two core orbitals are frozen. The minimum active space (2,2) is selected to contain the $3\sigma_g$ and $3\sigma_u$ orbitals. With the same basis set, the FCI PES (with two core orbitals and their corresponding virtual orbitals frozen) of this molecule is available [23] for comparison. The results from FCI, CAS-BCCC4, MR-CISD, and CASPT2 calculations are listed in Table 6-1. It can be observed that CAS-BCCC4 gives a uniformly good description for the PES over the entire range, with the MAE of 4.1 millihartree (mH) and the NPE of 1.8 mH.

Table 6-1. Comparison of ground-state energies from CAS-BCCC4, MR-CISD, and CASPT2 with FCI values for single bond dissociation in F_2. FCI energies are in a.u. The values for other methods are the deviations with respect to FCI values in mH. $R_e = 2.66816$ Bohr

$R_{FF}(R_e)$	FCI	CASPT2	MR-CISD	CAS-BCCC4
1.0	–198.968128	8.81	10.51	4.09
1.1	–198.976458	8.56	10.42	3.97
1.2	–198.972125	8.39	10.02	3.68
1.5	–198.952558	8.60	8.62	2.83
2.0	–198.945201	8.95	8.03	2.51
3.0	–198.944819	8.86	7.86	2.36
4.0	–198.944831	8.81	7.82	2.31

Table 6-2. Comparison of ground-state energies from CAS-BCCC4, MR-CISD, and CASPT2 with FCI values for simultaneous bond dissociation in H_2O. FCI energies are in a.u. The values for other methods are the deviations with respect to FCI values in mH. The bond angle is fixed at $\angle HOH = 109.57°$, and $R_e = 0.9929Å$

$R_{OH}(R_e)$	FCI	CASPT2	MR-CISD	CAS-BCCC4
1.0	−76.238850	13.56	5.67	3.51
1.4	−76.099020	12.32	5.44	3.47
1.8	−75.978140	9.43	4.36	2.70
2.2	−75.927220	8.30	3.44	2.07
2.6	−75.913410	8.38	3.06	1.84
3.0	−75.910030	8.48	2.95	1.78
3.4	−75.909080	8.51	2.92	1.76
3.8	−75.908780	8.52	2.91	1.75

For MR-CISD, the MAE is much larger than that of CAS-BCCC4, and the NPE is 2.7 mH. The CASPT2 method provides the smallest NPE (0.6 mH) in this molecule, although the absolute deviation is considerably larger than that of CAS-BCCC4.

The simultaneous dissociation in H_2O is a typical double-bond breaking model, which has been widely investigated [40, 45, 112, 113, 118, 159, 160]. In our calculations, we fix the bond angle at 109.57°, and stretch two O—H bonds symmetrically to the dissociation limit. The cc-pVDZ basis set [161] (with spherical d functions) is used, and the core orbital of the oxygen atom is frozen in all calculations. The minimum active space (4,4) contains two σ bonding orbitals and the corresponding anti-bonding orbitals. The results obtained from CAS-BCCC4, MR-CISD, and CASPT2 are listed in Table 6-2, together with the FCI data from the literature [112]. One can see that CASPT2 has much larger MAE and NPE than MR-CISD and CAS-BCCC4. The MAE and NPE are 5.7 and 2.8 mH for MR-CISD, 3.5 and 1.8 mH for CAS-BCCC4. Thus, the performance of CAS-BCCC4 is slightly better than that of MR-CISD.

The performance of the CAS-BCCC4 method for other systems has been discussed in detail in previous studies [126, 127, 133]. From the results presented here and previously, we can conclude that with the minimum active space for the broken bond, the CAS-BCCC4 approach provides quite accurate and balanced descriptions for the ground-state PESs of single-bond or multi-bond breaking processes. In most cases, the CAS-BCCC4 results are more accurate to some extent than those from the widely used CASPT2 and MR-CISD methods.

6.3.2. Spectroscopic Constants of Diatomic Molecules

The spectroscopic constants of diatomic molecules have been extensively studied with various theoretical methods. Here we show the performance of the CAS-BCCC4 method for three single-bond molecules (LiH, HF and F_2) and three

Table 6-3. Exact equilibrium distances (R_e), dissociation energies (D_e), and harmonic vibrational frequencies (ω_e) for the ground state of six diatomic molecules, and the corresponding deviations calculated by different theoretical methods with the 6-311G++(3*df*, 3*p*) basis set

	Method	LiH	HF	F_2	C_2	N_2	O_2	MAE
	Expt.[a]	1.596	0.917	1.412	1.243	1.098	1.208	
	CASSCF	0.039	–0.002	0.058	0.005	0.005	0.006	0.019
R_e (Å)	CAS-BCCC4	–0.002	–0.002	0.006	0.007	0.006	0.003	0.004
	CASPT2	0.018	0.000	0.012	0.007	0.006	0.004	0.008
	MR-CISD	0.012	–0.001	0.006	0.006	0.005	0.002	0.005
ω_e (cm^{-1})	Expt.[a]	1.406	4.138	917	1.855	2.359	1.580	
	CASSCF	–115	–1	–273	–184	–15	–25	102
	CAS-BCCC4	11	35	–52	–24	–31	2	26
	CASPT2	–45	27	–68	–24	–44	–8	36
	MR-CISD	–23	28	–56	–18	–28	4	26
	Expt.[a]	57.7	141.3	38.2	146.0	228.5	120.3	
	CASSCF	–13.2	–26.7	–22.8	2.0	–23.6	31.5	20.5
D_e (kcal/mol)	CAS-BCCC4	–0.8	–4.8	–6.5	–1.7	-10.3	–5.8	5.0
	CASPT2	–4.5	–3.8	–5.6	5.3	–18.8	–1.1	6.5
	MR-CISD	–4.5	–6.0	–7.9	–2.6	–10.4	–8.3	6.6

[a] References [162–166].

multi-bond molecules (C_2, N_2 and O_2), in which both nondynamic and dynamic correlation energies are important for quantitative descriptions. For single-bond molecules, the CASSCF function with the minimum active space (2,2) is sufficient for CAS-BCCC4 calculations. While for C_2, N_2 and O_2, the active spaces (4,6), (6,6), and (8,6), respectively, are used. The 6-311G+ + (3*df*, 3*p*) basis set is employed for all these molecules. The values of the equilibrium bond distance (R_e) and the harmonic vibrational frequency (ω_e) are obtained by fitting 16 points on the PESs around the equilibrium bond length to a cubic polynomial potential. The dissociation energy (D_e) is calculated by subtracting the energy at a large interatomic at a large interatomic distance (20Å) from that at R_e. As shown in Table 6-3, the mean absolute errors for R_e, ω_e, D_e predicted from CAS-BCCC4 calculations (with respect to the corresponding experimental values) are, respectively, 0.004 Å, 26 cm^{-1}, and 5.0 kcal/mol, which are comparable to the MR-CISD results (0.005 Å, 26 cm^{-1}, and 6.6 kcal/mol), and the CASPT2 results (0.008 Å, 36 cm^{-1}, and 6.5 kcal/mol). Thus, for these simple diatomic molecules, the CAS-BCCC4 method performs equally well as the widely used CASPT2 and MR-CISD methods.

6.3.3. Reaction Barriers

The prediction of reliable reaction barriers is very challenging for electronic structure methods since the transition states usually have strong multireference character. Several isomerization reactions have been studied with the CAS-BCCC4 method [130].

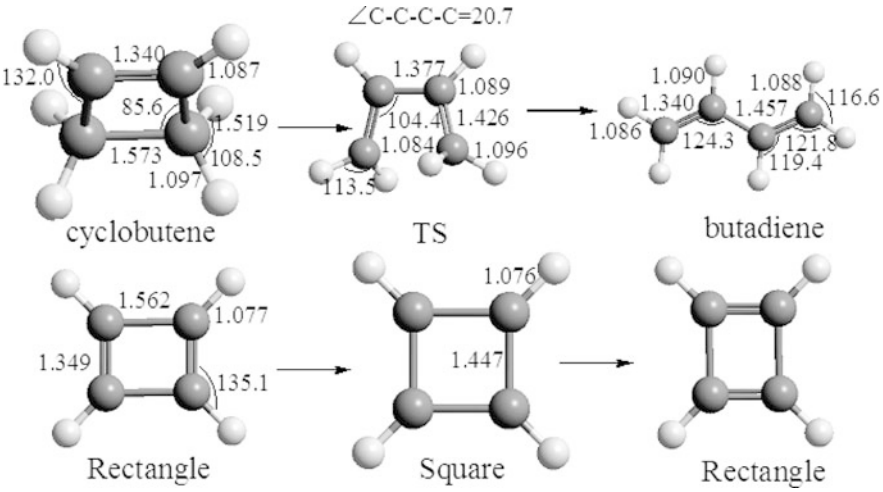

Figure 6-1. Geometric parameters of stationary points in the two isomerization reactions (Å for bond lengths and deg. for angles). The data related to the first reaction are from Ref. [175], and those related to the second reaction are from Ref. [178]

Here we will focus on two typical reactions, one is the isomerization of cyclobutene to butadiene, another is the automerization reaction of cyclobutadiene (CBD). For the first reaction, we perform single point CAS-BCCC4 calculations for all stationary points, whose structures (shown in Figure 6-1) are taken as those obtained at the B3LYP/6-31G(d) level [167]. The 6-311G++(d,p) basis set and the minimum active space (4,4) are used for CAS-BCCC4 calculations. The orbitals in the active space include four π orbitals for the transition state and the product, but two π orbitals plus two σ orbitals (in the breaking C—C bond) for the reactant.

As shown in Table 6-4, the calculated CAS-BCCC4 barrier height (with the zero-point energy corrections calculated at the B3LYP/6-31G(d) level) is 34.12 kcal/mol

Table 6-4. Total energies of the reactant and relative energies of the transition state, and the product (relative to the reactant) in the ring-opening reaction of cyclobutene calculated using different methods with the 6-311G++(d,p) basis set

Method	Reactant (a.u.)	E_a[a] (kcal/mol)	Product (kcal/mol)
CASSCF	−154.982313	36.12 (34.41)	−20.85 (− 21.77)
CAS-BCCC4	−155.547738	35.83 (34.12)	−12.87 (− 13.79)
CASPT2	−155.520442	32.69 (30.98)	−11.51 (− 12.43)
MR-CISD	−155.483865	35.70 (33.99)	−14.60 (− 15.52)
MR-CISD+Q	−155.562106	34.98 (33.27)	−12.56 (− 13.48)
Expt.[b]		31.9±0.2	

[a] Energy barriers with ZPE corrections (as described in the text) are included in the parenthesis.
[b] Reference [167].

Table 6-5. Total energies of the reactant and relative energies of the transition state (relative to the reactant) in the automerization reaction of cyclobutadiene calculated using different methods with the cc-pVTZ basis set

Method	Rectangle (a.u.)	E_a (kcal/mol)[a]
CASSCF	−153.761908	7.38 (4.88)
CAS-BCCC4	−154.353314	8.71 (6.21)
CASPT2	−154.341082	3.75 (1.25)
MR-CISD	−154.290699	8.45 (5.95)
MR-CISD+Q	−154.371872	8.99 (6.49)
MR-AQCC[b]		8.90 (6.40)
Expt.[c]		1.6–10

[a] Energy barriers with ZPE corrections (as described in the text) are included in the parenthesis.
[b] Reference [170].
[c] Reference [168, 169].

[167], reasonably close to the experimental value 31.9±0.2 kcal/mol. The energy barriers from CASPT2, MR-CISD, and MR-CISD+Q are also comparable to the CAS-BCCC4 value. In the automerization reaction of CBD, the transition state has a square structure (D_{4h} symmetry), which is an open shell diradical. The structures and energetics of this reaction have been studied with a number of theoretical methods. The energy barrier estimated from the experiment [168, 169] has a large uncertainty, being in the range of 1.6–10 kcal/mol. Our single point CAS-BCCC4 calculations are performed at the optimized geometries (shown in Figure 6-1) obtained with the multireference average-quadratic coupled cluster (MR-AQCC) method [170], and the active space contains four π electrons in four π orbitals (two π and two π^*), as used in the corresponding MR-AQCC calculations. The cc-pVTZ basis set is employed. The calculated energy barriers without and with ZPE corrections (the ZPE corrections at the MR-AQCC/cc-pVDZ level is −2.5 kcal/mol [170]) are listed in Table 6-5. The barrier height from CAS-BCCC4 calculations is 6.21 kcal/mol, quite close to the corresponding MR-AQCC value (6.4 kcal/mol) and MR-CISD+Q value (6.49 kcal/mol). However, the CASPT2 barrier height (1.25 kcal/mol) is considerably smaller than the barriers from other theoretical methods. On the other hand, for the closed-shell reactant (D_{2h} symmetry), the CCD energy (−154.35314 a.u) should also be a good estimate for its total energy. One can see that this value is almost identical to the CAS-BCCC4 energy, −154.35331 a.u. (CAS-BCCC4 without T_{2C} should be comparable to CCD for closed – shell molecules).

6.3.4. Singlet-Triplet Gaps of Diradicals

The CAS-BCCC4 method has been employed to study the singlet-triplet (S-T) gaps [128, 130, 131] for a number of typical diradicals including methylene (CH_2) and its isovalent species, substituted carbenes, benzyne isomer, and trimethylenemethane (TMM), etc. Here the adiabatic S-T gaps for methylene, halocarbenes (CF_2, CCl_2,

and CBr_2), and TMM calculated with the CAS-BCCC4 method are listed in Table 6-6, together with the corresponding values from CASPT2, MR-CISD, and MR-CISD+Q. For CH_2, the ground state is the triplet state ($\tilde{X}^3B_1$), and the first excited state is a singlet state ($\tilde{a}^1A_1$). However, each halocarbene has a singlet ground state ($\tilde{X}^1A_1$) and the triplet state ($\tilde{a}^3B_1$) as the first excited state. For TMM, its ground state is a triplet state $\left({}^3A_2{}'\right)$ with D_{3h} symmetry, and its lowest two singlet excited states ($^1A_1$ and $^1B_1$) are predicted to be of C_{2v} symmetry (not degenerate, due to the Jahn – Teller effect) [31, 171, 172]. In our CAS-BCCC4 calculations, the equilibrium structures in the ground- and lowest-excited states are from FCI/TZ2P optimizations [173] for CH_2, from CASSCF(18,12)/cc-pVTZ optimizations [174] for halocarbenes, and from SF-DFT/6-31G(d) optimizations [31] for TMM. The geometrical parameters of these molecules are displayed in Figure 6-2. For methylene and three halocarbenes, we employ the cc-pVTZ basis set and the CASSCF(2,2) reference function for CAS-BCCC4 calculations. For TMM, CAS-BCCC4 calculations are carried out with the active space (4,4) (four electrons in four π orbitals $1b_1$, $2b_1$, $1a_2$, and $3b_1$) and the DZP basis set (with five Cartesian d-like functions).

From Table 6-6, one can see that CAS-BCCC4 energies are always lower than MR-CISD values, and CASPT2 values (except for CF_2), implying that CAS-BCCC4 usually recovers more dynamical correlation energies than MR-CISD or CASPT2. Nevertheless, MR-CISD+Q energies are even lower than CAS-BCCC4 energies. In order to compare the energy gaps calculated at different theoretical levels with the experimental values, we need to add the zero-point energy (ZPE) difference between the ground state and its lowest excited state to the calculated electronic energy difference. The ZPE corrections obtained at the same level as in the geometry optimizations for these molecules are available from previous studies, and they will be employed to derive ZPE-corrected adiabatic S-T gaps (which will be used in the following discussions). The ZPE difference between the ground state and its lowest excited state was estimated to be -0.48, -0.10, 0.22, and 0.20 kcal/mol, respectively, for CH_2, CF_2, CCl_2, and CBr_2 [173, 174]. For TMM, the ZPE corrections at the SF-DFT/6-31G(d) level for the two lowest singlet excited states are -0.97 and -2.03 kcal/mol [31].

For CH_2, the ZPE-corrected S-T gaps from CAS-BCCC4, MR-CISD, MR-CISD+Q, and CASPT2 are 9.12, 9.32, 9.20, and 13.88 kcal/mol, respectively. Thus, the results from CAS-BCCC4, MR-CISD, and MR-CISD+Q are much closer to the experimental data (8.998 ± 0.014 kcal/mol [175]) than the CASPT2 value.

For each halocarbene, the S-T gaps from different theoretical methods are always in the order: CAS-BCCC4 > MR-CISD > CASPT2. For three halocarbenes, CAS-BCCC4 values are always very close to MR-CISD+Q values. For CF_2, the S-T gaps from four methods seem to be fairly close to each other and in good agreement with the experimental data (54 ± 3 kcal/mol [176]). For CCl_2 and CBr_2, the S-T separations predicted from all four methods used here are quite different from the experimental data [177] (3 ± 3 and -2 ± 3 kcal/mol, respectively). So our results will be compared with theoretical estimates obtained at the CCSD(T)/cc-pVQZ//CCSD(T)/cc-pVTZ level [174], which are 20.9 kcal/mol for CCl_2, and 16.6 kcal/mol for CBr_2. For these two molecules, it is clear that CAS-BCCC4 S-T

gaps are much closer to the CCSD(T) results than MR-CISD or CASPT2 values. Especially, the S-T gaps from CASPT2 are significantly smaller than those from CCSD(T) or CAS-BCCC4. For TMM, the calculated energy gaps for both singlet states (with respect to the ground triplet state) from four methods used here are comparable to each other, and the ${}^3A_2{}' - {}^1A_1$ gaps from all methods are quite consistent with the experimental value (16.1±0.1 kcal/mol) [178]. To conclude from the results presented here and in previous studies [128, 130, 131], one can find that the overall performance of CAS-BCCC4 and MR-CISD+Q methods are very competitive in predicting the singlet-triplet gaps of diradicals, significantly better than CASPT2 and MR-CISD. The performance of the CASPT2 method is even inferior to that of the MR-CISD method.

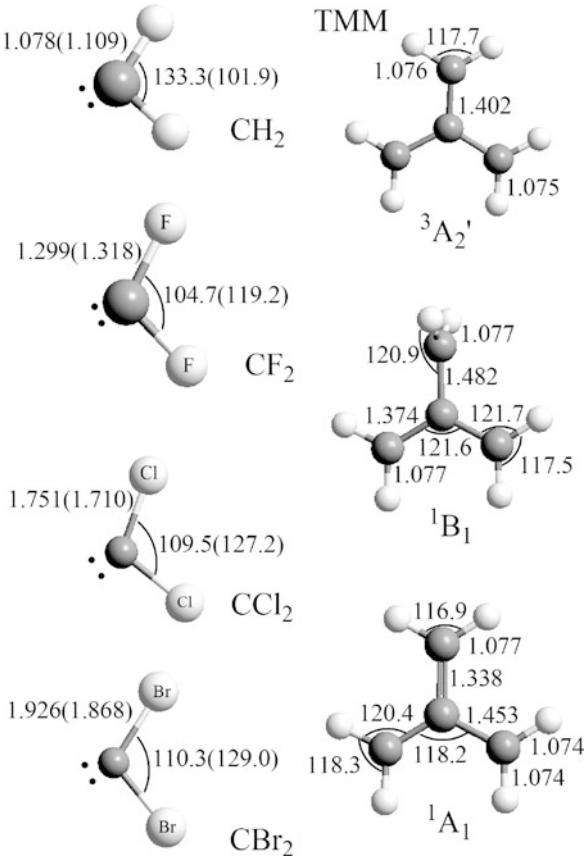

Figure 6-2. Geometric parameters for the ground states and lowest singlet (or triplet) states (the values in the parenthesis) of selected diradicals (Å for bond lengths and deg. for angles)

Table 6-6. The ground-state energies (a.u.) and adiabatic singlet-triplet gaps (kcal/mol) for several diradicals calculated with different methods

Species	Method	$\tilde{X}^3B_1$	$\tilde{a}^1A_1$ [a]	Expt.[b]
	CASSCF	−38.932325	10.66(10.18)	
	CAS-BCCC4	−39.073554	9.60(9.12)	
CH_2	CASPT2	−39.063919	14.36(13.88)	8.998±0.014
	MR-CISD	−39.071035	9.80(9.32)	
	MR-CISD+Q	−39.078580	9.68(9.20)	
		$\tilde{X}^1A_1$	$\tilde{a}^3B_1$ [a]	Expt.[c]
	CASSCF	−236.777249	48.61(48.52)	
	CAS-BCCC4	−237.396886	55.78(55.68)	
CF_2	CASPT2	−237.399631	51.28(51.18)	54±3
	MR-CISD	−237.347418	54.29(54.20)	
	MR-CISD+Q	−237.450219	55.62(55.52)	
	CASSCF	−956.828012	13.16(13.38)	
	CAS-BCCC4	−957.359421	19.16(19.38)	
CCl_2	CASPT2	−957.332392	12.43(12.65)	20.9
	MR-CISD	−957.295676	16.97(17.20)	
	MR-CISD+Q	−957.458818	18.21(18.43)	
	CASSCF	−5182.706556	7.78(7.99)	
	CAS-BCCC4	−5183.181327	13.96(14.16)	
CBr_2	CASPT2	−5183.157426	7.26(7.46)	16.6
	MR-CISD	−5183.124783	11.76(11.97)	
	MR-CISD+Q	−5183.191826	14.07(14.27)	
		$^3A_2{}'$	$^1B_1$ [a]	$^1A_1$ [a]
	CASSCF	−154.936880	14.80(13.83)	19.44 (17.41)
	CAS-BCCC4	−155.449617	15.59(14.62)	19.05 (17.02)
	CASPT2	−155.420386	15.38(14.41)	19.74 (17.71)
TMM	MR-CISD	−155.394006	15.20(14.23)	19.46 (17.43)
	MR-CISD+Q	−155.460780	15.05(15.08)	19.17 (17.14)
	MCQDPT2[d]	−155.423414	15.59(14.62)	19.90 (17.87)
	Expt.[e]			16.1±0.1

[a] Energy gaps with zero-point corrections (as described in the text) are included in the parenthesis.
[b] Reference [175].
[c] Reference [176] for CF_2, and theoretical estimates for CCl_2 and CBr_2 from Reference [174].
[d] Reference [31].
[e] Reference [178].

6.3.5. Low-Lying Excited States

The applicability of the CAS-BCCC4 approach for treating low-lying excited states has been demonstrated recently for several small molecules [129]. Here the results for excited-state PESs of HF and vertical excitation energies of N_2 will be presented.

In CAS-BCCC4 calculations for HF, core excitations (T_{2C}) and semi-internal excitations (T_{4E} and T_{4D}) are neglected since they contribute little to the CAS-BCCC4 energies. For these two molecules, we compare our results with the corresponding full CI values. For comparison, MR-CISD and CASPT2 results are also reported.

For HF, we have studied its five PESs, which include the $X^1\Sigma$ ground state, the lowest single and triple Σ excited states, and the lowest single and triple Π excited states. The Dunning-Hay DZV basis [179] is employed in all calculations. The CASSCF(2,2) reference functions are employed for all states, but the orbitals in the active space are different. For Σ states, the active space includes bonding σ and anti-bonding σ^* orbitals, while for Π states, the active space is composed of one bonding π orbital and one anti-bonding σ^* orbital. For the $^1\Sigma$ excited state, orbitals for CAS-BCCC4 calculations are from state-average CASSCF calculations (the target excited state and the ground state have the weights of 0.9 and 0.1, respectively). For all other states, the CASSCF orbitals are from single-state CASSCF calculations for the state of interest. In Tables 6-7 and 6-8, we have listed the FCI energies [121], and the deviations of CAS-BCCC4 and several other methods with respect to the FCI values. Among all methods, CAS-CCSD [121] (which is the most computationally expensive) provides the smallest absolute deviation, but CAS-BCCC4 gives the smallest NPE. The results from MR-CISD, CASPT2, and CR-EOM-CCSD(T) [180] are also quite comparable to the CAS-BCCC4 results. Among all five PESs, the PES of the $^1\Sigma$ excited state should be emphasized here, as all methods give the largest absolute deviation and NPE for this PES. The NPE is about 3.0 mH for CAS-BCCC4, 3.8 mH for CAS-CCSD, and even higher for other methods.

The vertical excitation energies of N_2 (at equilibrium distance = 2.068 Bohr) from FCI calculations with the cc-pVDZ basis set [161] have been reported [181]. To compare with the FCI results, our CAS-BCCC4 calculations are performed with the same basis set at the same geometry. The CASSCF(6,6) reference function is employed, where the active space consists of six valence orbitals ($3\sigma_g$, $1\pi_u$, $2\pi_u$, $1\pi_g$, $2\pi_g$, and $3\sigma_u$). Vertical excitation energies for $^1\Pi_g$, $^1\Sigma_u^-$, and $^1\Delta_u$ have been obtained with CAS-BCCC4, CASPT2, MR-CISD, and MR-CISD+Q methods. Frozen core approximation is used in all these post-CASSCF calculations. Results from these four different methods are listed in Table 6-9, with the results from EOM-CCSD, and CR-EOM-CCSD(T) reported previously [181, 182]. Among all these methods, CR-EOM-CCSD(T) gives the best performance, but it is also computationally the most expensive. CASPT2 gives less accurate descriptions for the $^1\Sigma_u^-$ state. Both MR-CISD and MR-CISD+Q methods give significant errors on the $^1\Pi_g$ state. The overall performance of CAS-BCCC4 is somewhat better than those of CASPT2, MR-CISD, and EOM-CCSD, and is comparable to that of MR-CISD+Q.

The results presented above and elsewhere have shown that the CAS-BCCC4 approach can give satisfactory descriptions for low-lying electronic excited states. It should be emphasized that, for excited state calculations, the accuracy of the CAS-BCCC4 approach is to some extent dependent on the quality of the CASSCF reference function. If the orbitals are from a single-state CASSCF calculation, the CAS-BCCC4 method usually gives quite accurate excitation energy for the state of

Table 6-7. Comparison of singlet state energies from CAS-BCCC4, MR-CISD, CASPT2, CAS-CCSD, and CR-EOM-CCSD(T) with FCI values for bond dissociation in HF. FCI energies are given as (E+99) in a.u. The values (in mH) for all other methods are the deviations with respect to FCI values

R_{H-F} (bohr)	1.40	1.733	2.50	3.40	4.175	5.00	6.00
	$X^1\Sigma$						
FCI	−1.075754	−1.146457	−1.088759	−1.011613	−0.982385	−0.973063	−0.970733
CAS-BCCC	2.11	2.29	2.68	2.43	1.99	1.83	1.79
MR-CISD[a]	5.36	5.31	5.15	4.99	5.10	5.24	5.23
CASPT2	3.54	3.32	3.99	4.68	4.53	4.49	4.51
CAS-CCSD[a]	−0.81	−0.24	0.63	1.24	1.35	1.56	1.63
CR-EOM-CCSD(T)[a]	0.09	0.23	0.60	1.24	1.89	2.14	1.87
	$2^1\Sigma$						
FCI	−0.397884	−0.552667	−0.682970	−0.745959	−0.751461	−0.732115	−0.703454
CAS-BCCC	1.30	1.73	3.96	4.33	3.95	3.80	3.82
MR-CISD[a]	4.89	6.79	8.40	9.26	9.64	9.67	9.64
CASPT2	−0.05	−4.09	−4.78	−2.20	−0.56	1.01	2.41
CAS-CCSD[a]	1.53	1.66	0.74	−0.29	−2.19	−1.89	−1.80
CR-EOM-CCSD(T)[a]	2.62	2.71	2.31	−0.24	−1.74	−1.24	−0.47
	$^1\Pi$						
FCI	−0.582928	−0.737204	−0.889068	−0.949385	−0.964420	−0.968949	−0.970129
CAS-BCCC	1.70	1.98	1.95	1.78	1.78	1.79	1.79
MR-CISD[a]	2.01	2.39	2.49	2.46	2.49	2.51	2.52
CASPT2	4.96	4.31	3.69	4.07	4.35	4.48	4.52
CAS-CCSD[a]	0.95	1.11	1.14	1.15	1.19	1.20	1.21
CR-EOM-CCSD(T)[a]	2.09	2.1	1.49	0.34	−0.31	−0.56	−1.16

[a] Reference [121].

Table 6-8. Comparison of triplet state energies from CAS-CCSD, MR-CISD, CASPT2, and CAS-BCCC4, with FCI values for bond dissociation in HF. FCI energies are given as (E + 99) in a.u. The values (in mH) for all other methods are the deviations with respect to FCI values

R_{H-F} (bohr)	1.40	1.733	2.50	3.40	4.175	5.00	6.00
	$^3\Pi$						
FCI	−0.604984	−0.761286	−0.905506	−0.955002	−0.966264	−0.969452	−0.970218
CAS-BCCC	1.72	2.00	2.00	1.81	1.79	1.79	1.79
CAS-CCSD[a]	0.94	1.11	1.11	1.13	1.18	1.20	1.21
MR-CISD[a]	2.21	2.62	2.81	2.62	2.55	2.53	2.53
CASPT2	4.98	4.19	3.90	4.35	4.48	4.52	4.53
	$^3\Sigma$						
FCI	−0.436232	−0.642808	−0.869191	−0.947667	−0.964545	−0.969077	−0.970142
CAS-BCCC	2.06	2.08	1.86	1.79	1.78	1.78	1.78
CAS-CCSD[a]	1.26	1.51	1.67	1.64	1.64	1.65	1.65
MR-CISD[a]	2.45	2.71	2.59	2.52	2.52	2.52	2.52
CASPT2	4.63	4.35	4.50	4.55	4.55	4.54	4.53

[a] Reference [121].

Table 6-9. Vertical excitation energies of N_2 from CAS-BCCC4, EOM-CCSD, MR-CISD, MR-CISD+Q, CASPT2, CR-EOM-CCSD(T), and FCI calculations. The FCI values are in eV, and the values (in eV) for all the other methods are the deviations with respect to FCI values

State	FCI[a]	EOM-CCSD[b]	CR-EOM-CCSD(T)[c]	MR-CISD	MR-CISD+Q	CASPT2	CAS-BCCC4
$^1\Pi_g$	9.584	−0.081	0.143	0.311	−0.206	−0.115	0.110
$^1\Sigma_u^-$	10.329	−0.136	0.013	0.076	0.003	−0.202	0.027
$^1\Delta_u$	10.718	−0.180	0.033	0.144	−0.022	−0.091	0.097

[a] Reference [181].
[b] Reference [182].
[c] Reference [180].

interest. If the orbitals are from a state-average CASSCF calculation, the relative weight of the state under study in the CASSCF calculation should be as large as possible.

6.3.6. Size-Extensivity Errors

As mentioned in the previous section, the CAS-BCCC4 approach is core- extensive, but not size-extensive with respect to the total number of electrons. To illustrate the core-extensivity of CAS-BCCC4, we perform a CAS-BCCC4 calculation for a model system, which contains two HF molecules separated from each other by 100 Å, with both H—F bond lengths of 1.0 Å. The 6-311 + +G** basis set is employed, and all operators up to the four-block correlation level are included in the

CAS-BCCC4 calculation. For this combined system, the active space includes the σ and σ* orbitals on one HF fragment. The CAS-BCCC4 energy is −200.600960 a.u. This value is equal to the sum of the CAS-BCCC4 energy (−100.300806 a.u.) for the HF with the same active space as in the combined system, and the CCSD energy (−100.300153 a.u.) for another HF. Hence, the CAS-BCCC4 method satisfies the core-extensivity.

However, CAS-BCCC4 is not fully size-extensive, and its size-extensivity error usually increases with increasing the size of the active space [130]. Here we take four diatomic molecules (C_2, N_2, O_2 and F_2) and four hydrocarbons (ethane, ethene, 2,3-dimethyl-butane, and 2,3-dimethyl-2-butene, as shown in Figure 6-3) as examples to demonstrate the size-extensivity errors for CAS-BCCC4, and other widely used multireference methods (CASPT2, MR-CISD, and MR-CISD+Q). For each molecule, the size-extensivity error is defined to be the energy difference between the energy calculated for the combined system containing two fragments by breaking a chemical bond (a central bond for polyatomic molecules) and the sum of energies obtained for two separated fragments. The 6-311G++$(3df, 3p)$ basis set is employed for diatomic molecules and 6-31G** for hydrocarbons. In CAS-BCCC4 calculations, operators T_{2C}, T_{4E} and T_{4D} are ignored to reduce the computation cost. For each molecule, the active space is chosen to be the minimum active space required for a qualitatively correct description of the broken bond. Some computational details were discussed previously [126, 128]. The size-entensivity errors obtained with four theoretical methods are listed in Table 6-10. It can be seen that the size-entensivity errors for CASPT2 are always close to zero, with the largest one being 0.08 kcal/mol for C_2. For CAS-BCCC4, the size-extensivity error for F_2

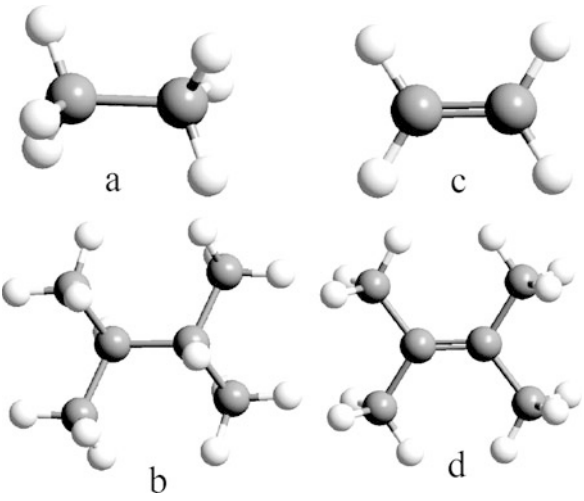

Figure 6-3. Schematic structures of the four studied hydrocarbons. (**a**) ethane; (**b**) 2,3-dimethyl- butane; (**c**) ethylene; d. 2,3-dimethyl-2-butene

Table 6-10. Size-extensivity errors (kcal/mol) of several molecules calculated with different theoretical methods

Molecule	Active space	CAS-BCCC4	CASPT2	MR-CISD	MR-CISD+Q
C_2	(6,6)	4.52	−0.08	5.36	1.11
N_2	(6,6)	4.17	−0.06	5.02	0.77
O_2	(8,6)	6.61	−0.01	7.26	1.18
F_2	(2,2)	0.87	0.01	−8.93	1.39
C_2H_6	(2,2)	−0.77	−0.01	8.65	1.62
C_6H_{14}	(2,2)	0.31	−0.01	48.85	19.09
C_2H_4	(4,4)	1.89	−0.01	5.69	0.95
C_6H_{12}	(4,4)	3.67	−0.04	43.91	16.74

with a small active space (2,2) is only 0.87 kcal/mol. Nevertheless, for O_2 with the larger active space (8,6), this value increases to 6.61 kcal/mol. The overall trend is that the size-extensivity error of the CAS-BCCC4 method increases with the size of the active space. However, due to the core-extensivity, the size-extensivity error of CAS-BCCC4 does not necessarily increase with the total number of electrons (or the size of the molecule). For instance, the size-extensivity error does not increase from ethane to 2,3-dimethyl-butane. For MR-CISD, the size-entensivity errors are always the largest among these methods, and increase rapidly with increasing the total number of electrons. The MR-CISD+Q method usually has very small size-entensivity errors for small molecules, regardless of the size of the active space. However, for relatively large molecules like 2,3-dimethyl-butane and 2,3-dimethyl-2-butene, the errors are 19.09 and 16.74 kcal/mol, respectively. Thus, the size-entensivity error of MR-CISD+Q increases also noticeably with the system size. It is expected that for relatively large molecules (with small active spaces) CAS-BCCC4 will have much smaller size-extensivity errors than MR-CISD+Q.

6.4. CONCLUDING REMARKS

In this chapter, we have presented the general formalism of block correlated coupled cluster method with a CASSCF reference function and a number of applications of this method for ground- and excited electronic states of molecules with multireference character. The CAS-BCCC4 method has several desirable properties: (1) free of the intruder state problem; (2) invariant with respect to orbital rotations within separated orbital subspaces (occupied, active, and virtual); (3) cost-effective, being much less expensive that most MRCC methods. Nevertheless, this method is only core-extensive, not size-extensive with respect to the total number of electrons. This drawback makes the CAS-BCCC4 method to be most applicable for systems with small active spaces. To assess the performance of the CAS-BCCC4 method, we have applied this method to investigate a number of chemical problems, which include bond breaking potential energy surfaces, singlet-triplet gaps of diradicals, reaction

barriers, spectroscopic constants of diatomic molecules, and low-lying excited states. Comparisons between CAS-BCCC4 results and those from FCI or other highly accurate theoretical methods demonstrate that the CAS-BCCC4 approach provides very accurate descriptions for all problems under study. The overall performance of CAS-BCCC4 is illustrated to be better than that of CASPT2 and MR-CISD methods. For small systems, the performance of CAS-BCCC4 and MR-CISD+Q is very competitive, but CAS-BCCC4 is expected to be even better than MR-CISD+Q when the system becomes relatively large, due to the core-extensivity of the CAS-BCCC4 method.

The future development of the CAS-BCCC method may proceed in several directions. One is to develop CAS-BCCC*n* with higher *n*-block correlation operators. The inclusion of perturbative triple excitations (only for core excitations) should be readily implemented within the CAS-BCCC framework, following a similar idea as in CCSD(T). Another is to develop a linear response or equation-of-motion CAS-BCCC4 method for treating more general excited states. This approach would allow more low-lying excited states to be treated in a more balanced way. On the other hand, as described above, the effectiveness of the CAS-BCCC4 approach will decrease with increasing the size of the active space. Thus, a more accurate way for treating systems with large active spaces is to use two (or more) smaller multi-orbital blocks instead a large multi-orbital block. If an electron pair is chosen as a block, then a GVB-based BCCC is expected to be more accurate than the CAS-BCCC method with a large active space. Our development along these directions is under progress.

ACKNOWLEDGMENTS

We would like to thank Prof. Mukherjee and his graduate student D. Datta for very helpful discussions, and graduate student Weijie Hua in our laboratory for his contribution to some of the work described in this chapter. The financial support was provided by the National Natural Science Foundation of China (Grant Nos. 20625309 and 20833003), the National Basic Research Program (Grant No. 2004CB719901), and the Chinese Ministry of Education (Grant No. NCET-04-0450).

REFERENCES

1. J. Čížek, J. Chem. Phys. **45**, 4256 (1966)
2. J. Čížek, J. Paldus, Int. J. Quantum Chem. **5**, 359 (1971)
3. G. D. Purvis, R. J. Bartlett, J. Chem. Phys. **76**, 1910 (1982)
4. K. Raghavachari, G. W. Trucks, J. A. Pople, M. Head-Gordon, Chem. Phys. Lett. **157**, 479 (1989)
5. J. Noga, R. J. Bartlett, J. Chem. Phys. **86**, 7041 (1987)
6. C. Sosa, J. Noga, R. J. Bartlett, J. Chem. Phys. **88**, 5974 (1988)
7. G. E. Scuseria, H. F. Schaeffer III, Chem. Phys. Lett. **152**, 382 (1988)
8. S. A. Kucharski, R. J. Bartlett, J. Chem. Phys. **97**, 4282 (1992)
9. N. Oliphant, L. Adamowicz, J. Chem. Phys. **95**, 6645 (1991)
10. M. Musial, R. J. Bartlett, J. Chem. Phys. **122**, 224102 (2005)

11. J. A. Pople, P. K. Nesbet, J. Chem. Phy. **22**, 571 (1954)
12. R. J. Bartlett, Annu. Rev. Phys. Chem. **32**, 359 (1981)
13. W. Chen, H. B. Schlegel, J. Chem. Phys. **101**, 5957 (1994)
14. A. I. Krylov, J. Chem. Phys. **113**, 6052 (2000)
15. X. Z. Li, J. Paldus, J. Chem. Phys. **107**, 6257 (1997)
16. X. Z. Li, J. Paldus, J. Chem. Phys. **108**, 637 (1998)
17. X. Z. Li, J. Paldus, J. Chem. Phys. **110**, 2844 (1999)
18. X. Z. Li, J. Paldus, J. Chem. Phys. **113**, 9966 (2000)
19. X. Li, J. Paldus, J. Chem. Phys. **115**, 5759 (2001); **115**, 5774 (2001)
20. X. Li, J. Paldus, J. Chem. Phys. **117**, 1941 (2002)
21. X. Li, J. Paldus, J. Chem. Phys. **118**, 2470 (2003)
22. X. Z. Li, J. Paldus, J. Chem. Phys. **124**, 174101 (2006)
23. X. Z. Li, J. Paldus, J. Chem. Phys. **125**, 164107 (2006)
24. J. Paldus, X. Li, in *Advances in Quantum Many-Body Theory*, vol. 5, Eds. R. F. Bishop, T. Brandes, K. A. Gernoth, N. R. Walet, Y. Xian (World Scientific, Singapore, 2002), pp. 393–404
25. A. I. Krylov, Chem. Phys. Lett. **338**, 375 (2001)
26. A. I. Krylov, Chem. Phys. Lett. **350**, 522 (2001)
27. A. I. Krylov, C. D. Sherrill, J. Chem. Phys. **116**, 3194 (2002)
28. J. S. Sears, C. D. Sherrill, A. I. Krylov, J. Chem. Phys. **118**, 9084 (2003)
29. Y. H. Shao, M. Head-Gordon, A. I. Krylov, J. Chem. Phys. **118**, 4807 (2003)
30. S. V. Levchenko, A. I. Krylov, J. Chem. Phys. **120**, 175 (2004)
31. L. V. Slipchenko, A. I. Krylov, J. Chem. Phys. **117**, 4694 (2002)
32. L. V. Slipchenko, A. I. Krylov, J. Chem. Phys. **123**, 084107 (2005)
33. A. I. Krylov, C. D. Sherrill, E. F. C. Byrd, M. Head-Gordon, J. Chem. Phys. **109**, 10669 (1998)
34. A. I. Krylov, C. D. Sherrill, M. Head-Gordon, J. Chem. Phys. **113**, 6509 (2000)
35. C. D. Sherrill, A. I. Krylov, E. F. C. Byrd, M. Head-Gordon, J. Chem. Phys. **109**, 4171 (1998)
36. R. C. Lochan, M. Head-Gordon, J. Chem. Phys. **126**, 164101 (2007)
37. S. R. Gwaltney, M. Head-Gordon, Chem. Phys. Lett. **323**, 21 (2000)
38. S. R. Gwaltney, C. D. Sherrill, M. Head-Gordon, A. I. Krylov, J. Chem. Phys. **113**, 3548 (2000)
39. S. R. Gwaltney, M. Head-Gordon, J. Chem. Phys. **115**, 2014 (2001)
40. S. R. Gwaltney, E. F. C. Byrd, T. Van Voorhis, M. Head-Gordon, Chem. Phys. Lett. **353**, 359 (2002)
41. P. Piecuch, K. Kowalski, I. S. O. Pimienta, M. J. McGuire, Int. Rev. Phys. Chem. **21**, 527 (2002)
42. K. Kowalski, P. Piecuch, J. Chem. Phys. **116**, 7411 (2002)
43. M. Włoch, J. R. Gour, K. Kowalski, P. Piecuch, J. Chem. Phys. **122**, 214107 (2005)
44. P. Piecuch, K. Kowalski, I. S. O. Pimienta, P. D. Fan, M. Lodriguito, M. J. McGuire, S. A. Kucharski, T. Kus, M. Musiał, Theor. Chem. Acc. **112**, 349 (2004)
45. P. Piecuch, M. Włoch, J. Chem. Phys. **123**, 224105 (2005)
46. A. Kinal, P. Piecuch, J. Phys. Chem. A **111**, 734 (2007)
47. M. Włoch, J. R. Gour, P. Piecuch, J. Phys. Chem. A **111**, 11359 (2005)
48. P. Piecuch, M. Włoch, K. Kowalski, A. J. C. Varandas, Theor. Chem. Acc. **120**, 59 (2008)
49. J. Zheng, J. R. Gour, J. J. Lutz, M. Włoch, P. Piecuch, D. G. Truhlar, J. Chem. Phys. **128**, 044108 (2008)
50. N. Oliphant, L. Adamowicz, J. Chem. Phys. **94**, 1229 (1991)
51. P. Piecuch, N. Oliphant, L. Adamowicz, J. Chem. Phys. **99**, 1875 (1993)
52. P. Piecuch, S. A. Kucharski, R. J. Bartlett, J. Chem. Phys. **110**, 6103 (1999)
53. M. Kallay, P. R. Surjan, J. Chem. Phys. **113**, 1359 (2000).
54. P. Piecuch, L. Adamowicz, J. Chem. Phys. **100**, 5792 (1994)
55. P. Piecuch, L. Adamowicz, Chem. Phys. Lett. **221**, 121 (1994)

56. K. Kowalski, S. Hirata, M. Włoch, P. Piecuch, T. L. Windus, J. Chem. Phys. **123**, 074319 (2005)
57. K. Kowalski, P. Piecuch, J. Chem. Phys. **113**, 8490 (2000)
58. K. Kowalski, P. Piecuch, Chem. Phys. Lett. **344**, 165 (2001)
59. K. Kowalski, P. Piecuch, J. Chem. Phys. **115**, 643 (2001)
60. P. Piecuch, S. Hirata, K. Kowalski, P. D. Fan, T. L. Windus, Int. J. Quantum Chem. **106**, 79 (2006)
61. J. R. Gour, P. Piecuch, M. Włoch, J. Chem. Phys. **123**, 134113 (2005)
62. J. Olsen, J. Chem. Phys. **113**, 7140 (2000)
63. P. Piecuch, S. A. Kucharski, V. Špirko, J. Chem. Phys. **111**, 6679 (1999)
64. T. Kinoshita O. Hino, R. J. Bartlett, J. Chem. Phys. **123**, 074106 (2005)
65. D. Mukherjee, R. K. Moitra, A. Mukhopadhyay, Mol. Phys. **33**, 955 (1977)
66. A. Haque, D. Mukherjee, J. Chem. Phys. **80**, 5058 (1984)
67. I. Lindgren, Int. J. Quantum Chem. **S12**, 33 (1978)
68. W. Kutzelnigg, J. Chem. Phys. **77**, 3081 (1982)
69. A. Haque, U. Kaldor, Chem. Phys. Lett. **117**, 347 (1986)
70. U. Kaldor, J. Chem. Phys. **87**, 467 (1987)
71. S. R. Hughes, U. Kaldor, Chem. Phys. Lett. **194**, 99 (1992)
72. R. Offerman, W. Ey, H. Kummel, Nucl. Phys. A **273**, 349 (1976)
73. R. Offerman, Nucl. Phys. A **273**, 368 (1976)
74. W. Ey, Nucl. Phys. A **296**, 189 (1978)
75. B. Jeziorski, H. J. Monkhorst, Phys. Rev. A **24**, 1668 (1981)
76. L. Stolarczyk, H. J. Monkhorst, Phys. Rev. A **32**, 743 (1985)
77. B. Jeziorski, J. Paldus, J. Chem. Phys. **88**, 5673 (1988)33
78. L. Meissner, K. Jankowski, J. Wasilewski, Int. J. Quantum Chem. **34**, 535 (1988)
79. J. Paldus, J. Pylypow, B. Jeziorski, Many Body Methods in Quantum Chemistry, Lecture Notes in Chemistry, vol. 52, Ed. U. Kaldor (Springer, Berlin, 1989)
80. P. Piecuch, J. Paldus, Theor. Chim. Acta **83**, 69 (1992)
81. A. Balkova, S. A. Kucharski, L. Meissner, R. J. Bartlett, Theor. Chim. Acta **80**, 335 (1991)
82. S. A. Kucharski, A. Balkova, P. G. Szalay, R. J. Bartlett, J. Chem. Phys. **97**, 4289 (1992)
83. X. Li, J. Paldus, J. Chem. Phys. **119**, 5320 (2003)
84. X. Li, J. Paldus, J. Chem. Phys. **119**, 5346 (2003)
85. X. Li, J. Paldus, J. Chem. Phys. **120**, 5890 (2004)
86. X. Li, J. Paldus, J. Chem. Phys. **124**, 034112 (2006)
87. D. Mukherjee, in *Recent Progress in Many-Body Theories*, vol. 4, Eds. E. Schachinger, R. Mitter, H. Stormann (Plenum, New York, 1995), pp. 127–133
88. U. S. Mahapatra, B. Datta, B. Bandyopadhyay, D. Mukherjee, Adv. Quantum Chem. **30**, 163 (1998)
89. U. S. Mahapatra, B. Datta, D. Mukherjee, J. Phys. Chem. A **103**, 1822 (1999)
90. U. S. Mahapatra, B. Datta, D. Mukherjee, J. Chem. Phys. **110**, 6171 (1999)
91. S. Chattopadhyay, U. S. Mahapatra, D. Mukherjee, J. Chem. Phys. **112**, 7939 (2000)
92. S. Chattopadhyay, D. Pahari, D. Mukherjee, U. S. Mahapatra, J. Chem. Phys. **120**, 5968 (2004)
93. S. Chattopadhyay, P. Ghosh, U. S. Mahapatra, J. Phys. B **37**, 495 (2004)
94. F. A. Evangelista, W. D. Allen, H. F. Schaefer III, J. Chem. Phys. **125**, 154113 (2006)
95. F. A. Evangelista, W. D. Allen, H. F. Schaefer III, J. Chem. Phys. **127**, 024102 (2007)
96. I. Hubač, P. Neogrady, Phys. Rev. **50**, 4558 (1994)
97. J. Mášik, I. Hubač, P. Mach, J. Chem. Phys. **108**, 6571 (1998)
98. J. Pittner, J. Chem. Phys. **118**, 10876 (2003)
99. J. Pittner, O. Demel, J. Chem. Phys. **122**, 181101 (2005)
100. J. Pittner, P. Nachtigall, P. Čársky, J. Mášik, I. Hubač, J. Chem. Phys. **110**, 10275 (1999)
101. I. Hubač, J. Pittner, P. Čársky, J. Chem. Phys. **112**, 8779 (2000)

102. M. Hanrath, J. Chem. Phys. **123**, 084102 (2005)
103. M. Hanrath, J. Chem. Phys. **128**, 154118 (2008)
104. J. Paldus, P. Piecuch, L. Pylypow, B. Jeziorski, Phys. Rev. A **47**, 2738 (1993)
105. P. Piecuch, J. Paldus, Phys. Rev. A **49**, 3479 (1994)
106. A. Banerjee, J. Simons, Int. J. Quantum Chem. **19**, 207 (1981)
107. A. Banerjee, J. Simons, J. Chem. Phys. **76**, 4548 (1982)
108. W. D. Laidig, R. J. Bartlett, Chem. Phys. Lett. **104**, 424 (1984)
109. W. D. Laidig, P. Saxe, R. J. Bartlett, J. Chem. Phys. **86**, 887 (1987)
110. D. Mukherjee, S. Pal, in *Advances in Quantum Chemistry*, vol. 20, Eds. P-O. Löwdin, J. R. Sabin, M. C. Zerner (Academic Press, Inc, San Diego, CA, 1989), pp. 291–373
111. M. R. Hoffmann, J. Simons, J. Chem. Phys. **88**, 993 (1988)
112. T. Yanai, G. K.-L. Chan, J. Chem. Phys. **124**, 194106 (2006)
113. T. Yanai, G. K.-L. Chan, J. Chem. Phys. **127**, 104107 (2007)
114. D. Mukherjee, Chem. Phys. Lett. **274**, 561 (1997)
115. W. Kutzelnigg, D. Mukherjee, J. Chem. Phys. **107**, 432 (1997)
116. L. Adamowicz, J. P. Malrieu, V. V. Ivanov, J. Chem. Phys. **112**, 10075 (2000)
117. V. V. Ivanov, L. Adamowicz, J. Chem. Phys. **112**, 9258 (2000)
118. D. I. Lyakh, V. V. Ivanov, L. Adamowicz, J. Chem. Phys. **122**, 024108 (2005)
119. V. V. Ivanov, L. Adamowicz, D. I. Lyakh, Int. J. Quantum Chem. **106**, 2875 (2006)
120. D. I. Lyakh, V. V. Ivanov, L. Adamowicz, Mol. Phys. **105**, 1335 (2007)
121. D. I. Lyakh, V. V. Ivanov, L. Adamowicz, J. Chem. Phys. **128**, 074101 (2008)
122. V. V. Ivanov, D. I. Lyakh, L. Adamowicz, Phys. Chem. Chem. Phys. **11**, 2355 (2009)
123. S. Li, J. Chem. Phys. **120**, 5017 (2004)
124. A. C. Hurley, J. Lennard-Jones, J. A. Pople, Proc. R. Soc. Lond., Ser. A **220**, 446 (1953)
125. F. W. Bobrowitcz, W. A. Goddard, III, in *Modern Theoretical Chemistry*, vol. 3, Ed. H. F. Schaefer III (Plenum, New York, 1977)
126. T. Fang, S. Li, J. Chem. Phys. **127**, 204108 (2007)
127. T. Fang, J. Shen, S. Li, J. Chem. Phys. **128**, 224107 (2008)
128. J. Shen, T. Fang, W. Hua, S. Li, J. Phys. Chem. A **112**, 4703 (2008)
129. T. Fang, J. Shen, S. Li, J. Chem. Phys. **129**, 234106 (2008)
130. J. Shen, T. Fang, S. Li, Y. Jiang, J. Phys. Chem. A **112**, 12518 (2008)
131. J. Shen, T. Fang, S. Li, Sci. China Ser. B-Chem. **51**, 1197 (2008)
132. J. Shen, T. Fang, S. Li, Y. Jiang, Chem. J. Chinese Univ. **29**, 2341 (2008)
133. J. Shen, T. Fang, S. Li, in *Progress in Theoretical Chemistry and Physics Frontiers in Quantum Systems in Chemistry Physics*, vol. 19, Eds. P. Piecuch, S. Wilson, P. J. Grout, J. Maruani, G. Delgado-Barrio (Springer, Berlin, 2009), pp. 241–255
134. S. Hirata, R. J. Bartlett, Chem. Phys. Lett. **321**, 216 (2000)
135. H. J. Monkhorst, Int. J. Quantum Chem., Quantum Chem. Symp. **11**, 421 (1977)
136. D. Mukherjee, P. K. Mukherjee, Chem. Phys. **39**, 325 (1979)
137. E. Dalgaard, H. J. Monkhorst, Phys. Rev. A **28**, 1217 (1983)
138. M. Takahashi, J. Paldus, J. Chem. Phys. **85**, 1486 (1986)
139. H. Nakatusji, K. Hirao, J. Chem. Phys. **68**, 2053 (1978)
140. H. Nakatsuji, Chem. Phys. Lett. **59**, 362 (1978)
141. H. Nakatsuji, Chem. Phys. Lett. **67**, 329 (1979)
142. H. Nakatsuji, Chem. Phys. Lett. **67**, 334 (1979)
143. K. Emrich, Nucl. Phys. A **351**, 379 (1981)
144. J. Geertsen, M. Rittby, R. J. Bartlett, Chem. Phys. Lett. **164**, 57 (1989)

145. D. C. Comeau, R. J. Bartlett, Chem. Phys. Lett. **207**, 414 (1993)
146. J. F. Stanton, R. J. Bartlett, J. Chem. Phys. **98**, 7029 (1993)
147. L. Kong, K. R. Shamasundar, O. Demel, M. Nooijen. J. Chem. Phys. **130**, 114101 (2009)
148. M. W. Schmidt, K. K. Baldridge, J. A. Boatz, S. T. Elbert, M. S. Gordon, J. H. Jensen, S. Koseki, N. Matsunaga, K. A. Nguyen, S. J. Su, T. L. Windus, M. Dupuis, J. A. Montgomery, J. Comput. Chem. **14**, 1347 (1993)
149. H.-J. Werner, E. A. Reinsch, J. Chem. Phys. **76**, 3144 (1982)
150. H.-J. Werner, P. J. Knowles, J. Chem. Phys. **89**, 5803 (1988)
151. P. J. Knowles, H. J. Werner, Chem. Phys. Lett. **145**, 514 (1988)
152. P. J. Knowles, H.-J. Werner, Theor. Chim. Acta **84**, 95 (1992)
153. H.-J. Werner, Mol. Phys. **89**, 645 (1996)
154. P. Celani, H.-J. Werner, J. Chem. Phys. **112**, 5546 (2000)
155. MOLPRO, version 2006.1, a package of ab initio programs, H.-J. Werner, P. J. Knowles, R. Lindh, F. R. Manby, M. Schütz, P. Celani, T. Korona, G. Rauhut, R. D. Amos, A. Bernhardsson, A. Berning, D. L. Cooper, M. J. O. Deegan, A. J. Dobbyn, F. Eckert, C. Hampel, G. Hetzer, A. W. Lloyd, S. J. McNicholas, W. Meyer, M. E. Mura, A. Nicklass, P. Palmieri, R. Pitzer, U. Schumann, H. Stoll, A. J. Stone, R. Tarroni, T. Thorsteinsson, see http://www.molpro.net
156. J. Pittner, J. Šmydke, P. Čársky, I. Hubač, J. Mol. Struct.: THEOCHEM **547**, 239 (2001)
157. T. H. Dunning, J. Chem. Phys. **53**, 2823 (1970)
158. S. Huzinaga, J. Chem. Phys. **42**, 1293 (1965)
159. R. J. Bartlett, M. Musial, J. Chem. Phys. **125**, 204105 (2006).
160. D. A. Mazziotti, Phys. Rev. A **76**, 052502 (2007)
161. T. H. Dunning, J. Chem. Phys. **90**, 1007 (1989)
162. J. Pérez-Jiménez, J. M. Pérez-Jordá, Phys. Rev. A **75**, 012503 (2007)
163. *NIST Chemistry WebBook, NIST Standard Reference Database Number 69*, Ed. Mallard, W. G. National Institute of Standards and Technology, http://webbook.nist.gov/chemistry, Release 69, June, 2005
164. *NIST Computational Chemistry Comparison and Benchmark Database, NIST Standard Reference Database Number 101*, Ed. Johnson III, R. D. National Institute of Standards and Technology, http://srdata.nist.gov/cccbdb, Release 12, August, 2005
165. G. Herzberg, *Molecular Spectra and Molecular Structure I. Spectra of Diatomic Molecules*, second reprinted edition (Krieger Publishing, Malabar, FL, 1989)
166. K. P. Huber, G. Herzberg, *Molecular Spectra and Molecular Structure IV. Constants of Diatomic Molecules* (van Nostrand, New York, 1979)
167. V. Guner, K. S. Khuong, A. G. Leach, P. S. Lee, M. D. Bartberger, K. N. Houk, J. Phys. Chem. A **107**, 11445 (2003)
168. D. W. Whitman, B. K. Carpenter, J. Am. Chem. Soc. **104**, 6473 (1982)
169. B. K. Carpenter, J. Am. Chem. Soc. **105**, 1700 (1983)
170. M. Eckert-Maksić, M. Vazdar, M. Barbatti, H. Lischka, Z. B. Maksić, J. Chem. Phys. **125**, 064310 (2006)
171. P. Dowd, J. Am. Chem. Soc. **88**, 2587 (1966)
172. R. J. Baseman, D. W. Pratt, M. Chow, P. Dowd, J. Am. Chem. Soc. **98**, 5726 (1976)
173. C. D. Sherrill, M. L. Leininger, T. J. Van Huis, H. F. Schaefer III, J. Chem. Phys. **108**, 1040 (1998)
174. K. Sendt, G. B. Bacskay, J. Chem. Phys. **112**, 2227 (2000)
175. P. Jensen, P. R. Bunker, J. Chem. Phys. **89**, 1327 (1998)
176. K. K. Murray, D. G. Leopold, T. M. Miller, W. C. Lineberger, J. Chem. Phys. **89**, 5442 (1988)
177. R. L. Schwartz, G. E. Davico, T. M. Ramond, W. C. Lineberger, J. Phys. Chem. A **103**, 8213 (1999)

178. P. G. Wenthold, J. S. Hu, R. R. Squires, W. C. Lineberger, J. Am. Chem. Soc. **118**, 475 (1996)
179. T. H. Dunning Jr., P. J. Hay, *Methods of Electronic Structure Theory*, Ed. H. F. Shaefer III (Plenum, New York, 1977), chap. 1, pp. 1–27
180. K. Kowalski, P. Piecuch, J. Chem. Phys. **120**, 1715 (2004)
181. O. Christiansen, H. Koch, P. Jørgensen, J. Olsen, Chem. Phys. Lett. **256**, 185 (1996)
182. M. Musial, R. J. Bartlett, J. Chem. Phys. **127**, 024106 (2007)

CHAPTER 7

A POSSIBILITY FOR A MULTI-REFERENCE COUPLED-CLUSTER: THE MRexpT ANSATZ

MICHAEL HANRATH

Institute for Theoretical Chemistry, University of Cologne, 50939 Cologne, Germany, e-mail: Michael.Hanrath@uni-koeln.de

Abstract: This contribution describes the derivation and analysis of the MRexpT ansatz. After a brief discussion of the fundamental difficulties with the generalization of the single-reference coupled-cluster ansatz to the multi-reference case (despite a significant number of research activities in various groups this process is to be considered still unfinished) this chapter gives a brief overview of the literature and shortly discusses a few selected approaches. Subsequently the MRexpT ansatz is introduced and theoretical properties are discussed in some detail. Apart from its lack of core/valence connectivity MRexpT offers many beneficial properties and shows a high numerical accuracy. The latter is illustrated by a number of selected applications.

Keywords: Multireference coupled cluster, MRexpT ansatz

7.1. INTRODUCTION

7.1.1. The Single-Reference Case

The single-reference coupled-cluster (SRCC) ansatz [1, 2] uses the ansatz

$$|\Psi_{\mathrm{CC}}\rangle = e^{\hat{T}}|0\rangle \tag{7-1}$$

with $|0\rangle$ the Fermi vacuum and the cluster operator $\hat{T} = \sum_{\nu=1}^{M} \hat{T}_\nu$ and

$$\hat{T}_\nu = \sum_{\substack{i_1<i_2<\ldots<i_\nu \\ a_1<a_2<\ldots<a_\nu}} t_{i_1\ldots i_\nu}^{a_1\ldots a_\nu}\, \hat{a}_{a_1}^\dagger \ldots \hat{a}_{a_\nu}^\dagger \hat{a}_{i_\nu} \ldots \hat{a}_{i_1} \tag{7-2}$$

where we used the common convention $i_\nu \in \mathbb{O}$ and $a_\nu \in \mathbb{V}$ with $\mathbb{O}$ and $\mathbb{V}$ the occupied and virtual orbitals with respect to the Fermi vacuum $|0\rangle$,

P. Čársky et al. (eds.), Recent Progress in Coupled Cluster Methods, 175–190.
DOI 10.1007/978-90-481-2885-3_7,

respectively. The choice of the creator and annihilator orbital sets is motivated by the observation

$$\begin{aligned} \hat{a}_i^\dagger|0\rangle &= 0 & \hat{a}_a^\dagger|0\rangle &\neq 0 \\ \hat{a}_i|0\rangle &\neq 0 & \hat{a}_a|0\rangle &= 0. \end{aligned} \tag{7-3}$$

The amplitudes $t^{\cdots}_{\cdots}$ within the cluster operator $\hat{T}$ allow to span the many-particle space. Inserting equation Eq. (7-1) into the Schrödinger equation, multiplication from left by $e^{-\hat{T}}$, and projection onto the Fermi vacuum and substituted determinants α delivers the common energy and amplitude equations

$$\langle 0|e^{-\hat{T}}\hat{H}e^{\hat{T}}|0\rangle = E \tag{7-4}$$

$$\langle \alpha|e^{-\hat{T}}\hat{H}e^{\hat{T}}|0\rangle = 0, \tag{7-5}$$

respectively.

The SRCC ansatz is potentially complete (for an untruncated cluster operator) and invariant with respect to occupied – occupied and virtual – virtual transformations. The crucial property for the success of the SRCC approach is however the size extensivity of the ansatz. It ensures the independence of the accuracy from the size of the system. Other methods like e.g. configuration interaction (CI) show a decreasing accuracy with growing system size.

The property of size extensivity (= connectivity) of the SRCC ansatz is often related to its exponential ansatz. However, it must be pointed out that the exponential ansatz itself does *not* guarantee size extensivity. In order for size extensivity to hold the cluster operators inserted into the exponential have to be connected themselves. This property of connectivity is sometimes also called irreducible. The term "connectivity" originates from the diagrammatic representation of the equations. The diagrammatic techniques introduced by Feynman are really genius since they allow for a very illustrative representation of very involved formulas. Although easily "seen" within a diagrammatic representation the practical meaning of connectivity is not quite obvious. Practically, connectivity relates to the statistical binding (locality) of indices.

After this discussion it should be obvious that the amplitudes may not be obtained arbitrarily. In order for the cluster operators to be connected (that is the amplitudes within them are connected) they must be obtained within the CC framework itself. It can be shown that the above mentioned projection technique insures the connectivity of the amplitudes. In contrast to this using e.g. adapted (disconnected) CI coefficients as cluster amplitudes fails to deliver a size extensive energy.

We discussed the connectivity issue in some detail since it turns out to be one of the crucial difficulties upon the generalization of the single-reference to the multi-reference approach.

7.1.2. The Multi-Reference Case

Turning to the multi-reference (MR) case there is no longer a unique Fermi vacuum $|0\rangle$ consisting of a single determinant. It has to be replaced by a linear combination of determinants

$$|\tilde{0}\rangle = \sum_{\mu} c_\mu |\mu\rangle. \tag{7-6}$$

7.1.2.1. Straightforward Generalization

Naively writing equation Eq. (7-1) with the reference function from Eq. (7-6) yields

$$|\Psi_{\mathrm{MRCC}_1}\rangle = e^{\hat{T}} \sum_{\mu} c_\mu |\mu\rangle. \tag{7-7}$$

Equation Eq. (7-7) contains a single cluster operator for all references $\{\mu\}$. However, it is not entirely clear how $\hat{T}$ should be assembled since there is no unique Fermi vacuum dividing the set of orbitals into an occupied and virtual set. In the SR case the creators were chosen from the set of virtual orbitals while the annihilators used the occupied orbitals. This was motivated by the observation that any other choice yields 0 (if only non-product terms are considered). Due to the MR structure of the reference the orbitals may now be classified into three distinct sets: inactive $\mathbb{I}$ (orbitals occupied in all reference determinants), virtual $\mathbb{V}$ (orbitals occupied in no reference determinant), and active $\mathbb{A}$ (the remaining ones). It can easily be seen that the inactive and virtual orbitals of the MR case map onto the occupied and virtual orbitals of the SR case in the sense that

$$\begin{array}{lll} \hat{a}_i^\dagger |\tilde{0}\rangle = 0 & \hat{a}_a^\dagger |\tilde{0}\rangle \neq 0 & \hat{a}_p^\dagger |\tilde{0}\rangle \neq 0 \\ \hat{a}_i |\tilde{0}\rangle \neq 0 & \hat{a}_a |\tilde{0}\rangle = 0 & \hat{a}_p |\tilde{0}\rangle \neq 0 \end{array} \tag{7-8}$$

with $i \in \mathbb{I}, a \in \mathbb{V}, p \in \mathbb{A}$. Equation Eq. (7-8) suggests the active orbitals to be treated differently from the others with respect to their association to creators or annihilators. More precisely following the previous arguments for the single reference case equation Eq. (7-8) suggests creators and annihilators to be taken from active orbitals in the sense

$$\hat{T}_\nu = \sum_{\substack{i'_1 < i'_2 < \ldots < i'_\nu \\ a'_1 < a'_2 < \ldots < a'_\nu}} t_{i'_1 \ldots i'_\nu}^{a'_1 \ldots a'_\nu} \, \hat{a}_{a'_1}^\dagger \ldots \hat{a}_{a'_\nu}^\dagger \hat{a}_{i'_\nu} \ldots \hat{a}_{i'_1} \tag{7-9}$$

with $i'_\nu \in \mathbb{I} \cup \mathbb{A}$ and $a'_\nu \in \mathbb{V} \cup \mathbb{A}$. This setup is in principle possible but there is a significant conceptual problem: The number of linear independent projections arising from

the application of the substitutions within the cluster operator onto the reference $|\tilde{0}\rangle$ and the number of independent amplitudes do no longer match in general. Another technical complication is that of the non-commuting algebra from the overlapping creator and annihilator sets.

A rather simple cure for this problem is to neglect all active orbitals from the association to creators and annihilators. That is setting $i'_\nu \in \mathbb{I}$ and $a'_\nu \in \mathbb{V}$. However, this is a very poor ansatz as it does not span the full function space. Especially the important active space is described insufficiently.

7.1.2.2. The Fock Space (Valence Universal) Approach

The Fock space (or valence universal (VUMRCC)) approach [3–8] reintroduces a unique Fermi vacuum $|0\rangle$. In order to set up a sufficient set of equations VUMRCC considers several states (indexed by i) and sectors (n, m) at once. The ordered pairs (n, m) classify the sectors by the number of particles n and holes m with respect to the formal Fermi vacuum $|0\rangle$. The VUMRCC wave function is given by

$$|\Psi_i^{(m,n)}\rangle = \{e^{\hat{S}}\}|\Psi_{i0}^{(m,n)}\rangle \tag{7-10}$$

with the curly braces denoting normal ordering and the reference states given by

$$|\Psi_{i0}^{(m,n)}\rangle = \sum_\mu c_{i\mu}|\mu^{(m,n)}\rangle \tag{7-11}$$

and the valence universal cluster operator

$$\hat{S} = \sum_{k=0}^{m}\sum_{l=0}^{n}\hat{T}^{(k,l)} \tag{7-12}$$

and $\hat{T}^{(k,l)} = \sum_{\nu=1}^{M}\hat{T}_\nu^{(k,l)}$ the cluster operators in the individual sectors. In contrast to a common $\hat{T}^{(0,0)}$ operator the $\hat{T}^{(0,1)}$ contains for instance one hole orbital as a creator. The sector (0, 1) corresponds to a to a singly ionized state while the (1, 0) sector corresponds to singly electron attached states. Naturally, the (1, 1) and (2, 2) sectors correspond to single and doubly excited states respectively and it is $|\mu^{(0,0)}\rangle = |0\rangle$. The reason for the introduction of the sectors lies in the fact that a direct determination of the amplitudes for an e.g. (2, 2) doubly excited state is not possible as it relies on amplitudes from sectors below. Actually, using the normal ordered form of the exponential in equation Eq. (7-10) avoids contractions within the active orbitals and insures that higher sectors depend only on lower sectors (and not the other way round) [9, 10]. This allows for a sector-wise construction of the solutions starting from the (0, 0) sector which corresponds to a usual single-reference coupled-cluster calculation. The actual determination of the coefficients involves the Bloch equation and shall not be discussed here in detail. It is important to note that although

VUMRCC introduces a formal Fermi vacuum all references in the desired sector are treated on the same footing. This is different from other formally single Fermi vacuum ansätze to be discussed later.

7.1.2.3. The Hilbert Space (State Universal) Approach

The Hilbert space (or state universal (SUMRCC)) approach [11] see also [12–16] is given by

$$|\Psi_\lambda\rangle = \sum_\mu c_{\lambda\mu} e^{\hat{T}(\mu)} |\mu\rangle, \quad \forall_\lambda \tag{7-13}$$

with the state label λ and the reference specific cluster operator

$$\hat{T}(\mu) = \sum_{\hat{\tau}(\mu)\in\mathbb{T}(\mu)} t_{\hat{\tau}(\mu)}(\mu)\hat{\tau}(\mu). \tag{7-14}$$

Equation (7-13) contains more variables than can be fixed by considering a single state only leading to similar problems as with the previous VUMRCC ansatz. The solution is similar: the SUMRCC ansatz considers several states at once. As these states consist of a single number of electrons only the ansatz is called Hilbert space ansatz. The state universal ansatz overcomes the problem of under-determinedness of the equations by employing the Bloch equation and considering as many states simultaneously as there are references. Since Eq. (7-13) is valid for all λ and the individual states $|\Psi_\lambda\rangle$ are distinguished by the coefficients $c_{\lambda\mu}$ only the set of cluster operators $\{\hat{T}(\mu)\}$ is state universal.

7.1.2.4. Variants and Additional Methods from the Literature

Both previously described approaches employ the Bloch equation and suffer (in their original formulation) from various limitations, mostly intruder states [12, 17]. The VUMRCC is related to later intermediate Hamiltonian IM-FSMRCC [18, 19], EOM-CC [20–22] (for details see [23, 24] presenting also new results) and ST-EOM-CC [25, 26] approaches. Very recent work [27] addresses the problem of the usually necessary completeness of the model space by the introduction of a suitably chosen normalization. The SUMRCC ansatz got further developed to general model space (GMS) SUMRCC variants [28, 29].

Since the "(state) universality" finally became less preferred the development of state selective methods started. Actually, a universal method has to treat several states at the same time with a limited number of amplitudes. In comparison to a state selective method the number of amplitudes per state is therefore smaller. This argumentation is not of a rigorous nature but the state selective methods proved to be typically more accurate in practice. The SUMRCC approach parents three state specific variants: (MkMRCC) [30–35], Brillouin-Wigner based ansätze (BWMRCC)

[36–40], and the multi-reference exponential (MRexpT) ansatz [41, 42] to be discussed in detail in the next section.

Since there are still various conceptual difficulties with the true multi-reference coupled cluster ansätze mentioned above another branch of approaches emerged. To circumvent the theoretical problems of the true MR approaches these ansätze rely on the single-reference ansatz and may be seen as some kind of augmentation of it. The first approach of this kind is the single-reference formalism based multi-reference coupled cluster approach (SRMRCC) [43]. Later it got extended to more general model spaces [44]. There are very similar variants of this approach in the literature: The CCSDt... family of methods [45, 46] and CASCC family of methods [47–49] and their excited state variants [50, 51]. For a recent review of these methods see [52]. Similarly, the method of moment (MM-CC) [53, 54] and completely renormalized (CR-CC) [55] ansätze rely on the SR ansatz as well. Another SR formalism based ansatz is the reduced MRCC (RMRCC) approach [56–58] which exists also in partially linearized form [59, 60]. Finally, Λ-CCSD [61, 62] improves SRCC with respect to MRCC type situations by the inclusion of de-excitation operators (Λ-equations). All single-reference formalism based approaches share the same problem: They are symmetry broken and not Fermi vacuum invariant.

7.2. THE MREXPT APPROACH

Similar to BWMRCC and MkMRCC the MRexpT ansatz [41, 42] is a state selective modification of the SUMRCC approach.

7.2.1. Ansatz

The main deficiency of the state and valence universal approaches is their need to calculate more states than desired simultaneously and the appearance of intruder states. The necessity to consider several states arises because a single substituted determinant may be reached from several references by distinct substitutions. In search for an ansatz which insures the match of free parameters and linear independent projections we require that for every amplitude t_j there must be a corresponding projection $|\beta\rangle \in \mathbb{Q}$. From the point of view of sufficiency it seems to be natural to use $|\beta\rangle$ to index the amplitudes t

$$t_j := t_{|\beta\rangle}. \tag{7-15}$$

Thereby we replace the excitation and reference related amplitude indexing of the state universal ansatz by an indexing which is based on excited determinants:

$$t_{\hat{\tau}(\mu)}(\mu) \longrightarrow t_{\hat{\tau}(\mu)|\mu\rangle}. \tag{7-16}$$

However there is still a sign to be fixed. Considering $\hat{a}_a^\dagger \hat{a}_p |pi\rangle = |ai\rangle$ and $\hat{a}_a^\dagger \hat{a}_q |iq\rangle = |ia\rangle$ we find the two substitution processes to yield the negative of each other. For symmetry reasons we define

$$t_{-|\beta\rangle} = -t_{|\beta\rangle}. \tag{7-17}$$

Finally, there is another sign issue that needs to be fixed. As the amplitudes are bound to the outcome of an excitation due to Eq. (7-16) and the reference coefficients enter the wave function directly it may happen that opposite signs of the references cause the coefficient of the resulting substituted determinant to vanish. In order to fix this problem the MRexpT ansatz introduces a reference phase compensation factor $\phi(z) = e^{-i \arg z}$, $z \in \mathbb{C}$, inside the exponential:

$$|\Psi\rangle = \sum_\mu c_\mu \exp\left(\phi(c_\mu) \sum_{\hat{\tau}_i(\mu) \in \mathbb{T}_\mu} t_{\hat{\tau}_i(\mu)|\mu\rangle} \hat{\tau}_i(\mu)\right) |\mu\rangle. \tag{7-18}$$

Upon linearization of the exponential series (*not* linearization of the equations!) ansatz Eq. (7-18) is equivalent to an MRCI type wave function in a non standard parameterization.

Finally we note that the excitation operators associated to a particular reference μ commute

$$[\hat{\tau}_{|\alpha\rangle}(\mu), \hat{\tau}_{|\beta\rangle}(\mu)] = 0. \tag{7-19}$$

Summarizing the MRexpT wave function is given by

$$|\Psi\rangle = \sum_\mu c_\mu e^{\hat{T}(\mu)} |\mu\rangle \tag{7-20}$$

with the cluster operator

$$\hat{T}(\mu) = \phi(c_\mu) \sum_{\hat{\tau}_i(\mu) \in \mathbb{T}_\mu} t_{\hat{\tau}_i(\mu)|\mu\rangle} \hat{\tau}_i(\mu). \tag{7-21}$$

Inserting Eq. (7-20) into the Schrödinger equation we get

$$\hat{H} \sum_\mu c_\mu e^{\hat{T}(\mu)} |\mu\rangle = E \sum_\mu c_\mu e^{\hat{T}(\mu)} |\mu\rangle. \tag{7-22}$$

Projecting Eq. (7-22) from the left onto $\langle\rho| \in \mathbb{P}^\dagger \cup \mathbb{Q}^\dagger$ we obtain a system of equations linear in the reference coefficients c_μ and non linear in the amplitudes $t_{|i\rangle}$

$$\sum_\mu c_\mu \langle\rho|(\hat{H} - E) e^{\hat{T}(\mu)} \mu\rangle = 0. \tag{7-23}$$

Since E enters Eq. (7-23) as an additional unknown explicitly there is still one equation missing. It may be easily obtained by the normalization of the reference weights

$$\sum_{\mu} |c_\mu|^2 = 1. \tag{7-24}$$

7.2.2. Theoretical and Technical Properties

At this place we shall briefly reiterate the crucial steps in the proofs of two major theoretical properties: size consistency and size extensivity.

7.2.2.1. Consistency

The algebraic proof of size consistency given in [41] relies on two major properties

1. the exponential law $e^{\hat{A}+\hat{B}} = e^{\hat{A}} e^{\hat{B}}$ for commuting operators $\hat{A}$ and $\hat{B}$
2. unique amplitude mapping from the fragments A and B to the compound system AB

The latter point is not trivial and different from the standard singe-reference coupled-cluster size consistency proof due to the changed amplitude indexing according to equation Eq. (7-16). It could be shown that the coefficient spaces for the fragments A and B map onto AB without any conflicts due to the assumption that there is no excitation generating one reference from another ($\langle\lambda|\hat{T}_\mu\mu\rangle = 0, \forall_{\lambda\neq\mu}$). It is important to notice that the latter assumption does not impose any restriction on the function space. Instead this assumption arises naturally from the necessity to create no redundant substitutions. The latter would result in an underdetermined equation system.

7.2.2.2. Connectivity

The proof of core connectivity of the MRexpT approach [63] shall be briefly summarized. The proof proceeds as follows: (i) elimination of E from the MRexpT working equations, (ii) setup of a perturbative cluster expansion, (iii) introduction of core/valence separation, (iv) processing of applicable simplifications.

After solving of Eq. (7-23) for E and reinsertion into Eq. (7-23) (for disjoint projections) we obtain

$$0 = \sum_{\mu} c_\mu \left[\langle\alpha|e^{-\hat{T}_\mu}\hat{H}e^{\hat{T}_\mu}\mu\rangle - B_\mu + C_\mu\right] \tag{7-25}$$

with the abbreviations

$$B_\mu := \langle\alpha|e^{\hat{T}_\mu}\mu\rangle \sum_{\mu'\neq\mu} \frac{c_{\mu'}}{c_\mu}\langle\mu|\hat{H}e^{\hat{T}_{\mu'}}\mu'\rangle \tag{7-26}$$

and

$$C_\mu := \sum_{i=1}^{\infty}\sum_{j=1}^{\infty}\sum_{|\omega\rangle\in\mathbb{Q}_{\mu j}}\frac{1}{i!}\langle\alpha|\hat{T}_\mu^i\omega\rangle\langle\omega|e^{-\hat{T}_\mu}\hat{H}e^{\hat{T}_\mu}\mu\rangle \tag{7-27}$$

and $\langle\alpha|$ projections from $\mathbb{Q}$.

A partitioning according to $\hat{H} = \hat{H}_0 + \hat{V}$ yields

$$0 = \sum_{\mu\in\mathbb{P}_\alpha}|c_\mu|\,t_{|\alpha\rangle}(\varepsilon_{|\alpha\rangle} - \varepsilon_{|\mu\rangle}) + \sum_\mu c_\mu\left[\langle\alpha|e^{-\hat{T}_\mu}\hat{V}e^{\hat{T}_\mu}\mu\rangle - B_\mu + C_\mu\right] \tag{7-28}$$

introducing $\mathbb{P}_\alpha = \{\mu \in \mathbb{P} \mid \alpha \in \mathbb{Q}_\mu\}$ constituting those references which may lead to substitution α. Solving Eq. (7-28) for $\hat{T}_\lambda$ yields

$$\frac{\hat{T}_\lambda}{\phi(c_\lambda)} = \sum_{|\alpha\rangle\in\mathbb{Q}_\lambda}\frac{\sum_\mu c_\mu\left[\langle\alpha|e^{-\hat{T}_\mu}\hat{V}e^{\hat{T}_\mu}\mu\rangle - B_\mu + C_\mu\right]}{\sum_{\mu\in\mathbb{P}_\alpha}|c_\mu|(\varepsilon_{|\mu\rangle} - \varepsilon_{|\alpha\rangle})}\hat{\tau}_{|\lambda\rangle\to|\alpha\rangle} \tag{7-29}$$

In deriving Eq. (7-29) there has been no approximation so far. We note: since the term B_μ in Eq. (7-29) is obviously disconnected, also $\hat{T}$ will be disconnected.

In the following we split the Hamiltonian and the cluster operator into their core (carrying no active orbital) and valence (carrying some active orbital) part

$$\hat{H} = \hat{H}^{\overline{\mathrm{v}}} + \hat{H}^{\mathrm{v}} \tag{7-30}$$

$$\hat{T} = \hat{T}^{\overline{\mathrm{v}}} + \hat{T}^{\mathrm{v}}. \tag{7-31}$$

and restrict the further analysis to the core Hamiltonian. After some manipulation [63] one arrives at

$$\hat{T}_\lambda^{\overline{\mathrm{v}}} = \sum_{|\alpha\rangle\in\mathbb{Q}_\lambda^{\overline{\mathrm{v}}}}\frac{\langle\alpha|e^{-\hat{T}_\lambda}\hat{V}^{\overline{\mathrm{v}}}e^{\hat{T}_\lambda}\lambda\rangle}{\left(\varepsilon_{|\lambda\rangle}^{\overline{\mathrm{v}}} - \varepsilon_{|\alpha\rangle}^{\overline{\mathrm{v}}}\right)}\hat{\tau}_{|\lambda\rangle\to|\alpha\rangle} \tag{7-32}$$

showing the core part of the cluster operator to be connected iff $\mathbb{Q}$ is closed with respect to de-excitations from $\mathbb{T}^\dagger$, that is $\hat{\tau}^\dagger|\alpha\rangle \in \mathbb{Q},\ \forall_{\hat{\tau}\in\mathbb{T},|\alpha\rangle\in\mathbb{Q}}$. A sufficient condition for the latter is that $\hat{T}$ contains a consecutive sequence of excitation levels (e.g. S, SD, SDT, ...).

The core connectivity is an important result as it guarantees the size extensivity of MRexpT with the number of core electrons which is very likely to become large.

7.2.2.3. Summary

The following enumeration summarizes the beneficial theoretical and technical properties of the MRexpT approach:

1. potential exactness (it converges to full CI with an untruncated cluster operator)
2. Fermi vacuum invariance (no particular reference)
3. size consistent [41, 42]
4. core (=inactive, doubly occupied) connected [63, 64]
5. properly corresponds to a projection of the Schrödinger equation (this issue was first mentioned in [65] and later analyzed in [66])
6. not symmetry broken
7. numerically very accurate
8. applicable to very difficult problems (e.g. dissociation of N_2 including excited states [67, 68])

Since MRexpT is not the "ultimate" solution (as none of currently existing proposals for MRCC ansätze is) there are also a few drawbacks:

1. not invariant with respect to active↔active unitary transformations
2. not core-valance connected [63, 64]
3. computationally more expensive than e.g. BWMRCC and MkMRCC (comparable to SRMRCC)

The lack of valence connectivity is the major bug of MRexpT. This error is present in any calculation but is typically of modest order as the size of the valence space is usually limited. However, for the core (=inactive) electrons MRexpT scales correctly. Molecular applications show the core space to grow much more rapidly and MRexpT should be a reasonable compromise.

7.3. SELECTED RECENT APPLICATIONS

Apart from other recent work [69, 70] we shall select a few applications from our recent research for a more detailed presentation in this section.

7.3.1. N_2

The nitrogen molecule dissociation including ground and excited states is a very difficult test case for any multi-reference theory. It offers a lot of spin and spatial symmetry properties and requires a balanced treatment of static and dynamic correlation. Due to the large amount of data the results on the nitrogen molecule were presented in two publications. Reference [67] reports on the correlation energy and degeneracy errors while [68] considers spin projection errors. For technical details please refer to these publications.

7.3.1.1. Correlation Energy Errors

In order to get an impression of the considered states Figure 7-1 shows the full CI potential surfaces including the dissociation channels. Figure 7-2 shows the actual

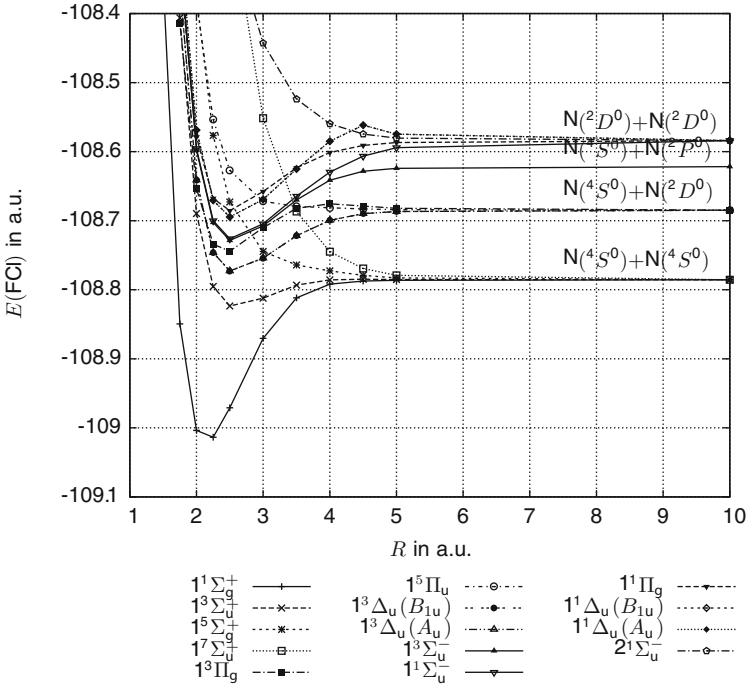

Figure 7-1. The full CI N_2 potential surface for ground and excited states

correlation energy errors with respect to full CI obtained with SRMRCC [43] and MRexpT approaches. Both approaches show errors of about 0.3 mE_h. The behavior of the errors along the surface is very similar. The errors become largest in the vicinity of the equilibrium. For the dissociation the calculations become more accurate as the effective number of electrons to be correlated decreases. At very small distances both approaches tend to overestimate the correlation energy for a few states. This

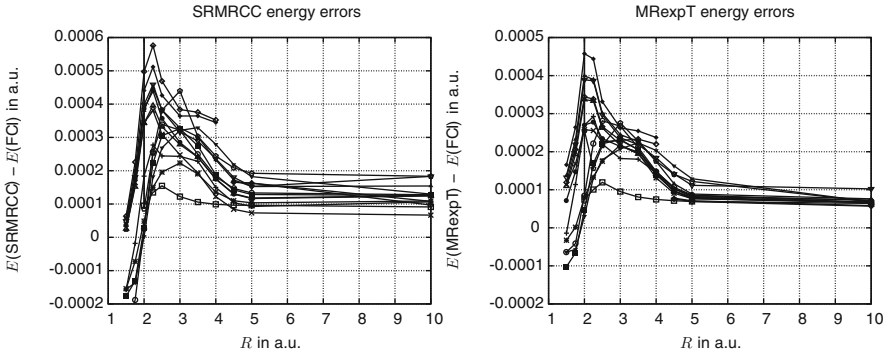

Figure 7-2. Energy differences of SRMRCC and MRexpT with respect to FCI

is due to the fact that the reference space description of these states becomes rather poor at short distances. Finally we note that the errors of the MRCC approaches are one order of magnitude smaller that for MRCI (results not shown here). This relation is likely to improve dramatically in favor of the MRCC methods for larger systems.

Due to the high symmetry of the nitrogen molecule the calculation has to meet several degeneracy criteria. They may be divided into two classes:

- Δ-state degeneracy: Among the 12 distinct states of the legend there are two Δ states. Each Δ state splits up into two irreducible representations of D_{2h} (the point group the calculation was carried out with) since the full symmetry of the molecule is $D_{\infty h}$. Nevertheless the two components should be perfectly degenerate. However, neither SRMRCC nor MRexpT reproduce this degeneracy exactly. A modest error of the order 10^{-5}–10^{-4} E_h remains.
- $R \to \infty$ degeneracy: There are two possibilities for the occurrence of $R \to \infty$ degeneracy: Upon dissociation the symmetry of the isolated atoms becomes the full rotation group. As this symmetry is larger than that of $D_{\infty h}$ there are several states ending in the same dissociation channel as shown in Figure 7-1. Additionally, there are different possible spin couplings of the atoms assembling a certain spin state of the molecule. For separated atoms these differing coupling patterns become degenerate. As before SRMRCC and MRexpT fail to reproduce this degeneracy exactly and the errors are of the same order of magnitude (10^{-5}–10^{-4} E_h).

7.3.1.2. Spin Projections Errors

Figure 7-3 shows the spin projection errors ε of SRMRCC and MRexpT. The spin projection error ε is given by $\varepsilon = \sqrt{1 - \langle \Psi^{S,S_z} | \Psi^{S,S_z} \rangle}$ with $|\Psi^{S,S_z}\rangle = \hat{P}^{S,S_z}_{\mathrm{CSF}} |\Psi_{\mathrm{MRCC}}\rangle$. $\hat{P}^{S,S_z}_{\mathrm{CSF}}$ projects onto the spin eigenfunctions associated with S and S_z while $|\Psi_{\mathrm{MRCC}}\rangle$ is the normalized MRCC coupled cluster wave function in determinantal basis. Consequently, any deviation of $\langle \Psi^{S,S_z} | \Psi^{S,S_z} \rangle$ from one measures the presence of spin components different from the desired S and S_z value. Therefore, it is $\varepsilon = 0 \Leftrightarrow \Psi_{\mathrm{MRCC}}$ is a spin eigenfunction. Please note that the alternative error criterion

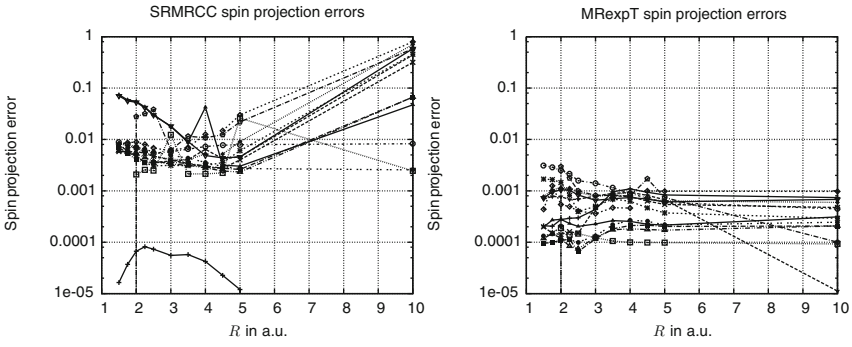

Figure 7-3. Spin projection errors of SRMRCC and MRexpT

$\tilde{\varepsilon} = \langle \Psi_{\mathrm{MRCC}} | \hat{S}^2 \Psi_{\mathrm{MRCC}} \rangle - S(S+1) = 0$ (although much simpler to evaluate) is not sufficient for Ψ_{MRCC} to be a spin eigenfunction.

According to Figure 7-3 MRexpT shows significantly smaller spin projection errors than SRMRCC. This is due to the symmetry breaking within SRMRCC caused by the arbitrarily selected particular Fermi vacuum. Especially in case of degeneracy the error becomes rather large.

7.3.2. Wave Function Quality and Variance

The previous results regarding the spin projection errors already gave some idea of the quality of the wave function. In this subsection we consider this quality more explicitly. The introduction of the error criterion $\Delta_{\mathrm{FCI}} = 1 - \langle \Psi_{\mathrm{FCI}} | \Psi_x \rangle$ constitutes a natural measurement of the quality of the wave function as it vanishes iff the trial wave function (in this case the MRCC wave function) becomes the full CI wave function itself. Alternatively, we may consider the wave function variance $\sigma^2 = \langle \Psi_x | \hat{H}^2 | \Psi_x \rangle - \langle \Psi_x | \hat{H} | \Psi_x \rangle^2$. Similarly to Δ_{FCI}, σ^2 vanishes for $\Psi_x = \Psi_{\mathrm{FCI}}$. However, the variance is not state selective in the sense that it compares in relation to a certain state. Any eigenfunction $|\Psi_x\rangle$ will result in $\sigma^2 = 0$. Especially in case of degeneracies this has to be taken into account.

Figure 7-4 shows the results from the calculations [71] on the H_4 model [72]. Additionally to the wave function error Δ_{FCI} and the variance σ^2 Figure 7-4 reports

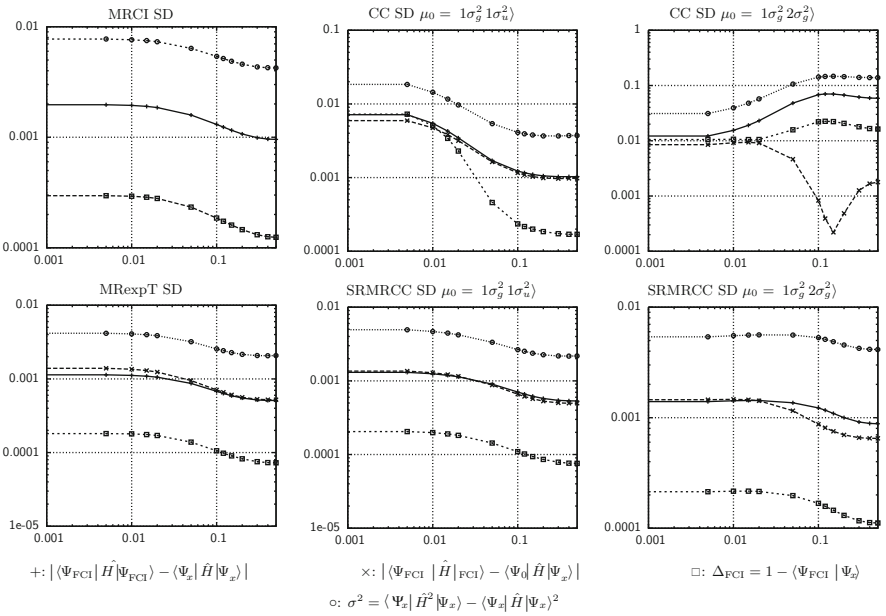

Figure 7-4. Energy expectation value (+) and projective energy (×) errors with respect to full CI in E_h, full CI wave function overlap errors (□), wave function variances (○) in E_h^2 for various methods at singles, doubles level, abscissa: Geometry parameter α, please note the differing logarithmic scalings

the projective and variational energy errors with respect to full CI (if applicable). The results for the Fermi vacuum dependent approaches (single-reference coupled-cluster and single-reference formalism based multi-reference coupled-cluster (SRM-RCC)) are reported for both possible Fermi vacua.

Obviously, the individual error criteria show a very strong correlation for any of the considered methods. As expected, being a single-reference method SRCC shows the largest errors, especially, if the non dominant reference determinant is taken as Fermi vacuum. MRCI behaves smoothly although the absolute errors are larger than for the MRCC approaches. SRMRCC for the dominating Fermi vacuum and MRexpT show a very good performance. Using SRMRCC with the "wrong" Fermi vacuum is usually still more accurate than SRCC although the absolute accuracy deteriorates significantly.

7.4. CONCLUSIONS

The conceptual difficulties of the generalization of the single-reference coupled-cluster ansatz to the multi-reference case were discussed and a few approaches from the literature were presented. After the derivation and motivation of the MRexpT approach its theoretical properties were analyzed. The most important features of MRexpT are its size consistency and core connectivity. The latter guarantees the correct scaling of the energy with the system size ensuring a high accuracy of the method. However, MRexpT does not scale properly with the number of valence electrons. This deficiency is subject to future research.

ACKNOWLEDGEMENTS

The author would like to thank Anna Engels-Putzka for carefully reading and commenting on the manuscript.

Support by the Deutsche Forschungsgemeinschaft (grants HA 5116/1-1, HA 5116/3-1 and SPP 1145) is gratefully acknowledged.

REFERENCES

1. F. Coester, H. Kümmel, Nucl. Phys. **17**, 477 (1960)
2. J. Čížek, J. Chem. Phys. **45**, 4256 (1966)
3. D. Mukherjee, R. K. Moitra, A. Mukhopadhyay, Mol. Phys. **30**, 1861 (1975)
4. D. Mukherjee, R. K. Moitra, A. Mukhopadhyay, Mol. Phys. **33**, 955 (1977)
5. I. Lindgren, Int. J. Quantum Chem. Symp. **12**, 33 (1978)
6. I. Lindgren, D. Mukherjee, Phys. Reports **151**, 93 (1987)
7. D. Mukherjee, S. Pal, Adv. Quantum Chem. **20**, 291 (1989)
8. B. Jeziorski, J. Paldus, J. Chem. Phys. **90**, 2714 (1989)
9. M. A. Hauque, D. Mukherjee, J. Chem. Phys. **80**, 5058 (1984)
10. U. Kaldor, Theor. Chim. Acta **80**, 427 (1991)
11. B. Jeziorski, H. J. Monkhorst, Phys. Rev. A **24**, 1668 (1981)

12. B. Jeziorski, J. Paldus, J. Chem. Phys. **88**, 5673 (1988)
13. J. Paldus, P. Piecuch, L. Pylypow, B. Jeziorski, Phys. Rev. A **47**, 2738 (1993)
14. S. A. Kucharski, R. J. Bartlett, J. Chem. Phys. **95**, 8227 (1991)
15. A. Balková, S. A. Kucharski, L. Meisner, R. J. Bartlett, Theor. Chem. Acc. **80**, 335 (1991)
16. A. Balková, S. A. Kucharski, L. Meissner, R. J. Bartlett, J. Chem. Phys. **95**, 4311 (1991)
17. P. Durand, J. P. Malrieu, Adv. Chem. Phys. **67**, 321 (1987)
18. L. Meissner, M. Nooijen, J. Chem. Phys. **102**, 9604 (1995)
19. J. P. Malrieu, P. Durand, J. P. Daudey, J. Phys. B **18**, 809 (1985)
20. K. Emrich, Nucl. Phys. **A351**, 379 (1981)
21. K. Emrich, Nucl. Phys. **A351**, 397 (1981)
22. J. F. Stanton, R. J. Bartlett, J. Chem. Phys. **98**, 7029 (1993)
23. M. Musial, R. J. Bartlett, J. Chem. Phys. **129**, 134105 (2009)
24. M. Musial, R. J. Bartlett, J. Chem. Phys. **129**, 044101 (2009)
25. M. Nooijen, R. J. Bartlett, J. Chem. Phys. **106**, 6441 (1997)
26. M. Nooijen, R. J. Bartlett, J. Chem. Phys. **106**, 6449 (1997)
27. R. Maitra, D. Datta, D. Mukherjee, Chem. Phys. **356**, 54 (2009)
28. X. Li, J. Paldus, J. Chem. Phys. **119**, 5320 (2003)
29. X. Li, J. Paldus, J. Chem. Phys. **119**, 5346 (2003)
30. U. S. Mahapatra, B. Datta, D. Mukherjee, Mol. Phys. **94**, 157 (1998)
31. U. S. Mahapatra, B. Datta, D. Mukherjee, J. Chem. Phys. **110**, 6171 (1999)
32. K. Bhaskaran-Nair, O. Demel, J. Pittner, J. Chem. Phys. **129**, 184105 (1991)
33. F. A. Evangelista, A. C. Simmonett, W. D. Allen, I. Henry F. Schaefer, J. Gauss, J. Chem. Phys. **128**, 124104 (2008)
34. E. Prochnow, F. A. Evangelista, I. Henry F. Schaefer, W. D. Allen, J. Gauss, J. Chem. Phys. **131**, 064109 (2009)
35. F. A. Evangelista, A. C. Simmonett, I. H. F. Schaefer, D. Mukherjee, W. Allen, Phys. Chem. Chem. Phys. **11**, 4728 (2009)
36. J. Mášik, I. Hubač, P. Mach, J. Chem. Phys. **108**, 6571 (1998)
37. I. Hubač, J. Pittner, P. Čársky, J. Chem. Phys. **112**, 8779 (2000)
38. J. Pittner, J. Chem. Phys. **118**, 10876 (2003)
39. J. Pittner, X. Li, J. Paldus, Mol. Phys. **103**, 2239 (2005)
40. J. Pitter, P. Piecuch, Mol. Phys. **107**, 1209 (2009).
41. M. Hanrath, J. Chem. Phys. **123**, 84102 (2005).
42. M. Hanrath, Chem. Phys. Lett. **420**, 426 (2006).
43. N. Oliphant, L. Adamowicz, J. Chem. Phys. **94**, 1229 (1991)
44. P. Piecuch, N. Oliphant, L. Adamowicz, J. Chem. Phys. **99**, 1875 (1993)
45. P. Piecuch, S. A. Kucharski, , R. J. Bartlett, J. Chem. Phys. **110**, 6103 (1999)
46. P. Piecuch, S. A. Kucharski, V. Špirko, J. Chem. Phys. **111**, 6679 (1999)
47. D. I. Lyakh, V. V. Ivanov, L. Adamowicz, J. Chem. Phys. **122**, 024108 (2005)
48. V. V. Ivanov, L. Adamowicz, D. I. Lyakh, Int. J. Quant. Chem. **106**, 2875 (2006)
49. D. I. Lyakhy, V. V. Ivanov, L. Adamowicz, Mol. Phys. **105**, 1335 (2007)
50. V. V. Ivanov, L. Adamowicz, D. I. Lyakh, J. Chem. Phys. **124**, 184302 (2006)
51. D. I. Lyakh, V. V. Ivanov, L. Adamowicz, J. Chem. Phys. **128**, 074101 (2008)
52. V. V. Ivanov, D. I. Lyakh, L. Adamowicz, Phys. Chem. Chem. Phys. **11**, 2355 (2009)
53. K. Kowalski, P. Piecuch, J. Chem. Phys. **113**, 18 (2000)
54. K. Kowalski, P. Piecuch, J. Chem. Phys. **115**, 2966 (2001)
55. K. Kowalski, P. Piecuch, J. Chem. Phys. **122**, 074107 (2005)
56. X. Li, J. Paldus, J. Chem. Phys. **107**, 6257 (1997)

57. X. Li, J. Paldus, J. Chem. Phys. **108**, 637 (1998)
58. X. Li, J. Paldus, J. Chem. Phys. **129**, 054104 (2008)
59. X. Li, J. Paldus, J. Chem. Phys. **128**, 144118 (2008)
60. X. Li, J. Paldus, J. Chem. Phys. **128**, 144119 (2008)
61. A. G. Taube, R. J. Bartlett, J. Chem. Phys. **128**, 044110 (2008)
62. A. G. Taube, R. J. Bartlett, J. Chem. Phys. **128**, 044111 (2008)
63. M. Hanrath, Theor. Chem. Acc. **121**, 187 (2008).
64. M. Hanrath, Chem. Phys. **356**, 31 (2009).
65. M. Hanrath, J. Chem. Phys. **128**, 154118 (2008).
66. L. Kong, Int. J. Quant. Chem. **109**, 441 (2008)
67. A. Engels-Putzka, M. Hanrath, Mol. Phys. **107**, 143 (2009)
68. M. Hanrath, A. Engels-Putzka, Theor. Chem. Acc. **122**, 197 (2009)
69. M. Hanrath, Mol. Phys. **106**, 1949 (2008).
70. A. Engels-Putzka, M. Hanrath, J. Mol. Struct.: THEOCHEM **902**, 59 (2009)
71. M. Hanrath, Chem. Phys. Lett. **466**, 240 (2008).
72. K. Jankowski, J. Paldus, Int. J. Quantum Chem. **18**, 1243 (1980)

CHAPTER 8

ECLECTIC ELECTRON-CORRELATION METHODS

SO HIRATA[1], TORU SHIOZAKI[1,2], EDWARD F. VALEEV[3], AND MARCEL NOOIJEN[4]

[1] *Quantum Theory Project, Departments of Chemistry and Physics, The Center for Macromolecular Science and Engineering, University of Florida, Gainesville, FL 32611-8435, USA, e-mail: hirata@qtp.ufl.edu*

[2] *Department of Applied Chemistry, Graduate School of Engineering, The University of Tokyo, Tokyo 113-8656, Japan, e-mail: shiozaki.toru@gmail.com*

[3] *Department of Chemistry, Virginia Tech, Blacksburg, VA 24061-0002, USA, e-mail: evaleev@vt.edu*

[4] *Department of Chemistry, University of Waterloo, Waterloo, ON N2L3G1, Canada, e-mail: nooijen@uwaterloo.ca*

Abstract: An eclectic combination of cluster, perturbation, and linear expansions often provides the most compact mathematical descriptions of molecular electronic wave functions. A general theory is introduced to define a hierarchy of systematic electron-correlation approximations that use two or three of these expansion types. It encompasses coupled-cluster and equation-of-motion coupled-cluster methods and generates various perturbation corrections thereto, which, in some instances, reduce to the standard many-body perturbation methods. Some of these methods are also equipped with the ability to use basis functions of interelectronic distances via the so-called R12 and F12 schemes. Two computer algebraic techniques are devised to dramatically expedite implementation, verification, and validation of these complex electron-correlation methods. Numerical assessments support the unmatched utility of the proposed approximations for a range of molecular problems.

Keywords: Coupled cluster, Equation-of-motion coupled cluster, Perturbation corrections, Explicitly correlated, Automated derivation and implementation

8.1. INTRODUCTION

Once a set of one-electron basis functions is chosen, it also defines a set of Slater determinants that constitutes a many-electron basis for a molecular electronic wave function. The task of electron-correlation theories is, therefore, to determine the coefficients (amplitudes) multiplying the Slater determinants that expand the wave function. There are three such expansions of fundamental significance – cluster, perturbation, and linear expansions. When used individually, they engender coupled-cluster (CC) theory [1, 2], many-body perturbation theory (MBPT) [2, 3], and

P. Čársky et al. (eds.), Recent Progress in Coupled Cluster Methods, 191–217.
DOI 10.1007/978-90-481-2885-3_8,

configuration-interaction (CI) theory [4], respectively, which are often viewed as competing methods. When used in combinations, however, they can lead to methods that are more accurate and economical than those based on just one expansion [5]. In fact, many popular methods for electron correlation occur at the intersections of two of these expansion types. The examples include coupled-cluster singles and doubles (CCSD) with noniterative triples [CCSD(T)] [6, 7] that combines cluster and perturbation expansions in this order, multireference perturbation theories [8, 9] that perform linear expansions followed by perturbation corrections, and equation-of-motion CC (EOM-CC) theory [10] (see also [11–17]), which is a joint cluster-linear expansion approach. Combining the three expansion types is, therefore, a fruitful technique that spawns a whole new array of useful and systematic approximations of wave functions.

To combine them effectively, one must recognize different physical processes that these expansions are well-suited to describe. A wave function Ψ in a cluster or perturbation expansion is written as

$$\Psi = \exp\left(\hat{T}\right)\Phi = \left(1 + \hat{T} + \tfrac{1}{2!}\hat{T}^2 + \tfrac{1}{3!}\hat{T}^3 + \cdots\right)\Phi, \tag{8-1}$$

where $\hat{T}$ is an excitation operator and Φ is a reference determinant. Owing to the property of the exponential function, this wave function and its associated total energy can scale asymptotically correctly with size (*size-extensive*). The exponential structure also implies that the amplitudes in $\hat{T}$ must be small (weak electron correlation). This is the basis on which a perturbation theory can be used to evaluate the amplitudes in $\hat{T}$. CC theory, on the other hand, determines these amplitudes by solving nonlinear equations and thus remains valid even when a perturbation treatment of $\hat{T}$ is no longer adequate. Nonetheless, it is fair to say that the applicable domain of cluster and perturbation expansions is fundamentally limited to weak (i.e., dynamical) electron correlation and to thermodynamically extensive quantities such as total energies.

In a linear expansion, a wave function is approximated by a linear combination of Slater determinants:

$$\Psi = \hat{R}\Phi, \tag{8-2}$$

where $\hat{R}$ is an excitation operator just like $\hat{T}$. Unlike $\hat{T}$, however, $\hat{R}$ can have a large amplitude since the amplitude does not affect the weights of any Slater determinants other than the one linked to that particular amplitude. Therefore, a linear expansion can describe massive changes in a wave function such as excitations, ionizations, and electron attachments as well as chemical reactions including bond breaking. Note that these changes, no matter how large, are spatially confined in a local area of a molecule and their associated energy changes are usually asymptotically independent of size (*size-intensive*). Therefore, a linear expansion is well-suited to describe strong

(i.e., nondynamical) electron correlation in thermodynamically intensive quantities such as those listed above.

One effective way of combining the three expansion types proceeds as follows. A cluster expansion is used to describe weak, size-extensive electron correlation in the wave function of a molecule in its ground state. A linear expansion is then introduced to characterize strong, size-intensive electron reorganization (if applicable) associated with an excitation, ionization, etc. Finally, a perturbation expansion is employed to capture the small remainder of electron correlation. In fact, a combination of cluster and linear expansions, in this order, arises naturally from an application of time-dependent linear response theory to a ground-state wave function described by CC theory [13–15]. It has been established as EOM-CC theory [10], which yields size-extensive total energies and size-intensive transition energies. In this chapter, therefore, we describe a general perturbation theory [18, 19] that defines converging series of corrections to the energies and wave functions of CC for the ground state and EOM-CC for excited states. Low-cost members of this hierarchy are of particularly interest [20–22] as they can potentially outperform today's most useful electron-correlation methods such as CCSD(T) by virtue of being derived more rigorously.

While the general theory is simple, it defines series of increasingly complicated perturbation expressions to CC and EOM-CC at various ranks. Characterizing the whole series requires a computer-assisted strategy [23] for implementing, verifying, and validating a large number of complex electron-correlation methods in a reasonable timeframe. We have introduced two such schemes – the determinant-based algorithm [24–26] and the computer algebra for electron correlation [27] (see a closely related approach of Kállay and Surján [28]). The determinant-based algorithm can implement any electron-correlation method with a well-defined determinantal wave function without having to first derive the algebraic equations, but sacrificing the intrinsic efficiency of the method. Efficient implementations of promising methods can then be realized expediently by computer algebra, which automates the entire development process – the formula derivation, algebraic transformation, and computer code synthesis – of a method definable by second quantization.

For total and correlation energies of most any molecules in the ground state, the perturbation corrections to CC are rapidly convergent toward full CI solutions within a basis set. However, these full CI limits are usually still far from the exact solutions of the Schrödinger equations because of the rather slow convergence of correlation energies with respect to basis-set size. Considerable advances have been made recently to accelerate the basis-set convergence via the so-called explicitly correlated (R12 and F12)[1] technique [29–32]. This technique introduces basis functions of

[1] The R12 and F12 methods refer to explicitly correlated methods that make use of linear and nonlinear functions of interelectronic distances, respectively, the latter performing considerably better than the former. The methods discussed in this chapter can use either and the terms "R12" and "F12" are used interchangeably in this chapter.

interelectronic distances within the framework of the existing electron-correlation theories and improves the convergence rate dramatically [29, 30]. This chapter also addresses the R12 extensions to the combination methods [33–39] as well as to the standard CC [33–53] and MBPT [54–66]. However, the details of the R12 technique itself are delegated to our review [32] and other chapters and will not be discussed in depth here. The resulting methods have perhaps the highest accuracy-versus-cost performance for energies and structures of molecules in the ground states whose wave functions are dominated by single reference determinants.

8.2. THEORY

This section reviews CC, EOM-CC, and the general perturbation theory [18, 19] that spawns the series of approximations that combine cluster, linear, and perturbation expansions. It also examines the most important, low-rank members of the series that have been implemented in efficient programs. See Table 8-1 for the definitions of many of the acronyms that appear in the following.

Table 8-1. CC, MBPT, and CI and their combinations implemented by computer algebra

Acronym	Definition	Cost[a]	References
CCD	CC doubles	m^6	[27]
LCCD	Linearized CCD	m^6	[27]
CCSD	CC singles and doubles	m^6	[27]
LCCSD	Linearized CCSD	m^6	[27]
QCISD	Quadratic CI singles and doubles	m^6	[27]
CCSDT	CC singles, doubles, and triples	m^8	[27]
CCSDTQ	CC singles, doubles, triples, and quadruples	m^{10}	[27]
CCSD*t*	CCSD with active-space triples	m^6	[67]
CCSD*tq*	CCSD with active-space triples and quadruples	m^6	[67]
CCSDT*q*	CCSDT with active-space quadruples	m^8	[67]
CCSD-R12	Explicitly correlated CCSD	m^6	[51]
CCSDT-R12	Explicitly correlated CCSDT	m^8	[53]
CCSDTQ-R12	Explicitly correlated CCSDTQ	m^{10}	[53]
CCSD(R12)	Explicitly correlated CCSD	m^6	[39]
MBPT(2)	Second-order MBPT	m^5	[27]
MBPT(3)	Third-order MBPT	m^6	[27]
MBPT(4)	Fourth-order MBPT	m^7	[27]
MBPT(2)-R12	Explicitly correlated MBPT(2)	m^6	[51]
CIS	CI singles	m^4	[21]
CISD	CI singles and doubles	m^6	[27]
CISDT	CI singles, doubles, and triples	m^8	[27]
CISDTQ	CI singles, doubles, triples, and quaduples	m^{10}	[27]
EOM-CCSD	EOM-CC singles and doubles	m^6	[16]
EOM-CCSDT	EOM-CC singles, doubles, and triples	m^8	[16]
EOM-CCSDTQ	EOM-CC singles, doubles, triples, and quadruples	m^{10}	[16]
IP-EOM-CCSD	Ionization-potential EOM-CCSD	m^6	[68]

Table 8-1. (*Continued*)

Acronym	Definition	Cost[a]	References
IP-EOM-CCSDT	Ionization-potential EOM-CCSDT	m^8	[68]
IP-EOM-CCSDTQ	Ionization-potential EOM-CCSDTQ	m^{10}	[68]
EA-EOM-CCSD	Electron-affinity EOM-CCSD	m^6	[69]
EA-EOM-CCSDT	Electron-affinity EOM-CCSDT	m^8	[69]
EA-EOM-CCSDTQ	Electron-affinity EOM-CCSDTQ	m^{10}	[69]
EOM-CCSDt	EOM-CCSD with active-space triples	m^6	[70]
EOM-CCSDtq	EOM-CCSD with active-space triples and quadruples	m^6	[70]
EOM-CCSDTq	EOM-CCSDT with active-space quadruples	m^8	[70]
CCSD(T)	CCSD with a noniterative triples correction	m^7	[20]
CCSD[T]	CCSD with a noniterative triples correction	m^7	[20]
CR-CCSD(T)	Completely renormalized CCSD(T)	m^7	[20]
CCSD(2)$_T$	CCSD with a second-order triples correction	m^7	[20]
CCSD(2)$_{TQ}$	CCSD with a second-order correction	m^9	[20]
CCSD(3)$_T$	CCSD with a third-order triples correction	m^8	[22]
CCSD(3)$_{TQ}$	CCSD with a third-order triples and quadruples correction	m^{10}	[22]
CCSDT(2)$_Q$	CCSDT with a second-order quadruples correction	m^{10}	[20]
CCSD(T)-R12	Explicitly correlated CCSD(T)	m^7	[39]
CCSD(2)$_T$-R12	Explicitly correlated CCSD(2)$_T$	m^7	[39]
CCSD(2)$_{TQ}$-R12	Explicitly correlated CCSD(2)$_{TQ}$	m^9	[39]
CCSD(3)$_T$-R12	Explicitly correlated CCSD(3)$_T$	m^8	[39]
CCSDT(2)$_Q$-R12	Explicitly correlated CCSDT(2)$_Q$	m^{10}	[39]
CCSD(2)$_T$(R12)	Explicitly correlated CCSD(2)$_T$	m^7	[39]
CCSD(2)$_{TQ}$(R12)	Explicitly correlated CCSD(2)$_{TQ}$	m^9	[39]
CIS(D)	CIS with a doubles correction	m^5	[21]
CIS(3)	CIS with a third-order correction	m^6	[21]
CIS(4)$_P$	CIS with a partial fourth-order correction	m^6	[21]
EOM-CCSD(2)$_T$	EOM-CCSD with a second-order triples correction	m^7	[22]
EOM-CCSD(2)$_{TQ}$	EOM-CCSD with a second-order correction	m^9	[22]
EOM-CCSD(3)$_T$	EOM-CCSD with a third-order triples correction	m^8	[22]

[a] Polynomial dependence of cost on the number of orbitals (m).

8.2.1. Coupled-Cluster Theory

The effective (similarity-transformed) Hamiltonian $\bar{H}$ of the rank-n CC method [1] ($n = 2$ for CCSD, $n = 3$ for CCSDT, $n = 4$ for CCSDTQ, and so forth) is defined by

$$\bar{H} = \exp(-\hat{T})\hat{H}\exp(\hat{T}) = \left[\hat{H}\exp(\hat{T})\right]_{\mathrm{C}}, \tag{8-3}$$

where $\hat{T}$ is the sum of one- through n-electron excitation operators, "C" means that the operators are diagrammatically connected, and $\hat{H}$ is the electronic Hamiltonian minus the reference energy,

$$\hat{H} = \hat{f} + \hat{v} = \sum_{p,q} f_q^p \{p^\dagger q\} + \frac{1}{4} \sum_{p,q,r,s} v_{rs}^{pq} \{p^\dagger q^\dagger sr\}. \tag{8-4}$$

Here, **f** and **v** are Fock and antisymmetrized two-electron integral matrices, p, q, r, and s label either occupied or virtual orbitals of the reference determinant, and brackets bring the second-quantized creation and annihilation operators in the normal order. The rank-n CC method is defined with $\bar{H}$ by

$$\hat{P}_m \bar{H} \left|\Phi\right\rangle = \hat{P}_m E_0^{(0)} \left|\Phi\right\rangle, \forall m = 0, \ldots, n, \tag{8-5}$$

where $E_0^{(0)}$ is the correlation energy[2] and $\hat{P}_k$ is a projector on the set of all k-electron excited determinants. Using i and j (and later k, l, m, and n also) for occupied orbitals and a and b (as well as c, d, and e) for virtual orbitals, $\hat{P}_2$, for instance, is written as

$$\hat{P}_2 = \sum_{i<j} \sum_{a<b} \left|\Phi_{ij}^{ab}\right\rangle\left\langle\Phi_{ij}^{ab}\right|, \tag{8-6}$$

where Φ_{ij}^{ab} is a two-electron excited determinant. The diagrammatic connectedness of Eq. (8-5), which is a result of Eq. (8-3), ensures the size-extensivity of $E_0^{(0)}$.

8.2.2. Equation-of-Motion Coupled-Cluster Theory

The rank-n EOM-CC method [10, 16, 71] can be regarded as an application of rank-n CI using rank-n CC effective Hamiltonian, $\bar{H}$, instead of $\hat{H}$. Let $\hat{R}_k^{(0)}$ be the linear excitation operator of this CI corresponding to the kth excited state. It must satisfy

$$\hat{P}_m \bar{H} \hat{R}_k^{(0)} \left|\Phi\right\rangle = \hat{P}_m E_k^{(0)} \hat{R}_k^{(0)} \left|\Phi\right\rangle, \forall m = 0, \ldots, n, \tag{8-7}$$

where E_k is the correlation energy of the kth state. Comparing Eqs. (8-7) and (8-5), we notice that $\hat{R}_0^{(0)} = 1$. Since $\bar{H}$ is not Hermitian, its matrix representation has distinct left and right eigenvectors. Let $\hat{L}_k^{(0)}$ be the linear de-excitation operator corresponding to $\hat{R}_k^{(0)}$. It is a solution of the following equation,

$$\left\langle\Phi\right| \hat{L}_k^{(0)} \bar{H} \hat{P}_m = \left\langle\Phi\right| \hat{L}_k^{(0)} E_k^{(0)} \hat{P}_m, \forall m = 0, \ldots, n \tag{8-8}$$

and

$$\left\langle\Phi\right| \hat{L}_k^{(0)} \hat{R}_l^{(0)} \left|\Phi\right\rangle = \delta_{kl}, \tag{8-9}$$

---

[2] The subscript indicates an electronic state and the superscript in the parenthesis is the order in a perturbation expansion.

where δ_{kl} is Kronecker's delta. These equations can be cast into the following equivalent expressions that underscore the size-intensivity of the EOM-CC excitation energy, $\omega_k^{(0)} = E_k^{(0)} - E_0^{(0)}$:

$$\hat{P}_m\big(\bar{H}\hat{R}_k^{(0)}\big)_{\mathrm{C}}|\Phi\rangle = \hat{P}_m\omega_k^{(0)}\hat{R}_k^{(0)}|\Phi\rangle, \forall m = 0,\ldots,n, \tag{8-10}$$

$$\langle\Phi|\big(\hat{L}_k^{(0)}\bar{H}\big)_{\mathrm{L}}\hat{P}_m = \langle\Phi|\hat{L}_k^{(0)}\omega_k^{(0)}\hat{P}_m, \forall m = 0,\ldots,n, \tag{8-11}$$

where "L" means that the operators are diagrammatically linked. Setting $n = 1$ and using the Hartree–Fock (HF) wave function as the reference, we arrive at the CIS method [72] because the rank-1 CC method has the trivial solution, $\hat{T} = 0$ and $E_0^{(0)} = 0$, and thus $\bar{H} = \hat{H}$. When $\hat{R}_k^{(0)}$ is a linear ionization (electron-attachment) operator and $\hat{L}_k^{(0)}$ is its adjoint, the above equations define the rank-n ionization-potential (electron-affinity) EOM-CC method [68, 69, 73, 74]. In that case, $\hat{P}_m$ should be understood to designate the projector on the manifold of the corresponding ionized (electron-attached) determinants.

8.2.3. General Perturbation Theory

We now define the whole series of perturbation corrections to CC and EOM-CC energies and wave functions [18] (see also [75–85]) using the standard Rayleigh–Schrödinger perturbation theory with the following partitioning of the Hamiltonian,

$$\bar{H} = \hat{H}^{(0)} + \hat{V}^{(1)}, \tag{8-12}$$

where $\hat{V}^{(1)}$ is the perturbation (fluctuation potential). The zeroth-order part, $\hat{H}^{(0)}$, is given by

$$\hat{H}^{(0)} = \hat{P}\bar{H}\hat{P} + \hat{Q}\big(E_0^{(0)} + \hat{f}^{(0)}\big)\hat{Q} \tag{8-13}$$

and

$$\hat{f}^{(0)} = \hat{f} - \sum_{a,i} f_i^a\{a^\dagger i\} - \sum_{i,a} f_a^i\{i^\dagger a\}. \tag{8-14}$$

Here $\hat{P} = \hat{P}_0 + \ldots + \hat{P}_n$ and $\hat{Q} = 1 - \hat{P} = \hat{P}_{n+1} + \ldots + \hat{P}_N$ (N is the number of electrons). We also require that

$$\hat{Q}\hat{R}_k^{(0)}|\Phi\rangle = \langle\Phi|\hat{L}_k^{(0)}\hat{Q} = 0. \tag{8-15}$$

It should be understood that, because $\bar{H}$ has the identical eigenvalues as $\hat{H}$, the perturbation series must converge at the corresponding full CI results (unless they diverge) regardless of the rank of the reference CC or EOM-CC method. This definition of

$\hat{H}^{(0)}$ also ensures that the invariance of the CC and EOM-CC energies and wave functions be maintained with respect to a unitary transformation among occupied orbitals or among virtual orbitals (but not across these two sets).

Expanding the exact (full CI) energy and wave function of the kth state in series

$$E_k = E_k^{(0)} + E_k^{(1)} + E_k^{(2)} + \cdots, \tag{8-16}$$

$$\hat{R}_k |\Phi\rangle = \hat{R}_k^{(0)} |\Phi\rangle + \hat{R}_k^{(1)} |\Phi\rangle + \hat{R}_k^{(2)} |\Phi\rangle + \cdots, \tag{8-17}$$

and substituting them into the Schrödinger equation

$$\big(\hat{H}^{(0)} + \hat{V}^{(1)}\big)\hat{R}_k|\Phi\rangle = E_k\hat{R}_k|\Phi\rangle \tag{8-18}$$

as well as separating terms according to their overall perturbation orders, we arrive at a recursive relation for $\hat{R}_k^{(i)}$:

$$\big(E_k^{(0)} - \hat{H}^{(0)}\big)\hat{R}_k^{(i)}|\Phi\rangle = \hat{V}^{(1)}\hat{R}_k^{(i-1)}|\Phi\rangle - \sum_{j=1}^{i} E_k^{(j)}\hat{R}_k^{(i-j)}|\Phi\rangle, \forall i \geq 1. \tag{8-19}$$

We furthermore impose the intermediate normalization on the exact wave function, which can be expressed as

$$\langle\Phi|\, \hat{L}_k^{(0)}\hat{R}_k\, |\Phi\rangle = 1, \tag{8-20}$$

implying

$$\langle\Phi|\, L_k^{(0)}R_k^{(i)}\, |\Phi\rangle = 0, \forall i \geq 1. \tag{8-21}$$

Using this relation and also Eq. (8-15), we can show that the perturbation corrections to the energy are simply,

$$E_k^{(i)} = \langle\Phi|\, \hat{L}_k^{(0)}\hat{V}^{(1)}\hat{R}_k^{(i-1)}\, |\Phi\rangle\,. \tag{8-22}$$

Apart from the special cases to be individually discussed below, the above expression generally has nonphysical size dependence. Our criterion for the correct size dependence of a perturbation correction to an excited-state total energy is as follows: the correction must consist of size-extensive and intensive parts and the size-extensive part must be equal to the correction in the ground state obtained by substituting $k = 0$ to the perturbation expression. See [86] for an in-depth discussion on other criteria for correct size dependence.

8.2.4. Low-Order Energy Corrections

The uncorrected (zeroth-order) correlation energies are, by construction, the energies of the parent CC or EOM-CC method. The first-order corrections vanish because of $\hat{P}\hat{V}^{(1)}\hat{P} = 0$ and Eq. (8-15). The first meaningful (nonvanishing) correction, therefore, occurs at the second order and can be expressed as

$$E_k^{(2)} = \langle\Phi|\,\hat{L}_k^{(0)}\hat{V}^{(1)}\bar{Q}\hat{V}^{(1)}\hat{R}_k^{(0)}\,|\Phi\rangle \tag{8-23}$$

with the resolvent operator defined by its components,

$$\bar{Q} = \hat{Q}\big(\omega_k^{(0)} - \hat{H}^{(0)}\big)^{-1}\hat{Q} = \sum_{m=n+1}^{N} \bar{Q}_{k,m}, \tag{8-24}$$

and

$$\bar{Q}_{k,m} = \frac{\big|\Phi_{i_1\cdots i_m}^{a_1\cdots a_m}\big\rangle\big\langle\Phi_{i_1\cdots i_m}^{a_1\cdots a_m}\big|}{\omega_k^{(0)} + e_{i_1} + \cdots + e_{i_m} - e_{a_1} - \cdots - e_{a_m}}. \tag{8-25}$$

Equation (8-25) assumes a canonical HF reference and e_{i_m} and e_{a_m} are its occupied and virtual orbital energies, respectively. This second-order expression is always size-extensive for the ground state ($k = 0$). This can be understood as follows. For Eq. (8-23) to be diagrammatically unlinked, it must have at least two pairs of excitation and de-excitation operators (vertexes), each forming a closed disconnected diagram. However, $\hat{R}_0^{(0)} = 1$ and cannot be a part of a closed diagram. There are only three operators, $\hat{L}_0^{(0)}$, $\hat{V}^{(1)}$, and $\hat{V}^{(1)}$ and Eq. (8.23) with $k = 0$ cannot be disconnected and, therefore, is size-extensive. Note that $\hat{V}^{(1)}$ is by itself connected because of Eq. (8-3).

Similarly, the third-order energy correction can be written in the following general form:

$$E_k^{(3)} = \langle\Phi|\,\hat{L}_k^{(0)}\hat{V}^{(1)}\bar{Q}\hat{V}^{(1)}\bar{Q}\hat{V}^{(1)}\hat{R}_k^{(0)}\,|\Phi\rangle\,. \tag{8-26}$$

This expression can also be shown to be size-extensive for the ground state ($k = 0$) as follows. For Eq. (8-26) to be unlinked, $\hat{L}_0^{(0)}$ and $\hat{V}^{(1)}$ must form a closed disconnected diagram and $\hat{V}^{(1)}$ and $\hat{V}^{(1)}$ another. Since $\hat{V}^{(1)}$ can de-excite only up to two electrons and $\hat{P}\hat{V}^{(1)}\hat{P} = 0$, two $\hat{V}^{(1)}$ can form a closed diagram only when $n \leq 1$. However, if $n \leq 1$, $\hat{L}_0^{(0)} = 1$ (assuming a HF reference) and there are too few operators to form two closed disconnected diagrams. Hence, Eq. (8-26) is always connected for $k = 0$ and size-extensive.

8.2.5. MBPT

When applied to a HF reference by setting $n = 0$ (rank-0 CC) and $k = 0$ (the ground state), the perturbation series ($i \geq 2$) introduced above reduces, order-by-order, to MBPT with the Møller–Plesset partitioning, which is size-extensive. For instance, the second- and third-order corrections in the canonical HF reference are

$$E_0^{\mathrm{MBPT}(2)} = \langle \Phi | \hat{H} \bar{Q}_{0,2} \hat{H} | \Phi \rangle \tag{8-27}$$

and

$$E_0^{\mathrm{MBPT}(3)} = \langle \Phi | \hat{H} \bar{Q}_{0,2} \hat{V}^{(1)} \bar{Q}_{0,2} \hat{H} | \Phi \rangle . \tag{8-28}$$

The same results can be obtained by using CC singles (CCS) based on a canonical HF reference ($n = 1$). The CCS equation can be satisfied by $\hat{T} = 0$ and thus $\bar{H} = \hat{H}$. Therefore, the only difference between the HF ($n = 0$) and CCS ($n = 1$) cases is the definition of $\hat{P}$: $\hat{P} = \hat{P}_0$ in the former and $\hat{P} = \hat{P}_0 + \hat{P}_1$ in the latter. However, this difference does not affect the perturbation expressions because of the Brillouin condition,

$$\hat{P}_1 \hat{H} | \Phi \rangle = 0, \tag{8-29}$$

when the HF reference is used.

8.2.6. Properties of Perturbation Series

Important general properties of the perturbation corrections can at this point be summarized as follows:

1. At each order, the wave function is well defined by Eq. (8.19).
2. The zeroth-order energies and wave functions are those of the parent CC and EOM-CC methods.
3. The first-order energy corrections are zero.
4. The second- and third-order corrections to ground-state energies are size-extensive.
5. The higher-order corrections to ground-state energies are generally not size-extensive.
6. The corrections to excited-state energies have nonphysical size dependence.
7. The perturbation series is convergent at the full CI limit.
8. The orbital invariance of the parent CC or EOM-CC method is maintained.
9. The perturbation theory with the rank-0 or rank-1 CC reference based on a canonical HF reference reproduces MBPT with the Møller–Plesset partitioning, which is size-extensive at any order.

The whole perturbation series based on the CC or EOM-CC method of any rank have been implemented by the determinant-based algorithm and their performance has been characterized (see Section 8.3). In the remainder of this section, we discuss the formalisms of some of the important members that have been implemented into efficient programs after some adjustments have been made (if necessary) to make them size-extensive or intensive.

8.2.7. Second-Order Corrections to CCSD

The second-order correction to CCSD [20] consists of two terms, each of which is size-extensive:

$$E_0^{\mathrm{CCSD}(2)} = \langle\Phi|\,\hat{L}_0^{(0)}\bar{H}\bar{Q}_{0,3}\bar{H}\,|\Phi\rangle + \langle\Phi|\,\hat{L}_0^{(0)}\bar{H}\bar{Q}_{0,4}\bar{H}\,|\Phi\rangle\,, \tag{8-30}$$

where $\bar{V}^{(1)}$ is replaced by the CCSD effective Hamiltonian $\bar{H}$ and $\hat{L}_0^{(0)}$ is the left eigenvector of $\bar{H}$ for the ground state. Five-electron and higher-rank excited determinants do not appear because $\bar{H}$ can de-excite only up to two electrons and $\hat{L}_0^{(0)}$ is an overall double de-excitation operator, allowing $\hat{L}_0^{(0)}\bar{H}$ to couple three- and four-electron excited determinants with the reference. We define two methods CCSD(2)$_T$ and CCSD(2)$_{TQ}$ by

$$E_0^{\mathrm{CCSD}(2)_T} = \langle\Phi|\,\hat{L}_0^{(0)}\bar{H}\bar{Q}_{0,3}\bar{H}\,|\Phi\rangle\,, E_0^{\mathrm{CCSD}(2)_{TQ}} = E_0^{\mathrm{CCSD}(2)}. \tag{8-31}$$

Both methods are size-extensive and their operation costs depend on the number of orbitals (m) as $O(m^7)$ and $O(m^9)$ asymptotically. A closely related method was proposed independently by Gwaltney and Head-Gordon [82, 84].

The widely used CCSD(T) [6, 7] and CCSD[T] [87] methods, both having the cost scaling of $O(m^7)$, can be viewed as diagrammatic simplifications of CCSD(2)$_T$. Approximating $\hat{L}_0^{(0)}$ by $1+\hat{T}_1^\dagger+\hat{T}_2^\dagger$, where $\hat{T}_i$ is an i-electron excitation operator, and retaining only the most important factors consisting of no more than two operators, we obtain the (T) correction to CCSD,

$$E_0^{\mathrm{CCSD(T)}} = \langle\Phi|\,\left(\hat{T}_1+\hat{T}_2\right)^\dagger\bar{H}\bar{Q}_{0,3}\left(\bar{H}\hat{T}_2\right)_{\mathrm{C}}\,|\Phi\rangle\,. \tag{8-32}$$

The CCSD[T] method is a further approximation of this method obtained by setting $\hat{T}_1 = 0$. Its energy correction is, therefore,

$$E_0^{\mathrm{CCSD[T]}} = \langle\Phi|\,\left(\bar{H}\hat{T}_2\right)_{\mathrm{C}}^\dagger\bar{Q}_{0,3}\left(\bar{H}\hat{T}_2\right)_{\mathrm{C}}\,|\Phi\rangle\,, \tag{8-33}$$

assuming a canonical HF reference.

8.2.8. Second-Order Correction to CCSDT

The second-order correction to CCSDT [20] also consists of two terms involving four- and five-electron excited determinants:

$$E_0^{\mathrm{CCSDT}(2)} = \langle\Phi|\,\hat{L}_0^{(0)}\bar{H}\bar{Q}_{0,4}\bar{H}\,|\Phi\rangle + \langle\Phi|\,\hat{L}_0^{(0)}\bar{H}\bar{Q}_{0,5}\bar{H}\,|\Phi\rangle\,, \tag{8-34}$$

where $\bar{H}$ is the CCSDT effective Hamiltonian and $\hat{L}_0^{(0)}$ is the corresponding left eigenvector for the ground state. We have reported an efficient implementation of CCSDT(2)$_Q$, which retains only the first term of Eq. (8.34) and is size-extensive:

$$E_0^{\mathrm{CCSDT}(2)_Q} = \langle\Phi|\,\hat{L}_0^{(0)}\bar{H}\bar{Q}_{0,4}\bar{H}\,|\Phi\rangle\,. \tag{8-35}$$

Its operation cost is $O(m^{10})$.[3]

8.2.9. Third-Order Corrections to CCSD

As many as seven individually size-extensive terms arise in the third-order correction to CCSD [22] according to Eq. (8.26).

$$\begin{aligned} E_0^{\mathrm{CCSD}(3)} = {} & \langle\Phi|\,\hat{L}_0^{(0)}\bar{H}\bar{Q}_{0,3}\hat{V}^{(1)}\bar{Q}_{0,3}\bar{H}\,|\Phi\rangle + \langle\Phi|\,\hat{L}_0^{(0)}\bar{H}\bar{Q}_{0,3}\hat{V}^{(1)}\bar{Q}_{0,4}\bar{H}\,|\Phi\rangle \\ & + \langle\Phi|\,\hat{L}_0^{(0)}\bar{H}\bar{Q}_{0,4}\hat{V}^{(1)}\bar{Q}_{0,3}\bar{H}\,|\Phi\rangle + \langle\Phi|\,\hat{L}_0^{(0)}\bar{H}\bar{Q}_{0,4}\hat{V}^{(1)}\bar{Q}_{0,4}\bar{H}\,|\Phi\rangle \\ & + \langle\Phi|\,\hat{L}_0^{(0)}\bar{H}\bar{Q}_{0,3}\hat{V}^{(1)}\bar{Q}_{0,5}\bar{H}\,|\Phi\rangle + \langle\Phi|\,\hat{L}_0^{(0)}\bar{H}\bar{Q}_{0,4}\hat{V}^{(1)}\bar{Q}_{0,5}\bar{H}\,|\Phi\rangle \\ & + \langle\Phi|\,\hat{L}_0^{(0)}\bar{H}\bar{Q}_{0,4}\hat{V}^{(1)}\bar{Q}_{0,6}\bar{H}\,|\Phi\rangle\,. \end{aligned} \tag{8-36}$$

Among them, we expect the first term to be numerically more important than the others. This term defines the CCSD(3)$_T$ method, whose operation cost scales as $O(m^8)$. The CCSD(3)$_{TQ}$ correction, on the other hand, is the sum of the first four terms of Eq. (8-36) that involve only the three- and four-electron excited determinants. The evaluation of these four terms requires $O(m^{10})$ arithmetic operations.

8.2.10. Second-, Third-, and Fourth-Order Corrections to CIS

For an excited state, our perturbation corrections generally have nonphysical size dependence. However, the application of an approximation introduced by Head-Gordon et al. [88] to these corrections has been shown to make them recover correct size dependence and at the same time reduce the computational cost. Let us consider the second-order correction to CIS. According to Eq. (8-23), it is

$$E_k^{\mathrm{CIS}(2)} = \langle\Phi|\,\hat{L}_k^{(0)}\hat{H}\bar{Q}_{k,2}\hat{H}\hat{R}_k^{(0)}\,|\Phi\rangle + \langle\Phi|\,\hat{L}_k^{(0)}\hat{H}\bar{Q}_{k,3}\hat{H}\hat{R}_k^{(0)}\,|\Phi\rangle \tag{8-37}$$

---

[3] The original paper reported the scaling incorrectly as $O(m^9)$.

in a HF reference, where $\hat{L}_k^{(0)\dagger} = R_k^{(0)}$ is the one-electron excitation operator whose amplitudes are determined by CIS. This is indeed the correction to a CIS total energy proposed by Foresman et al. [72] under the name CIS-MP2. The inspection of the terms shows that the first term is size-intensive and evaluated at an $O(m^5)$ cost, but the second term has ambiguous size dependence and its evaluation necessarily involves $O(m^6)$ operations because of the six-index denominator in $\bar{Q}_{k,3}$. The lack of size-intensivity in the second term can be explained diagrammatically [19, 21]: $\hat{L}_k^{(0)}$ and $\hat{R}_k^{(0)}$ can form a closed disconnected diagram and $\hat{H}$ and $\hat{H}$ another, making this term contain an unlinked diagram. This observation suggests the following approximation for the unlinked term (subscript "U") of Eq. (8-37):

$$\langle\Phi|\,\hat{L}_k^{(0)}\hat{H}\bar{Q}_{k,3}\hat{H}\hat{R}_k^{(0)}\,|\Phi\rangle_{\mathrm{U}} \approx \langle\Phi|\,\hat{L}_k^{(0)}\hat{R}_k^{(0)}\,|\Phi\rangle\,\langle\Phi|\,\hat{H}\bar{Q}_{0,2}\hat{H}\,|\Phi\rangle = E_0^{\mathrm{MBPT(2)}}, \quad (8\text{-}38)$$

where the orthonormality of CIS vectors $\langle\Phi|\,\hat{L}_k^{(0)}\hat{R}_l^{(0)}\,|\Phi\rangle = \delta_{kl}$ and Eq. (8-27) are used in the second equality. Incorporating this approximation into Eq. (8-37), we arrive at a more satisfactory second-order correction to CIS:

$$\begin{aligned} E_k^{\mathrm{CIS(D)}} &= \langle\Phi|\,\hat{L}_k^{(0)}\hat{H}\bar{Q}_{k,2}\hat{H}\hat{R}_k^{(0)}\,|\Phi\rangle + \langle\Phi|\,\hat{L}_k^{(0)}\hat{H}\hat{R}_k^{(0)}\bar{Q}_{0,2}\hat{H}\,|\Phi\rangle \\ &= \langle\Phi|\,\hat{L}_k^{(0)}\hat{H}\bar{Q}_{k,2}\hat{H}\hat{R}_k^{(0)}\,|\Phi\rangle + \langle\Phi|\,\hat{L}_k^{(0)}\hat{H}\hat{R}_k^{(0)}\bar{Q}_{0,2}\hat{H}\,|\Phi\rangle_{\mathrm{L}} + E_0^{\mathrm{MBPT(2)}}, \end{aligned} \quad (8\text{-}39)$$

which consists of the size-intensive corrections (the first two terms) to the CIS excitation energy and the size-extensive correction to the correlation energy in the ground state, which coincides with the MBPT(2) correction. Also, the elimination of the six-index denominator (i.e., $\bar{Q}_{k,3}$) permits the whole expression to be evaluated at an $O(m^5)$ cost. This method, proposed by Head-Gordon et al. [88] as CIS(D), can be viewed as an excited-state counterpart to MBPT(2).

The approximation of Head-Gordon et al. can be applied to higher-order corrections [21], awarding them correct size dependence and a considerably smaller computational cost. The third-order correction to CIS energy can be modified by this approximation as follows:

$$\begin{aligned} E_k^{\mathrm{CIS(3)}} &= \langle\Phi|\,\hat{L}_k^{(0)}\hat{H}\bar{Q}_{k,2}\hat{V}^{(1)}\bar{Q}_{k,2}\hat{H}\hat{R}_k^{(0)}\,|\Phi\rangle + \langle\Phi|\,\hat{L}_k^{(0)}\hat{H}\bar{Q}_{k,2}\hat{V}^{(1)}\bar{Q}_{k,3}\hat{H}\hat{R}_k^{(0)}\,|\Phi\rangle \\ &\quad + \langle\Phi|\,\hat{L}_k^{(0)}\hat{H}\bar{Q}_{k,3}\hat{V}^{(1)}\bar{Q}_{k,2}\hat{H}\hat{R}_k^{(0)}\,|\Phi\rangle + \langle\Phi|\,\hat{L}_k^{(0)}\hat{H}\bar{Q}_{k,3}\hat{V}^{(1)}\bar{Q}_{k,3}\hat{H}\hat{R}_k^{(0)}\,|\Phi\rangle \\ &\approx \langle\Phi|\,\hat{L}_k^{(0)}\hat{H}\bar{Q}_{k,2}\hat{V}^{(1)}\bar{Q}_{k,2}\hat{H}\hat{R}_k^{(0)}\,|\Phi\rangle + 2\,\langle\Phi|\,\hat{L}_k^{(0)}\hat{H}\bar{Q}_{k,2}\hat{V}^{(1)}\hat{R}_k^{(0)}\bar{Q}_{0,2}\hat{H}\,|\Phi\rangle \\ &\quad + \langle\Phi|\,\hat{H}\bar{Q}_{0,2}\hat{L}_k^{(0)}\hat{V}^{(1)}\hat{R}_k^{(0)}\bar{Q}_{0,2}\hat{H}\,|\Phi\rangle_{\mathrm{L}} + E_0^{\mathrm{MBPT(3)}}, \end{aligned} \quad (8\text{-}40)$$

where we have used the fact that the second and third terms in the right-hand side of the first equality are complex conjugate of each other and

$$\begin{aligned} &\langle\Phi|\,\hat{H}\bar{Q}_{0,2}\hat{L}_k^{(0)}\hat{V}^{(1)}\hat{R}_k^{(0)}\bar{Q}_{0,2}\hat{H}\,|\Phi\rangle_{\mathrm{U}} \\ &= \langle\Phi|\,\hat{L}_k^{(0)}\hat{R}_k^{(0)}\,|\Phi\rangle\,\langle\Phi|\,\hat{H}\bar{Q}_{0,2}\hat{V}^{(1)}\bar{Q}_{0,2}\hat{H}\,|\Phi\rangle = E_0^{\mathrm{MBPT(3)}}. \end{aligned} \quad (8\text{-}41)$$

Note that the approximate expression in Eq. (8-40) is the sum of size-intensive corrections to the excitation energy (the first three terms) and the size-extensive MBPT(3) correction to the ground-state energy (the last term). It can be evaluated by an $O(m^6)$ cost as opposed to an $O(m^8)$ cost without the approximation.

Similarly, a partial fourth-order correction to CIS [21] that consists of size-intensive corrections to the excitation energy and the size-extensive MBPT(4) correction to the ground-state energy can be defined by

$$\begin{aligned} E_k^{\mathrm{CIS}(4)_P} = {} & \langle\Phi|\,\hat{L}_k^{(0)}\hat{H}\bar{Q}_{k,2}\hat{V}^{(1)}\bar{P}_{k,0}\hat{V}^{(1)}\bar{Q}_{k,2}\hat{H}\hat{R}_k^{(0)}\,|\Phi\rangle \\ & + \langle\Phi|\,\hat{L}_k^{(0)}\hat{H}\bar{Q}_{k,2}\hat{V}^{(1)}\bar{P}_{k,1}\hat{V}^{(1)}\bar{Q}_{k,2}\hat{H}\hat{R}_k^{(0)}\,|\Phi\rangle \\ & + \langle\Phi|\,\hat{L}_k^{(0)}\hat{H}\bar{Q}_{k,2}\hat{V}^{(1)}\bar{P}_{k,1}\big(\hat{V}^{(1)}\hat{R}_k^{(0)}\bar{Q}_{0,2}\hat{H}\big)_{\mathrm{L}}\,|\Phi\rangle \\ & + \langle\Phi|\,\big(\hat{H}\bar{Q}_{0,2}\hat{L}_k^{(0)}\hat{V}^{(1)}\big)_{\mathrm{L}}\bar{P}_{k,1}\hat{V}^{(1)}\bar{Q}_{k,2}\hat{H}\hat{R}_k^{(0)}\,|\Phi\rangle \\ & + \langle\Phi|\,\big(\hat{H}\bar{Q}_{0,2}\hat{L}_k^{(0)}\hat{V}^{(1)}\big)_{\mathrm{L}}\bar{P}_{k,1}\big(\hat{V}^{(1)}\hat{R}_k^{(0)}\bar{Q}_{0,2}\hat{H}\big)_{\mathrm{L}}\,|\Phi\rangle + E_0^{\mathrm{MBPT}(4)}, \end{aligned} \tag{8-42}$$

where the resolvent operators $\bar{P}_{k,0}$ and $\bar{P}_{k,1}$ are given by

$$\bar{P}_{k,0} = \frac{|\Phi\rangle\langle\Phi|}{\omega_k^{(0)}}, \bar{P}_{k,1} = \sum_{j\in\Omega}\frac{\hat{R}_j^{(0)}\,|\Phi\rangle\langle\Phi|\,\hat{L}_j^{(0)}}{\omega_k^{(0)} - \omega_j^{(0)}}. \tag{8-43}$$

Here Ω represents a set of all CIS roots minus the ground-state and the kth excited-state roots as well as their degenerate roots (if any). The size-intensive corrections (the first five terms) in Eq. (8-42) can be evaluated at an $O(m^5)$ cost.

8.2.11. Second- and Third-Order Corrections to EOM-CCSD

It is straightforward to identify unlinked terms in the second- and third-order corrections to EOM-CCSD [19, 22] (see related studies by Watts and Bartlett [89, 90] and by Włoch et al. [91]). They contain closed disconnected diagrams resembling size-extensive corrections to the ground-state energy, as in the corrections to CIS. We replace them by the closest size-extensive diagrammatic analogues, which, in this case, are the corresponding approximations of $E_0^{\mathrm{CCSD}(2)}$ and $E_0^{\mathrm{CCSD}(3)}$. For instance, we define the second-order triples correction to EOM-CCSD by

$$E_k^{\mathrm{CCSD}(2)_T} = \langle\Phi|\,\hat{L}_k^{(0)}\bar{H}\bar{Q}_{k,3}\bar{H}\hat{P}_2\hat{R}_k^{(0)}\,|\Phi\rangle + \langle\Phi|\,\hat{L}_k^{(0)}\bar{H}\bar{Q}_{k,3}\bar{H}\hat{P}_1\hat{R}_k^{(0)}\,|\Phi\rangle + E_0^{\mathrm{CCSD}(2)_T}, \tag{8-44}$$

where $\bar{H}$ is the CCSD effective Hamiltonian, $\hat{L}_k^{(0)}$ and $\hat{R}_k^{(0)}$ are its left and right eigenvectors for the kth excited state, and we have used

$$\langle\Phi|\,\hat{L}_k^{(0)}\bar{H}\bar{Q}_{k,3}\bar{H}\hat{P}_0\hat{R}_k^{(0)}\,|\Phi\rangle \approx E_0^{\mathrm{CCSD}(2)_T}. \tag{8-45}$$

The first two terms in Eq. (8-44) are size-intensive (see [22] for a proof) and $E_0^{\mathrm{CCSD}(2)_T}$ is size-extensive. Equation (8-44) is in fact the definition of the EOM-CCSD($\tilde{\mathrm{T}}$) method proposed earlier by Watts and Bartlett [90]. The excited-state counterparts of CCSD(2)$_{TQ}$ and CCSD(3)$_T$ are defined by

$$\begin{aligned} E_k^{\mathrm{CCSD}(2)_{TQ}} &= \langle\Phi|\,\hat{L}_k^{(0)}\bar{H}\bar{Q}_{k,4}\bar{H}\hat{P}_2\hat{R}_k^{(0)}\,|\Phi\rangle + \langle\Phi|\,\hat{L}_k^{(0)}\bar{H}\bar{Q}_{k,4}\bar{H}\hat{P}_1\hat{R}_k^{(0)}\,|\Phi\rangle \\ &\quad + \langle\Phi|\,\hat{L}_k^{(0)}\bar{H}\bar{Q}_{k,3}\bar{H}\hat{P}_2\hat{R}_k^{(0)}\,|\Phi\rangle + \langle\Phi|\,\hat{L}_k^{(0)}\bar{H}\bar{Q}_{k,3}\bar{H}\hat{P}_1\hat{R}_k^{(0)}\,|\Phi\rangle \\ &\quad + E_0^{\mathrm{CCSD}(2)_{TQ}}, \end{aligned} \tag{8-46}$$

$$\begin{aligned} E_k^{\mathrm{CCSD}(3)_T} &= \langle\Phi|\,\hat{L}_k^{(0)}\bar{H}\bar{Q}_{k,3}\hat{V}^{(1)}\bar{Q}_{k,3}\bar{H}\hat{P}_2\hat{R}_k^{(0)}\,|\Phi\rangle \\ &\quad + \langle\Phi|\,\hat{L}_k^{(0)}\bar{H}\bar{Q}_{k,3}\hat{V}^{(1)}\bar{Q}_{k,3}\bar{H}\hat{P}_1\hat{R}_k^{(0)}\,|\Phi\rangle + E_0^{\mathrm{CCSD}(3)_T}. \end{aligned} \tag{8-47}$$

Again, they sum size-extensive and intensive corrections. The size dependence of their computational costs can be found in Table 8-1.

8.3. EXPLICITLY CORRELATED EXTENSIONS

8.3.1. Explicitly Correlated CC and EOM-CC

The slow basis-set convergence of correlation energies is caused by the inability of the products of one-electron basis functions to describe qualitatively correctly the cusps of the exact wave functions at electron-electron coalescence ($r_{12} = 0$), where the Coulomb operator $\left(r_{12}^{-1}\right)$ is divergent. The R12 scheme of Kutzelnigg [29] allows a basis function of interelectronic distances – the correlation factor (f_{12}) – to be incorporated into virtually any electron-correlation method [31, 32]. A carefully chosen, but universal, correlation factor can dramatically improve the description of the wave functions near these cusps and thereby reduce the basis-set truncation errors.

The R12 scheme introduces a two-electron excitation operator that promotes electrons from occupied orbitals spanned by a finite basis set (an orbital basis set or OBS) to virtual orbitals (α and β) spanned by a complete thus infinite set of basis functions. In the context of CC theory [33–53], $\hat{T}$ is replaced by $\hat{T} + \hat{\mathcal{T}}_2$ in the R12 scheme, where

$$\hat{\mathcal{T}}_2 = \sum_{\alpha<\beta}\sum_{i<j} t_{ij}^{\alpha\beta}\left\{\alpha^\dagger\beta^\dagger ji\right\} = \sum_{\alpha<\beta}\sum_{i<j}\sum_{k<l} F_{kl}^{\alpha\beta}t_{ij}^{kl}\left\{\alpha^\dagger\beta^\dagger ji\right\}. \tag{8-48}$$

Here $F_{kl}^{\alpha\beta}$ is an antisymmetrized two-electron integral of the correlation factor, which must satisfy $F_{kl}^{ab} = 0$ to avoid double counting of correlation. Hence, $\hat{\mathcal{T}}_2$ is to capture a complete-basis two-electron excitation effect with a relatively small number

of unknown coefficients $\{t_{ij}^{kl}\}$ [92]. Let $\hat{\mathcal{P}}_2$ be a projector on the determinant space accessible by $\hat{\mathcal{T}}_2$:

$$\hat{\mathcal{P}}_2 = \sum_{i<j} \sum_{k<l} \sum_{m<n} |\Phi_{ij}^{kl}\rangle (\mathbf{X}^{-1})_{kl}^{mn} \langle \Phi_{ij}^{mn}|, \tag{8-49}$$

where

$$|\Phi_{ij}^{kl}\rangle = \sum_{\alpha<\beta} F_{kl}^{\alpha\beta} \{\alpha^\dagger \beta^\dagger ji\} |\Phi\rangle \tag{8-50}$$

and its metric,

$$(\mathbf{X})_{mn}^{kl} = \langle \Phi_{ij}^{kl} \mid \Phi_{ij}^{mn} \rangle = \sum_{\alpha<\beta} F_{kl}^{\alpha\beta *} F_{mn}^{\alpha\beta}. \tag{8-51}$$

Using this projector, the rank-n CC-R12 and EOM-CC-R12 methods [48] are defined by Eqs. (8-7) and (8-8) as well as the following:

$$\hat{\mathcal{P}}_2 \bar{H} \hat{R}_k^{(0)} |\Phi\rangle = \hat{\mathcal{P}}_2 E_k^{(0)} \hat{R}_k^{(0)} |\Phi\rangle, \tag{8-52}$$

$$\langle \Phi| \hat{L}_k^{(0)} \bar{H} \hat{\mathcal{P}}_2 = \langle \Phi| \hat{L}_k^{(0)} E_k^{(0)} \hat{\mathcal{P}}_2, \tag{8-53}$$

where $\bar{H} = \left[\hat{H} \exp\left(\hat{T} + \hat{\mathcal{T}}_2\right)\right]_{\mathrm{C}}$ and $\hat{R}_k^{(0)}$ and $\hat{L}_k^{(0)}$ now have contributions in the space accessible by $\hat{\mathcal{P}}_2$.

Once these second-quantized expressions are evaluated [48], we arrive at equations that contain terms such as

$$\begin{aligned} \sum_{\alpha<\beta} v_{\alpha\beta}^{pq} F_{ij}^{\alpha\beta} &= \sum_{\kappa<\lambda} v_{\kappa\lambda}^{pq} F_{ij}^{\kappa\lambda} - \sum_{r<s} v_{rs}^{pq} F_{ij}^{rs} - \sum_{k,\bar{\alpha}} v_{k\bar{\alpha}}^{pq} F_{ij}^{k\bar{\alpha}} \\ &\approx \left(r_{12}^{-1} f_{12}\right)_{ij}^{pq} - \sum_{r<s} v_{rs}^{pq} F_{ij}^{rs} - \sum_{k,\bar{a}} v_{k\bar{a}}^{pq} F_{ij}^{k\bar{a}}, \end{aligned} \tag{8-54}$$

where κ or λ labels an occupied orbital or one of infinitely many virtual orbitals and $\bar{\alpha}$ labels a virtual orbital not contained in the set of virtual orbitals expanded by the OBS. The first sum in the right-hand side is taken over the infinite, complete space and is thus equal to the integral of the product of two operators r_{12}^{-1} and f_{12} because such summation constitutes resolution of the identity. If the form of f_{12} is chosen appropriately, the singularity of r_{12}^{-1} and hence the source of the slow basis-set convergence of correlation can be canceled analytically in this product. It is, therefore, essential that the two-electron integrals of $r_{12}^{-1} f_{12}$ are evaluated analytically. Other sums over infinite set of indexes in Eq. (8-54) are less important and can be approximated by replacing an infinite, incomplete set of virtual orbitals (labeled $\bar{\alpha}$)

by a large, finite auxiliary basis set (labeled $\bar{a}$) [55, 58]. In this way, equations of the CC-R12 methods can be obtained that no longer involve an infinite set and are computationally tractable.

8.3.2. Explicitly Correlated MBPT

MBPT-R12 can be derived by setting $\bar{H} = \hat{H}$ or $\hat{T} + \hat{\mathcal{T}}_2 = 0$ in our general perturbation theory and using the following partitioning:

$$\hat{P} = \hat{P}_0, \hat{Q} = \hat{\mathcal{P}}_2 + \hat{P}_1 + \ldots + \hat{P}_N. \tag{8-55}$$

Notice that the complete space ($1 = \hat{P} + \hat{Q}$) has been extended by the space accessible by $\hat{\mathcal{P}}_2$ and $\hat{H}$ is formally defined by an infinite set of creation and annihilation operators. Taking MBPT(2)-R12 [54–66] as an example, Eq. (8-19) becomes

$$-\left(\hat{P}_2 + \hat{\mathcal{P}}_2\right)\hat{f}^{(0)}\left(\hat{P}_2 + \hat{\mathcal{P}}_2\right)\hat{R}_0^{(1)}\left|\Phi\right\rangle = \left(\hat{P}_2 + \hat{\mathcal{P}}_2\right)\hat{H}\left|\Phi\right\rangle, \tag{8-56}$$

which has the formal solution

$$\hat{P}_2\hat{R}_0^{(1)}\left|\Phi\right\rangle = \bar{Q}_{0,2}\left(\hat{H} - \hat{f}^{(0)}\hat{\mathcal{P}}_2\hat{R}_0^{(1)}\right)\left|\Phi\right\rangle, \tag{8-57}$$

$$\hat{\mathcal{P}}_2\hat{R}_0^{(1)}\left|\Phi\right\rangle = -\hat{\mathcal{P}}_2\left(\hat{f}^{(0)} + \hat{f}^{(0)}\bar{Q}_{0,2}\hat{f}^{(0)}\right)^{-1}\hat{\mathcal{P}}_2\left(\hat{H} + \hat{f}^{(0)}\bar{Q}_{0,2}\hat{H}\right)\left|\Phi\right\rangle. \tag{8-58}$$

Substituting these into Eq. (8-22), we obtain

$$\begin{aligned} E_0^{\mathrm{MBPT(2)-R12}} &= \left\langle\Phi\right|\hat{H}\left(\hat{P}_2 + \hat{\mathcal{P}}_2\right)R_0^{(1)}\left|\Phi\right\rangle = \left\langle\Phi\right|\hat{H}\bar{Q}_{0,2}\hat{H}\left|\Phi\right\rangle \\ &- \left\langle\Phi\right|\left(\hat{H} + \hat{f}^{(0)}\bar{Q}_{0,2}\hat{H}\right)^{\dagger}\hat{\mathcal{P}}_2\left(\hat{f}^{(0)} + \hat{f}^{(0)}\bar{Q}_{0,2}\hat{f}^{(0)}\right)^{-1}\hat{\mathcal{P}}_2\left(\hat{H} + \hat{f}^{(0)}\bar{Q}_{0,2}\hat{H}\right)\left|\Phi\right\rangle. \end{aligned} \tag{8-59}$$

The first term in the right-hand side can be identified as $E_0^{\mathrm{MBPT(2)}}$ and the second term as an R12 correction that compensates for the basis-set incompleteness of $E_0^{\mathrm{MBPT(2)}}$.

8.3.3. Perturbation Corrections to Explicitly Correlated CC

Perturbation corrections [39] to the rank-n CC-R12 method are defined by setting

$$\hat{P} = \hat{\mathcal{P}}_2 + \hat{P}_0 + \ldots + \hat{P}_n, \hat{Q} = \hat{P}_{n+1} + \ldots + \hat{P}_N, \tag{8-60}$$

and using the CC-R12 effective Hamiltonian in our general perturbation theory. By virtue of including the R12 effects completely in the iterative CC step, these corrections need to capture only the higher-rank connected excitation effects. They are

thus defined by the identical expressions as the non-R12 counterparts, although they are different numerically because of the different $\bar{H}$ used. Equation (8-31) gives the second-order corrections in CCSD(2)$_T$-R12 and CCSD(2)$_{TQ}$-R12 [39]. Likewise, the corrections in CCSD(T)-R12 [33–39], CCSDT(2)$_Q$-R12 [39], and CCSD(3)$_T$-R12 [39] are obtained by evaluating Eqs. (8-32), (8-35) and the first term of Eq. (8-36), respectively. The cost scaling of each method remains the same as the corresponding non-R12 method. The approximate CC-R12 method called CC(R12) proposed by Fliegl et al. [43] can also be used to define $\bar{H}$, leading to the CCSD(2)$_T$(R12) and CCSD(2)$_{TQ}$(R12) methods [39].

Alternatively, perturbation corrections can be used to evaluate both higher-rank excitation and R12 effects on the non-R12 CC method. For the rank-n CC method, the partitioning of the Hamiltonian is as follows:

$$\hat{P} = \hat{P}_0 + \ldots + \hat{P}_n, \hat{Q} = \hat{\mathcal{P}}_2 + \hat{P}_{n+1} + \ldots + \hat{P}_N. \tag{8-61}$$

The second-order correction to CCSD consists of the higher-rank excitation terms and the R12 term that are now completely decoupled:

$$\begin{aligned} E_0^{\mathrm{CCSD(2)_{R12}}} = {} & \langle \Phi | \hat{L}_0^{(0)} \bar{H} \bar{Q}_{0,3} \bar{H} | \Phi \rangle + \langle \Phi | \hat{L}_0^{(0)} \bar{H} \bar{Q}_{0,4} \bar{H} | \Phi \rangle \\ & + \langle \Phi | \hat{L}_0^{(0)} \bar{H} \hat{\mathcal{P}}_2 \left(\hat{f}^{(0)} \right)^{-1} \hat{\mathcal{P}}_2 \bar{H} | \Phi \rangle , \end{aligned} \tag{8-62}$$

where $\bar{H}$ is the non-R12 CCSD effective Hamiltonian and $\hat{L}_0^{(0)}$ is the corresponding left eigenvector. The first and second terms of Eq. (8-62) are not just formally but also numerically identical to the corresponding terms in Eq. (8-30). The third term is an R12 correction. This method was originally proposed by Valeev et al. [47, 49, 50] and implemented as CCSD(T)$_{\mathrm{R12}}$. The complete CCSD(2)$_{\mathrm{R12}}$ method, as defined above, has yet to be implemented.

8.4. COMPUTER ALGEBRA

8.4.1. Determinant-Based Algorithms

The determinant-based algorithm [24–26] allows CI, CC, and MBPT at any rank and their various combinations [18] to be implemented into a single general computer code without having to derive algebraic formulas of individual methods. This algorithm manipulates higher mathematical constructs such as Slater determinants and electron creation and annihilation rather than just numbers and simple arithmetic. A determinant is computationally stored as a string of bits with each bit representing the occupancy of a spinorbital [93]. The action of a creation or annihilation operator on a determinant becomes a bit operation. Combinations of these algorithmic elements allow any electron-correlation theory that has a well-defined determinantal wave function to be implemented easily. However, a determinant-based implementation tends to incur a much greater computational cost. For instance, the scaling of the cost of rank-n CC is $O(m^{2n+4})$ in this algorithm instead of $O(m^{2n+2})$ of an optimal

algebraic implementation. Hence, a determinant-based implementation is ideal for an initial assessment of a whole hierarchy of approximations and generating benchmark data for the verification of more efficient implementations. It has been used for these purposes for many of the methods mentioned above including general-order CI [93], CC [24], MBPT [24, 94, 95], EOM-CC [96], IP-EOM-CC [97], EA-EOM-CC [97], and combined CI, CC, and MBPT [18].

8.4.2. Automated Formula Derivation and Implementation

An efficient implementation of an electron-correlation method entails the derivation of algebraic formulas from the expectation values of second-quantized operators, the determination of computational sequences, and the code synthesis. All of these are daunting tasks of symbol manipulations, taking many months to complete for one method. However, these manipulations are systematic and can be computerized to expedite the developments and at the same time improve the quality of the codes [23]. We have devised such computer algebra systems – TCE (Tensor Contraction Engine) and SMITH (Symbolic Manipulation Interpreter for Theoretical Chemistry) – [27, 48] that automate much of the entire development process of all of the electron-correlation methods discussed in this chapter including the R12 methods.

Given the definition expressed with expectation values of normal-ordered second-quantized operators in a determinant, the computer algebra systems transform them into sum-of-product matrix expressions by performing contractions of operators according to Wick's theorem, sometimes invoking diagrammatic techniques also. They subsequently determine the optimal order of multiplication for each of the matrix products and identify common multiplications in the sums of products and factor them. Then they find common subexpressions that can be precomputed, stored, and reused. Finally, the resulting computational sequences are translated into efficient codes that take into account the spin, spatial, and index-permutation symmetries and can adjust the maximum memory consumption at runtime. Many of these codes are also massively-parallel executable. With the aid of the computer algebra systems, an electron-correlation method can be developed within days.

Table 8-1 lists all the methods implemented by the computer algebra systems. Many of them, as stated earlier, have been verified by the determinant-based implementations. The formulas of the R12 methods in Table 8-1 have been derived and documented in our previous work [48]. In practical codes, the triples (quadruples) perturbation corrections are implemented so that a large array of triple (quadruple) excitation amplitudes needs not be stored; they are instead computed and discarded after their one-time use. The codes synthesized by the computer algebra systems also utilize this algorithmic optimization [20].

8.5. COMPARATIVE CALCULATIONS

Figure 8-1 shows the convergence of correlation energy of H_2O obtained by combined CC and MBPT (implemented in the determinant-based algorithms) as the rank of CC and/or the order of perturbation theory is raised [18]. The convergence is

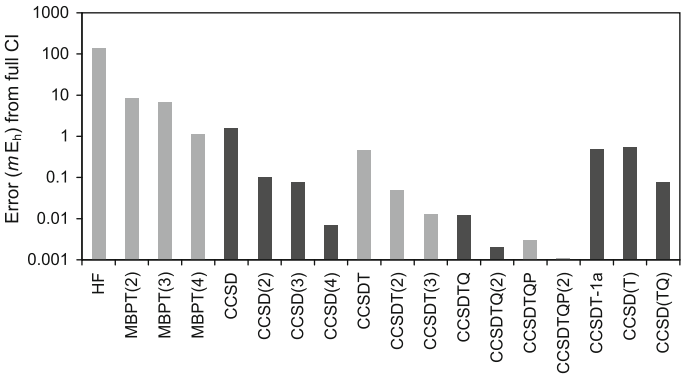

Figure 8-1. The errors (in mE$_h$) from full CI in correlation energies of H_2O obtained by CC, MBPT, and combined CC and MBPT [18]

monotonic and rapid. An order of magnitude reduction in errors is achievable by second-order perturbation corrections. MBPT shows the well-known staircase convergence. A similar trend can be observed in CCSD with perturbation corrections, suggesting that even-order corrections are particularly useful. Indeed, apart from MBPT(2), CCSD(2) and CCSDT(2) seem appealing and have been implemented into efficient codes by the computer algebra system TCE. Remarkably, CCSD(2) [CCSD(2)$_{TQ}$] achieves a noticeably smaller error than CCSDT or its approximations such as CCSDT-1a [98] or CCSD(T). This is because the former include the effect of connected quadruple excitations, which is neglected in the latter. CCSD(TQ) [75–77], on the other hand, yields a similar result as CCSD(2).

Perturbation corrections are not intended to work for strong correlation such as those encountered in broken bonds. Nonetheless, CCSD(2)$_T$, by virtue of its complete inclusion of all diagrammatic terms that are second order and evaluated at an $O(m^7)$ cost or less, has been found to resist a severe breakdown such as those seen in CCSD and CCSD(T). Figure 8-2 (obtained by the efficient computer-synthesized codes) demonstrates that the potential energy curves of HCl [99] computed by CCSD and CCSD(T) (both with a restricted HF reference) approach the wrong dissociation limits. The potential energy curve of CCSD(2)$_T$, in contrast, is within 4 mE$_h$ of the CCSDT curve. Note that this error is smaller than that obtained by CR-CCSD(T) [83, 85], which is not size-extensive.

Even in the case of two simultaneous single-bond stretch of H_2O, the perturbation corrections to CCSD and CCSDT largely remain an improvement over the respective parent methods, as shown in Figure 8-3 (obtained with the computer-synthesized codes) [20, 22]. Since the higher-rank connected excitation effects may not be a small perturbation in such situations, third-order corrections are more important in stretched geometries than in the equilibrium geometry. However, the CCSD(3)$_{TQ}$ result of this figure hints that the perturbation series may be divergent.

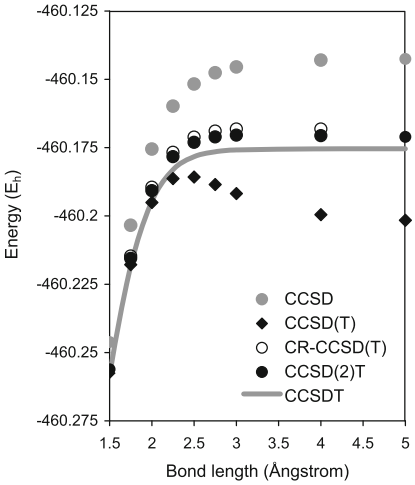

Figure 8-2. The dissociation curves of HCl obtained by CC and combined CC and MBPT with the aug-cc-pVDZ basis set in the frozen core approximation [99]

Figure 8-4 characterizes the whole hierarchy of combined EOM-CC and MBPT for CH^+ excitation energies [18] obtained with the determinant-based implementations. The additional approximations discussed above to make some of these methods size-intensive are not used here; the perturbation corrections to excitation energies have been obtained as the differences in corrections between the ground and excited states. While none of the corrected excitation energies are size-intensive, they are convergent at full CI. The convergence behavior is roughly exponential but is not as rapid as in ground states. Indeed, it takes four orders of perturbation corrections

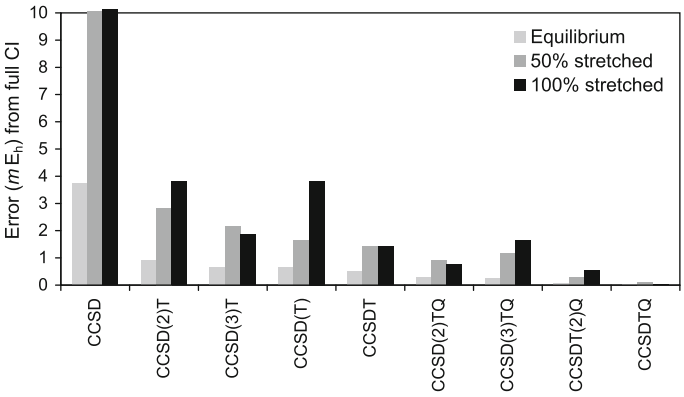

Figure 8-3. The errors (in mE_h) from full CI in correlation energies of H_2O at three bond lengths obtained by CC and combined CC and MBPT [20, 22]. The errors in CCSD are outside the range

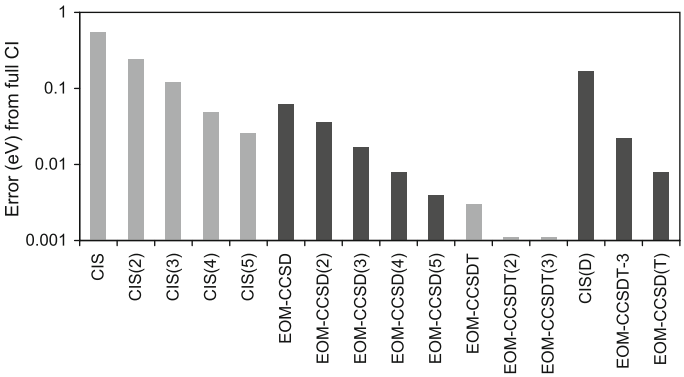

Figure 8-4. The errors (in eV) from full CI in excitation energies of CH^+ obtained by CIS, EOM-CC, and combined EOM-CC and MBPT [18]

for CIS to reach EOM-CCSD and more than five orders for EOM-CCSD to approach EOM-CCSDT. This observation may simply reflect the fact that the higher-order excitations are more important in excited states than in ground states.

Efficient implementations of size-intensive variants of CIS(2), CIS(3), and CIS(4) [21] as well as EOM-CCSD(2) and EOM-CCSD(3) [22] have been realized by the computer algebra system TCE. CIS with perturbation corrections have been applied to two representative cases: ethylene and formaldehyde [21]. The excited states of ethylene are reasonably well described by CIS and the perturbation corrections are expected to also work well. This expectation is substantiated by Figure 8-5 (entries labeled ET), in which gratifying convergence of the perturbation series toward EOM-CCSD can be seen. Considering the fact that these corrections can be evaluated at a noniterative $O(m^6)$ cost on a state-by-state basis, we consider them useful when EOM-CCSD is too cumbersome to apply. The results for formaldehyde (labeled FA)

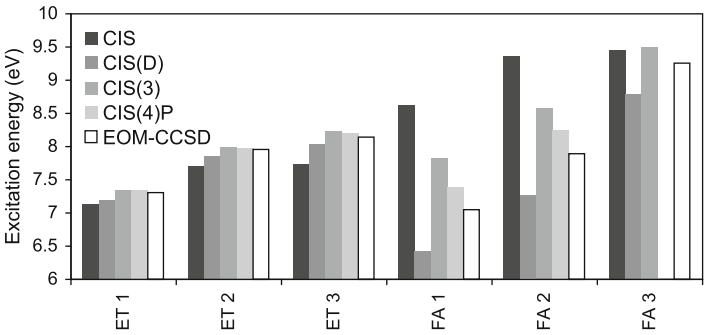

Figure 8-5. The excitation energies (in eV) of ethylene (labeled ET) and formaldehyde (labeled FA) obtained by CIS, EOM-CCSD, and combined CIS and MBPT [21]

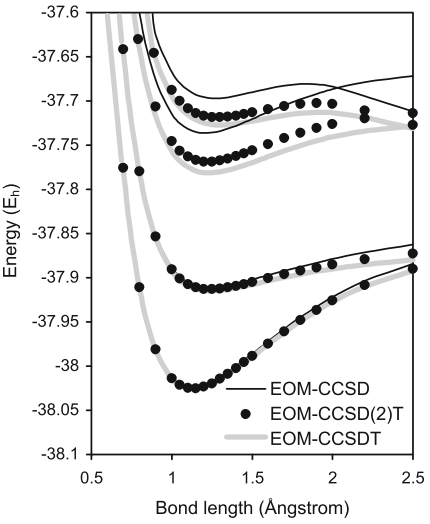

Figure 8-6. The potential energy curves of CH^+ obtained by EOM-CC and combined EOM-CC and MBPT [22]

reveal a problematic side of the perturbation series. CIS can no longer provide a good reference wave function for excited states of this molecule. For the two lowest-lying excited states, the corrections nonetheless manage to approach the respective EOM-CCSD results in an oscillatory fashion. For the third state, the series seems divergent. This result underscores the importance of having not just the second-order correction [CIS(D)] but also CIS(3) and CIS(4)$_P$ so that the convergence of the results can be checked.

Figure 8-6 plots the potential energy curves of CH^+ obtained by EOM-CCSD, EOM-CCSD(2)$_T$, and EOM-CCSDT, all implemented into efficient codes by the computer algebra system [22]. In the ground and first excited states, the EOM-CCSD and CCSDT curves are very close until the bond is significantly stretched, where EOM-CCSD(2)$_T$ is an improvement over EOM-CCSD. For the second and third excited states, the EOM-CCSD curves are visibly displaced from the EOM-CCSDT curves. The second-order triples correction can account for the majority of the differences between these two curves.

The R12 extension and a perturbation correction for higher-rank excitation effects are orthogonal – sometimes additive – enhancements and together lead to the most rapidly converging series of approximations with respect to both the excitation rank and basis-set size. Figure 8-7 plots the valence correlation energies of FH obtained by R12 and non-R12 methods as a function of the basis set [39, 53]. It is a striking demonstration of the dramatic improvement in the basis-set convergence of any correlation method achieved by the R12 extension. In this particular application, CCSD(2)$_T$-R12/aug-cc-pVTZ is the most economical model, yielding the correla-

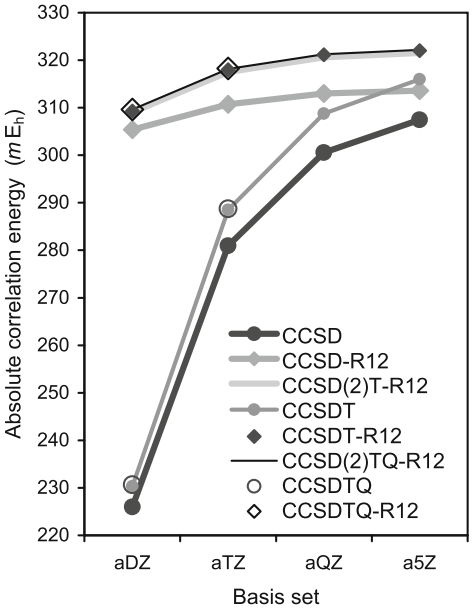

Figure 8-7. Basis-set dependence of the valence correlation energy of FH obtained by CC, CC-R12, and combined CC-R12 and MBPT [39, 53], where "aXZ" stands for the aug-cc-pVXZ basis set

tion energies obtained by CCSDT-R12/aug-cc-pV5Z and CCSD(2)$_{TQ}$-R12/aug-cc-pV5Z within 5 mE$_h$. The latter values are demonstratively converged within 1 mE$_h$ of the exact valence correlation energy of FH at its equilibrium geometry [39].

ACKNOWLEDGMENTS

S.H. thanks the financial support from the US Department of Energy (DE-FG02-04ER15621), the US National Science Foundation (CHE-0844448), and the American Chemical Society Petroleum Research Fund (48440-AC6). S.H. is a Camille Dreyfus Teacher-Scholar. T.S. thanks the Japan Society for the Promotion of Science Research Fellowship for Young Scientists. E.F.V. thanks the financial support from the American Chemical Society Petroleum Research Fund (46811-G6). E.F.V. is a Sloan Research Fellow.

REFERENCES

1. R. J. Bartlett, M. Musiał, Rev. Mod. Phys. **79**, 291 (2007)
2. I. Shavitt, R. J. Bartlett, *Many-Body Methods in Chemistry and Physics*. (Cambridge University Press, Cambridge, 2009)
3. R. J. Bartlett, Ann. Rev. Phys. Chem. **32**, 359 (1981)
4. I. Shavitt, Mol. Phys. **94**, 3 (1998)

5. S. Hirata, K. Yagi, Chem. Phys. Lett. **464**, 123 (2008)
6. K. Raghavachari, G. W. Trucks, J. A. Pople, M. Head-Gordon, Chem. Phys. Lett. **157**, 479 (1989)
7. J. D. Watts, J. Gauss, R. J. Bartlett, J. Chem. Phys. **98**, 8718 (1993)
8. K. Andersson, P.-Å. Malmqvist, B. O. Roos, A. J. Sadlej, K. Wolinski, J. Phys. Chem. **94**, 5483 (1990)
9. K. Hirao, Chem. Phys. Lett. **190**, 374 (1992)
10. J. F. Stanton, R. J. Bartlett, J. Chem. Phys. **98**, 7029 (1993)
11. H. Nakatsuji, K. Hirao, Int. J. Quantum Chem. **20**, 1301 (1981)
12. H. Nakatsuji, K. Ohta, K. Hirao, J. Chem. Phys. **75**, 2952 (1981)
13. H. Koch, P. Jørgensen, J. Chem. Phys. **93**, 3333 (1990)
14. H. Koch, H. J. A. Jensen, P. Jørgensen, T. Helgaker, J. Chem. Phys. **93**, 3345 (1990)
15. R. J. Rico, M. Head-Gordon, Chem. Phys. Lett. **213**, 224 (1993)
16. S. Hirata, J. Chem. Phys. **121**, 51 (2004)
17. M. Kállay, J. Gauss, J. Chem. Phys. **121**, 9257 (2004)
18. S. Hirata, M. Nooijen, I. Grabowski, R. J. Bartlett, J. Chem. Phys. **114**, 3919 (2001); **115**, 3967 (2001) (Erratum)
19. S. Hirata, P.-D. Fan, T. Shiozaki, Y. Shigeta, in *Radiation Induced Molecular Phenomena in Nucleic Acid: A Comprehensive Theoretical and Experimental Analysis*, Eds. J. Leszczynski, M. Shukla (Springer, New York, 2008), p. 15
20. S. Hirata, P.-D. Fan, A. A. Auer, M. Nooijen, P. Piecuch, J. Chem. Phys. **121**, 12197 (2004)
21. S. Hirata, J. Chem. Phys. **122**, 094105 (2005)
22. T. Shiozaki, K. Hirao, S. Hirata, J. Chem. Phys. **126**, 244106 (2007)
23. S. Hirata, Theor. Chem. Acc. **116**, 2 (2006)
24. S. Hirata, R. J. Bartlett, Chem. Phys. Lett. **321**, 216 (2000)
25. M. Kállay, P. R. Surján, J. Chem. Phys. **113**, 1359 (2000)
26. J. Olsen, J. Chem. Phys. **113**, 7140 (2000)
27. S. Hirata, J. Phys. Chem. A **107**, 9887 (2003)
28. M. Kállay, P. R. Surján, J. Chem. Phys. **115**, 2945 (2001)
29. W. Kutzelnigg, Theor. Chim. Acta **68**, 445 (1985)
30. W. Kutzelnigg, W. Klopper, J. Chem. Phys. **94**, 1985 (1991)
31. W. Klopper, F. R. Manby, S. Ten-no, E. F. Valeev, Int. Rev. Phys. Chem. **25**, 427 (2006)
32. T. Shiozaki, E. F. Valeev, S. Hirata, Ann. Rep. Comp. Chem. **5**, 131 (2009)
33. H. Fliegl, C. Hättig, W. Klopper, Int. J. Quantum Chem. **106**, 2306 (2006)
34. T. B. Adler, G. Knizia, H.-J. Werner, J. Chem. Phys. **127**, 221106 (2007)
35. D. Bokhan, S. Ten-no, J. Noga, Phys. Chem. Chem. Phys. **10**, 3320 (2008)
36. D. Bokhan, S. Bernadotte, S. Ten-no, Chem. Phys. Lett. **469**, 214 (2009)
37. G. Knizia, T. B. Adler, H. J. Werner, J. Chem. Phys. **130**, 054104 (2009)
38. A. Köhn, J. Chem. Phys. **130**, 131101 (2009)
39. T. Shiozaki, E. F. Valeev, S. Hirata, J. Chem. Phys. **131**, 044118 (2009)
40. J. Noga, W. Kutzelnigg, W. Klopper, Chem. Phys. Lett. **199**, 497 (1992)
41. J. Noga, W. Kutzelnigg, J. Chem. Phys. **101**, 7738 (1994)
42. J. Noga, P. Valiron, Chem. Phys. Lett. **324**, 166 (2000)
43. H. Fliegl, W. Klopper, C. Hättig, J. Chem. Phys. **122**, 084107 (2005)
44. D. P. Tew, W. Klopper, C. Neiss, C. Hättig, Phys. Chem. Chem. Phys. **9**, 1921 (2007)
45. D. P. Tew, W. Klopper, C. Hättig, Chem. Phys. Lett. **452**, 326 (2008)
46. J. Noga, S. Kedžuch, J. Šimunek, S. Ten-no, J. Chem. Phys. **128**, 174103 (2008)
47. E. F. Valeev, Phys. Chem. Chem. Phys. **10**, 106 (2008)
48. T. Shiozaki, M. Kamiya, S. Hirata, E. F. Valeev, Phys. Chem. Chem. Phys. **10**, 3358 (2008)
49. E. F. Valeev, T. D. Crawford, J. Chem. Phys. **128**, 244113 (2008)

50. M. Torheyden, E. F. Valeev, Phys. Chem. Chem. Phys. **10**, 3410 (2008)
51. T. Shiozaki, M. Kamiya, S. Hirata, E. F. Valeev, J. Chem. Phys. **129**, 071101 (2008)
52. A. Köhn, G. W. Richings, D. P. Tew, J. Chem. Phys. **129**, 201103 (2008)
53. T. Shiozaki, M. Kamiya, S. Hirata, E. F. Valeev, J. Chem. Phys. **130**, 054101 (2009)
54. W. Klopper, W. Kutzelnigg, Chem. Phys. Lett. **134**, 17 (1987)
55. W. Klopper, C. C. M. Samson, J. Chem. Phys. **116**, 6397 (2002)
56. F. R. Manby, J. Chem. Phys. **119**, 4607 (2003)
57. S. Ten-no, F. R. Manby, J. Chem. Phys. **119**, 5358 (2003)
58. E. F. Valeev, Chem. Phys. Lett. **395**, 190 (2004)
59. S. Ten-no, J. Chem. Phys. **121**, 117 (2004)
60. S. Ten-no, Chem. Phys. Lett. **398**, 56 (2004)
61. A. J. May, E. Valeev, R. Polly, F. R. Manby, Phys. Chem. Chem. Phys. **7**, 2710 (2005)
62. S. Kedžuch, M. Milko, J. Noga, Int. J. Quantum Chem. **105**, 929 (2005)
63. H.-J. Werner, F. R. Manby, J. Chem. Phys. **124**, 054114 (2006)
64. F. R. Manby, H. J. Werner, T. B. Adler, A. J. May, J. Chem. Phys. **124**, 094103 (2006)
65. H. J. Werner, T. B. Adler, F. R. Manby, J. Chem. Phys. **126**, 164102 (2007)
66. S. Ten-no, J. Chem. Phys. **126**, 014108 (2007)
67. P.-D. Fan, S. Hirata, J. Chem. Phys. **124**, 104108 (2006)
68. M. Kamiya, S. Hirata, J. Chem. Phys. **125**, 074111 (2006)
69. M. Kamiya, S. Hirata, J. Chem. Phys. **126**, 134112 (2007)
70. P.-D. Fan, M. Kamiya, S. Hirata, J. Chem. Theo. Comp. **3**, 1036 (2007)
71. J. D. Watts, in *Radiation Induced Molecular Phenomena in Nucleic Acid: A Comprehensive Theoretical and Experimental Analysis*, Eds. J. Leszczynski, M. Shukla (Springer, New York, 2008), p. 65
72. J. B. Foresman, M. Head-Gordon, J. A. Pople, M. J. Frisch, J. Phys. Chem. **96**, 135 (1992)
73. J. F. Stanton, J. Gauss, J. Chem. Phys. **101**, 8938 (1994)
74. M. Nooijen, R. J. Bartlett, J. Chem. Phys. **102**, 3629 (1995)
75. S. A. Kucharski, R. J. Bartlett, J. Chem. Phys. **108**, 5243 (1998)
76. S. A. Kucharski, R. J. Bartlett, J. Chem. Phys. **108**, 5255 (1998)
77. S. A. Kucharski, R. J. Bartlett, J. Chem. Phys. **108**, 9221 (1998)
78. J. F. Stanton, J. Gauss, J. Chem. Phys. **103**, 1064 (1995)
79. J. F. Stanton, J. Gauss, Theor. Chim. Acc. **93**, 303 (1996)
80. J. F. Stanton, J. Gauss, Theor. Chim. Acc. **95**, 97 (1997)
81. T. D. Crawford, J. F. Stanton, Int. J. Quantum Chem. **70**, 601 (1998)
82. S. R. Gwaltney, M. Head-Gordon, Chem. Phys. Lett. **323**, 21 (2000)
83. K. Kowalski, P. Piecuch, J. Chem. Phys. **113**, 5644 (2000)
84. S. R. Gwaltney, M. Head-Gordon, J. Chem. Phys. **115**, 2014 (2001)
85. K. Kowalski, P. Piecuch, Chem. Phys. Lett. **344**, 165 (2001)
86. M. Nooijen, K. R. Shamasundar, D. Mukherjee, Mol. Phys. **103**, 2277 (2005)
87. M. Urban, J. Noga, S. J. Cole, R. J. Bartlett, J. Chem. Phys. **83**, 4041 (1985)
88. M. Head-Gordon, R. J. Rico, M. Oumi, T. J. Lee, Chem. Phys. Lett. **219**, 21 (1994)
89. J. D. Watts, R. J. Bartlett, Chem. Phys. Lett. **233**, 81 (1995)
90. J. D. Watts, R. J. Bartlett, Chem. Phys. Lett. **258**, 581 (1996)
91. M. Włoch, J. R. Gour, K. Kowalski, P. Piecuch, J. Chem. Phys. **122**, 214107 (2005)
92. W. Klopper, Chem. Phys. Lett. **186**, 583 (1991)
93. P. J. Knowles, N. C. Handy, Chem. Phys. Lett. **111**, 315 (1984)

94. P. J. Knowles, K. Somasundram, N. C. Handy, K. Hirao, Chem. Phys. Lett. **113**, 8 (1985)
95. J. Olsen, O. Christiansen, H. Koch, P. Jørgensen, J. Chem. Phys. **105**, 5082 (1996)
96. S. Hirata, M. Nooijen, R. J. Bartlett, Chem. Phys. Lett. **326**, 255 (2000)
97. S. Hirata, M. Nooijen, R. J. Bartlett, Chem. Phys. Lett. **328**, 459 (2000)
98. Y. S. Lee, S. A. Kucharski, R. J. Bartlett, J. Chem. Phys. **81**, 5906 (1984)
99. S. Hirata, unpublished (2009)

CHAPTER 9

ELECTRONIC EXCITED STATES IN THE STATE – SPECIFIC MULTIREFERENCE COUPLED CLUSTER THEORY WITH A COMPLETE-ACTIVE-SPACE REFERENCE

VLADIMIR V. IVANOV[1], DMITRY I. LYAKH[1], AND LUDWIK ADAMOWICZ[2]

[1]*V. N. Karazin Kharkiv National University, Kharkiv, Ukraine, e-mail: vivanov@univer.kharkov.ua; lyakh@univer.kharkov.ua,*

[2]*University of Arizona, Tucson, AZ, USA, e-mail: ludwik@u.arizona.edu*

Abstract: The multireference state specific coupled cluster theory with CAS reference (CASCCSD) is generalized for calculations of electronically excited states. Test calculations have demonstrated high effectivity of the approach in comparison with other approximate approaches and with the full configuration interaction method.

Keywords: Multireference coupled cluster, Single Fermi vacuum, CAS reference, Excited states

9.1. INTRODUCTION

The success of the standard single-reference coupled cluster (CC) theory [1–5] in describing the ground states of molecular systems at their equilibrium structures and at geometries not much displaced from the equilibria has stimulated the search for a CC approach that is capable of describing molecules at non-equilibrium geometries and in electronically excited states. The inability of the standard CC theory to describe such important classes of chemical problems as open-shell systems and radicals, bond breaking and formation processes, etc., has limited the application of the CC method to studies of a rather narrow range of issues. Problems with configurational (determinantal) quasidegeneracies have been out of reach for the CC calculations. These types of quasidegeneracies are inherent to most of atomic and molecular electronically excited states rendering the single-reference CC theory inadequate and unable to correctly describe these states even at the lowest order of approximation.

There has been a considerable number of works devoted to the development of methods for describing electronic excited states (for a comprehensive review see, for example [6]). Both variational and non-variational (perturbational) approaches have been employed. There have also been a number of works devoted to the use of CC

P. Čársky et al. (eds.), Recent Progress in Coupled Cluster Methods, 219–249.
DOI 10.1007/978-90-481-2885-3_9,

methods in excited state calculations. A review of the single-reference (SR) CC and the multireference (MR) CC theories can be found, for instance, in [5].

A qualitatively correct description of a general excited state quasidegenerate situation can be achieved by using a MRCC approach where the ground state CC wave function is used to generate the excited states wave functions by applying excitation operators. If the exact ground-state wave function is used and if the set of the excitations is complete, in principle, exact solutions of the Schrödinder equation can be achieved for the excited states. However, if an approximate form of the ground state wave function is used and if an incomplete set of the excitations are included, the accuracy of the description of the excited states varies from state to state. For example, the equation-of-motion CC approach with singles and doubles excitations (EOM-CCSD), which is one of the MRCC theories based on the above-described approaches, produces very good results for excited states dominated by single electron excitations from the ground state wave function, but it fails to describe excited states with significant contributions from double excitations. It should be mentioned that the EOM-CCSD approach, as well as the other similar approaches, are multi-state methods, i.e. several excited states are determined in a single EOM-CCSD calculation.

In view of the above-described problems an approach that can bring a definite advantage over a multi-state MRCC approach, like EOM-CCSD, is the state – specific MRCC (SSMRCC) approach. The SSMRCC method by focusing on a single "target" state at a time provides the possibility of reaching high accuracy in describing that state. Our results, which we describe in this review, show that the SSMRCC approach fulfills these expectations.

9.2. STATE SPECIFIC MULTIREFERENCE COUPLED CLUSTER APPROACH WITH THE CAS REFERENCE

Let us start by shortly describing the standard CC theory. The CC wave function is represented as an exponential operator acting on a reference one-determinantal wave function (the so-called exponential *ansatz*):

$$|\Psi_{\mathrm{CC}}\rangle = \mathrm{e}^{\hat{\mathrm{T}}}|0\rangle, \tag{9-1}$$

where the CC $\hat{\mathrm{T}}$ operator generates a superposition of electronic excitations of different levels. The determinant $|0\rangle$ is the reference wave function. From this function all necessary excitations are generated. In the single reference CC theory the determinant $|0\rangle$ is usually the Hartree–Fock wave function. The $\hat{\mathrm{T}}$ operator can be represented as the following expansion:

$$\hat{\mathrm{T}} = \hat{\mathrm{T}}_1 + \hat{\mathrm{T}}_2 + \hat{\mathrm{T}}_3 + \ldots, \tag{9-2}$$

where the $\hat{T}_k$ term generates a superposition of k – fold excitations from $|0\rangle$. The CC method with the $\hat{T}$ operator including only single and double excitations:

$$\hat{T} \approx \hat{T}_1 + \hat{T}_2, \tag{9-3}$$

is termed the CCSD (CC with singles and doubles) approach.

One of the possible generalizations of Eq. (9-1) ansatz to a multireference case was proposed by Adamowicz and coworkers [7]. The approach was based on representing the wave MRCC wave function in a bi-exponential form:

$$|\Psi_{\mathrm{MRCC}}\rangle = e^{\hat{T}^{(\mathrm{ext})}} e^{\hat{T}^{(\mathrm{int})}} |0\rangle = e^{\hat{T}^{(\mathrm{ext})} + \hat{T}^{(\mathrm{int})}} |0\rangle. \tag{9-4}$$

In Eq. (9-4) the exponential *ansatz* is separated into two parts. The first part called "internal", ($\hat{T}^{(\mathrm{int})}$), generates a multi-determinantal reference function being a superposition of the determinants from the reference space. The second part called "external", ($\hat{T}^{(\mathrm{ext})}$), generates excitations from outside the reference space. The role of $\exp(T^{(\mathrm{ext})})$ is to describe the dynamic electron correlation, while the role of $\exp(T^{(\mathrm{int})})$ is to describe the nondynamic correlation (i.e. the correlation associated with electrons separating from each other not because of the repulsion but because, for example, in a dissociation of a diatomic molecule some of them follow the first nucleus and the other follow the second nucleus). In the original papers the approach based on Eq. (9-4) wave function was called the state – specific (SS) multireference coupled cluster theory (SSMRCC).

Two essential features of the SSMRCC theory are focusing on one state at a time and building the CC wave function for that state from a single reference determinant, $|0\rangle$, specific to the state. Choosing an appropriate "formal reference" determinant is key for the SSMRCC calculation. In Eq. (9-4) both cluster operators, $\hat{T}^{(\mathrm{int})}$ and $\hat{T}^{(\mathrm{ext})}$, act on the formal reference $|0\rangle$ to generate the complete SSMRCC wave function. As the two operators comprise separate sets of excitations from the formal reference determinant they commute:

$$[T^{(\mathrm{int})}, T^{(\mathrm{ext})}] = 0. \tag{9-5}$$

It should be mentioned that in the SSMRCC theory some excitations from the reference determinants are generated as the higher level "external" excitations (i.e. higher than double excitations) from the formal reference determinant.

In some situations it is convenient to represent the SSMRCC wave function (9-4) in a semi–linear form [8]:

$$|\Psi_{\mathrm{MRCC}}\rangle = e^{\hat{T}^{(\mathrm{ext})}} (1 + \hat{C}^{(\mathrm{int})}) |0\rangle, \tag{9-6}$$

where $\hat{C}^{(\mathrm{int})}$ is a configuration-interaction type operator that generates a linear superposition of reference determinants. The $\hat{T}^{(\mathrm{ext})}$ operator, as before, generates external

excitations from all reference determinants. Hence, the internal part of the CC operator in Eq. (9-6), $(1 + C^{(int)})$, generates the reference-space representation of the wave function of the considered state. The determinants forming this representation are single, double, etc. excitations from the formal reference determinant $|0\rangle$:

$$|0\rangle \quad |^{A}_{I}\rangle \quad |^{AB}_{I\,J}\rangle \quad |^{ABC}_{I\,J\,K}\rangle \quad \ldots . \tag{9-7}$$

Here the capital letters I,J,K,... designate the spin-orbitals which are occupied in $|0\rangle$ and letters A,B,C,... designate the unoccupied (vacant) spin-orbitals. $|^{A}_{I}\rangle$ designates the determinant where an electron is excited from the spin-orbital I to the spin-orbital A. $\left|^{AB}_{I\,J}\right\rangle$ designates a doubly excited determinant where the two electrons occupying the I and J spin-orbitals are excited to the A and B spinorbitals, etc.. The most important spin-orbitals in the wave function of the state under consideration constitute the so-called active orbital space.

The active orbital space in the SSMRCC approach is selected in the standard way schematically explained in Figure 9-1. As usual, the orbitals, which are occupied in all determinants, are called core orbitals. The orbitals which are not occupied in all reference determinants, but are important in describing the wave function of the state under consideration, are called active (valence) orbitals. As stated, these orbitals are designated by capital letters. The orbitals, which are either occupied in all determinants in the reference space or occupied in none of the reference-space determinants are called non-active orbitals and they are designated by small letters. Letters i, j, k, ... are used for occupied orbitals and letters a, b, c, ... are used for unoccupied orbitals. Arbitrary orbitals/spin – orbitals (active or non-active) are designated by italic style letters: *i, j, k,...* for the occupied orbitals and *a, b, c,...* for the vacant orbitals.

The SSMRCC method was implemented in our works in its most expeditious form termed the complete active space coupled cluster singles and doubles (CASCCSD) approach. All the necessary equations for the energy and the CC amplitudes in the CASCCSD method were derived using our automated computer program called

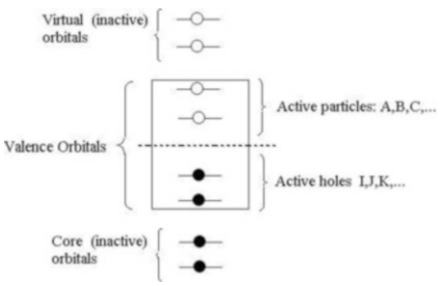

Figure 9-1. Partitioning of the orbital (spin-orbital) space used in the MRCC theory. The choice of the valence (active) orbitals is essential in correctly describing the state being the subject of the MRCC calculation

"CLUSTER" [9, 10]. In addition to generating the computational algorithms for the CASCCSD method the program also generated a computer code for calculating them. The CASCCSD code was interfaced with the quantum-chemical package GAMESS [11]. The results presented in this review have been obtained with this code.

As it was noted, all the excitations in the SS theory are represented as excitations from a single formal reference determinant. Let us describe in more detail how this works in the case where the active space contains four electrons distributed among four orbitals (4,4). This is a minimal active space that one needs to use to describe the dissociation process of a double covalent bond or a simultaneous dissociation of two single bonds [10]. The CASCCSD method which a (4,4) active space is designated as CAS(4,4)CCSD in our terminology. The CAS(4,4)CCSD reference space includes the following five types of configurations, which are distinct by their excitation levels from the formal reference determinant $|0\rangle$:

$$|0\rangle,\ |{}^{\mathrm{A}}_{\mathrm{I}}\rangle,\ |{}^{\mathrm{AB}}_{\mathrm{IJ}}\rangle,\ |{}^{\mathrm{ABC}}_{\mathrm{IJK}}\rangle,\ |{}^{\mathrm{ABCD}}_{\mathrm{IJKL}}\rangle. \tag{9-8}$$

All these determinants generated as one-, two-, three-, and four-electron excitations from the formal reference $|0\rangle$ are needed to describe the nondynamic electron correlation effects in the system. A correct description of the dynamic electron correlation requires including in the $\hat{\mathrm{T}}^{(\mathrm{ext})}$ operator in the CAS(4,4)CCSD wave function all single and double excitations from all reference determinants. As for the excitations contained in the $(1 + \mathrm{C}^{(\mathrm{int})})$ operator, the $\hat{\mathrm{T}}^{(\mathrm{ext})}$ excitations are also represented as excitations from the formal reference determinant. As the highest level of excitations from the formal reference determinant among the reference determinants is four ($|{}^{\mathrm{ABCD}}_{\mathrm{IJKL}}\rangle$), the highest excitation level in the $\hat{\mathrm{T}}^{(\mathrm{ext})}$ operator has to be six. Thus the complete CAS(4,4)CCSD wave function has the following form:

$$|\Psi_{\mathrm{CAS(4,4)CCSD}}\rangle = \mathrm{e}^{\hat{\mathrm{T}}_1+\hat{\mathrm{T}}_2+\hat{\mathrm{T}}_3\left({}^{ab\mathrm{C}}_{\mathrm{I}jk}\right)+\hat{\mathrm{T}}_4\left({}^{ab\mathrm{CD}}_{\mathrm{IJ}jk}\right)+\hat{\mathrm{T}}_5\left({}^{ab\mathrm{CDE}}_{\mathrm{IJK}jk}\right)+\hat{\mathrm{T}}_6\left({}^{ab\mathrm{CDEF}}_{\mathrm{IJKL}jk}\right)} (1 + \hat{\mathrm{C}}_1 + \hat{\mathrm{C}}_2 + \hat{\mathrm{C}}_3 + \hat{\mathrm{C}}_4)|0\rangle. \tag{9-9}$$

The set of the excited determinants in the CASCCSD wave function can be separated into two subsets. The first subset, which we term the "iterative space", contains the determinants whose contributions to the CASCCSD wave function include linear terms (i.e. single CC amplitudes). Thus, the "iterative space" includes the reference space and all single and double excitations from the reference determinants. All other determinants in the CASCCSD wave function (9-6) form the complementary "non-iterative" space. The contributions from these determinants to the wave function do not include linear terms but only terms which are products of amplitudes of the determinants from the "iterative space". As one can see, each important excitation in the CASCCSD wave function has a separate CC amplitude, while all other excitations are not assigned separate amplitudes.

The test calculations performed with the CASCCSD method on some quasidegenerate situations that occur in the ground states of molecular systems distorted from their equilibrium geometries demonstrated high accuracy of the method [10, 12]. The efficiency of the CASCCSD method to deal with inherently multireference problems encouraged us search for a generalized form of the method to calculate electronically excited states. In this generalization we had to address new issues such as dealing with open-shell electronic configurations and dealing with the spin adaptation of the CASCCSD wave function.

9.3. ELECTRONICALLY EXCITED STATES IN THE COUPLED CLUSTER THEORY

The major complication in describing electronic excited states is related with the inherent and usually significant multiconfigurationality of their wave functions. Thus the methods, which are capable of describing these states and the spectral transitions between them, must properly address the multireference character of their wave functions.

In this section we will briefly review the CC approaches developed for calculating excited states and for determining the transition energies associated with exciting/deexciting the system between the different states. First, it is important to note that most of these approaches (unlike the methods developed for the ground-state calculations) are not state-specific methods, i.e. many states are considered in a single calculation and the excited states are obtained as a "side-product" of the calculation of the wave function and the energy of the ground state. In the early 1990th Foresman et al. [13] suggested that the modern theories for excited state calculations can be grouped into two possible classes. The focus of the first class of methods is a direct calculation of the transition energies between different pairs of states (say a ground state and an excited state). The focus of the second group of methods is to calculate the excited state energies and their wave functions and from them determine the transition energies. First group is often referred to as "spectroscopy oriented" and the second group is referred to a "photophysically oriented". This terminology emphasizes the purpose of the method being either the calculation of the transition energies or the state energies.

Among the methods which are based on the CC *ansatz* we should first mention the Random Phase Approximation (RPA) approach [14–17], which can also be viewed as a generalization of the configuration interaction method with singles (CIS).[1] The RPA wave function can be expressed in the standard CC form as:

$$|\Psi_{\mathrm{RPA}}\rangle = \mathrm{e}^{\hat{\mathrm{T}}_1}|0\rangle, \tag{9-10}$$

[1] sometimes also called the Tamm-Dankov approximation; TDA

where the $\hat{T}_1$ generates single electron excitations from the reference $|0\rangle$. Different variants of RPA can be obtained from Eq. (9-10). Usually the $\hat{T}_1^2$ term resulting from expanding the exponent in Eq. (9-10) is included in the calculations. Naturally, the RPA method, while simple, is a very approximate approach that can only provide a qualitative representation of the spectral transitions. This is mainly due to the method not accounting for the electron correlation effects (for a discussion on this point see, for example [18]).

The standard way of accounting for the electron correlation effects in excited states is to include higher excitations in the CIS method. By including only doubles one gets the configuration interaction singles and doubles method (CISD). Some practical calculations of excited states and the corresponding transition energies using the CISD approach have demonstrated low effectivity of this method. As the orbitals in the CISD calculation come from the ground-state Hartree–Fock calculation, the excited states are usually significantly "under-correlated" in comparison to the ground state. As a result the spectral transition energies obtained from a CISD calculation are overestimated. To remedy this problem higher level excitations (triple, quadruple, etc.) can be included in the CI calculation resulting in a hierarchy of methods:

$$\text{CIS} \rightarrow \text{CISD} \rightarrow \text{CISDT} \rightarrow \ldots \rightarrow \text{FCI}, \tag{9-11}$$

where the full CI (FCI) method includes all excitations that can be generated within the given set of orbitals. However, the practical application of CI methods that include higher excitations is very limited due to high computational costs.

The development of non-variational methods for calculating excited states started in the middle 1980th. Among the approaches that were proposed we should mention the methods based on the one- and two-particle Green functions (e.g. the polarization propagator (PP) methods). Incorporating the cluster *ansatz* within the PP method gave rise to such methods as the coupled-cluster polarization propagator approach (CCPPA) and the second-order PP (SOPPA) approach [19]. These approaches have been the forerunners for the development of more general methods based on the CC theory. These methods are currently gaining grounds in the electronic structure calculations of excited states, transition energies, ionized states, etc. The formalism of most of the methods is based on the equation-of-motion (EOM) framework [20]. Thus, the approaches are a multi-state type (not state specific). It should be noted that the original formulation of the EOM theory is very general and includes a wide spectrum of different methods. The EOM-CC wave function can be written in the following form:

$$|\Psi_{\text{EOM–CC}}\rangle = \hat{R}\, e^{\hat{T}}|0\rangle, \tag{9-12}$$

where $e^{\hat{T}}|0\rangle$ is the ground-state CC wave function and the $\hat{R}$ operator generates excitations from it. $\hat{R}$ can be expressed in terms of spinorbital creation and annihilation operators as:

$$\hat{R} = \sum_{i,a} R_i^a a_a^+ a_i + \sum_{\substack{i>j \\ a>b}} R_{ij}^{ab} a_a^+ a_i a_b^+ a_j + \cdots . \tag{9-13}$$

In Eq. (9-13) R_i^a and R_{ij}^{ab} are the amplitudes of the corresponding determinants. An EOM-CCSD calculation requires solving the non-hermitian eigenvalue problem:

$$\overline{H}\mathbf{R} = \lambda \mathbf{R}, \tag{9-14}$$

where the right eigenvector **R** contains the following amplitudes:

$$\mathbf{R} = \begin{pmatrix} R_i^a \\ R_{ij}^{ab} \\ \cdots \end{pmatrix}, \tag{9-15}$$

and

$$\overline{H} = e^{-T} H e^{T}. \tag{9-16}$$

A large array of calculations has demonstrated effectiveness of the EOM method with singles and doubles excitations (EOM-CCSD) in describing some classes of excited states. A detailed description of the EOM-CC approaches and examples of using them in molecular calculations can be found in [21]. Some of the EOM-CC methods are implemented in the GAMESS package [22].

There are some other methods that are related to the EOMCC approach and should be mentioned here. One of them is the so-called symmetry-adapted cluster CI approach (SAC-CI) developed by Nakatsuji in the late 1970th [23]. The method employs the (9-12) wave function adapted for the spin and spatial symmetry of the state under consideration. The theoretical foundations of the EOM-CC and SAC-CI are very similar and the differences are in dealing with certain nonlinear terms in the CC components of the working equations (either ignoring or not ignoring them).

Another method with a close relation to EOMCC is the linear response (LR) CC theory approach (LRCC). The approach is derived based on the CC time-dependent theory. A general description of the time-dependent perturbation theory and its use in formulating the LR approach can be found in the paper by Langhoff et al. [24]. The CC implementations of the LR theory can be found in Refs. [25, 26]. A diagrammatic technique for the LRCC approach was developed by Sekino and Bartlett [27]. In general, it should be recognized that the LRCC and EOMCC approaches are virtually identical methods with some minor differences in their implementations. Same should be said about the SAC-CI approach, which is essentially identical to both the LRCC and EOMCC method with only a small difference concerning some nonlinear terms which SAC-CI neglects.

The more recent development of the EOMCC theory has involved the so-called similarity transformation (ST) of the Hamiltonian. In the method called STEOM-CCSD [28] a secondary transformation of the similarity transformed Hamiltonian is performed in order decrease the connectivity between the different blocks of the Hamiltonian matrix. As a result, in the doubly-transformed Hamiltonian matrix the blocks corresponding to different levels of excitations are approximately decoupled and the matrix is almost block-diagonal. Also, after the double transformation, the block corresponding to the single excitations contains some contributions from higher excitations. At the end the excited state energies are obtained by the diagonalization of the Hamiltonian block corresponding to the singly excited determinants. In general, the STEOMCCSD is a low-cost computational method that can be applied to relatively large systems (for example, see the calculations of the electronic spectrum of porphine [29]).

A shortcoming of the STEOMCCSD method (as well as with the EOM-CCSD method) is that *only excited states dominated by single-electron excitations* can be determined with a good accuracy in the STEOMCCSD calculations. States with significant contributions from doubly excited determinants are usually poorly described with the EOM-CCSD approach (a typical error in the estimation of the transition energies is about 1 eV or even higher). Even though there are fundamental reasons why the STEOMCCSD method is unable to describe transitions to double excited states, some progress has been made by the development of extended versions of the STEOMCC (ext-STEOMCC) approach [30]. The extension involves including higher order excitations (for example, this is done in the EOM-CCSDT method). However then the computational cost of the calculation significantly increases.

One should mention that Piecuch and Bartlett [31] proposed a variant of the EOMCC approach (called EOMXCC) where an additional transformation of the Hamiltonian is performed, which, according to the authors, allows for a better description of the effects due to higher excitations. Unfortunately the EOMXCC has not been developed beyond the prototype level.

An alternative to including the triple excitations on equal footing with single and double excitations is to use a non-iterative perturbative procedure developed by Piecuch et al. and termed the completely renormalized EOM-CCSD (CR-EOM-CCSD) approach [33]. The CR-EOM-CCSD(T) method is implemented in the GAMESS package [11]. The GAMESS package also includes other variants of the renormalized EOM-CCSD method differing from the original version of the method in the way the vertical transformation in the method is performed (see the GAMESS manual for a more detail description).

An option of combining the multireference SS method with the EOMCC approach was investigated by Piecuch [34]. In Piecuch's EOM-CCSDt method the triple excitations are only partially taken into account and limited to the determinants of the $|^{Abc}_{ijI}\rangle$ type. This is consistent with the spirit of the SS approach where the selection of the most important subsets of higher excitations (triple, quadruple, etc.) is a key element of the calculation. Such a selection is usually not difficult when only one state is being calculated, but it may become more complicated if the calculation

targets several states (as it is done in non-state specific approaches). Unusually in a multi-state calculation the active space has to be widened to facilitate an adequate description of all the considered states.

An interesting variant of the EOMCC method was recently proposed by Nooijen [35]. The method combines the SS approach with the EOM theory and was termed the Complete State Selective EOMCC (CSS-EOMCC) method. The CSS-EOMCC results obtained for some low-lying states of O_2 and F_2 molecules show some remarkable accuracy.

Finally, it is in order to mention "classical" multireference methods for the excited state calculations. Several papers provide comprehensive reviews of these methods (see, for example, [5]) and we will only briefly mention them in this review. In the so-called "Hilbert-space" (or state-universal (SU)) methods the ground-state is calculated along with a set of excited states. The energies of all these states are the result of the diagonalization of an effective Hamiltonian. The "Hilbert-space" MRCC theory is, in principle, flexible enough to describe any excited state. However, the well known "intruder state" often appears in the calculations and removing it is not an easy task especially if higher excited states are calculated. In addition to excited states also ionized states can be calculated using the so-called valency-universal (VU) method. Due to the complicated nature of both the "Hilbert-space" and valency-universal MRCC methods their popularity has been low. However, this can change with the development of such approaches as the one proposed by Chattopadhyay where the SU method was combined with the linear response theory [36]. Also Musiał et al. have recently developed a new approach for excited state calculations based on the VU method [37]. It utilizes the "intermediate Hamiltonian" technique to calculate the state energies. According to the authors [37] the "intruder state" problem was successfully overcame in their approach.

In conclusion, let us mention some important common features of the above-described CC theories for the excited state calculations.

1. The methods share many common features. The difference between them are mainly due to technical details related to their implementations and due to ignoring certain terms in the energy and/or amplitude equations to make the calculations simpler and less time consuming.
2. The methods (especially those EOMCC-based) are "Black-Box" approaches. Whether this should be perceived as a merit or a demerit depends on the point of view. "Black Box" approaches are usually successful in simple situations. However more complicated excited state problems usually necessitate a more detailed analysis of their nature and their treatment usually requires going beyond the "Black Box" approach.
3. An adequate accurate description of an arbitrary excited state can be attained only if higher-level excitations are included in the calculation. For example, the connected triple excitations (at least) are needed to adequately describe states in which two-electron excitations dominate.

In the next section we describe how the above mentioned features incorporated in the SSMRCC theory we developed to calculate excited states. For instance, our SSMRCC (CASCCSD) theory is not a "Black Box" approach. There are also differences in how the CASCCSD method approaches the single-excited and double-excited states because the calculations of these two types of states require the use of different reference spaces.

9.4. STATE SPECIFIC COUPLED CLUSTER APPROACH FOR EXCITED STATES

As mentioned, the standard existing CC theories for calculating excited states are not SS theories, i.e. the calculation is not focused on a single state. We will now discuss how a SSCC theory for calculating excited states can be formulated based the multireference method developed by us to describe bond dissociation processes and mentioned in the previous section. Naturally, a generalization of our method to excited states will have to involve a separate CC calculation of the ground state and each of the excited states. In these calculations different formal reference determinants can, in principle, be used. There is a certain advantage of using different formal references for different states which rests in making the treatment of all states more equivalent. Thus, there is no bias in the calculations towards a selected state; this usually being the ground state as it, for example, happens in the valence-universal MRCC approach. In general, if a theory relies on the results of the ground state calculation in describing the excited states (for example, if orbitals used to construct the excited-state wave functions come from the ground-state calculation), some perceptible errors often occur in the values of the spectral transitions. Even methods with high percentages of accounting for the electronic correlation effects, such as the CISD method, can significantly overestimate excitation energies by as much as $\approx$1–2 eV.

In general, even in calculating the simplest excited states, e.g. those dominated by single excitations, a one-determinant reference space is insufficient. The CC approach that works for the ground state of a closed-shell molecule is not applicable to excited states. The simplest, often appearing situation is when the excited state is dominated by two singly excited configurations with equal (or almost equal) weights:

$$|\Psi^*\rangle \approx \frac{1}{\sqrt{2}}(|^{a_1}_{i_1}\rangle \pm |^{a_2}_{i_2}\rangle). \tag{9-17}$$

A more difficult case appears when an electronically excited molecule undergoes a structural transformation (a photodissociation or a photochemical process). In such a situation a more general wave function has to be applied to obtain a correct "zero-order" description of the state under consideration along the whole PES:

$$|\Psi^{*}_{\mathrm{diss}}\rangle \approx \alpha \sum_{i_1,a_1} \pm|^{a_1}_{i_1}\rangle + \beta \sum_{\substack{i_1>i_2\\ a_1>a_2}} \pm|^{a_1a_2}_{i_1i_2}\rangle + \ldots, \tag{9-18}$$

where the α and β coefficients are large and comparable in values. In Eqs. (9-17) and (9-18) all the determinants are excitations from a single reference determinant (for example, the Hartree–Fock determinant). In order to construct a CC wave function for such a case a superposition of determinants (9-17) (or even (9-18)) has to be used as the reference.

One way of generalizing Eq. (9-1) to a multireference case is by using a multidimensional model space. With the general reference function (9-18) the MRCC wave function can be represented as:

$$|\Psi_{\mathrm{MRCC}}\rangle = \mathrm{e}^{\hat{\mathrm{T}}}\Big(\alpha \sum_{i_1,a_1} \pm|^{a_1}_{i_1}\rangle + \beta \sum_{\substack{i_1>i_2\\ a_1>a_2}} \pm|^{a_1a_2}_{i_1i_2}\rangle + \ldots\Big), \tag{9-19}$$

where the $\hat{\mathrm{T}}$ is an coupled cluster operator which generates excitations from determinants $|^{a_1}_{i_1}\rangle$ and $|^{a_1a_2}_{i_1i_2}\rangle$, etc. Some possible variants of the implementation of the wave function (9-19) in the SSMRCC framework were described in our recent papers [38, 39].

We will now describe our SSMRCC approach to excited states. In the first step one needs to assess the level of quasidegeneracy of the considered state (in some states an exact degeneracy may occur). Then, in order to apply the SSMRCC approach (or more specifically, its CASCCSD version) to calculate the state energy and the wave function, the following points need to be addressed:

1. An appropriate reference space needs to be defined. The space should include a minimal number of configurations to construct a good first-order representation of the wave function of the state under consideration. For excited states, the procedure for selecting adequate reference spaces is often not as straightforward as for the ground state where the selection is made based on clear physical principles.
2. In the ground state CASCCSD calculation a closed-shell determinant can be usually chosen as the formal reference determinant. However for excited states it may often happen that, due to symmetry reasons, closed-shell determinants do not contribute to the wave function or such determinants may give very small contributions. In such a case an open-shell determinant has to be chosen as the formal reference.
3. Choosing the formal reference determinant in the ground state calculation is usually simple. The reference determinant with the dominant contribution to the wave function is the obvious choice. In an excited state calculation several reference determinants, open- and/or closed-shell, may provide significant contributions. In principle, each of these determinants can be chosen as the formal reference. Thus, there is a certain degree of arbitrariness in choosing the formal reference in

such a situation. However, as the CASCCSD approach is a very accurate method, any of the choices should lead to an almost equally good result.

4. An exact configurational degeneracy rarely happens in the ground-state calculation, but it is often encountered in calculations of excited states. Also some excited states may be degenerate within a particular term. For example, Π- and Δ- states for a diatomic molecule may be degenerate. Also the states belonging to different terms may become degenerate or quasidegenerate at larger internuclear separations. The appearance of degeneracy may lead to a slow convergence (or lack of it) in solving the CC nonlinear equations.
5. The CASCCSD wave functions generated for different states in independent calculations are usually not strictly orthogonal. This may have some effect on the results and on their interpretation.
6. Not maintaining the strict orthogonality between the wave functions of different states can lead to root switching or even collapsing of an excited state to the ground state. This can happen when both states have the same spatial and spin symmetry.
7. Excited configurations of a certain level (say doubles) obtained for different (degenerate) reference determinants may have different excitation levels from the "formal reference" state. In order for the total CASCCSD wave function to represent a state with a certain spin multiplicity, the coefficients of some of these excited configurations should be coupled by spin-symmetry constraints. These constrains have to be implemented in the CASCCSD wave function at least for the most important configurations. This procedure is called the spin-adaptation and can be performed at various levels. It is relatively straightforward to apply it to the configurations from the iterative subspace, but its application to other configurations is not as simple because the amplitudes of those configurations are products of amplitudes of some iterative subspace configurations.

The above mentioned points (in particular 5 and 6) are more or less difficult to handle depending on the level of approximation used in the particular implementation of the CASCCSD method. For example, the nonorthogonality of the CASCCSD wave functions of different states can be a problem for a more approximate approach than for a more rigorous approach. In our view a SSMRCC calculation of an excited state is more justifiable if fewer approximations are made and the results have a high degree of absolute exactness (i.e. they are close to the FCI results). In such a case the nonorthogonality effects are insignificant and the convergence of the iterative procedure of solving the CASCCSD amplitude equations is usually faster provided a good initial guess for the configurational amplitudes is used. Also a good guess prevents the excited state roots to collapse to the ground state. One of the best possible initial guesses for the CASCCSD wave function is a renormalized multireference CI wave function.

We will now describe some model applications of the CASCCSD method to calculate excited states. The simplest model cases are lowest lying singlet and triplet

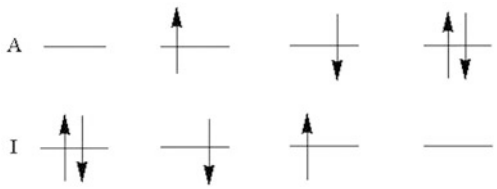

Figure 9-2. Distribution of two electrons among the two active orbitals

excited states of a closed-shell system. In these cases the active space comprises two electrons distributed among two molecular orbitals; the (2,2) space. There are four determinants in the (2,2) space. Two of them are closed-shell and two are open-shell determinants (Figure 9-2). In some cases one of the two closed-shell determinants can be chosen as the formal reference, $|0\rangle$. As before the capital letters are used to designate the active spin – orbitals; I, J, K, ... are used for the holes and A, B, C, ... for the particles. The four determinants of the (2,2) reference space which arise from all different distributions of two electrons among two orbitals (four spin-orbitals) are:

$$|0\rangle, \quad |^{A\bar{A}}_{I\bar{I}}\rangle \quad |^{A}_{I}\rangle, \quad |^{\bar{A}}_{\bar{I}}\rangle. \tag{9-20}$$

In general, the complete model space can contain determinants which are transformed differently with respect to the molecular symmetry elements of the system. In particular, the closed-shell determinants are always fully symmetric configurations. However, we should note that different linear combinations of such determinants can belong to terms with different projections of the electronic angular momentum of the system on the z axis (e.g. Δ and Σ states in homonuclear diatomic molecules). Also the determinants $|^{A}_{I}\rangle$ and $|^{\bar{A}}_{\bar{I}}\rangle$ can belong to representations which are not fully symmetric. If the symmetry of the state under consideration is the same as that of the $|^{A}_{I}\rangle$ determinant (and $|^{\bar{A}}_{\bar{I}}\rangle$), but different from the symmetry of $|0\rangle$ and $|^{A\bar{A}}_{I\bar{I}}\rangle$ determinants, the last two determinants should be excluded from the reference space. Thus the reference space for some states (non-fully symmetric singlets and triplets) will reduce to two determinants:

$$|^{A}_{I}\rangle, \quad |^{\bar{A}}_{\bar{I}}\rangle. \tag{9-21}$$

In general, the total wave function of the XCASCCSD approach for the (2,2) active space is represented in the following form:

$$|\Psi_{XCASCCSD}\rangle = e^{\hat{T}}\left(\delta + \lambda\left(a^{+}_{A}a_{I} \pm a^{+}_{\bar{A}}a_{\bar{I}}\right) + \gamma\, a^{+}_{A}a_{I}a^{+}_{\bar{A}}a_{\bar{I}}\right)|0\rangle, \tag{9-22}$$

where, as before, a^{+}_{A} and a_{I} are second quantized operators. Depending on the symmetry of the state, the δ, γ, and λ coefficients can have different values. $\delta \neq 0$ and

$\gamma \neq 0$ in Eq. (9-22) correspond to a fully symmetric singlet state, and $\delta = \gamma = 0$ corresponds to a non-fully symmetric singlet or triplet state. In the latter cases (9-22) simplifies to:

$$|\Psi^{s=0,1}_{CASCCSD}\rangle = e^{\hat{T}}(a^{+}_{A}a_{I} \pm a^{+}_{\bar{A}}a_{\bar{I}})|0\rangle, \tag{9-23}$$

or alternatively to:

$$|\Psi^{s=0,1}_{CASCCSD}\rangle = e^{\hat{T}}(|^{A}_{I}\rangle \pm |^{\bar{A}}_{\bar{I}}\rangle). \tag{9-24}$$

If the sign in the expressions (9-22), (9-23), and (9-24) is "minus", the wave function represents a triplet state with a zero S_z. The values of δ and γ can be calculated in the CASCCSD frameworks by using the standard spin-projection scheme or it can be taken from CASSCF, MRCI, CI, or perturbation theory calculations. As usual in the MRCC theory, the operator $\hat{T}$ should include singles and doubles excitations from the reference determinants. All these excitations (external and semiexternal) in Eqs. (9-22), (9-23), and (9-24) are expressed as excitations from the formal reference determinant. The structure of the wave function (9-22) for the singlet state can be written in a more compact form as:

$$|\Psi^{s=0}_{XCAS(2,2)CCSD}\rangle = e^{\hat{T}_1+\hat{T}_2}(\delta + \lambda E_{AI} + \gamma E^{2}_{AI})|0\rangle, \tag{9-25}$$

where $E_{AI} = a^{+}_{A_\alpha}a_{I_\alpha} + a^{+}_{A_\beta}a_{I_\beta}$ is a unitary group generator.

When $\delta = \gamma = 0$ in Eq. (9-23) a closed-shell determinant cannot be chosen as the formal reference. In this case one of the open-shell determinants, $|^{A}_{I}\rangle$ or $|^{\bar{A}}_{\bar{I}}\rangle$, can be used as the formal reference. The other reference determinant is then generated as a double electron excitation from the first determinant by a spin-flip excitation, $|^{A}_{I}\rangle \longleftrightarrow |^{\bar{A}}_{\bar{I}}\rangle$ (Figure 9-3). All the single and double excitations from the second reference determinant can be generated as single and double excitations $(\hat{T}_1 + \hat{T}_2)$, as well as some selected triple and quadruple excitations, from the formal reference determinant. If one chooses $|^{A}_{I}\rangle$ as the formal reference then the structure of the (2,2) active space can be represented in the form shown in Figure 9-4. The corresponding XCASCCSD wave function is:

$$|\Psi_{XCASCCSD}\rangle = e^{\hat{T}_1+\hat{T}_2+\hat{T}_3\binom{I\bar{A}a}{\bar{I}A\,i}+\hat{T}_4\binom{I\bar{A}ab}{\bar{I}A\,ij}}\left(1 \pm a^{+}_{I}a_{\bar{I}}a^{+}_{\bar{A}}a_{A}\right)|^{A}_{I}\rangle, \tag{9-26}$$

where indices i, j and a, b designate the occupied and vacant spin – orbitals, respectively. The orbital type (occupied or vacant) is determined with respect to the formal reference determinant. We should note that the reference function in Eq. (9-26) corresponds to either the singlet or the triplet state (depending on the sign), but no particular spin symmetry is implemented in the CC operator $\hat{T}$. Thus, while the linear combination of the reference part of the wave function is spin adapted, the CC part is not.

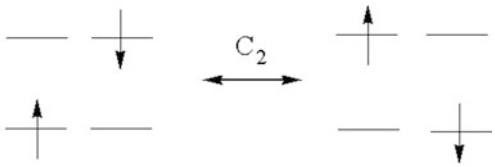

Figure 9-3. The second reference determinant can be generated as a double electron excitation from the "formal reference" determinant

We will now show some applications of the CASCCSD method in calculations of excited states. In the first example the calculations concerned fully symmetric states [38]. The configuration coefficients of the reference determinants were taken from a CASSCF calculation and, after the necessary renormalization, there values were kept constant during the XCASCCSD calculations. This type of approach is called "externally corrected" according to the terminology used by Paldus [40].

In the next example [39] we allow for the reference determinant coefficients to vary during the CASCCSD calculation. The initial values of the coefficients are taken from a MRCI (CASCISD) calculation. The renormalized CASCISD wave function can be written as the following expansion based on the single formal reference determinant $|0\rangle$:

$$|\Psi_{\mathrm{CASCISD}}\rangle = (1 + \hat{C}_1^{(\mathrm{ext})} + \hat{C}_2^{(\mathrm{ext})})(1 + \hat{C}^{(\mathrm{int})})|0\rangle, \tag{9-27}$$

where the operators $(1 + \hat{C}^{(\mathrm{int})})$ generates the reference wave function being a superposition of the reference determinants and $(\hat{C}_1^{(\mathrm{ext})} + \hat{C}_2^{(\mathrm{ext})})$ generates single and double excitations from the reference determinants. In this form the CASCISD wave function (9-27) resembles the CASCCSD wave function of CASCCSD. The difference between the two methods rests in the treatment of the external excitations.

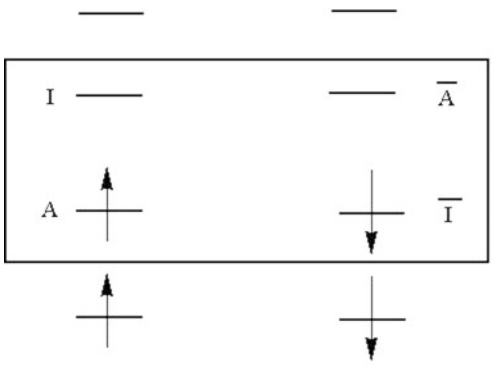

Figure 9-4. The active space for the (9-24) wave function

In the CASCISD wave function they are included in the linear form and in the XCASCCSD wave function the external excitation operators are exponentiated. Expanding the external excitation exponent generates strings of excitation operators which, when operating on the formal reference $|0\rangle$, generate higher order excitations. These higher-order excitations are not present in the CASCISD wave function. Due to the exponential form of wave function, the XCASCCSD method is size-extensive, as is the single-reference CC theory (e.g. CCSD), but the CASCISD method is not.

There is one point that needs to be mentioned regarding the dependency of the results of the CASCISD and XCASCCSD methods upon the choice of the formal reference determinant. The CASCISD method is invariant upon this choice. However, the results of the XCASCCSD method may depend on which reference determinant is chosen at the formal reference. This dependency is inherent to the CC theory. In our the XCASCCSD approach, for example, there are certain limits for the active indices. They lead to some asymmetry in the treatment of the determinants from the noniterative subspace. For example, there is a subset of triple excitations generated by the $\hat{T}^{(ext)}$ operator with the linear amplitudes $t_3(^{abC}_{Iij})$ (connected terms). However, the corresponding triple excitations from the second determinants do not have linear amplitudes, but their amplitudes are generated as products of "lower level" amplitudes $-t_2\,(^{ab}_{Ii})t_1(^{C}_{j}) + \frac{1}{3!}t_1(^{a}_{I})t_1(^{b}_{i})t_1(^{C}_{j})$ (disconnected terms). This brings some asymmetry to the approach. It can cause discontinuities in the CASCCSD solutions particularly when one calculates the potential energy surface for the system. In such calculations different reference determinants may be used as the formal references in different parts of the surface because the relative contributions of the reference determinants to the total wave function usually vary when the structure of the system is transformed. However, as the CASCCSD approach is a very accurate method and its absolute error relatively to FCI does not exceed $\approx$1–3 mHartree (as show by the calculations) the choice of the formal reference and its switching in the PES calculation is not a significant issue.

Also there is a possibility of spin contamination in the CASCCSD calculation. When a complete spin adaptation is perform of the CASCCSD wave function the configurational coefficients of some determinants with different levels of excitations from the formal reference determinant may need to be coupled to produce a spin-clean wave function (see, for example, Figure 9-3). When a partial spin-adaptation is performed, the spin-coupling of different determinants may be not strictly enforces and this is a situation when a spin contamination may arise. In the same way some spatial symmetry contamination of the wave function may also occur.

In order to eliminate (reduce) the symmetry contamination problem it is necessary to perform a complete or a partial symmetry adaptation of the CASCCSD wave function by imposing the appropriate coupling of configurational amplitudes. This can be achieved by a procedure involving parametrization of the cluster operators. The CC operators generated this way operate in the space of symmetry-adapted superpositions of determinants. However, such a scheme generally leads to a very complicated computational procedure and runs contradictory to the purpose

of our SS method which is to make the calculation as simple and time-efficient as possible.

To achieve this goal we use the following spin-adaptation approach in the CASCCSD calculation:

1. We first perform a RHF calculation or a CASSCF(n,m) calculation with the minimal active space adequate for the state under consideration.
2. Next we perform a CAS(n,m)CISD calculation to produce a good initial guess for the CC amplitudes of the XCASCCSD(n,m) wave function.
3. The determinant with the dominant contribution to the CAS(n,m)CISD wave function is selected as the formal reference. The CAS(n,m)CISD wave function is renormalized (by dividing all configurational amplitudes by the amplitude of the formal reference determinant) and transformed to the exponential form of the CAS(n,m)CCSD wave function.
4. The XCASCCSD(n,m) nonlinear amplitude equations are solved using the iterative procedure. A symmetry (spin and spatial) adaptation of the XCASCCSD wave function is performed in each iteration. This adaptation may be applied to only the reference determinants or may also involve determinants from outside the reference space.

In the iterative solution of the CC equations we use the standard procedure developed for the single-reference CC calculations. The symmetry adaptation step performed in each iteration is the only difference between the ground and excited state calculations.

Let us explain in more details how the symmetry adaptation works in a CAS(2,2)CCSD calculation. In this case there is a set of four equations to be solved obtained from projecting the Schrödinger equation on determinants with different excitation levels with respect to the formal reference:

$$\langle {}^{a}_{i}|(\hat{\mathrm{H}} - \mathrm{E})\mathrm{e}^{\hat{\mathrm{T}}^{(\mathrm{ext})}}\,\mathrm{e}^{\hat{\mathrm{T}}^{(\mathrm{int})}}|0\rangle_{\mathrm{C}} = 0, \tag{9-28}$$

$$\langle {}^{ab}_{ij}|(\hat{\mathrm{H}} - \mathrm{E})\mathrm{e}^{\hat{\mathrm{T}}^{(\mathrm{ext})}}\,\mathrm{e}^{\hat{\mathrm{T}}^{(\mathrm{int})}}|0\rangle_{\mathrm{C}} = 0, \tag{9-29}$$

$$\langle {}^{\mathrm{A}ab}_{ij\mathrm{I}}|(\hat{\mathrm{H}} - \mathrm{E})\mathrm{e}^{\hat{\mathrm{T}}^{(\mathrm{ext})}}\,\mathrm{e}^{\hat{\mathrm{T}}^{(\mathrm{int})}}|0\rangle_{\mathrm{C}} = 0, \tag{9-30}$$

$$\langle {}^{\mathrm{AB}ab}_{ij\mathrm{I}\,\mathrm{J}}|(\hat{\mathrm{H}} - \mathrm{E})\mathrm{e}^{\hat{\mathrm{T}}^{(\mathrm{ext})}}\,\mathrm{e}^{\hat{\mathrm{T}}^{(\mathrm{int})}}|0\rangle_{\mathrm{C}} = 0, \tag{9-31}$$

where the index C means that in the equations only connected terms are included. In each iterative step an amplitude symmetrization is performed. For the (2,2) reference space there are four types of CC amplitudes in the CASCCSD calculation:

$$\mathrm{t}_1,\ \ \mathrm{t}_2,\ \ \mathrm{t}_3^{'},\ \ \mathrm{t}_4^{'}, \tag{9-32}$$

where the prime indicates by $t_n^{'}$ that only a subset of excitations at that particular level is include in the wave function. In the first step of the symmetrization the following standard T $\rightarrow$ C transformation is performed:

$$c_1 = t_1, \tag{9-33}$$

$$c_2 = \frac{1}{2}t_1t_1 + t_2, \tag{9-34}$$

$$c_3^{'} = \frac{1}{6}t_1t_1t_1 + t_2t_1 + t_3^{'}, \tag{9-35}$$

$$c_4^{'} = \frac{1}{24}t_1t_1t_1t_1 + \frac{1}{2}t_2t_2 + \frac{1}{2}t_2t_1t_1 + t_3^{'}t_1 + t_4^{'}. \tag{9-36}$$

Using c's (not t's) the wave function can be represented in the linear form:

$$|\Psi_{\mathrm{XCASCCSD}}\rangle = (1 + \hat{C}_1 + \hat{C}_2 + \hat{C}_3^{'} + \hat{C}_4^{'} + \hat{Q})|0\rangle, \tag{9-37}$$

where the CI-like $\hat{Q}$ operator generates all remaining excitations (i.e. excitations from the non-iterative subspace). The linearized form of the XCASCCSD wave function (9-37) allow for an easier symmetry adaptation. After this is done a reverse $C \rightarrow T$ transformation is performed and the wave function is re-transformed back to the exponential form. The whole symmetrization procedure can be symbolically described with the following equation:

$$\langle \Psi_1 \pm \Psi_2 | (\hat{H} - E) e^{\hat{T}^{(\mathrm{ext})}} e^{\hat{T}^{(\mathrm{int})}} |0\rangle = 0. \tag{9-38}$$

In this equation the configurations Ψ_1 and Ψ_2 that need to be included in the wave function with equal weights, have different excitation levels. In the case of the (2,2) active space these can be double and quadruple excitations from the formal reference determinant. The amplitude symmetrization can be more or less complete. The simplest approach is to only symmetry adapt the configurational coefficients of the reference determinants. We denote such an approach as X_{Sr}CAS(n,m)CCSD. In a more complete case the symmetrization is also applied to the amplitudes of the determinants from the iterative subspace (i.e. the determinants with linear amplitudes). Such method is designated as X_{Sc}CAS(n,m)CCSD. Another variant of the symmetry adaptation method involves taking symmetrized amplitudes of the reference determinants from a non-CASCCSD calculation and not changing them during the CASCCSD calculation. We designate such an approach as X_fCAS(n,m)CCSD. A non-CASCCSD source of the amplitudes may be a CASSCF or CASCISD calculation. Other possibilities, such as the single reference or multireference perturbation theory, can also be considered.

The algorithms for solving the XCAS(n,m)CCSD equations have been implemented in our computer program called CLUSTER. CLUSTER is interfaced with the popular quantum chemistry package GAMESS [11].

In conclusion, some comments are in order regarding the computational cost of the XCASCCSD calculations. This cost strongly depends on the way the XCASCCSD algorithms are implemented especially if the code runs on a parallel computer with a shared or distributed memory. Regardless of the platform, the

overall computational cost for the XCASCCSD calculations scales as $O(n_o^2 n_v^4)$ when no higher than fivefold excitations from the formal reference are included.[2] For comparison, the standard CCSD also has the same asymptotic scaling, but, obviously, the proportionality coefficient is smaller in this case.

9.5. NUMERICAL EXAMPLES

In this section we will describe some examples of excite-state XCASCCSD calculations.

9.5.1. Excited States of the Water Molecule

The calculations were performed at the equilibrium ground-state geometry of the water molecule with the internuclear distance equal to $R_e = 0.95$ Å and the angle equal to $\angle = 104.5°$. All the calculations were performed with a double-zeta valence base set (Dunning-Hay, DZV [41], incorporated in the GAMESS package). We used this basis in order to be able to compare the XCASCCSD results with the FCI calculations available in the literature.

Choosing the active space is starting point of the XCASCCSD calculation. At first we will write down the symmetries of the Hartree–Fock (HF) molecular orbitals of the water molecule. If the C_2 symmetry axis is the z axis and the molecule is placed in the yz plane, the orbitals (ordered by increasing energy) are:

$$1a_1^2 2a_1^2 1b_2^2 3a_1^2 1b_1^2 \,||\, 4a_1 2b_2 2b_1 5a_1 3b_2 4b_2 6a_1 7a_1, \tag{9-39}$$

where the double vertical line separates the occupied and vacant orbitals. We use the natural orbital (NO) expansion obtained from a restricted CI calculation (CIS or CISD) for selecting the most important orbitals to form the active space for the XCASCCSD calculations of the state under consideration.

The occupation numbers and the symmetries of the natural orbitals obtained from the CI wave functions for some singlet and triplet excited states of the A_1 and A_2 symmetries considered in the present calculations are shown in Table 9-1. For the sake of comparison, we show the CIS, CISD, and FCI results in the table. The first two columns in the table describe the water ground state at the equilibrium geometry. Since the ground state is closed – shell, all highest occupied natural orbitals have occupation numbers (ON) equal to two. All other natural orbitals ($4a_1$ – $3b_2$ orbitals) have small ONs because they are involved in the part of the wave function that describes the electron correlation.

For the lowest $^1A_1$ excited state the $3a_1$ and $4a_1$ orbitals are singly – occupied and their ONs are close to one. Thus, the model space needed for describing the

[2] In the expression n_o and n_v are the numbers of the occupied and vacant orbitals, respectively.

Table 9-1. Occupation numbers of natural orbitals for the A_1 and A_2 excited singlet states of the water molecule obtained by different methods. Occupation numbers of singly occupied orbitals are underlined

Orbitals	X^1A_1 CISD	FCI	$^1A_1$ CIS	CISD	FCI	$^1A_2$ CIS	CISD	FCI
$1a_1$	2	2	2	2	2	2	2	2
$2a_1$	1.9895	1.9878	1.9997	1.9960	1.9868	2	1.9982	1.9889
$1b_2$	1.9729	1.9682	1.9889	1.9810	1.9602	2	1.9949	1.9778
$3a_1$	1.9757	1.9713	1.0166	1.1001	1.1095	2	1.9918	1.9692
$1b_1$	1.9819	1.9783	1.9948	1.9942	1.9785	1	0.9990	0.9942
$4a_1$	0.0227	0.0266	0.9834	0.8925	0.8803	0	0.0130	0.0338
$2b_2$	0.0240	0.0280	0.0111	0.0211	0.0384	1	0.9921	0.9946
$2b_1$	0.0171	0.0206	0.0052	0.0054	0.0202	0	0.0017	0.0069
$5a_1$	0.0111	0.0130	0.0003	0.0048	0.0114	0	0.0017	0.0120
$3b_2$	0.0026	0.0031	0.0	0.0015	0.0034	0	0.0055	0.0140
$4b_2$	0.0004	0.0005	0.0	0.0005	0.0026	0	0.0011	0.0036
$6a_1$	0.0019	0.0021	0.0	0.0020	0.0064	0	0.0007	0.0028
$7a_1$	0.0002	0.0004	0.0	0.0009	0.0023	0	0.0004	0.0021

$^1A_1$ state is a (2,2) space comprising determinants with all possible different occupations by two electrons of the $3a_1$ and $4a_1$ orbitals and includes the following four determinants:

$$|0\rangle, \quad |^{4a_1}_{3a_1}\rangle, \quad |^{\overline{4a_1}}_{\overline{3a_1}}\rangle, \quad |^{4a_1\,\overline{4a_1}}_{3a_1\,\overline{3a_1}}\rangle.$$

The *ansatz* for the CASCCSD wave function for this state is:

$$|\Psi_{\mathrm{XCAS(2,2)CCSD}[^1A_1]}\rangle = e^{\hat{T}}\left(\delta|0\rangle + \gamma|^{4a_1\,\overline{4a_1}}_{3a_1\,\overline{3a_1}}\rangle + |^{4a_1}_{3a_1}\rangle + |^{\overline{4a_1}}_{\overline{3a_1}}\rangle\right), \tag{9-40}$$

where δ and γ are the CI coefficients. As it was pointed out in the previous section, these coefficients can be either calculated by solving the CC amplitude equations or taken from a non–CC calculation. In the present work we used the latter option and we took the values of δ and γ from a CASSCF calculation. Such an approach can be called *unrelaxed* and we designate it as X_fCASCCSD.

The CAS(2,2)CCSD calculation for the A_1 triplet state can be carried out in a similar way as for the corresponding singlet state. The calculation requires that the signs of the CI coefficients of the two reference determinants, $|^{4a_1}_{3a_1}\rangle$ and $|^{\overline{4a_1}}_{\overline{3a_1}}\rangle$ are opposite:

$$|\Psi_{\mathrm{XCAS(2,2)CCSD}[^3A_1]}\rangle = e^{\hat{T}}\left(|^{4a_1}_{3a_1}\rangle - |^{\overline{4a_1}}_{\overline{3a_1}}\rangle\right), \tag{9-41}$$

(closed – shell model – space determinants $|0\rangle$ and $|^{4a_1\overline{4a_1}}_{3a_1\overline{3a_1}}\rangle$ do not contribute to the triplet state). Here again we used the $|^{4a_1}_{3a_1}\rangle$ determinant as the formal reference and we included all single and double excitations from both reference determinants in the $\hat{T}$ operator. This excitations are defined as single, double and some selected higher excitations from the formal reference determinant $|^{4a_1}_{3a_1}\rangle$.

The major contribution to the wave function of the $^1A_2$ state is the $1b_1 \rightarrow 2b_2$ one–electron excitation. Hence, the complete model space in this case contains two determinants:

$$|^{2b_2}_{3b_1}\rangle, \quad |^{\overline{2b_2}}_{\overline{3b_1}}\rangle.$$

The determinants with double occupations of the $1b_1$ and $2b_2$ orbitals (i.e., determinants $|0\rangle$ and $|^{2b_2\overline{2b_2}}_{1b_1\overline{1b_1}}\rangle$) do not contribute for the symmetry reason. Thus the XCASCCSD wave functions for the $^{1,3}A_2$ states have the following form:

$$|\Psi_{XCAS(2,2)CCSD[^{1,3}A_2]}\rangle = e^{\hat{T}}\left(|^{2b_2}_{3b_1}\rangle \pm |^{\overline{2b_2}}_{\overline{3b_1}}\rangle\right), \tag{9-42}$$

where the plus sign corresponds to the singlet state and the minus sign corresponds to the triplet. Here we used the $|^{2b_2}_{3b_1}\rangle$ determinant as the formal reference and in the $\hat{T}$ operator we included all single and double excitations from both reference determinants defined as single, double, and some selected triple and quadruple excitations from the formal reference determinant $|^{2b_2}_{3b_1}\rangle$.

In constructing the following XCAS(2,2)CCSD wave function for the $^{1,3}B_1$ singlet and triplet states we used the NO expansion:

$$|\Psi_{XCAS(2,2)CCSD[^{1,3}B_1]}\rangle = e^{\hat{T}}\left(|^{4a_1}_{1b_1}\rangle \pm |^{\overline{4a_1}}_{\overline{1b_1}}\rangle\right). \tag{9-43}$$

For the $^{1,3}B_2$ states the analogical procedure produced the following XCAS(2,2) CCSD wave functions:

$$|\Psi_{XCAS(2,2)CCSD[^{1,3}B_2]}\rangle = e^{\hat{T}}\left(|^{2b_2}_{3a_1}\rangle \pm |^{\overline{2b_2}}_{\overline{3a_1}}\rangle\right). \tag{9-44}$$

The XCASCCSD results for the $^{1,3}A_{1,2}$ states are presented in the Table 9-2. The table contains FCI energies (in a.u.) and the differences between the FCI and XCASCCSD.[3] Among the methods compared in the table, XCASCCSD produces

[3] for the $^3A_1$, $^1A_2$, $^3A_2$ states XCASCCSD is equivalent to X_{Sr}CASCCSD while for the $^1A_1$ state XCASCCSD $\equiv X_f$CASCCSD

Table 9-2. FCI energies (in a.u.; the sign is reversed) and absolute errors (in mHartree) of different methods relative to FCI for the different states of the water molecule. DZV basis set and the equilibrium geometry were used in the calculations

Method	$^1A_1$	$^3A_1$	$^1A_2$	$^3A_2$
FCI	75.730738	75.764810	75.742054	75.759576
CIS	163.11	143.86	155.08	149.96
CISD	67.36	68.45	68.10	69.40
CISDT	10.18	–	9.24	–
CASSCF(2,2)	115.54	104.97	104.29	106.41
MCQDPT	5.92	9.09	9.61	9.52
CCSD(s=s_z=1)	–	3.39	–	3.23
EOM-CCSD	−2.71	–	−2.13	–
X_{Sr}CASCCSD	0.91	1.35	1.33	1.35

results matching the FCI energies the best. The CASCCSD results are even better than the results of the CI method that includes up to three-electron excitations (CISDT). The comparison of the CASCCSD with the multi – configurational quasi – degenerate perturbation theory (MCQDPT)[4] was especially interesting for us, because that method has been described as being very accurate. The results presented in the table demonstrate that MCQDPT is significantly less exact than the XCASCCSD approach.

The calculations of the B_1 and B_2 states (shown in Table 9-3) also demonstrate high accuracy of XCASCCSD in comparison with FCI and are noticeably better than the CI and MCQDPT results. More detailed description of the calculations of excited states water molecule can be found in [38].

Table 9-3. A comparison of total energies (in a.u.; signs are reversed) and relative energies (in mHartrees) with respect to the FCI energy of various methods including the XCASCCSD method for the two lowest excited singlet and triplet states of the B_1 and B_2 symmetries of the water molecule

Method	$^1B_1$	$^3B_1$	$^1B_2$	$^3B_2$
FCI	75.818262	75.846183	75.643402	75.690767
CIS	165.06	156.54	152.67	132.01
CISD	69.35	69.95	65.69	68.56
CISDT	10.19	N/A	9.09	N/A
CASSCF(2,2)	105.93	105.83	101.30	106.02
MCQDPT	10.08	8.45	10.16	11.19
X_{Sr}CAS(2,2)CCSD	1.31	1.39	1.64	2.62

[4] Implemented in GAMESS

9.5.2. Excited States in Hydrogen Fluoride Molecule

Hydrogen Fluoride (HF) is another test example. For the sake of comparison of the XCASCCSD results with FCI we again use the small DZV basis set. The ground-state orbital ordering for the HF molecule is (at the equilibrium structure with R_e=1.733 a.u.):

$$(1\sigma^2 2\sigma^2)3\sigma^2 1\pi^4 || 4\sigma 2\pi 5\sigma 6\sigma 7\sigma. \tag{9-45}$$

The two core orbitals are in parentheses.

Before starting the XCASCCSD calculations we examine the structure of the wave functions for the different states considered in the study at different internuclear separations (R=R_e, 1.4, 2.50, 3.40, 4.175, 5.0, and 6 a.u.). The examination showed that the wave functions considerably change with the internuclear distance. To generate the initial wave-function guesses for the XCAS(2,2)CCSD calculations we used the CAS(2,2)CISD method. The analysis of the CAS(2,2)CISD wave function, is shown in the Table 9-4.

As one can see, the structure of the wave function strongly depends on the state. The reference functions (determinant) for the XCASCCSD calculation can be chosen based on the CASCISD results. The dominant reference determinant (or one of two degenerate determinants) can be selected as the formal reference.

In the calculation of the PES the formal reference determinant can change as the structure of the system is altered because the weights of the reference determinants usually vary with the structural transformations. As the formal reference determinant changes, all the excitation operators in the XCASCCSD wave function also change because they are defined with respect to this determinant. This may affect the accuracy of the PES calculation. A detailed analysis of the accuracy of the XCASCCSD method and of its performance in PES calculations was presented in [39].

Table 9-4. Dominant determinants for different states of the HF molecule as obtained from CAS(2,2)CISD calculations (with CASSCF orbitals). $1\sigma^2$ and $2\sigma^2$ are the core orbitals

State	Active orbitals	R(a.u.)	Reference function
$X^1\Sigma$	3σ,4σ	<4.175	$\|1\pi_x^2 1\pi_y^2 3\sigma^2\rangle$
		>4.175	$\|1\pi_x^2 1\pi_y^2 3\sigma^1(\alpha)4\sigma^1(\beta)\rangle - \|1\pi_x^2 1\pi_y^2 3\sigma^1(\beta)4\sigma^1(\alpha)\rangle$
$^1\Sigma$	3σ,4σ	<3.4	$\|1\pi_x^2 1\pi_y^2 3\sigma^1(\alpha)4\sigma^1(\beta)\rangle - \|1\pi_x^2 1\pi_y^2 3\sigma^1(\beta)4\sigma^1(\alpha)\rangle$
		>3.4	$\|1\pi_x^2 1\pi_y^2 3\sigma^2\rangle$
$^3\Sigma$	3σ,4σ	Whole interval	$\|1\pi_x^2 1\pi_y^2 3\sigma^1(\alpha)4\sigma^1(\beta)\rangle + \|1\pi_x^2 1\pi_y^2 3\sigma^1(\beta)4\sigma^1(\alpha)\rangle$
$^3\Pi$	1π,4σ	Whole interval	$\|1\pi_x^2 1\pi_y^1(\alpha)3\sigma^2 4\sigma^1(\beta)\rangle + \|1\pi_x^2 1\pi_y^1(\beta)3\sigma^2 4\sigma^1(\alpha)\rangle$
$^1\Pi$	1π,4σ	Whole interval	$\|1\pi_x^2 1\pi_y^1(\alpha)3\sigma^2 4\sigma^1(\beta)\rangle - \|1\pi_x^2 1\pi_y^1(\beta)3\sigma^2 4\sigma^1(\alpha)\rangle$

Table 9-5. Non-parallelity errors (first row) and maximal absolute deviation (second row) in mHartrees for the PES of different states HF molecule

Method	$X^1\Sigma$	$^1\Sigma$	$^3\Sigma$	$^3\Pi$	$^1\Pi$
CAS(2,2)CISD	0.373	4.787	1.894	0.521	0.506
	5.364	9.674	5.211	2.692	2.518
X_{Sc}CAS(2,2)CCSD	2.577	4.514	0.391	0.201	0.213
	1.770	2.326	1.787	1.225	1.231
X_{Sr}CAS(2,2)CCSD	2.440	3.851	0.404	0.265	0.258
	1.633	1.663	1.665	1.208	1.208
X_fCAS(2,2)CCSD	2.610	3.634	0.404	0.265	0.258
	1.740	1.862	1.665	1.208	1.208
EOM-CCSD	10.607	36.894	N/A	N/A	22.674
	11.976	29.939	N/A	N/A	14.546
CR-EOM-CCSD(T),III	2.047	4.449	N/A	N/A	3.262
	2.139	2.707	N/A	N/A	2.100

A useful tool to examine the accuracy of the PES calculation is the so-called non-parallelity error (NPE) [42]. It is determined based on the comparison of the PES calculated with a particular method and the FCI PES (see Table 9-5). It is interesting to examine how enforcing of the spin symmetry in the XCASCCSD wave function affects the NPE. The different variants of the CASCCSD method we proposed have different level of the spin adaptation (see Section 9.4). The maximal deviation from the FCI value in our XCASCCSD method is only 2.326 mHartree (≈1.46 kcal/mol). Interestingly, the X_f variant of the CASCCSD method shows a rather good performance for the ($^1\Sigma$) state, while the error in the EOM-CCSD data is rather significant. The situation is noticeable improved when the completely renormalized method is applied [33].

9.5.3. Excited States in C_2 Molecule

The XCASCCSD calculations of the C_2 molecule are compared here with the recent FCI results for the PES's of the ground $X^1\Sigma_g^+$ state and two excited $B^1\Delta_g$ and $B'^1\Sigma_g$ states of Abrams and Sherrill [43]. The 6-31G* basis set was used in our and their calculations. Abrams and Sherrill showed that all the three states of C_2 are essentially multireference with the wave functions either showing a strong mixing of the primary configuration $|(\text{core})2\sigma_g^2 2\sigma_u^2 1\pi_{u_x}^2 1\pi_{u_y}^2\rangle$ with some *doubly* excited configurations or being dominated by those *double* excitations. Moreover the $B^1\Delta_g$ excited state crosses the ground $X^1\Sigma_g^+$ state PES near ≈1.80 Å, whereas the $B'^1\Sigma_g^+$ and $X^1\Sigma_g^+$ states have an avoided crossing near ≈1.60 Å. All these features pose high demands on the method used in the PES calculation to obtain quantitatively correct description of all three states at all internuclear separations. Apart from the comparison of our results with the FCI results we are also comparing the with the results of other methods taken from the work of Sherrill and Piecuch [44].

In the XCASCCSD calculations of the $X^1\Sigma_g^+$ and $B'^1\Sigma_g^+$ states we used the equally-weighted "state-averaged" CASSCF orbitals also used in the work of Sherrill and Piecuch [44]. The active space in the CASSCF calculation consisted of eight active molecular orbitals occupied by eight electrons. In the calculations of the $B^1\Delta_g$ state we also used eight active orbitals (occupied by eight electrons) determined in state-specific CASSCF calculations performed for that state. As it was shown in the works of Abrams and Sherrill [43], the minimal active space needed for a post-CASSCF calculation to produce a quantitative description of the states of C_2 considered in the present calculations should contain at least six electrons and the following seven molecular orbitals (a (6,7) active space): $2\sigma_u$, $1\pi_{u_x}$, $1\pi_{u_y}$, $3\sigma_g$, $1\pi_{g_x}$, $1\pi_{g_y}$ and $3\sigma_u$. Note that the $2\sigma_g$ orbital is not included in the active space. We used this active space in the XCAS(6,7)CCSD calculations. In all calculations the electrons occupying the lowest two molecular orbitals were not correlated. Details of our calculations were presented in the Ref. [39]. Here we provide a summary of those results and a comparison with other methods.

Table 9-6 shows the NPEs and the maximal absolute value deviation from the FCI results. As one can notice, the XCAS(6,7)CCSD methods produce the most accurate

Table 9-6. NPE. (1st row) and maximal absolute value deviation (2nd row) for three electronic states of the C_2 molecule obtained with different methods with respect to the FCI results. The values are in mHartrees

Method	$X^1\Sigma_g^+$	$B^1\Delta_g$	$B'^1\Sigma_g^+$
CAS(6,7)CISD	0.437	0.666	0.890
	2.827	2.963	3.284
X_{S_c}CAS(6, 7)CCSD8	0.080	0.329	0.427
	0.844	0.797	1.117
X_{S_r}CAS(6, 7)CCSD8	0.168	0.370	0.237
	0.788	0.709	0.927
X_fCAS(6, 7)CCSD8	0.213	0.328	1.167
	0.427	0.552	1.085
X_{S_c}CAS(6, 7)CCSD6	0.193	0.403	0.383
	0.951	0.863	1.114
X_{S_r}CAS(6, 7)CCSD6	0.186	0.373	0.164
	0.791	0.765	0.895
CR − EOM − CCSD(T), III	18.426	43.585	31.504
	25.714	57.284	39.575
EOM-CCSD	37.997	49.792	35.220
	66.028	151.698	124.506
MCQDPT2	6.022	1.845	2.747
	11.813	12.284	11.162

results among all the methods compared in the table. However, it should be said that the XCAS(6,7)CCSD approach is also the most computationally demanding in this case (scales as $O(N^7)$ with a relatively large prefactor). The CAS(6,7)CISD approach produces results that have noticeably a higher absolute deviation because of the lack of the size-extensivity of this method. As it can be expected, the EOM methods produce much larger errors for C_2 than for the FH molecule because all three C_2 electronic states have "doubly excited multireference" character. It is more difficult to describe such states with the standard EOM schemes than states dominated by single excitations. An active-space based EOM approach would be more adequate in this situation.

The sextuple-limited XCAS(6,7)CCSD6 approximation (i.e. the XCAS(6,7) CCSD approach with the excitations from the formal reference limited to not higher than six-fold excitations) produces results only slightly worse than the results produced by the complete XCAS(6,7)CCSD8 approach. This indicates that the contributions from sevenfold and eightfold excited clusters can be very well approximated by products of lower-level clusters. Thus, an explicit account of the fully connected contributions from the t_7 and t_8 excited clusters is not very essential in this case.

9.5.4. Vertical Excitations in Formaldehyde

In this section we describe our XCASCCSD calculations of some vertical electronic excitations of the formaldehyde molecule (H_2CO). The electronic excited states of formaldehyde are rather typical for an organic molecule of this size. There have been a number of works describing these states both experimentally and theoretically (see, for example, Foresman et al. [13] and Moor et al. [45]).

In our calculations we used the experimental (C_{2v}) geometry of the formaldehyde molecule [46] with the bond lengths $R_{C=O}$=1.203 Å and $R_{C\text{-}H}$ = 1.099 Å and the bond angle $\angle_{HCO}$=116.5°. The calculations were performed with the cc-pVTZ basis set [51]. In all calculations the lowest two occupied orbitals and the highest two virtual orbitals were frozen (i.e. not used in the calculation of the correlation energy). The following six electronic states of formaldehyde were considered: the ground X^1A_1 state and the $^3(n\pi^*)$, $^1(n\pi^*)$, $^3(\pi\pi^*)$, $^1(\sigma\pi^*)$, and $^1(\pi\pi^*)$ excited states. In the Table 9-7 the excitation energies calculated for these states are presented. In the first step CASSCF calculations were performed with the active space comprising two electrons and the following pairs of orbitals: (σ, σ^*) for the ground state and (n, π^*), (π, π^*) and $(\sigma\pi^*)$ for the corresponding excited states. The CASSCF(2,2) orbitals were subsequently used in the CAS(2,2)CISD, MCQDPT2, and $X_{Sc}CAS(2,2)CCSD$ calculations. The EOM calculations were performed with the Hartree–Fock orbitals. All results, except the XCASCCSD ones, were obtained with the 2006 version of the GAMESS package [11] which does not allow for EOM computations for triplet states.

As one can see from Table 9-7 there are noticeable differences in the total XCASCCSD and CASCISD electronic energies. These differences are in the

Table 9-7. Total electronic energies (first row; in a.u.) and vertical excitation energies (second row; in eV) of ground and excited states of formaldehyde calculated with different methods and with the cc-pVTZ basis set. Two lowest occupied and two highest virtual orbitals are frozen. The experimental ground state geometry was used in the calculations [46]

Method	X^1A_1	$^3(n\pi^*)$	$^1(n\pi^*)$	$^3(\pi\pi^*)$	$^1(\sigma\pi^*)$	$^1(\pi\pi^*)$
CAS(2,2)SCF	−113.924119	−113.808788	−113.763952	−113.738833	−113.572681	−113.508586
	0	3.14	4.36	5.04	9.56	11.31
CAS(2,2)CISD	−114.286545	−114.157106	−114.136797	−114.070547	−113.946133	−113.904747
	0	3.52	4.07	5.88	9.26	10.39
X_{S_c}CAS(2, 2)CCSD	−114.314941	−114.182638	−114.166252	−114.092233	−113.975991	−113.940991
	0	3.60	4.05	6.06	9.22	10.18
EOM-CCSD	−114.311123	N/A	−114.162490	N/A	−113.971049	−113.925437
	0	N/A	4.04	N/A	9.25	10.50
CR-EOM-CCSD(T),III	−114.324331	N/A	−114.171972	N/A	−113.982120	−113.935747
	0	N/A	4.15	N/A	9.31	10.57
MCQDPT2	−114.290005	−114.172789	−114.181758	−114.076338	−113.988058	−113.954730
	0	3.19	2.95	5.81	8.22	9.12
Experimental	–	3.54[47]	4.1[48]	6.0[48]	9.0[49]	10.7[50]

range of 22-36 mHartree and should be attributed to the size-extensivity of the XCASCCSD method and lack of it in the CASCISD method.

9.6. CONCLUSION

In this article we review our state-specific coupled-cluster approach with the CASSCF reference for calculating electronically excited states (XCASCCSD). The method is a generalization of the CASCCSD approach we developed for ground state calculations. The key feature of the method, that is consistent with the SS approach, is the use of different reference functions for different states. The XCASCCSD calculations show high accuracy in comparison with the FCI results. We estimate that the average accuracy of the XCASCCSD method is only around 1–2 mHartree for states with the wave functions dominated by single excitations from the Hartree–Fock determinant, as well as for state dominated by double excitations. The XCASCCSD is not strictly invariant with respect to the choice of the formal reference. This, however, as shown by our calculations as well as by calculations performed by Kállay and Surján [52], causes only insignificant discontinuities of the energy. Thus, in general, the CASCCSD method can be used to calculate electronically excited states with different multiconfigurational characters with very high accuracy. The high efficiency of the method is due to it being based on the CASSCF reference and due to including all single and double excitations from the CAS configurations in the CC exponential operator that facilitates the size-extensivity of the results.

ACKNOWLEDGEMENT

This work was partially supported by NSF.

REFERENCES

1. J. Gauss, Coupled-Cluster Theory, in *Encyclopedia of Computational Chemistry*, Eds. P. v. R. Schlegel et al. (Wiley, Chichester, 2004), pp. 615–636
2. J. Paldus, X. Li, A Critical Assessment of the Coupled Cluster Method in Quantum Chemistry, Adv. Chem. Phys., **110**, 1 (1999)
3. J. Paldus, Coupled Cluster Methods, in *Handbook of Molecular Physics and Quantum Chemistry. V.2: Molecular Electronic Structure*, Ed. S. Wilson (Jhon Wiley and Sons, New York, 2003), pp. 272–313
4. R. J. Bartlett, in *Theory and Applications of Computational Chemistry: The first Forty Years*, Eds. C. E. Dykstra, G. Frenking, K. S. Kim, G. E. Scuseria (Elsevier, Amsterdam, 2005), pp. 1216–1221
5. R. J. Bartlett, M. Musiał, Rev. Mod. Phys. **79**, 291 (2007)
6. L. Serrano-Andrés, M. Merchán, J. Mol. Struct. (THEOCHEM), **729**, 99 (2005)
7. N. Oliphant, L. Adamowicz, J. Chem. Phys. **94**, 1229 (1991); P. Piecuch, N. Oliphant, L. Adamowicz, J. Chem. Phys. **99**, 1875 (1993); N. Oliphant, L. Adamowicz, Int. Rev. Phys. Chem. **12**, 339 (1993); P. Piecuch, L. Adamowicz, J. Chem. Phys. **100**, 1 (1994)
8. V. V. Ivanov, L. Adamowicz, J. Chem. Phys. **112**, 9258 (2000)

9. V. V. Ivanov, D. I. Lyakh, Kharkiv University Bulletin. Chemical Series. **549**, 15 (2002); D. I. Lyakh, V. V. Ivanov, L. Adamowicz, Kharkiv University Bulletin. Chemical Series. **596**, 9 (2003)
10. D. I. Lyakh, V. V. Ivanov, L. Adamowicz, J. Chem. Phys. **122**, 024108 (2005)
11. M. W. Schmidt, K. K. Baldridge, J. A. Boatz, S. T. Elbert, M. S. Gordon, J. H. Jensen, S. Koseki, N. Mastunada, K. A. Nguyen, S. Su, T. L. Windus, M. Dupuis, J. A. Montgomery, J. Comput. Chem. **14**, 1347 (1993)
12. V. V. Ivanov, L. Adamowicz, D. I. Lyakh, Int. J. Quant. Chem. **106**, 2875 (2006); D. I. Lyakh, V. V. Ivanov, L. Adamowicz, Teoret. Chem. Acta. **116**, 427 (2006); V. V. Ivanov, L. Adamowicz, D. I. Lyakh, Collect. Czech. Chem. Commun. **70**, 1017 (2005); D. I. Lyakh, V. V. Ivanov, L. Adamowicz, Mol. Phys. **105**, 1335 (2007)
13. J. B. Foresman, M. Head-Gordon, J. A. Pople, J. Phys. Chem. **96**, 135 (1992)
14. P. L. Altick, A. E. Glassgold, Phys. Rev. **133**, A632 (1964)
15. D. J. Rowe, Rev. Mod. Phys. **40**, 153 (1968)
16. T. H. Dunning, V. McKoy, J. Chem. Phys. **47**, 1735 (1967), **48**, 5263 (1968)
17. D. G. Truhlar, Int. J. Quantum Chem. **7**, 807, (1973)
18. R. J. Bartlett, F. Stanton, in *Reviews in Computational Chemistry*, vol. 5, Eds. K. B. Lipkowitz, D. B. Boyd (VCH Publishers, Inc., New York, 1994), pp. 65–169
19. J. Geertsen, S. Ericksen, J. Oddershede, Adv. Quantum. Chem. **22**, 167 (1991)
20. J. Geersten, M. Rittby, R. J. Bartlett, Chem. Phys. Lett., **164**, 57 (1989); D. C. Comeau, R. J. Bartlett, Chem. Phys. Lett., **207**, 414 (1993); J. F. Stanton, R. J. Bartlett, J. Chem. Phys., **98**, 7029 (1993); R. J. Bartlett, J. F. Stanton, Rev. Comput. Chem. Phys., **5**, 65 (1994); R. J. Rico, M. Head-Gordon, Chem. Phys. Lett **213**, 224 (1993); J. D. Watts, R. J. Bartlett, Chem. Phys. Lett, **233**, 81 (1995)
21. S. R. Gwaltney, R. J. Bartlett, Chem. Phys. Lett **241**, 26 (1995); O. Christiansen, H. Koch, P. Jørgensen, J. Chem. Phys. **97**, 1451 (1996); H. Koch, P. Jørgensen, J. Chem. Phys. **93**, 3333 (1990); O. Christiansen, H. Koch, P. Jørgensen, J. Chem. Phys. **103**, 7429 (1995); J. D. Watts, R. J. Bartlett, Spectrochim Acta A, **55**, 495 (1999).
22. P. Piecuch, S. A. Kucharski, K. Kowalski, M. Musiał, Comp. Phys. Commun. **149**, 71 (2002)
23. H. Nakatsuji, K. Hirao, J. Chem. Phys. **68**, 2053 (1978); H. Nakatsuji, K. Hirao, J. Chem. Phys. **69**, 4535 (1978); H. Nakatsuji, Chem. Phys. Lett. **67**, 334 (1979); H. Nakatsuji, J. Hasegawa, M. Hada, J. Chem. Phys. **104**, 2321 (1996)
24. P. W. Langhoff, S. T. Epstein, M. Karplus, Rev. Mod. Phys. **44**, 602 (1972)
25. H. J. Monkhorst, Int. J. Quant. Chem. Symp. **11**, 421 (1977); E. Dalgaard, H. J. Monkhorst, Phys. Rev. **28**, 1217 (1983)
26. H. Koch, H. A. Jensen, P. Jørgensen, T. Helgaker, J. Chem. Phys. **93**, 3345 (1990); O. Christiansen, H. Koch, P. Jørgensen, Chem. Phys. Lett. **243**, 409 (1995)
27. H. Sekino, R. J. Bartlett, Int. J. Quant. Chem.: Quant. Chem. Symp. **18**, 255 (1984)
28. M. Nooijen, R. J. Bartlett, J. Chem. Phys. **106**, 6441 (1997); M. Nooijen, R. J. Bartlett, J. Chem. Phys. **106**, 6449 (1997); M. Nooijen, J. Chem. Phys. **104**, 2638 (1996)
29. M. Nooijen, R. J. Bartlett, J. Chem. Phys. **107**, 6812 (1997)
30. M. Nooijen, V. Lotrich, J. Chem. Phys. **113**, 494 (2000)
31. P. Piecuch, R. J. Bartlett, Adv. Quant. Chem. **34**, 295 (1999)
32. J. D.Watts, R. J. Bartlett, Chem. Phys. Lett. **233**, 81 (1995); J. D.Watts, S. R. Gwaltney, R. J. Bartlett, J. Chem. Phys. **105**, 6979 (1996)
33. P. Piecuch, K. Kowalski, I. S. O. Pimienta, P.-D. Fan, M. Lodriguito, M. J. McGuire, S. A. Kucharski, T. Kus, M. Musiał, Theor. Chem. Acc. **112**, 349 (2004); K. Kowalski, P. Piecuch, J. Chem. Phys. **120**, 1715 (2004)
34. K. Kowalski, P. Piecuch, J. Chem. Phys. **115**, 643 (2001)

35. M. Nooijen, Int. J. Mol. Sci. **3**, 656 (2002)
36. S. Chattopadhyay, U. Mahapatra, D. Mukherjee, J. Chem. Phys. **112**, 7939 (2000)
37. M. Musiał, L. Meissner, S. A. Kucharski, R. J. Bartlett, J. Chem. Phys. **122**, 224110 (2005)
38. V. V. Ivanov, L. Adamowicz, D. I. Lyakh, J. Chem. Phys. **124**, 184302 (2006)
39. D. I. Lyakh, V. V. Ivanov, L. Adamowicz, J. Chem. Phys. **128**, 074101 (2008)
40. X. Li, J. Paldus. J. Chem. Phys. **115**, 5774 (2001)
41. T. H. Dunning Jr., P. J. Hay, in *Methods of Electronic Structure Theory*, Ed. H. F. Shaefer III (Plenum, New York, 1977), chap. 1, pp. 1–27
42. X. Li, J. Paldus, J. Chem. Phys. **103**, 1024 (1995)
43. M. L. Abrams, C. D. Sherrill, J. Chem. Phys. **121**, 9211 (2004)
44. C. D. Sherrill, P. Piecuch, J. Chem. Phys. **122**, 124104 (2005)
45. C. B. Moore, J. C. Weisshaar, Annu. Rev. Phys. Chem. **34**, 525 (1983)
46. K. Yamada, T. Nakagawa, K. Kuchitsu, Yo. Morino, J. Mol. Spectrosc. **38**, 70 (1971)
47. D. L. Yeager, V. McKoy, J. Chem. Phys. **60**, 2714 (1974)
48. L. B. Harding, W. A. Goddard III, J. Am. Chem. Soc. **99**, 677 (1977)
49. J. E. Mentall, E. P. Gentieu, M. Krauss, D. Neumann, J. Chem. Phys. **55**, 547 (1971)
50. M. J. Weiss, C. F. Kuyatt, S. Mielezarik, J. Chem. Phys. **54**, 4147 (1971)
51. T. H. Dunning Jr., J. Chem. Phys. **90**, 1007 (1989)
52. M. Kállay, P. Surján, J. Chem. Phys. **115**, 2945 (2001); M. Kállay, P. G. Szalay, P. Surján, J. Chem. Phys. **117**, 980 (2002)

CHAPTER 10

MULTIREFERENCE R12 COUPLED CLUSTER THEORY

STANISLAV KEDŽUCH[1], ONDŘEJ DEMEL[2], JIŘÍ PITTNER[2], AND JOZEF NOGA[1,3]

[1]*Institute of Inorganic Chemistry, Slovak Academy of Sciences, SK-84536 Bratislava, Slovakia, e-mail: stanislav.kedzuch@savba.sk*

[2]*J. Heyrovský Institute of Physical Chemistry, Academy of Sciences of the Czech Republic, CZ-18223 Prague 8, Czech Republic, e-mail: ondrej.demel@jh-inst.cas.cz; jiri.pittner@jh-inst.cas.cz*

[3]*Department of Inorganic Chemistry, Faculty of Natural Sciences, Comenius University, SK-84215 Bratislava, Slovakia, e-mail: jozef.noga@savba.sk*

Abstract: In order to account for static electron correlation, the explicitly correlated coupled cluster (CC) theory based on the R12 Ansatz is formulated with respect to a multi-determinantal reference using the Brillouin – Wigner (BW) approach. Though the latter avoids appearance of the intruder states, one pays for this desired feature by the loss of size extensivity. However, to some extent this can be remedied by an a posteriori correction. Since the BW-CC method offers simplest form of amplitude equations among Hilbert space MR CC ones, we have chosen it as the first step when developing MR CC-R12 approaches. It is shown that introducing of the basis set incompleteness correction via an explicit inclusion of the correlation factor into the wave function, separately for each reference, is easily realizable. Test calculations for the H4 model using the R12 optimized 9*s*6*p*4*d*3*f* basis and its subsets with increasing highest angular momentum show the potential of the MR CC-R12 approach. R12 results with mere *sp* functions are very close to values obtained by using a conventional approach and the full 9*s*6*p*4*d*3*f* basis set. We stress, however, that care must be taken to treat the R12 corrections with comparable accuracy for all the reference determinants.

Keywords: Multireference coupled cluster, Hilbert space, R12 approach, Explicitly correlated, Brillouin – Wigner coupled cluster

10.1. INTRODUCTION

Undoubtedly, the R12 Ansatz for the wave function, suggested a quarter of century ago by Kutzelnigg [1], launched an intensive and successful research leading to a number of approaches that treat the dynamical electron correlation by explicit inclusion of terms that are (at least in the leading term) linear in the inter-electronic coordinate (r_{12}) into the wave function. If L is the highest angular momentum involved in the one-particle orbital basis set, such approach can improve the formal

P. Čársky et al. (eds.), Recent Progress in Coupled Cluster Methods, 251–266.
DOI 10.1007/978-90-481-2885-3_10,

$\propto (L+1)^{-3}$ dependence of the conventional configuration interaction expansion error [2] to $\propto (L+1)^{-7}$ [3].

The basic idea is to extend a configuration interaction type expansion by r_{12} containing part resulting from the action of an operator $\hat{\mathcal{R}}$ onto the reference (Φ) resulting from the one-particle approximation solution.

$$|\Psi\rangle = \hat{\mathcal{R}}|\Phi\rangle + |\Psi_{\mathrm{CI-type}}\rangle. \tag{10-1}$$

$\hat{\mathcal{R}}$ is related to a (at this moment not necessarily specified) correlation factor $\hat{\mathcal{F}}$. While in the early development the correlation factor $\hat{\mathcal{F}}$ was simply an operator of the inter-electronic coordinate [4–6], the Slater type geminal (STG) plays the dominant role during the latest few years [7–20]. The former development has been recently reviewed by Klopper et al. [21].

Combination of the single reference coupled cluster (CC) theory with the idea of the R12 Ansatz gives rise to a more general description of the wave function than Eq. (10-1). Namely, $\hat{\mathcal{R}}$ becomes an integral part of the exponential wave operator

$$|\Psi\rangle = \hat{\Omega}|\Phi\rangle = \exp(\hat{T} + \hat{\mathcal{R}})|\Phi\rangle\,. \tag{10-2}$$

The operator $\hat{\mathcal{R}}$ can be expressed within the second quantized formalism and consequently the working CC-R12 equations using the diagrammatic techniques [22, 23] can be relatively easily derived. Unlike the early implementations, the latest ones do not strictly use an approximation that is known as "standard" and whose basic idea is derived from the fact that it is much easier to saturate the basis set at one particle level than at two-particle level [3]. Hence, if the basis set is close to saturation at the one-particle level, one can replace the exact one-particle resolution of identity by the projector into the space spanned by that one-particle basis set. In recent implementations, the exact one-particle resolution of identity is approximated by one described in an auxiliary basis set that can be substantially more extended than the main computational basis. More detailed overview of the latest development is summarized elsewhere in this book (Chapters 20 and 21).

As mentioned, the R12 approach treats the problem of the dynamical electron correlation (the proper description of the coulomb hole), and, in no case it can replace the need for treating the effect that is known as the non-dynamical electron correlation. The latter is related to a priori multireference character of the wave function in many situations (e.g. far from the equilibrium geometries). Combination of the MR CI with R12 [24, 25] has been announced soon after the CC-R12 [6], but the actual applications since are scarce. A simple F12 geminal correction in multi-reference perturbation theory has been recently proposed by Ten-no [26]. Irrespectively, it is highly desirable to introduce the R12 approach also within the MR CC theories.

There are basically two types of genuine MR CC methods, where the word "genuine" implies the use of the truly multi-reference wave operator formalism, namely, the Fock-space or valence universal MR CC approaches (see, e.g., [27, 28], and

references therein) and the Hilbert-space or state-universal (SU) MR CC schemes [29–34], which are based on the Jeziorski – Monkhorst (JM) Ansatz [29]. This work is based on the latter approach and employs the JM Ansatz with a cluster operator augmented by the R12 excitations to the complementary orbital basis. Nevertheless, it is a state-specific (SS) method. The SS methods employ formally the same definition of the effective Hamiltonian as SU methods, however, merely a single root of the effective Hamiltonian has a physical meaning in the SS context. So far, there have been three flavors of SS Hilbert-space MR CC suggested – the Brillouin-Wigner CC (BW-CC) [35–41], Mukherjee's CC method (MkCC) [42–45], and Hanrath's determinantal indexing approach (MRexpT) [46, 47]. The BW-CC method has the disadvantage that it is not exactly size-extensive, which makes a posteriori or iterative corrections necessary [40, 48]. On the other hand, it was able to yield results sufficiently accurate for practical purposes [49–62] and, from a practical point of view, it has the simplest form of amplitude equations among the three aforementioned SS approaches, coupled only via the eigenvalue of the effective Hamiltonian. This simplicity makes it an excellent candidate for the first step of the merger of MR CC and R12 theories, leaving the more complicated methods for future work. For simplicity, we also confine ourselves to the complete model space (CMS) throughout this work, acknowledging that an extension to general model spaces should be possible employing the C-conditions technique [63–66] developed already for the MR BW-CC method [67].

10.2. NOTATION AND CONVENTIONS

In the following, we shall use letters i, j, m, n to denote occupied spin-orbitals, a, b, c, d to denote virtual spin-orbitals and p, q, r, s to denote spin-orbitals from a unification of both these spaces. This indexing will always be related to a particular reference determinant $|\Phi_\mu\rangle$ which will be denoted in parenthesis following the pertinent matrix elements and/or operators. In the R12 theory, one works with a complete orthogonal complement to the aforementioned spin-orbital space. Referring to this complementary space is denoted by $\alpha, \beta, \gamma, \delta$. Whenever this complete complementary basis will be replaced by a finite auxiliary set of spin orbitals, we shall use p'', q'', r'', s'', while $p', q', \ldots$ refer to $p' \in p \cup p''$. Spin-orbitals within this unified space are assumed to be orthonormal, i.e. $|p'q'\rangle = \delta^{q'}_{p'}$. This corresponds to the concept of complementary auxiliary basis set (CABS) [68].

In our previous derivations of the (single reference) CC-R12 approach, it was convenient to work with second quantized normal ordered operators with respect to that reference used as a Fermi vacuum. With several reference determinants, any normal ordered n-body operator is expressed in terms of matrix elements and n-body replacement operators [69] related to a pertinent reference. Here, we shall only use one- and two-particle operators

$$\tilde{a}^{p_1}_{q_1}(\mu) = \left\{a^\dagger_{p_1} a_{q_1}\right\}_\mu; \qquad \tilde{a}^{p_1 p_2}_{q_1 q_2}(\mu) = \left\{a^\dagger_{p_1} a^\dagger_{p_2} a_{q_2} a_{q_1}\right\}_\mu, \tag{10-3}$$

where $a_p^\dagger$ and a_q are the creation and annihilation operators, respectively. The braces in Eq. (10-3) denote the normal ordering with respect to $|\Phi_\mu\rangle$.

A tensor notation will be used for integrals over any n-body operator $\hat{o}_n$,

$$o_{p_1}^{q_1} = \langle p_1|\hat{o}_1|q_1\rangle\,; \qquad o_{p_1p_2}^{q_1q_2} = \langle p_1p_2|\hat{o}_2|q_1q_2\rangle, \tag{10-4}$$

as well as for integral products. Einstein summation convention is considered throughout. Irrespectively of the particular correlation factor $\hat{\mathcal{F}}$, its matrix elements will be denoted by $F_{p_1p_2}^{q_1q_2}$.

The exact second quantized non-relativistic Hamiltonian ($\hat{H}$) comprises its part that is fully describable through the computational basis set ($\hat{H}^{\mathrm{ao}}$) and a complementary part ($\hat{H}^{\mathrm{comp}}$) that must be expressed in terms of the complete orthogonal complement to that basis [70]. Accordingly, the normal ordered Hamiltonian with respect to $|\Phi_\mu\rangle$ reads:

$$\hat{H}_N(\mu) = \hat{H} - \langle\Phi_\mu|\hat{H}|\Phi_\mu\rangle = \hat{H}_N^{\mathrm{ao}}(\mu) + \hat{H}_N^{\mathrm{comp}}(\mu) \tag{10-5}$$

$$\hat{H}_N^{\mathrm{ao}}(\mu) = f_p^q(\mu)\tilde{a}_q^p(\mu) + \tfrac{1}{4}\bar{g}_{pq}^{rs}\tilde{a}_{rs}^{pq}(\mu)\,, \tag{10-6}$$

$$\begin{aligned}\hat{H}_N^{\mathrm{comp}}(\mu) = {} & f_p^\alpha(\mu)\tilde{a}_\alpha^p(\mu) + f_\alpha^p(\mu)\tilde{a}_p^\alpha(\mu) + f_\beta^\alpha(\mu)\tilde{a}_\alpha^\beta \\ & + \tfrac{1}{2}\Big[\bar{g}_{\alpha q}^{rs}\tilde{a}_{rs}^{\alpha q}(\mu) + \bar{g}_{pq}^{\alpha s}\tilde{a}_{\alpha s}^{pq}(\mu) + \bar{g}_{\alpha\beta}^{\gamma s}\tilde{a}_{\gamma s}^{\alpha\beta}(\mu) + \bar{g}_{\alpha q}^{\gamma\delta}\tilde{a}_{\gamma\delta}^{\alpha q}(\mu)\Big] \\ & + \bar{g}_{\alpha q}^{\gamma s}\tilde{a}_{\gamma s}^{\alpha q}(\mu) + \tfrac{1}{4}\Big[\bar{g}_{\alpha\beta}^{rs}\tilde{a}_{rs}^{\alpha\beta}(\mu) + \bar{g}_{pq}^{\gamma\delta}\tilde{a}_{\gamma\delta}^{pq}(\mu) + \bar{g}_{\alpha\beta}^{\gamma\delta}\tilde{a}_{\gamma\delta}^{\alpha\beta}\Big]. \end{aligned} \tag{10-7}$$

Note that as soon as the normal ordered replacement operator relates merely to spin-orbitals of the complementary space, it becomes independent of the reference. Also matrix elements of the two-particle part, i.e. integrals over $\hat{g} = 1/r_{12}$, are independent of the reference, unlike the Fock matrix elements (f).

In fact, exact expression of any operator in its second quantized form can be written similarly as (10-5). Such partitioning enables an easy elimination of a part of the correlation factor that is describable by the given basis and should not be included in $\hat{\mathcal{R}}$ [Eq. (10-1)], since it creates determinants that are contained in the "conventional" configuration space (vide infra).

10.3. OUTLINE OF THE MR BW-CC METHOD

In this section, we recapitulate the basics of the traditional multireference Brillouin Wigner coupled cluster theory.

In accord with the JM Ansatz the model space is assumed to be spanned by M reference configurations $|\Phi_\mu\rangle$, whereas the projection of the exact wave function on the model space $|\Psi_\omega^P\rangle$ is expanded as a linear combination of references

$$|\Psi_\omega^P\rangle = \sum_{\mu=1}^{M} C_\mu^\omega |\Phi_\mu\rangle. \tag{10-8}$$

Here, the expansion coefficients C_μ^ω, which are a priori unknown, are determined in the subsequent calculation. P stands for the projection operator onto the model space, which is a sum of projection operators onto the individual references

$$\hat{P} = \sum_{\mu=1}^{M} |\Phi_\mu\rangle\langle\Phi_\mu|. \tag{10-9}$$

The exact wave function of the ω-th electronic state is then formally obtained from the reference function (10-8) using a wave operator $\hat{\Omega}_\omega$

$$|\Psi_\omega\rangle = \hat{\Omega}_\omega |\Psi_\omega^P\rangle, \tag{10-10}$$

while intermediate normalization

$$\langle\Psi_\omega|\Psi_\omega^P\rangle = 1 \tag{10-11}$$

must be fulfilled, which translates to the requirement of zero amplitudes for internal excitations in the complete model space case. Furthermore, let us assume existence of an effective Hamiltonian $\hat{H}^{\text{eff}}$ as an operator which gives the "exact" energy $\mathcal{E}_\omega$ when acting on the reference function

$$\hat{H}^{\text{eff}}|\Psi_\omega^P\rangle = \mathcal{E}_\omega|\Psi_\omega^P\rangle, \tag{10-12}$$

i.e. the exact energy $\mathcal{E}_\omega$ can be obtained as an eigenvalue of that effective Hamiltonian. Using the aforementioned wave operator, $\hat{H}^{\text{eff}}$ can be expressed as

$$\hat{H}^{\text{eff}} = \hat{P}\hat{H}\hat{\Omega}_\omega\hat{P}, \tag{10-13}$$

where the form of the wave operator is still unspecified and can vary due to a specific approach. In the MR BW-CC method, the wave operator is taken in the form of JM Ansatz

$$\hat{\Omega}_\omega = \sum_{\mu=1}^{M} e^{\hat{T}(\mu)} |\Phi_\mu\rangle\langle\Phi_\mu|. \tag{10-14}$$

Here, the operator $\hat{T}(\mu)$ is a global cluster operator consisting of excitations with respect to the reference configuration $|\Phi_\mu\rangle$. The cluster operators are specific for each

reference. Provided that the model space is complete, cluster amplitudes corresponding to internal excitations, i.e. excitations transforming one reference configuration to another one, are zero due to the requirement of intermediate normalization. For a general (incomplete) model space, this requirement leads to so called C-conditions for the internal amplitudes, which have been employed both in the state-universal [63–65] and state-specific Brillouin – Wigner [67] approaches. Since the active space is disjoint with the complement space, this technique can be extended to the R12 approach straightforwardly.

The equations for the cluster amplitudes can be derived from the generalized Bloch equation

$$\lambda\mathcal{E}_\omega\hat{\Omega}_\omega\hat{P}_\omega + (1-\lambda)\big[\hat{\Omega}_\omega,\hat{H}_0\big]\hat{P} = \lambda\hat{H}\hat{\Omega}_\omega\hat{P}_\omega + (1-\lambda)\big[\hat{V}\hat{\Omega}_\omega - \hat{\Omega}_\omega\hat{P}\hat{V}\Omega_\omega\big]\hat{P}\,, \tag{10-15}$$

where $\hat{P}_\omega$ denotes the projection operator $|\Psi_\omega^P\rangle\langle\Psi_\omega^P|$ and λ is an arbitrary real number from the interval $\langle 0,1\rangle$. For $\lambda = 1$, the equation corresponds to the Brillouin-Wigner perturbation theory, whereas $\lambda = 0$ leads to Rayleigh-Schrödinger theory and state-universal method. After insertion of the JM Ansatz into the generalized Bloch equation (10-15), the resulting equation is applied to the state $|\Psi_\omega\rangle$. Since for $\lambda \neq 0$ the method is state-specific, the sufficiency conditions are applied, splitting the equation system to individual equations sets for each reference $|\Phi_\mu\rangle$, in a consistent way with the $\lambda = 0$ limit. Division by C_μ^ω and projection onto the Slater determinants $|\Phi_\vartheta^{(\mu)}\rangle$ excited with respect to $|\Phi_\mu\rangle$ yields the cluster equations from which the amplitudes of $\hat{T}(\mu)$ are determined:

$$\begin{aligned}\lambda\ \ &\big(\mathcal{E}_\omega - H_{\mu\mu}^{\mathrm{eff}}\big)\big\langle\Phi_\vartheta^{(\mu)}\big|e^{\hat{T}(\mu)}\big|\Phi_\mu\big\rangle = \big\langle\Phi_\vartheta^{(\mu)}\big|\big[\hat{H}_N(\mu)e^{\hat{T}(\mu)}\big]_{\mathrm{C}}\big|\Phi_\mu\big\rangle \\ &+\big\langle\Phi_\vartheta^{(\mu)}\big|\big[\hat{H}_N(\mu)e^{\hat{T}(\mu)}\big]_{\mathrm{DC,L}}\big|\Phi_\mu\big\rangle - (1-\lambda)\sum_{\nu\neq\mu}\big\langle\Phi_\vartheta^{(\mu)}\big|e^{T(\nu)}\big|\Phi_\nu\big\rangle H_{\nu\mu}^{\mathrm{eff}}\,.\end{aligned} \tag{10-16}$$

Here, $H_{\mu\nu}^{\mathrm{eff}}$ are elements of the matrix representation of the effective Hamiltonian within the model space and can be evaluated from

$$H_{\mu\nu}^{\mathrm{eff}} = \langle\Phi_\mu|\hat{H}|\Phi_\mu\rangle\delta_{\mu\nu} + \big\langle\Phi_\mu\big|\big[\hat{H}_N(\nu)e^{T(\nu)}\big]_{\mathrm{C}}\big|\Phi_\nu\big\rangle\,. \tag{10-17}$$

The expression for the diagonal elements $H_{\mu\mu}^{\mathrm{eff}}$ is the same as for the CC energy in the single reference theory, when we use the amplitudes of the μ-th reference.

The off-diagonal elements of (10-17) can be viewed as the connected parts of the right hand sides of the cluster equations corresponding to the internal amplitude which transforms the ν-th reference to the μ-th reference. As long as the model space is restricted to mutually mono- and biexcited references, the off-diagonal elements of H^{eff} can be collected from the vector of the respective right hand sides at the CCSD level.

The correlation energy is obtained by the diagonalization of the $\mathbf{H}^{\text{eff}}$ matrix, while the coefficients in the corresponding eigenvector are the C_μ^ω coefficients from (10-8). Since the theory is state-specific, only the selected eigenvalue, for which we converge the equations, has a physical meaning.

For the purpose of obtaining BW-CC and size-extensivity corrections, the $(1-\lambda)$-scaled coupling terms are neglected and the disconnected linked (DC,L) terms are scaled by λ, giving rise to:

$$\lambda\left(\mathcal{E}_\omega - H^{\text{eff}}_{\mu\mu}\right)\left\langle \Phi^{(\mu)}_\vartheta \middle| e^{\hat{T}(\mu)} \middle| \Phi_\mu \right\rangle = \left\langle \Phi^{(\mu)}_\vartheta \middle| \left[\hat{H}_N(\mu) e^{\hat{T}(\mu)}\right]_{\text{C}} \middle| \Phi_\mu \right\rangle + \lambda \left\langle \Phi^{(\mu)}_\vartheta \middle| \left[\hat{H}_N(\mu) e^{\hat{T}(\mu)}\right]_{\text{DC,L}} \middle| \Phi_\mu \right\rangle. \tag{10-18}$$

The usually employed a posteriori size-extensivity correction [48] consists in solving this equation iteratively with $\lambda = 1$ until convergence is achieved and subsequently making one additional iteration with $\lambda = 0$, which yields corrected amplitudes, from which the corrected H^{eff} is computed and its diagonalization finally yields the corrected energy. This procedure is independent of the R12 Ansatz and will be performed analogously in the R12 method.

The theory can be used with an arbitrary truncation of the cluster operator. Truncating the cluster operator to single and double excitations, $\hat{T}(\mu) = \hat{T}_1(\mu) + \hat{T}_2(\mu)$, the cluster equations for the MR BW-CCSD variant reduce to:

$$\lambda\left(\mathcal{E}_\omega - \hat{H}^{\text{eff}}_{\mu\mu}\right)\left\langle \Phi_\mu \middle| \tilde{a}^i_a(\mu) e^{\hat{T}_1(\mu)} \middle| \Phi_\mu \right\rangle = \left\langle \Phi_\mu \middle| \tilde{a}^i_a(\mu) \left[\hat{H}_N(\mu) e^{\hat{T}(\mu)}\right]_{\text{C}} \middle| \Phi_\mu \right\rangle \tag{10-19}$$

$$\lambda\left(\mathcal{E}_\omega - H^{\text{eff}}_{\mu\mu}\right)\left\langle \Phi_\mu \middle| \tilde{a}^{ij}_{ab}(\mu) e^{\hat{T}(\mu)} \middle| \Phi_\mu \right\rangle = \left\langle \Phi_\mu \middle| \tilde{a}^{ij}_{ab}(\mu) \left[\hat{H}_N(\mu) e^{\hat{T}(\mu)}\right]_{\text{C}} \middle| \Phi_\mu \right\rangle + \lambda \left\langle \Phi_\mu \middle| \tilde{a}^{ij}_{ab}(\mu) \left[\hat{H}_N(\mu) e^{\hat{T}(\mu)}\right]_{\text{DC,L}} \middle| \Phi_\mu \right\rangle. \tag{10-20}$$

Since the action of $\hat{T}(\mu)$ creates determinants fully describable by the computational basis, $\hat{H}_N^{\text{comp}}$ contribution of $\hat{H}_N$ does not need to be considered and in Eqs. (10-16)-(10-20) $\hat{H}_N$ is essentially reduced to $\hat{H}_N^{\text{ao}}$.

10.4. MR CC-R12 ANSATZ

In the explicitly correlated multireference CC theory the form of the wave operator for the ω-th electronic state (10-10) is logically suggested by the combination of the basic idea of the CC-R12 given by Ansatz of Eq. (10-2) combined with the JM Ansatz of Eq. (10-14):

$$\hat{\Omega}_\omega = \sum_{\mu=1}^{M} e^{\hat{T}(\mu)+\hat{\mathcal{R}}(\mu)} |\Phi_\mu\rangle\langle\Phi_\mu|. \tag{10-21}$$

In analogy with the single reference case in the most general sense [9], distinct pseudo-excitation operators $\hat{\mathcal{R}}(\mu)$ related to each $|\Phi_\mu\rangle$ can be written as:

$$\hat{\mathcal{R}}(\mu) = \hat{\mathcal{R}}_1(\mu) + \hat{\mathcal{R}}_2(\mu) = c_k^i(\mu)\tilde{\mathcal{R}}_i^k(\mu) + \tfrac{1}{4}c_{kl}^{ij}(\mu)\tilde{\mathcal{R}}_{ij}^{kl}(\mu)\,; \tag{10-22}$$

$$\tilde{\mathcal{R}}_i^k(\mu) = \bar{F}_{\alpha j}^{kj}(\mu)\tilde{a}_i^\alpha(\mu) \equiv F_\alpha^k(\mu)\tilde{a}_i^\alpha(\mu), \tag{10-23}$$

$$\tilde{\mathcal{R}}_{ij}^{kl}(\mu) = \tfrac{1}{2}\bar{F}_{\alpha\beta}^{kl}(\mu)\tilde{a}_{ij}^{\alpha\beta}(\mu) + \bar{F}_{\alpha b}^{kl}(\mu)\tilde{a}_{ij}^{\alpha b}(\mu), \tag{10-24}$$

where c are variational parameters.

10.4.1. Working Equations

Amplitudes $c_k^i(\mu)$ and $c_{kl}^{ij}(\mu)$ of the pseudo-excitations created by the action of $\hat{\mathcal{R}}_1(\mu)$ and $\hat{\mathcal{R}}_2(\mu)$ upon $\langle\Phi_\mu|$ have to be determined along with the amplitudes of $\hat{T}$. Modification of Eq. (10-18) for MR BW-CCSD-R12 includes substitution of $\hat{T}(\mu)$ by $\hat{S}(\mu) = \hat{T}(\mu) + \hat{\mathcal{R}}(\mu)$ and, besides projections onto the $\langle\Phi_\vartheta^{(\mu)}|$, also projections onto $\langle\Phi_\mu|\big[\tilde{\mathcal{R}}_i^k(\mu)\big]^\dagger$ and $\langle\Phi_\mu|\big[\tilde{\mathcal{R}}_{ij}^{kl}(\mu)\big]^\dagger$. However, since

$$\langle\Phi_\vartheta^{(\mu)}|e^{\hat{\mathcal{R}}(\mu)}|\Phi_\mu\rangle = 0\,, \tag{10-25}$$

$$\langle\Phi_\mu|\hat{\mathcal{R}}^\dagger(\mu)e^{\hat{T}(\mu)}|\Phi_\mu\rangle = 0\,, \tag{10-26}$$

projections onto the "conventional" configuration subspaces give rise to

$$\begin{aligned}\lambda\big(\mathcal{E}_\omega - H_{\mu\mu}^{\mathrm{eff}}\big)\langle\Phi_\mu|\tilde{a}_a^i(\mu)e^{\hat{T}(\mu)}|\Phi_\mu\rangle &= \langle\Phi_\mu|\tilde{a}_a^i(\mu)\big[\hat{H}_N^{\mathrm{ao}}(\mu)e^{\hat{T}(\mu)}\big]_{\mathrm{C}}|\Phi_\mu\rangle \\ &+\langle\Phi_\mu|\tilde{a}_a^i(\mu)\big[\hat{H}_N^{\mathrm{comp}}(\mu)e^{\hat{S}(\mu)}\big]_{\mathrm{C}}|\Phi_\mu\rangle\,,\end{aligned} \tag{10-27}$$

$$\begin{aligned}\lambda\big(\mathcal{E}_\omega - H_{\mu\mu}^{\mathrm{eff}}\big)\langle\Phi_\mu|\tilde{a}_{ab}^{ij}(\mu)e^{\hat{T}(\mu)}|\Phi_\mu\rangle &= \langle\Phi_\mu|\tilde{a}_{ab}^{ij}(\mu)\big[\hat{H}_N^{\mathrm{ao}}(\mu)e^{\hat{T}(\mu)}\big]_{\mathrm{C}}|\Phi_\mu\rangle \\ &+\lambda\langle\Phi_\mu|\tilde{a}_{ab}^{ij}(\mu)\big[\hat{H}_N^{\mathrm{ao}}(\mu)e^{\hat{T}(\mu)}\big]_{\mathrm{DC,L}}|\Phi_\mu\rangle + \langle\Phi_\mu|\tilde{a}_{ab}^{ij}(\mu)\big[\hat{H}_N^{\mathrm{comp}}(\mu)e^{\hat{S}(\mu)}\big]_{\mathrm{C}}|\Phi_\mu\rangle \\ &+\lambda\langle\Phi_\mu|\tilde{a}_{ab}^{ij}(\mu)\big[\hat{H}_N^{\mathrm{comp}}(\mu)e^{\hat{S}(\mu)}\big]_{\mathrm{DC,L}}|\Phi_\mu\rangle\,,\end{aligned} \tag{10-28}$$

whereas projection onto the space of R12 pseudo-excitations results in

$$\lambda \ \left(\mathcal{E}_\omega - H^{\text{eff}}_{\mu\mu}\right)\left\langle \Phi_\mu \middle| \left[\tilde{\mathcal{R}}^k_i(\mu)\right]^\dagger e^{\hat{\mathcal{R}}(\mu)} \middle| \Phi_\mu \right\rangle = \left\langle \Phi_\mu \middle| \left[\tilde{\mathcal{R}}^k_i(\mu)\right]^\dagger \left[\hat{H}^{\text{comp}}_N(\mu) e^{\hat{S}(\mu)}\right]_{\text{C}} \middle| \Phi_\mu \right\rangle, \tag{10-29}$$

$$\begin{aligned}\lambda \ \left(\mathcal{E}_\omega - H^{\text{eff}}_{\mu\mu}\right)\left\langle \Phi_\mu \middle| \left[\tilde{\mathcal{R}}^{kl}_{ij}(\mu)\right]^\dagger e^{\hat{S}(\mu)} \middle| \Phi_\mu \right\rangle &= \left\langle \Phi_\mu \middle| \left[\tilde{\mathcal{R}}^{kl}_{ij}(\mu)\right]^\dagger \left[\hat{H}^{\text{comp}}_N(\mu) e^{\hat{S}(\mu)}\right]_{\text{C}} \middle| \Phi_\mu \right\rangle \\ &+ \lambda \left\langle \Phi_\mu \middle| \left[\tilde{\mathcal{R}}^{kl}_{ij}(\mu)\right]^\dagger \left[\hat{H}_N(\mu) e^{\hat{S}(\mu)}\right]_{\text{DC,L}} \middle| \Phi_\mu \right\rangle.\end{aligned} \tag{10-30}$$

The model space Hamiltonian also changes accordingly:

$$\begin{aligned}H^{\text{eff}}_{\mu\nu} &= \left\langle \Phi_\mu \middle| \hat{H} \middle| \Phi_\mu \right\rangle \delta_{\mu\nu} + \left\langle \Phi_\mu \middle| \left[\hat{H}^{\text{ao}}_N(\nu) e^{\hat{T}(\nu)}\right]_{\text{C}} \middle| \Phi_\nu \right\rangle \\ &+ \left\langle \Phi_\mu \middle| \left[\hat{H}^{\text{comp}}_N(\nu) e^{\hat{S}(\nu)}\right]_{\text{C}} \middle| \Phi_\nu \right\rangle.\end{aligned} \tag{10-31}$$

Again, $H^{\text{eff}}_{\mu\mu}$ formally corresponds to the total energy calculated separately for the reference $|\Phi_\mu\rangle$, using amplitudes of $\hat{T}(\mu)$ and $\hat{\mathcal{R}}(\mu)$.

In Eqs. (10-27), (10-28), and (10-31), parts that are identical with "conventional" MR BW-CCSD are clearly identified. For a single reference case, evaluation of the connected terms on the r.h.s. of Eqs. (10-27), (10-28), (10-29), (10-30), and (10-31) is given elsewhere [9]. Here, all the resulting matrix elements and intermediates must be just separately related to a specific reference determinant $|\Phi_\mu\rangle$. Products of integrals that involve summations over the complementary basis can be evaluated using insertions of the resolution of identity that can be in particular cases approximated by a large auxiliary basis [71]. It is convenient if this auxiliary basis is a unification of the computational AO basis and CABS [68]. Closely related to our formalism, more detailed principles of the derivations were shown in Ref. [72].

In addition to terms that are involved in the CCSD-R12 equations for the given reference, one has to evaluate the l.h.s. of Eqs. (10-27), (10-28), (10-29), and (10-30) and the disconnected terms on r.h.s. Their calculation is obvious for the "conventional" part. Less obvious, but still trivial is the evaluation of terms related to $\hat{\mathcal{R}}$ as they contain summations over the complementary basis. Namely,

$$\left\langle \Phi_\mu \middle| \left[\tilde{\mathcal{R}}^k_i(\mu)\right]^\dagger e^{\hat{\mathcal{R}}(\mu)} \middle| \Phi_\mu \right\rangle = F^\alpha_i(\mu) F^m_\alpha(\mu) c^k_m(\mu) = \mathcal{X}^m_i(\mu) c^k_m(\mu); \tag{10-32}$$

$$\begin{aligned}\langle \Phi_\mu \big| \big[\tilde{\mathcal{R}}^{kl}_{ij}(\mu)\big]^\dagger e^{\hat{S}(\mu)} \big| \Phi_\mu \rangle &= \tfrac{1}{2}\big[\tfrac{1}{2}\bar{F}^{\alpha\beta}_{ij}(\mu)\bar{F}^{mn}_{\alpha\beta}(\mu) + \bar{F}^{a\beta}_{ij}(\mu)\bar{F}^{mn}_{a\beta}(\mu)\big]c^{kl}_{mn}(\mu) \\ &+ \tfrac{1}{2}F^{\alpha\beta}_{ij}(\mu)F^{m}_{\alpha}(\mu)F^{n}_{\beta}(\mu)c^{k}_{m}(\mu)c^{l}_{n}(\mu) - F^{a\beta}_{ij}(\mu)t^{k}_{a}(\mu)F^{n}_{\beta}(\mu)c^{l}_{n}(\mu) \\ &= \tfrac{1}{2}\mathcal{X}^{mn}_{ij}(\mu)c^{kl}_{mn}(\mu) + \tfrac{1}{2}\mathcal{W}^{mn}_{ij}(\mu)c^{k}_{m}(\mu)c^{l}_{n}(\mu) - \mathcal{X}^{an}_{ij}(\mu)t^{k}_{a}(\mu)c^{l}_{n}(\mu)\,. \end{aligned} \tag{10-33}$$

The meaning of $\mathcal{X}$ and $\mathcal{W}$ is obvious. These amplitude-free intermediates can be easily calculated [9, 72] either using CABS or the standard approximation:

$$\begin{aligned}\mathcal{X}^{kl}_{ij}(\mu) &\overset{\text{cabs}}{=} (\bar{F}^2)^{kl}_{ij}(\mu) - \bar{F}^{mq''}_{ij}(\mu)\bar{F}^{kl}_{mq''}(\mu) - \tfrac{1}{2}\bar{F}^{pq}_{ij}(\mu)\bar{F}^{kl}_{pq}(\mu) \\ &\overset{\text{s.a.}}{=} (\bar{F}^2)^{kl}_{ij}(\mu) - \tfrac{1}{2}\bar{F}^{pq}_{ij}(\mu)\bar{F}^{kl}_{pq}(\mu) \end{aligned} \tag{10-34}$$

$$\mathcal{X}^{al}_{ij}(\mu) \overset{\text{cabs}}{=} \bar{F}^{aq''}_{ij}(\mu)F^{l}_{q''}(\mu) \overset{\text{s.a.}}{=} 0 \tag{10-35}$$

$$\mathcal{W}^{kl}_{ij}(\mu) \overset{\text{cabs}}{=} \bar{F}^{p''q''}_{ij}(\mu)F^{k}_{p''}(\mu)F^{l}_{q''}(\mu) \overset{\text{s.a.}}{=} 0 \tag{10-36}$$

The last term of Eq. (10-28) can be rewritten as:

$$\begin{aligned}&\langle \Phi_\mu \big| \tilde{a}^{ij}_{ab}(\mu)\big[\hat{H}^{\text{comp}}_N(\mu)e^{\hat{S}(\mu)}\big]_{\text{DC,L}} \big| \Phi_\mu \rangle \\ &\quad = \langle \Phi_\mu \big| \tilde{a}^{i}_{a}(\mu)\big[\hat{H}^{\text{comp}}_N(\mu)e^{\hat{S}(\mu)}\big]_{\text{C}} \big| \Phi_\mu \rangle\, t^{j}_{b}(\mu)\,. \end{aligned} \tag{10-37}$$

Finally, last term of Eq. (10-30) can be expressed as

$$\begin{aligned}&\langle \Phi_\mu \big| \big[\tilde{\mathcal{R}}^{kl}_{ij}(\mu)\big]^\dagger \big[\hat{H}_N(\mu)e^{\hat{S}(\mu)}\big]_{\text{DC,L}} \big| \Phi_\mu \rangle \\ &\quad = -\langle \Phi_\mu \big| \tilde{a}^{k}_{a}(\mu)\big[\hat{H}_N(\mu)e^{\hat{S}(\mu)}\big]_{\text{C}} \big| \Phi_\mu \rangle\, \mathcal{X}^{an}_{ij}c^{l}_{n}(\mu) \\ &\quad = \langle \Phi_\mu \big| \tilde{a}^{k}_{\alpha}(\mu)\big[\hat{H}_N(\mu)e^{\hat{S}(\mu)}\big]_{\text{C}} \big| \Phi_\mu \rangle \big[\bar{F}^{\alpha b}_{ij}(\mu)t^{l}_{b}(\mu) - \bar{F}^{\alpha\beta}_{ij}(\mu)F^{n}_{\beta}(\mu)c^{l}_{n}(\mu)\big]. \end{aligned} \tag{10-38}$$

In CABS approximation, it is legitimate to replace spin-orbitals from the complete complementary space (α) by those from the CABS space (p'') and evaluate the connected terms in brackets as in CCSD-R12. As soon as we assume the generalized Brillouin condition for each reference, i.e.

$$f^{\alpha}_{i}(\mu) = 0\,, \tag{10-39}$$

Equations (10-32) and (10-38) are identically equal to zero, which is the case within the standard approximation.

Validity of Eq. (10-39) is ensured when the (computational) basis set is saturated at the one-particle level for all the references. Then also $\hat{\mathcal{R}}_1(\mu)$ disappears. Hence, $\hat{\mathcal{R}}_1(\mu)$ reflects the basis set unsaturation error for occupied orbitals. In a sense, this operator treats the single-excitations into the complementary space as externally contracted. Alternatively, one can recover the deficiency of the one-particle basis by defining an additional single excitation operator onto the complementary space spanned by finite auxiliary basis that, together with the computational set, forms a one-particle basis close to the Hartree – Fock limit. Such approach involves more variational parameters, but it is computationally more demanding than treating of $\hat{\mathcal{R}}_1$ [73].

10.5. RESULTS AND DISCUSSION

Current implementation was based on our open shell UHF based code [74]. The potential of the suggested MR BW-CCSD-R12 ansatz was here preliminary tested on the H4 model. First suggested by Jankowski and Paldus [75], this model system consists of four hydrogen atoms arranged in an isosceles trapezoid geometry, with a fixed distance of 2 a.u. between the neighboring hydrogens. The geometry can be parameterized by the angle θ between the height and the side of the trapezoid. Hence, θ varies from 0 to $\pi/2$. The value of θ=0 corresponds to a square structure when the HOMO and LUMO orbitals are degenerate, which results in a strong multireference character. Conversely, θ=$\pi/2$ leads to a linear configuration when the HOMO and LUMO orbitals are well separated and single reference treatment is sufficient.

The calculations were performed using the parent 9*s*6*p*4*d*3*f* R12 suited basis set [76] and its subsets that remain after the subsequent removing of the highest angular momentum functions. Remaining basis sets will be (also) referred to as *s* (9*s*), *sp* (9*s*6*p*), *spd* (9*s*6*p*4*d*) and *spdf* (9*s*6*p*4*d*3*f*). Since the occupied molecular orbitals are dominantly built from atomic *s* orbitals, with these basis sets we could apply the standard approximation, although being aware that higher angular momentum functions are of non-negligible importance for occupied orbitals, too. With (properly used) standard approximation it does not make much difference if one uses r_{12} or STG as the correlation factor [9]. For these model results, we used r_{12} and hence eliminated the potential geometry dependence of the optimal STG exponent.

The model space included two reference configurations 220 and 202. The two monoexcited references could be omitted due to symmetry considerations. For our purpose, the size-extensivity correction was not employed.

Total energies calculated by both conventional and explicitly correlated MR BW-CCSD method are listed in Table 10-1. Let us consider the *spdf* R12 results as the reference ones. Much faster convergence of the R12 results in this basis set hierarchy towards the basis set limit values is evident in the whole range of the investigated geometries. With conventional MR BW-CCSD the maximum errors vary

Table 10-1. Geometry and basis set dependence of the total MR BW-CCSD energies for the H4 model. Energies are in E_h. For geometry and basis set specification see the text

θ/π	9s	9s6p	9s6p4d	9s6p4d3f
	MR BW-CCSD			
0.00	−2.060940	−2.093642	−2.099197	−2.099945
0.01	−2.066665	−2.099243	−2.104712	−2.105459
0.02	−2.075590	−2.108671	−2.114027	−2.114768
0.05	−2.107262	−2.141413	−2.146454	−2.147165
0.10	−2.150466	−2.184585	−2.189177	−2.189832
0.15	−2.178381	−2.211920	−2.216144	−2.216757
0.20	−2.195831	−2.228688	−2.232656	−2.233240
0.30	−2.213793	−2.245392	−2.249073	−2.249622
0.50	−2.223060	−2.253237	−2.256894	−2.257451
	MR BW-CCSD-R12			
0.00	−2.126476	−2.101485	−2.100409	−2.100515
0.01	−2.134080	−2.107145	−2.105988	−2.106051
0.02	−2.144353	−2.116592	−2.115355	−2.115386
0.05	−2.175869	−2.149112	−2.147820	−2.147815
0.10	−2.213502	−2.191568	−2.190495	−2.190480
0.15	−2.235512	−2.218008	−2.217395	−2.217391
0.20	−2.247468	−2.234145	−2.233851	−2.233857
0.30	−2.256754	−2.250125	−2.250196	−2.250217
0.50	−2.259192	−2.257913	−2.258016	−2.258039

from ∼40 mE_h for the *s* basis to ∼6, ∼1.3 and ∼0.5 mE_h for *sp*, *spd* and *spdf* basis sets, respectively, whereas with R12 approach these errors are reduced to ∼26, ∼1.0, and ∼0.1 mE_h, respectively, from *s* to *spd*. At the first glance, one can observe the inadequacy of the pure *s* basis. Even though the absolute error is significantly reduced with the R12 approach, the energies are overestimated too much. Such behavior occurs when the "standard approximation" is not fully justified. Nevertheless, we have included the latter results for illustration.

Of course, in the light of our knowledge of the performance of the R12 theory the aforementioned convergence within the basis set hierarchy has been expected. In an MR approach it is also desirable to investigate the relative performance with the changing ratio of the reference configurations. This is illustrated in Figure 10-1, where the errors relative the reference *spdf* numbers are monitored with respect to the changing angle θ. Ideal behavior would correspond to straight lines parallel to the *x*-axis. Note that both axes are in logarithmic scale which provided a meaningful comparison for all the results in a single figure. On the other hand, tiny differences at high accuracy level are more pronounced. Nevertheless, the figure clearly shows that, though the R12 *sp* results reach the absolute accuracy between conventional *spd*

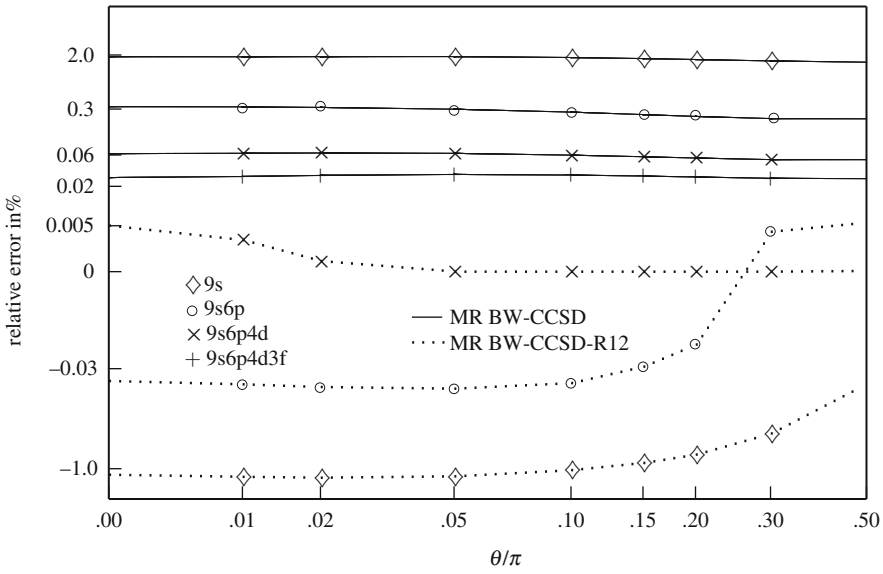

Figure 10-1. Relative energy errors with respect to *spdf* MR BW-CCSD-R12 values as functions of the basis set and the geometry of the H4 model. For description of geometries and basis sets see the text

and *spdf* values, relative error with the changing geometry varies little more than for the aforementioned conventional calculations. Despite the R12 *spd* curve is still not perfect, one has to realize that the relative error itself is essentially by an order of magnitude smaller than for the best conventional results. Generally, with all basis sets, the accuracy of the R12 corrected numbers is somewhat higher when a single reference determinant dominates.

Finally, in the MR R12 approach one is curious to see whether, and/or to which extent, the R12 corrections influence the relative importance of the reference configurations. The weights of these configurations are calculated as products of the corresponding elements of the right and left eigenvectors of the effective Hamiltonian. For selected geometries, the values are listed in Table 10-2. As seen, changes after inclusion of the R12 terms are small, but noticeable especially with smaller basis sets. Regardless of the ill-behaved *s* basis, with *sp* set the changes make as much as 2% for geometries of multireference character. From the theoretical point of view the weights of individual references should not change (too much), since via R12 approach the "dynamic correlation" is treated. Too large changes may indicate an unbalanced treatment for individual references. Indeed, the larger errors for *s* and *sp* R12 results seem to be related to this phenomenon.

Table 10-2. Comparison of the reference determinants weights for the H4 model at selected geometries using conventional and explicitly correlated MR BW-CCSD

		Reference configuration			
		220	202	220	202
Basis set	θ/π	MR BW-CCSD		MR BW-CCSD-R12	
9*s*	0.00	0.5695	0.4304	0.6496	0.3504
	0.02	0.8424	0.1575	0.8870	0.1130
	0.10	0.9859	0.0140	0.9894	0.0106
	0.20	0.9957	0.0042	0.9967	0.0033
	0.50	0.9986	0.0013	0.9989	0.0011
9*s*6*p*	0.00	0.5752	0.4247	0.5827	0.4173
	0.02	0.8781	0.1218	0.8832	0.1168
	0.10	0.9918	0.0081	0.9922	0.0078
	0.20	0.9976	0.0023	0.9977	0.0023
	0.50	0.9992	0.0007	0.9992	0.0008
9*s*6*p*4*d*	0.00	0.5766	0.4233	0.5799	0.4201
	0.02	0.8792	0.1207	0.8809	0.1191
	0.10	0.9931	0.0068	0.9932	0.0068
	0.20	0.9984	0.0015	0.9985	0.0015
	0.50	0.9996	0.0003	0.9996	0.0004
9*s*6*p*4*d*3*f*	0.00	0.5767	0.4232	0.5781	0.4219
	0.02	0.8793	0.1206	0.8802	0.1198
	0.10	0.9932	0.0067	0.9933	0.0067
	0.20	0.9985	0.0014	0.9985	0.0015
	0.50	0.9996	0.0003	0.9996	0.0004

10.6. CONCLUSION

In this chapter, we have shown that generalization of the CC-R12 theory to a multireference case is a relatively straightforward task. We have implemented and tested the MR BW-CCSD-R12 for the H4 model. Though the absolute energies converge much faster to the basis set limit values than using the conventional approach, special care should be devoted to a balanced treatment for all the reference determinants.

ACKNOWLEDGMENTS

This work has been supported by the Grant Agency of the Ministry of Education of the Slovak Republic and Slovak Academy of Sciences (VEGA project No. 2/0079/09) and by the Slovak Research and Development Agency (APVV 20-018405, LPP-0343-09), as well as by the Grant Agency of the Czech Republic (GACR Project No. 203/07/0070). Also, this work has benefited from the Centers of Excellence program of the Slovak Academy of Sciences (COMCHEM, Contract no. II/1/2007).

REFERENCES

1. W. Kutzelnigg, Theor. Chim. Acta **68**, 445 (1985)
2. W. Kutzelnigg, J. D. Morgan III, J. Chem. Phys. **96**, 4484 (1992)
3. W. Kutzelnigg, W. Klopper, J. Chem. Phys. **94**, 1985 (1991)
4. W. Klopper, W. Kutzelnigg, Chem. Phys. Lett. **134**, 17 (1987)
5. W. Klopper, R. Röhse, W. Kutzelnigg, Chem. Phys. Lett. **178**, 455 (1991)
6. J. Noga, W. Kutzelnigg, W. Klopper, Chem. Phys. Lett. **199**, 497 (1992)
7. S. Ten-no, Chem. Phys. Lett. **398**, 56 (2004)
8. S. Ten-no, J. Chem. Phys. **126**, 014108 (2007)
9. J. Noga, S. Kedžuch, J. Šimunek, S. Ten-No, J. Chem. Phys. **128**, 174103 (2008,); J. Chem. Phys. **130** 029901 (2009) (E)
10. D. Bokhan, S. Ten-no, J. Noga, Phys. Chem. Chem. Phys. **23**, 3320 (2008)
11. D. P. Tew, W. Klopper, C. Neiss, C. Hättig, Phys. Chem. Chem. Phys. **9**, 1921 (2007)
12. S. Hofener, F. A. Bischoff, A. Gloss, W. Klopper, Phys. Chem. Chem. Phys. **10**, 3390 (2008)
13. D. P. Tew, W. Klopper, C. Hättig, Chem. Phys. Lett. **452**, 326 (2008)
14. S. Hofener, D. P. Tew, W. Klopper, T. Helgaker, Chem. Phys. **356**, 25 (2009)
15. T. Shiozaki, M. Kamiya, S. Hirata, E. F. Valeev, J. Chem. Phys. **130**, 054101 (2009)
16. E. F. Valeev, Phys. Chem. Chem. Phys. **10**, 106 (2008)
17. F. R. Manby, H.-J. Werner, T. B. Adler, A. J. May J. Chem. Phys. **124**, 094103 (2006)
18. H.-J. Werner, T. B. Adler, F. R. Manby, J. Chem. Phys. **126**, 164102 (2007)
19. T. B. Adler, G. Knizia, H.-J. Werner, J. Chem. Phys. **127**, 221106 (2007)
20. A. Köhn, G. W. Richings, D. Tew, J. Chem. Phys. **129**, 201103 (2008)
21. W. Klopper, F. R. Manby, S. Ten-no, E. F. Valeev, Int. Rev. Phys. Chem. **25**, 427 (2006)
22. J. Noga, W. Kutzelnigg, J. Chem. Phys. **101**, 7738 (1994)
23. J. Noga, W. Kutzelnigg, W. Klopper, in *Recent Advances in Computational Chemistry*, vol. 3, Ed. R. J. Bartlett (World Scientific, Singapore, 1997), p. 1
24. J. R. Gdanitz, Chem. Phys. Lett. **210**, 253 (1993)
25. J. R. Gdanitz, R. Röhse, Int. J. Quantum Chem. **55**, 147 (1995), Int. J. Quantum Chem. **59** 505 (1996) (E)
26. S. Ten-no, Chem. Phys. Lett. **447**, 175 (2007)
27. I. Lindgren, D. Mukherjee, Phys. Rep. **151**, 93 (1987)
28. D. Mukherjee, S. Pal, Adv. Quant. Chem. **20**, 292 (1989)
29. B. Jeziorski, H. J. Monkhorst, Phys. Rev. A **24**, 1668 (1981)
30. P. Piecuch, J. Paldus, Theor. Chim. Acta **83**, 69 (1992)
31. J. Paldus, P. Piecuch, L. Pylypow, B. Jeziorski, Phys. Rev. A **47**, 2738 (1993)
32. P. Piecuch, J. Paldus, Phys. Rev. A **49**, 3479 (1994)
33. P. Piecuch, J. Paldus, J. Chem. Phys. **101**, 5875 (1994)
34. S. A. Kucharski, R. J. Bartlett, J. Chem. Phys. **95**, 8227 (1991)
35. I. Hubač, in *New Methods in Quantum Theory*, Eds. vol. 8 of *NATO ASI Series 3: High Technology*, A. Tsipis, V. S. Popov, D. R. Herschbach, J. S. Avery (Kluwer, Dordrecht, 1996), pp. 183–202
36. I. Hubač, J. Mášik, P. Mach, J. Urban, P. Babinec, in *Computational Chemistry. Reviews of Current Trends.*, vol. 3, Ed. J. Leszczynski (World Scientific, Singapore, 1999), pp. 1–48
37. J. Mášik, I. Hubač, Adv. Quant. Chem. **31**, 75 (1998)
38. J. Mášik, I. Hubač, in *Quantum Systems in Chemistry and Physics: Trends in Methods and Applications*, Eds. R. McWeeny, J. Maruani, Y. G. Smeyers, S. Wilson (Kluwer Academic Publishers, Dordrecht, 1997), pp. 283–308

39. J. Pittner, P. Nachtigall, P. Čársky, J. Mášik, I. Hubač, J. Chem. Phys. **110**, 10275 (1999)
40. J. Pittner, J. Chem. Phys. **118**, 10876 (2003)
41. J. Pittner, P. Piecuch, Mol. Phys. **107**, 1209 (2009)
42. U. S. Mahapatra, B. Datta, B. Bandyopadhyay, D. Mukherjee, Adv. Quant. Chem. **30**, 163 (1998)
43. U. S. Mahapatra, B. Datta, D. Mukherjee, J. Chem. Phys. **110**, 6171 (1999)
44. F. A. Evangelista, W. D. Allen, H. F. Schaefer III, J. Chem. Phys. **127**, 024102 (2007)
45. F. A. Evangelista, A. C. Simmonett, W. D. Allen, H. F. Schaefer III, J. Gauss, J. Chem. Phys. **128**, 124104 (2008)
46. M. Hanrath, J. Chem. Phys. **123**, 084102 (2005)
47. M. Hanrath, Chem. Phys. Lett. **420**, 426 (2006)
48. I. Hubač, J. Pittner, P. Čársky, J. Chem. Phys. **112**, 8779 (2000)
49. J. Pittner, O. Demel, P. Čársky, I. Hubač, Int. J. Mol. Sci. **2**, 281 (2002)
50. J. Pittner, P. Čársky, I. Hubač, Int. J. Quant. Chem. **90**, 1031 (2002)
51. J. Pittner, J. Šmydke, P. Čársky, I. Hubač, J. Molec. Struc. (Theochem) **547**, 239 (2001)
52. I. S. K. Kerkines, J. Pittner, P. Čársky, A. Mavridis, I. Hubač, J. Chem. Phys. **117**, 9733 (2002)
53. V. I. Teberekidis, I. S. K. Kerkines, C. A. Tsipis, P. Čársky, A. Mavridis, Int. J. Quant. Chem. **102**, 762 (2005)
54. S. Kardahakis, J. Pittner, P. Čársky, A. Mavridis, Int. J. Quant. Chem. **104**, 458 (2005)
55. M. Tobita, S. A. Perera, M. Musial, R. J. Bartlett, M. Nooijen, J. S. Lee, J. Chem. Phys. **119**, 10713 (2003)
56. J. C. Sancho-Garca, J. Pittner, P. Čársky, I. Hubač, J. Chem. Phys. **112**, 8785 (2000)
57. J. Pittner, P. Nachtigall, P. Čársky, I. Hubač, J. Phys. Chem. A **105**, 1354 (2001)
58. O. Rey-Puiggros, J. Pittner, P. Čársky, P. Stampfu, W. Wenzel, Collect. Czech. Chem. Commun. **68**, 2309 (2003)
59. O. Demel, J. Pittner, P. Čársky, I. Hubač, J. Phys. Chem. A **108**, 3125 (2004)
60. I. S. K. Kerkines, P. Čársky, A. Mavridis, J. Phys. Chem. A **109**, 10148 (2005)
61. J. Brabec, J. Pittner, J. Phys. Chem. A **110**, 11765 (2006)
62. L. Veis, P. Čársky, J. Pittner, J. Michl, Collect. Czech. Chem. Commun. **73**, 1525 (2008)
63. X. Li, J. Paldus, J. Chem. Phys. **119**, 5320 (2003)
64. X. Li, J. Paldus, J. Chem. Phys. **119**, 5334 (2003)
65. X. Li, J. Paldus, J. Chem. Phys. **119**, 5346 (2003)
66. X. Li, J. Paldus, Int. J. Quant. Chem. **99**, 914 (2004)
67. J. Pittner, X. Li, J. Paldus, Mol. Phys. **103**, 2239 (2005)
68. E. F. Valeev, Chem. Phys. Lett. **395**, 190 (2004)
69. J. Paldus, in *Relativistic and Electron Correlation Effects in Molecules and Solids*, Ed. G. I. Malli (Plenum Press, New York, 1994), p. 207
70. J. Noga, S. Kedžuch, J. Šimunek, J. Chem. Phys. **127**, 034106 (2007)
71. W. Klopper, C. C. M. Samson, J. Chem. Phys. **116**, 6397 (2002)
72. S. Kedžuch, M. Milko, J. Noga, Int. J. Quantum Chem. **105**, 929 (2005)
73. J. Noga, J. Šimunek, Chem. Phys. **356**, 1 (2009)
74. J. Noga, P. Valiron, Chem. Phys. Lett. **324**, 166 (2000)
75. K. Jankowski, J. Paldus, Int. J. Quantum Chem. **18**, 1243 (1980)
76. J. Noga, P. Valiron, Collect. Czech. Chem. Commun. **68**, 340 (2003)

CHAPTER 11

COUPLED CLUSTER TREATMENT OF INTRAMONOMER CORRELATION EFFECTS IN INTERMOLECULAR INTERACTIONS

TATIANA KORONA

Faculty of Chemistry, University of Warsaw, 02-093 Warsaw, Poland,
e-mail: tania@chem.uw.edu.pl

Abstract: An adequate account of the effects of intramonomer correlation is indispensable to obtain an accurate representation of intermolecular potentials in symmetry-adapted perturbation theory (SAPT) calculations. These intramonomer correlation effects have initially been taken into account by employing Møller-Plesset perturbation theory, i.e., using the SAPT(MP) method, and more recently by applying density functional theory within the SAPT(DFT) approach. In this review a new approach, called SAPT(CC), is presented, in which the intramonomer correlation effects are treated by coupled cluster (CC) theory. Specifically, in the SAPT(CC) method each interaction energy component predicted by SAPT is expressed via monomer properties (density matrices, density susceptibilities and their generalizations) obtained from coupled cluster theory. In practice, the expectation-value approach to coupled cluster properties has been found most useful. The SAPT(CC) approach was implemented in practice at the SAPT(CCSD) level by including only singly and doubly excited parts of the cluster operator. At this level, the theory is exact for the interaction of two-electron monomers, i.e., takes into account (connected) triple and quadruple excitation contributions appearing in the supermolecular CC calculations of the interaction energy. The results obtained thus far using the SAPT(CCSD) approach are reviewed and compared with results of the corresponding SAPT(MP) and SAPT(DFT) treatments. The quality of the SAPT(CCSD) method is also examined by comparison with high-level supermolecular calculations performed using the CCSD(T), CCSDT(Q) and CCSDTQ methods.

Keywords: Symmetry-adapted perturbation theory, Coupled cluster, Intermolecular interactions, Intramonomer correlation

11.1. INTRODUCTION

The concept of intermolecular interaction energy, or intermolecular potential, plays a central role in describing many phenomena in chemistry and physics, ranging from bulk properties of gases to biochemical processes [1]. A single point on the

P. Čársky et al. (eds.), Recent Progress in Coupled Cluster Methods, 267–298.
DOI 10.1007/978-90-481-2885-3_11,

intermolecular potential energy surface (PES) for a noncovalent complex (dimer) AB [2] is defined as the difference between the energy of a dimer and a sum of the energies of monomers A and B

$$E_{\text{int}} = E_{AB} - (E_A + E_B), \tag{11-1}$$

where the energies E_{AB}, E_A, and E_B are eigenvalues of the electronic Hamiltonians of a dimer (H_{AB}) and of monomers (H_A and H_B), respectively. In Eq. (11-1) the geometrical coordinates of monomers' nuclei are kept unchanged in the dimer, therefore the interaction energy defined by Eq. (11-1) is not identical with the so-called electronic binding energy [3]. Theoretical methods devoted for a calculation of the interaction energy can be divided into two classes: supermolecular (SM) and perturbational (PT) ones. In the first class Eq. (11-1) is directly applied with some approximate energies of a dimer and monomers used instead of the exact ones. For a detailed discussion of virtues and weaknesses of the SM method the reader is referred to, e.g., Refs. [1, 4]. Here we only mention that two necessary conditions for approximate energies in Eq. (11-1) are: the size-extensivity [5] of the selected method and a proper elimination of the basis-set superposition error (BSSE) [6].

Contrary to the SM approach, a PT interaction energy is obtained directly as a sum of some energy corrections. From several initial attempts to formulate a PT theory of intermolecular interactions, capable to describe the whole intermolecular potential energy surface, i.e. repulsion, minimum, and large-distance regions in a uniform way, the perturbational approach presented in Refs. [7–15] has proven to be the most successful. This approach, called symmetry-adapted perturbation theory (SAPT), has been used in numerous studies of noncovalent complexes after the first version of the SAPT program [16] has been released almost 20 years ago. For details of the historical development of SAPT the reader is referred to the reviews [1, 17] and references therein. In this place only a general overview of SAPT will be presented, necessary to establish key definitions and notation.

In perturbation theory of intermolecular interactions a natural candidate for the unperturbed part of the total Hamiltonian H_{AB} is the sum of the monomer Hamiltonians H_A and H_B. The perturbation V, usually called the intermolecular interaction operator, is thus defined as the difference between the Hamiltonian of a dimer and the Hamiltonians of monomers. If Rayleigh-Schrödinger perturbation theory (RSPT) is applied to such a division of the dimer's Hamiltonian, the so-called polarization theory of intermolecular interactions [18] is obtained. The RSPT interaction energy up to the second order in terms of V is composed of the first-order electrostatic ($E^{(1)}_{\text{elst}}$), and the second-order induction ($E^{(2)}_{\text{ind}}$) and dispersion ($E^{(2)}_{\text{disp}}$) energies. Unfortunately, the sum of polarization corrections alone fails to describe correctly these regions of PES, where the overlap between electron clouds of monomers is nonnegligible. This failure can be traced down to the improper permutational symmetry of approximate wave functions (i.e. RSPT wave functions of a finite kth order, $\Psi^{(k)}_{\text{pol}}$, are not antisymmetric with respect to transpositions of electrons belonging to

different monomers). As a solution of this problem, a forcing of the antisymmetry in the equations for energy and (in some variants of the method) for wave function corrections has been proposed [7, 8, 10, 19]. In the simplest case of the symmetrized Rayleigh-Schrödinger theory (SRS) [8] the unmodified RSPT wave functions are utilized and the symmetry-forcing is applied to the energy formulae only. Because of its simplicity and accuracy in a low order the SRS method is utilized in nearly all practical SAPT developments. The SRS interaction energy through the second order includes (in addition to the three polarization corrections mentioned above) the first-order exchange energy ($E^{(1)}_{\mathrm{exch}}$), and the second-order exchange-induction ($E^{(2)}_{\mathrm{exch-ind}}$) and exchange-dispersion ($E^{(2)}_{\mathrm{exch-disp}}$) energies.

It should be stressed that the convergence properties of polarization theory, as well as of SRS and other symmetry-forcing methods are far from being trivial. As a matter of fact, it is now well known that the SRS perturbation series for the energy and wave function diverge for all but for the smallest (one- and two-electron) monomers [20] (for a review see Refs. [1, 17] and references therein). From the perspective of years of applications one can say that the success of SAPT relies mostly on a fortunate circumstance that this divergent series usually provides an excellent approximation to the interaction energy in a low (usually second) order [21].

Another complication for a practical use of SRS arises from the fact that exact monomer energies and wave functions, appearing in the RSPT formulae, are not known, and their approximate counterparts should be used instead. The easiest solution to this problem consists in replacing the unknown exact monomer wave functions with Hartree-Fock (HF) determinants, leading to the approach denoted here as SAPT(HF). If such a replacement is performed, the *intra*monomer electron correlation effects resulting from the Coulomb repulsion are simply neglected in the SAPT interaction energy. However, it can be predicted that these effects play a significant role in the SAPT interaction energy, since on the one hand electron correlation contributes substantially to molecular properties and – on the other hand – there is a close relation between molecular properties and perturbation energy components (*vide infra*). So far the effect of intramonomer correlation has been treated on the level of Møller-Plesset (MP) theory or density functional theory (DFT), what gives methods denoted here as SAPT(MP) [9, 11–15, 22, 23] or SAPT(DFT) [24–31]. In SAPT(MP) the interaction energy is expanded in terms of three perturbations: V, W_A and W_B, where W_X is a fluctuation potential of the monomer X ($X = A, B$). This expansion gives rise to a triple perturbation series with expansion coefficients of the type $E^{(nij)}$, where n, i, j are powers of the perturbations V, W_A and W_B, respectively. The highest MP level used in practice for SAPT(MP) ranges from three (first-order electrostatics) through two (first-order exchange and second-order induction and dispersion energies) and down to zero (second-order exchange energies). The major disadvantage of the SAPT(MP) approach is its dependence on the convergence behavior of the MP perturbation series. If for some monomer in the complex under study the MP series is divergent [32], the reliability of the SAPT(MP) corrections for intramonomer correlation becomes questionable. A more recent SAPT(DFT) method has

been simultaneously developed in two groups: Misquitta, Jeziorski, and Szalewicz added the SAPT(DFT) functionality to the SAPT program [16], while Heßelmann and Jansen implemented their program into the MOLPRO suite of codes [33]. It should be noted that these two SAPT(DFT) formulations are not identical, since in the method of Misquitta et al. the uncoupled Kohn-Sham (KS) propagators are used for the calculation of the second-order exchange energy,[1] while the coupled KS propagators are utilized by Heßelmann and Jansen for this purpose.

Another popular way of accounting for electron correlation is provided by coupled cluster (CC) theory. If CC theory is applied to the intramonomer correlation effects of SAPT energy components, a new SAPT(CC) method is obtained [34–42]. This method will be described in detail in the next Sections.

11.2. LOW-ORDER SAPT TERMS AND THEIR RELATION TO MONOMER PROPERTIES

An important feature of SAPT is a possibility of expressing its energy components through monomer properties. This virtue of SAPT results in a deeper understanding of processes occurring in interacting molecules, and – from a practical point of view – allows the methods, which were originally designed for a treatment of molecular properties, to be easily adapted for needs of the SAPT approach. Noteworthy, a description of the polarization energy in terms of monomer properties facilitates a derivation of an asymptotic form of the interaction energy, which is consistent with finite-distance SAPT calculations. Monomer properties used as "building blocks" of SAPT corrections are: reduced density matrices, cumulants of reduced density matrices, frequency-dependent density susceptibilities and straightforward generalizations of the latter quantity, denoted as frequency-dependent density-matrix susceptibilities. All these quantities will be presented and discussed in a context of first- and second-order SAPT energy contributions. Since only reduced density matrices will be discussed here, the word *reduced* will be omitted in the rest of this article.

11.3. POLARIZATION ENERGIES

As already mentioned in Section 11.1, polarization energies are obtained by a direct application of RSPT to the dimer Hamiltonian H_{AB} divided into the unperturbed part $H_0 = H_A + H_B$ and the perturbation V. For a concise notation in the next sections, it will be convenient to express the operator V in terms of the generalized interaction potential $v(i,j)$ [22]

[1] The uncoupled KS exchange-induction and exchange-dispersion energies are then corrected by a scaling procedure to estimate the coupling effect.

$$V = \sum_{i=1}^{N_A} \sum_{j=1+N_A}^{N_A+N_B} v(i,j), \tag{11-2}$$

where N_A and N_B denote the numbers of electrons in monomers A and B, respectively, and the pair potential $v(i,j)$ is defined as

$$v(i,j) = \frac{1}{r_{ij}} - \frac{1}{N_B} \sum_{\beta \in B} \frac{Z_\beta}{r_{\beta i}} - \frac{1}{N_A} \sum_{\alpha \in A} \frac{Z_\alpha}{r_{\alpha j}} + \frac{1}{N_A N_B} \sum_{\alpha \in A} \sum_{\beta \in B} \frac{Z_\alpha Z_\beta}{R_{\alpha\beta}} \tag{11-3}$$

(i stands for coordinates of the ith electron, including spin, while $\mathbf{r}_i$ will denote spatial coordinates only).[2] The following energy corrections are obtained from RSPT, where E_X^n, Ψ_X^n ($X = A, B$) are eigenvalues and eigenvectors of H_X ($n = 0$ denotes the ground state)

$$E_{\text{elst}}^{(1)} = \langle \Psi_A^0 \Psi_B^0 | V \Psi_A^0 \Psi_B^0 \rangle, \tag{11-4}$$

$$E_{\text{ind}}^{(2)} = \langle \Psi_A^0 | V_{\text{B}} \Psi_{\text{ind,A}}^{(1)} \rangle + A \leftrightarrow B, \tag{11-5}$$

$$E_{\text{disp}}^{(2)} = \langle \Psi_A^0 \Psi_B^0 | V \Psi_{\text{disp}}^{(1)} \rangle. \tag{11-6}$$

Here $V_{\text{B}} = \left\langle \Psi_B^0 \middle| V \Psi_B^0 \right\rangle$ and $A \leftrightarrow B$ means that the second term should be added for the induction energy with A and B indices interchanged. The first-order induction and dispersion wave functions are defined through the following equations

$$\Psi_{\text{ind,A}}^{(1)} = -\sum_{n=1}^{\infty} \frac{\left|\Psi_A^n\right\rangle \left\langle \Psi_A^n \middle| V_{\text{B}} \Psi_A^0 \right\rangle}{\Delta E_A^n}, \tag{11-7}$$

$$\Psi_{\text{disp}}^{(1)} = -\sum_{n=1}^{\infty} \sum_{m=1}^{\infty} \frac{\left|\Psi_A^n \Psi_B^m\right\rangle \left\langle \Psi_A^n \Psi_B^m \middle| V \Psi_A^0 \Psi_B^0 \right\rangle}{\Delta E_A^n + \Delta E_B^m}, \tag{11-8}$$

where $\Delta E_X^n = E_X^n - E_X^0$. A total first-order polarization wave function is given by the formula

$$\Psi_{\text{pol}}^{(1)} = \Psi_{\text{ind,A}}^{(1)} \Psi_B^0 + \Psi_A^0 \Psi_{\text{ind,B}}^{(1)} + \Psi_{\text{disp}}^{(1)}. \tag{11-9}$$

Bearing in mind that V is a two-body operator (a "body" means an electron in this case), one can integrate r.h.s. of Eqs. (11-4), (11-5), (11-6), (11-7), and (11-8) over coordinates of all but two electrons. This procedure leads to formulae for polarization

[2] It is worthwhile to note that $v(i,j)$, unlike the pure interelectron repulsion operator r_{ij}^{-1}, is nonsymmetric, i.e. $v(i,j) \neq v(j,i)$.

energies described in terms of various monomer properties which will be analyzed in detail in Sections 11.3.1, 11.3.2, and 11.3.3.

11.3.1. Electrostatic Energy

The electrostatic energy is expressed through monomer properties by the following formula

$$E^{(1)}_{\mathrm{elst}} = \int \rho_A(1) v(1,1') \rho_B(1') d\tau_1 d\tau'_1, \tag{11-10}$$

where $\rho_X(i)$ denotes the one-electron density of the monomer X. The one-electron density can be viewed as a diagonal part of the one-electron density matrix $\rho(1|1')$ [43]

$$\rho(1|1') = N \int \Psi^0(1,2,\ldots,N)^* \Psi^0(1',2,\ldots,N) d\tau_2 \ldots \tau_N, \tag{11-11}$$

i.e. we have an identity $\rho(1) = \rho(1|1)$. In Eq. (11-11) Ψ^0 denotes the ground-state wave function for a system of N electrons. Eq. (11-10) validates a well-known interpretation of the electrostatic energy as being a result of the interaction between unperturbed electron clouds of monomers. Noteworthy, Eq. (11-10) in a somewhat different form (with a bare interelectron repulsion and with a total charge distribution) appeared in the literature already in 1956 [44].

Since first-order properties and therefore one-electron densities are available for many ab initio methods, it is relatively easy to apply them for a calculation of the electrostatic energy. As a result, there exist numerous calculations of the electrostatic energies for various electron-correlated methods, described in Ref. [22] for MPn ($n = 2, 3, 4$), Ref. [45] for BCCD, or Ref. [34] for LR-CCSD and QCISD(T) methods. In the present SAPT(CC) approach these densities are obtained from expectation-value coupled cluster theory XCC (X in the abbreviation comes from the word "expectation"), which has been proposed by Jeziorski and Moszynski some time ago [46].

In XCC theory the first-order property of an operator X is calculated from the following expression

$$\overline{X} = \langle e^{S^\dagger} e^{-T} X e^{T} e^{-S^\dagger} \rangle, \tag{11-12}$$

where the abbreviation $\langle Z \rangle = \langle \Phi | Z \Phi \rangle$ has been introduced (Φ is the reference determinant) and T denotes the usual cluster operator of CC theory. Equation (11-12) has been derived by inserting the normalized CC ansatz for the wave function into the formula for the expectation value of an operator X and by introducing a new excitation operator S, which is defined through the equation [46]

$$e^S \Phi = \frac{e^{T^\dagger} e^T \Phi}{\langle e^{T^\dagger} e^T \rangle}. \tag{11-13}$$

It has been proven [13, 46] that the S operator is a connected quantity, as it satisfies a linear equation containing a finite number of multiple commutators of T and $T^\dagger$. The connectedness of S and T operators implies that r.h.s. of Eq. (11-12) is also connected (provided that the operator X is connected itself). This feature can be most easily demonstrated by applying twice the nested-commutator expansion

$$e^{-A} B e^A = B + [B, A] + \frac{1}{2!}[[B, A], A] + \ldots, \tag{11-14}$$

to Eq. (11-12). The formula for a first-order property presented in Eq. (11-12) is therefore explicitly size-extensive.

An implementation of XCC theory has been reported in Ref. [36] for T limited to single and double excitations (CCSD theory). If the T operator is taken from CCSD theory, the expression for the first-order property $\overline{X}$ is simplified to

$$\begin{aligned} \overline{X} = \langle X \rangle + \langle S_1 | X \rangle + \langle X T_1 \rangle + \langle S_2 | [X, T_2] \rangle + \langle S_1 | [X, T_2] \rangle + \langle S_1 | [X, T_1] \rangle + \\ + \langle S_2 | [[X, T_1], T_2] \rangle + \mathcal{O}(W^5). \end{aligned} \tag{11-15}$$

In this formula the abbreviation $\langle Y | Z \rangle = \langle Y \Phi | Z \Phi \rangle$ has been used. The contributions of the fifth and higher orders in terms of the fluctuation operator W ($W = H - F$) have been also derived and implemented, but usually they contribute very little to the property $\overline{X}$. It should be noted that a proper factorization of Eq. (11-15) allows to make its computational cost insignificant in comparison to the time spent on the calculation of the cluster operator T.

The recursive formula for the S operator is highly nonlinear in T and $T^\dagger$ (see Eq. (23) of Ref. [46]) and needs to be truncated for practical reasons. A systematic way of selection of the most important terms in the equation for S has been proposed by Moszynski et al. [47]. The scheme presented in Ref. [47] is based on the neglect of contributions containing more than some prescribed number of T and $T^\dagger$ operators. For the case of CCSD theory the S operator up to cubic terms is presented below,

$$\begin{aligned} S = T + \widehat{\mathcal{P}}_1([T_1^\dagger, T_2]) + \frac{1}{2}\widehat{\mathcal{P}}_2([[T_2^\dagger, T_2], T_2]) + \widehat{\mathcal{P}}_2([[T_1^\dagger, T_2], T_1]) + \\ + \widehat{\mathcal{P}}_1\left(\frac{1}{2}[[T_1^\dagger, T_1], T_1] + [[T_2^\dagger, T_2], T_1]\right) + \frac{1}{2}\widehat{\mathcal{P}}_3([[T_1^\dagger, T_2], T_2]) + \mathcal{O}(T^4), \end{aligned} \tag{11-16}$$

where $\widehat{\mathcal{P}}_n$ is the superoperator projecting on the space spanned by n-tuple excitation operators,

$$\widehat{\mathcal{P}}_n(X) = \frac{1}{(n!)^2} \sum_{a_1 \ldots a_n} \sum_{i_1 \ldots i_n} \left\langle e^{i_1}_{a_1} \cdots e^{i_n}_{a_n} X \right\rangle \; e^{a_1}_{i_1} \cdots e^{a_n}_{i_n}, \tag{11-17}$$

with $e^p_q = a^p a_q$ being the spinorbital substitution operator (a^r and a_r are creation and annihilation operators for a spinorbital ϕ_r) [48].[3] Some terms of Eq. (11-16) can still be neglected without affecting the accuracy of the results. This fact can be deduced from an analysis of the importance of single and double excitations in CC theory interpreted as an infinite-order summation scheme for MP theory. It can be shown that e.g. the double-excitation operator T_2 is of the $\mathcal{O}(W^1)$ order, while the single-excitation operator T_1 appears for the first time in the second W order (i.e. $T_1 = \mathcal{O}(W^2)$). This means for instance that a term constructed from two T_2 and one T_1 operator is of the $\mathcal{O}(W^4)$ order, while a similar term built from three T_1 operators is much less important because of its $\mathcal{O}(W^6)$ order. Since the CCSD correlation energy is correct to the third W order and the first-order properties calculated from Eq. (11-12) with $T = T_1 + T_2$ are correct through the $\mathcal{O}(W^2)$ order only, the first three terms of Eq. (11-16) are sufficient in most applications.

The fact that Eq. (11-15) in spite of its visual complexity misses some $\mathcal{O}(W^3)$ terms (namely, those arising from a triple-excitation operator T_3 of CC theory), is somewhat disappointing. Fortunately enough, numerical results presented in Ref. [36] have shown that a lack of these terms does not affect the quality of the first-order molecular properties in the majority of cases. However, because of this formal problem, Jeziorski and Moszynski developed an alternative approach for an expectation-value CC molecular property, which starting from Eq. (11-12) arrives at the expression containing single- and double-excitation operators only, but nonetheless correct through the $\mathcal{O}(W^3)$ order [46]. For real orbitals the corresponding formula reads

$$\overline{X}_{\mathrm{resp}}(3) = \langle X \rangle + \langle T_2 | [X, T_2] \rangle + 2 \langle T_2 | [H, C_1(X)] \rangle + 2 \langle T_2 | [[H, C_1(X)], T_2] \rangle. \tag{11-18}$$

This method, called here just $\overline{X}_{\mathrm{resp}}(3)$, requires that an additional set of coupled HF equations with the perturbation operator X should be solved in order to obtain a new single-excitation operator $C_1(X)$. It should be stressed that the computational effort for first-order properties obtained from the XCCSD or $\overline{X}_{\mathrm{resp}}(3)$ methods is approximately two times smaller than the time required by the linear-response (LR) CCSD method [49–52], because in the latter case it is necessary to solve the left-hand CCSD equation to obtain the corresponding property.

In practice the operators and density matrices are expressed in a spinorbital basis $\{\phi_p\}$. For the one-electron density matrix the expansion in terms of spinorbitals is given by

[3] A convention for denoting occupied spinorbitals by letters i, j, k, l, virtual ones – by a, b, c, d, and generic by p, q, r, s will be used in the following.

$$\rho(1|1') = \sum_{pq} \rho_q^p \phi_p(1)^\star \phi_q(1'), \tag{11-19}$$

where the expansion coefficients are obtained as $\rho_q^p = \langle \Psi^0 | e_q^p \Psi^0 \rangle$. For the XCC case the e_q^p operators for all possible pairs (p,q) should be inserted as X into Eq. (11-15) to obtain the corresponding XCC one-electron density matrix. This matrix can be then used to calculate all one-electron first-order properties of a molecule. Of course, for the case of the electrostatic energy two such matrices, ρ_A and ρ_B, should be obtained.

11.3.2. Induction Energy

The second-order induction energy is composed of two terms, which describe the polarization of one monomer by the electrostatic field of another monomer and vice versa

$$E_{\text{ind}}^{(2)} = E_{\text{ind}}^{(2)}(A \leftarrow B) + E_{\text{ind}}^{(2)}(B \leftarrow A). \tag{11-20}$$

This interaction energy component can be expressed in terms of one-electron densities and static density susceptibilities of monomers as follows [53]

$$E_{\text{ind}}^{(2)} = -\frac{1}{2} \int v_{\text{eff,B}}(1) \alpha_A(1, 1'|0) v_{\text{eff,B}}(1') d\tau_1 d\tau_1' + A \leftrightarrow B. \tag{11-21}$$

The effective one-electron potential of the monomer B ($v_{\text{eff,B}}(1)$) entering into Eq. (11-21) is defined as

$$v_{\text{eff,B}}(1) = v_B(1) + \int \frac{\rho_B(1'|1')}{r_{11'}} d\tau_1', \tag{11-22}$$

where v_B and ρ_B are the one-electron potential and the one-electron density of the monomer B, respectively. Another monomer property appearing in Eq. (11-21) is a density susceptibility $\alpha(\mathbf{r}, \mathbf{r}'|\omega)$. This quantity is a particular case of a linear response function, denoted as $\langle\langle X;Y \rangle\rangle_\omega$, which describes a linear response of a molecule to perturbing operators (X or Y) oscillating with a frequency ω [54]

$$\langle\langle X;Y \rangle\rangle_\omega = -\langle \Psi_0 | Y \frac{Q}{H - E_0 + \omega} X \Psi_0 \rangle - \langle \Psi_0 | X \frac{Q}{H - E_0 - \omega} Y \Psi_0 \rangle. \tag{11-23}$$

In Eq. (11-23) H, E_0, and Ψ_0 are the Hamiltonian, energy and wave function of the unperturbed molecule, respectively, and $Q = 1 - |\Psi_0\rangle\langle\Psi_0|$ is the projection on the space orthogonal to Ψ_0. The linear response function is often called a polarization propagator. The density susceptibility is defined through linear response functions in the following way

$$\alpha(\mathbf{r},\mathbf{r}'|\omega) = -\langle\langle\hat{\rho}(\mathbf{r});\hat{\rho}(\mathbf{r}')\rangle\rangle_\omega = -\sum_{pqrs}\langle\langle G_q^p;G_s^r\rangle\rangle_\omega\,\phi_p(\mathbf{r})\phi_q(\mathbf{r})\phi_r(\mathbf{r}')\phi_s(\mathbf{r}'), \quad (11\text{-}24)$$

where the orbitals are assumed to be real and where $\hat{\rho}(\mathbf{r})$ is the electron-density operator [44],

$$\hat{\rho}(\mathbf{r}) = \sum_{i=1}^{N}\delta(\mathbf{r}-\mathbf{r}_i) = \sum_{pq}E_q^p\phi_p(\mathbf{r})\phi_q(\mathbf{r}). \quad (11\text{-}25)$$

In Eq. (11-24) an adaptation of spin, trivial for the closed-shell molecules, has been already performed, and $G_q^p = \frac{1}{2}\left(E_q^p + E_p^q\right)$ is the Hermitian combination of the usual orbital-replacement operator E_q^p $\left(E_q^p = a^{p\alpha}a_{q\alpha} + a^{p\beta}a_{q\beta}\right)$ [48].

The formulae (11-21) and (11-22) look very attractive at first glance since neither the susceptibility α_A, nor the one-electron density ρ_B depend on the presence of another monomer. This means that they can in principle be obtained separately for each interacting molecule and then used to calculate the whole PES of the intermolecular interaction. In spite of this, Eq. (11-21) is not well suited for a practical implementation, as it requires the knowledge of the full static monomer density susceptibility. In the algebraic approximation this means that the full 4-index propagator matrix constructed from coefficients $\langle\langle G_q^p;G_s^r\rangle\rangle_{\omega=0}$ should be available for SAPT calculations of the induction energy. In addition, it is a known problem that monomer properties obtained from monomer-centered basis sets (so-called MCBS) give a poor approximation of the SAPT interaction energy [55]. An augmentation of MCBS by basis functions placed on another monomer makes the quality of the SAPT energies considerably better, but this improvement has the price of making monomer properties dependent on the position of another monomer, what means that a costly step of obtaining the 4-index propagator matrices should be repeated for each geometry.

Fortunately enough, Eq. (11-5) can be recast into a form more suitable for computational purposes, provided that a concept of perturbed density matrices is utilized. The first-order one-electron density matrix is defined as

$$\rho^{(1)}(1|1') = N\int \Psi^0(1,2,\ldots,N)^*\Psi^{(1)}(1',2,\ldots,N)\,d\tau_2\ldots\tau_N, \quad (11\text{-}26)$$

where $\Psi^{(1)}$ describes the first-order response of a molecule to some perturbation. For the $E_{\mathrm{ind}}^{(2)}(A\leftarrow B)$ term the molecule A is perturbed by the $V_{\mathrm{eff,B}} = \sum_{i=1}^{N_A} v_{\mathrm{eff,B}}(i)$ operator, therefore the corresponding first-order density matrix of the monomer A will be denoted as $\rho^{(1)}_{A\leftarrow B}$. With these definitions the induction energy can be rewritten as

$$E_{\mathrm{ind}}^{(2)} = \int \rho^{(1)}_{\mathrm{A}\leftarrow\mathrm{B}}(1|1)v_{\mathrm{eff,B}}(1)d\tau_1 + A\leftrightarrow B. \quad (11\text{-}27)$$

It is noteworthy that the first-order one-electron density matrix has the form of a transition density matrix, where in place of the wave function for the final state the first-order wave function $\Psi^{(1)}$ is inserted.

For purposes of SAPT(CC), the ground-state and first-order one-electron densities of monomers are obtained from XCC theory. The ground-state density has been already presented in Section 11.3.1. The first-order density is retrieved from time-independent CC theory of the polarization propagator of Moszynski et al. [47]. In this theory the following ansatz for the first-order CC wave function is utilized

$$\Psi^X(\omega) = \frac{\left(\Omega_0^X(\omega) + \Omega^X(\omega)\right) e^T \Phi}{\langle e^T | e^T \rangle^{1/2}}, \tag{11-28}$$

where $\Omega_0^X(\omega)$ is a number and $\Omega^X(\omega)$ is an excitation operator which describes the first-order response of a molecule to the perturbation X oscillating with a frequency ω. The operator $\Omega^X(\omega)$ is identical with the first-order excitation operator of time-dependent CC theory (TD-CC) of molecular properties [49, 56] and satisfies the operator equation

$$\left[e^{-T} H e^T, \Omega^X(\omega)\right] \Phi + \omega \Omega^X(\omega) \Phi = -e^{-T} X e^T \Phi, \tag{11-29}$$

in the space orthogonal to Φ. The general formula for the frequency-dependent CC polarization propagator from Ref. [47] reads

$$\langle\langle X;Y \rangle\rangle_\omega = \langle e^{-S} e^{T^\dagger} Y e^{-T^\dagger} e^S \,|\, \widehat{\mathcal{P}}(e^{S^\dagger} \Omega^X(\omega) e^{-S^\dagger}) \rangle + \text{g.c.c.}, \tag{11-30}$$

where g.c.c. denotes the second term obtained by performing a complex conjugation of the first term calculated at frequency $-\omega^*$. The first term in Eq. (11-30) can be identified as $\langle \Psi | Y \Psi^X(\omega) \rangle$ with the wave function $\Psi^X(\omega)$ defined by Eq. (11-28). The elements of the first-order one-electron density matrix, $(\rho^{(1)}_{A \leftarrow B})^p_q$, are obtained by inserting $X = V_{\text{eff,B}}$ and $Y = e^p_q$ into the first term of the r.h.s. of Eq. (11-30) and by setting $\omega = 0$.

Similarly to the XCC first-order properties, Eq. (11-30) should be simplified for a practical use. To this end a systematic truncation procedure, proposed in Ref. [47], has been exploited in Ref. [35], resulting in three models denoted as CCSD(n), $n = 2, 3, 4$. Among these schemes the CCSD(3) model has been selected as an optimal choice for many-electron monomers. The CCSD(3) polarization propagator is calculated as

$$\begin{aligned} \langle\langle X;Y \rangle\rangle_\omega = {} & \left\langle Y \Omega_1^X(\omega) \right\rangle + \left\langle S | [Y, \Omega^X(\omega)] \right\rangle + \left\langle [Y, S_2] | \Omega_1^X(\omega) \right\rangle + \\ & + \langle [[T^\dagger, Y], S] | \Omega^X(\omega) \rangle + \text{g.c.c.}, \end{aligned} \tag{11-31}$$

with the S operator approximated by the first three terms of Eq. (11-16). This model contains all $\mathcal{O}(W^3)$ terms present in Eq. (11-30) for the T operator from CCSD theory, but it still misses some $\mathcal{O}(W^3)$ terms arising from the T_3 and $\Omega_3^X(\omega)$ triple-excitation operators. Nonetheless, the numerical experience shows that the CCSD(3) model performs well in comparison to the benchmark full configuration interaction (FCI) results [35] and that its accuracy is similar to that of time-dependent LR-CCSD theory [49–52]. It should be noted that LR-CCSD theory also misses some terms of the $\mathcal{O}(W^3)$ order, unless the orbital relaxation is explicitly taken into account. The orbital-relaxed version of LR-CCSD theory has been presented recently by Wheatley [57].

11.3.3. Dispersion Energy

The second-order dispersion energy can be expressed through monomer properties with the formula proposed by Longuet-Higgins [58]. This equation represents the dispersion energy through frequency-dependent density susceptibilities (FDDS) of monomers A and B (see Eq. (11-24)) calculated for imaginary frequencies $i\omega$

$$E_{\mathrm{disp}}^{(2)} = -\frac{1}{2\pi}\int_0^\infty \int \alpha_A(1,1'|i\omega)\alpha_B(2,2'|i\omega)\frac{1}{r_{12}}\frac{1}{r_{1'2'}}d\tau_1 d\tau_1' d\tau_2 d\tau_2' d\omega. \qquad (11\text{-}32)$$

Contrary to the case of the induction energy, the calculation of FDDS cannot be avoided by using some faster computational method for perturbed CCSD wave functions. For simpler models, like SAPT(HF) or SAPT(MP2), where the orbital summation ranges in Eq. (11-24) are restricted, it is advantageous to make use of the formula

$$\frac{1}{\Delta E_A^K + \Delta E_B^L} = \frac{2}{\pi}\int_0^\infty \frac{\Delta E_A^K}{\left(\Delta E_A^K\right)^2 + \omega^2}\frac{\Delta E_B^L}{\left(\Delta E_B^L\right)^2 + \omega^2}d\omega, \qquad (11\text{-}33)$$

and to calculate directly mixed AB amplitudes [12]. Monomer density susceptibilities can be conveniently obtained from the time-independent CC theory of the polarization propagator [47]. In a practical implementation the CCSD(3) model [35] has been used. The computation of 4-index coefficient matrices from Eq. (11-31) is the most time-consuming step in the computation of the CC dispersion energy. This is explained by the necessity of a calculation of a first-order perturbed operator $\Omega^{G_s^r}(i\omega)$ (see Eq. (11-29)) for all $r \geq s$ pairs of indices. For the CCSD case the computational cost of one such operator scales as iterative $\mathcal{O}(o^2v^4)$, where o and v denote the numbers of occupied and virtual orbitals, respectively. As a result, $\frac{1}{2}M(M+1)$ ($M = o + v$) operators $\Omega^{G_s^r}(i\omega)$ are needed to obtain a full FDDS at one frequency $i\omega$, what gives rise to an iterative $\mathcal{O}(o^2v^4M^2)$ scaling. In addition, a numerical quadrature over frequency requires usually about 8–12 integration points to achieve a 2–3 digit accuracy. This scaling behavior strongly limits the size of

complexes, for which the calculation of the CCSD dispersion energy is feasible. A way to overcome this limitation has been presented by Korona and Jeziorski [38], who proposed to expand density susceptibilities in an auxiliary basis set $\{\chi_K\}$ of a dimension N_{aux}

$$\alpha(\mathbf{r},\mathbf{r}'|i\omega) = -\sum_{KL} \langle\langle \hat{\chi}_K;\hat{\chi}_L\rangle\rangle_{i\omega}\ \chi_K(\mathbf{r})\,\chi_L(\mathbf{r}'). \tag{11-34}$$

New perturbing operators $\hat{\chi}_K$ are defined for each auxiliary orbital χ_K,

$$\hat{\chi}_K = \sum_{pq} D^K_{pq}\, E^p_q, \tag{11-35}$$

where the expansion coefficients D^K_{pq} are obtained by fitting the products of orbitals with the auxiliary basis set (orbitals are assumed to be real) and by using the Coulomb metric [59, 60]:

$$\phi_p(\mathbf{r})\phi_q(\mathbf{r}) \approx \sum_K D^K_{pq}\,\chi_K(\mathbf{r}). \tag{11-36}$$

The density-fitting procedure decreases the number of first-order operators $\Omega^X(\omega)$ for each frequency from M^2 to N_{aux}. Since N_{aux} is usually only 2–3 times larger than a dimension of the orbital basis M, the utilization of density-fitted FDDS reduces the computational effort by one order of magnitude (in terms of the orbital basis size), i.e. to an iterative $\mathcal{O}(o^2v^4N_{\text{aux}})$ scaling. It should be noted that the calculation of $\Omega^{\hat{\chi}_K}(i\omega)$ operators can be easily parallelized, since they are independent of each other and can be therefore obtained simultaneously for various K and ω's.

It should be noted that another CC-like treatment of the dispersion energy has been proposed some time ago by Williams et al. [61]. In this approach the dimer cluster operator $T = T_A + T_B + T_{AB}$ for a reference wave function $\Phi_A\Phi_B$ has been introduced. The T_A and T_B operators contain pure excitations from Φ_A or Φ_B to virtual orbitals of the monomers A and B, respectively, while the T_{AB} operator contains mixed excitations. Working expressions for these operators have been developed for the simplest nontrivial case of double excitations, giving rise to the dispersion energy named $E^{(2)}_{\text{disp}}$(CCD). This energy has been then augmented by noniterative single and triple corrections obtained in a spirit of the triples correction for CCSD(T) theory [62], what finally has resulted in the CCD+ST(CCD) method. The quality of the $E^{(2)}_{\text{disp}}$(CCD+ST(CCD)) energy is usually superior over the standard SAPT(MP) method. However, this energy cannot be expressed through monomer properties and therefore the CCD+ST(CCD) method has no well-defined asymptotics, i.e. the large-distance behavior of this approach cannot be related to the properties of monomers. On the contrary, the asymptotic form of the polarization energies obtained from Eqs. (11-10), (11-21), and (11-32) is readily available, if the expanded form of the intermolecular operator V is inserted into these expressions. The resulting formulae

will contain multipole moments and polarizabilities, which for a consistency should be calculated on the same level of theory, as used for the finite-distance energy components (see e.g. Ref. [35] for the calculation of the van der Waals dispersion coefficients from the CCSD(3) model).

11.4. EXCHANGE ENERGIES

The total SRS exchange corrections of first and second order in V are given by the formulae [8]

$$E^{(1)}_{\rm exch} = \langle \Psi^0_A \Psi^0_B | \mathcal{A} \Psi^0_A \Psi^0_B \rangle^{-1} \langle \Psi^0_A \Psi^0_B | V \mathcal{A} \Psi^0_A \Psi^0_B \rangle - E^{(1)}_{\rm pol}, \tag{11-37}$$

$$E^{(2)}_{\rm exch} = \langle \Psi^0_A \Psi^0_B | \mathcal{A} \Psi^0_A \Psi^0_B \rangle^{-1} \langle \Psi^0_A \Psi^0_B | (V - \overline{V}) \mathcal{A} \Psi^{(1)}_{\rm pol} \rangle - E^{(2)}_{\rm pol}, \tag{11-38}$$

where $\mathcal{A}$ denotes the antisymmetrizer and $\overline{Y}$ is the mean value of the operator Y with the zeroth-order wave function $\Psi^0_A \Psi^0_B$ (i.e. $\overline{V} = E^{(1)}_{\rm elst}$). The presence of $\mathcal{A}$ in Eqs. (11-37) and (11-38) makes the formulae fairly complicated for a general many-electron case. A technique to calculate such corrections has been developed only for the first-order exchange energy within the HF approximation [63]. Fortunately enough, it turns out that if the intermonomer distance is not too small, it is usually sufficient to take into account single exchanges of electrons between monomers only (a so-called S^2 approximation) [64, 65]. The S^2 approximation tremendously simplifies the expressions for exchange energies. Single-exchange formulae can be derived from Eqs. (11-37) and (11-38) if the expansion in terms of single- and higher-order exchanges of electrons is performed and then only terms linear in the single-exchange operator $\mathcal{P}_1$

$$\mathcal{P}_1 = -\sum_{i=1}^{N_A} \sum_{j=1+N_A}^{N_A+N_B} P_{ij}, \tag{11-39}$$

are taken into account (P_{ij} denotes here the transposition of electrons i and j). In the SAPT(CC) method only exchange corrections within the S^2 approximation will be considered. The formulae for the exchange energies up to the second order in V within the single-exchange approximation are listed below

$$E^{(1)}_{\rm exch} = \langle \Psi^0_A \Psi^0_B | (V - \overline{V}) \mathcal{P}_1 \Psi^0_A \Psi^0_B \rangle, \tag{11-40}$$

$$E^{(2)}_{\rm exch-ind} = \langle \Psi^0_A \Psi^0_B | (V - \overline{V}) (\mathcal{P}_1 - \overline{\mathcal{P}_1}) \Psi^{(1)}_{\rm ind,A} \Psi^0_B \rangle + A \leftrightarrow B, \tag{11-41}$$

$$E^{(2)}_{\rm exch-disp} = \langle \Psi^0_A \Psi^0_B | (V - \overline{V}) (\mathcal{P}_1 - \overline{\mathcal{P}_1}) \Psi^{(1)}_{\rm disp} \rangle, \tag{11-42}$$

where $E^{(2)}_{\rm exch-ind}$ and $E^{(2)}_{\rm exch-disp}$ are the induction and dispersion components of $E^{(2)}_{\rm exch}$. Similarly to the case of the polarization energies, the integration over most electron

coordinates can be performed in Eqs. (11-40), (11-41), and (11-42), since both V and $\mathcal{P}_1$ are 2-body operators. However, the presence of the $V\mathcal{P}_1$ term results in the emergence of more complicated monomer quantities, like e.g. two-electron density matrices. Nevertheless, a reformulation of Eqs. (11-40), (11-41), and (11-42) in terms of monomer properties is still possible, and will be presented in detail in Sections 11.4.1, 11.4.2, and 11.4.3.

11.4.1. First-Order Exchange Energy

The formula expressing the first-order exchange energy in terms of monomer properties has been proposed by Moszynski et al. [14]. In Ref. [14] an auxiliary quantity called the interaction density matrix has been introduced for this purpose. The interaction density matrix is constructed from one- and two-electron density matrices of the monomers A and B

$$\rho_{\mathrm{int}}(1|1') = -\rho_A(1|1')\rho_B(1'|1) - \int \rho_A(1|2')\Gamma_B(1'2'|1'1)d\tau_2' - \\ - \int \Gamma_A(12|11')\rho_B(1'|2)d\tau_2 - \int \Gamma_A(12|12')\Gamma_B(1'2'|1'2)d\tau_2 d\tau_2'. \quad (11\text{-}43)$$

A definition of a two-electron density matrix is given by the equation [43]

$$\Gamma(12|1'2') = N(N-1)\int \Psi^0(1,2,3,\ldots,N)^*\Psi^0(1',2',3,\ldots,N)d\tau_3\ldots\tau_N. \quad (11\text{-}44)$$

In the algebraic approximation the two-electron density matrix is expanded as

$$\Gamma(12|1'2') = \sum_{p_1q_1p_2q_2} \Gamma^{p_1p_2}_{q_1q_2}\phi^*_{p_1}(1)\phi^*_{p_2}(2)\phi_{q_1}(1')\phi_{q_2}(2'), \quad (11\text{-}45)$$

where the coefficients $\Gamma^{p_1p_2}_{q_1q_2}$ are obtained from the formula $\Gamma^{p_1p_2}_{q_1q_2} = \langle\Psi^0|e^{p_1p_2}_{q_1q_2}\Psi^0\rangle$ ($e^{p_1p_2}_{q_1q_2} = a^{p_1}a^{p_2}a_{q_2}a_{q_1}$ is a two-body spinorbital replacement operator). If the interaction density matrix $\rho_{\mathrm{int}}(1|1')$ is used, the first-order exchange energy can be represented in a following compact form [14]

$$E^{(1)}_{\mathrm{exch}} = \int \rho_{\mathrm{int}}(1|1')\Big(v(1,1') - \frac{\overline{V}}{N_AN_B}\Big)d\tau_1 d\tau_1'. \quad (11\text{-}46)$$

In the work of Moszynski et al. [14] the density matrices appearing in Eq. (11-43) have been obtained from MP theory, with a restriction that the cumulative order of W_A and W_B fluctuation operators should be not greater than 2. In this way the $E^{(1)}_{\mathrm{exch}}(2)$ correction has been obtained. Numerical results presented in Ref. [14] for this correction were only halfway satisfactory, therefore it has been proposed to use converged CCSD monomer amplitudes instead of their MP1 and MP2 counterparts

in the equations for $E^{(1)}_{\mathrm{exch}}(2)$. The first-order exchange energy obtained in this way is denoted as $E^{(1)}_{\mathrm{exch}}(\mathrm{CCSD})$. A utilization of the $E^{(1)}_{\mathrm{exch}}(\mathrm{CCSD})$ energy instead of the $E^{(1)}_{\mathrm{exch}}(2)$ one has become a standard in nearly all practical SAPT(MP) applications.

Equation 11-46 contains an explicitly disconnected part and it is not clear if this term cancels exactly with some parts of the first term, giving a size-extensive quantity (a correct definition of the first-order exchange energy should be of course size-extensive). In order to perform an explicit cancellation, a concept of the cumulant (denoted as Λ) of the two-electron density matrix is conveniently utilized. The cumulant is that part of a two-electron density matrix which cannot be described as the antisymmetrized product of one-electron density matrices [66]

$$\Gamma(12|1'2') = \rho(1|1')\rho(2|2') - \rho(1|2')\rho(2|1') + \Lambda(12|1'2'). \tag{11-47}$$

If a partitioning of Γ given in Eq. (11-47) is inserted into the definition of the interaction density matrix (Eq. (11-43)), one can show that the second term in Eq. (11-46) cancels with one of the terms arising from the part of the interaction density containing two-electron density matrices of monomers [40]. Since no other term can be factorized as a product of two or more integrals, the remaining expression is connected and therefore size-extensive. The resulting formula for the $E^{(1)}_{\mathrm{exch}}$ energy can be divided into four parts: (nn) – containing one-electron density matrices of monomers only, (cn) and (nc) – with a cumulant of the monomer A or B, and (cc) – with cumulants of both monomers simultaneously

$$\begin{aligned}
E^{(1)}_{\mathrm{exch}}(\mathrm{nn}) = &- \int \rho_A(1|1')\rho_B(1'|1)v(1,1')d\tau_1 d\tau_1' - \\
&- \int \rho_A(1|2')\big(\rho_B(1'|1')\rho_B(2'|1) - \rho_B(1'|1)\rho_B(2'|1')\big)v(1,1')d\tau_1 d\tau_1' d\tau_2' - \\
&- \int \big(\rho_A(1|1)\rho_A(2|1') - \rho_A(1|1')\rho_A(2|1)\big)\rho_B(1'|2)v(1,1')d\tau_1 d\tau_1' d\tau_2 - \\
&- \int \big(\rho_A(1|2')\rho_A(2|1)\rho_B(1'|2)\rho_B(2'|1') - \rho_A(1|1)\rho_A(2|2')\rho_B(1|2')\rho_B(2'|1') - \\
&-\rho_A(1|2')\rho_A(2|1)\rho_B(1'|1')\rho_B(2'|2)\big)v(1,1')d\tau_1 d\tau_1' d\tau_2 d\tau_2', \\
E^{(1)}_{\mathrm{exch}}(\mathrm{cn}) = &- \int \Lambda_A(12|11')\rho_B(1'|2)v(1,1')d\tau_1 d\tau_1' d\tau_2 - \\
&- \int \Lambda_A(12|12')\big(\rho_B(1'|1')\rho_B(2'|2) - \rho_B(1'|2)\rho_B(2'|1')\big)v(1,1')d\tau_1 d\tau_1' d\tau_2 d\tau_2', \\
E^{(1)}_{\mathrm{exch}}(\mathrm{nc}) = &- \int \rho_A(1|2')\Lambda_B(1'2'|1'1)v(1,1')d\tau_1 d\tau_1' d\tau_2' - \\
&- \int \big(\rho_A(1|1)\rho_A(2|1') - \rho_A(1|1')\rho_A(2|1)\big)\Lambda_B(1'2'|1'2)v(1,1')d\tau_1 d\tau_1' d\tau_2 d\tau_2', \\
E^{(1)}_{\mathrm{exch}}(\mathrm{cc}) = &- \int \Lambda_A(12|12')\Lambda_B(1'2'|1'2)v(1,1')d\tau_1 d\tau_1' d\tau_2 d\tau_2'.
\end{aligned} \tag{11-48}$$

Equations (11-48) are so far completely general and can be used for any theory with well-defined cumulants of two-electron density matrices. Unfortunately, the popular LR-CC theory does not belong to such a class of methods. This deficiency of LR-CC can be explained by the fact that both one- and two-electron LR-CC density matrices are linear in terms of the left-hand solution of CC equations, so one cannot define a cumulant according to the definition given in Eq. (11-47), since the resulting quantity would contain disconnected terms. On the other hand, it has been shown recently [40] that the two-electron CC density matrix obtained from expectation-value CC theory [46] correctly separates into the antisymmetrized product of the one-electron density matrices and the cumulant part, therefore this theory can be utilized to obtain molecular properties for the SAPT(CC) method. In the algebraic approximation the cumulant can be expanded in terms of spinorbitals, analogously to the density matrix (see Eq. (11-19)), with the expansion coefficients given by the equation

$$\begin{aligned}\Lambda^{p_1p_2}_{q_1q_2} = \langle e^{S^\dagger} e^{-T} e^{p_1}_{q_1} e^{T} e^{-S^\dagger} \widehat{\mathcal{P}} (e^{S^\dagger} e^{-T} e^{p_2}_{q_2} e^{T} e^{-S^\dagger}) \rangle - \\ - \langle e^{S^\dagger} e^{-T} \tilde{e}^{p_2}_{q_1} e^{T} e^{-S^\dagger} \rangle \langle e^{S^\dagger} e^{-T} e^{p_1}_{q_2} e^{T} e^{-S^\dagger} \rangle, \end{aligned} \tag{11-49}$$

where $\tilde{e}^p_q = a_q a^p$ denotes the one-hole substitution operator [48, 66].

In practice, a truncated form of Eq. (11-49) has to be used. The leading terms of the CCSD cumulant obtained by utilizing the same truncation schemes as in the case of the CCSD(3) polarization propagators are listed below

$$\begin{aligned}\Lambda^{p_1p_2}_{q_1q_2} = \langle e^{p_1}_{q_1} \widehat{\mathcal{P}}_1 ([e^{p_2}_{q_2}, T_2]) \rangle + \langle [S_2^\dagger, e^{p_1}_{q_1}] \widehat{\mathcal{P}}_1 (e^{p_2}_{q_2}) \rangle + \langle [S_2^\dagger, e^{p_1}_{q_1}] \widehat{\mathcal{P}}_1 ([e^{p_2}_{q_2}, T_2]) \rangle + \\ + \langle \{ [S_2^\dagger, e^{p_1}_{q_1}] \widehat{\mathcal{P}}_2 ([e^{p_2}_{q_2}, T_2]) \}_C \rangle + \langle \{ [S_2^\dagger, [e^{p_1}_{q_1}, T_2]] \widehat{\mathcal{P}}_1 (e^{p_2}_{q_2}) \}_C \rangle + \mathcal{O}(W^3), \end{aligned} \tag{11-50}$$

where the letter "C" in the subscript means that only connected diagrams should be taken into account. For one-electron density matrices entering Eq. (11-48) the expression from Eq. (11-15) is used. In this way the main (non-cumulant) part of the first-order exchange energy can be calculated very accurately (it is *exact* for two-electron monomers, for which CCSD is equivalent to FCI). The first-order exchange energy obtained from the expectation-value CC density matrices will be denoted as $E^{(1)}_{\mathrm{exch}}$(XCC), in order to differentiate it from the exchange energy obtained from the earlier approach of Moszynski et al. [13, 14]. A numerical experience shows that the non-cumulant part of the exchange energy is clearly a dominant contribution (it gives over 90% of the total correction), therefore the truncation performed in Eq. (11-50) is fully justified. It can be noted that differences between the $E^{(1)}_{\mathrm{exch}}$(XCCSD) and $E^{(1)}_{\mathrm{exch}}$(CCSD) energies are of the $\mathcal{O}(W^3)$ order.

11.4.2. Second-Order Exchange-Induction Energy

A closer look at Eqs. (11-40) and (11-41) reveals that the $E^{(1)}_{\mathrm{exch}}$ and $E^{(2)}_{\mathrm{exch-ind}}$ energies presented there have a very similar structure. Basically, the main term of the formula for $E^{(2)}_{\mathrm{exch-ind}}(A \leftarrow B)$ is obtained from Eq. (11-40) if the second Ψ^0_A wave function is replaced by $\Psi^{(1)}_A$. Therefore the approach, which closely resembles that described in Section 11.4.1, can be also proposed for the exchange-induction energy. An analog of the interaction density matrix $\rho^{(1)}_{\mathrm{int}}(1|1')$ for the $A \leftarrow B$ component of the exchange-induction energy is the first-order interaction density matrix of the monomer A defined as [41]

$$\rho^{(1)}_{\mathrm{int,A}}(1|1') = -\rho^{(1)}_{\mathrm{A\leftarrow B}}(1|1')\rho_B(1'|1) - \int \rho^{(1)}_{\mathrm{A\leftarrow B}}(1|2')\Gamma_B(1'2'|1'1)d\tau'_2 -$$
$$- \int \Gamma^{(1)}_{\mathrm{A\leftarrow B}}(12|11')\rho_B(1'|2)d\tau_2 - \int \Gamma^{(1)}_{\mathrm{A\leftarrow B}}(12|12')\Gamma_B(1'2'|1'2)d\tau_2 d\tau'_2, \quad (11\text{-}51)$$

where the one-electron first-order density matrix of the monomer A, $\rho^{(1)}_{\mathrm{A\leftarrow B}}(i|j)$, has been introduced in Section 11.3.2 and the two-electron first-order density matrix is defined analogously to Eq. (11-44) with the ket wave function Ψ^0_A replaced by the first-order wave function $\Psi^{(1)}_A$. With these definitions the exchange-induction energy can be expressed by the formula

$$E^{(2)}_{\mathrm{exch-ind}} = \int \rho^{(1)}_{\mathrm{int,A}}(1|1')v(1,1')d\tau_1 d\tau'_1 - \frac{\overline{V}}{N_A N_B}\int \rho^{(1)}_{\mathrm{int,A}}(1|1')d\tau_1 d\tau'_1 -$$
$$-\overline{\mathcal{P}_1}\int \rho^{(1)}_{\mathrm{A\leftarrow B}}(1|1)v(1,1')\rho_B(1'|1')d\tau_1 d\tau'_1 + A \leftrightarrow B. \quad (11\text{-}52)$$

As in the case of the first-order exchange energy, Eq. (11-52) contains explicitly disconnected terms, which should be removed by the first part of the formula in order to preserve size-extensivity. An explicitly connected form of Eq. (11-52) can be obtained if the first-order perturbed cumulant $\Lambda^{(1)}(12|1'2')$ is inserted to Eq. (11-51). For the sake of brevity of the next few formulae some permutation symbols acting on electron coordinates must be introduced, which will serve to generate parts of formulae with transposed electron coordinates. For a given product of two functions f and g of electron coordinates, $f(i|j)g(k|l)$, the symbol π^*_{ik} will denote the permutation of left coordinates, while the symbol π_{jl} will permute right coordinates in the product fg, e.g. $\pi^*_{12}f(1|1)g(2|2) = f(2|1)g(1|2)$, while $\pi_{12}f(1|1)g(2|2) = f(1|2)g(2|1)$. Additionally, let us define the antisymmetrizers $\mathcal{A}^*_{ik} = 1 - \pi^*_{ik}$ and $\mathcal{A}_{jl} = 1 - \pi_{jl}$. Finally, the superscript A or B will denote an operator acting on the quantities belonging to the monomer A or B only. With these definitions the partitioning of the first-order two-electron density matrix into the non-cumulant and cumulant parts takes the form

$$\Gamma^{(1)}(12|1'2') = \mathcal{A}^*_{12}\mathcal{A}_{1'2'}\rho^{(1)}(1|1')\rho(2|2') + \Lambda^{(1)}(12|1'2'). \quad (11\text{-}53)$$

By inserting Eq. (11-53) into Eqs. (11-51) and (11-52) the second-order exchange-induction energy can be expressed through the connected terms only, which, in a full analogy to the first-order exchange energy, can be separated into four types, depending on the presence of monomer cumulants in the expressions

$$
\begin{aligned}
E^{(2)}_{\mathrm{exch-ind}}(\mathrm{nn}) = &- \int v(1,1')\rho_A^{(1)}(1|1')\rho_B(1'|1)d\tau_1 d\tau_1' - \\
&- \int v(1,1')\rho_A^{(1)}(1|2')\mathcal{A}^B_{1'1}\rho_B(1'|1')\rho_B(2'|1)d\tau_1 d\tau_1' d\tau_2' - \\
&- \int v(1,1')\mathcal{A}^{*A}_{12}\mathcal{A}^{A}_{11'}\rho_A^{(1)}(1|1)\rho_A(2|1')\rho_B(1'|2)d\tau_1 d\tau_1' d\tau_2 - \\
&- \int v(1,1')\left(\mathcal{A}^{*A}_{12}\mathcal{A}^{A}_{12'}\mathcal{A}^B_{1'2} - 1 - \pi^{*A}_{12}\pi^{A}_{1'2'}\right)\rho_A^{(1)}(1|1)\rho_A(2|2') \times \\
&\times \rho_B(1'|1')\rho_B(2'|2)d\tau_1 d\tau_1' d\tau_2 d\tau_2' + A \leftrightarrow B, \\
E^{(2)}_{\mathrm{exch-ind}}(\mathrm{nc}) = &- \int \rho_A^{(1)}(1|2')\Lambda_B(1'2'|1'1)v(1,1')d\tau_1 d\tau_1' d\tau_2' - \\
&- \int v(1,1')\mathcal{A}^{*A}_{12}\mathcal{A}^{A}_{11'}\rho_A^{(1)}(1|1)\rho_A(2|1')\Lambda_B(1'2'|1'2)d\tau_1 d\tau_1' d\tau_2 d\tau_2' + A \leftrightarrow B, \\
E^{(2)}_{\mathrm{exch-ind}}(\mathrm{cn}) = &- \int \Lambda^{(1)}{}_A(12|11')\rho_B(1'|2)v(1,1')d\tau_1 d\tau_1' d\tau_2 - \\
&- \int v(1,1')\Lambda^{(1)}{}_A(12|12')\mathcal{A}^B_{1'2}\rho_B(1'|1')\rho_B(2'|2)d\tau_1 d\tau_1' d\tau_2 d\tau_2' + A \leftrightarrow B, \\
E^{(2)}_{\mathrm{exch-ind}}(\mathrm{cc}) = &- \int v(1,1')\Lambda^{(1)}{}_A(12|12')\Lambda_B(1'2'|1'2)d\tau_1 d\tau_1' d\tau_2 d\tau_2' + A \leftrightarrow B.
\end{aligned}
\tag{11-54}
$$

For the SAPT(CC) method the one- and two-electron first-order density matrices are obtained from the formula for the time-independent coupled cluster polarization propagator [47] (see Eq. (11-30)), where X is set to $V_{\mathrm{eff,B}}$ and $\omega = 0$. As in the ground-state case, it can be demonstrated [41] that the two-electron first-order matrices defined by setting $Y = e^{p_1p_2}_{q_1q_2}$ in Eq. (11-30) exhibit a correct behavior, i.e. that one can define the first-order cumulant according to Eq. (11-53).

The second-order exchange-induction energy is of a lesser importance than the first-order exchange energy, so in practical applications a more approximate treatment of this contribution is possible. To this end all terms in the first-order cumulant expansion of order $\mathcal{O}(W^2)$ and higher have been neglected. This truncation procedure leads to the following form of the perturbed cumulant

$$
\begin{aligned}
(\Lambda^{(1)})^{\,p_1p_2}_{q_1q_2} = &\langle e^{p_1p_2}_{q_1q_2}\Omega_2^{V_{\mathrm{eff,B}}}(0)\rangle + \langle S_2^\dagger e^{p_1}_{q_1}\widehat{\mathcal{P}}_1(e^{p_2}_{q_2}\Omega_1^{V_{\mathrm{eff,B}}}(0))\rangle + \\
&+\langle S_2^\dagger e^{p_2}_{q_2}\widehat{\mathcal{P}}_1(e^{p_1}_{q_1}\Omega_1^{V_{\mathrm{eff,B}}}(0))\rangle + \mathcal{O}(W^2).
\end{aligned}
\tag{11-55}
$$

Also for the ground-state cumulant only terms of the $\mathcal{O}(W^1)$ order, i.e. the first two terms of Eq. (11-50), have been used. Since the $E^{(2)}_{\mathrm{exch-ind}}(\mathrm{cc})$ contribution is of a total $\mathcal{O}(W^2)$ order, it has been neglected in the present SAPT(CCSD) implementation. The first-order one-electron density matrices needed in Eq. (11-54) are the same as used for the induction energy (see Section 11.3.2).

The exchange-induction energy can be formulated through monomer properties independent of another monomer, similarly to the induction energy expressed through monomer static density susceptibilities (see Eq. (11-21)). This formulation requires an introduction of the electron density-matrix operator $\rho(1|1')$, which in the algebraic approximation is given by the equation

$$\hat{\rho}(1|1') = \sum_{pq} e^p_q \phi^*_p(1)\phi_q(1'). \tag{11-56}$$

Then a generalization of the polarization propagator, denoted here as a half-propagator, should be defined for purely imaginary frequencies $i\omega$ as

$$\langle\langle X;Y\rangle\rangle^+_{i\omega} = 2\langle\Psi_0|XRe\ \Psi^Y(i\omega)\rangle. \tag{11-57}$$

Note that the CC half-propagator $\langle\langle Y;X\rangle\rangle^+_{i\omega}$ is obtained as a doubled first term of Eq. (11-30). With definitions from Eqs. (11-56) and (11-57) a new quantity, called a density-matrix susceptibility $\alpha(1|1';2|i\omega)$, can be introduced as

$$\alpha(1|1';2|i\omega) = -\langle\langle\hat{\rho}(1|1');\hat{\rho}(2)\rangle\rangle^+_{i\omega} = -\sum_{p_1q_1p_2q_2}\langle\langle e^{p_1}_{q_1};g^{p_2}_{q_2}\rangle\rangle^+_{i\omega}\phi_{p_1}(1)\phi_{q_1}(1')\phi_{p_2}(2)\phi_{q_2}(2), \tag{11-58}$$

where $g^p_q = \frac{1}{2}\left(e^p_q + e^q_p\right)$ is the Hermitian combination of the usual spinorbital replacement operators. With the just defined density-matrix susceptibilities and one-electron density matrices of monomers the non-cumulant part of the exchange-induction energy can be expressed in a following way [42]

$$\begin{aligned}
E^{(2)}_{\mathrm{exch-ind}}(\mathrm{nn}) = {} & \frac{1}{2}\int v(1,1')v_{\mathrm{eff,B}}(3)\alpha_A(1|1';3|0)\rho_B(1'|1)d\tau_1 d\tau'_1 d\tau_3 + \\
& + \frac{1}{2}\int v(1,1')v_{\mathrm{eff,B}}(3)\alpha_A(1|2';3|0)\mathcal{A}^B_{1'2'}\rho_B(1'|1')\rho_B(2'|1)d\tau_1 d\tau'_1 d\tau'_2 d\tau_3 + \\
& + \frac{1}{2}\int v(1,1')v_{\mathrm{eff,B}}(3)\mathcal{A}^{*A}_{12}\mathcal{A}^A_{1'2'}\alpha_A(1|1;3|0)\rho_A(2|1')\rho_B(1'|2)d\tau_1 d\tau'_1 d\tau_2 d\tau_3 + \\
& + \frac{1}{2}\int v(1,1')v_{\mathrm{eff,B}}(3)\left(\mathcal{A}^{*A}_{12}\mathcal{A}^A_{12'}\mathcal{A}^B_{1'2} - 1 - \pi^{*A}_{12}\pi^A_{1'2'}\right)\alpha_A(1|1;3|0)\rho_A(2|2') \times \\
& \times\rho_B(1'|1')\rho_B(2'|2)d\tau_1 d\tau'_1 d\tau_2 d\tau'_2 d\tau_3 + A \leftrightarrow B.
\end{aligned} \tag{11-59}$$

Similar expressions can be derived also for cumulant-containing quantities [42]. As in the case of the induction energy, Eq. (11-59) is not suitable for a practical

implementation, although it can possibly serve for devising better trial functions in a fitting procedure of potential energy surfaces obtained by SAPT.

11.4.3. Second-Order Exchange-Dispersion Energy

The second-order exchange-dispersion energy has been recently expressed [42] through monomer properties, such as one-electron density matrices and frequency-dependent density-matrix susceptibilities introduced at the end of Section 11.4.2. In this review only the main (non-cumulant) part of the corresponding formula will be presented. The omitted part of $E^{(2)}_{\mathrm{exch-disp}}$ contains unimplemented cumulant quantities, which in the algebraic approximation lead to 6-index expansion coefficients. A numerical experience gained from the calculations of analogous cumulant parts of the first-order exchange and the second-order exchange-induction energies, as well as a comparison with the exact (FCI) exchange-dispersion energy for a helium dimer [67] allows us to estimate the importance of the neglected terms at level of a couple percent of the total $E^{(2)}_{\mathrm{exch-disp}}$ contribution for the attractive region of PES. The expression for the exchange-dispersion energy bears some similarity to the Longuet-Higgins formula for the dispersion energy (see Eq. (11-32))

$$
\begin{aligned}
E^{(2)}_{\mathrm{exch-disp}}(\mathrm{nn}) = \frac{1}{2\pi}\int_0^\infty \Bigg[& \int v(1,1')\alpha_A(1|1';3|i\omega)\alpha_B(1'|1;3'|i\omega)\frac{1}{r_{33'}}d\tau_1 d\tau_1' d\tau_3 d\tau_3' + \\
& + \int v(1,1')\alpha_A(1|2';3|i\omega)\mathcal{A}^{*B}_{1'2'}\mathcal{A}^{B}_{1'1}\alpha_B(1'|1';3'|i\omega)\rho_B(2'|1)\frac{1}{r_{33'}}d\tau_1 d\tau_1' d\tau_2' d\tau_3 d\tau_3' + \\
& + \int v(1,1')\mathcal{A}^{*A}_{12}\mathcal{A}^{A}_{11'}\alpha_A(1|1;3|i\omega)\rho_A(2|1')\alpha_B(1'|2;3'|i\omega)\frac{1}{r_{33'}}d\tau_1 d\tau_1' d\tau_2 d\tau_3 d\tau_3' + \\
& + \int v(1,1')\big(\mathcal{A}^{*A}_{12}\mathcal{A}^{A}_{12'}\mathcal{A}^{*B}_{1'2'}\mathcal{A}^{B}_{1'2} - 1 - \pi^{*A}_{12}\pi^{A}_{12'}\pi^{*B}_{1'2'}\pi^{B}_{1'2}\big)\alpha_A(1|1;3|i\omega)\rho_A(2|2') \times \\
& \times \alpha_B(1'|1';3'|i\omega)\rho_B(2'|2)\frac{1}{r_{33'}}d\tau_1 d\tau_1' d\tau_2 d\tau_2' d\tau_3 d\tau_3' \Bigg] d\omega. \qquad (11\text{-}60)
\end{aligned}
$$

From Eq. (11-57) it is clear that the density susceptibility and density-matrix susceptibility share the same first-order wave functions $\Psi^{G^p_q}(i\omega)$. Since for the CC case the calculation of these functions dominates the CPU time, the computational requirements for the dispersion and exchange-dispersion energies are basically the same. For density-matrix susceptibilities one can still apply the density fitting to the second pair of orbitals in Eq. (11-58), so the same scaling of the computational effort is preserved also for the density-fitted version of the exchange-dispersion energy. The expansion coefficients for one-electron density matrices and density-matrix susceptibilities of monomers at the CCSD level are calculated according to Eq. (11-15) and the first part of Eq. (11-31), respectively.

It should be stressed that the second-order exchange energies in SAPT(MP), as implemented in the SAPT program [16], are so far treated on the uncorrelated level,

i.e. the SAPT(HF) values for these terms are used.[4] The SAPT(CC) method represents therefore the first implementation of the second-order exchange contributions with the inclusion of the intramonomer electron correlation.

11.5. TOTAL SAPT(CCSD) INTERACTION ENERGY

The energy components described in Sections 11.3 and 11.4 give the SAPT(CCSD) interaction energy up to the second order in terms of the intermolecular operator V. A derivation of higher-order corrections is quite involved even for monomers described by HF determinants [68] and – on the other side – a systematic improvement of the SAPT interaction energy by adding these corrections cannot be guaranteed in view of a divergence of the SRS series for many-electron monomers. To circumvent this difficulty, it has been proposed some time ago to approximately account for some of these missing contributions by adding the so-called HF "delta" correction term δE_{HF}, which is calculated as a difference between the HF supermolecular interaction energy and the SAPT(HF) electrostatic, first-order exchange, induction, and exchange-induction terms (the last two components obtained within the CHF approach) [69, 70]. Due to its simplicity and a visible improvement of the results for many noncovalent complexes, the utilization of the δE_{HF} correction has become a standard in the SAPT(MP) and SAPT(DFT) applications. However, very recently it has been postulated that this term should be added only for interactions involving polar or polarizable molecules [68], since only in these cases the δE_{HF} correction can be approximately identified with a sum of the third-order induction and exchange-induction terms, $E_{\mathrm{ind}}^{(3)} + E_{\mathrm{exch-ind}}^{(3)}$. Therefore, in numerical examples presented in Section 11.6 the utilization of the δE_{HF} term will depend on the polarity of a system under study.

For the case of the SAPT(CCSD) method one more correction term should be added. Let us first remind that multiple exchanges of electrons between the interacting monomers are neglected for all exchange components of the interaction energy. Although the contributions beyond the S^2 approximation are small in the attractive region of PES, they can be nonetheless more significant in the repulsive part of the potential. In order to approximately account for this effect, a missing multiple-exchange part of the $E_{\mathrm{exch}}^{(1)}$ term is estimated on the HF level by calculating a difference

$$\delta E_{\mathrm{exch}}^{(100)}(S^2) = E_{\mathrm{exch}}^{(100)} - E_{\mathrm{exch}}^{(100)}(S^2), \tag{11-61}$$

where $E_{\mathrm{exch}}^{(100)}(S^2)$ and $E_{\mathrm{exch}}^{(100)}$ denote the HF first-order exchange energies calculated with and without the S^2 approximation, respectively.

---

[4] For the exchange-induction energy a scaling procedure has been proposed to estimate the missing intramonomer correlation part, ${}^t E_{\mathrm{exch-ind}}^{(22)} = \frac{{}^t E_{\mathrm{ind}}^{(22)}}{E_{\mathrm{ind,resp}}^{(20)}} E_{\mathrm{exch-ind,resp}}^{(20)}$.

Summarizing, the total SAPT(CCSD) interaction energy is composed of the following terms

$$E_{\rm int} = E^{(1)}_{\rm elst}({\rm XCCSD}) + E^{(2)}_{\rm ind}({\rm XCCSD}) + E^{(2)}_{\rm disp}({\rm XCCSD}) + E^{(1)}_{\rm exch}({\rm XCCSD}) + \\ + E^{(2)}_{\rm exch-ind}({\rm XCCSD}) + E^{(2)}_{\rm exch-disp}({\rm XCCSD}) + \delta E^{(100)}_{\rm exch}(S^2) + (\delta E_{\rm HF}). \quad (11\text{-}62)$$

The parenthesis around the $\delta E_{\rm HF}$ term emphasizes that in order to utilize this corrections the conditions listed at the beginning of this Section and in Ref. [68] should be fulfilled. All six SAPT components are used in the form and within approximations discussed earlier.

11.5.1. Accuracy of SAPT(CCSD) – Theoretical Considerations

The quality of the SAPT(CCSD) interaction energy can be most easily gauged by an analysis of electron configurations, which are included in this approach for large distances between interacting molecules. Both monomers in SAPT(CCSD) are described by CCSD theory, so the part of the interaction resulting from simultaneous single and double excitations on A and B is correctly reproduced. Quite on the contrary, in the available SAPT(MP) corrections (with the exception of the $E^{(211)}_{\rm disp}$ and $E^{(111)}_{\rm exch}$ terms) one monomer is always treated on the HF level. Since simultaneous double excitations on both monomers mean a *quadruple* excitation for a dimer, the SAPT(CCSD) interaction energy should be compared with the supermolecular interaction energy obtained from CCSDTQ theory (coupled cluster theory limited to single, double, triple, and quadruple excitations) [71] (or at least with a somewhat cheaper CCSDT(Q) theory [72]), rather than with the popular CCSD(T) approach [62].

On the other hand, the molecular properties described by CC theory limited to single and double excitations only may not be accurate enough for needs of SAPT energy components. The deficiencies of the XCCSD properties can be (somewhat artificially) divided into problems related to the orbital relaxation and to the connected triple and higher excitations in monomers' wave functions. One of the known shortcomings of the XCCSD first- and second-order properties, already discussed in Sections 11.3.1 and 11.3.2, is an absence of some $\mathcal{O}(W^3)$ terms, appearing within the XCC approach only after triple amplitudes (T_3) are included. As already mentioned, a solution of this problem for the case of the first-order one-electron properties has been provided by Jeziorski and Moszynski in Ref. [46] through the $\overline{X}_{\rm resp}(3)$ model. Since in this method a CHF-type equation has to be solved, the $\overline{X}_{\rm resp}(3)$ approach incorporates explicitly the effect of orbital relaxation, while the original XCCSD method includes the orbital response only implicitly through the e^{T_1} operator [73]. On the other hand, the absence of the T_1 operator in the $\overline{X}_{\rm resp}(3)$ formula (see Eq. (11-18)) may lead to a lower accuracy for molecules with a large admixture of single excitations in the exact wave functions. Finally, neither XCCSD, nor $\overline{X}_{\rm resp}(3)$

approaches are expected to be accurate for molecules with a large contribution from connected triple (and higher) excitations (e.g. molecules with multiple bonds).

11.5.2. Numerical Details

The SAPT(CCSD) calculations presented here have been performed with a local developer version of the MOLPRO suite of codes [33]. The SAPT(MP) results have been obtained with the SAPT [16] program, using the standard level of approximations [74]. For CCSDT(Q) and CCSDTQ supermolecular calculations the MRCC code [75, 76] of Kállay has been used. The SAPT(DFT) results have been obtained with the program of Heßelmann et al. [27, 28, 30, 31, 77] which is a part of MOLPRO. The functional similar to PBE0 [78, 79], which differs from the original PBE0 by replacing the PBEc functional with PW91, with the asymptotic correction of Grüning et al. [80] has been used to describe the intramonomer correlation in SAPT(DFT). The ionization potentials needed to calculate this correction have been taken from Ref. [81]. In all supermolecular calculations the Boys-Bernardi counterpoise correction for BSSE has been used [6].

The Be$\cdots$H$_2$, (HF)$_2$, Ne$_2$, and (CO)$_2$ noncovalent complexes have been selected as examples of various limiting cases discussed above. For the first three complexes the aug-cc-pVTZ basis set has been utilized, while for the dimer of carbon monoxide a smaller aug-cc-pVDZ basis has been applied [82]. For the (HF)$_2$ and (CO)$_2$ complexes the mutual orientations of monomers correspond to those at the global minima (see Refs. [83, 84], respectively), while distances between monomers (as defined in respective references) have been varied. For density-fitted SAPT(CCSD) components the corresponding aug-cc-pVXZ/MP2fit ($X = D, T$) auxiliary basis sets [85] have been used, with the exception of the Be atom where the cc-pVTZ/MP2fit basis has been utilized. It has been verified that the CCSD(T) and CCSDT(Q) interaction energies for the dimers of HF and Ne differ by at most few tenths of percent, therefore only the CCSD(T) energy was used for a comparison in these two cases.

11.6. PERFORMANCE OF SAPT(CCSD)

11.6.1. Be$\cdots$H$_2$ Complex

Figure 11-1 presents interaction energies for the complex of the beryllium atom and the hydrogen molecule obtained from the SAPT(CCSD), SAPT(MP), and SAPT(DFT) methods, as well as from CCSDTQ and CCSD(T) supermolecular theories. Since beryllium is a highly polarizable species, the δE_{HF} term has been used in the SAPT approach.

The CCSD(T) and CCSDTQ interaction energies differ noticeably for the case of the Be$\cdots$H$_2$ complex (the error of the CCSD(T) energy amounts to 9% at the minimum and 5% for large distances). This fact can be explained qualitatively by the importance of a low-energy doubly-excited configuration $1s^2 2p^2$ of beryllium. Because

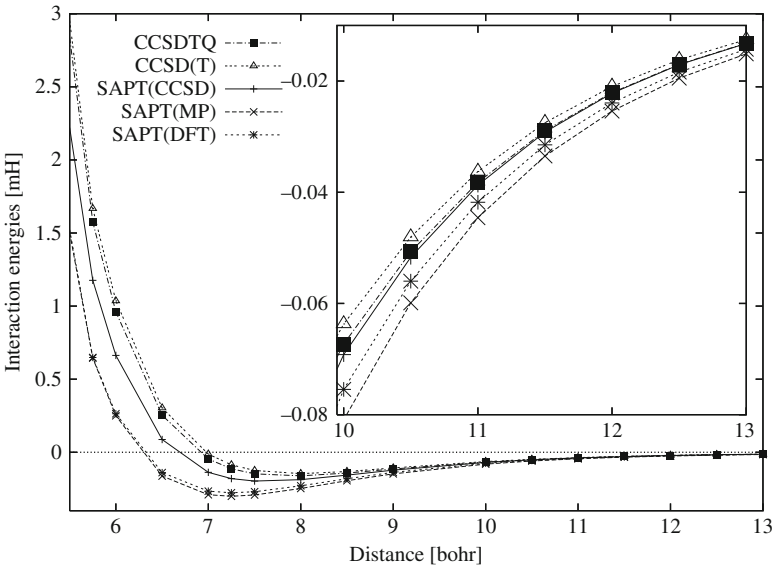

Figure 11-1. Interaction energies for the Be$\cdots$H$_2$ complex (linear configuration, R$_{H-H}$=1.449 bohr) calculated by various perturbational and supermolecular methods. All electrons are correlated

of its significant weight in the exact wave function of beryllium this configuration should be treated on an equal footing with the ground-state configuration $1s^2 2s^2$ in supermolecular calculations of beryllium-containing complexes. In particular, configurations which are doubly-excited on the Be atom and singly- or doubly-excited on H_2 should be available for the supermolecular method. Evidently, such a treatment is not possible within the supermolecular CCSD(T) theory, and a more advanced CC approach is necessary in this case.

Similar considerations allow to explain the observed behavior of the SAPT(CCSD) interaction energies, which are close to the CCSDTQ energies for large distances. For $R \geq 11$ bohr errors of SAPT(CCSD) with respect to CCSDTQ drop below the 1% threshold. A generally poor performance of all SAPT approaches for smaller distances can be explained by a high polarizability of beryllium, what makes the second-order perturbation theory inadequate in this case. It should be stressed, however, that the SAPT(DFT) and SAPT(MP) methods perform substantially worse than SAPT(CCSD), what for the case of SAPT(MP) can be rationalized by an insufficient inclusion of intramonomer correlation. A behavior of SAPT(CCSD) for large separations between monomers in the Be$\cdots$H$_2$ complex is an illustration of the limit case where the contributions from *inter*monomer triple and quadruple excitations are large on the one side, and a role of *intra*monomer triple and quadruple excitations is very small on the other.

11.6.2. Dimers of HF, CO, and Ne

Table 11-1 presents the interaction energies obtained with various SAPT methods and compared to the supermolecular CCSDT(Q) and CCSD(T) interaction energies for $(HF)_2$, $(CO)_2$, and Ne_2 complexes (distances $R = 5$, 6, and 8 bohr for $(HF)_2$, Ne_2, and $(CO)_2$ correspond to the minimum region, respectively). The δE_{HF} term has been used for the dimer of hydrogen fluoride. The individual SAPT energy components for the same complexes are listed in Table 11-2.

Let us first examine the hydrogen fluoride dimer. It can be seen from Table 11-1 that the SAPT(CCSD) approach performs disappointingly bad for a smaller distance, especially in comparison to SAPT(MP), while the agreement with CCSD(T) becomes substantially better for a larger distance. As discussed in Section 11.5, the source of this behavior can be traced down either to an insufficient inclusion of orbital relaxation or to a large contribution of connected triple amplitudes for monomer properties. For a highly polar HF molecule the first explanation is more plausible. Indeed, if the $\overline{X}_{\mathrm{resp}}(3)$ density matrices are used instead of the XCCSD ones in the formulae for the first-order energies (see Eqs. (11-10) and (11-46)), the agreement with the CCSD(T) interaction energies remarkably improves. For the $(HF)_2$ complex the first-order SAPT components are dominant contributions to the interaction energy (see Table 11-2), therefore it is not unexpected that a better treatment of these two energies improves the overall result. On the other hand, a small error of the SAPT(MP) interaction energy should be regarded as a result of some error cancellation, since the differences between SAPT(MP) and SAPT(CCSD) exchange-induction energies are close to the differences between the corresponding total SAPT energies.

Table 11-1. A comparison of total SAPT and supermolecular interaction energies. The row with CCSD(T) energies is followed by percent errors of this method with respect to CCSDT(Q). For the $(CO)_2$ complex the rows with SAPT energies are followed by percent errors with respect to CCSDT(Q) and with CCSD(T) (the value in parenthesis), while for two other complexes just the error with respect to CCSD(T) is listed. Energies are in millihartrees, distances in bohr

Molecule	$(HF)_2$		$(CO)_2$		Ne_2		
Method/R	5	7	8	10	4	6	7
CCSDT(Q)	–	–	–0.454	–0.286	–	–	–
CCSD(T)	−6.436	−3.052	–0.430	–0.278	7.575	−0.081	−0.053
	–	–	–5.3	–2.8	–	–	–
SAPT(CCSD)	−5.895	−3.012	–0.466	–0.313	7.728	−0.082	−0.054
	−8.4	−1.3	2.8(8.6)	9.5 (12.7)	2.0	1.5	3.1
SAPT(MP)	−6.575	−3.126	–0.484	–0.304	7.954	−0.078	−0.053
	2.2	2.4	6.7(12.6)	6.4(9.5)	5.0	−3.7	0.6
SAPT(DFT)	−5.733	−3.051	–0.393	–0.275	8.136	−0.082	−0.053
	−10.9	0.0	–13.4(–8.6)	–3.8(–1.0)	7.4	1.0	0.9
SAPT(CCSD)[a]	−6.492	−3.083	–0.380	–0.295	7.369	−0.088	−0.055
	0.9	1.0	–16.2(–11.5)	3.2(6.2)	−2.7	8.7	4.3

[a] This row contains the SAPT(CCSD) energies obtained if the XCCSD one-electron density matrices are replaced by $\overline{X}_{\mathrm{resp}}(3)$ for the first-order components of the interaction energy.

Table 11-2. Individual components of interaction energies obtained with various SAPT approaches. The SAPT(HF) terms, denoted as HF, are followed by intramonomer correlation contributions from the SAPT(CCSD), SAPT(MP), and SAPT(DFT) methods, which are denoted as CCSD, MP, and DFT, respectively. For SAPT(CCSD) also the cumulant corrections [CCSD(c)] are given. All exchange contributions are presented within the S^2 approximation. The corrections for multiple exchanges for the $E^{(1)}_{\mathrm{exch}}$ energy are listed at the bottom of the table

Molecule	$(HF)_2$		$(CO)_2$		Ne_2		
Method/R	5	7	8	10	4	6	7
	$E^{(1)}_{\mathrm{elst}}$						
HF	−12.5116	−2.9354	−0.5077	−0.0746	−3.2658	−0.0203	−0.0014
CCSD	0.4997	0.3222	−0.2758	−0.0686	−0.8932	−0.0117	−0.0011
MP	0.4111	0.2200	−0.2107	−0.0550	−0.5575	−0.0064	−0.0007
DFT	0.3580	0.2757	−0.1656	−0.0427	−0.7927	−0.0084	−0.0008
	$E^{(1)}_{\mathrm{exch}}$						
HF	11.7908	0.1545	1.1797	0.0358	12.0546	0.0857	0.0070
CCSD	2.4375	0.0674	0.2274	0.0108	2.4112	0.0411	0.0045
MP[a]	2.4712	0.0634	0.1984	0.0094	2.4237	0.0382	0.0041
DFT	2.3382	0.0557	0.1376	0.0066	2.6283	0.0333	0.0035
CCSD(c)	0.2119	0.0049	0.0607	0.0015	−0.1052	−0.0014	−0.0002
	$E^{(2)}_{\mathrm{ind}}$						
HF	−6.2091	−0.2303	−0.2625	−0.0057	−3.7943	−0.0151	−0.0006
CCSD	−1.2358	−0.0255	−0.0474	−0.0027	−1.4561	−0.0109	−0.0008
MP	−1.0421	−0.0209	−0.0086	0.0004	−1.1703	−0.0081	−0.0006
DFT	−1.1847	−0.0201	−0.0224	−0.0008	−1.2614	−0.0074	−0.0006
	$E^{(2)}_{\mathrm{exch-ind}}$						
HF	3.2101	0.0236	0.2125	0.0031	3.8882	0.0154	0.0006
CCSD	1.1738	0.0167	0.0581	0.0014	1.4759	0.0112	0.0008
MP[b]	0.5387	0.0021	0.0070	−0.0002	1.1993	0.0083	0.0006
DFT	1.1101	0.0125	0.0266	0.0007	1.3071	0.0075	0.0006
CCSD(c)	0.0753	0.0016	0.0157	0.0003	0.0013	0.0001	0.0000
	$E^{(2)}_{\mathrm{disp}}$						
HF	−3.4920	−0.3052	−1.0668	−0.2039	−2.4274	−0.1467	−0.0520
CCSD	−0.7919	−0.0946	−0.1000	−0.0138	−0.4965	−0.0362	−0.0119
MP	−0.7677	−0.0839	−0.1030	−0.0165	−0.4633	−0.0314	−0.0103
DFT	−0.6622	−0.0768	−0.0292	0.0020	−0.4475	−0.0306	−0.0100
	$E^{(2)}_{\mathrm{exch-disp}}$						
HF	0.5959	0.0111	0.0762	0.0031	0.4904	0.0041	0.0003
CCSD	0.2074	0.0085	0.0382	0.0021	0.1641	0.0029	0.0003
DFT	0.1840	0.0079	0.0270	0.0016	0.1579	0.0024	0.0002
δE_{HF}	−1.6421	−0.0253	−0.1088	−0.0023	−0.4732	−0.0017	−0.0001
$\delta E^{(100)}_{\mathrm{exch}}(S^2)$	0.0720	0.0000	0.0016	0.0000	0.0499	0.0000	0.0000
$\delta E^{(1)}_{\mathrm{exch}}(S^2)$(DFT)	0.0997	0.0000	0.0020	0.0000	0.0719	0.0000	0.0000

[a] The $E^{(1)}_{\mathrm{exch}}$(CCSD) energy has been used [14].

[b] The estimated correction, see the footnote on the page 288.

The second complex in Tables 11-1 and 11-2 is the dimer of carbon monoxide. A triple bond between carbon and oxygen atoms makes the CO molecule a notoriously difficult example for theories of electron correlation and requires an inclusion of higher excitations in order to achieve a good accuracy. It is also well known that electron correlation changes the sign of the dipole moment of the carbon monoxide molecule. Therefore it is not surprising that the role of intramonomer correlation is large also for a dimer of this molecule. From Table 11-2 is can be observed that the intramonomer correlation corrections are often of the same order of magnitude as their uncorrelated (HF) counterparts. For instance, the SAPT(CCSD) electrostatic intramonomer correction for the electrostatic energy amounts to 92% of the $E_{\mathrm{elst}}^{(100)}$ term for the larger distance considered. Table 11-1 shows that the SAPT(CCSD) error with respect to CCSDT(Q) is equal to 3% for the smaller distance while it becomes as high as 10% for the larger R. The differences with respect to the CCSD(T) energy are much larger. Table 11-2 reveals that three major energy components can be identified for $(CO)_2$. These components are: the first-order electrostatic and exchange energies and the second-order dispersion energy. As in the HF dimer case, the first-order energies have been also calculated with the $\overline{X}_{\mathrm{resp}}(3)$ monomer density matrices (see the last two lines of Table 11-1). This approach improves the agreement with CCSDT(Q) for a larger distance, but increases the error substantially for the minimum region. Note, however, that for $R = 10$ bohr the electrostatic energy has the largest intramonomer correlation contribution, so a smaller error of the SAPT(CCSD) energy calculated with $\overline{X}_{\mathrm{resp}}(3)$ densities can be explained by an improvement in the description of the electrostatic component. On the other hand, for the smaller distance an insufficient inclusion of the intramonomer correlation into the second-order SAPT(CCSD) components may play a role. Based on these results a preliminary conclusion can be reached that the $(CO)_2$ dimer requires both triple excitations and orbital relaxation effects to be included in the description of density matrices and density susceptibilities in order to obtain a better agreement with the CCSDT(Q) benchmark interaction energies. This complex shows therefore limitations of the present implementation of the SAPT(CC) method.

The last complex examined in Tables 11-1 and 11-2 is a neon dimer. In this case the SAPT(CCSD) interaction energy agrees well with the CCSD(T) values, but the utilization of the $\overline{X}_{\mathrm{resp}}(3)$ density matrices for the first-order SAPT(CCSD) components results in larger errors with respect to CCSD(T), especially in the minimum region. It can be therefore concluded that the $\overline{X}_{\mathrm{resp}}(3)$ density matrices should be rather used for cases with dominant first-order contributions to the interaction energy, i.e. for polar monomers. Asymptotically, the Ne_2 complex is bound by the dispersion energy, although for smaller distances also other, short-range, energy contributions are equally important. In particular, for the first distance in Table 11-2, which corresponds to the repulsive part of PES, almost all energy components are of the same order of magnitude. The leading correction for this distance is the first-order exchange energy, for which the intramonomer correlation amounts to about 20% of the HF value. The induction and exchange-induction contributions are also quite large, but they cancel each other almost perfectly, giving the net zero contribution.

For two larger distances the dispersion energy becomes a dominant component of the interaction energy, and its intramonomer correlation part is well described by all three SAPT methods. It is interesting to note that for other components the relative importance of the intramonomer electron correlation becomes more pronounced for larger distances, e.g. the intramonomer correlation part of the exchange-dispersion energy amounts to about 70% of $E^{(200)}_{\mathrm{exch-disp}}$ for $R = 7$ bohr.

The individual energy components listed in Table 11-2 allow us to make some general conclusions about the accuracy of the intramonomer correlation corrections. An examination of this table reveals that the agreement between intramonomer correlation corrections calculated by the SAPT(CCSD), SAPT(MP), and SAPT(DFT) methods is usually good, especially for the dimers of HF and Ne. Larger differences occur mostly for the problematic case of $(CO)_2$. As a rule, the cumulant contributions in SAPT(CCSD) are quite small in comparison to the total exchange corrections, but they should be nonetheless included into the SAPT(CC) energy if a high accuracy is desired.

11.7. CONCLUSIONS

The presented SAPT(CC) approach allows for an accurate treatment of intramonomer electron correlation, and is in addition free from the uncertainties plaguing two other available SAPT methods, which are caused either by the possible divergence of the MP series or by an ambiguity in the choice of the DFT functional. However, the high accuracy comes always at a price of a high cost of the computations, therefore the new method can be applied only for small, few-atom monomers. Among three available treatments of intramonomer correlation only the SAPT(DFT) method has the capabilities to tackle large noncovalent complexes. It is therefore very reassuring that the agreement between SAPT(CCSD) and SAPT(DFT) energy components is quite good in nearly all cases. In particular, a closeness of the first-order exchange energies obtained from both methods indicates that the one-electron density matrix composed of KS orbitals provides a good estimate of the exact density matrix (note parenthetically that this fact is not so evident, since in density functional theory only densities, but not density *matrices*, can be in principle exact). The smallness of the cumulant part of the exchange energy, which is absent in SAPT(DFT), is also important in justifying the SAPT(DFT) treatment of the exchange contributions to the interaction energy. It is interesting to note that the non-cumulant parts of the SAPT(CCSD) exchange energies agree even better with the corresponding SAPT(DFT) values. The second-order exchange components calculated by SAPT(CCSD) and SAPT(MP) are quite different, what can be explained by the neglect of the intramonomer correlation effect for the exchange-induction and exchange-dispersion energies in the current version of SAPT(MP). On the other hand, the agreement between SAPT(CCSD) and SAPT(DFT) for these two energy components is very good, what justifies the use of the CKS monomer propagators [31, 77] for the calculation of the discussed quantities. It should be stressed that the

agreement of the exchange-dispersion term obtained from the uncoupled KS propagators is usually substantially worse [42].

ACKNOWLEDGMENTS

The author thanks Prof. Bogumił Jeziorski for reading and commenting on the manuscript.

REFERENCES

1. K. Szalewicz, K. Patkowski, B. Jeziorski, Structure and Bonding **116**, 43 (2005)
2. P. Hobza, R. Zahradník, K. Müller-Dethlefs, Coll. Czech. Chem. Commun. **71**, 443 (2006)
3. K. Szalewicz, B. Jeziorski, J. Chem. Phys. **109**, 1198 (1998)
4. G. Chalasinski, M. M. Szczesniak, Chem. Rev. **94**, 1723 (1994)
5. R. J. Bartlett, J. Phys. Chem. **93**, 1697 (1989)
6. S. F. Boys, F. Bernardi, Mol. Phys. **19**, 553 (1970)
7. B. Jeziorski, W. Kolos, Int. J. Quantum Chem. Suppl. **12**(1), 91 (1977)
8. B. Jeziorski, G. Chalasinski, K. Szalewicz, Int. J. Quantum Chem. **14**, 271 (1978)
9. K. Szalewicz, B. Jeziorski, Mol. Phys. **38**, 191 (1979)
10. B. Jeziorski, W. Kolos, Perturbation Approach to the Study of Weak Intermolecular Interactions. In *Molecular Interactions*, vol. 3, Eds. H. W. J. Ratajczak, W. J. Orville-Thomas (Wiley, New York, 1982), pp. 1–46
11. B. Jeziorski, R. Moszynski, S. Rybak, K. Szalewicz, Many-Body Theory of van der Waals Interactions. In *Many-Body Methods in Quantum Chemistry*, Lecture Notes in Chemistry, vol. 52, Ed. U. Kaldor (Springer, New York, 1989), pp. 65–94
12. S. Rybak, B. Jeziorski, K. Szalewicz, J. Chem. Phys. **95**, 6576 (1991)
13. R. Moszynski, B. Jeziorski, K. Szalewicz, J. Chem. Phys. **100**, 1312 (1994)
14. R. Moszynski, B. Jeziorski, S. Rybak, K. Szalewicz, H. L. Williams, J. Chem. Phys. **100**, 5080 (1994)
15. R. Moszynski, S. M. Cybulski, G. Chalasinski, J. Chem. Phys. **100**, 4998 (1994)
16. R. Bukowski, W. Cencek, P. Jankowski, M. Jeziorska, B. Jeziorski, S. A. Kucharski, V. F. Lotrich, A. J. Misquitta, R. Moszyński, K. Patkowski, R. Podeszwa, S. Rybak, K. Szalewicz, H. L. Williams, R. J. Wheatley, P. E. S. Wormer, P. S. Żuchowski, SAPT2008: An Ab Initio Program for Many-Body Symmetry-Adapted Perturbation Theory Calculations of Intermolecular Interaction Energies. University of Delaware and University of Warsaw (2008). URL http://www.physics.udel.edu/∼szalewic/SAPT/SAPT.html
17. B. Jeziorski, R. Moszynski, K. Szalewicz, Chem. Rev. **94**, 1887 (1994)
18. J. O. Hirschfelder, I. Chem. Phys. Lett. **1**, 325 (1967)
19. B. Jeziorski, W. A. Schwalm, K. Szalewicz, J. Chem. Phys. **73**, 6215 (1980)
20. W. H. Adams, Int. J. Quantum Chem. **72**, 393 (1999)
21. K. Patkowski, T. Korona, B. Jeziorski, J. Chem. Phys. **115**, 1137 (2001)
22. R. Moszynski, B. Jeziorski, A. Ratkiewicz, S. Rybak, J. Chem. Phys. **99**, 8856 (1993)
23. R. Moszynski, B. Jeziorski, K. Szalewicz, Int. J. Quantum Chem. **45**, 409 (1993)
24. H. L. Williams, C. F. Chabalowski, J. Phys. Chem. A **105**, 646 (2001)
25. G. Jansen, A. Heßelmann, J. Phys. Chem. A **105**, 11156 (2001)
26. A. J. Misquitta, K. Szalewicz, Chem. Phys. Lett. **357**, 301 (2002)
27. A. Heßelmann, G. Jansen, Chem. Phys. Lett. **357**, 464 (2002)
28. A. Heßelmann, G. Jansen, Chem. Phys. Lett. **362**, 319 (2002)

29. A. J. Misquitta, B. Jeziorski, K. Szalewicz, Phys. Rev. Lett. **91**, 033201 (2003)
30. A. Heßelmann, G. Jansen, Chem. Phys. Lett. **367**, 778 (2003)
31. A. Heßelmann, G. Jansen, Phys. Chem. Chem. Phys. **5**, 5010 (2003)
32. J. Olsen, P. Jørgensen, T. Helgaker, O. Christiansen, J. Chem. Phys. **112**, 9736 (2000)
33. H. J. Werner, P. J. Knowles, R. Lindh, F. R. Manby, M. Schütz, P. Celani, T. Korona, A. Mitrushenkov, G. Rauhut, T. B. Adler, R. D. Amos, A. Bernhardsson, A. Berning, D. L. Cooper, M. J. O. Deegan, A. J. Dobbyn, F. Eckert, E. Goll, C. Hampel, G. Hetzer, T. Hrenar, G. Knizia, C. Köppl, Y. Liu, A. W. Lloyd, R. A. Mata, A. J. May, S. J. McNicholas, W. Meyer, M. E. Mura, A. Nicklass, P. Palmieri, K. Pflüger, R. Pitzer, M. Reiher, U. Schumann, H. Stoll, A. J. Stone, R. Tarroni, T. Thorsteinsson, M. Wang, A. Wolf, Molpro, version 2008.2, a package of ab initio programs (2008). See http://www.molpro.net
34. T. Korona, B. Jeziorski, R. Moszynski, Mol. Phys. **100**, 1723 (2002)
35. T. Korona, M. Przybytek, B. Jeziorski, Mol. Phys. **104**, 2303 (2006)
36. T. Korona, B. Jeziorski, J. Chem. Phys. **125**, 184109 (2006)
37. T. Korona, Phys. Chem. Chem. Phys. **9**, 6004 (2007)
38. T. Korona, B. Jeziorski, J. Chem. Phys. **128**, 144107 (2008)
39. T. Korona, J. Chem. Phys. **122**, 224104 (2008)
40. T. Korona, Phys. Chem. Chem. Phys. **10**, 5698 (2008)
41. T. Korona, Phys. Chem. Chem. Phys. **10**, 6509 (2008)
42. T. Korona, J. Chem. Theory Comp. **5**, 2663 (2009)
43. P. O. Löwdin, Phys. Rev. **97**, 1474 (1955)
44. H. C. Longuet-Higgins, Proc. R. Soc. Lond. A **235**, 537 (1956)
45. A. Heßelmann, G. Jansen, J. Chem. Phys. **112**, 6949 (2000)
46. B. Jeziorski, R. Moszynski, Int. J. Quantum Chem. **48**, 161 (1993)
47. R. Moszynski, P. S. Żuchowski, B. Jeziorski, Coll. Czech. Chem. Commun. **70**, 1109 (2005)
48. J. Paldus, B. Jeziorski, Theor. Chim. Acta **73**, 81 (1988)
49. H. J. Monkhorst, Int. J. Quantum Chem. Symp. **11**, 421 (1977)
50. L. Adamowicz, W. D. Laidig, R. J. Bartlett, Int. J. Quantum Chem. Symp. **18**, 245 (1984)
51. R. J. Bartlett, Analytical Evaluation of Gradients in Coupled Cluster and Many Body Perturbation Theory. In *Geometrical Derivatives of Energy Surfaces and Molecular Properties*, Eds. P. Jørgensen, J. Simons (Reidel, Dordrecht, The Netherlands, 1986), p. 35.
52. P. Jørgensen, T. Helgaker, J. Chem. Phys. **89**, 1560 (1988)
53. J. G. Ángyán, G. Jansen, M. Loos, C. Hättig, B. A. Heß, Chem. Phys. Lett. **219**, 267 (1994)
54. J. Oddershede, Adv. Quant. Chem. **11**, 275 (1978)
55. H. L.Williams, E. M. Mas, K. Szalewicz, B. Jeziorski, J. Chem. Phys. **103**, 7374 (1995)
56. O. Christiansen, P. Jørgensen, C. Hättig, Int. J. Quantum Chem. **68**, 1 (1998)
57. R. J. Wheatley, J. Comput. Chem. **29**, 445 (2008)
58. H. C. Longuet-Higgins, Chem. Soc. **40**, 7 (1965)
59. B. I. Dunlap, J. W. D. Connolly, J. R. Sabin, J. Chem. Phys. **71**, 4993 (1979)
60. B. I. Dunlap, Phys. Chem. Chem. Phys. **2**, 2113 (2000)
61. H. L. Williams, K. Szalewicz, R. Moszynski, B. Jeziorski, J. Chem. Phys. **103**, 4586 (1995)
62. K. Raghavachari, G. W. Trucks, J. A. Pople, M. Head-Gordon, Chem. Phys. Lett. **157**, 479 (1989)
63. B. Jeziorski, M. Bulski, L. Piela, Int. J. Quantum Chem. **10**, 281 (1976)
64. M. Bulski, G. Chalasinski, B. Jeziorski, Theor. Chim. Acta **52**, 93 (1979)
65. P. Jankowski, B. Jeziorski, S. Rybak, K. Szalewicz, J. Chem. Phys. **92**, 7441 (1990)
66. W. Kutzelnigg, D. Mukherjee, J. Chem. Phys. **107**, 432 (1997)
67. T. Korona, H. L. Williams, R. Bukowski, B. Jeziorski, K. Szalewicz, J. Chem. Phys. **106**, 5109 (1997)
68. K. Patkowski, K. Szalewicz, B. Jeziorski, J. Chem. Phys. **125**, 154107 (2006)

69. M. Jeziorska, B. Jeziorski, J. Čížek, Int. J. Quantum Chem. **32**, 149 (1987)
70. R. Moszynski, T. G. A. Heijmen, B. Jeziorski, Mol. Phys. **88**, 741 (1996)
71. S. A. Kucharski, R. J. Bartlett, J. Chem. Phys. **97**, 4282 (1992)
72. Y. J. Bomble, J. F. Stanton, M. Kállay, J. Gauss, J. Chem. Phys. **123** (2005)
73. D. J. Thouless, Nucl. Phys. **21**, 225 (1960)
74. B. Jeziorski, K. Szalewicz, Symmetry-Adapted Perturbation Theory. In *Handbook of Molecular Physics and Quantum Chemistry*, vol. 3, Ed. S. Wilson (Wiley, New York, 2003), p. 232.
75. M. Kállay, MRCC, a String-Based Quantum Chemical Program Suite Written by M. Kállay. See http://www.mrcc.hu
76. M. Kállay, R. J. Surján, J. Chem. Phys. **115**, 2945 (2001)
77. A. Heßelmann, G. Jansen, M. Schütz, J. Chem. Phys. **122**, 014103 (2005)
78. J. P. Perdew, K. Burke, M. Ernzerhof, Phys. Rev. Lett. **77**, 3865 (1996)
79. C. Adamo, V. Barone, J. Chem. Phys. **110**, 6158 (1999)
80. M. Grüning, O. V. Gritsenko, S. J. A. van Gisergen, E. J. Baerends, J. Chem. Phys. **114**, 652 (2001)
81. Computational Chemistry Comparison and Benchmark DataBase. `http://cccbdb.nist.gov` (accessed July 1, 2008)
82. T. H. Dunning Jr., J. Chem. Phys. **90**, 1007 (1989)
83. M. P. Hodges, A. J. Stone, E. C. Lago, J. Phys. Chem. A **102**, 2455 (1998)
84. G. W. M. Vissers, P. E. S. Wormer, A. van der Avoird, Phys. Chem. Chem. Phys. **5**, 4767 (2003)
85. F. Weigend, M. Häser, H. Patzelt, R. Ahlrichs, Chem. Phys. Lett. **294**, 143 (1998)

CHAPTER 12

UNCONVENTIONAL ASPECTS OF COUPLED-CLUSTER THEORY

WERNER KUTZELNIGG

Lehrstuhl für Theoretische Chemie, Ruhr-Universität Bochum, D-44780 Bochum, Germany, e-mail: werner.kutzelnigg@ruhr-uni-bochum.de

Abstract: The formalism of *Quantum chemistry in Fock space* is used to analyse coupled-cluster (CC) theory for a closed-shell state. A main aspect is the challenge of generally accepted wisdom. The theoretical background of CC theory is the separation theorem in Fock space. This applies to systems that are separable in a localized representation. In three main parts (a) the traditional coupled cluster (TCC) method, based on a non-unitary similarity transformation of the Hamiltonian, (b) variational coupled cluster (VCC) in intermediate normalization, and (c) unitary coupled cluster (UCC) approaches are analyzed. The infinite summation of diagrams from many-body perturbation theory (MBPT) is studied. It is stressed that higher-order non-linear (multi-commutator) terms are dominated by *diagonal* EPV contributions with repeated hole labels, that lead to an *individual normalization* of the pair functions, familiar from the *coupled electron pair approximation* (CEPA). This concept is generalizable to clusters of higher particle rank. An estimation of the difference between TCC and VCC is presented. The most promising reformulation of CC theory appears to be in terms of UCC, for which a closed summation of the bulk contributions is derived.

Keywords: Traditional coupled cluster, Variational coupled cluster, Unitary coupled cluster, Extended coupled cluster, Diagram summation, Coupled electron pair approximation, Exclusion principle violating terms, Fock space

12.1. INTRODUCTION

Coupled-Cluster (CC) theory is one of the most powerful methods of ab-initio Quantum Chemistry, and is a kind of standard for accurate calculations. It is, nevertheless, not yet fully satisfactory in some respects. There is the challenge to revisit CC theory in the light of more recent insight into the basis of the molecular many-electron problem, especially for large molecules.

Traditional CC theory for *closed-shell* states with a single Slater determinant reference state Φ has been guided by essentially the following paradigms.

P. Čársky et al. (eds.), Recent Progress in Coupled Cluster Methods, 299–356.
DOI 10.1007/978-90-481-2885-3_12,

(1) We search for a wave operator W, which changes the reference wave function Φ to the *exact* wave function Ψ, where *exact* always means *full CI* (configuration interaction). This W is written as an exponential

$$\Psi = W\Phi; W = e^S; S = \sum_{k=1}^{n} S_{(k)} \tag{12-1}$$

where $S_{(k)}$ is a k-particle excitation operator, and n the particle number. For the upper summation limit n in (12-1) replaced by $m < n$, the ansatz (12-1) represents an m-particle approximation.

(2) The theory should be *invariant* with respect to unitary transformations among the spin orbitals ψ_i occupied in the reference function Φ.

(3) A *non-variational* formalism in terms of a wave operator W in *intermediate normalization* is preferable to a *variational* theory, because the power series expansion of the wave operator terminates only for the former, such that variational CC requires a *double hierarchy* in terms of the *particle rank* and the *truncation of the exponential*, while a single hierarchy is sufficient for the non-variational formalism.

(4) Many-body perturbation theory (MBPT) is a good guiding line for the construction of approximate CC.

(5) One should be as accurate as possible, i.e. not make additional approximations, at the *lowest level* of the CC hierarchy, either CCD (CC with *d*ouble excitations) or CCSD (CC with *s*ingle and *d*ouble excitations), while even serious approximations are regarded as legitimate at the next-higher level, CCSDT (CC with *s*ingle, *d*ouble, and *t*riple excitations), such that the *approximate* CCSD(T) is by far more common than *full* CCSDT.

(6) CC for open-shell or multiconfiguration reference states has not been in the center of interest, and is not yet in a fully standardized form [1].

Of these paradigms only the first one (1) is still uncontested. However, if one bases the CC ansatz on the separation theorem (Section 12.3), the relation of CC theory to a description in a *localized basis* becomes obvious, and it appears imperative to take advantage of a localized description.

The paradigm (2) must, in view of our present knowledge, be relaxed in the sense outlined in Section 12.8.2, as it is required to achieve scaling of the computational effort with a low power of the system size (keyword *linear scaling*) [2].

In this context the relations between CC theory and methods known as IEPA (*independent electron pair approximation*) [3, 4] or CEPA (*coupled electron pair approximation*) [5, 6] need to be reconsidered. The closeness between CC and CEPA [7], forgotten for a while, is likely to find more attention in the future.

The preference of the non-variational formulation in the sense of paradigm (3) also needs a reexamination. One pays a rather high price for the termination of the expansion of the exponential, such as the lack of a variation principle. The error of the CC energy does not decrease quadratically with that of the wave function [8], but only approximatively so (with a nonvanishing linear term), which makes traditional

CC theory rather uneconomic, when it goes to really high accuracy. The lack of a genuine Hellmann – Feynman theorem must be compensated by a rather complicated formalism for energy derivatives [9]. Alternative CC ansaetze have been considered previously, but usually with pessimistic conclusions [10].

One must further realize that MBPT as a guide for suggesting approximations according to paradigm (4) is *dangerous*. There is no guarantee that MBPT converges [11], and if it does, the convergence is often slow. The convergence in terms of the excitation rank, on which CC theory is based, is usually much faster. We shall see, that there are, e.g. terms of 4th order in MBPT that are more important than others of 3rd order, and further that in CCSDT there are 6th order terms neglected in CCSD(T), which are possibly more important than the 5th terms taken care of in CCSD(T) [12]. CCSD(T) does not describe a genuine three-electron system exactly. In going from CCSD to CCSDT one introduces energy contributions of 4th and higher orders due to triple excitations, but one misses the *variational* 2-particle terms of 5th order, that are ignored in CCSD. A good criterion for CCD or CCSD is that it should be exact for genuine 2-electrons systems, while CCSDT should be exact for genuine 3-electron systems. This is the case for CCSD and CCSDT, but not for CCSD(T). This aspect has recently been considered by Bartlett and Musial [13].

Most curious is the paradigm (5), to be as accurate as possible at the CCD or CCSD level, but not to mind problematic simplifications of CCSDT. Why should one care for all terms of 4th order in CCSD, if one is willing to miss terms of the same order that arise first in CCSDT? If one cares about 5th order terms in CCSD(T), why does one ignore 5th order contributions to variational CCSD? Is one well advised to evaluate contributions which are cheap and to ignore others of the same order, which are expensive?

The aim of the present chapter is to look behind the scene and shed light on the aspects of CC theory, that usually found less interest. For this purpose a compact Fock space formalism is used, that has, unfortunately, not yet become as popular, as it would deserve. We start with a recapitulation of this formalism in Section 12.2. This is easily generalized beyond closed-shell reference states, for which it was originally conceived [14–20]. However, the available space does not allow us to go into details about this.

The *separation theorem* in Fock space is presented in Section 12.3 as the basis of CC theory. In this context the importance of a description in a localized representation is stressed. After a review of some often ignored historic aspects, CC theory is studied in three contexts, namely (a) the *traditional* CC theory (TCC) in terms of a non-unitary similarity transformation of the Fock space Hamiltonian in intermediate normalization, (b) *expectation value* CC theory and *variational* CC theory (XCC and VCC) in intermediate normalization, (c) *unitary* CC theory (UCC).

For an analysis of TCC theory the *Arponen functional* [21] turns out to be useful (see Section 12.5.5). The partial summation of certain classes of MBPT diagrams is studied in detail (see Section 12.5.6). The natural emergence of IEPA and CEPA as well as their linearized versions IEPA_0 and CEPA_0 plays a key role. Unlike IEPA_0 and CEPA_0, IEPA and CEPA are exact for a supersystem of non-interacting electron

pairs. In part (b) the focus is on the estimation of the *variational error* of TCC theory (Section 12.7). The last part (c) concentrates on a general linearized CC theory and a *normalized CC theory* based on an infinite-order summation of the bulk contributions to unitary CC theory, which looks as the most promising aspect of the present paper.

A complementary paper on many-body perturbation theory (MBPT) in the language of *Quantum Chemistry in Fock space* has just been published [22]. This is especially recommended for non-initiated readers. Unfortunately, the space available does not allow us to address the *important* topics of multiconfiguration CC [1], and of explicitly correlated CC both in terms of Gaussian Geminals [23] and with linear terms in r_{12} [24].

12.2. THE FOCK SPACE HAMILTONIAN

A more detailed account of this topic is found in Ref. [22].

12.2.1. Excitation Operators

We construct a Fock space built up from a *finite-dimensional* one-particle Hilbert space, spanned by an *orthonormal* spin-orbital basis $\{\psi_p\}$. The basic quantities are the *creation operators* $a^p = a_p^\dagger$ and the *annihilation operators* a_p corresponding to this basis. Both together are called *elementary fermion operators*.

A product of fermion operators is said to be in *normal order*, if all creation operators are left of all annihilation operators, like e.g.

$$a^p a_q a_r a_s \tag{12-2}$$

The vacuum expectation value of a normal order operator vanishes, e.g.

$$\langle 0|a^p a_q a_r a_s|0\rangle = 0 \tag{12-3}$$

Of special interest are the *excitation operators* (a more appropriate, but rather lengthy, name might be spin-orbital replacement [or substitution] operator [25]), such as the one-particle excitation operators a_q^p or the two-particle excitation operators [14–20] a_{rs}^{pq}

$$a_q^p = a^p a_q;\ a_{rs}^{pq} = a^p a^q a_s a_r \tag{12-4}$$

They are *particle-number conserving* and in *normal order*.

Density matrix elements are expectation values of excitation operators [15, 16]

$$\gamma_q^p = \langle \Psi | a_q^p | \Psi \rangle \tag{12-5}$$

$$\gamma_{rs}^{pq} = \langle \Psi | a_{rs}^{pq} | \Psi \rangle; \text{ etc.} \tag{12-6}$$

Consider a configuration space Hamiltonian

$$H_n(1,2,3\ldots.n) = \sum_{k=1}^{n} h(k) + \sum_{k<l=1}^{n} \frac{1}{r_{kl}} \tag{12-7}$$

with the matrix elements

$$h_q^p = \langle \psi_q | h | \psi_p \rangle; \tag{12-8}$$

$$V_{rs}^{pq} = \langle \psi_r(1)\psi_s(2) | \frac{1}{r_{12}} | \psi_p(1)\psi_q(2) \rangle; \tag{12-9}$$

The corresponding *Fock space Hamiltonian* is then

$$H = h_q^p a_p^q + \frac{1}{2} V_{rs}^{pq} a_{pq}^{rs} \tag{12-10}$$

with the *Einstein summation convention* [15].

The Hamiltonians H_n and H have the same matrix elements with respect to n-electron Slater determinants. H has eigenstates for all n, H_n only for a specified n. The eigenstates of H are the *full-CI states*. The particle number n is a quantum number.

It is convenient (especially if one wants to apply perturbation theory) to choose the one-electron basis such that the one-electron part h of H is diagonal

$$H = h + V; h = \varepsilon_p a_p^p; V = \frac{1}{2} V_{rs}^{pq} a_{pq}^{rs} = \frac{1}{4} \bar{V}_{rs}^{pq} a_{pq}^{rs}; \bar{V}_{rs}^{pq} = V_{rs}^{pq} - V_{sr}^{pq} \tag{12-11}$$

12.2.2. Inversion of a Commutator

In order to transform the Fock space Hamiltonian to *diagonal* form by means of a similarity transformation, we have to be able to *invert* a commutator with the one-electron operator $h = \varepsilon_p a_p^p$.

The commutator of a_{rs}^{pq} with $h = \varepsilon_p a_p^p$ is obtained if one multiplies a_{rs}^{pq} with an energy difference

$$[a_{rs}^{pq}, \varepsilon_t a_t^t] = (\varepsilon_r + \varepsilon_s - \varepsilon_p - \varepsilon_q) a_{rs}^{pq} \tag{12-12}$$

Hence if B has the matrix elements B_{pq}^{rs}, those of $A = [B, h]$ are $A_{pq}^{rs} = B_{pq}^{rs}(\varepsilon_r + \varepsilon_s - \varepsilon_p - \varepsilon_t)$. If A is known, we get the elements of B as

$$B_{pq}^{rs} = A_{pq}^{rs}(\varepsilon_r + \varepsilon_s - \varepsilon_p - \varepsilon_q)^{-1} \tag{12-13}$$

We must, of course, require that $(\varepsilon_r + \varepsilon_s - \varepsilon_p - \varepsilon_t) \neq 0$, otherwise the commutator inverse does not exist. We symbolize the commutator inverse by the subscript H and define [15]

$$(A_H)^{rs}_{pq} = \left\{ \begin{array}{c} A^{rs}_{pq}(\varepsilon_r + \varepsilon_s - \varepsilon_p - \varepsilon_q)^{-1} \; if \; (\varepsilon_r + \varepsilon_s - \varepsilon_p - \varepsilon_q) \neq 0 \\ = 0 \; \text{otherwise} \end{array} \right\} \tag{12-14}$$

With this definition the commutator inverse is not unique. One can add to A_H any operator that commutes with h and it is still a commutator inverse. We shall use this freedom to impose a *normalization condition for the wave operator*.

A generalization of the inverse of the commutator with h to operators of arbitrary particle rank is straightforward. An example is

$$(A_H)^{stu}_{pqr} = \left\{ \begin{array}{c} A^{stu}_{pqr}(\varepsilon_s + \varepsilon_t + \varepsilon_u - \varepsilon_p - \varepsilon_q - \varepsilon_r)^{-1} \\ if \; (\varepsilon_s + \varepsilon_t + \varepsilon_u - \varepsilon_p - \varepsilon_q - \varepsilon_r) \neq 0 \\ = 0 \; \text{otherwise} \end{array} \right\} \tag{12-15}$$

12.2.3. Particle-Hole Picture

The switch to the particle-hole picture means a change of the reference state Φ. In the original Fock space formulation the reference is the genuine vacuum $|0\rangle$. The wave operator W generates the n-electron wave function Ψ from the vacuum

$$\Psi = W|0\rangle \tag{12-16}$$

In the particle-hole picture the reference is a single Slater determinant n-electron wave function Φ, and W is a particle number conserving operator that generates Ψ from Φ

$$\Psi = W\Phi \tag{12-17}$$

The reference wave function Φ is a Slater determinant with the spin-orbitals $\psi_i, \psi_j, ...$ occupied. These are complemented by the unoccupied spin orbitals $\psi_a, \psi_b, ...$ to an orthonormal set $\psi_p, \psi_q, ...$

In the traditional particle-hole picture one defines first *hole creation* and *hole annihilation* operators. This is, however, a *dead end*, since it destroys the tensor notation, and since it is not generalizable to arbitrary (non-single-Slater -determinant) reference functions.

We prefer to define *excitation operators in particle-hole picture* [17–20, 26] (with a tilde on a) as

$$\tilde{a}^p_r = a^p_r - \gamma^p_r \tag{12-18}$$

$$\tilde{a}^{pq}_{rs} = a^{pq}_{rs} - \gamma^p_r a^q_s + \gamma^p_s a^q_r + \gamma^q_r a^p_s - \gamma^q_s a^p_r + \gamma^{pq}_{rs}; \; \gamma^{pq}_{rs} = \gamma^p_r \gamma^q_s - \gamma^p_s \gamma^q_r \tag{12-19}$$

with γ^p_r etc. defined as (12-5) and (12-6) with Ψ replaced by Φ. While operators in the original normal ordering satisfy

$$0 = \langle 0|a^p_r|0\rangle; \; 0 = \langle 0|a^{pq}_{rs}|0\rangle \tag{12-20}$$

$$h_a^i\,\tilde{a}_i^a \qquad \overline{V}_{ab}^{ci}\,\tilde{a}_{ci}^{ab} \qquad \overline{V}_{ab}^{ci}\,\tilde{a}_{ci}^{ab}/\Delta e$$

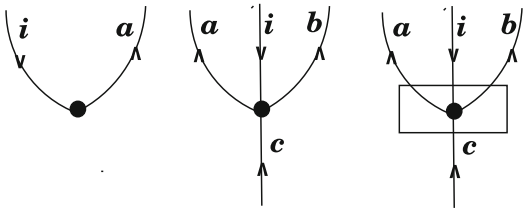

$$\overline{V}_{rs}^{pq} = V_{rs}^{pq} - V_{rs}^{qp}\,;\ \Delta e = e_c + e_i - e_a - e_b$$

Figure 12-1. Graphs for operators in particle-hole picture

operators in normal ordering in the particle-hole sense satisfy

$$0 = \langle\Phi|\tilde{a}_r^p|\Phi\rangle;\ 0 = \langle\Phi|\tilde{a}_{rs}^{pq}|\Phi\rangle \tag{12-21}$$

The notation using a tilde on operators is an alternative to the more traditional one where one includes an operator product in braces or double dots.

Operators in the particle hole picture are illustrated by diagrams, in which lines with labels $i, j, \ldots$ (corresponding to occupied spin orbitals) are going downwards (hole lines). An example is on Figure 12-1.

12.2.4. Generalized Wick Theorem

To evaluate *products* of excitation operators (in particle-hole picture) as *sums* of excitation operators (in particle-hole picture) and possibly a constant, we need a generalization [17, 26] of Wick's theorem [27]. On Figure 12-2 the special case for two matching labels is illustrated. Signs are part of the diagrams.

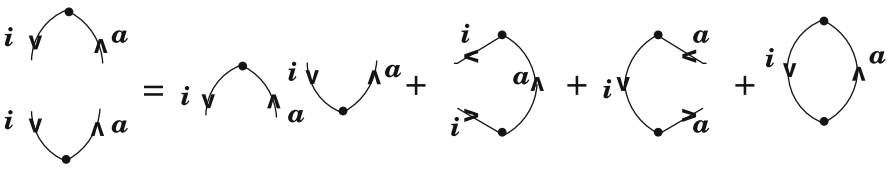

Figure 12-2. Wick theorem in the particle-hole picture

The Wick theorem in the particle-hole sense contains hole contractions and combined contractions (even full contractions) in addition to particle contractions e.g.

$$\tilde{a}_a^i \tilde{a}_j^b = \tilde{a}_{aj}^{ib} + \delta_a^b \tilde{a}_j^i - \delta_j^i \tilde{a}_a^b - \delta_a^b \delta_j^i \tag{12-22}$$

(see also Figure 12-2)

Particle labels contract *from upper right to lower left* in the formula (with up-going arrows in the figure), while hole labels contract *from upper left to lower right* (with down-going arrows). Hole contractions are associated with a factor (-1).

Only *full contractions* contribute to the expectation value w.r.t. Φ.

12.2.5. Fock Space Hamiltonian in Particle-Hole Picture

In particle-hole picture the Hamiltonian becomes [17]

$$H = E^{(0)} + f_q^p \tilde{a}_p^q + \frac{1}{2} V_{rs}^{pq} \tilde{a}_{pq}^{rs};\ E^{(0)} = h_q^p \gamma_p^q + \frac{1}{2} V_{rs}^{pq} \gamma_{pq}^{rs};\ f_q^p = h_q^p + \bar{V}_{qs}^{pr} \gamma_r^s \tag{12-23}$$

The zeroth order ground state energy $E^{(0)}$

$$E^{(0)} = \langle \Phi | H | \Phi \rangle = E_0 + E_1;\ E_0 = h_q^p \gamma_p^q;\ E_1 = \frac{1}{2} V_{rs}^{pq} \gamma_{pq}^{rs} \tag{12-24}$$

appears as a constant. This $E^{(0)}$ must be distinguished from E_0, the zeroth order in a perturbation expansion.

In (12-23) one recognizes the Fock operator $\mathbf{f}$, that contains the effective field created by the electrons in addition to the nuclear field.

It is recommended to determine Φ so that the expectation value (12-24) is minimized, such that the Brillouin condition [28]

$$\langle \Phi | [\tilde{a}_q^p, H] | \Phi \rangle = 0;\ [\mathbf{f}, \boldsymbol{\gamma}] = 0 \tag{12-25}$$

is satisfied. This defines Hartree – Fock theory, and implies that $\mathbf{f}$ is diagonal in the basis of the occupied spin orbitals.

Then V does not contain self-contractions (tadpoles) as illustrated in Figure 12-3.

It appears natural to regard

$$H_0 = f_q^p a_p^q \tag{12-26}$$

as unperturbed Hamiltonian for a perturbative treatment, as it has first been proposed by Møller and Plesset [29]. Sometimes one wants to consider the *bare nuclear Hamiltonian*

$$h = h_q^p a_p^q \tag{12-27}$$

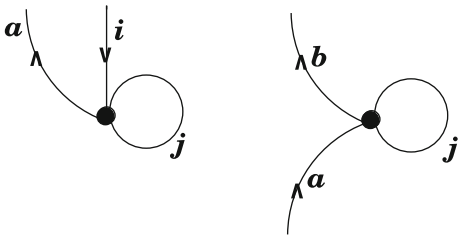

Figure 12-3. Interactions with self-contractions (tadpoles)

as unperturbed H_0. For this choice the perturbation does contain tadpoles. Our formalism covers both cases. We shall point out simplifications that arise for PT in the Møller – Plesset case. CC theory will usually be based on MP.

We do not consider *open-shell* states, for which not all possible Brillouin conditions are satisfied, and we must consider single excitations to lowest order.

12.2.6. Definition of Diagonal for Closed-Shell States

We want to apply a similarity transformation to the Fock space operator H, such that the transformed operator L is *diagonal*. For the present purpose, namely the evaluation of the ground state energy of a closed-shell state, the following definition is convenient. We call a diagram in the particle-hole picture [17]

C: closed, if it has no external line (only full contractions)

B: closed from below, if there are only particle creations and/or hole annihilations

A: closed from above, if there are only particle annihilations and/or hole creations

O: open for another possibilities.

A graphical illustration is given on Figure 12-4.

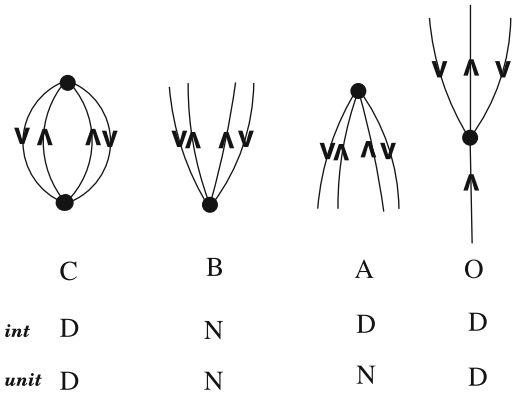

Figure 12-4. Definition of the subscripts C, B, A, O, D, N for operators

An operator of type B is also called non-diagonal (N), while operators of the types C, A, O are also called diagonal (D), see the line *int* in Figure 12-4. Note that operators of type C are just numbers (expectation values with respect to Φ).

These definitions are appropriate if we choose the *intermediate* normalization of the wave operator. For the *unitary* normalization (see Section 12.9) a different definition of D and N must be used. It is also indicated on Figure 12-4 in the line *unit*. While the definition of B, A, C, O remains unchanged, now D is the sum of C and O, while N is the sum of B and A.

Different definitions of D and N are also needed if we consider a degenerate or quasi-degenerate state [16]. This is out of the scope of the present chapter.

The nomenclature of the present subsection has the disadvantage that, in the literature, the label C is often used for *connected* rather than *closed*. Misunderstandings are hardly possible in this paper, since we always use a formalism, in which diagrams are connected by construction. We hence do not need a subscript for *connected*.

Jeziorski and Moszynski [30] have used a superoperator formalism, that is, to some extent, equivalent to the present one.

12.3. THE SEPARATION THEOREM

We start from a Fock space Hamiltonian, built up from a finite one-electron basis (as explained in Section 12.2.5). Suppose that the space of one-electron basis functions can be divided into *two subspaces A and B*, such that all matrix elements h_q^p and g_{rs}^{pq} vanish, unless p and q, or p, q, r, s, belong to the same subspace A or B.

Then the Fock space Hamiltonian is *additively separable*:

$$H = H_A + H_B \tag{12-28}$$

The solution of the Schrödinger equation is essentially equivalent to the *block diagonalization* of H by means of a *similarity transformation* with the wave operator W.

$$L = W^{-1}HW = L_D \tag{12-29}$$

The subscript D means *diagonal*. There are *various options for the definition* of D (diagonal) [15, 19], e.g. that given at the end of the preceding subsection. The results of this section hold for all acceptable definitions of D (diagonal).

We must, of course, require that the definition of *diagonal* is compatible with separability. It is here where the fact comes into play that electrons are fermions.

Let us assume that we have achieved the block diagonalization in either subspace

$$L_A = W_A^{-1}H_AW_A = L_{AD}; L_B = W_B^{-1}H_BW_B = L_{BD} \tag{12-30}$$

Using that operators commute, if they act in different subspaces, we get

$$L_A = W_B^{-1} W_A^{-1} H_A W_A W_B \tag{12-31}$$

$$L_B = W_B^{-1} W_A^{-1} H_B W_A W_B \tag{12-32}$$

$$L = L_A + L_B = W^{-1} H W;\ W = W_A W_B \tag{12-33}$$

While L is additively separable, W is multiplicatively separable. Let us write

$$W = \exp(S) \tag{12-34}$$

$$W_A = \exp(S_A);\ W_B = \exp(S_B);\ S = S_A + S_B \tag{12-35}$$

Then the *cluster amplitude S* is *additively separable.*

Separability implies *extensivity* and a *connected-diagram theorem*. If we formulate the theory in terms of H, S, and L, we deal with only additively separable quantities, that can be represented by connected diagrams. A diagram is *connected* if without cutting at least one fermion (particle or hole) line it cannot be decomposed into two distinct parts. An example of both a connected and a disconnected diagram is given on Figure 12-5.

Let us divide the space of one-particle functions into two subspaces, the interaction of which can be gradually switched off. Then, in the limit of vanishing interaction, a disconnected diagram, describing L, E, or S, consisting of two parts in the two subspaces, will not vanish, as it should. It must therefore be absent, even if the interaction is switched on.

The separation theorem is both fundamental and almost trivial. So it is hard to say when it has first been formulated. The earliest reference known to the author is a paper by Primas [31].

It is curious that the ansatz (12-34), associated with the names of Coester and Kümmel [32], which is a manifestation of the separation theorem, is older than this theorem, and that this ansatz was first formulated in an indirect and tedious way going through the machinery of *many-body perturbation theory* (MBPT) [33].

The Gedanken-Experiment to divide the one-electron Hilbert space into two *non-interacting* parts, requires that we can use a localized one-electron basis. *Separability* is closely related to *localizability*.

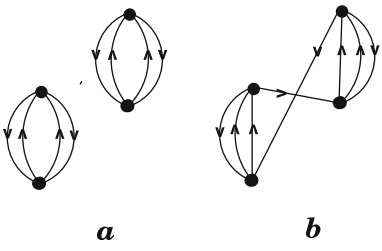

Figure 12-5. Examples of a disconnected (**a**) and a connected (**b**) diagram

In terms of a *delocalized basis*, separability is *not* really meaningful. The requirement of invariance between a formulation in a localized or a delocalized basis, would therefore be counterproductive. This is now trivial for anyone who tries to describe large systems in a satisfactory way [2], which is only possible in a localized basis. This was not familiar to Pople [34] when he formulated his *criteria* that a good many-electron theory should satisfy. The requirement of unitary invariance should be somewhat attenuated. For details see Section 12.8.1.

12.4. SHORT HISTORY OF ELECTRON PAIR THEORY

The concept of *electron pairs* has always played a great role in Theoretical Chemistry [35–39]. Valence bond (VB) theory is, to a large extent, a theory of electron pairs, though a rather rudimentary one. The first systematic formulation of an electron pair theory is the theory of *separated pairs* of Hurley et al. [40]. The Separated Pair ansatz became later known as APSG [41], for *antisymmetrized product of strongly orthogonal geminals*. This ansatz has a few nice features, and it can, at least in principle, be applied in variational calculations, but it is, of course, approximate. It could be shown, that in those cases, where this ansatz is exact (e.g. for a supersystem of n He atoms at mutually infinite distances), the various pair functions can be treated independently, and *normalized individually*, just in the effective field of the other electrons and nuclei, and that the exact correlation energy is a *sum of pair correlation energies*.

The APSG ansatz is actually a special case of a CC ansatz [36]. In terms of this ansatz one minimizes the total energy of a $(2n)$-electron system, subject to normalization conditions for n pairs. This leads to n eigenvalue equations. To understand the APSG ansatz is a prerequisite for understanding CC theory [36].

We can only mention briefly that an alternative ansatz, called APIG (antisymmetrized product of identical geminals) [41] or AGP (antisymmetrized geminal power) [42] has found some interest, mainly in the context of the theory of superconductivity, and that a geminal product ansatz without the restriction of strong orthogonality has recently been studied with promising results [43].

Even before it became feasible to implement the APSG ansatz in a large-scale ab-initio context [44], it was obvious, that this ansatz is *not general enough* and that one ought to go beyond it. With the APSG ansatz one considers n electron pairs for $2n$ electrons, e.g. for the Be ground state (with $2n = 4$) the $1s^2$ pair and the $2s^2$ pair, while a more refined treatment would require to consider also the $1s2s$ pairs, for 4 possible spin pairings, i.e. a total of 6 pairs. It has been observed [45] that to the lowest order of Møller – Plesset perturbation theory, to 2nd order for the energy (MP2), the total correlation energy appears as the sum of $\binom{2n}{2}$ pair correlation energies. It is plausible to combine this result with that for the APSG ansatz and to conjecture, that a good approximation to the correlation energy of a closed-shell $2n$ electron state can be constructed as the sum of $\binom{2n}{2}$ pair correlation energies in the

effective field of the other pairs. Sinanoğlu [46] has based his *many-electron theory* on an intuitive argument of this kind. Independently, and even earlier Nesbet [47, 48] has suggested the same approximation under the name Bethe – Goldstone theory. He based this on a study by Bethe and Goldstone [49], who proposed to sum all *ladder diagrams* of many-body perturbation theory (MBPT), which leads to an effective pair equation (see Section 12.5.6). Actually the motivation of Bethe and Goldstone was not the derivation of a pair theory, but the construction of a *reaction operator*, that is less singular than the *hard-core* pair interaction, and that allowed a mean-field treatment of nuclear matter and nuclei, for cases where Hartree – Fock diverged.

Both names *many-electron theory* and *Bethe – Goldstone theory* are somewhat misleading and they were replaced by the neutral term *independent electron pair theory* (IEPA) [3]. Nesbet's access has not only the advantage that his derivation of IEPA is at least justified in terms of MBPT, but he has moreover defined this approximation as a *member of a hierarchy* of approximations, that eventually lead to an exact theory. The next step is a theory of *electron triples*. Nesbet and others [50] did also consider this next step numerically, but this strategy was not further considered. Nesbet's ideas have actually survived in the *incremental scheme* of Stoll, Dolg, and others [51].

IEPA was combined with the concept of the expansion of electron pair functions into *pair natural orbitals* (PNO) and became for a few years the most powerful approximation towards the evaluation of the electron correlation for small molecules [4]. One of the merits of IEPA is that it is exact for a supersystem of non-interacting two-electron systems. IEPA is not invariant with respect to a unitary transformation among the hole orbitals. One must therefore recommend a particular choice of these. Localized orbitals represent usually the best choice, because in terms of them the neglected coupling terms become minimal. All published IEPA-PNO calculations [4] were based on Boys-localized orbitals.

The simple alternative to implement straight 2nd order Møller – Plesset perturbation theory (MP2) [29] rather than IEPA was only considered much later [52]. Both IEPA and MP2 are approximations, IEPA is more accurate, but also somewhat more expensive. Sometimes it was reproached to IEPA, that it often overshoots the correlation energy. This also applies to MP2, but was hardly used as an argument against it. Some people preferred MP2 over IEPA, because it is unitary invariant [36], but this is not a strong argument. See the comments on the unitary invariance of CEPA later in this section and in Section 12.8.3. MP2 will survive for some time, as the simplest approach to account for electron correlation.

It was a rather small, but important step from IEPA [3] to the *coupled electron pair approximation* (CEPA) [5, 6]. This step can be justified by an analogy to that from MP2 and MP3. It was also seen as an approximation to CP-MET. IEPA merged into CEPA and became just the first step in a CEPA treatment. The IEPA results for the total correlation energy became obsolete, but the *pair increments* to the IEPA energy (documented in many early studies [4, 53]) remained meaningful, especially if one wanted to explain changes in the correlation energy, e.g. on a reaction path.

Actually, pair energies are also defined within CEPA. Even these days IEPA is still alive and has been used as an intermediate step in CC theory [54].

One can justify CEPA (like IEPA) starting from MBPT in terms of a selection of diagrams (see Section 12.5.6). It has usually been made plausible starting from CID, i.e. configuration interaction with double substitutions [36], as we shall see later in more detail (Section 12.8.3).

CEPA became available for large-scale ab-initio calculations at about the same time as routine MP2 calculations, but long before the first comparable calculations in terms of CCD, then still called CP-MET, for *coupled-pair many-electron theory*, an obvious tribute to Sinanoglu's *(un-coupled-pair) many-electron theory, synonymous with IEPA*.

Coupled cluster (CC) theory, originally called e^S theory, goes back to nuclear physics [32, 33]. The early history of the e^S theory has been reviewed by Paldus [55].

This theory was adapted to molecular applications by Čížek [56]. First implementations of the Čížek formalism were in a semiempirical context. Preliminary ab-initio CC calculations were published in 1972 [57], while first large-scale CCD calculations [58] of the type that is now standard, appeared in 1978, at a time when CEPA was already on the market. The very first large-scale CCD calculation by Taylor et al. [59] of 1976 (still under the older name CP-MET [56]) was actually built upon CEPA, using the Karlsruhe CEPA program [6], with extra coupling terms on top of it. This was cited in Bartlett's review [60], but has otherwise found little attention, as is also happened to the few studies published on the relation between CEPA and CC [36, 61–63]. Especially the message that CCD and CEPA differ only marginally [59, 63], did not become popular.

As already pointed out, CEPA was originally justified from an analysis of the CI (configuration interaction) equations with *unlinked products* of pair excitations included. Earlier attempts to *derive* CEPA from CCD were reviewed by the present author [36]. The key point, to which we come in detail in Section 12.8.3, is that the leading pair coupling terms are those of EPV (exclusion-principle violating) type, and that the summation over these terms leads to CI-like pseudo-eigenvalue equations with different eigenvalues, corresponding to independent normalization, for the different pairs, as they are familiar from CEPA. The non-EPV terms only lead to usually small and physically rather meaningless corrections.

In spite of the obvious closeness of CCD and CEPA, the opinion was widespread that CCSD is more sophisticated and better founded, and hence superior to CEPA. One of the arguments against CEPA has been that it is not invariant with respect to a unitary transformation among the occupied spin orbitals. This reputation has not been the result of systematic numerical studies. Actually (see Section 12.8.3) for "normal" molecules at least the CEPA_1 variant is *very close to invariant* with respect to a switch from canonical to localized orbitals (see also Section 12.8.3).

Even former protagonists of CEPA abandoned CEPA in favor of CCD or CCSD, and CEPA was practically forgotten for decades [7], although both some old and

some recent studies indicated that CEPA often performs, e.g. for spectroscopic constants, even better than CCD or CCSD [64, 65].

Curiously, until very recently [66], CC theory had its greatest success in chemistry and never became very popular in physics, although some important formal studies were published by nuclear physicists [21, 67]. The earliest use of the name *coupled cluster* theory, that has also been adopted in nuclear physics, has probably been in a series of papers by Harris, Zivkovic, and Monkhorst, which would deserve to be better known [68–70].

12.5. MANY-BODY ASPECTS OF MBPT AND CC THEORY

12.5.1. Similarity Transformation

Many-Body perturbation theory (MBPT) and coupled-cluster (CC) theory have a common history and some common features. This is not so obvious from the original papers in nuclear theory, because the e^S ansatz [32] was meant as a counterpoint in spirit to MBPT, formulated willingly in algebraic form, not using diagrams. The adaptation of the e^S ansatz to chemistry [56] was formulated in terms of diagrams and had more similarities with MBPT than the original e^S theory.

In order to understand the essential features of MBPT and CC, a look at the history is hardly helpful, and is, in fact rather confusing [71]. A modern formulation of MBPT (see also Ref. [72]) has recently been given by the present author [22, 71, 73], using the language of *Quantum Chemistry in Fock space* [15]. The same formalism is applied here to CC theory. In order for this review to be self-contained, the essentials of this formalism are here recapitulated. For more details the reader is referred to the companion paper [22].

In a modern language the basis of both MBPT and CC is very simple. We search for a *similarity transformation* of the Fock space Hamiltonian H in normal order in particle hole picture by means of a non-unitary wave operator $W = e^S$ to an operator that is *diagonal* in the sense of the definition given in Section 12.2.6, which means that the desired eigenstate with the energy eigenvalue E, equal to the *closed* part L_C of the transformed Hamiltonian $L = W^{-1}HW$, is *decoupled* from the rest. We use the symbol S for the *cluster amplitude* in agreement with the original literature [32] rather than T, which is popular in chemistry.

$$L = e^{-S}He^S; S = S_B; L_B = 0; E = L_C \tag{12-36}$$

The choice $S = S_B$ is no loss of generality, but leads to important simplifications, because all basis operators with subscript B commute with each other.

In MBPT one expands in powers of the perturbation parameter λ

$$\begin{aligned} &H = H_0 + \lambda V; S = \lambda S_1 + \lambda^2 S_2 + ...; L = H_0 + \lambda L_1 + \lambda^2 L_2 + ... \\ &E = E_0 + \lambda E_1 + \lambda^2 E_2 + ... \end{aligned} \tag{12-37}$$

In (traditional) CC theory one expands S in (12-34) in terms of excitation operators of particle rank k, i.e.

$$S = \sum_{k}^{m} S_{(k)} \tag{12-38}$$

A CC hierarchy consists in solving (12-36) first for S replaced by $S_{(2)}$, then with the upper summation index in (12-38) $m = 2$, $m = 3$ etc. For $m = n$ one arrives at the full-CI result. Expanding (12-36) we get the CC equations

$$0 = H_B + [H,S]_B + \frac{1}{2}[[H,S],S]_B + \frac{1}{6}[[[H,S],S],S]_B + \frac{1}{24}[[[[H,S],S],S],S]_B \tag{12-39}$$

$$E = H_C + [H,S]_C + \frac{1}{2}[[H,S],S]_C \tag{12-40}$$

The Hausdorff expansion in (12-40) terminates, because a triple (or higher) commutator $[[[H,S],S],S]$ with $S = S_B$ cannot be *closed*. The three S factors mean at least a threefold excitation, the factor H at most a twofold de-excitation. The expansion in (12-39) terminates, because a quintuple (or higher) commutator cannot be *connected* and must hence vanish.

Using that (for operators X_B and Y_B closed from below, but arbitrary otherwise)

$$[H_0, X_B] = [H_0, X_B]_B; [X_B, Y_B] = 0 \tag{12-41}$$

and introducing the formal commutator inverse (12-14), (12-39) and (12-40) can be reformulated to

$$S = V_{BH} + [V,S]_{BH} + \frac{1}{2}[[V,S],S]_{BH} + \frac{1}{6}[[[V,S],S],S]_{BH} + \frac{1}{24}[[[[V,S],S],S],S]_{BH} \tag{12-42}$$

$$E = E_0 + V_C + [V,S]_C + \frac{1}{2}[[V,S],S]_C \tag{12-43}$$

This is the basis of *traditional coupled-cluster* (TCC) theory, outlined in more detail in Section 12.6.

12.5.2. Two Possible Choices of H_0

We consider two possible options for the choice of the Hamiltonian of Section 12.2.5:

(a) The energy expectation value is minimized with respect to variation of Φ. Then the unperturbed Hamiltonian H_0 is that of Hartree – Fock theory, and

the perturbation term V in the Hamiltonian does not contain single-particle interactions (diagrams with *tadpoles*). This is the case for Møller – Plesset based CC or PT.

(b) We keep Φ arbitrary, e.g. possibly as the solution of the bare-nuclear Hamiltonian (BNH) problem. Then tadpoles must be included.

In a recent review on MBPT [22] we have considered the general case (b), and indicated the simplifications that arise for the special choice (a). We shall here only consider the Møller – Plesset option (a), because the BNH case hardly plays a role in CC theory. One should realize however, that it may be advantageous to base CC theory on so-called *Brueckner orbitals* (see Section 12.6.2). These don't make the energy expectation value stationary, such that the general case (b) must be the starting point.

12.5.3. Connected-Diagram Theorem

In the formalism based on a similarity transformation we only consider operators such as H, L, S, which are *additively separable*. All derived quantities are obtained in Lie algebraic form, i.e. as commutators or multiple commutators. In a diagrammatic representation all these expressions can be represented by *connected diagrams*, because a commutator of two operators represented by connected diagrams is also represented by a connected diagram (see Section 12.3).

It is essential that we consider operators in Fock space, and also that we *ignore restrictions on spin-orbital labels* (as they must be made in a traditional formulation in fixed-particle-number Hilbert space), and distinguish only particle and hole lines.

The anticommutation relations of the fermion operators take care, that all results for observables are in perfect agreement with the Pauli principle. However, *individual diagrams* may apparently be in conflict with the Pauli principle, e.g. two or more particle (or hole) lines in a diagram may have the same label. One can achieve, that all such EPV diagrams cancel. However, usually connected EPV diagrams cancel with disconnected ones. If one wants to take advantage of the connected-diagram theorem, one must *not* cancel connected EPV diagrams with disconnected diagrams, but keep the connected EPV diagrams. The connected diagram theorem only holds, if all connected EPV diagrams are taken care of. For an illustration see Section 12.8.3.

We rely here on a constructive approach, in which connectedness at each step is guaranteed by a Lie-algebraic formulation. One can alternatively proceed in a non-constructive way, where at the end one selects only connected diagrams. For more details see Ref. [22].

12.5.4. Perturbation Expansion

Since in CC theory one often uses arguments from perturbation theory, it is recommended to have look at the perturbation expansion of TCC [22, 71–73]. We expand

$$H = H_0 + \lambda V \tag{12-44}$$
$$S = \lambda S_1 + \lambda^2 S_2 + \ldots = S_B \tag{12-45}$$
$$E = E_0 + \lambda E_1 + \lambda^2 E_2 + \ldots \tag{12-46}$$

and get (orders in PT are indicated by *subscripts*) immediately from (12-42) and (12-43).

$$S_1 = V_{BH} \tag{12-47}$$
$$S_2 = [V, S_1]_{BH} \tag{12-48}$$
$$S_3 = [V, S_2]_{BH} + \frac{1}{2}[[V, S_1], S_1]_{BH} \tag{12-49}$$
$$S_4 = [V, S_3]_{BH} + [[V, S_1], S_2]_{BH} + \frac{1}{6}[[[V, S_1], S_1], S_1]_{BH} \tag{12-50}$$
$$S_5 = [V, S_4]_{BH} + [[V, S_1], S_3]_{BH} + \frac{1}{2}[[V, S_2], S_2]_{BH} + \frac{1}{2}[[[V, S_1], S_1], S_2]_{BH} + \frac{1}{24}[[[[V, S_1], S_1], S_1], S_1]_{BH} \tag{12-51}$$
$$E_1 = V_C \tag{12-52}$$
$$E_2 = [V, S_1]_C \tag{12-53}$$
$$E_3 = [V, S_2]_C + \frac{1}{2}[[V, S_1], S_1]_C \tag{12-54}$$
$$E_4 = [V, S_3]_C + [[V, S_1], S_2]_C \tag{12-55}$$
$$E_5 = [V, S_4]_C + [[V, S_1], S_3]_C + \frac{1}{2}[[V, S_2], S_2]_C \tag{12-56}$$

We have used that S_k and S_l commute, and that hence

$$[[V, S_k], S_l] = [[V, S_l], S_k] \tag{12-57}$$

We can reformulate these expressions such that, in the spirit of the Wigner $(2n + 1)$ rule, E_3 is expressible through S_1, and E_4 and E_5 in terms of S_1 and S_2 [30]. E_5 gets a more compact form, if one does not eliminate S_3. The most compact expressions for the low orders of the MBPT energy are [22, 74] (12-52) and (12-53), and:

$$E_3 = [S_1^\dagger, [V, S_1]]_C \tag{12-58}$$
$$E_4 = [S_1^\dagger, [V, S_2]]_C + \frac{1}{2}[S_1^\dagger, [[V, S_1], S_1]_C \tag{12-59}$$
$$E_5 = [S_1^\dagger, [V, S_3]]_C + [S_1^\dagger, [[V, S_1], S_2]]_C + \frac{1}{2}[[V, S_2], S_2]_C \tag{12-60}$$

A diagrammatic expression of the E_k of MBPT is given in ref. [22]. The E_k given here, hold for MP, starting from Hartree Fock. More general results are found in Ref. [22].

12.5.5. The Arponen Functional and Related Functionals

An alternative formulation of the traditional CC theory (12-36) is to require that $S = S_B$ satisfies

$$(X^\dagger e^{-S} H e^S)_C = 0, \textit{ for all } X^\dagger = (X^\dagger)_A \tag{12-61}$$

and that E is constructed from this S as

$$E = (e^{-S} H e^S)_C \tag{12-62}$$

A further step is to consider the functional, introduced by Arponen [21]

$$F_{CC}(T^\dagger, S) = \{(1 + T^\dagger) e^{-S} H e^S\}_C; S = S_B; T^\dagger = (T^\dagger)_A \tag{12-63}$$

We could also write $S^\dagger$ for $T^\dagger$, if we insist that $S^\dagger$ and S are *independent* operators.

This functional has the following properties:

(1) Stationarity of F_{CC} with respect to all possible variations of $T^\dagger$ is achieved, if S satisfies the TCC equations (12-42) and (12-43).

(2) The stationary F_{CC} is equal to the TCC energy E, and is exact (i.e. equivalent to full CI), if F_{CC} is stationary with respect to *all possible* variations of $T^\dagger$ (within our finite-dimensional Fock space).

(3) F_{CC} does, unlike a variational functional, *not* provide an upper bound for the exact E.

This is a somewhat unusual functional. It depends on the two operators S and $T^\dagger$ in an asymmetric way. Let us consider another functional, namely that corresponding to *configuration interaction* (CI), with the CI wave function generated from the reference function Φ by means of the wave operator $(1 + U)$ with $U = U_B$

$$F_{CI}(U^\dagger, U) = \frac{\{(1 + U^\dagger) H (1 + U)\}_C}{\{(1 + U^\dagger)(1 + U)\}_C} \tag{12-64}$$

Stationarity with respect to variation of $U^\dagger$ is achieved if U is determined so, that

$$\{X^\dagger (H - E)(1 + U)\}_C = 0; E = F_{CI}(U^\dagger, U) \tag{12-65}$$

for the set of operators X into which U is expanded. The stationarity condition (12-65) is an eigenvalue equation and implies

$$0 = \{U^\dagger(H-E)(1+U)\}_C \tag{12-66}$$

$$\{(H-E)(1+U)\}_C = \{(1+U^\dagger)(H-E)(1+U)\}_C \tag{12-67}$$

$$E = F(U^\dagger, U) = E + \frac{\{H(1+U)-E\}_C}{\{(1+U^\dagger)(1+U)\}_C} \tag{12-68}$$

$$E = H_C + (HU)_C \tag{12-69}$$

The eigenvalue equation (12-65) can be rewritten as a nonlinear system of equations

$$\{X^\dagger(H + (H - H_C - [HU]_C)U)\}_C = 0; E = H_C + (HU)_C \tag{12-70}$$

that can be solved iteratively, starting with $[HU]_C = 0$, i.e. with the linear system

$$\{X^\dagger(H + (H - H_C)U)\}_C = 0; E = H_C + (HU)_C \tag{12-71}$$

Let us now consider the Arponen functional for CCD, i.e. for only double excitations

$$\begin{aligned} & F_{CCD}(T^\dagger_{(2)}, S_{(2)}) \\ &= \{H + HS_{(2)} + T^\dagger_{(2)}H + T^\dagger_{(2)}[H, S_{(2)}] + \frac{1}{2}T^\dagger_{(2)}, [[H, S_{(2)}], S_{(2)}]\}_C \\ &= \{H + [H, S_{(2)}] + [T^\dagger_{(2)}, H] + [T^\dagger_{(2)}, [H, S_{(2)}]] \\ &\quad + \frac{1}{2}[T^\dagger_{(2)}, [[H, S_{(2)}], S_{(2)}]\}_C \end{aligned} \tag{12-72}$$

which has the stationarity condition

$$\{X^\dagger_{(2)}(H + [H, S_{(2)}] + \frac{1}{2}[[H, S_{(2)}], S_{(2)}])\}_C = 0; E = H_C + [H, S_{(2)}]_C \tag{12-73}$$

This is also a non-linear system of equations. The linear part, e.g. for an iteration start, is

$$\{X^\dagger_{(2)}(H + [H, S_{(2)}]\}_C = 0; E = H_C + [H, S_{(2)}]_C \tag{12-74}$$

If we identify $S_{(2)}$ with $U_{(2)}$ and realize that

$$\{X^\dagger_{(2)}([H, S_{(2)}]\}_C = \{X^\dagger_{(2)}(HS_{(2)} - S_{(2)}H)\}_C = \{X^\dagger_{(2)}(H_{(2)}S - S_{(2)}H_C)\}_C \tag{12-75}$$

we see that the *linear approximation* for CCD and CID is the same. It can also be written

$$\{X^{\dagger}_{(2)}(V + [H_0, S_{(2)}] + [V, S_{(2)}]\}_C = 0; E = H_C + [V, S_{(2)}]_C \tag{12-76}$$

This linear system can be derived in many different ways and is now usually called $CEPA_0$ [36]. It has the formal solution

$$S_{(2)} = V_{BH} + [V, S_{(2)}]_{BH} \tag{12-77}$$

The linear $CEPA_0$ system misses only those terms of CCD, which are of 4th order in MBPT and which are bilinear in S such as

$$\frac{1}{2}\{X^{\dagger}_{(2)}[[H, S_{(2)}], S_{(2)}]\}_C \tag{12-78}$$

We shall have a closer look at these terms in Section 12.8.3. In the moment we note that these terms are rather small in absolute value, and are certainly much smaller than the respective terms of CID

$$-\{X^{\dagger}_{(2)}(HU_{(2)})_C U_{(2)}\}_C = -(X^{\dagger}_{(2)}U_{(2)})_C(HU_{(2)})_C \tag{12-79}$$

While (12-78) is in Lie algebraic form, hence separable and representable by only connected diagrams, (12-79) factorizes, is not additively separable, and consists of *products* of closed diagrams, i.e. of *only disconnected* diagrams. We know that CID is not acceptable. $CEPA_0$ is usually a better approximation to CCD than is CID. Nevertheless, even $CEPA_0$ is not fully satisfactory, because it does not describe a genuine 2-electron system exactly, nor a supersystem of non-interacting 2-electron systems. For this the extra term (12-78) is needed. However, a simple compact approximation as in $CEPA_2$ (see Section 12.8.3) will be sufficient.

$CEPA_0$ as it stands, has hardly been used as an approximation to CCD, mainly because it can suffer from singularities, especially in situations of near-degeneracy [63], (where, anyway, a pair theory based on a single reference is not recommended). A way to avoid these singularities has been found by Taube and Bartlett by means of a Tichonov regularization [75].

For a genuine 2-electron system CCD and CID must be indistinguishable. This is not immediately obvious from the expressions (12-78) and (12-79). It requires a closer look at the respective diagrams (see Section 12.8.3).

12.5.6. Infinite Summation of Classes of MBPT Diagrams

If one solves the CC equations in a finite one-electron basis exactly, one gets the full-CI result. One can usually not afford this and one must make approximations.

The simplest approximation consists in taking the lowest order of PT or the first iteration cycle, i.e.

$$S = V_{BH}; E = E^{(0)} + V_C + [V, V_{BH}]_C \tag{12-80}$$

This is MP2 (2nd order Møller – Plesset).

Attempts to improve the theory by going to successively higher orders of MBPT, i.e. from MP2 via MP3 to MP4 etc. were disappointing. An alternative to classifying the diagrams of MBPT by the *order in the perturbation parameter* λ, and collecting those of the same order, is to consider certain *classes of diagrams*, that one regards as important, and to sum them to infinite order.

It is useful to follow an idea that goes back to Bethe and Goldstone [49], though introduced for a different purpose.

Let us look at all MBPT diagrams, that carry *two hole lines*, labeled i and j. In terms of Goldstone vertices these diagrams look like ladders. They are therefore called (particle-line) ladder diagrams. They are illustrated on Figure 12-6 in terms of Hugenholtz vertices. We have used square dots for the antisymmetrized matrix elements of the interaction potential V, to be consistent with diagrams used later in this chapter.

Note that in an algebraic expression operators are counted *from right to left*, while the corresponding vertices in a diagram go *from bottom to top*. Energy denominators are indicated by rectangular boxes (see Section 12.2.3).

Let us now try to sum all these diagrams. The sum of all ladder diagrams is

$$\Delta E = \sum_{i<j} \varepsilon_{ij} \tag{12-81}$$

with ε_{ij} the partial sum over diagrams for a particular pair of hole labels. We can write

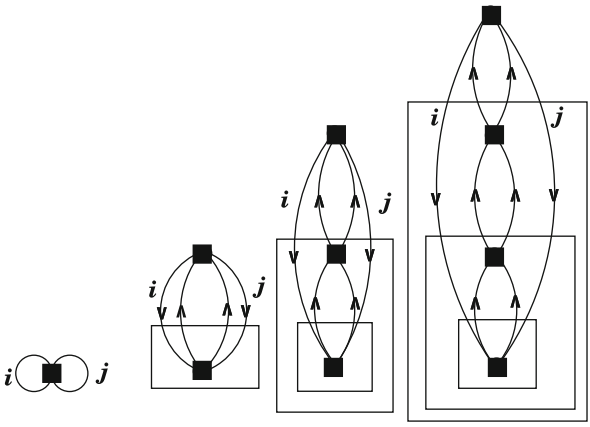

Figure 12-6. Ladder diagrams

$$\begin{aligned}
\varepsilon_{ij} &= V_{Cij} + [V, V_{BHij}]_{Cij} + [V, [V, V_{BHij}]_{BHij}]_{Cij} + \ldots \\
&= V_{Cij} + [V, S_{ij}]_{Cij} && \text{(12-82)} \\
S_{ij} &= V_{BHij} + [V, V_{BHij}]_{BHij} + \ldots \\
&= V_{BHij} + [V, S_{ij}]_{BHij} && \text{(12-83)} \\
-[H_0, S_{ij}] &= V_{Bij} + [V, S_{ij}]_{Bij} && \text{(12-84)} \\
[H_0 + V_{ij}, S_{ij}] &= -V_{Bij} && \text{(12-85)}
\end{aligned}$$

where the labels ij indicate that the only hole labels present are i and j.

We get S_{ij} as solution of a *linear system of equations*, and ε_{ij} immediately in terms of S_{ij}. We call this IEPA$_0$. Like CEPA$_0$, mentioned in Section 12.5.5 it is linear (whence the subscript 0), while IEPA stands for *independent electron pair approximation*. IEPA$_0$ differs from CEPA$_0$ in the neglect of the pair interaction terms $\{S_\mu^\dagger V S_\nu\}_C$ (for $\mu \neq \nu$). Like CEPA$_0$ (see Section 12.5.5), also IEPA$_0$ fails for a genuine 2-electron system. For this the only allowed hole labels are i and j as in the partial sum ε_{ij} of ladder diagrams. We must, include *additional* diagrams, namely EPV diagrams with repeated hole lines for any pair of hole labels. A typical EPV diagram is shown on Figure 12-7.

Adding all the EPV diagrams with two repeated hole labels, one gets a *nonlinear* system of equations, that is equivalent to an eigenvalue equation, which describes a 2-electron system correctly. EPV diagrams must be included to get the *correct normalization*. To sum up just the ladder diagrams is not sufficient.

Generally, the summation of a perturbation series to infinite order leads to a *linear system* of equations, if only direct (non-EPV) terms are summed up, while renormalization (EPV) terms have to be included in order to get the correct eigenvalue equation, or a non-linear equation equivalent to it.

It would be too tedious at this point to discuss how the inclusion of EPV diagrams leads from IEPA$_0$ to IEPA, i.e. to a nonlinear theory of independent electron pairs.

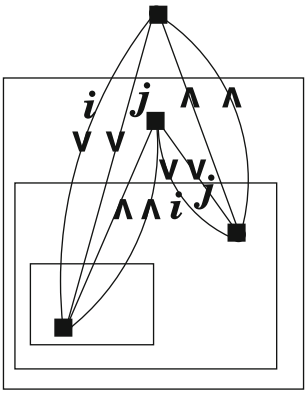

Figure 12-7. A typical EPV diagram with two repeated hole labels. Only *hole lines* are labeled

It is easier to wait until we have derived CEPA (Section 12.8.3). Then we can simply omit the pair coupling terms from CEPA or $CEPA_0$ to arrive at IEPA or $IEPA_0$ respectively.

It is an interesting challenge to sum all diagrams with *three hole lines*, to construct a theory of independent or coupled *electron triples*. We shall, however, find an easier access to this (Section 12.8.5).

12.6. TRADITIONAL COUPLED CLUSTER THEORY (TCC)

This section is devoted to *traditional* coupled cluster theory, based on a non-unitary similarity transformation in intermediate normalization, i.e. we try to solve the Eqs. (12-39) and (12-40). We do this in terms of a hierarchy in the particle rank. Starting point is the expansion of the cluster amplitude S in a basis of two-particle operators $X_{(2)}$, known as CCD (D for doubles). The basis is then augmented to $X_{(2)}$ and $X_{(1)}$, which defines CCSD (S for singles). With additional triply exciting basis operators $X_{(3)}$ we have CCSDT (T for triples). The next step in the hierarchy, CCSDTQ (Q for quadruples) has hardly played a significant role in practice [76]. If we want to distinguish between traditional CC and other CC variants, we put a letter T in front of the respective acronym, e.g. TCCD in the same meaning as CCD.

The CC equations are usually solved iteratively, because it is relatively easy to *invert a commutator with the one electron operator* H_0. This does not mean that the iterative solution is the only, or the preferable option. Little attention has been spent to this point.

12.6.1. Coupled-Cluster Theory with Double Excitations (CCD)

We chose $S = S_{(2)}$ as a 2-particle operator. The particle rank of an operator is now indicated by a subscript in parenthesis. This somewhat unconventional notation is chosen to be consistent with the paper on MBPT [22] where a simple subscript (normally chosen for the particle rank) was used for the orders in the perturbation expansion. Then we have to solve:

$$S = S_{(2)} = V_{BH} + [V, S_{(2)}]_{(2)BH} + \frac{1}{2}[[V, S_{(2)}], S_{(2)}]_{(2)BH} \tag{12-86}$$

$$E = E_0 + V_C + [V, S_{(2)}]_C \tag{12-87}$$

This compact system of equations can be solved iteratively, starting with $S = 0$. We like the commutator formulation, because it makes the connectedness immediately obvious. Sometimes only one term in the commutator is nonvanishing, and one can, as well write products instead of commutators, such as

$$S = S_{(2)} = V_{BH} + (V_A S_{(2)})^c_{(2)BH} + \frac{1}{2}(V S_{(2)} S_{(2)})^c_{(2)BH} \tag{12-88}$$

$$E = E_0 + V_C + (V_A S_{(2)})^c_C \tag{12-89}$$

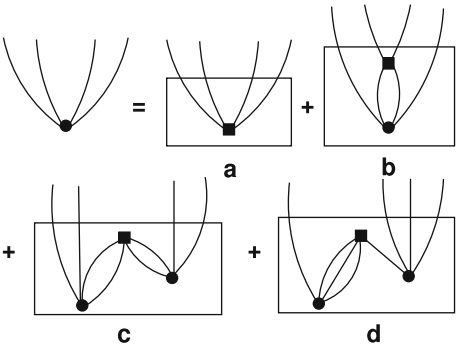

Figure 12-8. Graphical representation of the basis equation for CCD in terms of skeletons. *Spherical dots* represent cluster amplitudes S, *square dots* the electron interaction V

In this formulation one needs to specify that only the connected part has to be taken. We have done this tentatively in term of the superscript c. This is the only place in this chapter, where this notation is used. It is not needed if one expresses everything in terms of commutators.

While both S and V are 2-electron operators, and of the single commutators only the 2-electron parts are taken, in the construction of the double commutator intermediate 3-electron operators (say, in the commutator $[V, S_{(2)}]$) must not be ignored, although the final result is a 2-electron operator.

A graphical representation of the Eq. (12-86) is given on Figure 12-8 for skeletons [56, 71], i.e. for Hugenholtz type diagrams without explicit distinction of particle and hole lines. For the skeleton (b) of Figure 12-8 the possible explicit diagrams are shown on Figure 12-9, for the skeletons (c) and (d) on Figure 12-10. We symbolize a vertex representing an element of S by a spherical dot, one of the electron interaction V by a square dot.

The skeletons (a), (b), (c), and (d) represent contributions to 1st, 2nd, 3rd, and 3rd order of PT respectively. The corresponding contributions to the energy are of 2nd, 3rd, 4th, and 4th order respectively. If one neglects the 4th order terms, the formalism is greatly simplified. In fact this defines CEPA_0, that has been mentioned in Section 12.5.5.

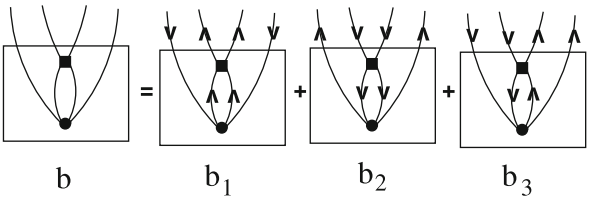

Figure 12-9. Hugenholtz type diagrams for the skeleton **(b)** on Figure 12-8

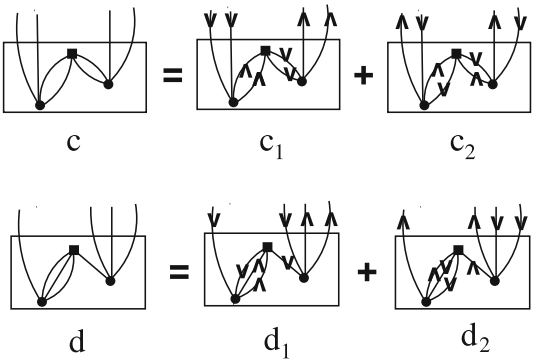

Figure 12-10. Hugenholtz type diagrams for the skeletons **(c)** and **(d)** on Figure 12-8

The converged result of traditional CCD (TCCD) differs from that of variational CCD (VCCD) by a term of $O(\lambda^5)$ (see Section 12.7.3). This may not matter as long as one is only interested in CCD or CCSD, but in CCSDT one will worry about terms of $O(\lambda^5)$, and the difference between TCCD and VCCD starts to be relevant.

12.6.2. Coupled-Cluster Theory with Single and Double Excitations (CCSD)

If we choose $S = S_{(1)} + S_{(2)}$ the system to be solved becomes a little lengthy

$$\begin{aligned} S_{(2)} = {} & V_{BH} + [V, S_{(2)}]_{(2)BH} + [V, S_{(1)}]_{(2)BH} + \frac{1}{2}[[V, S_{(2)}], S_{(2)}]_{(2)BH} \\ & + [[V, S_{(2)}], S_{(1)}]_{(2)BH} + \frac{1}{2}[[V, S_{(1)}], S_{(1)}]_{(2)BH} \\ & + \frac{1}{6}[[[V, S_{(1)}], S_{(1)}], S_{(1)}]_{(2)BH} + \frac{1}{2}[[[V, S_{(2)}], S_{(1)}], S_{(1)}]_{(2)BH} \\ & + \frac{1}{24}[[[[V, S_{(1)}], S_{(1)}], S_{(1)}], S_{(1)}]_{(2)BH} \qquad (12\text{-}90) \\ S_{(1)} = {} & [V, S_{(2)}]_{(1)BH} + [V, S_{(1)}]_{(1)BH} + [[V, S_{(2)}], S_{(1)}]_{(1)BH} \\ & + \frac{1}{2}[[V, S_{(1)}], S_{(1)}]_{(1)BH} + \frac{1}{6}[[[V, S_{(1)}], S_{(1)}], S_{(1)}]_{(1)BH} \qquad (12\text{-}91) \\ E = {} & E_0 + V_C + [V, S_{(2)}]_C + \frac{1}{2}[[V, S_{(1)}], S_{(1)}]_C \qquad (12\text{-}92) \end{aligned}$$

An iterative solution requires that both the equations for $S_{(1)}$ and $S_{(2)}$ must be solved self-consistently. Starting from CCD one must update $S_{(2)}$, since it depends on $S_{(1)}$, and so forth. There are two types of contributions of $S_{(1)}$ to the energy,

$$\Delta E^{a}_{(1)} = [V, \Delta S^{(1)}_{(2)}]_C = [V, [V, S_{(1)}]_{(2)BH}]_C + O(\lambda^5) \tag{12-93}$$

$$\Delta E^{b}_{(1)} = \frac{1}{2}[[V, S_{(1)}], S_{(1)}]_C \tag{12-94}$$

$$S_{(1)} = [V, S_{(2)}]_{(1)BH} + O(\lambda^3) \tag{12-95}$$

$$\Delta S^{(1)}_{(2)} = [V, S_{(1)}]_{(2)BH} = [V, [V, S_{(2)}]_{(1)BH}]_{(2)BH} + O(\lambda^4) \tag{12-96}$$

where $\Delta S^{(1)}_{(2)}$ is the change of $S_{(2)}$ due to the presence of $S_{(1)}$. If one has updated $S_{(2)}$, the *indirect* contribution $\Delta E^{a}_{(1)}$ is included and need not be evaluated explicitly. It starts with $O(\lambda^4)$. The direct contribution $\Delta E^{b}_{(1)}$ must be included explicitly. It goes with $O(\lambda^5)$.

The many terms containing $S_{(1)}$ are somewhat embarrassing. Their contributions to the energy vary between $O(\lambda^4)$ and $O(\lambda^7)$. Most of them could be safely be neglected. Fortunately, it is possible to *absorb* the single excitation into the reference function. Having constructed $S_{(1)}$ one can apply a similarity transformation to the reference function Φ, such that the transformed reference function is a Slater determinant constructed from modified spin-orbitals (often called *Brueckner* orbitals) such that no single excitations are explicitly present. One must then update $S_{(1)}$ and proceed until self-consistency. We cannot go into details here [77].

Although arguments from perturbation theory let single excitations appear rather unimportant, this applies mainly to the energy. They are quite important for one-electron properties

12.6.3. Coupled-Cluster with Doubles and Triples (CCDT)

Both single excitations and triple excitations contribute to the energy to 4th order in MBPT. One may therefore want to treat them on the same footing. Since the treatment of single excitations is so much easier (though lengthy), it is customary to start with CCSD and build the triple excitations, usually treated only approximately, upon a quasi-exact CCSD.

To understand the role of triples, it is nevertheless recommended to consider, at least preliminarily, a CCDT approach, in which singles are ignored. The stationarity conditions with respect to variation of $T^{\dagger}$ are

$$0 = \left\{ X^{\dagger}_{(2)} \left(V + [H_0, S_{(2)}] + [V, S_{(2)}]_{(2)} + [V, S_{(3)}]_{(2)} + \frac{1}{2}[[V, S_{(2)}], S_{(2)}]_{(2)} \right) \right\}_C \tag{12-97}$$

$$0 = \left\{ X^{\dagger}_{(3)} \Big(H + [H_0, S_{(3)}] + [V, S_{(2)}]_{(3)} + [V, S_{(3)}]_{(3)} + \frac{1}{2}[[V, S_{(2)}], S_{(2)}]_{(3)} + \frac{1}{2}[[V, S_{(2)}], S_{(3)}]_{(3)} + \frac{1}{2}[[V, S_{(3)}], S_{(2)}]_{(3)} \Big) \right\}_C \tag{12-98}$$

A consequence of stationarity is

$$E = H_C + [V, S]_C = E^{(0)} + [V, S_{(2)}]_C \tag{12-99}$$

The correlation energy is a *sum of pair energies* as in CCD. $S_{(3)}$ enters only indirectly, insofar as it changes $S_{(2)}$ with respect to that constructed in CCD.

We can formally solve (12-97) and (12-98) for $S_{(2)}$ and $S_{(3)}$ and get

$$S_{(2)} = V_{BH} + [V, S_{(2)}]_{(2)BH} + [V, S_{(3)}]_{(2)BH} + \frac{1}{2}[[V, S_{(2)}], S_{(2)}]_{(2)BH} \tag{12-100}$$

$$S_{(3)} = [V, S_{(2)}]_{(3)BH} + [V, S_{(3)}]_{(3)BH} + \frac{1}{2}[[V, S_{(2)}], S_{(2)}]_{(3)BH} + [[V, S_{(2)}], S_{(3)}]_{(3)BH} \tag{12-101}$$

The Eqs. (12-100) and (12-101) can be solved iteratively. In the *first iteration* for $S_{(3)}$ one keeps the 1st and the 3rd term of (12-101), i.e. one constructs

$$S_{(3)} = [V, S_{(2)}]_{(3)BH} + \frac{1}{2}[[V, S_{(2)}], S_{(2)}]_{(3)BH} \tag{12-102}$$

In this first iteration cycle one gets the leading term of $O(\lambda^2)$ of $S_{(3)}$ and another term of $O(\lambda^3)$. If one omits the second term in (12-102), one still gets the leading term of $S_{(3)}$. This defines an approximation that one can call CCD[T], in analogy to the approximation CCSD[T], also called CCSD+T(CCSD) of Urban, Noga, and Bartlett [78] to full CCSDT (see Section 12.6.4).

$S_{(3)}$ does not enter the energy directly, but only via its effect on $S_{(2)}$. The change $\Delta S^{(3)}_{(2)}$ of $S_{(2)}$ induced by $S_{(3)}$ is dominated by a term of $O(\lambda^3)$

$$\Delta S^{(3)}_{(2)} = [V, S_{(3)}]_{(2)BH} + O(\lambda^4) \tag{12-103}$$

which implies the leading *triples contribution* to the energy of $O(\lambda^4)$

$$\Delta E_{(3)} = [V, \Delta S^{(3)}_{(2)}]_C = [V, [V, S_{(3)}]_{(2)BH}]_C + O(\lambda^5) \tag{12-104}$$

One can reformulate this to

$$\Delta E_{(3)} = [V_{AH}, [V, S^{(2)}_{(3)}]]_C + O(\lambda^5) = [S^{\dagger}_{(2)}, [V, S_{(3)}]]_C + O(\lambda^5) \tag{12-105}$$

In the approximation CCD[T] (12-104) simplifies to

$$\begin{aligned}\Delta E_{(3)} &= [V,[V,[V,S_{(2)}]_{(3)BH}]_{(2)BH}]_C + O(\lambda^5)\\ &= [S^{\dagger}_{(2)},[V,[V,S_{(2)}]_{(3)BH}]]_C + O(\lambda^5)\end{aligned} \tag{12-106}$$

In CCD[T] one misses terms of 5th and 6th order in the energy, which, except for one 5th order term, require an *iterative solution*. One wants to avoid this, since it involves a formal N^8 step, while the non-iterative procedure scales only with N^7.

Another term of 5th order, that is included in CCSD(T) (see Section 12.6.4), has no counterpart in CCDT.

Unfortunately, arguments in terms of orders of perturbation theory have only limited value. We come back to this in Section 12.8.5.

12.6.4. Coupled-Cluster with Singles, Doubles and Triples (CCSDT)

The expressions of CCSDT are rather lengthy. We therefore consider S only to $O(\lambda^3)$

$$\begin{aligned}S_{(2)} &= V_{BH} + [V,S_{(2)}]_{(2)BH} + [V,S_{(3)}]_{(2)BH} + [V,S_{(1)}]_{(2)BH}\\ &\quad + \frac{1}{2}[[V,S_{(2)}],S_{(2)}]_{(2)BH} + O(\lambda^4)\end{aligned} \tag{12-107}$$

$$\begin{aligned}S_{(1)} &= [V,S_{(2)}]_{(1)BH} + [V,S_{(3)}]_{(1)BH} + [V,S_{(1)}]_{(1)BH}\\ &\quad + \frac{1}{2}[[V,S_{(2)}],S_{(2)}]_{(1)BH} + O(\lambda^4)\end{aligned} \tag{12-108}$$

$$\begin{aligned}S_{(3)} &= [V,S_{(2)}]_{(3)BH} + [V,S_{(1)}]_{(3)BH} + [V,S_{(3)}]_{(3)BH}\\ &\quad + \frac{1}{2}[[V,S_{(2)}],S_{(2)}]_{(3)BH} + O(\lambda^4)\end{aligned} \tag{12-109}$$

$$E_{\mathrm{CCSDT}} = [V,S_{(2)}]_C + \frac{1}{2}[[V,S_{(1)}],S_{(1)}]_C \tag{12-110}$$

In a full CCSDT treatment the equations for $S_{(1)}, S_{(2)}$, and $S_{(3)}$ are solved iteratively and self-consistently. Then only $S_{(2)}$ and $S_{(1)}$ are needed for the evaluation of E_{CCSD}. $S_{(3)}$ acts indirectly, via the dependence of $S_{(2)}$ and $S_{(1)}$ on $S_{(3)}$.

In approximations to CCSDT one starts from CCSD treated self-consistently, i.e. the influence of $S_{(1)}$ on $S_{(2)}$ is taken care of. However, the influence of $S_{(3)}$ on $S_{(2)}$ is only treated to the lowest order of perturbation theory. The leading change $\Delta S_{(2)}$ of $S_{(2)}$ under the influence of $S_{(3)}$ is of $O(\lambda^3)$ and the same (12-103) as in CCDT. It gives rise to an energy contribution (12-104) or (12-106) of $O(\lambda^4)$. This term is taken care of in the non-iterative full CCSDT formalism.

The second term of $O(\lambda^3)$ in (12-101) or (12-110), which gives rise to an energy contribution of $O(\lambda^5)$ is neglected in all non-iterative schemes.

In the rather popular CCSD(T) approach [12] one term of $O(\lambda^5)$ for the energy is explicitly taken care of, which does not even show up explicitly in the full CCSDT. If one does not update $S_{(1)}$ and $S_{(2)}$ under the influence of $S_{(3)}$, i.e. one starts from

CCSD and adds triple excitations *perturbatively*, one must not only take care of $\Delta S^{(3)}_{(2)}$ as one does in CCSD[T], but also of $\Delta S^{(3)}_{(1)}$, i.e. the change of $S_{(1)}$ under the influence of $S_{(3)}$. This $\Delta S^{(3)}_{(1)}$ leads to a change $\Delta S^{(31)}_{(2)}$ of $S_{(2)}$

$$\Delta S^{(3)}_{(1)} = [V, S_{(3)}]_{(1)BH} + O(\lambda^4) \tag{12-111}$$

$$\begin{aligned}\Delta S^{(31)}_{(2)} &= [V, \Delta S^{(3)}_{(1)}]_{(2)BH}] + O(\lambda^5) \\ &= [V, [V, S_{(3)}]_{(1)BH}]_{(2)BH}] + O(\lambda^5)\end{aligned} \tag{12-112}$$

$$\begin{aligned}\Delta E^{(3)}_{(1)} &= [V, \Delta S^{(31)}_{(2)}]_C + O(\lambda^6) \\ &= [V, [V, [V, S_{(3)}]_{(1)BH}]_{(2)BH}]_C + O(\lambda^6)\end{aligned} \tag{12-113}$$

One can reformulate this to

$$\Delta E^{(3)}_{(1)} = [S^{\dagger}_{(2)}, [V, [V, S_{(3)}]_{(1)BH}]]_C + O(\lambda^6) = [S^{\dagger}_{(1)}, [V, S_{(3)}]]_C + O(\lambda^6) \tag{12-114}$$

The two terms (12-105) and (12-114), which characterize CCSD(T) in the most compact way, are shown on Figure 12-11.

It looks somewhat arbitrary to select one of several contributions to the energy of $O(\lambda^5)$ and neglect others. Support for this choice came mainly from numerical calculations.

Among the attempts to justify this choice, a study by Stanton [79] (see also Ref. [80]) is interesting, where he showed, that CCSD(T) comes out automatically, if one tries to formulate CCSDT, starting from CCSD (rather than Hartree – Fock) as the reference state and constructing the effect of triple substitutions to the lowest order of perturbation theory based on CCSD. This perturbative approach can be

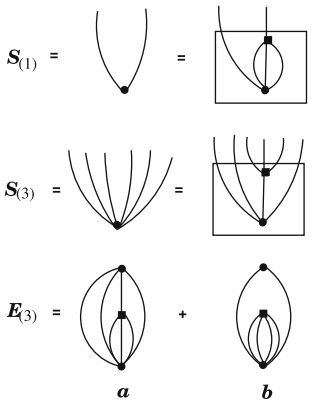

Figure 12-11. Contributions of $S_{(3)}$ and $S_{(1)}$ in CCSD(T)

formulated using the theory of CCSD gradients [9], for a non-hermitian unperturbed operator. The extra term in CCSD(T) is a direct consequence of the non-hermiticity of the CCSD Hamiltonian and would not show up in a hermitian perturbation theory. The extra term is often called a *non-Hartree Fock term*, to indicate that in a Hartree – Fock based theory it arises to higher order than in PT based on CCSD.

Müller et al. [81] have observed that, at least in one special case (the HF molecule) CCSD(T) performed better in a CC calculation with a conventional basis expansion, but that in terms of an explicitly correlated basis CCSD[T]-R12 appeared superior to CCSD(T)-R12. Unfortunately, this has not been checked in other calculation, since most available program packages do not allow to use CCSD[T].

There has been an enormous effort in the literature to derive approximations that are almost as effective as CCSDT at the cost of CCSD(T) [82].

If one remembers that the main merit of CCD or CCSD is that it is *non-perturbative*, one may wonder, why in the next step beyond CCSD, one uses perturbative approaches almost without hesitation. Both popular approximations to CCSDT, namely CCSD[T] and CCSD(T) are *not even* at the level of $CETA_0$, the linear version of CETA, the *coupled electron-triples approximation*, or the 3-particle generalization of $CEPA_0$, see Section 12.8.5. While CCSDT is at least exact for a genuine 3-electron system, this is neither the case for CCSD[T] nor for CCSD(T) (see Section 12.8.5).

A simplification CCSDT(Q) of CCSDTQ, with a perturbative inclusion of quadruples in the same spirit as CCSD(T) was proposed by Kállay et al. [76].

12.7. TOWARDS VARIATIONAL CC

12.7.1. Why Should One Care for Variational CC?

Traditional coupled cluster (TCC) theory has some attractive features, mainly that the basis operators S_μ *commute*, and that the *Hausdorff expansion* terminates. As a consequence we need only consider *one hierarchy*, namely that in terms of the *excitation rank*, with the steps TCCD, TCCSD, TCCSDT etc.

One of the drawbacks of TCC theory is, that it is not variational, i.e. does not provide an upper bound to the ground state energy and does not fulfill *hypervirial relations* such as a Hellmann Feynman theorem.

In a variational formulation, the error of the energy is *quadratic* in the error of the wave function (or wave operator), in TCC it has a *linear* term and is only approximatively quadratic [8]. If one cares for really high accuracy (i.e. if CCSDT is not sufficient), one should worry about VCC, because it should converge much faster with respect to the excitation rank.

If one tries a variational CC (VCC) in the intermediate normalization for the wave operator, one has still a basis of commuting operators, but not automatically manifest separability and no longer a terminating Hausdorff expansion, One has to consider a combination of *two hierarchies*, one in terms the *excitation rank*, one in terms of

the *truncation of the exponential*. One can use arguments from perturbation theory, to combine the hierarchic guidelines in a consistent way.

It is difficult, but possible [30], to formulate an expectation value of a CC ansatz, such that it is in Lie algebraic form and hence manifestly connected.

In terms of a perturbation expansion, TCCD and VCCD are consistent up to 4th order of the energy. The TCCD error starts with $O(\lambda^5)$.

If one formulates variational coupled cluster theory in terms of a unitary ansatz (UCC), to which we come in the last part of this paper (Section 12.9), it is almost trivial to reconcile variational behavior and manifest separability. There we shall also be in the fortunate situation, that the bulk of the non-terminating Hausdorff expansion can be evaluated as a closed summation, with a surprisingly simple result.

A question that has not yet found much attention is, whether the conventional hierarchy of CC theory, based on the excitation rank of the cluster amplitude is really the best choice, or whether one should, e.g. follow the suggestion of Nooijen [83–85] in favor of the generalized coupled cluster ansatz with singles and doubles (GCCSD).

XCC (expectation-value coupled-cluster theory), VCC, and UCC methods have been considered by Bartlett and Noga [86]. They differ from those studied here, insofar as H_0 and V are treated as separate quantities, somewhat in the spirit of perturbation theory. So they are not directly comparable with those of the present and an earlier study [8], where H is *not* decomposed into H_0 and V.

A rather extensive comparative study of XCC, VCC, and UCC as well as various variants of them, in terms of criteria that a good theory should satisfy, was published by Szalay et al. [10]. They recommend a method called SC-XCC (strongly connected expectation value coupled cluster), but the general conclusions are rather pessimistic.

Unfortunately little is known about results of VCC calculations. A benchmark study [87] treats very untypical situations, for which neither TCCD nor VCCD are good approximations. Benchmark calculations for *normal* molecules are badly needed.

12.7.2. The Expectation Value of a CC Ansatz in Intermediate Normalization

On can try a variational formulation of CC theory in two ways, either – as done in this subsection – in the intermediate normalization, starting from the expectation value

$$E = \frac{(e^{S^\dagger} H e^S)_C}{(e^{S^\dagger} e^S)_C} \tag{12-115}$$

or – as outlined later (Section 12.9) in unitary normalization.

Condition for stationarity of (12-115) is [8]

$$\{X^\dagger e^{S^\dagger} (H - E) e^S\}_C = 0; X = X_B \tag{12-116}$$

A problem is that we have to consider a twofold hierarchy, namely with respect to the excitation rank of the contributions to S and the truncation of the power series.

Unfortunately, the expression (12-115) is not in a Lie algebraic formulation. A manifestly connected, but a bit complicated formulation, has been given by Jeziorski and Moszynski [30] in terms of a series of commutators.

There is an expression equivalent to (12-115) [88]

$$E = \frac{(e^{S^\dagger} e^S L)_C}{(e^{S^\dagger} e^S)_C} = \frac{(e^{S^\dagger} e^S L)_C + (L^\dagger e^{S^\dagger} e^S)_C}{2(e^{S^\dagger} e^S)_C}; L = e^{-S} H e^S \tag{12-117}$$

Both formulations for E are hermitian, the latter is manifestly so. This can further be written as

$$E = L_C + \frac{\{(e^{S^\dagger} e^S)_A L_B)_C + (L_A^\dagger (e^{S^\dagger} e^S)_B\}_C}{2(e^{S^\dagger} e^S)_C} \tag{12-118}$$

i.e. as the sum of the energy L_C of TCC, plus a correction term which changes L_C to an upper bound. If $L = L_C$ or $L_B = 0$, we get $E = L_C$, but this is only achieved at the end of the CC hierarchy.

One can try to make E stationary with respect to variation of S, but this will be very tedious. A more modest possibility is to construct S from TCC and to insert this into (12-115) and get so an upper bound for E (though not the best possible one). These two variants can be referred to as VCC (V for variational) and XCC (X for expectation value).

12.7.3. Almost Variational CC Theory

Let us rewrite the energy functional as [88]

$$E = L_C + \frac{\{(e^{-S} e^{S^\dagger} e^S)_A L_B\}_C}{\{e^{-S} e^{S^\dagger} e^S\}_C} \tag{12-119}$$

We define a hierarchy of functionals, in which $e^{S^\dagger}$ is replaced successively by 1, $1 + S^\dagger$, $1 + S^\dagger + \frac{1}{2} S^{\dagger 2}$ etc. The first members are

$$E^{[0]} = L_C \tag{12-120}$$

$$E^{[1]} = L_C + \frac{\{S_A^\dagger L_B\}_C}{\{1 + [S^\dagger, S]\}_C} \tag{12-121}$$

$$E^{[2]} = L_C + \frac{\{(S^\dagger + \frac{1}{2} S^{\dagger 2} + \frac{1}{2}[S^{\dagger 2}, S])_A L_B\}_C}{\{1 + [S^\dagger, S] + \frac{1}{4}[[S^{\dagger 2}, S], S]\}_C} \tag{12-122}$$

The superscripts count members of a hierarchy. $E^{[0]}$ is stationary if S is that of TCC theory. Let us now *specify* that we consider CCD. Then we get $E^{[1]} = E^{[0]}$, i.e. the same S makes also $E^{[1]}$ stationary. If we now insert this S into (12-122), in the spirit of XCCD, we get

$$E = L_C + \frac{1}{2}\{S^{\dagger 2} L_B\} + O(\lambda^6) = L_C + \frac{1}{4}\{S^{\dagger 2}[[V, S], S]\} + O(\lambda^6) \tag{12-123}$$

The correction is of $O(\lambda^5)$. The part of $O(\lambda^5)$ is a generalized expectation value of a positive operator, and is likely to be positive. This does not mean that the total variational correction is necessarily positive. It is only so if the leading term of $O(\lambda^5)$ dominates. It is not unexpected that the TCCD energy *cheats*, i.e. is lower than the expectation value obtained with the same wave function.

This correction term has been considered previously [30, 88, 89].

Let us now go one step further. In (12-123) we have made L_C stationary, i.e. determined S so that $(S^\dagger L_B)_C = 0$. Let us now consider (12-123) as a functional of $S^\dagger$ and make it stationary with respect to variation of $S^\dagger$, in the spirit of VCC. We do not require that L_C ist stationary. We have, hence to add the term $(S^\dagger L_B)_C$. Our functional is then

$$E = L_C + (S^\dagger L_B)_C + \frac{1}{2}\{S^{\dagger 2} L_B\}_C + O(\lambda^6) \tag{12-124}$$

The stationarity condition is

$$0 = (X^\dagger L_B)_C + (X^\dagger S^\dagger L_B)_C + O(\lambda^6) \tag{12-125}$$

which implies

$$0 = (S^\dagger L_B)_C + (S^{\dagger 2} L_B)_C + O(\lambda^6) \tag{12-126}$$

$$E = L_C - \frac{1}{2}(S^{\dagger 2} L_B)_C + O(\lambda^6) = L_C - \frac{1}{4}(S^{\dagger 2}[[V, S], S]) + O(\lambda^6) \tag{12-127}$$

Of course, L_C has changed, since it is evaluated in terms of a different S, but the main change is in the sign of the correction term.

The VCCD energy is then, at least to the leading order, not only lower than the XCCD energy, but even lower than the TCCD energy. This needs numerical checks.

From TCC to XCC the energy rises apparently by a certain amount, then from XCC to VCC it decreases by roughly twice the same amount, provided that the leading term dominates, i.e. in situations without near-degeneracies.

The hierarchy presented in this subsection looks too complicated, to be applicable in practice. It is, however, useful to estimate how the TCC energy differs from an expectation value and the variational result for the same operator basis. It has

been suggested [88] to evaluate the correction term routinely, to get a feeling for the difference between TCC, XCC, and VCC.

At the level of CCD the *non-variational error* of the energy is of the order $O(\lambda^5)$ in perturbation theory. Since CCD is only correct to $O(\lambda^3)$, one is tempted not to worry about this error. However, if one goes to CCSDT, which is correct to $O(\lambda^4)$, neglect of the *non-variational error* for the CC-SD part does matter. The stationarity condition for CCSDT does not imply vanishing of this correction term. For this the stationarity condition for CCSDTQ would be necessary.

12.7.4. Extended Coupled Cluster Theory (ECC)

In extended coupled-cluster theory (ECC) [21] one applies two successive non-unitary similarity transformation to the Hamiltonian H

$$\tilde{L} = \{e^{T^\dagger} e^{-S} H e^{S} e^{-T^\dagger}\}_C; S = S_B; T^\dagger = (T^\dagger)_A \tag{12-128}$$

The double Hausdorff expansion terminates, but at much higher order in S and $T^\dagger$ than for the single similarity transformation of TCC. To the lower orders we get for ECCD

$$\begin{aligned}\tilde{L} = \{H + [H,S] + [T^\dagger,H] + \frac{1}{2}[[H,S],S] + \frac{1}{2}[T^\dagger,[T^\dagger,H]] + [T^\dagger,[H,S]\\ + \frac{1}{2}[T^\dagger,[[H,S],S]] + \frac{1}{2}[T^\dagger,[T^\dagger,[H,S]]] + \frac{1}{4}[T^\dagger,[T^\dagger,[[H,S],S]]\}_C\end{aligned} \tag{12-129}$$

plus terms of 5th and higher order in T or S. To low orders this looks like a symmetrized version of the Arponen functional. To higher order asymmetries between S and T arise. ECC is somehow half between TCC and VCC. What interests us here, is that the next term beyond the Arponen functional is actually the correction term (12-123)

$$\frac{1}{4}\{[T^\dagger,[T^\dagger,[[H,S],S]]\}_C \tag{12-130}$$

that we have derived as the leading variational correction to CCD.

12.8. ADVANCED CC THEORY

12.8.1. Change of Paradigm

So far, a paradigm of CC theory has been that an acceptable formalism should be invariant with respect to a unitary transformation of the hole states, i.e. the spin orbitals occupied in the reference state [34]. It has turned out that this paradigm can sometimes be even counterproductive. If one wants to construct a formalism

that scales linearly with the particle number [2], one must use a localized basis, and renounce on unitary invariance. In this case one is better advised to take advantage of the freedom in the choice of the basis to care for an *optimal basis*.

We know that the separation theorem, on which the justification of an exponential ansatz for the wave operator is based, makes explicitly use of a localized description (see Section 12.3). Although the CC ansatz is unitarily invariant, and so are all expectation values constructed from it, the *decomposition* of expectation values into physically meaningful parts is not. At least for very large molecules a physically meaningful analysis and a distinction between relevant and irrelevant contributions is possible only in the localized representation, which allows one either to ignore or approximate the latter.

A message of this chapter is that on the way to construct the wave operator in exponential form, the first step is a *linear theory*, of the type CEPA_0, but generalized to arbitrary particle rank. This step happens to be unitary invariant. In a second step (not strictly, but often practically unitary invariant) one achieves that the various electron pairs and higher order clusters are *normalized individually*, which leads to CEPA-like equations. This requires to sum over the EPV contributions to certain coupling terms.

Only in a next step, if at all, the non-EPV contributions to higher order couplings, which are small in absolute value and of random sign, can be taken care of. These terms hardly contain physical information. They represent *separability defects* related to a slight incompatibility of ideal localization with the general antisymmetry of the wave function, and are the price to pay for the virtues of the CC expansion.

There are further serious problems related to the non-hermiticity of the effective Hamiltonian of traditional CC theory, which strongly suggest to switch to a variational, preferentially unitary CC theory (see Sections 12.7 and 12.9).

12.8.2. Unitary Invariance and Linear Scaling

Let us consider an energy expression of the form

$$E = \sum_{i,j,k,l} E_{ijkl} \tag{12-131}$$

where the terms in this sum depend on 4 spin-orbital labels i, j, k, l, referring to holes (occupied spin orbitals). Each of them is an implicit sum over particle (virtual spin orbital) labels a, b, c, d. Let the sum be *unitary invariant* with respect to the hole labels, i.e. depend only on the space spanned by the virtual spin orbitals i, j, k, l and let further each term E_{ijkl} depend only on the space spanned by the virtual spin orbitals a, b, c, d. (This *virtual-virtual unitary invariance* will not be disputed.)

Let us now decompose E into a diagonal and a non-diagonal part (with a different meaning of these terms than in Section 12.2.6)

$$E = E_d + E_n; E_d = \sum_{i,j} E_{ijij}; E_n = \sum_{(i,j)\neq(k,l)} E_{ijkl} \tag{12-132}$$

This decomposition is *not necessarily* unitary invariant, i.e. E_d and E_n individually are then not invariant under a unitary transformation among the occupied spin orbitals.

When we refer in this chapter to *unitary invariance*, or the lack of it, we mean this precisely with respect to a decomposition of a totally unitary invariant sum such as (12-132).

There are choices of the hole labels for which E is dominated by the diagonal term E_d, and this is usually the case if the hole orbitals are *localized*. If there is a choice of the hole orbitals, for which E_n is negligible, the computational effort is reduced. It is then of the order n_{occ}^2, where n_{occ} is the number of occupied spin orbitals (holes), while the full expression contains $O\left(n_{\text{occ}}^4\right)$ terms. A better scaling with the number of hole labels (in the direction of linear scaling) is possible if one *relaxes the requirement of unitary invariance*. If one wants to take advantage of this possibility, one must, of course, have criteria of how to choose the hole orbitals, in order that E_d is a sufficiently good approximation to E. We have this in mind when we refer to *incompatibility of unitary invariance and linear scaling*.

One can go even one step further and consider an energy expression in terms of *hole pair* labels μ, ν

$$E = \sum_{\mu,\nu} E_{\mu,\nu} = E_d + E_n \tag{12-133}$$

and search for an orthogonal set of hole-pair functions in terms of which E_d is a good approximation to E. These pair functions belong to the family of extremal pair functions [90].

We shall see that the contribution of those terms by which CCD differs from CEPA_0, are of the type just discussed. The sum of these terms can be decomposed into contributions of EPV diagrams and non-EPV diagrams.

Often this decomposition is not strictly, but practically, unitary invariant. There are probably cases with a stronger deviation from unitary invariance, where the non-diagonal terms are negligible only for a special choice of the occupied spin orbitals, namely localized ones. In this situation one will want to relax the paradigm of unitary invariance and rather care for an optimal set of occupied spin orbitals.

One can then still decide whether one wants to neglect E_n altogether or to construct first E_d, and to evaluate finally E_n in terms of parameters optimized for E_d, and so get close to the result of a manifestly unitary invariant calculation.

12.8.3. From CCD to CEPA

Let us start from the Arponen functional (12-72) for CCD and let us decompose it into the CEPA_0 functional

$$F_{CEPA_0}(T^\dagger_{(2)}, S_{(2)}) = \{H + [H, S_{(2)}] + [T^\dagger_{(2)}, H] + [T^\dagger_{(2)}, [H, S_{(2)}]] \qquad (12\text{-}134)$$

and an additional term

$$F_{\Delta CCD}(T^\dagger_{(2)}, S_{(2)}) = \frac{1}{2}\{[T^\dagger, [[H, S_{(2)}], S_{(2)}]]'_C \qquad (12\text{-}135)$$

$$F_{CCD}(T^\dagger_{(2)}, S_{(2)}) = F_{CEPA_0}(T^\dagger_{(2)}, S_{(2)}) + F_{\Delta CCD}(T^\dagger_{(2)}, S_{(2)}) \qquad (12\text{-}136)$$

This triple-commutator term is represented graphically on Figure 12-12, without the factor $\frac{1}{2}$.

The diagrams c_1, c_2, d_1, d_2 correspond to the diagrams with the same labels as in Figure 12-10.

One may think that they represent the interaction between *triples of pairs (as the name coupled-cluster may suggest)*. In reality they play a much simpler and physically very meaningful role.

The algebraic equivalents of these diagrams are

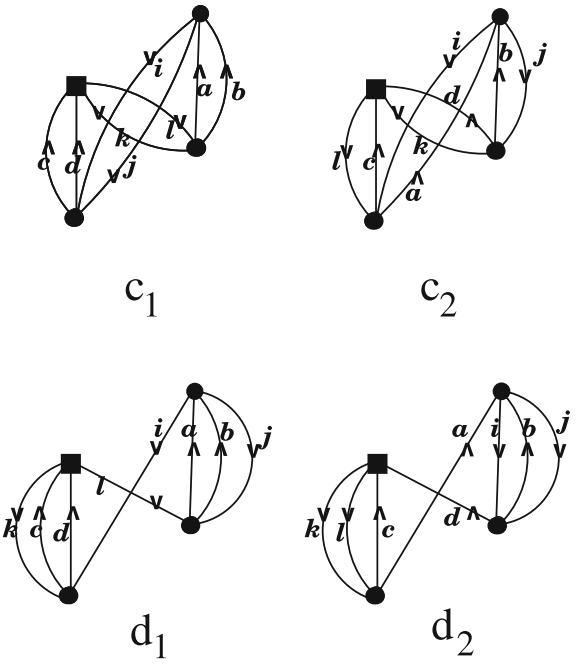

Figure 12-12. Terms bilinear in $S_{(2)}$ of the Arponen functional for CCD. *Spherical dots* for $T^\dagger$ or S, *square dots* for V. In c_2 the labels k and l should be exchanged

$$c_1 : \quad \tilde{T}_{ij}^{ab}\tilde{V}_{kl}^{cd}\tilde{S}_{ab}^{kl}\tilde{S}_{cd}^{ij} = (\tilde{T}_{ij}^{ab}\tilde{S}_{ab}^{kl})(\tilde{V}_{kl}^{cd}\tilde{S}_{cd}^{ij}) \tag{12-137}$$

$$c_2 : \quad \tilde{T}_{ij}^{ab}\tilde{V}_{kl}^{cd}\tilde{S}_{db}^{lj}\tilde{S}_{ca}^{ji} \tag{12-138}$$

$$d_1 : \quad -\tilde{T}_{ij}^{ab}\tilde{V}_{kl}^{cd}\tilde{S}_{ab}^{lj}\tilde{S}_{cd}^{ki} = -(\tilde{T}_{ij}^{ab}\tilde{S}_{ab}^{lj})(\tilde{V}_{kl}^{cd}\tilde{S}_{cd}^{ki}) \tag{12-139}$$

$$d_2 : \quad -\tilde{T}_{ij}^{ab}\tilde{V}_{kl}^{cd}\tilde{S}_{db}^{ij}\tilde{S}_{ca}^{kl} \tag{12-140}$$

The fact that one ought to include diagrams with T and V exchanged, cancels the factor $\frac{1}{2}$. One must note that the diagrams c_1 and d_2 are invariant with respect to the exchange $i \leftrightarrow j$ and $k \leftrightarrow l$ independently, such that we can sum over $i < j, k < l$, while those of d_1 and c_2 are only invariant with respect to a simultaneous exchange $i \leftrightarrow j, k \leftrightarrow j$, such that one must also include $i < j, k > l$ (or $i > j, k < l$).

It is not trivial to extract the sign from our diagrams. For this, diagrams with line vertices would be preferable, but even for point vertices one can distinguish between lines that enter or leave on the left or right side of the vertex. The diagrams c_1 and c_2 have 2 and 4 closed loops respectively, hence a +sign, the diagrams d_1 and d_2 have 3 closed loops, hence a $-$sign.

The most detailed numerical studies on the relative importance of these diagrams found in the literature, are the relatively old ones by Paldus et al. [61] and Dykstra et al. [62] on some realistic systems and some model systems. The counterparts of our Hugenholtz type diagrams c_2 and d_2 are the Goldstone type diagrams 1, 2, and 3 respectively in Ref. [61], while our c_1 and d_1 correspond to 5 and 4 respectively in Ref. [61].

One interesting observation has been that the *non-factorizable* diagrams c_2 and d_2 give very small absolute contributions. If one only adds c_2 and d_2 to CEPA$_0$ (this approach has been called ACP-D$_{123}$ [61], with ACP for *approximate coupled pair*), the results are hardly different from CEPA$_0$. Apparently the individual diagrams in c_2 and d_2 have random sign and cancel to a large extent. This is independent of whether one uses a localized or a delocalized basis, since the sum of the diagrams of one class is unitary invariant. One can argue that the diagrams c_2 and d_2 represent some *noise* and have no real physical meaning.

The diagrams c_2 and d_2 contain EPV diagrams with repeated hole labels, but these are *non-factorizable* (not equivalent to disconnected diagrams). Each of these in c_2 cancels with a partner in d_2. The sum of the d_2 EPV diagrams is just the same expression with a minus sign. For the sum of the two sets of diagrams c_2 and d_2 it does not matter whether or not one includes the EPV diagrams.

One sees this cancellation on Figure 12-12 if one looks at the diagrams for c_2 and d_2 with $i = k$.

Conversely to the approach just considered, we can take only the diagrams c_1 and d_1 and add them to CEPA$_0$, in the sense of ACP-D$_{45}$ in Ref. [61] or ACC (approximate CC) in Ref. [62]. One then nearly duplicates the CCD results. Apparently the diagrams c_1 and d_1 do not show significant sign oscillations, their sums even factorize. Although preliminary experiences with ACC or ACP-D$_{45}$ were very encouraging, this approximation has never become popular. In CC theory in terms

of Gaussian geminals [23] a *factorized version* FCCD has played an important role. It is the counterpart of ACC, and has turned out very powerful in the study of the He dimer [91]. See also the comment on the 2CC method [13] at the end of this subsection.

The author was successful in convincing Frank Neese (private communication) to perform similar studies at the present state of the art, taking some small molecules such as CH_4, NH_3, H_2O, HF, CO, N_2 and F_2, as well as two larger ones, adenine and cyclodecane, as examples. He confirmed that the sums of the terms of type c_2 and d_2 practically cancel in all cases, giving rise to less than 2% of the full correlation energy. They appear to carry *hardly any physical information*. The diagrams with the smallest contribution happen also to be the computationally most expensive ones.

The situation is slightly different for the diagrams c_1 and d_1. Their sums are not negligible, but are entirely dominated by the *EPV diagrams*. The non-EPV diagrams of c_1 and d_1 contribute by less than 1% to the overall correlation energy. In this respect the old studies by Paldus et al. [61] were perfectly confirmed by Neese (private communication).

The behavior of the diagrams c_2 and d_2 is independent of whether or not one uses a canonical or a localized basis, and is essentially based on the random sign of the respective diagrams. On the other hand there is some preliminary evidence that the non-EPV diagrams of c_1 and d_1 are negligible only in a localized basis. This needs a further check, but is, at least, suggested by the following argument.

Let us refer to *ideal* localization if the basis can be decomposed into as many subsets $\mathcal{S}(i)$ as there are occupied spin orbitals ψ_i in the reference function, with each subset $\mathcal{S}(i)$ associated with one ψ_i, such that the matrix elements S_{ab}^{ij} are non-vanishing only if ψ_a and ψ_b belong to $\mathcal{S}(i)$ and $\mathcal{S}(j)$ or vice versa.

Let us postulate ideal localization, and let us assume that $a \in \mathcal{S}(i); b \in \mathcal{S}(j); c \in \mathcal{S}(k), d \in \mathcal{S}(l)$, and let us consider the case that the labels i,j,k,l are *all different*. Then in all 4 types of diagrams the first two factors are non-vanishing. The third and forth factors vanish to forth order in the overlap between subsets for diagrams c_1 and to second order in d_1. A factor S_{cd}^{ij} is e.g. *small to second order*, because $c \in \mathcal{S}(k)$ and $d \in \mathcal{S}(l)$. So these terms will be small, even if there is no *ideal* localization.

This is no longer the case, if at least *one hole label is repeated*, i.e. for EPV diagrams. On Figure 12-13 we show the diagrams of type d_1 with one repeated hole line (i), namely the connected EPV diagram on the r.h.s. and the corresponding disconnected, but joint (with one common label) renormalization diagram. These diagrams sum to 0.

Let us define the normalization integral s_{ij}^2 and the pair correlation energy ε_{ij}

$$s_{ij}^2 = \sum_{a<b} \tilde{T}_{ij}^{ab} \tilde{S}_{ab}^{ij}; \; \varepsilon_{ij} = \sum_{c<d} \tilde{V}_{ji}^{cd} \tilde{S}_{cd}^{ji} \tag{12-141}$$

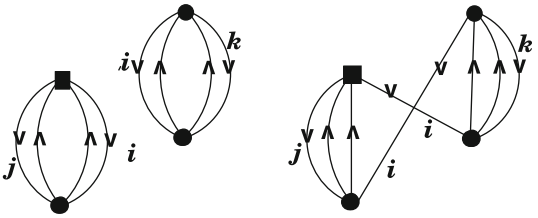

Figure 12-13. EPV diagrams of type d_1 with one repeated hole label (r.h.s.), and equivalent disconnected diagram (l.h.s.)

Then the algebraic equivalent of the EPV diagram on Figure 12-13, and the sum over a, b, c, d is:

$$-\sum_{a<b,\ c<d} \tilde{T}_{ij}^{ab} \tilde{V}_{ki}^{cd} \tilde{S}_{ab}^{ij} \tilde{S}_{cd}^{ki} = -\sum_{a<b} (\tilde{T}_{ij}^{ab} \tilde{S}_{ab}^{ij}) \sum_{c<d} (\tilde{V}_{ki}^{cd} \tilde{S}_{cd}^{ki}) = -s_{ij}^2 \varepsilon_{ik} \quad (12\text{-}142)$$

One can symmetrize to

$$-\frac{1}{2} s_{ij}^2 (\varepsilon_{ik} + \varepsilon_{jk}) \quad (12\text{-}143)$$

and one gets the sum

$$-\sum_{i<j} s_{ij}^2 \sum_{k \neq (i,j)} (\varepsilon_{ik} + \varepsilon_{jk}) \quad (12\text{-}144)$$

The sum of all EPV diagrams on Figure 12-14 (with two repeated hole labels i, j) is the negative of the disconnected diagram, hence

$$-s_{ij}^2 \varepsilon_{ij} \quad (12\text{-}145)$$

with the sum

$$-\sum_{i<j} s_{ij}^2 \varepsilon_{ij} \quad (12\text{-}146)$$

For the sum of all EPV diagrams we get finally

$$-\sum_{i<j} s_{ij}^2 \tilde{\varepsilon}_{ij};\ \tilde{\varepsilon}_{ij} = \varepsilon_{ij} + \sum_{k \neq j} \varepsilon_{ik} + \sum_{k \neq i} \varepsilon_{kj} \quad (12\text{-}147)$$

with $\tilde{\varepsilon}_{ij}$ the pair correlation energy of the pair ij plus the sum of the pair correlation energies of all pairs that are semi-joint with ij, i.e. have a common spin-orbital label.

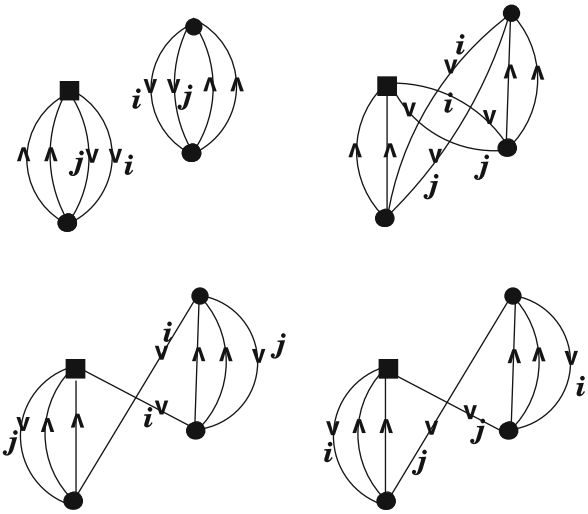

Figure 12-14. EPV diagrams of type c_1 and d_1 with two repeated hole labels (r.h.s.), and equivalent disconnected diagram

Like for c_2 and d_2 there are also non-factorizable EPV diagrams of c_1 and d_1, which do not cancel with disconnected diagrams, but between the two sets c_1 and d_1. Consider, e.g. the diagram d_1 on Figure 12-12 with $k = j$. It cancels with the corresponding c_1 diagram. Again it does not matter for the sum of c_1 and d_1, whether or not one includes these non-factorizable EPV diagrams.

The result (12-146) was first found in a different context by Kelly [38] and later, starting from CCD by Taylor et al. [59] as well as Paldus et al. [61], though in terms of spin-adapted pairs, where it needs a slight modification. The EPV concept is strictly applicable only in terms of spin orbitals. It leads to the CEPA variant CEPA_3 [36].

We get so a simplified form of the functional $F_{\Delta\mathrm{CCD}}$, namely (we omit the subscript (2) on $T^\dagger$ and S)

$$F_{\Delta\mathrm{CEPA}_3}(T^\dagger, S) = -\sum_\mu T_\mu^\dagger \tilde{\varepsilon}_\mu S_\mu \tag{12-148}$$

where $\mu = i < j$ is a label that counts pairs.

If we add this to the CEPA_0 functional (12-134) we get the CEPA_3 functional

$$F_{\mathrm{CEPA}_3}(T^\dagger, S) = \{H + \sum_\mu [H, S_\mu] + \sum_\mu [T_\mu^\dagger, H] + \sum_{\mu,\nu} [T_\mu^\dagger, [H, S_\nu]] - \sum_\mu T_\mu^\dagger \tilde{\varepsilon}_\mu S_\mu\}_C \tag{12-149}$$

The stationarity condition with respect to variation of $T^\dagger$ is

$$0 = \{X_\mu^\dagger (V + [H_0, S_\mu] + \sum_\nu [V, S_\nu] - \tilde{\varepsilon}_\mu S_\mu)\}_C \tag{12-150}$$

Due to the last term this is no longer a linear system. The nonlinearity is in the energy shift $\tilde{\varepsilon}_\mu$ for the pair μ.

Before we come to other CEPA variants, let us compare the extra functional $F_{\Delta\mathrm{CEPA}_1}$ with the difference (12-79) between the CI and the CEPA_0 functional

$$F_{\Delta\mathrm{CI}} = -\sum_{\mu,\nu} s_\mu^2 \varepsilon_\nu \tag{12-151}$$

This is a sum of products of normalization integrals of pairs and pair correlation energies, taking care of *all pairs of electron pairs* μ, ν. This is obviously *non-physical* and in conflict with the connected-diagram theorem (except, of course, for a genuine 2-electron system). The main advantage of CEPA_3 with respect to CID is that only those products $s_\mu^2 \varepsilon_\nu$ enter, for which the pairs ν, μ have at least one common orbital label.

One can go one step further, and replace $\tilde{\varepsilon}_\mu$ by ε_μ, i.e. consider only products $s_\mu^2 \varepsilon_\mu$ for the same pair. This defines CEPA_2, while CEPA_1 is a compromise with the choice

$$\tilde{\varepsilon}_{ij} = \varepsilon_{ij} + \frac{1}{2}\sum_{k\neq j} \varepsilon_{ik} + \frac{1}{2}\sum_{k\neq i} \varepsilon_{kj} \tag{12-152}$$

i.e. just the mean of CEPA_2 and CEPA_3. The subscripts of the CEPA variants have not always been used unambiguously. The now generally accepted [36] nomenclature is slightly unsystematic, since the ordering is CEPA_0, CEPA_2, CEPA_1, CEPA_3.

CEPA_2 (often just called CEPA) is the simplest variant (after CEPA_0). Its motivation was that the standard IEPA had exactly this energy shift [6]. CEPA_1 was proposed as a variant which is invariant with respect to a switch between the canonical and the localized representation in a special case [5].

If one wants to approximate CCD, CEPA_3 (which is generally very close to ACC (Neese, private communication)) appears to be the best choice, while CEPA_1 is probably closer to experiment. It has been speculated (see below) that CEPA_1 and CEPA_2 perform better than CEPA_3 because they simulate some 3-particle correlations.

One can argue in terms of a plausibility argument. The *energy shift* of CID contains the products $s_\mu^2 \varepsilon_\nu$ for *all* pairs of pairs μ, ν. In CCD, i.e. by simulating the inclusion of the unlinked clusters of pair excitations, one removes all products $s_\mu^2 \varepsilon_\nu$ for μ and ν *disjoint*, i.e. with no common spin-orbital label [6], but keeps those for a single pair $s_\mu^2 \varepsilon_\mu$ and those for μ and ν *semi-joint* i.e. with a common spin orbital label [6]. In the limit of independent pairs only $s_\mu^2 \varepsilon_\mu$ survives. It is plausible that the effect of correlations beyond CCD reduces the interaction terms for *semi-joint*

pairs, multiplying them by a factor $0 < p < 1$, which leads to something between $CEPA_3$ ($p = 1$) and $CEPA_2$ ($p = 0$). This means that by switching from $CEPA_3$ (which appears to be the best approximation to CCD) to $CEPA_1$ or even $CEPA_2$ on can simulate to some extent the effect of higher excitations. This possibly explains why $CEPA_1$ or $CEPA_2$ often perform better than CCD in real calculations.

Had CEPA survived longer on the market (and had not been practically eliminated in favor of by CC), one would certainly have agreed on a standard, which would make the argument obsolete, that CEPA is not uniquely defined. I have never heard, by the way, that DFT is invalid, because there are so many variants of it on the market.

Heully and Malrieu [92] have presented a more rigorous formulation for the treatment of the effect of triples in terms of a *dressed* 2-particle Hamiltonian, which is equivalent to CCSD(T).

If one wants to take CEPA as an approximation to CCD, and keep e.g. the option to treat triple excitations on top of it, one should probably prefer $CEPA_3$. If one wants to end with CEPA, and cares for practical performance, $CEPA_1$, or $CEPA_2$ would probably be the methods of choice.

It has often been argued that CEPA, unlike CCD, CID or $CEPA_0$ is *not unitary invariant*. This argument has probably mainly been based on the fact that rigorous unitary invariance of $CEPA_k$ with $k = 1,\ 2,\ 3$ cannot be proven, than on systematic numerical investigations. Recent studies by Neese (private communication) on some small and medium-sized molecules, including adenine, have shown that the switch from a canonical to a localized representation leads to changes of the order of only 0.1% of the total correlation energy, at least for $k = 1$ or 3 . Of course, the bulk of the latter is in the $CEPA_0$ part, which is unitary invariant anyway. This precludes very strong deviations from unitary invariance. The new results (private communication) confirm in this and other respects old conclusions [63]. For a formal discussion of unitary invariance in CC theory see Ref. [8].

From a practical point of view unitary invariance does not appear to be a problem for CEPA. Noticeable deviations from unitary invariance are observed in cases of near-degeneracy (where CC based on a single Slater determinant reference is problematic anyway) [63]. Then CEPA is closest to CCD for *localized* hole orbitals. One further expects stronger deviations from unitary invariance for really large molecules. More systematic studies are needed.

The CEPA theory, with the two variants $CEPA_1$ and $CEPA_2$ was first derived on a different route [5, 35, 36], starting from an analysis of the CI equations.

The CEPA conditions imply

$$E = E^{(0)} + [H, S]_C = E^{(0)} + \sum_{\mu} \varepsilon_{\mu} \tag{12-153}$$

i.e. the total correlation energy in this approximation can be written as a sum of pair correlation energies.

A reader may object that, by neglecting the non-EPV contributions to $[T^{\dagger}, [[H, S], S]]$, one ignores an essential ingredient of CC theory, even if these terms

hardly matter numerically. In reality, what the exp(S) ansatz achieves is that it *removes spurious couplings* that plague the linear ansatz of CI and cares for an *independent normalization* of the various pairs. This is physics, while the presence of the non-EPV contributions to the quadruple commutators are *the price to pay* for the physical decoupling. This indicates that the name *coupled cluster* may be slightly misleading. What matters is that kind of coupling (or rather *interaction*) of the pairs, of $O(\lambda^3)$, by which CEPA differs from IEPA, and which is also present in CID, while the coupling, of $O(\lambda^4)$, through the normalization of the pairs is minimized in CCD relative to CID.

One can, of course, after one has performed a CEPA calculation, look at those diagrams, which do not enter CEPA, and evaluate them in a perturbative way, i.e. as simple expectation values. This may make sense, if one wants to go beyond CCSD. Since the triple contributions in CCSDT start with $O(\lambda^4)$, one may want to have taken care earlier of all terms of $O(\lambda^4)$ in CCSD. However, if one ignores triples, the effort to be complete with $O(\lambda^4)$ in CCSD will usually not pay, since the bulk of the $O(\lambda^4)$ terms is taken care of in CEPA anyway. Numerical studies, both old and recent ones [63–65] have not indicated any superiority of CCSD with respect to CEPA, as far as e.g. spectroscopic constants are concerned.

If we omit the *pair interaction* terms in CEPA_3 (12-150), we arrive at the IEPA_3 system:

$$0 = \{X_\mu^\dagger (V + [H_0, S_\mu] + [V, S_\mu] - \tilde{\varepsilon}_\mu S_\mu)\}_C \tag{12-154}$$

The variant with $\tilde{\varepsilon}_\mu$ replaced by ε_μ is then IEPA_2. This does describe a supersystem of non-interacting pairs exactly, as does IEPA_1, CEPA_2, or CEPA_1. The acronyms IEPA_k have, so far, not been used, only IEPA, in the meaning of IEPA_2.

The non-linear system (12-154) is then equivalent to a coupled eigenvalue system.

$$0 = \{X_\mu^\dagger (H + [H, S_\mu] - E_\mu S_\mu)\}_C \tag{12-155}$$

The same stationarity condition is obtained if we minimize the following functional

$$E^{(0)} + \sum_\mu \frac{\{[S_\mu^\dagger, H] + [H, S_\mu] + [S_\mu^\dagger, [H, S_\mu]]\}_C}{\{1 + S_\mu^\dagger S_\mu\}_C} \tag{12-156}$$

One can also ignore the denominators, and require individual normalization of the various pairs. Then the energy shifts ε_μ for the pairs play the role of Lagrange multipliers.

This functional for IEPA can be generalized to a functional proposed by Ahlrichs [39] for coupled electron pairs. We shall (Section 12.9.5) later get a more direct access to the Ahlrichs functional. As to a precursor of this functional see Ref. [35].

Recently Bartlett and Musial [13] have considered a hierarchy *n*CC of approximations, such that with *n*CC one describes an *n*-particle systems or supersystems of non-interacting *n*-particle systems exactly, but that one ignores terms from full CC theory that are not needed for this property. 2CC turns out to be essentially the same as ACC. The authors [13] regard this explicitly as a counterpart of CEPA, that is *unitary invariant*.

12.8.4. The Variational CCD Corrections and CEPA

We have earlier (Section 12.7.3) derived a variational correction to CCD

$$\frac{1}{4}[T^\dagger,[T^\dagger,[[V,S],S]]]_C \tag{12-157}$$

We must now study what this correction becomes in the same spirit as that which led us from CCD to CEPA. We argue that in (12-157) three factors combine to a pair interaction term

$$[T^\dagger,[V,S]]_C=\sum_{\mu,\nu}[T^\dagger_\mu,[V,S_\nu]]_C=\sum_{\mu,\nu}v_{\mu,\nu} \tag{12-158}$$

while two factors combine to a pair normalization integral

$$[T^\dagger,S]_C=\sum_{\mu}[T^\dagger_\mu,S_\mu]_C=\sum_{\mu}s^2_\mu \tag{12-159}$$

such that an approximation to (12-157) is

$$\sum_{\mu,\nu}v_{\mu,\nu}(s^2_\mu+s^2_\nu)/2 \tag{12-160}$$

Details have to be worked out, it matters especially whether the two interacting pairs μ and ν have a common orbital label. The interaction of semijoint pairs is usually more important than that between disjoint pairs. Most important is the electron interaction within a single pair, such that terms like $v_{\mu,\mu}s^2_\mu$ deserve special attention.

One expects a functional, that can be constructed from the CEPA_0 functional with some normalization corrections

$$F=\sum_\mu\{H+([H,S_\mu]+[S^\dagger_\mu,H])(1-s^2_\mu)+[S^\dagger_\mu,[H,S_\nu](1-s^2_\mu/2-s^2_\nu/2)\}_C \tag{12-161}$$

It is an open question whether one should make this correction to the CEPA functional. In the way, how we have derived CEPA in the Section 12.8.3, CEPA shares with TCCD that it is non-variational.

We shall find an easier access to variational CEPA in Section 12.9.5. One notes the relation of the functional (12-161) to the coupled-pair functional of Ahlrichs et al. [39], to which we shall come back in a different context (Section 12.9.5).

12.8.5. Beyond CEPA. Electron Triple Approximations

In Section 12.8.3 we have shown that the attempt to solve the CCD equations in a localized basis leads in a first approximation to a *linear system* of equations, namely $CEPA_0$, and in the next approximation to a nonlinear eigenvalue-like system $CEPA_2$ with individual energy shifts for the various pairs. What can we learn from this for the corresponding treatment of CCDT? Again, in order to simplify things, we ignore single excitations.

First we must try to formulate the corresponding linear system, that one may call $CETA_0$ (coupled-electron *t*riple approximation, linear version). Starting from the CCDT stationarity condition (12-98) we have two possibilities

$$0=\left\{X^{\dagger}_{(3)}\left(H+[H_0,S_{(3)}]+[V,S_{(2)}]_{(3)}+[V,S_{(3)}]_{(3)}+\frac{1}{2}[[V,S_{(2)}],S_{(2)}]_{(3)}\right)\right\}_C \tag{12-162}$$

or

$$0=\left\{X^{\dagger}_{(3)}\left(H+[H_0,S_{(3)}]+[V,S_{(2)}]_{(3)}+[V,S_{(3)}]_{(3)}\right)\right\}_C \tag{12-163}$$

In both cases we have a linear system for $S_{(3)}$. In Section 12.9.3 we will get support for the second choice. The formal solution for this is

$$S_{(3)}=[V,S_{(2)}]_{(3)BH}+[V,S_{(3)}]_{(3)BH} \tag{12-164}$$

It requires an iterative solution, and is, therefore, more demanding than CCD[T]. It requires an N^8 step like full CCSDT. This is a challenge.

We also need to update $S_{(2)}$, because $S_{(3)}$ does not enter the energy expression directly. In the spirit of a linear theory we get this from

$$S_{(2)}=V_{BH}+[V,S_{(2)}]_{(2)BH}+[V,S_{(3)}]_{(2)BH} \tag{12-165}$$

As a linear theory, $CETA_0$ does not describe a genuine three-electron system correctly. Approximate versions of CCSDT or CCSDT, such as CCD[T] or CCSD(T) fail in this respect as well, but full CCSDT works. For a correct description of a 3-electron system the EPV contributions to the neglected terms are required to care for an energy shift. Let us look at the contributions of the Arponen functional of CCSDT that go beyond $CETA_0$.

$$F_{\Delta\mathrm{CCDT}}(T^\dagger) = \frac{1}{2}\{T^\dagger([[V,S],S]\}_C$$
$$= \frac{1}{2}\{T^\dagger_{(3)}([[V,S_{(2)}],S_{(2)}] + [[V,S_{(2)}],S_{(3)}] + [[V,S_{(3)}],S_{(2)}]$$
$$+[[V,S_{(3)}],S_{(3)}])\}_C + \frac{1}{2}\{T^\dagger_{(2)}([[V,S_{(2)}],S_{(3)}]$$
$$+[[V,S_{(3)}],S_{(2)}] + [[V,S_{(3)}],S_{(3)}])\}_C \qquad (12\text{-}166)$$

It looks as if the term

$$\{T^\dagger_{(3)}[[V,S_{(2)}],S_{(3)}]\}_C \qquad (12\text{-}167)$$

were a candidate for containing normalization corrections. Its EPV contributions could be factorized as

$$\sum\nolimits_{\mu\kappa}[VS_{(2)\mu}]_C[T^\dagger,S_{(2)\kappa}]_C = \sum\nolimits_{\mu\kappa}\varepsilon_\mu s^2_\kappa \qquad (12\text{-}168)$$

Where the sum over κ goes over all triples, and that over μ over all pairs belonging to a given triple.

Further work is needed in order to formulate a 3-particle generalization of CEPA. A possible candidate for this is the 3CC method of Bartlett and Musial [13] or some modification of it.

Another question arises at this point. Does one really want a hierarchy in terms of *coupled* k-tuples, i.e. CEPA, CETA etc. or CCD, CCSDT etc.? Would it not make more sense to care for a hierarchy in terms of *independent* k-tuples, like IEPA, IETA, etc. in the spirit of Nesbet [47]?

Going back to the old idea of summing classes of diagrams to infinite order, one arrives at IEPA by summing all diagrams (including those of EPV type) with two distinct hole labels i and j. If in a next step one takes all diagrams with three hole labels i,j,k, one describes independent 3-particle correlations, but at the same time couplings between semi-joint pairs like i,j and k,j. The couplings between disjoint pairs i,j and k,l are treated at the same level as genuine 4-particle correlations, and the couplings between semijoint correlation functions.

12.9. A CLOSED SHELL REFERENCE STATE IN UNITARY NORMALIZATION

12.9.1. Formulation of the Problem

We start from the same Hamiltonian (12-23) as in Section 12.2.5, but we subject it to a unitary transformation [36]

$$L = e^{-\sigma}He^{\sigma} = L_D; \sigma = \sigma_N; \sigma^\dagger = -\sigma; E = L_C \qquad (12\text{-}169)$$

Now a different definition of *diagonal* and *nondiagonal* than in Section 12.6 is needed (see Section 12.2.6). We call an operator diagonal (D) if it is either closed (C) or open (O), and non-diagonal (N) if it is either closed from below (B) or closed from above (A).

The expansion of the energy is

$$E = H_C + [H,\sigma]_C + \frac{1}{2}[[H,\sigma],\sigma]_C + \frac{1}{6}[[[H,\sigma],\sigma],\sigma]_C + \frac{1}{24}[[[[H,\sigma],\sigma],\sigma],\sigma]_C + ... \tag{12-170}$$

while the operator σ is obtained as solution of

$$0 = H_N + [H,\sigma]_N + \frac{1}{2}[[H,\sigma],\sigma]_N + \frac{1}{6}[[[H,\sigma],\sigma],\sigma]_N + \frac{1}{24}[[[[H,\sigma],\sigma],\sigma],\sigma]_N + ... \tag{12-171}$$

Unlike the counterparts (12-40) and (12-39) in intermediate normalization the expansions (12-170) and (12-171) *do not terminate*. Further the basis operators, into which σ is expanded, do not commute, but they constitute a Lie algebra. We shall see that the unitary coupled cluster theory (UCC) theory is superior to TCC, nevertheless.

12.9.2. Perturbation Expansion

For perturbation theory it does not matter that the Hausdorff expansion does not terminate. The various terms in the perturbation expansion terminate order by order. We expand

$$H = H_0 + \lambda V \tag{12-172}$$

$$\sigma = \lambda\sigma_1 + \lambda^2\sigma_2 + ... = \sigma_N \tag{12-173}$$

$$E = E_0 + \lambda E_1 + \lambda^2 E_2 + ... \tag{12-174}$$

The expansion of (12-171) is to the lowest order

$$0 = V_N + [H_0,\sigma_1] \tag{12-175}$$

$$0 = [V,\sigma_1]_N + [H_0,\sigma_2] + \frac{1}{2}[[H_0,\sigma_1],\sigma_1]_N = [V - \frac{1}{2}V_N,\sigma_1]_N + [H_0,\sigma_2] \tag{12-176}$$

$$0 = [V,\sigma_2]_N + \frac{1}{2}[[V,\sigma_1],\sigma_1]_N + [H_0,\sigma_3] + \frac{1}{2}[[H_0,\sigma_2],\sigma_1]_N + \frac{1}{2}[[H_0,\sigma_1],\sigma_2]_N + \frac{1}{6}[[[H_0,\sigma_1],\sigma_1],\sigma_1]_N$$

$$= [V - \frac{1}{2}V_N, \sigma_2]_N + \frac{1}{2}[[V - \frac{1}{3}V_N, \sigma_1], \sigma_1]_N - \frac{1}{2}[[V - \frac{1}{2}V_N, \sigma_1]_N, \sigma_1]_N + [H_0, \sigma_3] \quad (12\text{-}177)$$

We solve for the σ_k, making again use of the formal commutator inverse (12-14)

$$\sigma_1 = V_H \quad (12\text{-}178)$$

$$\sigma_2 = [V - \frac{1}{2}V_N, \sigma_1]_H \quad (12\text{-}179)$$

$$\sigma_3 = [V - \frac{1}{2}V_N, \sigma_2]_H + \frac{1}{2}[[V - \frac{1}{3}V_N, \sigma_1], \sigma_1]_H - \frac{1}{2}[[V - \frac{1}{2}V_N, \sigma_1]_N, \sigma_1]_H \quad (12\text{-}180)$$

We insert the stationarity conditions into the energy expressions and get, noting that the commutator of two operators has a closed (C) part only if both factors are non-diagonal (N)

$$E_1 = V_C \quad (12\text{-}181)$$

$$E_2 = \frac{1}{2}[V_N, \sigma_1]_C \quad (12\text{-}182)$$

$$E_3 = \frac{1}{2}[V_O, \sigma_1], \sigma_1]_C + \frac{1}{3}[V_N, \sigma_1], \sigma_1]_C \quad (12\text{-}183)$$

$$E_4 = \frac{1}{2}[V - \frac{1}{3}V_N, \sigma_2], \sigma_1]_C + \frac{1}{12}[V_N, \sigma_1], \sigma_2]_C + \frac{1}{6}[[[V - \frac{1}{4}V_N, \sigma_1], \sigma_1], \sigma_1]_C - \frac{1}{6}[[[V - \frac{1}{2}V_N, \sigma_1]_N, \sigma_1], \sigma_1]_C \quad (12\text{-}184)$$

These expressions are a little more lengthy than the counterparts in intermediate normalization. However, they are manifestly both connected (extensive) and variational, i.e. a Wigner ($2n$+1) rule holds. Knowing σ_1 and σ_2 we get the energy up to E_5. In intermediate normalization we had to choose between either manifest separability (via a Lie algebraic structure) or variational behavior but could not get both properties at the same time.

12.9.3. Linearized Unitary Coupled-Cluster Theory

Let us consider the simplest *non-trivial truncation* of the UCC expansion. For the sake of simplicity we assume that single excitations can be ignored. We decompose σ as

$$\sigma = T - T^\dagger; T = T_B \quad (12\text{-}185)$$

The first non-trivial choice is (a superscript in brackets indicates the order of the truncation of the Hausdorff expansion)

$$E^{[2]} = \{H + [H,\sigma] + \frac{1}{2}[[H,\sigma]\sigma]\}_C = \{H + 2\mathrm{Re}[H,T] + [T^\dagger,[H,T]]\}_C \quad (12\text{-}186)$$

The stationarity condition is

$$0 = \{[X^\dagger,H] + [X^\dagger,[H,T]]\}_C; X = X_B \quad (12\text{-}187)$$

If we expand

$$T = \sum_k c_k X_k \quad (12\text{-}188)$$

this is a linear system of equations for the construction of the coefficients c_k, and obviously a generalization of CEPA_0 to arbitrary particle rank. It implies

$$0 = \{[T^\dagger,H] + [T^\dagger,[H,T]]\}_C \quad (12\text{-}189)$$

$$E^{[2]} = H_C + \mathrm{Re}[H,T]_C = H_C + \mathrm{Re}\sum_k c_k [H,X_k]_C \quad (12\text{-}190)$$

We consider a hierarchy in the excitation rank of the operators T. We start with $T_{(2)}$ for UCCD, continue with $T_{(1)} + T_{(2)}$ for UCCSD etc. The formalism is simpler, if we ignore single excitations, what we shall henceforth do.

The stationarity condition for $\mathrm{UCCD}^{[2]}$ is

$$\begin{aligned} 0 = \{&[X^\dagger_{(2)},V] + [X^\dagger_{(2)},[H_0,T_{(2)}]] \\ &+[X^\dagger_{(2)},[V,T_{(2)}]]\}_C \end{aligned} \quad (12\text{-}191)$$

with the solution

$$T_{(2)} = V_{BH} + [V,T_{(2)}]_{BH}; E^{[2]} = H_C + \mathrm{Re}[H,T_{(2)}]_C \quad (12\text{-}192)$$

This is, of course, CEPA_0. The stationarity conditions for $\mathrm{UCCDT}^{[2]}$ are

$$\begin{aligned} 0 = \{&[X^\dagger_{(2)},V] + [X^\dagger_{(2)},[H_0,T_{(2)}]]. \\ &+[X^\dagger_{(2)},[V,T_{(2)}]] + [X^\dagger_{(2)},[V,T_{(3)}]]\}_C \end{aligned} \quad (12\text{-}193)$$

$$\begin{aligned} 0 = \{&[X^\dagger_{(3)},[H_0,T_{(3)}]] \\ &+[X^\dagger_{(3)},[V,T_{(2)}]] + [X^\dagger_{(3)},[V,T_{(3)}]]\}_C \end{aligned} \quad (12\text{-}194)$$

with the solution

$$T_{(2)} = V_{BH} + [V, T_{(2)}]_{(2)BH} + [V, T_{(3)}]_{(2)BH} \tag{12-195}$$

$$T_{(3)} = [V, T_{(2)}]_{(3)BH} + [V, T_{(3)}]_{(3)BH} \tag{12-196}$$

$$E^{[2]} = H_C + \mathrm{Re}[H, T_{(2)}]_C \tag{12-197}$$

The contribution of $T_{(3)}$ to the energy is

$$\mathrm{Re}[V, [V, T_{(3)}]_{(2)BH}]_C \tag{12-198}$$

We have so the linearized version of UCCDT.

12.9.4. EPV Contributions

Like in the study of TCC we can argue, that the dominant contributions to the terms with higher than double commutators are of EPV type, with repeated hole labels.

To simplify the situation we only consider those EPV diagrams that are necessary to describe isolated k-electron systems exactly. More general EPV diagrams can be added at a later stage, possibly in a perturbative way.

Let us first consider the UCCD ansatz, for which σ always means $\sigma_{(2)}$ and $T = T_{(2)}$.

We note that the term

$$[H, \sigma]_C = 2\sum_{\mu} \varepsilon_\mu = \sum_{\mu} [H, \sigma_\mu]_C = 2\mathrm{Re}[H, T_\mu]_C \tag{12-199}$$

is a sum of pair contributions $2\varepsilon_\mu$. The next term is a sum of pair interactions (including interactions within a pair) and a renormalization term

$$\{[[H, \sigma], \sigma]\}_C = \sum_{\mu,\nu} (T_\mu^\dagger H T_\nu)_C - H_C \sum_{\mu} (T_\mu^\dagger T_\mu)_C \tag{12-200}$$

In higher-order commutators we consider only EPV type renormalization terms. For triple commutators we follow essentially Section 12.8.4

$$\{[[[H, \sigma], \sigma], \sigma]\}_C \approx 2\sum_{\mu} \varepsilon_\mu (T_\mu^\dagger T_\mu)_C \tag{12-201}$$

Analogously we get for the quadruple commutator

$$\{[[[[H,\sigma],\sigma],\sigma],\sigma]\}_C \approx \sum_{\mu,\nu}(T_\mu^\dagger H T_\nu)_C \frac{1}{2}\{(T_\mu^\dagger T_\mu)_C + (T_\nu^\dagger T_\nu)_C\}$$

$$\approx \sum_{\mu,\nu}(T_\mu^\dagger H T_\nu)_C \sqrt{(T_\mu^\dagger T_\mu)_C (T_\nu^\dagger T_\nu)_C} = \sum_{\mu,\nu}(T_\mu^\dagger H T_\nu)_C s_\mu s_\nu \tag{12-202}$$

The replacement of the arithmetic mean by the geometric mean is justified, since contributions dominate in which $s_\mu \approx s_\nu$, including those with $\mu = \nu$.

12.9.5. Partial Summation of the Hausdorff Expansion to Infinite Order

Limiting higher-order commutators to the *diagonal* EPV terms, the Hausdorff expansion for UCC-D becomes

$$E = H_C + \sum_\mu(-t_\mu^2 + \frac{t_\mu^4}{3} + ...)H_C + \sum_\mu(1 - \frac{2t_\mu^2}{3} + \frac{2t_\mu^4}{15} + ...)(HT_\mu + T_\mu^\dagger H)_C$$
$$+ \sum_{\mu,\nu}(1 - \frac{t_\mu^2}{6} + \frac{t_\nu^2}{6} + \frac{t_\mu^4}{120} + \frac{t_\nu^4}{120} + \frac{t_\mu^2 t_\mu^2}{36} - ...)(T_\mu^\dagger H T_\nu)_C \tag{12-203}$$

$$t_\mu^2 = (T_\mu^\dagger T_\mu)_C \tag{12-204}$$

$$E = H_C - \sum_\mu \sin^2 t_\mu H_C + \sum_\mu \frac{\cos t_\mu \sin t_\mu}{t_\mu}(HT_\mu + T_\mu^\dagger H)_C$$
$$+ \sum_{\mu,\nu}\frac{\sin t_\mu \sin t_\nu}{t_\mu t_\nu}(T_\mu^\dagger H T_\nu)_C \tag{12-205}$$

Apparently a closed summation is possible. This summation has been known for a long time [36]. It has been derived for an isolated 2-electron system and it was not realized, how general it is, at least as a good approximation.

One can derive conditions for stationarity with respect to variation of the T_μ and insert this into the energy expression to get a stationary energy.

One may alternatively construct the T_μ from the $CEPA_0$ system and insert them into the sum (12-205). There is, however, a simpler and more accurate way. Let us define

$$S_\mu = T_\mu \frac{\tan t_\mu}{t_\mu};\ s_\mu^2 = (S_\mu^\dagger S_\mu)_C = \tan^2 t_\mu \tag{12-206}$$

then we get

$$
\begin{aligned}
& E \\
&= H_C - \sum_\mu \frac{s_\mu^2}{1+s_\mu^2} H_C + \sum_\mu \frac{1}{1+s_\mu^2}(HS_\mu + S_\mu^\dagger H)_C + \sum_{\mu,\nu} \frac{(S_\mu^\dagger H S_\nu)_C}{\sqrt{(1+s_\mu^2)(1+s_\nu^2)}} \\
&= \sum_\mu \frac{1}{1+s_\mu^2}([H,S_\mu] + [S_\mu^\dagger, H])_C + \sum_{\mu,\nu} \frac{([S_\mu^\dagger,[H,S_\nu]]}{\sqrt{(1+s_\mu^2)+(1+s_\nu^2)}} \qquad (12\text{-}207)
\end{aligned}
$$

This is essentially the coupled-pair functional of Ahlrichs et al. [39], at least the variant appropriate for $CEPA_2$, that was originally derived in a heuristic way, and that, at variance with the Arponen functional, to which it slightly resembles, defines a variational method. All pairs are normalized individually. The conditions for stationarity are not exactly the CEPA system, but they are close to it.

A generalization of this scheme to arbitrary particle rank will be given elsewhere [93].

12.10. CONCLUSIONS

This chapter contains a few take-home messages.

Coupled-cluster (CC) theory is, at the same time, both much simpler and more sophisticated than is often claimed. The main merit of the CC ansatz is that it is *separable* and correctly describes extensive properties, such as the energy of a molecule. In this respect CC is by far superior to truncated CI (configuration interaction), which is not separable. Separability is meaningful in a localized representation, and CC becomes most powerful in a localized context, which is also essential to achieve *linear scaling*.

The simplest form of coupled cluster theory is a linear pair theory, in which the zeroth oder pair functions are obtained from a linear system of equations, usually called $CEPA_0$. The next improvement over $CEPA_0$ is $CEPA_3$, where the non-EPV contributions to 4th order terms of CCD are neglected. This leads to an individual normalization of the various pair functions. All further corrections, by which CCD differs from $CEPA_0$, are numerically marginal. $CEPA_1$ and $CEPA_2$ apparently perform better than CCD, possibly because they simulate the effect of triples to some extent.

If one wants to use CC theory (we consider here only closed-shell states), one must distinguish three regimes. In the first of these one cares for modest accuracy, for which CEPA is a good choice. It hardly matters whether one uses $CEPA_1$, $CEPA_2$, or $CEPA_3$. Straight CCD or CCSD is just more complicated, but not more accurate. Users have just to wait until the CEPA option becomes a standard in the leading program packages. The ORCA program package offers this choice.

At the next level of sophistication one will want to take care of triple excitations, but one cannot afford full CCSDT. Although the standard solution to choose CCSD(T) does not appear to be the best possible choice, it is likely to survive for some time, until possibly CETA or IETA will take over.

Finally one may care for really high accuracy and want to push CC to its limit. Then one cannot but choose a scheme, where the error of the energy is quadratic in the error of the wave function. This means that one will have to abandon TCC in intermediate normalization and switch to UCC, even if previous studies on these lines did not lead to optimistic conclusions [10, 87]. This is a challenge for the more distant future.

Another message is that the formalism introduced long ago under the name *quantum chemistry in Fock space* is very powerful, both for the formulation of CC theory and MBPT. Its main potential, that it is a Fock space theory, and easily applicable to multiconfiguration reference states, has not been exploited here. This aspect had to be left out of the present chapter. We also did not have the space to discuss explicitly correlated CC theory, both the older one in terms of Gaussian geminals [23], and the more recent combination of CC theory with the R12-method [24].

ACKNOWLEDGMENTS

The author thanks R. Ahlrichs, K. Jankowski, B. Jeziorski, W. Liu, D. Mukherjee, F. Neese, J. Noga, and V. Staemmler, for valuable comments on this manuscript. He is particularly grateful to F. Neese for a starting cooperation on this topic.

REFERENCES

1. R. Maitra, D. Datta, D. Mukherjee, Chem. Phys. **356**, 54 (2009)
2. C. Hampel, H. J. Werner, J. Chem. Phys. **104**, 6286 (1996); P. J. Ayala, G. Scuseria, J. Chem. Phys. **111**, 830 (1999); R. A. Mata, H. J. Werner, M. Schütz, J. Chem. Phys. **128**, 144106 (2008)
3. R. Ahlrichs, W. Kutzelnigg, J. Chem. Phys. **48**, 1819 (1968); M. Jungen, R. Ahlrichs, Theor. Chim. Acta **17**, 339 (1970)
4. M. Gelus, R. Ahlrichs, V. Staemmler, W. Kutzelnigg, Chem. Phys. Lett. **7**, 503 (1970); W. Kutzelnigg, V. Staemmler, C. Hoheisel, Chem. Phys. **1**, 27 (1973); F. Driessler, R. Ahlrichs, V. Staemmler, W. Kutzelnigg, Theor. Chim. Acta **30**, 315 (1973); B. Zurawski, R. Ahlrichs, W. Kutzelnigg, Chem. Phys. Lett. **21**, 309 (1973); F. Keil, W. Kutzelnigg, J. Am. Chem. Soc. **97**, 3623 (1975); H. Lischka, Theor. Chim. Acta **31**, 39 (1973)
5. W. Meyer, Int. J. Quantum Chem. **5**, 341 (1971), J. Chem. Phys. **58**, 1017 (1973); W. Meyer, P. Rosmus, J. Chem. Phys. **63**, 2356 (1975)
6. R. Ahlrichs, H. Lischka, V. Staemmler, W. Kutzelnigg, J. Chem. Phys. **62**, 1225 (1975); R. Ahlrichs, F. Driessler, H. Lischka, V. Staemmler, W. Kutzelnigg, J. Chem. Phys. **62**, 1235 (1975); R. Ahlrichs, F. Keil, H. Lischka, W. Kutzelnigg, J. Chem. Phys. **63**, 455 (1975); R. Ahlrichs, H. Lischka, B. Zurawski, W. Kutzelnigg, J. Chem. Phys. **63**, 4685 (1975); B. Zurawski, W. Kutzelnigg, J. Am. Chem. Soc. **100**, 2654 (1978); H. Wallmeyer, W. Kutzelnigg, J. Am. Chem. Soc. **101**, 2804 (1979); V. Staemmler, R. Jaquet, Theor. Chim. Acta **59**, 48 (1981); R. Jaquet, V. Staemmler,

M. D. Smith, D. R. Flower, J. Phys. B **25**, 285 (1992), Chim. Acta **59**, 48 (1981); R. Fink, V. Staemmler, Theor. Chim. Acta **87**, 129 (1993)
7. W. Kutzelnigg, P. v. Herigonte, Adv. Quantum Chem. **36**, 185 (2000)
8. W. Kutzelnigg, Theor. Chim. Acta **80**, 349 (1991)
9. L. Adamowicz, W. D. Laidig, R. J. Bartlett, Int. J. Quantum Chem. Symp **18**, 245 (1984); E. A. Salter, G. W. Trucks, R. J. Bartlett, J. Chem. Phys. **90**, 1752 (1989)
10. P. G. Szalay, M. Nooijen, R. J. Bartlett, J. Chem. Phys. **103**, 281 (1995)
11. J. Olsen, O. Christiansen, H. Koch, P. Jørgensen, J. Chem. Phys. **105**, 5082 (1996); J. Olsen, P. Jørgensen, T. Helgaker, O. Christiansen, J. Chem. Phys. **112**, 9736 (2000)
12. K. Raghavachari, G. W. Trucks, J. A. Pople, M. Head-Gordon Chem. Phys. Letters **157**, 479 (1989)
13. R. J. Bartlett, M. Musial, J. Chem. Phys. **125**, 204105 (2006)
14. W. Kutzelnigg, Chem. Phys. Letters **83**, 156 (1981)
15. W. Kutzelnigg, J. Chem. Phys. **77**, 3081 (1982)
16. W. Kutzelnigg, S. Koch J. Chem. Phys. **79**, 4315 (1983)
17. W. Kutzelnigg, J. Chem. Phys. **80**, 822 (1984)
18. W. Kutzelnigg, J. Chem. Phys. **82**, 4166 (1985)
19. W. Kutzelnigg, 'Quantum Chemistry in Fock Space', in *Aspects of Many-Body Effects in Molecules and Extended Systems*, Lecture Notes in Chemistry, vol. 50, Ed. D. Mukherjee (Springer, Berlin, 1989)
20. W. Kutzelnigg, 'Theory of Electron Correlation', in *Explicitly Correlated Wave Functions in Chemistry and Physics*, Ed. J. Rychlewski (Kluwer, Dordrecht, 2003)
21. J. Arponen, Ann. Phys. NY **151**, 301 (1983), Phys. Rev. A **55**, 2686 (1997); R. F. Bishop, J. Arponen, E. Pajanne, in *Aspects of Many-Body Effects in Molecules and Extended Systems*, Lecture Notes in Chemistry, **50**, Ed. D. Mukherjee (Springer, Berlin, 1989)
22. W. Kutzelnigg, Int. J. Quantum Chem. **109**, 3858(2009)
23. B. Jeziorski, H. J. Monkhorst, K. Szalewicz, J. G. Zabolitzky, J. Chem. Phys. **81**, 368 (1984)
24. J. Noga, W. Kutzelnigg, J. Chem. Phys. **101**, 7738 (1994)
25. J. Paldus, B. Jeziorski, Theor. Chim. Acta **73**, 81 (1988)
26. W. Kutzelnigg and D. Mukherjee, J. Chem. Phys. **107**, 432 (1997)
27. G. C. Wick, Phys. Rev. **80**, 268 (1951)
28. L. Brillouin, Acualités Sci. Ind. 71 (1933), 159 (1934)
29. C. Møller, M. S. Plesset, Phys. Rev. **46**, 618 (1934)
30. B. Jeziorski, R. Moszynski, Int. J. Quantum Chem. **48**, 161 (1993)
31. H. Primas, in *Modern Quantum Chemistry*, vol. 2, Ed. O. Sinanoğlu (Academic Press, New York, 1965), p. 45
32. F. Coester, Nucl. Phys. **7**, 421 (1958); F. Coester, H. Kümmel, Nucl. Phys. **17**, 477 (1960); H. Kümmel, Nucl. Phys. **22**, 177 (1961)
33. J. Hubbard, Proc. R. Soc. Lond. A **240**, 539 (1957)
34. J. A. Pople, R. Krishnan, H. B. Schlegel, J. S. Binkley, Int. J. Quantum Chem. **14**, 545 (1978)
35. W. Kutzelnigg, Fortschr. Chem. Forsch. (Top. Curr. Chem.) **41**, 31, (1973)
36. W. Kutzelnigg, 'Pair Correlation Theories' in *Modern Theoretical Chemistry*, vol. III, Ed. H. F. Schaefer III (Plenum, New York, 1977)
37. R. Ahlrichs, Comput. Phys. Commun. **17**, 31 (1979)
38. H. P. Kelly, Phys. Rev. **131**, 684 (1963), **134**, 1450 (1964), **144**, 39; H. P. Kelly, A. H. Sessler, Phys. Rev. **132**, 2091 (1963)
39. R. Ahlrichs, P. Scharf, C. Ehrhardt, J. Chem. Phys. **82**, 890 (1985)
40. A. C. Hurley, J. E. Lennard-Jones, J. A. Pople, Proc. R. Soc. Lond. A **220**, 446 (1953)
41. W. Kutzelnigg, J. Chem. Phys. **40**, 3640 (1964)
42. A. J. Coleman, Rev. Mod. Phys. **35**, 668 (1963)

43. P. Cassam-Chenai, J. Chem. Phys. **124**, 104109 (2006)
44. D. M. Silver, K. Ruedenberg, E. L. Mehler, J. Chem. Phys. **52**, 1206 (1970)
45. O. Sinanoğlu, Proc. R. Soc. Lond. A **260**, 379 (1961)
46. O. Sinanoğlu, J. Chem. Phys. **36**, 706, 3198 (1962)
47. R. K. Nesbet, Proc. R. Soc. Lond. A **230**, 312 (1955)
48. R. K. Nesbet, Phys. Rev. **109**, 1632 (1958), Adv. Chem. Phys. **14**, 1 (1969); C. M. Moser, R. K. Nesbet, Phys. Rev. A **6**, 1710 (1972)
49. H. A. Bethe, J. Goldstone, Proc. R. Soc. Lond. A **238**, 551 (1957)
50. G. A. van der Velde, W. C. Nieuwpoort, Chem. Phys. Lett. **13**, 409 (1972)
51. H. Stoll, Chem. Phys. Lett. **191**, 548 (1992); J. Friedrich, M. Dolg, J. Chem. Theory Comput. **5**, 287 (2009); J. Friedrich, K. Walczak, M. Dolg, Chem. Phys. **356**, 47 (2009)
52. R. J. Bartlett, D. M. Silver, J. Chem. Phys. **62**, 3258 (1975); J. S. Binkley, J. A. Pople, Int. J. Quantum Chem. **9**, 229 (1975); J. A. Pople, R. Krishnan, H. B. Schlegel, J. S. Binkley, Int. J. Quantum Chem. Symp. **13**, 225 (1979)
53. W. Kutzelnigg, 'Localization and Correlation', in *Localization and Delocalization in Quantum Chemistry*, Eds. O. Chalvet et al. (Reidel, Dordrecht, 1975)
54. M. Przybytek, B. Jeziorski, K. Szalewicz, Int. J. Quantum Chem. **109**, 2872 (2009)
55. J. Paldus, in *Theory and Applications of Computational Chemistry. The First Forty Years*, Eds. C. E. Dykstra et al. (Elsevier, Amsterdam 2005)
56. J. Čížek, J. Chem. Phys. **45**, 4256 (1966), Adv. Chem. Phys. **14**, 35 (1969)
57. J. Paldus, J. Čížek, I. Shavitt, Phys. Rev. A **5**, 50 (1972)
58. R. J. Bartlett, G. D. Purvis, Int. J. Quantum Chem. **14**, 561 (1978); J. A. Pople, R. Krishnan, H. B. Schlegel, H. B. Binkley, Int. J. Quantum Chem. **14**, 545 (1978)
59. P. R. Taylor, G. B. Bacsay, N. S. Hush, A. C. Hurley, Chem. Phys. Lett. **41**, 444 (1976), J. Chem. Phys. **69**, 46 (1978)
60. R. J. Bartlett, J. Phys. Chem. **93**, 1697 (1989)
61. J. Paldus, J. Chem. Phys. **67**, 303 (1977); K. Jankowski, J. Paldus, Int. J. Quantum Chem. **18**, 1243 (1980), Phys. Rev. A **24**, 2316 (1981); B. G. Adams, K. Jankowski, J. Paldus, Phys. Rev. A **24**, 2330 (1981); J. Paldus, Phys. Rev. B **30**, 2193 (1984), J. Paldus, Phys. Rev. A **30**, 4267 (1984)
62. R. A. Chiles, C. E. Dykstra, Chem. Phys. Lett. **80**, 69 (1981); R. A. Chiles, C. E. Dykstra, J. Chem. Phys. **74**, 4544 (1981); S. M. Bachrach, R. A. Chiles, C. E. Dykstra, J. Chem. Phys. **75**, 2270 (1981)
63. S. Koch, W. Kutzelnigg, Theor. Chim. Acta **59**, 387 (1981)
64. P. Botschwina, M. Oswald, J. S. Flügge, R. Oswald, Chem. Phys. Lett. **209**, 117 (1993); P. Botschwina, M. Horn, J. S. Flügge, **67**, 303 (1977); S. Seeger, J. Chem. Soc. Faraday Trans. **89**, 2219 (1993)
65. F. Wennmohs,F. Neese, Chem. Phys. **343**, 217 (2008); F. Neese, F. Wennmohs, A. Hansen, J. Chem. Phys. **130**, 114108 (2009)
66. J. R. Gour, M. Horoi, P. Piecuch, B. A. Brown, Phys. Rev. Lett. **101**, 052501 (2008)
67. H. Kümmel, H. Lührmann, Nucl. Phys. A **191**, 525 (1972), **194**, 225 (1972); H. Kümmel, H. Lührmann, K. H. Zabolitzky, Phys. Rep. **36**, 1 (1978) Phys. Rev. A **55**, 2686 (1997); R. F. Bishop, J. Arponen, E. Pajanne, in *Aspects of Many-Body Effects in Molecules and Extended Systems*, Lecture Notes in Chemistry, vol. 50, Ed. D. Mukherjee (Springer, Berlin, 1989)
68. F. Harris, Int. J. Quantum Chem. Symp. **11**, 403 (1977)
69. T. Zivkovic, Int. J. Quantum Chem. Symp. **11**, 413 (1977)
70. H. Monkhorst,Int. J. Quantum Chem. Symp. **11**, 421 (1977)
71. W. Kutzelnigg, 'The Many-Body Perturbation Theory of Brueckner and Goldstone', in *Applied Many-Body Methods in Spectroscopy and Electronic Structure*, Ed. D. Mukherjee (Plenum, New York, 1992)
72. H. J. Monkhorst, B. Jeziorski, F. E. Harris, Phys. Rev. A **23**, 1639 (1981)

73. W. Kutzelnigg, in: *Recent Progress in Many-Body Theory*, Lecture notes in physics, vol. 198, Eds. H. Kümmel, M. L. Ristig (Springer, Berlin, 1984), p. 361
74. K. Szalewicz, B. Jeziorski, H. J. Monkhorst, J. G. Zabolitzky, J. Chem. Phys. **79**, 5543 (1983)
75. A. G. Taube, R. J. Bartlett, J. Chem. Phys. **130**, 144112 (2009)
76. J. Noga, S. A. Kucharski, R. J. Bartlett, J. Chem. Phys. **90**, 3399 (1989); Y. J. Bomble, J. F. Stanton, M. Kállay, J. Gauss, J. Chem. Phys. **123**, 054101 (2005); M. Kállay, J. Gauss, J. Chem. Phys. **123**, 214105 (2005); M. Kállay, J. Gauss, J. Chem. Phys. **129**, 144101 (2008)
77. W. Kutzelnigg, Theor. Chim. Acta **86**, 41 (1993)
78. M. Urban, J. Noga, S. J. Cole, R. J. Bartlett, J. Chem. Phys. **83**, 404 (1985); J. Noga, R. J. Bartlett, M. Urban, Chem. Phys. Lett. **134**, 128 (1987); J. Noga, R. J. Bartlett, J. Chem. Phys. **86**, 7041 (1987), J. Chem. Phys. **89**, 3401 (1988) Erratum
79. J. F. Stanton, Chem. Phys. Lett. **281**, 130 (1997)
80. R. J. Bartlett, M. Musial, Rev. Mod. Phys. **79**, 291 (2007)
81. H. Müller, R. Franke, St. Vogtner, R. Jaquet, W. Kutzelnigg, Theor. Chem. Acc. **100**, 85 (1998)
82. O. Christiansen, H. Koch, P. Jørgensen Chem. Phys. Lett. **243**, 409 (1995); H. Koch, O. Christiansen, P. Jørgensen, A. M. Sanches de Merás, T. Helgaker, J. Chem. Phys. **106**, 1808 (1997); S. A. Kucharski, R. J. Bartlett, J. Chem. Phys. **108**, 5243 (1998); K. Kowalski, P. Piecuch, J. Phys. Chem. A **113**, 18 (2000) P. Piecuch, M. Włoch, J. Chem. Phys. **123**, 224105 (2005); M. Włoch, J. R. Gour, P. Piecuch, J. Phys. Chem. A **111**, 11359 (2007)
83. M. Nooijen, Phys. Rev. Lett. **84**, 2108 (2000)
84. W. Kutzelnigg, D. Mukherjee, Phys. Rev. A **71**, 022502 (2005)
85. P. Piecuch, J. Mol. Struct. (THEOCHEM) **771**, 89 (2006)
86. R. J. Bartlett, J. Noga, Chem. Phys. Lett. **150**, 29 (1988)
87. T. van Voorhis, M. Head-Gordon J. Chem. Phys. **113**, 8873 (2000)
88. W. Kutzelnigg, Mol. Phys. **94**, 65 (1998)
89. R. J. Bartlett, J. D. Watts, S. A. Kucharski, J. Noga, Chem. Phys. Lett. **165**, 513 (1990); S. A. Kucharski, R. J. Bartlett,Chem. Phys. Lett. **237**, 264 (1995)
90. W. Kutzelnigg, St. Vogtner, Int. J. Quantum Chem. **60**, 235 (1996) W. Klopper, W. Kutzelnigg, H. Müller, J. Noga, St. Vogtner, Top. Curr. Chem. **203**, 21 (1999)
91. K. Patkowski, W. Cencek, M. Jeziorska, B. Jeziorski, K. Szalewicz, J. Phys. Chem. A **111**, 7611 (2007)
92. J. L. Heully, J.-P. Malrieu, J. Mol. Struct. (THEOCHEM) **768**, 53 (2006)
93. W. Kutzelnigg, to be published

CHAPTER 13

COUPLED CLUSTERS AND QUANTUM ELECTRODYNAMICS

INGVAR LINDGREN[1], STEN SALOMONSON[2], AND DANIEL HEDENDAHL[3]

[1]*Department of Physics, University of Gothenburg, Sweden, e-mail: ingvar.lindgren@physics.gu.se*
[2]*Department of Physics, University of Gothenburg, Sweden, e-mail: sten.salomonson@physics.gu.se*
[3]*Department of Physics, University of Gothenburg, Sweden, e-mail: daniel.hedendahl@physics.gu.se*

Abstract: We start by reviewing, as a background, the standard non-relativistic and relativistic many-body perturbative and coupled-cluster approaches in the way we have implemented them. The covariant-evolution-operator method that we introduced more recently for quantum-electrodynamical (QED) calculations is then described, and it is demonstrated how this method can be extended to combine electron-correlation and QED effects in a covariant manner. This can be included in a many-body calculation of coupled-cluster type, and it is demonstrated that this leads for two-particle systems eventually to the full Bethe–Salpeter equation. It is indicated how this procedure can also be applied to systems with more than two electrons. Preliminary numerical results are given for the ground state of some heliumlike ions.

Keywords: Relativistic coupled cluster, Quantum electrodynamics

13.1. INTRODUCTION

The Coupled-Cluster procedure has for about half a century proved itself to be an extremely efficient way of handling the correlation problem of electronic and nuclear systems. In the last couple of decades there has been an increased interest also in quantum-electrodynamical (QED) problems, particularly in connection with experiments on highly-charged ions. Also here – for systems with more than one electron – the electron correlation problem plays an important role [1]. We shall demonstrate here that the coupled-cluster approach is also in such cases a very good base.

The standard approach to include QED effects into many-body calculations is to add to the final non-QED energy the first-order QED effects [2], taken from analytical calculations [3]. To go beyond that approximation requires a more sophisticated approach, where the QED effects are included directly into the wave function, leading to a more *covariant procedure*. We have developed and applied a *covariant-evolution-operator* (CEO) technique for QED calculations [4], which has been found

P. Čársky et al. (eds.), Recent Progress in Coupled Cluster Methods, 357–374.
DOI 10.1007/978-90-481-2885-3_13,

to be suitable as a basis also for such a more advanced procedure, where QED and electron-correlation effects are combined in a more systematic fashion.

In the present chapter we shall first present the many-body and coupled-cluster procedures in the way we implemented them some time ago, and then demonstrate how this can be further developed in order to include QED effects in a covariant way.

13.2. TIME-INDEPENDENT PERTURBATION PROCEDURE

13.2.1. Linked-Diagram Expansion

The first steps towards a many-body perturbation theory (MBPT) were taken by Brueckner and Goldstone in developing the *linked-diagram or linked-cluster expansion* [5, 6]. They demonstrated that – for a degenerate model space – the non-linear terms of the Rayleigh–Schrödinger expansion must cancel, leaving only so-called *linked* terms, which can be expressed by means of the *Bloch equation* [7] as

$$\left(E_0 - H_0\right)\Omega P = \left(V\Omega - \Omega V_{\text{eff}}\right)_{\text{linked}} P \tag{13-1}$$

(A term or diagram is said to be "linked", if it does not contain any disconnected part that is closed, i.e., operating entirely within the *model space*, where the model states are located.) Here, the Hamiltonian of the system is partitioned into a model Hamiltonian and a perturbation

$$H = H_0 + V \tag{13-2}$$

and

$$V_{\text{eff}} = PV\Omega P \tag{13-3}$$

is the *effective interaction* (in intermediate normalization) and P is the projection operator for the model space. The perturbation expansion starts from an unperturbed (model) state, eigenstate of H_0 with the eigenvalue E_0 that might be *degenerate*,

$$H_0\Psi_0 = E_0\Psi_0 \tag{13-4}$$

The procedure can be generalized to the treatment of several target states simultaneously with model states that do not need to be degenerate – so-called *quasi-degeneracy*

$$H\Psi^\alpha = E^\alpha\Psi^\alpha \quad (\alpha = 1, 2, \cdots d) \tag{13-5}$$

A *wave operator* can be defined that transforms all degenerate model states to the corresponding full (target) states

$$\Omega\,\Psi_0^\alpha = \Psi^\alpha \quad (\alpha = 1, 2, \cdots d) \tag{13-6}$$

The model states are eigenvectors of an *effective Hamiltonian*, and the corresponding eigenvalues are the exact energies of the target states,

$$H_{\text{eff}}\Psi_0^\alpha = E^\alpha \Psi_0^\alpha \quad (\alpha = 1, 2, \cdots d) \tag{13-7}$$

In intermediate normalization the effective Hamiltonian becomes

$$H_{\text{eff}} = PH\Omega P = PH_0P + V_{\text{eff}} \tag{13-8}$$

It was demonstrated by Brandow [8] – by using a double perturbation expansion – that the linked-diagram theorem of Brueckner and Goldstone could be extended to the case of quasi-degeneracy by introducing so-called *folded diagrams*. This was somewhat later demonstrated by Lindgren [9] in a more direct way by means of a generalization of the original Bloch equation

$$\boxed{\big[\Omega, H_0\big]P = \big(V\Omega - \Omega V_{\text{eff}}\big)_{\text{linked}}P} \tag{13-9}$$

In lowest orders this leads to ($Q = 1 - P$)

$$\begin{cases} \big[\Omega^{(1)}, H_0\big]P = VP - PVP = QVP \\ \big[\Omega^{(2)}, H_0\big]P = Q\big(V\Omega^{(1)} - \Omega^{(1)}V_{\text{eff}}^{(1)}\big)_{\text{linked}}P \end{cases} \tag{13-10}$$

The second-order equation is illustrated in Figure 13-1. The single-electron orbitals are here generated in the potential of the nucleus (or some other external potential) – known as the *Furry picture*. The last diagram is the *folded diagram* that represents the contribution due to an intermediate state in the model space, *model-space contribution* (MSC). Such a state leads to a *(quasi)singularity* that is automatically eliminated by the Bloch equation. We shall see that this kind of singularity plays an important role also in the formalism we shall describe later.

The formalism above is based upon the *intermediate normalization*, implying that the overlap between the target and model functions is normalized, $\langle\Psi_0^\alpha|\Psi^\alpha\rangle = 1$. Then a condition for the linked-diagram theorem to hold is that the model space

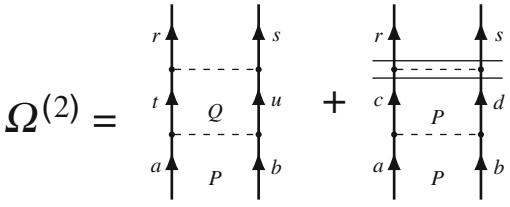

Figure 13-1. Diagrammatic representation of the second-order equation (13-10). The heavy *vertical lines* represent electron orbitals and propagators in the *Furry picture*. The last diagram is the "folded" diagram, which has a double denominator, associated with the last interaction (represented by a double bar)

is *complete*, i.e., contains all configurations that can be formed by distributing the valence electrons among the valence orbitals in all possible ways.

13.2.2. All-Order and Coupled-Cluster Approaches

By means of second quantization the wave operator can be separated into one-, two-, ... body effects

$$\Omega = 1 + \Omega_1 + \Omega_2 + \cdots \tag{13-11}$$

This leads to the corresponding partitioning of the Bloch equation

$$\big[\Omega_n, H_0\big]P = \big(V\Omega - \Omega V_{\text{eff}}\big)_{\text{linked},n}P \tag{13-12}$$

and solving a number of these coupled sub-equations iteratively, yields the corresponding effects essentially to all orders. This is known as the *all-order perturbation approach*, which is frequently employed.

The simplest approach is to include only double excitations (pair correlation), $\Omega \approx 1 + \Omega_2$, leading to the *pair equation*

$$\big[\Omega_2, H_0\big]P = Q\big(V(1 + \Omega_2) - \Omega_2 V_{\text{eff}}\big)_{\text{linked},2}P \tag{13-13}$$

illustrated in Figure 13-2. The expansion of this equation, when there are no core states, is indicated in Figure 13-3, and we can generally express this function as

$$|\rho_{ab}\rangle = \Gamma_Q(\mathcal{E})I^{\text{Pair}}|ab\rangle \tag{13-14}$$

where $\mathcal{E}$ is the unperturbed energy of the state $|ab\rangle$ and

$$\Gamma(\mathcal{E}) = \frac{1}{\mathcal{E} - H_0}; \qquad \Gamma_Q(\mathcal{E}) = \frac{Q}{\mathcal{E} - H_0} \tag{13-15}$$

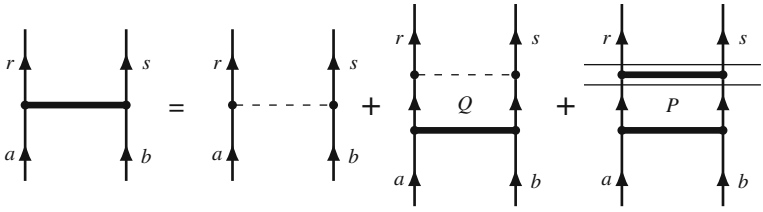

Figure 13-2. Graphical representation of the self-consistent pair equation (13-13) with the "folded" diagram (*last*)

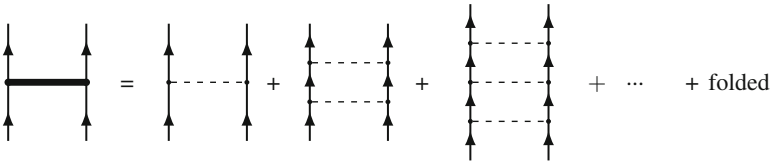

Figure 13-3. Expansion of the pair function in Figure 13-2

are the *resolvent* and *reduced resolvent*, respectively, and I^{Pair} represents the series of Coulomb interactions (with folds). The effective interaction, V_{eff}, becomes with this notation

$$V_{\text{eff}} = PI^{\text{Pair}}P \tag{13-16}$$

An even more effective way of treating electron correlation is the *coupled-cluster approach* or *exponential Ansatz*, developed for closed-shell systems in nuclear physics by Coster and Kümmel [10, 11] and introduced into quantum chemistry by Čížek [12]. Here, the wave operator is expressed as an exponential

$$\Omega = \exp(T) = 1 + T + \frac{1}{2}T^2 + \cdots \tag{13-17}$$

By separating the *cluster operator* into one-, two-, ... body parts

$$T = T_1 + T_2 + \cdots \tag{13-18}$$

the wave operator can be expanded as

$$\Omega = 1 + T_1 + T_2 + \cdots + \frac{1}{2}T_1^2 + T_1T_2 + \frac{1}{2}T_2^2 + \cdots \tag{13-19}$$

The last term indicated above represents normally the most important correlation effect, next to the pair correlation T_2. This effect is included in the simplest CCA approximation, the pair-correlation approach CCD with $T = T_2$. An effective and frequently used approximation is the CCSD with singles and doubles, $T = T_1 + T_2$.

For open-shell systems it is often convenient to express the wave operator in *normal-ordered exponential form* [13, 14]

$$\Omega = \{\exp(T)\} \tag{13-20}$$

which eliminates unwanted contractions between the clusters. It can be shown that for a complete model space this operator is completely *connected*, which can be expressed by means of the generalized Bloch theorem (13-9) as [13]

$$\left[T_n, H_0\right]P = \left(V\Omega - \Omega V_{\text{eff}}\right)_{\text{conn},n}P \tag{13-21}$$

(It should be noted that a "linked" diagram can be disconnected if all parts are "open", acting outside the model space.) Mukherjee has shown that the theorem also holds for an incomplete model space, if the intermediate–normalization condition is abandoned [15, 16].

In the CCSD approximation

$$T = T_1 + T_2 \tag{13-22}$$

the cluster operators satisfy the coupled equations

$$\begin{aligned} \left[T_1, H_0\right]P &= \left(V\Omega - \Omega V_{\text{eff}}\right)_{\text{conn},\,1}P \\ \left[T_2, H_0\right]P &= \left(V\Omega - \Omega V_{\text{eff}}\right)_{\text{conn},\,2}P \end{aligned} \tag{13-23}$$

illustrated in analogy with Figure 13-2 in Figure 13-4. These equations lead to one- and two-particle equations, analogous to the pair equation given above (13-13). Also these equations have to be solved *iteratively*, and we observe that they are *coupled*, as are the corresponding equations (13-10) for the full wave operator.

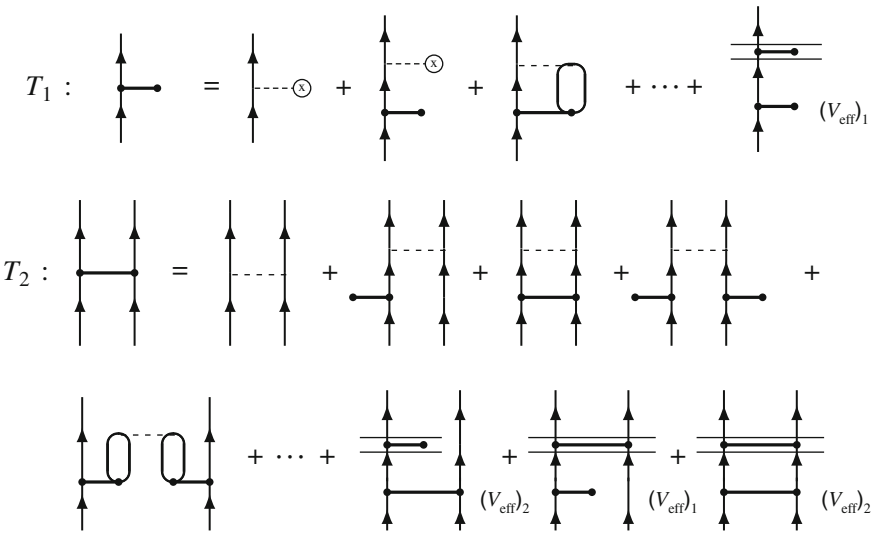

Figure 13-4. Diagrammatic representation of the equations for the cluster operators T_1 and T_2 Eq. (13-23). The *circle* with a cross represents the "effective potential" [17], which vanishes when Hartree–Fock orbitals are used. The last diagram in the second row and the first diagram in the third row are examples of coupled-cluster diagrams. The last diagram in the first row and the last three diagrams in the last row represent folded terms (c.f. Figure 13-2)

13.2.3. Versions of MBPT/CCA

What is indicated here is a *multi-reference* approach, in which a multiple of states are treated simultaneously. This is particularly advantageous in calculating transition energies. The *valence universal* version, valid also for different stages of ionization, is particularly useful in evaluating ionization energies or electron affinities. A serious disadvantage with the multi-reference approach is that it often leads to so-called *intruder states*, i.e., states that do not belong to the group of target states under study but penetrate into the energy range of target states of the same symmetry when the perturbation is turned on. When this happens, the perturbation expansion no longer converges.

For simple atomic systems that we are mainly interested in, the intruder problem is usually not a serious one, and we therefore prefer the multi-reference approach. The situation is different for molecular systems, due to more dense energy levels. Therefore, single-reference approaches are becoming more popular for such systems, as described in other chapters of this book.

13.2.4. Standard Relativistic MBPT: Definition of QED Effects

In the present chapter our main focus is relativity and QED problems, and the starting point is here the standard relativistic MBPT procedures, based upon the *projected Dirac-Coulomb-Breit approximation* [18][1]

$$H = \Lambda_+\Big[\sum_{i=1}^{N} h_D(i) + \sum_{i<j}^{N} \frac{e^2}{4\pi r_{ij}} + H_B\Big]\Lambda_+ \tag{13-24}$$

h_D is here the single-electron Dirac Hamiltonian and H_B is the *instantaneous Breit interaction*

$$H_B = -\frac{e^2}{8\pi}\sum_{i<j}\Big[\frac{\alpha_i\cdot\alpha_j}{r_{ij}} + \frac{(\alpha_i\cdot r_{ij})(\alpha_j\cdot r_{ij})}{r_{ij}^3}\Big] \tag{13-25}$$

Λ_+ is a projection operator that eliminates the negative-energy solutions of the Dirac equation. This approximation is also known as the *No-Virtual-Pair Approximation* (NVPA).

Effects beyond the NVPA are conventionally referred to as *QED effects*, and the lowest-order diagrams are depicted in Figure 13-5. The first row represents so-called *non-radiative effects*, or Araki-Sucher effects [19, 20], and the second row *radiative effects* (self energy, vacuum polarization and vertex correction).

---

[1] Using natural or relativistic units: $c = \hbar = m_e = \epsilon_0 = 1$, $e^2 = 4\pi\alpha$, α being the fine-structure constant.

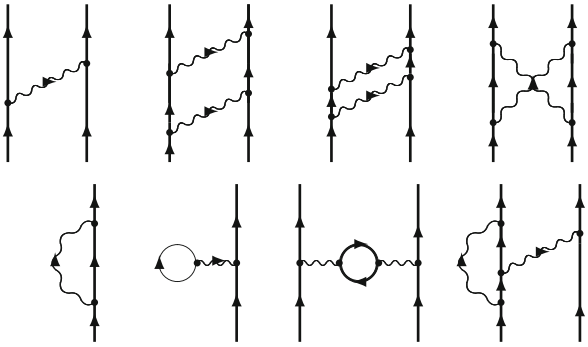

Figure 13-5. Some low-order non-radiative (*upper line*) and radiative (*lower line*) "QED effects". These diagrams are *Feynman diagrams*, and the *heavy lines* represent particle as well as hole or anti-particle states in the *Furry picture*. The *wavy lines* represent the covariant photon exchange. The second diagram is, when the intermediate states are *particle* states, *reducible*, since it can be separated into two single-photon-exchange diagrams, while all the remaining diagrams are *irreducible*

13.2.5. Implementation

In this subsection we shall briefly indicate the development and applications of the many-body theory of the Göteborg group. The development started in the early 1970s by Ingvar Lindgren and John Morrison and is summarized in their book *Atomic Many-Body Theory* [17]. The calculations were first based on first-order single-particle and pair programs, introduced into the group by Morrison [21, 22]. This was then developed into numerical all-order programs in the late 1970s by Sten Garpman, Lindgren and Ann-Marie Mårtensson-Pendrill [23–25]. This technique was later converted into a coupled-cluster program with doubles (CCD) by Sten Salomonson [26] and applied to various atomic systems. It was also applied to open-shell systems [27, 28] – in the application to the beryllium atom the above-mentioned "intruder problem" was probably observed for the first time in an atomic system. The procedure was extended to the full CCSD procedure and applied by Lindgren [29] (see Table 13-1) and Salomonson et al. [31, 39] (see Tables 13-2 and 13-3).

A relativistic version of the linear all-order pair program (LD) was developed by Eva Lindroth [32], and applied to the helium atom. A new numerical, highly accurate technique, referred to as the *discretization technique*, was developed by Salomonson and Per Öster [33] and applied to full atomic coupled-cluster calculations, relativistically as well as non-relativistically [30, 31]. This technique has been the basis for all later works of our group.

In Tables 13-1, 13-2 and 13-3 we have compared some of our coupled-cluster calculations for lithium, sodium, beryllium and Li^- with results from other groups. The calculations on Be and Li^- demonstrates clearly the importance of single excitations for such systems. The results for sodium show the importance of triple excitations in this case. (The results by Safronova et al. are probably fortuitous, indicating that effects of non-linear coupled-cluster terms and triples accidentally cancel.)

Table 13-1. Binding energies of the two lowest states of the lithium atom (in μH)

Lithium atom			
	$2\,^2S$	$2\,^2P$	References
Expt'l	198, 159	130, 246	
Hartree–Fock	196, 304	128, 637	
Difference	1, 854	1, 609	
LSD	1, 855	1, 582	Blundell et al. [34]
CCSD	1, 850	1, 584	Lindgren [29]
CCSD	1, 835	1, 534	Eliav et al. [35]

Table 13-2. Correlation energy of some low-lying states of the sodium atom (in μH) (from Ref. [36])

Sodium atom					
	$3\,^2S$	$3\,^2P_{1/2}$	$3\,^2P_{3/2}$	$4\,^2S$	References
Expt'l	6, 825	2, 121	2, 110	1, 415	
LSD	6, 835	2, 118	2, 108	1, 418	Safronova et al. [36]
CCSD	6, 458				Salomonson–Ynnerman [31]
CCSD	6, 385				Eliav et al. [35]
CCSD(T)	6, 840				Salomonson–Ynnerman [31]

Table 13-3. Correlation energy of the ground state of the beryllium atom and the negative lithium ion (in μH) (from Ref. [37])

Beryllium atom and negative lithium ion			
	Be	Li^-	References
CCD	92.960	71.148	Bukowski et al. [37]
CCD	92.961	71.266	Salomonson–Öster [30]
CCSD	93.665	72.015	Bukowski et al. [37]
CCSD	93.667	72.142	Salomonson–Öster [30]

13.3. COVARIANT EVOLUTION OPERATOR

We shall now go over into the later developments in our group towards a covariant many-body procedure. This will be described in more detail in a separate publication [38].

13.3.1. Single-Photon Exchange

In the *interaction picture* (IP) the state vectors and operators are related to those in the Schrödinger picture (SP) by

$$|\chi_{\mathrm{I}}(t)\rangle = \mathrm{e}^{\mathrm{i}H_0 t}\,|\chi_{\mathrm{S}}(t)\rangle; \qquad V_{\mathrm{I}}(t) = \mathrm{e}^{\mathrm{i}H_0 t}\,V\,\mathrm{e}^{-\mathrm{i}H_0 t} \tag{13-26}$$

It then follows that the Schrödinger equation becomes in IP

$$\mathrm{i}\frac{\partial}{\partial t}|\chi_{\mathrm{I}}(t)\rangle = V_{\mathrm{I}}(t)\,|\chi_{\mathrm{I}}(t)\rangle \tag{13-27}$$

The *time-evolution operator* in IP, $U(t, t_0)$, is defined by[2]

$$|\chi(t)\rangle = U(t, t_0)\,|\chi(t_0)\rangle \qquad (t > t_0) \tag{13-28}$$

and it satisfies the differential equation

$$\mathrm{i}\frac{\partial}{\partial t}U(t, t_0) = V(t)\,U(t, t_0) \tag{13-29}$$

This leads to the expansion [39]

$$U_\gamma(t, t_0) = \sum_{n=0}^{\infty} \frac{(-\mathrm{i})^n}{n!} \int_{t_0}^{t} \mathrm{d}t_1 \ldots \int_{t_0}^{t} \mathrm{d}t_n\, T\big[V(t_1)\ldots V(t_n)\big]\,\mathrm{e}^{-\gamma(|t_1|+|t_2|\ldots+|t_n|)} \tag{13-30}$$

where T is the *time-ordering operator* and γ is an *adiabatic damping factor*.

The perturbation is represented by the interaction between an electron and the radiation fields

$$V(t) = \int \mathrm{d}^3x\,\mathcal{H}(t, x) \tag{13-31}$$

with

$$\mathcal{H}(x) = -e\hat{\psi}^\dagger(x)\alpha^\mu A_\mu(x)\hat{\psi}(x) \tag{13-32}$$

where $x = (t, x)$ is the four-dimensional space-time coordinate and $\hat{\psi}(x)$, $\hat{\psi}^\dagger(x)$ and A_μ are the electron-field and the photon-field operators, respectively. The expansion (13-30) then becomes

$$U(t, t_0) = \sum_{n=0}^{\infty} \frac{(-\mathrm{i})^n}{n!} \int_{t_0}^{t} \mathrm{d}^4x_1 \ldots \int_{t_0}^{t} \mathrm{d}^4x_n\, T\big[\mathcal{H}(x_1)\ldots\mathcal{H}(x_n)\big]\,\mathrm{e}^{-\gamma(|t_1|+|t_2|\ldots+|t_n|)} \tag{13-33}$$

---

[2] In the following we shall work mainly in the interaction picture and leave out the subscript "I"

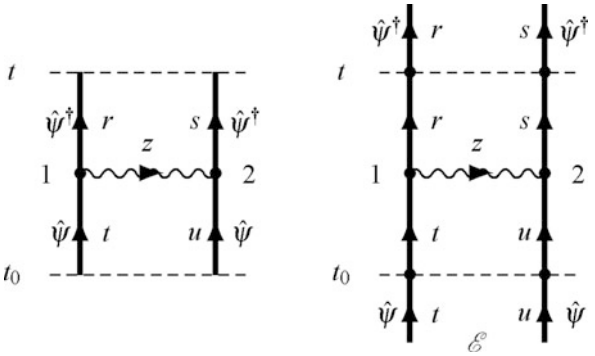

Figure 13-6. Comparison between the standard and the covariant evolution operator for single-photon exchange. In the latter there are electron propagators on the in- and outgoing lines, implying that they can represent particle *or* hole with time running both ways

where the integrations are performed over all space and over time as indicated. The perturbation operates here in the *extended photonic Fock space*, where the number of photons is no longer constant. The exchange of a single (virtual) photon is represented by TWO perturbations of this kind.

The evolution operator (13-28) is *non-covariant*, since time evolves only in the *positive* direction ($t > t_0$). In relativistic applications we must allow time to run also *backwards* in the negative direction, which represents the propagation of *hole or antiparticle states* with negative energy. This leads to the *covariant evolution operator* (CEO), introduced by Lindgren, Salomonson and coworkers [4]. In Figure 13-6 we compare the standard and the covariant evolution operators for the single-photon exchange between the electrons.

The single-photon CEO is in the adiabatic limit $\gamma \to 0$

$$U_{\rm sp}(t,t_0) = \mathrm{e}^{-\mathrm{i}t(\mathcal{E}-H_0)}\,\mathrm{i}\,\Gamma(\mathcal{E})\,V_{\rm sp}(\mathcal{E})\Gamma(\mathcal{E})\,\mathrm{e}^{-\mathrm{i}t_0(\mathcal{E}-H_0)} \tag{13-34}$$

where $V_{\rm sp}$ is the single-photon potential, and $\mathcal{E}$ is the energy of the initial unperturbed state. The energy-dependent potential becomes [4, 38]

$$\langle rs|V_{\rm sp}(\mathcal{E})|tu\rangle = \langle rs|\int_0^\infty \mathrm{d}k f(k) \times\Big[\frac{1}{\mathcal{E}-\varepsilon_r-\varepsilon_u-k}+\frac{1}{\mathcal{E}-\varepsilon_s-\varepsilon_t-k}\Big]|tu\rangle \tag{13-35}$$

when all states are *particle states*. Here, ε_x represent the orbital energies, and $f(k)$ is a gauge-dependent function of the photon momentum.

The diagram of the covariant evolution operator in Figure 13-6 is a *Feynman diagram*, involving all possible time orderings of the vertices. In the general case this corresponds to 16 combinations of particles and holes. A potential has been

constructed also for this general case, although this obviously becomes more complicated than that given above and will not be reproduced here [38].

13.3.2. Connection to MBPT

The covariant evolution operator contains *singularities* in higher orders, when there is an intermediate state in the model space (c.f. Figure 13-2). Eliminating these singularities leads to what we have referred to as the *reduced covariant evolution operator* [4] or the *Green's operator* [40], since this object is quite analogous to the *Green's function*.

We separate the Green's operator, $\mathcal{G}(t, t_0)$, into

$$\mathcal{G}(t, t_0) = 1 + \mathcal{G}_{\rm op}(t, t_0) + \mathcal{G}_{\rm cl}(t, t_0) \tag{13-36}$$

where the subscripts "op" and "cl" refer to the *open* and *closed* parts, respectively. The open part is closely related to the wave operator of standard MBPT (13-6)

$$\boxed{\Omega_{\rm Cov} = 1 + \mathcal{G}_{\rm op}(0, -\infty)} \tag{13-37}$$

and the closed part to the effective interaction (13-3)

$$\boxed{V_{\rm eff}^{\rm Cov} = P\Big(\mathrm{i}\frac{\partial}{\partial t}\,\mathcal{G}_{\rm cl}(t, -\infty)\Big)_{t=0} P} \tag{13-38}$$

The covariant wave operator satisfies a "Bloch-like" equation, and in lowest orders we have in analogy with the corresponding equation in standard MBPT (13-10)[3]

$$\begin{cases} \Omega^{(1)} P_{\mathcal{E}} = \Gamma_Q(\mathcal{E}) V(\mathcal{E}) P_{\mathcal{E}} \\ \Omega^{(2)} P_{\mathcal{E}} = \Gamma_Q(\mathcal{E}) \Big[V(\mathcal{E}) \Omega^{(1)} - \Omega^{(1)} V_{\rm eff}^{(1)} + \frac{\delta V(\mathcal{E})}{\delta \mathcal{E}}\, V_{\rm eff}^{(1)} \Big]_{\rm linked} P_{\mathcal{E}} \end{cases} \tag{13-39}$$

where $P_{\mathcal{E}}$ is the projection operator of the part of the model space with energy $\mathcal{E}$ we operate on. The second term on the rhs of the second-order equation is identical to the folded term of MBPT, and the last term is an additional contribution from the intermediate model-space state due to the energy dependence of the potential. This equation can also be expressed

$$\Omega_{\rm Cov}^{(2)} P_{\mathcal{E}} = \left[\Gamma_Q(\mathcal{E})\, V(\mathcal{E})\, \Omega^{(1)} + \frac{\delta \Omega^{(1)}}{\delta \mathcal{E}}\, V_{\rm eff}^{(1)} \right]_{\rm linked} P_{\mathcal{E}} \tag{13-40}$$

[3] In the following we leave out the subscript "Cov".

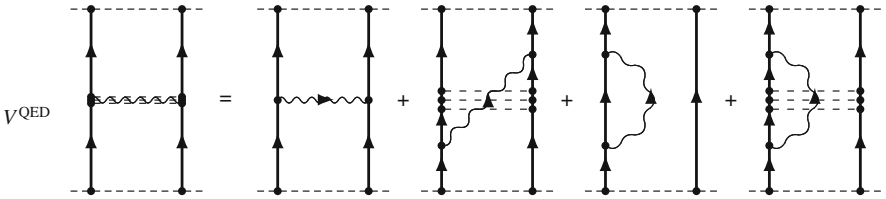

Figure 13-7. Feynman diagram representing the "QED potential", containing also radiative QED effects

13.3.3. QED Potential

In addition to the general potential of the exchange of a single retarded photon, we have also constructed (although not yet fully implemented) potentials for the photon with crossed Coulomb interactions as well as of electron self energy and vertex correction, illustrated in Figure 13-7. This potential contains the most important QED corrections (which, of course, have to be properly renormalized). Below we shall indicate how this potential can be incorporated into MBPT calculations.

13.4. COUPLED-CLUSTER-QED APPROACH

The QED potential, shown in Figure 13-7, can be combined with the non-QED many-body procedure, described above. A single QED potential, combined with the pair function in Figure 13-2, leads to the evolution operator

$$U_{\mathrm{QED}}(t)|ab\rangle = \frac{\mathrm{e}^{-\mathrm{i}t(\mathcal{E}-H_0)}}{\mathcal{E}-H_0}\, V^{\mathrm{QED}}(\mathcal{E})\Gamma_Q(\mathcal{E})\, I^{\mathrm{Pair}}|ab\rangle \tag{13-41}$$

where I^{Pair} represents the iterated Coulomb interactions (Eq. 13-14). Removing the singularities, due to intermediate model-space states, leads to the corresponding wave operator [38]

$$\Omega|ab\rangle = \left[\Gamma_Q(\mathcal{E})V^{\mathrm{QED}}\Gamma_Q(\mathcal{E})\, I^{\mathrm{Pair}} + \frac{\delta^*\Omega}{\delta\mathcal{E}}\, V_{\mathrm{eff}}\right]|ab\rangle \tag{13-42}$$

illustrated in Figure 13-8. This is a generalization of the second-order result (13-40). In the last folded term we have introduced the symbol δ^*, implying that *only the last interaction, including the associated resolvent, is differentiated*,

$$\frac{\delta^*\big(\Gamma(\mathcal{E})V_1(\mathcal{E})\Gamma(\mathcal{E})V_2(\mathcal{E})\cdots\big)}{\delta\mathcal{E}} = \frac{\delta\big(\Gamma(\mathcal{E})V_1(\mathcal{E})\big)}{\delta\mathcal{E}}\,\Gamma(\mathcal{E})V_2(\mathcal{E})\cdots \tag{13-43}$$

V_{eff} above is the corresponding effective interaction (13-38).

We can also insert the QED potential in the CC equations (13-23) and at the same time insert the single-electron QED interactions (vacuum polarization and electron

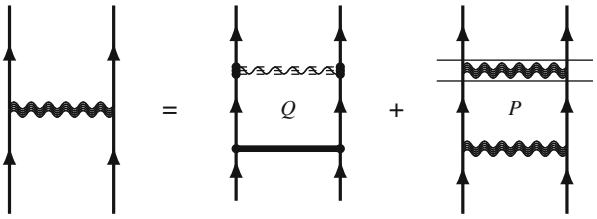

Figure 13-8. Combining the QED potential in Figure 13-7 with standard pair-function input (*heavy line*), yields to the *QED pair function* after removing the singularity (last folded diagram) (see Eq. 13-42)

self energy) into the single-particle equation. This corresponds to the replacements illustrated in Figure 13-9. By continuing this procedure and including more and more *irreducible* interactions (see Figure 13-5), this will eventually lead to the solution of the two-particle *Bethe–Salpeter equation* [41, 42]. (Then, of course, the Coulomb interactions will automatically be part of the covariant interactions and do not have to be included separately.) Treating the full Bethe–Salpeter equation, however, is a very tedious way of handling the electron correlation. Therefore, the procedure described here, is a much more effective way of gradually including QED into MBPT calculations.

The CC-QED procedure can also be applied to systems with more than two electrons. For instance, if we consider the simple approximation

$$\Omega = 1 + T_2 + \frac{1}{2}T_2^2$$

then we will have in addition to the pair function also the coupled-cluster term, illustrated in Figure 13-10 (left). Here, one or both of the pair functions can be replaced by the QED pair function in Figure 13-8 in order to insert QED effects on this level.

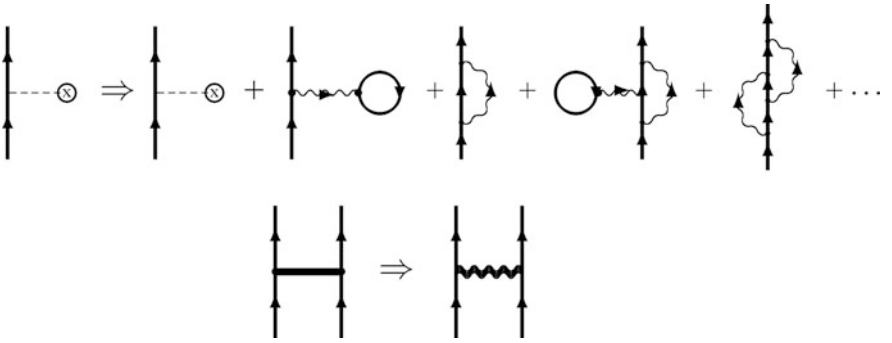

Figure 13-9. Replacements to be made in the CC equations in Figure 13-4 in order to generate the corresponding CC-QED equations

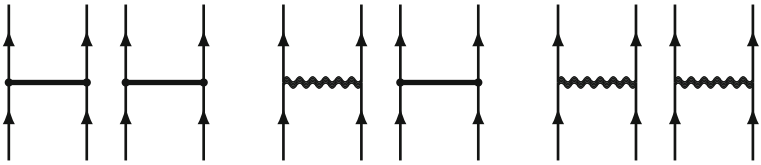

Figure 13-10. Feynman diagram representing coupled-cluster term $\frac{1}{2}T_2^2$ with standard pair functions (*left*) and one and two inserted QED pair function (defined in Figure 13-8)

In the CCSD approximation, $T = T_1 + T_2$, also the single-particle QED effects will be included in the orbitals, as illustrated in Figure 13-9.

It is a consequence of the complete compatibility between the standard MBPT/CC approach and the covariant approach described here that the insertion of QED effects can be restricted to places where they are expected to be most significant. This fact can be utilized to optimize the computing efficiency.

13.5. IMPLEMENTATION AND FUTURE OUTLOOK

The combined many-body/coupled-cluster-QED procedure, described above, is now being implemented at our laboratory. The single-photon exchange, represented by the first diagram in the rhs of Figure 13-7 is fully implemented in our procedure (with all combinations of particles and holes) and the second diagram in the no-pair approximation. Calculations have been performed for the ground state of a number of light and medium-heavy heliumlike ions, and some results are given in the second part of Table 13-4. These results, here presented for the first time, represent effects *beyond two-photon exchange*, i.e., one virtual, covariant photon and at least two Coulomb interactions (with and without crossing). Our present results are compared in the first part of the table with corresponding two-photon S-matrix results,

Table 13-4. Comparison in the ground state of some heliumlike ions between two-photon Coulomb-Breit (unretarded no-pair, retarded no-pair, and virtual pairs) and correspondingly WITH electron correlation, beyond two photons (in μH).

	Two-photon Coul-Breit			Beyond two-photon Coul-Breit		
Z	Unretarded	Retarded	Virtual pairs	Unretarded	Retarded	Virtual pairs
6	−1,054	31	−10	137	−9.0	2.6
10	−2,870	122	−46	223	−21	7.3
14	−5,514	293	−122	301	−36	13
18	−8,947	553	−248	372	−51	21
30	−23,629	1,910	−1,010	553	−102	46
42	−44,490	4,118	−2,435	688	−147	71

published by our group in 1995 [43] (Figure 13-11). More detailed results will be published shortly [38].

The calculations we have performed correspond to the first two diagrams in Figure 13-12 (up to three Coulomb crossings). The next two diagrams, including one retarded and one unretarded Breit interaction, are also quite feasible to evaluate, while the last two – with TWO retarded interactions – are beyond reach for the time being. It should be noted, though, that the corresponding effects would be quite small. In Figure 13.11 we have indicated the effect of doubly retarded two-photon exchange, and the corresponding effect with correlation would be one order of magnitude smaller.

In the pipeline is also to implement the radiative part of the potential in the Figure 13-7. This will require regularization and renormalization in the Coulomb gauge, which is not straightforward.

Our intention is also to apply the procedure to excited states of heliumlike ions in order to evaluate fine-structure splitting. Very accurate experimental results are here available that presently have no matching theoretical counterpart [44, 45]. In order to reach sufficient accuracy, our numerical procedure has to be further improved, a

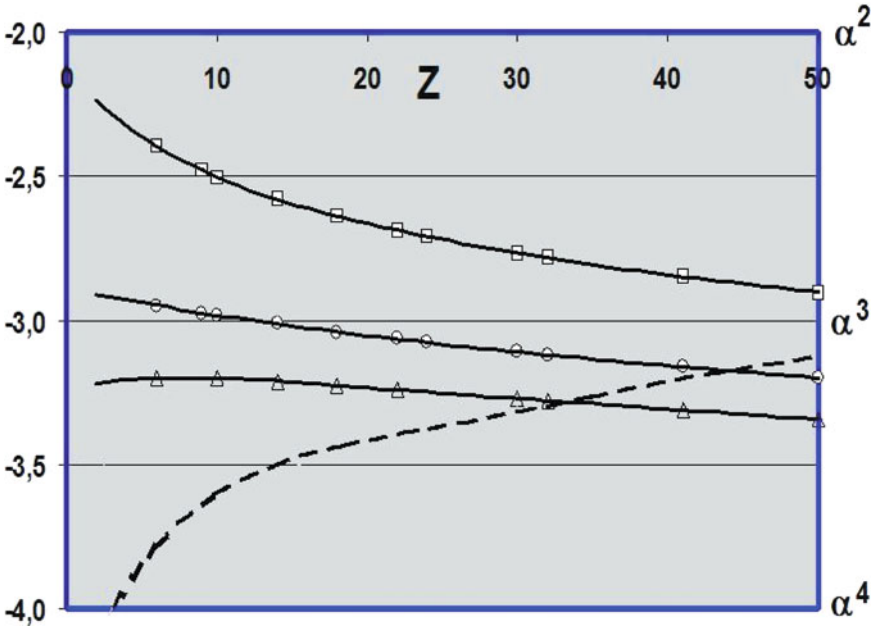

Figure 13-11. The Coulomb-Breit interaction with electron correlation beyond two-photon exchange, unretarded (*squares*), retarded no-pair (*circles*), and virtual pairs (*triangles*). Shown is also the (estimated) two-photon Breit-Breit interaction with DOUBLE retardation (*dashed*). The values are normalized to the ionization energy. The vertical scale is logarithmic with one unit corresponding to a factor of the fine-structure constant $\alpha \approx 1/137$

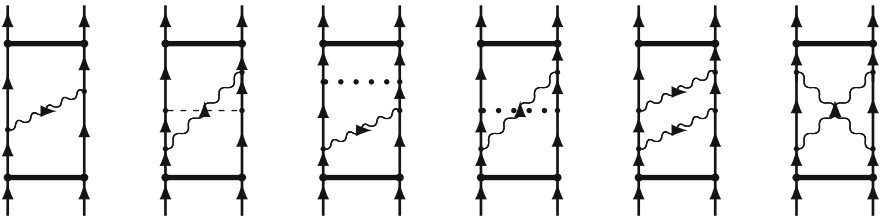

Figure 13-12. One- and two-photon exchange diagrams with electron correlation, represented by incoming and/or outgoing pair functions with one or several Coulomb interactions

procedure that is presently under way in collaboration with the mathematical department at our university.

To what extent we will be able to realize the ambitious program indicated here, will largely depend on the economical and personal resources that we can access in the future.

REFERENCES

1. S. Fritzsche, P. Indelicato, T. Stöhlker, J. Phys. B **38**, S707 (2005)
2. D. R. Plante, W. R. Johnson, J. Sapirstein, Phys. Rev. A **49**, 3519–3530 (1994)
3. G. W. F. Drake, Can. J. Phys. **66**, 586–611 (1988)
4. I. Lindgren, S. Salomonson, B. Åsén, Phys. Rep. **389**, 161–261 (2004)
5. K. A. Brueckner, Phys. Rev. **100**, 36–45 (1955)
6. J. Goldstone, Proc. R. Soc. London, Ser. A **239**, 267–279 (1957)
7. C. Bloch, Nucl. Phys. **6/7**, 329/451 (1958)
8. B. H. Brandow, Rev. Mod. Phys. **39**, 771–828 (1967)
9. I. Lindgren, J. Phys. B **7**, 2441–2470 (1974)
10. F. Coster, Nucl. Phys. **7**, 421–424 (1958)
11. H. Kümmel, K. H. Lührman, J. G. Zabolitsky, Phys. Rep. **36**, 1–135 (1978)
12. J. Čížek, J. Chem. Phys. **45**, 4256–4266 (1966)
13. I. Lindgren, Int. J. Quantum Chem. **S12**, 33–58 (1978)
14. W. Ey, Nucl. Phys. A **296**, 189–204 (1978)
15. D. Mukherjee, Chem. Phys. Lett. **125**, 207–212 (1986)
16. I. Lindgren, D. Mukherjee, Phys. Rep. **151**, 93–127 (1987)
17. I. Lindgren, J. Morrison, in *Atomic Many-Body Theory*, Second edition (Springer, Berlin, 1986, reprinted 2009)
18. J. Sucher, Phys. Rev. A **22**, 348–362 (1980)
19. H. Araki, Prog. Theor. Phys. (Japan) **17**, 619–642 (1957)
20. J. Sucher, Phys. Rev. **109**, 1010–1011 (1957)
21. J. Morrison, J. Phys. B **6**, 2205–2212 (1973)
22. S. Garpman, I. Lindgren, J. Lindgren, J. Morrison, Phys. Rev. A **11**, 758–781 (1975)
23. S. Garpman, I. Lindgren, J. Lindgren, J. Morrison, Z. Phys. A **276**, 167–177 (1976)
24. I. Lindgren, J. Lindgren, A. M. Mårtensson, Z. Phys. A **279**, 113–125 (1976)
25. A. M. Mårtensson, J. Phys. B **12**, 3995–4012 (1980)

26. I. Lindgren, S. Salomonson, in *A Numerical Coupled-Cluster Procedure Applied to the Closed-Shell Atoms Be and Ne*. Presented at the Nobel Symposium on Many-Body Effects in Atoms and Solids, Lerum, 1979. Physica Scripta **21**, 335–342 (1980)
27. J. Morrison, S. Salomonson, in *Many-Body Perturbation Theory of the Effective Electron–Electron Interaction for Open-Shell Atoms*. Presented at the Nobel Symposium, Lerum, 1979. Physica Scripta **21**, 343–350 (1980)
28. S. Salomonson, I. Lindgren, A. M. Mårtensson, in *Numerical Many-Body Perturbation Calculations on Be-like Systems Using a Multi-Configurational Model Space*. Presented at the Nobel Symposium on Many-Body Effects in Atoms and Solids, Lerum, 1979. Physica Scripta **21**, 335–342 (1980)
29. I. Lindgren, *Accurate many-body calculations on the lowest ^2S and ^2P states of the lithium atom*. Phys. Rev. A **31**, 1273–1286 (1985)
30. S. Salomonson, P. Öster, Phys. Rev. A **41**, 4670–4681 (1989)
31. S. Salomonson, A. Ynnerman, Phys. Rev. A **43**, 88–94 (1991)
32. E. Lindroth, Phys. Rev. A **37**, 316–328 (1988)
33. S. Salomonson, P. Öster, Phys. Rev. A **40**, 5548, 5559 (1989)
34. S. A. Blundell, W. R. Johnson, Z. W. Liu, J. Sapirstein, Phys. Rev. A **40**, 2233–2246 (1989)
35. E. Eliav, U. Kaldor, Y. Ishikawa, Phys. Rev. A **50**, 1121–1128 (1994)
36. M. S. Safronova, J. Sapirstein, W. R. Johnson, Phys. Rev. A **58**, 1016–1028 (1998)
37. R. Bukowski, B. Jeziorski, K. Szalewicz, J. Chem. Phys. **110**, 4165–4183 (1999)
38. D. Hedendahl, S. Salomonson, I. Lindgren, Phys. Rev. (to be published) (2010)
39. A. L. Fetter, J. D. Walecka, in *The Quantum Mechanics of Many-Body Systems* (McGraw-Hill, New York, 1971)
40. I. Lindgren, S. Salomonson, D. Hedendahl, in *Field-Theoretical Approach to Many-Body Perturbation Theory: Combining MBPT and QED*. Invited talk at the Sixth International Conference of Computational Methods in Sciences and Engineering, Corfu, Greece, September 2007. Adv. Quantum Chem. (2008)
41. I. Lindgren, S. Salomonson, D. Hedendahl, Einstein centennial review paper. Can. J. Phys. **83**, 183–218 (2005)
42. I. Lindgren, S. Salomonson, D. Hedendahl, Phys. Rev. A **73**, 062,502 (2006)
43. I. Lindgren, H. Persson, S. Salomonson, L. Labzowsky, Phys. Rev. A **51**, 1167–1195 (1995)
44. E. G. Myers, H. S. Margolis, J. K. Thompson, M. A. Farmer, J. D. Silver, M. R. Tarbutt, Phys. Rev. Lett. **82**, 4200–4203 (1999)
45. T. R. DeVore, D. N. Crosby, E. G. Myers, Phys. Rev. Lett. **100**, 243,001 (2008)

CHAPTER 14

ON SOME ASPECTS OF FOCK-SPACE MULTI-REFERENCE COUPLED-CLUSTER SINGLES AND DOUBLES ENERGIES AND OPTICAL PROPERTIES

PRASHANT UDAY MANOHAR[1], KODAGENAHALLI R. SHAMASUNDAR[2], ARIJIT BAG[3], NAYANA VAVAL[4], AND SOURAV PAL[5]

[1]*Department of Chemistry, University of Southern California, Los Angeles, CA 90089-0482, USA, e-mail: pumanohar@gmail.com*

[2]*Universität Stuttgart, Institut für Theoretische Chemie, Pfaffenwaldring 55, D-70569 Stuttgart, Germany, e-mail: sham@theochem.uni-stuttgart.de*

[3]*Physical Chemistry Division, National Chemical Laboratory, Pune 411008, India, e-mail: bagarijit@gmail.com*

[4]*Physical Chemistry Division, National Chemical Laboratory, Pune 411008, India, e-mail: np.vaval@ncl.res.in*

[5]*Physical Chemistry Division, National Chemical Laboratory, Pune 411008, India, e-mail: s.pal@ncl.res.in*

Abstract: Multi-reference coupled cluster methods are established as accurate and efficient tools for describing electronic structure of quasi degenerate states. Recently we have developed multi-reference coupled cluster linear response approach based on the constrained variation method. The method is very general and can describe challenging problems due to the multiple-root nature of effective Hamiltonian. Calculation of response properties for the ionized/electron attached or excited state molecules is a challenging task. With this formulation it is possible to accurately predict the higher order molecular properties of the open shell molecules. In this article we review the response approaches for quasi degenerate cases with emphasis on Fock space multi-reference coupled cluster method.

Keywords: Multireference coupled cluster, Fock space, Optical properties, Linear response

14.1. INTRODUCTION

Spectacular success of the standard single reference coupled-cluster (SRCC) method in the last few decades in explaining a wide variety of chemical phenomena is well documented in the quantum chemistry literature [1]. Its ability to treat dynamical electron correlation accurately for closed shell molecules and satisfy size-extensivity features, makes it an attractive candidate for electronic structure calculations. Another reason for the emergence of SRCC as the state-of-the-art method is

P. Čársky et al. (eds.), Recent Progress in Coupled Cluster Methods, 375–393.
DOI 10.1007/978-90-481-2885-3_14,

the successful development of efficient analytic energy derivative techniques for the calculation of molecular properties [2–7]. The response approach in the SRCC context was first attempted by Monkhorst [8]. This was originally formulated in a non-stationary framework, and hence, this did not have the simplicities introduced by the generalized Hellmann – Feynman theorem and the $(2n + 1)$ rule. As a result, evaluation of first-order property in SRCC depended explicitly on first-derivatives of cluster amplitudes with respect to the external perturbation. Thus, to satisfy the necessary condition for Hellmann – Feynman theorem and get the full use of $(2n+1)$ rule, several attempts have been made to formulate stationary coupled cluster theory [9–12]. All such attempts have ended in more complicated theories. This apparent impediment was overcome by Bartlett and coworkers [3, 13]. They used the idea of algebraic Z-vector method introduced by Handy and Schaefer [14] in the analysis of analytic orbital derivatives introduced in the configuration interaction method. They have shown that the requirement of first derivative of cluster amplitudes for such mode of perturbation may be replaced by a single perturbation independent quantity, known as Z-vector. This and the subsequent developments by Bartlett and coworkers substantially facilitated efficient implementation of molecular energy gradients for SRCC, and significantly contributed to its success in quantum chemistry. However, Z-vector type of approach turned out to be a tedious job for higher-order properties such as Hessians, polarizabilities, etc. On the other hand, a conceptually different approach, using a constrained variation approach, proposed by Jørgensen and coworkers, has incorporated all such developments in a single formulation through the formation of Lagrangian functional which is easily applicable to higher order energy derivative [15–18]. This approach involved recasting of standard SRCC theory in a stationary framework by introducing an extra set of de-excitation amplitudes. It was shown that this method includes the Z-vector method as a zeroth-order result and transparently extends its benefits to higher-order properties. While SRCC method has been routinely used for energy and energy derivatives for closed shell like systems, where a single determinant can be identified to be the most important part of the wave-function. Description of molecular excited states, open shell and potential energy surfaces in general, demand a description beyond SRCC theories. These are the cases where reference state may not be described by a single Slater determinant. A linear combination of determinants may be more appropriate to describe non-dynamic correlation associated with such states. The use of multi-determinantal reference space to incorporate non-dynamical electron correlation is in general known as multi-reference (MR) theories [19, 20]. There have been several approaches developed in last two decades among which the effective Hamiltonian approaches [21, 22] are dominating. An effective Hamiltonian is diagonalized with in a suitably chosen model space to approximately reproduce a part of the spectrum associated with the exact Hamiltonian.

The development of coupled cluster methods incorporating the non-dynamical electron correlation is known as multi-reference coupled cluster (MRCC). There are two subclasses of MRCC methods, which have been studied extensively. One is the multi root description via effective Hamiltonian approach [23, 24] and the other

describes a specific root, known as the state-specific MRCC approach [25]. In multi-root effective Hamiltonian approach, exact energies of the corresponding strongly interacting near-degenerate states are obtained as roots of effective Hamiltonian via diagonalization. This class of methods is further subdivided into Hilbert space and Fock space approach depending on the way the dynamical part of electron correlation is described [23, 26–36]. In Hilbert space approach a state-universal wave operator which contains different cluster operators for each of the reference determinants in the model space [26, 30, 31]. It is based on the concept of multiple vacua and the different cluster operators are hole-particle creation operators with respect to different vacua. This method has been used for studying PES, bond-dissociation, etc. However for PES, state-selective MRCC method developed by Mukherjee and co-workers [25] has been found to be more suitable from the point of view of circumventing the important problems of intruder states. The Fock-space (FS) MRCC [26–30, 32–36] in general, is suitable for energy difference calculations i,e ionization, electron-attachment and electronic excitation of molecules and is based on the concept of common-vacuum and a valence universal wave-operator. The model space is composed of near degenerate configurations obtained by combinations of electron occupancies among what are called active orbitals. The occupancies of the active orbitals are denoted in terms of number of active particles and active holes with respect to the vacuum. The wave operator in this approach must be able to destroy a set of active holes and/or particles apart from hole particle excitation. The explicit form of inverse of normal ordered exponential is not known. Therefore, Bloch equation approach is the only approach that can be followed to obtain the cluster amplitude equations. It has been shown that this leads to a connected set of equations for each valence sector and equations for different Fock space sectors are decoupled from each other. This decoupling of the different Fock space sectors is known as subsystem embedding condition (SEC). This emerges naturally as consequence of normal-ordered form of ansatz. Because of these simplifications, the normal-ordered exponential ansatz has become the standard ansatz for FSMRCC theories and their applications. The effective Hamiltonian theory aims at a simultaneous description of a manifold of strongly interacting states. A zeroth-order approximation to this manifold is provided by the chosen model space. It is further assumed that this model space is energetically well-separated from its orthogonal complement and weakly interacts with it. This means that determinants from orthogonal complement are not dominant in any of the targeted states.Thus, the choice of the model space is very important the wrong choice of model space may lead to intruder state problem. However, the intruder state problem may be overcome by the Fock-space (FS) effective Hamiltonian scheme of Meissner [24] which is very efficient from the computational point of view.

Parallel to this, methods like equations-of-motion (EOM) CC [37–43], coupled cluster linear response (CC-LR) [44], symmetry adapted clusters configuration interaction (SAC-CI) [45, 46], etc. are also known to handle certain classes of quasi-degeneracy. Bartlett [38] and co-workers implemented EOMCC method for calculation of excitation energies for atoms and molecules. Stanton and Bartlett [40] used EOMCC method for excitation energies, transition probabilities and excited

state properties. Nooijen and Bartlett [47] implemented it for electron attached systems. Later, Watts and Bartlett [48] included triples excitation to EOMCC for excitation energies. Similarity transformed EOMCC method (STEOMCC) was developed by Nooijen and Bartlett [49] for ionized, electron attached and excited states. More recently, spin-flip EOMCC has been introduced by Krylov [50] for description of excited states, bond breaking, diradicals and triradicals. For one valence system in Fock space i.e. for ionization potential and electron affinity calculation it has been shown that both EOMCC and FSMRCC are equivalent [49]. However, for excitation energy calculation, such equivalency disappears. It was shown by Bartlett [51] that while the size-extensivity is maintained in FSMRCC, the same is not true in case of EOM-CC for higher valence cases. However, recently developed similarity transformed (ST) EOM-CC method of Nooijen and co-workers [52, 53] is size-extensive. CC-LR method developed by Jørgensen's group [54] has also been used extensively for the calculation of excitation energies. The excitation energies obtained by CC-LR are identical to the EOM-CC excitation energies.

EOMCC derivatives for property calculation was also initiated and implemented by Stanton [54] first and then by Stanton and Gauss [41, 55]. Analytic energy derivatives for ionized states were described by Stanton and Gauss [41] in EOMCC formalism. Subsequently, analytic second derivative for excited state was also introduced by Stanton and Gauss [55]. Gradients using STEOM-CC was implemented by Nooijen and coworkers [56] using Lagrange undetermined multiplier, which is similar to the method followed in the work which is to be reviewed in this article. In STEOM-CC method, two more Z vector like quantities are required to be evaluated for the response of the $S^{\pm}$ coefficients to the perturbation along with the Lagrange multiplier lambda (Λ). The role of Λ is equivalent in both cases.

However, obtaining energy derivatives in the context of multi-root MRCC methods was a challenge. Along the lines of SRCC, the analytic linear response for MRCC method based on Monkhorst's approach [8] was initiated by Pal [57] long back. The computational developments and implementation of the method was done later by Ajitha et al. [58–60] for obtaining dipole moment of doublet radicals and low-lying excited states of molecules. However, the approach was quite unsatisfactory, since it required expensive evaluation of cluster amplitude derivatives for every mode of perturbations.

In SRCC context, this problem was solved by incorporation of Z-vector technique [4] or equivalently, the constrained variational approach (CVA) [7], which was based on the method of Lagrange undetermined multipliers. The CVA method in FSMRCC framework was studied by Szalay [61], independently. However, this method was applicable for complete model spaces (CMS) only. Similar developments for both Fock and Hilbert space MRCC [62, 63] for ionic, electron attached and excited states was pursued by Pal and co-workers in recent years [62]. The CVA formulation of Shamasundar et al. [62]. is applicable for a general incomplete model space (IMS) cases and simplifies to Szalay's formulation in the case of CMS. This single root method provides a cost-effective tool to obtain higher order energy derivatives with

the knowledge of lower order cluster amplitude derivatives and a set of perturbation independent vectors, the Lagrange multipliers.

The computational developments of FSMRCC using CVA were recently started by Manohar et al. [64, 65] and Bag et al. [66] using singles and doubles (SD) truncation of the wave operator. The implementation for analytic dipole moments and polarizabilities of doublet radicals has been done by Manohar et al. [64] and Bag et al. [66, 67]. Implementation of CVA-FSMRCC method for the energy derivatives of the singlet and the triplet excited states have been done by Bag et al. [66]. In this review article, we present an overview of the FSMRCC method for energy derivatives. In particular, we review the Lagrangian based formulation using CVA which is the most efficient implementation of the method. We review the basic theory and discuss some of the results obtained using the state of the art CVA based analytic derivative formulation.

14.2. FOCK-SPACE MULTI-REFERENCE COUPLED-CLUSTER METHOD

We now present the developments so far in FSMRCC and related methods. As mentioned earlier, FSMRCC is based on the concept of a common vacuum. We choose an N-electron RHF configuration as vacuum, which defines the holes and particles. In the Fock-space, the model space determinants contain h-holes and p-particles distributed within a set of what are termed as active holes and active particles, usually around the Fermi level. We denote the above p-active particle, h-active hole model space determinant by $\left\{\Phi_i^{(p,h)}\right\}$. Thus, the model space of a (p,h) valence Fock-space can be written as

$$\left|\Psi_{(0)\mu}^{(p,h)}\right\rangle = \sum_i C_{i\mu}^{(p,h)} \left|\Phi_i^{(p,h)}\right\rangle \tag{14-1}$$

The dynamical electron correlation arises due to comparatively weak interactions of the model-space configurations with the virtual space configurations. This interaction is brought in through a universal wave operator Ω which is parameterized such that the states generated by its action on the reference function satisfy Schrödinger equation. To generate the exact states for the (p,h) valence system, the wave operator must generate all valid excitations from the model space. The correlated μth wave function in the MRCC formalism is written as

$$\left|\Psi_{\mu}^{(p,h)}\right\rangle = \Omega \left|\Psi_{(0)\mu}^{(p,h)}\right\rangle \tag{14-2}$$

where

$$\Omega = \left\{e^{\tilde{T}^{(p,h)}}\right\} \tag{14-3}$$

The brace-bracket indicates normal ordering of the cluster-operators. In the Fock-space approach $\tilde{T}^{(p,h)}$ amplitudes contain the lower valence amplitudes and thus give the additional flexibility in the theory.

$$\tilde{T}^{(p,h)} = \sum_{k=0}^{p} \sum_{l=0}^{h} T^{(k,l)} \tag{14-4}$$

The super scripted bracket in the right hand side of the above expression indicates that the cluster operator T is capable of destroying exactly k active particles and l active holes, in addition to creation of holes and particles. The $\tilde{T}^{(p,h)}$ operator subsumes all such lower $T^{(k,l)}$ operators.

The Schrödinger equation for the manifold of quasi-degenerate states can be written as

$$\begin{aligned} H\big|\Psi_i^{(p,h)}\big\rangle &= E_i\big|\Psi_i^{(p,h)}\big\rangle \\ &\text{which leads to} \\ H\Omega\Big(\sum_i C_{i\mu}^{(p,h)}\Phi_i^{(p,h)}\Big) &= E_\mu\Omega\Big(\sum_i C_{i\mu}^{(p,h)}\Phi_i^{(p,h)}\Big) \end{aligned} \tag{14-5}$$

The projection operator for model space is defined as

$$P^{(p,h)} = \sum_i \big|\Phi_i^{(p,h)}\big\rangle\big\langle\Phi_i^{(p,h)}\big| \tag{14-6}$$

The orthogonal component of the model space, i.e. the virtual space is defined as

$$Q = 1 - P \tag{14-7}$$

The effective Hamiltonian for (p,h) valence system can be defined such that

$$\sum_j \big(H_{\text{eff}}^{(p,h)}\big)_{ij} C_{j\mu} = E_\mu C_{i\mu} \tag{14-8}$$

$$\big(H_{\text{eff}}^{(p,h)}\big)_{ij} = \big\langle\Phi_i^{(k,l)}\big|\Omega^{-1}H\Omega\big|\Phi_j^{(k,l)}\big\rangle$$

which can be written as

$$H_{\text{eff}}^{(p,h)} = P^{(p,h)}\Omega^{-1}H\Omega P^{(p,h)} \tag{14-9}$$

The form the inverse of Ω, in general may not be well defined. Hence, above definition is seldom used to obtain the effective Hamiltonian. Instead, the Bloch – Lindgren approach is commonly used to define the effective Hamiltonian. The Bloch equation is just a modified form of Schrödinger equation.

$$H\Omega P = \Omega H_{\text{eff}} P \tag{14-10}$$

The Bloch-Lindgren approach not only eliminates the requirement of Ω^{-1}, but also provides an important criterion the effective Hamiltonian must fulfill. The effective Hamiltonian is, in general, non-hermitian. Mainly two approaches are used to obtain Ω and the effective Hamiltonian. One of them, known as Bloch projection approach, involves left projection of above equation by P and Q.

$$\begin{aligned} P^{(k,l)}\big(H\Omega - \Omega H_{\text{eff}}^{(k,l)}\big)P^{(k,l)} &= 0 \\ Q^{(k,l)}\big(H\Omega - \Omega H_{\text{eff}}^{(k,l)}\big)P^{(k,l)} &= 0; \\ \forall\ k = 0,\ldots,p; \\ l = 0,\ldots,h \end{aligned} \tag{14-11}$$

The normalization condition is specified indirectly through parameterization of Ω. In case of complete model spaces (CMS), the intermediate normalization is commonly employed.

The diagonalization of the effective Hamiltonian within the P space gives the energies of the corresponding states and the left and the right eigenvectors.

$$H_{\text{eff}}^{(p,h)} C^{(p,h)} = C^{(p,h)} E$$

$$\tilde{C}^{(p,h)} H_{\text{eff}}^{(p,h)} = E\tilde{C}^{(p,h)} \tag{14-12}$$

$$\tilde{C}^{(p,h)} C^{(p,h)} = C^{(p,h)} \tilde{C}^{(p,h)} = 1 \tag{14-13}$$

Because of normal ordering, the contractions amongst different cluster operators within the exponential are avoided, leading to partial hierarchical decoupling of cluster equations. This is commonly referred to as sub-system embedding condition (SEC). The lower valence cluster equations are completely decoupled from the higher valence cluster equations because of SEC. Hence, the Bloch equations are solved progressively from the lowest valence $(0,0)$ sector upwards up to (p,h) valence sector.

14.3. FSMRCC LINEAR RESPONSE

14.3.1. The Explicit Differentiation Method

The LR in FSMRCC framework was initiated by Pal and then implemented by Pal and co-workers for dipole moments of doublet radicals and excited states of closed-shell molecules. The method is non-variational and involves explicit differentiation of Bloch equation with respect to uniform external field. In presence of time-independent uniform external field, the parameters $\Upsilon = \left\{H_{\text{eff}}^{(p,h)}, C^{(p,h)}, \tilde{C}^{(p,h)}, E, \Omega\right\}$ become perturbation dependent and can be expanded in Taylor series of g.

$$\Upsilon(g) = \Upsilon^{(0)} + g\Upsilon^{(1)} + \frac{1}{2!}g^2\Upsilon^{(2)} + \frac{1}{3!}g^3\Upsilon^{(3)} + \ldots \tag{14-14}$$

The differentiation of the Bloch equations following left projections by model space and virtual space configurations with respect to g yields the equations for wave-function derivatives and the derivative effective Hamiltonian.

$$P^{(k,l)}\left(H^{(1)}\Omega^{(0)} + H^{(0)}\Omega^{(1)} - \Omega^{(1)}H_{\text{eff}}^{(k,l)^{(0)}} - \Omega^{(0)}H_{\text{eff}}^{(k,l)^{(1)}}\right)P^{(k,l)} = 0 \quad (14\text{-}15)$$

$$Q^{(k,l)}\left(H^{(1)}\Omega^{(0)} + H^{(0)}\Omega^{(1)} - \Omega^{(1)}H_{\text{eff}}^{(k,l)^{(0)}} - \Omega^{(0)}H_{\text{eff}}^{(k,l)^{(1)}}\right)P^{(k,l)} = 0 \quad (14\text{-}16)$$

$$;\forall k = 0, \ldots, p; l = 0, \ldots, h$$

The equations are linear in the perturbation dependent quantities. It is interesting to note that the homogeneous parts of the Ω derivative equations are identical to the linear homogeneous part of the undifferentiated cluster equations. The SEC transparently holds at every order. The method provides multiple roots of derivative effective-Hamiltonian which can be obtained simultaneously by solving following equations.

$$\sum_i \left\{\left(H_{\text{eff}}^{(1)}\right)_{ji} C_{i\mu}^{(0)} + \left(H_{\text{eff}}^{(0)}\right)_{ji} C_{i\mu}^{(1)}\right\} = E_\mu^{(1)} C_{j\mu}^{(0)} + E_\mu^{(0)} C_{j\mu}^{(1)} \quad (14\text{-}17)$$

However, due to its non-variational nature, the method does not obey the generalized Hellmann – Feynman theorem for energy derivatives. Therefore, the evaluation of nth order energy derivatives demands the knowledge of cluster amplitudes and their derivatives up to nth order.

14.3.2. The Z-vector Method

The explicit differentiation method described in the last subsection, although straight forward, is cumbersome, particularly for higher order derivatives. Before discussing z-vector method for multi-reference problem we will briefly state formalism for single reference first. The response approach for SRCC was formulated by Monkhorst [8] to enable analytic computation of such properties. The SRCC was originally formulated in a non-stationary framework, and due to this it did not have the simplicities introduced by the generalized Hellmann – Feynman theorem and the $(2n + 1)$ -rule. As a result, the expression for a first-order property in SRCC depended explicitly on first- derivatives of cluster amplitudes with respect to the external perturbation, which means it is necessary calculate these cluster amplitude derivatives for all modes of perturbation. Bartlett and coworkers [3, 13] introduced what is known as a z-vector method For first-order properties, this problem was overcome by Bartlett and coworkers using the idea of algebraic Z-vector method based on Dalgarno's interchange theorem [68]. This substantially facilitated efficient implementation of molecular energy gradients for SRCC, and significantly contributed to its success in quantum chemistry. In lines of Z-vector formalism in SRCC, Pal and co-workers proposed Z-vector technique for FSMRCC response [58–60]. Expanding Ω and its

derivatives in terms of $T^{(p,h)}$ and absorbing the lower valence T operators in the transformed Hamiltonian $\bar{H}$ ($\bar{H} = [H \exp(\tilde{T}^{(i,j)})]_c$), the equations for $H_{\text{eff}}^{(p,h)^{(1)}}$ and $T^{(p,h)^{(1)}}$ can be simplified and rearranged. The $H_{\text{eff}}^{(p,h)^{(1)}}$ can thus be rewritten as.

$$\begin{aligned} P^{(p,h)}\big(\bar{H}^{(1)} + \bar{H}^{(1)}T^{(p,h)^{(0)}} - T^{(p,h)^{(0)}}\bar{H}^{(1)} + \bar{H}^{(0)}T^{(p,h)^{(1)}} - T^{(p,h)^{(1)}}\bar{H}^{(0)}\big)P^{(p,h)} \\ = P^{(p,h)}\big(H_{\text{eff}}^{(p,h)^{(1)}}\big)P^{(p,h)} \end{aligned} \tag{14-18}$$

Similarly, from Eq. (14-15) we arrive to

$$\begin{aligned} Q^{(p,h)}\big(\bar{H}^{(0)}T^{(k,l)^{(1)}} - T^{(k,l)^{(1)}}\bar{H}^{(0)} - T^{(k,l)^{(1)}}H_{\text{eff}}^{(p,h)^{(0)}} - T^{(k,l)^{(0)}}H_{\text{eff}}^{(p,h)^{(1)}}\big)P^{(p,h)} \\ = Q^{(p,h)}\big(\bar{H}^{(1)} + \bar{H}^{(1)}T^{(k,l)^{(0)}} - T^{(k,l)^{(0)}}\bar{H}^{(1)}\big)P^{(p,h)} \end{aligned} \tag{14-19}$$

Applying the resolution of identity it follows

$$\begin{aligned} &\langle Q^{(p,h)}|\bar{H}^{(0)}|Q^{(p,h)}\rangle\langle Q^{(p,h)}|T^{(p,h)^{(1)}}|P^{(p,h)}\rangle \\ &-\langle Q^{(p,h)}|T^{(p,h)^{(1)}}|P^{(p,h)}\rangle\langle P^{(p,h)}|\bar{H}^{(0)}|P^{(p,h)}\rangle \\ &-\langle Q^{(p,h)}|T^{(p,h)^{(1)}}|P^{(p,h)}\rangle\langle P^{(p,h)}|H_{\text{eff}}^{(p,h)^{(0)}}|P^{(p,h)}\rangle \\ &\quad = \langle Q^{(p,h)}|\bar{H}^{(1)} + \bar{H}^{(1)}T^{(k,l)^{(0)}} - T^{(k,l)^{(0)}}\bar{H}^{(1)}|P^{(p,h)}\rangle \end{aligned} \tag{14-20}$$

Substituting Eq. (14-18) in the above equation, it follows

$$\begin{aligned} &\langle Q^{(p,h)}|\bar{H}^{(0)}|Q^{(p,h)}\rangle\langle Q^{(p,h)}|T^{(p,h)^{(1)}}|P^{(p,h)}\rangle \\ &-\langle Q^{(p,h)}|T^{(p,h)^{(1)}}|P^{(p,h)}\rangle\langle P^{(p,h)}|\bar{H}^{(0)}|P^{(p,h)}\rangle \\ &-\langle Q^{(p,h)}|T^{(p,h)^{(1)}}|P^{(p,h)}\rangle\langle P^{(p,h)}|H_{\text{eff}}^{(p,h)^{(0)}}|P^{(p,h)}\rangle \\ &\quad = \langle Q^{(p,h)}|(\bar{H}^{(0)} + \bar{H}^{(1)}T^{(p,h)^{(0)}} - T^{(p,h)^{(0)}}\bar{H}^{(1)}|P^{(p,h)}\rangle \\ &\qquad +\langle Q^{(p,h)}|T^{(p,h)^{(0)}}|P^{(p,h)}\rangle\langle P^{(p,h)}|(\bar{H}^{(0)} + \bar{H}^{(1)}T^{(p,h)^{(0)}}|P^{(p,h)}\rangle \end{aligned} \tag{14-21}$$

From the above equation, one can see that $T^{(p,h)^{(1)}}$ in the left hand side appears in the right of $\bar{H}$ in the Q-space and to the left of H_{eff} in P-space. Since, in general, H_{eff} has a matrix structure, the factorization of the $T^{(p,h)^{(1)}}$ can be effected only upon a diagonal assumption of H_{eff}. In the limit of single reference due to single-root of the model-space, this approximation becomes exact. In case of degenerate states and states with different symmetries also, the diagonal approximation is appropriate. Thus, under the diagonal approximation, the equations for $T^{(p,h)^{(1)}}$ can be written as

$$
\begin{aligned}
&(\langle Q^{(p,h)}|(\bar{H}^{(0)}|Q^{(p,h)}\rangle - \langle P^{(p,h)}|(\bar{H}^{(0)}|P^{(p,h)}\rangle \\
&-\langle P^{(p,h)}|H_{\text{eff}}^{(p,h)^{(0)}}|P^{(p,h)}\rangle + \langle Q^{(p,h)}\big|\bar{H}^{(1)}T^{(p,h)^{(0)}} \\
&-T^{(p,h)^{(0)}}\bar{H}^{(1)}|P^{(p,h)}\rangle)\langle Q^{(p,h)}|T^{(p,h)^{(1)}}|P^{(p,h)}\rangle \\
&\quad = \langle Q^{(p,h)}|(\bar{H}^{(1)} + \bar{H}^{(1)}T^{(p,h)^{(0)}} - T^{(p,h)^{(0)}}\bar{H}^{(1)}) \\
&\quad\quad +T^{(p,h)^{(0)}}(\bar{H}^{(1)} + \bar{H}^{(1)}T^{(p,h)^{(0)}})|P^{(p,h)}\rangle
\end{aligned}
\tag{14-22}
$$

Rearranging the above equation, it follows

$$
\begin{aligned}
\langle Q^{(p,h)}|T^{(p,h)^{(1)}}|P^{(p,h)}\rangle = \langle Q^{(p,h)}|(\bar{H}^{(1)} + [\bar{H}^{(1)}, T^{(p,h)^{(0)}}]) + T^{(p,h)^{(0)}}(\bar{H}^{(1)} \\
+\bar{H}^{(1)}T^{(p,h)^{(0)}})|P^{(p,h)}\rangle * A^{(p,h)^{(-1)}}
\end{aligned}
\tag{14-23}
$$

where,

$$
\begin{aligned}
A^{(p,h)} = \langle Q^{(p,h)}|\bar{H}^{(0)}|Q^{(p,h)}\rangle - \langle P^{(p,h)}|\bar{H}^{(0)}|P^{(p,h)}\rangle \\
-\langle P^{(p,h)}|H_{\text{eff}}^{(p,h)^{(0)}}|P^{(p,h)}\rangle - \langle Q^{(p,h)}|T^{(p,h)^{(0)}}\bar{H}^{(0)}|P^{(p,h)}\rangle
\end{aligned}
\tag{14-24}
$$

Ajitha and Pal proposed a perturbation independent set of amplitudes ζ such that for every $Q^{(p,h)}T^{(p,h)}P^{(p,h)}$ sector amplitude, there is a corresponding $P^{(p,h)}\zeta^{(p,h)}Q^{(p,h)}$ amplitude. Defining the ζ vectors as

$$
\begin{aligned}
\langle P^{(p,h)}|\zeta^{(p,h)}|Q^{(p,h)}\rangle = \langle P^{(p,h)}|(\bar{H}^{(1)} + [\bar{H}^{(1)}, T^{(p,h)^{(0)}}]) + T^{(p,h)^{(0)}}(\bar{H}^{(1)} \\
+\bar{H}^{(1)}T^{(p,h)^{(0)}})|Q^{(p,h)}\rangle * A^{(p,h)^{-1}};
\end{aligned}
\tag{14-25}
$$

the derivative effective Hamiltonian equation can be written in terms of these ζ vectors as

$$
\begin{aligned}
\langle P^{(p,h)}|H_{\text{eff}}^{(p,h)^{(0)}}|P^{(p,h)}\rangle = \langle P^{(p,h)}|(\bar{H}^{(1)} + \bar{H}^{(1)}T^{(p,h)^{(0)}})|P^{(p,h)}\rangle \\
\langle Q^{(p,h)}|\zeta^{(p,h)}|Q^{(p,h)}\rangle\langle Q^{(p,h)}|\bar{H}^{(0)}|P^{(p,h)}\rangle
\end{aligned}
\tag{14-26}
$$

This equation is a consequence of Dalgarno's interchange theorem. We observe that the derivative effective Hamiltonian equation is independent of the derivative T-amplitudes of the (p,h)-sector of the Fock space.

14.3.3. The Constrained-Variation Method

In the lines of SRCC, the constrained-variational approach (CVA) for energy derivatives was introduced in FSMRCC context by Szalay and was applicable for complete model spaces (CMS). Later, Pal and co-workers independently formulated the

CVA-FSMRCC for general incomplete model spaces (IMS) and showed that the functional simplifies to the one proposed by Szalay if applied for CMS and quasi-complete model space (QMS). The CVA-FSMRCC method of Pal an co-workers provides response of a specific root of the multiple roots of FSMRCC. One has to project a single desired state (root of effective Hamiltonian) for doing constrained variation. In FSMRCC context, the energy of a specific state of the (p,h) FS sector is given by

$$E_\mu = \sum_{ij} \tilde{C}^{(p,h)}_{\mu i} (H_{\text{eff}})^{(p,h)}_{ij} C^{(p,h)}_{j\mu} \tag{14-27}$$

We construct the Lagrangian to minimize the energy expression given above, with the constraint that the MRCC equations (Eqs. 14-11 and 14-13) are satisfied for the state μ.

$$\begin{aligned}\Im = \sum_{ij} \tilde{C}^{(p,h)}_{\mu i} (H_{\text{eff}})^{(p,h)}_{ij} C^{(p,h)}_{j\mu} + \sum_{k=0}^{p} \sum_{l=0}^{h} \{ & P^{(k,l)} \Lambda^{(k,l)} P^{(k,l)} P^{(k,l)} \big[H\Omega - \Omega H^{(k,l)}_{\text{eff}} \big] P^{(k,l)} \\ & + P^{(k,l)} \Lambda^{(k,l)} Q^{(k,l)} Q^{(k,l)} \big[H\Omega - \Omega H^{(k,l)}_{\text{eff}} \big] P^{(k,l)} \} + E_\mu \big[\sum_{ij} \tilde{C}^{(p,h)}_{\mu i} C^{(p,h)}_{j\mu} - 1 \big]\end{aligned} \tag{14-28}$$

The Λs in the above equation are the undetermined Lagrange multipliers obtained by applying stationarity condition on the Lagrangian $\Im$ with respect to the cluster amplitudes of the corresponding sectors. The stationarity condition on $\Im$ with respect to the Λ vectors yields the MRCC equations for the cluster amplitude. Obviously, the cluster-amplitudes are completely decoupled from the Λ vectors. The Λ vectors follow the partial sector wise decoupling exactly in the reverse SEC, i.e., the Λ vectors of the highest sector are totally decoupled from the lowest ones. The lowest sector Λ vectors are coupled with the Λs of all the higher sectors through the inhomogeneous part of the linear equations. The eigenvectors and effective Hamiltonian can be obtained by applying stationarity condition on the $\Im$. In case of CMS and IMS, since the effective Hamiltonian can be explicitly defined in terms of the cluster amplitudes, the CVA method simplifies to the one proposed by Szalay.

14.3.3.1. First Order Properties Using CVA-FSMRCC

For simplicity, we consider the ionization problem. In FSMRCC context, the model-space configurations belong to (0,1) sector of the FS, with the unionized RHF reference as vacuum. One can easily extend the algebra for general (p,h) valence case. The configurations of the ionized states are given by

$$|\Psi_{\mu}^{(0,1)}\rangle = \sum_{i} C_{i\mu}|\Phi_{i}^{(0,1)}\rangle \tag{14-29}$$

The dynamical electron correlation effects are brought in through a universal wave operator Ω.

$$\Omega = \{e^{\tilde{T}^{(0,1)}}\} \tag{14-30}$$

$$\tilde{T}^{(0,1)} = T^{(0,1)} + T^{(0,0)} \tag{14-31}$$

The wave operator Ω is parameterized such that the states generated by its action on the reference function satisfy Bloch – Lindgren equation for effective Hamiltonian given by Eq. (14-10). From the earlier definition (14-28), the Lagrangian can be defined as

$$\begin{aligned}\Im = &\sum_{ij} \tilde{C}_{\mu i}^{(0,1)} (H_{\text{eff}})_{ij}^{(0,1)} C_{j\mu}^{(0,1)} \\ &+P^{(0,1)} \Lambda^{(0,1)} P^{(0,1)} P^{(0,1)} \left[H\Omega - \Omega H_{\text{eff}}^{(0,1)}\right] P^{(0,1)} \\ &+P^{(0,1)} \Lambda^{(0,1)} Q^{(0,1)} Q^{(0,1)} \left[H\Omega - \Omega H_{\text{eff}}^{(0,1)}\right] P^{(0,1)} \\ &+P^{(0,0)} \Lambda^{(0,0)} P^{(0,0)} P^{(0,0)} H\Omega P^{(0,0)} \\ &+P^{(0,0)} \Lambda^{(0,0)} Q^{(0,0)} Q^{(0,0)} H\Omega P^{(0,0)} \\ &-E_{\mu} \left(\sum_{ij} \tilde{C}_{\mu i}^{(0,1)} C_{j\mu}^{(0,1)} - 1 \right)\end{aligned} \tag{14-32}$$

Being the CMS, the effective Hamiltonian has explicit expression in terms of the cluster amplitudes due to which, the closed part of the Lagrangian vanishes and the above equation reduces to

$$\begin{aligned}\Im = &\sum_{ij} \tilde{C}_{\mu i}^{(0,1)} (H_{\text{eff}})_{ij}^{(0,1)} C_{j\mu}^{(0,1)} \\ &+P^{(0,1)} \Lambda^{(0,1)} Q^{(0,1)} Q^{(0,1)} \left[H\Omega - \Omega H_{\text{eff}}^{(0,1)}\right] P^{(0,1)} \\ &+P^{(0,0)} \Lambda^{(0,0)} Q^{(0,0)} Q^{(0,0)} H\Omega P^{(0,0)} \\ &-E_{\mu} \left(\sum_{ij} \tilde{C}_{\mu i}^{(0,1)} C_{j\mu}^{(0,1)} - 1 \right)\end{aligned} \tag{14-33}$$

In presence of external field, the Lagrangian and the parameters $\Upsilon = \{H_{\text{eff}}, C, \tilde{C}, E, \Omega, \Lambda\}$ become perturbation dependent. These can be expanded in Taylor series.

$$\Upsilon(g) = \Upsilon^{(0)} + g\Upsilon^{(1)} + \frac{1}{2!}g^2\Upsilon^{(2)} + \frac{1}{3!}g^3\Upsilon^{(3)} + \ldots \tag{14-34}$$

The Lagrangian defined in Eq. (14-33) can be differentiated with respect to the field g to obtain the Lagrangians at every order. The zeroth order and the first order Lagrangians can therefore, be written as

$$\begin{aligned}
\Im^{(0)} = & \left(\tilde{C}^{(0,1)(0)} H_{\text{eff}}^{(0,1)(0)} C^{(0,1)(0)}\right)_{\mu\mu} \\
& + P^{(0,1)} \Lambda^{(0,1)(0)} \left[H^{(0)}\Omega^{(0)} - \Omega^{(0)} H_{\text{eff}}^{(0,1)(0)}\right] P^{(0,1)} \\
& + P^{(0,0)} \Lambda^{(0,0)(0)} \left[H^{(0)}\Omega^{(0)}\right] P^{(0,0)} \\
& - E_\mu \left(\sum_{ij} \tilde{C}_{\mu i}^{(0,1)(0)} C_{j\mu}^{(0,1)(0)} - 1 \right)
\end{aligned} \tag{14-35}$$

$$\begin{aligned}
\Im^{(1)} = & \left(\tilde{C}^{(0,1)(1)} H_{\text{eff}}^{(0,1)(0)} C^{(0,1)(0)}\right)_{\mu\mu} + \left(\tilde{C}^{(0,1)(0)} H_{\text{eff}}^{(0,1)(1)} C^{(0,1)(0)}\right)_{\mu\mu} \\
& + \left(\tilde{C}^{(0,1)(0)} H_{\text{eff}}^{(0,1)^{(0)}} C^{(0,1)^{(1)}}\right)_{\mu\mu} \\
& + P^{(0,1)} \Lambda^{(0,1)(1)} \left[H^{(0)}\Omega^{(0)} - \Omega^{(0)} H_{\text{eff}}^{(0,1)(0)}\right] P^{(0,1)} \\
& + P^{(0,1)} \Lambda^{(0,1)(0)} \left[H^{(1)}\Omega^{(0)} + H^{(0)}\Omega^{(1)} - \Omega^{(1)} H_{\text{eff}}^{(0,1)(0)} - \Omega^{(0)} H_{\text{eff}}^{(0,1)(1)}\right] P^{(0,1)} \\
& + P^{(0,0)} \Lambda^{(0,0)(1)} H^{(0)}\Omega^{(0)} P^{(0,0)} + P^{(0,0)} \Lambda^{(0,0)(0)} H^{(1)}\Omega^{(0)} + H^{(0)}\Omega^{(1)} P^{(0,0)} \\
& - E_\mu^{(0)} \sum_{ij} \left(\tilde{C}_{\mu i}^{(0,1)(0)} C_{j\mu}^{(0,1)(1)} + \tilde{C}_{\mu i}^{(0,1)(1)} C_{j\mu}^{(0,1)(0)} \right) \\
& - E_\mu^{(1)} \left(\sum_{ij} \tilde{C}_{\mu i}^{(0,1)(0)} C_{j\mu}^{(0,1)(0)} - 1 \right)
\end{aligned} \tag{14-36}$$

The Eqs. (14-35) and (14-36) give the energy and the first order energy derivative for the state μ. Because of stationarity of Lagrangian with respect to Λ and Ω, the above expressions are further simplified. The energy derivatives follow $(2n+1)$ rule with respect to the Ω amplitudes and $(2n+2)$ rule with respect to Λ amplitudes. There is a $(2n+1)$ rule for the eigenvectors $\tilde{C}^{(0,1)}$ and $C^{(0,1)}$ for evaluation of energy derivatives. With these, the expressions for Lagrangians given in Eqs. (14-35) and (14-36) simplify. We denote this simplified Lagrangian as $\Im_{\text{opt}}$.

$$\Im_{\text{opt}}^{(0)} = \left(\tilde{C}^{(0,1)(0)} H_{\text{eff}}^{(0,1)(0)} C^{(0,1)(0)}\right)_{\mu\mu} \tag{14-37}$$

$$\begin{aligned}\Im^{(1)}_{\text{opt}} = &\left(\tilde{C}^{(0,1)(0)} H^{(0,1)(1)}_{\text{eff}\Omega^{(0)}} C^{(0,1)(0)}\right)_{\mu\mu} \\ &+P^{(0,1)} \Lambda^{(0,1)(0)} \left[H^{(1)}\Omega^{(0)} - \Omega^{(0)} H^{(0,1)(1)}_{\text{eff}\Omega^{(0)}}\right] P^{(0,1)} \\ &+P^{(0,0)} \Lambda^{(0,0)(0)} H^{(1)} \Omega^{(0)} P^{(0,0)} \end{aligned} \tag{14-38}$$

The subscript $\Omega^{(0)}$ indicates that the derivative effective Hamiltonian does not contain any term formed from derivatives of the cluster amplitudes. The first order properties can thus be obtained simply with the knowledge of Ω and Λ amplitudes only.

14.3.3.2. Second Order Properties Using CVA-FSMRCC

Now, we differentiate the Lagrangian (Eq. 14-33) twice with respect to the external field.

$$\begin{aligned}\Im^{(2)} = &\left(\tilde{C}^{(0,1)(2)} H^{(0,1)(0)}_{\text{eff}} C^{(0,1)(0)}\right)_{\mu\mu} + \left(\tilde{C}^{(0,1)(1)} H^{(0,1)(1)}_{\text{eff}} C^{(0,1)(0)}\right)_{\mu\mu} \\ &+2\left(\tilde{C}^{(0,1)(1)} H^{(0,1)(0)}_{\text{eff}} C^{(0,1)(1)}\right)_{\mu\mu} + \left(\tilde{C}^{(0,1)(0)} H^{(0,1)(2)}_{\text{eff}} C^{(0,1)(0)}\right)_{\mu\mu} \\ &+\left(\tilde{C}^{(0,1)(0)} H^{(0,1)(1)}_{\text{eff}} C^{(0,1)(1)}\right)_{\mu\mu} + \left(\tilde{C}^{(0,1)(0)} H^{(0,1)(0)}_{\text{eff}} C^{(0,1)(2)}\right)_{\mu\mu} \\ &+P^{(0,1)} \Lambda^{(0,1)(2)} \left[H^{(0)}\Omega^{(0)} - \Omega^{(0)} H^{(0,1)(0)}_{\text{eff}}\right] P^{(0,1)} \\ &+P^{(0,1)} \Lambda^{(0,1)(1)} \left[H^{(1)}\Omega^{(0)} + H^{(0)}\Omega^{(1)} - \Omega^{(0)} H^{(0,1)(1)}_{\text{eff}} - \Omega^{(1)} H^{(0,1)(0)}_{\text{eff}}\right] P^{(0,1)} \\ &+P^{(0,1)} \Lambda^{(0,1)(0)} \left[H^{(2)}\Omega^{(0)} + H^{(1)}\Omega^{(1)} + H^{(0)}\Omega^{(2)}\right] P^{(0,1)} \\ &-P^{(0,1)} \Lambda^{(0,1)(0)} \left[\Omega^{(0)} H^{(0,1)(2)}_{\text{eff}} + \Omega^{(1)} H^{(0,1)(1)}_{\text{eff}} + \Omega^{(2)} H^{(0,1)(0)}_{\text{eff}}\right] P^{(0,1)} \\ &+P^{(0,0)} \Lambda^{(0,0)(2)} \left[H^{(0)}\Omega^{(0)}\right] P^{(0,0)} + P^{(0,0)} \Lambda^{(0,0)(1)} \left[H^{(1)}\Omega^{(0)} + H^{(0)}\Omega^{(1)}\right] P^{(0,0)} \\ &+P^{(0,0)} \Lambda^{(0,0)(0)} \left[H^{(2)}\Omega^{(0)} + H^{(1)}\Omega^{(1)} + H^{(0)}\Omega^{(2)}\right] P^{(0,0)} \\ &-E^{(0)}_{\mu} \sum_{ij} \left(\tilde{C}^{(0,1)(2)}_{\mu i} C^{(0,1)(0)}_{j\mu} + 2\tilde{C}^{(0,1)(1)}_{\mu i} C^{(0,1)(1)}_{j\mu} + \tilde{C}^{(0,1)(0)}_{\mu i} C^{(0,1)(2)}_{j\mu}\right) \\ &-E^{(1)}_{\mu} \sum_{ij} \left(\tilde{C}^{(0,1)(1)}_{\mu i} C^{(0,1)(0)}_{j\mu} + \tilde{C}^{(0,1)(0)}_{\mu i} C^{(0,1)(1)}_{j\mu}\right) \\ &-E^{(2)}_{\mu} \sum_{ij} \left(\tilde{C}^{(0,1)(0)}_{\mu i} C^{(0,1)(0)}_{j\mu} - 1\right) \end{aligned} \tag{14-39}$$

The $\Lambda^{(1)}$ containing terms in the above expressions vanish as they are the products of the $\Lambda^{(1)}$ with the derivative MRCC equations (Eqs. 14-15 and 14-16). Similarly, the $\Lambda^{(2)}$ containing terms are the MRCC equations multiplied to the $\Lambda^{(2)}$ equations and hence, vanish. Analogously, the $C^{(2)}$ and $\tilde{C}^{(2)}$ terms also vanish. With these cancellations, the energy second derivative equation reduces to the form which contains only undifferentiated Λ vectors and up to first derivatives of cluster amplitudes and eigen-

vectors. single-root nature of the CVA method, one has to obtain the Λ amplitudes separately for every state unlike the non-variational response of FSMRCC structure. However, the expensive evaluation of wave-function derivatives for each mode of perturbation is avoided in CVA-FSMRCC. This feature becomes more prominent while obtaining higher order properties like polarizability. Also, the single-root feature makes CVA more attractive for the cases like curve-crossing studies of excited states, etc. than the non-variational response method.

14.4. IMPLEMENTATIONS AND RESULTS AND DISCUSSIONS

In the initial implementation of the FSMRCC response for the first order properties Ajitha et al. used the formulation which involved explicit differentiation method as discussed in section III A. of the cluster amplitudes. Using this approach dipole moments of the OH, OOH, HCOO, CH , SiH and NO radicals [58–60]. However, this is not the efficient way of the calculation of molecular properties in particular higher order properties. The Z-vector method described in Section 14.3.2 was quite complicated in structure and has not been implemented yet for practical applications. On the other hand, Pal and co-workers have implemented most efficient approach in this article. CVA-FSMRCCSD has been implemented for the first and second order properties of the one valence radicals as well and N electron excited states [64–67]. Bag et al. have also implemented the third order property i.e. first hyperpolarizability for the one valence problem [69]. These implementations are presented in the references [64–67]. Taking the advantage of SEC, first the $(0,0)$ sector amplitudes are calculated. Before solving for the valence sector amplitudes, the $(He^{T^{(0,0)}})_c$, intermediates are calculated and stored these are denoted as $\bar{H}$. The closed part of $\bar{H}$, i.e. $\bar{H}_{cl}$ is the ground state energy. The open parts of $\bar{H}$ can be further classified into one body, two body, three body parts and so on. Under the singles and doubles (SD) approximation, only up to three body parts of $\bar{H}$ contribute to the $T^{(0,1)}$, $T^{(1,0)}$ and $T^{(1,1)}$ as well as to the $\Lambda^{(0,1)}$, $\Lambda^{(1,0)}$ and $\Lambda^{(1,1)}$ equations. Because of the large dimensions, the three body parts of the $\bar{H}$ cannot be stored in the hard disk. These are, therefore, evaluated in the code as and when required. The one and two-body parts of $\bar{H}$ are calculated only once and are stored. The equations for Λ amplitudes are linear simultaneous equations. However, unlike the T amplitudes Λ amplitudes follow reverse decoupling. Thus, first equations for the Λ amplitudes of the highest sector are solved, followed by the solution of the lower sectors of the Λ. The Jacobi iterative procedure has been used for the obtaining Λ amplitudes and the cluster amplitudes. The first derivatives of cluster amplitudes are obtained in the similar way using differentiated FSMRCC equations for cluster amplitude derivatives and derivative effective Hamiltonian. Taking the advantage of SEC, the derivative $\bar{H}$ are obtained and stored in the similar way. The terms arising from $\frac{\partial \Lambda \Omega H_{\text{eff}}}{\partial \Omega}$ in which, there is $\Lambda - \Omega$ contraction, have been merged together, since, the differentiation of Ω contained in Heff is structurally identical for these terms. The $\Lambda - \Omega$ contractions for these terms is programmed and stored in an array of dimensions of the

effective Hamiltonian, for computational simplicity. To validate the implementation of Lagrange based code for the (1,1) sector Pal and co-workers [66] implemented the non-relaxed finite field calculations for the first and second order properties. Each Fock space sector starting from (0,0) each sector results were checked with the analytic code till the desired accuracy.

14.4.1. Ionized and Electron Attached States

As mentioned earlier the lagrangian based constrained response approach was implemented for the ionized, electron attached and excited state first and second order properties [64–67]. For the one valence problem, the OH, OOH, HCOO, NO, NO_2, *CH*, and *SiH* radicals were studied. If the RHF of the closed shell anion is considered as a vacuum, the model space configuration of the radical belongs to the (0,1)/(1,0) sector of the Fock space. For the Hydroxy radical, results of the CVA FSMRCC method were compared with the EOMCC non-relaxed as well as Full CI results available. CC-pVDZ basis used was used for the calculation. The RHF of the of hydroxide was chosen as a vacuum and removal of the electron from HOO leads to degenerate doublet $^2\Pi$ state of the radical. The dipole moment result (0.634 au) was in good agreement with the FCI (0.663 au) as well as EOMCC (0.639 au) [64]. However, for polarizabilities no other results we available for the same. Manohar et al. compared analytic results with the non-relaxed finite field calculations. Analytic polarizability diagonal value along the inter-nuclear axis using CVA FSMRCC method yields 6.61 au which is in good agreement with the finite field results 6.0 au. Thus, it can be concluded that the effect of relaxation is marginal. The model space configurations of a radical belonging to this class corresponds to the (1,0) sector of the Fock space with the RHF of the corresponding cation as a vacuum. Two systems chosen in this category are CH and SiH radicals. For the dipole moment and polarizabilities of the CH and SiH, Sadlej basis optimized for the properties was used. For both the radicals CVAFSMRCC results were compared with finite field as well as UGA-CCSD results[70]. The dipole moment for CH radical was found to be 0.543 au using analytic FSMRCC, where as finite field FSMRCC was 0.520 au the UGA-CCSD gives 0.535 au. For SiH dipole moment was very small. The value using analytic FSMRCC was 0.063 au and UGA-CCSD (0.037 au) [70].

14.4.2. Excited State Dipole Moment and Polarizabilities

The excited state properties of CH^+, H_2O and Ozone have been computed using a reference space of one hole one particle excited determinants with respect to the restricted Hartree Fock of the ground state of the molecules as vacuum. The code for (1,1) FS sector was validated using non-relaxed finite field calculations for CH+ molecule [67]. Basis set convergence of the properties was also studied for the CH+ molecule. It was observed that both singlet and triplet state dipole moments increase from DZ to TZ basis, DZP to TZP basis and so on, but the trend is just opposite

for polarizabilities. It was observed that singlet dipole moments decrease with the addition of polarization functions, where as triplet dipole moments increase with the addition of polarization functions. However, polarizabilities of both singlet and triplet states increase with the addition of polarization functions. The dipole moments and polarizabilities of both the states virtually converged after the addition of a second polarization function. The adiabatic excited state dipole moment and polarizabilities for the water and ozone were also studied by the method [66].

ACKNOWLEDGMENTS

One of us (SP) acknowledges partial financial assistance from J. C. Bose Fellowship grand of DST and Shanti Swarup Bhatnagar (SSB) prize grant of CSIR towards this work. Authors also acknowledge Center of Excellence at N.C.L Pune.

REFERENCES

1. J. Čížek, Adv. Quantum Chem. **14**, 35 (1969); R. J. Bartlett, Annu. Rev. Phys. Chem. **32**, 359 (1981); J. Paldus, in *Methods in Computational Molecular Physics*, NATO ASI Series B, Eds. S. Wilson, G. H. F. Diercksen (Plenum, New York, 1992)
2. T. Helgaker, P. Jørgensen, Adv. Quantum Chem. **19**, 183 (1988)
3. R. J. Bartlett, in *Geometrical Derivatives of Energy Surface and Molecular Properties*, Eds. P. Jørgensen, J. Simons (Reidel, Dordrecht, 1986)
4. E. A. Salter, G. Trucks, R. J. Bartlett, J. Chem. Phys. **90**, 1752 (1989); E. A. Salter, R. J. Bartlett, J. Chem. Phys. **90**, 1767 (1989)
5. S. Pal, M. D. Prasad, D. Mukherjee, Theor. Chim. Acta **62**, 523 (1983)
6. N. Vaval, S. Pal, Phys. Rev. A **54**, 250 (1996); N. Vaval, A. B. Kumar, S. Pal, Int. J. Mol. Sci. **2**, 89 (2001); P. U. Manohar, N. Vaval, S. Pal, Chem. Phys. Lett. **387**, 442 (2004)
7. J. Gauss, J. F. Stanton, J. Chem. Phys. **104**, 2574 (1996); T. Helgaker, M. Jaszunski, K. Ruud, Chem. Rev. **99**, 293 (1999)
8. H. J. Monkhorst, Int. J. Quantum Chem. **S11**, 421 (1977)
9. R. J. Bartlett, J. Noga, Chem. Phys. Lett. **150**, 29 (1988); R. J. Bartlett, S. A. Kucharski, J. Noga, Chem. Phys. Lett. **155**, 133 (1989)
10. S. Pal, K. B. Ghosh, Curr. Sci. **63**, 667 (1992)
11. J. S. Arponen, Ann. Phys. **151**, 311 (1983); J. S. Arponen, R. F. Bishop, E. Pajanne, Phys. Rev. A **36**, 2519 (1987)
12. T. V. Voorhis, M. Head-Gordon, Chem. Phys. Lett. **330**, 585 (2000); M. Head-Gordon, T. V. Voorhis, J. Chem. Phys. **113**, 8873 (2000)
13. L. Adamowicz, W. D. Ladig, R. J. Bartlett, Int. J. Quantum Chem. Symp. **18**, 245 (1984)
14. N. C. Handy, H. F. Scaefer III, J. Chem. Phys. **81**, 5031 (1984)
15. P. Jørgensen, T. Helgaker, J. Chem. Phys. **89**, 1560 (1988)
16. T. Helgaker, P. Jørgensen, Theor. Chim. Acta **75**, 111 (1989)
17. H. Koch, H. J. Aa. Jensen, P. Jørgensen, T. Helgaker, G. E. Scuseria, H. F. Schaefer III, J. Chem. Phys. **92**, 4924 (1990)
18. H. Koch, P. Jørgensen, J. Chem. Phys. **93**, 3333 (1990)
19. D. Mukherjee, I. Lindgren, Phys. Rep. **151**, 93 (1987)
20. D. Mukherjee, S. Pal, Adv. Quantum Chem. **20**, 291 (1989)

21. P. Durand, J. P. Malrieu, Adv. Chem. Phys. **67**, 321 (1987)
22. V. Hurtubise, K. F. Freed, Adv. Chem. Phys. **83**, 465 (1993)
23. P. Durand, J. P. Malrieu, Adv. Chem. Phys. **67**, 321 (1987); S. Evangelisti, J. P. Daudey, J. P. Malrieu, Phys. Rev. A **35**, 4930 (1987)
24. L. Meissner, K. Jankowski, J. Wasilewski, Int. J. Quantum Chem. **34**, 535 (1988); L. Meissner, Chem. Phys. Lett. **255**, 244 (1996); L. Meissner, J. Chem. Phys. **108**, 9227 (1998)
25. S. Chattopadhyay, U. Sinha Mahapatra, B. Datta, D. Mukherjee, Chem. Phys. Lett. **357**, 426 (2002)
26. D. Mukherjee, Pramana **12**, 203 (1979)
27. H. Reitz, W. Kutzelnigg, Chem. Phys. Lett. **66**, 11 (1979); W. Kutzelnigg, J. Chem. Phys. **77**, 3081 (1981)
28. M. Haque, U. Kaldor, Chem. Phys. Lett. **117**, 347 (1985), **120**, 261 (1985)
29. I. Lindgren, Phys. Scr. **32**, 291 (1985)
30. D. Mukherjee, Proc. Ind. Acad. Sci. **96**, 145 (1986), Chem. Phys. Lett. **125**, 207 (1986), Int. J. Quantum Chem. Symp. **20**, 409 (1986)
31. B. Jezioroski, H. J. Monkhorst, Phys. Rev. A **24**, 1668 (1982); A. Balkova, S. A. Kucharski, L. Meissner, R. J. Bartlett, J. Chem. Phys. **95**, 4311 (1991)
32. D. Sinha, S. Mukhopadhyay, D. Mukherjee, Chem. Phys. Lett. **129**, 369 (1986)
33. S. Pal, M. Rittby, R. J. Bartlett, D. Sinha, D. Mukherjee, Chem. Phys. Lett. **137**, 273 (1987)
34. I. Lindgren, D. Mukherjee, Phys. Rep. **151**, 93 (1987)
35. S. Pal, M. Rittby, R. J. Bartlett, D. Sinha, D. Mukherjee, J. Chem. Phys. **88**, 4357 (1988)
36. D. Mukherjee, S. Pal, Adv. Quantum. Chem. **20**, 291 (1989)
37. R. J. Bartlett, J. F. Stanton, in *Reviews in Computational Chemistry*, vol. 5, Eds. K. B. Lipkowitz, D. B. Boyd (VCH, New York, 1994), p. 65
38. J. Geertsen, M. Rittby, R. J. Bartlett, Chem. Phys. Lett. **164**, 57 (1989); D. C. Comeau, R. J. Bartlett, Chem. Phys. Lett. **207**, 414 (1993)
39. D. C. Comeau, R. J. Bartlett, Chem. Phys. Lett. **207**, 414 (1993)
40. J. F. Stanton, R. J. Bartlett, J. Chem. Phys. **98**, 7029 (1993)
41. J. F. Stanton, J. Gauss, J. Chem. Phys. **101**, 8938 (1994)
42. M. Nooijen, R. J. Bartlett, J. Chem. Phys. **102**, 3629 (1995), **102**, 6735 (1995)
43. A. I. Krylov, Ann. Rev. Phys. Chem. **59**, 433 (2008)
44. H. Koch, P. Jørgensen, J. Chem. Phys. **93**, 3345 (1990)
45. H. Nakatsuji, O. Kitao, M. Komori, in *Aspects of Many Body Effects in Molecules and Extended Systems*, Lecture Notes in Chemistry, vol. 50, Ed. D. Mukherjee (Springer-Verlag, Heidelberg, 1989), p. 101
46. H. Nakatsuji, K. Hirao, J. Chem. Phys. **68**, 2053 (1978); H. Nakatsuji, Chem. Phys. Lett. **67**, 324 (1979), **67**, 329 (1979); K. Hirao, Y. Hatano, Chem. Phys. Lett. **111**, 533 (1984); K. Hirao, J. Chem. Phys. **83**, 1433 (1985), Theor. Chim. Acta **71**, 231 (1987); H. Wasada, K. Hirao, Chem. Phys. Lett. **139**, 155 (1987); H. Nakatsuji, K. Hirao, Y. Mizukami, Chem. Phys. Lett. **179**, 555 (1991)
47. M. Nooijen, R. J. Bartlett, J. Chem. Phys. **102**, 291 (1995)
48. J. D. Watts, R. J. Bartlett, Chem. Phys. Lett **233**, 81 (1995)
49. M. Nooijen, R. J. Bartlett, J. Chem. Phys. **106**, 6449 (1997); M. Nooijen, R. J. Bartlett, J. Chem. Phys. **107**, 6812 (1997)
50. A. I. Krylov, Chem. Phys. Lett. **338**, 375 (2001); A. I. Krylov, Acc. Chem. Res. **39**, 83 (2006)
51. R. J. Bartlett, in *Modern Electronic Structure Theory, Part II*, Advanced Series in Physical Chemistry, vol. 2, Ed. D. R. Yarkony (World Scientific, Singapore, 1995), p. 1047
52. M. Nooijen, R. J. Bartlett, J. Chem. Phys. **106**, 6441 (1997), **107**, 6812 (1997); S. R. Gwaltney, R. J. Bartlett, M. Nooijen, J. Chem. Phys. **111**, 58 (1999)

53. M. Wladyslawski, M. Nooijen, in *Low-Lying Potential Energy Surfaces*, ACS Symposium Series, vol. 828, Eds. M. R. Hoffmann, K. G. Dyall (ACS, Washington, DC, 2002), pp. 65–92; M. Tobita, S. A. Perera, M. Musial, R. J. Bartlett, M. Nooijen, J. S. Lee, J. Chem. Phys. **119**, 10713 (2003); A. I. Krylov, Ann. Rev. Phys. Chem. **59**, 433 (2008)
54. J. F. Stanton, J. Chem. Phys. **99**, 8840 (1993)
55. J. F. Stanton, J. Gauss, J. Chem. Phys. **103**, 88931 (1995)
56. S. R. Gwaltney, R. J. Bartlett, M. Nooijen, J. Chem. Phys. **111**, 58 (1999)
57. S. Pal, Phys. Rev. A **39**, 39 (1989), Int. J. Quantum. Chem. **41**, 443 (1992)
58. D. Ajitha, S. Pal, Phys. Rev. A **56**, 2658 (1997), Chem. Phys. Lett. **309**, 457 (1999), J. Chem. Phys. **114**, 3380 (2001)
59. D. Ajitha, N. Vaval, S. Pal, J. Chem. Phys. **110**, 2316 (1999)
60. D. Ajitha, S. Pal, J. Chem. Phys. **114**, 3380 (2001)
61. P. Szalay, Int. J. Quantum. Chem. **55**, 151 (1995)
62. K. R. Shamasundar, S. Asokan, S. Pal, J. Chem. Phys. **120**, 6381 (2004)
63. K. R. Shamasundar, S. Pal, Int. J. Mol. Sci. **3**, 710 (2002)
64. P. U. Manohar, N. Vaval, S. Pal, J. Mol. Struct. (THEOCHEM) **768**, 91 (2006); P. U. Manohar, S. Pal, Chem. Phys. Lett. **438**, 321 (2007)
65. P. U. Manohar, S. Pal, AIP Conference Proceedings, Computational Methods in Science and Engineering: Theory and Computation: Old Problems and New Challenges **963**, 337 (2007)
66. A. Bag, P. U. Manohar, N. Vaval, S. Pal, J. Chem. Phys. **131**, 024102 (2009)
67. A. Bag, P. U. Manohar, S. Pal, Comp. Lett. **3**, 351 (2007)
68. A. Dalgarno, A. L. Stewart, Proc. R. Soc. Lond. A **238**, 269 (1957)
69. A. Bag, S. Bhattacharyay, S. Pal, in Recent Advances in Spectroscopy: Astrophysical, Theoretical and Experimental perspectives (in press)
70. X. Li, J. Paldus, in *Recent Advances in Computational Chemistry, Recent Advances in Coupled-Cluster Methods*, vol. 3, Ed. R. J. Bartlett (World Scientific, Singapore, 1997), p. 183
71. J. F. Stanton, R. J. Bartlett, J. Chem. Phys. **98**, 7029 (1993); J. Stanton, J. Gauss, J. Chem. Phys. **101**, 8938 (1994)
72. I. Lindgren, J. Morrison, in *Atomic Many-Body Theory* (Springer-Verlag, Berlin, 1982)

CHAPTER 15

INTERMEDIATE HAMILTONIAN FORMULATIONS OF THE FOCK-SPACE COUPLED-CLUSTER METHOD: DETAILS, COMPARISONS, EXAMPLES

LESZEK MEISSNER[1] AND MONIKA MUSIAŁ[2]

[1] *Institute of Physics Nicholas Copernicus University, 87-100 Toruń, Poland, e-mail: meissner@fizyka.umk.pl*

[2] *Institute of Chemistry University of Silesia, 40-006 Katowice, Poland e-mail: monika.musial@us.edu.pl*

Abstract: The single-reference approaches such as many-body perturbation expansions and coupled-cluster methods, have been very successful in describing many-particle systems. Their applicability is, however, limited to the cases when the degree of quasi-degeneracy is rather weak. Unfortunately, their generalization to multi-reference cases, that would enable us to deal efficiently with quasi-degenerate and open-shell systems turned out nontrivial. The difficulties that have been encountered are of both theoretical and numerical nature. In spite of tremendous progress that has been made the problem still remains one of the main challenges for theoretical physics and quantum chemistry. In this paper we present one of the developments that, in our opinion, is very promising. It concerns one of the two basic multi-reference coupled-cluster formulations, namely, the so-called Fock-space coupled-cluster method. We would like to show that by employing the intermediate Hamiltonian technique it is possible to overcome many of the problems the standard effective Hamiltonian formulations have to face. The approach is presented in a broader context, relations with other methods of similar type are discussed and some numerical examples showing the effectiveness of the method are presented.

Keywords: Multireference coupled cluster, Fock space, Intermediate Hamiltonian

15.1. INTRODUCTION

The single-reference (SR) methods for describing electron correlation effects are now being used in routine calculations [1]. Among them the coupled-cluster (CC) method [2–4] has proved to be the most powerful tool for the treatment of electron correlation especially when high accuracy results are required [5–7]. However, the applicability of the single-reference approaches is limited to the cases when a single determinant gives reliable zeroth-order approximation to the wave function. In order to be able to describe quasi-degenerate and open-shell systems a generalization

P. Čársky et al. (eds.), Recent Progress in Coupled Cluster Methods, 395–428.
DOI 10.1007/978-90-481-2885-3_15,

of the SR methods to a multi-reference (MR) case is required. Only for very few methods this generalization is straightforward and easy, like, for example, for the configuration interaction (CI) method. The MR generalization of CI retains formal and computational simplicity of its SR counterpart and is one of very few MR methods that are routinely used in calculations. The reason is that both dynamic and nondynamic electron correlation effects are treated in the same manner in the CI wave function, i.e. via linear expansion. For approaches that use other expansion than the linear one for describing dynamic correlation the generalization turned out non-trivial. That concerns, first of all, many-body perturbation [8, 9] and CC expansions [10–14]. The necessity of employing two different ways for determination of both types of electron correlation calls for two-step procedures and such a procedure is provided by the effective Hamiltonian formalism [15–19]. Here the first step is the determination of the wave operator that describes dynamic correlation effects while the second step gives non-dynamic correlation contributions to the energies via diagonalization of the effective Hamiltonian. Unfortunately, within the effective Hamiltonian formulation eigenvalue problems for several states are coupled and that requires to consider them simultaneously. That makes schemes based on the effective Hamiltonian approach numerically demanding.

It is essential for the CC methods to have excitations described thought second-quantized operators and for that the Fermi vacuum must be chosen. While in the SR-case the natural selection is the reference determinant, there is no such an obvious choice in the MR case. Two different strategies in selecting Fermi vacuum resulted in two basic versions of MR-CC formulations. The first one is the so-called Fock-space (FS) CC method that follows the strategy of having one Fermi vacuum [10–12], the other defines different Fermi vacua for excitations from different reference determinants and is known as the Hilbert-space CC method [13, 14]. The FS-CC approach seems well suited for description of open shell systems and calculation of excitation energies and is the main focus of our paper.

Besides of the difficulties in formulating MR-CC approaches described above, the MR-CC methods have faced many problems in their practical applications. The effectiveness of iterative procedures for solving equations for cluster amplitudes depends much on clear separation of dynamic and non-dynamic correlation effects [20–22]. Cluster operators that generate contributions from the orthogonal space while acting on the reference space should be, in principle, responsible for description of the dynamic part of correlation. Thus wave functions of all states described by the effective Hamiltonian should be dominated by the reference space contribution and that can be difficult to satisfy in many practical situations. If the requirement is not satisfied then we have to deal with the problem of large amplitudes that can hurt convergence of iterative schemes employed. It is known that the CC expansion can handle even a large contribution of non-dynamic correlation. Examples are given by the SR-CC schemes that are capable of providing quite good results even when the degree of quasi-degeneracy is not so low [23]. However, iterative schemes, especially those based on Jacobi-type methods seem less effective in dealing with multi-reference situations. The reason is that these situations are more complex than

the SR ones where we have only one state to describe. The MR-CC applications are frequently plagued with the so-called intruder state problem [20, 21] or problem of multiple solutions [22].

In the following we show how the intermediate Hamiltonian (IH) [19, 24] reformulation of the Fock-space CC method eliminates many drawbacks of the standard effective Hamiltonian FS-CC formulation. The reason for concentrating on the FS-CC approach is that some specific features of the method allow us to obtain very simple and at the same time numerically efficient scheme for solving the FS-CC equations [25, 26]. Over the last several years different variants of the FS-CC method have been reformulated using the intermediated Hamiltonian technique. The one designated for description of quasi-degenerate ground states has been implemented and applied to the beryllium atom [27]. The Be atom is a well-known example of the failure of the traditionally formulated FS-CC method caused by intruder states [20, 21]. Only with the help of the Newton–Raphson iterative method the equations have been finally solved after many years of unsuccessful attempts [28]. The Newton–Raphson method is, however, numerically demanding thus its applicability is very limited. With our intermediate Hamiltonian version of FS-CC method we are able to obtain not only the so-called standard FS-CC solutions for Be but also alternative ones without any problem. The other variant of the IH FS-CC method that has been implemented is the one that is convenient for direct calculations of vertical excitation energies from the closed-shell ground state [29]. Two levels of approximation are now available, the basic one that includes one- and two-body components in the cluster operator (CCSD) [26, 30] and the one that also contains the three-body part (CCSDT) [31].

The next section is devoted to multi-reference approaches. Some aspects of the situation when single reference determinant must be replaced with the combination of several reference determinants to obtain a reliable zeroth-order approximation to the wave function are discussed. That leads to the concept of effective Hamiltonian. The subsequent section describes basics of the standard effective Hamiltonian FS-CC method in its version designed for excitation energy calculations. Then the intermediate Hamiltonian scheme is introduced through similarity transformations of the Hamiltonian. Besides the IH FS-CC version used by us so far [26, 27, 30] also another possible variant of the method is presented. Next we present an alternative route to the IH FS-CC formulation that perhaps is not so appealing as that using similarity transformations but might be very instructive to show the link between connected form of the FS-CC equations and the IH FS-CC matrix. The staring point is the standard FS-CC equations expressed through connected diagrams. We show a method of transforming connected FS-CC equations to the so-called canonical form. The canonical form allows us to reduce the problem of solving the FS-CC equations to the eigenvalue problem of a certain operator that can be identified as the intermediate Hamiltonian [32]. Finally some numerical examples are presented demonstrating numerical efficiency of the IH technique as well as the performance of the FS-CC method on both CCSD and CCSDT levels of approximation.

15.2. MULTI-REFERENCE APPROACHES

Single-reference approaches can be successfully applied when the wave function is dominated by a single determinant usually the Hartree–Fock one. If this is not the case then we have to use several determinants ($\Phi_i,\ i = 1,\ldots,m$) to construct a reliable zeroth-order approximation to the wave function. The single reference determinant Φ must be replaced with the linear combination of several determinants

$$\tilde{\Psi} = \sum_{i=1}^{m} c_i \Phi_i. \tag{15-1}$$

Usually the combination contains not only determinants that are important to create the good zeroth-order description but also those necessary to have the so-called complete active space (CAS). Orbitals that are used to construct CAS function are partitioned into two categories, The first one consists of those which are occupied in all Φ_i while the second one contains the so-called active orbitals that are occupied in some but not all of them. To have CAS all possible occupancies of active orbitals must be allowed in the set of Φ_i. Having $\tilde{\Psi}$ one can try to generate the exact wave function Ψ in a way similar to that in the single-reference case, i.e., by employing the wave operator Ω

$$\Psi = \Omega\tilde{\Psi}. \tag{15-2}$$

The difference here is that the reference function $\tilde{\Psi}$ is not completely determined since the linear combination of Φ_i contains unknown coefficients c_i. One can consider several options. The first one is to obtain the c_i coefficients, for example, from diagonalization of the matrix representation of the Hamiltonian H within the space spanned by reference determinants Φ_i. That would fix $\tilde{\Psi}$ and make the problem more similar to that in the single-reference case. However, a closer look at excitations that must be included in the wave operator Ω to reproduce the part of the exact wave function Ψ that is orthogonal to the reference component $\tilde{\Psi}$ shows that the situation is not so simple. Since active orbitals are occupied in some but unoccupied in other Φ_i determinants then excitation operators can produce linearly dependent contributions and this linear dependence must then be eliminated. Moreover, also the so-called internal excitations that lead to other combinations of reference determinants must be admitted . That can cause problems when we deal with degenerate or nearly degenerate situations. In spite of these difficulties some approaches based on this scheme have been developed like, for example, the CC method by Banerjee and Simons [33], internally contracted CI methods [34], perturbative approaches [35], in particular the CAS PT2 method [36]. It follows that it would be convenient to exclude internal excitations by leaving the c_i coefficients in Eq. (15-1) to be determined. In this way the full similarity to the single-reference case is lost but

only external excitations must be considered. If so then the wave function can be expressed as

$$\Psi = \sum_{i=1}^{m} c_i \Phi_i + \sum_{i=1}^{m} X c_i \Phi_i = (1+X) \sum_{i=1}^{m} c_i \Phi_i, \tag{15-3}$$

where the X operator generates external excitations only so they must involve at least one inactive unoccupied or core (occupied in all determinants Φ_i) spin orbital. Inserting this form of Ψ to the Schrödinger equation

$$H(1+X) \sum_{i=1}^{m} c_i \Phi_i = E(1+X) \sum_{i=1}^{m} c_i \Phi_i, \tag{15-4}$$

and projecting on the M_0 space spanned by the reference determinants Φ_i and on its orthogonal complement $M_\perp$ we have

$$P_0 H(1+X) P_0 \sum_{i=1}^{m} c_i \Phi_i = E P_0 \sum_{i=1}^{m} c_i \Phi_i, \tag{15-5}$$

$$Q H(1+X) P_0 \sum_{i=1}^{m} c_i \Phi_i = E Q X P_0 \sum_{i=1}^{m} c_i \Phi_i, \tag{15-6}$$

where P_0 and Q are projection operators on M_0 and $M_\perp$, respectively. The quantities to determine are $X \equiv QXP_0$, c_i and the energy E. There are several ways one can proceed. First, one may find attractive to eliminate X from Eq. (15-5) by determining it from Eq. (15-6). From Eq. (15-6) we have

$$QXP_0 \tilde{\Psi} = Q[P_0 + Q(E-H)Q]^{-1} QHP_0 \tilde{\Psi}. \tag{15-7}$$

Now, inserting Eqn.(15-7) into Eqn.(15-5) we obtain

$$P_0 \{H + HQ[P_0 + Q(E-H)Q]^{-1} QH\} P_0 \tilde{\Psi} = E \tilde{\Psi}. \tag{15-8}$$

This is a pseudo-eigenvalue problem since the operator

$$P_0 \{H + HQ[P_0 + Q(E-H)Q]^{-1} QH\} P_0, \tag{15-9}$$

depends on one of its eigenvalues. The action of the operator is restricted to the reference space M_0. This pseudo-eigenvalue equation must be solved iteratively because of the energy dependence. Starting with some initial guess for the energy the operator (15-9) can be diagonalized providing a set of eigenvalues from which one must be selected for the subsequent iteration. The procedure is continued till convergence. In the final set of eigenvalues only one of them represents the solution of the

Schrödinger equation the remaining ones are a by-product of the procedure. It is seen that the scheme involves the inversion of matrix representation of $Q(E-H)Q$ thus may not be found numerically very attractive here but it has been frequently used in some specific situations. The method has been proposed by Löwdin and it is known as the partitioning technique [37]. The partitioning technique can provide many solutions of the Schrödinger equation but for each of them a separate calculation is required.

The partitioning technique is state specific, i.e. the calculation is performed for one selected state at a time. Another technique that is quite similar in this respect is the so-called Brillouin–Wigner-type approach [38] in which instead of inverting the $Q(E-H)Q$ matrix the idea of solving eigenvalue dependent Eq. (15-6) in an iterative manner is used. Indeed, from Eq. (15-6) we have

$$[QHP_0 + Q(H-E)QXP_0]\tilde{\Psi} = 0, \tag{15-10}$$

that together with Eq. (15-5) form a set of equations suitable for an iterative scheme. When the Hamiltonian is partitioning into the zeroth-order part H_0 and the perturbation V

$$H = H_0 + V, \tag{15-11}$$

and assuming that determinants spanning the space are eigenvectors of H_0 we have

$$QXP_0 = \frac{Q}{E-H_0} V(1+X)P_0. \tag{15-12}$$

Now the coupled set of Eqs. (15-12) and (15-5) can be used for solving for X and E. X obtained from Eq. (15-12) is energy-dependent and so is the $P_0H(1+X)P_0$ operator in Eq. (15-5). Diagonalization of the latter again provides only one meaningful eigenvalue. This approach is used in the so-called multi-reference Brillouin–Wigner coupled cluster method [39]. There are several characteristic features of this scheme. First, the number of unknowns in X exceeds the number of parameters required for determination of only one energy. This is associated with the above mentioned problem of linear dependence of excitation operators which is manifested here by the fact that the same orthogonal space ($M_\perp$) determinant can be reached by excitations from each reference function Φ_i. In fact, the number of parameters in X would be sufficient for determining wave functions for $m = \dim M_0$ states but here, because of the state-dependence of X, only single-state description is obtained. On the other hand it can be seen that the set of equations (15-12) is decoupled into subsets corresponding to different reference determinants Φ_i so in each iteration the QXP_i components, where P_i is the projection on Φ_i, can be calculated separately. All of them are coupled, however, by Eq. (15-5) that provides updated energy for the next iterative step. It should be noted that this energy dependence usually leads to size-inextensivity of approximate schemes originating from this approach.

It is seen from the above that the number of parameters in X is sufficient to describe several states at a time or more precisely $m = \dim M_0$ states. Hence, let us consider such a set of m states with the wave functions Ψ_j $(j = 1, \ldots, m)$ dominated by the reference space determinants. We have

$$H\Psi_j = E_j\Psi_j. \tag{15-13}$$

Introducing the model functions

$$\tilde{\Psi}_j = \sum_{i=1}^{m} c_i^j \Phi_i, \tag{15-14}$$

and imposing the intermediate normalization condition

$$\langle \Psi_j | \tilde{\Psi}_j \rangle = \langle \tilde{\Psi}_j | \tilde{\Psi}_j \rangle = 1, \tag{15-15}$$

we have

$$\Psi_j = (1 + X)\tilde{\Psi}_j, \quad (j = 1, \ldots, m), \tag{15-16}$$

and

$$H(1 + X)\tilde{\Psi}_j = E_j(1 + X)\tilde{\Psi}_j, \quad (j = 1, \ldots, m). \tag{15-17}$$

Projection of the equation on M_0 and $M_\perp$ gives

$$P_0H(1 + X)P_0\tilde{\Psi}_j = E_jP_0\tilde{\Psi}_j, \tag{15-18}$$

$$Q[H(1 + X) - XE_j]P_0\tilde{\Psi}_j = 0. \tag{15-19}$$

Now, unlike the previous case, the $P_0H(1 + X)P_0$ that acts within the M_0 space provides m exact eigenvalues of H. The operator is called the effective Hamiltonian

$$H_{\mathit{eff}} = P_0H(1 + X)P_0. \tag{15-20}$$

and its eigenvectors are $\tilde{\Psi}_j$. The effective Hamiltonian allows us to remove the energy dependence from the equations. Assuming that $\tilde{\Psi}_j$ are linearly independent Eq. (15-19) can be written as

$$Q[H(1 + X) - XP_0H(1 + X)]P_0 = 0. \tag{15-21}$$

Eq. (15-21) is quadratic in X and can be solved for X iteratively. Having X, the effective Hamiltonian (15-20) can be constructed and its eigenvalues obtained.

The effective Hamiltonian formalism gives us opportunity to deal efficiently with the linear-dependence problem that appears when the orthogonal space component has to be generated by excitation operator from the multi-determinantal reference function. The obvious disadvantage of the approach is the necessity of solving the eigenvalue problem of H for several states at a time which makes calculations very expensive. Moreover, for the success of methods based on the effective Hamiltonian formulation it is important to have components from M_0 significant in all Ψ_j thus X small and easy to find in iterative procedures. That can be difficult to achieve in practical applications and can cause convergence problems. Usually along with this the problem of so-called intruder states appears meaning that there is an additional state that also tends to be described by the method. This is because Eq. (15-21) can have many different solutions for X. The one that leads to the desired subset $\{E_j\}_{j=1}^{m}$ of all eigenvalues of H is only one of them.

In the following we discuss multi-reference CC approaches that employ the effective Hamiltonian technique. The focus is on the Fock-space CC method. We show how serious disadvantages of the effective Hamiltonian formulation can be overcome by reformulating the method using the concept of intermediate Hamiltonian.

15.3. MULTI-REFERENCE FOCK-SPACE COUPLED-CLUSTER METHOD

For the CC approaches it is essential to express excitation operators in the second-quantized form and for that the choice of Fermi vacuum must be made. In the single-reference case the Hartree–Fock determinant is the obvious choice for the vacuum. In multi-reference situations there is no such a natural selection and basically two strategies can be followed. The first one is to define one Fermi vacuum for excitations from all Φ_i. This is historically the older concept that can be seen quite sensible when atomic and nuclear systems are considered. For them the core determinant built from spin orbitals that are occupied in all Φ_i seems natural. On the other hand when looking at Eq. (15-21) another possibility can be seen. That is when different Fermi vacua are defined for excitations originating from different Φ_i. That can make the MR-CC equations corresponding to each reference determinant quite similar to that in the SR-case. The main deference is caused by the second term in (15-21), the so-called renormalization term, that couples equations corresponding to different Φ_i. Both strategies have their advantages and drawbacks. For example, the common vacuum leads to a universal X operator meaning that again there are many different many-body excitation operators that, while acting on a particular reference determinant, lead to the same excited function and introduction of additional equations is necessary to solve the problem. Also the second choice has its disadvantages. For example, excitation operators of the same excitation-rank generate different spaces while acting on different Φ_i which in many cases unable us to obtain wave functions of proper spin-symmetry [40].

In this paper the focus is on the first kind of MR-CC developments, i.e. those based on the common Fermi vacuum. This general idea does not assume any specific choice for the vacuum and various options can be considered. The most obvious is to use the core determinant. Another possibility for the Fermi vacuum has been considered by Lindgren [12, 41] and then, more extensively, by Haque and Mukherjee, and others [29, 42, 43]. The aim was to obtain a method suitable for calculation of excitation energies from the closed-shell ground state. Thus, like in the single-reference ground state calculation, the Hartree–Fock determinant Φ for the neutral system is used for the vacuum but both hole and particle levels are additionally partitioned into two categories of active and inactive ones (Figure 15-1). The reference space determinants are now obtained by creating k particles and l holes on active orbital levels in all possible ways. The reference space spanned by such determinants is usually denoted by $M_0^{(k,l)}$. For excited states dominated by singly excited determinants the reference space determinants should be all those having one active hole and one active particle and that was considered as a primary application of the approach [12, 41].

Let us assume that we are interested in the above mentioned (1, 1) case. To generate reference determinants spanning the $M_0^{(1,1)}$ space we have to act with a pair of particle-hole creation operators on the Hartree–Fock determinant that create one active hole and one active particle. Excitations giving outer space contributions are

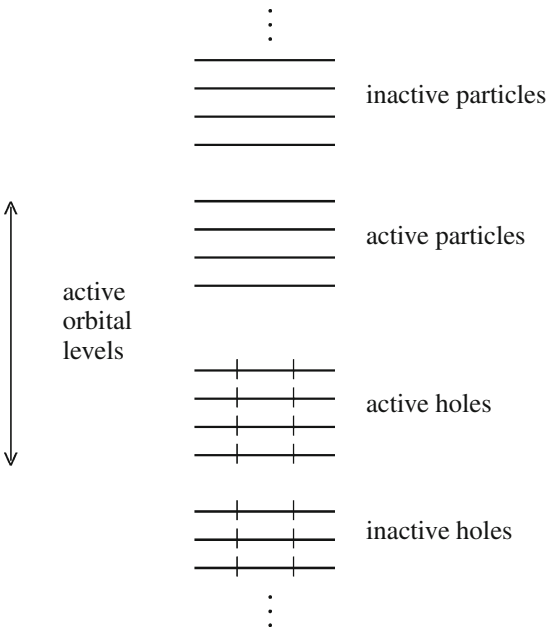

Figure 15-1. Classification of the orbital levels in the Fock-space coupled-cluster approaches designated for excitation energy calculations

defined as second-quantized operators in the normal-ordered form with respect to the Fermi vacuum. They can contain at most two active particle-hole annihilation operators. This is because they can annihilate only one active hole and one active particle that are used to create the reference functions. We can have three types of excitation operators: (i) having no particle-hole annihilation operators, (ii) having one such an operator and here two cases can be considered, annihilation of active particle or of active hole, (iii) having a pair of annihilation operators, one annihilating active particle and another one annihilating active hole. The particle-hole creation operators generate excited states. It is convenient to use graphical representation for second-quantized normal-ordered excitation operators. Their diagrams can be found in Figure 15-2. For details of diagrammatic techniques we refer, for example, to Ref. [44]. Each diagram has a vertex that is associated with the matrix element of a given operator, oriented lines represent annihilation and creation operators defined with respect to the physical vacuum. Outgoing and incoming lines are used for creation and annihilation operators, respectively. Up-going lines are of particle character while down-going ones are hole lines. Particle-hole creation operators are represented by oriented lines above the vertex while lines below the vertex are those corresponding to particle-hole annihilation operators. It follows that our excitation operators can have at most two lines at the bottom and they all must be active which is marked by double arrows. The excitations are particle-conserving operators so the number of incoming lines equals the number of outgoing lines. Particle-hole creation operators (above the vertex) are responsible for generating outer space functions so if their number is equal to the number of particle-hole annihilation operators they cannot be exclusively active. Up to two-body contributions to excitation operators are depicted in Figure 15-2 and they are partitioned according to the categories discussed above. They are denoted by $\bar{S}^{(k,l)}$ where k and l correspond to the number of active particle annihilation and active hole annihilation lines in the diagram, respectively. Also a subscript is sometimes added to denote the body-rank of the operator. One can notice that the one-body part that contains only particle-hole annihilation operators is missing in $\bar{S}^{(1,1)}$. Such a contribution should be included since the excitation leads to the Hartree–Fock determinant that does not belong to the reference functions. However, it can be proved that such an operator is not necessary for the CC excitation energy calculation in spite of the fact that it can be required for obtaining the wave function of excited state. Thus we exclude the Hartree–Fock determinant from the orthogonal space determinants and address the problem later on.

Having the excitation operators defined one can try to use them to construct a coupled-cluster-type of expansion. The usual way is to use them in the exponent

$$\exp(\bar{S})P_0^{(1,1)}, \quad \bar{S} = \bar{S}^{(0,0)} + \bar{S}^{(1,0)} + \bar{S}^{(0,1)} + \bar{S}^{(1,1)}, \tag{15-22}$$

where $P_0^{(1,1)}$ is the projection operator on $M_0^{(1,1)}$. However, the structure of the exponential expansion becomes very complicated because second-quantized $\bar{S}$ operators can be contracted with other $\bar{S}$ operators in the expansion. The normal-ordered form of $\exp(\bar{S})P_0^{(1,1)}$ can be made simpler when the $\bar{S}$ operators are redefine to obtain

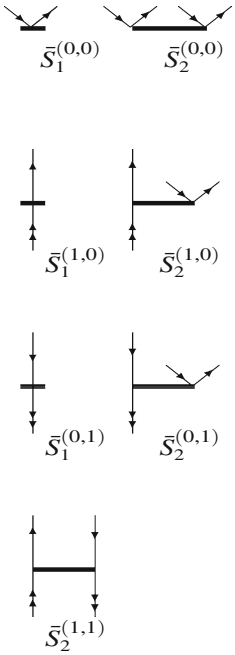

Figure 15-2. Graphical representation of cluster amplitudes $\bar{S}$. Diagrams are partitioned into categories according to the number of active lines at the bottom for which *double arrow* is used . The *superscript* (m, n) stands for the number of the active particle lines and the number of the active hole lines, respectively. The *subscript* is used to indicate the particle-rank of the operator. *Thick horizontal lines* are used for matrix elements of $\bar{S}$

$$\{\exp(\bar{S})\}P_0^{(1,1)}, \tag{15-23}$$

where { } stands for the normal-ordered form and the new $\bar{S}$ operators are defined through connected structures obtained after applying Wick's theorem in Eq. (15-22). The normal-ordered form of the expansion has been proposed by Offermann et al. [11], and by Lindgren [12]. Because of the normal-ordering contractions between $\bar{S}$ operators are no longer possible in the expansion. A disadvantage of this form is that the inverse operator of $\{\exp(\bar{S})\}$ is not easy to find. Such is required when one would like to perform similarity transformation of the Hamiltonian. This difficulty can be, however, overcome by determining the transformed Hamiltonian directly as it is done in the similarity transformed equation of motion (STEOM) method [45]. Expansion (15-23) allows us, however, for a partial transformation of the Hamiltonian in the Fock-space. Indeed, we can write

$$\{\exp(\bar{S})\}P_0^{(1,1)} = \exp(\bar{S}^{(0,0)})\{\exp(\bar{S}^{(1,0)} + \bar{S}^{(0,1)} + \bar{S}^{(1,1)})\}P_0^{(1,1)}, \tag{15-24}$$

since the $\bar{S}^{(0,0)}$ operator contains only particle-hole creation operators. For $\exp(\bar{S}^{(0,0)})$ the inverse is, of course, $\exp(-\bar{S}^{(0,0)})$. The $\bar{S}^{(0,0)}$ part of $\bar{S}$ is similar to the cluster operator T used in the single-reference CC approach. Within the single-reference CC scheme similarity transformation of the Hamiltonian using $\exp(T)$ is very convenient to justify the elimination of disconnected contributions to the CC equations (due to Hausdorff formula) and to prove size-extensivity of the method.

It is easy to notice that in each $\bar{S}^{(k,l)}$ subgroup of $\bar{S}$ there is an operator that, while acting on a given Φ_i, gives the same excited determinant. These are, for example, $\bar{S}_1^{(0,0)}$, $\bar{S}_2^{(1,0)}$, and $\bar{S}_2^{(0,1)}$ shown in Figure 15-2. The number of the effective Hamiltonian equations (15-21) that is the number of reference functions times the dimension of the orthogonal space is not sufficiently large to determine all them. The problem can be solved when the many-body structure of terms contributing to Eq. (15-21) is analyzed.

Since $\bar{S}^{(0,0)}$ is specific let us introduce more convenient notation for the cluster operators

$$T = \bar{S}^{(0,0)}, \quad S = \bar{S} - T, \tag{15-25}$$

thus the expansion reads now

$$\exp(T)\{\exp(S)\}P_0^{(1,1)}. \tag{15-26}$$

By inserting (15-26) into the effective Hamiltonian equations (15-21), multiplying them by $\exp(-T)$ from the left and applying Wick's theorem we can obtain the following form of the equations as shown by Lindgren [12]

$$Q^{(1,1)}\{[\bar{H}\{\exp(S)\} - \{\exp(S)\}(\bar{H}\{\exp(S)\})_{\mathrm{cl}}]_{\mathrm{conn}}\{\exp(S)\}\}P^{(1,1)} = 0, \tag{15-27}$$

where

$$\bar{H} = \exp(-T)H\exp(T), \tag{15-28}$$

and $(\,)_{\mathrm{cl}}$ and $(\,)_{\mathrm{conn}}$ stand for the closed and connected part of the resulting operators (diagrams), respectively. The closed part must have the number of particle-hole annihilation operators equal to the number of particle-hole creation operators and all of them must carry indices of active spin orbitals. For diagrams that means that the number of lines at the bottom of the diagram must be equal to the number of lines at the top of the diagram and all of them must be active. Operators or diagrams which are not closed are called open and will be denoted by $(\,)_{\mathrm{op}}$. Connected contribution to the normal-ordered product of second-quantized operators must be such that each operator has at least one common summation index with one of the others. In diagrammatic language that means that all vertices are connected via orbital or interaction lines.

Equation (15-27) represents a product of the connected operator and $\{\exp(S)\}$. It is easy to see that the closed part of the connected operator is equal to zero, so finally the so-called is linked diagram theorem can be shown for the method, where linked means that there are no contributions to the equation having disconnected closed parts. Equation (15-27) is satisfied if the connected operator, that is open, is equal to zero. The operator can be partitioned into several parts according to the number of active particle and the number of active hole annihilation operators. We require each part to be equal to zero

$$(\bar{H})^{(0,0)}_{\text{op}} = 0, \tag{15-29}$$

$$[\bar{H}\{\exp(S^{(1,0)})\} - \{\exp(S^{(1,0)}) - 1\}(\bar{H}\{\exp(S^{(1,0)}))_{\text{cl}}]^{(1,0)}_{\text{op,conn}} = 0, \tag{15-30}$$

$$[\bar{H}\{\exp(S^{(0,1)})\} - \{\exp(S^{(0,1)}) - 1\}(\bar{H}\{\exp(S^{(0,1)}))_{\text{cl}}]^{(0,1)}_{\text{op,conn}} = 0, \tag{15-31}$$

$$[\bar{H}\{\exp(S^{(1,0)} + S^{(0,1)} + S^{(1,1)})\} - \{\exp(S^{(1,0)} + S^{(0,1)} + S^{(1,1)}) - 1\} \times(\bar{H}\{\exp(S^{(1,0)} + S^{(0,1)} + S^{(1,1)}))_{\text{cl}}\}]^{(1,1)}_{\text{op,conn}} = 0, \tag{15-32}$$

where the superscript associated with each equation has the same meaning as for the $\bar{S}$ operators shown in Figure 15-2. The requirement provides the additional equations that allow us to determine all cluster amplitudes. The effective Hamiltonian (15-20) can be expressed in a similar manner

$$h^{(0,0)}_{\text{eff}} = (\bar{H})^{(0,0)}_{\text{cl}}, \tag{15-33}$$

$$h^{(1,0)}_{\text{eff}} = [\bar{H}\{\exp(S^{(1,0)})\}]^{(1,0)}_{\text{cl,conn}}, \tag{15-34}$$

$$h^{(0,1)}_{\text{eff}} = [\bar{H}\{\exp(S^{(0,1)})\}]^{(0,1)}_{\text{cl,conn}}, \tag{15-35}$$

$$h^{(1,1)}_{\text{eff}} = [\bar{H}\{\exp(S^{(1,0)} + S^{(0,1)} + S^{(1,1)})\}]^{(1,1)}_{\text{cl,conn}}, \tag{15-36}$$

where we have only closed parts contributing. We have all these four many-body components in the effective Hamiltonian for the (1,1) case. It is seen from the above that a hierarchical way of solving the S equations can be established. The hierarchy starts with Eq. (15-29) that contains only T and can be solved for T. Then, using T already determined in the first step, Eqs. (15-30) and (15-31) can be separately solved for $S^{(1,0)}$ and $S^{(0,1)}$, respectively. Finally, having T, $S^{(1,0)}$ and $S^{(0,1)}$ obtained in the previous steps, $S^{(1,1)}$ can be calculated from Eq. (15-32). This is the so-called valence universal strategy of solving the CC equations proposed by Mukherjee [46]. A closer look at the additional equations required by the strategy for the $(1, 1)$ problem shows that these contain a significant physical information about the system. Eq. (15-29) together with Eq. (15-33) constitute the standard single-reference CC equations for the neutral system. Then, having the ground state correlation effects determined, a systems with one extra electron is considered. By solving Eq. (15-30) for $S^{(1,0)}$ and diagonalizing $h^{(1,0)}_{\text{eff}}$ electron affinities are obtained due to neglecting $(\bar{H})^{(0,0)}_{\text{cl}}$. Usually $\bar{H}_N = \bar{H} - (\bar{H})^{(0,0)}_{\text{cl}}$ is used instead of $\bar{H}$ to obtain excitation

energies from the ground state directly. Similarly, ionization energies are given when Eq. (15-31) is solved for $S^{(0,1)}$ and used for constructing $h_{\mathrm{eff}}^{(0,1)}$. Finally, knowing T, $S^{(1,0)}$, and $S^{(0,1)}$ Eq. (15-32) can be solved for $S^{(1,1)}$. Excitation energies are obtained as eigenvalues of the effective Hamiltonian

$$H_{\mathrm{eff}}^{(1,1)} = P^{(1,1)} \left(h_{\mathrm{eff}}^{(1,0)} + h_{\mathrm{eff}}^{(0,1)} + h_{\mathrm{eff}}^{(1,1)} \right) P_0^{(1,1)}. \tag{15-37}$$

The above procedure is an example of the valence-universal strategy for solving the FS-CC equations. For the problem which requires the (k, l) reference space valence-universal strategy assumes performing a sequence of calculations. The sequence contains all problems with (m, n) reference spaces in order of growing number of quasi-particles (defined as $m + n$) with $m \leq k$ and $n \leq l$. In each step only $S^{(m,n)}$ cluster operators have to be determined, the remaining operators that enter the equations are known from lower quasi-particle problems. The hierarchy of problems that must be solved to reach the final one involves calculations for systems with different number of electrons and for this reason the approach is called the Fock-space CC method. For some specific problems like $(k, 0)$ or $(0, l)$ the hierarchy really contains different sectors of the Fock-space but for the more general choices different (m, n) spaces can correspond to problems with the same number of electrons. For example, the $(0, 0)$ and $(1, 1)$ sectors describe a system with the same number of electrons and here we would like to return to the problem of the so-called deexcitation operator that has been omitted in $\bar{S}^{(1,1)}$. The operator generates excitations to the Hartree–Fock determinant ($M_0^{(0,0)}$ space) while acting on $M_0^{(1,1)}$. Definitely, the operator is necessary if the cluster expansion is assumed to reproduce the exact wave function since excited states can have contribution from the Hartree–Fock determinant. However, for the energy calculation the deexcitation operator is not required. To see this let us go back to the effective Hamiltonian equations (15-20) and (15-21). These equations possess many solutions and, in principle, are capable of describing all states that have non-zero overlap with the reference space functions. Thus in the valence-universal strategy involving $(0, 0)$ and $(1, 1)$ problems the same state can be described twice. That is avoided if the transformed Hamiltonian $\bar{H}$ Eq. (15-28) is used in the $(1, 1)$ calculation. The right eigenfunction of $\bar{H}$ is the ground state Hartree–Fock determinant Φ and its eigenvalue is one of the exact energies, usually the ground state one E_0

$$\bar{H}\Phi = E_0\Phi. \tag{15-38}$$

The remaining eigenvalues of H can be found as eigenvalues of $\bar{H}$ in the space orthogonal to Φ, thus, the deexcitation operator is not required. Then, if necessary, a simple calculation can be performed to recover the exact wave function. These simple facts are not so obvious when the wave function expansion is considered. For example, in early applications of the FS-CC method this elimination of deexcitation operator was considered as an approximation [29]. The use of similarity

transformations makes some aspects of the method more transparent and more convenient for further developments.

It is worth mentioning here that other similarity transformations of the Hamiltonian can be introduced to utilize information about states, which description have already been obtained, to reduce the number of cluster operators. For example, for the $(2,2)$ problem in such a way the excitation operators to $M_0^{(0,0)}$ and $M_0^{(1,1)}$ can be excluded from $S^{(2,2)}$. For more details we refer to Ref. [47].

15.4. INTERMEDIATE HAMILTONIAN FORMULATIONS OF THE FOCK-SPACE CC METHOD

Similarity transformations of the Hamiltonian can be considered as an attractive alternative way of introducing the effective Hamiltonian scheme. One can look at the effective Hamiltonian technique as a way of extracting problem corresponding to several eigenvalues from the complete eigenvalue problem for the Hamiltonian. As before we assume that the functional space is divided into two subspaces: M_0 and $M_\perp$. Using simple similarity transformation the eigenvalue problem of the Hamiltonian can be split into two subproblems [19]. Defining

$$X \equiv QXP_0, \tag{15-39}$$

we can transform the Hamiltonian H to the form

$$e^{-X}He^{X} = (1-X)H(1+X). \tag{15-40}$$

Requiring X to satisfy the equation

$$Q(1-X)H(1+X)P_0 = 0, \tag{15-41}$$

we divide the problem of finding all eigenvalues of H into two subproblems. Now all eigenvalues of H can be obtained by looking for eigenvalues of the $P_0 - P_0$ and $Q - Q$ parts of the transformed Hamiltonian separately. The $P_0 - P_0$ part of the transformed Hamiltonian is the effective Hamiltonian which diagonalization provides $m = \dim M_0$ energies

$$H_{\text{eff}} = P_0(1-X)H(1+X)P_0 = P_0H(1+X)P_0. \tag{15-42}$$

The set of Eqs. (15-41) and (15-42) is identical with that obtained previously for the effective Hamiltonian. The difference is that we still can consider the complete eigenvalue problem knowing how the remaining energies can be obtained.

Similarity transformations are also convenient to introduce another formulation of the FS-CC method that is formally simpler and more effective in practical applications. The standard FS-CC formalism that is based on the effective Hamiltonian

formulation has many disadvantages. First of all this is a two step procedure. In each (m,n) sector first the cluster amplitudes must be determined in an iterative way and then, using them, the effective Hamiltonian is constructed. The energies are given by its diagonalization. The iterative procedure can be slowly convergent or divergent and that can be related to the intruder state problem. In some cases the alternative solution can be reached instead of the standard one. Moreover, the method is not state specific, i.e. we have to perform calculations for all m states at a time in spite of the fact that we can be interested only in some of them. Thus, it would be desirable to have a method that provides an efficient and dependable way of solving the FS-CC equations and does not require to find all cluster amplitudes and energies simultaneously.

The CC expansion shows its advantages when approximate variants are considered, when no approximation is made the exponential expansion is equivalent to the linear one. If some truncation scheme is imposed on $\bar{S}$, for example, the one shown in Figure 15-2 where only at most two-body operators are included, then two types of contributions are present in the exponential expansion. There are contributions from the orthogonal space that are generated directly by S but also contributions that are given by products of S operators. Most of these products generate excitations that cannot be reached directly by S. Thus, higher excitations than those given by S are approximated by products of lower excitation-rank cluster operators and that is the main advantage the CC ansatz. The effectiveness of this approximation depends, however, on fulfilling the so-called cluster conditions. If the cluster conditions are satisfied then the CC expansion is very effective and leads to high-quality results.

A specific feature of the FS-CC approach allowing us to find more efficient formulation than the standard one is that the FS-CC cluster expansion is linear in the unknown cluster amplitudes at each (m,n) level of the calculations beyond the $(0,0)$ one. Indeed, a closer look at $\{\exp(S)\}P_0^{(m,n)}$ shows that nonlinear terms are generated only by cluster amplitudes from lower sectors. Since these are already known then the expansion is linear in the unknown amplitudes. That indicates that the FS-CC equations can be solved by diagonalization of some operator. To be more specific let us consider the $(1,1)$ case in which higher than two-body $\bar{S}$ operators are neglected, i.e., the FS-CCSD method (see Figure 15-2). We extract from the orthogonal space a subspace that is spanned by those determinants that are reached by applying the $S^{(m,n)}$ excitation operators on the (m,n) reference space determinants at the $(1,0)$, $(0,1)$ and $(1,1)$ levels. Those subspaces will be denoted by $M_I^{(m,n)}$ and called the intermediate spaces. For the corresponding projection operators we use $P_I^{(m,n)}$. The transformed Hamiltonian reads

$$\tilde{H}^{(m,n)} = (1 - X^{(m,n)})\bar{H}_N(1 + X^{(m,n)}), \tag{15-43}$$

where

$$X^{(m,n)} = \{\exp S - 1\}P_0^{(m,n)}. \tag{15-44}$$

In the standard effective Hamiltonian approach we require

$$P_I^{(m,n)} \tilde{H}^{(m,n)} P_0^{(m,n)} = 0, \tag{15-45}$$

and that provides us with the set of equations for the $S^{(m,n)}$ amplitudes. The hierarchy of equations that must be solved for the (1,1) problem is given by

$$P_I^{(0,0)} \bar{H}_N P_0^{(0,0)} = 0, \tag{15-46}$$

$$P_I^{(1,0)} (1 - X^{(1,0)}) \bar{H}_N (1 + X^{(1,0)}) P_0^{(1,0)} = 0, \tag{15-47}$$

$$P_I^{(0,1)} (1 - X^{(0,1)}) \bar{H}_N (1 + X^{(0,1)}) P_0^{(0,1)} = 0, \tag{15-48}$$

$$P_I^{(1,1)} (1 - X^{(1,1)}) \bar{H}_N (1 + X^{(1,1)}) P_0^{(1,1)} = 0, \tag{15-49}$$

These are the standard FS-CCSD equations that must be solved iteratively. To obtain another possibility of solving the equations than that involving standard iterative procedures we split the transformations into sequences of two similarity transformations by dividing $X^{(m,n)}$ into two parts. One can relate this to the idea that has been put forward by Malrieu et al. [24] suggesting a partition of contributions generated by the wave operator into two parts and obtaining the trouble making part not via iterations but by diagonalization of an operator that acts in a larger space than the effective Hamiltonian but has a subset of eigenvalues identical with the set of eigenvalues of H_{eff}. The operator has been called the intermediate Hamiltonian and different intermediate Hamiltonian schemes can be considered since this general idea gives us a lot of flexibility [19, 24]. Also here different variants can be taken into account but two of them seem sensible. The choice is determined by partitioning of $X^{(m,n)}$

$$X^{(m,n)} = Y^{(m,n)} + Z^{(m,n)}, \tag{15-50}$$

where, in order to obtain similarity transformation within the $M^{(m,n)}$ space being a sum of the model space $M_0^{(m,n)}$ (also called the main model space by Malrieu et al. in this context) and the intermediate space $M_I^{(m,n)}$ we assume that $Z^{(m,n)}$ generates excitations to the intermediate space $M_I^{(m,n)}$ only while acting on $M_0^{(m,n)}$

$$Z^{(m,n)} \equiv P_I^{(m,n)} Z^{(m,n)}. \tag{15-51}$$

Having $X^{(m,n)}$ partitioned the transformed Hamiltonian can be rewritten as

$$\tilde{H}^{(m,n)} = (1 - Z^{(m,n)})(1 - Y^{(m,n)}) \bar{H}_N (1 + Y^{(m,n)})(1 + Z^{(m,n)}). \tag{15-52}$$

Its structure in the $M^{(m,n)}$ space is, of course, characteristic for the transformation that leads to the effective Hamiltonian. Namely, its off-diagonal $P_I^{(m,n)} - P_0^{(m,n)}$ part is equal to zero according to Eqs. (15-47)–(15-49) and then diagonalization of the

$P_0^{(m,n)} - P_0^{(m,n)}$ part that is the effective Hamiltonian gives the desired excitation energies. The remaining eigenvalues of the transformed Hamiltonian (15-52) in the $M^{(m,n)}$ space can be obtained by diagonalization of the $P_I^{(m,n)} - P_I^{(m,n)}$ block. Now, let us consider the operator

$$\tilde{\bar{H}}^{(m,n)} = (1 - Y^{(m,n)})\bar{H}_N(1 + Y^{(m,n)}). \tag{15-53}$$

Denoting by $P^{(m,n)}$ the projection operator on $M^{(m,n)}$ one can see that both

$$\begin{aligned} &P^{(m,n)}\tilde{H}^{(m,n)}P^{(m,n)} \\ &\quad = P^{(m,n)}(1 - Z^{(m,n)})(1 - Y^{(m,n)})\bar{H}_N(1 + Y^{(m,n)})(1 + Z^{(m,n)})P^{(m,n)}. \end{aligned} \tag{15-54}$$

and

$$P^{(m,n)}\tilde{\bar{H}}^{(m,n)}P^{(m,n)} = P^{(m,n)}(1 - Y^{(m,n)})\bar{H}_N(1 + Y^{(m,n)})P^{(m,n)}. \tag{15-55}$$

operators have the same eigenvalues since, due to the requirement (15-51), they are related through similarity transformation within the $M^{(m,n)}$ space. Thus, the energies given by the effective Hamiltonian are among those of the operator (15-55). The operator can be called the intermediate Hamiltonian since it has been derived following the idea of obtaining a part of effects from the orthogonal space by diagonalization. Let us recall here that the intermediate Hamiltonian contains only those cluster amplitudes that have already been determined at lower quasi-particle levels. The intermediate Hamiltonian allows us to avoid iterative calculations associated with finding $Z^{(m,n)}$. The two step procedure of solving the equations is replaced by diagonalization of the intermediate Hamiltonian (15-55). Eigenvalues of the intermediate Hamiltonian can be found by using diagonalization procedures that permit single-root calculations and in this sense the method becomes state selective. The required eigenvalues and eigenvectors can be calculated one by one if necessary.

There are different choices possible for the $Z^{(m,n)}$ operator. The one that has been used by us so far [26, 27, 30] is

$$Z^{(m,n)} = P_I^{(m,n)}\{\exp(S)\}P_0^{(m,n)}. \tag{15-56}$$

It follows from Eqs. (15-44) and (15-51) that

$$P_I^{(m,n)}Y^{(m,n)} = 0, \tag{15-57}$$

so the intermediate Hamiltonian can be given by a very simple expression that is similar to the effective Hamiltonian one with the only difference being that $P_0^{(m,n)}$ and $X^{(m,n)}$ are replaced with $P^{(m,n)}$ and $Y^{(m,n)}$

$$H_I^{(m,n)} = P^{(m,n)}\bar{H}_N(1 + Y^{(m,n)})P^{(m,n)}. \tag{15-58}$$

That can be further simplified

$$H_I^{(m,n)} = P^{(m,n)}\bar{H}_N P^{(m,n)} + P^{(m,n)}\bar{H}_N Y^{(m,n)} P_0^{(m,n)}, \tag{15-59}$$

showing that the basic part of the $H_I^{(m,n)}$ matrix is the matrix representation of $\bar{H}_N$ and the additional contributions coming from $\bar{H}_N Y^{(m,n)}$ enter only the first columns corresponding to the reference space $M_0^{(m,n)}$.

The other choice that can be consider for $Z^{(m,n)}$ is

$$Z^{(m,n)} = S^{(m,n)} P_0^{(m,n)}. \tag{15-60}$$

The $Z^{(m,n)}$ component generates excitations to $M_I^{(m,n)}$ as it should but $Y^{(m,n)}$ gives contributions from both $M_I^{(m,n)}$ and a part of the orthogonal space that is not included in $M_I^{(m,n)}$. Having this in mind we can analyze terms that enter different blocks of the intermediate Hamiltonian

$$P_0^{(m,n)} H_I^{(m,n)} P_0^{(m,n)} = P_0^{(m,n)} \bar{H}_N (1 + Y^{(m,n)} P_0^{(m,n)}, \tag{15-61}$$

$$P_I^{(m,n)} H_I^{(m,n)} P_0^{(m,n)} = P_I^{(m,n)} \bar{H}_N (1 + Y^{(m,n)}) - Y^{(m,n)} \bar{H}_N (1 + Y^{(m,n)})] P_0^{(m,n)}, \tag{15-62}$$

$$P_0^{(m,n)} H_I^{(m,n)} P_I^{(m,n)} = P_0^{(m,n)} \bar{H}_N P_I^{(m,n)}, \tag{15-63}$$

$$P_I^{(m,n)} H_I^{(m,n)} P_I^{(m,n)} = P_I^{(m,n)} (1 - Y^{(m,n)}) \bar{H}_N P_I^{(m,n)}. \tag{15-64}$$

At first glance $H_I^{(m,n)}$ looks complicated which is not surprising. Because of reducing $Z^{(1,1)}$ to $S^{(1,1)} P_0^{(1,1)}$ many additional term must contribute to the intermediate Hamiltonian. The question is, however, whether all these terms are irreducible.

Using diagrams introduced in Figure 15-2 we can discuss the FS-CCSD method in more detail. The first problem in the hierarchy, the $(0, 0)$ one, remains unchanged. For the one-quasi-particle sectors, $(1, 0)$ and $(0, 1)$, that are next to consider, the intermediate Hamiltonian has very simple form. This is because

$$X^{(1,0)} = S^{(1,0)} P_0^{(1.0)}, \quad X^{(0,1)} = S^{(0,1)} P_0^{(0.1)}, \tag{15-65}$$

and, thus,

$$Y^{(1,0)} = 0, \quad Y^{(0,1)} = 0, \tag{15-66}$$

For the one quasi-particle problem both choices for the $Z^{(m,n)}$ operator considered above are equivalent leading to the same intermediate Hamiltonians

$$H_I^{(1,0)} = P^{(1,0)}\bar{H}_N P^{(1,0)}, \quad H_I^{(0,1)} = P^{(0,1)}\bar{H}_N P^{(0,1)}. \tag{15-67}$$

The problem is reduced to finding eigenvalues of $\bar{H}_N$ in the $M^{(1,0)}$ space and in the $M^{(0,1)}$ space. It follows from the above that the eigenvalues do not dependent on the choice of active orbital levels. However, that does not concern the cluster amplitudes, $S^{(1,0)}$ and $S^{(0,1)}$, that are needed to construct the intermediate Hamiltonian in the $(1, 1)$ sector. To obtain the $S^{(1,0)}$ cluster amplitudes we need $m = \dim M_0^{(1,0)}$ eigenvectors of $H_I^{(1,0)}$. They are used as columns to construct matrix $\mathbf{V^{(1,0)}}$. The matrix is partitioned into an $m \times m$ submatrix $\mathbf{V_0^{(1,0)}}$ consisting of reference determinant coefficients and submatrix $\mathbf{V_I^{(1,0)}}$ consisting of the intermediate space coefficients. The $\mathbf{Z^{(1,0)}}$ matrix can be obtained as

$$\mathbf{Z^{(1,0)}} = \mathbf{V_I^{(1,0)}} \left(\mathbf{V_0^{(1,0)}}\right)^{-1}, \tag{15-68}$$

where we assume that $\mathbf{V_0^{(1,0)}}$ is nonsingular. The $S^{(1,0)}$ cluster amplitudes are given directly by matrix elements of $\mathbf{Z^{(1,0)}}$. In a similar manner the $S^{(0,1)}$ cluster amplitudes are obtained for a given choice of active hole levels.

Having the T, $S^{(1,0)}$ and $S^{(1,0)}$ amplitudes determined the intermediate Hamiltonian for the $(1, 1)$ sector can be constructed. Two different partitioning of $X^{(1,1)}$ are shown in Figure 15-3 in a schematic way (line directions are omitted and circles are used for active lines). The first choice is shown in Figure 15-3a and diagrammatic representation of terms contributing to the intermediate Hamiltonian is

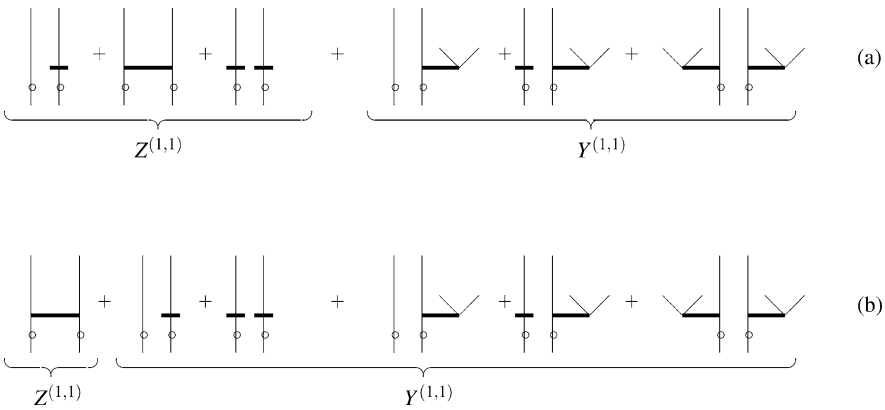

Figure 15-3. Two different partitioning of the $X^{(1,1)}$ operator into the $Z^{(1,1)}$ and $Y^{(1,1)}$ discussed in the text. Diagram are shown in a schematic ways with line directions omitted

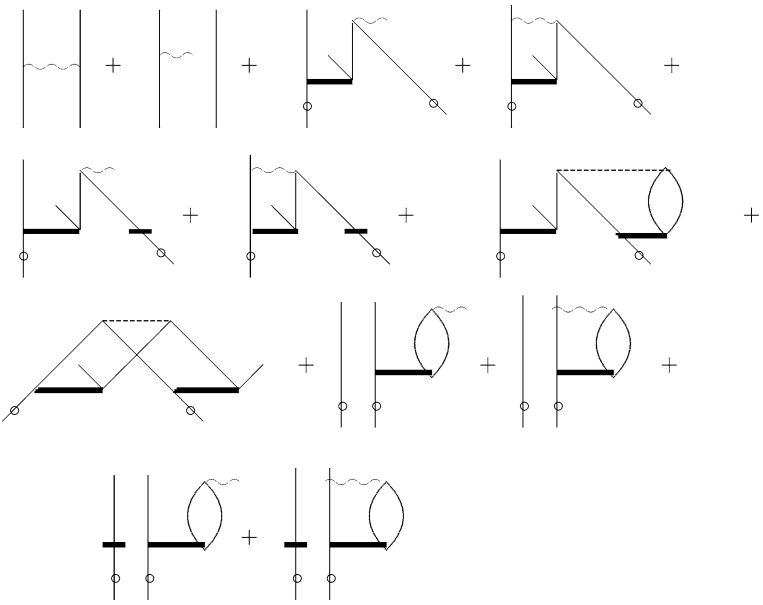

Figure 15-4. Diagrammatic representation of the intermediate Hamiltonian corresponding to choice **(a)** for $Z^{(1,1)}$ in Figure 15-3. The wavy line is used for matrix elements of $\bar{H}_N$

depicted in Figure 15-4. The wavy line is used for matrix elements of $\bar{H}_N$. The number of diagrams that must be constructed for matrix elements of the intermediate Hamiltonian is significantly reduced compared to the standard FS-CCSD equations. First of all there are no diagrams representing the renormalization term since this contribution is generated in the process of diagonalization. Also some diagrams originating from the principal part in the FS-CCSD equations are not present in the intermediate Hamiltonian. The additional contributions that have to be included are simple and they are represented by the last four diagrams in Figure 15-4. They can be disconnected but that does not hurt extensivity of the method that is completely equivalent to the standard one as far as the results are concerned. In fact, the disconnected diagrams are really necessary to maintain size-extensivity since they are required to cancel those disconnected terms that are given by diagonalization of the intermediate Hamiltonian. So, unlike the standard FS-CC approach, the cancellation of disconnected terms is numerical. Also the $S^{(1,1)}$ amplitudes can be obtained from the $Z^{(1,1)}$ matrix elements in the way similar to that in the $(1,0)$ and $(0,1)$ sectors. The difference is that matrix elements of $Z^{(1,1)}$ do not give the $S^{(1,1)}$ amplitudes directly but must be obtained from

$$S_2^{(1,1)}P_0^{(1,1)} = (Z_2^{(1,1)} - S_1^{(1,0)} + S_1^{(0,1)} + \{S_1^{(1,0)}S_1^{(0,1)}\})P_0^{(1,1)}. \tag{15-69}$$

They are, however, not really needed in the final sector calculation.

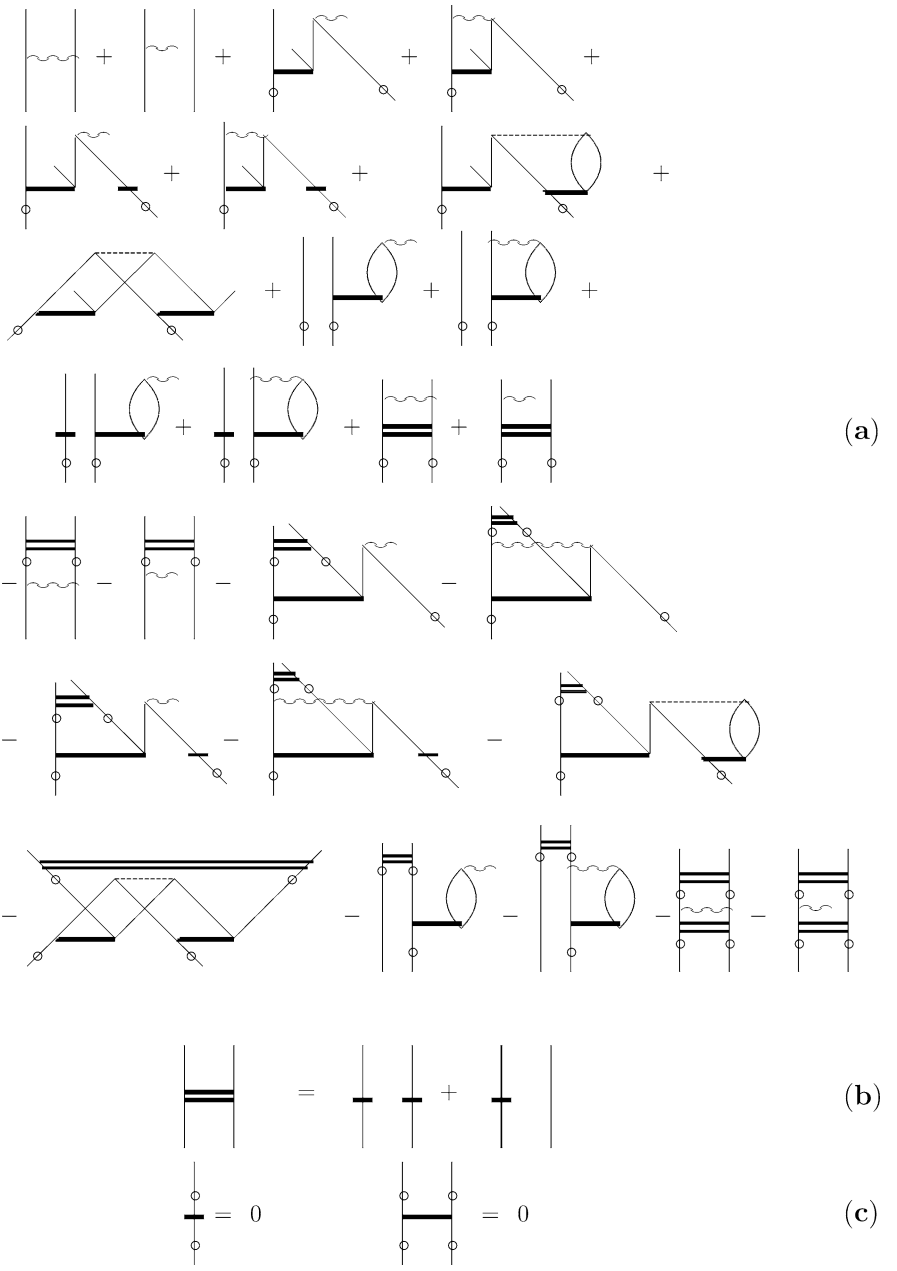

Figure 15-5. **(a)** Diagrammatic representation of the intermediate Hamiltonian corresponding to choice **(b)** for $Z^{(1,1)}$ in Figure 15-3. An additional vertex, marked by *double horizontal line*, is introduce to reduce the number of diagrams and its definition is given by **(b)**. The fact that internal excitations are not allowed in S is depicted in **(c)**

The second choice for $Z^{(1,1)}$ given by Eq. (15-60) and shown in Figure 15-3b might be seen as not very attractive. Although it gives the $S^{(1,1)}$ amplitudes directly from the $\mathbf{Z^{(1,1)}}$ matrix but the intermediate Hamiltonian corresponding to this choice looks quite complicated. Its diagrammatic representation is presented in Figure 15-5. To reduce the number of diagrams an additional vertex is introduced and the fact that $S_1^{(1,0)}$, $S_1^{(0,1)}$ and $S_2^{(1,1)}$ must excite outside the reference space thus all their diagrams having exclusively active lines are equal to zero is shown.

The intermediate Hamiltonian formalism, as it has been introduced here, does not make use of the connected diagram theorem and rely on the numerical cancellation of disconnected contributions. In the next section we present another route to the intermediate Hamiltonian FS-CC formulations for which the starting point is the connected form of the standard FS-CC equations. For the second choice for $Z^{(1,1)}$ that permits elimination of reducible contributions and provides simpler expressions for matrix elements of the corresponding $H_I^{(1,1)}$.

15.5. CANONICAL FORM OF THE FS-CCSD EFFECTIVE HAMILTONIAN EQUATIONS

The effective Hamiltonian formulations resulted from the necessity of describing two types of electron correlation effects. These formulations postulate a specific structure for the wave function and introduce approximate schemes. After this it would be convenient to decouple equations for all states under consideration and solve them for each state separately. That is possible if the problem of solving the effective Hamiltonian equations can be reduced to the eigenvalue problem of some operator. In the following we would like to show how the standard FS-CC equations can be transformed to a form that is suitable for going back to the single-eigenvalue problem. This form has been called canonical [32] but can be also related to the so-called eigenvalue independent partitioning technique [48]. A characteristic feature of the canonical form is that the equations are expressed in the way characteristic for the effective Hamiltonian equations

$$H_{\text{eff}} = P_0 H_I (1 + Z) P_0, \tag{15-70}$$

$$QH_I(1 + Z)P_0 - QZH_{\text{eff}} = 0, \tag{15-71}$$

where H_I is some operator that is obtained by rearranging the effective Hamiltonian equations and $Z \equiv QZP$ is an excitation operator. If such a form is obtained then the problem of solving the equations can be reduced to the eigenvalue problem but this time of H_I instead of H. A comparison between Eqs. (15-20) and (15-21) and Eqs. (15-70) and (15-71) shows that H and H_I must be related through some similarity transformation.

Let us now consider the FS-CCSD method. The equations are given by (15-29)–(15-37) where only connected terms contribute. It is easy to notice that the $(1,0)$ and $(0,1)$ equations are already in the canonical form since they can be written as

$$P_I^{(1,0)}\bar{H}_N(1+S^{(1,0)})P_0^{(1,0)} - S^{(1,0)}H_{\text{eff}}^{(1,0)} = 0,$$
$$H_{\text{eff}}^{(1,0)} = P_0^{(1,0)}\bar{H}_N(1+S^{(1,0)})P_0^{(1,0)}, \tag{15-72}$$

$$P_I^{(0,1)}\bar{H}_N(1+S^{(0,1)})P_0^{(0,1)} - S^{(0,1)}H_{\text{eff}}^{(0,1)} = 0,$$
$$H_{\text{eff}}^{(0,1)} = P_0^{(0,1)}\bar{H}_N(1+S^{(0,1)})P_0^{(0,1)}. \tag{15-73}$$

The equations are expressed in the diagrammatic form in Figure 15-6. One can easily see that the H_I operator is simply $\bar{H}_N$ and Z is either $S^{(1,0)}$ or $S^{(0,1)}$ depending on the case. Thus the eigenvalues of the effective Hamiltonian for the $(1,0)$ case can be obtained by diagonalization of $\bar{H}_N$ in the space spanned by determinants with one extra electron placed on unoccupied level (reference determinants plus determinants generated from them by $S_1^{(1,0)}$) and two extra electrons and one hole (generated by $S_2^{(1,0)}$). Such a space is usually called the p 2p-h space. The diagonalization gives electron affinities. For the $(0,1)$ sector $\bar{H}_N$ must be diagonalized in the h p-2h space

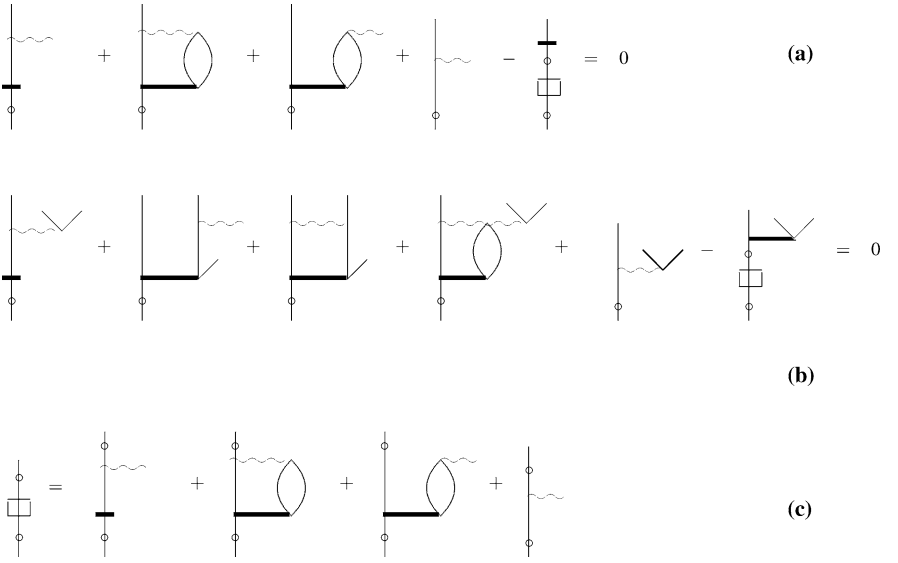

Figure 15-6. Diagrammatic representation of the standard FS-CCSD equations in the $(1,0)$ and $(0,1)$ sectors. The first two equations, **(a)** and **(b)**, are the amplitude equations, **(c)** shows the one-body contribution to the effective Hamiltonian

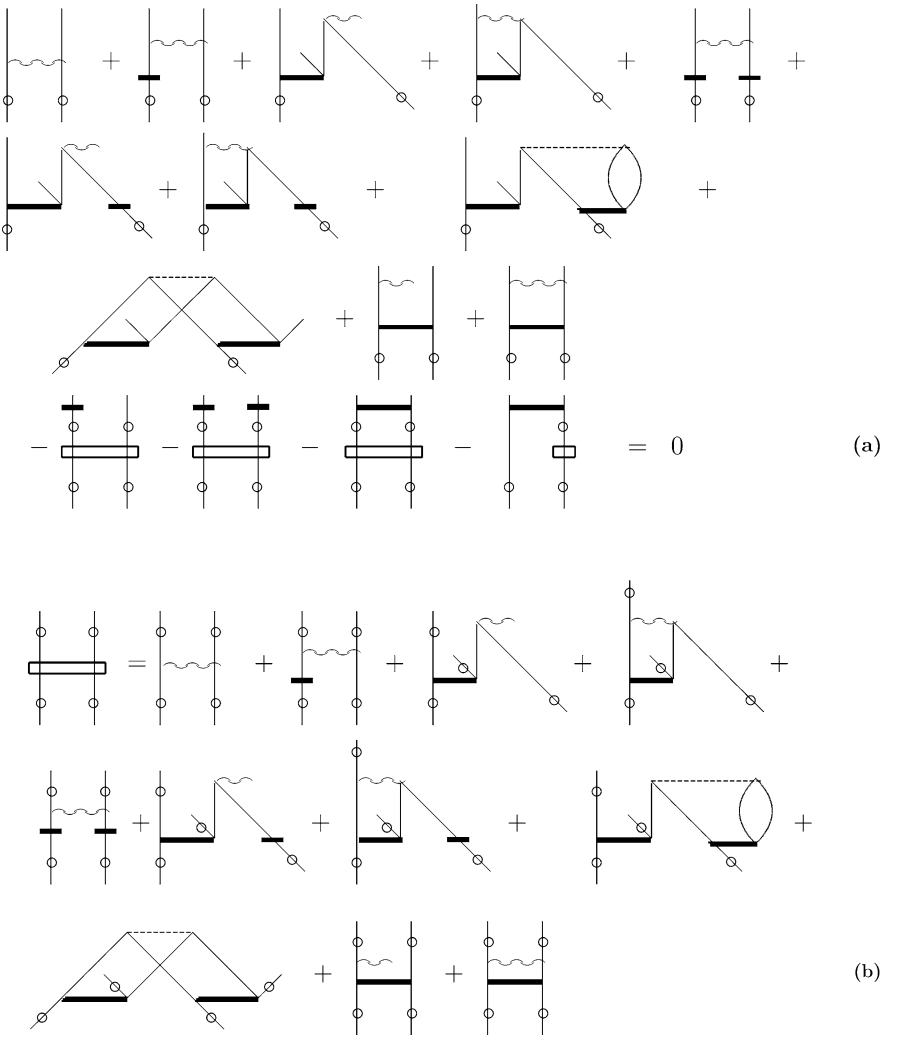

Figure 15-7. Diagrammatic representation of the standard FS-CCSD equations in the $(1,1)$ sector. The first equation **(a)** represents the set of equations for $S^{(1,1)}$ while **(b)** shows the two-body contribution to the effective Hamiltonian

and that provides ionization potentials. So the situation here does not differ from that described in the previous section.

The $(1,1)$ case is, however, much more complicated. Diagrammatic representation of the connected FS-CCSD equations is shown in Figure 15-7. As before, different possibilities of reaching the canonical form can be considered. Let us start with the choice for $Z^{(1,1)}$ that is shown diagrammatically in Figure 15-8a and is identical with the first choice for $Z^{(1,1)}$ considered in the previous section. In order

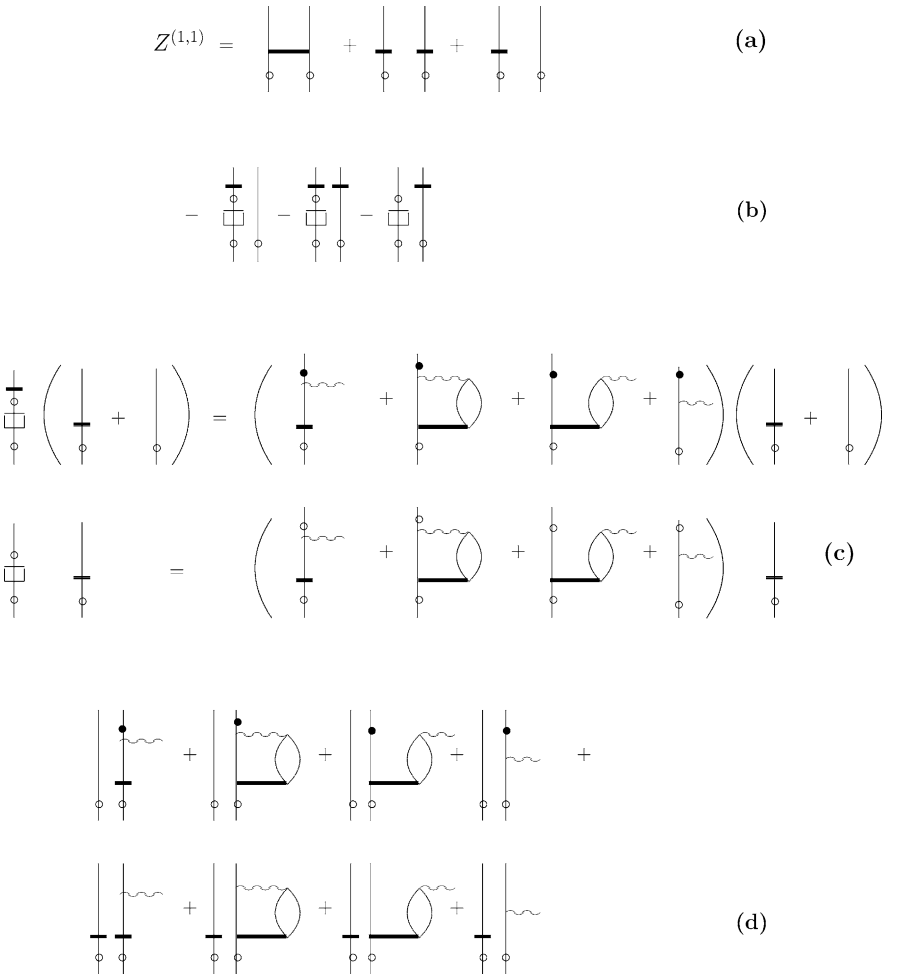

Figure 15-8. **(a)** The first choice for $Z^{(1,1)}$. **(b)** Diagrams that are lacking in the renormalization term in the $(1,1)$ amplitude equations shown in Figure 15-7a to obtain the canonical form. **(c)** Transformation of diagrams **(b)** with the use if $(1,0)$ and $(1,0)$ equations presented in Figure 15-6. *Filled circles* are used to denote inactive lines. **(d)** Diagrams that must be included in the principal part of the $(1,1)$ FS-CCSD equations in Figure 15-7 a to have the renormalization part in the canonical form

to have canonical form of the renormalization term with such a choice, diagrams that are shown in Figure 15-8b must be added. Thus, the renormalization term suits the canonical form if diagrams Figure 15-8b with the opposite sign are added to those generated by the first principal term in Eq. (15-71). Unfortunately, they do not support the canonical form of the first term. However, when the $(1,0)$ and $(0,1)$ equations from Figure 15-6 are used to transform them, as shown in Figure 15-8c, then the canonical form, pictured in Figure 15-8d, is reached. To see diagrams

representing $H_I^{(1,1)}$ resulting from the canonical form we have to collect all diagrams entering the amplitude equations shown in Figure 15-7a except those representing the renormalization term and supply them with those shown in Figure 15-8d. If some diagram has one of the $Z^{(1,1)}$ vertices shown in Figure 15-8a then such a part of the diagram must be removed but the remaining part should be kept. Diagrams obtained in this way represent the $P_I^{(1,1)} - P^{(1,1)}$ part of $H_I^{(1,1)}$.

The same should be done with the one- and two-particle contributions to the effective Hamiltonian shown in Figures 15-6c and 15-7b. Again we should remove $Z^{(1,1)}$ vertices from the two-particle diagrams of the effective Hamiltonian. These diagrams contribute to the $P_0^{(1,1)} - P^{(1,1)}$ of $H_I^{(1,1)}$. If this is done then one can see that diagrams derived in this way are identical with those obtained in the previous section for the same choice of $Z^{(1,1)}$. This derivation is, however, more tedious than the one presented before. It is worth mentioning that one can also use the $(1,0)$ and $(0,1)$ equations in a slightly different manner and obtain a different diagrammatic representation but the same numerical values for the intermediate Hamiltonian matrix elements as presented in Ref. [32].

Now the question is whether for the second choice of $Z^{(1,1)}$, i.e., $Z^{(1,1)} = S^{(1,1)}P^{(1,1)}$, the canonical form is also so much difficult to obtain. It should be recalled here that in the previous section the intermediate Hamiltonian was represented by relatively large number of diagrams. Surprisingly, a closer look at the FS-CCSD equations in Figure 15-7a shows that this is not the case since the equations are already in the canonical form, The only operation that must be done is to identify $H_I^{(1,1)}$ for this case. The renormalization term in (15-71) is given by the last two diagrams in the equation for the cluster amplitudes in Figure 15-7a. That definitely represents what is required by the canonical form. The only problem is that the remaining two diagrams with effective Hamiltonian vertices must be expressed in the explicit form to divide their contribution into the constant part and the part that is linear in $S^{(1,1)}$. Now collecting several diagrams in one intermediate diagram (filled box) as shown in Figure 15-9b, contributions to different blocks of $H_I^{(1,1)}$ entering Eqs. (15-70)–(15-71) can be expressed in a compact form as shown in Figure 15-9c. A similar structure can be obtained from diagrams derived in the previous section if the $(1,0)$ and $(0,1)$ equations, depicted in Figure 15-6, are used. Indeed it can be seen that some disconnected diagrams that are shown in Figure 15-5 give the net contribution equal to zero if the fact that $S^{(1,0)}$ and $S^{(0,1)}$ satisfy equations shown in Figure 15-6 is taken into account.

To summarize let us emphasize the main features of the intermediate Hamiltonian versions of the FS-CC method. First, the intermediate Hamiltonian approach is equivalent to the standard one in the sense that provides the same energies and cluster amplitudes, however, the way of reaching the solution is completely different. Unlike the effective Hamiltonian FS-CC method, the intermediate Hamiltonian version is based on one-step procedure which gives the eigenvalues and the corresponding eigenvectors at the same time. Diagonalization allows us to find single eigenvalues and in this sense the approach is state-selective. Also alternative solutions are easy

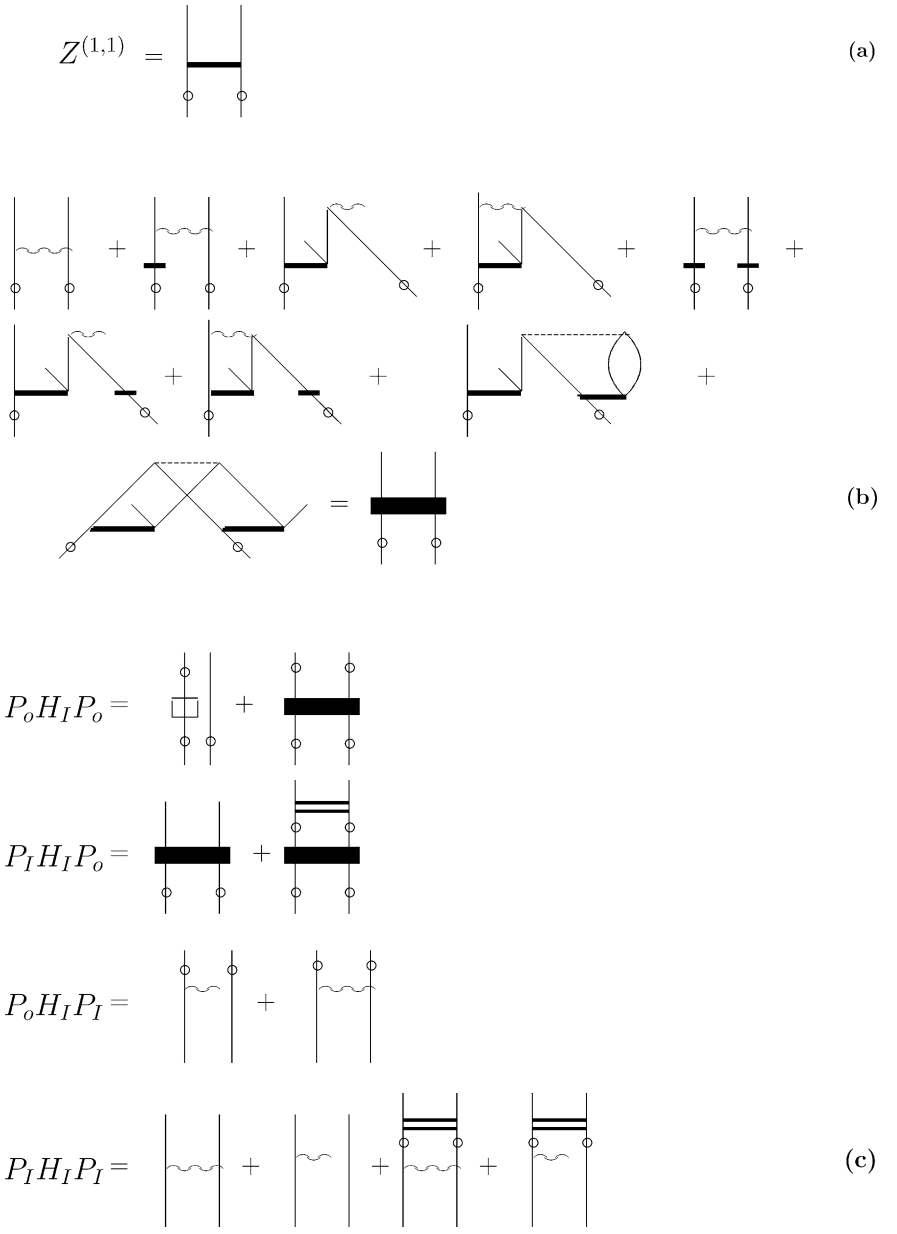

Figure 15-9. **(a)** The second choice for $Z^{(1,1)}$. **(b)** Definition of the filled rectangle vertex. **(c)** Diagrams contributing to different blocks of the intermediate Hamiltonian

to access [25]. As has been demonstrated the effective Hamiltonian MR-CC iterative schemes can lead to some solutions that are not our primary goal [22]. That usually happens when the chosen reference space can be considered as a relatively good selection for another set of m states. The ability of obtaining an alternative solution depends on the starting vector as well as on the iterative scheme used. It has been shown that the quality of description of some states given by alternative solutions is quite good [22, 27]. It is easy to see that all possible energies that can be obtained by the effective Hamiltonian FS-CC approach with all possible solutions for X are eigenvalues of the intermediate Hamiltonian. Each solution for X provides a set of m eigenvalues and these are always m-element subsets of eigenvalues of the intermediate Hamiltonian. Also it follows that the energy corresponding to a particular state is the same in all possible solutions of the effective Hamiltonian approach. Another aspect of the intermediate Hamiltonian formulation is that the method introduces many formal simplifications. The number of diagrams that must be considered is significantly reduced.

In the next section numerical examples showing the efficiency of the intermediate Hamiltonian version of the FS-CC method are presented. The method has been implemented on the CCSD and CCSDT level [30, 31]. Also the standard effective Hamiltonian codes are available to compare the performance of the two approaches [49].

15.6. NUMERICAL EXAMPLES

The intermediate Hamiltonian FS-CC codes can be easily obtained from those for the standard FS-CC method. The intermediate Hamiltonian scheme requires, however, some reorganization of the calculation. Diagrams that are used to constructed the FS-CC amplitude equations now contribute to the matrix elements of the intermediate Hamiltonian. It is seen from Figures 15-7 and 15-4 that only a part of them is needed. They must be supplemented with a very few that are not present in the standard equations but these are easy to code and calculate (Figure 15-4). Moreover, the iterative schemes for solving equations for cluster amplitudes must be replaced with diagonalization procedure. Usually very effective Hirao–Nakatsuji generalization [50] of the Davidson algorithm [51] is employed that permits diagonalization of non-hermitian matrices.

Having the effective Hamiltonian FS-CC codes we can examine the behavior of the standard iterative schemes: the Jacobi-type of iterations as well as the scheme with iterations damped. Three examples are presented. These are the C_2, H_2O and O_3 molecules. Calculations are performed on the CCSD level. Results are collected in Tables 15-1, 15-2, and 15-3 where the basis sets and geometries can also be found. The basis sets employed are either the correlation-consistent basis sets by Dunning (aug-cc-pVTZ [52]) or the Poli basis sets by Sadlej [53], both with spherical d functions. The experimental geometries for the ground state are used and the core electrons are kept frozen. The ability to reach convergence within the standard

Table 15-1. Vertical excitation energies (eV) of the C_2^a molecule with FS-CCSD method[b] (aug-cc-pVTZ basis set [c]; R = 1.243 Å[d]). NC means no convergence

	(1,3)[b]			(3,3)[b]			(5,3)[b]			
Sym.	H_{eff}	H_{eff} with damp.	IH	H_{eff}	H_{eff} with damp.	IH	H_{eff}	H_{eff} with damp.	IH	Exp.[e]
$^1\Pi_u$	NC	1.335	1.335	NC	NC	1.280	NC	NC	1.279	1.23
$^1\Sigma_u^+$	NC	5.941	5.941	NC	NC	1.1086	NC	NC	5.789	5.36

[a] Valence electrons correlated.
[b] (m,n) is used to describe active spaces. m is the number of lowest unoccupied orbitals and n is the number of highest occupied orbitals used as active in the calculation.
[c] Ref. [52].
[d] Ref. [54].
[e] Ref. [55].

Table 15-2. Vertical excitation energies (eV) of the H_2O^a molecule with FS-CCSD method[b] (POL1 basis set [c]; R = 0.975 Å, angle = 104.5°[d]). NC means no convergence

	(2,3)[b]			(3,3)[b]			(6,3)[b]			
Sym.	H_{eff}	H_{eff} with damp.	IH	H_{eff}	H_{eff} with damp.	IH	H_{eff}	H_{eff} with damp.	IH	Exp.[d]
$^1B_1$	NC	7.656	7.656	NC	7.602	7.602	NC	NC	7.349	7.4
$^1A_2$	NC	9.500	9.500	NC	9.500	9.500	NC	NC	9.235	9.1
$^1A_1$	NC	10.087	10.087	NC	10.062	10.062	NC	NC	9.772	9.7

[a] Valence electrons correlated.
[b] (m,n) is used to describe active spaces. m is the number of lowest unoccupied orbitals and n is the number of highest occupied orbitals used as active in the calculation.
[c] Ref. [53].
[d] Ref. [60].

Table 15-3. Vertical excitation energies (eV) of the O_3^a molecule with FS-CCSD method[b] (POL1 basis set[c]; R = 1.272 Å, angle = 116.8°[d]). NC means no convergence

	(1,3)[b]			(3,3)[b]			(4,3)[b]			
Sym.	H_{eff}	H_{eff} with damp.	IH	H_{eff}	H_{eff} with damp.	IH	H_{eff}	H_{eff} with damp.	IH	Exp.[e]
$^1A_2$	NC	2.075	2.075	NC	NC	2.075	NC	NC	2.075	1.92
$^1B_1$	NC	2.143	2.143	NC	NC	2.143	NC	NC	2.143	2.1
$^1B_2$	NC	5.302	5.302	NC	NC	5.268	NC	NC	5.257	4.86

[a] Valence electrons correlated.
[b] (m,n) is used to describe active spaces. m is the number of lowest unoccupied orbitals and n is the number of highest occupied orbitals used as active in the calculation.
[c] Ref. [53].
[d] Ref. [57, 58].
[e] Ref. [56, 59].

FS-CCSD scheme very much depends on the reference space size. In non of the cases the straight Jacobi-type iterations lead to convergence but with the use of the damp factor (usually 0.8 or 0.9) we are able to reach the convergence for the smallest reference spaces considered. Only in one case of the medium-size reference space the solution is obtained (H_2O) while for the largest reference spaces the damping technique does not help at all. To have an idea about cluster amplitude magnitudes we should mention that in all presented cases there are cluster amplitudes which absolute values are slightly above 1. That can explain the convergence problems of the standard iterative schemes. It can be observed that with the growing size of the reference space the accuracy of excitation energies given by the method increases. To have high quality results relatively large reference spaces are required and for them obtaining solutions within the standard effective Hamiltonian FS-CC iterative schemes may be out of reach. The intermediate Hamiltonian technique provides solutions of the FS-CCSD equations in all cases without any problems. It must be noted that we employ here simple but most commonly used Jacobi-type iterative schemes. There are also more sophisticated methods like, for example, that based on the Newton – Raphson scheme. However, the Newton–Raphson scheme is very numerically demanding and, moreover, depends very much on the starting vector so in practice can be used only for small systems. But even with the Newton–Raphson method we have experienced difficulties in calculations for the Be atom, namely, some non-standard solutions were reached only when we used starting vectors obtained from the results provided by the intermediate Hamiltonian FS-CC approach [27].

The next two tables (Tables 15-4 and 15-5) contain results of more extensive calculations for C_2 and H_2O. Using the same basis sets as before we show how the accuracy of the results can be increased by enlarging the reference space and including three-body operators in the exponent. The IH formulation of the basic FS-CCSD approximation discussed in this paper in more detail can be easily extended to the FS-CCSDT scheme that includes additional three-body components in the cluster operator at each level of calculation required by the valence-universal strategy [31]. Results for two different reference spaces are presented in both cases. Also results of the equation-of-motion (EOM) CC method which is more frequently used in excitation energy calculations than the FS-CC one are shown at both CCSD and CCSDT levels. It is seen that the extension of reference space can have a significant impact on the accuracy of the FS-CC results and it looks that the effect is more profound at the CCSD level than at the CCSDT one. Inclusion of triples generally improves the accuracy of excitation energies leading to better agreement with the experimental data. In some cases the improvement is particularly well seen like, for example, for the ${}^1\Sigma_u^+$ state for C_2 when the energy gap is reduced by 0.38–0.29 eV. For the H_2O calculation with smaller reference space the difference between CCSD and CCSDT results varies from 0.12 to 0.25 while for the larger space is less significant. Comparison with the EOMCC results shows that FS-CC method can be considered slightly more accurate than the EOMCC one. It must be mentioned that the EOMCC method requires diagonalization of much larger matrix than the IH one but does not need calculations in the $(1,0)$ and $(0,1)$ sectors. Another important

Table 15-4. Vertical excitation energies (eV) for C_2[a] as obtained with the IH-FS-CC[b] and EOM-CC methods at the CCSD and CCSDT level with the aug-cc-pVTZ[c] basis set ($R = 1.243$ Å[d]).

	IH-FS				EOM		
	(3,3)		(8,3)				
Sym.	CCSD	CCSDT	CCSD	CCSDT	CCSD	CCSDT	Exp.[e]
$^1\Pi_u$	1.280	1.252	1.263	1.251	1.313	1.287	1.23
$^1\Sigma_u^+$	5.907	5.531	5.789	5.500	5.577	5.532	5.36

[a] Valence electrons correlated.
[b] (m,n) is used to describe active spaces. m is the number of lowest unoccupied orbitals and n is the number of highest occupied orbitals used as active in the calculation.
[c] Ref. [52].
[d] Ref. [54].
[e] Ref. [55].

Table 15-5. Vertical excitation energies (eV) for H_2O[a] as obtained with the IH-FS-CC[b] and EOM-CC methods at the CCSD and CCSDT level with the POL1[c] basis set ($R = 0.957$ Å, angle $= 104.5°$[d]).

	IH-FS				EOM		
	(3,3)		(6,3)				
Sym.	CCSD	CCSDT	CCSD	CCSDT	CCSD	CCSDT	Exp.[d]
$^1B_1$	7.602	7.476	7.349	7.463	7.609	7.603	7.4
$^1A_2$	9.500	9.246	9.235	9.238	9.368	9.374	9.1
$^1A_1$	10.062	9.887	9.772	9.873	9.899	9.901	9.7

[a] Valence electrons correlated.
[b] (m,n) is used to describe active spaces. m is the number of lowest unoccupied orbitals and n is the number of highest occupied orbitals used as active in the calculation.
[c] Ref. [53].
[d] Ref. [60].

feature of EOM-CC is the lack of size-extensivity. As discussed the FS-CC approach is fully size-extensive.

15.7. CONCLUSION

In the paper we show advantages of the intermediate Hamiltonian version of the Fock-space CC method. Drawbacks of the effective Hamiltonian CC approaches are well-known. These are mainly formal complexity, high numerical cost of the

calculations, necessity of describing several states at a time, convergence and intruder state problems. They cause that the MR-CC methods are not as popular as their single-reference counterparts and rarely used in routine calculations for physically and chemically interesting systems. We show that the intermediate Hamiltonian reformulation of FS-CC helps to overcome many of difficulties the traditionally formulated FS-CC methods have to face. It makes the equations simpler, allows for performing calculations for single states, introduces a powerful computation scheme for solving the equations. All solutions that are difficult or impossible to obtain within the standard approach are easily accessible within the intermediate Hamiltonian formulation. That also includes nonstandard solutions of the effective Hamiltonian scheme. The effectiveness and accuracy of the approach are shown on several numerical examples. The numerical performances of the standard and reformulated version of FS-CC method are compared, the accuracy of calculations at the CCSD and CCSDT level of approximation with different choices for the reference space is discussed. The results are also compared with those given by the EOMCC method.

ACKNOWLEDGMENTS

We thank the Institute for Nuclear Theory at the University of Washington for its hospitality and the Department of Energy for partial support during the completion of this work. One of the authors (M.M.) acknowledges the financial support by the Ministry of Science and Higher Education under Grant No. N N204 218934.

REFERENCES

1. R. McWeeny, in *Methods of Molecular Quantum Mechanics*, second edition (Academic Press, New York, 1998)
2. F. Coester, Nucl. Phys. **7**, 421 (1958)
3. J. Čížek, J. Chem. Phys. **45**, 4256 (1966)
4. G. D. Purvis, R. J. Bartlett, J. Chem. Phys. **76**, 1910 (1982)
5. R. J. Bartlett, in *Modern Electronic Structure Theory*, Ed. D. R. Yarkony (World Scientific, New York, 1995), p. 1047
6. J. Paldus, X. Li, Adv. Chem. Phys. **110**, 1 (1999)
7. R. J. Bartlett, M. Musiał, Rev. Mod. Phys. **79**, 291 (2007)
8. B. H. Brandow, Rev. Mod. Phys. **39**, 771 (1967)
9. G. Hose, U. Kaldor, J. Phys. B **12**, 3827 (1979)
10. D. Mukherjee, R. K. Moitra, A. Mukhopadhay, Mol. Phys. **33**, 955 (1977)
11. R. Offermann, W. Ey, H. Kümmel, Nucl. Phys. A **273**, 349 (1976)
12. I. Lindgren, Int. J. Quantum Chem. Symp. **12**, 33 (1978)
13. B. Jeziorski, H. J. Monkhorst, Phys. Rev. A **24**, 1668 (1981)
14. L. Meissner, K. Jankowski, J. Wasilewski, Int. J. Quantum Chem. **34**, 535 (1988)
15. D. J. Klein, J. Chem. Phys. **61**, 786 (1974)
16. F. Jørgensen, Mol. Phys. **29**, 1137 (1975)
17. Ph. Durand, Phys. Rev. A **29**, 3184 (1983)
18. V. Hurtubise, K. F. Freed, Adv. Chem. Phys. **83**, 541 (1993)

19. L. Meissner, M. Nooijen, J. Chem. Phys. **102**, 9604 (1995)
20. S. Salomonson, I. Lindgren, A.-M. Mårtensson, Phys. Scr. **21**, 351 (1980)
21. U. Kaldor, Phys. Rev. A **38**, 6013 (1988)
22. J. Paldus, L. Pylypow, B. Jeziorski, in *Many-Body Methods in Quantum Chemistry*, Lecture Notes in Chemistry, vol. 52, Ed. U. Kaldor (Springer, Berlin, 1989), pp. 151–170
23. K. Jankowski, J. Paldus, Int. J. Quantum Chem. **18**, 1243 (1980)
24. J.-P. Malrieu, Ph. Durand, J.-P. Dauday, J. Phys. A **18**, 809 (1985)
25. L. Meissner, Chem. Phys. Lett. **255**, 244 (1996)
26. L. Meissner, J. Chem. Phys. **108**, 9227 (1998)
27. L. Meissner, P. Malinowski, Phys. Rev. A **61**, 062510 (2000)
28. K. Jankowski, P. Malinowski, Chem. Phys. Lett. **205**, 471 (1993)
29. M. A. Haque, D. Mukherjee, J. Chem. Phys. **80**, 5058 (1984)
30. M. Musiał, L. Meissner, S. A. Kucharski, R. J. Bartlett, J. Chem. Phys. **122**, 224110 (2005)
31. M. Musiał, R. J. Bartlett, J. Chem. Phys. **129**, 044110 (2008)
32. M. Musiał, R. J. Bartlrtt, J. Chem. Phys. **129**, 134105 (2008)
33. A. Banerjee, J. Simons, J. Chem. Phys. **76**, 4548 (1982)
34. H.-J. Werner, P. J. Knowles, J. Chem. Phys. **89**, 5803 (1988)
35. K. Woliński, P. Pulay, J. Chem. Phys. **90**, 3647 (1989)
36. K. Andersson, P. A. Malmqvist, B. O. Roos, J. Chem. Phys. **96**, 1218 (1992)
37. P.-O. Löwdin, J. Math. Phys. **3**, 969 (1962)
38. I. Lindgren, J. Phys. B **7**, 2441 (1974)
39. J. Mášik, I. Hubač, Adv. Quantum Chem. **31**, 75 (1999)
40. S. Berkovic, U. Kaldor, Chem. Phys. Lett. **199**, 42 (1992)
41. I. Lindgren, Phys. Scr. **32**, 611, 291 (1985)
42. A. Haque, U. Kaldor, Chem. Phys. Lett. **120**, 261 (1985)
43. S. Pal, M. Rittby, R. J. Bartlett, D. Sinha, D. Mukherjee, Chem. Phys. Lett. **137**, 273 (1987)
44. J. Paldus, J. Čížek, Adv. Quantum Chem. **9**, 105 (1975)
45. M. Noojen, J. Chem. Phys. **104**, 2638 (1996)
46. D. Mukherjee, Pramãna **12**, 203 (1979)
47. L. Meissner, J. Chem. Phys. **103**, 8014 (1995)
48. D. Sinha, S. K. Mukhopadhyay, R. Chaudhuri, D. Mukherjee, Chem. Phys. Lett. **154**, 544 (1989)
49. M. Musiał, R. J. Bartlett, J. Chem. Phys. **121**, 1670 (2004)
50. K. Hirao, H. Nakatsuji, J. Comput. Phys. **45**, 246 (1982)
51. E. R. Davidson, J. Comput. Phys. **17**, 87 (1975)
52. T. H. Dunning Jr., J. Chem. Phys. **90**, 1007 (1989); R. A. Kendall, T. H. Dunning Jr., R. J. Harrison, J. Chem. Phys. **96**, 6796 (1992); D. E. Woon, T. H. Dunning Jr., J. Chem. Phys. **103**, 4572 (1995)
53. A. J. Sadlej, Collect. Czech. Chem. Commun. **53**, 1995 (1988)
54. K. P. Huber, G. Herzberg, in *Constants of Diatomic Molecules* (Van Nostrand Reinhold, New York, 1979)
55. X. Li, J. Paldus, J. Chem. Phys. **124**, 034112 (2006)
56. O. Christiansen, H. Koch, P. Jørgensen, J. Olsen, Chem. Phys. Lett. **256**, 185 (1996)
57. A. Barbe, C. Secroun, P. Jouve, J. Mol. Spectrosc. **49**, 171 (1974)
58. T. Tanaka, Y. Morino, J. Mol. Phys. **33**, 538 (1970)
59. K.-H. Thunemann, S. D. Peyerimhoff, R. J. Buenker, J. Mol. Spectrosc. **70**, 432 (1978)
60. A. Banichevich, S. D. Peyerinhoff, Chem. Phys. **174**, 93 (1993)

CHAPTER 16

COUPLED CLUSTER CALCULATIONS: OVOS AS AN ALTERNATIVE AVENUE TOWARDS TREATING STILL LARGER MOLECULES

PAVEL NEOGRÁDY[1], MICHAL PITOŇÁK[1,2], JAROSLAV GRANATIER[1], AND MIROSLAV URBAN[1,3]

[1] *Department of Physical and Theoretical Chemistry, Faculty of Natural Sciences, Comenius University, SK-842 15 Bratislava, Slovakia, e-mail: palo@fns.uniba.sk; pitonak@fns.uniba.sk; granatier@fns.uniba.sk; urban@fns.uniba.sk*

[2] *Institute of Organic Chemistry and Biochemistry, Academy of Sciences of the Czech Republic, v.v.i. and Center for Biomolecules and Complex Molecular Systems, Flemingovo nám. 2, 166 10 Praha 6, Czech Republic*

[3] *Faculty of Materials Science and Technology in Trnava, Institute of Materials Science, Slovak University of Technology in Bratislava, Bottova 25, 917 24 Trnava, Slovakia*

Abstract: An overview of basic principles and different concepts of the Optimized Virtual Orbital Space (OVOS) method and its applications is presented. The objective is to show that the OVOS is a tool that allows extending the applicability of Coupled Cluster calculations to larger systems with larger basis sets it was possible before. We describe some instruments which serve as a measure of the accuracy of the CC calculation upon the OVOS truncation supplemented with a short outline of how to get a balanced reduction of virtual orbital space for all species participating in, e.g., calculation of reaction or interaction energies. We demonstrate the performance of the OVOS technique in different areas, including molecular electric properties, electron affinities, intermolecular interactions and some other applications. We also present some examples of large scale CCSD(T) calculations, which illustrate the computational efficiency of the OVOS approach.

Keywords: Coupled cluster, Optimized virtual orbital space, Large molecules, Intermolecular interactions

16.1. INTRODUCTION

Past few decades brought vigorous progress in the development and applications of the Coupled Cluster (CC) [1] methods. Most frequently, CC methods are applied to relatively small molecules which can be well represented by a single-determinant Hartree – Fock reference. Nowadays, along with extensive applications of a single-reference CC calculations to numerous molecular properties a large variety of

P. Čársky et al. (eds.), Recent Progress in Coupled Cluster Methods, 429–454.
DOI 10.1007/978-90-481-2885-3_16,

different models based on the exponential parametrization of the correlated wave functions, capable of treating general multi-reference (MR) systems (Fock and Hilbert space approaches), excited states (EOM), molecular properties (analytic derivatives and response techniques) and many other interesting aspects [2–8] have appeared. These achievements help in extending the applicability of CC methods into areas previously dominated by other methods, like MR CI (Configuration Interaction) or CASPT2 (Complete Active Space Perturbation Theory) [9]. Nevertheless, highly accurate calculations of "well behaved" single-reference systems still remain one of the most important areas of applications of the CC approach. In spite of the splendid progress in the applicability of CC and other wave function methods [9] to larger and more general systems, a vast majority of quantum chemical calculations are nowadays done using methods based on the Density Functional Theory (DFT). The admirable progress and the success of DFT methods in many areas of chemistry, physics and even biology is indisputable. Yet, we should not forget that DFT is still lacking suitable control of accuracy in terms of a systematic hierarchy of increasing level of the theory. This extends a space for methods like CC which may serve as a reliable tool for accurate predictions of molecular properties, intermolecular interaction energies, chemical reactivity etc. but, also, as valuable benchmarks for DFT and other more approximate methods applicable to truly large molecules. To serve this purpose better there is a need for the availability of CC calculations of model molecules which are closer to species which need to be treated in real chemical applications. This may help in approaching a desired symbiosis of the wave function methods, like CC methods, DFT methods and experiment. Such efforts seem to be quite promising [10–12].

For obtaining results with high and controlled accuracy, only a few ab-initio wave function techniques are available. In general, all such methods are computationally demanding. Moreover, widely accepted methods should be robust enough, i.e. they should allow explicit correlation of "many" electrons (say up to 50–100 electrons; actually much larger number would be advisable) with large enough basis sets, which guarantee results close to the Complete Basis Set (CBS) limit. If this is not feasible, calculations should be done with a series of systematically improved basis sets allowing the extrapolation to the CBS limit. Within CC methods the basic approach is represented by the CCSD method in which the amplitudes of the T_1 and T_2 operators are calculated iteratively [1, 3–5]. Of course, for highly accurate results rigorous treatment of higher than T_2 connected excitation operators must be considered. Theoretical and computational implementation of T_3, T_4 and even higher excitation operators is available [13–15], but iterative CCSDT, CCSDTQ and higher methods are for larger molecules prohibitively demanding. Important progress in extending CC methods with higher that T_1 and T_2 operators was initiated by the introduction of the perturbative calculation of effects due to higher excitation operators by utilizing amplitudes arising from the rigorous iterative treatment of the lower-order amplitudes. An order-by-order analysis of the perturbative sequence of such approximations is a basic instrument for a controlled accuracy arising from a systematic improvement of the wave function representation. Far most important is the CCSD(T) method which

appears to be the well balanced compromise between the accuracy and computational effort. This approach, where relatively feasible iterative CCSD method is corrected by more demanding, but a single-step perturbative treatment of the T_3 contribution [16, 17] nowadays represents the "golden standard" for single reference, highly correlated calculations. Perturbative incorporation of quadruples and even quintuples can be achieved in a similar way leading to a hierarchical wave-function based analysis of the respective theoretical tools for these contributions.

In most applications the CCSD(T) method leads to very accurate results and can be used as a predictive tool for obtaining highly reliable molecular properties. Also, it is frequently used as a benchmark for less controllable DFT calculations. Yet, when using CCSD(T) in a single-reference framework, its performance should not be blindly overestimated. Quality of results should be controlled via the T_1 diagnostics [18], which together with careful inspection of the largest T_1 and T_2 amplitudes [19, 20] allow to safely identify eventual multireference behavior of the system. When T_1 and T_2 amplitudes are approaching a limiting value of about 0.2, one should be careful in using CCSD itself and resulting T_1 and T_2 amplitudes as a source for obtaining the triples contributions. In that case, a simple perturbative T_3 treatment may not be accurate enough and can even lead to unphysical behavior. As was already mentioned, the T_3 contribution to the correlation energy appears to be crucial in achieving the chemical accuracy, as it completes the CCSD energy by the missing fourth-order terms [5]. For systems which exhibit large quasidegeneracy higher excitations, at least quadruples, become important. Obtaining iterative triples or quadruples, is, unfortunately, very demanding when we need to correlate large number of electrons. When combined with large basis sets and large number of virtual orbitals, computational demands increase truly painfully. A remedy can be achieved, e.g, by reducing the number of virtuals in a controlled way.

Returning to CCSD(T) we should stress that scaling of the CCSD(T) method with the size of the problem is still very disfavorable. Iterative CCSD procedure scales generally as N^6 (N is a general symbol for the number of occupied and virtual orbitals). The most time consuming steps scale as o^3v^3 and o^2v^4 (o and v is the number of occupied and virtual orbitals, respectively). Non-iterative perturbative T_3 contributions scale as N^7, namely as o^3v^4 and o^4v^3. For systems with large number of electrons, the T_3 step starts to be computationally most demanding. Thus, reducing of the computational efforts of the CCSD(T) method represents an important challenge which is crucial for extending the applicability of highly accurate ab-initio methods to larger systems.

The computational demands of CCSD(T) or higher level CC methods can be reduced employing methodological and technical innovations. From the methodological improvements the following routes are very promising: accelerating of the basis set convergence by R12 techniques [21–23], reducing the size of the virtual orbital space by OVOS [24, 25] or FNO techniques [26–29] or using localized orbitals [30–32]. Innovative technical tools cover different numerical methods which allow approaching final results with a controlled accuracy in computationally more efficient way. Among several of those, let us mention techniques based on the sparsity of matrices [33, 34], different prescreening methods [35], methods based on direct

evaluation of atomic integrals [36], etc. Approximate formulations based on the Cholesky Decomposition (CD) of 2-electron integrals (or other objects [37–39]) and Density fitting (DF, also known as the Resolution-of-the-Identity, RI) techniques employing auxiliary basis sets [40, 41] enable reformulation of CC algorithms into more efficient form, even if they can not reduce the overall scaling of CC methods. A specific class of purely technical innovations represent parallelization or incorporation of highly-optimized algebraic routines (BLAS).

16.2. OUTLINE OF THE OVOS METHOD

One of the approaches that enable reduction of overall computational demands of the Coupled Cluster methods (as well as other correlated methods heavily dependent on the size of the virtual orbital space – VOS) is the method of Optimized Virtual Orbital Space – OVOS [24, 25, 42]. The objective of this method is truncating the original set of virtual orbitals by an unitary transformation in such a way, that a reduced part of suitably rotated VOS is able to represent the complete VOS in the subsequent correlated calculations. In other words, we try to accumulate most of the flexibility of the complete VOS into a subspace of a smaller dimension, while the rest of the rotated VOS do not contribute to the expansion of the correlated wave function anymore. Using of OVOS with sufficiently truncated dimension obviously leads to the reduction of numerical demands of CC calculations – in fact it leads not only to the reduction of the computer time, but in many cases it principally opens the feasibility of calculations, which would be otherwise intractable with the available computational software and hardware using the original virtual space. Truncated OVOS also saves considerable disc space and the amount of the input/output operations. From this point of view, OVOS technique is one of the methods extending the applicability of the CC approach in general. Overall speedup of the subsequent correlated calculation depends both on the method and on the measure of the reduction of OVOS. For the "golden standard" – the CCSD(T) method, which scales as v^3 and v^4 (the CCSD part) and v^4 (the triples part), reduction of OVOS to 60% of its original dimension may reduce computational demands roughly by an order of magnitude.

Our introduction to the essence of the OVOS method was rather intuitive so far. Now, we will present the method in a more exact way. Let us divide the VOS into three parts: V1-orbitals, which remain unchanged (unrotated) during the VOS optimization procedure; V2-optimized virtual orbitals, which will be employed in the subsequent calculations instead of the full VOS; V3-remaining part of optimized virtual orbitals, which will be deleted in subsequent calculations. Any unitary rotation of the space of virtual orbitals should not affect the results of quantum chemical methods – these methods should be invariant with respect to the unitary rotation of VOS. The structure of the orbital space is illustrated in Figure 16-1.

Introducing the V1 block is a straightforward concept for the treatment of both closed- and open-shell systems (or possibly other more general reference space) within the same framework. V1 block is usually empty for closed shell systems. For the ROHF reference, V1 typically contains spatial complements of the singly

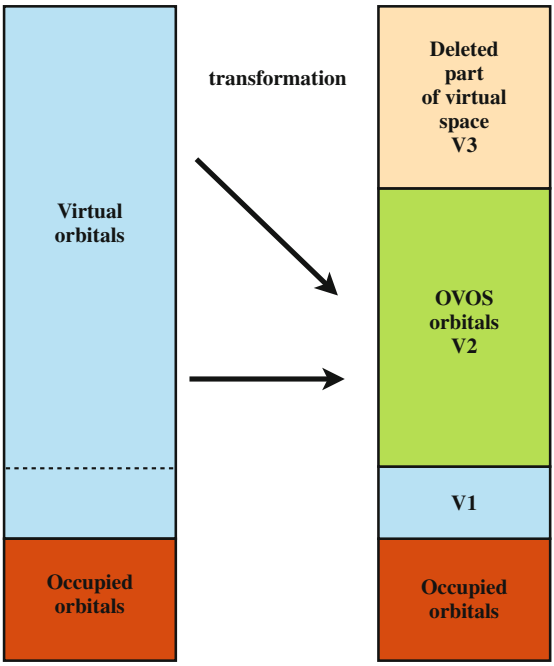

Figure 16-1. Structure of the orbital space

occupied orbitals. Since those are occupied only with α spin electrons, they do not belong exclusively to the occupied or the virtual space. Obviously, they cannot be mixed with V2 or V3 orbitals, because, as mentioned above, mutual mixing of occupied and virtual orbitals violates renormalized vacuum state, making CC energy no longer invariant with respect to such rotation. We note, that the V1 block can include also other orbitals, which need to be, for some reason, kept unchanged during the optimization of VOS.

Let us consider the simplest correlation level, say MBPT2 (Many-body second-order perturbation theory, or in short, MP2). The original VOS uses the whole space of virtuals, with dimension of V1 + V2 + V3, to describe the energy or other property at the MP2 level. With OVOS, the overall capability of the original VOS in describing any selected property is redistributed among virtuals in such a way, that the capability of the V2+V3 set is condensed into the truncated V2 space as much as possible. When reproducing the flexibility of the original VOS in a truncated set of optimized orbitals, reproducing the MP2 energy or, preferably, the overlap of the first-order wave function can be considered as examples of the optimization criteria. Our aim is to maximize the match between the full VOS and truncated (i.e. V2 OVOS) MP2 energy, or the overlap of the first order wave function. Optimization of orbitals proceeds via an unitary rotation among the virtuals from V2+V3 subspaces. Standard correlated methods like CC, CI and MP are invariant to so called "canonical" transformation (i.e. unitary transformation which does not "mix" occupied and virtual

orbitals). Thus, without deleting the V3 space, this rotation has no effect on the total correlation energy as calculated in the full VOS of HF-SCF canonical orbitals. However, deleting the V3 OVOS space deteriorates the correlation energy much less than a naive deletion of equally large subspace of the original, canonical VOS (i.e. simple deletion of virtuals with highest orbital energies).

The key point in the OVOS method is specifying the functional, which will be optimized in order to obtain desired reorganization of the VOS. In pioneering papers, Refs. [24, 25], the authors used the second-order Hylleraas functional, J_2, which gives an upper estimate of the second-order MBPT energy $E^{(2)}$ for a arbitrary trial wave function. Optimization with respect to this functional tends to modify the trial wave function toward the first order MBPT wave function $|\Psi^{(1)}\rangle$, since it has its global minimum there. In our later works, Refs. [42–44], we introduce slightly different functionals, first of which is based on the optimization of the CCSD energy with truncated OVOS, or more precisely, the minimization of the quantity

$$\mathcal{L} = (E_{\mathrm{CCSD}} - E_{\mathrm{CCSD}}^{\mathrm{OVOS}})^2 \tag{16-1}$$

where E_{CCSD} stands for CCSD energy in complete VOS, and $E_{\mathrm{CCSD}}^{\mathrm{OVOS}}$ is CCSD energy expressed expanded in V1+V2 subspace of OVOS. In the similar spirit we also defined, even more successful alternative optimization functional, based on optimization of the overlap of linearized CCSD wave function

$$\mathcal{L} = \langle \Phi_0 | T_{\mathrm{CCSD}} | T_{\mathrm{CCSD}}^{\mathrm{OVOS}} | \Phi_0 \rangle \tag{16-2}$$

where T_{CCSD} stands for CCSD mono- and biexcitations in complete VOS, while $T_{\mathrm{CCSD}}^{\mathrm{OVOS}}$ are defined as

$$T_1^{\mathrm{OVOS}} = \sum_{i,a^*} t_i^{a^*} a^{*\dagger} i \qquad T_2^{\mathrm{OVOS}} = 1/4 \sum_{\substack{i,j \\ a^*,b^*}} t_{ij}^{a^* b^*} a^{*\dagger} i b^{*\dagger} j \tag{16-3}$$

with an asterisk assigning virtuals from the V1+V2 subspace.

Once we have the optimization functional, we can easily express it in terms of rotational parameters. From this expression we derive final scheme for determination of optimized rotational parameters. In the pioneering works [24, 25] an exponential parametrization of the orbital transformation was used, $\mathbf{U} = \exp(\mathbf{R})$, where $\mathbf{R}$ is an antisymmetric matrix. In this formulation, matrix elements of the $R_{\mathrm{V2,V3}}$ block need to be determined to define the transformation uniquely. This rotation is automatically unitary, although sometimes with problematic convergence. To improve the convergence and overall applicability of the OVOS method, we introduced an alternative optimization scheme [42], where direct parametrization of the orbital transformation was used, i.e. U_{ab} were directly treated as rotational parameters. Since this parametrization does not guarantee the unitarity of the transformation, additional orthogonality conditions need to be taken into consideration. We used Lagrangian

multipliers to guarantee the orthogonality of new, optimized virtual orbitals. Varying the optimization functional (16-2) supplemented by the orthogonality constrains leads to the iterative diagonalization of the **Q** matrix (only the closed shell scheme is presented, for details see Ref. [42, 43])

$$\mathbf{U}^{\mathbf{T}}\mathbf{Q}\mathbf{U} = \lambda \tag{16-4}$$

in the V2+V3 subspace, assigned by the superscript +,

$$Q_{a^+b^+} = \sum_{ij}\sum_{cd} t_{ij}^{ca^+} t_{ij}^{db^+} P_{cd} \tag{16-5}$$

$$P_{cd} = \sum_{e^*} U_{e^*c} U_{e^*d} \tag{16-6}$$

Also here, only the $U_{\mathrm{V2,V3}}$ block is important, because V1 orbitals are not changed and the mutual V2 $\leftrightarrow$ V2 and V3 $\leftrightarrow$ V3 rotations have no effect on optimization functional value. Final OVOS orbitals have to diagonalize the $F_{\mathrm{V2,V2}}$ block of the Fock matrix, defining new orbital energies for the V2 OVOS subspace. Resulting iterative procedure is very similar to the HF-SCF procedure and leads to the significantly faster and more stable convergence of the method.

OVOS approach is closely related to the Frozen Natural Orbitals (FNO) method [26–29]. FNO approach can be viewed as an approximation to the OVOS method, based on the (16-2) functional, setting $P = 1$ instead of (16-6). In this case, procedure (16-4) is not iterative, because Q does not depend on U anymore. Thus, in the FNO approach there is no need to define the VOS splitting into V2 and V3 a priori. However, limited summation in Eq. (16-6) in the OVOS method slightly enhances the flexibility of the reorganization of the virtuals, i.e. OVOS represents the optimization tailored specifically to the selected truncated V2 subspace. So, in FNO there is no initial setting of V2 and V3 subspaces, V3 subspace is deleted a posteriori, without V2 $\leftrightarrow$ V3 splitting feedback. Generally, FNO is very efficient approximation to OVOS, perhaps up to the substantial truncations of optimized VOS, where P is not well approximated by the unity matrix anymore.

Overlap functional, defined in Eq. (16-2), can be used in a straightforward way for the post-CCSD calculations. However, if we wish to use the truncated OVOS already in the CCSD step, we must use a simplification, in which converged T_{CCSD} amplitudes are substituted by their first order estimates, ${}^{(1)}T$. Optimization functional becomes actually an overlap of the first-order wave function in the full and truncated OVOS, respectively.

$$\mathcal{L} = \langle \Phi_0^{(1)} T | {}^{(1)}T_{\mathrm{OVOS}} \Phi_0 \rangle \tag{16-7}$$

Accuracy of the OVOS approach for any target method, e.g. CCSD(T), can be significantly improved, by taking only the higher than the second order

contributions from the calculation in OVOS. $E_{\mathrm{MBPT(2)}}$ is taken from the full VOS, since it is available prior to the OVOS CCSD/CCSD(T) calculation anyway.

$$E^{\mathrm{OVOS}}_{\mathrm{CCSD}(T),2} = E^{\mathrm{Full}}_{\mathrm{MBPT(2)}} + X_2 \tag{16-8}$$

$$X_2 = E^{\mathrm{OVOS}}_{\mathrm{CCSD}(T)} - E^{\mathrm{OVOS}}_{\mathrm{MBPT(2)}} \tag{16-9}$$

This idea goes back to initial OVOS papers [24, 25] and is based on the fact, that most of the correlation energy originates from the second order. In this way we can eliminate major source of error by taking this term from complete VOS calculation. The OVOS CCSD(T) energy corrected using Eq. (16-8) will be denoted in the application part simply as $\mathrm{CCSD(T)}_2$. It is convenient to use an alternative notation

$$E^{\mathrm{OVOS}}_{\mathrm{CCSD}(T),2} = E^{\mathrm{OVOS}}_{\mathrm{CCSD}(T)} + Y_2 \tag{16-10}$$

$$Y_2 = E^{\mathrm{Full}}_{\mathrm{MBPT(2)}} - E^{\mathrm{OVOS}}_{\mathrm{MBPT(2)}} \tag{16-11}$$

where Y_2 is approaching zero if error of the second order in OVOS is approaching zero as well. Thus, Y_2 parameter serves as an indicator of the quality of OVOS optimization [43, 44].

16.2.1. Applications of OVOS: A few Hints for Practical Calculations

OVOS is not a true "black-box" method for several reasons. First, the dimension of OVOS must be set somehow prior to the calculation by, for instance, defining percentage of VOs (Virtual Orbitals) to be deleted or by specifying exact number of VOs to be retained in each irreducible representation. This might seem trivial, but in more complicated cases like highly-symmetric systems, bond dissociation, calculation at the reaction energy profile or non-covalent interactions, balanced distribution of optimized VOs in each symmetry species is crucial.

Perhaps the most demonstrative example is the BSSE (Basis Set Superposition Error) corrected OVOS calculation of the interaction energy. The most commonly used approach to eliminate BSSE is the Boys–Bernardi [45] counterpoise scheme, where the same AO (Atomic Orbital) basis set for the supersystem and subsystems is used. Since the supersystem (for simplicity a dimer), and monomers have different number of occupied orbitals, number of VOs must be also different. Efficiency, to which the truncated optimized VOs reproduce the original VOS, changes with both the dimension and the percentage of truncation of the full size VOS. This is the reason, why the "desired" truncation of OVOS for dimer cannot be the same as for the monomers. Using the same truncation would lead to unbalanced recovery of correlation energy and thus to inaccurate results.

There is a way of how to overcome this difficulty, applicable also in other similar situations when simultaneous treatment of several species is necessary (e.g. finite field calculation of electric properties, reaction energies, etc.). Specifying

the truncation and carrying out OVOS optimization for any of involved species, for instance dimer, we obtain an quantitative information about the "efficiency" of optimization. As this quantity, we use the ratio of value of the optimization functional in truncated optimized and the full VOS. Based on this ratio we can act "backwards" and determine the truncation in all other involved species (e.g. monomers). This is done by insisting on the best possible agreement of the ratios, mentioned above, for each particular species (e.g. monomers) with the "reference", obtained independently (e.g. dimer).

Furthermore, obtaining OVOS according to the scheme described above, leads to essentially BSSE-free calculation of interaction energies at subsequent CCSD(T) step. Effect of BSSE, i.e. using of the supermolecular AO basis for monomers, is almost completely absorbed into the optimized VOs, meaning that their resulting number is almost equal to the number corresponding to genuine original AO basis sets for each monomer.

16.2.2. Prerequisites for Large-Scale CCSD(T) Calculations

When talking about extending limits of applicability of CC methods, it is useful mentioning also the progress in the area of development of more efficient computer programs. It is mainly the synergic effect of using the OVOS technique combined with more powerful computer implementation of the CCSD(T) method that enables calculations of larger problems within this framework. Several robust CCSD(T) codes in different program packages appeared recently [46–50]. Among those, we will shortly describe our new implementation [46] in the MOLCAS program package [9, 51], where both OVOS and CCSD(T) methods are implemented in the efficient and highly parallelized way.

For large-scale CC calculations several crucial aspects need to be addressed at the same time. First, it is the huge disk and internal memory requirements. Even quantities like CCSD T_2 amplitudes, scaling as o^2v^2, can not be stored at once in-core. The two electron integrals, mainly $(ab|cd)$ integrals over virtuals (scaling as v^4, where a,b,c and d are indexes of virtual orbitals) are usually too large to be stored even on disk. Another problem is the rapidly increasing number of I/O operations, but mainly the arithmetics, scaling as o^2v^4 and o^3v^3 for the single CCSD step and o^3v^4 and o^4v^3 for the noniterative triples step.

Ideas of the Cholesky decomposition (CD) of the 2-electron integrals, segmentation of the virtual orbitals and efficient matrix-multiplication (BLAS) oriented algorithms are basic concepts our new CCSD(T) implementation profits from. CD of 2-electron integrals, which is the leading concept of the new generation of the MOLCAS modules (SCF, CASSCF, CASPT2) [9] is expression of 4-index AO integrals in terms of 3-index quantities [37–39]

$$(\mu\nu|\lambda\sigma) \approx \sum_{J=1}^{M} L^J_{\mu\nu} L^J_{\lambda\sigma} \,, \tag{16-12}$$

where the Mulliken notation was used. CD (which is analogous to the DF/RI techniques) opens a possibility for much simpler handling with the 2-electron AO and MO integrals, thus enabling more efficient factorization of several terms in the CC equations. Another important tool, enabling elimination of the memory storage requirements and at the same time splitting of the CC equations into independent tasks (within a single CCSD iteration) is the segmentation, or blocking, of virtual orbitals. If we divide virtual orbitals into N' blocks, with the number of virtuals in each block being roughly $v' \approx v/N'$, corresponding block of e.g. T_2 amplitudes $\left(t_{ij}^{a'b'}\right)$ requires only $o^2v'^2$ words. Similarly, other larger arrays and intermediates split into smaller blocks, since they are labeled by at least one virtual orbital index.

We can reformulate the CCSD procedure assuming, that only such fragments of arrays can be kept in-core. This reduces the memory requirements practically to any extent, since N' can be chosen large enough to fit the blocks into a particular memory. Moreover, whole procedure splits into $\approx N'^2$ independent tasks (in single CCSD iteration), which is beneficial in parallelization, since each task can be performed on separate node or parallel process (PP). Unfortunately, such segmentation introduces an extra penalty in the form of additional I/O, proportional to $N'^2o^2v^2$. As in any other CCSD parallel algorithms, there is also a significant data transfer among nodes – a complete set of amplitudes (also proportional to o^2v^2) need to be interchanged and updated among all nodes after each CCSD iteration. Obviously, these additional processes, proportional to o^2v^2 are asymptotically insignificant compared to $o^2v'^4$ and $o^3v'^3$, if the computed system becomes large.

In our CCSD code two variants of handling of the most difficult $(ab|cd)$ integrals are implemented. First is the "pre-calculation" algorithm, where $(ab|cd)$ integrals are recalculated from Cholesky vectors prior to the iterative procedure. These integrals are stored on disk and read in each CCSD iteration. In massively parallel run, certain combination of occupied/virtual indices are locked to particular parallel task, which mean that the number of integrals needed to be stored on each node decreases with the number of PP, roughly as 1/PP. Second is the "on-the-fly" algorithm, where direct reconstruction of desired blocks of these integrals from Cholesky vectors are done on-the-fly whenever needed, without storing them. The efficiency of both algorithms depends on the size of calculated system and the setup of the available computer hardware. Since the dimension of the Cholesky vector is typically quite large, it is usually faster to read $(a'b'|c'd')$ block than to recalculate it from Cholesky vectors (according to Eq. 16-12). However, this is true mostly for PPs with single, or smaller number of CPUs/cores (1–2), while with increasing this number direct recalculation of integrals starts to be more efficient. Another limitation is the disk capacity. If we perform large calculation on small number of nodes, the portion of $(ab|cd)$ integrals, that need to be stored on each node can easily exceed the disk capacity. In such case, "on-the-fly" algorithm is the only choice. However, as mentioned above, with increasing number of nodes – N, disk space requirements decrease proportionally to $1/N$. Thus, for massively parallel runs, required portion of $(ab|cd)$ integrals can be stores on local disks and the "pre-calculation" remains feasible.

Our CCSD implementation is completed by noniterative T_3 program taken from DIRCCR12OS code [52], with the memory requirement optimized also via segmentation of virtual orbitals. Triples (T) step is typically the most time consuming part of the whole CCSD(T) calculation, mainly for systems with large number of correlated electrons. On the other hand, (T) step can be almost ideally parallelized, without any significant data transfer. Our CCSD(T) code was tested so far mostly on distributed memory clusters with typically one to eight cores, 1GB memory per core and several hundreds of GB of local scratch disk on each node. In this setup, CCSD(T) calculations scaled almost linearly up to hundreds of nodes. Details of implementation and performance can be found in Ref. [46].

16.3. TESTING THE OVOS PERFORMANCE

In the following two sections we will present few typical applications in which the OVOS technique allows more extended CCSD(T) calculations than it was possible with a standard approach. Applications go either to larger molecules or to CCSD(T) calculations with large basis sets needed for obtaining accurate benchmark results. Before applying the OVOS CCSD(T) technique to large-scale problems, careful verification of its accuracy and reliability is needed. The usefulness of the OVOS approach was demonstrated in our previous papers [42–44, 53–55] on reaction energies as, e.g., the dissociation energy of pentane to propene and ethane, spectroscopic constants, dipole moments and dipole polarizabilities of small and medium molecules, interaction energies of the hydrogen-bonded molecules like the formamide and formamidine dimers, van der Waals interactions of typical stacking structures which serve as a model of interactions in biological systems etc. In this section we will present a few examples showing the performance of OVOS in CCSD(T) calculations of molecular electric properties, intermolecular interactions and electron affinities of relatively small molecules. These properties are mostly quite sensitive to the quality of the method and may serve as a touchstone of the performance of OVOS. For all these testing examples OVOS results were confronted with the full virtual space CCSD(T) results. Subsequently, in Section 16.4 we will provide benchmark calculations on a few properties of biologically important molecules. All CCSD(T) calculations were performed by the computer program developed in our laboratory, which is a part of the MOLCAS package [9, 51].

16.3.1. Molecular Properties

First testing examples documenting the performance of OVOS were accurate CCSD(T) calculations of the dipole moment and dipole polarizabilities of a series of atoms and their anions, simple molecules like CO and formaldehyde, followed by larger push-pull 1-amino-4-nitrobutadiene molecule [42, 53, 54]. In this section we summarize in Table 16-1 the frozen-core CCSD(T) finite field calculations of the dipole moment and dipole polarizabilities of thiophene with a medium aug-cc-pVTZ

Table 16-1. CCSD(T)$_2$ dipole moment and dipole polarizabilities (a.u.) of thiophene with differently truncated OVOS

% of OVOS	No. of VOs	μ	α_{zz}	$\bar{\alpha}$	$\triangle\alpha$
aug-cc-pVTZ					
100	304	0.204	77.75	64.71	30.29
60	182	0.204	77.77	64.73	30.26
50	152	0.202	77.78	64.73	30.27
40	121	0.203	77.67	64.73	30.32
aug-cc-pVQZ					
100	566	0.214	77.76		
60	339	0.212	77.74		
50	283	0.212	77.78		
40	226	0.213	77.87		

and a larger aug-cc-pVQZ basis sets [56–58]. CCSD(T) calculations of thiophene with the aug-cc-pVQZ basis set (566 virtual orbitals) are not quite effortless with a routine workstation so it is beneficial to consider less demanding approach. The dipole moment of thiophene is surprisingly insensitive to the truncation of OVOS. Even when truncated to 40% of the full VOS the result differs from the full VOS by only 0.001 a.u. and can be obtained by about 40 times faster. The dipole moment with smaller aug-cc-pVTZ basis is underestimated by almost 5% with all OVOS truncations. The dipole moment can be obtained faster and more accurately (in full agreement with experiment [59]) with larger aug-cc-pVQZ basis with OVOS truncated to, say, 50% of the full VOS. CCSD(T) dipole moment of thiophene with small basis sets, as 6-31G+pd or 6-31G+pdd are unreliable, being overestimated by a factor of almost two [44, 60].

Dipole polarizabilities of thiophene are almost insensitive to the basis set when using at least aug-cc-pVTZ and aug-cc-pVQZ bases. CCSD(T)$_2$ results with OVOS truncated down to 50% of the full VOS of both basis sets are accurate to within 0.03 a.u. Again, calculations with smaller basis sets lead to inaccurate results [60] and are clearly outperformed by CCSD(T)$_2$ calculations with larger bases and properly selected OVOS. More details can be found in Refs. [44, 54].

16.3.2. Intermolecular Interactions

Intermolecular interactions, particularly weak van der Waals interactions, are very sensitive to the quality of the method. When using OVOS we must be very careful in proper balancing the truncation of the virtual space for the supersystem and for subsystems. Some hints were described in Section 16.2.1. Particular attention must be paid to the treatment of BSSE within OVOS. Among most desired applications belong benchmark calculations of H-bonded and stacking interactions, typical in molecules participating in biological systems. Recently [55], we have demonstrated

good performance of OVOS in calculations of CCSD(T)$_2$ interaction energies of the model H-bonded complexes, the formamide and formamidine dimers as well as stacked formaldehyde and the ethylene dimers. With the space of virtual orbitals reduced to 50% of the full space, which means reducing computational demands by an order of magnitude, the interaction energy for both H-bonded and stacking dimers is affected no more than by 0.1 kcal/mol. This error is much smaller than is the error when interaction energies are calculated using limited basis sets. In the next section we will show benchmark calculations on relative interaction energies of different structures of the van der Waals benzene and uracil dimers. Quite large basis sets could be used thanks to our efficient parallelized computer code employing Cholesky decomposition combined with reasonably reduced OVOS. To ensure that we are obtaining "good results for a good reason" we present at least one testing example of using OVOS in similar applications in Figure 16-2. It is seen that the part of the CCSD(T) energy hypersurface which represents parallel displacement of the ethylene dimer is represented by OVOS excellently. There is a slight shift of interaction energies but main features of the surface are preserved with OVOS truncated to 50% with just 10% of the computer time needed for the full VOS calculation. The minimum CCSD(T) energy is calculated at $R_1 = 3.301$ and $R_2 = 3.040$ Å, respectively, with the full VOS. With OVOS truncated to 50% are optimized distances practically the same, $R_1 = 3.299$ and $R_2 = 3.044$ Å. Interaction energies with the full VOS and OVOS are -0.71 and -0.73 kcal/mol, respectively. For $R_2 = 3.04$ Å and $R_1 = 0.0$ Å (sandwich D_{2h} structure of the dimer) the energy

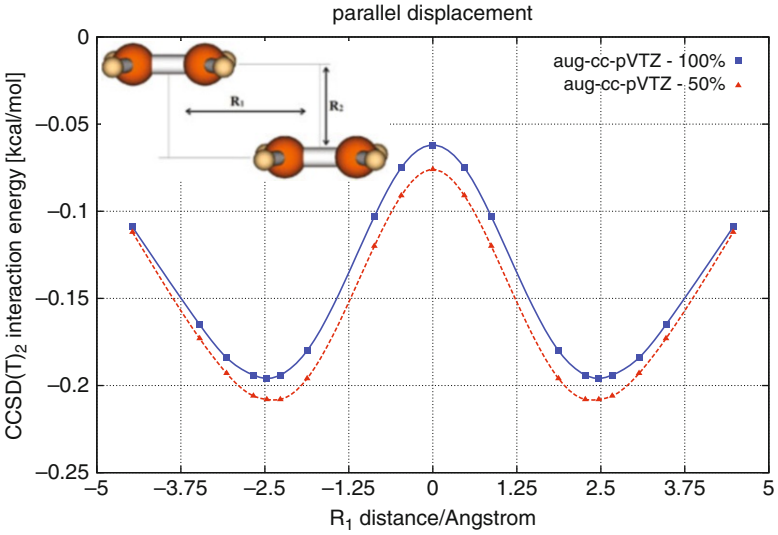

Figure 16-2. CCSD(T)$_2$ interaction energies [kcal/mol] of the stacked ethylene dimer with full VOS (100%) and OVOS reduced to 50% with aug-cc-pVTZ basis set. R_2 distance is fixed at 4.6 Å. Results are based on data in Ref. [55]

is repulsive. We do not present this part of the energy hypersurface in Figure 16-2. For details see Ref. [55].

Quite different is another testing example, namely interactions between coinage metals (M) and the SCH_3 radical. From the point of view of applications of OVOS to intermolecular interactions the $M\cdots SCH_3$ complex differs from those treated in Ref. [55] in several aspects. First, included are scalar relativistic effects using the second-order Douglas–Kroll–Hess CCSD(T)-DK approach. Second, both interacting species are open-shells. Consequently, the interaction of a metal with SCH_3 in its ground state, $^2A'$ (assuming simplified C_{3v} structure) leads to at least two different products, namely the closed shell singlet $^1A'$ and the triplet $^3A''$ state of the $M\cdots SCH_3$ complex. Open-shell complex and separated species were treated by the approximate spin-adapted ROHF-CCSD(T) method developed in our laboratory [61]. Calculations of the Cu, Ag, and Au interacting with the SCH_3 radical follow up investigations of the bonding mechanism between the coinage metals (M) and the lone-pair closed shell ligands (L), $M\cdots L$, like NH_3, H_2O, or H_2S published some time ago [62, 63].

Based on the analysis of relativistic effects, we were able to provide a consistent interpretation of trends in $M\cdots L$ interactions which is based on the idea of *partial* charge transfer from the lone pair carrier L (employing a molecular orbital picture of a ligand) to the coinage metal atom. The molecular orbital picture requires also that there is certain overlap between the electron donor (lone pair orbital of L) and the electron acceptor (valence n*s* orbital of M). This requirement makes the interaction pattern symmetry-dependent and is the main cause of the distinction between the geometric structures of the $M\cdots NH_3$ (C_{3v}) and non-planar $M\cdots OH_2$ and $M\cdots SH_2$ complexes. Applying this picture to $M\cdots SCH_3$ we expect that the M–S–C bond is bent. Precisely this is seen in Figure 16-3. The bond angles optimized using the ROHF-CCSD(T) method [61] with the full VOS and with OVOS truncated to 60%, respectively, agree to within 0.04° for the singlet and the triplet states of $M\cdots SH_2$. Relying on the experience with the bond angle optimization for $Cu\cdots SCH_3$ were bond angles in remaining $Ag\cdots SCH_3$ and $Au\cdots SCH_3$ complexes optimized only using OVOS truncated to 60%.

Similarly, so truncated OVOS reproduces the full VOS ROHF-CCSD(T) M–S optimized bond length in both states of $M\cdots SCH_3$ excellently, Figure 16-4. For the $^1A'$ state of $Au\cdots SCH_3$ are R_e with the full VOS and the OVOS, 2.241 and 2.242 Å, respectively, while the corresponding bond lengths R_e for the $^3A''$ state are 2.327 and 2. 329 Å. For a general use for obtaining optimized geometries of larger systems Taube and Bartlett [66] developed the gradient technique based on the Frozen Natural Orbitals (FNO), which is closely related to OVOS.

We note that the usual long-range model fails in describing the bonding features of $M\cdots L$ complexes, with the exception of very large distances. The transfer of the electronic charge to M depends on the ionization potential (IP) of the lone pair electron in L and the electron affinity (EA) of M. The importance of these factors for $M\cdots NH_3$, $M\cdots OH_2$ and $M\cdots SH_2$ complexes has been discussed in our earlier papers [62, 63]. Relativistic effects enhance EA of the metal and support the stability of

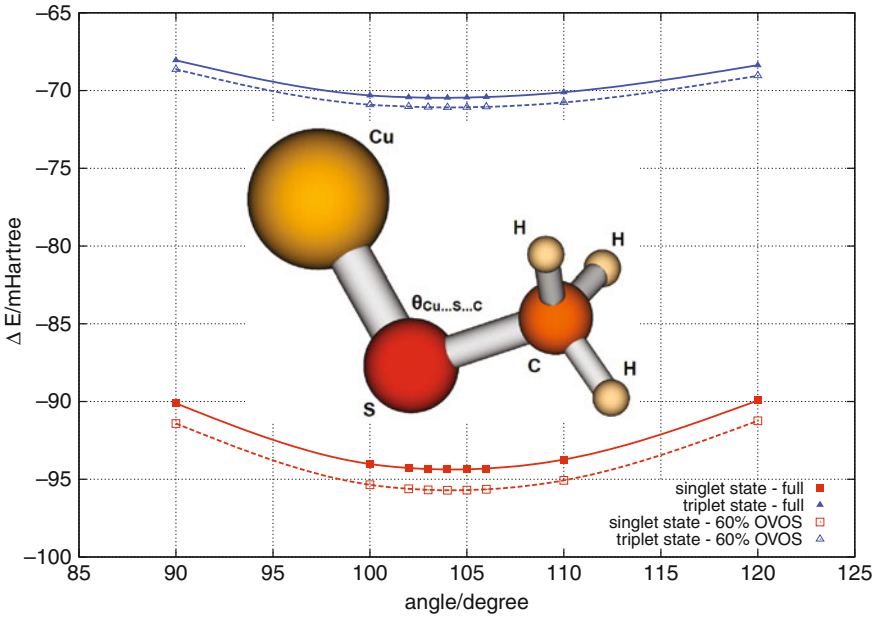

Figure 16-3. The CCSD(T)-DK optimization of the Cu–S–C angle in $^1A'$ and $^3A''$ states of Cu$\cdots$SCH$_3$ complexes. The full VOS and OVOS of the aug-cc-pVTZ-DK basis set [57, 64, 65] truncated to 60%. Energies for the $^3A''$ state are shifted down by 50 mHartree to fit into the plot

these complexes significantly, particularly with gold. Previously studied complexes have a closed shell ligand. The SCH_3 radical may interact with the coinage metal either with its doubly or singly occupied lone-pair orbital. The same mechanism as in M$\cdots$L complexes with a closed shell ligand is also valid for the Au$\cdots$SCH$_3$ complex (and similarly with other coinage metals) in the $^3A''$ state. It results from the partial charge transfer of electrons in the *doubly occupied* $10a'$ lone pair orbital (IP=9.2 eV) to the metal, leaving a single electron in the second lone pair of SCH_3. The bond in the $^1A'$ state of the Au$\cdots$SCH$_3$ complex is essentially a covalent bond created by electrons in the singly occupied lone pair of SCH_3 and the valence n*s* electron of the metal. Detailed description of the bonding mechanism in both states of M$\cdots$SCH$_3$ will be presented elsewhere. For the purpose of this paper it is important that OVOS works very well in describing the structural features of these complexes. CCSD(T) interaction energies represented by OVOS are satisfactorily accurate as well. With the full VOS is the CCSD(T)-DK interaction energy of the $^1A'$ state of the Au$\cdots$SCH$_3$ complex 87.17 mHartree (54.7 kcal/mol) and with OVOS it is 88.41 mHartree (55.5 kcal/mol). Full VOS and OVOS interaction energies for the $^3A''$ state are 28.39 and 29.24 mHartree (17.8 and 18.3 kcal/mol, respectively) with the aug-cc-pVTZ-DK basis set. This accuracy is fully satisfactory for considering structural and energetic aspects of medium inorganic complexes tractable with the

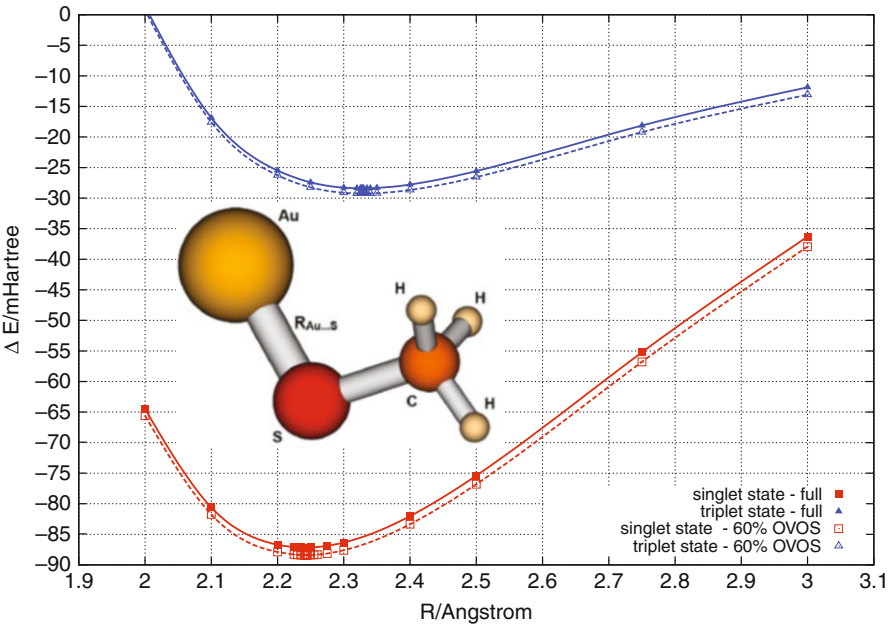

Figure 16-4. The CCSD(T)-DK optimization of the Au–S bond length [Å] in $^1A'$ and $^3A''$ states of $Au\cdots SCH_3$ complexes. The full VOS and OVOS of the aug-cc-pVTZ-DK basis set truncated to 60%

single-determinant reference closed shell or open-shell CCSD(T). Basis set effects are much larger than is the inaccuracy caused by the OVOS truncation. $M\cdots SCH_3$ complexes are microscopic representatives of bonding features encountered in the Self-Assembled-Monolayers (SAMs) or in various compact metal-ligand species participating in some biological processes. OVOS allows CCSD(T) calculations with satisfactorily diffuse (i.e. large) basis sets, which may hopefully serve as benchmark results for DFT calculations for larger complexes of this kind.

16.3.3. Electron Affinities

Calculations of electron affinities (EA) require sophisticated treatment of the electron correlation and large diffuse basis sets. Unfavorable scaling of CCSD(T) with the number of virtual orbitals can be alleviated by OVOS, but finding well balanced truncation of the virtual space for the neutral and the anionic species is difficult. Therefore, calculation of EA is a good testing example of the OVOS method.

Seemingly a simple task, adiabatic electron detachment energy of the oxygen molecule has an interesting story of difficulties in obtaining this property accurately, both experimentally and theoretically. Theoretical difficulties are summarized in, e.g., Ref. [43]. Experimental measurements have also undergo a long series of improvements [67]. Finally, by employing CCSD(T) calculations with extrapolation

to the CBS limit, vibrational ZPE, core correlation, scalar and spin-orbit relativistic corrections we have succeeded [68] in obtaining a highly accurate electron affinity of this molecule in the ground state at 0 K, 0.449±0.008 eV, which is in superb agreement with the most recent photoelectron spectroscopy (PES) electron affinity of O_2 measured by Ervin et al. [67], 0.448±0.006 eV.

ROHF-CCSD(T) calculation with the largest d-aug-cc-pV6Z basis (415 virtuals) used in the full VOS study of O_2 [67] is relatively demanding but can be performed more effectively by truncating the virtual space. Results are presented in Table 16-2. $CCSD(T)_2$ calculations [43] with the (d)-aug-cc-pVXZ series [56–58] show that OVOS reproduces the trend with increasing X in both series quite well, even if EA with OVOS truncated to 50% is slightly overestimated with respect to the full VOS. OVOS with truncation to 60% gives EA which deviates from the full VOS by about 0.01 eV (or even less with d-aug-cc-pVXZ basis sets). Considering the error bars of best experimental measurements (and theoretical calculations as well) this is quite satisfactory for most applications of the OVOS method to electron affinities. For bases smaller than (d)-aug-cc-pV5Z is the basis set effect larger than is the error due to the OVOS truncation.

Now, let us take EA=0.407 eV, calculated with our best d-aug-cc-pV6Z basis set as a reference for some comparisons of CCSD(T) results with OVOS and full VOS, both having similar number of virtual orbitals, v. We note, e.g., that EA with aug-cc-pV6Z with OVOS reduced to 50% ($v = 171$) or with d-aug-cc-pV5Z ($v = 158$) are closer to the best result than are full VOS results with smaller basis sets, as d-aug-cc-pVQZ ($v = 201$) or aug-cc-pVQZ ($v = 151$).

Table 16-2. Electronic contribution to adiabatic EA (in eV) of the oxygen molecule with the full VOS CCSD(T) method and $CCSD(T)_2$ using differently truncated OVOS[a]

	% of OVOS[b]			
basis set	100	70	60	50
aug-cc-pVTZ	0.358	0.359	0.343	0.344
aug-cc-pVQZ	0.385	0.395	0.389	0.390
aug-cc-pV5Z	0.401	0.406	0.408	0.413
aug-cc-pV6Z	0.405	0.412	0.417	0.419
CBS[c]	0.415	0.419	0.428	0.432
d-aug-cc-pVTZ	0.365	0.364	0.366	0.367
d-aug-cc-pVQZ	0.389	0.388	0.395	0.401
d-aug-cc-pV5Z	0.403	0.408	0.410	0.411
d-aug-cc-pV6Z	0.407	0.408	0.412	0.418
CBS[c]	0.415	0.420	0.421	0.424

[a] For more details, see Ref. [43].
[b] With respect to the full VOS of the O_2^- anion.
[c] Extrapolated using the three-point fit with respect to $1/X^3$.

16.4. LARGE SCALE CALCULATIONS WITH OVOS

16.4.1. Benzene Dimer

An interesting application of the OVOS CCSD(T) methodology is the recently published benchmark calculation of relative stability of various structures of benzene dimer [69]. It is based on the pilot study on performance of OVOS for different hydrogen bonded systems and some typical stacking interactions, as summarized in Section 16.3.2. In Figure 16-5, three lowest lying structures are shown. Their geometries were obtained by full gradient optimization using BLYP-D/TZV [69], with the empirical dispersion term optimized against the T and PD CCSD(T)/aug-cc-pVTZ PES cuts [69].

It is known for some time [70], that the so-called "sandwich" structure of D_{6h} symmetry, not show in the figure, is relatively well energetically separated from the almost isoenergetic TT, T and PD structures. However, which of TT/T/PD structures is the lowest in energy, was quite widely discussed [71] and none of methodologies used so-far were convincing enough to deliver the "ultimate" answer. Meanwhile, on-the-fly ab-initio dynamics of benzene dimer at the DFT-D level [72] revealed,

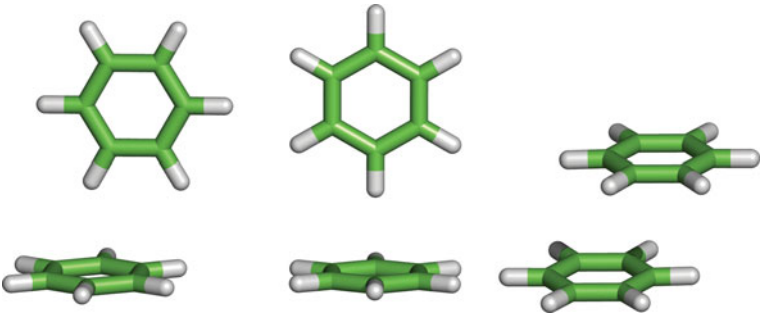

Figure 16-5. C_s TT (T-shaped Tilted, *left*), C_{2v} T (T-shaped, *middle*) and C_{2h} PD (Parallel-Displaced, *right*) structures of benzene dimer

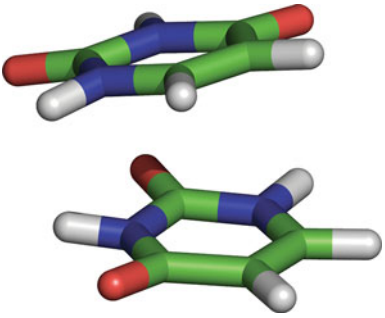

Figure 16-6. Stacked uracil dimer

that the barrier between the TT, T and PD structures can be overcome already at 10K, thus making discussion about relative stability of TT/T/PD based solely on the electronic energy only academic. Nevertheless, knowledge of high-accuracy interaction energies is extremely beneficial in designing, parameterizing and testing of novel, typically approximate, methods.

In Table 16-3 the plain CCSD(T), OVOS CCSD(T)$_2$ and hybrid extrapolated values of stabilization energies for T, TT and PD structures are shown. Structure "PD$_p$" served as a reference for calibrating our OVOS CCSD(T) methodology with respect to QCISD(T) data published by Janowski et al. [73]. Effect of basis set for all structures is quite significant, stabilization energies change by almost 0.5 kcal/mol (i.e. ~20%). At the aug-cc-pVDZ level, T structure seems to be stabilized by ~0.13 kcal/mol more than the PD, while TT structure by almost 0.3 kcal/mol. At the CBS level, T and PD became degenerate within the accuracy of our methodology, which was estimated to be ±0.03 kcal/mol. TT structure, at the CBS, is only by ~0.8 kcal/mol more stable that the other structures. Comparing to the results of other groups (see Table 16-3), nice agreement (i.e. ±0.05 kcal/mol) is achieved. It must be, however, emphasized, that significant part of these energy differences can be attributed to use of different geometries obtained in various ways (see References in the table).

Table 16-3. Benzene dimer stabilization energies [kcal/mol] for various structures, methods, basis sets and CBS extrapolations. Geometry of the PD$_p$ structure was taken from Ref. [73]

Method/Basis set	PD	TT	T	PD$_p$
CCSD(T)/aug-cc-pVDZ	2.15	2.44	2.28	2.29 (2.30)[a]
CCSD(T)$_2$/aug-cc-pVTZ 70% OVOS	2.49	2.66	2.57	2.53 (2.55)
CCSD(T)$_2$/aug-cc-pVQZ 60% OVOS	2.63	2.75	2.65	2.64 (2.61)
CCSD(T)$_2$/(Q→5)[b]	2.74	2.81	2.71	
CCSD(T)$_2$/(Q→5)[c]	2.70	2.78	2.69	
Sherrill et al. [74]	2.63	–	2.61	
Szalewicz et al. [75]	2.70	2.80	2.68	
Werner et al. [76]	2.72	–	2.68	
Hobza and Kim et al. [71]	2.73	2.83	2.77	
Bludský et al. [77]	2.73	2.82	2.70	
Pulay et al. [73]	2.66	–	2.68	
DFT-D/BLYP[d]/TZVP	2.88	2.93	2.80	
DFT-D[e]/BLYP/TZVP	2.57	2.33	2.03	

[a] In parenthesis, "reference" QCISD(T) full VOS energies calculated by Janowski et al. [73].
[b] (Q→5) extrapolation using Helgaker's formula [78] in the form: SCF/5 + corr. MP2/(Q→5) + Δ CCSD(T)^{OVOS}/(T→Q). See Ref. [69] for details.
[c] Kim's scheme [71] with interaction energies calculated as SCF/X + corr. MP2/X + Δ CCSD(T)^{OVOS}/(X-1), where X stands for Q, 5 and X-1 for T, Q. See Ref. [69] for details.
[d] Empirical dispersion term optimized on the T and PD CCSD(T)/aug-cc-pVTZ PES cuts [69].
[e] Empirical dispersion term with the original parameters fitted to S22 test set [10].

Error of the OVOS CCSD(T)$_2$ approach can be seen from comparison with the full VOS QCISD(T) data by Pulay et al. [73]. However, certain facts have to be realized before making any conclusions. It was demonstrated, that for the benzene dimer QCISD(T) and CCSD(T) stabilization energies agree to within 0.004 kcal/mol in aug-cc-pVTZ basis set[73], which means that neglecting of certain terms in CCSD(T) does not lead to significant errors. Real sources of error, besides using OVOS technique, are the use of approximate, Cholesky-decomposed 2-electron integrals and the elimination of linear-dependent AO basis functions. From our experience, CD can lead to errors in interaction energy not larger than 0.01 kcal/mol, if 1×10^{-5} threshold is applied in the decomposition. Larger errors can be attributed to the elimination of linear-dependent basis functions, which can be ~0.03 kcal/mol, if 1×10^{-5} threshold is applied in elimination. Summing up all these arguments, error of OVOS CCSD(T)$_2$ is within the error bars of the applied methodology and does not significantly worsen the results.

So far we have demonstrated, that OVOS CCSD(T) approach is accurate enough to compete with the full VOS calculations. What is not shown in the Table 16-3, is the number of VOs, determining the cost of the correlation energy calculation. For instance, number of VOs for the TT structure in aug-cc-pVQZ (after deleting of certain number of linear dependent AO basis functions) is 1,416, which was reduced by OVOS to 851 (~60%) without significant loss of accuracy. In combination with efficient parallelization and Cholesky decomposition, for this system (60 correlated electrons, 851 virtual orbitals, 6,940 Cholesky vectors) 16 iteration of CCSD were finished in 82 h on 4 computational nodes (Intel Core2 quad-core 2.4 GHz CPUs, parallelization within computational node was done only by threaded BLAS routines) and the perturbative triples step in 408 h. In terms of quartic scaling of CCSD(T) with respect to the number of VOs, this leads to speedup of almost an order of magnitude. To keep the accuracy below a few hundredths of kcal/mol, we used very "conservative" truncation of OVOS at the aug-cc-pVTZ level, 70%, reducing number of VOs from 786 to 541. 16 iteration of CCSD were finished in 10 h on 6 computational nodes and the perturbative triples step in 48 h.

16.4.2. Uracil Dimer

Another example demonstrating robustness of OVOS CCSD(T) approach based on Cholesky decomposed 2-electron integrals is the uracil dimer in the "stacked" arrangement, studied in the work of Pitoňák et al. [79].

As shown in Table 16-4 stabilization energies obtained by various methods (MP2, MP3, SCS-MP2 [81], SCS(MI)-MP2 [82] and DFT-SAPT [83]) close to the CBS range from 7.92 (MP3) to 11.08 (MP2) kcal/mol, i.e. they are lying within the interval of 3.2 kcal/mol. Excluding the MP3 method and taking into account only those methods, which are routinely used for calculation of non-covalent interactions, this interval reduces only slightly, to 2.8 kcal/mol.

Table 16-4. Stabilization energy (in kcal/mol) of stacked uracil dimer obtained by various methods, basis sets and CBS extrapolations. (a)XZ stands for Dunning's (aug-)cc-pVXZ basis set [80]. X→Y represents CBS extrapolation from basis X to Y according to Helgaker et al. [78]

Method	Stabilization energy	
MP2(aTZ → aQZ)	11.08	
MP3(aTZ → aQZ)	7.92	
SCS-MP2(TZ → QZ)	8.30	
SCS(MI)-MP2(TZ → QZ)	9.60	
DFT-SAPT/aTZ[a]	9.26	
CCSD(T)/6-31G*(0.25)	7.59	(10.17)[b]
CCSD(T)/6-31G**(0.25,0.15)	7.75	(10.27)
CCSD(T)/aDZ	8.54	(9.82)
CCSD(T)/aTZ OVOS 60%	9.33	(9.79)
CCSD(T)/(aDZ → aTZ OVOS)	9.77	

[a] For details see Ref. [79].
[b] Values in parenthesis obtained according to Eq. (16-13).

In order to obtain the "benchmark" value of the stabilization energy, we carried out a series of CCSD(T) calculations in several basis sets up to the largest, aug-cc-pVTZ (920 basis functions) basis set. As advocated by Hobza et al. [84–86], quite reliable estimates of CCSD(T)/CBS interaction energies can be obtained by combining relatively "cheap" MP2/CBS energy with the CCSD(T) one, calculated in small or medium size basis set according to the following equation:

$$\mathrm{CCSD(T)/CBS} \approx \mathrm{MP2/CBS} + \Delta\mathrm{CCSD(T)/small\ basis}, \tag{16-13}$$

where

$$\Delta\mathrm{CCSD(T)/small\ basis} = \mathrm{CCSD(T)/small\ basis} - \mathrm{MP2/small\ basis}. \tag{16-14}$$

Comparing errors of CCSD(T) energies calculated in 6-31G* (0.25) and 6-31G** (0.25,0.15) with respect to CCSD(T)/CBS, i.e. −2.18 and −2.02 kcal/mol, with errors of estimated CCSD(T)/CBS (see Eq. 16-13 and values in parenthesis in Table 16-4), calculated in the same basis sets, i.e. 0.4 and 0.5 kcal/mol, the benefit of using (16-13) is obvious. Deviation of estimated CCSD(T)/CBS with respect to the "benchmark" CCSD(T)/CBS is thus reduced to only 0.5 kcal/mol in all used basis sets.

In order to obtain the best estimate of CCSD(T)/CBS, calculation of CCSD(T) correlation energy was done in aug-cc-pVTZ basis set in the OVOS truncated to 60%. This calculation employed 558 optimized VOs and 84 correlated electron. Though it might seem, that the calculation with about 500 virtual orbital should not be "too" demanding, opposite is true. The perturbative triples step, scaling as o^3v^4,

becomes time-determining for systems with large number of correlated electrons. While 21 CCSD iteration on 4 computation nodes (same specification as for benzene dimer, see above) took 41 h, calculation of perturbative triples took almost 168 h on 5 of these computational nodes. Without using truncated OVOS, computational time could be expected to be over 1,000 h in this setup.

16.4.3. Towards More Accurate Electron Affinity of Uracil

When Bachorz, Klopper and Gutowski [87] have published their paper on the electron affinity of the uracil molecule, it was clear that this is a challenge for CCSD(T) with OVOS. One reason is the importance of EA of the nuclear acid bases (NBA), linked to the discovery of damage to single stranded DNA induced by low-energy electrons. This has stimulated much research on electron attachment of electrons to NBA [88, 89]. Clearly, electron attachment to the isolated NBA itself can not explain the mechanism of damage to DNA. Environmental effects are substantial, see Ref. [88, 89] and references therein. While it is difficult to calculate accurately EA of a single NBA by the ROHF-CCSD(T) method, it is nearly impossible to perform calculations for NBA surrounded by realistic environment. It appears that EA of NBA's can be significantly enhanced by interaction with a single water molecule. This can be tractable with CCSD(T) provided that the OVOS performs better than other methods. Obviously, for larger systems only DFT methods combined with the molecular mechanics treatment can help in solving the problem of damage to DNA by low-energy electrons. Having all this in mind it appears to be useful to tune DFT methods by providing accurate EA's of at least simple systems. We note that results of calculations of electron affinities with more simple methods, like DFT or MP2 overestimate EA of, e.g., uracil, by as much as 0.2 eV. Therefore, as a first step, we try to show how OVOS performs in obtaining accurate adiabatic EA of a single uracil molecule by large basis set CCSD(T) calculation. We calculate the valence-bound EA with an extra electron attached to the antibonding π^* orbital. Our results, summarized in Table 16-5, should be understood as an extension of accurate calculations by Bachorz et al. [87] and as demanding validation of OVOS. First, we note, that using OVOS reduced to 60% of the full VOS, the error in EA is 11 meV in the aug-cc-pVDZ basis set and only 7 meV with larger aug-cc-pVTZ basis set. Therefore, we

Table 16-5. Spin-adapted ROHF CCSD(T)$_2$ contribution to EA (the adiabatic electron detachment) of the uracil molecule [eV]. Dunning's et al. aug-cc-pVXZ basis sets [56]

	Electron affinity of the uracil molecule		
% of OVOS	aug-cc-pVDZ	aug-cc-pVTZ	aug-cc-pVQZ
100	−0.189	−0.150	
60	−0.200	−0.157	−0.141

can expect that OVOS can be safely used with even larger aug-cc-pVQZ basis. Such calculation was not tractable before with standard CC approach. When going from the aug-cc-pVTZ to larger QZ basis the electronic contribution to EA is less negative by 16 meV. Upon extending the basis set, the extra electron tends to be attached to the uracil molecule. Taking vibrational, core correlation and other corrections (altogether +0.155 eV) and the CBS limit from our ROHF-CCSD(T) aug-cc-pVTZ and QZ results, we arrive at AEA of −15 meV. This means, that the extra electron is unbound in the isolated uracil. Bachorz et al. [87] report the final value of +40 meV. The difference is, that we used the spin-adapted ROHF-CCSD(T) method, which reduces the correlation energy of the anion. This would reduce their EA by about 30 meV arriving therefore to the value of just 10 meV. Second, Bachorz et al. [87] extrapolated second-order MP2 correlation energies. In any case, both results lead to unbound or to very weakly bound electron attached to the uracil. Difficulties in accurate calculations of the AEA of uracil are, that large basis sets must be used in conjunction with sophisticated treatment of the electron correlation. The problem also is that the uracil anion has puckered structure, while the neutral molecule has a symmetry plane. Therefore, we can not employ the symmetry implemented in our open-shell CCSD(T) code. Residual basis set effects, spin adaptation, core correlation effects are small, but even small effects matter in accurate calculation of the electron affinity of uracil. We expect, however, that with OVOS we will be able to treat EA of the hydrated uracil and provide benchmark results for DFT and other more approximate methods.

16.5. CONCLUSIONS

The progress in the implementation of efficient algorithms, efficient treatment of the two-electron integrals and high level of parallelism extend the feasibility of CCSD(T) single-reference calculations towards calculations of gradually larger molecules. When combined with methods like OVOS or FNO allowing substantial truncation of the virtual orbital space in a controllable way, the painful computational consequences of the scaling of CCSD(T) with the number of virtual orbitals can be alleviated substantially. Using of OVOS is particularly useful when applied to calculations with extended basis sets aimed at accurate predictions of molecular properties of relatively large molecules not amenable to CCSD(T) calculations by a standard way. We have demonstrated the viability of OVOS in highly accurate calculations of molecular electric properties, electron affinities, reaction energies, interaction energies and other applications. Reliable results can be obtained with OVOS truncated to 50–60% of the full virtual space with computer time reduced by an order of magnitude. We believe that even larger computer effectivity can be achieved when using OVOS in higher level CC calculations, particularly for the iterative treatment of triples and iterative or approximate calculations of quadruples. First such results were obtained by Kallay [90] who demonstrated in higher level CC calculations the OVOS technique may lead to more that two order of magnitude shorter computer

time in comparison with calculations with the full virtual space. We believe that OVOS can be combined also with the MR CC calculations. The OVOS method can be considered as a viable alternative of other methods which extend applicability of CC methods to larger molecules with larger basis sets enhancing their predictive power substantially.

ACKNOWLEDGMENTS

We acknowledge the support of the Slovak Research and Development Agency (Contract No. APVV-20-018405) and the Slovak Grant Agency VEGA under the contracts No. 1/0428/09 and 1/0520/10. This work was also part of the research project No. Z40550506 of the Institute of Organic Chemistry and Biochemistry, Academy of Sciences of the Czech Republic and it was supported by Grants No. LC512 and MSM6198959216 from the Ministry of Education, Youth and Sports of the Czech Republic.

REFERENCES

1. J. Čížek, J. Chem. Phys. **45**, 4256 (1966)
2. R. J. Bartlett, M. Musiał, Rev. Mod. Phys. **79**, 291 (2007)
3. J. Paldus, X. Li, Adv. Chem. Phys. **110**, 1 (1999)
4. R. J. Bartlett, in *Modern Electronic Structure Theory, Part II*, Ed. D. R. Yarkony (World Scientific, Singapore, 1995), pp. 1047–1131
5. M. Urban, I. Černušák, V. Kellö, J. Noga, in *Methods in Computational Chemistry*, vol. 1, Ed. S. Wilson (Plenum Press, New York, 1987), pp. 117–250
6. J. Pittner, P. Piecuch, Mol. Phys. **107**, 1209 (2009)
7. X. Li, J. Paldus, J. Chem. Phys. **119**, 5320 (2003)
8. N. Bera, S. Ghosh, D. Mukherjee, S. Chattopadhyay, J. Phys. Chem. A **109**, 11462 (2005)
9. F. Aquilante, L. De Vico, N. Ferre, G. Ghigo, P.-Å. Malmquist, P. Neogrády, T. Pedersen, M. Pitoňák, M. Reiher, B. Roos, L. Serrano-Andres, M. Urban, V. Veryazov, R. Lindh, J. Comput. Chem. **31**, 224 (2010)
10. P. Jurečka, J. Černý, P. Hobza, D. R. Salahub, J. Comput. Chem. **28**, 555 (2007)
11. Y. Zhao, D. G. Truhlar, Theor. Chem. Acc. **120**, 215 (2008)
12. T. Schwabe, S. Grimme, Phys. Chem. Chem. Phys. **9**, 3397 (2007)
13. J. Noga, R. J. Bartlett, J. Chem. Phys. **86**, 7041 (1987)
14. M. Musiał, S. A. Kucharski, R. J. Bartlett, J. Chem. Phys. **116**, 4382 (2002)
15. M. Kallay, P. R. Surjan, J. Chem. Phys. **115**, 2945 (2001)
16. K. Raghavachari, G. W. Trucks, J. A. Pople, M. Head-Gordon, Chem. Phys. Lett. **157**, 479 (1987)
17. M. Urban, J. Noga, S. J. Cole, R. J. Bartlett, J. Chem. Phys. **83**, 4041 (1985)
18. T. J. Lee, G. E. Scuseria, in *Quantum Mechanical Electronic Structure Calculations with Chemical Accuracy*, Ed. S. R. Langhoff (Kluwer Academic, Dordrecht, 1995), pp. 47–108
19. J. Watts, M. Urban, R. J. Bartlett, Theor. Chim. Acta **90**, 341 (1995)
20. M. Urban, P. Neogrády, J. Raab, G. H. D. Diercksen, Collect. Czech. Chem. Commun. **63**, 1409 (1998)
21. W. Kutzelnigg, Theor. Chim. Acta **68**, 445 (1985)

22. W. Klopper, F. R. Manby, S. Ten-no, E. F. Valeev, Int. Rev. Phys. Chem. **25**, 427 (2006)
23. J. Noga, S. Kedžuch, J. Šimunek, S. Ten-no, J. Chem. Phys. **128**, 174103 (2008)
24. L. Adamowicz, R. J. Bartlett, J. Chem. Phys. **86**, 6314 (1987)
25. L. Adamowicz, R. J. Bartlett, A. J. Sadlej, J. Chem. Phys. **88**, 5749 (1988)
26. C. Edmiston, M. Krauss, J. Chem. Phys. **45**, 1833 (1966)
27. T. L. Barr, E. R. Davidson, Phys. Rew. A **1**, 644 (1970)
28. C. Sosa, J. Geertsen, G. W. Trucks, R. J. Bartlett, J. A. Franz, Chem. Phys. Lett. **159**, 148 (1989)
29. A. G. Taube, R. J. Bartlett, Collect. Czech. Chem. Commun. **70**, 837 (2005)
30. M. Schütz, G. Hetzer, H. J. Werner, J. Chem. Phys. **111**, 5691 (1999)
31. M. Schütz, J. Chem. Phys. **113**, 9986 (2000)
32. M. Schütz, H.-J. Werner, J. Chem. Phys. **114**, 661 (2001)
33. P. Sałek, S. Høst, L. Thøgersen, P. Jørgensen, P. Manninen, J. Olsen, B. Jansík, S. Reine, F. Pawłowski, E. Tellgren, T. Helgaker, S. Coriani, J. Chem. Phys. **126**, 114110 (2007)
34. V. Weijo, P. Manninen, P. Jørgensen, O. Christiansen, J. Olsen, J. Chem. Phys. **127**, 074106 (2007)
35. P. Constans, P. Y. Ayala, G. E. Scuseria, J. Chem. Phys. **113**, 10451 (2000)
36. H. Koch, A. Sánchez de Merás, T. Helgaker, O. Christiansen, J. Chem. Phys. **104**, 4157 (1996)
37. C. E. Benoit, Bull. Geodesique **7**, 67 (1924)
38. N. H. F. Beebe, J. Linderberg, Int. J. Quantum. Chem. **12**, 683 (1977)
39. H. Koch, A. Sánchez de Merás, T. B. Pedersen, J. Chem. Phys. **118**, 9481 (2003)
40. J. L. Whitten, J. Chem. Phys. **58**, 4496 (1973)
41. M. Feyereisen, G. Fitzgerald, A. Komornicki, Chem. Phys. **208**, 359 (1993)
42. P. Neogrády, M. Pitoňák, M. Urban, Mol. Phys. **103**, 2141 (2005)
43. M. Šulka, M. Pitoňák, P. Neogrády, M. Urban, Int. J. Quantum. Chem. **108**, 2159 (2008)
44. M. Urban, M. Pitoňák, P. Neogrády, in *Lecture Series on Computer and Computational Science, Trends and Perspectives in Modern Computational Science*, Eds. G. Maroulis, T. Simos (Brill Academic Publishers, Leiden, 2006), pp 265–285
45. S. F. Boys, F. Bernardi, Mol. Phys. **100**, 65 (2002), reprinted from Mol. Phys. **19**, 553 (1970)
46. P. Neogrády, M. Pitoňák, F. Aquilante, J. Noga, In preparation
47. V. Lotrich, N. Flocke, M. Ponton, A. D. Yau, A. Perera, E. Deumens, R. J. Bartlett, J. Chem. Phys. **128**, 194104 (2008)
48. T. Janowski, A. R. Ford, P. Pulay, J. Chem. Theory Comput. **3**, 1368 (2007)
49. T. Janowski, P. Pulay, J. Chem. Theory Comput. **4**, 1585 (2008)
50. R. M. Olson, J. L. Bentz, R. A. Kendall, M. W. Schmidt, M. S. Gordon, J. Chem. Theory Comput. **3**, 1312 (2007)
51. G. Karlström, R. Lindh, P.-Å. Malmquist, R. O. Roos, U. Ryde, V. Veryazov, P. O. Widmark, M. Cossi, B. Schimelpfennig, P. Neogrády, L. Seijo, Comput. Mat. Science **28**, 222 (2003)
52. J. Noga, P. Valiron, Mol. Phys. **103**, 2123 (2005)
53. M. Pitoňák, P. Neogrády, V. Kellö, M. Urban, Mol. Phys. **104**, 2277 (2006)
54. M. Pitoňák, F. Holka, P. Neogrády, M. Urban, J. Mol. Struct. (THEOCHEM) **768**, 79 (2006)
55. P. Dedíková, M. Pitoňák, P. Neogrády, I. Černušák, M. Urban, J. Phys. Chem. A **112**, 7115 (2008)
56. R. A. Kendall, T. H. Dunning, R. J. Harrison, J. Chem. Phys. **96**, 6796 (1992)
57. D. E. Woon, T. H. Dunning, J. Chem. Phys. **98**, 1358 (1993)
58. A. K. Wilson, T. van Mourik, T. H. Dunning, J. Mol. Struct. (THEOCHEM) **388**, 339 (1996)
59. F. Fringuelli, G. Marino, A. Taticchi, Adv. Heterocycl. Chem. **21**, 119 (1977)
60. K. Kamada, M. Ueda, H. Nagao, K. Tawa, T. Sugino, Y. Shmizu, K. Ohta, J. Phys. Chem. A **104**, 4723 (2000)
61. P. Neogrády, M. Urban, Int. J. Quantum Chem. **55**, 187 (1995)
62. A. Antušek, M. Urban, A. J. Sadlej, J. Chem. Phys. **119**, 7247 (2003)

63. J. Granatier, M. Urban, A. J. Sadlej, J. Phys. Chem. A **111**, 13238 (2007)
64. N. B. Balabanov, K. A. Peterson, J. Chem. Phys. **123**, 064107 (2005)
65. K. A. Peterson, C. Puzzarini, Theor. Chem. Acta **114**, 283 (2005)
66. A. G. Taube, R. J. Bartlett, J. Chem. Phys. **128**, 164101 (2008)
67. K. M. Ervin, I. Anusiewicz, P. Skurski, J. Simons, W. C. Lineberger, J. Phys. Chem. A **107**, 8521 (2003)
68. P. Neogrády, M. Medved', I. Černušák, M. Urban, Mol. Phys. **100**, 541 (2002)
69. M. Pitoňák, P. Neogrády, J. Řezáč, P. Jurečka, M. Urban, P. Hobza, J. Chem. Theory Comput. **4**, 1829 (2008)
70. M. O. Sinnokrot, E. F. Valeev, C. D. Sherrill, J. Am. Chem. Soc. **124**, 10887 (2002)
71. E. C. Lee, D. Kim, P. Jurečka, P. Tarakeshwar, P. Hobza, K. S. Kim, J. Phys. Chem. A **111**, 3446 (2007)
72. J. Řezáč, P. Hobza, J. Chem. Theory Comput. **4**, 1835 (2008)
73. T. Janowski, P. Pulay, Chem. Phys. Lett. **447**, 27 (2007)
74. M. O. Sinnokrot, C. D. Sherrill, J. Phys. Chem. A **108**, 10200 (2004)
75. R. Podeszwa, R. Bukowski, K. Szalewicz, J. Phys. Chem. A **110**, 10345 (2006)
76. J. G. Hill, J. A. Platts, H.-J. Werner, Phys. Chem. Chem. Phys. **8**, 4072 (2006)
77. O. Bludský, M. Rubeš, P. Soldán, P. Nachtigall, J. Chem. Phys. **128**, 114102 (2008)
78. A. Halkier, T. Helgaker, P. Jørgensen, W. Klopper, H. Koch, J. Olsen, A. K. Wilson, Chem. Phys. Lett. **286**, 243 (1998)
79. M. Pitoňák, K. E. Riley, P. Neogrády, P. Hobza, Chem. Phys. Chem. **9**, 1636 (2008)
80. T. H. Dunning, K. A. Peterson, J. Chem. Phys. **113**, 7799 (2000)
81. S. Grimme, J. Chem. Phys. **118**, 9095 (2003)
82. R. A. Distasio, M. Head-Gordon, Mol. Phys. **105**, 1073 (2007)
83. G. Jansen, A. Hesselmann, J. Phys. Chem. A **105**, 11156 (2001)
84. P. Jurečka, P. Hobza, Chem. Phys. Lett. **365**, 89 (2002)
85. P. Jurečka, P. J. Šponer, J. Černý, P. Hobza, Phys. Chem. Chem. Phys. **8**, 1985 (2006)
86. J. Řezáč, P. Jurečka, K. E. Riley, J. Černý, H. Valdes, K. Pluháčková, K. Berka, T. Řezáč, M. Pitoňák, J. Vondrášek, P. Hobza, Collect. Czech. Chem. Commun. **73**, 1261 (2008)
87. R. A. Bachorz, W. Klopper, M. Gutowski, J. Chem. Phys. **126**, 085101 (2007)
88. J. Simons, Acc. Chem. Res. **39**, 772 (2006)
89. J. D. Gu, Y. M. Xie, H. F. Schaefer III, Chem. Phys. Lett. **473**, 213 (2009)
90. M. Kallay, Proceedings, 13th ICQC, Helsinki, Finland (2009)

CHAPTER 17

MULTIREFERENCE COUPLED-CLUSTER METHODS: RECENT DEVELOPMENTS

JOSEF PALDUS[1], JIŘÍ PITTNER[2], AND PETR ČÁRSKY[2]

[1]*Department of Applied Mathematics, Department of Chemistry, and Guelph-Waterloo Center for Graduate Work in Chemistry (GWC)*[2]*-Waterloo Campus, University of Waterloo, Waterloo, Ontario N2L 3G1, Canada, e-mail: paldus@scienide2.uwaterloo.ca*

[2]*J. Heyrovský Institute of Physical Chemistry v.v.i., Dolejškova 3, CZ-18223 Praha, Czech Republic, e-mail: jiri.pittner@jh-inst.cas.cz; petr.carsky@jh-inst.cas.cz*

Abstract: The objective of this paper is to provide an overview of various multi-reference (MR) coupled-cluster (CC) approaches, particularly those relating to our own research. Although MR CC methods have been around for almost three decades and much work has been expended on their development and implementation, no general purpose codes are presently available. In view of the complexity, inherent difficulties, and computational demands of both genuine valence and state universal (VU and SU) MR CC methods, attention has been directed towards the state selective or state specific (SS) approaches that focus on one state at a time. These methods are based on either the genuine MR CC formalism or on a single-reference (SR) CC Ansatz, in which higher-than-pair clusters are accounted for by relying on basic ideas of general MR approaches. This is achieved either *internally* by relying on CC or MBPT formalism or by exploiting some *external* source providing approximate values of these clusters and accomplished by either correcting equations yielding the cluster amplitudes or directly by evaluating the corrections to the CCSD energy. Nowadays there exists a whole plethora of such various approaches for handling of quasi-degenerate states with a various degree of MR character and our goal is to outline their basic features and comment on their pro's and con's, their usefulness and weaknesses, as well as point out their mutual relationship.

Keywords: Multireference coupled cluster, Hilbert space, State universal, state specific, Brillouin – Wigner coupled cluster, Effective Hamiltonian, Jeziorski – Monkhorst Ansatz, Completely renormalized coupled cluster, Externally corrected, Internally corrected

17.1. INTRODUCTION

Coupled-cluster (CC) methods represent highly-accurate and reliable approaches that are often exploited in molecular electronic structure calculations. This is particularly the case for non-degenerate ground states of closed-shell systems near their equilibrium geometry, but less so for general open-shell systems. Although much

P. Čársky et al. (eds.), Recent Progress in Coupled Cluster Methods, 455–489.
DOI 10.1007/978-90-481-2885-3_17,

progress has been achieved in this regard during the past couple of decades, there are no "black-box"-type packages that could be relied upon in the presence of a strong, or even an intermediate quasi-degeneracy due to a multireference (MR) nature of the state considered. This is particularly the case when we wish to generate potential energy surfaces (PESs) in the entire range of geometries, including various dissociation channels involving the breaking of genuine chemical bonds. We thus devote this chapter to CC methods that address this type of problems, which invariably lead to a multireference-type formalism of one kind or another. It is however beyond the scope of this chapter to provide concrete illustrations of the performance of such methods. Neither shall we deal with the equation-of-motion (EOM) or relativistic approaches and will focus our attention on the energy rather than other properties. These aspects will be handled in other chapters of this monograph.

17.2. SINGLE-REFERENCE COUPLED-CLUSTER APPROACHES

The single-reference (SR) coupled-cluster (CC) methods are based on the exponential Ansatz for the wave operator U that generates an exact non-relativistic state $|\Psi\rangle$ when acting on an independent particle model (IPM) reference (usually a Slater determinant) $|\Phi_0\rangle$,

$$|\Psi\rangle = U\,|\Phi_0\rangle\,, \qquad U = \exp(T)\,, \tag{17-1}$$

where T designates the so-called *cluster operator*

$$T = \sum_{\mu} t_\mu G_\mu\,, \tag{17-2}$$

which can be expressed as a linear combination of excitation operators G_μ with coefficients t_μ, representing the *cluster amplitudes*, both associated with all possible excitations μ from the spin orbitals that are occupied in $|\Phi_0\rangle$ (labeled by capitals $A, B, C, \cdots$) to the unoccupied ones $(R, S, T, \cdots)$,

$$G_\mu = X_R^\dagger X_S^\dagger X_T^\dagger \cdots X_C X_B X_A \cdots\,, \qquad \mu{:}ABC\cdots \rightarrow RST\cdots\,, \tag{17-3}$$

with $X_I^\dagger$ (X_I) designating the creation (annihilation) operators. Classifying G_μ and t_μ by their excitation order i, we can rewrite (17-2) as

$$T = \sum_{i=1}^{N} T_i\,, \qquad T_i = \sum_{\mu(i)} t_\mu^{(i)} G_\mu^{(i)}\,, \qquad G_\mu^{(i)} = \prod_{j=1}^{i} \left(X_{R_j}^\dagger X_{A_j}\right) \tag{17-4}$$

(for recent reviews, see, e.g., [1–5]; for a historical overview, see [6, 7]).

The source of this Ansatz stems from the general MBPT (many-body perturbation theory) as developed by Brueckner [8], Goldstone [9], Hugenholtz [10], and others

(see [11] for a time-independent version). They showed that the exact wave function $|\Psi\rangle$ and the corresponding energy is given by *linked* MBPT terms or diagrams, the fact referred to as the *linked cluster theorem*. But it was Hubbard [12–14] who formulated the *connected cluster theorem*, which states that the exact $|\Psi\rangle$ can be expressed in the exponential form given by Eq. (17-1), with the $(T|\Phi_0\rangle)$ consisting of all possible *connected* MBPT wave function diagrams, usually designated as $(T|\Phi_0\rangle)_C$. The contribution from disconnected, but *linked*, terms is then generated by the exponential Ansatz. The vacuum version of these linked diagrams then gives the corresponding energy.

The first suggestion to exploit the cluster expansion form for $|\Psi\rangle$ in solving the non-relativistic stationary Schrödinger equation was made in nuclear physics by Coester and Kümmel [15, 16]. At this time, however, the issuing formalism looked too formidable to be of a practical use, not to mention the peculiarities of nuclear Hamiltonians (hard core, tensor forces, absence of fundamental internuclear potentials, etc.). For these reasons a further development has been delayed and more or less abandoned till its recent revival (see, e.g., [17]). In the meantime, the cluster expansion was exploited in the context of the molecular electronic structure by Čížek [18, 19], who formulated general rules for the derivation of *explicit* CC equations and illustrated them on the most important case when T is truncated to pair clusters T_2 (yielding, in today's parlance, the CCD method; see also [20]).

In general, relying either on the diagrammatic or algebraic formalism, one finds that

$$H_N \exp(T)|\Phi_0\rangle = \{H_N \exp(T)\}_C \exp(T)|\Phi_0\rangle = \exp(T)\{H_N \exp(T)\}_C|\Phi_0\rangle\,, \tag{17-5}$$

where the subscripts N and C indicate the N-product form of the Hamiltonian [11] and the connected component, respectively. We also immediately see that $\{H_N \exp(T)\}_C$ involves at most four cluster amplitudes [or the four fold commutators; see Eq. (17-10) below], since the two-electron interaction has at most four fermion lines. Premultiplying the Schrödinger equation $H_N|\Psi\rangle = \Delta E|\Psi\rangle$, $\Delta E = E - \langle\Phi_0|H|\Phi_0\rangle$ with $\exp(-T)$ from the left gives

$$\{H_N \exp(T)\}_C|\Phi_0\rangle = \Delta E|\Phi_0\rangle\,, \tag{17-6}$$

so that

$$\Delta E = \langle\Phi_0|\{H_N \exp(T)\}_C|\Phi_0\rangle\,, \qquad \text{and} \qquad \langle G_\mu^{(i)}\Phi_0|\{H_N \exp(T)\}_C|\Phi_0\rangle = 0, \tag{17-7}$$

yielding the correlation energy ΔE and equations for the CC amplitudes $t_\mu^{(i)}$, respectively. Equivalently, using the algebraic formalism we can write

$$\Delta E = \langle\Phi_0|\bar{H}_N|\Phi_0\rangle = \langle\Phi_0|H_N\big(T_1 + T_2 + \tfrac{1}{2}T_1^2\big)|\Phi_0\rangle\,, \tag{17-8}$$

and

$$\langle G_\mu^{(i)} \Phi_0 | \bar{H}_N | \Phi_0 \rangle = 0 \,, \tag{17-9}$$

where

$$\begin{aligned} \bar{H}_N &\equiv \exp(-T) H_N \exp(T) \\ &= \sum_{n=0}^{4} (n!)^{-1} [\cdots [[H_N, \underbrace{T], T], \cdots T}_{n}] = \sum_{n=0}^{4} (n!)^{-1} \{H_N T^n\}_C \\ &= \{H_N \exp(T)\}_C \,, \end{aligned} \tag{17-10}$$

is referred to as a similarity transformed normal-product Hamiltonian H_N.

Although the initial ab initio test example, which also approximately accounted for the T_1 and T_3 components, yielded most encouraging results [21], a wider exploitation had to await the appearance of more efficient computational tools. Six years later, almost simultaneously, general purpose codes were developed for the CCD method [22, 23] and, shortly afterwards, for the CCSD method [24]. In the meantime, several powerful packages that can handle the standard SR CC method have become available [25–31] and are currently widely exploited.

Since the complexity of the implementation of CC methods grows rapidly with the excitation rank of the cluster operator, at most pentuple excitations have been derived and coded in a "traditional way" [32]. Implementations of higher excitations with proper computational scaling have been developed in two ways, both involving computer manipulation of expressions, pioneered in the MBPT [33, 34] and CC [35–37] formalisms already some time ago. The task of diagram generation and factorization of the resulting expressions is passed to the computer in both approaches, however, they differ in the way how the resulting tensor contractions are evaluated. One possibility is an automatic generation of Fortran (or other language) code for each particular case, which is then compiled and linked into the final program [38–43]. Another possibility is the string-based CC approach, which implements contractions of tensors with arbitrary number of indices within one (human-written) code [44–46]. Both approaches are able to achieve proper computational scaling and take advantage of the antisymmetry of amplitudes and spin symmetry for any CC excitation level. Approximate non-iterative schemes of general order and analytic gradients have been implemented using the string approach as well [47–50].

While the CCSD approach, accounting for T_1 and T_2, represents an excellent approximation, it turned out that in order to achieve the chemical accuracy of 1 kcal/mol, it is necessary to also account for T_3, at least in an approximate way, since a full account of triples via the CCSDT method [51–53] is computationally very demanding, not to mention CCSDTQ or higher-order versions [54]. In many cases it is thus sufficient to treat the triples perturbatively via the CCSD(T) method [55–58].

Indeed, this approach has often been referred to as the "gold standard" of quantum chemistry [59–61].

Unfortunately, CCSD(T) fails in quasi-degenerate situations – these invariably arise when dealing with open-shell systems, as when breaking genuine chemical bonds or when handling radicaloid or excited state species – as does even CCSD itself when the basic assumption of non-degeneracy of the reference $|\Phi_0\rangle$ is violated (see, e.g., Figure 1 of [62], Figure 1 of [63], and Figures 1–4 of [64]). In such cases, the role of higher-than-pair clusters becomes essential and, in general, calls for a multireference (MR) type formalism. Much work has been devoted to this problem (see, e.g., an overview in [3, 65–68]) and two *bona fide* MR CC methodologies were formulated (see below), yet their routine exploitation has yet to be realized. For this reason much attention has been devoted to approaches that focus on one state at a time. There exists nowadays a whole plethora of such methods to which we turn our attention in this chapter. We should also mention, at least in passing, a version exploiting, in general, a multi-determinantal reference of the Clifford algebra unitary group approach (CAUGA) [69–73] that can handle open-shell singlet, doublet, and triplet states and is fully spin adapted [36, 37, 74].

17.3. GENERAL ASPECTS OF MULTIREFERENCE CC APPROACHES

In contrast to configuration interaction (CI) methods, an extension of the SR CC theory to the MR case is far from being straightforward, since there is no unique way how to generalize the SR exponential Ansatz, Eq. (17-1). The MR CC or MBPT approaches are, generally, based on *the effective Hamiltonian formalism* (see Section 17.4), which employs a *model space* $\mathcal{M}_0$ that is spanned by M suitable orthonormal configurations $|\Phi_i\rangle$, $(i = 1, 2, \cdots, M)$ – consisting of either Slater determinants or configuration state functions (CSFs) – representing a zero-order approximation to M exact states $|\Psi_i\rangle$ we are interested in, the latter spanning the *target space* $\mathcal{M}$. The projections of $|\Psi_i\rangle$ into $\mathcal{M}_0$ are thus given by a linear combination of model space configurations $|\Phi_i\rangle$ and are designated by a tilde, i.e., as $|\tilde{\Phi}_i\rangle$.

The next task is to find a wave operator U that transforms the model space CSFs into the target states. Here we have essentially two options: we can either aim for a *single* cluster operator, defining the *valence universal* (VU) or Fock space [65, 75, 76] wave operator U (often designated by Ω), transforming the model states $|\Phi_i\rangle$ into the target states $|\Psi_i\rangle$ (or, rather, their linear combinations $|\tilde{\Psi}_i\rangle$) or, alternatively, we can define *different* cluster operators $T[i]$, one for each $|\Phi_i\rangle$, leading to the *state universal* (SU) or Hilbert space Ansatz [77]. The desired exact states $|\Psi_i\rangle$ are then obtained by diagonalizing the Hamiltonian $H^{(\mathrm{eff})}$ of the effective Hamiltonian formalism (see below; for more details see [2, 3, 67, 68]).

Each of these approaches has its own peculiarities. Yet, one common obstacle is represented by the so-called *intruder states* (cf., e.g., [78]). These are the states from the orthogonal complement of the model space $\mathcal{M}_0$ whose energy is generally much higher than the energy of configurations spanning the model space at one (say,

equilibrium) geometry, but becomes sufficiently lowered at stretched geometries, so much so, that they fall (or intrude) within the interval of energies associated with the model space configurations or lie close to this interval. Just as we require the reference of the SR CC formalism not to be degenerate or quasi-degenerate, it is important that the energies of the references of a MR formalism be well separated from those belonging to the orthogonal complement of $\mathcal{M}_0$. Intruder states mainly arise due to the *complete model space* (CMS) requirement ($\mathcal{M}_0$ involving all possible valence or active orbital occupancies) in order to warrant the size extensivity. For this reason other MR CC approaches, including those that may slightly violate the size extensivity, but avoid the intruder state problem, or focus on one state at a time, have been explored.

We shall thus distinguish between the *genuine* MR CC approaches that consider all M states simultaneously (usually restricted to low dimensional model spaces [79, 80] or employing the so-called *C-conditions* as in the generalized model space (GMS) MR CC method [81–87]) and the so-called *state selective* or *state specific* (SS) methods that focus on one state at a time. These SS-type approaches may then again be classified into those that employ genuine MR CC equations, represented primarily by MkCC (Mukherjee et al. MR CC [88–95]), KB-MRCC (using Kucharski and Bartlett coupling [96]), and by the BWCC (Brillouin – Wigner MR CC [97, 98]) methods, as well as by a large group of approaches that are essentially of a SR-type, but employ some MR CC ideas in accounting for higher-than-pair clusters. Amongst the latter we may then distinguish the *internally* (*ic*) and *externally* (*ec*) corrected approaches [99–101]: the former ones rely solely on the CC or MBPT formalism, while the *ec* methods also employ external sources, such as CI or CAS SCF, to supply the information about higher-than-pair clusters.

The ubiquitous CCSD(T) method may thus be regarded as a prime example of *ic*-type approaches, as is its CCSD(TQ) generalization treating perturbatively also quadruples [102–104]. Another straightforward SS approaches simply truncate CCSDT or CCSDTQ to CCSDt, CCSDtq or similar versions [105, 106] by considering only a certain subset of triples and quadruples, implied by the MRCC formalism, while employing standard SR CC equations.

Yet another successful generalization of CCSD(T) that avoids many of its shortcomings is represented by the CCSD(2) method [107] and especially by the renormalized (R) or completely renormalized (CR) CCSD approaches [62, 63, 108–110] or their fully size-extensive version, the CR-CC(m, n) method [111–113]. We must also mention recently proposed partially-linearized MRCC (plMR CC) method, [114, 115] which is an *ic* version of the *ec* RMR CC approach (see below) and is somewhat related to the CCSDT-1 method [116], representing a linearized version of CCSDT and the first of the CCSDT-n series of approximations [51, 117].

The *ec* methods may then again be subdivided into the *amplitude-corrected* approaches [represented mainly by the reduced multireference (RMR) CCSD method [118–122] that employs a subset of approximate triples and quadruples as supplied by a modest-size MR CISD] and the *energy-corrected* ones that employ the MR CISD wave function in the asymmetric energy formula [64, 123]. In fact, the latter

approach is methodologically closely related to the CR-type methods [64, 123], while the former one can also be employed in the context of genuine MR CC methods [124]. We should also point out that most MR CC approaches are based on the SU formalism [77]; for this reason we focus our attention on SU rather than VU cluster Ansatz. The essence of such approaches will be described in the following sections.

For a nonexpert, the variety and complexity of these various MRCC approaches may be bewildering. We will thus try to summarize this chapter by providing our personal opinion concerning the merits and domains of application of these individual methods and of their relationship, advantages, and shortcoming in comparison with the CI-type and other approaches.

17.4. EFFECTIVE HAMILTONIAN FORMALISM

We consider a model space $\mathcal{M}_0$ together with a target space $\mathcal{M}$,

$$\begin{aligned} \mathcal{M}_0 &= \mathrm{Span}\{\Phi_i\} = \mathrm{Span}\{\tilde{\Phi}_i\}\,, \\ \mathcal{M} &= \mathrm{Span}\{\Psi_i\} = \mathrm{Span}\{\tilde{\Psi}_i\}\,, \qquad \dim \mathcal{M}_0 = \dim \mathcal{M} = M\,, \end{aligned} \tag{17-11}$$

with the relevant states interrelated via the projector P onto $\mathcal{M}_0$, $P = \sum_{i=1}^{M} P_i$, and $P_i = |\Phi_i\rangle\langle\Phi_i|$, as well as its "inverse", the wave operator U, as follows (for details see, e.g., [67, 68])

$$P\Psi_i = \tilde{\Phi}_i\,, \qquad U\tilde{\Phi}_i = \Psi_i\,, \tag{17-12}$$

$$P\tilde{\Psi}_i = \Phi_i\,, \qquad U\Phi_i = \tilde{\Psi}_i\,, \tag{17-13}$$

where both P and U are idempotent, yet P is Hermitian while U is not. Assuming the intermediate normalization $\langle\Phi_i|\tilde{\Psi}_j\rangle = \delta_{ij}$, we also find the identities

$$UPU = UP = U\,, \quad PUP = PU = P\,, \quad \text{and} \quad UQ \equiv U(1-P) = 0\,. \tag{17-14}$$

Note that while $\langle\Phi_i|\Phi_j\rangle = \delta_{ij} = \langle\Psi_i|\Psi_j\rangle$, the projections $|\tilde{\Phi}_i\rangle$ of $|\Psi_i\rangle$ into $\mathcal{M}_0$ are, generally, no longer orthogonal, yet span the same space $\mathcal{M}_0$. The operator U may then be thought of as an "inverse" of P from $\mathcal{M}_0$ to $\mathcal{M}$, so that

$$|\tilde{\Phi}_i\rangle = \sum_j c_{ij}|\Phi_j\rangle \quad \text{and} \quad |\Psi_i\rangle = \sum_j c_{ij}|\tilde{\Psi}_j\rangle \quad \text{or} \quad |\tilde{\Psi}_i\rangle = \sum_j (\mathbf{C}^{-1})_{ij}|\Psi_j\rangle\,, \tag{17-15}$$

where $\mathbf{C} = ||c_{ij}||$.

It is now straightforward to derive the key equations of the effective Hamiltonian formalism: First, projecting the Schrödinger equation for the target states $|\Psi_i\rangle$, $H|\Psi_i\rangle = E_i|\Psi_i\rangle$, $(i = 1, \cdots, M)$ onto $\mathcal{M}_0$ immediately gives

$$H^{(\mathrm{eff})}|\tilde{\Phi}_i\rangle = E_i|\tilde{\Phi}_i\rangle\,, \quad (i = 1, \cdots, M) \quad \text{with} \quad H^{(\mathrm{eff})} = PHU = PHUP\,. \tag{17-16}$$

Next, acting with U on the same Schrödinger equation leads to the (generalized) Bloch equations that determine the operator U, namely

$$UHU = HU \quad \text{or} \quad HU = UH^{(\text{eff})} . \tag{17-17}$$

A rather surprising result that $H^{(\text{eff})}$ acting within $\mathcal{M}_0$ yields the same exact eigenvalues $\{E_i\}$ as the original Hamiltonian, Eq. (17-16), is made possible thanks to the fact that we consider only a *finite* subset of M eigenvalues E_i. The Bloch equation, Eq. (17-17), can be cast into different equivalent forms (see, e.g., [67, 68]). In particular, when we partition H into the unperturbed part H_0 and a perturbation W, $H = H_0 + W$, $[H_0, P] = 0$, we then arrive at the following often used form of Bloch equation [76]

$$[U, H_0]P = (WU - UPWU)P . \tag{17-18}$$

17.5. GENUINE MRCC METHODS

As implied by the effective Hamiltonian formalism, the cluster Ansatz for the MR wave operator U cannot take a simple SR form, Eq. (17-1), since the idempotency of U would require that $U = \hat{1}$. As pointed out in Section 17.3, we have basically two options here, leading to the so-called *valence universal* (VU) and the *state universal* (SU) formalisms.

In the VU case, the operator U must be defined on a suitably larger space than $\mathcal{M}_0$, namely on a general Fock space $\mathcal{F}$ engendered by a one-particle space defining the ab initio model employed. We then require that its restriction to $\mathcal{M}_0$ yields U, i.e., $UP = U$, but differs from U in its action on the orthogonal complement $\mathcal{M}_0^{\perp}$ of $\mathcal{M}_0$. Thus, we have to consider a family of model spaces involving a varying number of electrons, leading to the concept of valence universality. This in turn requires that we replace the definition of a standard N-product by its "commutative" version which preserves the number of particles and holes and leads to the "normal ordered" exponential function, usually designated by a bold face symbol, i.e., $\mathbf{exp}(T)$. The precise formulation of these concepts is rather involved (see, e.g., [125]; see also [3, 65–68, 76, 126]). Since in this work we deal with methods that are based on the SU Ansatz [77], we refer the reader who is interested in VU-type approaches to appropriate literature (for an overview and references, see, e.g., [2, 5, 67, 68, 76]).

17.5.1. SU MRCC Formalism

The Jeziorski–Monkhorst (JM) or SU cluster Ansatz for the wave operator U, Eqs. (17-12), (17-13), and (17-14), and for the corresponding exact wave functions $|\Psi_j\rangle$, $(j = 1, \cdots, M)$, have the form [77]

$$U = \sum_{i=1}^{M} \exp\left(T[i]\right) P_i \quad \text{and} \quad |\Psi_j\rangle = \sum_{i=1}^{M} c_{ij} \exp\left(T[i]\right) |\Phi_i\rangle \,, \tag{17-19}$$

with the coefficients c_{ij} given by the eigenvectors of $H^{(\mathrm{eff})}$, the corresponding eigenvalues E_i, $(i = 1, \cdots, M)$ providing the desired exact energies, Eq. (17-16). Hereafter the bracketed argument in $T[i]$ will indicate that this cluster operator is defined relative to the reference $|\Phi_i\rangle$ from $\mathcal{M}_0$.

The matrix elements $H_{ij}^{(\mathrm{eff})}$ of $H^{(\mathrm{eff})}$ are given by similar expressions as in the SR case

$$H_{ij}^{(\mathrm{eff})} = \langle \Phi_i | \{ H_{N_j} \exp\left(T[j]\right) \}_C | \Phi_j \rangle \,, \tag{17-20}$$

where N_j indicates the N-product form relative to $|\Phi_j\rangle$. The cluster amplitudes are then obtained by exploiting the Bloch equation (17-17). Thus, using the Ansatz (17-19) in (17-17) gives

$$\begin{aligned} HU|\Phi_i\rangle = H \exp\left(T[i]\right)|\Phi_i\rangle = UH^{(\mathrm{eff})}|\Phi_i\rangle = \\ \sum_j \exp\left(T[j]\right)|\Phi_j\rangle\langle\Phi_j|H^{(\mathrm{eff})}|\Phi_i\rangle = \\ \sum_j \exp\left(T[j]\right)|\Phi_j\rangle H_{ji}^{(\mathrm{eff})} \quad , \end{aligned} \tag{17-21}$$

and projecting onto $|\Phi_\alpha^\rho[i]\rangle \in \mathcal{M}_0^\perp$ after multiplying on the left with $\exp(-T[i])$ and realizing that $\langle \Phi_\alpha^\rho[i]|\Phi_i\rangle = 0$, we finally obtain SU MRCC equations [77]

$$\langle \Phi_\alpha^\rho[i]|\bar{H}[i]|\Phi_i\rangle = \sum_{j(\neq i)} H_{ji}^{(\mathrm{eff})}\, \Gamma^{ij}(\Phi_\alpha^\rho[i]) \,, \tag{17-22}$$

where

$$\bar{H}[i] \equiv \exp(-T[i]) H_{N_i} \exp\left(T[i]\right) \,, \qquad \text{and} \tag{17-23}$$

$$\Gamma^{ij}(\Phi_\alpha^\rho[i]) \equiv \langle \Phi_\alpha^\rho[i]| \exp(-T[i]) \exp\left(T[j]\right)|\Phi_j\rangle \,. \tag{17-24}$$

Here α and ρ represent the sets of (spin) orbital hole and particle labels relative to $|\Phi_i\rangle$, $\alpha \equiv \{P_1, P_2, \cdots, P_m\}$ and $\rho \equiv \{Q_1, Q_2, \cdots, Q_m\}$, respectively.

Note that the left-hand-side of (17-22) has the same form as the SR CC equations relative to one of the references from $\mathcal{M}_0$ and $|\Phi_\alpha^\rho[i]\rangle$ does not involve excitations within the active orbitals, which are now taken care of via the right-hand-side coupling terms $\Gamma^{ij}(\Phi_\alpha^\rho[i])$. Clearly, when numerous reference configurations are involved, which is particularly the case when we adhere to CMS, the SU MRCC

equations (17-22) represent a challenging complex problem. This is certainly the reason why very few applications of this formalism are available, except possibly for the simplest two-reference case [79, 80].

17.5.1.1. General Model Space Approach

In the standard SU CC approach it is important that one employs a CMS that is spanned by all possible configurations involving active orbitals and electrons, warranting the size-extensivity and the intermediate normalization property $\langle \Phi_i | \tilde{\Psi}_j \rangle = \delta_{ij}$. However, the use of CMS has a disadvantage not only due to a rapidly increasing dimensionality of $\mathcal{M}_0$ with the number of active orbitals, but also as a source of intruder states. It is thus desirable to truncate CMS to a suitable *incomplete model space* (IMS). We refer to such IMS as a *general model space* (GMS) in order to emphasize its arbitrariness, at least in principle. Indeed, our GMS is spanned by suitably selected configurations that are not necessarily based on the division of MOs into the core, active, and virtual ones, but rather on the role they play in the states of interest, as implied, e.g., by a small-scale CI.

The challenge of GMS SU CC approach [81] is thus the handling of those cluster amplitudes that are associated with the so-called *internal* excitations, i.e., those that interrelate configurations spanning $\mathcal{M}_0$ (see also [77]). If we wish to preserve the intermediate normalization then the corresponding internal amplitudes cannot be simply set to zero as in the CMS case, but must be determined via the so-called *C-conditions* (*C* for constrained or connected).

To briefly indicate the source of the *C*-conditions for the internal amplitudes [81, 83, 84], consider the FCI form of the exact state $|\Psi_i\rangle$

$$|\Psi_i\rangle = \sum_{|\Phi_j\rangle \in \mathcal{M}_0} c_{ij} |\Phi_j\rangle + \sum_{|\Xi_j\rangle \in \mathcal{M}_0^\perp} d_{ij} |\Xi_j\rangle \,, \tag{17-25}$$

with $|\Phi_j\rangle$ spanning the model space $\mathcal{M}_0$ and $|\Xi_j\rangle$ its orthogonal complement $\mathcal{M}_0^\perp$, so that $\mathbf{C} = ||c_{ij}||$ is a square invertible matrix and $\mathbf{D} = ||d_{ij}||$ is a rectangular matrix. The corresponding state $|\tilde{\Psi}_i\rangle$ then takes the form

$$\begin{aligned} |\tilde{\Psi}_i\rangle &= U|\Phi_i\rangle = \exp\left(T[i]\right)|\Phi_i\rangle \\ &= |\Phi_i\rangle + \sum_{|\Xi_j\rangle \in \mathcal{M}_0^\perp} b_{ij} |\Xi_j\rangle \,, \end{aligned} \tag{17-26}$$

where now $\mathbf{B} = \mathbf{C}^{-1}\mathbf{D}$ and the corresponding $\tilde{\mathbf{C}} = ||\tilde{c}_{ij}|| = \mathbf{C}^{-1}\mathbf{C} = \mathbf{I}$ becomes identity. Thus, for the internal excitations $G_\alpha^\rho[i]|\Phi_i\rangle \in \mathcal{M}_0$ we must require that the corresponding coefficients vanish, i.e., $\tilde{c}_\alpha^\rho[i] \equiv 0$. This immediately implies that all such singly-excited internal cluster amplitudes vanish, while the higher-excited ones are determined by the above requirement $\tilde{c}_\alpha^\rho[i] = 0$. Thus, for example, assuming that

$|\Phi_i\rangle \in \mathcal{M}_0$, $(i = 1, 2)$, are related via the excitation operator $G^{Q_1,Q_2}_{P_1,P_2}$, i.e., $|\Phi_2\rangle = G^{Q_1,Q_2}_{P_1,P_2}[1]|\Phi_1\rangle$, we require that $\tilde{c}^{Q_1,Q_2}_{P_1,P_2}[1] = 0$, so that we must set

$$t^{Q_1,Q_2}_{P_1,P_2}[1] \equiv t^{Q_2}_{P_1}[1]t^{Q_1}_{P_2}[1] - t^{Q_1}_{P_1}[1]t^{Q_2}_{P_2}[1]\,, \tag{17-27}$$

and similarly for $t^{P_1,P_2}_{Q_1,Q_2}[2]$, as well as for higher-than-pair cluster amplitudes [82] [81]. The *external* cluster amplitudes that are associated with the excitation operators $G^{\rho}_{\alpha}[i]$, $G^{\rho}_{\alpha}[i]|\Phi_i\rangle \in \mathcal{M}^{\perp}_0$ are then determined using the standard SU CC equations (17-22). Finally, as in the RMR CCSD case (Section 17.6.2.1), we can perturbatively account for secondary triples by modifying the diagonal elements of $H^{(\mathrm{eff})}$ (see [127]).

This approach enabled us to handle relatively large model spaces while avoiding the problem of intruder states, and yielded excellent results in test calculations [86].

17.5.2. Kucharski – Bartlett Formulation of SU MRCC

An alternative formulation of the SU MRCC method has been proposed by Kucharski and Bartlett [96, 128–130], henceforth referred to as the KB approach. It starts with Eq. (17-21), but in contrast to the JM SU formalism, no multiplication by $\exp(-T[i])$ is performed before the projection onto the excited states $|\Phi^{\rho}_{\alpha}[i]\rangle \in \mathcal{M}^{\perp}_0$. This leads to amplitude equations in the following form

$$\left\{\langle\Phi^{\rho}_{\alpha}[i]|H_{N_i}\exp(T[i])|\Phi_i\rangle\right\}_{C+DC,L} = \sum_{j\neq i}\langle\Phi^{\rho}_{\alpha}[i]|\exp(T[j])|\Phi_j\rangle H^{(\mathrm{eff})}_{ji}\,. \tag{17-28}$$

Notice that in contrast to (17-22), where the vanishing $i = j$ term is absent from the sum over j, here it is not included since it cancels with an unlinked term on the left hand side, which involves only connected and linked disconnected diagrams, as indicated by the subscript $C + DC, L$. Using the method of moments technique, it can be proved that this formulation is equivalent to the SU MRCC method, as long as we employ a CMS [131]. We can thus view the KB approach as a generalization of the equivalence between the connected and linked formulations of the SR CC method. Moreover, as shown by Kucharski and Bartlett [96], who performed a detailed diagrammatic analysis of the expressions in Eq. (17-28), the cancellation of disconnected terms yields

$$\langle\Phi^{\rho}_{\alpha}[i]|\bar{H}[i]|\Phi_i\rangle = \sum_{j\neq i}\left\{\langle\Phi^{\rho}_{\alpha}[i]|\exp(T[j])|\Phi_j\rangle H^{(\mathrm{eff})}_{ji}\right\}_C\,, \tag{17-29}$$

where the subscript C indicates that only connected diagrams are involved. The removal of disconnected terms preserves the size-extensivity, but breaks the equivalence of the resulting method with FCI in the FCC limit. However, with a CMS, the

variant including disconnected terms, Eq. (17-28), is already size-extensive thanks to the equivalence with the JM approach (17-22).

The computation of coupling terms in the KB scheme [in either (17-28) or (17-29) version] is simpler than in the SU MRCC formalism, Eq. (17-24), thanks to the presence of a single exponential. In the KB case, one only has to compute a product of the coupling term $\langle \Phi_\alpha^\rho[i]|e^{T[j]}|\Phi_j\rangle$ and an effective Hamiltonian matrix element $H_{ji}^{(\mathrm{eff})}$. The evaluation of the latter is analogous to obtaining a higher CI coefficient from CC amplitudes. Concerning the implementation of Eq. (17-29), it is not necessary to explicitly evaluate the connected diagrams corresponding to the entire coupling term, since it is simpler to evaluate disconnected terms and subtract them from the product on the right-hand-side of (17-29) [132]. However, the computation of coupling terms does not represent a bottleneck, which lies in the handling of the left-hand-side terms $\langle \Phi_\alpha^\rho[i]|\bar{H}[i]|\Phi_i\rangle$, so that the KB formulation does not bring any advantage in this regard. Moreover, its convergence may be influenced by the presence of intruder states, as in the SU MRCC method. Nonetheless, the main advantage of the KB formalism lies in a simpler form of the coupling terms, facilitating their implementation. We also note that the KB formulation can be generalized to an IMS by exploiting the *C*-conditions described in the preceding section.

Note also, that the analytic gradient theory has been developed for the SU MRCC method [133–137], but has not yet achieved a widespread use due to the lack of an efficient black-box implementation, with the exception of a special low-spin singlet two-determinantal case [134].

17.5.3. Brillouin – Wigner MR CC Method

Before we turn our attention to SS MRCC methods, we point out some basic properties of the JM Ansatz as it pertains to the state-specific formalism. It is well-known that in model-space-based MR approaches, be they of the CI or CC variety, the excitations from distinct reference configurations $|\Phi_i\rangle \in \mathcal{M}_0$ may lead to identical excited state configurations from $\mathcal{M}_0^\perp$. This, however, does not imply any ambiguity of the JM Ansatz in the SU context (as is sometimes erroneously intimated), since in this case the operator equation resulting from the insertion of the JM Ansatz into Bloch equation can be applied to all determinants $|\Phi_i\rangle$ from the model space $\mathcal{M}_0$ and projected onto appropriate excited bras $\langle \Phi_\alpha^\rho[i]|$ for each such ket, yielding exactly as many equations as there are unknowns in the JM Ansatz. Therefore, in the SU methods all the relevant cluster amplitudes are uniquely defined and, if desired, may be recovered by the cluster analysis of the FCI wave function for any target state $|\Psi_i\rangle$ (see, e.g., [138]). Thus, inserting the JM Ansatz into Bloch equation yields perfectly consistent MRCC equations at any level of truncation.

However, an entirely different situation arises when we exploit the JM Ansatz in the MR SS-type methods, which focus on one state at a time. In this case we have to rely on the Schrödinger equation for *a single* target state, rather than on Bloch equation, so that we do not have enough conditions for the number of cluster

amplitudes in the JM Ansatz to be uniquely determined. The resulting ambiguity may be usually avoided by invoking suitable sufficiency conditions which replace the general requirement $\sum_{i\in\mathcal{M}_0} A(i) = 0$ by setting each term to zero, i.e.,

$$\sum_{i\in\mathcal{M}_0} A(i) = 0 \qquad \Leftarrow \qquad A(i) = 0\,, \quad \forall i \in \mathcal{M}_0\,. \tag{17-30}$$

This idea was used only implicitly in the original derivation of BWCC and later has been formulated explicitly by Mukherjee et al. [89] in the context of his approach (cf. Section 17.5.4).

Historically, the derivation of the MR Brillouin – Wigner coupled-clusters method (BWCC), as originally proposed by Hubač, Čársky, and Mášik [97, 98, 139, 140], was based on the state-specific Lippmann – Schwinger-like equation

$$U_i = 1 + B_i W U_i\,, \qquad B_i = \sum_{\Phi_j\in\mathcal{M}_0^\perp} \frac{|\Phi_j\rangle\langle\Phi_j|}{E_i - E_j'}\,, \tag{17-31}$$

where B_i is the BW resolvent, which is responsible for the SS nature of this approach. In contrast to the SU CC methods, the wave operator U_i (as well as the cluster operator) now carries the index of the target state i. This equation played the role of Bloch equation for the BWCC theory [141] and it is, of course, equivalent to the Schrödinger equation for the state $|\Psi_i\rangle$.

It turns out that the derivation of the amplitude equations is actually simpler if one inserts the JM Ansatz (17-19) with a SS wave operator U_j directly into the Schrödinger equation $(H - E_j)|\Psi_j\rangle = 0$, which yields

$$\sum_{i\in\mathcal{M}_0} (H - E_j) \exp(T[i])|\Phi_i\rangle c_{ij} = 0. \tag{17-32}$$

Application of the sufficiency conditions (17-30) and a few algebraic manipulations lead to BWCC amplitude equations

$$\{\langle\Phi_\alpha^\rho[i]|H_{N_i} \exp(T[i])|\Phi_i\rangle\}_{C+DC,L} = (E_j - H_{ii}^{(\mathrm{eff})})\langle\Phi_\alpha^\rho[i]| \exp(T[i])|\Phi_i\rangle\,. \tag{17-33}$$

Notice that for a notational simplicity we have omitted the state index j from the cluster operator, which acquires different values $T_j[i]$ for each state. The effective Hamiltonian keeps the same form as in the SU MRCC method, Eq. (17-20), but now only its jth eigenvalue has a physical meaning. The iterative solution of the amplitude equations (17-33) requires a diagonalization of $H^{(\mathrm{eff})}$ in each iteration, and the resulting eigenvalue E_j is then used in the next iteration.

The advantage of the BWCC method over the SU methods lies in a greater simplicity of its amplitude equations, which are coupled only via the exact energy E_j.

Another important advantage is its insensitivity to intruder states, which in turn leads to a superior convergence characteristics in comparison with the standard SU CC methods. However, it has a serious drawback in not being size-extensive, thus lacking the most valuable trait of CC methods. Trying to restore the size-extensivity by left-multiplication with $e^{-T[i]}$ leads to uncoupled system of equations

$$\left\{\langle \Phi_\alpha^\rho[i]|H_{N_i}\exp(T[i])|\Phi_i\rangle\right\}_C = 0\,, \tag{17-34}$$

which are not equivalent to (17-33), since the term with the exact energy E_j vanishes. Thus, an *a posteriori* size-extensivity correction to BWCC energies has been suggested [142], which consists in an iterative solution of the amplitude equations (17-33), followed by a single iteration of (17-34) and a final assembly and diagonalization of the effective Hamiltonian matrix, yielding the corrected energy. This correction is, of course, not exact, but in numerous tests and applications it turned out to yield sufficiently accurate results for practical purposes [143–156].

Another way how to introduce the size-extensivity corrections to BWCC is to exploit a continuous transition between the BW and Rayleigh – Schrödinger (RS) perturbation theories, which yields [131, 132]

$$\lambda E_i U_i \tilde{P}_i + (1-\lambda)[U_i, H_0]P = \lambda H U_i \tilde{P}_i + (1-\lambda)[WU_i - U_i PWU_i]P, \tag{17-35}$$

where $\tilde{P}_i = |\tilde{\Phi}_i\rangle\langle\tilde{\Phi}_i|$ is a state-specific projection operator on a one-dimensional subspace of the model space and λ is a real scaling parameter ranging from zero to one. The $\lambda = 1$ limit corresponds to the BW perturbation theory, while $\lambda = 0$ to the RS theory. Insertion of the JM Ansatz into this equation leads, after some algebra, to amplitude equations for a λ-scaled transition between the SU MRCC and BWCC. The iterative size-extensivity correction to BWCC then corresponds to a continuous change of λ from one to zero during the CC iterative process while neglecting the SU MRCC coupling terms in the amplitude equations. The iterative correction leads to exact size-extensivity, but unfortunately reintroduces the intruder state problem and related convergence difficulties.

Recently, the connected triple excitations have been included in the MR BWCC method [157–159], considerably increasing its accuracy thanks to a more precise description of dynamic correlation effects, similarly as in the SR case, where one also has to account – at least approximately – for connected triply-excited clusters in order to achieve the chemical accuracy. For a recent detailed account of BW MBPT-based approaches we refer the reader to a forthcoming monograph by Hubač and Wilson [141].

17.5.4. Mukherjee's Approach to MRCC

Similarly to BWCC, the derivation of MkCC [89, 91, 160, 161] starts by substituting the JM Ansatz (17-19) for $|\Psi_j\rangle$ into the Schrödinger equation for that state, which yields (17-32). Then, however, additional transformations of this equation are

performed before the sufficiency conditions (17-30) are applied. Inserting resolution of the identity in the form

$$1 = e^{T[i]} P e^{-T[i]} + e^{T[i]} Q e^{-T[i]} \tag{17-36}$$

into Eq. (17-32), where again $P = \sum_{k \in \mathcal{M}_0} |\Phi_k\rangle\langle\Phi_k|$ and $Q = 1 - P$ are projectors onto the model space $\mathcal{M}_0$ and its orthogonal complement $\mathcal{M}_0^{\perp}$, respectively, we obtain

$$\sum_{ik} e^{T[i]} |\Phi_k\rangle\langle\Phi_k| \bar{H}[i] |\Phi_i\rangle c_{ij} + \sum_i e^{T[i]} Q \bar{H}[i] |\Phi_i\rangle c_{ij} - E_j \sum_i e^{T[i]} |\Phi_i\rangle c_{ij} = 0\,. \tag{17-37}$$

The next essential step is an interchange of the summation indices i and k in the first term and the subsequent application of the above mentioned sufficiency conditions (17-30), equating each term in the sum over i to zero. A left-multiplication by $e^{-T[i]}$ and a projection onto the excited bra manifold then yields

$$\langle \Phi_\alpha^\rho[i] | \bar{H}[i] | \Phi_i\rangle c_{ij} = -\sum_{k(\neq i)} \langle \Phi_\alpha^\rho[i] | e^{-T[i]} e^{T[k]} | \Phi_i\rangle H_{ik}^{(\mathrm{eff})} c_{kj}\,, \tag{17-38}$$

assuming a CMS in evaluating the effective Hamiltonian matrix elements.

Note that in contrast to the standard SU CC equations (17-22), the MkCC equations (17-38) for the cluster amplitudes involve both the effective Hamiltonian matrix elements and the eigenvector coefficients c_{ij} for a selected state j, indicating the state-specificity of the resulting method. Thus, as in the BWCC approach, the effective Hamiltonian must be diagonalized in each iteration, providing in this case the j-th eigenvector coefficients c_{ij}. Note also that should we invoke the sufficiency conditions (17-30) to (17-37) without first interchanging the order of summations in the first term, we would recover uncoupled SR CC-type equations relative to references $|\Phi_i\rangle$. Mukherjee et al. [89, 160] have also shown how BW-type denominators can be obtained by expanding the coupling terms, implying a robustness of the method relative to the intruder states while preserving the size-extensivity.

An important advantage of this approach stems from the structure of the coupling coefficients which, in contrast to those characterizing the standard SUCC method, involve the same configuration in the bra and the ket. This distinction was noticed by Evangelista, Allen, and Schaefer, who derived explicit formulas for these coefficients enabling them to develop an efficient implementation of the method accounting for up to triexcitations [94, 95, 162]. A non-iterative approximation to MkCCSDT has been proposed and implemented by Bhaskaran-Nair et al. [163].

An alternative formulation of Mukherjee's method – that is similarly related to the above presented MkCC, Eq. (17-38), as is the Kucharski – Bartlett SU MRCC to the Jeziorski – Monkhorst SU MRCC – is obtained if instead of premultiplying

Eq. (17-37) by $e^{-T[i]}$ we analyze the disconnected terms arising via the projection onto the bra configurations, yielding

$$\left(E_j - H_{ii}^{(\mathrm{eff})}\right)\langle \Phi_\alpha^\rho[i]|e^{T[i]}|\Phi_i\rangle c_{ij} = \left\{\langle \Phi_\alpha^\rho[i]|He^{T[i]}|\Phi_i\rangle\right\}_{C+DC,L,EXT} c_{ij} + \sum_{k\neq i}\langle \Phi_\alpha^\rho[i]|e^{T[k]}|\Phi_i\rangle H_{ik}^{(\mathrm{eff})} c_{kj}\,. \quad (17\text{-}39)$$

The subscript $C + DC, L, EXT$ denotes the inclusion of connected as well as disconnected linked diagrams, with at least one external line carrying an inactive orbital index. Note a similarity of this approach with the BWCC method, Eq. (17-33), thanks to the presence of the exact energy E_j. This approach is equivalent with (17-38), as long as a CMS is employed [164]. Its advantages stem from the fact that the coupling terms in (17-39) involve a single exponential and thus require coding of a much smaller number of terms. However, the computational costs of both approaches scales in the same way, since the computation is not dominated by the evaluation of coupling terms. The convergence properties of this alternative formulation remain to be investigated, since its efficient implementation has been developed only recently [165].

17.5.5. Hanrath's MR Exponential Ansatz

In lieu of invoking sufficiency conditions (17-30) in order to eliminate redundancies in the SU Ansatz when used in the SS-type approaches, Hanrath [166–169] proposed their explicit avoidance a priori by modifying the structure of the cluster operators $T[j]$ by writing

$$T[j] = e^{\mathrm{i}\arg c_{ij}} \sum_{\hat{\tau}_\mu(j)} t_{\hat{\tau}_\mu(j)|\Phi_j\rangle}\hat{\tau}_\mu(j)\,, \quad (17\text{-}40)$$

where c_{ij} designate the coefficients defining the appropriate effective Hamiltonian eigenvector, Eq. (17-19). The excitation operators $\hat{\tau}_\mu(j)$ run again over mono-, bi-, and higher excitations relative to a reference $|\Phi_j\rangle$, but the cluster amplitudes are labeled by configurations (or determinants) generated by these operators. In other words, if the two distinct excitations $\hat{\tau}_\mu(j)$ and $\hat{\tau}_\nu(k)$, $j \neq k$, generate the same determinant, i.e., if $\hat{\tau}_\mu(j)|\Phi_j\rangle = \pm\hat{\tau}_\nu(k)|\Phi_k\rangle$, there will be only one amplitude $t_{\hat{\tau}_\mu(j)|\Phi_j\rangle} \equiv \pm t_{\hat{\tau}_\nu(k)|\Phi_k\rangle}$ in the Ansatz (17-40). This "brute force" a priori elimination of redundancies leads, however, to a complex indexing scheme requiring computer assisted code generation, particularly when higher-level excitations are to be included [169]. The phase factor $e^{\mathrm{i}\arg c_{ij}}$ prevents a cancellation of amplitudes when the coefficients c_{ij} happen to be equal for the two references (e.g., due to the symmetry) [166].

Insertion of the MRexpT ansatz (17-40) into the Schrödinger equation and projection onto the bra manifold of both the reference and excited determinants yields the system of equations

$$\sum_{i\in\mathcal{M}_0} c_i\langle\rho|(H-E)e^{T[i]}|\Phi_i\rangle = 0\,, \tag{17-41}$$

which is fully determined, provided the normalization is fixed by requiring $\sum_i |c_i|^2 = 1$. Hanrath has shown the MRexpT Ansatz to be size-consistent [166] and core-extensive [168, 170, 171], which indicates that the method has a potential to be accurate for large molecules. Presently, only results for small model systems are available [167, 169, 172], probably due to the higher complexity of the working equations resulting from the determinantal indexing. See Chapter 7 for more detail.

17.6. STATE-SPECIFIC MRCC-LIKE METHODS BASED ON SR CC ANSATZ

Although a proper account of both dynamic and nondynamic correlations in the presence of quasi-degeneracy calls for a genuine MR description, much can be often achieved by SS approaches that rely on SR CC Ansatz, while exploiting at the same time the basic ideas and concepts of MR-type Ansätze. The major shortcomings of the standard SR CCSD method arise due to the neglect of higher-than-pair clusters, namely of the terms $\Lambda_i^{(k)}$, $(k = 1, 2)$

$$\begin{aligned}\Lambda_i^{(1)} &\equiv \langle\Phi_i^{(1)}|H_N\, T_3||\Phi_0\rangle_C\,,\\ \Lambda_i^{(2)} &\equiv \langle\Phi_i^{(2)}|H_N(T_3+T_4+T_1T_3)|\Phi_0\rangle_C\,,\end{aligned} \tag{17-42}$$

whose importance increases with the degree of quasi-degeneracy. Thus, all SS methods that are based on SR CC Ansatz account, in one way or another, for these clusters, which were neglected in decoupling of CCSD equations from the rest of the CC chain. Here it is important to realize that T_3 and T_4 clusters do not contribute directly to the energy as given by the asymmetric energy formula

$$\mathcal{E}(\Xi,\Psi) = \langle\Xi|H|\Psi\rangle/\langle\Xi|\Psi\rangle\,, \quad \langle\Xi|\Psi\rangle \neq 0\,, \tag{17-43}$$

but via their interaction with the T_1 and T_2 clusters. Thus, in the CC case, $|\Xi\rangle = |\Phi_0\rangle$ and $|\Psi\rangle = \exp(T)|\Phi_0\rangle$, and the correlation energy ΔE is given by Eq. (17-8).

It is important to realize that $\mathcal{E}(\Xi,\Psi)$ yields the exact (i.e., FCI) energy E when either $|\Xi\rangle$ or $|\Psi\rangle$ are exact. Clearly, in practice, both $|\Xi\rangle$ and $|\Psi\rangle$ are approximate. Thus, in CCSD $|\Xi\rangle = |\Phi_0\rangle$ and $|\Psi\rangle \equiv |\mathrm{CCSD}\rangle = |\exp(T_1+T_2)\Phi_0\rangle$. With the increasing quasi-degeneracy or MR character, the weight of $|\Phi_0\rangle$ in the FCI wave function decreases and, at the same time, the overlap $\langle\mathrm{FCI}|\mathrm{CCSD}\rangle$, and

especially the norm $\langle \mathrm{CCSD}|\mathrm{CCSD}\rangle$ rapidly increase. Yet, the renormalized overlap $\langle \mathrm{FCI}|\mathrm{CCSD}\rangle/\sqrt{\langle \mathrm{CCSD}|\mathrm{CCSD}\rangle}$ stays almost constant (cf. Figure 2 and Table I of [115]). Moreover, MBPT treatment of T_3 and T_4 further aggravates the situation (cf., e.g., Figure 1 of [62]). We shall see that either a suitable renormalization (Section 17.6.1.2) or an approximate treatment of higher-than-pair clusters (Sections 17.6.2.1 and 17.6.3.1) can go a long way towards the achievement of a useful, while computationally affordable, description.

The account of T_3 and T_4 clusters can be achieved in two qualitatively distinct ways, which we refer to as the *internal* and *external* ones. The latter approaches rely on some independent or external source of information about the T_3 and T_4 clusters, while the former ones employ the CC or MBPT formalism for this purpose.

17.6.1. Internally Corrected Methods

The prototype of these methods is a basic "workhorse" of CC approaches, namely the CCSD(T) method [55–58]), often referred to as the "gold standard" of quantum chemistry [59–61], which relies on a perturbative estimate of triples. One can obtain a good approximation to $T_3|\Phi_0\rangle = \{R^{(3)}V_N \sum_{n=1}^{\infty} (RV_N)^n|\Phi_0\rangle\}_C$ that is compatible with the CCSD method by retaining those higher-order terms that are generated via the two-body clusters, i.e.,

$$\Lambda_i^{(2)} = \langle \Phi_i^{(2)}|H_N T_3|\Phi_0\rangle_C \approx \Lambda_i'^{(2)} = \langle \Phi_i^{(2)}|V_N R^{(3)} V_N T_2|\Phi_0\rangle_C = \sum_j W_{ij}^{(2)} t_j^{(2)} ,$$

$$W_{ij}^{(2)} = -\sum_k^{(3)} H_{ik} H_{jk}^*/\Delta\varepsilon_k , \qquad H_{ij} = \langle \Phi_i^{(2)}|V_N|\Phi_j^{(3)}\rangle , \tag{17-44}$$

where V_N designates the two-electron part of H_N and $R^{(3)}$ and $\Delta\varepsilon_k$ are, respectively, the MBPT resolvent and denominator (cf. [3, 11]). The additive triple correction to the CCSD energy,

$$\Delta E^{(T)} = \sum_{i,j} t_i^{(2)} W_{ij}^{(2)} t_j^{(2)} , \tag{17-45}$$

then yields the CCSD[T] method [56, 57] or CCSD(T) method when also accounting for singles via the $\langle \Phi_i^{(1)}|H_N T_3|\Phi_0\rangle_C$ term.

The $\Lambda_i'^{(2)}$ term can also be employed to design an amplitude-correcting algorithm, either of the iterative kind, yielding various CCSDT-n approximations [51, 116, 117] or noniterative ones by evaluating the $W_{ij}^{(2)}$ terms a priori and using them to modify CCSD equations.

17.6.1.1. Truncated SRCC Approaches

Since a complete account of T_3 and T_4 clusters via, respectively, the CCSDT and CCSDTQ methods is computationally too demanding, we can obtain a suitable approximation by relying on a truncated version of these methods, which consider only a subset of the most important triples and quadruples. This type of approaches was pioneered by Adamowicz et al. [105, 106], particularly in the so-called CCSDt and CCSDtq methods [173, 174]. To find suitable subsets of triples and quadruples one relies on MR CC concepts, while further subdividing the set of active orbitals and allowing higher-than-double excitations involving these subsets. Unfortunately, even these truncated approaches can quickly become computationally demanding.

17.6.1.2. Renormalized and Completely Renormalized CC Methods

A breakdown of the standard CCSD(T) method in the presence of quasi-degeneracy may be remedied to a large degree by a suitable renormalization, as indicated in Section 17.6. This led Kowalski and Piecuch [62, 63, 108–110] to design the *renormalized* (R-) and *completely renormalized* (CR-) CCSD(T) approaches (as well as other perturbatively corrected approaches, such as CCSD(TQ), EOM-CC, or CCSD[T], etc.) by relying on the method of moments (MM) (see, also [175]). The basis of this and related formalisms, leading to both *ic* or *ec* approaches, is most simply understood when based on the asymmetric energy formula, Eq. (17-43). In the CC case we have

$$\mathcal{E}(\Xi,\Psi) = D^{-1}\langle \Xi|H|\exp(T)\,\Phi_0\rangle\,, \qquad D = \langle \Xi|\exp(T)\,\Phi_0\rangle\,. \tag{17-46}$$

Inserting resolution of the identity in the form $e^T \sum_{k=0}^{N}\sum_{i\in(k)} |\Phi_i^{(k)}\rangle\langle\Phi_i^{(k)}|\,e^{-T}$, and assuming the truncation of T at the nth order, $T \approx T^{[n]} = \sum_{i=1}^{n} T_i$, we easily find in view of Eq. (17-9) that [62, 108, 123]

$$\begin{aligned}\mathcal{E}(\Xi,\mathrm{CC}[n]) &= E_{\mathrm{CC}[n]} + D^{-1}\sum_{k=n+1}^{N}\sum_{i\in(k)}\langle\Xi|\exp(T^{[n]})|\Phi_i^{(k)}\rangle\langle\Phi_i^{(k)}|\bar{H}^{[n]}|\Phi_0\rangle \\ &\equiv E_{\mathrm{CC}[n]} + D^{-1}\sum_{k=n+1}^{N}\sum_{i\in(k)}\mathcal{C}_i^{(k)}[n]\,M_i^{(k)}[n]\,.\end{aligned} \tag{17-47}$$

Note that the moments $M_i^{(k)}[n]$ represent the left-hand side of standard CC equations projected onto $|\Phi_i^{(k)}\rangle$, $k > n$. In the CCSD $\equiv$ CC[2] case $T \approx T^{[2]} = T_1 + T_2$, we thus have

$$\mathcal{E}(\Xi,\mathrm{CCSD}) = E_{\mathrm{CCSD}} + D^{-1}\sum_{k=3}^{N}\sum_{i\in(k)}\mathcal{C}_i^{(k)}[2]\,M_i^{(k)}[2]\,, \tag{17-48}$$

which can be rewritten as [62, 108, 123]

$$\mathcal{E}(\Xi, \mathrm{CCSD}) = E_{\mathrm{CCSD}} + D^{-1}\langle\tilde{\Xi}|(H_N - \Delta E_{\mathrm{CCSD}})\exp(T^{[2]})|\Phi_0\rangle\,, \qquad (17\text{-}49)$$

where $|\tilde{\Xi}\rangle$ represents higher-than-doubly-excited part of $|\Xi\rangle$ and ΔE_{CCSD} is the CCSD correlation energy {cf. Eqs. (12) and (15) of [62] and Eq. (17) of [123]}. Equation (17-48) or (17-49) serves as a basis of the energy-corrected approaches of either the *ic* or *ec* type (see Section 17.6.2.2). When the bra state $\langle\Xi|$ is now evaluated via a CC-analogue of MBPT to an appropriate order [by associating the cluster amplitudes with the rightmost interaction vertices] and noting that $\mathcal{C}^{(0)}[2] = 1$, we obtain the CR-CCSD(T) or CR-CCSD[T] method. These can be similarly extended to CCSD(TQ), CCSDT(Q) and other approaches. The corresponding R-CC methods then result by considering only the leading term in the momenta [62, 108].

While CR-CCSD(T) approach corrects for the shortcomings of the standard CCSD(T) for states having a strong MR character and, in fact, for those of CCSD as well (that are responsible for, e.g., an artificial hump on potential energy curves, cf. [176]), it is slightly less accurate than CCSD(T) in the neighborhood of equilibrium geometry and slightly ($\sim$ 0.5%) violates the size-extensivity. These shortcomings are eliminated in the so called CR-CC(n_A, n_B) methods, which exploit an extended CC Ansatz by representing the bra state as $\langle\Xi| = \langle\Lambda\exp(-T^{[n_A]})|$. This in turn requires the evaluation of components of the Λ operator, as in the analytic gradient CC theory, as well as a more laborious evaluation of denominators [111]. Thus, the most useful CR-CC(2,3) method, correcting CCSD ($n_A = 2$) for triples ($n_B = 3$), yields results that optimally approximate CCSDT. Likewise, when quadruples are required (see, e.g., [177]) one can employ CR-CC(2,4) which, however, is already computationally quite demanding.

17.6.1.3. Partially Linearized MR CC Method

This method [114], referred to by the acronym plMR CCSD, represents an *ic* alternative to the *ec* RMR CCSD method (see Section 17.6.2.1). It employs again a small subset of higher-than-pair cluster amplitudes, which in this case are generated by relying on a linear version of higher-order CC equations. In fact, by considering all triples, we would obtain the CCSDT-1 method [116]. However, in contrast to the latter, plMR CCSD considers only a small subset of important triples, as well as higher order amplitudes (possibly up to hextuples). Again, the remaining triples may be accounted for perturbatively, yielding plMR CCSD(T) method [114, 115, 178].

Although plMR methods are fully size extensive, the corresponding RMR approaches always yield superior results [115]. This is likely due to the absence of nonlinear terms in higher than doubles equations. The computational requirements for both plMR and RMR methods are very similar, yet the former approach is more difficult to converge, especially in the presence of a strong quasi-degeneracy [115]. However, plMR would allow a relatively easy development of codes for gradients and Hessians.

17.6.2. Externally Corrected Methods

In *ec* approaches of the *amplitude-correcting* type one exploits the fact that the electronic Hamiltonian involves at most two-body terms. As a consequence, the energy is fully determined by one- and two-body cluster amplitudes, Eq. (17-8), and the SD-projected CC equations are coupled to the rest of the chain via the terms $\Lambda_i^{(k)}$, $(k = 1, 2)$, Eq. (17-42), that involve triples and quadruples. Now, rather than decoupling the CC chain by setting $T_3 = T_4 = 0$, yielding the standard CCSD equations, one should be able to achieve a physically more meaningful decoupling by approximating the T_3 and T_4 terms by relying on some external, yet easily accessible source that is capable to account for nondynamic correlation effects. Since the importance of triples and quadruples increases with the increasing quasi-degeneracy, their account should help to overcome the shortcomings of CCSD and yield more accurate one- and two-body amplitudes and, consequently, a better energy. In fact, when the "exact" (i.e., FCI) T_3 and T_4 clusters are available (i.e., via the cluster analysis of the FCI wave function), then *ec*CCSD will return the exact FCI energy.

The first attempt along these lines exploited a singlet-projected UHF (or PUHF) wave function as a source of four-body clusters (note that PUHF cannot provide triples). This led to the so-called ACPQ (approximate coupled-pairs with quadruples) method [179, 180], which is closely related to ACC(S)D [approximate CC with (singles and) doubles] approach proposed at the same time by Dykstra's group [181, 182] and the ACP-D45 and similar methods developed by Jankowski and Paldus [183, 184] that emphasize the role of EPV (exclusion principle violating) terms, which play also the crucial role in CEPA-type approaches [185–187].

In fact, neither ACPQ nor ACCD or ACP-D45 actually evaluate T_4 amplitudes but, instead, discard certain quadratic $\frac{1}{2}T_2^2$ terms (keeping only those associated with diagrams (4) and (5) of Figure 1 in [183] that separate over one or two hole lines) in CCSD equations. It can be shown [179, 180] that under certain conditions (e.g., the exactness of the PUHF wave function) the neglected quadratic terms are in fact canceled by the terms arising from the T_4 clusters. Only later on were the t_4 amplitudes actually extracted from the PUHF wave function, yielding the so-called CCSD′ method [188].

The inability of these approaches to account for triples represents definitely a drawback. Nonetheless, numerous applications testify that the ACPQ results are always superior to the CCSD ones, while being computationally less demanding. Recently the attention was again turned to this topic (see, e.g., the 2CC approach [189, 190] or an empirical handling of quadratic terms [191–194]).

To account for both triples and quadruples in *ec*CCSD one relies on a small subset of the most important $t^{(3)}$ and $t^{(4)}$ amplitudes obtained via the cluster analysis of a suitable, easily accessible wave function that efficiently describes nondynamic correlations that are lacking in SR CCSD. Initially, VB, CAS FCI, and CAS SCF wave functions were employed for this purpose: The first one (exploited only at a semi-empirical level [99–101, 195, 196]) represents an ideal source but, unfortunately, no suitable general purpose codes are available at the ab initio level, while

both CAS-type wave functions (particularly CAS SCF) require a large active space, rapidly increasing the cost [101, 195–197]. Finally, it was a modest size MR CISD that proved to be an optimal source, resulting in the reduced MR (RMR) CCSD method. While *ec*CCSD represents an amplitude-corrected approach, described in the next section, the same external source can also be employed for the energy-corrected version (see Section 17.6.2.2).

17.6.2.1. Amplitude-Corrected ecCCSD

As alluded to above, an optimal choice for the amplitude-corrected *ec*CCSD turned out to be a modest-size MR CISD wave function thanks to the following facts [198–201]: (i) the complementarity of the CC and CI approaches in their ability to describe, respectively, the dynamic and nondynamic correlation effects; (ii) a simple relationship between the CC and CI Ansätze, facilitating the extraction of the $t^{(3)}$ and $t^{(4)}$ amplitudes via the cluster analysis [138] (following a trivial transformation of the MR CISD wave function into the SR CISD form); (iii) the fact that the approximate $T_i \approx T_i^{(0)}$, $(i = 3, 4)$ clusters automatically account for higher-order T_i, $i > 4$ clusters [recall that with the exact (i.e., FCI) three- and four-body clusters *ec*CCSD returns the exact result] and, finally, (iv) the fact that *ec*CCSD requires only a very small subset of triples and quadruples (referred to as the primary ones) as provided by a modest-size MR CISD.

Moreover, the resulting RMR CCSD method will at most very slightly violate the size-extensivity, since it is again based on the exponential cluster Ansatz, namely

$$U = \exp\left(T_1 + T_2 + T_3^{(0)} + T_4^{(0)}\right), \tag{17-50}$$

the superscript (0) indicating the approximate external cluster components. Evaluating the $\Lambda_i^{(k)}$, $(k = 1, 2)$ terms, Eq. (17-42), once and for all, and using them to correct the absolute term in CCSD equations (for the treatment of the $T_1 T_3$ term, see [100, 195–197, 202]), the resulting *ec*CCSD equations have the same algebraic form as the standard CCSD ones and can be solved with the same ease.

Finally, it is often useful to also correct for the secondary triples that are generally very small, yet very large in number. This can be done as in the standard SR CCSD(T) method, yielding the RMR CCSD(T) approach [203, 204]. Moreover, when we consider larger systems or employ large basis sets, even the number of primary triples and quadruples becomes significant and it may be useful to truncate this subset based on suitable criteria [205] (see also [206]) and account for the eliminated triples via RMR CCSD(T).

On a practical side, the 2R-RMR CCSD (based on 2R-CISD) is often all that is required to handle the breaking of a single bond (note that in that case the number of primary $t^{(4)}$ amplitudes is the same as the number of $t^{(2)}$ amplitudes). However, for a proper description of a triple-bond breaking in N_2 [176], we require a high-dimensional $\mathcal{M}_0$. Once the references spanning $\mathcal{M}_0$ are decided upon, the available

codes [207] will automatically perform the corresponding RMR CCSD calculation, requiring roughly 20% more time than the standard CCSD.

17.6.2.2. Energy-Corrected ecCCSD

As pointed out in Section 17.6.1.2, instead of approximating the bra state $\langle \Xi |$ using a CC-based MBPT, leading to R- and CR-CC approaches, we can employ an external source for this purpose. This leads to the energy-corrected *ec*CCSD methods [64, 123, 202, 208].

Thus, using as an optimal source a CI-type wave function

$$|\Xi\rangle = |\Phi_0\rangle + \sum_{k=1}^{m} {\sum_{i\in(k)}}' c_i^{(k)} |\Phi_i^{(k)}\rangle \,, \tag{17-51}$$

where the prime indicates that only a subset of k-times excited configurations may be involved, the energy correction $\Delta\mathcal{E}$ of Eqs. (17-48) or (17-49) becomes

$$\Delta\mathcal{E}(\Xi, \mathrm{CCSD}) = \sum_{k=3}^{m} {\sum_{i\in(k)}}' \Delta\mathcal{E}_i^{(k)}(\Xi, \mathrm{CCSD}) \,, \tag{17-52}$$

where

$$\Delta\mathcal{E}_i^{(k)}(\Xi, \mathrm{CCSD}) = D^{-1} c_i^{(k)} \sum_{n=3}^{k} {\sum_{j\in(n)}}' \langle \Phi_i^{(k)} | \exp(T^{[2]}) | \Phi_j^{(n)} \rangle \, M_j^{(n)}[2], \tag{17-53}$$

$$D \equiv \langle \Xi | \exp(T^{[2]}) | \Phi_0 \rangle = 1 + \sum_{k} {\sum_{i\in(k)}}' c_i^{(k)} \, \langle \Phi_i^{(k)} | \exp(T^{[2]}) | \Phi_0 \rangle \,. \tag{17-54}$$

Thus, e.g., $\Delta\mathcal{E}_i^{(3)}(\Xi, \mathrm{CCSD}) = D^{-1} c_i^{(3)} \, M_i^{(3)}$(see ref. [2]).

In general, both the energy-corrected *ec*CCSD and amplitude-corrected RMR CCSD approaches that employ the same MR CISD wave function yield very similar results, the former one being slightly superior at large internuclear separations [64]. In fact, one can combine both approaches to obtain even better results. Nonetheless, to achieve an accurate description of the triple-bond breaking requires very large reference space and is most easily carried out using the RMR approach [176].

17.6.2.3. ec-GMS MRCC

The idea of amplitude-corrected *ec*CCSD (Section 17.6.2.1) can be easily extended to GMS CCSD (Section 17.5) yielding the (N, M)-CCSD method [124], which employs M-dimensional GMS SU CCSD while exploiting the relevant M states MR CISD that is based on N-dimensional reference space, $N \geq M$. The cluster analysis is again easily accomplished [138], but has to be carried out relative to each reference

separately after a transformation with the inverse of the **C** matrix, Eq. (17-25). Note that SR RMR CCSD $\equiv (N,1)$-CCSD and SU CCSD $\equiv (0,M)$-CCSD represent special cases of a general (N,M)-CCSD method. Conceptually, the most useful version is represented by (M,M)-CCSD, since it deals with a singly- and doubly-excited manifold of $\mathcal{M}_0$ and no additional model space is required. However, the advantage of a general $M \neq N$ version gives the possibility to account for important configurations, including intruders, in MR CCSD and not in GMS CCSD itself.

17.6.3. Other SR-Based Methods

17.6.3.1. String-Based MRCC Method

The above mentioned idea of Oliphant and Adamowicz [105] to truncate the number of triples and quadruples in the SR CCSDT and CCSDTQ approaches was further extended by Kállay et al. [209]. They consider a CMS and select one determinant as a formal Fermi vacuum. Mono-, bi-, and higher-excited determinants relative to the individual references are then considered as higher-excited configurations from that Fermi vacuum. The required CC equations are generated in terms of antisymmetrized diagrams while eliminating the amplitudes that carry an undesirable number of inactive indices. The implementation has been based on the string CC approach [45], which eliminates the need for manual generation of diagrams, factorization of the resulting expressions, and coding of tensor contractions [45]. An advantage of this approach is the elimination of problems that are inherent to genuine-MRCC methods, such as the intruder states or redundancy of the SS MRCC Ansatz. On the other hand an arbitrariness in the choice of a reference Fermi vacuum may lead to problems in highly degenerate situations, since it may cause the non-invariance of the energy with respect to this choice or, in particular, may break the spin symmetry of, e.g., the low-spin, open-shell singlet states.

17.7. DISCUSSION

In the preceding sections we attempted to present an overview of various MR CC approaches to many-electron correlation problem, particularly those that are based, at least tangentially, on the effective Hamiltonian formalism and the SU CC Ansatz of Jeziorski and Monkhorst. We payed only a cursory, if any, attention to those methods which are surveyed in greater detail in other chapters of this monograph, and passed over those SR approaches that exploit, either explicitly or implicitly, a multi-determinantal reference, such as various spin-adapted approaches (e.g., the CAUGA based CC [36, 37, 74], spin-flip approaches [210–213], etc.). We shall now try to assess the merits and limitations of the above reviewed methods by relying on the available results. The lack of evidence in some cases will be compensated by a personal view of the authors.

The introduction of genuine MR CC methods has represented an important step forward in the development of CC methodology. It supplied the need for a CC paral-

lel to the MR CI methods, which would eliminate the shortcomings of the standard SR CC theory in the presence of a quasi-degeneracy and was able to treat multiple states belonging to the same symmetry species. However, in spite of the ingenuity and subtlety of the MR CC formalism, its practical implementation turned out to be difficult and most of the existing applications have been limited to simple models or small molecules. It became soon obvious that suitable simplifications are necessary if these methods are to be exploited with the present state of the computing technology. Of course, such simplifications bring about more or less serious approximations and deficiencies. For example, an important simplification results by relying on the Brillouin – Wigner MBPT, however, at the price of loosing the size-extensivity.

The SU CC methods in either the JM or KB version, representing the genuine Hilbert-space MR CC approaches [77, 96], have never been widely applied in their full generality. One of the reasons is certainly the absence of efficient codes and a high computational cost (which was especially prohibitive at the time of their inception, but is becoming acceptable today, at least for mid-size molecules at the CCSD level). The most severe limitation, however, turned out to be the intruder states, causing a poor convergence, or even divergence, of the available algorithms. In some cases these difficulties may be avoided by exploiting incomplete model spaces rather that a CMS [81, 82]. Another disadvantage of SU MRCC (as well as of BWCC and MkCC that also employ the JM Ansatz) is the non-invariance of the energy with respect to rotations among the active orbitals, which in some cases may lead to artifactual results, e.g., when computing vibrational frequencies for modes that lower the symmetry of the system.

In view of its desirable property of a fast convergence, thanks to the BW energy denominator shifts which simultaneously enable to avoid intruder states, as well as to the size-extensivity corrections, the basic BW CCSD method has yielded reasonably accurate results for systems in which the nondynamic correlation plays a significant role [143–155]. Recently, the connected triple excitations have been included in the MR BWCC theory [157–159], resulting in a considerable increase in the accuracy of the method thanks to a more precise description of dynamical correlation effects, similarly as in the SR case. As already mentioned, the main shortcoming of BWCC is the lack of the exact size-extensivity, only partly remedied by the non-iterative correction [142]. The method thus cannot a priori guarantee reliability for larger systems in spite of its many successful applications. Another problem with the a posteriori corrections is that the resulting amplitudes do not obey converged amplitude equations. This would considerably complicate the development of the analytic gradient formalism that is available for uncorrected BWCC [137]. Unfortunately, the iterative size-extensivity correction [132] reverts back to the state-universality and reintroduces the intruder state problem.

The MkCC approach seems to represent the only fully size-extensive variant of the Hilbert-space MRCC method that is capable to avoid intruders thanks to its SS nature and provides useful and reliable results. This has been enabled thanks to an efficient implementation accounting for up to triexcitations, including non-iterative triples variant [94, 95, 162, 164]. However, according to our experience, BWCC

usually converges faster, often considerably so. One might thus perform a BWCC study and employ MkCC as a check of the BWCC size-extensivity error. We also point out that practically all MkCC applications that we are aware of has been to the lowest state of a given symmetry (except for the first excited state of the H4 model [183], in which case MkCC slightly underperforms standard SU CCSD [94]). It would be certainly very interesting to test its capabilities for more and higher lying excited states of real systems.

The dominant part of the computational cost of all Hilbert-space MRCC methods scales as an M-multiple of the SR CC scaling at the same truncation level, where M is the dimension of the model space. With the exception of BWCC, this cost also includes a term proportional to $M(M-1)/2$ due to the coupling terms. However, the scaling with the basis set size for the evaluation of the coupling terms is lower than that required for the connected terms, so that for small values of M that have been employed so far the cost of the coupling term evaluation does not represent a bottleneck.

An appealing possibility how to cope with quasidegeneracies of electronic states exploits the idea of external corrections [99–101, 195–197], which proved to be very fertile in both the SR and MR CC approaches. At the SR-level, it has been especially the RMR CCSD approach [118, 121, 206] and its truncated [205] and RMR CCSD(T) [203] versions that proved to be very useful in actual applications, enabling us to handle even rather strong quasi-degeneracies and thus providing an accurate treatment of a number of both important and challenging systems, including open-shells [121]. Indeed, these methods turned out to be very efficient not only in generating of entire potential energy surfaces or curves for small species [119, 214–216] (e.g., HF, F_2, H_2O, LiH, BN, C_2, BNB, N_3, etc.), including a very demanding case of the triple-bond breaking in the nitrogen molecule [176, 217] (see also [122]), but also enabled the handling of relatively large systems, such as nickel-carbonyls [218] and transition metal ion – methylene complexes [219]. Likewise, they enabled a reliable determination of the spin-multiplicity of the ground state in radicaloid systems with a small singlet-triplet splittings between the lowest-lying states, again in both small species [177, 220, 221] (such as CH_2, BN, and C_2) and in relatively large systems, such as benzynes [178], pyridynes [222], naphthynes [223], and linear di-dehydro-polyenes [224]. Particularly remarkable turned out to be the RMR handling of a triple-bond dissociation of N_2 [176] using a 56-dimensional reference space for MR CISD (including hextuples).

In most cases just mentioned the standard CCSD(T) breaks down or is unreliable. Nonetheless, in applications to reaction barriers in a series of heavy-atom transfer, nucleophilic substitution, association, and unimolecular reactions [225] the standard CCSD(T) method performs very well [differing, in a few cases, from the RMR-CCSD(T) result by only about 1 kJ/mol]. This is perhaps due to the fact that in the relevant transition complexes the original chemical bonds are not yet completely broken while the new bonds are being formed, so that the MR or quasi-degeneracy effects are sufficiently small to be handled by the standard CCSD(T) method. Indeed,

while the RMR-type approaches enable one to overcome the CCSD(T) breakdown in the presence of a strong quasi-degeneracy, in most instances the CCSD(T) approach provides excellent results, deserving its designation as the "gold standard" in molecular electronic structure calculations.

A simultaneous handling of a number of states via SU-type MRCC has been enabled by the GMS-type approaches [81–87, 124, 127, 226], which also indicate a considerable potential in view of the existing test calculations. Yet, their computational implementation could be greatly improved, particularly when exploiting parallel processing.

Let us also point out here that the R- and CR-CCSD(T) methods are equally capable of handling significant quasi-degeneracy effects, at least when dissociating single bonds [62, 108–113]. Moreover, the CR-CC(2,3) version is fully size-extensive and generally provides an excellent approximation to the full CCSDT. In some instances, however, the role of quadruples may be significant [177]. While the RMR approaches also account for primary quadruples, one has to turn to CR-CC(2,4) in the case of renormalized approaches, which significantly increases the computational cost.

The above listed applications attest to the efficacy of the RMR-type approaches, which generally exceeds the computational demands of the standard CCSD or CCSD(T) by only about 20%. Once the desired model space for the relevant MR CISD is chosen, the existing codes have a black-box character [207]. Of course, the principal shortcoming of RMR CCSD is the same as for any SR-type approach, namely that it can only handle the lowest-lying state of each symmetry species. This shortcoming may be overcome by exploiting the GMS CCSD method and its *ec* version (N,M)-CCSD, which consider simultaneously several states of the same symmetry species in the spirit of general MR SU CCSD approaches [81–87, 124, 127, 226]. However, this very much increases the computational demands and the available codes are of an *ad hoc* nature. In this regard, the SS-versions of the SU CCSD approach [92–95] are computationally much more efficient, although we are not aware of applications that treat several states of the same symmetry, as already pointed out.

In contrast, both GMS CCSD and its *ec* version (N,M)-CCSD enable a simultaneous handling of several states of the same symmetry in the spirit of general MR SU CCSD approaches. At the same time they can avoid the intruder state problem while preserving size-extensivity to a very high degree of accuracy [82, 83]. Test calculations on diatomic and triatomic systems, as well as a realistic exploration of singlet and triplet excited states, examining either the entire PECs or vertical and equilibrium excitation energies, showed that these methods can handle both the equilibrium and highly stretched geometries and are able to describe at the SD level – in contrast to EOM CCSD – all types of excited states, including those having a doubly-excited character [78, 82, 85–87, 124, 201, 226]. The C-conditions of the GMS method enabled for the first time to consider relatively large model spaces (up to 14-dimensional one in the case of the water molecule [86]), as well as to generate highly accurate singlet and triplet excitation energies for all the symmetry species.

It was also demonstrated that a simple diagonal correction for secondary triples can often achieve the same goal as the (N, M)-CCSD approach.

More recent additions to MRCC methodology that were briefly mentioned (e.g., Section 17.5.5) bring a welcome extension to the available repertoire of MR techniques. Although in most cases the required algorithms may be rather daunting, so that their general implementation is difficult without a computer assisted code generation, which proved to be indispensable already in earlier cases (cf., e.g., Ref. [36]), they seem to deliver encouraging results. We refer the reader to respective Chapters in this monograph for an up to date description and assessment of these recent developments.

17.8. SUMMARY

In general, the developments described in this review represent useful tools for the exploration of the molecular electronic structure when the SR approaches are either inapplicable or inadequate. Numerous successful applications, as briefly pointed out in the preceding section, witness the capabilities of these methods and their viability. It is encouraging that most of these approaches can handle both closed- and open-shell systems with the same ease, be they excited states of various spin multiplicity or the low-lying states of radicaloid or diradicaloid species. Moreover, most of these approaches can successfully handle intruder states, even at the general MR SU level.

We did not pay attention to VU MRCC methods, but instead attempted a comprehensive overview of the SU MRCC approaches. Some of them were developed only recently and there is not yet much evidence on their performance and feasibility of the respective calculations. Nonetheless, we endeavored to provide their critical assessment from the viewpoint of practical applications. In the family of genuine MRCC methods, the SS approaches of Sections 17.5.3 and 17.5.4 proved to be very useful, even though so far mostly for the lowest states of a given symmetry. The BWCC method with a posteriori size-extensivity correction has the advantage of simplest amplitude equations and excellent convergence properties, at the expense of being only approximately size-extensive. In contrast, MkCC method is exactly size-extensive, but sometimes requires considerably more iterations to converge than does BWCC, probably due to the presence of more complex coupling terms. Unfortunately, we are unable to reliably judge the performance of the MRexpT approach of Hanrath due to the lack of applications to larger systems.

The MR CC methods of either the SS or SU type that are internally or externally corrected for higher-than-two-body clusters offer a multitude of possibilities, leading to methods that enable applications even to relatively large systems. As we showed in Sections 17.6.1 and 17.6.2, there are many ways how to proceed, and only further applications will show which of these methods are the most general and profitable ones. Some of these methods are already available in quantum chemical software packages and we are convinced that this will also be the case for more recent additions, thus providing a useful complement to MR CI approaches.

ACKNOWLEDGMENTS

This paper presents a part of work done in the projects supported by the COST Action D37 and the Grant Agency of the Czech Republic (grant 203/07/0070). One of us (J. Paldus) wishes to acknowledge a continued support by the Natural Sciences and Engineering Research Council of Canada. We would also like to thank Professor Bogumil Jeziorski for enlightening discussions.

REFERENCES

1. R.J. Bartlett, in *Modern Electronic Structure Theory, Part I*, Eds. D. R. Yarkony (World Scientific, Singapore, 1995), pp. 1047–1131
2. J. Paldus, X. Li, Adv. Chem. Phys. **110**, 1 (1999)
3. J. Paldus, in *Handbook of Molecular Physics and Quantum Chemistry*, vol. 2, Ed. S. Wilson (Wiley, Chichester, 2003), pp. 272–313
4. J. Gauss, in *The Encyclopedia of Computational Chemistry*, Eds. P. v. R. Schleyer, N. L. Allinger, T. Clark, J. Gasteiger, P. A. Kollman, H. F. Schaefer III, P. R. Scheiner (Wiley, Chichester, 1998), pp. 615–636
5. R. J. Bartlett, M. Musiał, Rev. Mod. Phys. **79**, 291 (2007)
6. J. Paldus, in *Theory and Applications of Computational Chemistry: The First Forty Years*, Eds. C. E. Dykstra, G. Frenking, K. S. Kim, G. E. Scuseria (Elsevier, Amsterdam, The Netherlands, 2005), pp. 115–147
7. R. J. Bartlett, in *Theory and Applications of Computational Chemistry: The First Forty Years*, Eds. C. E. Dykstra, G. Frenking, K. S. Kim, G. E. Scuseria (Elsevier, Amsterdam, The Netherlands, 2005), pp. 1191–1221
8. K. A. Brueckner, Phys. Rev. **100**, 36 (1955)
9. J. Goldstone, Proc. R. Soc. Lond. A **239**, 267 (1957)
10. N. M. Hugenholtz, Physica (Utrecht) **23**, 481 (1957)
11. J. Paldus, J. Čížek, Adv. Quant. Chem. **9**, 105 (1975)
12. J. Hubbard, Proc. R. Soc. Lond. A **240**, 539 (1957)
13. J. Hubbard, Proc. R. Soc. Lond. A **243**, 336 (1958)
14. J. Hubbard, Proc. R. Soc. Lond. A **244**, 199 (1958)
15. F. Coester, Nucl. Phys. **7**, 421 (1958)
16. F. Coester, H. Kümmel, Nucl. Phys. **17**, 477 (1960)
17. K. Kowalski, D. J. Dean, M. Hjorth-Jensen, T. Papenbrock, P. Piecuch, Phys. Rev. Lett. **92**, 132501 (2004)
18. J. Čížek, J. Chem. Phys. **45**, 4256 (1966)
19. J. Čížek, Adv. Chem. Phys. **14**, 35 (1969)
20. J. Čížek, J. Paldus, Int. J. Quantum Chem. **5**, 359 (1971)
21. J. Paldus, J. Čížek, I. Shavitt, Phys. Rev. A **5**, 50 (1972)
22. R. J. Bartlett, G. D. Purvis III, Int. J. Quantum Chem. Symp. **14**, 561 (1978)
23. J.A. Pople, R. Krishnan, H.B. Schlegel, J.S. Binkley, Int. J. Quant. Chem. Symp. **14**, 545 (1978)
24. R. J. Bartlett, G. D. Purvis III, Phys. Scripta **21**, 255 (1980)
25. M. W. Schmidt, K. K. Baldridge, J. A. Boatz, S. T. Elbert, M. S. Gordon, J. H. Jensen, S. Koseki, N. Matsunaga, K. A. Nguyen, S. J. Su, T. L. Windus, M. Dupuis, J. Montgomery, J. Comp. Chem. **14**, 1347 (1993)

26. ACES II is a program product of Quantum Theory Project, University of Florida, J. F. Stanton, J. Gauss, J. D. Watts, M. Nooijen, N. Oliphant, S. A. Perera, P. G. Szalay, W. J. Lauderdale, S. R. Gwaltney, S. Beck, A. Balková, D. E. Bernholdt, K.-K. Baeck, P. Rozyczko, H. Sekino, C. Huber, R. J. Bartlett. Integral packages included are VMOL (J. Almlöf, P. R. Taylor); VPROPS (P. R. Taylor); ABACUS (T. Helgaker, H. J. Aa. Jensen , P. Joergensen, J. Olsen, P. R. Taylor)
27. M. J. Frisch, G. W. Trucks, H. G. Schlegel, G. E. Scuseria, M. A. Robb, J. R. Cheeseman, V. G. Zakrzewski, J. J. A. Montgomery, R. E. Stratmann, J. C. Burant, S. Dapprich, J. M. Millam, A. D. Daniels, K. N. Kudin, M. C. Strain, D. Farkas, J. Tomasi, V. Barone, M. Cossi, R. Cammi, B. Mennucci, C. Pomelli, C. Adamo, S. Clifford, J. Ochterski, G. A. Petersson, P. Y. Ayala, Q. Cui, K. Morokuma, D. K. Malick, A. D. Rabuck, K. Raghavachari, J. B. Foresman, J. Cioslowski, J. V. Ortiz, A. G. Baboul, B. B. Stefanov, G. Liu, A. Liashenko, P. Piskorz, I. Komaromi, R. Gomperts, R. L. Martin, D. J. Fox, T. Keith, M. A. Al-Laham, C. Y. Peng, A. Nanayakkara, C. Gonzales, M. Challacombe, P. M. W. Gill, B. Johnson, W. Chen, M. W. Wong, J. L. Andres, M. Head-Gordon, E. S. Replogle, J. A. Pople, GAUSSIAN98: Revision A.7 (Gaussian Inc., Pittsburgh, PA, 1998)
28. MOLPRO is a package of ab initio programs written by H.-J. Werner, P. J. Knowles, with contributions from J. Almlöf, R. D. Amos, A. Berning, D. L. Cooper, M. J. O. Deegan, A. J. Dobbyn, F. Eckert, S. T. Elbert, C. Hampel, R. Lindh, A. W. Lloyd, W. Meyer, A. Nicklass, K. Peterson, R. Pitzer, A. J. Stone, P. R. Taylor, M. E. Mura, P. Pulay, M. Schütz, H. Stoll, T. Thorsteinsson
29. G. Karlström, R. Lindh, P.-Å. Malmqvist, B. O. Roos, U. Ryde, V. Veryazov, P.-O. Widmark, M. Cossi, B. Schimmelpfennig, P. Neogrády, L. Seijo, Comput. Mat. Sci. **28**, 222 (2003)
30. F. Aquilante, L. D. Vico, N. Ferré, G. Ghigo, P.-Å. Malmqvist, P. Neogrády, T. B. Pedersen, M. Pitoňák, M. Reiher, B. O. Roos, L. Serrano-Andrés, M. Urban, V. Veryazov, R. Lindh, J. Comput. Chem. **31**, 224 (2010)
31. CFOUR, Coupled Cluster Techniques for Computational Chemistry, a quantum-chemical program package by J. F. Stanton, J. Gauss, M. E. Harding, P. G. Szalay with contributions from A. A. Auer, R. J. Bartlett, U. Benedikt, C. Berger, D. E. Bernholdt, O. Christiansen, M. Heckert, O. Heun, C. Huber, D. Jonsson, J. Jusélius, K. Klein, W. J. Lauderdale, D. Matthews, T. Metzroth, D. P. O'Neill, D. R. Price, E. Prochnow, K. Ruud, F. Schiffmann, S. Stopkowicz, A. Tajti, M. E. Varner, J. Vázquez, F. Wang, J. D. Watts and the integral packages MOLECULE (J. Almlöf, P. R. Taylor), PROPS (P. R. Taylor), ABACUS (T. Helgaker, H. J. Aa. Jensen, P. Jørgensen, J. Olsen), and ECP routines by A.V. Mitin, C. van Wüllen. For the current version, see http://www.cfour.de
32. M. Musiał, S. A. Kucharski, R. J. Bartlett, J. Chem. Phys. **116**, 4382 (2002)
33. J. Paldus, H. C. Wong, Comp. Phys. Commun. **6**, 1 (1973)
34. H. C. Wong, J. Paldus, Comp. Phys. Commun. **6**, 9 (1973)
35. C. L. Janssen, H. F. Schaefer III, Theor. Chim. Acta **79**, 1 (1991)
36. X. Li, J. Paldus, J. Chem. Phys. **101**, 8812 (1994)
37. P. Jankowski, B. Jeziorski, J. Chem. Phys. **111**, 1857 (1999)
38. P. Sadayappan, G. Baumgartner, D. E. Bernholdt, R. J. Harrison, S. Hirata, M. Nooijen, R. M. Pitzer, J. Ramanujam, The Tensor Contraction Engine, `http://www.cse.ohio-state.edu:/~gb/TCE`
39. S. Hirata, J. Phys. Chem. A **107**, 9887 (2003)
40. P. Piecuch, S. Hirata, K. Kowalski, P.-D. Fan, T. L. Windus, Int. J. Quantum Chem. **106**, 79 (2005)
41. S. Hirata, P. D. Fan, A. A. Auer, M. Nooijen, P. Piecuch, J. Chem. Phys. **121**, 12197 (2004)
42. S. Hirata, J. Chem. Phys. **122**, 094105 (2005)
43. A. A. Auer, G. Baumgartner, D. E. Bernholdt, A. Bibireata, V. Choppella, D. Cociorva, X. Gao, R. Harrison, S. Krishnamoorthy, S. Krishnan, C.-C. Lam, Q. Lu, M. Nooijen, R. Pitzer, J. Ramanujam, P. Sadayappan, A. Sibiryakov, Mol. Phys. **104**, 211 (2006)
44. M. Kállay, P. R. Surján, J. Chem. Phys. **113**, 1359 (2000)

45. M. Kállay, P. R. Surján, J. Chem. Phys. **115**, 2945 (2001)
46. J. Olsen, J. Chem. Phys. **113**, 7140 (2000)
47. M. Kállay, J. Gauss, P. G. Szalay, J. Chem. Phys. **119**, 2991 (2003)
48. M. Kállay, J. Gauss, J. Chem. Phys. **120**, 6841 (2004)
49. M. Kállay, J. Gauss, J. Chem. Phys. **123**, 214105 (2005)
50. M. Kállay, J. Gauss, J. Chem. Phys. **129**, 144101 (2008)
51. J. Noga, R. J. Bartlett, J. Chem. Phys. **86**, 7041 (1987)
52. G. E. Scuseria, H. F. Schaefer III, Chem. Phys. Lett. **152**, 382 (1988)
53. M. R. Hoffmann, H. F. Schaefer III., Adv. Quantum Chem. **17**, 207 (1986)
54. S. A. Kucharski, R. J. Bartlett, J. Chem. Phys. **97**, 4282 (1992)
55. K. Raghavachari, J. Chem. Phys. **82**, 4607 (1985)
56. M. Urban, J. Noga, S. J. Cole, R. J. Bartlett, J. Chem. Phys. **83**, 4041 (1985)
57. M. Urban, J. Noga, S. J. Cole, R. J. Bartlett, J. Chem. Phys. **85**, 5383 (1986). Erratum
58. K. Raghavachari, G. W. Trucks, J. A. Pople, M. Head-Gordon, Chem. Phys. Lett. **157**, 479 (1989)
59. C. J. Cramer, *Essentials of Computational Chemistry: Theories and Models*, Second edition (Wiley, New York, 2004) p. 226
60. S. I. Lu, J. Chem. Phys. **121**, 10495 (2004)
61. See also *Wikipedia*, `http://en.wikipedia.org/wiki/Coupled_cluster`
62. K. Kowalski, P. Piecuch, J. Chem. Phys. **113**, 18 (2000)
63. K. Kowalski, P. Piecuch, J. Mol. Struc. (THEOCHEM) **547**, 191 (2001)
64. X. Li, J. Paldus, J. Chem. Phys. **115**, 5774 (2001)
65. I. Lindgren, D. Mukherjee, Phys. Rep. **151**, 93 (1987)
66. D. Mukherjee, S. Pal, Adv. Quantum Chem. **20**, 292 (1989)
67. J. Paldus, in *Methods in Computational Molecular Physics*, *NATO ASI Series B: Physics*, vol. 293, Eds. S. Wilson, G. H. F. Diercksen (Plenum, New York, 1992), pp. 99–194
68. J. Paldus, in *Relativistic and Correlation Effects in Molecules and Solids*, *NATO ASI Series B: Physics*, vol. 318, Ed. G. L. Malli (Plenum, New York, 1994), pp. 207–282
69. J. Paldus, J. Chem. Phys. **61**, 5321 (1974)
70. J. Paldus, in *Mathematical Frontiers in Computational Chemical Physics*, *IMA Series*, vol. 15, Ed. D. G. Truhlar (Springer, Berlin, 1988), pp. 262–299
71. J. Paldus, C. R. Sarma, J. Chem. Phys. **83**, 5135 (1985)
72. J. Paldus, M. J. Gao, J. Q. Chen, Phys. Rev. A **35**, 3197 (1987)
73. X. Li, Q. Zhang, Int. J. Quantum Chem. **36**, 599 (1989)
74. B. Jeziorski, J. Paldus, P. Jankowski, Int. J. Quantum Chem. **56**, 129 (1995)
75. I. Lindgren, Int. J. Quantum Chem. Symp. **12**, 33 (1978)
76. I. Lindgren, J. Morrison, in *Atomic Many-Body Theory* (Springer, Berlin, 1982)
77. B. Jeziorski, H. J. Monkhorst, Phys. Rev. A **24**, 1668 (1981)
78. J. Paldus, X. Li, Collect. Czech. Chem. Commun. **69**, 90 (2004)
79. B. Jeziorski, J. Paldus, J. Chem. Phys. **88**, 5673 (1988)
80. J. Paldus, P. Piecuch, L. Pylypow, B. Jeziorski, Phys. Rev. A **47**, 2738 (1993)
81. X. Li, J. Paldus, J. Chem. Phys. **119**, 5320 (2003)
82. X. Li, J. Paldus, J. Chem. Phys. **119**, 5346 (2003)
83. X. Li, J. Paldus, Int. J. Quantum Chem. **99**, 914 (2004)
84. J. Paldus, X. Li, N. D. Petraco, J. Math. Chem. **35**, 215 (2004)
85. X. Li, J. Paldus, J. Chem. Phys. **120**, 5890 (2004)
86. X. Li, J. Paldus, Mol. Phys. **104**, 661 (2006)
87. X. Li, J. Paldus, J. Chem. Phys. **124**, 034112 (2006)

88. U. S. Mahapatra, B. Datta, B. Bandyopadhyay, D. Mukherjee, Adv. Quantum Chem. **30**, 163 (1998)
89. U. S. Mahapatra, B. Datta, D. Mukherjee, J. Chem. Phys. **110**, 6171 (1999)
90. S. Chattopadhyay, U. S. Mahapatra, D. Mukherjee, J. Chem. Phys. **112**, 7939 (2000)
91. S. Chattopadhyay, D. Pahari, D. Mukherjee, U. S. Mahapatra, J. Chem. Phys. **120**, 5968 (2004)
92. S. Chattopadhyay, P. Ghosh, U. S. Mahapatra, J. Phys. B **37**, 495 (2004)
93. U. S. Mahapatra, B. Datta, D. Mukherjee, in *Recent Advances in Coupled Cluster Methods*, Ed. R. J. Bartlett (World Scientific, Singapore, 1997), pp. 155–181
94. F. A. Evangelista, W. D. Allen, H. F. Schaefer III, J. Chem. Phys. **125**, 154113 (2006)
95. F. A. Evangelista, W. D. Allen, H. F. Schaefer III, J. Chem. Phys. **127**, 024102 (2007)
96. S. A. Kucharski, R. J. Bartlett, J. Chem. Phys. **95**, 8227 (1991)
97. I. Hubač, in *New Methods in Quantum Theory*, *NATO ASI Series 3: High Technology*, vol. 8, Eds. A. Tsipis, V. S. Popov, D. R. Herschbach, J. S. Avery (Kluwer, Dordrecht, 1996), pp. 183–202
98. J. Mášik, I. Hubač, Adv. Quant. Chem. **31**, 75 (1998)
99. J. Paldus, J. Planelles, Theor. Chim. Acta **89**, 13 (1994)
100. J. Planelles, J. Paldus, X. Li, Theor. Chim. Acta **89**, 33 (1994)
101. L. Z. Stolarczyk, Chem. Phys. Lett. **217**, 1 (1994)
102. N. Oliphant, L. Adamowicz, J. Chem. Phys. **96**, 3739 (1992)
103. N. Oliphant, L. Adamowicz, Int. Rev. Phys. Chem. **12**, 339 (1993)
104. L. Adamowicz, P. Piecuch, K. B. Ghose, Mol. Phys. **94**, 225 (1998)
105. N. Oliphant, L. Adamowicz, J. Chem. Phys. **95**, 6645 (1991)
106. P. Piecuch, L. Adamowicz, J. Chem. Phys. **100**, 5792 (1994)
107. S. R. Gwaltney, M. Head-Gordon, J. Chem. Phys. **115**, 2014 (2001)
108. K. Kowalski, P. Piecuch, J. Chem. Phys. **113**, 5644 (2000)
109. K. Kowalski, P. Piecuch, Chem. Phys. Lett. **344**, 165 (2001)
110. P. Piecuch, S. A. Kucharski, K. Kowalski, Chem. Phys. Lett. **344**, 176 (2001)
111. P. Piecuch, M. Włoch, J. Chem. Phys. **123**, 224105 (2005)
112. P. Piecuch, M. Włoch, J. R. Gour, A. Kinal, Chem. Phys. Lett. **418**, 463 (2005)
113. M. Włoch, M. D. Lodriguito, P. Piecuch, J. R. Gour, Mol. Phys. **104**, 2149 (2006)
114. X. Li, J. Paldus, J. Chem. Phys. **128**, 144118 (2008)
115. X. Li, J. Paldus, J. Chem. Phys. **128**, 144119 (2008)
116. Y. S. Lee, S. A. Kucharski, R. J. Bartlett, J. Chem. Phys. **81**, 5906 (1984)
117. J. Noga, R. J. Bartlett, J. Chem. Phys. **89**, 3401 (1988)
118. X. Li, J. Paldus, J. Chem. Phys. **107**, 6257 (1997)
119. X. Li, J. Paldus, J. Chem. Phys. **108**, 637 (1998)
120. X. Li, J. Paldus, J. Chem. Phys. **110**, 2844 (1999)
121. X. Li, J. Paldus, Mol. Phys. **98**, 1185 (2000)
122. X. Li, J. Paldus, J. Chem. Phys. **113**, 9966 (2000)
123. X. Li, J. Paldus, J. Chem. Phys. **115**, 5759 (2001)
124. X. Li, J. Paldus, J. Chem. Phys. **119**, 5334 (2003)
125. B. Jeziorski, J. Paldus, J. Chem. Phys. **90**, 2714 (1989)
126. W. Kutzelnigg, D. Mukherjee, S. Koch, J. Chem. Phys. **87**, 5902 (1987)
127. X. Li, J. Paldus, Mol. Phys. **104**, 2047 (2006)
128. A. Balková, S. A. Kucharski, R. J. Bartlett, Chem. Phys. Lett. **182**, 511 (1991)
129. A. Balková, S. A. Kucharski, L. Meissner, R. J. Bartlett, J. Chem. Phys. **95**, 4311 (1991)
130. A. Balková, S. A. Kucharski, L. Meissner, R. J. Bartlett, Theor. Chim. Acta **80**, 335 (1991)
131. J. Pittner, P. Piecuch, Mol. Phys. (2009). Mol. Phys. **107**, 1209 (2009)
132. J. Pittner, J. Chem. Phys. **118**, 10876 (2003)

133. P. G. Szalay, Int. J. Quantum Chem. **55**, 151 (1995)
134. P. G. Szalay, R. J. Bartlett, J. Chem. Phys. **101**, 4936 (1994)
135. K. R. Shamasundar, S. Pal, J. Chem. Phys. **114**, 1981 (2001)
136. K. R. Shamasundar, S. Pal, J. Chem. Phys. **115**, 1979 (2001)
137. J. Pittner, J. Šmydke, J. Chem. Phys. **127**, 114103 (2007)
138. J. Paldus, X. Li, J. Chem. Phys. **118**, 6769 (2003)
139. I. Hubač, J. Mášik, P. Mach, J. Urban, P. Babinec, in *Computational Chemistry. Reviews of Current Trends*, vol. 3, Ed. by J. Leszczynski (World Scientific, Singapore, 1999), pp. 1–48
140. J. Mášik, I. Hubač, in *Quantum Systems in Chemistry and Physics: Trends in Methods and Applications*, Eds. R. McWeeny, J. Maruani, Y. G. Smeyers, S. Wilson (Kluwer Academic Publishers, Dordrecht, 1997), pp. 283–308
141. I. Hubač, S. Wilson, *Brillouin-Wigner Methods for Many-Body Systems* (Springer, Berlin, 2010)
142. I. Hubač, J. Pittner, P. Čársky, J. Chem. Phys. **112**, 8779 (2000)
143. J. Pittner, O. Demel, P. Čársky, I. Hubač, Int. J. Mol. Sci. **2**, 281 (2002)
144. J. Pittner, P. Čársky, I. Hubač, Int. J. Quantum Chem. **90**, 1031 (2002)
145. J. Pittner, J. Šmydke, P. Čársky, I. Hubač, J. Mol. Struct. (THEOCHEM) **547**, 239 (2001)
146. I. S. K. Kerkines, J. Pittner, P. Čársky, A. Mavridis, I. Hubač, J. Chem. Phys. **117**, 9733 (2002)
147. V. I. Teberekidis, I. S. K. Kerkines, C. A. Tsipis, P. Čársky, A. Mavridis, Int. J. Quantum Chem. **102**, 762 (2005)
148. S. Kardahakis, J. Pittner, P. Čársky, A. Mavridis, Int. J. Quantum Chem. **104**, 458 (2005)
149. M. Tobita, S. A. Perera, M. Musiał, R. J. Bartlett, M. Nooijen, J. S. Lee, J. Chem. Phys. **119**, 10713 (2003)
150. J. C. Sancho-García, J. Pittner, P. Čársky, I. Hubač, J. Chem. Phys. **112**, 8785 (2000)
151. J. Pittner, P. Nachtigall, P. Čársky, I. Hubač, J. Phys. Chem. A **105**, 1354 (2001)
152. O. Rey-Puiggros, J. Pittner, P. Čársky, P. Stampfuß, W. Wenzel, Collect. Czech. Chem. Commun. **68**, 2309 (2003)
153. O. Demel, J. Pittner, P. Čársky, I. Hubač, J. Phys. Chem. A **108**, 3125 (2004)
154. I. S. K. Kerkines, P. Čársky, A. Mavridis, J. Phys. Chem. A **109**, 10148 (2005)
155. J. Brabec, J. Pittner, J. Phys. Chem. A **110**, 11765 (2006)
156. L. Veis, P. Čársky, J. Pittner, J. Michl, Collect. Czech. Chem. Commun. **73**, 1525 (2008)
157. J. Pittner, O. Demel, J. Chem. Phys. **122**, 181101 (2005)
158. O. Demel, J. Pittner, J. Chem. Phys. **124**, 144112 (2006)
159. O. Demel, J. Pittner, J. Chem. Phys. **128**, 104108 (2008)
160. U. S. Mahapatra, B. Datta, D. Mukherjee, Chem. Phys. Lett. **299**, 42 (1999)
161. D. Pahari, S. Chattopadhyay, A. Deb, D. Mukherjee, Chem. Phys. Lett. **386**, 307 (2004)
162. F. A. Evangelista, A. C. Simmonett, W. D. Allen, H. F. Schaefer III, J. Gauss, J. Chem. Phys. **128**, 124104 (2008)
163. K. Bhaskaran-Nair, O. Demel, J. Pittner, J. Chem. Phys. **129**, 184105 (2008)
164. J. Pittner, J. Chem. Phys. (2008). J. Pittner, unpublished (2010)
165. K. Bhaskaran-Nair, O. Demel, J. Pittner, J. Chem. Phys. **132**, 154105 (2010)
166. M. Hanrath, J. Chem. Phys. **123**, 084102 (2005)
167. M. Hanrath, Chem. Phys. Lett. **420**, 426 (2006)
168. M. Hanrath, Theor. Chem. Acc. **121**, 187 (2008)
169. M. Hanrath, J. Chem. Phys. **128**, 154118 (2008)
170. M. Nooijen, K. R. Shamasundar, D. Mukherjee, Mol. Phys. **103**, 2277 (2005)
171. M. Hanrath, Chem. Phys. **356**, 31 (2009)
172. M. Hanrath, Chem. Phys. Lett. **466**, 240 (2008)

173. P. Piecuch, S. A. Kucharski, R. J. Bartlett, J. Chem. Phys. **110**, 6103 (1999)
174. P. Piecuch, S. A. Kucharski, V. Špirko, J. Chem. Phys. **111**, 6679 (1999)
175. K. Jankowski, P. Piecuch, J. Paldus, Theor. Chim. Acta **80**, 223 (1991)
176. X. Li, J. Paldus, J. Chem. Phys. **129**, 054104 (2008)
177. X. Li, J. R. Gour, J. Paldus, P. Piecuch, Chem. Phys. Lett. **461**, 321 (2008)
178. X. Li, J. Paldus, J. Chem. Phys. **129**, 174101 (2008)
179. J. Paldus, J. Čížek, M. Takahashi, Phys. Rev. A **30**, 2193 (1984)
180. J. Paldus, M. Takahashi, R. W. H. Cho, **30**, 4267 (1984)
181. R. A. Chiles, C. E. Dykstra, Chem. Phys. Lett. **80**, 69 (1981)
182. C. E. Dykstra, S. Y. Liu, M. F. Daskalakis, J. P. Lucia, M. Takahashi, Chem. Phys. Lett. **137**, 266 (1987)
183. K. Jankowski, J. Paldus, Int. J. Quantum Chem. **18**, 1243 (1980)
184. B. G. Adams, K. Jankowski, J. Paldus, Phys. Rev. A **24**, 2330 (1981)
185. W. Meyer, Int. J. Quantum Chem. **5**, 341 (1971)
186. W. Meyer, Theor. Chim. Acta **35**, 277 (1974)
187. W. Kutzelnigg, in *Methods of Electronic Structure Theory*, Ed. H. F. Schaefer III (Plenum, New York, 1977), p. 129
188. P. Piecuch, R. Tobola, J. Paldus, Phys. Rev. A **54**, 1210 (1996)
189. R. J. Bartlett, M. Musiał, J. Chem. Phys. **125**, 204105 (2006)
190. J. Paldus, J. Čížek, B. Jeziorski, J. Chem. Phys. **93**, 1485 (1990)
191. L. Meissner, I. Grabowski, Chem. Phys. Lett. **300**, 53 (1999)
192. L. Meissner, J. Gryniakow, I. Hubač, Chem. Phys. Lett. **397**, 34 (2004)
193. L. Meissner, M. Nooijen, Chem. Phys. Lett. **316**, 501 (2000)
194. M. Nooijen, R. J. LeRoy, J. Mol. Struct. (THEOCHEM) **768**, 25 (2006)
195. X. Li, G. Peris, J. Planelles, F. Rajadell, J. Paldus, J. Chem. Phys. **107**, 90 (1997)
196. G. Peris, F. Rajadell, X. Li, J. Planelles, J. Paldus, Mol. Phys. **94**, 235 (1998)
197. G. Peris, J. Planelles, J. Paldus, Int. J. Quantum Chem. **62**, 137 (1997)
198. J. Paldus, X. Li, in *Correlation and Localization*, *Topics in Current Chemistry*, vol. 203, Ed. P. Surján (Springer, Berlin, 1999), pp. 1–20
199. J. Paldus, X. Li, in *Low-Lying Potential Energy Surfaces*, ACS Symposium Series, vol. 828, Eds. M. R. Hoffmann, K. G. Dyall (ACS Books, Washington, DC, 2002), pp. 10–30
200. J. Paldus, X. Li, in *Quantum Many-Body Theory*, vol. 5, Eds. R. F. Bishop, T. Brandes, K. A. Gernoth, N. R. Walet, Y. Xian (World Scientific, Singapore, 2002), pp. 393–404
201. J. Paldus, X. Li, in *Recent Advances in the Theory of Chemical and Physical Systems*, *Progress in Theoretical Chemistry and Physics*, vol. 15, Eds. J.-P. Julien, J. Maruani, D. Mayou, G. Delgado-Barrio, S. Wilson (Springer, Berlin, 2006), pp. 13–44
202. J. Paldus, X. Li, Collect. Czech. Chem. Commun. **68**, 554 (2003)
203. X. Li, J. Paldus, J. Chem. Phys. **124**, 174101 (2006)
204. J. Paldus, X. Li, Collect. Czech. Chem. Commun. **72**, 100 (2007)
205. X. Li, J. Paldus, Int. J. Quantum Chem. **80**, 743 (2000)
206. X. Li, I. Grabowski, K. Jankowski, J. Paldus, Adv. Quantum Chem. **36**, 231 (2000)
207. X. Li. GMR CC Manual (University of Waterloo, internal document)
208. X. Li, J. Paldus, J. Chem. Phys. **117**, 1941 (2002)
209. M. Kállay, P. G. Szalay, P. R. Surján, J. Chem. Phys. **117**, 980 (2002)
210. A. I. Krylov, Chem. Phys. Lett. **338**, 375 (2001)
211. L. V. Slipchenko, A. I. Krylov, J. Chem. Phys. **117**, 4694 (2002)
212. L. V. Slipchenko, A. I. Krylov, J. Chem. Phys. **118**, 6874 (2003)

213. L. V. Slipchenko, A. I. Krylov, J. Chem. Phys. **123**, 084107 (2005)
214. X. Li, J. Paldus, J. Chem. Phys. **118**, 2470 (2003)
215. X. Li, J. Paldus, J. Chem. Phys. **126**, 224304 (2007)
216. X. Li, J. Paldus, Int. J. Quantum Chem. **108**, 2117 (2008)
217. X. Li, J. Paldus, Chem. Phys. Lett. **286**, 145 (1998)
218. X. Li, J. Paldus, J. Chem. Phys. **125**, 164107 (2006)
219. X. Li, J. Paldus, J. Chem. Phys. **126**, 234303 (2007)
220. X. Li, J. Paldus, Collect. Czech. Chem. Commun. **63**, 1381 (1998)
221. X. Li, J. Paldus, Chem. Phys. Lett. **431**, 179 (2006)
222. X. Li, J. Paldus, J. Theor. Comput. Chem. **7**, 805 (2008)
223. X. Li, J. Paldus, Can. J. Chem. (2009). **87**, 917 (2009)
224. X. Li, J. Paldus, Int. J. Quantum Chem. **109**, 3305 (2009)
225. X. Li, J. Paldus, J. Phys. Chem. A **111**, 11189 (2007)
226. X. Li, Collect. Czech. Chem. Commun. **70**, 755 (2005)

CHAPTER 18

VIBRATIONAL COUPLED CLUSTER THEORY

PETER SEIDLER AND OVE CHRISTIANSEN

The Lundbeck Foundation Center for Theoretical Chemistry and Center for Oxygen Microscopy and Imaging, Department of Chemistry, Aarhus University, Langelandsgade 140, 8000 Aarhus C, Denmark, e-mail: seidler@chem.au.dk; ove@chem.au.dk

Abstract: Vibrational coupled cluster (VCC) theory is introduced as a method for solving the time-independent vibrational Schrödinger equation within the Born-Oppenheimer approximation. The first part of this chapter introduces the basic foundations of the theory, including the vibrational self-consistent field method and an appropriate second quantization formalism. The VCC method is then defined and shown to provide good accuracy when compared with vibrational configuration interaction calculations. The second part of the chapter provides a detailed treatment of the form and evaluation of the VCC equations in terms of amplitudes and integrals. Along these lines, strategies for efficient implementations are discussed.

Keywords: Vibrational coupled cluster, Anharmonic vibrations, Vibrational spectroscopy

18.1. INTRODUCTION

As evidenced by the other contributions to this monograph, coupled cluster (CC) theory has proven to be an accurate, yet affordable, method for obtaining electronic wave functions, energies, and properties in molecular science. However, describing the electronic motion in a molecule is only half the story. Most often the Born – Oppenheimer approximation is invoked and the electronic equations are solved for fixed nuclear coordinates. In this way, a potential energy surface (PES) on which the nuclei move can be obtained by varying these coordinates. The nuclear motion is the second half of the story. In this chapter, we explore how CC theory can be applied to this problem. More specifically, we consider the solution of the time-independent vibrational Schrödinger equation using an exponential ansatz for the wave function based on excitations out of a mean field reference state. The method is denoted vibrational coupled cluster (VCC) theory and was introduced as recently as 2004 [1, 2].

P. Čársky et al. (eds.), Recent Progress in Coupled Cluster Methods, 491–512.
DOI 10.1007/978-90-481-2885-3_18,

Though this chapter is very focused on VCC, we acknowledge the large number of other methods available for calculating vibrational energies and wave functions, see e.g. Refs. [3–5] for entries into the literature.

18.2. PRELIMINARIES

The nuclear problem is rather different from the electronic case. We focus in this chapter only on the internal vibrational motion, though extension to the rovibrational problem is interesting and possible. In this section we discuss two basic subjects: The construction of the Schrödinger equation for internal nuclear motion, and the vibrational self-consistent field method which is the vibrational analogue to Hartee-Fock theory. Together with the next section on a second quantization formalism suitable for vibrational wave functions, this forms the basis for a formulation and implementation of VCC theory.

18.2.1. The Vibrational Schrödinger Equation

The vibrational Schrödinger equation in the Born-Oppenheimer approximation is given by

$$\Big(T + V(\mathbf{Q})\Big)\Psi_i(\mathbf{Q}) = E_i\Psi_i(\mathbf{Q}). \tag{18-1}$$

Here T is the kinetic energy operator for the internal motion of the nuclei, and $V(\mathbf{Q})$ is the PES obtained from the solution of the electronic problem as a function of the nuclear coordinates, $\mathbf{Q}$, describing the relative arrangement of the nuclei.

In general, $V(\mathbf{Q})$ is a complicated function coupling all the vibrational degrees of freedom (modes). A common approximation is to use a hierarchical expansion of $V(\mathbf{Q})$ in terms of functions coupling only a limited number of modes,

$$V(\mathbf{Q}) = \sum_{\mathbf{m}\in \mathrm{MCR}[V]} \bar{V}^{\mathbf{m}}(\mathbf{Q}_{\mathbf{m}}). \tag{18-2}$$

In this expression, $\mathbf{m}$ is a mode combination (MC), i.e. the set of modes coupled by the function $\bar{V}^{\mathbf{m}}(\mathbf{Q}_{\mathbf{m}})$, and $\mathbf{Q}_{\mathbf{m}}$ denotes the coordinates for the modes in $\mathbf{m}$. Note that the $\bar{V}^{\mathbf{m}}$ functions only describe the couplings and therefore are defined to be vanishing whenever one or more coordinates are zero, i.e. $\bar{V}^{\mathbf{m}}(\ldots, Q_m = 0, \ldots) = 0$. For instance, $\bar{V}^{\{m_1 m_2\}} = V^{\{m_1 m_2\}}(Q_{m_1}, Q_{m_2}) - V^{\{m_1\}}(Q_{m_1}) - V^{\{m_2\}}(Q_{m_2})$. The set of all MCs used in the PES representation is given by the mode combination range, MCR[V]. A common approximation is to include in MCR[V] all MCs up to a given level, for instance all one-, two-, and three-mode couplings. The MC and MCR concepts are used throughout this chapter to describe quantities acting on a limited set of modes.

For the efficient implementation of VCC theory, we have chosen to represent each $\bar{V}^{\mathbf{m}}$ function as a sum of products over one mode operators,

$$\bar{V}^{\mathbf{m}} = \sum_{t}^{N_t} c_t \prod_{m \in \mathbf{m}} h^{mo^{tm}}, \tag{18-3}$$

where N_t is the number of terms in the given $\bar{V}^{\mathbf{m}}$ function and $h^{mo^{tm}}$ is a one-mode operator for mode m of type o^{tm}. For instance, a three mode coupling function may be written as a polynomial expansion,

$$\bar{V}^{\mathbf{m}} = \bar{V}^{\{m_1 m_2 m_3\}} = \sum_{t}^{N_t} c_t \prod_{m \in \{m_1, m_2, m_3\}} h^{mo^{tm}} = \sum_{t}^{N_t} c_t \, Q_{m_1}^{r_t} Q_{m_2}^{s_t} Q_{m_3}^{u_t}, \tag{18-4}$$

where r_t, s_t, and u_t specify the exponents used in each term. The coefficients c_t may be obtained from derivative information in the case of a Taylor expansion or from polynomial fitting to a grid representation of the $\bar{V}^{\mathbf{m}}$ function. PESs can nowadays be automatically constructed from single point electronic structure calculations and expressed in the form of Eqs. (18-2), (18-3), and (18-4). We refer to Refs. [6, 7] for further details on this particular approach and Refs. [5, 8–10] for more general overviews.

The representation of the kinetic energy operator, T, is very dependent on the choice of nuclear coordinates. In mass-weighted normal coordinates, the Watson operator must in principle be used [11]. However, if the terms originating from rovibrational couplings are neglected it reduces to the simple form

$$T = -\frac{1}{2} \sum_{m=1}^{M} \frac{\partial^2}{\partial Q_m^2}, \tag{18-5}$$

where M is the number of modes. Though only normal coordinates have been considered so far, the theory and implementation of VCC does not depend on the specific coordinates used. In case of more involved expressions for the kinetic energy operator, a MC expansion similar to the one used for the PES may be employed.

18.2.2. Vibrational Self-Consistent Field Theory

In analogy to the Hartree–Fock method in electronic structure theory, the vibrational self-consistent field (VSCF) method can account for the interaction between different modes in a mean field sense. Below follows a brief account of the method, see e.g. Refs. [5, 12, 13] for further details.

Since the vibrational modes are distinguishable, the ansatz for the VSCF wave function is a simple Hartree product of one-mode functions,

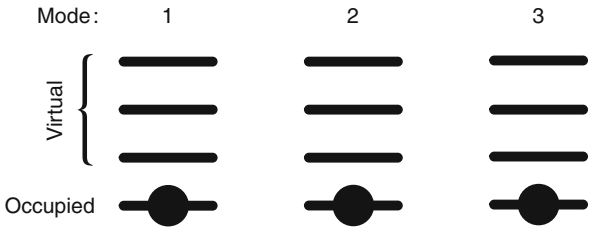

Figure 18-1. The occupied and virtual modals obtained in a VSCF calculation. The vertical lines represent modals and the circles indicate which ones enter the Hartree product being optimized, in this case the ground state

$$\Psi_i(\mathbf{Q}) \approx \Phi_{\mathbf{i}}(Q_1, Q_2, \ldots, Q_M) = \prod_{m=1}^{M} \phi_{i_m}^m(Q_m), \tag{18-6}$$

where $\phi_{i_m}^m(Q_m)$ is a one-mode function for mode m and $\mathbf{i} = (i_1, i_2, \ldots, i_M)$ is a vector specifying the occupied level in each mode. The one-mode functions are commonly denoted *modals* in analogy to the orbitals of electronic structure theory. The optimal modals are obtained by minimizing the energy expectation value, $E_{\mathbf{i}} = \langle \Phi_{\mathbf{i}} | H | \Phi_{\mathbf{i}} \rangle$, with respect to arbitrary variations in $\phi_{i_m}^m$.

Each modal can be expanded in a primitive basis, for instance a set of harmonic oscillator functions or a set of distributed Gaussians. This translates the minimization problem into a set of eigenvalue problems which must be solved self-consistently. In the end, a set of optimal modals is obtained. In addition, one also obtains a set of virtual modals for each mode as illustrated for a ground state VSCF calculation in Figure 18-1.

The treatment of one-mode anharmonicity is exact in VSCF theory provided a complete one-mode basis is used. However, the correlated motion of the nuclei is only treated in a mean-field sense. To include explicit correlation, an expansion in multiple Hartree products generated by excitations into the virtual modals may be used. The next section describes a second quantization formalism that is particularly useful for representing and manipulating Hartree products generated from the VSCF modals. This paves the wave for the formulation of CC theory in a vibrational context.

18.3. SECOND QUANTIZATION FOR MANY-MODE VIBRATIONAL SYSTEMS

To represent a Hartree product in second quantization, we introduce an occupation number vector (ONV). This vector contains an integer, k_p^m, for every modal, p, in every mode, m, specifying how many times the modal enters the Hartree product,

$$|\mathbf{k}\rangle = |\{k_1^1, k_2^1, \ldots, k_{N_1}^1\}, \ldots, \{k_1^m, k_2^m, \ldots, k_{N_m}^m\}, \ldots, \{k_1^M, k_2^M, \ldots, k_{N_M}^M\}\rangle. \quad (18\text{-}7)$$

Here N_m is the size of the modal basis for mode m, and M is the total number of modes. Since a Hartree product must contain exactly one modal for each mode, only the subspace of all $|\mathbf{k}\rangle$ vectors with exactly one k_i^m equal to 1 and all others equal to 0 for each mode is of physical relevance to us here. An ONV for an example Hartree product is illustrated in Figure 18-2.

The special ONV with all elements equal to zero is denoted the vacuum state, $|\text{vac}\rangle$. The inner product between two ONVs is defined as

$$\langle \mathbf{k}|\mathbf{l}\rangle = \prod_{m=1}^{M} \prod_{p=1}^{N_m} \delta_{k_p^m l_p^m}. \quad (18\text{-}8)$$

To manipulate the ONVs, we introduce the creation and annihilation operators,

$$a_p^{m\dagger}|\ldots, k_p^m, \ldots\rangle = \sqrt{k_p^m + 1}|\ldots, k_p^m + 1, \ldots\rangle, \quad (18\text{-}9)$$

$$a_p^m|\ldots, k_p^m, \ldots\rangle = \sqrt{k_p^m}|\ldots, k_p^m - 1, \ldots\rangle. \quad (18\text{-}10)$$

Note that the result of a_p^m acting on an ONV with $k_p^m = 0$ is vanishing. Letting the operators work on arbitrary ONVs, the following basic commutator relations are obtained,

$$[a_p^{m\dagger}, a_q^{m'\dagger}] = [a_p^m, a_q^{m'}] = 0, \quad (18\text{-}11)$$

$$[a_p^m, a_q^{m'\dagger}] = \delta_{mm'}\delta_{pq}. \quad (18\text{-}12)$$

It is worth noting that the present formalism is different from a formulation in terms of the usual harmonic oscillator step up and down ladder operators. As is

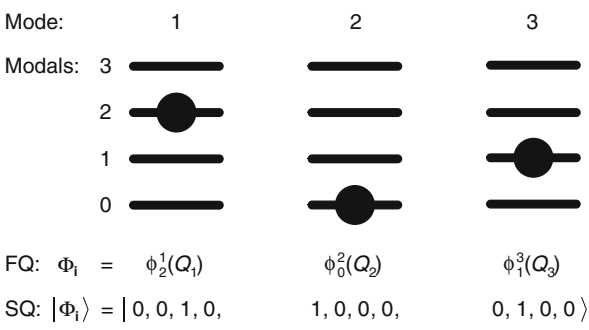

Figure 18-2. Using an ONV to represent a Hartree product in second quantization. FQ: first quantization representation in terms of one-mode functions. SQ: the corresponding second quantization ONV

evident from Eq. (18-9), the application of a creation operator does not excite the molecule to a higher vibrational level. Instead, it simply adds a modal to the Hartree product it represents. One advantage of this formalism is that there is no restriction to a particular basis or reference state. CC theory based on the harmonic oscillator second quantization has been proposed by other authors for one-dimensional [14–16] as well as coupled anharmonic oscillators [17, 18]. However, these methods are very different from the theory presented in this chapter.

To see how physical excitations can be introduced, we first define a reference Hartree product described by the vector $\mathbf{i} = (i_1, i_2, \ldots, i_M)$. In second quantization, this product is expressed as

$$|\Phi_{\mathbf{i}}\rangle = \prod_{m=1}^{M} a_{i_m}^{m\dagger} |\mathrm{vac}\rangle. \tag{18-13}$$

For the ground state illustrated in Figure 18-1, we would choose $\mathbf{i} = (0, 0, 0)$. In the remainder of this chapter, we use the notation that modal indices $i, j, k, \ldots$ correspond to modals occupied in the reference Hartree product while $a, b, c, \ldots$ correspond to unoccupied modals. To denote general modals, the indices $p, q, r, \ldots$ are used. To generate excited states, we introduce the excitation operators

$$\tau_{\mu^{\mathbf{m}}} = \prod_{m \in \mathbf{m}} a_{a_m}^{m\dagger} a_{i_m}^{m}, \tag{18-14}$$

where $\mathbf{m}$ is the MC for the operator, i.e. the set of modes in which it excites, and $\mu^{\mathbf{m}}$ is a compound index specifying exactly what modals the operator excites to. For instance, the one- and two-mode excitation operators can be written explicitly using general mode indices m_1 and m_2 as

$$\tau_{a^{m_1}} = a_{a_1}^{m_1\dagger} a_{i_1}^{m_1}, \tag{18-15}$$

$$\tau_{a^{m_1} a^{m_2}} = a_{a_1}^{m_1\dagger} a_{i_1}^{m_1} a_{a_2}^{m_2\dagger} a_{i_2}^{m_2}. \tag{18-16}$$

Since there will always only be one occupied modal for each mode in the reference state, the corresponding i_m index is omitted on the left-hand side. The two-mode excitation operator is illustrated in Figure 18-3. From the basic commutator relations, (18-11) and (18-12), it is seen that all excitation operators commute,

$$[\tau_{\mu^{\mathbf{m}}}, \tau_{\nu^{\mathbf{m}'}}] = 0. \tag{18-17}$$

A key feature of second quantization is that both states and operators can be represented in terms of creation and annihilation operators. The representation of the Hamiltonian becomes particularly simple for the sum over products form introduced in Section 18.2.1. Defining the second quantized operator as

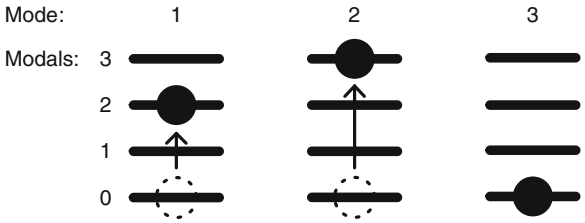

Figure 18-3. The action of the two-mode excitation operator $\tau_{\mu\mathbf{m}} = \tau_{a^{m_1}a^{m_2}}$ with $\mathbf{m} = \{m_1, m_2\} = \{1, 2\}$ and $a^{m_1} = 2, a^{m_2} = 3$

$$H^{\mathrm{SQ}} = \sum_t c_t \prod_{m \in \mathbf{m}^t} h^{mo^{tm}}, \quad h^{mo^{tm}} = \sum_{p,q} h_{pq}^{mo^{tm}} a_p^{m\dagger} a_q^m, \tag{18-18}$$

where $\mathbf{m}^t$ is the MC for the term t and $h_{pq}^{mo^{tm}} = \int \phi_{p_m}^m(Q_m) h^{mo^{tm}} \phi_{q_m}^m(Q_m) dQ_m$ are one-mode integrals, we obtain a one-to-one correspondence between first and second quantization. Thus, with either representation, a matrix element between two Hartree products simply turns into a sum of products of one-dimensional integrals times a number of Kronecker deltas for the modes not included in the specific term,

$$\langle \Phi_{\mathbf{p}} | H | \Phi_{\mathbf{q}} \rangle = \sum_t c_t \prod_{m \in \mathbf{m}^t} h_{pq}^{mo^{tm}} \prod_{m \notin \mathbf{m}^t} \delta_{p_m q_m}. \tag{18-19}$$

Figure 18-4 illustrates how the second quantization representation picks out the correct one mode integrals based on the occupation numbers in the bra and ket ONVs.

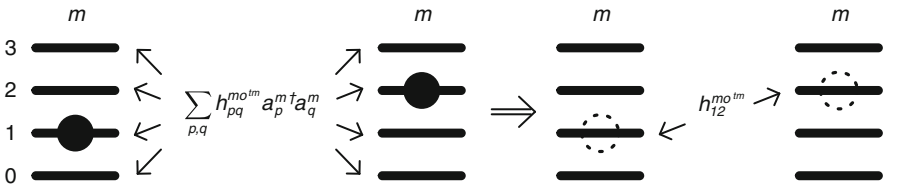

Figure 18-4. The second quantization representation of an operator. For each mode in a given term in the Hamiltonian, the annihilation operators will work on each modal. This will give zero for all modals except the ones occupied in the ONV. Thus, the result will be a product of the correct one mode integrals

18.4. VIBRATIONAL COUPLED CLUSTER THEORY

To correct for the neglect of correlation beyond the mean-field in VSCF theory, we have to include more Hartree products than just the VSCF reference state. The conceptually simplest way of doing this is through a variational linear expansion

approach in the Hartree product space giving the standard vibrational configuration interaction (VCI) [5, 8] method. Including all possible configurations, we obtain the full VCI (FVCI) wave function. For molecules with more than four atoms corresponding to $M = 6$ vibrational modes, dealing with the FVCI wave function is most often impractical due to its exponential N^M scaling in the number of parameters where N is the number of one-mode basis functions per mode. Though approximate VCI methods can be devised [19, 20], we now turn to the alternative VCC approach.

The VCC wave function is based on the exponential ansatz

$$|\mathrm{VCC}\rangle = \exp(T)|\Phi_{\mathbf{i}}\rangle, \tag{18-20}$$

where the cluster operator, T, is defined as

$$T = \sum_{\mathbf{m}\in \mathrm{MCR}[T]} T^{\mathbf{m}}, \qquad T^{\mathbf{m}} = \sum_{\mu^{\mathbf{m}}} t_{\mu^{\mathbf{m}}} \tau_{\mu^{\mathbf{m}}}. \tag{18-21}$$

In this expression, MCR[T] is used to specify the MCs included in the excitation space. The $T^{\mathbf{m}}$ operator then contains all excitation operators and their associated amplitudes, $t_{\mu^{\mathbf{m}}}$, for the MC $\mathbf{m}$.

If MCR[T] contains all possible MCs for a given system, Eq. (18-20) is just an alternative parameterization of the FVCI wave function. However, since the number of possible excitations increases rapidly with the number of simultaneously excited modes, the cluster operator must often be truncated. The simplest approach is to include only MCs containing at most n modes. This results in a hierarchy of VCC[n] methods analogously to the CCS, CCSD, CCSDT, ... hierarchy in electronic structure theory. However, since the molecular vibrations are distinguishable, more elaborate excitation spaces may be of relevance. Consider for instance two vibrational modes, m_0 and m_1, which turn out to be only weakly coupled through the Hamiltonian. In such a case, the corresponding amplitudes $\mathbf{t}^{\{m_0 m_1\}}$ are expected to be small and one may choose to exclude these entirely from the excitation space.

The determination of the cluster amplitudes is carried out as usual by solving the projected Schrödinger equation after a transformation with $\exp(-T)$,

$$0 = e_{\mu^{\mathbf{m}}} = \langle \mu^{\mathbf{m}}| \exp(-T) H \exp(T)|\Phi_{\mathbf{i}}\rangle. \tag{18-22}$$

The energy is in turn obtained from

$$E_{\mathrm{VCC}} = \langle \Phi_{\mathbf{i}}| H \exp(T)|\Phi_{\mathbf{i}}\rangle. \tag{18-23}$$

The solution of Eq. (18-22) is achieved in an iterative manner. The time-limiting step in this case is the evaluation of the error vector, $e_{\mu^{\mathbf{m}}}$, using a given set of trial amplitudes. This will be described more carefully in Section 18.6.

18.4.1. Excited States

Two basic strategies exist for obtaining vibrational excited states: A state specific and a response approach.

In the state specific approach, a separate VCC calculation is carried out based on an optimized VSCF reference for each state. In other words, the calculation of each state is based on a modal basis which is optimal for the state in question. The VCC excitation level is furthermore counted relative to the reference describing the excited state. The advantage of this approach is the use of optimized modals which may reduce the size of the required VCC excitation space. On the other hand, CC methods based on a single reference function are not well suited for states with multireference character, especially at lower excitation levels. Often, excited vibrational states will be strongly multireference due to the vast number of possible resonances. In these cases, the state specific method may run into trouble. A related issue is solving the non-linear equations for the excited states in practice. Contrary to the ground state, the convergence of iterative methods has proved troublesome is some cases. Another problem is the non-orthogonality of the obtained states. This complicates the evaluation of for instance transition moments which may be of great interest in addition to the excitation energies. Due to the issues discussed here, the state specific method will not be considered further in this chapter.

The response method is fundamentally different from the state-specific approach in that it is based only on a ground state optimization of the VCC wave function. CC response theory for electronic structure theory has been extensively described, see Ref. [21] and references therein. The generalization to VCC theory is provided in Ref. [22]. In this chapter we shall not go through the derivation but simply quote the result that excitation energies may be approximated by the eigenvalues of the Jacobian of the VCC error vector,

$$A_{\mu^{\mathbf{m}}\nu^{\mathbf{m}'}} = \langle \mu^{\mathbf{m}} | \exp(-T)[H, \tau_{\nu^{\mathbf{m}'}}] \exp(T) | \Phi_{\mathbf{i}} \rangle. \tag{18-24}$$

Due to the large dimension of the excitation space, the calculation of the full spectrum of $\mathbf{A}$ is not feasible. Instead, iterative subspace methods are used to obtain only a limited number of eigenstates. These methods all rely on the ability to transform a given vector with the Jacobian. Once again, this transformation is the time-limiting step and can be carried out using similar approaches as those described in Section 18.6.

The response method provides a framework for obtaining not only excitation energies but also many other properties like expectation values, polarizabilities, and transition moments. These features are, however, beyond the scope of the present chapter.

18.5. NUMERICAL EXAMPLES

The VCC method is still in its infancy. Therefore, it is important to asses to accuracy of the method by means of benchmark calculations. This is especially true due to the large diversity of PESs. First of all, the physical degree of mode coupling will vary between molecules. Second, the number of modes coupled simultaneously in the model description of the PES is limited by computational resources. The excitation level needed in VCC will depend on both of these factors. This situation should be contrasted to electronic theory where the correlation always arises from the universal two-body Coulomb repulsion.

So far, VCC has only been applied to a limited number of molecules. In this section we compare ground-state based calculations for two molecules: Formaldehyde and ethylene. We only present graphical illustrations of average errors relative to FVCI. The full set of results and a more elaborate discussion is available in Ref. [22].

The first three panels of Figure 18-5 show the average absolute errors for the fundamentals, overtones, and combination bands of formaldehyde. The fourth panel shows the same results but for the fundamentals of ethylene. Note the logarithmic scale. It is seen that the accuracy is systematically improved in the VCC hierarchy at each excitation level. The accuracy is higher for the one-mode excitations, i.e. the fundamentals and overtones, compared to the combinations. It is also seen that VCC is superior to VCI at all excitation levels. These facts can all be justified by perturbation theory arguments, see Ref. [22]. The relative performance is as expected and experience is similar with other molecules. More extensive benchmarking of the VCC method to quantify further the accuracy obtainable for given computational levels is a high priority at the time of this writing.

Though VCC is clearly theoretically favorable over VCI in the sense that higher accuracy is achieved using the same number of parameters, the VCC equations are much more complicated to implement in a computationally efficient manner. The rest of this chapter deals more carefully with this issue.

18.6. A CLOSER LOOK AT THE VCC EQUATIONS

In this section we consider the evaluation of the VCC error vector, Eq. (18-22), in terms of amplitudes and integrals. The discussion presented here can quite straightforwardly be translated into a computer implementation of a general excitation level VCC method. Though the efficiency of such an implementation has proven not to be adequate for larger systems, the discussion is nevertheless relevant since it serves to introduce a number of basic concepts. It illustrates how VCC works and underlines the differences relative to electronic CC and VCI.

We begin by introducing the resolution of the identity,

$$1 = \sum_{\mathbf{m},\mu^{\mathbf{m}}} |\mu^{\mathbf{m}}\rangle\langle\mu^{\mathbf{m}}| = |\Phi_{\mathbf{i}}\rangle\langle\Phi_{\mathbf{i}}| + \sum_{\mathbf{m}\neq\{\}} \sum_{\mu^{\mathbf{m}}} |\mu^{\mathbf{m}}\rangle\langle\mu^{\mathbf{m}}|, \tag{18-25}$$

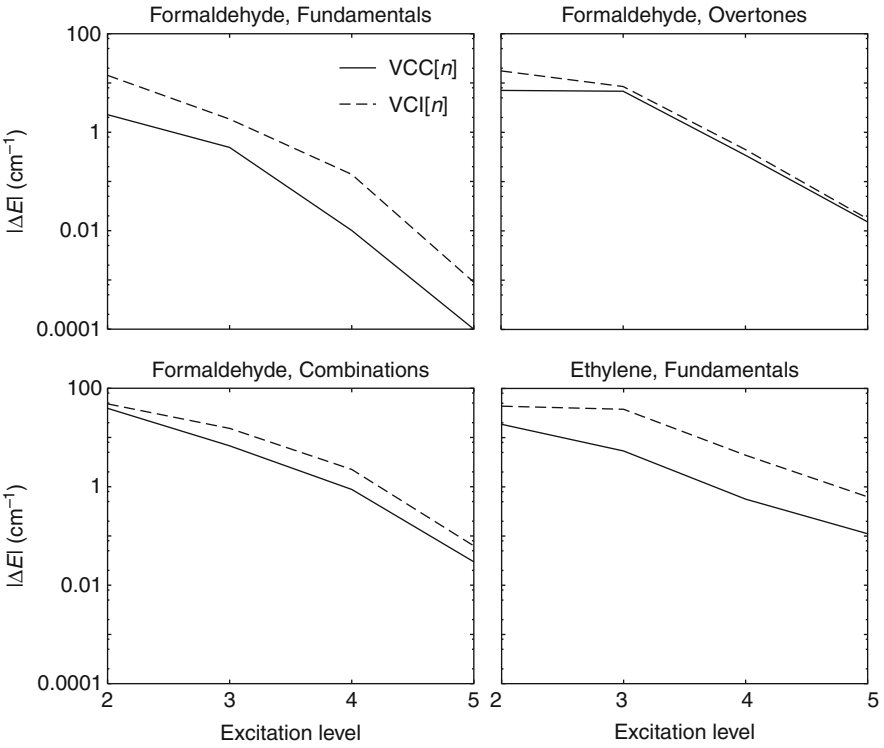

Figure 18-5. The convergence of VCC response and VCI ground-state based excitation energies. For formaldehyde the PES is a fourth order Taylor approximation with up to four-mode couplings [23]. The primitive basis consists of seven harmonic oscillator functions per mode and all virtual modals are used in the VCI and VCC calculations. For ethylene, the PES is a fourth order Taylor approximation restricted to include only up to three-mode couplings [24]. While 21 harmonic oscillator functions were used as the primitive basis, only the 3 lowest VSCF modals per mode was used in the VCI and VCC calculations to facilitate the FVCI calculation (531,411 coefficients)

twice into Eq. (18-22):

$$e_{\mu^{\mathbf{m}}} = \sum_{\mathbf{m}^p,\nu^{\mathbf{m}^p}} \sum_{\mathbf{m}^q,\sigma^{\mathbf{m}^q}} \langle \mu^{\mathbf{m}} | \exp(-T) | \nu^{\mathbf{m}^p} \rangle \langle \nu^{\mathbf{m}^p} | H | \sigma^{\mathbf{m}^q} \rangle \langle \sigma^{\mathbf{m}^q} | \exp(T) | \Phi_{\mathbf{i}} \rangle, \quad (18\text{-}26)$$

Note that the summations are formally over all possible MCs (including the empty one) and not restricted to the particular VCC excitation space. The evaluation of the error vector may now be performed in three separate steps:

1. Evaluation of the effect of $\exp(T)$ on the reference state,

$$c_{\sigma^{\mathbf{m}^q}} = \langle \sigma^{\mathbf{m}^q} | \exp(T) | \Phi_{\mathbf{i}} \rangle. \quad (18\text{-}27)$$

2. Transformation of $c_{\sigma^{\mathbf{m}^q}}$ with the Hamiltonian,

$$d_{\nu^{\mathbf{m}^p}} = \sum_{\mathbf{m}^q, \sigma^{\mathbf{m}^q}} \langle \nu^{\mathbf{m}^p} | H | \sigma^{\mathbf{m}^q} \rangle c_{\sigma^{\mathbf{m}^q}}. \tag{18-28}$$

3. A final transformation with $\exp(-T)$,

$$e_{\mu^{\mathbf{m}}} = \sum_{\mathbf{m}^p, \nu^{\mathbf{m}^p}} \langle \mu^{\mathbf{m}} | \exp(-T) | \nu^{\mathbf{m}^p} \rangle d_{\nu^{\mathbf{m}^p}}. \tag{18-29}$$

In the next two subsections we discuss the $\exp(T)$ and Hamiltonian transformations. We then discuss the assembly of these separate steps into a working entity.

18.6.1. The Exponential Transformations

The exponential transformations can be carried out based on the Taylor expansion of the exponential function. We first consider the case of $\exp(T)$ acting on the reference state,

$$\exp(T)|\Phi_{\mathbf{i}}\rangle = \left(1 + T_1 + (T_2 + \frac{1}{2}T_1^2) + (T_3 + T_1T_2 + \frac{1}{6}T_1^3) + \ldots\right)|\Phi_{\mathbf{i}}\rangle. \tag{18-30}$$

The three-mode excited configurations resulting from this transformation are generated from a combination of the T_1, T_2, and T_3 cluster operators, $C_3 = T_3 + T_1T_2 + \frac{1}{6}T_1^3$. The coefficients of the individual configurations generated by C_3 are obtained by combining the amplitudes. For instance, the vector of three-mode coefficients for the MC $\{m_1m_2m_3\}$ is given by

$$\begin{aligned}\mathbf{c}^{\{m_1m_2m_3\}} = {} & \mathbf{t}^{\{m_1m_2m_3\}} + \mathbf{t}^{\{m_1\}}\mathbf{t}^{\{m_2m_3\}} + \mathbf{t}^{\{m_2\}}\mathbf{t}^{\{m_1m_3\}} + \mathbf{t}^{\{m_3\}}\mathbf{t}^{\{m_1m_2\}} \\ & + \mathbf{t}^{\{m_1\}}\mathbf{t}^{\{m_2\}}\mathbf{t}^{\{m_3\}}.\end{aligned} \tag{18-31}$$

Notice that the factor of $1/6$ disappears when the actual coefficient are calculated due to the six possible ways the modes can be distributed on the three T_1 operators.

In the above equation, the product of two amplitude vectors should be considered as a direct product, i.e.

$$\mathbf{t}^{\{m_1\}}\mathbf{t}^{\{m_2\}} = \begin{bmatrix} t_1^{m_1} \\ t_2^{m_1} \end{bmatrix} \otimes \begin{bmatrix} t_1^{m_2} \\ t_2^{m_2} \end{bmatrix} = \begin{bmatrix} t_1^{m_1}t_1^{m_2} \\ t_1^{m_1}t_2^{m_2} \\ t_2^{m_1}t_1^{m_2} \\ t_2^{m_1}t_2^{m_2} \end{bmatrix}. \tag{18-32}$$

In general, it can be realized that the **c** coefficients for a given MC can be obtained from

$$\mathbf{c}^{\mathbf{m}} = \sum_{\mathrm{MCR}\in \mathrm{SMCR}[\mathbf{m}]} \prod_{\mathbf{m}^k \in \mathrm{MCR}} \mathbf{t}^{\mathbf{m}^k}. \tag{18-33}$$

Here SMCR[**m**] is the set of all partitions of **m**, i.e. the set of all possible sets of mutually disjoint subsets of **m** whose union is **m**. Since the cluster operator is usually truncated, the additional restriction that all MCs in each MCR must be part of the excitation space naturally applies. The product is again to be considered as a direct product. Using Eq. (18-33) it is possible to construct the entire $c_{\sigma^{\mathbf{m}^q}}$ vector in Eq. (18-27).

The above equations describe how to transform the reference state. Transforming a general state with $\exp(\pm T)$ as is needed in Eq. (18-29) is only slightly more complicated. Let the initial state be written as

$$|D\rangle = \sum_{\mathbf{m}^p \in \mathrm{MCR}[D]} \sum_{\nu^{\mathbf{m}^p}} d_{\nu^{\mathbf{m}^p}} |\nu^{\mathbf{m}^p}\rangle. \tag{18-34}$$

The coefficients, $\mathbf{e}^{\mathbf{m}}$, of the transformed state $|E\rangle = \exp(T)|D\rangle$ are then given by

$$\mathbf{e}^{\mathbf{m}} = \sum_{\mathbf{m}'\in \mathrm{MCR}[D]} \Big(\sum_{\mathrm{MCR}\in \mathrm{SMCR}[\mathbf{m}\setminus\mathbf{m}']} \prod_{\mathbf{m}^k \in \mathrm{MCR}} \mathbf{t}^{\mathbf{m}^k} \Big) \mathbf{d}^{\mathbf{m}'}. \tag{18-35}$$

It is seen that in contrast to Eq. (18-33) which generates all excitations necessary to arrive at the MC **m**, this form only generates the excitations not already present in the $\mathbf{d}^{\mathbf{m}'}$ coefficients.

To finish this discussion, we merely note that doing $\exp(-T)$ as opposed to $\exp(T)$ is simply a matter of multiplying $(-1)^n$ on each term in Eqs. (18-33) and (18-35) where n is the number of **t**-factors entering.

18.6.2. The Hamiltonian Transformation

To allow large excitation spaces, the transformation with the Hamiltonian, Eq. (18-28), is carried out in a direct fashion, i.e. the Hamiltonian matrix is never explicitly constructed. Instead, an algorithm is used to carry out a transformation of the coefficients equivalent to a matrix multiplication.

The core of a direct transformer is the ability to transform the coefficients corresponding to excitations in a given MC, $c_{\sigma^{\mathbf{m}^p}}$, by a single term, $H_t^{\mathbf{m}}$, in the Hamiltonian,

$$d'_{\nu^{\mathbf{m}^p}} = \sum_{\sigma^{\mathbf{m}^q}} \langle \nu^{\mathbf{m}^p} | H_t^{\mathbf{m}} | \sigma^{\mathbf{m}^q} \rangle c_{\sigma^{\mathbf{m}^p}} \tag{18-36}$$

$$= \sum_{\sigma^{\mathbf{m}^q}} \langle \nu^{\mathbf{m}^p} | \prod_{m\in\mathbf{m}} h^{mo^{tm}} | \sigma^{\mathbf{m}^q} \rangle c_{\sigma^{\mathbf{m}^p}}, \tag{18-37}$$

where $d'_{\nu,\mathbf{m}^p}$ is the set of coefficients corresponding to the MC $\mathbf{m}^p$ in the result.

Since each term in the Hamiltonian is a product of one-mode operators, the result of the transformation may be determined by applying each operator in turn. This will lead to a sequence of one-index transformations of the coefficients. Depending on the mode, m_h, associated with the operator and the modes included in $\mathbf{m}^q$ and $\mathbf{m}^p$, four kinds of transformations are possible:

- $m_h \notin (\mathbf{m}^p \cup \mathbf{m}^q)$
  In this case, mode m_h in neither excited in $\langle \nu^{\mathbf{m}^p}|$ or $|\sigma^{\mathbf{m}^q}\rangle$. Considering the second quantization form of the one-mode operator, Eq. (18-18), we see that only the term $h_{ii}^{m_h o^{tm_h}} a_i^{m_h\dagger} a_i^{m_h}$ will give a non-zero results. Therefore, the integral $h_{ii}^{m_h o^{tm_h}}$ should simply be multiplied on every coefficient. This is known as a *passive* contraction.
- $m_h \in (\mathbf{m}^q \setminus \mathbf{m}^p)$
  If mode m_h is excited in $|\sigma^{\mathbf{m}^q}\rangle$ but not in $\langle \nu^{\mathbf{m}^p}|$, the excitation must be removed. Considering again the second quantized operator, we see that this is accomplished when $p = i$ and $q = a$ in Eq. (18-18). The corresponding transformation of the coefficients is denoted a *down* contraction,

$$d'^{\{m_1 m_2 \cdots m_{h-1} m_{h+1} \cdots m_K\}}_{a_1 a_2 \cdots a_{h-1} a_{h+1} \cdots a_K} = \sum_{a_h} h_{i_h a_h}^{m_h o^{tm_h}} c^{\{m_1 m_2 \cdots m_{h-1} m_h m_{h+1} \cdots m_K\}}_{a_1 a_2 \cdots a_{h-1} a_h a_{h+1} \cdots a_K}. \tag{18-38}$$

- $m_h \in (\mathbf{m}^p \setminus \mathbf{m}^q)$
  This situation is the opposite of the previous, i.e. excitations in mode m_h must be generated. We denote this an *up* contraction,

$$d'^{\{m_1 m_2 \cdots m_{h-1} m_h m_{h+1} \cdots m_{K+1}\}}_{a_1 a_2 \cdots a_{h-1} a_h a_{h+1} \cdots a_{K+1}} = h_{a_h i_h}^{m_h o^{tm_h}} c^{\{m_1 m_2 \cdots m_{h-1} m_{h+1} \cdots m_{K+1}\}}_{a_1 a_2 \cdots a_{h-1} a_{h+1} \cdots a_{K+1}}. \tag{18-39}$$

- $m_h \in (\mathbf{m}^p \cap \mathbf{m}^q)$
  The final possibility is that m_h is excited in both $\langle \nu^{\mathbf{m}^p}|$ and $|\sigma^{\mathbf{m}^q}\rangle$. In this case the excitation must be retained but the second quantized operator connects different modals, i.e. annihilates one modal and creates another. The result is a *forward* contraction,

$$d'^{\{m_1 m_2 \cdots m_h \cdots m_K\}}_{a_1 a_2 \cdots a_h \cdots a_K} = \sum_{b_h} h_{a_h b_h}^{m_h o^{tm_h}} c^{\{m_1 m_2 \cdots m_h \cdots m_K\}}_{a_1 a_2 \cdots b_h \cdots a_K}. \tag{18-40}$$

To implement the transformation (18-37) efficiently, the scaling of the different types of contractions must be considered. If N is the number of virtual modals, and K is the number of excited modes on the right-hand sides of Eqs. (18-38), (18-39) and (18-40), it can be seen that down contractions scale as N^K while forward and up contractions scale as $N^{(K+1)}$. Due to the basic commutator relations, Eqs. (18-11) and (18-12), the order in which the one-mode operators are applied does not matter. It is therefore advantageous to do the contractions in the order down, forward, up, since this will minimize the number of excited modes and thereby the operation count in all steps.

We now give a specific example to illustrate a simple transformation in practice. Consider a set of coefficients, $c_{\sigma^{\mathbf{m}^q}}$, describing excitations in $\mathbf{m}^q = \{m_1 m_2\}$, transformed with a three-mode term in the Hamiltonian,

$$d'_{\nu^{\{m_2 m_3\}}} = \sum_{\sigma^{\{m_1 m_2\}}} \langle \nu^{\{m_2 m_3\}} | h^{m_1 o_1} h^{m_2 o_2} h^{m_3 o_3} | \sigma^{\{m_1 m_2\}} \rangle c_{\sigma^{\{m_1 m_2\}}}. \tag{18-41}$$

As is seen, in this case we want the result corresponding to $\mathbf{m}^p = \{m_2 m_3\}$. The evaluation of the result vector can now be performed in a sequence of steps. In the simple case of only three modals per mode (with the occupied numbered as 0 and the virtuals as 1 and 2), these are given as

$$\begin{bmatrix} x_1^{m_2} \\ x_2^{m_2} \end{bmatrix} = \begin{bmatrix} h_{01}^{m_1 o_1} c_{11}^{m_1 m_2} + h_{02}^{m_1 o_1} c_{21}^{m_1 m_2} \\ h_{01}^{m_1 o_1} c_{12}^{m_1 m_2} + h_{02}^{m_1 o_1} c_{22}^{m_1 m_2} \end{bmatrix} \xleftarrow{h^{m_1 o_1},\ \text{down}} \begin{bmatrix} c_{11}^{m_1 m_2} \\ c_{12}^{m_1 m_2} \\ c_{21}^{m_1 m_2} \\ c_{22}^{m_1 m_2} \end{bmatrix}, \tag{18-42}$$

$$\begin{bmatrix} y_1^{m_2} \\ y_2^{m_2} \end{bmatrix} = \begin{bmatrix} h_{11}^{m_2 o_2} x_1^{m_2} + h_{12}^{m_2 o_2} x_2^{m_2} \\ h_{21}^{m_2 o_2} x_2^{m_2} + h_{22}^{m_2 o_2} x_2^{m_2} \end{bmatrix} \xleftarrow{h^{m_2 o_2},\ \text{forward}} \begin{bmatrix} x_1^{m_2} \\ x_2^{m_2} \end{bmatrix}, \tag{18-43}$$

$$\begin{bmatrix} d'^{m_2 m_3}_{11} \\ d'^{m_2 m_3}_{12} \\ d'^{m_2 m_3}_{21} \\ d'^{m_2 m_3}_{22} \end{bmatrix} = \begin{bmatrix} h_{10}^{m_3 o_3} y_1^{m_2} \\ h_{20}^{m_3 o_3} y_1^{m_2} \\ h_{10}^{m_3 o_3} y_2^{m_2} \\ h_{20}^{m_3 o_3} y_2^{m_2} \end{bmatrix} \xleftarrow{h^{m_3 o_3},\ \text{up}} \begin{bmatrix} y_1^{m_2} \\ y_2^{m_2} \end{bmatrix}. \tag{18-44}$$

We have now described how the partial transformation (18-37) can be carried out. The transformation with the full Hamiltonian, Eq. (18-28), is a simple matter of accounting for all MCs and all terms in the Hamiltonian as described by the following algorithm:

Algorithm for evaluating Eq. (18-28):

- Loop over all $\mathbf{m}^p$
  - Loop over all $\mathbf{m}^q$ coupled to $\mathbf{m}^p$ through H
    - Loop over all terms, t, in H coupling $\mathbf{m}^p$ and $\mathbf{m}^q$
      - Evaluate $d'_{\nu^{\mathbf{m}^p}}$ using Eq. (18-37) and add to the final result, $d_{\nu^{\mathbf{m}^p}}$.

18.6.3. Putting the Pieces Together

In Sections 18.6.1 and 18.6.2 the individual steps required for the evaluation of the VCC error vector, Eq. (18-26), were described. In this section, we discuss the resolution of the identity in greater detail, or rather, the requirements on the intermediate spaces $|\nu^{\mathbf{m}^p}\rangle$ and $|\sigma^{\mathbf{m}^q}\rangle$.

To be specific, start from the left in Eq. (18-26). The MCR of the error vector is given by MCR[T]. Since $\exp(-T)$ can only create excitations, the MCR of the intermediate space $|\nu^{\mathbf{m}^p}\rangle$ can be set equal to MCR[T] with the restriction that the space should be closed under deexcitation. To see why this last restriction applies, let $\exp(-T)$ work to the left on $\langle\mu^{\mathbf{m}}|$. This will deexcite the bra and generate a set of $|\nu^{\mathbf{m}^p}\rangle$ states. Since $\langle\nu^{\mathbf{m}^p}|H|\sigma^{\mathbf{m}^q}\rangle$ will not in general be zero for any of the resulting states, these have to be included as well.

Consider next the $|\sigma^{\mathbf{m}^q}\rangle$ space. The Hamiltonian may both excite and deexcite and thus the MCR of the $|\sigma^{\mathbf{m}^q}\rangle$ space has to be larger than MCR[T]. For a VCC[n] calculation with a h-mode Hamiltonian the $|\sigma^{\mathbf{m}^q}\rangle$ space must contain up to $(n+h)$-mode excitations. Once the two intermediate spaces are set up, the steps described in the previous subsections can be applied. The entire process for the case of VCC[2] with a two-mode Hamiltonian is illustrated in Figure 18-6.

The explicit construction of the excitation coefficients in the larger intermediate $|\sigma^{\mathbf{m}^q}\rangle$ space has unfortunate consequences in terms of performance. As noted above, down contractions scale as N^K while ups and forwards scale as $N^{(K+1)}$. Although only down contractions are relevant for the highest excitation part of the $|\sigma^{\mathbf{m}^q}\rangle$ vector since we must arrive in the $|\nu^{\mathbf{m}^p}\rangle$ space, these will still scale as $N^{(n+h)}$. This is a significant factor of $N^{(h-1)}$ more than a corresponding VCI[n] calculation and first of all it can be avoided.

Instead of constructing the larger $|\sigma^{\mathbf{m}^q}\rangle$ space, we may use it only as a formal utility. Thus, instead of employing the resolution of the identity between H and $\exp(T)$ in the error vector, Eq. (18-22), we use a direct formula for the exponential transformation equivalent to Eq. (18-33),

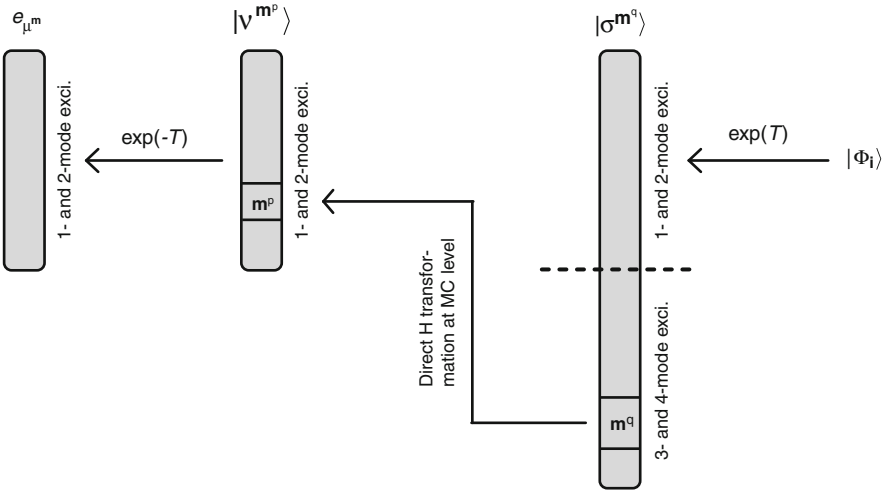

Figure 18-6. Schematic overview of the evaluation of the VCC [2] error vector with a two-mode Hamiltonian

$$e_{\mu^{\mathbf{m}}} = \sum_{\mathbf{m}^p, \nu^{\mathbf{m}^p}} \langle \mu^{\mathbf{m}} | \exp(-T) | \nu^{\mathbf{m}^p} \rangle \langle \nu^{\mathbf{m}^p} | H \exp(T) | \Phi_{\mathbf{i}} \rangle \tag{18-45}$$

$$= \sum_{\mathbf{m}^p, \nu^{\mathbf{m}^p}} \langle \mu^{\mathbf{m}} | \exp(-T) | \nu^{\mathbf{m}^p} \rangle \times \langle \nu^{\mathbf{m}^p} | H \sum_{\mathbf{m}^q} \left(\sum_{\mathrm{MCR} \in \mathrm{SMCR}[\mathbf{m}^q]} \prod_{\mathbf{m}^k \in \mathrm{MCR}} T^{\mathbf{m}_k} \right) | \Phi_{\mathbf{i}} \rangle. \tag{18-46}$$

Now remember that the Hamiltonian is written in terms of products of one-mode operators. Instead of doing the direct product of the cluster amplitudes followed by a series of contractions, it is therefore possible to reverse the order. Thus, in this scheme we perform the contractions with the individual amplitude vectors first and then do the direct product of the resulting vectors. The two methods are compared in Figure 18-7. The advantage is two-fold. First, the contractions will scale at most like $N^{(n+1)}$ since the maximum excitation level of any amplitude vector is n. This is no higher than in the case of VCI. In addition, the dimensions of the quantities entering the direct product will usually be smaller since down contractions have reduced their size. This increases efficiency as well.

Though the above modification reduces the scaling of the individual contractions, a VCC implementation using this strategy is still significantly more expensive than a VCI at the same excitation level. This is due to the fact that the number of subsets in SMCR[$\mathbf{m}^q$] grows quickly as the size of $\mathbf{m}^q$ increases. The number of partitions of a set of size n is given by the Bell numbers [25], B_n, not to be discussed further here. Suffice is to say that the first few numbers starting at $n = 1$ are 1, 2, 5, 15, 52, 203, 877, 4140, 21147, 115975, ... Moreover, since the MCs partitioned are the ones in the larger $|\sigma^{\mathbf{m}^q}\rangle$ space, the excitation level will generally be higher than in the T-space. The problem can be somewhat alleviated by absorbing the one-mode part of the cluster operator in the Hamiltonian as described in Ref. [26]. Defining $T = T_1 + T_r$, we obtain

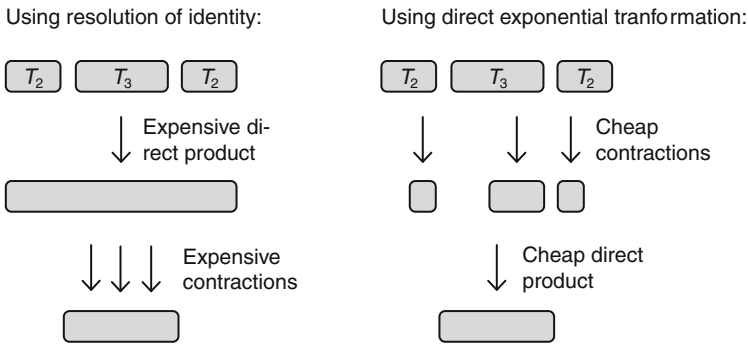

Figure 18-7. Two different strategies for the evaluation of the error vector

$$e_{\mu^{\mathbf{m}}} = \langle \mu^{\mathbf{m}} | \exp(-T_1 - T_\mathrm{r}) H \exp(T_1 + T_\mathrm{r}) | \Phi_\mathbf{i} \rangle \tag{18-47}$$

$$= \langle \mu^{\mathbf{m}} | \exp(-T_\mathrm{r}) \tilde{H} \exp(T_\mathrm{r}) | \Phi_\mathbf{i} \rangle, \tag{18-48}$$

where $\tilde{H} = \exp(-T_1) H \exp(T_1)$. The T_1 transformation of the Hamiltonian preserves the particle rank of the operator (which would not be the case for higher excitation level cluster operators) and using the $\tilde{H}$ operator in place of H is a simple matter of transforming the one-mode integrals, see Ref. [26] for details. Since T_r contains no one-mode operators, all partitions containing one or more MCs with only one mode can be discarded. This reduces the number of possible partitions to 0, 1, 1, 4, 11, 41, 162, 715, 3425, 17722, ... Thus, the number of partitions and thereby contractions and direct products can be significantly reduced. For the very relevant example of VCC [3] with three-mode couplings in the Hamiltonian, the intermediate MCs in the $|\sigma^{\mathbf{m}^q}\rangle$ space contain up to 6 mode excitations. In this case the original 203 partitions are reduced to only 41 for which contractions and direct products must be made.

In this section, some basic concepts and issues relevant for the implementation of VCC theory has been discussed. As is evident, the inner details of VCC are very different from those in electronic CC theory due to the distinguishability of the modes, the resulting differences in the associated second quantization, and the different form of the Hamiltonian operator which frequently contain higher-mode couplings. Electronic single-reference CI and CC can be implemented such that roughly identical computational scalings are obtained. To arrive at this situation is more difficult in the VCC case. The above implementation based on the resolution of the identity brings us only part of the way in this respect. However, the value of a general excitation level transformer, in particular for benchmark purposes, should not be underestimated for a new theory such as VCC. Furthermore, much of the analysis and important steps (direct products and contractions) are key elements in the quest for more efficient but also more specialized implementations which we will turn to now.

18.7. TOWARDS EFFICIENT IMPLEMENTATIONS

In this section we present a brief overview of an alternative method for evaluating the VCC error vector. The method is based on the Baker–Campbell–Hausdorff (BCH) commutator expansion commonly employed in electronic CC theory. Though designing an efficient general excitation level implementation in terms of a commutator expansion is possible and work is underway, it is a tremendous challenge, as should be clear from the previous sections.[1] We therefore restrict ourselves in this section to the case of a VCC [2] model with a two-mode Hamiltonian operator. A full account of the theory and implementation is given in Ref. [26] and this section merely introduces the basic concepts.

---

[1] A general implementation with optimal scaling was recently published, see J. Chem. Phys. 131, 234109 (2009).

Since we include only one- and two-mode couplings in the excitation space and the Hamiltonian, the BCH expansion terminates after three terms,

$$e_{\mu^{\mathbf{m}}} = \langle \mu^{\mathbf{m}} | \exp(-T_2)\tilde{H}\exp(T_2)|\Phi_{\mathbf{i}}\rangle \tag{18-49}$$

$$= \langle \mu^{\mathbf{m}} | \tilde{H} + [\tilde{H}, T_2] + \frac{1}{2}[[\tilde{H}, T_2], T_2]|\Phi_{\mathbf{i}}\rangle, \tag{18-50}$$

where the T_1- transformed Hamiltonian, Eq. (18-48), has been used. The termination after three terms can be understood by noting that higher nested commutators will contain at least three T_2 operators generating at least six-mode excitations. The Hamiltonian can remove at most two excitations (by down contractions), and the resulting four-mode excited configurations will be outside the VCC[2] space used in the $\langle \mu^{\mathbf{m}}|$ projection.

The evaluation of the error vector proceeds by expanding the commutators,

$$e_{\mu^{\mathbf{m}}} = \langle \mu^{\mathbf{m}} | \tilde{H} + \tilde{H}T_2 + T_2\tilde{H} + \frac{1}{2}\tilde{H}T_2T_2 + T_2\tilde{H}T_2|\Phi_{\mathbf{i}}\rangle. \tag{18-51}$$

The final step is now to perform contractions of the amplitudes with the one-mode operators in the Hamiltonian as described in the previous section. To express this in a formal way, we introduce a notation where a given one-mode operator is written as a sum of operators corresponding to either passive, down, up, or forward contractions,

$$\tilde{h}^{mo} = \tilde{h}^{mo}_p + \tilde{h}^{mo}_d + \tilde{h}^{mo}_u + \tilde{h}^{mo}_f. \tag{18-52}$$

In this way, a contribution to the error vector arising from a down contracted set of amplitudes may be written like

$$e_{\mu^{\{m_0\}}} \leftarrow \langle \mu^{\{m_0\}}| \sum_{m_1 o_1} c^{m_1}_{o_1} \tilde{h}^{m_1 o_1}_d T^{\{m_0 m_1\}}|\Phi_{\mathbf{i}}\rangle, \tag{18-53}$$

where $c^{m_1}_{o_1}$ is the coefficient of the given term in the Hamiltonian and $\leftarrow$ indicates that this is only one of many contributions to the error vector. To evaluate the full error vector, we simply have to figure out all possible contributions. This is done in Ref. [26].

Of course, the result of a Taylor expansion of the exponential functions could be evaluated in the same way, i.e. by writing products of H and T operators and determining all possible contributions. However, the commutator expansion has a slight advantage: Due to the basic commutator relations, (18-11) and (18-12), each T operator must have at least one mode in common with the Hamiltonian. This reduces the number of possible contributions. In the case of a Taylor expansion, there is no such restriction. However, the result will be the same since some terms will cancel out in the end.

The major advantage of the strategy presented in this section relative to the use of the resolution of the identity is the possibility of using intermediates to reduce the scaling. In the VCC [2] model, one of the most demanding contributions turns out to be

$$e_{\mu^{\{m_0 m_1\}}} = \langle \mu^{\{m_0 m_1\}} | \sum_{m_2 o_2} \sum_{m_3 o_3} c_{o_2 o_3}^{m_2 m_3} \tilde{h}_d^{m_2 o_2} \tilde{h}_d^{m_3 o_3} T^{\{m_0 m_2\}} T^{\{m_1 m_3\}} | \Phi_{\mathbf{i}} \rangle. \tag{18-54}$$

The scaling of this contribution is formally $M^4 L^2 N^2$ where M is the number of modes, L is the number of one-mode operators, and N is the number of virtual modals. However, by introducing an intermediate,

$${}_{m_2 o_2} I^{m_1} = \sum_{m_3 o_3} c_{o_2 o_3}^{m_2 m_3} \tilde{h}_d^{m_3 o_3} T^{m_1 m_3}, \tag{18-55}$$

the construction of which scales as $M^3 L^2 N^2$, the contribution may be evaluated with $M^3 L N^2$ effort as

$$e_{\mu^{\{m_0 m_1\}}} = \langle \mu^{\{m_0 m_1\}} | \sum_{m_2 o_2} {}_{m_2 o_2} I^{m_1} \tilde{h}_d^{m_2 o_2} T^{\{m_0 m_2\}} | \Phi_{\mathbf{i}} \rangle. \tag{18-56}$$

Using such tricks the scaling of all contributions to the VCC[2] error vector can be reduced to at most M^3. This is no higher than the corresponding VCI[2] model.

A very efficient implementation of VCC[2] has been made based on the above principles. An illustrative example of the capabilities is provided by a sequence of calculations on duplicated (non-interacting) polyaromatic hydrocarbons, each consisting of seven benzene rings. The timings for a single evaluation of the error vector are shown in Figure 18-8. The "Full MCR" calculation includes all possible two-mode couplings. In this case, the algorithmic scaling is M^3 as argued above.

As previously noted, the MCR concept in the definition of the cluster operator, Eq. (18-21), allows for more elaborate excitation spaces than simply defining a specific excitation level. This is potentially useful for larger systems where the nuclear motion may in some sense be localized. The case of duplicated monomers represents an idealized case of such a system in the sense that each vibration is localized on a single monomer. The calculation labeled ISO1 (interaction space order 1) in Figure 18-8 takes advantage of this artificial localization. Thus, only MCs coupled directly to the reference state by the Hamiltonian are included in MCR[T]. This means that no two-mode cluster operators containing modes from different monomers are included and hence the number of these operators only increases linearly with the number of monomers. The result is a linear scaling of the computational time. We note that this reduction in computational cost does not change the numerical results, i.e. the calculated ground state energies are identical to those obtained from the "Full MCR" calculations. This is due to the exponential parameterization of the wave function. Thus, simultaneous one-mode excitations in different monomers are accounted for

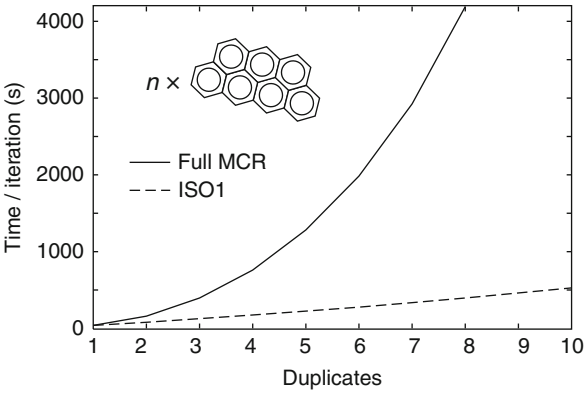

Figure 18-8. Scaling of the VCC [2] algorithm when applied to a set of duplicated, non-interacting polyaromatic hydrocarbon monomers. Each monomer consists of seven benzene rings and has 114 modes. The largest system thus has 1,140 modes. Full MCR refers to a calculation where all two-mode couplings are included. ISO1 includes only couplings also present in the Hamiltonian giving a linear scaling with no loss in accuracy due to the size-extensivity of CC theory.

by the disconnected doubles, i.e. $T_1 T_1$. This manifestation of size-extensivity is another strong argument in favor of VCC over VCI and can only be expected to be of increasing importance as the treatment of larger systems becomes possible.

18.8. SUMMARY

In this chapter, a formulation of CC theory for solving the vibrational Schrödinger equation has been introduced. The theory is build on top of a second quantization formalism appropriate for treating systems with distinguishable degrees of freedom. Compared to the VCI approach which is a standard method in vibrational structure theory, VCC provides a higher accuracy given identical excitation spaces. However, both the derivation and implementation of the VCC equations are significantly more complicated than the corresponding ones in VCI. Different implementation strategies have been discussed in relation to generality and efficiency. While VCC is a relatively new method and still needs much further development and testing, it has much to offer due to its high accuracy, its size-extensivity, and its applicability to large systems. We believe there are good reasons to hope that VCC will open many new possibilities in the study of the internal dynamics of molecules.

ACKNOWLEDGMENTS

O.C. acknowledges support from the Danish Center for Scientific Computing (DCSC), the Danish National Research Foundation, the Lundbeck Foundation, and EUROHORCs for a EURYI award.

REFERENCES

1. O. Christiansen, J. Chem. Phys. **120**, 2140 (2004)
2. O. Christiansen, J. Chem. Phys. **120**, 2149 (2004)
3. P. Jensen, P. Bunker, in *Computational Molecular Spectroscopy* (Wiley, Chichester, 2000)
4. J. M. Bowman, T. Carrington, H. Meyer, Mol. Phys. **106**, 2145 (2008)
5. O. Christiansen, Phys. Chem. Chem. Phys. **9**, 2942 (2007)
6. J. Kongsted, O. Christiansen, J. Chem. Phys. **125**, 124108 (2006)
7. D. Toffoli, J. Kongsted, O. Christiansen, J. Chem. Phys. **127**, 204106 (2007)
8. J. M. Bowman, S. Carter, X. Huang, Int. Rev. Phys. Chem. **22**, 533 (2003)
9. A. Jackle, H. Meyer, J. Chem. Phys. **109**, 3772 (1998)
10. J. O. Jung, R. B. Gerber, J. Chem. Phys. **105**, 10332 (1996)
11. J. K. G. Watson, Mol. Phys. **15**, 479 (1968)
12. J. M. Bowman, Acc. Chem. Res. **19**, 202 (1986)
13. M. A. Ratner, R. B. Gerber, J. Phys. Chem. **90**, 20 (1986)
14. U. B. Kaulfuss, M. Altenbokum, Phys. Rev. D **33**, 3658 (1986)
15. R. F. Bishop, M. F. Flynn, Phys. Rev. A **38**, 2211 (1988)
16. R. F. Bishop, M. C. Bosca, M. F. Flynn, Phys. Rev. A **40**, 3484 (1989)
17. V. Nagalakshmi, V. Lakshminarayana, G. Sumithra, M. D. Prasad, Chem. Phys. Lett. **217**, 279 (1994)
18. S. Banik, S. Pal, M. D. Prasad, J. Chem. Phys. **129**, 134111 (2008)
19. N. Gohaud, D. Begue, C. Darrigan, C. Pouchan, J. Comput. Chem. **26**, 743 (2005)
20. G. Rauhut, J. Chem. Phys. **127**, 184109 (2007)
21. O. Christiansen, P. Jřrgensen, C. Hättig, Int. J. Quantum Chem. **68**, 1 (1998)
22. P. Seidler, O. Christiansen, J. Chem. Phys. **126**, 204101 (2007)
23. H. Romanowski, J. M. Bowman, L. B. Harding, J. Chem. Phys. **82**, 4155 (1985)
24. O. Christiansen, J. M. Luis, Int. J. Quantum Chem. **104**, 667 (2005)
25. E. T. Bell, Am. Math. Month. **41**, 411 (1934)
26. P. Seidler, M. B. Hansen, O. Christiansen, J. Chem. Phys. **128**, 154113 (2008)

CHAPTER 19

ON THE COUPLED-CLUSTER EQUATIONS. STABILITY ANALYSIS AND NONSTANDARD CORRECTION SCHEMES

PÉTER R. SURJÁN AND ÁGNES SZABADOS

Eötvös University, Institute of Chemistry, Laboratory of Theoretical Chemistry, e-mail: surjan@chem.elte.hu; szabados@chem.elte.hu

Abstract: (i) The coupled-cluster equations being nonlinear, they have to be solved iteratively. An insight into the convergence properties of this iteration can be obtained by analyzing the stability of the converged solutions as fixed points. (ii) The usual form of coupled-cluster equations represents an example to the method of moments, with the number of unknown amplitudes being equal to the number of equations. The method of moments generates non-symmetric equations loosing the variational character of the coupled-cluster method, but enabling efficient evaluation of the matrix elements. Taking higher moments into account, one may obtain more equations than parameters, thus the latter must be determined by minimizing the sum-of-squares of all moments. This leads to additional effort but improved coupled-cluster wave functions and/or energies. (iii) Another way of improving the coupled-cluster method is perturbation theory, which needs special formulations due to the nonsymmetric nature of the formalism. An efficient way to do this is offered by multi-configuration perturbation theory.

Keywords: Coupled cluster, Stability analysis, Perturbative corrections

19.1. INTRODUCTION

Most fundamental equations of physics are linear. The basic equation of quantum mechanics, Schrödinger equation, is also linear. Nonlinearity in nature usually appears as a consequence of complexity, often caused by dissipative forces, cf. the field equations of condensed matter (fluid mechanics).

The mathematics of linear equations is relatively simple and well developed. Standard variational tools and eigenproblems offer the solution in most cases. In turn, nonlinear equations usually lack standard methods to solve, and dealing with them one often encounters numerical and conceptual difficulties. Here the variational methods are often replaced by the method of moments, and one may attain the solution only via complicated iteration schemes. One easily gets the impression that whenever the physics of the problem permits, one should rely on linear formulations.

P. Čársky et al. (eds.), Recent Progress in Coupled Cluster Methods, 513–534.
DOI 10.1007/978-90-481-2885-3_19,

A fundamental approximate method of the many-electron problem, however, deals with genuinely nonlinear equations. Coupled-cluster (CC) theory involves exponential wave operators to ensure the extensivity of approximate energies, and generating nonlinearity at the same time. In this review, we emphasize the following issues.

1. The nonlinear nature of the CC equations deserves an analysis of the stability of the solutions. This will offer an insight into the convergence feature of iterative solutions.
2. The CC equations emerge as a trivial application of the method of moments. Improved results can be expected when higher moments, neglected in the standard formulation, are considered.
3. The nonsymmetric nature of the method of moments makes it necessary to develop special perturbation schemes to obtain systematic corrections to a given level of CC theory.

19.2. STABILITY ANALYSIS OF ITERATION SCHEMES

Owing to the size and the nonlinear nature of the CC equations, one uses, almost exclusively, iterative procedures to locate their solutions representing the fixed points of the iteration scheme. To ensure and accelerate convergence, one often applies control parameters or extrapolation techniques such as DIIS [1]. Nonlinearity of the equations represents a complication not only because of iterative solutions, but also by generating spurious solutions. Analysis in this line has been carried out by Jankowski [2]. Here, we begin this review with a standard tool for analyzing convergence features of nonlinear iterative schemes.

The theory of stability matrices and Ljapunov exponents is well established [3]. A general iteration procedure for an m-component vector $\mathbf{x}$ is given as

$$x_i^{(n+1)} = f_i\left(\mathbf{x}^{(n)}\right), \quad i = 1, 2, \ldots m. \tag{19-1}$$

Let vector $\mathbf{a}$ be a fixed point of this iteration:

$$a_i = f_i(\mathbf{a}), \quad i = 1, 2, \ldots m. \tag{19-2}$$

Small deviations around this fixed point are written as

$$\mathbf{x}^{(n)} = \mathbf{a} + \boldsymbol{\xi}^{(n)}. \tag{19-3}$$

Substitution into (19-1) and expanding the m-variable function f into Taylor series up to the first order gives

$$\xi_i^{(n+1)} = \sum_{j=1}^{m} J_{ij}\xi_j^{(n)} + \mathcal{O}(2) \tag{19-4}$$

with the definition of the Jacobian at point **a**

$$J_{ij} = \left.\frac{\partial f_i}{\partial x_j}\right|_{\mathbf{a}}. \tag{19-5}$$

The Jacobi matrix **J** is, in this context, the *stability matrix*. Solution of (19-4) can be looked for in the form

$$\boldsymbol{\xi}^{(n)} = e^{\lambda n}\boldsymbol{\xi}^{(0)} \tag{19-6}$$

which, after substitution into (19-4) and writing $\lambda = \log \mu$ provides the eigenvalue problem

$$\mathbf{J}\boldsymbol{\xi}^{(0)} = \mu\boldsymbol{\xi}^{(0)} \tag{19-7}$$

Modes $\boldsymbol{\xi}^{(0)}$ are eigenvectors of the stability matrix while the logarithm of the eigenvalues give parameters λ which are related to the Ljapunov exponents of the problem.[1]

Analysis of convergence properties of the iteration process (19-1) can be based on the value of the Ljapunov exponents λ, or on their exponentials μ. If all μ-s are positive so all λ-s are real, the procedure converges only if all Ljapunov exponents are negative, that is, if all eigenvalues of the stability matrix satisfy

$$0 < \mu < 1.$$

When one or more exponents are positive, i.e., $\mu > 1$, the iteration will diverge along the corresponding trajectory.

It may happen that one or more eigenvalues of the Ljapunov matrix are negative, generating complex Ljapunov exponents: $\lambda = \lambda_1 + i\lambda_2$. To have a real μ, we require that

$$\mathrm{Im}\, e^{\lambda} = e^{\lambda_1} \sin\lambda_2 = 0,$$

which is satisfied by $\lambda_2 = k\pi$ with any integer k. However, $\mu = \cos\lambda_2\, e^{\lambda_1}$ is negative only for odd k values, thus we may choose $k = 1$. Therefore, the Ljapunov exponent for real, negative μ can be written as

$$\lambda = \log|\mu| + i\pi$$

[1] The more common "dynamical" definition of Ljapunov exponents works with the limit $n \to \infty$; we adopt here a "static" definition based on the converged solution **a**.

leading to the convergence condition

$$\mathrm{Re}\,\lambda = \log|\mu| < 0,$$

which requires the moduli of all eigenvalues to be smaller than unity:

$$|\mu| < 1. \tag{19-8}$$

The iterations in this case are not monotonic, but exhibit oscillatory convergence:

$$\boldsymbol{\xi}^{(n)} = e^{\lambda n}\boldsymbol{\xi}^{(0)} = e^{i\pi n}e^{n\log|\mu|}\boldsymbol{\xi}^{(0)}. \tag{19-9}$$

As the Jacobian is not symmetric, its eigenvalues μ may also become complex. Let us have $\mu = a + ib$. Then, from $e^{\lambda} = a + ib$ we get

$$\left.\begin{aligned} e^{\lambda_1}\cos\lambda_2 &= a \\ e^{\lambda_1}\sin\lambda_2 &= b \end{aligned}\right\}$$

resulting

$$e^{\lambda_1} = \sqrt{a^2 + b^2} = |\mu|,$$

which leads again to (19-8).

All above cases can be summarized in the condition of convergence:

$$|\mu| < 1$$

Violating this condition, the procedure usually diverges, but on the borderline of convergence and divergence, nonlinear systems may also exhibit chaotic iterations [4]. This is manifested in irregular and stochastic iteration patterns.

19.3. THE CC EQUATIONS

Previously [5], we have applied the above theory to study iteration characteristics of the Bloch equation [6, 7] and the idempotency-conserving density matrix iteration [8, 9]. Here we apply it to the CCSD equations.

Using the CC Ansatz $\Psi = \mathrm{e}^{T}\Phi$, we write the Schrödinger equation as

$$\mathrm{e}^{-T}H\,\mathrm{e}^{T}\Phi = E\Phi \tag{19-10}$$

where Φ is the reference state, typically the Hartree-Fock solution. The cluster operator for k-fold excitations T_k is formally written as

$$T_k = \frac{1}{k!} \sum_{\mu} {}^k t_\mu \hat{E}_\mu, \tag{19-11}$$

where ${}^k t_\mu$ are the cluster amplitudes to be determined, and $\hat{E}_\mu$-s are excitation operators which, for closed shell systems, can be written as

$$\hat{E}_\mu = E_u^\beta = \sum_\sigma a_{\beta,\sigma}^\dagger a_{u,\sigma} \tag{19-12}$$

for single and

$$\hat{E}_\mu = E_{uv}^{\beta\gamma} = E_u^\beta E_v^\gamma \tag{19-13}$$

for double excitations. From (19-10), the CC equations for the amplitudes emerge as

$$F_\nu \;=\; \langle \Phi | \hat{E}_\nu^\dagger \, \mathrm{e}^{-T} H \, \mathrm{e}^{T} | \Phi \rangle \;=\; 0. \tag{19-14}$$

Substituting the Hamiltonian, the above forms of the excitation operators and evaluating the matrix elements, this equation can be reduced to its orbital form ${}^1F_u^\beta = 0$ and ${}^2F_{uv}^{\beta\gamma} = 0$. The resulting formulae for CCSD were originally tabulated in Ref. [10], and recollected in the Appendix of Ref. [11]. Both ${}^1t$ and ${}^2t$ equations detailed there are of the shape

$$F(\mathbf{t}) = 0,$$

and there are several ways to recast them into an iterative form $t = f(t)$, e.g. using the scheme

$$t = t + kF(t)$$

where k is a t-independent arbitrary parameter or expression. We consider here the form of the CCSD equations which uses Møller – Plesset-type denominators:

$$t_u^\beta \;=\; t_u^\beta \;-\; \frac{{}^1F_u^\beta}{\varepsilon_\beta - \varepsilon_u - \eta} \tag{19-15}$$

$$t_{uv}^{\beta\gamma} \;= t_{uv}^{\beta\gamma} \;-\; \frac{{}^2F_{uv}^{\beta\gamma}}{\varepsilon_\beta + \varepsilon_\gamma - \varepsilon_u - \varepsilon_v - 2\eta} \tag{19-16}$$

for the ${}^1t$ and ${}^2t$ amplitudes, respectively. Parameter η is introduced merely to control the iteration by damping or accelerating the sequence.[2] In these equations, ε denote orbital energies.

19.4. THE STABILITY MATRIX OF THE CCSD EQUATION

The stability matrix of the CCSD problem can be obtained by taking the derivatives of the iterative equations with respect to the independent parameters. In our case, the latter are represented by the cluster amplitudes ${}^1t_\mu$ and ${}^2t_\mu$. Since the CCSD equations for these amplitudes are coupled, the stability matrix will be composed of four blocks which we denote by ${}^{11}\mathbf{J}$, ${}^{12}\mathbf{J}$, ${}^{21}\mathbf{J}$, ${}^{22}\mathbf{J}$, respectively, where ${}^{mn}\mathbf{J}$ stands for the derivatives of the m-equations with respect to the ${}^nt$ amplitudes. The four blocks of the stability matrix are obtained as

$$
\begin{aligned}
\mathbf{J}^{11}_{u\beta,l\lambda} &= \delta_{ul}\delta_{\beta\lambda} - \frac{\frac{\partial\, {}^1F_{u\beta}}{\partial t^{\lambda}_{l}}}{\varepsilon_\beta - \varepsilon_u - \eta} \\
\mathbf{J}^{12}_{u\beta,lm\lambda\mu} &= -\frac{\frac{\partial\, {}^1F_{u\beta}}{\partial t^{\lambda\mu}_{lm}}}{\varepsilon_\beta - \varepsilon_u - \eta} \\
\mathbf{J}^{21}_{uv\beta\gamma,l\lambda} &= -\frac{\frac{\partial\, {}^2F_{uv\beta\gamma}}{\partial t^{\lambda}_{l}}}{\varepsilon_\beta + \varepsilon_\gamma - \varepsilon_u - \varepsilon_v - 2\eta} \\
\mathbf{J}^{22}_{uv\beta\gamma,lm\lambda\mu} &= \delta_{ul}\delta_{vm}\delta_{\beta\lambda}\delta_{\gamma\mu} - \frac{\frac{\partial\, {}^2F_{uv\beta\gamma}}{\partial t^{\lambda\mu}_{lm}}}{\varepsilon_\beta + \varepsilon_\gamma - \varepsilon_u - \varepsilon_v - 2\eta}.
\end{aligned}
\tag{19-17}
$$

The explicit results for these derivatives are listed in Ref. [11].

The above equations show that the stability matrix $\mathbf{J}$ is in close connection to the Jacobi matrix $\mathbf{J}^0$ of the CCSD equations. The structure of Eq. (19-17) is

$$
J_{ab} = \delta_{ab} - \frac{J^0_{ab}}{\Delta_a - \eta} \tag{19-18}
$$

where Δ_a stands for the energy denominator in the iterative equations. Using Eq. (19-14), we obtain

$$
J^o_{ab} = \frac{\partial F_a}{\partial t_b} = \langle \Phi | \hat{E}^\dagger_a \, \mathrm{e}^{-T} [H, \hat{E}_b] \, \mathrm{e}^{T} | \Phi \rangle
$$

[2] Negative (positive) values for η will damp (accelerate) the iteration by increasing (decreasing) the denominators, respectively.

The eigenvalue equation of this matrix is known as the EOM-CC equation for excitation energies [12–16].

It is important to emphasize the following two features of the above analysis:

- It is valid only if no extrapolation techniques like DIIS are used to govern the iteration. While the DIIS method is known to be highly efficient in accelerating convergence, it does not change the *nature* of the fixed point. If, by a wrongly chosen value for η, the fixed point of the iteration becomes repellent, neither DIIS nor any other extrapolation technique can be expected to ensure convergence.
- The Ljapunov exponents as defined above characterize the nature of the fixed point, rather than the process of the iteration. We always assume that the initial amplitudes lie in the sufficient proximity of the fixed point.

Numerical illustrations of the above theory published in Ref. [11] seem to suggest that a sufficiently large value of the damping parameter η always ensures convergence. We cannot provide a formal proof for this statement. Even if one finds a sufficiently large value for η so that all Ljapunov exponents are negative, this means only that the fixed point of the iteration is attractive. Starting from a set of amplitudes far from the converged ones, the iteration may diverge or may converge to another fixed point. However, we have not yet treated any cases in which convergence was impossible to achieve. (Note that a convergent iteration does not mean that one has reached the desired state.)

In concluding, the nature of the fixed points of the CCSD equations can be analyzed by finding the eigenvalue of the stability matrix which has the largest absolute value. The logarithm of the modulus of the eigenvalue (admitting complex solutions) can be regarded as the Ljapunov exponent of the problem which should be negative to ensure convergence. The nature of the fixed points can be effectively controlled by denominator shifts which may either damp or accelerate the iteration. Connection between the stability matrix $\mathbf{J}$ and the Jacobian $\mathbf{J}^0$ reveals an interesting relation between excitation energies (eigenvalues of $\mathbf{J}^0$) and the Ljapunov exponents (eigenvalues of $\mathbf{J}$).

19.5. IMPROVING CC RESULTS: METHOD OF MOMENTS

In this section, following an idea by Jankowski et al. [17], we investigate a possibility to improve the cluster amplitudes. Emphasizing the close connection between CC theory and the theory of moments, CC amplitudes are determined by minimizing the sum-of-squares of the moments of the Hamiltonian constructed with the CCSD trial function. In addition to standard moments with SD excitations, we include all moments with excitations higher than doubles in an unconstrained minimization. This procedure is computationally demanding thus it does not lead to any practical

method. To circumvent the computational difficulties of amplitude minimization, Jankowski et al. [17] substituted the exponential of the cluster operator by the linearized CCD (LCCD) Ansatz, reducing thereby the moment optimization problem to a solution of a linear system of equations. In this work, keeping the nonlinear e^T Ansatz, we rely on a numerical minimization procedure.

Since the publication of the original work [17], many papers have appeared exploring higher moments in CC theory [18–35]. A common feature of these works is that they, with a given CC Ansatz, use the higher moments either to modify the amplitude equations or derive (noniterative) corrections to the CC energy. For a theoretical comparison of various CC Ansätze, see [36].

Owing to the recent success of utilizing higher moments in CC theory, it appears to be interesting to revisit the problem of moment optimization with the simplest, traditional CCSD Ansatz.

19.5.1. The Method of Moments

The method of moments has been introduced in quantum chemistry a long time ago [37–39]. It can be summarized as follows. If Ψ is an exact eigenvector of H, and E is the associated eigenvalue, any quantities of the form

$$m_\nu = \langle f_\nu \,|H - E|\, \Psi \rangle \quad \nu = 1, 2, \ldots p \tag{19-19}$$

are identically zero for arbitrary well-behaved testing functions f_ν. Quantities m_ν are the moments of the Hamiltonian. If the exact wave function is substituted by an approximate wave function Φ, the above moments are not necessarily zero. Considering Φ to depend on the parameter set t_μ, $\mu = 1, 2, \ldots n$, the best trial function Φ can be determined by minimizing the functional for a given set of testing functions f_ν,

$$M = \sum_{\nu=1}^{p} m_\nu^2 \tag{19-20}$$

with respect to parameters t_μ in Φ. The necessary condition for this minimum is

$$\frac{\partial M}{\partial t_\mu} = 2 \sum_{\nu=1}^{p} m_\nu \frac{\partial m_\nu}{\partial t_\mu} = 0 \qquad \mu = 1, 2, \ldots n \tag{19-21}$$

which constitutes an $n \times n$ system of equations for the n unknown parameters t_μ. One may show that in the special case where (i) the testing functions f_ν are obtained from a common bra generator function depending on the same set of parameters as the ket function Φ, and (ii) the bra generator and the ket trial function are the same, then the method of moments reduces to the variational method.

The accuracy of the method of moments depends on (i) the number of parameters in the trial ket function, n, and (ii) the number of moments considered, p. In general,

p can be much larger than n. The method has a trivial variant when $p = n$ which corresponds to the standard CCSD equations. In this case the functional M can be set exactly zero, since the equations

$$m_\nu = 0$$

can be solved for all ν. This is, of course, not the exact solution if the set of testing functions f_ν-s is restricted.

19.5.2. CC Theory and the Method of Moments

The standard CC method accomplishes the trivial version of the method of moments. To see this, we introduce the similarity-transformed Hamiltonian

$$\overline{H} = e^{-T} H e^{T},$$

and choose the bra test functions as $\langle f_\nu| = \langle 0|\, T_\nu^\dagger$. Therefore, all moments

$$m_\nu \;=\; \langle 0|\, T_\nu^\dagger\, (\overline{H} - E)|0\rangle \;=\; \langle 0|\, T_\nu^\dagger\, \overline{H}\, |0\rangle \;=\; 0 \qquad \text{(19-22)}$$

are required to vanish for $\nu = 1, 2, \ldots n$. Here we used the orthogonality of the test functions to the reference state to get rid of the energy.

Having n amplitudes e.g. in a CCSD wave function, we eliminate only the moments which are projected by single and double substitutions $\langle 0|T_\nu^\dagger$. However, the exponential wave operator e^T and the Hamiltonian H, when acting on the reference state $|0\rangle$, generate moments which correspond to triple, quadruple, etc. excitations. These moments are completely neglected in standard amplitude equations, making CCSD theory non-exact, as many of these moments are nonzero in general.

Stimulated by the theory of moments, one may ask what happens when trying to achieve a balance between the moments emerging from SD and higher excitations. That is, what kind of CCSD amplitudes result by minimizing the functional

$$M = \sum_{\nu=1}^{p} m_\nu^2 \;=\; \sum_{\nu=1}^{p} \left(\langle 0|\, T_\nu^\dagger\, \overline{H}\, |0\rangle\right)^2 \qquad \text{(19-23)}$$

with respect to the CCSD amplitudes t_μ, when

$$\nu = 1, 2, \ldots p \quad (p > n)$$

runs over S, D, T, Q, ... excitations. In the following section a numerical procedure is outlined that is used to perform an unconstrained minimization of the sum of squared moments.

19.5.3. Amplitude Optimization

Solution of the problem represented by the minimization of functional M in Eq. (19-23) can be performed in a general way by numerical optimization techniques. To this end, derivation of the gradients (derivatives of M with respect to the amplitudes) is highly desirable. Components of the gradient vector g

$$g_\lambda = \frac{\partial M}{\partial t_\lambda}$$

were defined in Eq. (19-21). Using the shorthand

$$\langle \nu | = \langle 0 | T_\nu^\dagger$$

and the decomposition

$$T = \sum_\mu t_\mu T_\mu,$$

the derivatives of the individual moments read as

$$\begin{aligned} \frac{\partial m_\nu}{\partial t_\lambda} &= \langle \nu | \frac{\partial e^{-T}}{\partial t_\lambda} H\, e^T | 0 \rangle \; + \; \langle \nu | e^{-T} H \, \frac{\partial e^T}{\partial t_\lambda} | 0 \rangle \\ &= \langle \nu | e^{-T} [H, T_\lambda] e^T | 0 \rangle \end{aligned} \tag{19-24}$$

where the square bracket stands for the commutator.

Evaluation of the matrix elements occurring in (19-24), in principle, can be performed by standard many-body techniques or by applying the more recent automated implementation philosophy [40–45]. The only non-usual ingredient of these formulae is that state $\langle \nu |$ denotes not only an SD, but also higher excited configurations. Fortunately, sixfold excitations are the highest which may contribute [17]. One can also restrict $\langle \nu |$ at a selected lower maximal excitation level, quadruples for example. The need for higher excitations makes the evaluation of matrix elements quite involved, and the string based algorithm [40] can be very helpful.

Having the gradients, one can invoke one of the standard optimization routines to get optimized amplitudes. We have examined the performance of the Broyden – Fletcher – Goldfarb – Shanno (BFGS) procedure [46] and the optimally conditioned (OC) method by Davidon [47]. They were found to perform similarly. As starting parameters for the optimization, standard CCSD amplitudes are convenient to use in most cases.

19.5.4. Numerical Results

The model studies reported so far [48] were obtained not exactly with the above formulae, but with the energy-dependent form of the CC equations. Due to the complexity of the problem, small systems in very small basis sets were considered. Two-electron systems are of course excluded, since for them CCSD is equivalent to full CI.

Consider first a simple four-electron example, the Be atom. Table 19-1 presents standard and moment-optimized CCSD energies in comparison with full CI. The expectation value of the Hamiltonian computed with the actual wave function is also tabulated. To measure the accuracy of the wave function, we give the norm of the

$$|r\rangle = (H - \langle H\rangle)\,|\Psi\rangle$$

residual vector.

Table 19-1 clearly shows that balancing SD and higher moments, results in a slight energy loss. However, the residual norm indicates that overall accuracy of the wave function improves. For Be, this improvement is quite small, it is some 8% in the minimal basis, only 1% in the split shell basis, and less than 4% in the polarized basis set. Similar experience was gained on other small systems.

Table 19-1. Effect of moment-optimized amplitudes on the Be atom. E(CCSD) corresponds to the standard CC energy formula, $\langle H\rangle$ is the expectation value of the Hamiltonian computed by the given wave function, $\sqrt{\langle r|r\rangle}$ is the norm of the residual vector

basis set	level	E(CCSD)	$\langle H\rangle$	$\sqrt{\langle r\|r\rangle}$
STO-6G				
	HF		−14.503361	0.16097
	CCSD	−14.556084	−14.556086	0.00510
	opt-CCSD	−14.556076	−14.556086	0.00472
	FCI		−14.556089	0.0
6-31G				
	HF		−14.566764	0.17153
	CCSD	−14.613518	−14.613518	0.01399
	opt-CCSD	−14.613085	−14.613515	0.01383
	FCI		−14.613545	0.0
6-31G**				
	HF		−14.566944	0.26110
	CCSD	−14.616483	−14.616487	0.03588
	opt-CCSD	−14.614763	−14.616413	0.03462
	FCI		−14.616635	0.0

The slight improvement shown by the residual norm may become important in special cases. Dissociation curves computed by breaking more than one bond at a time were found to constitute such an example. We report here the results for the nitrogen molecule, where a triple bond rupture is monitored. Figure 19-1 shows the case of the N_2 molecule in 6-31G** basis, with the four lowest canonical molecular orbitals (MO) kept frozen. The standard CCSD curve is quite pathologic in this case, an effect well known from previous studies [19, 25, 27, 30, 49–52]. When determining CCSD amplitudes from moment minimization, the erratic behavior of the curve is greatly improved, and the moment optimized CCSD potential curve gets much closer to full CI. The curves can be compared to those showing the expectation value with the CCSD wave function, depicted also in Figure 19-1. With standard CCSD wave function the expectation value gives an acceptable estimation till about $R \sim 2$ Å. When computing the expectation value with moment-optimized CCSD, one gets a curve that is the closest to full CI.

It is notable that in all basis sets collected in Table 19-1 we see an increase of the CCSD energy (often getting away from the exact value). At the same time the wave function improves in the residual norm sense. This fact is tolerable, regarding the non-variational character of the CC Ansatz. However, it is interesting that not only the moment-like CC energy, but also the expectation value of the Hamiltonian may increase (cf. Figure 19-1). This clearly indicates that we are still far from the region

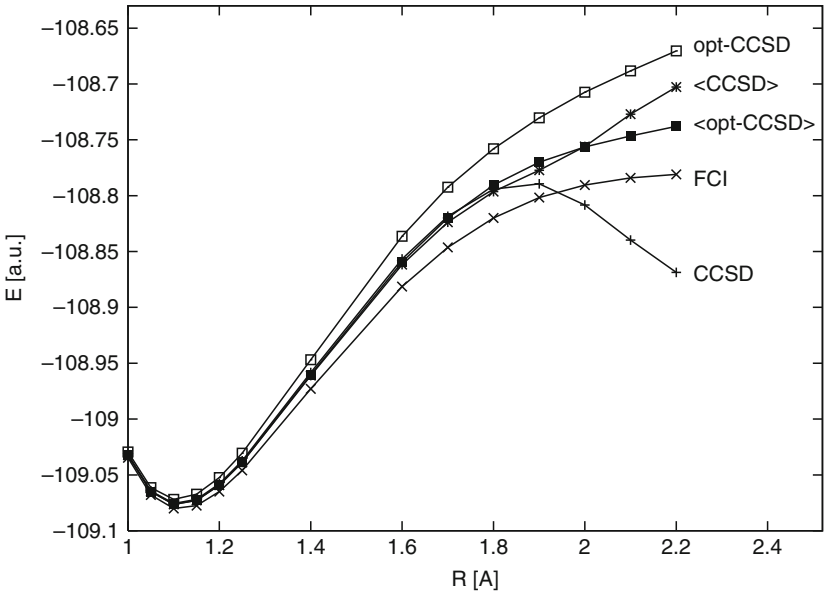

Figure 19-1. Potential curve of the nitrogen molecule in split-valence polarized basis set. Methods used are standard and moment-optimized CCSD. Expectation values taken with both wave functions are also depicted. For abbreviations see text

Table 19-2. Collection of the largest moments for the water molecule at stretched geometry, R_{OH}=2.5 Å, before and after optimization (minimal basis set). Excitations are identified by the serial numbers of the MOs involved. MOs 4 and 5 are the symmetric and antisymmetric combinations of OH bonding orbitals, 6 and 7 are their virtual counterparts. MO 2 is the σ lone pair on the oxygen atom

Excitation	Standard CCSD	Moment-optimized CCSD
$45 \rightarrow 67\ (\alpha,\alpha)$	0.0000	0.0197
$45 \rightarrow 67\ (\alpha,\beta)$	0.0000	–0.0146
$55 \rightarrow 66$	0.0000	0.0249
$55 \rightarrow 77$	0.0000	–0.0178
$44 \rightarrow 66$	0.0000	–0.0179
$44 \rightarrow 77$	0.0000	0.0239
$4545 \rightarrow 6767$	0.2461	0.0130
$2525 \rightarrow 6767$	0.0169	0.0007
$2424 \rightarrow 6767$	0.0183	0.0023

of validity of the Eckart theorem [53] which, for non-degenerate states would require the simultaneous improvement of the energy and the wave function.

To gain a better insight into the effect of moment optimization, we have collected the moments larger than 0.005 in absolute value for water in Table 19-2. First few lines of the Table show various double excitations. The associated moments are exactly zero in standard CCSD, as they should be. The last three lines correspond to quadruple excitations, among which the $4545 \rightarrow 6767$ frontier excitation has an enormous moment, almost 0.25. Certainly, in this small basis set appearance of this huge moment is responsible for the failure of CCSD at this geometry. Upon minimizing all moments democratically, we find that this large moment is greatly reduced, at the price of generating small moments in the SD space. Upon minimization the other two quadruple moments also diminish by an order of magnitude.

In summarizing, we have investigated the quality of the CCSD wave function and the associated energy upon performing an unconstrained optimization of the sum of moment squares with respect to CCSD amplitudes. The numbers presented above permit us to draw two general conclusions: (i) in each case studied the CCSD energy raises when computed with moment-optimized amplitudes, while (ii) the wave function improves in a residual norm sense, if compared with standard CCSD. This observation is quite significant, particularly when CCSD fails due to its non-variational behavior, like the cases of stretched multiple bonds.

19.6. IMPROVING CC RESULTS: PERTURBATION THEORY

The usual formulation of Rayleigh – Schrödinger perturbation theory (PT) relies on the availability of the full set of right- and left eigenvectors of a zero order Hamiltonian. In multi-reference perturbation theory this requirement is relaxed, and perturbed wave functions are often expanded in auxiliary bases. In most formulations, the symmetry between bra and ket vectors is kept, however. In coupled cluster theory, it is appropriate to abandon this latter constraint too, owing to the essentially non-symmetric (moment-like) nature of the formalism. A general perturbative tool that can be routinely applied even is such cases is the so-called multi-configuration perturbation theory (MCPT) [54–56]. A short review of this formalism as applied to a coupled cluster wave function is presented below.

19.6.1. Nonsymmetric PT Formulation

Consider a multiconfigurational reference state $|\mathrm{CC}\rangle$ in intermediate normalization:

$$|\mathrm{CC}\rangle \;=\; |\mathrm{HF}\rangle \;+\; \sum_{k=1} d_k \,|k\rangle \;,$$

where $|k\rangle$ denotes determinants obtained by applying single, double etc. excitations to the Fermi vacuum $|\mathrm{HF}\rangle$. Determinant $|k\rangle$ with $k = 0$ will be identified as the Fermi vacuum. Coefficients d_k can be obtained by conversion of CC amplitudes to CI coefficients [57], e.g.

$$d_{ij}^{ab} \;=\; t_{ij}^{ab} + t_i^a t_j^b - t_i^b t_j^a$$

if determinant k is associated with excitation $i,j \to a,b$.

A skew-projector $\hat{O}$ can be taken down in terms of the coupled-cluster wave function and the Fermi-vacuum in the following form

$$\hat{O} \;=\; |\mathrm{CC}\rangle\langle\mathrm{HF}| \;.$$

It is easily seen that operator $\hat{O}$ is idempotent and leaves $|\mathrm{CC}\rangle$ and $\langle\mathrm{HF}|$ intact. The projector orthogonal and complementary to $\hat{O}$ can be defined as

$$\hat{P} \;=\; \hat{1} - \hat{O}$$

It is also trivially verified that $\hat{P}|\mathrm{CC}\rangle$ results zero as well as $\langle\mathrm{HF}|\hat{P}$ while

$$\hat{P}|k\rangle \;=\; |k\rangle$$

for $k \geq 1$. A spectral form of projector $\hat{P}$ can be constructed, starting from the representation of the identity

$$\hat{1} = \sum_{k=0} |k\rangle\langle k|$$

and writing

$$\hat{P} = \hat{1}\hat{P} = \sum_{k=1} |k\rangle\langle k|\hat{P} \tag{19-25}$$

where $k = 0$ is omitted from the sum since $\langle \mathrm{HF}|\hat{P} = 0$. Expression (19-25) is in fact a biorthogonal spectral resolution of operator $\hat{P}$ formulated in terms of direct space vectors $|k\rangle$ and reciprocal space vectors

$$\langle\tilde{k}| = \langle k|\hat{P} = \langle k| - d_k\langle \mathrm{HF}| \, .$$

It is indeed straightforward to see, that vectors $|\mathrm{CC}\rangle$ and $|k\rangle$ for $k \geq 1$ form a biorthogonal set with vectors $\langle \mathrm{HF}|$ and $\langle\tilde{k}|$, satisfying the conditions

$$\begin{aligned} \langle \mathrm{HF}|\mathrm{CC}\rangle &= 1 \qquad \langle \mathrm{HF}|l\rangle = 0 \\ \langle\tilde{k}|\mathrm{CC}\rangle &= 0 \qquad \langle\tilde{k}|l\rangle = \delta_{kl} \end{aligned}$$

with $k, l \geq 1$. In terms of the above direct and reciprocal space vectors a non-Hermitean zero-order Hamiltonian can be taken down in the form

$$\hat{H}^0 = E_{\mathrm{CC}} \, |\mathrm{CC}\rangle\langle \mathrm{HF}| + \sum_{k=1} E_k \, |k\rangle\langle\tilde{k}| \tag{19-26}$$

where $E_{\mathrm{CC}} = \langle \mathrm{HF}|\hat{H}|\mathrm{CC}\rangle$ is the coupled-cluster energy. The excited state energies E_k are parameters of the theory. They are in principle arbitrary quantities that define $\hat{H}^0$, i.e. the *partitioning*. The above definition of $\hat{H}^0$ possesses the properties

$$\hat{H}^0 \, |\mathrm{CC}\rangle = E_{\mathrm{CC}} \, |\mathrm{CC}\rangle \tag{19-27}$$

and

$$\hat{H}^0 \, |k\rangle = E_k \, |k\rangle \, .$$

One can similarly see, that left eigenvectors of operator (19-26) are vectors $\langle\tilde{k}|$ and the principal determinant $\langle \mathrm{HF}|$.

Perturbation theory using a biorthogonal vector set as constructed above differs from usual Rayleigh – Schrödinger PT only in that reciprocal (biorthogonal)

functions are used in the bra vectors of each matrix element. (For applications of biorthogonal PT in the theory of chemical bond and intermolecular interactions, see Refs. [58–60].) Accordingly, for the first order energy correction of the ground state E_{CC} we get:

$$E^{(1)} \;=\; \langle \mathrm{HF}|\hat{W}|\mathrm{CC}\rangle \;=\; 0$$

having utilized Eq. (19-27). The second order looks

$$E^{(2)} = -\sum_{k=1} \frac{\langle \mathrm{HF}|\hat{W}|k\rangle\langle\tilde{k}|\hat{W}|\mathrm{CC}\rangle}{E_k - E_{\mathrm{CC}}} \tag{19-28}$$

with $\hat{W} = \hat{H} - \hat{H}^0$. Higher order PT corrections can be put down similarly.

Before discussing the question of partitioning, let us analyse the numerator of the second order energy (19-28). One readily sees that $\hat{W}$ can be substituted for $\hat{H}$ in the matrix elements, regarding that $|\mathrm{CC}\rangle$ and $\langle \mathrm{HF}|$ are eigenvectors to $\hat{H}^0$ from the right and left, respectively. Matrix element $\langle \mathrm{HF}|\hat{H}|k\rangle$ ensures that at most doubly excited determinants can contribute to the expression, while matrix element

$$\langle\tilde{k}|\hat{H}|\mathrm{CC}\rangle \;=\; \langle k|\hat{H} - E_{\mathrm{CC}}|\mathrm{CC}\rangle = 0 \tag{19-29}$$

sets all the terms zero as a result of the converged CCSD equations. The first nonzero energy correction of the theory is therefore the third order term

$$E^{(3)} = \sum_{kl} \frac{\langle \mathrm{HF}|\hat{W}|k\rangle\langle\tilde{k}|\hat{W}|l\rangle\langle\tilde{l}|\hat{W}|\mathrm{CC}\rangle}{(E_k - E_{\mathrm{CC}})\,(E_l - E_{\mathrm{CC}})} \,.$$

Energy corrections obtained by the above theory are tabulated up to order 5 for the HF molecule in 6-31G* basis set in Table 19-3. Partitioning used in this calculation is given by e.g.

$$E_k \;=\; E_{\mathrm{CC}} + \varepsilon_a + \varepsilon_b - \varepsilon_i - \varepsilon_j \tag{19-30}$$

if determinant k arises upon excitation $i,j \to a,b$ acting on the Fermi vacuum. One particle energies ε_p are Hartree – Fock orbital energies. When willing to describe a situation where single-reference theories fail, e.g. bond breaking, it is wise to make a different choice for one particle energies. In this case ionization potentials and electron affinities have been successfully used instead of Koopmans values [61–63].

Inspecting data of Table 19-3 one sees that the third order correction represents a considerable improvement upon the CCSD energy. As the covalent bond is stretched, the third order energy deteriorates, which is a consequence of the partitioning choice. The error increases from about a tenth of a milliHartree around equilibrium distance to about one milliHartree at twice the equilibrium length. At $2.0R_e$ the third order

Table 19-3. PT energy errors $E - E_{\mathrm{FCI}}$ [mHartree] for the H-F molecule in 6-31G* basis set, frozen core approximation ($R_e = 0.917$ Å). Reference function is a CCSD wave function. Full CI energies in Hartree are -100.188421 (R_e), -100.108796 ($1.5R_e$), -100.034004 ($2.0R_e$)

	Geometry		
Order	R_e	$1.5R_e$	$2.0R_e$
Nonsymmetric theory			
0	2.146	4.313	9.474
3	−0.074	0.146	1.386
4	0.312	1.108	3.773
5	−0.080	−0.155	−0.170
Symmetric theory			
0	1.93	3.939	8.437
2	0.279	0.636	1.553
3	0.160	0.427	1.121
CCSD(T)	0.457	0.840	0.275

approximation is worse than the CCSD(T) result. Regarding higher orders, it is notable that correction of order 4 does not represent any improvement, and the PT series manifestly oscillates around the exact value.

19.6.2. Symmetric PT Formulation

A somewhat better behaving PT series is obtained if turning to a more symmetrical PT framework. This is however computationally demanding as it starts with a symmetrical projector of the form

$$\hat{Q} \;=\; \frac{|\mathrm{CC}\rangle\langle\mathrm{CC}|}{\langle\mathrm{CC}|\mathrm{CC}\rangle}$$

where the norm of the coupled-cluster wave function is not computable for anything but small model problems. If pursuing the theory even with such computational limitations in mind, one takes down the orthogonal and complementary projector to $\hat{Q}$

$$\hat{R} \;=\; \hat{1} \;-\; \hat{Q}\,.$$

To find a spectral form of projector $\hat{R}$ let us evaluate the product $\hat{P}\hat{R}$, which leads to

$$\begin{aligned}\hat{P}\hat{R} &= (\hat{1} \;-\; |\mathrm{CC}\rangle\langle\mathrm{HF}|)\left(\hat{1} \;-\; \frac{|\mathrm{CC}\rangle\langle\mathrm{CC}|}{\langle\mathrm{CC}|\mathrm{CC}\rangle}\right)\\ &= \hat{1} \;-\; |\mathrm{CC}\rangle\langle\mathrm{HF}| \;=\; \hat{P}\,,\end{aligned}$$

while if multiplying the two projectors in reverse order, one gets

$$\hat{R}\hat{P} \;=\; \hat{R}\,.$$

Let us then write projector $\hat{R}$ as

$$\hat{R} \;=\; \hat{R}\hat{1}\hat{P} \;=\; \sum_{k=1} \hat{R}|k\rangle\langle k|\hat{P} \tag{19-31}$$

where again the term $k = 0$ is omitted from the sum, because $\langle k|\hat{P} = 0$. Just as in the previous case, one can observe the right hand side of expression (19-31) being of the form of a biorthogonal spectral resolution with direct space vectors

$$|k'\rangle \;=\; \hat{R}|k\rangle$$

and reciprocal vectors

$$\langle\tilde{k'}| \;=\; \langle k|\hat{P}\,.$$

In fact it can be verified that biorthogonal relations

$$\begin{aligned} \langle \mathrm{CC}|\mathrm{CC}\rangle/\langle \mathrm{CC}|\mathrm{CC}\rangle = 1 \qquad & \langle \mathrm{CC}|l'\rangle = 0 \\ \langle\tilde{k'}|\mathrm{CC}\rangle = 0 \qquad & \langle\tilde{k'}|l'\rangle = \delta_{kl} \end{aligned}$$

indeed hold for $k, l \geq 1$.

Zero-order Hamiltonian in terms of these direct and reciprocal space vectors is now formulated as

$$\hat{H}^0 \;=\; \overline{E}_{\mathrm{CC}}\,\frac{|\mathrm{CC}\rangle\langle\mathrm{CC}|}{\langle\mathrm{CC}|\mathrm{CC}\rangle} \;+\; \sum_{k=1} E_k\,|k'\rangle\langle\tilde{k'}| \tag{19-32}$$

with $\overline{E}_{\mathrm{CC}} = \langle \mathrm{CC}|\hat{H}|\mathrm{CC}\rangle/\langle \mathrm{CC}|\mathrm{CC}\rangle$. Using biorthogonal PT the energy terms arising from this zero-order choice are

$$\begin{aligned} E^{(1)} \;&=\; \langle \mathrm{CC}|\hat{W}|\mathrm{CC}\rangle/\langle \mathrm{CC}|\mathrm{CC}\rangle \;=\; 0 \\ E^{(2)} &= -\frac{1}{\langle \mathrm{CC}|\mathrm{CC}\rangle}\sum_{k=1}\frac{\langle \mathrm{CC}|\hat{W}|k'\rangle\langle\tilde{k'}|\hat{W}|\mathrm{CC}\rangle}{E_k - E_{\mathrm{CC}}} \end{aligned} \tag{19-33}$$

with $\hat{W} = \hat{H} - \hat{H}^0$. Higher orders can be constructed analogously.

Inspecting second order expression (19-33), one immediately sees, that matrix element $\langle\tilde{k'}|\hat{W}|\mathrm{CC}\rangle$ in the numerator is zero for singly or doubly excited determinants, for the reason (19-29). However, at difference with the previous PT formulation, the states contributing to $E^{(2)}$ are not restricted to singles and doubles. In this latter approach every determinant that may interact with the coupled-cluster function

via the Hamiltonian contributes to the second order correction. This may involve the full configuration space and therefore it is highly impractical.

Note, that this approach is symmetric only as what concerns projector $\hat{Q}$. Projector $\hat{R}$ is still represented in the form of a biorthogonal spectral resolution, i.e. direct and reciprocal vectors are different. When computing the illustrative examples shown in Table 19-3, we neglected primes and tildes in expression (19-33), and also in the third order formula. Hence the presented numbers should be considered only approximate. Second and third order energies shown in the table are obtained by the partitioning of Eq. (19-30). The results indicate that in the symmetric formulation the errors slowly but systematically decrease with increasing order. Note however that the first nonvanishing correction is better in the case of the nonsymmetric theory. The difference between second order by the symmetric theory and third order by the nonsymmetric approach is diminished as the interatomic distance is enlarged.

19.6.3. Connected Moment Expansion

The marked difference between symmetric and moment-like formulation of corrections to the coupled-cluster wave function has been observed in a different context also [64]. In this study the Horn – Weinstein function

$$f(\alpha) \;=\; \frac{\langle \mathrm{CC}|\hat{H}e^{-\alpha\hat{H}}|\mathrm{CC}\rangle}{\langle \mathrm{CC}|e^{-\alpha\hat{H}}|\mathrm{CC}\rangle}$$

and its momentum-type analogue

$$\tilde{f}(\alpha) \;=\; \frac{\langle \mathrm{HF}|\hat{H}e^{-\alpha\hat{H}}e^{\hat{T}}|\mathrm{HF}\rangle}{\langle \mathrm{HF}|e^{-\alpha\hat{H}}e^{\hat{T}}|\mathrm{HF}\rangle}$$

constitute the basis of the approximations. Both of the above functions tend to the ground state eigenvalue of $\hat{H}$ as $\alpha \to \infty$. Derivative of f with respect to α evaluated at $\alpha = 0$ are related to the so-called connected moments of the Hamiltonian

$$\begin{aligned} f(0) = I_1 \;&=\; \langle\hat{H}\rangle/\mathcal{N} \\ -\left.\frac{\mathrm{d}f}{\mathrm{d}\alpha}\right|_{\alpha=0} = I_2 \;&=\; \langle\hat{H}^2\rangle/\mathcal{N} \;-\; \langle\hat{H}\rangle^2/\mathcal{N}^2 \\ -\left.\frac{\mathrm{d}^2f}{\mathrm{d}\alpha^2}\right|_{\alpha=0} = I_3 \;&=\; \langle\hat{H}^3\rangle/\mathcal{N} \;-\; 3\langle\hat{H}^2\rangle\langle\hat{H}\rangle/\mathcal{N}^2 \;+\; 2\langle\hat{H}\rangle^3/\mathcal{N}^3 \end{aligned}$$

and similarly for higher derivatives. Here, we used $\langle \mathrm{CC}|\hat{H}^k|\mathrm{CC}\rangle = \langle\hat{H}^k\rangle$ and the squared norm of the coupled cluster function is denoted by $\mathcal{N}$. The connected moments can be used for constructing a successive approximation to the ground state energy e.g. in the form [65]

$$E = I_1 - I_2^2/I_3 - \ldots \tag{19-34}$$

The analogous treatment of function $\tilde{f}$ leads to another infinite series for the ground state energy,

$$E = \tilde{I}_1 - \tilde{I}_2^2/\tilde{I}_3 - \ldots \tag{19-35}$$

which is considerably cheaper to compute as the coupled-cluster function never figures in the bra vectors of the modified connected moments

$$\begin{aligned} \tilde{f}(0) = \tilde{I}_1 &= \langle e^{-\hat{T}} \hat{H} e^{\hat{T}} \rangle = \langle \overline{H} \rangle \\ -\left.\frac{\mathrm{d}\tilde{f}}{\mathrm{d}\alpha}\right|_{\alpha=0} &= \tilde{I}_2 = \langle \overline{H}^2 \rangle - \langle \overline{H} \rangle^2 \\ -\left.\frac{\mathrm{d}^2 f}{\mathrm{d}\alpha^2}\right|_{\alpha=0} &= I_3 = \langle \overline{H}^3 \rangle - 3\langle \overline{H}^2 \rangle \langle \overline{H} \rangle + 2\langle \overline{H} \rangle^3 \end{aligned}$$

where we used $\overline{H} = e^{-\hat{T}} \hat{H} e^{\hat{T}}$ and $\langle \mathrm{HF}|\overline{H}^k|\mathrm{HF}\rangle = \langle \overline{H}^k \rangle$. In analogy with the PT formulation, it can be shown that the second connected moment in the nonsymmetric theory is exactly zero due to the fulfillment of the coupled-cluster equations. As it was found in Ref. [64], only the impractical symmetric expansion (19-34) offers good corrections, while the accuracy of the nonsymmetric expansion (19-35) is insufficient.

Regarding the coupled cluster wave function as a multiconfigurational reference, systematic improvement is possible to obtain by the MCPT approach, either following the symmetric or the nonsymmetric formulation. Noniterative corrections can be also derived by means of connected moments. Both schemes show that numbers obtained from a symmetric version are more reliable, though these methods can not be used in practice. The third (first nonvanishing) order of the nonsymmetric MCPT seems to offer a reliable and practical tool.

ACKNOWLEDGMENTS

The authors thank D. Mukherjee, Z. Rolik and P. Szakács for extensive discussions. Partial support from grants OTKA K-81588, K-81590, NI-67702 and TetIndo4/2006 is acknowledged.

REFERENCES

1. G. E. Scuseria, T. J. Lee, H. F. Schaefer III, Chem. Phys. Lett. **130**, 236 (1986)
2. K. Kowalski, K. Jankowski, Phys. Rev. Lett. **81**, 1195 (1998)

3. Granino A. Korn and Thresa M. Korn, in *Mathematical Handbook for Scientists and Engineers* (McGraw Hill, New York, 1968)
4. E. Ott, in *Chaos in Dynamical Systems* (Cambridge University Press, Cambridge, 1993)
5. P. Szakács, P. R. Surján, J. Math. Chem. **43**, 314 (2008)
6. I. Lindgren, J. Morrison, in *Atomic Many-Body Theory* (Springer, Berlin, 1986)
7. P. O. Löwdin, Int. J. Quantum Chem. **72**, 370 (1999)
8. D. Kőhalmi, Á. Szabados, P. R. Surján, Phys. Rev. Lett. **95**, 13002 (2005)
9. Z. Szekeres, P. G. Mezey, P. R. Surján, Chem. Phys. Lett. **424**, 420 (2006)
10. G. E. Scuseria, C. L. Janssen, H. F. Schaefer, J. Chem. Phys. **89**, 7382 (1988)
11. P. Szakács, P. R. Surján, Int. J. Quantum Chem. **108**, 2043 (2008)
12. J.Geertsen, M. Rittby, R. J. Bartlett, Chem. Phys. Lett. **164**, 57 (1989)
13. J. F. Stanton, R. J. Bartlett, J. Chem. Phys. **98**, 7029 (1993)
14. L. Meissner, R. J. Bartlett, J. Chem. Phys. **102**, 7490 (1995)
15. O. Christiansen, H. Koch, P. Jørgensen, Chem. Phys. Lett. **243**, 409 (1995)
16. H. Koch, O. Christiansen, P. Jørgensen, A. M. S. de Meras, T. Helgaker, J. Chem. Phys. **106**, 1808 (1997)
17. K. Jankowski, J. Paldus, P. Piecuch, Theor. Chim. Acta **80**, 223 (1991)
18. X. Li, J. Paldus, J. Chem. Phys. **115**, 5759 (2001)
19. X. Li, J. Paldus, J. Chem. Phys. **115**, 5774 (2001)
20. X. Li, J. Paldus, J. Chem. Phys. **117**, 1941 (2002)
21. X. Li, J. Paldus, J. Chem. Phys. **118**, 2470 (2003)
22. J. Paldus, X. Li, Collec. Czech. Chem. Commun. **68**, 554 (2003)
23. J. Paldus, X. Li, Int. J. Mod. Phys. B **17**, 5379 (2003)
24. K. Kowalski, P. Piecuch, Mol. Phys. **102**, 2425 (2004)
25. K. Kowalski, P. D. Fan, P. Piecuch, Mol. Phys. **103**, 2191 (2005)
26. K. Kowalski, P. Piecuch, J. Chem. Phys. **113**, 18 (2000)
27. K. Kowalski, P. Piecuch, J. Chem. Phys. **113**, 5644 (2000)
28. P. Piecuch, K. Kowalski, I. S. O. Pimienta, M. J. McGuire, Int. Rev. Phys. Chem. **21**, 527 (2002)
29. I. S. O. Pimienta, K. Kowalski, P. Piecuch, J. Chem. Phys. **119**, 2951 (2003)
30. P. Piecuch, K. Kowalski, I. S. O. Pimienta, P. D. Fan, M. Lodriguito, M. J. McGuire, S. A. Kucharski, T. Kuś, M. Musiał, Theor. Chem. Acc. **112**, 349 (2004)
31. P. Piecuch, M. Włoch, J. R. Gour, A. Kinal, Chem. Phys. Lett. **418**, 463 (2005)
32. P. Piecuch, M. Włoch, J. Chem. Phys. **123**, 224105 (2005)
33. I. Ozkan, A. Kinal, M. Balci, J. Phys. Chem. A **108**, 507 (2004)
34. M. J. McGuire, P. Piecuch, J. Am. Chem. Soc. **127**, 2608 (2005)
35. C. J. Cramer, M. Włoch, P. Piecuch, C. Puzzarini, L. Gagliardi, J. Phys. Chem. A **110**, 1991 (2006)
36. P. G. Szalay, M. Nooijen, R. J. Bartlett, J. Chem. Phys. **103**, 281 (1995)
37. E. Szondy, T. Szondy, Acta Phys. Hung. **20**, 253 (1966)
38. M. Hegyi, M. Mezei, T. Szondy, Theor. Chim. Acta **21**, 168 (1971)
39. K. Ladányi, V. Lengyel, T. Szondy, Theor. Chim. Acta **21**, 176 (1971)
40. M. Kállay, P. R. Surján, J. Chem. Phys. **115**, 2945 (2001)
41. S. Hirata, P. D. Fan, A. A. Auer, M. Nooijen, P. Piecuch, J. Chem. Phys. **121**, 12197 (2004)
42. A. Hartono, A. Sibiryakov, M. Nooijen, G. Baumgartner, D. E. Bernholdt, S. Hirata, C. C. Lam, R. M. Pitzer, J. Ramanujam, P. Sadayappan, Lect. Notes Comput. Sci. **3514**, 155 (2005)
43. S. Hirata, J. Phys. Chem. A **107**, 9887 (2003)
44. S. Hirata, J. Chem. Phys. **121**, 51 (2004)
45. P. Piecuch, S. Hirata, K. Kowalski, P. D. Fan, T. L. Windus, Int. J. Quantum Chem. **106**, 79 (2006)
46. R. Fletcher, Comput. J. **13**, 317 (1970)
47. W. C. Davidon, Math. Prog. **9**, 1 (1975)

48. Z. Rolik, D. K. Á. Szabados, P. R. Surján, J. Mol. Struct. (THEOCHEM) **768**, 1723 (2006)
49. T. V. Voorhis, M. Head-Gordon, Chem. Phys. Lett. **317**, 575 (2000)
50. T.V. Voorhis, M. Head-Gordon, J. Chem. Phys. **115**(17), 7814 (2001)
51. P. Piecuch, V. Spirko, A. E. Kondo, J. Paldus, J. Chem. Phys. **104**, 4699 (1996)
52. W. D. Laidig, P. Saxe, R. J. Bartlett, J. Chem. Phys. **86**, 887 (1987)
53. C. E. Eckart, Phys. Rev. **36**, 878 (1930)
54. P. R. Surján, Á. Szabados, Z. Szekeres, Int. J. Quantum Chem. **90**, 1309 (2002)
55. Z. Rolik, Á. Szabados, P.R. Surján, J. Chem. Phys. **119**, 1922 (2003)
56. Á. Szabados, Z. Rolik, G. Tóth, P. R. Surján, J. Chem. Phys. **122**, 114104 (2005)
57. I. Mayer, in *Simple Theorems, Proofs, and Derivations in Quantum Chemistry* (Kluwer, New York, 2003)
58. P. R. Surján, I. Mayer, I. Lukovits, Phys. Rev. A **32**, 748 (1985)
59. P. R. Surján, I. Mayer, I. Lukovits, Chem. Phys. Lett. **119**, 538 (1985)
60. P. R. Surján, I. Mayer, J. Mol. Struct. (THEOCHEM) **226**, 47 (1991)
61. A. Zaitevskii, J. P. Malrieu, Chem. Phys. Lett. **233**, 597 (1995)
62. P. R. Surján, Á. Szabados, Int. J. Quantum Chem. **69**, 713 (1998)
63. Y. Mochizuki, Chem. Phys. Lett. **472**, 143 (2009)
64. J. Noga, Á. Szabados, P. R. Surján, Int. J. Mol. Sci. **3**, 508 (2002)
65. J. Cioslowski, Phys. Rev. Lett. **58**, 83 (1987)

CHAPTER 20

EXPLICITLY CORRELATED COUPLED-CLUSTER THEORY

DAVID P. TEW[1], CHRISTOF HÄTTIG[2], RAFAŁ A. BACHORZ[3], AND WIM KLOPPER[3]

[1] *School of Chemistry, University of Bristol, Bristol BS8 1TS, UK, e-mail: david.tew@bristol.ac.uk*
[2] *Lehrstuhl für Theoretische Chemie, Ruhr-Universität Bochum, D-44780 Bochum, Germany, e-mail: christof.haettig@theochem.ruhr-uni-bochum.de*
[3] *Institut für Physikalische Chemie, Karlsruhe Institute of Technology, KIT Campus South, Kaiserstr. 12, D-76131 Karlsruhe, Germany, e-mail: rafal.bachorz@chem-bio.uni-karlsruhe.de; klopper@kit.edu*

Abstract: The theoretical prediction of molecular energies and properties to chemical accuracy is often achieved using coupled-cluster methods and large orbital basis sets. Through recent advances in F12 explicitly correlated methods it is now possible to obtain the same high accuracy far more efficiently, using much smaller orbital basis sets. In CCSD(T)-F12 methods, the basis set truncation error is almost entirely eliminated by introducing a small set of two-particle basis functions that depend explicitly on the inter-electronic distances and closely resemble the correlation hole. The computational expense of including the F12 geminals can be reduced to a fraction of that of the underlying CCSD(T) calculation through judicious insertions of resolution of the identity approximations and further simplifications. In this chapter we present CCSD(T)-F12 theory and review the simplified models CCSD(T)(F12), CCSD(T)-F12x and CCSD(T)$_{\overline{\text{F12}}}$, demonstrating their utility for practical applications. In contrast to standard CCSD(T), the Hartree–Fock basis set error may limit the accuracy of a CCSD(T)-F12 calculation and we therefore also describe methods for improving the Hartree–Fock energy within an F12 calculation. A brief discussion on the extension of F12 theory to reduce basis set errors in connected triples and response properties is also presented.

Keywords: Coupled cluster, R12 approach, F12 approach, Explicitly correlated

20.1. INTRODUCTION

The success of coupled-cluster methods for the computational investigation of chemical phenomena lies in the rapid and systematic convergence of the hierarchy of coupled-cluster models [1–5] towards the exact solution of the Schrödinger equation. The CCSD(T) method [6], which accounts for one- and two-electron interactions

P. Čársky et al. (eds.), Recent Progress in Coupled Cluster Methods, 535–572.
DOI 10.1007/978-90-481-2885-3_20,

with a perturbative treatment of the simultaneous interaction of three electrons, has long been a standard tool for quantum chemists, providing reliably high accuracy for predictions of molecular energies and properties. For example, atomization energies computed using CCSD(T) are generally within 5 kJ mol^{-1} of experimental values for light molecules. The corresponding accuracy for bond lengths is typically 0.1–0.2 pm and harmonic frequencies are accurate to 6–10 cm^{-1}.

However, the intrinsic accuracy of the coupled-cluster models is only realized if they are used in combination with sufficiently large orbital basis sets. Even when using basis sets of quadruple-ζ quality, the basis set errors in frozen-core CCSD(T) calculations of reaction energies are typically larger than the influence of post-CCSD(T) corrections and thus limit the accuracy of the calculation. When aiming for 1 kJ mol^{-1} accuracy [7–10], by combining CCSD(T) energies with corrections for relativistic and non-adiabatic effects and higher-order correlation (including core-valence correlation), it is necessary to reduce the CCSD(T) basis set error below that remaining from cc-pV6Z calculations. Indeed, the basis set errors in the post-CCSD(T) corrections are also problematic. Since the computational resources required for a coupled-cluster calculation scale with basis size as N_{AO}^4 at least, where N_{AO} is the number of basis functions per atom, the necessity for large basis sets severely limits the applicability of coupled-cluster approaches.

Extrapolation techniques [11–14], which exploit the relatively smooth convergence of the energy with basis set cardinal number X, are widely applied to reduce the basis set error. For example, extrapolations based on cc-pVTZ and cc-pVQZ calculations are generally as accurate as cc-pV5Z calculations. Although extrapolation goes some way to alleviating the basis set problem, it is still necessary to use relatively large basis sets to realize the intrinsic accuracy of the coupled-cluster methods and the extension of extrapolation techniques to molecular properties is not always clear cut. F12 explicitly correlated methods are a far more direct and efficient solution to the basis set problem. Based on the ideas of Kutzelnigg [15], the coupled-cluster wave function is expanded using one- and two-particle basis functions, which depend explicitly on the inter-electronic distance r_{12}. In this chapter, we present the current status of F12 explicitly correlated coupled-cluster theory, demonstrating that near basis set limit accuracy is obtained with comparatively small orbital basis sets and a low computational cost.

20.2. R12 AND F12 EXPLICITLY CORRELATED METHODS

The root of the basis set problem lies in the inefficient description of the shape of the correlation hole at short inter-electronic distances. Since the Coulomb singularity must be canceled by an equal and opposite singularity in the kinetic energy, all correlated wave functions formally exhibit a linear dependence on r_{12} when two electrons approach each other, which culminates in a cusp at electron coalescence for singlet spin-coupled pairs (Kato's cusp condition – see Section 20.6.1). For MP2, the spin-adapted first order pair functions $|u_{ij}^{(s)}\rangle$ satisfy

$$|u_{ij}^{(s)}\rangle = \frac{1}{2(1+s)}\hat{Q}_{12}r_{12}\frac{1}{\sqrt{2}}(\phi_i\phi_j + (1-2s)\phi_j\phi_i) + \mathcal{O}\left(r_{12}^{(2+s)}\right), \tag{20-1}$$

where i,j denote different spin-free occupied Hartree–Fock orbitals and the spin s is 0 or 1.[1] While atom centered functions are well suited to the description of Hartree–Fock orbitals and the nuclear cusps, they are poorly suited to the description of the correlation cusp, which is electron centered. The conventional expansion of $|u_{ij}^{(s)}\rangle$ in terms of virtual orbital pairs amounts to a partial wave expansion of linear-r_{12}, which is slowly convergent. Indeed, the correlation energy increment for each successive angular momentum l in such a partial wave expansion can be shown to be proportional to $(l+\frac{1}{2})^{-4}$ [16, 17]. The total error for a set truncated at l is then proportional to l^{-3}, which also accounts for the slow X^{-3} convergence behavior of the correlation-consistent basis sets [18].

The central, distinguishing idea of the R12 approach is to augment the orbital expansion with a small set of R12 geminals, two particle functions with explicit r_{12} dependence that directly and efficiently describe the cusp regions of the wave function [15]. From Eq. (20-1) it is clear that the set of spatial functions

$$\hat{Q}_{12}f_{12}\phi_i\phi_j \tag{20-2}$$

can explicitly satisfy the correlation cusp for restricted closed-shell MP2 wave functions, where $f_{12} = f(r_{12}) = r_{12} + \mathcal{O}\left(r_{12}^2\right)$ and i,j run over the set of occupied orbitals. The inclusion of these functions accelerates the convergence with orbital basis from l^{-3} to l^{-7} [15], which is sufficient to eliminate the basis set problem from almost all practical applications of modern quantum chemistry. The details for how to practically incorporate these functions as double orbital replacements in MP2 and CCSD wave functions were worked out by Kutzelnigg and co-workers [19–23] and relies chiefly on inserting resolution-of-the-identity (RI) approximations to reduce three- and four-electron integrals to sums of products of two-electron integrals (see Section 20.5).

In the original R12 methods, f_{12} was set to r_{12} and the orbital basis was used for the RI. The early R12 methods have been very successful for benchmark calculations on small to medium sized molecules with a hitherto unobtainable sub mE_h accuracy in total energies [24–39]. Indeed, the basis set limits provided by R12 calculations made it possible to develop and assess extrapolation methods. However, the fact that linear-r_{12} accurately describes a rather small region around the cusp, and the requirement that the orbital basis be sufficiently complete for an accurate RI, meant that it was not possible to use small orbital basis sets with the original R12 methods.

---

[1] $\hat{Q}_{12}$ is the strong orthogonality projector, which ensures intermediate normalization and zero contribution to $|u_{ij}^{(s)}\rangle$ from single excitations (see Sections 20.3.2 and 20.5).

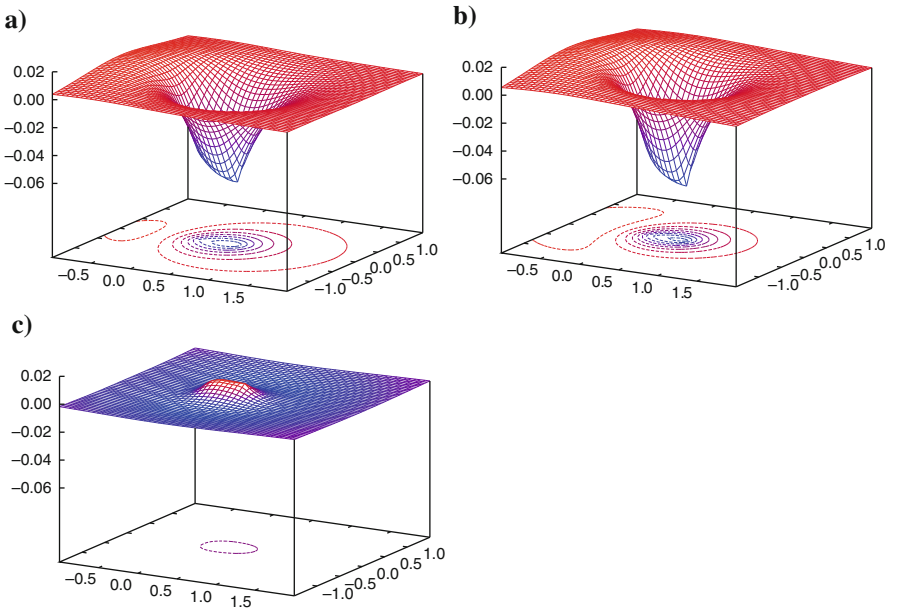

Figure 20-1. **(a)** The correlation hole $\Psi_{\mathrm{CCSD}} - \Psi_{\mathrm{HF}}$ for ^1S helium plotted as a function of electron 2 with electron 1 positioned 0.5 a_0 from the nucleus. Ψ_{CCSD} and Ψ_{HF} have been computed with Hylleraas expansions and are numerically exact on this scale. **(b)** The F12 basis function $-\frac{1}{2}\hat{Q}_{12}e^{-r_{12}}\Psi_{\mathrm{HF}}$. **(c)** The difference between the exact correlation hole and the F12 basis function

Today, the predominant choice for f_{12} is a Slater-type function[2] [40]

$$f_{12} = -\gamma^{-1}(1 - \exp(-\gamma r_{12})), \tag{20-3}$$

which accounts for screening in the inter-electronic interaction and accurately describes a much larger region of the correlation hole than linear-r_{12}. Indeed, 80% of the CCSD dynamic correlation energy can be recovered using Slater-type geminal functions (STGs) alone, that is, without the conventional orbital expansion for double excitations (see Figure 20-1 and Ref. [41]). Furthermore, a complementary auxiliary basis set (CABS) is used in addition to the orbital basis for the RI [42, 43]. Combined, these two developments have transformed R12 theory into a method capable of recovering over 98% of the basis set limit correlation energy with specially optimized double-zeta basis sets, which is as accurate as conventional quintuple-zeta calculations. R12 methods where the correlation factor f_{12} is non-linear are generally referred to as F12 methods.

---

[2] Practical calculations actually use $f_{12} = -\gamma^{-1}\exp(-\gamma r_{12})$, or a STG-$n$G fit using Gaussian geminals. Note that the projection operator $\hat{Q}_{12}$ eliminates the constant.

These key advances appeared 5–10 years ago at the MP2 level of theory [44] and since then there has been rapid development in many aspects of R12 methodology, including systematic approximations [42, 45–47], robust density fitting for the R12 integrals [48, 49], combination with local methods [50–54], efficient integral evaluation [40, 53, 55, 56], improvements in RI through numerical quadrature [55, 57], specially optimized orbital and auxiliary basis sets [58–60], as well as the extension of MP2-F12 theory to CASPT2-F12 [61] and several coupled-cluster models for ground state energies and response properties.

In this chapter we review the current status of CCSD-F12 theory, for which MP2-F12 is the precursor. We will not discuss local [50–54] or multi-reference methods [61–63] and refer the reader to the literature for information on these topics. In Section 20.3 we introduce the formalism and notation, and in Section 20.4 we present the CCSD-F12 method and review several approximations to it. The various integrals and intermediates required for CCSD-F12 and MP2-F12 calculations are discussed in Section 20.5 and the choice of correlation factor f_{12} is explained in more detail in Section 20.6. In Sections 20.7 and 20.8 we address the issue of basis set incompleteness in single and triple excitations, respectively. Finally in Section 20.9 we present the current status of CCSD-F12 response theory, before concluding with some thoughts on the future of F12 methods in Section 20.10.

20.3. FORMALISM AND NOTATION

20.3.1. Orbital Spaces

Coupled-cluster methods are most conveniently discussed in second quantization. In standard canonical coupled-cluster theory, the set of orbitals underlying the occupation number representation is determined by a Hartree–Fock calculation in the (finite) orbital basis. For a second quantization representation of F12 functions, which extend beyond the space spanned by the orbital basis, it is necessary to introduce a formally complete set of orbitals. The orbital spaces are depicted in Figure 20-2. We adhere to the usual convention, with i, j, k, l, m, n referring to orbitals occupied in the Hartree–Fock state and a, b, c, d to virtual orbitals within the finite basis set. p, q, r, s

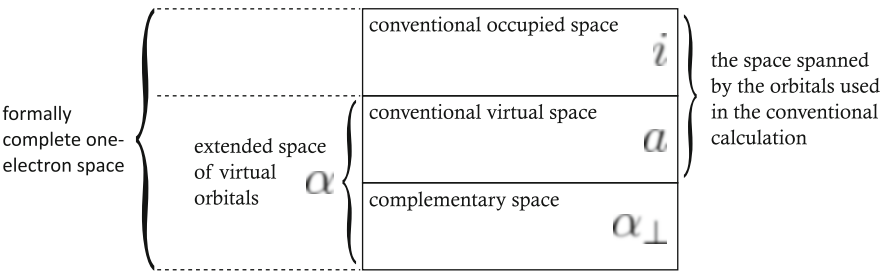

Figure 20-2. Orbital space notation

refer to orbitals (occupied or virtual) in the finite basis set. $\alpha_\perp, \beta_\perp$ denote the set of complementary orbitals that are orthogonal to the finite set and complete the basis, while α, β are used for the full set of virtuals. The CABS orbitals used to improve the RI fall in the complementary space $\alpha_\perp$ and the indices p', q' are used to denote CABS orbitals.

The occupied orbitals are not eigenfunctions of the Fock operator since they are obtained from a finite basis calculation and the Fock matrix elements $F_i^{\alpha_\perp} = \langle i|\,\hat{F}\,|\alpha_\perp\rangle \neq 0$. In F12 methods these matrix elements that couple F12 geminals and occupied orbitals are sometimes neglected. This is referred to as assuming the generalized Brillouin condition (GBC). Alternatively, they are included in an approximate manner by treating them as a perturbation (see Section 20.7). The more drastic assumption that the elements $F_a^{\alpha_\perp} = 0$ is referred to as the extended Brillouin condition (EBC). For calculations where core orbitals are not included in the correlation treatment, we use the abbreviation fc (frozen-core).

20.3.2. Excitation Operators

The CCSD-F12 wave function is defined as

$$|\mathrm{CC}\rangle = \exp(\hat{T})|\mathrm{HF}\rangle = \exp(\hat{T}_1 + \hat{T}_2 + \hat{T}_{2'})|\mathrm{HF}\rangle, \tag{20-4}$$

where $|\mathrm{HF}\rangle$ is the Hartree–Fock wave function and the cluster operators are given by

$$\hat{T}_1 = \sum_{ia} t_a^i \hat{E}_{ai}, \tag{20-5}$$

$$\hat{T}_2 = \tfrac{1}{2} \sum_{aibj} t_{ab}^{ij} \hat{E}_{ai}\hat{E}_{bj}, \tag{20-6}$$

$$\hat{T}_{2'} = \tfrac{1}{2} \sum_{kilj} c_{kl}^{ij} \sum_{\alpha\beta} w_{\alpha\beta}^{kl} \hat{E}_{\alpha i}\hat{E}_{\beta j}. \tag{20-7}$$

To simplify later discussions, we adopt the spin-free (closed-shell) formalism and in terms of creation and annihilation operators the excitation operator is

$$\hat{E}_{ai} = \sum_{\sigma} a_{a\sigma}^{\dagger} a_{i\sigma}. \tag{20-8}$$

t_a^i and t_{ab}^{ij} are the usual singles and doubles amplitudes, respectively. The F12 basis functions enter the wave function as additional double excitations, representing a replacement of an orbital pair $|ij\rangle$ with the geminal $\hat{Q}_{12} f_{12}\,|kl\rangle$ with an amplitude c_{kl}^{ij}. A F12 basis function is a specific linear combination of orbitals in the complete basis

that describes the correlation hole. The coefficients $w_{kl}^{\alpha\beta}$ are the (spin-free) matrix elements

$$w_{\alpha\beta}^{kl} = \langle kl|f_{12}\hat{Q}_{12}|\alpha\beta\rangle \tag{20-9}$$

The choice for the strong orthogonality operator $\hat{Q}_{12}$ defines the Ansatz of the F12 method. The best choice, referred to as Ansatz 2, is[3]

$$\hat{Q}_{12} = (1 - \hat{O}_1)(1 - \hat{O}_2) - \hat{V}_1\hat{V}_2, \tag{20-10}$$

where

$$\hat{O} = \sum_i |\phi_i\rangle \langle\phi_i| , \tag{20-11}$$

$$\hat{V} = \sum_a |\phi_a\rangle \langle\phi_a| . \tag{20-12}$$

In first quantization, $\hat{Q}_{12}$ projects out the overlap of the function $f_{12}|kl\rangle$ with all occupied pairs $|ij\rangle$ and all singly excited pairs $|i\alpha\rangle$, which ensures that the excitations into F12 geminals are pure double excitations. Furthermore, the overlap with the conventional double excitations into the finite basis is also projected out, minimizing the coupling between $\hat{T}_2$ and $\hat{T}_{2'}$. The resulting space of F12 double excitations is depicted in Figure 20-3.

An alternative choice, Ansatz 1, is

$$\hat{Q}_{12}^1 = (1 - \hat{P}_1)(1 - \hat{P}_2), \tag{20-13}$$

$$\hat{P} = \sum_p |\phi_p\rangle\langle\phi_p|. \tag{20-14}$$

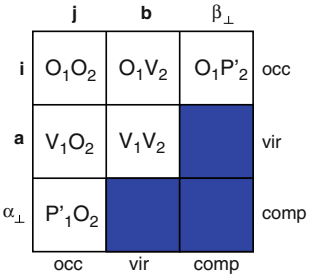

Figure 20-3. The space of orbital pairs. The space of F12 double excitations for Ansatz 2 is shaded

[3] Some researchers refer to this as Ansatz 3, reserving Ansatz 2 for $(1 - \hat{O}_1)(1 - \hat{O}_2)$.

Here the F12 geminals fall only in the space of $|\alpha_\perp\beta_\perp\rangle$ and do not contain any contributions from $|a\beta_\perp\rangle$, which lead to coupling terms between $\hat{T}_2$ and $\hat{T}_{2'}$ in the amplitude equations. Although Ansatz 1 results in much simpler working equations, Ansatz 2 is far more accurate and Ansatz 1 is rarely used in modern F12 methods. The practical evaluation of integrals involving F12 geminals usually involves RI techniques to avoid three- and four-electron integrals and is discussed in Section 20.5.

20.3.3. Projection Manifolds and Similarity Transformation

In our approach to coupled-cluster methods, the projection manifolds, the biorthogonal bra states for single, double and F12 double excitations, which are used to set up the CCSD-F12 amplitude equations, are given by

$$\langle\mu_1| = \langle\mathrm{HF}|\tfrac{1}{2}\hat{E}_{ia}, \tag{20-15}$$

$$\langle\mu_2| = \langle\mathrm{HF}|\left(\tfrac{1}{3}\hat{E}_{ia}\hat{E}_{jb} + \tfrac{1}{6}\hat{E}_{ja}\hat{E}_{ib}\right), \tag{20-16}$$

$$\langle\mu_{2'}| = \sum_{\alpha\beta} w^{kl}_{\alpha\beta}\langle\mathrm{HF}|\left(\tfrac{1}{3}\hat{E}_{i\alpha}\hat{E}_{j\beta} + \tfrac{1}{6}\hat{E}_{j\alpha}\hat{E}_{i\beta}\right). \tag{20-17}$$

The energy and amplitude equations are obtained by projecting the Schrödinger equation onto the states $\langle\mathrm{HF}|\exp(-\hat{T})$ and $\langle\mu|\exp(-\hat{T})$.

$$E = \langle\mathrm{HF}|\exp(-\hat{T})\hat{H}\exp(\hat{T})|\mathrm{HF}\rangle, \tag{20-18}$$

$$0 = \langle\mu|\exp(-\hat{T})\hat{H}\exp(\hat{T})|\mathrm{HF}\rangle. \tag{20-19}$$

The Campbell–Baker–Hausdorff expansion of the similarity transformed Hamiltonian $\exp(-\hat{T})\hat{H}\exp(\hat{T})$ truncates at four nested commutators and the expansion is term-wise size extensive.

$$\exp(-\hat{T})\hat{H}\exp(\hat{T}) = \hat{H} + [\hat{H},\hat{T}] + \tfrac{1}{2}[[\hat{H},\hat{T}],\hat{T}] + \cdots. \tag{20-20}$$

The coupled-cluster equations are greatly simplified by absorbing the single excitations into the integrals and using $\hat{T}_1$-transformed operators, defined as

$$\tilde{H} = \exp(-\hat{T}_1)\hat{H}\exp(\hat{T}_1). \tag{20-21}$$

In the Lagrangian formulation of coupled-cluster theory, or in the equation of motion (EOM) coupled-cluster approach, both the left and right eigenvectors of the similarity transformed Hamiltonian are required. The ground state right eigenvector is obviously the Hartree–Fock state. The left eigenvector, $\langle\Lambda| = \langle\mathrm{HF}| + \langle\bar{\mathbf{t}}|$, is defined by the Lagrange multipliers. In CCSD-F12 theory, $\langle\bar{\mathbf{t}}|$ contains singles, doubles and F12 doubles components,

$$\langle \bar{\mathbf{t}}_1| = \sum_{ia} \bar{t}_a^i \langle \mathrm{HF}| \tfrac{1}{2}\hat{E}_{ia}, \tag{20-22}$$

$$\langle \bar{\mathbf{t}}_2| = \tfrac{1}{2} \sum_{aibj} \bar{t}_{ab}^{ij} \langle \mathrm{HF}| \left(\tfrac{1}{3}\hat{E}_{ia}\hat{E}_{jb} + \tfrac{1}{6}\hat{E}_{ja}\hat{E}_{ib} \right), \tag{20-23}$$

$$\langle \bar{\mathbf{c}}| = \tfrac{1}{2} \sum_{kilj} \bar{c}_{kl}^{ij} \sum_{\alpha\beta} w_{\alpha\beta}^{kl} \langle \mathrm{HF}| \left(\tfrac{1}{3}\hat{E}_{i\alpha}\hat{E}_{j\beta} + \tfrac{1}{6}\hat{E}_{j\alpha}\hat{E}_{i\beta} \right). \tag{20-24}$$

To first order, the doubles amplitudes and multipliers are related through

$$\bar{t}_{ab}^{ij} = 2t_{ab}^{ij} - t_{ab}^{ji}. \tag{20-25}$$

20.3.4. Basis Sets

The correlation-consistent basis sets of Dunning and co-workers, cc-pVXZ [64, 65] are not appropriate for F12 calculations. The F12 geminal basis functions are used for the short range description of the correlation hole and thus the exponents of the polarization functions in an F12 calculation should be much smaller than for a conventional calculation [66]. It has therefore been customary to use augmented sets for F12 calculations, aug-cc-pVXZ [65, 67]. Recently, Peterson and co-workers have constructed correlation-consistent basis sets explicitly for use with F12 methods, cc-pVXZ-F12 [58]. Although these sets are somewhat larger than the sister cc-pVXZ sets, being closer in size to the cc-pV(X+1)Z sets, they give significantly improved relative energies [68]. The cc-pVXZ-F12 sets were optimized specifically for use with the STG choice for f_{12} with the exponent $\gamma = 0.9\ \mathrm{a}_0^{-1}$, $1.0\ \mathrm{a}_0^{-1}$ and $1.1\ \mathrm{a}_0^{-1}$ for X = D, T and Q, respectively. Auxiliary basis sets for the CABS RI approach have also been constructed for combination with the cc-pVXZ-F12 [59] and the aug-cc-pVXZ orbital basis sets [60]. All of Peterson's F12 basis sets are available from his web server [69].

20.4. CCSD-F12 MODELS

Partitioning the Hamiltonian into the one-electron part, the Fock operator, and the two-electron part, the fluctuation potential,

$$\hat{H} = \hat{F} + \hat{\Phi}, \tag{20-26}$$

the equations for the CCSD-F12 energy and amplitudes are given by

$$E = E_{\mathrm{HF}} + \langle \mathrm{HF}| \tfrac{1}{2}[[\hat{\Phi}, \hat{T}_1], \hat{T}_1] + [\hat{\Phi}, \hat{T}_2 + T_{2'}]\,|\mathrm{HF}\rangle\,, \tag{20-27}$$

$$0 = \langle \mu_1|\,[\hat{F}, \hat{T}_1] + [\hat{F}, \hat{T}_{2'}] + \tilde{\Phi} + [\tilde{\Phi}, \hat{T}_2 + \hat{T}_{2'}]\,|\mathrm{HF}\rangle\,, \tag{20-28}$$

$$0 = \langle \mu_2 | \, [\tilde{F}, \hat{T}_2 + \hat{T}_{2'}] + \tilde{\Phi} + [\tilde{\Phi}, \hat{T}_2 + \hat{T}_{2'}] + \tfrac{1}{2}[[\tilde{\Phi}, \hat{T}_2 + \hat{T}_{2'}], \hat{T}_2 + \hat{T}_{2'}] \, | \mathrm{HF} \rangle \, , \tag{20-29}$$

$$0 = \langle \mu_{2'} | \, [\tilde{F}, \hat{T}_2 + \hat{T}_{2'}] + \tilde{\Phi} + [\tilde{\Phi}, \hat{T}_2 + \hat{T}_{2'}] + \tfrac{1}{2}[[\tilde{\Phi}, \hat{T}_{2'}], 2\hat{T}_2 + \hat{T}_{2'}] \, | \mathrm{HF} \rangle \, . \tag{20-30}$$

The above equations assume the Brillouin condition (see Section 20.4.4) and Ansatz 2 ($\langle \mu_2 | \, [[\tilde{\Phi}, \hat{T}_{2'}], \hat{T}_{2'}] \, | \mathrm{HF} \rangle = 0$ for Ansatz 1). These equations are formally identical to conventional CCSD, except that there are two types of double excitations, those into orbital pairs and those into F12 geminals. All of the properties of CCSD, such as size extensivity and orbital invariance, are retained.[4] The procedure for solving the amplitude equations is also completely analogous to standard CCSD, with an MP2-F12 calculation providing the initial guess for the iterative solution of the amplitude equations.

An attractive alternative to optimizing the F12 amplitudes is provided by the SP Ansatz [57, 70, 71], where the F12 amplitudes are predetermined to satisfy the singlet (s-wave) and triplet (p-wave) coalescence conditions for the first-order wave function (see Section 20.6.1),

$$c_{kl}^{ij} = \tfrac{3}{8}\delta_{ik}\delta_{jl} + \tfrac{1}{8}\delta_{il}\delta_{jk}. \tag{20-31}$$

The amplitudes for conventional excitations are optimized in the presence of this fixed geminal contribution. The SP approach is numerically less sensitive to the accuracy of the RI approximations and many F12 contributions can be pre-contracted, significantly reducing the computational cost. The energy for the SP Ansatz is computed from the Lagrange functional

$$E = \langle \mathrm{HF} | \exp(-\hat{T}) \hat{H} \exp(\hat{T}) \, | \mathrm{HF} \rangle + \langle \bar{\mathbf{c}} | \exp(-\hat{T}) \hat{H} \exp(\hat{T}) \, | \mathrm{HF} \rangle \, . \tag{20-32}$$

The F12 Lagrange multipliers are approximated to first order by replacing them with the F12 amplitudes according to Eq. (20-25). This ensures that orbital invariance is retained. Although the accuracy in total energies suffers due to the reduced flexibility, relative energies are often at least as accurate as when optimizing the F12 amplitudes. Moreover, there is no direct geminal contribution to the basis set superposition error (BSSE) for the SP Ansatz, and traditional counterpoise corrections can be applied to remove the orbital BSSE. This leads to much improved predictions for weak interactions [70].

Availability: At the time of writing, the CCSD-F12 model with CABS and Ansatz 2 had only been implemented using automated techniques, due to the large number of terms that arise when evaluating the commutators. In particular, CCSD-F12 has been implemented in the MPQC program using the SMITH package [72–74]

[4] In the original MP2-R12 method, the geminal excitations were restricted to c_{ij}^{ij} and c_{ij}^{ji}, which is not orbital invariant [21] unless the amplitudes are the same for every ij [55].

for automatic code generation and in the GECCO program [75–77], based on generalized contraction routines. If the orbital basis is used for the RI, that is without the CABS, the CCSD-F12 equations become very much simpler. The CCSD-F12 method without CABS has been implemented in DIRCCR12-OS [78].

Computational cost: The computational effort required for the F12 terms makes a CCSD-F12 calculation somewhat more expensive than a CCSD calculation with the same orbital basis set. In particular, the commutators $\langle \mu_{2'} | \, [\tilde{\Phi}, \hat{T}_{2'}] \, | \mathrm{HF} \rangle$ and $\langle \mu_{2'} | \, [[\tilde{\Phi}, \hat{T}_{2'}], \hat{T}_{2'}] \, | \mathrm{HF} \rangle$ contain terms that scale as O^3X^3, where O is the number of occupied orbitals and X is the number of CABS orbitals used for the RI. The size of the CABS is typically 2–3 times larger than the size of the orbital basis. For the single commutator, the O^3X^3 scaling can be replaced by an O^6V step, where V is the number of virtual orbitals, by precomputing the Z intermediate with O^5VX^2 cost [23, 75, 78, 79]. For the SP Ansatz, where the F12 residual is only computed once, the cost of the $\langle \mu_2 | \, [[\tilde{\Phi}, \hat{T}_{2'}], \hat{T}_{2'}] \, | \mathrm{HF} \rangle$ term is critical: it contains terms that scale as $O^2V^2X^2$.

Apart from the high computational expense, two further observations regarding the terms quadratic in $\hat{T}_{2'}$ are noteworthy. The F12 amplitudes vanish in the limit of an infinite orbital basis and the quadratic terms are therefore small, even for relatively small orbital basis sets. The evaluation of these terms requires multiple RI insertions, which may lead to an increased numerical sensitivity to the quality of the CABS. In short, computing these terms is more trouble than it is worth. In the following sections we discuss several approximate CCSD-F12 methods, where the scaling is reduced to O^3N^2X or O^2N^4 in the iterations ($N = O + V$). These simplified models have been shown to be almost as accurate as the full CCSD-F12 while the simplest are only a few percent more expensive than a conventional CCSD calculation in the same orbital basis.

20.4.1. CCSD(F12)

In the CCSD(F12) model, introduced by Fliegl et al. [80], the treatment of the F12 amplitudes is reduced to second order in the fluctuation potential using analogous arguments to those used to simplify the treatment of conventional doubles from CCSD to CC2 [81]. In particular, the Fock operator and the conventional singles and doubles amplitudes and multipliers are taken to be zeroth order. The fluctuation potential and the F12 amplitudes and multipliers are then first order. The amplitude equations of the CCSD(F12) model are obtained by discarding all terms in the CCSD-F12 Lagrange functional that are higher than second order. This gives

$$0 = \langle \mu_1 | \, [\hat{F}, \hat{T}_1] + [\hat{F}, \hat{T}_{2'}] + \tilde{\Phi} + [\tilde{\Phi}, \hat{T}_2 + \hat{T}_{2'}] \, | \mathrm{HF} \rangle \,, \tag{20-33}$$

$$0 = \langle \mu_2 | \, [\hat{F}, \hat{T}_2 + \hat{T}_{2'}] + \tilde{\Phi} + [\tilde{\Phi}, \hat{T}_2 + \hat{T}_{2'}] + \tfrac{1}{2}[[\tilde{\Phi}, \hat{T}_2], \hat{T}_2 + 2\hat{T}_{2'}] \, | \mathrm{HF} \rangle \,, \tag{20-34}$$

$$0 = \langle \mu_{2'} | \, [\hat{F}, \hat{T}_2 + \hat{T}_{2'}] + \tilde{\Phi} + [\tilde{\Phi}, \hat{T}_2] \, | \mathrm{HF} \rangle \,. \tag{20-35}$$

The energy is evaluated using Eq. (20-27) if the F12 amplitudes are optimized. If the SP Ansatz is used, then the energy is evaluated using the simplified Lagrange functional [70]

$$E = \langle \mathrm{HF}| \exp(-\hat{T})\hat{H}\exp(\hat{T})\,|\mathrm{HF}\rangle + \langle \bar{\mathbf{c}}|\,[\hat{F}, \hat{T}_2 + \hat{T}_{2'}] + \tilde{\Phi} + [\tilde{\Phi}, \hat{T}_2]\,|\mathrm{HF}\rangle\,. \tag{20-36}$$

Compared to the full CCSD-F12 model, Eqs. (20-28), (20-29) and (20-30), all terms quadratic in the F12 amplitudes have been neglected, as has the commutator $\langle \mu_{2'}|\,[[\hat{F}, \hat{T}_1] + \tilde{\Phi}, \hat{T}_{2'}]\,|\mathrm{HF}\rangle$. Although this simplification leads to a slight loss in accuracy (see below), this is a very small price to pay for the significant reduction in computational cost and increased numerical stability associated with the CCSD(F12) method. Furthermore, since the model is consistent from the point of view of perturbational analysis, the CCSD(F12) method is appropriate for use in response calculations (see Section 20.9).

Computational cost: Beyond the O^2N^4 scaling of conventional CCSD, the F12 terms in the CCSD(F12) iterations scale at worst as O^3N^2X. Depending on the size of the CABS, a CCSD(F12) calculation can take approximately 3 times longer than a conventional CCSD calculation in the same orbital basis and the cost (but not scaling) can be significantly reduced by employing the SP Ansatz.

Availability: The pilot implementation of the CCSD(F12) model including STGs and CABS with Ansatz 2 was in a developmental version of the DALTON program package [82, 83]. This implementation was restricted to closed-shell calculations with restricted references and has been verified by comparison with the automated routines in the GECCO program. Subsequently Ten-no has presented an implementation of the CCSD(F12) model using the SP ansatz and numerical quadratures [84] and Bachorz et al. have recently completed an efficient implementation of CCSD(F12) in the TURBOMOLE package using a combination of integral direct routines and density fitting. Naturally the CCSD(F12) model is also available in the automated codes SMITH and GECCO, and also in DIRCCR12-OS, but, at the time of writing this chapter, without the CABS orbitals.

Performance: The CCSD(F12) method is an accurate, robust and efficient approximation to CCSD-F12 and can be used to compute near basis set limit CCSD correlation energies at relatively low cost using small orbital basis sets [83, 85]. The loss of accuracy due to the CCSD(F12) simplifications is illustrated in Table 20-1, where we list fc-CCSD correlation energies of water from CCSD-F12 and CCSD(F12) calculations, taken from Ref. [75]. For comparison we also include energies from the CCSD-F12(lin) model, where only the terms quadratic in $\hat{T}_{2'}$ are neglected from the CCSD-F12 equations. The loss of accuracy due to the simplified F12 treatment is below 0.3 mE_h for these correlation energies, and below 0.1 kJ mol^{-1} for equivalent calculations for the reaction energy for $H_2 + CO_2 \longrightarrow H_2O + CO$ (see Ref. [75]).

Table 20-1. Valence correlation energies of H_2O in mE_h for various CCSD-F12 models, computed with a STG exponent of 1.3 a_0^{-1} [75]

Basis	CCSD(F12)	CCSD-F12(lin)	CCSD-F12
aug-cc-pVDZ	−291.005	−291.300	−291.190
aug-cc-pVTZ	−296.097	−295.959	−295.950
aug-cc-pVQZ	−297.820	−297.655	−297.654

In Table 20-2 we present statistics for the deviation of fc-CCSD(F12) energies from the basis set limit using the cc-pVXZ-F12 basis sets and CABS sets, with the recommended STG exponents.[5] The basis set limit CCSD energies of 58 small molecules of H, C, N, O and F [86] have been computed to 99.95% accuracy using the CCSD(F12) method with the basis sets from Ref. [68]. The CCSD correlation energy, ΔCCSD, computed using the CCSD(F12) method and the cc-pVDZ-F12 basis is more accurate than conventional CCSD using the cc-pV5Z basis. Considering that the scaling with orbital basis is always N^4 for any given system, and considering that the cc-pV5Z basis is 3 times larger than the cc-pVDZ-F12 basis, the cost of the CCSD(F12) calculation is ∼30 times less than the conventional calculation in the large basis.

In Table 20-2 we have also listed the basis set errors arising due to the Hartree–Fock (HF) and (T) contributions to the energy. These have been calculated using the Hartree–Fock energy in the given basis and evaluating the (T) energy correction using the conventional singles and doubles amplitudes from a converged CCSD or CCSD(F12) calculation, that is, without any explicit F12 dependence (see Section 20.8). For the CCSD(F12)/cc-pVDZ-F12 calculations, the dominant contribution to the total error is from the Hartree–Fock energies, whereas for the CCSD(F12)/cc-pVQZ-F12 calculations, the slow convergence of the triples

Table 20-2. Basis set error statistics of conventional CCSD(T) and CCSD(T)(F12) methods over a set of 58 small molecules (kJ mol^{-1} per valence electron). Core orbitals have not been correlated

		HF		ΔCCSD		CCSD		(T)		CCSD(T)	
CCSD(T)	Basis	Mean	Std.	Mean	Std.	Mean	Std.	Mean	Std.	Mean	Std.
Conv.	cc-pVDZ	11.40	2.66	27.00	5.45	38.40	8.04	2.22	0.45	40.62	8.40
	cc-pVTZ	2.75	0.69	9.69	2.37	12.43	3.05	0.66	0.15	13.09	3.19
	cc-pVQZ	0.63	0.17	3.85	1.06	4.48	1.22	0.22	0.06	4.70	1.27
	cc-pV5Z	0.08	0.02	1.80	0.51	1.88	0.53	0.06	0.02	1.93	0.54
(F12)	cc-pVDZ-F12	3.22	0.75	1.35	0.29	4.56	1.00	1.07	0.22	5.64	1.19
	cc-pVTZ-F12	0.60	0.14	0.21	0.07	0.81	0.21	0.36	0.08	1.18	0.26
	cc-pVQZ-F12	0.06	0.01	−0.04	0.01	0.02	0.02	0.12	0.03	0.15	0.04

[5] The GBC was assumed in these calculations.

Table 20-3. Basis set error statistics of CCSD(T), CCSD(T)(F12) and CCSD(T)(F12)-SP methods over a set of 53 reactions (kJ mol^{-1} per valence electron). Core orbitals have not been correlated

		HF		ΔCCSD		CCSD		(T)		CCSD(T)	
CCSD(T)	Basis	Mean	Std.	Mean	Std.	Mean	Std.	Mean	Std.	Mean	Std.
Conv.	cc-pVDZ	−0.27	0.37	−0.95	0.86	−1.22	1.07	−0.11	0.08	−1.33	1.10
	cc-pVTZ	−0.08	0.12	−0.26	0.29	−0.34	0.34	−0.04	0.03	−0.39	0.35
	cc-pVQZ	−0.04	0.04	−0.07	0.10	−0.12	0.11	−0.01	0.01	−0.13	0.11
	cc-pV5Z	0.00	0.01	−0.03	0.05	−0.03	0.04	−0.00	0.00	−0.03	0.04
(F12)	cc-pVDZ-F12	−0.03	0.20	−0.07	0.09	−0.11	0.22	−0.05	0.06	−0.16	0.25
	cc-pVTZ-F12	−0.03	0.03	−0.01	0.02	−0.04	0.04	−0.02	0.02	−0.06	0.04
	cc-pVQZ-F12	−0.00	0.00	−0.00	0.00	−0.00	0.01	−0.01	0.01	−0.01	0.01
(F12)-SP	cc-pVDZ-F12	−0.03	0.20	−0.10	0.08	−0.13	0.23	−0.05	0.06	−0.18	0.27
	cc-pVTZ-F12	−0.03	0.03	−0.01	0.01	−0.03	0.04	−0.02	0.02	−0.05	0.04
	cc-pVQZ-F12	−0.00	0.00	−0.00	0.00	−0.00	0.01	−0.01	0.01	−0.01	0.01

correction means that this contribution to the basis set error dominates. Methods for reducing the basis set errors in the Hartree–Fock and triples contributions are discussed in Sections 20.7 and 20.8, respectively.

In Table 20-3 we present analogous statistical measures for the basis set errors for the decomposition of 53 molecules into H_2, CO, CO_2, N_2 and F_2. The comments concerning total energies apply equally well to relative energies. The basis set error for the fc-CCSD(F12) correlation energies is only 0.1 kJ mol^{-1} per valence electron with the cc-pVDZ-F12 basis, which is sufficient for chemical accuracy in a wide range of applications (provided that the Hartree–Fock error is reduced to a similar level). The cc-pVQZ-F12 basis provides near benchmark accuracy with errors less than 0.01 kJ mol^{-1} per valence electron. In Table 20-3 we also present statistics for the SP Ansatz, which performs at least as well as the fully optimized approach for relative energies. Indeed, the loss of accuracy in total energies due to the fewer variational parameters is compensated by the absence of geminal basis set superposition error when computing relative energies. This advantage of the SP Ansatz is particularly important when computing weak interactions [70, 87, 88].

20.4.2. CCSD-F12x

In the CCSD-F12x methods of Werner and co-workers [89, 90], the CCSD-F12 equations are reduced to the minimal set of terms required to capture the dominant F12 contributions so that the additional computational cost of including the explicitly correlated functions is only a fraction of the underlying cost of the CCSD calculation. To this end the SP Ansatz is adopted in the CCSD-F12x methods. In the CCSD-F12x methods, the conventional single and double equations are determined using

$$0 = \langle \mu_1 | \, [\hat{F}, \hat{T}_1] + [\hat{F}, \hat{T}_{2'}] + \tilde{\Phi} + [\tilde{\Phi}, \hat{T}_2] + [\hat{\Phi}, \hat{T}_{2'}] \, | \mathrm{HF} \rangle \,, \tag{20-37}$$

$$0 = \langle \mu_2 | \, [\tilde{F}, \hat{T}_2] + [\hat{F}, \hat{T}_{2'}] + \tilde{\Phi} + [\tilde{\Phi}, \hat{T}_2] + [\tilde{\Phi}, \hat{T}_{2'}] + \tfrac{1}{2}[[\tilde{\Phi}, \hat{T}_2], \hat{T}_2] \, | \mathrm{HF} \rangle \,. \tag{20-38}$$

For all but the $\langle\mu_2|\,[\hat{F},\hat{T}_{2'}]\,|\mathrm{HF}\rangle$ term, which appears in MP2-F12 theory, the strong orthogonality projection operator is approximated as

$$\hat{Q}_{12} \approx 1 - \hat{P}_1\hat{P}_2. \tag{20-39}$$

This is equivalent to using only the orbital basis for the RI for these terms[6] instead of the combined basis of orbital plus CABS and greatly simplifies the resulting equations. In the CCSD-F12a method, the energy is computed from the Lagrange functional

$$\langle\mathrm{HF}|\exp(-\hat{T})\hat{H}\exp(\hat{T})\,|\mathrm{HF}\rangle + \langle\bar{\mathbf{c}}|\,[\hat{F},\hat{T}_2+\hat{T}_{2'}]+\hat{\Phi}\,|\mathrm{HF}\rangle\,, \tag{20-40}$$

where the F12 terms are identical to those of MP2-F12 (in the Hylleraas functional) and are evaluated using the full $\hat{Q}_{12}$, that is Eq. (20-10), not (20-39). In the CCSD-F12b method, the Lagrangian is extended to

$$\langle\mathrm{HF}|\exp(-\hat{T})\hat{H}\exp(\hat{T})\,|\mathrm{HF}\rangle + \langle\bar{\mathbf{c}}|\,[\hat{F},\hat{T}_2+\hat{T}_{2'}]+\tilde{\Phi}+[\tilde{\Phi},\hat{T}_2]\,|\mathrm{HF}\rangle\,, \tag{20-41}$$

where the approximate $\hat{Q}_{12}$ is used to evaluate the additional term.

The CCSD-F12x methods can be considered as approximations to the CCSD(F12) approach. By replacing $\hat{Q}_{12}$ with the approximate form for all terms that do not appear in MP2-F12, the CCSD(F12)-SP equations reduce to essentially the CCSD-F12b model. The only further simplification required to recover the above equations is then to assume the GBC and to neglect the $\hat{T}_1$ contributions to the commutator $\langle\mu_1|\,[\tilde{\Phi},\hat{T}_{2'}]\,|\mathrm{HF}\rangle$. To recover the unlinked equations in Ref. [90] it is also necessary to delete some of the $\hat{T}_1$ contributions to $\langle\mu_2|\,[\tilde{\Phi},\hat{T}_{2'}]\,|\mathrm{HF}\rangle$ and $\langle\mu_{2'}|\,\tilde{\Phi}\,|\mathrm{HF}\rangle$, but the effect of this is probably small. The approximation used for $\hat{Q}_{12}$ could be seen as rather severe, particularly for double-zeta basis sets where the approximate RI is far from complete, but the authors of the CCSD-F12x approaches report that the effect for relative energies is small. It should be noted that for the CCSD-F12a approach, contributions computed with the approximate $\hat{Q}_{12}$ do not enter the final energy expression, affecting it only indirectly through the amplitudes.

Computational cost: In the CCSD-F12x methods, the expense of computing the F12 terms in the coupled-cluster iterations is only a fraction of the cost of the conventional terms. The effect of the approximation for $\hat{Q}_{12}$ is to remove almost all coupling terms between conventional and F12 doubles and in doing so, to avoid all terms in the iterations that depend on the size of the CABS. Formally, the most expensive contraction scales as O^2N^4, but this is computed almost for free by adding F12 amplitudes to the conventional amplitudes before the contraction involving four externals in the conventional calculation. The additional cost of a CCSD-F12x calculation over conventional CCSD lies predominantly in the computation of the integrals and intermediates required for MP2-F12, which scales as ON^2X^2 for the

[6] This is known as the *standard approximation* in the literature.

SP approach, and the computation of the final energy, which requires a further O^2N^4 contraction for CCSD-F12b. To summarize, for systems with around 20 valence electrons, the computation time for a CCSD-F12x calculation is only a few percent longer than that of a CCSD calculation in the same basis.

Availability: The CCSD-F12x methods have been developed within the MOLPRO quantum chemistry package. Since they are essentially a simplified version of the CCSD(F12) method, it is highly probable that it will become possible to use the CCSD-F12x methods within the CCSD(F12) programs mentioned in the previous section.

Performance: In Table 20-4 we compare CCSD-F12x correlation energies for H_2O, taken from Ref. [90], with CCSD-F12 values computed using GECCO. The CCSD-F12 values differ from Table 20-1 because, although the same orbital and CABS were used, the calculations reported in Table 20-4 were performed with a STG exponent of 1.5 a_0^{-1}. The CCSD-F12a method overestimates the correlation energy, because the F12 contribution is computed using an MP2-like functional. The convergence of CCSD-F12b with orbital basis is more in line with the full CCSD-F12 model. For the CCSD-F12b/aug-cc-pVDZ calculations, the loss of accuracy of 3 mE_h in the total correlation energy compared to CCSD-F12 is significant, since it corresponds to 5% of the F12 contribution to the correlation energy, and increases the total basis set error by 40%.

Due to the use of an approximate $\hat{Q}_{12}$, it is not appropriate to judge the CCSD-F12x methods based on total energies, but rather for relative energies. To date, no fair and direct comparison between the CCSD-F12x methods and other approximate models exists in the literature. However, the basis set errors of the CCSD-F12x models for reaction energies, atomization energies, ionization potentials and electron affinities have been extensively investigated [90]. The results are summarized in Table 20-5. Compared to a conventional calculation in the same basis, the basis set errors for the CCSD-F12x methods are an order of magnitude smaller. Even using aug-cc-pVDZ basis sets, the CCSD-F12x basis set errors are below 5 kJ mol^{-1} for reaction energies. In this method this important reduction in the basis set error has been achieved by including F12 basis functions at almost no extra cost compared to the conventional calculation. It should be noted that to obtain these excellent results, the CCSD-F12x energies were combined with a correction for the Hartree–Fock basis set error, using Eqs. (20-81), (20-82) and (20-83) of Section 20.7. Examples

Table 20-4. Valence correlation energies of H_2O in mE_h for the CCSD-F12x and CCSD(2)$_{\overline{F12}}$ models, computed with a STG exponent of 1.5 a_0^{-1}. The basis set limit is −297.9 mE_h

Basis	CCSD-F12a	CCSD-F12b	CCSD(2)$_{\overline{F12}}$	CCSD-F12
aug-cc-pVDZ	−293.22	−287.27	−290.72	−290.18
aug-cc-pVTZ	−298.50	−294.33	−294.75	−295.58
aug-cc-pVQZ	−299.37	−296.88	−296.94	−297.35

Table 20-5. CCSD and CCSD-F12x RMS basis set errors for open- and closed-shell reaction energies and atomization energies (kJ mol^{-1}), and ionization potentials and electron affinities (meV). Taken from Ref [90]

Method	Basis	RE(cs)	RE(os)	AE	IP	EA
CCSD	aug-cc-pVDZ	18.74	51.97	80.49	245.72	177.76
	aug-cc-pVTZ	6.80	18.65	24.94	98.10	72.18
	aug-cc-pVQZ	2.46	6.71	8.84	40.10	28.00
	aug-cc-pV5Z	1.23	3.09	4.17	20.54	14.64
CCSD-F12a	aug-cc-pVDZ	2.68	4.68	7.03	51.96	34.93
	aug-cc-pVTZ	1.28	1.29	1.86	9.23	11.76
	aug-cc-pVQZ	0.51	1.24	2.17	9.10	11.38
CCSD-F12b	aug-cc-pVDZ	2.34	5.00	10.23	70.84	50.22
	aug-cc-pVTZ	1.18	1.81	2.14	21.80	14.83
	aug-cc-pVQZ	0.59	0.68	0.70	5.20	3.76

for the performance of the CCSD-F12x methods for potential energy surfaces can be found in Ref. [91].

20.4.3. CCSD(2)$_{\overline{\text{F12}}}$

In Valeev's CCSD(2)$_{\overline{\text{F12}}}$ model,[7] rather than solving for the geminal amplitudes iteratively, the geminal contributions are included *a posteriori* on the basis of perturbation theory, using a Löwdin partitioning of the CCSD similarity transformed Hamiltonian [92–94]. This approach is thus analogous to the perturbative rather than iterative treatment of connected triples in the (T) method [95]. The particular choice of Löwdin and perturbation partitionings that is used to define the CCSD(2)$_{\overline{\text{F12}}}$ model is

$$\bar{H} = \bar{H}^{(0)} + \bar{H}^{(1)} = \begin{pmatrix} \bar{H}_{PP} & 0 \\ 0 & \bar{H}^{(0)}_{QQ} \end{pmatrix} + \begin{pmatrix} 0 & \bar{H}_{PQ} \\ \bar{H}_{QP} & \bar{H}^{(1)}_{QQ} \end{pmatrix}, \tag{20-42}$$

where $\bar{H} = e^{-\hat{T}_1-\hat{T}_2}\hat{H}e^{\hat{T}_1+\hat{T}_2}$ and the singles and doubles amplitudes are those of a converged CCSD calculation. The Löwdin partitioning of the Hamiltonian into a reference space P and external space Q, for the perturbation, is chosen such that P refers to the space of ket states $|\text{HF}\rangle \oplus \hat{E}_{ai}|\text{HF}\rangle \oplus \hat{E}_{ai}\hat{E}_{bj}|\text{HF}\rangle$ or the biorthogonal bra states, and Q refers to the space of kets $\hat{E}_{\alpha i}\hat{E}_{\beta_\perp j}|\text{HF}\rangle$ or the biorthogonal bra states. The choice of zeroth order Hamiltonian for the QQ space is $\hat{F} + E^{(0)} - \varepsilon$, where $\varepsilon = \langle\text{HF}|\hat{F}|\text{HF}\rangle$. The zeroth order energy $E^{(0)}$ is the CCSD energy and the

[7] Valeev himself uses the moniker CCSD(2)$_{\overline{\text{R12}}}$ irrespective of the correlation factor, but for consistency we use F12 in this chapter.

zeroth order bra and ket states are simply the left and right eigenvectors of the CCSD similarity transformed Hamiltonian, $\langle \Lambda|$ and $|\mathrm{HF}\rangle$. Applying perturbation theory, the first order energy correction vanishes and the second-order correction defines the CCSD(2)$_{\mathrm{F12}}$ method,

$$E^{(2)} = -\Lambda_P \bar{H}_{PQ} \left(\bar{H}^{(0)}_{QQ} - E^{(0)} S_{QQ} \right)^{-1} \bar{H}_{Q0}. \tag{20-43}$$

$\bar{H}^{(0)}_{QQ}$ and S_{QQ} are the familiar B and X matrices required for the F12 Fock matrix elements in MP2-F12 theory (see Section 20.5.1). $\bar{H}_{Q0}$ and $\Lambda_P \bar{H}_{PQ}$ are given by

$$\bar{H}_{Q0} = \langle \mu_{2'} | \bar{H} | \mathrm{HF} \rangle , \tag{20-44}$$

$$\Lambda_P \bar{H}_{PQ} = \langle \Lambda | \bar{H} | \mu_{2'} \rangle . \tag{20-45}$$

To arrive at the CCSD(2)$_{\overline{\mathrm{F12}}}$ model, several simplifications are required, which are referred to as screening approximations in the literature and are very similar in nature to those used to construct the CCSD-F12x methods. In particular, the HF, singles and doubles components of $\langle \Lambda | \bar{H} | \mu_{2'} \rangle$ are approximated as

$$\langle \mathrm{HF} | \bar{H} | \mu_{2'} \rangle \approx \langle \mathrm{HF} | \hat{\Phi} | \mu_{2'} \rangle , \tag{20-46}$$

$$\langle \mu_1 | \bar{H} | \mu_{2'} \rangle \approx 0, \tag{20-47}$$

$$\langle \mu_2 | \bar{H} | \mu_{2'} \rangle \approx \langle \bar{\mathbf{t}}_2 | \hat{\Phi} | \mu_{2'} \rangle . \tag{20-48}$$

In keeping with (T) theory, the Lagrange multipliers are approximated to first order only (see Eq. (20-25)). The neglected terms are either higher than second order in the fluctuation potential from the point of view of standard Møller–Plesset perturbation theory, or would disappear if $\hat{Q}_{12} \approx 1 - \hat{P}_1 \hat{P}_2$, or correspond to GBC terms. Similar approximations are applied to the $\langle \mu_{2'} | \bar{H} | \mathrm{HF} \rangle$ term. The resulting energy expression is very simple in form,

$$E^{(2)} = -\langle \mathrm{HF} + \bar{\mathbf{t}}_2 | \hat{\Phi} | \mu_{2'} \rangle \langle \mu_{2'} | \hat{F} - \varepsilon | \nu_{2'} \rangle^{-1} \langle \nu_{2'} | \hat{\Phi} + [\hat{\Phi}, \hat{T}_2] | \mathrm{HF} \rangle . \tag{20-49}$$

Summation over the indices of adjacent $\mu_{2'}$ or $\nu_{2'}$ is implied. The CCSD(2)$_{\overline{\mathrm{F12}}}$ energy can be equivalently obtained by minimizing a modified Hylleraas functional, which can then also be used with the SP Ansatz,

$$L^{(2)} = \langle \bar{\mathbf{c}} | [\hat{F}, \hat{T}_{2'}] | \mathrm{HF} \rangle + 2 \langle \bar{\mathbf{c}} | \hat{\Phi} + [\hat{\Phi}, \hat{T}_2] | \mathrm{HF} \rangle . \tag{20-50}$$

This is very similar to the energy functional of the CCSD-F12b method. All that is required to obtain the CCSD(2)$_{\overline{\mathrm{F12}}}$ functional is to neglect terms from EBC and

single amplitudes[8] and to introduce into Eq. (20-41) a factor of 2 in front of the commutator $\langle \bar{\mathbf{c}}| [\tilde{\Phi}, \hat{T}_2] |\mathrm{HF}\rangle$, which is the difference between CCSD-F12b and CCSD-F12a. However, in contrast to the CCSD-F12x methods, the full projector $\hat{Q}_{12}$ is used to evaluate the terms in the CCSD(2)$_{\overline{\mathrm{F12}}}$ approach, that is, Eq. (20-10) is used, not Eq. (20-39).

Computational cost: Since the CCSD equations are solved without any reference to the geminal basis, the cost of the iterations is identical to that of conventional CCSD. Just as for the CCSD-F12x methods, the additional computational effort for the F12 contributions lies in the construction of the MP2-F12 intermediates and the evaluation of the final energy. In contrast to the CCSD-F12b method, the CABS contributions to the commutator $\langle \mathrm{HF}| [\hat{\Phi}, \hat{T}_2] |\mathrm{HF}\rangle$ are not neglected, which leads to a step with O^3N^2X scaling in addition to the O^2N^4 contractions required for CCSD-F12b.

Availability: The CCSD(2)$_{\overline{\mathrm{F12}}}$ model was developed using the MPQC and PSI3 programs. So far, the CCSD(2)$_{\overline{\mathrm{F12}}}$ method has also been implemented in MOLPRO, but, due to its simplicity, it is very likely to find its way into almost every program where full or approximate CCSD-F12 methods are available.

Performance: For total energies, the CCSD(2)$_{\overline{\mathrm{F12}}}$ method appears to be more reliable than the CCSD-F12a or CCSD-F12b approaches. The valence correlation energies of water computed using the CCSD(2)$_{\overline{\mathrm{F12}}}$ method are listed in Table 20-4 along side CCSD-F12 and CCSD-F12x values. The CCSD(2)$_{\overline{\mathrm{F12}}}$ and CCSD-F12x values were both computed using the MOLPRO package, with the same basis sets. These values were taken from Ref. [90]. It would appear that the improvement of CCSD(2)$_{\overline{\mathrm{F12}}}$ over CCSD-F12b for total energies is independent of whether the SP Ansatz is used or not [90, 93] and results both from the better treatment of $\hat{Q}_{12}$ and, fortuitously, from the neglect of the EBC terms. For relative energies, the CCSD(2)$_{\overline{\mathrm{F12}}}$ and CCSD-F12x methods appear to perform similarly. Although no direct comparison has yet been published, the impressive results in Table 20-5 could probably equally well have been obtained using the CCSD(2)$_{\overline{\mathrm{F12}}}$ method. However, the differing treatment of single excitations may lead to differences in performance for ionization potentials and electron affinities.

20.4.4. Further Simplifications

In standard canonical theory, the Brillouin condition implies that

$$\langle \mathrm{HF}| [\hat{F}, \hat{T}_1] |\mathrm{HF}\rangle = \langle \mu_1| \hat{F} |\mathrm{HF}\rangle = \langle \mu_1| [\hat{F}, \hat{T}_2] |\mathrm{HF}\rangle = \\ \langle \mu_1| [[\hat{F}, \hat{T}_1], \hat{T}_1] |\mathrm{HF}\rangle = \langle \mu_2| [[\hat{F}, \hat{T}_1], \hat{T}_2] |\mathrm{HF}\rangle = 0. \qquad (20\text{-}51)$$

[8] All contributions from single excitations are neglected in the CCSD(2)$_{\overline{\mathrm{F12}}}$ model: the singles amplitudes have been assumed to be second order in the fluctuation potential, which is reasonable for ground state energies computed using RHF and UHF references, but not ROHF [94].

If the GBC is assumed, then the following terms are additionally zero

$$\langle \mu_1 | \, [\hat{F}, \hat{T}_{2'}] \, | \mathrm{HF} \rangle = \langle \mu_2 | \, [[\hat{F}, \hat{T}_1], \hat{T}_{2'}] \, | \mathrm{HF} \rangle = \langle \mu_{2'} | \, [[\hat{F}, \hat{T}_1], \hat{T}_{2'}] \, | \mathrm{HF} \rangle = 0. \tag{20-52}$$

Assumption of the EBC zeros the coupling terms

$$\langle \mu_2 | \, [\hat{F}, \hat{T}_{2'}] \, | \mathrm{HF} \rangle = \langle \mu_{2'} | \, [\hat{F}, \hat{T}_2] \, | \mathrm{HF} \rangle = 0. \tag{20-53}$$

At the level of MP2-F12 theory, neglect of GBC and particularly EBC terms can lead to significant computational savings. The effect of neglecting the GBC terms is usually less than 0.1% of the correlation energies and is comparable in magnitude to the other approximations employed in integral evaluation [96]. The EBC terms have an order of magnitude larger effect on the MP2-F12 correlation energy, and probably should not be neglected, although relative energies do not deteriorate significantly when the EBC is assumed. Valeev has shown that using a Fock operator built from imprecise Hartree–Fock orbitals has only a minor effect on the MP2 correlation energy when the GBC and EBC terms are computed [97]. In CCSD-F12 calculations, the cost of computing the GBC and EBC terms is completely insignificant.

20.4.5. Open-Shell Extensions

The CCSD-F12 equations are straightforwardly written in terms of spin-orbitals, which defines the UCCSD-F12 approach for use with UHF references or ROHF references with semi-canonical orbitals. Just as for conventional calculations, the ROHF Fock elements F_i^{α} are treated as first order and therefore do not appear in the zeroth-order Hamiltonian for MP2-F12 [90, 98].

There is, however, a complication that arises when applying the SP Ansatz to open-shell molecules. It is not possible to satisfy both the *s*- and *p*-wave coalescence conditions for the opposite-spin pairs for UHF references using the geminal basis defined through the occupied orbitals. Spin-flipped geminal basis functions are also required [71],

$$f_{12} \bar{\phi}_{i\sigma} \bar{\phi}_{j\tau}, \tag{20-54}$$

where, for example, $\bar{\phi}_i$ is the spatial function for the orbital with τ spin. For ROHF references, the additional set of geminals only differ from the ones of the occupied orbitals for pairs where one of the orbitals is singly occupied. By expanding the geminal basis to include these orbital pairs, the usual SP amplitudes in Eq. (20-31) can be applied. At the time of writing this chapter, this had been implemented for the CCSD-F12x methods in MOLPRO [90] and at the CCSD(F12) level of theory in TURBOMOLE.

20.5. INTEGRALS AND INTERMEDIATES

20.5.1. MP2-F12

The F12 intermediates involved in a CCSD-F12 calculation may be divided into those required for the initial MP2-F12 calculation and those that are only needed for the coupled-cluster residuals. The MP2-F12 equations are given by

$$E = \langle \mathrm{HF}| \hat{F} + \hat{\Phi} + [\Phi, \hat{T}_2 + \hat{T}_{2'}] \, |\mathrm{HF}\rangle \,, \tag{20-55}$$

$$0 = \langle \mu_2| \, [\hat{F}, \hat{T}_2 + \hat{T}_{2'}] + \hat{\Phi} \, |\mathrm{HF}\rangle \,, \tag{20-56}$$

$$0 = \langle \mu_{2'}| \, [\hat{F}, \hat{T}_2 + \hat{T}_{2'}] + \hat{\Phi} \, |\mathrm{HF}\rangle \,, \tag{20-57}$$

and are usually solved by minimizing the Lagrangian (Hylleraas functional) for each pair ij (Ref. [44] contains a review of MP2-F12 theory). In addition to the conventional Fock and Coulomb integrals, four further intermediates are required:

$$V_{ij}^{kl} = \langle kl| f_{12} \hat{Q}_{12} r_{12}^{-1} |ij\rangle, \tag{20-58}$$

$$B_{mn}^{kl} = \langle kl| f_{12} \hat{Q}_{12} (\hat{F}_1 + \hat{F}_2) \hat{Q}_{12} f_{12} |mn\rangle, \tag{20-59}$$

$$X_{mn}^{kl} = \langle kl| f_{12} \hat{Q}_{12} f_{12} |mn\rangle, \tag{20-60}$$

$$C_{ab}^{kl} = \langle kl| f_{12} \hat{Q}_{12} (\hat{F}_1 + \hat{F}_2) |ab\rangle. \tag{20-61}$$

The particular way in which the Fock matrix elements B and C are evaluated, regarding whether or not certain terms are neglected or treated approximately is responsible for the bewildering array of acronyms in MP2-F12 theory, such as A, A′ B, C, with or without an appended asterisk etc. We will not concern ourselves with all the details of the derivation or evaluation of these intermediates here and refer the reader to the numerous accounts in the literature [20, 42, 45–47, 98, 99]. Refs. [47] and [98] contain particularly thorough discussions on this topic for RHF and ROHF references, respectively. Here it is sufficient to mention that for CCSD-F12 theories no real saving is gained by using the more approximate versions of MP2-F12 theory and that almost all programs employ the variant B or C, where no terms are neglected.[9]

Two salient points regarding MP2-F12 intermediates, however, do need to be discussed here. Taking the V intermediate as an example and expanding $\hat{Q}_{12}$ using Eq. (20-10), one sees that three-electron integrals arise,

$$\langle kl| f_{12} \hat{O}_1 r_{12}^{-1} \, |ij\rangle = \sum_m \langle klm| f_{12} r_{23}^{-1} \, |mji\rangle \,. \tag{20-62}$$

---

[9] For consistency with the CABS singles approach, the Fock elements $F_i^{\alpha\perp}$ should be considered as part of the first-order Hamiltonian. Since these Fock contributions do not formally contribute to the B or C matrices, this choice has no effect on the above equations.

Four-electron integrals are required for the evaluation of B. Although these integrals are straightforward to evaluate for particular choices of f_{12}, their sheer number means that the cost of their evaluation would severely restrict the size of system that could be treated. One of the primary features that distinguish the R12 and F12 methods from other geminal based approaches, such as GTG [100–106] or GGn [107–110], is the use of RI approximations to compute these integrals by decomposing them into sums of products of two-electron integrals (see Ref. [111] for an overview of explicitly correlated approaches). In the CABS approach, the basis for the RI is the union of the orbital basis and a complementary auxiliary basis, which leads to the following compact expressions for $\hat{Q}_{12}$:

$$\hat{Q}_{12} \approx 1 - \hat{P}_1\hat{P}_2 - \hat{O}_1\hat{P}'_2 - \hat{P}'_1\hat{O}_2, \tag{20-63}$$

$$\hat{Q}_{12} \approx \hat{P}'_1\hat{P}'_2 + \hat{V}_1\hat{P}'_2 + \hat{P}'_1\hat{V}_2. \tag{20-64}$$

The first is more accurate since the CABS orbitals are used only to approximate the $|i\alpha_\perp\rangle$ region of the geminal space, which can be seen by identifying the parts of $\hat{Q}_{12}$ in Figure 20-3. The second expression is only used when the evaluation of the integrals for the unity result in three-electron integrals, for example in the exchange contribution to B, $\langle kl|f_{12}(\hat{K}_1 + \hat{K}_2)f_{12}|mn\rangle$. The use of either of these expressions for $\hat{Q}_{12}$ in Eq. (20-58) obviously results in sums of products of two-electron integrals.

The second point that should be highlighted is the accuracy of the RI approximation. For the Fock matrix elements, B, direct insertion of the RI approximated $\hat{Q}_{12}$ leads to expressions that converge slowly with the size of CABS [20]. However, a reformulation involving commutators results in terms that either truncate or are rapidly convergent with CABS. Nevertheless, for the approximate RI to be accurate, the orbital plus CABS must be saturated to at least $3L_{\mathrm{occ}}$, where L_{occ} is the maximum angular momentum of the atomic functions contributing to the occupied orbitals.[10] With appropriately chosen CABS the approximate RI leads to errors similar in magnitude or slightly larger than density fitting errors, that is around 0.01 mE_h for 10 electron systems [112]. Solving the MP2-F12 equations implicitly involves inverting B, which is diagonally dominant in spin-adapted form. Too small CABS can result in significant errors in the small off-diagonal elements, leading to non-positive definiteness of B and positive F12 contributions to pair energies. This numerical problem is circumvented through use of the SP Ansatz.

Most F12 programs currently apply the CABS approach, where the computational expense for computing the MP2-F12 intermediates is O^4X^2, which can be reduced to O^4NX by employing so called hybrid approximations [45, 47]. For the SP Ansatz, only the diagonal spin-adapted matrices are required and the scaling reduces to the cost of computing the two-electron integrals. This is at most ON^2X^2

[10] This can be reduced to $2L_{\mathrm{occ}}$ using a combined RI and density fitting approximation [49].

and many programs employ density fitting techniques to reduce the pre-factor significantly [48].

RI is not the only device capable of avoiding many-electron integrals: numerical quadrature can also be applied [57, 113]. This method represents electron repulsion integrals, for example, as sums of two- and three-center objects over grid points,

$$\langle pq|r_{12}^{-1}|rs\rangle \approx \sum_g \bar{\phi}_p(\mathbf{r}_g)\bar{\phi}_r(\mathbf{r}_g)\langle q|r_{1g}^{-1}|s\rangle, \tag{20-65}$$

where $\bar{\phi}_p(\mathbf{r}_g) = w_g\phi_p(\mathbf{r}_g)$ denotes the weighted value of the orbital ϕ_p at the quadrature grid point $\mathbf{r}_g$ (w_g is the weight of that grid point). Applied to three-electron integrals, numerical quadrature yields

$$\langle pqr|f_{12}r_{23}|stu\rangle \approx \sum_g \bar{\phi}_q(\mathbf{r}_g)\bar{\phi}_t(\mathbf{r}_g)\langle p|f_{2g}|s\rangle\langle r|r_{2g}^{-1}|u\rangle. \tag{20-66}$$

By combining numerical quadrature and CABS RI techniques, the requirements on the CABS basis can be reduced. Such hybrid approaches have been suggested by Ten-no [55].

20.5.2. CCSD-F12

The simplified CCSD-F12x and CCSD(2)$_{\overline{\text{F12}}}$ models require only one additional intermediate beyond those of MP2-F12, namely the integral

$$V_{pq}^{kl} = \langle kl|f_{12}\hat{Q}_{12}r_{12}^{-1}|pq\rangle. \tag{20-67}$$

The cost of evaluation for this intermediate is O^2N^4 and Coulomb integrals with four external indices are required, irrespective of whether Eq. (20-10) or Eq. (20-39) is used for $\hat{Q}_{12}$. Just as for conventional CCSD, integral direct schemes can be applied to avoid storage of the Coulomb integrals with four external indices. Storage of four-index Coulomb integrals with CABS indices can be avoided through density fitting.

For the CCSD(F12) approach, $\hat{T}_1$ dependent contributions to V are required, which have been combined into a new intermediate $\tilde{V}$ in the literature [83],

$$\tilde{V}_{pq}^{kl} = \langle kl|f_{12}\hat{Q}_{12}\big(1 - \hat{T}_1 - \tfrac{1}{2}\hat{T}_1^2\big)r_{12}^{-1}|pq\rangle. \tag{20-68}$$

This is term is used to evaluate $\langle\mu_{2'}|\,\tilde{\Phi}\,|\text{HF}\rangle$ and $\langle\mu_{2'}|\,[\tilde{\Phi},\hat{T}_2]\,|\text{HF}\rangle$ and the $\hat{T}_1$ dependent contributions must be reevaluated in every iteration.

The evaluation of the commutator $\langle\mu_{2'}|\,[\tilde{\Phi},\hat{T}_{2'}]\,|\text{HF}\rangle$ for the full CCSD-F12 method requires intermediates of the type [23]

$$P_{ij}^{kl} = \langle kl|f_{12}\hat{Q}_{12}r_{12}^{-1}\hat{Q}_{12}f_{12}|ij\rangle, \tag{20-69}$$

$$Z_{ij;p}^{kl;m} = \langle klm|f_{12}\hat{Q}_{12}r_{23}^{-1}\hat{Q}_{12}f_{12}i|jp\rangle, \tag{20-70}$$

where the Z intermediate is needed, for example, for the $\hat{T}_1$ dependency. Several other intermediates also appear, but the above two require special attention because, unlike the other terms, straightforward insertion of RI leads to expressions that converge slowly with the size of CABS. For an accurate implementation these must be reformulated into terms that either truncate or converge rapidly (see Ref. [78], and also [77], which contains numerical examples and a corrected expression for Z).

20.5.3. Two-Electron Integrals

Evaluation of the MP2-F12 intermediates requires the computation of two-electron integrals over r_{12}^{-1}, f_{12}, $f_{12}r_{12}^{-1}$, f_{12}^2 and $(\nabla_1 f_{12})^2$.[11] The full CCSD-F12 model requires additional integrals over $f_{12}^2 r_{12}^{-1}$. The cost of computing these integrals makes a MP2-F12 calculation rather more expensive than a conventional MP2 calculation in the same orbital basis, but for the CCSD-F12 models, the cost is dominated by the iterations, or by the triples correction in a CCSD(T)-F12 calculation. Most programs employ robust density fitting techniques [48] to reduce the cost of the integral evaluation.

Three choices of correlation factor f_{12} are prevalent in the literature:

$$f_{12} = r_{12}, \tag{20-71}$$

$$f_{12} = -\gamma^{-1}\exp(-\gamma r_{12}), \tag{20-72}$$

$$f_{12} = \sum_i^n c_i \exp\left(-\gamma_i r_{12}^2\right) \approx -\gamma^{-1}\exp(-\gamma r_{12}). \tag{20-73}$$

R12 methods refer to choosing linear-r_{12} and F12 methods to non-linear correlation factors. For all three choices, the required two-electron integrals may be computed analytically. The integrals for linear-r_{12} are related to conventional Coulomb integrals and the integrals for the STG can be found in Ref. [40] within the Obara–Saika recursive scheme. The integrals for Gaussian geminals in the STG-nG contraction are also well known and date back to Boys and Singer [114, 115]. The particular integrals required for MP2-F12 theory have been reported in Refs. [116] and [56] for the McMurchy–Davidson and Obara–Saika recursive schemes, respectively and coefficients for the STG-nG fit with $n = 3, 4, 5$ and 6 can be found in Ref. [66], or, alternatively, computed using the prescription in Ref. [47].

Due to the higher accuracy of the F12 methods, linear-r_{12} is rarely chosen in modern calculations. Furthermore, the STG correlation factors are shorter range and

[11] If approximation B is used rather than C, then integrals over $[\nabla_1^2, f_{12}]$ are also needed.

thus more amenable to density fitting and local approximations. The computational cost of selecting STG or STG-*n*G would appear to be comparable [55].

20.6. THE CORRELATION FACTOR

The role of the F12 geminal basis functions is to efficiently describe the correlation hole in correlated wave functions, which is defined as $\Psi_{\text{corr.}} - \Psi_{\text{HF}}$. Due to the nature of the Coulomb potential the correlation hole must be linear in r_{12} at short range r_{12}. This fact is embodied in Kato's well known cusp condition (see below). At longer range r_{12}, the correlation hole deviates from linear-r_{12}, as illustrated for helium in Figure 20-1. In F12 methods, the correlation hole for each correlated orbital pair function is represented as a correlation factor f_{12} multiplying a Hartree–Fock orbital pair. Both the orbital and f_{12} components give rise to deviation from linear-r_{12}. The choice of the orbital pair is chosen such that Kato's cusp condition can be satisfied for MP2 wave functions. In this section we examine the choice of f_{12} in more detail.

20.6.1. Coalescence Conditions

In the limit $r_{12} \to 0$ the form of the correlation hole is determined by the singularity of the Coulomb potential. For the local energy not to diverge, the correlated wave function must exhibit a derivative discontinuity at $r_{12} = 0$ such that the singularity in the kinetic energy exactly cancels that of the Coulomb repulsion. Mathematical analysis of the exact wave function leads to [117–119]

$$\frac{\partial \widetilde{\Psi}^{0}}{\partial r_{12}}\bigg|_{r_{12}=0} = \tfrac{1}{2}\,\Psi_{r_{12}=0}, \tag{20-74}$$

$$\frac{\partial^2 \widetilde{\Psi}^{1}}{\partial r_{12}^2}\bigg|_{r_{12}=0} = \tfrac{1}{2}\,\frac{\partial \widetilde{\Psi}^{1}}{\partial r_{12}}\bigg|_{r_{12}=0}. \tag{20-75}$$

The first equation is Kato's cusp condition and is valid when $\Psi_{r_{12}=0} \neq 0$, that is, when the coalescing electrons have different spins. For triplet coupled electrons, the wave function vanishes at coalescence and the derivative discontinuity is in the second derivative. The notation $\widetilde{\Psi}^{l}$ indicates a spherical average weighted with a spherical harmonic Y_{lm}. Equations (20-74) and (20-75) are referred to as *s*-wave and *p*-wave cusp conditions, respectively and have the integrated forms

$$\Psi = \Psi_{r_{12}=0}\big(1 + \tfrac{1}{2}r_{12}\big) + \mathcal{O}\big(r_{12}^2\big), \tag{20-76}$$

$$\Psi = \mathbf{r}_{12} \cdot \frac{\partial \Psi}{\partial \mathbf{r}_{12}}\bigg|_{r_{12}=0} \big(1 + \tfrac{1}{4}r_{12}\big) + \mathcal{O}\big(r_{12}^3\big). \tag{20-77}$$

The equivalent conditions for the first order pair functions in MP2 theory have been given in Eq. (20-1). In comparing Eq. (20-1) with Eqs. (20-76) and (20-77), it is helpful to identify the spatial part of singlet Hartree–Fock orbital pairs $\frac{1}{\sqrt{2}}(\phi_i\phi_j + \phi_j\phi_i)$ with the s-wave expression and triplet pairs $\frac{1}{\sqrt{2}}(\phi_i\phi_j - \phi_j\phi_i)$ with the p-wave expression. The coalescence conditions only give information regarding the linear-r_{12} dependence of the correlation hole. The form of the hole at medium to long range r_{12} is expected to be system dependent. Indeed, analysis of the $\mathcal{O}\left(r_{12}^2\right)$ and $\mathcal{O}\left(r_{12}^3\right)$ terms in Eqs. (20-76) and (20-77) indicates an early deviation from linearity and that different correlation factors are appropriate for different orbital pairs. However, there is strong numerical evidence suggesting that the Slater-type correlation factor is close to optimal in F12 methods [66, 120].

20.6.2. Slater-Type Correlation Factors

The R12 basis functions, where $f_{12} = r_{12}$, give an exact description of the MP2 correlation hole at short r_{12}, but they do not decay quickly enough to give a reasonable description for longer range r_{12}.[12] This is demonstrated in Figure 20-4 where we have plotted the optimum F12 correlation factor for a CCSD calculation on the ^1S and ^3S states of helium, computed numerically using Hylleraas coordinates (see Refs. [66, 121]). The Slater-type correlation factor is very close to the optimum correlation factor for helium for a wide range of r_{12}. A natural interpretation for this is that the Slater function models the screened interaction between the two electrons.

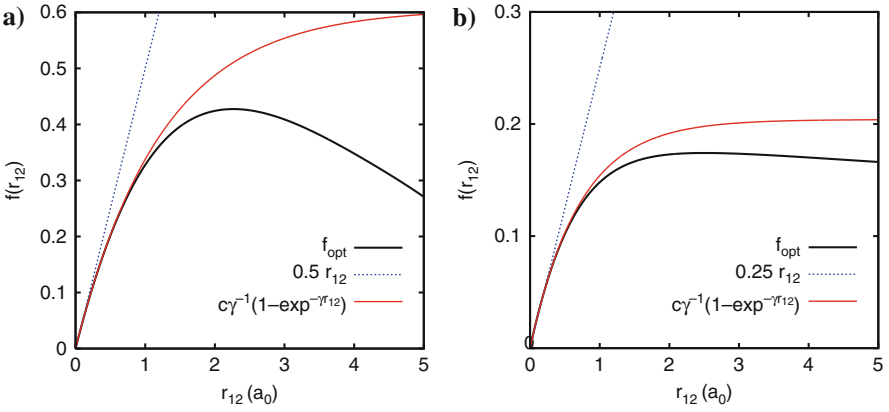

Figure 20-4. **(a)** R12 and F12 correlation factors $\left(c = 0.49, \gamma = 0.81\ \mathrm{a}_0^{-1}\right)$ compared to the optimum factor for ^1S helium. **(b)** R12 and F12 correlation factors $\left(c = 0.29, \gamma = 1.40\ \mathrm{a}_0^{-1}\right)$ compared to the optimum factor for ^3S helium

[12] Note that the orbital component of the R12 basis functions ensures that they do decay with r_{12} and are zero at infinite r_{12}.

Table 20-6. Parameters for the fit $c\gamma^{-1}(1-e^{-\gamma r_{12}})$ to the optimum correlation factor for He and its isoelectronic series of cations. γ closely follows $a(Z-b)$ with $a = 0.7177$ and $b = 0.8481$

Z	2	3	4	5	6	7	8
c	0.49	0.49	0.49	0.49	0.49	0.49	0.49
γ (a_0^{-1})	0.81	1.55	2.27	2.99	3.70	4.42	5.12
$a(Z-b)$	0.83	1.54	2.26	2.98	3.70	4.42	5.13

In Table 20-6 we list the coefficients c and exponents γ in a STG fit to the optimum correlation factors for the helium isoelectronic series of cations in their ^1S ground states. These differ slightly from those of Ref. [66] because here the fits only used the range $r_{12} < 0.1$ a_0. The size of the correlation hole shrinks with increasing nuclear charge Z and the value of γ thus increases proportionally. The function $a(Z-b)$ in Table 20-6 models the screened nuclear charge acting on the correlating electrons. Variations in the effective nuclear charge for valence shell electrons are relatively weak for neutral atoms and molecules. Thus a single correlation factor with a single exponent is sufficient for many purposes. However, an exponent chosen for valence correlation is sub-optimal for core correlation, or correlation in anions or cations. If one wants to avoid including additional STGs with adapted exponents, these deficiencies must be made up through the orbital basis set.

In fact, there is a large redundancy between the orbital basis and the F12 basis functions, which helps to reduce the sensitivity of F12 calculations to the choice of γ. The cc-pVXZ-F12 basis sets were optimized for a particular STG exponent and it is recommended to use the correct exponent with the correct basis (see Section 20.3.4).

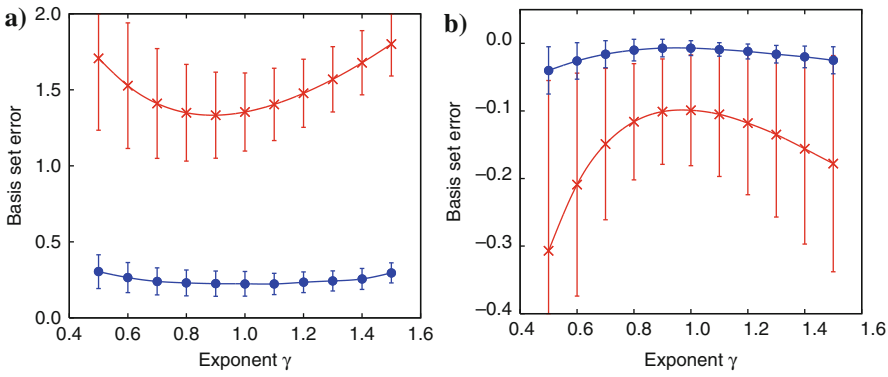

Figure 20-5. **(a)** Mean basis set errors (kJ mol^{-1} per valence electron) in the valence CCSD(F12)/cc-pVXZ-F12 correlation energies over 58 molecules for X = D (×) and T (●) as a function of γ (a_0^{-1}). The standard deviation is given as an error bar. **(b)** Mean basis set errors (kJ mol^{-1} per valence electron) in the valence CCSD(F12)-SP/cc-pVXZ-F12 correlation contribution to 53 reaction energies for X = D (×) and T (●) as a function of γ (a_0^{-1}). The standard deviation is given as an error bar

In Figure 20-5 we have plotted statistical measures of the basis set errors in the CCSD(F12) correlation energy as a function of the exponent γ in the STG correlation factor. We plot the mean and standard deviations for the basis set errors for total and relative correlation energies over the set of 58 molecules used for Table 20-2, where we have used the SP Ansatz for the relative energies. For the cc-pVDZ-F12 basis set, the accuracy is rather sensitive to the exponent γ and the lowest errors are obtained using the recommended value of 0.9 a_0^{-1}. For the cc-pVTZ-F12 basis, the absolute accuracy is much less sensitive to the choice of exponent and again the recommended value of 1.0 a_0^{-1} gives the best results. It should, however, be noted that these statistics only include molecules with elements H, C, N, O and F.

20.7. AUXILIARY SINGLE EXCITATIONS

The F12 geminals reduce the basis set errors in the CCSD correlation energies to such an extent that the basis set error in the Hartree–Fock energy becomes the limiting factor for CCSD/cc-pVDZ-F12 calculations (see Table 20-3 and the discussion in Section 20.4.1). One obvious solution to this problem would be to compute the Hartree–Fock energy using a larger basis. Indeed very efficient Hartree–Fock programs exist and this is usually possible. However, an additional calculation is unnecessary, since a Hartree–Fock correction can be computed essentially for free using Fock matrix elements that form part of an MP2-F12 calculation. Perhaps more importantly, separate calculations for Hartree–Fock and correlation energies is undesirable when energy derivatives are required for structure optimization or the computation of response properties.

The CABS orbitals of a MP2-F12 or CCSD-F12 calculation form a convenient basis for improving the Hartree–Fock description [89]. The CABS singles Hartree–Fock energy correction is obtained from a second-order perturbative treatment of the CCS equations, where the conventional single excitations are combined with single excitations into CABS orbitals, defined through

$$\hat{T}_{1'} = \sum_{ip'} t^i_{p'} \hat{E}_{p'i}, \tag{20-78}$$

$$\langle \mu_{1'}| = \langle \mathrm{HF}| \tfrac{1}{2} \hat{E}_{ip'}. \tag{20-79}$$

Using the orbitals from a finite basis Hartree–Fock calculation, the GBC Fock matrix elements $F_i^{q'}$ form the perturbation [122],

$$F = F^{(0)} + F^{(1)} = \begin{pmatrix} F_i^j & 0 & 0 \\ 0 & F_a^b & F_a^{q'} \\ 0 & F_{p'}^b & F_{p'}^{q'} \end{pmatrix} + \begin{pmatrix} 0 & F_i^b & F_i^{q'} \\ F_a^j & 0 & 0 \\ F_{p'}^j & 0 & 0 \end{pmatrix}. \tag{20-80}$$

We have also treated the off-diagonal Fock matrix elements F_i^a as first order to define a single set of equations for RHF, UHF and ROHF references and to be consistent with standard ROHF-MBPT. The CABS singles Hartree–Fock energy correction is given by [90, 123],

$$E^{(S2)} = E_{HF} + \langle HF|\,[\hat{F}^{(1)}, \hat{T}_1 + \hat{T}_{1'}]\,|HF\rangle = E_{HF} + 2F_i^a t_a^i + 2F_i^{p'} t_{p'}^i, \tag{20-81}$$

$$0 = \langle \mu_1|\,\hat{F}^{(1)} + [\hat{F}^{(0)}, \hat{T}_1 + \hat{T}_{1'}]\,|HF\rangle = F_a^i + F_a^b t_b^i - F_j^i t_a^j + F_a^{q'} t_{q'}^i, \tag{20-82}$$

$$0 = \langle \mu_{1'}|\,\hat{F}^{(1)} + [\hat{F}^{(0)}, \hat{T}_1 + \hat{T}_{1'}]\,|HF\rangle = F_{p'}^i + F_{p'}^{q'} t_{q'}^i - F_j^i t_{p'}^j + F_{p'}^b t_b^i. \tag{20-83}$$

Summation over repeated indices is implied. These equations may be solved analytically with OX^3 effort, or iteratively with OX^2 scaling. This perturbative approach to Hartree–Fock can be formally incorporated into an MP2-F12 treatment without complication and the corrections for Hartree–Fock and correlation energies are uncoupled to second order. Furthermore, the Fock matrix elements in the unified orbital plus CABS space are available from an MP2-F12 calculation because they are required for evaluating the B matrix. The cost of evaluating the CABS singles correction is entirely negligible compared to the cost of an MP2-F12 calculation. Based on a different partitioning in the original work of Noga et al. [122], a simpler correction was also suggested [89], where the EBC elements $F_a^{q'}$ were included in $F^{(1)}$ rather than treated as zeroth order. Here the energy correction has the very simple form

$$E^{(S2*)} = -2\sum_{ip'} \frac{|F_i^{p'}|^2}{\varepsilon_{p'} - \varepsilon_i}, \tag{20-84}$$

where it is assumed that $F_i^j = \delta_i^j \varepsilon_i$ and $F_{p'}^{q'} = \delta_{p'}^{q'} \varepsilon_{p'}$. However, the EBC terms are rather large for small basis sets and the Hartree–Fock energies obtained when treating them as zeroth order are far superior. The above expressions are for RHF calculations but the UHF formulae are entirely analogous. Knizia et al. have derived spin-free expressions for high-spin ROHF references [98].

Table 20-7 is taken from Ref. [90] and lists the RMS basis set errors for Hartree–Fock calculations on reaction energies, atomization energies, ionization potentials and electron affinities, with and without the CABS singles correction. Equations (20-81) (20-82) and (20-83) were used for the correction, denoted (S2), and for a HF/aug-cc-pVXZ calculation, the cc-pVXZ JKFIT basis set was used for CABS. The basis set limit was taken as the aug-cc-pV6Z value and the ROHF method was used for all open-shell calculations. The CABS singles correction reduces the Hartree–Fock basis set errors by an order of magnitude and, despite its perturbative rather than variational nature, it is sufficient to ensure that the accuracy of the Hartree–Fock energies matches that of the CCSD-F12 correlation energies.

The basis set errors for the singles contribution to correlation energies is much less important than the Hartree–Fock or doubles basis set errors. Nevertheless, this basis set error can also be reduced by including the $\hat{T}_{1'}$ cluster operator into the CCSD-F12

Table 20-7. Hartree–Fock RMS basis set errors for open- and closed-shell reaction energies and atomization energies (kJ mol^{-1}), and ionization potentials and electron affinities (meV), with and without the CABS singles correction. Taken from Ref. [90]

Method	Basis	RE(cs)	RE(os)	AE	IP	EA
RHF	aug-cc-pVDZ	13.45	28.88	24.39	65.14	76.22
	aug-cc-pVTZ	2.07	3.61	3.47	11.07	11.80
	aug-cc-pVQZ	0.49	1.17	0.82	2.27	3.58
	aug-cc-pV5Z	0.17	0.35	0.25	0.59	0.98
$E^{(S2)}$	aug-cc-pVDZ	1.79	2.22	1.64	8.16	8.04
	aug-cc-pVTZ	0.48	0.54	0.29	2.76	1.80
	aug-cc-pVQZ	0.18	0.17	0.13	1.04	1.01

wave function [123]. However, simplified methods analogous to the CCSD(F12) approach are required to avoid terms that have worse scaling than O^2N^3X [124].

20.8. CONNECTED TRIPLES

The CCSD method alone is insufficient for a robust and accurate description of electron correlation. Reliable predictions and a quantitative agreement with experiment requires a treatment of the simultaneous correlation of three electrons and, for high accuracy, higher order correlation must also be taken into account. For many applications the CCSD(T) model is sufficient. The (T) energy correction for a CCSD-F12 wave function is given by

$$\Delta E_{(\mathrm{T})} = \langle \bar{\mathbf{t}}_1 | [\hat{\Phi}, \hat{T}_3] | \mathrm{HF} \rangle + \langle \bar{\mathbf{t}}_2 | [\hat{F}, \hat{T}_3] + [\hat{\Phi}, \hat{T}_3] | \mathrm{HF} \rangle + \langle \bar{\mathbf{c}} | [\hat{\Phi}, \hat{T}_3] | \mathrm{HF} \rangle, \quad (20\text{-}85)$$

$$0 = \langle \mu_3 | \, [\hat{F}, \hat{T}_3] + [\hat{\Phi}, \hat{T}_2 + \hat{T}_{2'}] \, | \mathrm{HF} \rangle \,, \quad (20\text{-}86)$$

where $\hat{T}_3$ is the usual three-electron excitation operator

$$\hat{T}_3 = \tfrac{1}{6} \sum_{ijkabc} t_{abc}^{ijk} \hat{E}_{ai} \hat{E}_{bj} \hat{E}_{ck}. \quad (20\text{-}87)$$

Equation (20-86) for the triples amplitudes differs from that of a conventional calculation only through $\langle \mu_3 | \, [\hat{\Phi}, \hat{T}_{2'}] \, | \mathrm{HF} \rangle$. Neglecting this term and the contribution to $\Delta E_{(\mathrm{T})}$ from $\langle \bar{\mathbf{c}} | [\hat{\Phi}, \hat{T}_3] | \mathrm{HF} \rangle$, the (T) energy correction may be computed in exactly the same way as for a conventional CCSD(T) calculation, taking the singles and doubles amplitudes from a converged CCSD-F12 calculation [125]. The effect of neglecting the F12 contribution is to deteriorate the (T) energy slightly compared to a conventional CCSD(T) calculation in the same basis, but this effect is small (compare columns CCSD(T) and CCSD(T)(F12)-SP in Table 20-8). To date, this is the way in which the (T) correction is computed in the CCSD(T)(F12) and CCSD(T)-F12x models [83, 89, 90, 125]. For the CCSD(T)$_{\mathrm{F12}}$ approach, the Löwdin partitioning has been chosen such that the (T) correction

Table 20-8. Valence (T) correlation energies of FH in mE_h from CCSD(T) and CCSD(T)(F12)-SP calculations, with and without F12 triple excitations [77]. The basis set limit is −8.8 mE_h

Basis	CCSD(T)	(F12)-SP	(F12)-XSP
aug-cc-pVDZ	−4.132	−4.004	−8.203
aug-cc-pVTZ	−7.505	−7.299	−8.504
aug-cc-pVQZ	−8.271	−8.170	−8.674
aug-cc-pV5Z	−8.580		
aug-cc-pV6Z	−8.692		

and F12 correction are uncoupled and F12 has rigorously zero contribution in this case [94].

It is straightforward, at least formally, to include F12 basis functions into any coupled-cluster model. All that is required is to introduce F12 double excitations into the cluster operator. Indeed, in the initial development of R12 coupled-cluster methods, formulae were presented up to CCSDT-R12 within the standard approximation, that is, without CABS [23]. The powerful automated programs GECCO and SMITH are currently capable of performing CCSDTQ-F12 calculations [74] and work is in progress to ensure that the additional *P*- and *Z*-type intermediates that occur are appropriately treated.

Although the basis set error for the doubles amplitudes is greatly reduced by F12, these basis functions do not accelerate the convergence of connected triple excitations, or indeed higher order excitations. Table 20-3 demonstrates that the basis set error for the (T) correction in a CCSD(T)(F12) calculation dominates over that of the CCSD correlation energy when a cc-pVQZ-F12 basis set is used. To use F12 methodology to solve the basis set problem for triple excitations, it is necessary to include additional three-body basis functions that are suitable for describing the wave function when at least two of the three interacting electrons are close together. For higher excitations, analogous many-body F12-type basis functions are required.

Köhn has recently proposed the following generalization of the F12 approach to generate arbitrarily high many-body F12 basis functions [76, 77]. Motivated by the cusp condition in first quantization

$$\left.\frac{\partial \Psi_{\mathrm{CC}}}{\partial r_{12}}\right|_{r_{12}=0} = \tfrac{1}{2} r_{12} \Psi_{\mathrm{CC}} + \mathcal{O}\left(r_{12}^2\right), \tag{20-88}$$

Köhn defines a generalized geminal operator $\hat{R}$, representing the action of the correlation factor on the whole orbital space, rather than just the occupied space

$$\hat{R} = \tfrac{1}{2} \sum_{rpsq} c_{rs}^{pq} \sum_{\alpha\beta} w_{\alpha\beta}^{rs} \hat{E}_{\alpha p} \hat{E}_{\beta q}. \tag{20-89}$$

For the SP Ansatz, $c_{rs}^{pq} = \frac{3}{8}\delta_{pr}\delta_{qs} + \frac{1}{8}\delta_{ps}\delta_{qr}$. In second quantization, $r_{12}\Psi_{\mathrm{CC}}$ is represented by $e^{\hat{R}}e^{\hat{T}}\,|\mathrm{HF}\rangle$. Combining the exponentials leads to the generalized cluster operator

$$\hat{T} + \hat{R} + [\hat{R}, \hat{T}] + \tfrac{1}{2}[[\hat{R}, \hat{T}], \hat{T}], \tag{20-90}$$

where only the parts that are excitation operators from the point of view of the Hartree–Fock reference are retained. The linear term $\hat{R}$ is simply $\hat{T}_{2'}$ and the next term $[\hat{R}, \hat{T}] = [\hat{R}, \hat{T}_1 + \hat{T}_2 + \dots\,]$ leads to excitations of the type

$$\hat{T}_{2''} = \sum_{ijb\alpha\beta} t_b^j \left(\tfrac{3}{8} w_{\alpha\beta}^{ib} + \tfrac{1}{8} w_{\alpha\beta}^{bi}\right) \hat{E}_{\alpha i}\hat{E}_{\beta j}, \tag{20-91}$$

$$\hat{T}_{3'} = \sum_{ijkbc\alpha\beta} t_{bc}^{jk} \left(\tfrac{3}{8} w_{\alpha\beta}^{ib} + \tfrac{1}{8} w_{\alpha\beta}^{bi}\right) \hat{E}_{\alpha i}\hat{E}_{\beta j}\hat{E}_{ck}, \tag{20-92}$$

etc. The SP Ansatz has been used. The $\hat{T}_{2''}$ operator represents the action of f_{12} on singly excited orbital pairs, contracted with the singles amplitudes, and is appropriate for describing singly excited states in response calculations [76]. $\hat{T}_{3'}$ is the natural parameterization for triple excitations in ground state energies because it corresponds to satisfying the cusp in the commutator $\langle \mu_{3'}|\,[\hat{\Phi}, \hat{T}_2]\,|\mathrm{HF}\rangle$ in the generalized amplitude Eq. (20-86). Using the SP Ansatz with this definition of $\hat{T}_{3'}$, the (T) energy is given by [77]

$$\begin{aligned}
\Delta E_{(\mathrm{T})} =& \langle \bar{\mathbf{t}}_{\mathbf{1}}|[\hat{\Phi}, \hat{T}_3 + \hat{T}_{3'}]|\mathrm{HF}\rangle \\
&+ \langle \bar{\mathbf{t}}_{\mathbf{2}}|[\hat{F}, \hat{T}_3 + \hat{T}_{3'}] + [\hat{\Phi}, \hat{T}_3 + \hat{T}_{3'}]|\mathrm{HF}\rangle \\
&+ \langle \bar{\mathbf{c}}|[\hat{F}, \hat{T}_{3'}] + [\hat{\Phi}, \hat{T}_3 + \hat{T}_{3'}]|\mathrm{HF}\rangle \\
&+ \langle \bar{\mathbf{t}}_{\mathbf{3'}}|[\hat{F}, \hat{T}_3 + \hat{T}_{3'}] + [\hat{\Phi}, \hat{T}_2 + \hat{T}_{2'}]|\mathrm{HF}\rangle, \qquad (20\text{-}93) \\
0 =& \langle \mu_3|\,[\hat{F}, \hat{T}_3 + \hat{T}_{3'}] + [\hat{\Phi}, \hat{T}_2 + \hat{T}_{2'}]\,|\mathrm{HF}\rangle\,. \qquad (20\text{-}94)
\end{aligned}$$

No new amplitudes are associated with $\hat{T}_{3'}$, so no new amplitude equations need be solved. In Table 20-8 we list valence (T) energies for FH computed using this method, denoted XSP, together with energies computed using the standard (T) expression, that is without any direct F12 contribution. These values are taken from Ref. [77] and in both cases, the singles and doubles amplitudes are those of a CCSD(F12)-SP calculation. For comparison, we also list valence (T) energies from a conventional CCSD(T) calculation. Inclusion of the $\hat{T}_{3'}$ basis functions greatly accelerates the convergence of the (T) correction. 92% of the (T) energy is obtained with the aug-cc-pVDZ basis, which although somewhat less than the 97% recovered for the CCSD(F12) correlation energy, is more than sufficient to ensure that the accuracy in the triples is not the limiting factor. One possible source of the remaining basis set error in (T) is that corresponding to the missing description of three-electron

coalescence. However, this contribution is expected to be small both because the volume element is small and also because the wave function is always zero at the coalescence point.

At the time of writing the CCSD(T)(F12)-XSP method had only been applied in pilot calculations using a preliminary implementation in GECCO. The computational cost is formally O^3VX^3, but this can be somewhat reduced by the application of screening or hybrid approximations similar to those used for CCSD-F12x and CCSD(2)$_{\overline{\text{F12}}}$. Furthermore, the ideas are readily extended to quadruple and higher excitations and work is in progress to address the basis set errors for these higher-order correlation effects.

20.9. RESPONSE PROPERTIES

The CCSD-F12 model can be used to compute response properties in much the same way as for conventional CCSD [126]. In particular, the ket response functions for frequency-dependent response properties are computed as right eigenvectors of the similarity transformed Hamiltonian $\bar{H} = e^{\hat{T}}\hat{H}e^{\hat{T}}$, expanded in the space of singly and doubly excited determinants,

$$\begin{pmatrix} \bar{H}_{PP} & \bar{H}_{PQ} \\ \bar{H}_{QP} & \bar{H}_{QQ} \end{pmatrix} \begin{pmatrix} R_P \\ R_Q \end{pmatrix} = E \begin{pmatrix} 1 & 0 \\ 0 & S_{QQ} \end{pmatrix} \begin{pmatrix} R_P \\ R_Q \end{pmatrix}. \tag{20-95}$$

The eigenvalues are the ground and excited state energies. We use an analogous notation to that of Section 20.4.3, but here $\bar{H}$ denotes the similarity transformation with the entire CCSD-F12 cluster operator, not just the conventional singles and doubles. The only difference between Eq. (20-95) and that of conventional CCSD linear response theory is that the F12 basis functions are not orthogonal and require the metric

$$S_{\mu_{2'}\nu_{2'}} = \langle \mu_{2'} | \nu_{2'} \rangle. \tag{20-96}$$

Apart from this, the CCSD-F12 response equations are solved in an entirely analogous way to those of CCSD. Furthermore, the iterative second and third order methods CC2 [81] and CC3 [127] can also be combined with the F12 approach. The detailed response equations for CC2-F12 have been presented by Fliegl et al. [82] and response equations for CCSD(F12) have been given by Neiss et al. [128], where the simplifications used for the ground state CCSD(F12) equations are applied to Eq. (20-95).

Contrary to expectation, the CC2-F12 excitation energies do not always converge more rapidly with basis set than conventional CC2 calculations [82]. Analysis of the different contributions reveals that the geminal basis functions $f_{12}\phi_i\phi_j$ are biased towards the ground state. In some cases the basis set error for excited states is relatively unaffected by including these F12 basis functions, which results in a

slow convergence with basis size for the excitation energies. Similarly, properties such as frequency-dependent polarizabilities also exhibit slow convergence for some molecules. Expanding the geminal basis to include functions $f_{12}\phi_x\phi_y$, where ϕ_x and ϕ_y denote semi-natural virtual orbitals, significantly reduces this problem [129, 130]. An alternative approach has been proposed by Köhn [76], where the F12 excitations are generalized in a different way, essentially corresponding to a t_b^j contraction of the set of geminals $f_{12}\phi_i\phi_b$. This approach avoids the near linear dependencies between the functions $f_{12}\phi_x\phi_y$ and can also be combined with the SP Ansatz.

20.10. SUMMARY AND OUTLOOK

In this chapter we have presented the current status of explicitly correlated coupled-cluster theory. For CCSD theory, we have demonstrated that the inclusion of a small set of F12 two-particle basis functions into standard CCSD approaches reduces the basis set error of the calculation by an order of magnitude, which means that the accuracy of a CCSD-F12 calculation using a cc-pVDZ-F12 basis set is equivalent to that of conventional CCSD using a cc-pV5Z basis. Furthermore, we have discussed three approaches to simplifying the CCSD-F12 method, demonstrating that the cost of the most accurate simplified model, CCSD(F12), is only a factor of 2–3 times that of standard CCSD in the same basis. The cost of the slightly less accurate models CCSD-F12x and CCSD(2)$_{\overline{\text{F12}}}$ is only a few percent larger than that of the conventional calculation. Contrary to all experience with standard coupled-cluster methods, the basis set error for the Hartree–Fock energy dominates that of the correlation energy in a CCSD-F12 calculation and it is necessary to include a correction for the Hartree–Fock basis set error, which can be computed with very low cost using quantities available in a CCSD-F12 calculation. Combination of the simplified CCSD-F12 approaches with standard perturbative triples corrections results in highly accurate and efficient CCSD(T)-F12 methods, capable of predicting energetics to chemical accuracy for much larger molecules than previously possible, due to the reduced basis set requirements. Moreover, F12 approaches are well suited to local approximations, which opens the door to an even larger range of applicability.

Explicitly correlated approaches have undergone rapid development over the past 5–10 years and are constantly evolving. Although the approach to ground state energies is now fairly well established, appropriate extensions to excitation energies and response properties are only now becoming clear and further developments are expected in this direction. Similarly, the implementation of analytic derivatives has begun [131] and we can reasonably expect simplified CCSD-F12 analytic gradients in the near future. Recent work has also extended to the reduction in the basis set error for higher excitations, important for calculations aiming at sub-kJ mol^{-1} accuracy, by including explicitly correlated basis functions for triples excitations etc. Indeed, to date, F12 methods have focused on CCSD valence correlation energies of light atoms and there is much to be done to extend F12 methods to be able to

treat heavy atoms, where relativistic effects are important, and core orbitals, which require F12 functions with a shorter length scale.

ACKNOWLEDGMENTS

The development of explicitly correlated coupled-cluster methods has been supported by the Priority Program 1145 (Modern and Universal First-Principles Methods for Many-Electron Systems in Chemistry and Physics) of the Deutsche Forschungsgemeinschaft (DFG, projects HA 2588/3 and KL 721/2). D.P.T. acknowledges support by the DFG through project TE 644/1. The authors thank Andreas Köhn for helpful comments on the manuscript.

REFERENCES

1. G. D. Purvis III, R. J. Bartlett, J. Chem. Phys. **76**, 1910 (1982)
2. J. Noga, R. J. Bartlett, J. Chem. Phys. **86**, 7041 (1987)
3. G. E. Scuseria, H. F. Schaefer III, Chem. Phys. Lett. **152**, 382 (1988)
4. J. Olsen, J. Chem. Phys. **113**, 7140 (2000)
5. M. Kállay, J. Gauss, J. Chem. Phys. **123**, 214105 (2005)
6. K. Raghavachari, G. W. Trucks, J. A. Pople, M. Head-Gordon, Chem. Phys. Lett. **157**, 479 (1989)
7. A. D. Boese et al., J. Chem. Phys. **120**, 4129 (2004)
8. A. Karton, E. Rabinovich, J. M. L. Martin, B. Ruscic, J. Chem. Phys. **125**, 144108 (2006)
9. A. Tajti et al., J. Chem. Phys. **121**, 11599 (2004)
10. Y. J. Bomble et al., J. Chem. Phys. **125**, 064108 (2006)
11. T. Helgaker, W. Klopper, H. Koch, J. Noga, J. Chem. Phys. **106**, 9639 (1997)
12. A. Halkier et al., Chem. Phys. Lett. **286**, 243 (1998)
13. A. Halkier, T. Helgaker, W. Klopper, P. Jørgensen, A. G. Császár, Chem. Phys. Lett. **310**, 385 (1999)
14. D. W. Schwenke, J. Chem. Phys. **122**, 014107 (2005)
15. W. Kutzelnigg, Theor. Chim. Acta **68**, 445 (1985)
16. R. N. Hill, J. Chem. Phys. **83**, 1173 (1985)
17. W. Kutzelnigg, J. D. M. III, J. Chem. Phys. **96**, 4484 (1992)
18. W. Kutzelnigg, Phys. Chem. Chem. Phys. **10**, 3460 (2008)
19. W. Klopper, W. Kutzelnigg, Chem. Phys. Lett. **134**, 17 (1987)
20. W. Kutzelnigg, W. Klopper, J. Chem. Phys. **94**, 1985 (1991)
21. W. Klopper, Chem. Phys. Lett. **186**, 583 (1991)
22. J. Noga, W. Kutzelnigg, W. Klopper, Chem. Phys. Lett. **199**, 497 (1992)
23. J. Noga, W. Kutzelnigg, J. Chem. Phys. **101**, 7738 (1994)
24. H. M. Sulzbach, H. F. Schaefer III, W. Klopper, H. P. Lüthi, J. Am. Chem. Soc. **118**, 3519 (1996)
25. W. Klopper, H. P. Lüthi, Chem. Phys. Lett. **262**, 546 (1996)
26. G. Tarczay et al., J. Chem. Phys. **110**, 11971 (1999)
27. W. Klopper, J. G. C. M. van Duijneveldt-van de Rijdt, F. B. van Duijneveldt, Phys. Chem. Chem. Phys. **2**, 2227 (2000)
28. E. F. Valeev, W. D. Allen, H. F. Schaefer III, A. G. Császár, J. Chem. Phys. **114**, 2875 (2001)
29. M. O. Sinnokrot, E. F. Valeev, C. D. Sherrill, J. Am. Chem. Soc. **124**, 10887 (2002)
30. E. F. Valeev, W. D. Allen, R. Hernandez, C. D. Sherrill, H. F. Schaefer III, J. Chem. Phys. **118**, 8594 (2003)

31. J. P. Kenny, W. D. Allen, H. F. Schaefer III, J. Chem. Phys. **118**, 7353 (2003)
32. T. Rajamäki, J. Noga, P. Valiron, L. Halonen, Mol. Phys. **102**, 2259 (2004)
33. T. Rajamäki, M. Kállay, J. Noga, P. Valiron, L. Halonen, Mol. Phys. **102**, 2297 (2004)
34. M. S. Schuurman, S. R. Muir, W. D. Allen, H. F. Schaefer III, J. Chem. Phys. **120**, 11586 (2004)
35. A. Faure et al., J. Chem. Phys. **122**, 221102 (2005)
36. M. O. Sinnokrot, C. D. Sherrill, J. Phys. Chem. A **110**, 10656 (2006)
37. P. Valiron et al., J. Chem. Phys. **129**, 134306 (2008)
38. J. Aguilera-Iparraguirre, A. D. Boese, W. Klopper, B. Ruscic, Chem. Phys. **346**, 56 (2008)
39. J. Aguilera-Iparraguirre, H. J. Curran, W. Klopper, J. M. Simmie, J. Phys. Chem. A **112**, 7047 (2008)
40. S. Ten-no, Chem. Phys. Lett. **398**, 56 (2004)
41. S. Höfener, D. P. Tew, W. Klopper, T. Helgaker, Chem. Phys. **356**, 25 (2009)
42. W. Klopper, C. C. M. Samson, J. Chem. Phys. **116**, 6397 (2002)
43. E. F. Valeev, Chem. Phys. Lett. **395**, 190 (2004)
44. W. Klopper, F. R. Manby, S. Ten-No, E. F. Valeev, Int. Rev. Phys. Chem. **25**, 427 (2006)
45. W. Klopper, J. Chem. Phys. **120**, 10890 (2004)
46. S. Kedžuch, M. Milko, J. Noga, Int. J. Quantum Chem. **105**, 929 (2005)
47. H.-J. Werner, T. B. Adler, F. R. Manby, J. Chem. Phys. **126**, 164102 (2007)
48. F. R. Manby, J. Chem. Phys. **119**, 4607 (2003)
49. S. Ten-no, F. R. Manby, J. Chem. Phys. **119**, 5358 (2003)
50. H.-J. Werner, F. R. Manby, J. Chem. Phys. **124**, 054114 (2006)
51. F. R. Manby, H.-J. Werner, T. B. Adler, A. J. May, J. Chem. Phys. **124**, 094103 (2006)
52. H.-J. Werner, J. Chem. Phys. **129**, 101103 (2008)
53. T. B. Adler, H.-J. Werner, F. R. Manby, J. Chem. Phys. **130**, 054106 (2009)
54. T. B. Adler, H.-J. Werner, J. Chem. Phys. **130**, 241101 (2009)
55. S. Ten-no, J. Chem. Phys. **126**, 014108 (2007)
56. S. Höfener, F. A. Bischoff, A. Glöß, W. Klopper, Phys. Chem. Chem. Phys. **10**, 3390 (2008)
57. S. Ten-no, J. Chem. Phys. **121**, 117 (2004)
58. K. A. Peterson, T. B. Adler, H.-J. Werner, J. Chem. Phys. **128**, 084102 (2008)
59. K. E. Yousaf, K. A. Peterson, J. Chem. Phys. **129**, 184108 (2008)
60. K. E. Yousaf, K. A. Peterson, Chem. Phys. Lett. (2009), doi:1016/j.cplett.2009.06.003
61. S. Ten-no, Chem. Phys. Lett. **447**, 175 (2007)
62. R. J. Gdanitz, Chem. Phys. Lett. **210**, 253 (1993)
63. R. J. Gdanitz, Chem. Phys. Lett. **283**, 253 (1998)
64. T. H. Dunning Jr., J. Chem. Phys. **90**, 1007 (1989)
65. D. E. Woon, T. H. Dunning Jr., J. Chem. Phys. **98**, 1358 (1993)
66. D. P. Tew, W. Klopper, J. Chem. Phys. **123**, 074101 (2005)
67. R. A. Kendall, T. H. Dunning Jr., R. J. Harrison, J. Chem. Phys. **96**, 6796 (1992)
68. F. A. Bischoff, S. Wolfsegger, D. P. Tew, W. Klopper, Mol. Phys. **107**, 963 (2009)
69. http://tyr0.chem.wsu.edu/~kipeters/basissets/basis.html
70. D. P. Tew, W. Klopper, C. Hättig, Chem. Phys. Lett. **452**, 326 (2008)
71. D. Bokhan, S. Ten-no, J. Noga, Phys. Chem. Chem. Phys. **10**, 3320 (2008)
72. T. Shiozaki, M. Kamiya, S. Hirata, E. F. Valeev, Phys. Chem. Chem. Phys. **10**, 3358 (2008)
73. T. Shiozaki, M. Kamiya, S. Hirata, E. F. Valeev, J. Chem. Phys. **129**, 071101 (2008)
74. T. Shiozaki, M. Kamiya, S. Hirata, E. F. Valeev, J. Chem. Phys. **130**, 054101 (2009)
75. A. Köhn, G. W. Richings, D. P. Tew, J. Chem. Phys. **129**, 201103 (2008)
76. A. Köhn, J. Chem. Phys. **130**, 104104 (2009)
77. A. Köhn, J. Chem. Phys. **130**, 131101 (2009)
78. J. Noga, S. Kedžuch, J. Šimunek, S. Ten-no, J. Chem. Phys. **128**, 174103 (2008)

79. J. Noga, P. Valiron, Chem. Phys. Lett. **324**, 166 (2000)
80. H. Fliegl, W. Klopper, C. Hättig, J. Chem. Phys. **122**, 084107 (2005)
81. O. Christiansen, H. Koch, P. Jørgensen, Chem. Phys. Lett. **243**, 409 (1995)
82. H. Fliegl, C. Hättig, W. Klopper, J. Chem. Phys. **124**, 044112 (2006)
83. D. P. Tew, W. Klopper, C. Neiss, C. Hättig, Phys. Chem. Chem. Phys. **9**, 1921 (2007)
84. D. Bokhan, S. Bernadotte, S. Ten-no, Chem. Phys. Lett. **469**, 214 (2009)
85. D. P. Tew, W. Klopper, C. Neiss, C. Hättig, Phys. Chem. Chem. Phys. **10**, 6325 (2008)
86. D. Bakowies, J. Chem. Phys. **127**, 084105 (2007)
87. D. P. Tew, W. Klopper, J. Chem. Phys. **125**, 094302 (2006)
88. O. Marchetti, H.-J. Werner, Phys. Chem. Chem. Phys. **10**, 3400 (2008)
89. T. B. Adler, G. Knizia, H.-J. Werner, J. Chem. Phys. **127**, 221106 (2007)
90. G. Knizia, T. B. Adler, H.-J. Werner, J. Chem. Phys. **130**, 054104 (2009)
91. G. Rauhut, G. Knizia, H.-J. Werner, J. Chem. Phys. **130**, 054105 (2009)
92. E. F. Valeev, Phys. Chem. Chem. Phys. **10**, 106 (2008)
93. M. Torheyden, E. F. Valeev, Phys. Chem. Chem. Phys. **10**, 3410 (2008)
94. E. F. Valeev, T. D. Crawford, J. Chem. Phys. **128**, 244113 (2008)
95. J. F. Stanton, Chem. Phys. Lett. **281**, 130 (1997)
96. A. J. May, E. Valeev, R. Polly, F. R. Manby, Phys. Chem. Chem. Phys. **7**, 2710 (2005)
97. E. F. Valeev, Chem. Phys. Lett. **418**, 333 (2006)
98. G. Knizia, H.-J. Werner, J. Chem. Phys. **128**, 154103 (2008)
99. F. A. Bischoff, S. Höfener, A. Glöß, W. Klopper, Theor. Chem. Acc. **121**, 11 (2008)
100. K. Szalewicz, B. Jeziorski, H. J. Monkhorst, J. G. Zabolitzky, Chem. Phys. Lett. **91**, 169 (1982)
101. K. Szalewicz, B. Jeziorski, H. J. Monkhorst, J. G. Zabolitzky, J. Chem. Phys. **78**, 1420 (1983)
102. K. Szalewicz, B. Jeziorski, H. J. Monkhorst, J. G. Zabolitzky, J. Chem. Phys. **79**, 5543 (1983)
103. B. Jeziorski, H. J. Monkhorst, K. Szalewicz, J. G. Zabolitzky, J. Chem. Phys. **81**, 368 (1984)
104. K. B. Wenzel, J. G. Zabolitzky, K. Szalewicz, B. Jeziorski, H. J. Monkhorst, J. Chem. Phys. **85**, 3964 (1986)
105. R. Bukowski, B. Jeziorski, K. Szalewicz, J. Chem. Phys. **108**, 7946 (1998)
106. K. Patkowski, W. Cencek, M. Jeziorska, B. Jeziorski, K. Szalewicz, J. Phys. Chem. A **111**, 7611 (2007)
107. R. Polly, H.-J. Werner, P. Dahle, P. R. Taylor, J. Chem. Phys. **124**, 234107 (2006)
108. P. Dahle, T. Helgaker, D. Jonsson, P. R. Taylor, Phys. Chem. Chem. Phys. **9**, 3112 (2007)
109. D. P. Tew, W. Klopper, F. R. Manby, J. Chem. Phys. **127**, 174105 (2007)
110. P. Dahle, T. Helgaker, D. Jonsson, P. R. Taylor, Phys. Chem. Chem. Phys. **10**, 3377 (2008)
111. T. Helgaker, W. Klopper, D. P. Tew, Mol. Phys. **106**, 2107 (2008)
112. P. Wind, W. Klopper, T. Helgaker, Theor. Chem. Acc. **107**, 173 (2002)
113. S. F. Boys, N. C. Handy, Proc. R. Soc. Lond. A **310**, 43 (1969)
114. S. F. Boys, Proc. R. Soc. Lond. A **258**, 402 (1960)
115. K. Singer, Proc. R. Soc. Lond. A **258**, 412 (1960)
116. C. C. M. Samson, W. Klopper, T. Helgaker, Comp. Phys. Commun. **149**, 1 (2002)
117. T. Kato, Commun. Pure Appl. Math. **10**, 151 (1957)
118. R. T. Pack, W. Byers Brown, J. Chem. Phys. **45**, 556 (1966)
119. D. P. Tew, J. Chem. Phys. **129**, 014104 (2008)
120. E. F. Valeev, J. Chem. Phys. **125**, 244106 (2006)
121. E. A. Hylleraas, Z. Phys. **54**, 347 (1929)
122. J. Noga, S. Kedžuch, J. Šimunek, J. Chem. Phys. **127**, 034106 (2007)
123. J. Noga, J. Šimunek, Chem. Phys. **356**, 1 (2009)
124. A. Köhn, D. P. Tew, **132**, 024101 (2010)

125. H. Fliegl, C. Hättig, W. Klopper, Int. J. Quantum Chem. **106**, 2306 (2006)
126. O. Christiansen et al., J. Chem. Phys. **105**, 6921 (1996)
127. H. Koch, O. Christiansen, P. Jørgensen, A. M. Sanchez de Merás, T. Helgaker, J. Chem. Phys. **106**, 1808 (1997)
128. C. Neiss, C. Hättig, J. Chem. Phys. **126**, 154101 (2007)
129. C. Neiss, C. Hättig, W. Klopper, J. Chem. Phys. **125**, 064111 (2006)
130. J. Yang, C. Hättig, J. Chem. Phys. **130**, 124101 (2009)
131. E. Kordel, C. Villani, W. Klopper, Mol. Phys. **105**, 2565 (2007)

CHAPTER 21

EFFICIENT EXPLICITLY CORRELATED COUPLED-CLUSTER APPROXIMATIONS

HANS-JOACHIM WERNER[1], THOMAS B. ADLER[1], GERALD KNIZIA[1], AND FREDERICK R. MANBY[2]

[1] *Institut for Theoretical Chemistry, University of Stuttgart, Pfaffenwaldring 55, D-70569 Stuttgart, Germany, e-mail: werner@theochem.uni-stuttgart.de; adler@theochem.uni-stuttgart.de; knizia@theochem.uni-stuttgart.de*

[2] *School of Chemistry, University of Bristol, Cantocks Close, Bristol BS8 1TS, UK, e-mail: fred.manby@bristol.ac.uk*

Abstract: Explicitly correlated MP2-F12 and CCSD(T)-F12 methods are reviewed. We focus on the CCSD(T)-F12x ($x = a, b$) approximations, which are only slightly more expensive than their non-F12 counterparts. Furthermore, local approximations in the LMP2-F12 and LCCSD-F12 methods are described, which make it possible to treat larger molecules than with standard coupled-cluster methods. We demonstrate the practicability of F12 methods by large benchmark calculations for various properties, including reaction energies, vibrational frequencies, and intermolecular interactions. In these calculations, the newly developed V*n*Z-F12 orbital and OPTRI auxiliary basis sets by Peterson et al. are compared to other previously used basis sets. The accuracy and efficiency of local approximations is demonstrated for reactions of large molecules.

Keywords: Coupled cluster, F12 approach, Explicitly correlated, Perturbation theory, Local approximations

21.1. INTRODUCTION

The coupled-cluster method with single and double excitations and a perturbative treatment of triple excitations [CCSD(T)] is nowadays considered to be the gold standard of quantum chemistry. As long as a single-reference treatment is sufficient, it yields highly accurate results for many properties, and chemical accuracy can be reached for energy differences such as reaction enthalpies [1, 2]. However, the method suffers from two major problems: the very steep scaling of the computational cost with increasing molecular size, and the extremely slow convergence of the correlation energy with respect to the basis set size. The latter problem is severe even for

P. Čársky et al. (eds.), Recent Progress in Coupled Cluster Methods, 573–619.
DOI 10.1007/978-90-481-2885-3_21,

very small molecules, since the computational cost increases with the fourth power of the basis set size N_{AO}, while the errors in the energy decrease only with N_{AO}^{-1}.

The slow convergence of the correlation energy with basis set size is due to the fact that the shape of the wave function cusp for small to intermediate values of r_{12} is not well described by an expansion in products of one-electron functions (orbitals). Already in 1929 Hylleraas realized that for the helium atom this problem can be avoided by including terms in the wave function that depend explicitly on the interelectronic distance r_{12} [3]. However, extensions to many-electron systems proved difficult since very numerous many-electron integrals appear in the formalism. The various early approaches, such as Gaussian-type geminal theories and transcorrelated methods, have recently been nicely reviewed by Helgaker et al. [4], and we refer to this paper for further information and references. Since most of these methods require the calculation of three-electron and four-electron integrals, they are applicable only to very small systems.

A way out of this problem was opened almost 25 years ago by the seminal work of Kutzelnigg [5]. He proposed to use resolutions of the identity (RIs) to factorize the many-electron integrals into sums of products of two-electron integrals. Furthermore, he proposed to augment the conventional pair functions by a single explicitly correlated term that is proportional to $r_{12}\Phi_{\mathrm{HF}}$. Since the conventional expansion in terms of orbital products (Slater determinants) is flexible enough to describe the correlation hole for medium values of r_{12}, the explicitly correlated terms need only correct the wave function in the region near the wave function cusp, which is poorly represented by the orbital products. This leads to a much simpler formalism than many of the older theories in which the whole wave function was written in terms of r_{ij}-dependent functions.

This so-called R12-method was first implemented by Kutzelnigg and Klopper [6–11] for MP2 (second-order Møller–Plesset perturbation theory), and was later extended to CISD (configuration interaction with single and double excitations) and CEPA (coupled electron pair approximation) [12] as well as to coupled cluster [13, 14] and MRCI [15] (multireference configuration interaction) wave functions. In all these early methods the atomic orbital (AO) basis set was used to approximate the RIs (within the so-called standard approximation). In order to represent the resolution of the identity accurately, very large orbital basis sets were needed, and the method was therefore mainly applied to obtain highly accurate correlation energies for atoms and small molecules.

An important next step towards the goal to obtain accurate results with small basis sets was made by Klopper and Samson in 2002, who implemented for the first time an MP2-R12 method in which the RIs were approximated by an auxiliary basis set [16]. An improved scheme, using the union of the AO and auxiliary basis sets, was later proposed by Valeev [17] (complementary auxiliary basis set (CABS) approach). It turned out, however, that the accuracy of the correlation energies was still rather unsatisfactory when small or medium size basis sets were used. The origin of this problem is the linear r_{12} correlation factor. Even though this makes it possible to describe the wave function cusp for $r_{12} \rightarrow 0$ correctly, its linear increase with

the interelectronic distance is unphysical and must be compensated by the standard orbital product expansion. This not only requires large basis sets, but may also lead to numerical problems in calculations for larger molecules.

A breakthrough came when it was realized that non-linear short-range correlation factors, such as a Slater-type function $F_{12} = \exp(-\gamma r_{12})$, yields much better basis set convergence and numerical stability than the linear r_{12} factor. This was first proposed and demonstrated by Ten-no [18]. At about the same time, May and Manby [19] implemented an MP2-F12 method in which an arbitrary function $F_{12}(r_{12})$ could be approximated by a frozen linear combination of Gaussians $F_{12} = \sum_i c_i \exp\left(-\alpha_i r_{12}^2\right)$. In Ref. [19] $F_{12} = r_{12}$ was assumed, but soon afterwards it was found that even with a single Gaussian much better results are obtained than with $F_{12} = r_{12}$ [20]. In the subsequent years, several other MP2-F12 implementations followed [21–29]. Various other functional forms of the correlation factor F_{12} (fitted to an expansion of Gaussians) were tested by Tew and Klopper [22], but the simple Slater function as proposed by Ten-no turned out to be most suitable.

Using the Slater-type geminal it is possible to compute the integrals exactly [18, 30], but no chemically significant error is introduced by an approximate expansion of the correlation factor in Gaussians. The efficiency of the integral evaluation can also be enhanced by robust density fitting approximations [19, 31, 32]. Furthermore, Peterson et al. optimized new orbital [33] and RI [34, 35] basis sets that are specially designed for F12 calculations. All these advances greatly increased the efficiency and numerical stability of F12-methods, which can now be used by non-experts routinely. Many benchmark calculations with the MP2-F12 method showed that with triple-zeta basis sets quintuple zeta or even better accuracy can be obtained [21, 24, 27–29]. Extensions to the calculations of excitation energies [36, 37] and of non-linear response properties[38] were also reported.

Most of the above mentioned methods were limited to MP2, which is not sufficiently accurate for reliable predictions. Extensions to coupled-cluster theory are therefore the focus of current research. Formally complete treatments of CCSD-R12 methods were described many years ago by Noga et al. [13, 14, 39, 40], but these methods were complicated and suffered from the fact that the AO basis was used to approximate the RIs. For CCSD-R12 methods this is even more severe than for MP2-R12, since many terms which require multiple RIs appear in the CCSD-R12 formalism. Therefore very large basis sets were necessary for numerically accurate results. In 2008, two independent full CCSD-F12 implementations which use auxiliary basis sets were described [41–43]. Even higher-order methods, up to CCSDTQ-F12, have recently been developed [44, 45], using automatic programming tools. All these methods include r_{12}-dependent terms only in the doubles excitation operators, and therefore they do not improve the basis set convergence of the energy contributions of higher excitations. This problem has recently been addressed by Köhn, who presented the first method which also improves the accuracy of the triples energy [46].

The CCSD-R12 and CCSD-F12 methods described above are computationally up to two orders of magnitude more expensive than the standard CCSD method. This

is because in CCSD-F12 many terms arise that scale with the second or third power of the size of the auxiliary basis. In order to reduce the computational effort Fliegl et al. introduced simplified CC2(R12) [37] and CCSD(T)(R12) [47, 48] methods (initially without an auxiliary basis set), which have more recently been extended to CCSD(T)(F12) by Tew et al. [49, 50] using the CABS approach. In these treatments terms that are non-linear in the amplitudes of the explicitly correlated configurations as well as some other small contributions are neglected. Even simpler CCSD(T)-F12 approximations, denoted CCSD(T)-F12a and CCSD(T)-F12b, were proposed and implemented by our group [51, 52]. In these methods the only additional effort as compared to the standard CCSD(T) is an initial MP2-F12 calculation. Since this scales as $\mathcal{O}(N^5)$, where N is a measure of the molecular size, while CCSD(T) scales as $\mathcal{O}(N^7)$, the additional effort becomes negligible for larger molecules. Many benchmark calculations [52–56] have shown that, despite the approximations, these methods achieve virtually the same accuracy as the CCSD(T)(F12) or the much more expensive full CCSD(T)-F12 methods. Our methods will be reviewed in Section 21.2.2.

It should be noted that Valeev independently proposed an approximation that is closely related to our CCSD-F12b method [57, 58]. In Valeev's approximation the coupling between the explicitly correlated and conventional terms is not taken into account in the CCSD iterations as in our methods, but added a posteriori using a perturbative approach.

The steep scaling of the computational cost with molecular size can be avoided by local approximations [59–67], and linear cost scaling has been achieved in our group for most single reference correlation methods [64–67]. This has made it possible to perform local CCSD(T) calculations for much larger molecules than with the conventional CCSD(T) method. For example, some enzyme reactions have been studied using combined quantum mechanics and classical molecular mechanics (QM/MM) methods. The QM region with up to 49 atoms was treated accurately with LCCSD(T) using triple-zeta basis sets [68, 69]. Recently, we have demonstrated that it is possible to include explicitly correlated terms into the LMP2 and LCCSD(T) wave functions without much additional cost and no increase of the scaling [27, 70, 71]. Moreover, the errors due to the local approximations are to a large extent eliminated by the explicitly correlated terms in the wave function [70–72]. These methods will be reviewed in Section 21.2.4.

In another contribution to this volume Tew et al. discuss explicitly correlated coupled cluster theory from a different point of view, providing an overview of the approximate CCSD(T)-F12 models in the current literature. They present general expressions of the coupled cluster equations in terms of commutator expansions, which is very elegant and compact. However, it neither shows the expressions which actually have to be programmed, nor in detail which approximations are introduced into the working equations. We have chosen a complementary approach and will present the working equations explicitly. We describe the approximations made in our CCSD(T)-F12x methods in detail and this should make it possible for other groups to reproduce these methods exactly.

21.2. THEORY

In this section we will summarize the theory and working equations for the MP2-F12 and CCSD-F12 methods, as implemented in the MOLPRO quantum chemistry program [73]. For simplicity, we will only consider the closed-shell wave functions. The corresponding open-shell methods are also available and are described in Refs. [29, 52]. The various orbital spaces used in our formalism with their associated indices are summarized in Table 21-1. We distinguish occupied orbitals (any orbital contained in the HF determinant), valence orbitals (correlated occupied orbitals), virtual orbitals (unoccupied in the HF determinant), and complementary auxiliary (CA) orbitals. The occupied and virtual molecular orbitals (MOs) are represented in the AO basis set. The complementary auxiliary orbitals, which are orthogonal to all MOs, are represented in the union of the AO basis and an auxiliary (RI) basis set. In addition, we will use the indices α, β for a complete (infinitely large) orbital space. It is assumed that this contains all the orbital spaces in Table 21-1 as subspaces and that all orbitals are orthonormal.

Table 21-1. Orbital spaces and their indices

Occupied molecular orbitals	p, q
Valence molecular orbitals	i, j, k, l, m, n, o
Virtual molecular orbitals	a, b, c, d
Any molecular orbitals (MO)	r, s, t, u
Complementary auxiliary (CA) orbitals	x, y
Any MO or CA orbitals	α', β'
Complete space	α, β

21.2.1. MP2-F12 Theory

21.2.1.1. Definition of the First Order Wave Function

The MP2-F12 first-order wave function is defined as [11]

$$\Psi^{(1)} = \frac{1}{2}\sum_{ij}^{\text{val}}\left[\sum_{a,b}^{\text{virt}} \Phi_{ij}^{ab} T_{ab}^{ij} + \sum_{k,l}^{\text{val}} \Phi_{ij}^{kl} T_{kl}^{ij}\right] \equiv \frac{1}{2}\left[\Phi_{ij}^{ab} T_{ab}^{ij} + \Phi_{ij}^{kl} T_{kl}^{ij}\right], \quad (21\text{-}1)$$

$$\Phi_{ij}^{\alpha\beta} = \hat{E}_{\alpha i}\hat{E}_{\beta j}\Phi_{\text{HF}}, \quad (21\text{-}2)$$

$$\Phi_{ij}^{kl} = \sum_{\alpha,\beta}^{\text{complete}} \Phi_{ij}^{\alpha\beta}\langle\alpha\beta|\hat{Q}_{12}F_{12}|kl\rangle \equiv \Phi_{ij}^{\alpha\beta}\langle\alpha\beta|\hat{Q}_{12}F_{12}|kl\rangle. \quad (21\text{-}3)$$

In the following, summations over repeated dummy indices will always be implied, as indicated in the above equations. $\hat{E}_{\alpha i} = \eta_\alpha^\dagger \eta_i + \bar{\eta}_\alpha^\dagger \bar{\eta}_i$ are spin-summed one-electron excitation operators, and F_{12} is the r_{12}-dependent correlation factor,

$$F_{12} = -\frac{1}{\gamma} e^{-\gamma r_{12}} \tag{21-4}$$

with γ a length-scale parameter. The projector $\hat{Q}_{12}$ keeps the explicitly correlated terms strongly orthogonal to the Hartree–Fock (HF) reference function and orthogonal to the conventional singly and doubly excited configurations Φ_i^a and Φ_{ij}^{ab}. In the literature, the following alternative forms of the projector have been discussed [16, 28]:

$$\text{Ansatz } \mathbf{1}\text{: } \hat{Q}_{12} = (1 - \hat{r}_1)(1 - \hat{r}_2), \tag{21-5}$$

$$\text{Ansatz } \mathbf{2}\text{: } \hat{Q}_{12} = (1 - \hat{o}_1)(1 - \hat{o}_2), \tag{21-6}$$

$$\text{Ansatz } \mathbf{3}\text{: } \hat{Q}_{12} = (1 - \hat{o}_1)(1 - \hat{o}_2) - \hat{\mathrm{v}}_1 \hat{\mathrm{v}}_2, \tag{21-7}$$

where the operators $\hat{o} = \sum_p^{\text{occ}} |p\rangle\langle p| \equiv |p\rangle\langle p|, \hat{\mathrm{v}} = \sum_a^{\text{virt}} |a\rangle\langle a| \equiv |a\rangle\langle a|$, and $\hat{r} = \hat{o} + \hat{\mathrm{v}}$ project onto the occupied, virtual, and full orbital spaces, respectively. Their subscripts denote the electron coordinate on which they act. Ansatz **1** turned out to be unsatisfactory because configurations where one electron is excited to a virtual orbital and the other into an orbital outside the MO basis are neglected. The ansätze **2** and **3** are equivalent if no further approximations are introduced. However, ansatz **2** leads to more complicated working equations and yields slightly different results if certain approximations are introduced (for details see Ref. [28]). Therefore we like to keep the distinction, even though this is not made by all authors. Our formalism is based on ansatz **3**.

In principle, the range of orbitals k, l in Eq. (21-1) is arbitrary and further specifies the wave function ansatz. In the current work, k, l are taken to be valence orbitals only (in open-shell cases with RHF reference functions, k, l run over all valence spatial orbitals that are either occupied with alpha or beta spin). With this ansatz, the optimized wave function is invariant with respect to unitary transformations among the closed-shell or open-shell valence orbitals (e.g., orbital localization). However, it has been found that this ansatz can lead to problems due to geminal basis set superposition effects (GBSSE) [23]. Furthermore, when the orbitals k, l are far away from i, j, near-singularities of the zeroth-order Hamiltonian may arise, which can lead to serious numerical problems in larger molecules. These problems can be avoided by using the "diagonal" (D) ansatz, in which kl is restricted to ij or ji:

$$T_{kl}^{ij} \overset{\text{D}}{=} \delta_{ik}\delta_{jl} T_{ij} + \delta_{jk}\delta_{il} T_{ji}. \tag{21-8}$$

In most cases, this more restricted ansatz gives even more accurate results than the full ansatz [28, 29]. However, it is not orbital invariant and is only size consistent if localized orbitals are used. Ten-no proposed to use fixed coefficients $T_{ij}^S = 1/2$ and $T_{ij}^T = 1/4$ for all singlet and triplet pairs, respectively [18, 74]. These coefficients follow from the wave function cusp conditions [75, 76]. In the current formalism, which does not use singlet and triplet coupling of the external electrons, this means

$$T_{kl}^{ij} \overset{\text{FIX}}{=} \frac{3}{8}\delta_{ik}\delta_{jl} + \frac{1}{8}\delta_{jk}\delta_{il}. \tag{21-9}$$

The fixed-amplitude ansatz avoids GBSSE as well as singularities, and is orbital invariant and size consistent. Furthermore, it has the advantage that no amplitude equations have to be solved for the coefficients T_{kl}^{ij}. This is particularly important for the CCSD-F12 method discussed in Section 21.2.2. Usually, the loss of accuracy by fixing the amplitudes is negligible for valence-shell correlation. However, if inner-shell orbitals are also correlated, the errors may be significant, since larger values of γ are required and the fixed-amplitude method is more sensitive to the choice of γ than the methods with optimized amplitudes.

In Eq. (21-3) the explicitly correlated configurations Φ_{ij}^{kl} are formally expanded in the complete set of doubly excited configurations $\Phi_{ij}^{\alpha\beta}$, and the integrals $\langle\alpha\beta|\hat{Q}_{12}F_{12}|kl\rangle$ can be viewed as fixed contraction coefficients. In the MP2-F12 formalism the summations over the complete orbital space mostly lead to exact resolutions of the identity that can be removed when deriving the explicit working equations. For example, $\langle kl|F_{12}|\alpha\beta\rangle\langle\alpha\beta|r_{12}^{-1}|ij\rangle$ is replaced by the integral $\langle kl|F_{12}r_{12}^{-1}|ij\rangle$. In some less important terms, where such replacements are not possible, the auxiliary basis set is used to approximate the summations over the complete space. This will be discussed in more detail in Section 21.2.2.

The configurations $\Phi_{ij}^{\alpha\beta}$ as defined in Eq. (21-2) are pairwise non-orthogonal. In order to write the working equations in the most compact form, it is convenient to define the contravariant (biorthogonal) configurations $\tilde{\Phi}_{ij}^{\alpha\beta}$ and their associated amplitudes $\tilde{T}_{\alpha\beta}^{ij}$:

$$\tilde{\Phi}_{ij}^{\alpha\beta} = \frac{1}{6}\left(2\Phi_{ij}^{\alpha\beta} + \Phi_{ij}^{\beta\alpha}\right) \tag{21-10}$$

$$\tilde{T}_{\alpha\beta}^{ij} = 2T_{\alpha\beta}^{ij} - T_{\beta\alpha}^{ij} \tag{21-11}$$

The contravariant configurations have the properties

$$\langle\tilde{\Phi}_{ij}^{ab}|\Phi_{kl}^{cd}\rangle = \delta_{ik}\delta_{jl}\delta_{ac}\delta_{bd} + \delta_{il}\delta_{jk}\delta_{ad}\delta_{bc}, \tag{21-12}$$

$$\langle\tilde{\Phi}_{ij}^{ab}|\Psi^{(1)}\rangle = T_{ab}^{ij}. \tag{21-13}$$

21.2.1.2. Choice of the Zeroth-Order Hamiltonian

The zeroth-order Hamiltonian can be defined as [29]

$$\hat{H}^{(0)} = g_{\alpha\beta}\hat{E}_{\alpha\beta} \tag{21-14}$$

$$\hat{g} = \hat{o}\hat{f}\hat{o} + (1-\hat{o})\hat{f}(1-\hat{o}) \tag{21-15}$$

where $\hat{f}$ is the closed-shell Fock operator with matrix elements $f_{\alpha\beta} = \langle\alpha|\hat{f}|\beta\rangle$. Due to Brillouin's theorem $f_{ai} = 0$ if the molecular orbitals are fully optimized. We will not assume, however, that the Fock matrix is diagonal in the occupied and/or virtual orbital subspaces. The projected operator $\hat{g}$ is introduced in order to make the HF wave function $\Phi_{\rm HF} \equiv \Psi^{(0)}$ an exact eigenfunction of $\hat{H}^{(0)}$. This means that contributions of f_{ix} are treated as part of the perturbation. The projection is needed in spin-restricted open-shell cases [29], since then the orbitals are not eigenfunctions of the Fock operator. For closed-shell wave functions this choice of $\hat{H}^{(0)}$ leads to exactly the same result as if $\hat{f}$ is used instead of $\hat{g}$, if the amplitude equations are derived by minimizing the Hylleraas functional. It turns out, however, that the formalism is somewhat simpler when $\hat{g}$ is used (cf. Section 21.2.1.3). Other choices of $\hat{H}^{(0)}$ have been discussed by Noga et al. [26].

21.2.1.3. Explicit Formulation of the MP2-F12 Amplitude Equations

The amplitudes T_{ab}^{ij} and T_{kl}^{ij} can be optimized by minimizing the Hylleraas functional

$$\begin{aligned} E_2 &= \langle\Psi^{(1)}|\hat{H}^{(0)} - E^{(0)}|\Psi^{(1)}\rangle + 2\langle\Psi^{(1)}|\hat{H}|\Psi^{(0)}\rangle \\ &= \tilde{T}_{ab}^{ij}\big(K_{ab}^{ij} + R_{ab}^{ij}\big) + \tilde{T}_{kl}^{ij}\big(V_{kl}^{ij} + R_{kl}^{ij}\big), \end{aligned} \tag{21-16}$$

where

$$K_{ab}^{ij} = \langle\tilde{\Phi}_{ij}^{ab}|\hat{H}|\Psi^{(0)}\rangle = \langle ab|r_{12}^{-1}|ij\rangle, \tag{21-17}$$

$$V_{kl}^{ij} = \langle\tilde{\Phi}_{ij}^{kl}|\hat{H}|\Psi^{(0)}\rangle = \langle kl|F_{12}\hat{Q}_{12}r_{12}^{-1}|ij\rangle, \tag{21-18}$$

$$R_{ab}^{ij} = K_{ab}^{ij} + \langle\tilde{\Phi}_{ij}^{ab}|\hat{H}^{(0)} - E^{(0)}|\Psi^{(1)}\rangle, \tag{21-19}$$

$$R_{kl}^{ij} = V_{kl}^{ij} + \langle\tilde{\Phi}_{ij}^{kl}|\hat{H}^{(0)} - E^{(0)}|\Psi^{(1)}\rangle. \tag{21-20}$$

For the optimized amplitudes the residuals R_{ab}^{ij} and R_{kl}^{ij} must vanish. Their explicit form is

$$\begin{aligned} R_{ab}^{ij} &= K_{ab}^{ij} + f_{ac}T_{cb}^{ij} + T_{ac}^{ij}f_{cb} \\ &\quad - f_{io}T_{ab}^{oj} - T_{ab}^{io}f_{oj} + T_{mn}^{ij}C_{ab}^{mn}, \end{aligned} \tag{21-21}$$

$$\begin{aligned} R_{kl}^{ij} &= V_{kl}^{ij} + B_{kl,mn}T_{mn}^{ij} \\ &\quad - S_{kl,mn}\left[f_{io}T_{mn}^{oj} + T_{mn}^{io}f_{oj}\right] + C_{ab}^{kl}T_{ab}^{ij}, \end{aligned} \tag{21-22}$$

where the matrix elements are formally defined as

$$B_{kl,mn} = \langle kl|F_{12}\hat{Q}_{12}\hat{g}_{12}\hat{Q}_{12}F_{12}|mn\rangle, \tag{21-23}$$

$$S_{kl,mn} = \langle kl|F_{12}\hat{Q}_{12}F_{12}|mn\rangle\,, \tag{21-24}$$

$$C_{ab}^{kl} = \langle kl|F_{12}\hat{Q}_{12}\hat{f}_{12}|ab\rangle. \tag{21-25}$$

Here and in the following, we use the notation $\hat{f}_{12} = \hat{f}_1 + \hat{f}_2$ and $\hat{g}_{12} = \hat{g}_1 + \hat{g}_2$. Note that in previous papers $\langle kl|F_{12}\hat{Q}_{12}F_{12}|mn\rangle$ was denoted $X_{kl,mn}$, but since we will need the symbol $\mathbf{X}$ later in the context of coupled-cluster theory we changed the notation. Using the additional definition

$$A_{kl,mn} = \langle kl|F_{12}\hat{g}_{12}\hat{Q}_{12}F_{12}|mn\rangle \tag{21-26}$$

the matrix $B_{kl,mn}$ can be rewritten as

$$B_{kl,mn} = \frac{1}{2}\left(A_{kl,mn} + A_{mn,kl} - F^{kl}_{ab}C^{mn}_{ab} - C^{kl}_{ab}F^{mn}_{ab}\right). \tag{21-27}$$

It should be noted that due to the use of the projected Fock operator in Eq. (21-15) the matrix elements $Z_{kl,mn}$ in Eqs. (31) and (33) of Ref. [28] are zero. In the present formulation, this contribution is contained in $A_{kl,mn}$ and does not require any additional computational effort. Furthermore, the GBC (generalized Brillouin condition, i.e. $f_{ix} = 0$) approximation is not needed.

Up to this point no approximations beyond the wave function ansatz and the second-order Møller–Plesset treatment have been made. The difficulty is to compute the matrix elements explicitly, because the one-electron projectors in Eq. (21-7) lead to 3- and 4-electron integrals, e.g.

$$\langle ij|r_{12}^{-1}\hat{o}_1F_{12}|kl\rangle = \langle ijp|r_{12}^{-1}F_{23}|plk\rangle. \tag{21-28}$$

As first proposed by Kutzelnigg [5], the many-electron integrals can be avoided by inserting (approximate) resolutions of the identity (RIs) $\hat{u}$ into the projector $\hat{Q}_{12}$:

$$\hat{Q}_{12} = 1 - \hat{o}_1 - \hat{o}_2 + \hat{o}_1\hat{o}_2 - \hat{\mathrm{v}}_1\hat{\mathrm{v}}_2 \tag{21-29}$$

$$\approx 1 - \hat{o}_1\hat{u}_2 - \hat{u}_1\hat{o}_2 + \hat{o}_1\hat{o}_2 - \hat{\mathrm{v}}_1\hat{\mathrm{v}}_2, \tag{21-30}$$

$$\hat{u} = |\alpha'\rangle\langle\alpha'|. \tag{21-31}$$

The many-electron integrals then factorize into sums of products of 2-electron integrals, e.g.,

$$\langle ij|r_{12}^{-1}\hat{o}_1\hat{u}_2F_{12}|kl\rangle \approx \langle ij|r_{12}^{-1}|p\alpha'\rangle\langle p\alpha'|F_{12}|kl\rangle. \tag{21-32}$$

In practice, the RIs are approximated using the union of the orbital basis and an auxiliary basis set. The operator $\hat{u}$ can then be written as a sum of a contribution $|r\rangle\langle r|$ from the orbital basis, and a remainder $|x\rangle\langle x|$, where x are orthonormal complementary auxiliary (CA) orbitals which are orthogonal to the MO basis, $\langle r|x\rangle = 0$ for all x, r (CABS approach [17]):

$$\hat{u} = |r\rangle\langle r| + |x\rangle\langle x|. \tag{21-33}$$

Writing the projector as $\hat{Q}_{12} = 1 - \hat{P}_{12}$ it follows

$$\hat{P}_{12} = |rs\rangle\langle rs| + |px\rangle\langle px| + |xp\rangle\langle xp|. \tag{21-34}$$

In the following, we will use the short-hand notation

$$\hat{P}_{12} = |\alpha\beta\rangle P_{\alpha\beta}\langle\alpha\beta|, \tag{21-35}$$

where $P_{rs} = P_{px} = P_{xp} = 1$, and all other elements $P_{\alpha\beta}$ are zero. This definition implies that the orbitals α, β are contained in the MO or CA basis, and therefore the primes on α or β have been omitted.

The advantage of the CABS approach is not only that the accuracy of the RI is improved, but also that it leads to simpler equations since various terms cancel. If the auxiliary basis set alone were used to represent the RI, these cancellations would only be approximate, leading to spurious contributions. Furthermore, $1 - |rs\rangle\langle rs|$ is the dominant contribution in the projector, and the contributions of the CA orbitals in the last two terms of Eq. (21-34) are only rather small corrections. As will be shown later, these can be neglected in some terms without significant loss of accuracy.

The evaluation of the matrix elements V_{kl}^{ij} and $S_{kl,mn}$ is now straightforward and does not require further approximations:

$$V_{kl}^{ij} = K_{ij,kl}^{\mathrm{F}} - K_{\alpha\beta}^{ij} P_{\alpha\beta} F_{\alpha\beta}^{kl}, \tag{21-36}$$

$$S_{kl,mn} = F_{kl,mn}^{2} - F_{\alpha\beta}^{kl} P_{\alpha\beta} F_{\alpha\beta}^{mn}, \tag{21-37}$$

where the integrals are defined as

$$K_{\alpha\beta}^{ij} = \langle\alpha\beta|r_{12}^{-1}|ij\rangle, \tag{21-38}$$

$$F_{\alpha\beta}^{kl} = \langle\alpha\beta|F_{12}|kl\rangle, \tag{21-39}$$

$$K_{ij,kl}^{\mathrm{F}} = \langle ij|r_{12}^{-1}F_{12}|kl\rangle, \tag{21-40}$$

$$F_{kl,mn}^{2} = \langle kl\,|F_{12}F_{12}|mn\rangle. \tag{21-41}$$

These integrals can be evaluated analytically or using density fitting approximations [27, 31].

The matrix elements which contain the Fock operator are more difficult, since integrals over the product of $\hat{f}_{12}F_{12}$ cannot be computed analytically. There are different possibilities to solve this problem. One way (approximation C, proposed by Kedžuch et al. [77]) is to straightforwardly use RIs to factorize most of these products. For example, for the matrix elements C_{ab}^{kl} this leads to

$$C_{ab}^{kl} = f_{ax}F_{xb}^{kl} + F_{ax}^{kl}f_{xb}. \tag{21-42}$$

Alternatively, Kutzelnigg and Klopper [8, 16] have used commutator expressions to reformulate the matrix elements such that the RI is only needed to factorize the smaller products $\hat{k}_{12}F_{12}$, where $\hat{k}$ is the exchange operator (approximation B). Since no products with the kinetic energy operator arise, RI approximations for $\hat{k}_{12}F_{12}$ should converge faster than for $\hat{f}_{12}F_{12}$. However, approximation B leads to more complicated expressions (for details, see Ref. [28]), and an additional price one has to pay is the evaluation of integrals over the commutator $[F_{12}, \hat{t}_{12}]$, which are quite expensive ($\hat{t}_{12} = \hat{t}_1 + \hat{t}_2$ is the kinetic energy operator). Many tests have shown that in practice there is no significant improvement of the accuracy by using approximation B, provided appropriate RI basis sets are used. Therefore approximation B has mainly historical value and is hardly used any more. We note that there is also an approximation A [16], which is obtained from approximation B by neglecting the exchange operator entirely. Nevertheless, due to the need for the expensive commutator integrals, calculations with approximation A are still more expensive than with approximation C (at least with our program). Approximation A turned out to be useful, however, when local approximations are introduced. We will come back to this in Section 21.2.4.

All that remains is to evaluate the matrix elements $A_{kl,mn}$. Here we will use approximation C. Apart from the replacement of r_{12} by F_{12} our formulation is exactly equivalent to the one in Ref. [77], but the derivation is different and the final working expressions are much simpler. The commutator trick is used only in one place to avoid slowly convergent double RIs when evaluating the matrix elements $\langle kl|F_{12}(\hat{g}_1 + \hat{g}_2)F_{12}|mn\rangle$. For this we define

$$\hat{g} = \hat{t} + \hat{\mathrm{v}} + 2\hat{j} - \hat{n} \equiv \hat{h} - \hat{n}, \tag{21-43}$$

$$\hat{n} = \hat{k} - (2\hat{o}\hat{f}\hat{o} - \hat{o}\hat{f} - \hat{f}\hat{o}). \tag{21-44}$$

where $\hat{t}$, $\hat{\mathrm{v}}$, $\hat{j}$, and $\hat{k}$ are the kinetic energy, external potential, Coulomb, and exchange contributions to the Fock operator. Since $\hat{\mathrm{v}} + 2\hat{j}$ commutes with F_{12} we can write:

$$F_{12}\hat{g}_{12}\hat{Q}_{12}F_{12} = \hat{U}^F_{12} - F_{12}\hat{h}_{12}\hat{P}_{12}F_{12} + \hat{h}_{12}F^2_{12} - \hat{Y}_{12}, \tag{21-45}$$

$$\hat{U}^F_{12} = [F_{12}, \hat{t}_{12}]F_{12}, \tag{21-46}$$

$$\hat{Y}_{12} = F_{12}\hat{n}_{12}\hat{Q}_{12}F_{12}. \tag{21-47}$$

Defining the *intermediate orbitals*

$$|\bar{\alpha}\rangle = \hat{h}|\alpha\rangle \approx |\beta\rangle h_{\beta\alpha}, \tag{21-48}$$

$$|\widetilde{\alpha}\rangle = \hat{n}|\alpha\rangle \approx |\beta\rangle n_{\beta\alpha}, \tag{21-49}$$

one obtains

$$A_{kl,mn} = U^F_{kl,mn} - \left(F^{kl}_{\tilde{\alpha}\beta} + F^{kl}_{\alpha\tilde{\beta}}\right)P_{\alpha\beta}F^{mn}_{\alpha\beta} + F^2_{\tilde{kl},mn} + F^2_{k\tilde{l},mn} - Y_{kl,mn}, \quad (21\text{-}50)$$

$$U^F_{kl,mn} = \langle kl|\hat{U}^F_{12}|mn\rangle, \quad (21\text{-}51)$$

$$Y_{kl,mn} = \langle kl|\hat{Y}_{12}|mn\rangle \approx \left(F^{kl}_{\tilde{x}a} + F^{kl}_{x\tilde{a}}\right)F^{mn}_{xa} + \left(F^{kl}_{\tilde{a}x} + F^{kl}_{a\tilde{x}}\right)F^{mn}_{ax} + \left(F^{kl}_{\tilde{x}y} + F^{kl}_{x\tilde{y}}\right)F^{mn}_{xy}. \quad (21\text{-}52)$$

The most expensive part is the evaluation of the matrix $Y_{kl,mn}$. The computational effort to evaluate this matrix grows as $\mathcal{O}\left(N_o^4 N_x^2\right)$, where N_o and N_x are the number of valence and CA orbitals, respectively. If the diagonal approximation [cf. Eq. (21-8)] is used, the scaling reduces to $\mathcal{O}\left(N_o^2 N_x^2\right)$. Further reductions of the computational effort can be achieved by using so called hybrid approximations [28] that either neglect the matrix elements $Y_{kl,mn}$ entirely (HY1 approximation), or only the last term (HY2 approximation). The HY1 approximation is closely related (but not identical) to the hybrid approximation proposed earlier by Klopper [78]. It should be noted that even with the HY1 approximation integrals with two indices in the RI basis are needed in order to compute quantities like $F^{kl}_{\tilde{m}x}$. Nevertheless, the savings achieved by this approximation are significant.

21.2.1.4. Solving the MP2-F12 Equations

The F12 amplitude equations $R^{ij}_{kl} = 0$ [cf. Eq. (21-22)] can be solved iteratively by using the amplitude update formula

$$\Delta\mathbf{T}^{ij} = -\left[\mathbf{B} - (f_{ii} + f_{jj})\mathbf{S}\right]^{-1}\mathbf{R}^{ij}. \quad (21\text{-}53)$$

In this expression, the F12 intermediates $S_{kl,mn}$ and $B_{kl,mn}$ are regarded as matrices with the combined (kl) labels as row index and (mn) as column indices, and the vectors $\mathbf{T}^{ij}$ and $\mathbf{R}^{ij}$ correspond to T^{ij}_{kl} and R^{ij}_{kl}, respectively.

Exactly evaluating the inverse matrices $\left[\mathbf{B} - (f_{ii} + f_{jj})\mathbf{S}\right]^{-1}$ for each ij pair is a process with an unfavorable $\mathcal{O}\left(N_o^8\right)$ scaling, where N_o is the number of correlated orbitals. However, the term can be estimated efficiently by using approximate spectral decompositions of both $\mathbf{S}$ and $\mathbf{B}$ in terms of a *common* eigensystem $\mathbf{Q} = (\mathbf{q}_p)$:

$$\mathbf{S} \approx \sum_p s_p\,\mathbf{q}_p\mathbf{q}_p^T, \quad (21\text{-}54)$$

$$\mathbf{B} \approx \sum_p b_p\,\mathbf{q}_p\mathbf{q}_p^T. \quad (21\text{-}55)$$

With this approximation, Eq. (21-53) turns into

$$\Delta\mathbf{T}^{ij} = -\sum_p \mathbf{q}_p \frac{1}{b_p - (f_{ii} + f_{jj})s_p}\mathbf{q}_p^T\mathbf{R}^{ij}, \quad (21\text{-}56)$$

which can be evaluated completely in terms of matrix multiplications ($\mathcal{O}\left(N_o^6\right)$) and scalar-vector multiplication ($\mathcal{O}\left(N_o^4\right)$). The eigensystem of $\mathbf{S}+\mathbf{B}$ works well for representing both $\mathbf{S}$ and $\mathbf{B}$ at the same time. The expansion coefficients b_p and s_b are then given by the diagonal elements of $\mathbf{Q}^T\mathbf{B}\mathbf{Q}$ and $\mathbf{Q}^T\mathbf{S}\mathbf{Q}$, respectively. In practical calculations this update scheme works nearly as well as when using exact pair specific matrix inversions, even if core orbitals are correlated (i.e., if large diagonal elements f_{ii} and f_{jj} occur).

In general, the conventional amplitude equations $R_{ab}^{ij}=0$ [cf. Eq. (21-21)] also need to be solved iteratively due to the coupling to the F12 amplitudes. This can be done in the standard way (e.g., Ref. [79]). It is recommendable to solve the F12 amplitude equations (21-22) exactly in micro-iterations for each conventional macro-iteration. However, when fixed F12 amplitudes and canonical orbitals are used, or when EBC (extended Brillouin condition, i.e. neglect of the coupling matrices C_{ab}^{kl}) is employed, a non-iterative closed form solution of the coupled MP2-F12 equations is also possible.

21.2.2. Explicitly Correlated Coupled Cluster Methods

In this section we will first summarize the general CCSD-F12 theory and then describe our CCSD-F12a and CCSD-F12b approximations [51]. As for MP2, the discussion will be restricted to the closed-shell case. An open-shell implementation is also available and described in Ref. [52].

The CCSD-F12 wave function is defined as

$$\Psi_{\text{CCSD-F12}}=\exp\left(\hat{T}_1+\hat{T}_2\right)|\Phi_{\text{HF}}\rangle, \tag{21-57}$$

where $\hat{T}_1$ and $\hat{T}_2$ are one and two particle excitation operators:

$$\hat{T}_1=t_a^i\hat{E}_{ai}, \tag{21-58}$$

$$\hat{T}_2=\frac{1}{2}\left[T_{ab}^{ij}\hat{E}_{ai}\hat{E}_{bj}+\mathcal{T}_{\alpha\beta}^{ij}\hat{E}_{\alpha i}\hat{E}_{\beta j}\right], \tag{21-59}$$

with

$$\mathcal{T}_{\alpha\beta}^{ij}=\langle\alpha\beta|\hat{Q}_{12}F_{12}|kl\rangle T_{kl}^{ij}. \tag{21-60}$$

The operator $\hat{T}_1$ and the first part of $\hat{T}_2$ are the same as in the standard CCSD. Note that there are no single excitations into the CA orbitals, i.e., $t_x^i=0$. The second term in Eq. (21-59) adds the explicitly correlated contributions, in the same way as in the first-order wave function in MP2-F12. For the further discussion it is useful to unify the two terms and to write $\hat{T}_2$ as

$$\hat{T}_2=\frac{1}{2}\mathcal{U}_{\alpha\beta}^{ij}\hat{E}_{\alpha i}\hat{E}_{\beta j}, \tag{21-61}$$

$$\mathcal{U}_{\alpha\beta}^{ij} = \delta_{\alpha a}\delta_{\beta b}T_{ab}^{ij} + \mathcal{T}_{\alpha\beta}^{ij}. \tag{21-62}$$

Here $\mathcal{U}_{\alpha\beta}^{ij}$ are generalized amplitude matrices defined in the complete orthonormal orbital space. They are zero if either α or β or both correspond to an occupied orbital. In the following, we will use the fixed amplitude ansatz, i.e., the amplitudes T_{kl}^{ij} are determined by Eq. (21-9), and therefore no extra amplitude equations need to be solved for them.

21.2.2.1. General Formulation of the full CCSD-F12 Amplitude Equations

The singles and doubles amplitudes t_a^i and T_{ab}^{ij} are determined by the conditions $r_a^i = 0$ and $R_{ab}^{ij} = 0$, where r_a^i and R_{ab}^{ij} are the CCSD-F12 singles and doubles residuals obtained by projecting the Schrödinger equation from the left with the contravariant configurations $\tilde{\Phi}_{ab}^{ij}$ [cf. Eq. (21-10)] and $\tilde{\Phi}_i^a = \frac{1}{2}\hat{E}_{ai}\Phi_{\rm HF}$:

$$\tilde{r}_a^i = \langle\tilde{\Phi}_i^a|\hat{H} - E|\Psi_{\text{CCSD-F12}}\rangle, \tag{21-63}$$

$$\tilde{R}_{ab}^{ij} = \langle\tilde{\Phi}_{ij}^{ab}|\hat{H} - E|\Psi_{\text{CCSD-F12}}\rangle. \tag{21-64}$$

If the explicit form of these residuals is derived, the energy dependent terms cancel out. The resulting equations for CCSD were presented in Ref. [79]; they form the basis for the original CCSD implementation in MOLPRO.

Alternatively, as preferred by many authors, one can use the similarity transformed Hamiltonian ($\hat{T} = \hat{T}_1 + \hat{T}_2$)

$$r_a^i = \langle\tilde{\Phi}_i^a|e^{-\hat{T}}\hat{H}e^{\hat{T}}|\Phi_{\rm HF}\rangle, \tag{21-65}$$

$$R_{ab}^{ij} = \langle\tilde{\Phi}_{ij}^{ab}|e^{-\hat{T}}\hat{H}e^{\hat{T}}|\Phi_{\rm HF}\rangle. \tag{21-66}$$

It is straightforward to show that $r_a^i = \tilde{r}_a^i$ and

$$R_{ab}^{ij} = \tilde{R}_{ab}^{ij} - t_a^i\tilde{r}_b^j - \tilde{r}_a^i t_b^j. \tag{21-67}$$

Since for the optimized amplitudes the last two terms in the latter expression vanish, the solutions of the amplitude equations $R_{ab}^{ij} = 0$ or $\tilde{R}_{ab}^{ij} = 0$ are the same, as long as no further approximations are introduced. Computationally there is no significant advantage of using one or the other form, and also convergence of the iterative solution of the amplitude equations is virtually the same. It should be noted, however, that there is a difference if local approximations are introduced. In this case the singles residuals $\tilde{r}_a^i$ vanish only in the orbital domain $[i]$, and since this is smaller than the pair domain $[ij]$ the optimized LCCSD energies are slightly different if either Eqs. (21-64) or (21-66) are used. Therefore, and also in order to be consistent with the formulation of most other authors, we will in the following only use R_{ab}^{ij} [Eq. (21-66)] (this is also the current default in MOLPRO).

The most compact and computationally efficient form of the CCSD equations is based on the matrix/tensor formulation as first introduced by Meyer in the self-consistent electron pair (SCEP) theory [80, 81] (which corresponds to CISD). The corresponding tensor expressions for CCSD, QCISD (quadratic configuration interaction), and BCCD (Brueckner coupled cluster doubles) were given in Ref. [79] using Eq. (21-64). Here we will use a similar matrix formulation based on Eq. (21-66).

In order to keep the presentation most compact, we will absorb all contributions of single excitations into the integrals, using "dressed" orbitals

$$|\tilde{r}\rangle = |r\rangle + |c\rangle t_c^r, \tag{21-68}$$

$$|\bar{s}\rangle = |s\rangle - |k\rangle t_s^k, \tag{21-69}$$

where it is assumed that $t_c^a = 0$ and $t_i^k = 0$, i.e., $|\tilde{a}\rangle = |a\rangle$ and $|\bar{i}\rangle = |i\rangle$. Furthermore, the singles amplitudes t_β^α are assumed to be zero if either α or β corresponds to a CA orbital. Note that the dressed orbitals $|\tilde{r}\rangle$ and $|\bar{s}\rangle$ are unrelated to the intermediate orbitals $|\tilde{\alpha}\rangle$ and $|\bar{\alpha}\rangle$ in Eqs. (21-49) and (21-48).

Using dressed integrals corresponds to employing a similarity transformed Hamiltonian $\bar{H} = e^{-\hat{T}_1}\hat{H}e^{\hat{T}_1}$ and writing the residuals as

$$r_a^i = \langle \tilde{\Phi}_i^a | e^{-\hat{T}_2} \bar{H} e^{\hat{T}_2} | \Phi_{\mathrm{HF}} \rangle, \tag{21-70}$$

$$R_{ab}^{ij} = \langle \tilde{\Phi}_{ij}^{ab} | e^{-\hat{T}_2} \bar{H} e^{\hat{T}_2} | \Phi_{\mathrm{HF}} \rangle. \tag{21-71}$$

For the sake of simplicity in the following expressions, we define dressed integrals and a dressed Fock matrix

$$\bar{K}_{tu}^{rs} = \langle \bar{t}\bar{u} | r_{12}^{-1} | \tilde{r}\tilde{s} \rangle, \tag{21-72}$$

$$\bar{f}_{rs} = h_{\tilde{r}\tilde{s}} + 2\langle \bar{r}\bar{k} | r_{12}^{-1} | \tilde{s}\tilde{k} \rangle - \langle \bar{k}\bar{r} | r_{12}^{-1} | \tilde{s}\tilde{k} \rangle. \tag{21-73}$$

Furthermore, to preserve the matrix structure of the equations, it is convenient to define integral matrices and vectors

$$\left[\mathbf{K}^{kl}\right]_{\alpha\beta} = \langle \alpha\beta | r_{12}^{-1} | kl \rangle, \tag{21-74}$$

$$\left[\mathbf{L}^{kl}\right]_{\alpha\beta} = 2K_{\alpha\beta}^{kl} - K_{\alpha\beta}^{lk}, \tag{21-75}$$

$$\left[\hat{\mathbf{K}}^{kl}\right]_{\alpha b} = \langle \alpha \bar{b} | r_{12}^{-1} | k \tilde{l} \rangle, \tag{21-76}$$

$$\left[\hat{\mathbf{J}}^{kl}\right]_{\alpha b} = \langle k\alpha | r_{12}^{-1} | \tilde{l}\bar{b} \rangle, \tag{21-77}$$

$$\left[\bar{\mathbf{I}}^{kli}\right]_{\alpha} = 2\langle kl | r_{12}^{-1} | \alpha\tilde{i} \rangle - \langle lk | r_{12}^{-1} | \alpha\tilde{i} \rangle, \tag{21-78}$$

as well as amplitude matrices

$$\left[\mathbf{U}^{ij}\right]_{\alpha\beta} = \mathcal{U}_{\alpha\beta}^{ij}, \tag{21-79}$$

$$\left[\tilde{\mathbf{U}}^{ij}\right]_{\alpha\beta} = 2\mathcal{U}^{ij}_{\alpha\beta} - \mathcal{U}^{ji}_{\alpha\beta}. \tag{21-80}$$

The CCSD-F12 residuals are obtained from the standard CCSD ones by replacing the amplitudes T^{ij}_{ab} by the generalized amplitudes $\mathcal{U}^{ij}_{\alpha\beta}$. This yields

$$r^i_a = \bar{f}_{ai} + \tilde{\mathcal{U}}^{ik}_{a\beta}\bar{f}_{k\beta} + K^{\alpha\beta}_{\bar{a}k}\tilde{\mathcal{U}}^{ik}_{\alpha\beta} - \mathcal{U}^{kl}_{a\beta}\bar{l}^{lki}_{\beta}, \tag{21-81}$$

$$R^{ij}_{ab} = \bar{K}^{ij}_{ab} + \bar{K}^{\alpha\beta}_{ab}\mathcal{U}^{ij}_{\alpha\beta} + \alpha_{ij,kl}T^{kl}_{ab} + G^{ij}_{ab} + G^{ji}_{ba}, \tag{21-82}$$

where the intermediates are defined as

$$\alpha_{ij,kl} = \bar{K}^{ij}_{kl} + K^{\alpha\beta}_{kl}\mathcal{U}^{ij}_{\alpha\beta}, \tag{21-83}$$

$$\beta_{ki} = \bar{f}_{ki} + K^{\alpha\beta}_{kl}\tilde{\mathcal{U}}^{il}_{\alpha\beta}, \tag{21-84}$$

$$\mathbf{X} = \bar{\mathbf{f}}^{\dagger} - \mathbf{L}^{kl}\mathbf{U}^{lk}, \tag{21-85}$$

$$\mathbf{Y}^{kj} = \hat{\mathbf{K}}^{kj} - \frac{1}{2}\hat{\mathbf{J}}^{kj} + \frac{1}{4}\mathbf{L}^{kl}\tilde{\mathbf{U}}^{lj}, \tag{21-86}$$

$$\mathbf{Z}^{kj} = \hat{\mathbf{J}}^{kj} - \frac{1}{2}\mathbf{K}^{lk}\mathbf{U}^{jl}, \tag{21-87}$$

$$\mathbf{G}^{ij} = \mathbf{U}^{ij}\mathbf{X} + \tilde{\mathbf{U}}^{ik}\mathbf{Y}^{kj} - \frac{1}{2}\mathbf{U}^{ki}\mathbf{Z}^{kj} - (\mathbf{U}^{ki}\mathbf{Z}^{kj})^{\dagger} - \mathbf{T}^{ik}\beta_{kj}. \tag{21-88}$$

In the matrix multiplications with $\mathbf{U}^{ij}$ the summations run formally over the complete virtual space (occupied orbitals do not contribute due to the strong orthogonality projector), e.g.,

$$\left[\mathbf{U}^{ij}\mathbf{X}\right]_{ab} = U^{ij}_{a\gamma}X_{\gamma b}. \tag{21-89}$$

When substituting the definition of $\mathcal{U}^{ij}_{\alpha\beta}$ [cf. Eq. (21-62)] into these expressions we can distinguish two types of terms:

Type 1: The exact resolution of the identity $|\alpha\beta\rangle\langle\alpha\beta|$ arising from the unity operator in $\hat{Q}_{12}$ can be eliminated. This is only possible for the trace-like terms

$$K^{\alpha\beta}_{rs}\mathcal{U}^{ij}_{\alpha\beta} = [\mathbf{K}(\mathbf{T}^{ij})]_{rs} + \bar{V}^{ij}_{rs}, \tag{21-90}$$

where

$$[\mathbf{K}(\mathbf{T}^{ij})]_{rs} = \langle rs|r_{12}^{-1}|cd\rangle T^{ij}_{cd}, \tag{21-91}$$

$$\bar{V}^{ij}_{rs} = \langle rs|r_{12}^{-1}\hat{Q}_{12}F_{12}|kl\rangle T^{ij}_{kl}. \tag{21-92}$$

The contributions $\bar{V}_{rs}^{ij}$ can be evaluated as

$$\bar{V}_{rs}^{ij} = \bar{W}_{rs}^{ij} - K_{\alpha\beta}^{rs} P_{\alpha\beta} \bar{F}_{\alpha\beta}^{ij}, \tag{21-93}$$

where

$$\bar{F}_{\alpha\beta}^{ij} = \langle \alpha\beta | F_{12} | kl \rangle T_{kl}^{ij}, \tag{21-94}$$

$$\bar{W}_{rs}^{ij} = \langle rs | r_{12}^{-1} F_{12} | kl \rangle T_{kl}^{ij}. \tag{21-95}$$

They occur in Eq. (21-81) for $rs = ak$ (contributions of integrals over 3 external orbitals), in Eq. (21-82) for $rs = ab$ (contributions of integrals over 4 external orbitals), and in Eqs. (21-83) and (21-84) for $rs = kl$ (contributions of integrals over 2 external orbitals). Defining

$$\bar{T}_{rs}^{ij} = \delta_{rc}\delta_{sd} T_{cd}^{ij} - \bar{F}_{rs}^{ij} \tag{21-96}$$

one can write Eq. (21-90) as

$$\begin{aligned} K_{rs}^{\alpha\beta} \mathcal{U}_{\alpha\beta}^{ij} = {} & [\bar{\mathbf{W}}^{ij} + \mathbf{K}(\bar{\mathbf{T}}^{ij})]_{rs} \\ & - \langle rs | r_{12}^{-1} | px \rangle \bar{F}_{px}^{ij} - \langle rs | r_{12}^{-1} | xp \rangle \bar{F}_{xp}^{ij}. \end{aligned} \tag{21-97}$$

The external exchange operators $\mathbf{K}(\bar{\mathbf{T}}^{ij})$ can be computed directly from the two-electron integrals in the AO basis by first transforming the amplitudes into the AO basis:

$$\bar{T}_{\rho\sigma}^{ij} = C_{\rho c} T_{cd}^{ij} C_{\sigma d} - C_{\rho r} \bar{F}_{rs}^{ij} C_{\sigma s}, \tag{21-98}$$

then contracting these with the integrals, and finally transforming the resulting matrices back into the MO basis:

$$[\mathbf{K}(\bar{\mathbf{T}}^{ij})]_{\mu\nu} = \langle \mu\nu | r_{12}^{-1} | \rho\sigma \rangle \bar{T}_{\rho\sigma}^{ij}, \tag{21-99}$$

$$[\mathbf{K}(\bar{\mathbf{T}}^{ij})]_{rs} = C_{\mu r} [\mathbf{K}(\bar{\mathbf{T}}^{ij})]_{\mu\nu} C_{\nu s}. \tag{21-100}$$

The transformation of the matrices $\bar{F}_{rs}^{ij}$ into the AO basis [cf. Eq. (21-98)] can be carried out before the CCSD-F12 iterations and is therefore required only once. The same holds for the last two terms of Eq. (21-97). These terms can be efficiently evaluated using density fitting approximations (for details see Ref. [52]). Even more efficient is to neglect the terms involving the CA orbitals entirely. As will be discussed in Section 21.2.2.3, this is an excellent approximation. The effort for the remaining first term in Eq. (21-97), which needs to be computed in each iteration, is then virtually the same as in standard CCSD.

Type 2: These are all contributions where only one index of $\mathbf{U}^{ij}$ matches an integral label, i.e., all cases where $\mathbf{U}^{ij}$ occurs in a matrix product. In these terms the unit operator in $\hat{Q}_{12}$ cannot be treated exactly as for type 1, but must be approximated by a double RI, yielding

$$\hat{Q}_{12} = |ax\rangle\langle ax| + |xa\rangle\langle xa| + |xy\rangle\langle xy|. \tag{21-101}$$

For example, this leads to contributions like

$$\left[\mathbf{U}^{ik}\mathbf{J}^{kj}\right]_{ab} = T^{ik}_{ac}J^{kj}_{cb} + \bar{F}^{ik}_{ax}J^{kj}_{xb}, \tag{21-102}$$

$$\left[\mathbf{U}^{ik}\mathbf{K}^{kl}\mathbf{U}^{lj}\right]_{ab} = T^{ik}_{ac}K^{kl}_{cd}T^{lj}_{db} + \bar{F}^{ik}_{ax}K^{kl}_{xy}\bar{F}^{lj}_{yb} + \bar{F}^{ik}_{ax}K^{kl}_{xd}T^{lj}_{db} + T^{ik}_{ac}K^{kl}_{cx}\bar{F}^{lj}_{xb}. \tag{21-103}$$

Hence, the first index of the intermediates $\mathbf{X}$, $\mathbf{Y}^{kj}$ and $\mathbf{Z}^{kj}$ must run over the virtual and CA spaces. For the dominant terms this leads to an overall computational cost of $N_o^3\left(4N_\mathrm{v}^3 + 6N_\mathrm{v}^2N_x + 4N_\mathrm{v}N_x^2\right)$. Thus, the computational effort scales quadratically in the size of the CA basis. Assuming that $N_x \approx 3N_\mathrm{v}$ it follows that the evaluation of these terms in CCSD-F12 is about one order of magnitude more expensive than in standard CCSD. However, as will be shown in Section 21.2.2.3, it is an excellent approximation to neglect all type 2 contributions of the CA orbitals, and then the overall effort for the CCSD-F12 residual is virtually the same as for standard CCSD.

Even though the above formulation of the CCSD-F12 amplitude equations in terms of dressed integrals is very simple and compact, it should be noted that it is not the computationally most efficient one. This is because the rather numerous dressed integrals have to be recomputed and stored in each iteration. The integral transformation scales with $\mathcal{O}\left(N_oN_\mathrm{AO}^4\right)$, where N_o is the number of occupied (correlated) orbitals, and N_AO is the number of basis functions. On the other hand, the additional terms arising in the explicit treatment of the singles take very little time and scale at most with $\mathcal{O}\left(N_\mathrm{v}^3N_o^2\right)$ (N_v being the number of virtual orbitals). One might argue that integrals over three virtual and one occupied orbitals (3-external integrals) are not needed if dressed integrals are used, but these integrals are required for the perturbative triples (T) correction anyway, and therefore there is no overall saving. The generation and storage of transformed 4-external integrals can be avoided in both cases by computing these contributions directly from the two-electron integrals in the AO basis as explained above. The expanded form of the CCSD residuals, as implemented in MOLPRO, is given in the Appendix [note that the matrices $\mathbf{G}^{ij}$ in the appendix [Eq. (21-144)] are not identical to the ones in Eq. (21-88), since some singles terms in Eq. (21-144) are included in the dressed integrals in the first two terms of Eq. (21-82)].

21.2.2.2. The CCSD(T)-F12 Energy Expression

Assuming that fully optimized HF orbitals and fully optimized amplitudes T_{ab}^{ij} and T_{kl}^{ij} are used, the CCSD-F12 correlation energy expression simply reads

$$E_{\text{CCSD-F12}} = \tilde{D}_{ab}^{ij} K_{ab}^{ij} + \tilde{T}_{kl}^{ij} V_{kl}^{ij}. \tag{21-104}$$

Here and in the following, we employ composite amplitude matrices D_{ab}^{ij}, which are defined as

$$D_{rs}^{ij} = \delta_{rc}\delta_{sd}\left(T_{cd}^{ij} + t_c^i t_d^j\right) + \delta_{ri} t_s^j + \delta_{sj} t_r^i, \tag{21-105}$$

$$\tilde{D}_{rs}^{ij} = 2D_{rs}^{ij} - D_{rs}^{ji}. \tag{21-106}$$

For fixed amplitudes T_{kl}^{ij}, however, Eq. (21-104) should not be used, since it depends in first order on the deviations of the amplitudes from their fully optimized values. It is then necessary to use an energy functional that depends only quadratically on the deviations of the T_{kl}^{ij} from the fully optimized values. This can be achieved by adding to Eq. (21-104) a contribution

$$\Delta E_{\text{CCSD-F12}} = \Lambda_{kl}^{ij} \langle kl | F_{12} \hat{Q}_{12} | \alpha\beta \rangle R_{\alpha\beta}^{ij}, \tag{21-107}$$

where Λ_{kl}^{ij} is a vector of Lagrange multipliers (the so-called Λ-vector or Z-vector), and $R_{\alpha\beta}^{ij}$ is the CCSD-F12 doubles residual in the complete orbital basis. To a good approximation one can assume $\Lambda_{kl}^{ij} = 2T_{kl}^{ij} - T_{kl}^{ji}$. This is exactly true for MP2-F12 or variational approaches like CI or coupled pair functional (CPF). The correlation energy can then be written as

$$\begin{aligned}\mathcal{E}_{\text{CCSD-F12}} = {} & \tilde{D}_{ab}^{ij} K_{ab}^{ij} + \tilde{T}_{kl}^{ij}\left(V_{kl}^{ij} + R_{kl}^{ij}\right) + \tilde{D}_{rs}^{ij} \bar{V}_{rs}^{ij} + \bar{S}_{ij,kl}\gamma_{ij,kl} \\ & + \tilde{T}_{mn}^{ij} H_{mn,op} T_{op}^{ij} + 2\tilde{F}_{xa}^{ij} \bar{V}_{xk}^{ij} t_a^k \\ & + 2\left(\tilde{F}_{ax}^{ij} \bar{G}_{ax}^{ij} + \tilde{F}_{xa}^{ij} \bar{G}_{xa}^{ij} + \tilde{F}_{xy}^{ij} \bar{G}_{xy}^{ij}\right),\end{aligned} \tag{21-108}$$

where R_{kl}^{ij} is the MP2-F12 residual given in Eq. (21-22) but evaluated with CCSD-F12 amplitudes, and

$$\tilde{F}_{\alpha\beta}^{ij} = 2\bar{F}_{\alpha\beta}^{ij} - \bar{F}_{\alpha\beta}^{ji}, \tag{21-109}$$

$$H_{mn,op} = \langle mn | F_{12} \hat{Q}_{12} r_{12}^{-1} \hat{Q}_{12} F_{12} | op \rangle, \tag{21-110}$$

$$\gamma_{ij,kl} = \alpha_{ij,kl} - \delta_{ik}(\beta_{lj} - f_{lj}) - \delta_{jl}(\beta_{ki} - f_{ki}), \tag{21-111}$$

$$\bar{S}_{ij,kl} = \tilde{T}_{mn}^{ij} S_{mn,op} T_{op}^{kl}, \tag{21-112}$$

$$\bar{\mathbf{G}}^{ij} = \mathbf{U}^{ij}(\mathbf{X} - \mathbf{f}) - \sum_k [\mathbf{K}(\mathbf{D}^{ij})^{(k)} + \mathbf{k}^{ijk}]\mathbf{t}^{k\dagger} + \sum_k \left[\tilde{\mathbf{U}}^{ik}\mathbf{Y}^{kj} - \frac{1}{2}\mathbf{U}^{ki}\mathbf{Z}^{kj} - (\mathbf{U}^{ki}\mathbf{Z}^{kj})^{\dagger}\right]. \quad (21\text{-}113)$$

The intermediates $\alpha_{ij,kl}$, β_{ki}, $\mathbf{X}$, $\mathbf{Y}^{kj}$, and $\mathbf{Z}^{kj}$ are defined in Eqs. (21-83), (21-84), (21-85), (21-86) and (21-87). The Fock matrix contributions are subtracted from $\mathbf{X}$ and β_{ki} since these are included in the MP2-F12 residuals R_{kl}^{ij}. Again, there are type 1 and type 2 contributions. The type 1 contributions occur in R_{kl}^{ij}, $\bar{V}_{rs}^{ij}$, $S_{mn,op}$, and $H_{mn,op}$ (here m, n, o, p run over the valence space only). The contribution of $H_{mn,op}$ to the energy takes the explicit form

$$\tilde{T}_{mn}^{ij} H_{mn,op} T_{op}^{ij} = \tilde{T}_{mn}^{ij} \langle mn|F_{12} r_{12}^{-1} F_{12}|op\rangle T_{op}^{ij} - \tilde{F}_{\alpha\beta}^{ij} P_{\alpha\beta} \left(\bar{V}_{\alpha\beta}^{ij} + \bar{W}_{\alpha\beta}^{ij}\right). \quad (21\text{-}114)$$

The quantities $\bar{V}_{\alpha\beta}^{ij}$ and $\bar{W}_{\alpha\beta}^{ij}$ are defined in analogy to Eqs. (21-92) and (21-95), respectively.

However, all contributions of the matrices $\bar{G}_{\alpha\beta}^{ij}$ can only be evaluated in the type 2 way using multiple RIs and by approximating the amplitude matrices $\mathbf{U}^{ij}$ as $U_{ab}^{ij} = T_{ab}^{ij}$, $U_{ax}^{ij} = \bar{F}_{ax}^{ij}$, $U_{xa}^{ij} = \bar{F}_{xa}^{ij}$, and $U_{xy}^{ij} = \bar{F}_{xy}^{ij}$. This requires large auxiliary basis sets and leads to $\mathcal{O}\left(N_x^3\right)$ scaling of the computational cost. In fact, if one adds the blocks $\bar{G}_{ab}^{ij}$, which are needed for the CCSD-F12 doubles residual, the evaluation of the $\bar{\mathbf{G}}^{ij}$ matrices proceeds exactly as in a standard CCSD calculation but using the combined virtual and CA orbital basis, and the total effort is approximately proportional to $4N_o^3(N_\mathrm{v}+N_x)^3$. If the amplitudes T_{kl}^{ij} were not fixed but fully optimized in the CCSD-F12, similar quantities would be required in each iteration. Thus, the computational effort would be about two orders of magnitude larger than in CCSD, even in a most efficient implementation which makes fully use of the simple matrix structure of the equations.

A (T) perturbative energy correction for triple excitations can be added in the standard way, using the CCSD-F12 amplitudes. This correction is not explicitly correlated, and therefore the F12 treatment does not reduce the basis set incompleteness error of the triples energy (there is a small indirect effect by the singles and doubles amplitudes, which are affected by the coupling terms in the CCSD-F12x equations). A proper treatment of explicitly correlated (T) corrections, as recently proposed by Köhn[46], is complicated but may be considered at a later time. For the time being, we optionally correct for the basis set error of the triples approximately by scaling the triples energy as [52, 56]

$$\Delta E_{(\mathrm{T}^*)} = \Delta E_{(\mathrm{T})} \frac{E_{\mathrm{corr}}^{\mathrm{MP2\text{-}F12}}}{E_{\mathrm{corr}}^{\mathrm{MP2}}}. \quad (21\text{-}115)$$

This assumes that the relative basis set error is similar for the MP2 and (T) correlation energy contributions. The methods with scaled triples contribution are denoted by a star on the T, e.g., CCSD(T*)-F12.

21.2.2.3. The CCSD-F12x Approximations

The quadratic or cubic dependence of the computational effort on the size of the CA basis can be avoided by neglecting most type 2 contributions in the CCSD-F12 residuals and in the energy expression. The only exceptions are the type 2 terms in the MP2-F12 residuals, which also contribute to the CCSD-F12 residuals. By default, the contribution of the CA orbitals is also neglected in Eqs. (21-93) and (21-97) (but these contributions can be included optionally). The matrix $\bar{V}_{rs}^{ij}$ in Eq. (21-93) then takes the form

$$\bar{\mathbf{V}}^{ij} = \bar{\mathbf{W}}^{ij} - \mathbf{K}(\bar{\mathbf{F}}^{ij}). \tag{21-116}$$

The approximations CCSD-F12a and CCSD-F12b only differ in approximations in the energy expression:

$$\mathcal{E}_{\text{CCSD-F12a}} = \tilde{D}_{ab}^{ij} K_{ab}^{ij} + \tilde{T}_{kl}^{ij}\left(V_{kl}^{ij} + R_{kl}^{ij}\right), \tag{21-117}$$

$$\mathcal{E}_{\text{CCSD-F12b}} = \mathcal{E}_{\text{CCSD-F12a}} + \tilde{D}_{rs}^{ij} \bar{V}_{rs}^{ij}, \tag{21-118}$$

where again R_{kl}^{ij} is the MP2-F12 residual defined in Eq. (21-22) evaluated with CCSD-F12 amplitudes. All further terms in Eq. (21-108) are neglected. The computational effort for these approximations is essentially that of a standard CCSD plus an MP2-F12 calculation (in addition to the MP2-F12, one needs to evaluate the matrix elements $\bar{V}_{rs}^{ij}$; these can be easily obtained from the half transformed integrals $V_{\mu\nu}^{ij}$ that are also computed at an intermediate stage in MP2-F12). Since the effort of MP2-F12 scales only with $\mathcal{O}(N^5)$ while CCSD(T) scales with $\mathcal{O}(N^7)$, the additional time for the MP2-F12 becomes negligible in CCSD(T)-F12x calculations for larger molecules.

Extensive benchmarks have shown that CCSD-F12a somewhat overestimates the exact CCSD-F12 correlation energy, and this leads to a favorable and systematic error compensation when small (double or triple zeta) basis sets are used. The CCSD-F12b energy expression is closer to the exact CCSD-F12 but slightly underestimates it. CCSD-F12b is recommended for large basis sets (quadruple-zeta or larger). In most cases, however, relative energies computed with both approximations are of rather similar accuracy.

21.2.3. Perturbative CABS Singles Correction

In MP2-F12 and CCSD-F12 calculations the basis set errors of the Hartree–Fock energy are often much larger than the errors of the correlation energy. The error

of the HF contribution can be much reduced by including single excitations into the complementary auxiliary (CA) orbital space and by computing the second-order energy contribution perturbatively[29, 51]. For closed-shell cases the CABS singles amplitudes are obtained by solving

$$0 = f^i_{\alpha'} + f_{\alpha'\beta'} t^i_{\beta'} - f_{ik} t^k_{\alpha'}, \tag{21-119}$$

where $f_{\alpha'\beta'}$ are the matrix elements of the closed-shell Fock operator and the indices α', β' run over the virtual and CA orbitals. This equation can easily be solved by block diagonalizing the Fock matrix in the occupied and virtual+CA spaces. Note that the standard virtual orbitals need to be included, since the couplings f_{xa} are non-zero. The energy correction is then computed as

$$\Delta E_s = 2 t^i_{\alpha'} f^i_{\alpha'}. \tag{21-120}$$

A spin-free extension for high-spin open-shell cases has been discussed in Ref. [29].

We consider the CABS singles correction as a correction to the HF energy and not as a correlation effect. The Fock matrix elements $f_{\alpha'\beta'}$ and $f_{\alpha' i}$ are needed in MP2-F12 calculations anyway and therefore the additional effort for this correction is negligible. It should be noted that this energy correction is entirely distinct from the CCSD-F12 calculations, and the singles amplitudes t^i_β used here are not the same as those in the CCSD-F12.

Noga et al. [26] have proposed another way to include singles in the MP2-F12 method. This is different and more complex than our simple approach. One could also include the CABS singles in the CCSD-F12 equations. However, this would require many additional integrals and cause a large additional cost, at least within the F12x framework. The effect would probably be small and not worth the additional effort.

21.2.4. Explicitly Correlated Local Methods

Local correlation methods [59, 62, 63] exploit the short range character of dynamic electron correlation through the use of localized orbital basis sets. In the current work the correlated (valence) Hartree–Fock orbitals (LMOs) are localized using the Pipek–Mezey scheme [82], but Foster–Boys localization or natural localized orbitals (NLMOs) can also be employed in our program [83]. The choice of the localization method usually has only a small effect on the results. Pipek–Mezey localization has the advantage that $\sigma - \pi$ separation is kept in planar or linear molecules, and that analytical energy gradients can be computed [84, 85]. A disadvantage is that sometimes poor localization is achieved if diffuse basis sets are used. This can be cured by removing the diffuse functions from the localization criterion, or by using NLMOs, which are more stable with respect to variations of the basis set [83].

Since the orthogonal virtual orbitals cannot be well localized, projected atomic orbitals (PAOs) are used to span the virtual space

$$|\tilde{\mu}\rangle \equiv |\tilde{\phi}_\mu^{\mathrm{PAO}}\rangle = \sum_a |a\rangle\langle a|\chi_\mu^{\mathrm{AO}}\rangle, \tag{21-121}$$

where $|\chi_\mu^{\mathrm{AO}}\rangle$ are atomic orbitals. Note that in the current section we use tilde to indicate quantities in the PAO basis. This is entirely distinct from the intermediate orbitals or the dressed orbitals used earlier. The AOs can either be individual basis functions, or atomic orbitals that are represented by a linear combination of basis functions at one atom. In the current work, we use correlation consistent basis sets, and the functions $|\chi_\mu^{\mathrm{AO}}\rangle$ either correspond to atomic valence orbitals or to correlation/polarization functions. PAOs resulting from atomic core orbitals are omitted, since they have a very small norm. The PAOs are orthogonal to all occupied orbitals, but non-orthogonal among themselves. Since there are more AOs than virtual orbitals, the PAOs form a redundant set with N_{v} linearly independent vectors.

The use of local orbital spaces makes it possible to introduce two kinds of approximations: first, the conventional double excitations are restricted to pair domains $[ij]$, which are spanned by subsets of PAOs that are spatially close to the LMOs from which the electrons are excited (*domain approximation*). The pair domain $[ij]$ is defined as the union of orbital domains $[i]$ and $[j]$. The orbital domain $[i]$ includes all PAOs located at a subset of atoms that is associated to the LMO i. Automatic procedures to select the subsets of atoms that are associated to an orbital domain have been proposed by Boughton and Pulay (BP) [86] and Mata and Werner [83]. The latter method is based on natural population analysis (NPA) and has the advantage of being much more stable with respect to changes of the basis set. However, the calculations presented in the present paper were still carried out with the older BP method. Details of this method, as implemented in MOLPRO, can be found in Refs. [63, 87].

Secondly, one can introduce a hierarchy of pair classes, dependent on the distance of the LMOs i and j (*pair approximation*). Correlation effects between very distant pairs are small, and their contribution to the energy can be neglected. On the other hand, strong pairs, in which the orbitals i and j share at least one atom, usually contribute more than 90% of the correlation energy. In many cases it is sufficient to treat only these strong pairs at the highest level, e.g., LCCSD(T), and the remaining ones by LMP2.

For what follows it is convenient to define orthonormalized functions $\tilde{a}$, $\tilde{b}$ spanning the domain $[ij]$, and these are obtained from the PAOs $\tilde{\mu}$ by transformations

$$|\tilde{a}\rangle = \sum_{\tilde{\mu}\in[ij]} |\tilde{\mu}\rangle W_{\tilde{\mu}\tilde{a}}^{(ij)}. \tag{21-122}$$

Thus, the orbitals $|\tilde{a}\rangle$ are pair-specific and should in principle be indexed with the pair label ij. However, since it is always obvious to which domain they belong, we will omit this index. The transformation matrices $W_{\tilde{\mu}\tilde{a}}^{(ij)}$ are obtained by solving the projected Fock equations

$$\tilde{\mathbf{f}}^{(ij)}\mathbf{W}^{(ij)} = \tilde{\mathbf{S}}^{(ij)}\mathbf{W}^{(ij)}\mathbf{e}^{(ij)}, \tag{21-123}$$

where $\tilde{\mathbf{f}}^{(ij)}$ and $\tilde{\mathbf{S}}^{(ij)}$ are the Fock and overlap matrices, respectively in the basis of the PAOs of the domain $[ij]$, and $\mathbf{e}^{(ij)}$ is a diagonal matrix holding the orbital energies. Due to the fact that the PAO basis is redundant, the overlap matrix $\tilde{\mathbf{S}}^{(ij)}$ may have zero or very small eigenvalues. These are removed using singular value decomposition. Thus, the resulting transformation matrices $W^{(ij)}_{\tilde{\mu}\tilde{a}}$ may be rectangular with fewer columns ($\tilde{a}$) than rows ($\tilde{\mu}$).

Naturally, the restriction of the excitations to domains leads to a reduction of the computed correlation energy. This is called the *domain error* and in conventional local correlation calculations amounts to 1–2% of the correlation energy. Even though this relative error is rather small, its absolute value is significant and can cause non-negligible errors when energy differences are computed. In the following it will be shown that these errors are much reduced in explicitly correlated local correlation methods [70–72].

21.2.4.1. LMP2-F12

The LMP2-F12 wave function is defined as

$$\Psi_{\text{LMP2-F12}} = (1 + \hat{T}_2)\Phi_{\text{HF}}, \tag{21-124}$$

where $\hat{T}_2$ is defined as

$$\hat{T}_2 = \frac{1}{2}\left[\sum_{ij\in P_d}\sum_{\tilde{a},\tilde{b}\in[ij]} T^{ij}_{\tilde{a}\tilde{b}}\hat{E}_{\tilde{a}i}\hat{E}_{\tilde{b}j} + \sum_{ij\in P_c}\sum_{\alpha,\beta} \mathcal{T}^{ij}_{\alpha\beta}\hat{E}_{\alpha i}\hat{E}_{\beta j}\right], \tag{21-125}$$

with

$$\mathcal{T}^{ij}_{\alpha\beta} = \sum_{k,l}\langle\alpha\beta|\hat{Q}^{ij}_{12}\hat{F}_{12}|kl\rangle T^{ij}_{kl}. \tag{21-126}$$

As compared to the standard MP2-F12 ansatz the following approximations are introduced:

(i) Orbital pairs ij where the LMOs i and j are very distant are neglected (pair approximation). This is indicated by the lists P_d and P_c. P_d is the list of all pairs that are included in the conventional LMP2 (strong, close, weak and distant pairs [63, 67]). The list of explicitly correlated pairs P_c may optionally be smaller and exclude the weak and distant pairs (cf. Section 21.3.5).

(ii) The conventional double excitations are restricted to the pair domains $[ij]$ (domain approximation).

(iii) Since the excitations are restricted to domains, a pair-specific projector $\hat{Q}_{12}^{ij}$ [70] is used in Eq. (21-126):

$$\hat{Q}_{12}^{ij} = (1 - \hat{o}_1)(1 - \hat{o}_2) - \sum_{\tilde{c},\tilde{d} \in [ij]} |\tilde{c}\tilde{d}\rangle\langle\tilde{c}\tilde{d}|. \tag{21-127}$$

The only difference to the ordinary projector in standard MP2-F12 or CCSD-F12 theory is that the summation in the last term is restricted to the pair domain $\tilde{c}, \tilde{d} \in [ij]$. This is not an additional approximation but is implied by the local ansatz in the conventional part of the wave function.

Our LMP2-F12 and LCCSD-F12 methods use the diagonal or fixed amplitude ansatz with approximation 3*A. The latter is simpler and more suitable for a linear scaling algorithm [27, 71] than the more rigorous approximation 3C as described in the previous sections. In approximation 3*A the extended Brillouin condition (EBC) is implied (i.e. $C_{ab}^{kl} = 0$) and the contributions of $Y_{kl,mn}$ [cf. Eq. (21-52)] are neglected. Furthermore, the $S_{kl,mn}$-matrix as well as exchange terms are neglected (for details see Refs. [16, 28]). The only quantities needed for LMP2-F12 are then

$$V_{kl}^{ij} = K_{ij,kl}^{F} + \sum_{p,q} K_{pq}^{ij} F_{pq}^{kl} - \sum_{\alpha,p} \left(K_{\alpha p}^{ij} F_{\alpha p}^{kl} + K_{p\alpha}^{ij} F_{p\alpha}^{kl} \right) - \sum_{\tilde{a},\tilde{b} \in [ij]} K_{\tilde{a}\tilde{b}}^{ij} F_{\tilde{a}\tilde{b}}^{kl}, \tag{21-128}$$

$$B_{kl,mn}^{(ij)} = U_{kl,mn}^{F} + \sum_{p,q} U_{pq}^{kl} F_{pq}^{mn} - \sum_{\alpha,p} \left(U_{\alpha p}^{kl} F_{\alpha p}^{mn} + U_{p\alpha}^{kl} F_{p\alpha}^{mn} \right) - \sum_{\tilde{a},\tilde{b} \in [ij]} U_{\tilde{a}\tilde{b}}^{kl} F_{\tilde{a}\tilde{b}}^{mn} \tag{21-129}$$

where $U_{kl,mn}^{F}$ is defined in Eq. (21-51), $U_{\alpha\beta}^{kl} = \langle kl|[F_{12}, \hat{t}_1 + \hat{t}_2]|\alpha\beta\rangle$ and $P_{\alpha\beta}^{ij} = \langle\alpha\beta|1 - \hat{Q}_{12}^{ij}|\alpha\beta\rangle$. Approximation 3*A leads to a slight overestimation of the correlation energies, but this has only a minor impact on energy differences such as reaction energies (see, e.g., Ref. [28]).

The use of the pair-specific projectors has two important advantages. First, the integrals $K_{\tilde{a}\tilde{b}}^{ij}$, $F_{\tilde{a}\tilde{b}}^{mn}$, and $U_{\tilde{a}\tilde{b}}^{kl}$ in the last summations of Eqs. (21-128) and (21-129) are only needed for $\tilde{a}$, $\tilde{b} \in [ij]$, and thus the number of these integrals scales linearly with molecular size (provided distant pairs ij are neglected and the diagonal ansatz is used, i.e. $kl = ij$ or $kl = ji$, and $mn = ij$ or $mn = ji$). This leads to a strong reduction of the computation time and disk space. Further savings can be achieved by also using local RI approximations in the other summations of Eqs. (21-128) and (21-129) (cf. Section 21.2.4.3). It is then possible to achieve linear scaling of the computational cost with molecular size.

Secondly, due to the modified pair specific projector, the double excitations into virtual orbitals *outside* the domain $[ij]$ are not entirely excluded as in standard local

correlation methods, but for a pair ij implicitly approximated by

$$\Delta\hat{T}_2^{ij} = \sum_{\tilde{c},\tilde{d}\notin[ij]} \bar{F}^{ij}_{\tilde{c}\tilde{d}} \hat{E}_{\tilde{c}i}\hat{E}_{\tilde{d}j}, \tag{21-130}$$

where $\bar{F}^{ij}_{\tilde{c}\tilde{d}} = \sum_{k,l}\langle\tilde{c}\tilde{d}|\hat{F}_{12}|kl\rangle T^{ij}_{kl}$. This can be viewed as an externally contracted excitation scheme, i.e., instead of fully optimized amplitudes $T^{ij}_{\tilde{c}\tilde{d}}$ the fixed matrix elements $\bar{F}^{ij}_{\tilde{c}\tilde{d}}$ are used. As will be demonstrated in Section 21.3.5, these additional terms very successfully correct for the domain error [70–72].

One of the main reasons for using approximation 3*A is that type 2 matrix elements (cf. Section 21.2.2) are entirely avoided. In type 2 matrix elements, which arise in the C^{kl}_{ab} [cf. Eq. (21-42)] and $Y_{mn,kl}$ [cf. Eq. (21-52)] terms, the unity operator in $\hat{Q}_{12}$ is approximated by a double RI, which leads without local approximations to Eq. (21-101). However, if the pair specific projector $\hat{Q}^{ij}_{12}$ is used, one obtains

$$\hat{Q}^{ij}_{12} = |ax\rangle\langle ax| + |xa\rangle\langle xa| + |xy\rangle\langle xy| + \sum_{\tilde{c},\tilde{d}\notin[ij]} |\tilde{c}\tilde{d}\rangle\langle\tilde{c}\tilde{d}|. \tag{21-131}$$

The additional last term arises because the contributions of the virtual orbitals in the double RI are only partly canceled by the last term in Eq. (21-127). Here, $\tilde{c}$, $\tilde{d}$ run over an orthonormal set of virtual orbitals that does not contain the domain $[ij]$. If they were included, much of the computational saving in the LMP2-F12 method would be lost.

21.2.4.2. LCCSD-F12

In the LCCSD-F12 method the excitation operators $\hat{T}_1$ and $\hat{T}_2$ are defined as

$$\hat{T}_1 = \sum_i \sum_{\tilde{a}\in[i]} t^i_{\tilde{a}} \hat{E}_{\tilde{a}i}, \tag{21-132}$$

$$\hat{T}_2 = \frac{1}{2}\sum_{ij\in P_s}\sum_{\alpha,\beta} \mathcal{U}^{ij}_{\alpha\beta}\hat{E}_{\alpha i}\hat{E}_{\beta j}, \tag{21-133}$$

where, in analogy to Eq. (21-62),

$$\mathcal{U}^{ij}_{\alpha\beta} = \sum_{c,d\in[ij]} \delta_{\alpha c}\delta_{\beta d}T^{ij}_{cd} + \sum_{k,l}\langle\alpha\beta|\hat{Q}^{ij}_{12}\hat{F}_{12}|kl\rangle T^{ij}_{kl}. \tag{21-134}$$

Optionally, only strong pairs, as defined by a list P_s, are included in $\hat{T}_2$. The remaining pairs are then treated by LMP2-F12, as outlined in the previous section. Again, we use the approximation LCCSD-F12x (cf. Section 21.2.2.3) with ansatz 3*A in the LMP2-F12. The LCCSD amplitude equations differ from the standard CCSD ones

by additional multiplications with the overlap matrix $\tilde{\mathbf{S}}$, which take into account the non-orthogonality of the PAOs. Furthermore, the sparse structure of the amplitude and integral tensors must be consistently taken into account. For details see Refs. [63], [67].

The only difference of the LCCSD-F12 and LCCSD amplitude equations are the terms $\Delta R^{ij}_{\tilde{a}\tilde{b}} = \langle \tilde{a}\tilde{b}|r_{12}^{-1}\hat{Q}^{ij}_{12}\hat{F}_{12}|kl\rangle T^{ij}_{kl}$. Neglecting the contributions of the complementary auxiliary orbitals in Eq. (21-97) yields explicitly in the non-orthogonal PAO basis

$$\begin{aligned}\Delta R^{ij}_{\tilde{\mu}\tilde{\nu}} \approx \bar{W}^{ij}_{\tilde{\mu}\tilde{\nu}} &- \sum_{p,q}\langle\tilde{\mu}\tilde{\nu}|r_{12}^{-1}|p,q\rangle\bar{F}^{ij}_{pq} \\ &- \sum_{p,c}\left[\langle\tilde{\mu}\tilde{\nu}|r_{12}^{-1}|pc\rangle\bar{F}^{ij}_{pc} + \langle\tilde{\mu}\tilde{\nu}|r_{12}^{-1}|cp\rangle\bar{F}^{ij}_{cp}\right] \\ &- \sum_{\tilde{\rho},\tilde{\sigma}\in[ij]}\langle\tilde{\mu}\tilde{\nu}|r_{12}^{-1}|\tilde{\rho}\tilde{\sigma}\rangle\sum_{\tilde{a},\tilde{b}\in[ij]} W^{(ij)}_{\tilde{\rho}\tilde{a}}\bar{F}^{ij}_{\tilde{a}\tilde{b}}W^{(ij)}_{\tilde{\sigma}\tilde{b}} \quad \text{for } \tilde{\mu},\tilde{\nu}\in[ij].\end{aligned} \tag{21-135}$$

An important observation is that in the last term of Eq. (21-135) the use of the local projector directly leads to linear scaling of the number of two-electron integrals $\langle\tilde{\mu}\tilde{\nu}|r_{12}^{-1}|\tilde{\rho}\tilde{\sigma}\rangle$ over four PAOs. This is true because $\tilde{\mu},\tilde{\nu},\tilde{\rho},\tilde{\sigma}\in[ij]$ and the number of PAOs in a given domain is independent of the molecular size. In fact, exactly the same integrals are needed in standard LCCSD theory, where similar contractions with the amplitudes $T^{ij}_{\tilde{\rho}\tilde{\sigma}}$ occur. Thus, both contractions can be done together with virtually no extra cost by forming $T^{ij}_{\tilde{\rho}\tilde{\sigma}} - \sum_{\tilde{a},\tilde{b}\in[ij]} W^{(ij)}_{\tilde{\rho}\tilde{a}}\bar{F}^{ij}_{\tilde{a}\tilde{b}}W^{(ij)}_{\tilde{\sigma}\tilde{b}}$. The contraction of these quantities with the integrals $\langle\tilde{\mu}\tilde{\nu}|r_{12}^{-1}|\tilde{\rho}\tilde{\sigma}\rangle$ scales linearly with molecular size, without introducing any additional approximations. Unfortunately, this is not automatically true for the first two summations in Eq. (21-135). Their treatment will be discussed in the next section.

21.2.4.3. Local RI Approximations

In the previous sections it has been shown that the local ansatz leads to linear scaling of the terms in the last summations of Eqs. (21-128), (21-129), and (21-135). However, this is not the case for the other summations in these equations, which arise from the occupied-occupied and occupied-virtual terms in the projector and are not automatically affected by the local ansatz.

In a local orbital basis the integrals $F^{ij}_{\mu' p}$ will be small unless the RI basis functions μ' and the LMOs p are spatially close to the LMOs i and j. Therefore, we can restrict the summations to domains, and approximate the first summation in Eq. (21-128) as

$$\sum_{\alpha,p} K^{ij}_{\alpha p}F^{kl}_{\alpha p} \approx \sum_{\bar{\alpha}\in[ij]_{\mathrm{RI}}}\sum_{p\in[ij]_{\mathrm{MO}}} K^{ij}_{\bar{\alpha}p}F^{kl}_{\bar{\alpha}p}, \tag{21-136}$$

where $[ij]_{\mathrm{RI}}$ is a domain of RI basis functions μ associated to pair ij, and $\bar{\alpha}$ are orthogonalized functions that span this domain. Similarly, $[ij]_{\mathrm{MO}}$ is a domain of LMOs p. In large molecules, this leads to linear scaling of the number of integrals to be computed, and at least in principle to linear scaling of the computational cost for LMP2-F12. Currently, we have implemented only the RI domains and always use all occupied orbitals p. This formally leads to quadratic scaling. The remaining terms in Eqs. (21-128) and (21-129) can be approximated in a similar way. The impact of this local RI approximation on relative energies will be demonstrated in Section 21.3.5.

The overhead for using local RI approximations is that *for each pair* the RI basis functions α in the domain $[ij]_{\mathrm{RI}}$ must be orthogonalized and the operators $K^{ij}_{\alpha p}$, $F^{ij}_{\alpha p}$, and $U^{ij}_{\alpha p}$ ($\alpha \in [ij]_{\mathrm{RI}}$) have to be transformed into this basis. Even though this scales linearly with molecular size (provided that distant pairs are neglected), this additional effort pays off only for large molecules, i.e., there is a cross-over point below which making these approximations is more expensive than the standard procedure.

Similar approximations can be used for LCCSD-F12 in the first two summations of Eq. (21-135). Again, the summations over p, q are restricted to MO domains $[ij]_{\mathrm{MO}}$. We found that it is sufficient to include in these domains the LMOs whose domains overlap with the orbital domains $[i]$ or $[j]$; furthermore, it is possible to neglect the contributions of core orbitals. The summation over the virtual orbitals c can be restricted to the pair domain $[ij]$. The corresponding terms can then be written as

$$\sum_{p,c} \langle \tilde{\mu}\tilde{\nu}|r_{12}^{-1}|cp\rangle \bar{F}^{ij}_{cp} \approx \sum_{p\in[ij]_{\mathrm{MO}}} \sum_{\tilde{\rho}\in[ij]} \langle \tilde{\mu}\tilde{\nu}|r_{12}^{-1}|\tilde{\rho}p\rangle \bar{F}^{ij}_{\tilde{\rho}p} \tag{21-137}$$

where $\bar{F}^{ij}_{\tilde{\rho}p} = \sum_{\tilde{a}\in[ij]} W^{(ij)}_{\tilde{\rho}\tilde{a}} \bar{F}^{ij}_{\tilde{a}p}$. If these approximations are made, the number of transformed two-electron integrals $\langle \tilde{\mu}\tilde{\nu}|r_{12}^{-1}|pq\rangle$ and $\langle \tilde{\mu}\tilde{\nu}|r_{12}^{-1}|\tilde{\rho}p\rangle$ and the computational effort will scale linearly with molecular size. These integrals are a subset of those needed in the standard LCCSD method [67], and therefore overall linear scaling of the computational cost should be possible. As will be demonstrated in Section 21.3.5, the errors introduced by these approximations are very small.

21.2.4.4. Local Density Fitting

Density fitting (DF) approximations are widely used nowadays in electronic structure theory. After the method was pioneered by Boys and Shavitt [88] and refined by Whitten [89] it was very successfully used to accelerate the treatment of the Coulomb problem in density functional theory (DFT) [90]. The method has now spread from MP2 [32, 91–95] and CC2 [96] over (local) CCSD(T) [97] to MP2-F12 [19, 27, 28, 31, 98–102]. The overall scaling with respect to system size is not affected by standard DF, but it significantly reduces the prefactor and reduces the scaling with respect to $N_{\mathrm{AO}}/N_{\mathrm{atoms}}$ from quartic to cubic. If integrals other than

Coulomb integrals are computed, it is essential to use robust fitting approximations [31, 103] to ensure integral accuracy.

For the AO integrals like $K^{ij}_{\mu\nu}$ or $F^{ij}_{\mu\nu}$ a local variant of DF can be applied [95, 99]. The summation over the inherently local fitting functions A, B can be restricted to domains $[i]_{\text{fit}}$, very similar to the RI summations discussed in the previous section. The domain $[i]_{\text{fit}}$ consists of those fitting functions within a distance R_{fit} (or a certain number of bonds) from the AOs in the orbital domain $[i]$. The local density-fitted integrals then take the form

$$F^{ij}_{\mu\nu} \approx \sum_{A\in[i]_{\text{fit}}} D^A_{\mu i} F^A_{\nu j} + \sum_{B\in[j]_{\text{fit}}} F^B_{\mu i} D^B_{\nu j} - \sum_{A\in[i]_{\text{fit}}} \sum_{B\in[j]_{\text{fit}}} D^A_{\mu i} F_{AB} D^B_{\nu j}. \quad (21\text{-}138)$$

The fitting coefficients $D^B_{\mu i}$ are obtained by solving the linear equations

$$\sum_{B\in[i]_{\text{fit}}} J_{AB} D^B_{\mu i} = J^A_{\mu i} \qquad (\forall A \in [i]_{\text{fit}}). \quad (21\text{-}139)$$

Similar, but slightly more complicated expressions hold for the commutator integrals $U^{ij}_{\alpha\beta}$ (for details see Refs. [19, 31, 99]). The 2-index and 3-index integrals are defined as

$$J_{AB} = (A|r_{12}^{-1}|B) = \int d\mathbf{r}_1 \int d\mathbf{r}_2 \; \chi_A(\mathbf{r}_1) r_{12}^{-1} \chi_B(\mathbf{r}_2), \quad (21\text{-}140)$$

$$J^A_{\mu\nu} = (A|r_{12}^{-1}|\mu\nu) = \int d\mathbf{r}_1 \int d\mathbf{r}_2 \; \chi_A(\mathbf{r}_1) r_{12}^{-1} \chi_\mu(\mathbf{r}_2) \chi_\nu(\mathbf{r}_2), \quad (21\text{-}141)$$

$$J^A_{\mu i} = (A|r_{12}^{-1}|\mu\nu) C_{\nu i}, \quad (21\text{-}142)$$

where χ_A are the fitting basis functions, and $C_{\mu i}$ are the molecular orbital coefficients. The integrals F_{AB} and $F^A_{\mu i}$ are defined analogously by replacing the integral kernels r_{12}^{-1} by F_{12}.

The overhead of the local fitting is that for each orbital domain $[i]_{\text{fit}}$ the Coulomb submatrix J_{AB}, $A, B \in [i]_{\text{fit}}$ must be inverted (or the corresponding LU-decomposition be performed). Thus, as for local RI approximations, there will be a certain molecular size below which local DF will be more expensive than standard DF.

21.3. BENCHMARKS

In several previous papers [28, 29, 52–54, 56] we have presented benchmarks for atomization energies, reaction energies, ionization potentials, electron affinities, equilibrium distances, vibrational frequencies, and intermolecular interaction energies. All these calculations were performed with the augmented correlation consistent orbital basis sets (aug-cc-pVnZ) of Kendall et al. [104]. For the second long row atoms,

we used the aug-cc-pV($n+d$)Z basis sets of Dunning et al. [105]. For simplicity, the aug-cc-pVnZ and aug-cc-pV($n+d$)Z basis sets will in the following be denoted AVnZ. As RI basis, we used the VnZ/JKFIT basis sets of Weigend [106], which turned out to work well for this purpose.

Recently, Peterson et al. optimized new AO basis sets [33] that are specifically designed for F12 calculations. These are denoted VnZ-F12. Furthermore, new auxiliary (RI) basis sets for the VnZ-F12 as well as for the aug-cc-pVnZ orbital basis were presented [34, 35]. Here we will repeat the benchmarks presented in Ref. [52] using these new basis sets and compare the performance of the VnZ-F12 sets with the aug-cc-pVnZ ones. For the latter, we will also compare the JKFIT sets with the new OPTRI auxiliary basis sets which were very recently published [35].

The new OPTRI basis sets [34, 35] are slightly smaller than the JKFIT bases and are specially constructed for the CABS approach (they cannot be used without CABS unless they are augmented by the orbital basis). In particular, they contain fewer s and p functions, but instead contain higher angular momentum functions than in the JKFIT basis sets. Their main advantage is that they minimize the linear dependencies between the AO and the RI basis sets, which leads to improved numerical stability. For the density fitting, which is used to compute all integrals in the MP2-F12 part, the MP2FIT basis sets of Weigend et al. [107] are used. These were also employed in the previous calculations.

Peterson et al. recommended to use for the length scale parameter γ in the F12 function values of 0.9, 1.0, and 1.1 a_0^{-1} for the VDZ-F12, VTZ-F12, and VQZ-F12 basis sets, respectively. For the sake of simplicity, we chose $\gamma = 1.0a_0^{-1}$ for all basis sets; this value was also used in all previous benchmarks. It is possible that slightly better results could be obtained with the recommended values for the VDZ-F12 and VQZ-F12 basis sets, but the dependence on the value of this parameter is rather weak.

The molecular systems used in the next three subsections were the same as in Ref. [52]. For atomization energies, electron affinities, and ionization potentials the original G2 set [108] was used, with the exception that molecules containing alkali and alkali-earth elements were omitted, because no JKFIT basis sets were available. For the benchmarks of reaction energies, a total of 104 reactions were studied, among which 54 involved only closed-shell molecules and the remaining 50 also open-shell molecules. A list of these reactions and molecules can be found in Ref. [52]. Except for the choice of the basis sets, only default parameters as implemented in the current generally available production version of MOLPRO (version 2009.1) were used. Thus, such calculations can be performed in a black-box manner.

The error statistics presented in the following sections refer to the same reference values as in [52]. Wherever possible, these were obtained by extrapolating the correlation energies of the AV5Z and AV6Z sets to the complete basis set limit (CBS[56]). For some of the larger molecules, only the AVQZ and AV5Z results could be used for the extrapolation (CBS [45]). The Hartree-Fock energies were not extrapolated, and the values from the largest employed basis set were used directly. In the tables we will present mean absolute deviations (MAD), root means square deviations (RMS),

and the absolute maximum errors (MAX). All energy differences are computed from the total energies, including the Hartree-Fock contribution with the CABS singles correction.

21.3.1. Benchmarks for the CABS Singles Correction

In Table 21-2 the improvement of the Hartree–Fock energy differences by using the CABS singles correction is demonstrated. It is of interest to check how the new OPTRI basis sets perform in this respect, because they contain fewer *s* and *p* functions than the JKFIT basis sets. In particular, functions with larger exponents are missing. As a result, the absolute values for the perturbative corrections are much smaller than for the JKFIT basis sets. Nevertheless, as seen in Table 21-2, the performance for energy differences is very good. The comparisons also show that for all properties the V*n*Z-F12/OPTRI basis-set combination is slightly more accurate than either AV*n*Z/JKFIT or AV*n*Z/OPTRI. The last two combinations are almost equally accurate. The better performance of the V*n*Z-F12 basis sets is probably due to the fact that for these the total energy was optimized, including the Hartree-Fock and correlation energies. Furthermore, the V*n*Z-F12 orbital basis sets are slightly larger than the AV*n*Z sets (except for hydrogen).

21.3.2. Benchmarks with RMP2-F12

Table 21-3 shows a comparison of standard RMP2 and RMP2-F12 results. The fixed amplitude ansatz has been used. It should be noted that these results cannot be compared directly with those in [29], since the wave function ansatz has been changed: in our original work on RMP2-F12, the summation over k, l in Eq. (21-1) included only the spin orbitals that are occupied in the RHF wave function. In our current methods, the summation includes both spin orbitals that can be formed from any occupied spatial orbital. It was found that this significantly improves the accuracy [52]. Furthermore, it is more consistent if the fixed amplitude ansatz is used [109]. Table 21-3 demonstrates for RMP2-F12 the dramatic improvements by the F12 treatment. For all properties, the double-zeta F12 results are better than the standard quadruple zeta ones.

Again, the performance of the V*n*Z-F12 and AV*n*Z sets is comparable, except for the electron affinities. For the latter, the V*n*Z-F12 are not diffuse enough and yield much larger errors. There is no significant difference in the performance of the JKFIT and OPTRI auxiliary basis sets.

21.3.3. Benchmarks with CCSD(T)-F12x

Table 21-4 shows the results for the RCCSD(T*)-F12a and RCCSD(T*)-F12b methods. Again the accuracy is excellent, even though the errors are somewhat larger than in the RMP2-F12 case. This is mainly due to the fact that the basis set error

Table 21-2. Error statistics for the Hartree–Fock contribution to various properties with and without the CABS singles contribution

		Hartree–Fock			HF+singles		
Orbital basis	RI basis	MAD	RMS	MAX	MAD	RMS	MAX
Ionization potentials (meV)							
AVDZ	JKFIT	45.9	65.1	220.4	7.9	9.9	20.7
AVTZ	JKFIT	8.2	11.1	28.5	2.1	2.8	7.7
AVQZ	JKFIT	1.6	2.3	7.7	0.8	1.0	2.2
AVDZ	OPTRI	45.9	65.1	220.4	9.4	11.6	21.6
AVTZ	OPTRI	8.2	11.1	28.5	2.7	3.4	7.3
AVQZ	OPTRI	1.6	2.3	7.7	1.0	1.2	2.2
VDZ-F12	OPTRI	21.8	33.4	113.8	4.5	5.4	11.3
VTZ-F12	OPTRI	2.2	3.7	14.9	1.2	1.4	2.7
VQZ-F12	OPTRI	0.4	0.5	2.2	0.2	0.3	0.5
Electron affinities (meV)							
AVDZ	JKFIT	42.2	76.2	325.5	6.3	11.1	48.4
AVTZ	JKFIT	8.1	11.8	35.1	2.4	3.2	8.8
AVQZ	JKFIT	2.4	3.6	12.8	1.4	1.9	5.4
AVDZ	OPTRI	42.2	76.2	325.5	6.7	10.5	42.4
AVTZ	OPTRI	8.1	11.8	35.1	2.4	3.2	6.7
AVQZ	OPTRI	2.4	3.6	12.8	1.2	1.6	3.7
VDZ-F12	OPTRI	26.6	51.7	233.4	5.4	8.5	31.3
VTZ-F12	OPTRI	3.5	5.4	21.2	2.2	2.7	5.5
VQZ-F12	OPTRI	1.4	2.0	5.4	1.2	1.7	4.8
Atomization energies (kJ/mol)							
AVDZ	JKFIT	20.66	24.39	84.60	1.58	1.98	5.33
AVTZ	JKFIT	2.90	3.47	11.37	0.23	0.30	1.10
AVQZ	JKFIT	0.58	0.82	3.91	0.10	0.13	0.46
AVDZ	OPTRI	20.66	24.39	84.60	2.47	3.17	8.56
AVTZ	OPTRI	2.90	3.47	11.37	0.36	0.50	1.58
AVQZ	OPTRI	0.58	0.82	3.91	0.11	0.14	0.30
VDZ-F12	OPTRI	9.95	12.17	45.68	1.30	1.53	4.63
VTZ-F12	OPTRI	1.61	1.90	6.75	0.19	0.23	0.52
VQZ-F12	OPTRI	0.22	0.25	0.78	0.04	0.06	0.32
Reaction energies (kJ/mol)							
AVDZ	JKFIT	12.14	21.01	144.08	1.85	2.60	11.49
AVTZ	JKFIT	1.84	2.91	17.27	0.40	0.52	2.02
AVQZ	JKFIT	0.45	1.03	6.72	0.13	0.18	0.67
AVDZ	OPTRI	12.14	21.01	144.08	1.54	2.77	16.11
AVTZ	OPTRI	1.84	2.91	17.27	0.28	0.49	2.83
AVQZ	OPTRI	0.45	1.03	6.72	0.14	0.21	0.85
VDZ-F12	OPTRI	7.35	12.38	68.45	1.01	1.76	9.13
VTZ-F12	OPTRI	1.00	1.63	9.52	0.17	0.30	1.58
VQZ-F12	OPTRI	0.15	0.21	0.98	0.07	0.12	0.66

Table 21-3. Error statistics using RMP2-F12 for various properties. The fixed amplitude ansatz was used

		RMP2			RMP2-F12		
Orbital basis	RI basis	MAD	RMS	MAX	MAD	RMS	MAX
Ionization potentials (meV)							
AVDZ	JKFIT	251.0	266.8	453.0	32.2	34.8	66.7
AVTZ	JKFIT	113.2	122.7	207.6	5.3	6.1	12.4
AVQZ	JKFIT	56.0	61.2	109.1	1.5	1.8	5.2
AVDZ	OPTRI	251.0	266.8	453.0	33.0	35.7	64.1
AVTZ	OPTRI	113.2	122.7	207.6	5.9	6.7	15.8
AVQZ	OPTRI	56.0	61.2	109.1	1.3	1.6	3.8
VDZ-F12	OPTRI	234.8	252.3	484.3	30.3	34.4	78.9
VTZ-F12	OPTRI	111.1	120.8	205.2	5.6	6.3	14.8
VQZ-F12	OPTRI	55.9	61.3	105.4	1.1	1.4	3.4
Electron affinities (meV)							
AVDZ	JKFIT	209.8	223.7	375.4	43.0	45.9	81.6
AVTZ	JKFIT	94.2	104.8	160.4	10.8	13.0	28.2
AVQZ	JKFIT	47.3	52.6	79.8	3.2	5.5	15.8
AVDZ	OPTRI	209.8	223.7	375.4	42.2	45.9	83.6
AVTZ	OPTRI	94.2	104.8	160.4	9.6	12.2	29.2
AVQZ	OPTRI	47.3	52.6	79.8	3.3	5.4	15.6
VDZ-F12	OPTRI	237.8	251.2	430.6	67.9	72.6	138.9
VTZ-F12	OPTRI	117.9	127.8	201.0	30.2	32.3	56.5
VQZ-F12	OPTRI	61.4	66.8	106.1	14.4	15.9	27.4
Atomization energies (kJ/mol)							
AVDZ	JKFIT	79.43	87.70	166.86	3.13	3.78	9.99
AVTZ	JKFIT	26.87	29.60	56.33	0.57	0.77	2.32
AVQZ	JKFIT	10.94	12.14	23.84	0.58	0.71	1.79
AVDZ	OPTRI	79.43	87.70	166.86	3.82	4.68	11.49
AVTZ	OPTRI	26.87	29.60	56.33	0.44	0.58	1.52
AVQZ	OPTRI	10.94	12.14	23.84	0.54	0.66	1.63
VDZ-F12	OPTRI	60.66	66.37	130.01	2.44	3.09	7.97
VTZ-F12	OPTRI	27.03	29.68	61.29	0.45	0.59	1.69
VQZ-F12	OPTRI	12.73	14.02	29.07	0.21	0.27	0.84
Reaction energies (kJ/mol)							
AVDZ	JKFIT	25.60	39.60	194.10	2.48	3.30	14.75
AVTZ	JKFIT	9.88	14.27	54.03	0.91	1.29	5.93
AVQZ	JKFIT	4.86	6.66	23.91	0.49	0.69	2.93
AVDZ	OPTRI	25.60	39.60	194.10	2.10	3.31	18.96
AVTZ	OPTRI	9.88	14.27	54.03	0.59	0.80	2.89
AVQZ	OPTRI	4.86	6.66	23.91	0.52	0.72	2.09
VDZ-F12	OPTRI	23.38	32.53	113.79	1.80	2.98	16.75
VTZ-F12	OPTRI	9.44	13.22	44.14	0.44	0.65	2.79
VQZ-F12	OPTRI	5.15	6.68	19.86	0.34	0.53	2.17

Table 21-4. Error statistics using RCCSD(T*)-F12x for various properties. The fixed amplitude ansatz was used. The triples energies were scaled using Eq. (21-115)

		CCSD(T)-F12a			CCSD(T)-F12b		
Orbital basis	RI basis	MAD	RMS	MAX	MAD	RMS	MAX
Ionization potentials (meV)							
AVDZ	JKFIT	66.0	74.8	170.8	87.8	96.1	204.1
AVTZ	JKFIT	9.6	13.3	33.4	26.3	30.3	59.8
AVQZ	JKFIT	4.6	5.0	8.9	7.4	8.9	18.0
AVDZ	OPTRI	67.6	75.3	168.4	89.4	96.6	201.7
AVTZ	OPTRI	10.1	13.4	33.9	27.0	30.5	60.3
AVQZ	OPTRI	4.5	4.9	8.8	7.5	8.7	17.6
VDZ-F12	OPTRI	63.3	75.6	176.3	84.1	94.5	208.6
VTZ-F12	OPTRI	9.1	12.3	30.3	24.1	27.7	55.1
VQZ-F12	OPTRI	4.8	5.4	11.7	7.2	8.0	15.0
Electron affinities (meV)							
AVDZ	JKFIT	61.5	67.8	137.2	88.7	94.7	170.4
AVTZ	JKFIT	10.3	12.5	29.4	28.1	31.1	49.5
AVQZ	JKFIT	5.7	6.6	12.5	9.3	11.2	25.5
AVDZ	OPTRI	60.6	66.8	139.4	87.8	94.0	172.6
AVTZ	OPTRI	9.5	11.7	27.1	26.9	29.9	50.3
AVQZ	OPTRI	6.1	7.2	14.1	8.8	10.7	25.5
VDZ-F12	OPTRI	98.3	105.5	203.8	121.1	127.2	232.2
VTZ-F12	OPTRI	32.9	35.7	58.1	50.0	52.8	83.8
VQZ-F12	OPTRI	12.4	13.8	25.9	24.2	25.8	41.8
Atomization energies (kJ/mol)							
AVDZ	JKFIT	7.88	9.42	18.68	12.67	14.76	31.22
AVTZ	JKFIT	0.96	1.33	4.01	3.57	3.97	8.96
AVQZ	JKFIT	1.13	1.36	3.49	0.70	0.97	3.57
AVDZ	OPTRI	9.69	11.76	24.99	14.76	17.20	36.98
AVTZ	OPTRI	1.14	1.54	3.77	3.96	4.39	8.59
AVQZ	OPTRI	1.11	1.33	3.43	0.72	0.95	3.41
VDZ-F12	OPTRI	6.26	7.42	15.41	10.45	11.90	26.56
VTZ-F12	OPTRI	1.10	1.42	3.77	3.91	4.28	8.31
VQZ-F12	OPTRI	1.07	1.28	3.10	1.29	1.42	3.01
Reaction energies (kJ/mol)							
AVDZ	JKFIT	2.43	3.48	16.45	2.78	3.86	17.53
AVTZ	JKFIT	0.97	1.25	3.06	1.37	1.85	5.59
AVQZ	JKFIT	0.73	0.99	2.81	0.70	0.93	3.14
AVDZ	OPTRI	3.44	4.78	21.33	3.96	5.67	22.41
AVTZ	OPTRI	0.89	1.21	3.80	1.37	1.98	6.64
AVQZ	OPTRI	0.78	1.06	3.35	0.70	0.96	3.16
VDZ-F12	OPTRI	3.05	4.25	16.96	3.62	5.10	19.18
VTZ-F12	OPTRI	1.02	1.40	5.30	1.55	2.19	7.75
VQZ-F12	OPTRI	0.47	0.70	2.80	0.48	0.75	3.53

of the triples contribution is not removed by the F12 treatment. For the CCSD(T)-F12b method, significant improvements of all results are achieved by scaling the triples contribution, as explained in Section 21.2.2.3. For CCSD(T)-F12a, which somewhat overestimates the correlation energy, the improvements by the scaling are less systematic, since there is an error compensation between the overshooting of the CCSD-F12a correlation energy and the underestimation of the triples energy. Overall, for the double and triple zeta basis sets the F12a method yields more accurate results, due to the above-mentioned error compensation. For larger basis sets the F12b approximation is preferable, since it converges more smoothly to the basis set limit.

The RMS errors of the reaction energies obtained with the double-zeta basis sets (relative to the basis set limit) amount to about 1 kcal/mol, which corresponds to chemical accuracy. The errors obtained with the triple-zeta basis sets are smaller than 1.5 kJ/mol (CCSD(T*)-F12a). This corresponds to the intrinsic accuracy of CCSD(T) if only valence electrons are correlated. To obtain higher accuracy, higher excitations, core correlation effects, and relativistic effects should be taken into account.

Table 21-5 shows computed CCSD(T)-F12a and CCSD(T)-F12b equilibrium distances and harmonic vibrational frequencies for the same 13 diatomic molecules studied in Ref. [52]. The accuracy is outstanding, in particular for CCSD(T)-F12b. Already with the VDZ-F12 basis set the RMS error of the vibrational frequencies is less than 3 cm^{-1}. This is about the same accuracy as achieved with CCSD(T) and the AV5Z basis set [52]. Also the RMS error for the equilibrium distances obtained with CCSD(T)-F12b/VDZ-F12 is smaller than the one for CCSD(T)/AVQZ. Somewhat surprisingly, CCSD(T)-F12b yields for these properties with all basis sets more accurate results than CCSD(T)-F12a. Furthermore, in contrast to most other properties, the scaling of the triples energy does not improve the frequencies and distances. The reason for this behavior is not yet understood in detail.

Table 21-5. Error statistics using CCSD(T)-F12x harmonic vibrational frequencies and equilibrium distances for 13 diatomic molecules

	CCSD(T)-F12a			CCSD(T)-F12b		
Orbital basis	MAD	RMS	MAX	MAD	RMS	MAX
Harmonic vibrational frequencies (cm^{-1})						
VDZ-F12	5.1	5.6	8.5	2.2	2.9	5.7
VTZ-F12	3.1	3.4	6.3	1.7	2.1	4.9
VQZ-F12	0.8	1.1	2.1	0.6	0.7	1.3
Equilibrium distances (pm)						
VDZ-F12	0.14	0.17	0.40	0.09	0.11	0.27
VTZ-F12	0.07	0.09	0.23	0.05	0.07	0.18
VQZ-F12	0.02	0.02	0.06	0.01	0.01	0.04

The RMS deviations of the CCSD(T)/CBS values from the experimental equilibrium distances and harmonic frequencies amount to 0.17 pm and 10.3 cm^{-1}, respectively. Thus, already for the VDZ-F12 basis set, the basis set incompleteness errors are smaller than the intrinsic errors of the CCSD(T) method. As for the reaction energies, it would be necessary to include higher excitations, core correlation, and relativistic effects to obtain higher accuracy.

Similar accuracy was also achieved in Ref. [54] for nine polyatomic molecules with up to 6 atoms. Due to the efficiency of the CCSD(T)-F12x methods, it was possible to generate many-dimensional potential energy surfaces around the equilibrium geometries and to compute anharmonic frequencies using vibrational configuration interaction methods. Using CCSD(T)-F12a/AVTZ, the mean absolute deviation of all computed frequencies from experimental values was only 4 cm^{-1}.

21.3.4. Intermolecular Interaction Energies

Intermolecular interaction energies are of much current interest due to their importance in many biological systems. For example, hydrogen bonding and π-stacking interactions between nucleic acid base pairs are crucial for the folding of nucleic acids such as DNA and RNA. A particular challenge is the accurate prediction of dispersion energies, which dominate π-stacking interactions. The calculation of dispersion interactions is difficult because they are pure electron correlation effects, which cannot be described by simple methods such as Hartree–Fock or standard density functional theory.

We have applied the explicitly correlated MP2-F12 and CCSD(T)-F12a methods to calculate intermolecular interaction energies for the S22 benchmark set of Jurečka et al. [110]. This includes clusters which are either hydrogen (electrostatic) bonded or predominantly dispersion bonded, as well as mixed ones. The interaction energies range from less than 1 kcal/mol to over 20 kcal/mol. In some clusters with strong dispersion interactions, the correlation contribution to the interaction energy is larger than the total interaction energy and may exceed 25 kcal/mol.

In all calculations, the counterpoise correction [111] was applied to reduce basis set superposition errors (BSSE). For high accuracy, this is even needed in explicitly correlated calculations, since the BSSE of the Hartree–Fock contribution may still be significant (even with the CABS singles correction, which is always applied). The BSSE of the correlation contributions are much smaller than in conventional MP2 or CCSD(T) calculations, but still not entirely negligible.

The deviations of the MP2 and DF-MP2 interaction energies from MP2/ CBS[45] reference values are shown in Figure 21-1 (from Ref. [53]). In the standard MP2 calculations the diffuse functions on the hydrogen atoms were omitted. This reduces the BSSE and has little effect on the results. The resulting mixed basis sets are denoted AVnZ′. In the MP2-F12 calculations the diagonal approximation was used. Figure 21-1 shows that the conventional MP2 results converge very slowly with increasing basis set size. In contrast, the MP2-F12 method yields amazingly accurate

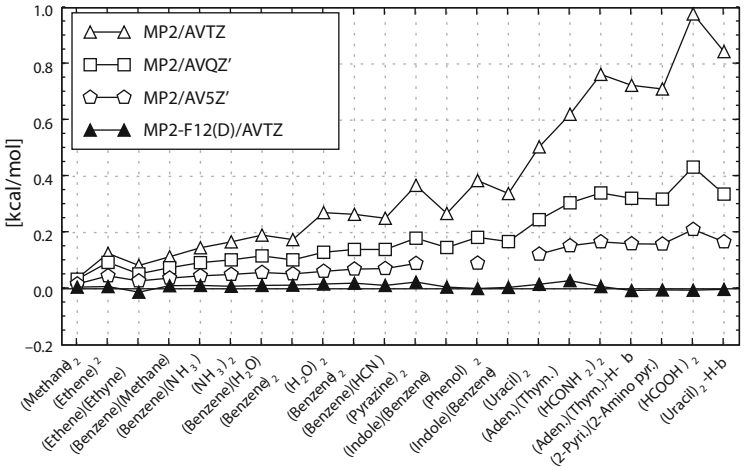

Figure 21-1. Errors of the total MP2/AV*n*Z′ and MP2-F12/AVTZ interaction energies for the S22 set relative to the MP2/CBS [45] estimates of the basis set limits

results already with small basis sets. Using the triple zeta basis set, the MP2-F12 interaction energies are much more accurate than the MP2/AV5Z′ results.

Figure 21-2 shows a similar comparison for CCSD(T*)-F12a [56]. In this case the CCSD(T) reference calculations were only possible for a reduced set of 11 dimers. The results are similar to MP2-F12: Using the AVTZ basis, CCSD(T*)-F12a yields

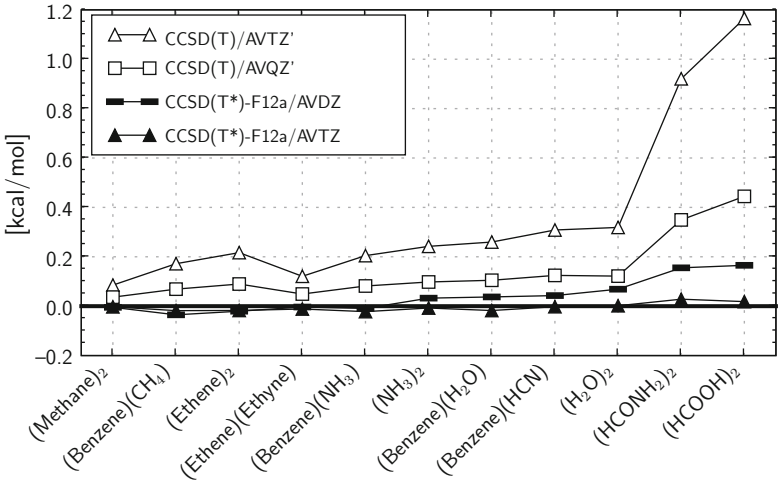

Figure 21-2. Errors of CCSD(T) and CCSD(T*)-F12 interaction energies relative to CCSD(T)/CBS [34] results for different basis sets

highly accurate results. Even with the AVDZ basis set the errors are smaller than 0.2 kcal/mol for all dimers.

21.3.5. Benchmarks with LMP2-F12 and LCCSD-F12

In this section we will summarize and extend our results from Refs. [71], [72]. In all cases, the domains were determined using the method of Boughton and Pulay [86], using a completeness criterion of 0.985 (triple zeta basis sets) or 0.98 (double zeta basis sets). Unless otherwise noted, in all F12 calculations the diagonal ansatz with approximation 3*A has been used, and the VTZ/JKFIT basis sets were employed for the RI.

Table 21-6 shows the computed correlation energies for selected large molecules (cf. Ref. [71]). The F12 energy contributions as well as the total correlation energies are compared. It can be seen that the F12 energy contributions in the MP2-F12 and LMP2-F12 calculations differ by about 100 mHartree. This is due to the fact that in the LMP2-F12 method this contribution corrects for the domain errors in the LMP2 wave function. However, the total correlation energies differ in all cases by less than 10 mHartree. This shows that the explicitly correlated terms remove the domain errors very efficiently. Table 21-7 demonstrates for a reaction involving large

Table 21-6. Comparison of MP2-F12 and LMP2-F12 correlation energies ($-E_{\mathrm{corr}}$ in mHartree) for selected large molecules. The AVTZ orbital basis was used and all pairs apart from very distant pairs were treated in F12. No local DF or local RI approximations were employed

	MP2-F12		LMP2-F12	
Molecule	F12	Total	F12	Total
Progesterone ($C_{21}H_{30}O_2$)	397.7	4466.9	477.9	4460.5
Cholesterol ($C_{27}H_{46}O$)	470.6	5457.1	576.3	5448.7
Borrelidin ($C_{28}H_{43}NO_6$)	654.0	7100.4	763.1	7091.8

Table 21-7. The effects of pair approximations and of local RI, DF approximations on the correlation contributions ΔE_{corr} (in kJ/mol) to the DF-LMP2-F12/AVTZ′ reaction energy of the androstenedione ring closure reaction shown in Figure 21-3

Pairs	Full RI and DF	Local RI and DF
Strong (no bond)	19.56	19.58
Close (up to 1 bond)	22.01	22.05
Weak (up to 3 bonds)	23.07	23.14
Weak (up to 4 bonds)	23.98	24.07
Weak (up to 5 bonds)	24.21	24.31
All	24.32	24.37

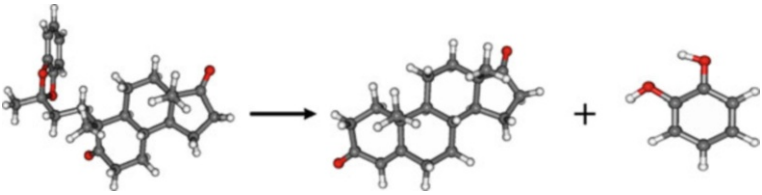

Figure 21-3. A ring closure reaction yielding androstenedione

molecules how the correlation contribution to the reaction energy depends on the pair approximation in the explicitly correlated part (i.e., the list P_c in Eq. (21-125) has been varied). The pairs *ij* are classified according to the minimum number of bonds between any atom in the orbital domain [*i*] and any atom in domain [*j*]. In strong pairs the two orbital domains share at least one atom; close pairs are those were the shortest distance is one bond, and so on. The number of pairs included in the conventional LMP2 part is always the same (only very distant pairs are neglected). Somewhat surprisingly, the F12 correlation contributions converge rather slowly with extension of the pair list. If only strong pairs are included, an error of about 5 kJ/mol results. If close pairs are also explicitly correlated, the error is reduced to 2.3 kJ/mol (0.55 kcal/mol). For many applications involving large molecules this may be sufficient. Further reductions of the error are possible by including weak pairs. Table 21-7 also demonstrates that the effect of local DF and local RI approximations on the reaction energy is negligible. These approximations lead to almost linear scaling of the overall computational cost with molecular size. For details and timings we refer to Ref. [71].

Table 21-8 presents a comparison of CCSD and LCCSD correlation energies with and without explicit correlation [72]. All pairs are fully included in the LCCSD and LCCSD-F12 calculations, i.e., the difference between the local and non-local results solely reflects the domain error. The conventional CCSD and LCCSD energies differ by several mHartree, but this error is reduced to about 0.1 mHartree in the explicitly correlated methods. This demonstrates that the domain error is also efficiently removed in LCCSD-F12. As compared to the estimated complete basis set limits,

Table 21-8. LCCSD-F12a correlation energies ($-E_{\mathrm{corr}}$ in mHartree) obtained with the VTZ-F12 basis set in comparison to the extrapolated CCSD/CBS[45] values. The fixed amplitude Ansatz was used

Molecule	CCSD	LCCSD	CCSD-F12	LCCSD-F12	CBS
C_2H_4O	611.8	609.2	658.0	658.1	650.4
CH_3CHO	606.1	603.8	651.6	651.7	643.9
C_2H_5OH	648.2	644.3	697.3	697.3	689.1
NH_2CONH_2	851.9	847.6	918.0	917.9	908.2
$HCOOCH_3$	844.7	841.1	911.7	911.7	901.7

Table 21-9. Error statistics for reaction energies (in kJ/mol) computed using the LMP2-F12 and LCCSD-F12 methods. The fixed amplitude ansatz with approximation 3*A and the V*n*Z/OPTRI auxiliary basis sets were used in the F12 calculations

	VDZ-F12			VTZ-F12		
Method	MAD	RMS	MAX	MAD	RMS	MAX
MP2	10.1	10.8	68.9	4.3	4.7	31.9
LMP2	14.5	13.8	78.3	6.1	5.9	35.1
MP2-F12	1.2	1.1	6.6	0.5	0.5	2.8
LMP2-F12	1.3	1.2	6.5	0.6	0.7	3.3
CCSD	10.5	10.0	57.5	4.6	4.4	27.8
LCCSD	14.3	13.6	66.5	6.1	5.4	30.2
CCSD-F12	1.8	1.5	6.2	0.7	0.6	2.6
LCCSD-F12	1.8	1.5	6.1	0.7	0.6	2.4

the CCSD-F12 and LCCSD-F12 correlation energies are somewhat too large. This is mainly due to the 3*A approximation used in these calculations. Previous studies have shown that this has little effect on computed energy differences. This is confirmed by the results presented below.

Finally, in Table 21-9 we present the error statistics for the 54 closed-shell reactions, computed with various local and non-local methods. The fixed amplitude ansatz with approximation 3*A has been used in all these explicitly correlated calculations, while the results in Tables 21-3 and 21-4 were obtained with the theoretically more accurate approximation 3C. Nevertheless, the errors of the 3*A results are equally small. The local and non-local variants yield virtually the same accuracy, both for MP2-F12 and CCSD-F12x, i.e., the domain errors are almost fully removed. This is a very promising result for future applications of the LCCSD(T)-F12x methods for large molecules. The implementation of a fully local linear scaling LCCSD(T)-F12x implementation is currently in progress.

21.4. CONCLUSIONS

In this paper we have presented in detail the theory of the exact MP2-F12 and CCSD-F12 methods and discussed the CCSD(T)-F12x approximations as implemented in the MOLPRO package of ab initio programs. In these approximations the MP2-F12 part is treated without any approximations (apart from the RI). In the additional terms occurring in the CCSD-F12 amplitude equations and in the energy functional, all contributions arising from the complementary auxiliary orbital basis are neglected. Thus, apart from the initial MP2-F12, the computational effort is very similar as for a standard CCSD(T) calculation with the same basis set. While the additional effort for

MP2-F12 relative to MP2 is still significant (typically a factor of 10), the additional effort becomes negligible for CCSD(T)-F12x calculations on larger molecules. This is because the cost of the MP2-F12 calculation becomes small relative to the triples calculation, which scales much more steeply with molecular size. Overall, for the largest systems presented in this work, the CCSD(T)-F12x calculations are only a few percent more expensive than standard CCSD(T) calculations with the same basis. Of course, such comparisons depend on the efficiency of the CCSD(T) itself. In this respect we may note that our CCSD(T) program is considered to be one of the fastest currently available. This is due to the consequent formulation of the theory in terms of matrix multiplications, which run near the theoretical maximum speed of modern processors. For example, the complete CCSD(T)-F12/AVTZ calculation for the T-structure of the benzene dimer (including counterpoise correction) took 118 h on a single Xeon 3.0 GHZ processor (MacPro). Of this time, 5.9 h was spent for the MP2-F12 parts, i.e., the additional effort for the F12 correction is only 5% of the corresponding CCSD(T)/AVTZ calculation [53].

Extensive benchmark results for atomization energies, reaction energies, ionization potentials, electron affinities, intermolecular interaction energies, harmonic vibrational frequencies, and equilibrium structures have demonstrated the outstanding accuracy of the new F12 methods. New AO V*n*Z-F12 orbital basis sets, that were especially optimized for F12 methods, were compared to the standard augmented correlation consistent basis sets of Dunning and co-workers. Furthermore, new RI basis sets of Yousaf and Peterson [34, 35] were tested. For most properties the results obtained with the V*n*Z-F12 and aug-cc-pV*n*Z basis sets are of the same quality, and also the choice of the RI basis has a rather small effect. This is consistent with a very recent study of Bischoff et al. [112]. Only for electron affinities the more diffuse aug-cc-pV*n*Z basis sets are preferable. Whatever basis set is used and property is considered, the explicitly correlated results are uniformly much more accurate than those obtained with the conventional MP2 and CCSD(T) methods and the same basis set. Typically, the F12 results obtained with the AV*n*Z basis are equally or more accurate as conventional calculations with the AV($n + 2$)Z basis.

Local variants of the MP2-F12 and CCSD-F12 methods have also been reviewed. These are very promising to extend the applicability of the CCSD(T)-F12 method to larger molecules. It has been demonstrated that the error caused by the domain approximation is almost entirely removed by the explicitly correlated terms. Preliminary investigations for LMP2-F12 have shown how the F12 energy correction depends on pair approximations. Future work is necessary to determine what is the best choice of pair approximations in LCCSD(T)-F12 calculations in order to obtain a best compromise between cost and accuracy.

All the (non-local) calculations presented in this paper were performed with default values as implemented in the public version 2009.1 of the MOLPRO quantum chemistry package [73] and require no special input. Thus, they can be performed in a black box manner, similar to standard MP2 and CCSD(T) calculations. In conclusion, these methods are ready for public use and are highly recommended for future applications.

ACKNOWLEDGMENTS

This work was funded in the priority program 1145 of the Deutsche Forschungsgemeinschaft. Further support by the Fonds der Chemischen Industrie is gratefully acknowledged. T.B.A. would also like to thank the Studienstiftung des deutschen Volkes.

APPENDIX: THE CCSD EQUATIONS IN EXPANDED FORM

The CCSD residuals take the explicit form

$$R_{ab}^{ij} = K_{ab}^{ij} + [\mathbf{K}(\mathbf{D}^{ij})]_{ab} + \sum_{k,l} \alpha_{ij,kl} D_{ab}^{kl} + G_{ab}^{ij} + G_{ba}^{ji}, \tag{21-143}$$

$$\mathbf{G}^{ij} = \mathbf{T}^{ij}\mathbf{X} - \sum_k \mathbf{T}^{ik}\beta_{kj} - \sum_k [\mathbf{K}(\mathbf{D}^{ij})^{(k)} + \mathbf{k}^{ijk}]\mathbf{t}^{k\dagger} + \sum_k \left[\tilde{\mathbf{T}}^{ik}\mathbf{Y}^{kj} - \frac{1}{2}\mathbf{T}^{ki}\mathbf{Z}^{kj} - (\mathbf{T}^{ki}\mathbf{Z}^{kj})^{\dagger}\right], \tag{21-144}$$

$$\mathbf{r}^{i} = \mathbf{f}^{i} + [\mathbf{R}^{\dagger} - \sum_k (2\mathbf{J}^{kk} - \mathbf{K}^{kk})]\mathbf{t}^{i} - \sum_{k,l} \mathbf{T}^{lk}\mathbf{l}^{kli} + \sum_k \left[\mathbf{K}(\tilde{\mathbf{D}}^{ik})^{(k)} + \tilde{\mathbf{T}}^{ik}\bar{\mathbf{f}}^{k} - \mathbf{t}^{k}\beta_{ki}\right], \tag{21-145}$$

with the intermediates:

$$\alpha_{ij,kl} = K_{kl}^{ij} + \mathrm{tr}(\mathbf{C}^{ij}\mathbf{K}^{lk}) + (\mathbf{t}^{i\dagger}\mathbf{k}^{klj} + \mathbf{t}^{j\dagger}\mathbf{k}^{lki}), \tag{21-146}$$

$$\beta_{ki} = f_{ki} + \mathbf{f}^{k\dagger}\mathbf{t}^{i} + \sum_l \left[\mathrm{tr}(\mathbf{L}^{kl}\mathbf{T}^{li}) + \mathbf{t}^{l\dagger}(\mathbf{l}^{lki} + \mathbf{L}^{lk}\mathbf{t}^{i})\right], \tag{21-147}$$

$$\bar{\mathbf{f}}^{k} = \mathbf{f}^{k} + \sum_l \mathbf{L}^{kl}\mathbf{t}^{l}, \tag{21-148}$$

$$\mathbf{R} = \mathbf{f} - \sum_{k,l} \mathbf{L}^{kl}\mathbf{T}^{lk}, \tag{21-149}$$

$$\mathbf{X} = \mathbf{R} - \sum_k \bar{\mathbf{f}}^{k}\mathbf{t}^{k\dagger} + \sum_k [2\mathbf{J}(\mathbf{E}^{kk}) - \mathbf{K}(\mathbf{E}^{kk})], \tag{21-150}$$

$$\mathbf{Y}^{kj} = \mathbf{K}^{kj} + \mathbf{K}(\mathbf{E}^{kj}) - \frac{1}{2}\left[\mathbf{J}^{kj} + \mathbf{J}(\mathbf{E}^{kj})\right] + \frac{1}{4}\sum_l \mathbf{L}^{kl}\tilde{\mathbf{T}}^{lj} - \frac{1}{2}\sum_l (\mathbf{l}^{klj} + \mathbf{L}^{kl}\mathbf{t}^j)\mathbf{t}^{l\dagger}, \tag{21-151}$$

$$\mathbf{Z}^{kj} = \mathbf{J}^{kj} + \mathbf{J}(\mathbf{E}^{kj}) - \sum_l \left[\frac{1}{2}\mathbf{K}^{lk}\mathbf{T}^{jl} + (\mathbf{k}^{lkj} + \mathbf{K}^{lk}\mathbf{t}^j)\mathbf{t}^{l\dagger}\right]. \tag{21-152}$$

GLOSSARY

$A_{kl,mn} = \langle kl\|F_{12}\hat{g}_{12}\hat{Q}_{12}F_{12}\|mn\rangle$	Part of MP2-F12 B-matrix
$B_{kl,mn} = \langle kl\|F_{12}\hat{Q}_{12}\hat{g}_{12}\hat{Q}_{12}F_{12}\|mn\rangle$	MP2-F12 B-matrix
$C_{\mu i}$	MO coefficients
$C_{ab}^{kl} = \langle kl\|F_{12}\hat{Q}_{12}\hat{f}_{12}\|ab\rangle$	MP2-F12 coupling terms
$D_{rs}^{ij} = \delta_{rc}\delta_{sd}\left(T_{cd}^{ij} + t_c^i t_d^j\right) + \delta_{ri}t_s^j + \delta_{sj}t_r^i,$	Composite amplitudes
$\tilde{D}_{rs}^{ij} = 2D_{rs}^{ij} - D_{rs}^{ji}$	
$E_{rs}^{ij} = \delta_{ri}t_s^j$	Used in contractions of integrals with singles
$F_{\alpha\beta}^{ij} = \langle\alpha\beta\|F_{12}\|ij\rangle$	Integrals over F_{12}
$\bar{F}_{\alpha\beta}^{ij} = \langle\alpha\beta\|F_{12}\|kl\rangle T_{kl}^{ij}$	Contracted integrals over F_{12}
$\tilde{F}_{\alpha\beta}^{ij} = 2\bar{F}_{\alpha\beta}^{ij} - \bar{F}_{\alpha\beta}^{ji}$	
$G_{\alpha\beta}^{ij}$	Intermediates in CCSD-F12 residuals
$H_{mn,op} = \langle mn\|F_{12}\hat{Q}_{12}r_{12}^{-1}\hat{Q}_{12}F_{12}\|op\rangle$	Matrix elements in CCSD-F12 energy expression
$J_{\alpha\beta}^{kl} = \langle\alpha k\|r_{12}^{-1}\|\beta l\rangle$	Two-external Coulomb integrals
$K_{\alpha\beta}^{kl} = \langle\alpha\beta\|r_{12}^{-1}\|kl\rangle$	Two-external exchange integrals
$\bar{K}_{\alpha\beta}^{rs} = \langle\bar{\alpha}\bar{\beta}\|r_{12}^{-1}\|\tilde{r}\tilde{s}\rangle$	Dressed integrals
$K_{ij,kl}^{F} = \langle ij\|r_{12}^{-1}F_{12}\|kl\rangle$	Integrals over $r_{12}^{-1}F_{12}$
$L_{\alpha\beta}^{kl} = 2K_{\alpha\beta}^{kl} - K_{\alpha\beta}^{lk}$	
$R_{\alpha\beta}$	Intermediates in CCSD-F12 residual
R_{kl}^{ij}	MP2-F12 residual for explicitly correlated amplitudes
R_{ab}^{ij}	MP2-F12 or CCSD-F12 doubles residual

$S_{mn,op} = \langle mn\|F_{12}\hat{Q}_{12}F_{12}\|op\rangle$	Overlap of explicitly correlated configurations
$\bar{S}_{ij,kl} = \tilde{T}^{ij}_{mn} S_{mn,op} T^{kl}_{op}$	Contracted overlap matrix
$\tilde{S}^{(ij)}_{rs} = \langle\tilde{r}\|\tilde{s}\rangle, \quad r,s \in [ij]$	Overlap matrix of PAOs in domain $[ij]$
T^{ij}_{kl}	Amplitudes of explicitly correlated configurations
$\tilde{T}^{ij}_{kl} = 2T^{ij}_{kl} - T^{ji}_{kl}$	
T^{ij}_{ab}	Doubles amplitudes, virtual space
$\tilde{T}^{ij}_{ab} = 2T^{ij}_{ab} - T^{ji}_{ab}$	
$\mathcal{T}^{ij}_{\alpha\beta} = \langle\alpha\beta\|\hat{Q}_{12}F_{12}\|kl\rangle T^{ij}_{kl}$	Amplitudes of explicitly correlated terms in the complete virtual space
$\mathcal{U}^{ij}_{\alpha\beta} = \delta_{\alpha c}\delta_{\beta d} T^{ij}_{cd} + \mathcal{T}^{ij}_{\alpha\beta}$	Composite doubles amplitudes in complete space
$\tilde{\mathcal{U}}^{ij}_{\alpha\beta} = 2\mathcal{U}^{ij}_{\alpha\beta} - \mathcal{U}^{ji}_{\alpha\beta}$	
$U^{kl}_{\alpha\beta} = \langle kl\|[F_{12}, \hat{t}_1 + \hat{t}_2]\|\alpha\beta\rangle$	Commutator integrals used in MP2-F12
$U^{F}_{kl,mn} = \langle kl\|[F_{12}, \hat{t}_1 + \hat{t}_2]F_{12}\|mn\rangle$	Commutator integrals used in MP2-F12
$V^{ij}_{kl} = \langle kl\|F_{12}\hat{Q}_{12}r_{12}^{-1}\|ij\rangle$	Integrals used in MP2-F12
$\bar{V}^{ij}_{\alpha\beta} = \langle\alpha\beta\|r_{12}^{-1}\hat{Q}_{12}F_{12}\|kl\rangle T^{ij}_{kl}$	Contracted integrals used in CCSD-F12
$\bar{W}^{ij}_{\alpha\beta} = \langle\alpha\beta\|r_{12}^{-1}F_{12}\|kl\rangle T^{ij}_{kl}$	Contracted integrals used in CCSD-F12
$W^{(ij)}_{\tilde{\mu}\tilde{a}}, \quad \tilde{\mu},\tilde{a} \in [ij]$	Transformation from PAO basis to orthonormal basis in domain $[ij]$
$X_{\alpha\beta}, Y^{kj}_{\alpha\beta}, Z^{kj}_{\alpha\beta}$	Intermediates in CCSD-F12 residuals
$Y_{kl,mn} = \langle kl\|F_{12}\hat{n}_{12}\hat{Q}_{12}F_{12}\|mn\rangle$	Intermediates in MP2-F12 residuals
$f_{\alpha\beta} = h_{\alpha\beta} + 2J^{kk}_{\alpha\beta} - K^{kk}_{\alpha\beta}$	Closed-shell Fock matrix
$f^{i}_{\alpha} = f_{\alpha i}$	One-external Fock matrix elements
$\bar{f}_{\alpha\beta}$	Dressed Fock matrix

$\bar{f}^i_\alpha = \bar{f}_{i\alpha}$	One-external dressed Fock matrix elements
$\tilde{f}^{(ij)}_{rs} = f_{\tilde{r}\tilde{s}},\ \ \tilde{r},\tilde{s} \in [ij]$	Fock matrix in PAO basis in domain $[ij]$
$k^{kli}_\alpha = K^{kl}_{\alpha i}$	One-external integrals
$l^{kli}_\alpha = 2k^{kli}_\alpha - k^{lki}_\alpha$	
t^i_a	CCSD singles amplitudes
r^i_a	CCSD singles residuals

Contractions of integrals with amplitudes:

$$[\mathbf{J}(\mathbf{E}^{ij})]_{ab} = \langle ai|r_{12}^{-1}|bc\rangle t^j_c$$
$$[\mathbf{K}(\mathbf{E}^{ij})]_{ab} = \langle ab|r_{12}^{-1}|ic\rangle t^j_c$$
$$[\mathbf{K}(\mathbf{T}^{ij})]_{rs} = \langle rs|r_{12}^{-1}|cd\rangle T^{ij}_{cd}$$
$$[\mathbf{K}(\mathbf{D}^{ij})]_{rs} = \langle rs|r_{12}^{-1}|tu\rangle D^{ij}_{tu}$$
$$[\mathbf{K}(\mathbf{D}^{ij})]^{(k)}_a = [\mathbf{K}(\mathbf{D}^{ij})]_{ak}$$

REFERENCES

1. A. Karton, E. Rabinovich, J. M. L. Martin, B. Ruscic, J. Chem. Phys. **125**, 144108 (2006)
2. A. Tajti, P. G. Szalay, A.G. Császár, M. Kállay, J. Gauss, E. F. Valeev, B. A. Flowers, J. Vázquez, J. F. Stanton, J. Chem. Phys. **121**, 11599 (2004)
3. E. A. Hylleraas, Z. Phys. **54**, 347 (1929)
4. T. Helgaker, W. Klopper, D. P. Tew, Mol. Phys. **106**, 2107 (2008)
5. W. Kutzelnigg, Theor. Chim. Acta **68**, 445 (1985)
6. W. Klopper, W. Kutzelnigg, Chem. Phys. Lett. **134**, 17 (1987)
7. W. Klopper, W. Kutzelnigg, J. Phys. Chem. **94**, 5625 (1990)
8. W. Kutzelnigg, W. Klopper, J. Chem. Phys. **94**, 1985 (1991)
9. V. Termath, W. Klopper, W. Kutzelnigg, J. Chem. Phys. **94**, 2002 (1991)
10. W. Klopper, W. Kutzelnigg, J. Chem. Phys. **94**, 2020 (1991)
11. W. Klopper, Chem. Phys. Lett. **186**, 583 (1991)
12. W. Klopper, R. Röhse, W. Kutzelnigg, Chem. Phys. Lett. **178**, 455 (1991)
13. J. Noga, W. Kutzelnigg, W. Klopper, Chem. Phys. Lett. **199**, 497 (1992)
14. J. Noga, W. Kutzelnigg, J. Chem. Phys. **101**, 7738 (1994)
15. R. J. Gdanitz, J. Chem. Phys. **109**, 9795 (1998)
16. W. Klopper, C. C. M. Samson, J. Chem. Phys. **116**, 6397 (2002)
17. E. F. Valeev, Chem. Phys. Lett. **395**, 190 (2004)
18. S. Ten-no, Chem. Phys. Lett. **398**, 56 (2004)
19. A. J. May, F. R. Manby, J. Chem. Phys. **121**, 4479 (2004)
20. F. R. Manby, A. J. May, Abstr. Pap. Am. Chem. Soc. **228**, 273 (2004)
21. A. J. May, E. Valeev, R. Polly, F. R. Manby, Phys. Chem. Chem. Phys. **7**, 2710 (2005)
22. D.P. Tew, W. Klopper, J. Chem. Phys. **123**, 074101 (2005)
23. D.P. Tew, W. Klopper, J. Chem. Phys. **125**, 094302 (2006)

24. E. F. Valeev, J. Chem. Phys. **125**, 244106 (2006)
25. W. Klopper, F. R. Manby, S. Ten-no, E. F. Valeev, Int. Rev. Phys. Chem. **25**, 427 (2006)
26. J. Noga, S. Kedžuch, J. Šimunek, J. Chem. Phys. **127**, 034106 (2007)
27. F. R. Manby, H. J. Werner, T. B. Adler, A. J. May, J. Chem. Phys. **124**, 094103 (2006)
28. H. J. Werner, T. B. Adler, F. R. Manby, J. Chem. Phys. **126**, 164102 (2007)
29. G. Knizia, H. J. Werner, J. Chem. Phys. **128**, 154103 (2008)
30. S. Ten-no, J. Chem. Phys. **126**, 014108 (2007)
31. F. R. Manby, J. Chem. Phys. **119**, 4607 (2003)
32. S. Ten-no, F. R. Manby, J. Chem. Phys. **119**, 5358 (2003)
33. K. A. Peterson, T. B. Adler, H. J. Werner, J. Chem. Phys. **128**, 084102 (2008)
34. K. E. Yousaf, K. A. Peterson, J. Chem. Phys. **129**, 184108 (2008)
35. K. E. Yousaf, K. A. Peterson, Chem. Phys. Lett. **476**, 303 (2009)
36. C. Neiss, C. Hättig, W. Klopper, J. Chem. Phys. **125**, 064111 (2006)
37. H. Fliegl, C. Hättig, W. Klopper, J. Chem. Phys. **124**, 044112 (2006)
38. C. Neiss, C. Hättig, J. Chem. Phys. **126**, 154101 (2007)
39. J. Noga, P. Valiron, Chem. Phys. Lett. **324**, 166 (2000)
40. J. Noga, S. Kedžuch, J. Šimunek, S. Ten-no, J. Chem. Phys. **128**, 174103 (2008)
41. T. Shiozaki, M. Kamiya, S. Hirata, E. F. Valeev, Phys. Chem. Chem. Phys. **10**, 3358 (2008)
42. T. Shiozaki, M. Kamiya, S. Hirata, E. F. Valeev, J. Chem. Phys. **129**, 071101 (2008)
43. A. Köhn, G. W. Richings, D. P. Tew, J Chem Phys **129**, 201103 (2008)
44. T. Shiozaki, M. Kamiya, S. Hirata, E. F. Valeev, J. Chem. Phys. **130**, 054101 (2009)
45. T. Shiozaki, E. F. Valeev, S. Hirata, J. Chem. Phys. **131**, 044118 (2009)
46. A. Köhn, J. Chem. Phys. **130**, 131101 (2009)
47. H. Fliegl, W. Klopper, C. Hättig, J. Chem. Phys. **122**, 084107 (2005)
48. H. Fliegl, C. Hättig, W. Klopper, Int. J. Quantum Chem. **106**, 2306 (2006)
49. D. P. Tew, W. Klopper, C. Neiss, C. Hättig, Phys. Chem. Chem. Phys. **9**, 1921 (2007)
50. D. P. Tew, W. Klopper, C. Hättig, Chem. Phys. Lett. **452**, 326 (2008)
51. T. B. Adler, G. Knizia, H. J. Werner, J. Chem. Phys. **127**, 221106 (2007)
52. G. Knizia, T. B. Adler, H. J. Werner, J. Chem. Phys. **130**, 054104 (2009)
53. O. Marchetti, H. J. Werner, Phys. Chem. Chem. Phys. **10**, 3400 (2008)
54. G. Rauhut, G. Knizia, H. J. Werner, J. Chem. Phys. **130**, 054105 (2009)
55. P. Botschwina, R. Oswald, G. Knizia, H. J. Werner, Z. Phys. Chem. **223**, 447 (2009)
56. O. Marchetti, H. J. Werner, J. Chem. Phys. A **113**, 11580 (2009)
57. E. F. Valeev, Phys. Chem. Chem. Phys. **10**, 106 (2008)
58. E. F. Valeev, T. D. Crawford, J. Chem. Phys. **128**, 244113 (2008)
59. P. Pulay, Chem. Phys. Lett. **100**, 151 (1983)
60. S. Saebø, P. Pulay, Chem. Phys. Lett. **113**, 13 (1985)
61. S. Saebø, P. Pulay, J. Chem. Phys. **86**, 914 (1987)
62. S. Saebø, P. Pulay, Annu. Rev. Phys. Chem. **44**, 213 (1993)
63. C. Hampel, H. J. Werner, J. Chem. Phys. **104**, 6286 (1996)
64. M. Schütz, G. Hetzer, H. J. Werner, J. Chem. Phys. **111**, 5691 (1999)
65. M. Schütz, H. J. Werner, Chem. Phys. Lett. **318**, 370 (2000)
66. M. Schütz, J. Chem. Phys. **113**, 9986 (2000)
67. M. Schütz, H. J. Werner, J. Chem. Phys. **114**, 661 (2001)
68. F. Claeyssens, J. N. Harvey, F. R. Manby, R. A. Mata, A. J. Mulholland, K. E. Ranaghan, M. Schütz, S. Thiel, W. Thiel, H. J. Werner, Angew. Chem. **118**, 7010 (2006)
69. R.A. Mata, H. J. Werner, S. Thiel, W. Thiel, J. Chem. Phys. p. 025104 (2008)
70. H. J. Werner, J. Chem. Phys. **129**, 101103 (2008)

71. T. B. Adler, H. J. Werner, F. R. Manby, J. Chem. Phys. **130**, 054106 (2009)
72. T. B. Adler, H. J. Werner, J. Chem. Phys. **130**, 241101 (2009)
73. H. J. Werner, P. J. Knowles, R. Lindh, F. R. Manby, M. Schütz et al., Molpro, version 2009.1, a package of ab initio programs (2009). See http://www.molpro.net
74. S. Ten-no, J. Chem. Phys. **121**, 117 (2004)
75. T. Kato, Comm. Pure Appl. Math. **10**, 151 (1957)
76. R. T. Pack, W. Byers Brown, J. Chem. Phys. **45**, 556 (1966)
77. S. Kedžuch, M. Milko, J. Noga, Int. J. Quantum Chem. **105**, 929 (2005)
78. W. Klopper, J. Chem. Phys. **120**, 10890 (2004)
79. C. Hampel, K. A. Peterson, H. J. Werner, Chem. Phys. Lett. **190**, 1 (1992)
80. W. Meyer, J. Chem. Phys. **64**, 2901 (1976)
81. P. Pulay, S. Saebø, W. Meyer, J. Chem. Phys. **81**, 1901 (1984)
82. J. Pipek, P. G. Mezey, J. Chem. Phys. **90**, 4916 (1989)
83. R. Mata, H. J. Werner, Mol. Phys. **105**, 2753 (2007)
84. A. ElAzhary, G. Rauhut, P. Pulay, H. J. Werner, J. Chem. Phys. **108**, 5185 (1998)
85. M. Schütz, H. J. Werner, R. Lindh, F. R. Manby, J. Chem. Phys. **121**, 737 (2004)
86. J. W. Boughton, P. Pulay, J. Comput. Chem. **14**, 736 (1993)
87. H. J. Werner, K. Pflüger, Ann. Rep. Comput. Chem. **2**, 53 (2006)
88. S. F. Boys, I. Shavitt, University of Wisconsin, Report WIS-AF-13 (1959)
89. J. L. Whitten, J. Chem. Phys. **58**, 4496 (1973)
90. E. J. Baerends, D. E. Ellis, P. Ros, Chem. Phys. **2**, 41 (1973)
91. O. Vahtras, J. Almlöf, M. W. Feyereisen, Chem. Phys. Lett. **213**, 514 (1993)
92. M. W. Feyereisen, G. Fitzgerald, A. Komornicki, Chem. Phys. Lett. **208**, 359 (1993)
93. F. Weigend, M. Häser, H. Patzelt, R. Ahlrichs, Chem. Phys. Lett. **294**, 143 (1998)
94. F. Weigend, A. Köhn, C. Hättig, J. Chem. Phys. **116**, 3175 (2002)
95. H. J. Werner, F. R. Manby, P. Knowles, J. Chem. Phys. **118**, 8149 (2003)
96. C. Hättig, F. Weigend, J. Chem. Phys. **5154**, 2000 (113)
97. M. Schütz, F. R. Manby, Phys. Chem. Chem. Phys. **5**, 3349 (2003)
98. C. Villani, W. Klopper, J. Phys. B **38**, 2555 (2005)
99. H. J. Werner, F. R. Manby, J. Chem. Phys. **124**, 054114 (2006)
100. G. Knizia, H. J. Werner, J. Chem. Phys. **128**, 154103 (2008)
101. F. A. Bischoff, S. Höfener, A. Glöss, W. Klopper, Theor. Chem. Acc. **121**, 11 (2008)
102. S. Höfener, F. A. Bischoff, A. Glöss, W. Klopper, Phys. Chem. Chem. Phys. **10**, 3390 (2008)
103. B. I. Dunlap, Phys. Chem. Chem. Phys. **2**, 2113 (2000)
104. R. A. Kendall, T. H. Dunning, R.J. Harrison, J. Chem. Phys. **96**, 6796 (1992)
105. T. Dunning Jr., K. A. Peterson, A. Wilson, J. Chem. Phys. **114**, 9244 (2001)
106. F. Weigend, Phys. Chem. Chem. Phys. **4**, 4285 (2002)
107. F. Weigend, A. Köhn, C. Hättig, J. Chem. Phys. **116**, 3175 (2002)
108. L. A. Curtiss, K. Raghavachari, G. W. Trucks, J. A. Pople, J. Chem. Phys. **94**, 7221 (1991)
109. D. Bokhan, S. Ten-no, J. Noga, Phys. Chem. Chem. Phys. **10**, 3320 (2008)
110. P. Jurečka, J. Šponer, J. Černý, P. Hobza, Phys. Chem. Chem. Phys. **8**, 1985 (2006)
111. F. Bernardi, S. F. Boys, Mol. Phys. **19**, 553 (1970)
112. F. A. Bischoff, S. Wolfsegger, D. P. Tew, W. Klopper, Mol. Phys. **107**, 963 (2009)

CHAPTER 22

INSTABILITY IN CHEMICAL BONDS: UNO CASCC, RESONATING UCC AND APPROXIMATELY PROJECTED UCC METHODS TO QUASI-DEGENERATE ELECTRONIC SYSTEMS

SHUSUKE YAMANAKA[1], SATOMICHI NISHIHARA[2], KAZUTO NAKATA[3], YASUSHIGE YONEZAWA[1], YASUTAKA KITAGAWA[2], TAKASHI KAWAKAMI[2], MITSUTAKA OKUMURA[2], TOSHIKAZU TAKADA[4], HARUKI NAKAMURA[1], AND KIZASHI YAMAGUCHI[5]

[1] *Protein Institute, Osaka University, 3-2 Yamadaoka, Suita, Osaka 565-0871, Japan*
[2] *Graduate School of Science, Osaka University, 1-1 Machikaneyama, Toyonaka, Osaka 560-0043, Japan*
[3] *HPC Marketing Promotion Division, NEC Corporation, 1-10, Nisshincho, Fuchu, Toyoko, 183-8501, Japan*
[4] *RIKEN Next-Generation Supercomputer R&D Center, Chiyodaku, Tokyo, 100-0005, Japan*
[5] *TOYOTA Physical & Chemical Research Institute, Nagakute, Aichi, 480-1192, Japan*

Abstract: We review several versions of coupled-cluster (CC) methods based on spin-unrestricted Hartree–Fock (UHF) approximation. A multireference (MR) CC theory by the use of UHF natural orbitals (UNO), UNO CASCC, is revisited to elucidate scope and limitation of UHF coupled-cluster (CC) methods and two types of quantum corrections for UHF CC (UCC) solutions: first one is the approximate spin-projected UCC scheme (AP UCC) based on Heisenberg model Hamiltonian, and second one is the recently developed resonating UCC configuration interaction (Res-UCC CI) approach. In this article, we examine these CC-based approaches for quasi-degenerate electronic systems such as dissociation of covalent bonds. The computational results are discussed in comparison with those of the MR-CC theory. Our methods have been applied to exchange-coupled systems and ion-radical systems, which have been accepted current interests.

Keywords: Coupled cluster, Spin-unrestricted, Resonating configuration interaction, Instability in chemical bonds, Dissociation limits

22.1. INTRODUCTION

In the past decades quasi-degenerate electronic systems attracted great interest in the fields of chemical reactions and material sciences. Among multideterminant wavefunction theories, the configuration interaction (CI) theory is the most

P. Čársky et al. (eds.), Recent Progress in Coupled Cluster Methods, 621–648.
DOI 10.1007/978-90-481-2885-3_22,

fundamental and straightforward theory for strongly correlated systems with such quasi-degenerate electronic states [1–7]. However, practical truncated CI methods suffer the inextensitivity of electron correlation effects [8]. On the other hand, it is known that the coupled-cluster (CC) theory is a size-extensive electron-correlation theory and therefore a promising theory towards large systems. The progress of the CC theories has been achieved through many computational and theoretical studies since Sinanoglu, Cizek, Paldus and others introduced the CC ansatz in the field of quantum chemistry [9–57]. Recent treatments such as the local correlation method [44] and fragment molecular orbital method [49] are proposed as "an accurate theory for large systems". Also, for the biomolecular systems such as enzymes, a multilayer theoretical framework such as CC plus the second-order Møller–Plesset perturbation theory (MP2) is proposed on the basis of the many-body perturbation theory [55]. From the theoretical viewpoint, CC theories involving explicit interelectronic distances have been developed for the pursuit of preciseness for short-range correlation effects [9, 10, 35, 55]. A more remarkable progress has been made in the computational method: development of an automatic code generation for ab initio many-body perturbation theories [53] might become a turning point towards the next generation of the high-quality ab initio studies. In fact, simplifying the complicated and tedious manipulations of equations for programming, Hirata and coworkers have implemented several higher-order coupled-cluster theories [57].

Towards the coupled-cluster theory for quasi-degenerate electronic systems, various multireference formulations [14–18, 20–24, 29, 30, 34–37, 39, 41–43, 45, 46, 48, 50, 51, 56] have been developed. The MR-CC theory is expected to provide reliable results for almost all cases: those might be more reliable than the experimental results when the instrument or the method of measurement involves artifacts. However, MR-CC calculations are still computationally demanding as compared with other wavefunction methods, although the remarkable advances in theoretical and computational contexts have been achieved. Also, it is pointed out that MR-CC theories suffer active-orbital orbital rotation issues, and can not yield the correct "size-consistent" potential surfaces [54]. So in applications to exchange-coupled systems, we should be careful to choose appropriately specific versions of MR-CC and the orbitals used for the MRCC calculations [54]. Thus, more convenient approaches are needed if we treat with the large molecular systems containing open-shell electrons. Since we have investigated molecular magnetic systems, our direction might be slightly different from that of many other developers of CC theories. As described above, we can expect from the analysis of UMP2 APUMP2 and MRMP2 that spin-unrestricted CC (UCC) theory could be an alternative to the MR-CC theory if some quantum corrections is applied appropriately to recover its symmetry-broken feature. This "quantum correction using symmetry-broken solutions" is a fundamental scheme behind the spin-projection method proposed by one of the authors (K.Y.) [58–64], and a resonating CI theory [65–67] based on UCC solutions that is now developed. In this article, we reviewed the coupled-cluster theory for the open-shell systems,

rather emphasizing on the UCC, and UCC based quantum corrected theories and its relation with the quantum fluctuations.

22.2. THEORETICAL BACKGROUND

22.2.1. Independent Particle Model and Mean-Field Approximation

Independent particle model for many-boby systems permits several mean-field approximations such as the Hartree–Fock (HF) approach, which provide qualitative pictures and concepts for lucid understanding of complex phenomena. Here, we start to define what the "explicit" correlation effects are. The explicit electron correlation effects are results from the non-commutative relationship between an effective one-electron Hamiltonian and the remaining electron correlation operator,

$$\left[\hat{H}_0 + \hat{V}_{\text{eff}}, \quad \hat{H}_0 + \hat{V}_{ee}\right] \neq 0. \tag{22-1}$$

Here, $\hat{H}_0$ and $\hat{V}_{ee}$, two terms of the non-relativistic ab initio Hamiltonian, $\hat{H}$, are the core Hamiltonian consisting of kinetic and external potential operators and the inter-electron repulsion operator, respectively. $\hat{V}_{\text{eff}}$ is a mean-field potential operator, which is the sum of classical Coulomb-repulsion operator and the exchange operator for the HF approximation. An important point is that, even if we determine a ground-state solution $|\Phi_0\rangle$ of $\hat{H}_0 + \hat{V}_{\text{eff}}$ exactly, transitions from $|\Phi_0\rangle$ to the excited configurations are inevitable due to the relation given by Eq. (22-1). This type of effects is obviously a kind of quantum fluctuations since it is due to a noncommutative (uncertainty) relation of quantum mechanics. We call these effects "explicit" electron correlation effects for many-body systems. Thus, the resulting solution is beyond the scope of "noninteracting picture", namely independent particle model, in other words, beyond any single-determinant wavefunction [68].

Such explicit correlation effects are important for molecular magnetism and the homolysis type of bond breaking. Here, let us first consider the simplest system, i.e. hydrogen molecule. The "noninteracting picture" type of wavefunction is expressed with molecular orbital (MO) model

$$\left|\Phi_0^{\text{R}}\right\rangle = \left|\phi_{\text{bond}}\bar{\phi}_{\text{bond}}\right\rangle = \frac{1}{\sqrt{2}}|S\rangle + \frac{1}{\sqrt{2}}|I\rangle \tag{22-2}$$

where ϕ_{bond} and $\bar{\phi}_{\text{bond}}$ are α and β molecular orbitals (MO), respectively. The rightest side in Eq. (22-2) indicates that the noninteracting wavefunction is an equivalent superposition of covalent (quantum singlet: S) state and ionic (I) configurations in the valence-bond (VB) CI approach [63].

This picture is appropriate for the stable chemical bond, but not appropriate for dissociation of the chemical bond. A ground-state configuration, $\left|\Phi_0^{\text{R}}\right\rangle$ that is determined for a mean-field Hamiltonian, $\hat{H}_0 + \hat{V}_{\text{eff}}$, is always disturbed by transitions to excited configurations as described above, resulting in a multideterminant

ground-state wavefunction. Since the most important transition is from the bonding state $|\phi_{\rm bond}\bar{\phi}_{\rm bond}\rangle$ to the antibonding state $|\phi_{\rm antibond}\bar{\phi}_{\rm antibond}\rangle$ in this case, the resulting wavefunction becomes the 2×2 CI form.

$$\begin{aligned}|\Phi_0^{CI}\rangle &= C_{\rm bond}|\phi_{\rm bond}\bar{\phi}_{\rm bond}\rangle - C_{\rm antibond}|\phi_{\rm antibond}\bar{\phi}_{\rm antibond}\rangle \\ &= \frac{C_{\rm bond} - C_{\rm antibond}}{\sqrt{2}}|S\rangle + \frac{C_{\rm bond} + C_{\rm antibond}}{\sqrt{2}}|I\rangle \end{aligned} \tag{22-3}$$

The weight of pseudo double excitation in Eq. (22-3) is a measure of diradical character in chemistry. Under the above situation, the closed-shell HF (RHF) solution $|\phi_{\rm bond}\bar{\phi}_{\rm bond}\rangle$ suffers the triplet instability, and it is reorganized into a more stable unrestricted HF (UHF) solution [69–71], $|\Psi_0^U\rangle$ consisted of the different orbital for different spins (DODS) type of molecular orbitals,

$$\psi_\alpha^U = \cos\theta\phi_{\rm bond} + \sin\theta\phi_{\rm antibond}, \quad \psi_\beta^U = \cos\theta\phi_{\rm bond} - \sin\theta\phi_{\rm antibond} \tag{22-4}$$

We then have a plain expression of $|\Psi_0^U(I)\rangle$ with using the triplet term $|T\rangle$,

$$|\Psi_0^{U1}\rangle = |\psi_\alpha^U\bar{\psi}_\beta^U\rangle = \frac{2\cos^2\theta - 1}{\sqrt{2}}|I\rangle + \frac{1}{\sqrt{2}}|S\rangle + \frac{\sin 2\theta}{\sqrt{2}}|T\rangle, \tag{22-5}$$

Eq. (22-5) can be further transformed into another expression using a classical spin term, $|C\rangle = (|S\rangle + |T\rangle)/\sqrt{2}$ [63],

$$|\Psi_0^{U1}\rangle = \frac{2\cos^2\theta - 1}{\sqrt{2}}|I\rangle + \frac{1 - \sin 2\theta}{\sqrt{2}}|S\rangle + \frac{\sin 2\theta}{\sqrt{2}}|C\rangle. \tag{22-6}$$

This expression shows that the UHF solution reduces to the RHF solution for the noninteracting limit ($\theta \to 0$) and the classical spin solution for the strongly correlated limit ($\theta \to \pi/4$), respectively.

$$\mathrm{Lim}_{\theta\to 0}\left[|\Psi_0^{U1}\rangle\right] = \mathrm{Lim}_{\theta\to 0}\left[|\Psi_0^{U2}\rangle\right] = |\Phi_0^R\rangle. \tag{22-7}$$

$$\mathrm{Lim}_{\theta\to \pi/4}\left[|\Psi_0^{\rm U1}\rangle\right] = -\mathrm{Lim}_{\theta\to \pi/4}\left[|\Psi_0^{\rm U2}\rangle\right] = |C\rangle. \tag{22-8}$$

where $|\Psi_0^{U2}\rangle$ is the other UHF solution which is, as a partner of $|\Psi_0^{U1}\rangle$, given by

$$|\Psi_0^{U2}\rangle = |\psi_\beta^U\bar{\psi}_\alpha^U\rangle = \frac{2\cos^2\theta - 1}{\sqrt{2}}|I\rangle + \frac{1}{\sqrt{2}}|S\rangle - \frac{\sin 2\theta}{\sqrt{2}}|T\rangle. \tag{22-9}$$

At the dissociation limit ($\theta \to \pi/4$), the ionic term correctly vanishes and Neel-ordered classical configuration develops.

Since UHF(I) and UHF(II) solutions are degenerate in energy, the in-phase combination of them provides the pure singlet wavefunction which corresponds to Eq. (22-3), whereas the out of phase combination gives the triplet wavefunction $|T\rangle$. The resonating UHF solution for the singlet state reduces to the pure covalent term in the VB theory at the dissociation limit.

$$\mathrm{Lim}_{\theta\to\pi/4}\left[\left|\Psi_0^{\mathrm{Res-HF}}\right\rangle\right] = \mathrm{Lim}_{\theta\to\pi/4}\left[\left(\left|\Psi_0^{U1}\right\rangle + \left|\Psi_0^{U2}\right\rangle\right)\Big/\sqrt{2}\right] = |S\rangle\,. \quad (22\text{-}10)$$

Therefore Eq. (22-10) is just the zero-th order description of the antiferromagnetically coupled diradicals in the theory of the kinetic exchange mechanism [72, 73]. Then, the ionic configuration, $|I\rangle$, is mixed with $|S\rangle$, yielding a multideterminant (valence-bond (VB) configuration interaction (CI)) wavefunction, $C_S\,|S\rangle + C_I\,|I\rangle$ ($|C_S| >> |C_I|$) that is similar to the wavefunction given by Eq. (22-3).

The orbital mixings in Eq. (22-4) become necessary for several chemical bonds in quasi-degenerate electronic systems, providing UHF and more general HF (GHF) solutions depending on electron and spin correlation effects for systems under consideration [74]. A lot of electronic and spin states become feasible for these systems, and these states are often nearly degenerate in energy. This entails the multiconfiguration theory for appropriate description of these quasi-degenerate electronic states.

22.2.2. MR CI for Nondynamical Correlations

The electronic and spin states of quasi-degenerated electronic systems can be described using full configuration interaction (FCI) method as shown in standard textbooks of quantum chemistry [8],

$$\left|\Phi_0^{FCI}\right\rangle = \left(c_0 + \sum\nolimits_{ar} c_a^r a_r^+ a_a + \sum\nolimits_{abrs} c_{ab}^{rs} a_r^+ a_s^+ a_b a_a + \ldots\right)\left|\Phi_0^{\mathrm{R}}\right\rangle. \quad (22\text{-}11)$$

The second and third terms in the parenthesis indicate that electrons in the ground-state configuration excite from the occupied orbitals (a, b, ...) to the unoccupied orbitals ($r, s, \ldots$). However, applicability of FCI is limited to rather small molecules, indicating the necessity of reduction of number of configurations for large molecules. In fact, selection of active orbitals and active electrons is crucial for so-called MR CI approach [1–3]. To this end, the first order density matrix of the UHF and generalized HF (GHF) solutions has been diagonalized [4–7] as a first step to consider quantum correction to the broken-symmetry (BS) (unrestricted) Hartree-Fock (UHF or GHF) mean-field solution [69–71].

$$\rho\,(\mathbf{r}_1;\mathbf{r}_2) = \sum\nolimits_{\sigma}^{\alpha,\beta} \psi_\sigma^{U+}\,(\mathbf{r}_1)\,\psi_\sigma^{U}\,(\,\mathbf{r}_2) = \sum\nolimits_i n_i \phi_i^+\,(\mathbf{r}_1)\,\phi_i\,(\mathbf{r}_2). \quad (22\text{-}12)$$

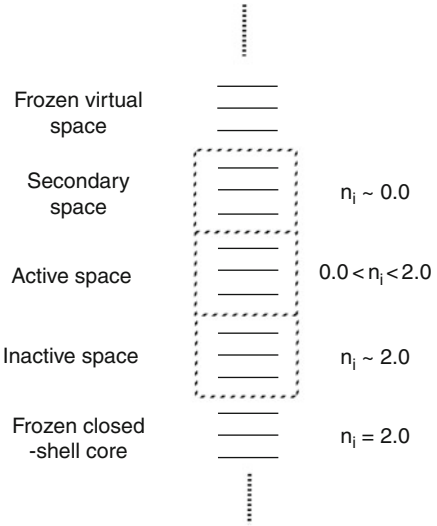

Figure 22-1. Division of orbital space based on UHF natural orbital analysis

where ϕ_i and n_i denote, respectively, UHF (GHF) natural orbitals (U(G)NOs) and their occupation numbers. The U(G)NOs are classified into five groups using occupation numbers as illustrated in Figure 22-1

(1) Frozen closed-shell orbitals (FCO)
(2) Inactive space consisting of closed-shell orbitals (CO) for which $n_i \cong 2.0$.
(3) Active space (AO) consisting of partially filled orbitals ($0.0 < n_i < 2.0$), which are closely related to nondynamical correlations responsible for instability of the mean-field HF solution.
(4) Secondary space consisting of virtual orbitals (VO) for which $n_i \cong 0.0$.
(5) Frozen virtual orbitals (FVO).

The full CI is usually performed within active space (AO) in the group (22-3) of the above classification, leading to reduction of FCI in Eq. (22-11) into UNO complete active space (CAS) CI.

$$\Psi_0^{FCI(\text{group 3})} = \Psi_0^{\text{UNO CAS}} = \sum\nolimits_i a_i \Phi_i. \tag{22-13}$$

The CAS (MO) CI wavefunction can be transformed into the VB CI one [5]. To this end, the localized natural orbitals (LNO) for active orbital space were defined as the broken symmetry molecular orbitals (Eq. 4) at the strong correlation limit.

$$\phi_a = (\phi_{\text{bond}} + \phi_{\text{antibond}})/\sqrt{2}, \phi_b = (\phi_{\text{bond}} - \phi_{\text{antibond}})/\sqrt{2} \tag{22-14}$$

The LNO are indeed useful for VB type explanation of UNO CAS CI [6].

The UNO CAS space in the group (22-13) is relatively small since it is only responsible for nondynamical correlation relating to triplet instability [4–6, 20]. For well-balanced description of both ground and excited states, the CAS space is expanded with covering all of the excitations among valence electrons in valence orbitals,

$$\left|\Psi_0^{\mathrm{CASSCF}}\right\rangle = \left(c_0 + \sum_{ar}^{\substack{\text{active}\\ \text{orbitals}}} c_a^r a_r^+ a_a + \sum_{abrs}^{\substack{\text{active}\\ \text{orbitals}}} c_{ab}^{rs} a_r^+ a_s^+ a_b a_a + \ldots\right) \left|\Phi_0^{\mathrm{R}}\right\rangle, \tag{22-15}$$

where trial MOs such as UNO are re-optimized using the multiconfiguration self-consistent field (MCSCF) technique. This method is now called complete-active-space (CAS) SCF [75]. In the CASSCF wavefunction, all of low-lying electronic configurations are included so that it is appropriate for describing qualitative features of chemical reactions and excited states. In fact, if the active space is large enough, the CASSCF wavefunction includes all effects related to chemical bonding, other than relativistic effects and finite-temperature effects. However, as the number of active orbitals and active electrons increases linearly if the system size increases, the CASSCF method becomes at least an NP-hard problem [76, 77]. Also, from the viewpoint of ab initio theory, dynamical correlations that are missed in Eq. (22-15) should be covered for the quantitative discussions. Of course, if we cover such remaining effects using CI, i.e., use multireference CI (MRCI), we turn back to the size-extensivity problem [8]. Then the second-order perturbations based on CAS are used for the purpose [78, 79].

22.2.3. Coupled-Cluster Method and Size Consistency Condition

The coupled-cluster (CC) theory [10–57] is, on the other hand, based on an exponential type of expansion, and therefore covers higher-order excitations

$$\left|\Psi^{CC}\right\rangle = \exp\left(\hat{T}\right)|\Phi\rangle. \tag{22-16}$$

Here T consists of excitation operators with normal order from the reference function, $|\Phi\rangle$. The CC equations to obtain $\left|\Psi^{CC}\right\rangle$ is given by

$$\langle\Phi|\exp\left(-\hat{T}\right)\hat{H}\exp\left(\hat{T}\right)|\Phi\rangle = E, \tag{22-17}$$

$$\langle\Phi|\hat{O}\exp\left(-\hat{T}\right)\hat{H}\exp\left(\hat{T}\right)|\Phi\rangle = 0, \tag{22-18}$$

where $\hat{O}$ is an arbitrary excitation operator. A remarkable point is that in the CC theory, in contrast to the CI theory, the energy is not equivalent to the expectation value for Hamiltonian of the CC wavefunction given by Eq. (22-16). There are many excellent review articles and textbooks for coupled-cluster theories [22–43], in which

theoretical foundations, various versions, and applications of the CC theories are described in detail. An important point here is that, if the reference function is a single-determinant or the complete-active-space (CAS) type of wavefunction, the linked-cluster theorem holds, the CC theories being size-extensive theories. Thanks to this size-extensive feature of the electron correlation effects, this type of expansion is superior to the usual type of CI expansion such as SDCI and MRCI for large-size systems. If we employ the excitation operator T including all possible single excitations, the CC calculations provide better densities than the CI calculations do. This is also highly desirable for molecular dynamics studies based on ab initio theories since the accuracy of the forces relies on the densities calculated by ab initio theories due to the Feynman's electrostatic theorem. Further, because the CC theory includes infinite series of expansion, this theory could treat with the correlated systems, for which the same order perturbation theory does not work due to the large remaining electron correlation effects beyond $|\Phi\rangle$. For this reason, the CC theory is not only well-established high-quality one for molecular systems, but also effective one for the condensed matter-systems. In fact, this type of approximation is also used to cover the quantum spin effects of magnetic systems within model spin Hamiltonians [27]. However, the correct dissociation of chemical bonding is another issue for the CC theory. If we persist in spin-restricted single-determinant CC (RCC), the "size-consistency" in total meaning is not achieved because of the perturbative treatment of the CC equation. In fact, we showed that the RCCSD method fails to describe the correct dissociation limits of covalent bonds where the orbital energies of bonding and corresponding antibonding orbitals become quasi-degenerate [32]. The convenient prescription for this problem is to remove the restriction of symmetry, i.e. to use spin-unrestricted CC (UCC) method [18, 19]. If we have to care about the symmetry of the systems (for instance to investigate stable geometries of radical species), it is better to apply quantum corrections described later. Otherwise we have to select a "CI compromise" [39, 75] or MR-CC described just below.

22.2.4. MR CC for Nondynamical and Dynamical Correlations

Here, we describe a minimum review of the MRCC theory for the convenience of later discussions. For the complete description and other recently developed methods related to MRCC theories, please refer to review excellent articles and comprehensive comparative studies (for example refs. [18, 23, 25, 37, 46, 56]). Late 1970's, several versions of MR CC have been presented for quasi-degenerate electronic systems [14–16, 18]. We have proposed use of UNO CASCI zero-order wavefunctions as trials of MR CC approach for the purpose [20]. The UNO CASSCF (MCSCF) wavefunction has been expressed with the MRCC formulae by the use of the single (T_1) excitation operator:

$$\Psi_i^{\text{UNO CASSCF}} = \Psi_i^{\text{UNO CASCCS}} = e^{T_1}\Psi_0^{\text{UNO CAS}}. \tag{22-19}$$

The orbital relaxation effects for UNO CASCI can be incorporated with the T_1 operator. The dynamical correlation correction is further considered for quantitative purpose. The double-excitation operator is used as

$$\Psi_i^{\mathrm{MRCCSD}} \cong \Psi_i^{\mathrm{UNO\ CASCCSD}} = e^{T_1+T_2}\Psi_0^{\mathrm{UNO\ CAS}}. \tag{22-20}$$

Thus UNO CASCC is regarded as a direct extension of UNO CAS CI starting from broken-symmetry (BS) UHF and GHF calculations for qausi-degenerated systems [19, 20]. However, since MRCCSD computations were too difficult at that time, MRCI with Davidson correction [2] was employed to obtain the higher-order correction for excitation spectra of several peroxides [7, 20, 80].

Early 1980's, the multireference version of coupled-cluster (MRCC) theories for open-shell systems has been formulated extensively. Since the theoretical foundation of the MR-CC theory is not straightforward, many formulae have been derived recently. In addition, as the numerical treatment is also complicated, the various procedures are proposed and implemented. Lindgren and Mukherjee [23] classified various MR-CC theories with respect to (i) the model space and (ii) the wave operator. In particular, the choice of the model space determines the theoretical framework of the MRCC theory: if the number of valence electrons is fixed as in the usual ab initio theories, the formulation of the MR-CC theory is based on the n-valence Hilbert space. On the other hand, it is possible to formulate the MR-CC theory, with which the systems with the numbers of valence electrons ranging from zero to n are treated simultaneously. In this case, the theory is based on the Fock space. Therefore the two types of the MR-CC theories are referred to as the Hilbert-space and the Fock-space approaches, respectively. Theorists of MRCC have taken special cares for the diagrammatic connectivity that is directly related to the size-extensivity, a most fundamental characteristic of the CC theory. Our present interest is on systems with fixed-number electrons, so we here describe only the Hilbert-space MRCC theory briefly.

In the Hilbert space MR-CC theory, we first divide the Hilbert space into the model space and its complementary space using projection operators, P, and Q,

$$\hat{I} = \hat{P} + \hat{Q}, \tag{22-21}$$

where P is a projection operator to a specific zero-order reference space, $\left\{\left|\Phi_0^i\right\rangle\right\}_i$,

$$\hat{P} = \sum\nolimits_i \left|\Phi_0^i\right\rangle\left\langle\Phi_0^i\right|. \tag{22-22}$$

Then it is assumed that the exact wavefunction, $\left|\Psi_0^i\right\rangle$ can be written as a cluster expansion around a reference function, $\left|\Phi_0^i\right\rangle$ using an wave operator, $\hat{\Omega}$,

$$\left|\Psi_0^i\right\rangle = \hat{\Omega}\left|\Phi_0^i\right\rangle. \tag{22-23}$$

We then have an effective multireference equation given by,

$$\hat{H}_{\text{eff}} \left|\Psi_0^i\right\rangle = \hat{\Omega}^{-1}\hat{H}\hat{\Omega}E^i \left|\Phi_0^i\right\rangle. \tag{22-24}$$

with a Bloch equation to determine the wave operator,

$$\hat{H}\hat{\Omega}\hat{H} = \hat{\Omega}\hat{P}\hat{H}_{\text{eff}}\hat{P}. \tag{22-25}$$

An explicit form of the wave operator Ω is given by Jeziorski and Monkhorst

$$\hat{\Omega} = \sum\nolimits_{i=1}^{P} \exp\left(\hat{T}^i\right) \left|\Psi_0^i\right\rangle\left\langle\Psi_0^i\right|, \tag{22-26}$$

in which different exponential operators are applied on every reference functions, $\left\{\left|\Phi_0^i\right\rangle\right\}_i$ [22]. Thus the wavefunction is given by,

$$\left|\Psi_0^j\right\rangle = \sum\nolimits_{i=1}^{P} C_{ji} \exp\left(\hat{T}^i\right) \left|\Psi_0^i\right\rangle. \tag{22-27}$$

The MR-CC based on the Jeziorski and Monkorst's ansatz is called state universal (SU) type. The SU formalism provides the accurate results on each state [19, 23, 48, 51] but leads to the complicated situations that is difficult to control, for example spin quantum number of each state simultaneously.

To reduce the manipulative complexity, a straightforward way is a state-specific (or state-selective) (SS) method where an effective Hamiltonian is constructed as SU formalism, but just the specific exponential is used in the state-specific wave operator. Note that the problem (the effective equation) is for multistates (MS), so this is referred to as SS-MS MR-CC. The SS-MS MR-CC involves a redundancy problem to determine the CC amplitudes. To resolve the problem using manipulations on the wavevector and the CC equation, there are several branches within SS MR-CC such as Mk-MRCC [39] and Brillouin–Wigner (BW) MRCC [41].

Further simplifications are possible with reducing the set of reference functions, $\left\{\left|\Phi_0^i\right\rangle\right\}_i$ to one reference function, $|\Phi_0\rangle$, being "state-specific single-state MR-CC (SS-SS MR-CC)". Even within this simplest subgroup of MRCC theories, there are many variants with respect to the cluster operator, the reference function, and other devices [32, 43, 45]. Since we would like to use MRCC to provide the precise description of exchange-coupled systems, the CAS-CC type of methods in Eq. (22-13) is desirable. For this case, the formulation is similar to the single-reference restricted CC theory, of which the energy of the state is given by,

$$E_0 = \left\langle \Psi_0^{\text{CAS}} \right| \exp\left(-\hat{T}\right)\hat{H}\exp\left(\hat{T}\right) \left|\Psi_0^{\text{CAS}}\right\rangle. \tag{22-28}$$

As the implementation of the SS-SS MRCC is similar to that of MRCI [1–7], the size-extensive correction to MRCI would be closely related to the SS-SS MRCC

[18, 20]. Szalay and Bartlett have developed an intermediate method between SS-SS MRCC and MRCI methods called as multi-reference averaged quadratic coupled-cluster (MRAQCC) method, in which size-extensivity of MRCI is improved [29]. One might argue that there is a problem due to the simplification to the single-state version, which is known as the intruder states problem for the single-state CAS based perturbation theory (CAS-PT2) [76, 77] for geometry changes that make several states quasi degenerate. However judging from their applications [43], missing "multistate" characteristics in the SS-SS MR-CC theory is not severe compared with the CAS-PT2, leading to a relatively small CAS in Eq. (22-13).

22.2.5. Spin Unrestricted Coupled-Cluster Method

Besides the MR-CC theories described above, the spin-unrestricted CC (UCC) theory also correctly describes the homolysis of covalent bonds and polyradicals. The UCC wavefunction becomes closer and closer to the full CI if the excitation operators are expanded as single (S), double (D), triple (T) and so on, though the broken symmetry UHF solution is taken as the zero-th order reference function.

We can see from Eq. (22-8) that the description of diradicals becomes a classical like spin ordering (C), which is different from Eq. (22-10) that represents a quantum singlet spin ordering. This is due to the third term at the rightest side in Eq. (22-5) that is the well-known triplet (T) contaminant term of the UHF solution, implying that this UHF wavefunction $\left|\Phi_0^U\right\rangle$ is a spin "broken-symmetry" solution. The UCC wavefunction is generated with a coupled-cluster expansion of the UHF reference,

$$\left|\Psi_0^{\mathrm{UCC}}\right\rangle = \exp\left(\hat{T}\right)\left|\Phi_0^U\right\rangle. \tag{22-29}$$

Although the spin-contaminations are suppressed due to the quasi-multiconfiguration nature of coupled-cluster expansions of UCC, the broken-symmetry feature remains if the excitation operators are truncated.

The use of the broken-symmetry solutions to describe radical species, homolysis of chemical bonds, and the open-shell transition metal systems [19, 69–71] are now widely accepted. In particular, spin-unrestricted DFT, of which solutions have characteristics similar to Eqs. (22-4), (22-5), (22-6), (22-7) and (22-8), become a standard tool [81, 82]. In fact, magnetic states in transition metal systems often involve spin-orbit interactions so that we do not have to insure the spin-symmetry of the solutions. In addition, the quantum spin effects decrease as the system size increases, because the frequency of spin axis rotation of each sub-lattice that is required to recover the quantum spin state is a function, $J/(\hbar N)$, of magnetic interaction J and the number of magnetic sites N, reducing to zero as the N increases [72]. For this reason, the classical spin ordering (Neel ordering: broken-symmetry state) is actually observed as the most stable spin state in antiferromagnetic solids [72, 73]. Also for molecular systems, quantum effects depend on the molecular sizes, the spin magnitudes on the spin sources, and environments including finite temperature effects. For instance,

the ESR spectrum of phenalenyl radical dimer in solution indicates that the dimeric unit forms the quantum spin singlet [83]. For chromium dimers, it was reported that the quantum spin correction for UB3LYP solutions considerably affects equilibrium geometries [63, 64]. For the molecular systems that quantum spin effects are strong, the quantum corrections for UCC solutions are needed. In the following sections, we shall describe several quantum corrections we proposed.

22.2.6. Approximated Spin-Projected UCC (APUCC) theory

In the field of quantum chemistry and nuclear physics, several types of quantum correction techniques [58–64, 84–87] have been proposed to recover the broken-symmetry solutions since spin and angular momentum are good quantum numbers for small molecular systems and nuclear systems, respectively. The first is the usual projection operator technique of quantum mechanics that is known as the Löwdin projection [84] in quantum chemistry. The method usually truncates up to some low-lying spin states to project out [85], which sometimes causes some errors: for instance the effective interactions computed with the projected UMP do not reduce to zero at the no magnetic interaction limit [88]. The second is called the Peierls–Yoccoz scheme [86], which is originally used to recover the angular momentum of the deformed nucleus in the field of nuclear physics. This method is also introduced in molecular systems, but it requires an additional numerical integration in practice [86].

We have proposed several versions of spin-projection schemes based on spin-multiplets energy levels with the Heisenberg (HB) model, which is generally used in the theory of molecular magnetism [58–64]. It is the most convenient projection method concerning the procedure and the computational cost. Now we again consider the simplest model consisting of two magnetic sites for simplicity. This system can be described with the Heisenberg Hamiltonian,

$$\hat{H}_{\mathrm{HB}} = -2J\hat{\mathbf{S}}_1 \cdot \hat{\mathbf{S}}_2. \tag{22-30}$$

Assuming we can use ab initio results for energies and spin-correlation functions of the Heisenberg model,

$$E_{\mathrm{HB}}^{\mathrm{LS}} = -2J\left\langle \hat{\mathbf{S}}_1 \cdot \hat{\mathbf{S}}_2 \right\rangle_{\mathrm{HB}}^{\mathrm{LS}}, E_{\mathrm{HB}}^{\mathrm{HS}} = -2J\left\langle \hat{\mathbf{S}}_1 \cdot \hat{\mathbf{S}}_2 \right\rangle_{\mathrm{HB}}^{\mathrm{HS}}, \tag{22-31}$$

we obtain the J value of the ab initio results [63],

$$J = \frac{E_{\mathrm{X}}^{\mathrm{LS}} - E_{\mathrm{X}}^{\mathrm{HS}}}{2\left(\left\langle \hat{\mathbf{S}}_1 \cdot \hat{\mathbf{S}}_2 \right\rangle_{\mathrm{X}}^{\mathrm{HS}} - \left\langle \hat{\mathbf{S}}_1 \cdot \hat{\mathbf{S}}_2 \right\rangle_{\mathrm{X}}^{\mathrm{LS}}\right)}, \mathrm{X} = \text{any ab initio method.} \tag{22-32a}$$

As we treated with the magnetic states described by the Heisenberg model, we can assume that the on-site spin expectation value of the low-spin state is identical to that of the high-spin state,

$$2\left\langle \hat{\mathbf{S}}_1 \cdot \hat{\mathbf{S}}_2 \right\rangle_{\mathrm{X}}^{\mathrm{LS}} - 2\left\langle \hat{\mathbf{S}}_1 \cdot \hat{\mathbf{S}}_2 \right\rangle_{\mathrm{X}}^{\mathrm{HS}} = \left\langle \hat{\mathbf{S}}^2 \right\rangle_{\mathrm{X}}^{\mathrm{LS}} - \left\langle \hat{\mathbf{S}}^2 \right\rangle_{\mathrm{X}}^{\mathrm{HS}} - \sum_i^{1,2} \left(\left\langle \hat{\mathbf{S}}_{\mathrm{i}}^2 \right\rangle_{\mathrm{X}}^{\mathrm{LS}} - \left\langle \hat{\mathbf{S}}_{\mathrm{i}}^2 \right\rangle_{\mathrm{X}}^{\mathrm{HS}} \right), \\ \cong \left\langle \hat{\mathbf{S}}^2 \right\rangle_{\mathrm{X}}^{\mathrm{LS}} - \left\langle \hat{\mathbf{S}}^2 \right\rangle_{\mathrm{X}}^{\mathrm{HS}} \tag{22-33}$$

we finally have

$$J = \frac{E_{\mathrm{X}}^{\mathrm{LS}} - E_{\mathrm{X}}^{\mathrm{HS}}}{\left\langle \hat{\mathbf{S}}^2 \right\rangle_{\mathrm{X}}^{\mathrm{HS}} - \left\langle \hat{\mathbf{S}}^2 \right\rangle_{\mathrm{X}}^{\mathrm{LS}}}, \mathrm{X} = \text{any ab initio method.} \tag{22-32b}$$

Exploiting the Heisenberg model further, we obtain the approximated $U - X$ ($X =$ DFT, MP, CC) corrected energy for the low-spin state,

$$E_{\mathrm{APU}-X}^{\mathrm{LS}} = E_{U-X}^{\mathrm{LS}} - J\left(S(S+1) - \left\langle \hat{\mathbf{S}}^2 \right\rangle_{U-X}^{\mathrm{LS}} \right), \tag{22-34}$$

where $S(S+1)$ is the correct spin eigenvalue for the low-spin state.

This method is easy to be implemented and applicable to any types of spin broken-symmetry theories [58–64]. For the coupled-cluster theories, however, it is not trivial to compute $\left\langle \hat{\mathbf{S}}^2 \right\rangle_{\mathrm{UCCSD}}$. In the following, we use an approximated expression of $\left\langle \hat{\mathbf{S}}^2 \right\rangle_{\mathrm{UCCSD}}$ proposed by Purvis et al. (PSB) [24]. A more accurate expression of $\left\langle \hat{\mathbf{S}}^2 \right\rangle_{\mathrm{UCCSD}}$, which is based on the Helllmann–Feynman theorem, is derived by Chen and Schlegel (CS) [31], but the differences between PSB and CS are smaller than 0.004 on values for a wide range of interatomic distances of hydrogen fluoride. Therefore hereafter we employ the PSB estimation of $\left\langle \hat{\mathbf{S}}^2 \right\rangle_{\mathrm{UCCSD}}$ for the APUCC theory.

22.3. RESONATING CONFIGURATION INTERACTION METHOD BASED ON SPIN-UNRESTRICTED COUPLED CLUSTER SOLUTIONS

22.3.1. Resonating Hartree–Fock Configuration Interaction Method

Next we turn to the resonating configuration interaction (Res-CI) approach based on broken symmetry solutions. We first proposed this method [65–67] as a simplified version of the resonating Hartree–Fock SCF theory developed by Fukutome [89]. After the publications of refs [65–67], we noticed that there are several approaches

similar to Res-HF CI implemented by the precursors [90–93]. However, since the Res-CI based on broken-symmetry UCC solutions has not been reported, we would like to present it here.

In the context of the applications to biradical systems, the resonating CI theory works as a spin-projection method. As touched in Eqs. (22-5), (22-9) and (22-10), there are two solutions that compensate each other as shown in Figure 22-2a.

$$\left|\Phi_1^U\right\rangle = \left|\phi_\alpha^U \bar{\phi}_\beta^U\right\rangle, \left|\Phi_2^U\right\rangle = \left|\phi_\beta^U \bar{\phi}_\alpha^U\right\rangle \tag{22-35}$$

Using these two UHF solutions, we immediately have the Res-CI solution as,

$$\left|\Psi_0^{\mathrm{ResCI}}\right\rangle = \frac{1}{\sqrt{2}}\left(\left|\phi_\alpha^U \bar{\phi}_\beta^U\right\rangle + \left|\phi_\alpha^U \bar{\phi}_\beta^U\right\rangle\right) = \sqrt{\frac{2}{3+\cos\left[4\theta\right]}}\left(\cos\left[2\theta\right]|I\rangle + |S\rangle\right). \tag{22-36}$$

This Res-CI wavefunction obviously includes the resonating effects among $\left|\phi_\alpha^U \bar{\phi}_\beta^U\right\rangle$ and $\left|\phi_\beta^U \bar{\phi}_\alpha^U\right\rangle$ and is equivalent to a spin-projected UHF (APUHF) solution in this case [70, 71]. The relation among RHF, UHF, and Res-CI (= APUHF) solutions for this case is summarized in the Figure 22-2A.

The ion-radical system is another important target of the Res-CI theory. For this type of systems, weak points of theories we examine are exposed. The quantum chemists using traditional MR wavefunction methods such as MCSCF and MRCI have struggled to describe relative stabilities among several low-lying states of formyloxyl radical, nitrogen dioxide, and other ion-radical species [92–96]. Their

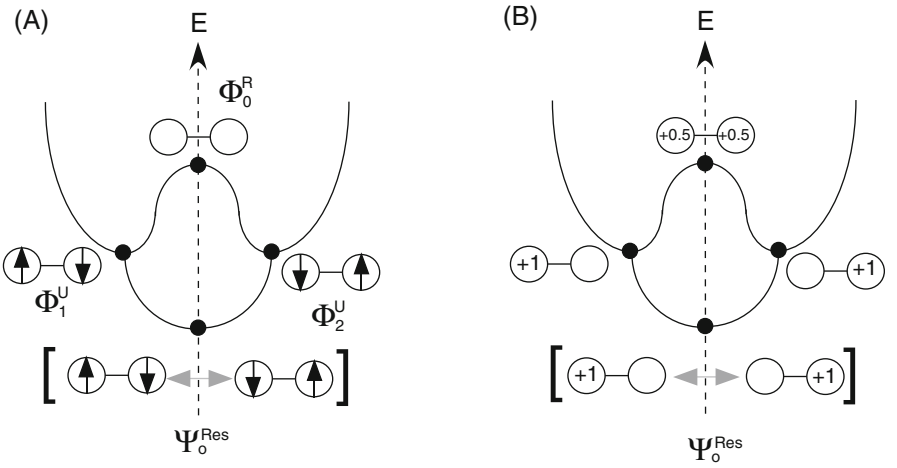

Figure 22-2. Schematic illustrations of the bifurcation to broken-symmetry (BS) solutions and quantum corrections using complementary BS solutions

studies show that it is required to employ the awful computer-demanding method for many systems if the conventional wavefunction theories based on orthogonal configurations. In particular, the problem is that the charge-distributions calculated by ab initio methods often exhibit artificially symmetry-broken feature. Even for the case of molecular systems consisting of such as HCO_2 and NO_2, the problem is complicated because the spatially broken-symmetry of the charge distributions are coupled with the geometry distortions.

For simplicity we consider cation-radical systems consisting of two sites, in which we do not limit any conditions for molecular geometries, whether these two sites are connected via through-space or through-bond interaction paths, and types of environments (gas, liquid, protein etc.). In order to clarify the electronic structure, we pick out the fundamental two parameters, i.e., the transfer between left and right sides, and the asymmetric degree between left and right sides, illustrating the two-dimensional space in Figure 22-3. Basically, there are four limits in this space. The first one is the two-center three electron systems consisting of two equivalent sites as shown in Figure 22-3i. This is a robust chemical bond with the bond-order 0.5 that can be described by the open-shell restricted Hartree-Fock (ROHF) method. As the degree of asymmetry increases, the deviation of charge distribution increases. Then we reach at the ionic chemical bond Figure 22-3ii. The third one Figure 22-3iii corresponds to the dissociation limit of this ionic bond where the system can be

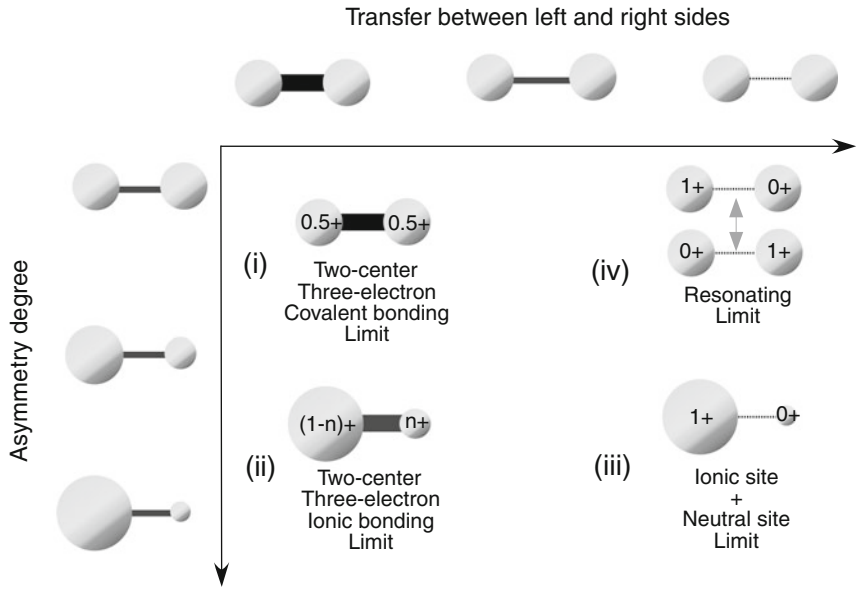

Figure 22-3. Two-dimensional parameter space including four limits for two-site ion-radical systems

described as the sum of cation site and neutral site. The last one is the dissociation limit of the two-center three electron systems consisting of two equivalent sites as shown in Figure 22-3iv. From the viewpoint of quantum mechanics, this state is straightforwardly described as the equivalent superposition of the left (L)-and-right (R) localized states, $(|L\rangle + |R\rangle)/\sqrt{2}$. In spite of such a straightforward character, it is not easy task to reproduce this state by ab initio method, because the delocalization and localization errors involved in the electronic structure theories we examined are exposed here [66, 67, 96]. However, the small deviations lift the equivalent superposition between $|L\rangle$ and $|R\rangle$, leading to the other limit, Figure 22-3iii.

Recently, we investigated a simplest example of the ion-radical system, He_2^+ using various electronic structure methods, and showed that almost all wavefunction theories such as UHF, UCCSD, CASSCF, fail to describe the limit Figure 22-3iv. All of these methods lead to two types of charge-localized solutions, the left localized type, $|L\rangle$ and the right localized type, $|R\rangle$. We then presented that the resonating CI using $|L\rangle$ and $|R\rangle$ solutions yields the correct resonating limit Figure 22-3iv. The bifurcation to $|L\rangle$ and $|R\rangle$ solutions and restoration of the delocalized state via the resonating effects are similar to those of diradical states as shown in Figure 22-2B. In addition we showed that the Res-CI solutions, satisfy the Perdew–Parr–Levy–Balduz relation that is an essential condition to describe the limit Figure 22-3iv of the ion-radical systems [66, 67, 97]. After that we found that some precursors applied the nonorthogonal CI treatments for this type of problems [90–93]. Of course, the valence bond (VB) CI is another option [97–99], which is particularly suitable for radical systems, in which the ionic character of the electronic structure is small. A CI based on the VB picture has been implemented since the early days of quantum chemistry [97, 98] and is now a sub-branch of electronic structure theory [99]. A superior point of the UHF-based Res-CI is the use of UHF canonical orbitals. In fact, the Res-CI requires smaller number of configurations than the VB CI does. Furthermore it is possible to efficiently extend the Res-HF CI to resonating-"post-HF" CI methods as described later.

We assume the systems where there are several types of broken-symmetry solutions, which are described by spin density wave, charge-density wave, bond-order wave, and even the two-and-three-dimensional spin density waves [89, 100]. For simplicity, we limit our discussion to the ion-radical type of molecules as presented in refs. [66, 67]. In this case, the Res-HF CI equation is given by,

$$\begin{bmatrix} \langle L|\hat{H}|L\rangle & \langle R|\hat{H}|L\rangle \\ \langle L|\hat{H}|R\rangle & \langle R|\hat{H}|R\rangle \end{bmatrix} \begin{bmatrix} C_L \\ C_R \end{bmatrix} = E_0 \begin{bmatrix} \langle L \mid L\rangle & \langle R \mid L\rangle \\ \langle L \mid R\rangle & \langle R \mid R\rangle \end{bmatrix} \begin{bmatrix} C_L \\ C_R \end{bmatrix}. \tag{22-37}$$

Since $\langle L|\hat{H}|L\rangle \neq \langle R|\hat{H}|R\rangle$ in general, the Res-CI solution takes the form,

$$|\mathrm{Res}\rangle = C_L|L\rangle + C_R|R\rangle\,. \tag{22-38}$$

The CI coefficients, $\{C_L, C_R\}$, covers the all range from the completely delocalized state $\{1/\sqrt{2}, 1/\sqrt{2}\}$, to the completely localized state ($\{1,0\}$ or $\{0,1\}$). Since the Res-CI equation is just a 2×2 CI in this case, it could be solved easily.

$$E_{\text{Res-CI}} = \frac{1}{S^2 - 1} \times \left(E_{\text{UHF}} + \frac{\Delta E}{2} - St - \sqrt{\left(\frac{\Delta E}{2}\right)^2 - S\,t\,(2E_{\text{UHF}} + \Delta E) + S^2 E_{\text{UHF}} \Delta E + t^2} \right). \tag{22-39}$$

Here $t \equiv \langle R|\,\hat{H}\,|L\rangle$, $S \equiv \langle R|L\rangle$, $E_{\text{UHF}} \equiv Min\left[\langle L|\,\hat{H}\,|L\rangle, \langle R|\,\hat{H}\,|R\rangle\right]$, and $\Delta E \equiv \left|\langle L|\,\hat{H}\,|L\rangle - \langle R|\,\hat{H}\,|R\rangle\right|$. Then all we have to compute are $t \equiv \langle R|\,\hat{H}\,|L\rangle$ and $S \equiv \langle R|L\rangle$ to correct the UHF energy, E_{UHF}.

One advantage of using a resonating type of CI is its ability to include both spin-polarized type of correlations and the quantum many-body fluctuations, which are usually missed in the spin-unrestricted methods, within the small CI expansion. However, if the spin-polarization effects are too strong to reduce the transfer and overlap matrices in Eq. (22-39), the resonating CI energy reduces to the low-lying UHF energy as,

$$\text{Lim}_{t\to 0, S\to 0} E_{\text{Res-CI}} = E_{\text{UHF}}. \tag{22-40}$$

As is known, the CC expansion around the UHF solution usually suppresses the spin-polarization effects, so is expect to improve this situation, which is the motivation to develop the resonating CC CI.

22.3.2. A Straightforward Res-CC CI Method

There are two possible formulation of the Res-CC CI. The first formulation is a straightforward extension of the Res-HF CI. All we have to do is to replace the UHF elements by the UCC elements in Eqs. (22-38), (22-39) and (22-40). For instance, the transfer integral in Eq. (22-40) is given by,

$$\begin{aligned}\left\langle \Psi_R^{\text{UCCSD}} \middle|\, \hat{H} \,\middle| \Psi_L^{\text{UCCSD}} \right\rangle &= \sum\nolimits_{R_I} \sum\nolimits_{L_J} C_{R_I} C_{L_J} \left\langle \Phi_{R_I} \middle|\, \hat{H} \,\middle| \Phi_{L_J} \right\rangle \\ &= \sum\nolimits_{R_I} \sum\nolimits_{L_J} \Big[C_{R_I} C_{L_J} \sum\nolimits_{R_i} \sum\nolimits_{L_j} \\ &\quad + \sum\nolimits_{R_k} \sum\nolimits_{L_l} \rho_{L_j L_l R_i R_k} \left\langle \psi_{R_i} \psi_{R_k} \middle|\, \hat{V}_{ee} \,\middle| \psi_{L_j} \psi_{L_l} \right\rangle \Big] \end{aligned} \tag{22-41}$$

for the Res-CC CI method. This method is the convenient version of the cluster expanded CI method for the following energy.

$$E = Min_{C_I,C_J,\hat{T}_I,\hat{T}_J}\left[\frac{\sum_{IJ}^{LR} C_I^* C_J \left\langle \Phi_I^{\mathrm{UHF}}\right| \exp\left[\hat{T}^{I+}\right]\hat{H}\exp\left[\hat{T}^{J}\right]\left|\Phi_J^{\mathrm{UHF}}\right\rangle}{\sum_{IJ}^{LR} C_I^* C_J \left\langle \Phi_I^{\mathrm{UHF}}\right| \exp\left[\hat{T}^{I+}\right]\exp\left[\hat{T}^{J}\right]\left|\Phi_J^{\mathrm{UHF}}\right\rangle}\right] \tag{22-42}$$

Actually, as we fix the amplitudes $\hat{T}^L, \hat{T}^R$ to those of left-and-right UCC solutions in the Res-CC CI method, the Res-CI energy is given by,

$$E = \mathrm{Min}_{C_I,C_J}\left[\frac{\sum_{IJ}^{LR} C_I^* C_J \left\langle \Phi_I^{\mathrm{UHF}}\right| \exp\left[\hat{T}^{I+}\right]\hat{H}\exp\left[\hat{T}^{J}\right]\left|\Phi_J^{\mathrm{UHF}}\right\rangle}{\sum_{IJ}^{LR} C_I^* C_J \left\langle \Phi_I^{\mathrm{UHF}}\right| \exp\left[\hat{T}^{I+}\right]\exp\left[\hat{T}^{J}\right]\left|\Phi_J^{\mathrm{UHF}}\right\rangle}\right] \tag{22-43}$$

Technically, the energy expression given by Eq. (22-42) differs from that of MRCC, because we don't remove the unlinked diagram. In practice, we can not only resolve the size-extensitivity problem, but also yield the correct potential surfaces for any case, if we choose appropriately the left-and-right UCC solutions.

The problem is that we must resolve is the non-orthogonality of two sets of UHF orbitals in order to use the Slater–Condon rule for Eq. (22-41), i.e.

$$\left\langle \psi_{Li}^{\sigma} \middle| \psi_{Rj}^{\sigma}\right\rangle \neq \delta_{ij}, \quad \sigma = \alpha, \beta. \tag{22-44}$$

The developers of valence-bond CI theories have confronted with and considerably worked out the non-orthogonality problem of atomic orbitals they have employed as a one-electron basis set for CI [100]. We can take a most simple and straightforward prescription for the specific Res-CI, by exploiting the fact that two sets of nonorthogonal orbitals are UHF canonical orbitals and similar to each other.

In such case, we can apply the corresponding molecular orbital transformation [101], i.e. a singular value decomposition between two sets of UHF orbitals. In the following, we shall use "a,b,..." and "p,q,..." for orbital indices, and "O" and "V" for subscripts to distinguish occupied and virtual sets. In order to diagonalize the overlap orbitals between two sets of UHF occupied orbitals, $[\mathbf{O}_{OO\,\sigma}]_{ab} \equiv \left\langle \psi_{La}^{\sigma} \middle| \psi_{Rb}^{\sigma}\right\rangle$, the Hermitian matrix, $\mathbf{O}_{OO\,\sigma}^{+}\mathbf{O}_{OO\,\sigma}$ is first diagonalized,

$$\mathbf{O}_{OO\sigma}^{+}\mathbf{O}_{OO\sigma}\mathbf{V}_{OO\sigma} \equiv \mathbf{V}_{OO\sigma}\Lambda_{OO\sigma}. \tag{22-45}$$

$\mathbf{U}_{OO\,\sigma}$ is defined using the eigenvalues matrix, $\Lambda_{OO\,\sigma}$, and the eivenvector matrix, $\mathbf{V}_{OO\,\sigma}$ as

$$\mathbf{U}_{OO\sigma} \equiv \mathbf{O}_{OO\sigma}\mathbf{V}_{OO\sigma}\Lambda_{OO\sigma}^{-1/2}. \tag{22-46}$$

Using $\mathbf{U}_{OO\,\sigma}$ and $\mathbf{V}_{OO\,\sigma}$, the overlap matrix can be transferred into a diagonal matrix,

$$[\mathbf{o}_{OO\sigma}]_{ab} \equiv \langle \psi'^{\sigma}_{La} \mid \psi'^{\sigma}_{Rb} \rangle = \left[\mathbf{U}^{+}_{OO\sigma}\mathbf{O}_{OO\sigma}\mathbf{V}_{OO\sigma}\right]_{ab} = \delta_{ab\sigma}\lambda^{1/2}_{a\sigma}. \tag{22-47}$$

In the similar manner, the virtual orbitals are transformed by $\mathbf{U}^{+}_{V\sigma}$ and $\mathbf{V}_{V\sigma}$ for L and R types of UHF orbital sets respectively. Strictly speaking, the remaining overlap matrices, $\left[\mathbf{O}_{OV\sigma}\right] \equiv \left[\langle \psi^{\sigma}_{La} | \psi^{\sigma}_{Rp} \rangle\right]_{a,p}$ and $\left[\mathbf{O}_{VO\sigma}\right]_{pa} \equiv \langle \psi^{\sigma}_{Lp} | \psi^{\sigma}_{Ra} \rangle$, are not zero in general, but those are expected to be nearly zero matrices because the occupied and virtual orbital spaces are expected not to overlap considerably each other. In fact, we confirmed [102] that $\langle \psi^{\sigma}_{La} | \psi^{\sigma}_{Rp} \rangle \sim 0$ and $\langle \psi^{\sigma}_{Lp} | \psi^{\sigma}_{Ra} \rangle \sim 0$ for any pair of (a,p) for several parallel-stacking configurations of ethylene dimmer cation [66].

Using these CMOs, we can obtain the left-and-right localized types of the UCCSD solutions. These are equivalent to those using the canonical UHF orbitals, but enable us to use the Slater-Condon rule to estimate the transfer matrix of Res-CC CI given by Eq. (22-41). Unfortunately, the UCC program, by which CC calculations using arbitrary non-canonical UHF orbitals are possible, is not available at the present time. Instead, we choose the second type of the Res-CC CI theory as described in the next section.

22.3.3. A Res-CC CI Method Based on the Ayala and Schlegel Treatment

The second formulation is similar to that of Res-CI MP2 developed by Ayala and Schlegel [90]. As described above, they developed the nonorthogonal CI that is equivalent to the Res-HF CI and applied it to the formyloxyl radical. Further they adopted a second-order perturbation correction to include correlation effects. Following their treatment, we solve the equation

$$\begin{bmatrix} E^{L}_{\mathrm{UCC}} & t^{RL}_{\mathrm{UCC}} \\ t^{LR}_{\mathrm{UCC}} & E^{L}_{\mathrm{UCC}} \end{bmatrix} \begin{bmatrix} C_L \\ C_R \end{bmatrix} = E_0 \begin{bmatrix} 1 & S^{RL}_{\mathrm{UCC}} \\ S^{LR}_{\mathrm{UCC}} & 1 \end{bmatrix} \begin{bmatrix} C_L \\ C_R \end{bmatrix}. \tag{22-48}$$

in order to obtain the Res-CC energy. Here the diagonal terms of the Hamiltonian matrix are the CC energies given by,

$$E^{\mathrm{UCCSD}}_{L} = \left\langle \Phi^{\mathrm{UHF}}_{L} \middle| \hat{H} \middle| \Psi^{\mathrm{UCCSD}}_{L} \right\rangle, \quad E^{\mathrm{UCCSD}}_{R} = \left\langle \Phi^{\mathrm{UHF}}_{R} \middle| \hat{H} \middle| \Psi^{\mathrm{UCCSD}}_{R} \right\rangle. \tag{22-49}$$

The point is that the intermediate normalization is employed. The transfer term and overlap term are then taken as the average of two possible forms as,

$$t^{RL}_{UCC} = t^{LR}_{UCC} = \left(\left\langle \Phi^{\mathrm{UHF}}_{R} \middle| \hat{H} \middle| \Psi^{\mathrm{UCCSD}}_{L} \right\rangle + \left\langle \Phi^{\mathrm{UHF}}_{L} \middle| \hat{H} \middle| \Psi^{\mathrm{UCCSD}}_{R} \right\rangle \right) \Big/ 2, \tag{22-50}$$

$$S^{RL}_{\mathrm{UCC}} = S^{LR}_{\mathrm{UCC}} = \left(\left\langle \Phi^{\mathrm{UHF}}_{R} \mid \Psi^{\mathrm{UCCSD}}_{L} \right\rangle + \left\langle \Phi^{\mathrm{UHF}}_{L} \mid \Psi^{\mathrm{UCCSD}}_{R} \right\rangle \right) \Big/ 2. \tag{22-51}$$

The matrix elements between nonorthogonal determinants are evaluated with expanding one canonical orbital in terms of the other canonical orbitals. Thus, as the

one determinant is also expanded in terms of the other determinant and its excited configurations, the Hamiltonian element between Φ_L^{UHF} and Φ_R^{UHF} is given by,

$$\left\langle \Phi_L^{\mathrm{UHF}} \middle| \hat{H} \middle| \Psi_R^{\mathrm{UHF}} \right\rangle = c_0 \left\langle \Phi_L^{\mathrm{UHF}} \middle| \hat{H} \middle| \Phi_L^{\mathrm{UHF}} \right\rangle + \sum c_{ab}^{pq} \left\langle \Phi_L^{\mathrm{UHF}} \middle| \hat{H} a_p^+ a_q^+ a_b a_a \middle| \Phi_L^{\mathrm{UHF}} \right\rangle. \quad (22\text{-}52)$$

Other terms between one-ground configuration and the other excited configurations can be calculated using similar equations. The expansion coefficients in Eq. (22-52) can be estimated using cofactors [90]. In this formalism, diagonal elements in Eq. (22-48) are consistent with those obtained from the UCCSD calculations as shown in Eq. (22-49). This is slightly different from the straightforward implementation of the Res-CC CI method described in the previous section, in which the diagonal terms of Res-CC CI Hamiltonian are given by, $\left\langle \Psi_L^{\mathrm{UCCSD}} \middle| \hat{H} \middle| \Psi_L^{\mathrm{UCCSD}} \right\rangle$ and $\left\langle \Psi_R^{\mathrm{UCCSD}} \middle| \hat{H} \middle| \Psi_R^{\mathrm{UCCSD}} \right\rangle$. In the following Res-CC calculations, we employed this Ayala and Schlegel type of Res-CC CI method.

To our knowledge, this type of theory has not been presented yet. We shall examine the computational results of this Res-CC CI method, comparing with those of other methods for simple radical systems in the next section.

22.4. COMPUTATIONAL RESULTS AND DISCUSSIONS

We here present the comparative calculations of several versions of coupled-cluster theories for simple examples. The programs used are as follows. The RCCSD and UCCSD calculations are done with using Gaussian 03 [103] and Aces2 [104]. The later is used to obtain $\left\langle \hat{S}^2 \right\rangle_{\mathrm{UCCSD}}$ values. The multireference averaged quadratic coupled-cluster (MR-AQCC) calculations [28] are performed with COLUMBUS [105]. Further, the multireference coupled-cluster (MRCC) calculations are done the *PSIMRCC* code developed by Evangelista and Simmonett [106]. Finally, the resonating CC theory is implemented in the original Res-CI code developed by Nishihara [66, 67].

22.4.1. Fluorine Molecule

First, we consider singlet states of F_2, for which the dynamical correlation corrections are essential. The valence electrons that contribute to the covalent bond are just two electrons in the σ-orbital. However, the binding energy estimated by CASCI [2,2] calculation with 6–311 + +G [2d, 2p] basis set yields the 11.8 kcal/mol that is less than one third of the experimental value, 38.3 kcal/mol [107]. This is caused by the fact that the dynamical correlation effects are essential to reproduce the binding energies of F_2 where many valence closed-shell electrons exist.

In fact, the CAS [2,2]-DFT treatment with using on-top pair density to estimate spin-polarization effects of DFT correlations enhanced the BE to approximately

27 kcal/mol, but this is partially due to the semi-empirical feature of Lee–Yang–Parr (LYP) correlation functional employed [108]. Now we performed the BW-MRCC, Mk-MRCC, MR-AQCC, UCCSD, and Res-UCCSD CI calculations with using 6-31G basis set, for which the full CI calculation is feasible. For MRCC, we employed the CAS[2,2] reference and examined both canonical orbitals and localized orbitals for reference active orbitals. The results are summarized in Figure 22-4 (A) together with MR-AQCC and full CI results. As we can see from this figure that the potential surfaces of both Mk-MRCC and BW-MRCC do not dissociate correctly when the canonical active orbitals are employed. Evangelista et al. reported that this "size-inconsistent behavior" is caused by the lack of invariance under unitary transformation of active orbitals in the MRCC procedure and pointed out that this behavior is corrected by the use of localized orbitals [54]. In fact, Mk-MRCC and BW-MRCC results with employing localized active orbitals (LAO) (see Eq. (22-14)) show remarkable improvement for this problem. The BE of Mk-MRCC with LAO results is similar to those of full CI and MR-AQCC,

The potential curve of F_2 with UMP2 exhibits a hump at the intermediary stage of the dissociation. On the other hand, the Res-MP2 CI by Ayala and Schelegel [90] provides a smooth curve without the hump for the F_2 dissociation. APUMP2 also reproduces the Res-MP2 CI curve. In contrast to UMP2 and complicated situations concerning reference orbitals in MRCC results, the UCCSD results provide the smooth (no hump) and "size-consistent" potential surface as shown in Figure 22-4b. The BEs of these two results are, however, considerably smaller than that of full CI. The resonating CI treatment followed the UCCSD calculations does not change the situation. Rather, the spin-projected UCCSD (APUCCSD) yields BE of 21.4 kcal/mol, which is a better value than that of Res-CC CI: note that the spin correction term in Eq. (22-34) is crucial even at UCCSD level. For degenerate (magnetic) systems, it is noteworthy that APUCCSD and Res-CC CI results give the correct dissociation limit.

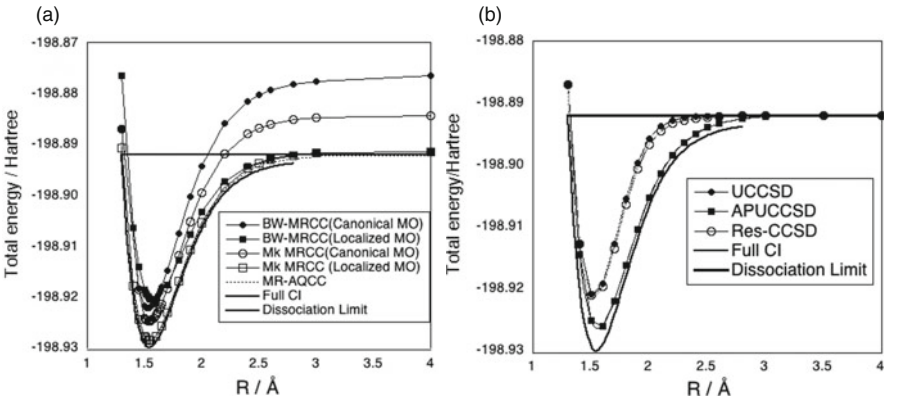

Figure 22-4. Potential surfaces of F_2 calculated by (**a**) MRCC, MRAQCC, and (**b**) UCCSD, APUCCSD, Res-CCSD, together with Full CI methods

22.4.2. Manganese Dimer

As a typical example for strong correlated systems with weak magnetic interacting systems, we calculate manganese dimmer (Mn_2). Up to a few years ago, chemical bonding and magnetic interaction of this species were in controversy [109, 110]. The stability of the singlet state had been shown by several experiments in the rage-gas matrix [109], while the DFT researchers had suggested that the high-spin coupling is favorable for the Mn–Mn interaction [110]. Recently, it was reported that multireference perturbation theory (MRMP2) calculations yield spectroscopic constants similar to those of experimentally reported values and the singlet ground state of Mn_2, supporting experimental data [109]. After that, we examined various types of DFTs and concluded that the high-spin stability of the DFT results is due to the self-interaction error, which causes overstabilizing a high-spin state [110]. A reason of this confusing situation is that the straightforward covalent bonding is hindered by four 4s electrons, resulting in the weak antiferromagnetic interactions. To describe this system correctly, both nondynamical and dynamical correlation effects have to be covered accurately. However, the MRCC calculations are not feasible for this system, because there are 14 active electrons in 12 active orbitals. Figure 22-5 shows the potential surfaces of ${}^1\Sigma_g^+$ and ${}^{11}\Sigma_u^+$ states calculated by UCCSD(T) with the Wachter set with f orbital. Also APUCCSD(T) results are presented where the UMP2 spin expectation values are used for spin-projection. As shown in this figure, ${}^1\Sigma_g^+$ and ${}^{11}\Sigma_u^+$ states are nearly degenerate, so spin-projection correction is small for this system with local spin ($S_{1(2)} = 5/2$) (see Eq. (22-30)). In other word, UCCSD(T)∼APUCCSD(T)∼Res-CCSD(T) CI holds in this case. This result is consistent with the

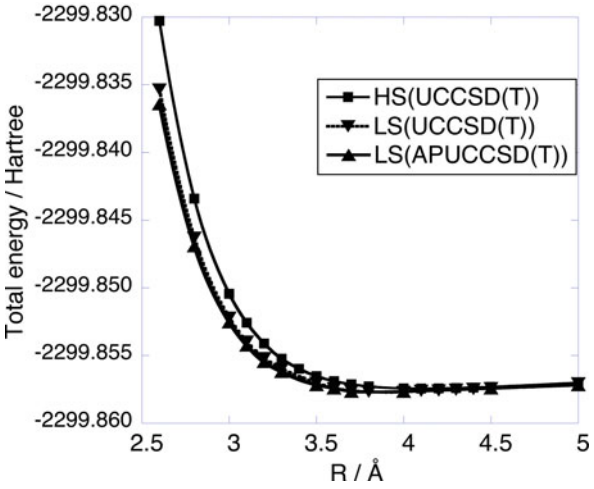

Figure 22-5. Potential surfaces of low-spin (LS) and high-spin (HS) states of Mn_2 calculated by UCCSD(T) and APUCCSD(T) methods

weak antiferromagnetic interaction $J \sim -9 \pm 3\,\mathrm{cm}^{-1}$: note that $J = -9\,\mathrm{cm}^{-1}$ with ESR and $J = \sim -10.3 \pm 0.6\,\mathrm{cm}^{-1}$ with MCD [109]. In addition, the binding energy is approximately 0.05 eV, being also comparable to the experimental one (0.1 eV).

These results show that APUCCSD(T) is efficient for describing the strong correlated low-spin systems with weak antiferromagnetic interaction and UCCSD(T) involving lower-lying paramagnetic configurations is responsible for temperature-dependent paramagnetic state, namely broken-symmetry (BS) one. On the other hand, applicability of DFT is often limited in the case of strongly correlated electron systems.

22.4.3. He_2^+ Systems

Next we shall turn to $He_2{}^+$ system. This is a simplest example of ion-radical systems, which have been accepted great interest in relation to many-electron self-interaction errors of DFT [66, 67, 111]. We present the potential surfaces calculated by UHF, UB3LYP, CASSCF [3, 12] and UCCSD methods with employing aug-cc pVTZ basis in Figure 22-6a. As is known, the potential surface of UB3LYP does not correctly dissociate to the dissociation limit energetically, because of the many-electron self-interaction error of the UB3LYP functional. The delocalized charge distributions of B3LYP shown in Figure 22-6b are also the results of this error. On the other hand, the UHF, CASSCF [3, 12], and UCCSD methods yield correct potential surfaces. However the localization errors in these solutions are shown as Mulliken charges of the relatively anionic site of $He_2{}^+$ for large intersite distances in Figure 22-6b. In other worlds, these methods are not effective for the resonating limit (iv) in Figure 22-3. A noteworthy point is that the localized CASSCF solutions become most stable for large intersite distances, although 1s, 2s, 2p, and 3s orbitals are included in the variational space.

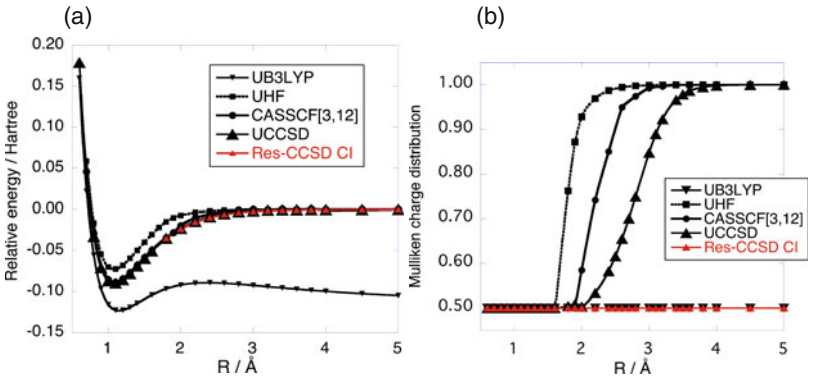

Figure 22-6. (**a**) Potential surfaces and (**b**) Charge distributions at relatively negative site of $He_2{}^+$ calculated by UB3LYP, UHF, CASSCF, UCCSD, and Res-CCSD CI methods.

Interestingly, the coupled-cluster expansion for UHF solutions improves the sudden charge-separation for the change of intersite distance, but it also leads to completely localized solutions for the distances larger than 4 Å. Then we implemented Res-CCSD CI calculations with employing the left-and-right localized UCCSD solutions. Although, as shown in Figure 22-6a, the stabilization energies with resonating CI treatment is considerably small, the Res-CC CI provides the correct energy surface and correct charge distributions for $He_2{}^+$ system. We further examined the energy dependence of the Res-CC CI binding energy on charge distribution of $He_2{}^+$. It can be seen in Figure 22-7 that the energy profile for the various charge distributions becomes approximately flat at the intersite distance 10 Å, i.e.,

$$\begin{aligned} E_{\text{Res-CC CI}}\left(\text{He} + \text{He}^+\right) &= E_{\text{Res-CC CI}}\left(\text{He}^{\omega+} + \text{He}^{(1-\omega)+}\right) \\ &= E_{\text{Res-CC CI}}\left(\text{He}^+ + \text{He}\right). \end{aligned} \tag{22-54}$$

This implies that the Res-CC CI satisfies the PPLB condition [8], which is essential to describe the region near the resonating limit, (iv) in Figure 22-3.

Next we intend to examine the small perturbation effects on these Res-CC CI solutions due to asymmetric degree of freedom in Figure 22-3. For this purpose, we introduce an artificial negative point charge placed at 10 Å from the one site on the line of $He_2{}^+$, which is illustrated in Figure 22-8. The point charges examined are $X = 0$ (no point charge), -0.01, and -0.0001 Hartree, of which the energy scales as perturbations are approximately 0, 0.001, and 0.00001 Hartree, respectively for the total energy, but it does not have significant impact on the potential surface because the deviations are expected to be mostly cancelled over the potential surface. On the

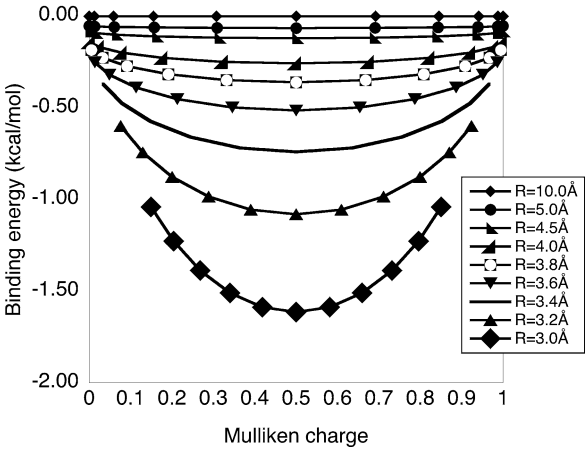

Figure 22-7. Dependence of the Res-CCSD CI binding energies on charge distributions for $He_2{}^+$

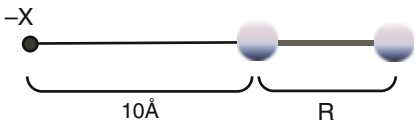

Figure 22-8. Schematic illustration of He_2^+ + point charge model

other hand, there are significant features for responses of the charge distributions to these perturbations.

Figure 22-9 shows the charge distributions of UHF, UCCSD, Res-CC CI solutions on relatively anionic site of He_2^+ plus a point charge system. For asymmetric cases, we also present the full CI results. As we can see from this figure, UHF and UCCSD results are not affected by these point charges, implying that the localization errors of these approximations dominate over small asymmetric perturbations near the symmetric region of Figure 22-3. On the other hand, the response of Res-CC CI charges to the perturbations is remarkably large, which is quite similar to that of full CI. These results imply that the Res-CI treatment followed UCCSD calculations is essential to cover the quantum fluctuations around the resonating limits (iv) in Figure 22-3.

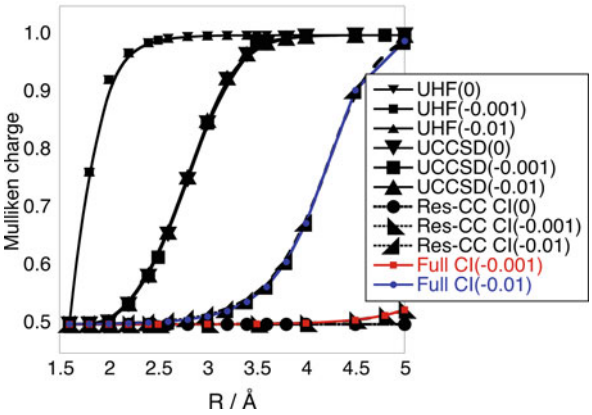

Figure 22-9. Mulliken distributions of the cationic site for the He_2^+ + point charge model. The numbers in parentheses are the magnitudes of the point charges

ACKNOWLEDGMENTS

The authors acknowledge the Ministry of Education, Culture, Sports, Science and Technology (MEXT) for a grant-in-aid for Research and Development of the Next-Generation Integrated Simulation of Living Matter, a part of the Development and Use of the Next-Generation Supercomputer Project. We would also like to thank

Professor H. Lischka, Dr. M. E. Harding, R. J. Bartlett, Professor M. Kallay and other developers for providing him COLUMBUS, Aces II (QTP and Mainz-Austin-Budapest versions), mrcc (although not used for this article), and PSI3 programs. S. Y. further thanks Dr. F. Evangelista for helpful information of his work and PSIM-RCC.

REFERENCES

1. A. Pipano, I. Shavitt, Int. J. Quantum Chem. **II**, 741–749 (1968)
2. S. R. Langhoff, E. R. Davidson, Int. J. Quantum Chem. **VIII**, 61–72 (1974)
3. R. J. Buenker, S. Peyerimhoff, Theor. Chim. Acta (Berl) **35**, 33–58 (1974)
4. K. Yamaguchi, K. Ohta, S. Yabushita, T. Fueno, Chem. Phys. Lett. **49**, 555–559 (1977)
5. K. Yamaguchi, T. Fueno, Chem. Phys. **23**, 375–386 (1977)
6. K. Yamaguchi, K. Ohta, S. Yabushita, T. Fueno, J. Chem. Phys. **68**, 4323–4325 (1977)
7. K. Yamaguchi, Int. J. Quantum Chem. **18**, 101–106 (1980)
8. A. Szabo, N. S. Ostlund, *Modern Quantum Chemistry*, (Macmillan Publishing Co., Inc., New York, 1982)
9. F. Coester, H. Kummel, Nucl. Phys. **17**, 477–485 (1960)
10. O. Sinanoglu, J. Chem. Phys. **36**, 706–718 (1961)
11. O. Sinanoglu, J. Chem. Phys. **36**, 3198–3208 (1962)
12. J. Cizek, J. Chem. Phys. **45**, 4256–4266 (1966)
13. J. Paldus, I. Shavitt, J. Cizek, Phys. Rev. A **5**, 50–67 (1972)
14. D. Mukherjee, R. K. Moitra, A. Mukhopadhyay, Mol. Phys. **30**, 1861–1888 (1975)
15. R. Offermann, W. Ey, H. Kummel, Nucl. Phys. A **273**, 349–367 (1976)
16. R. Offermann, Nucl. Phys. A **273**, 368–382 (1976)
17. W. Kutzelnigg, In *Methods of Electronic Structure Theory*, Ed. H. F. Schaefer III (Plenum Press, New York, 1977)
18. B. H. Brandow, Adv. Quantum Chem. **10**, 187–249 (1977)
19. K. Yamaguchi, Chem. Phys. Lett. **68**, 477–482 (1979)
20. K. Yamaguchi, Int. J. Quantum Chem. **S14**, 269–284 (1980)
21. A. Benerjee, J. Simons, Int. J. Quantum Chem. **XIX**, 207–216 (1981)
22. B. Jeziorski, H. J. Monkhorst, Phys. Rev. A **24**, 1668–1681 (1981)
23. I. Lindgren, D. Mukherjee, Phys. Rep. **151**, 93–127 (1987)
24. G. D. Purvis, H. Sekino, R. J. Bartlett, Collect. Czech. Chem. Commun. **53**, 2203–2213 (1988)
25. D. Mukherjee, S. Pal, Adv. Quantum Chem. **20**, 91–373 (1989)
26. K. Yamaguchi, In *Self-consistent Field, Theory and Applications*, Eds. R. Carbo, M. Klobukowski (Elsevier, Amsterdam, 1990)
27. R. F. Bishop, J. B. Parkinson, Y. Xian, Phys. Rev. B **41**, 200–219 (1990)
28. J. F. Stanton, J. Gauss, J. D. Watts, W. J. Lauderdale, R. J. Bartlett, Int. J. Quantum Chem. Symp. **26**, 879–894 (1992)
29. P. G. Szalay, R. J. Bartlett, Chem. Phys. Lett. **214**, 481–488 (1993)
30. P. Piecuch, N. Oliphant, L. Adamowicz, J. Chem. Phys. **99**, 1875–1900 (1993)
31. W. Chen, H. B. Schlegel, J. Chem. Phys. **101**, 5957–5968 (1994)
32. S. Yamanaka, M. Okumura, M. Nakano, K. Yamaguchi, J. Mol. Struct. (THEOCHEM) **310**, 205–218 (1994)
33. R. J. Bartlett (Ed.), *Recent Advances in Coupled-Cluster Methods* (World Scientific, Singapore, 1997)

34. J. Noga, W. Klopper, W. Kutzelnigg, In *Self-consisent Field, Theory and Applications*, Eds. R. Carbo, M. Klobukowski (Elsevier, Amsterdam, 1997)
35. D. Cremer, J.-L. Calais, In *Conceptual Perspectives in Quantum Chemistry*, vol. 3, Eds. J.-L. Calais, E. Kryachko (Kluwer Publishing Co, Dordrecht, 1997)
36. X. Li, J. Paldus, J. Chem. Phys. **107**, 6257–6269 (1997)
37. U. Mahapatra, B. Datta, B. Bandyopadhyay, D. Mukherjee, Adv. Quantum Chem. **30**, 163–193 (1998)
38. J. Paldus, Li, X, Adv. Chem. Phys. **110**, 1–175 (1999)
39. U. S. Mahapatra, B. Datta, D. Mukherjee, J. Chem. Phys. **110**, 6171–6188 (1999)
40. T. D. Crawford, H. F. Schaefer III, In *Reviews in Computational Chemistry*, vol. 17, Eds. K. B. Lipkowitz, D. B. Boyd (Wiley-VCH, New York, 2000), pp. 33–136
41. I. Hubac, J. Pittner, P. Carsky, J. Chem. Phys. **112**, 8779–8784 (2000)
42. L. Adamowicz, J.-P. Malrieu, V. V. Ivanov, J. Chem. Phys. **112**, 10075–10084 (2000)
43. J. Olsen, J. Chem. Phys. **113**, 7140–7148 (2000)
44. M. Schütz, H.-J. Werner, J. Chem. Phys. **114**, 66 (2001)
45. M. Kállay, P. G. Szalay, P. R. Surján, J. Chem. Phys. **117**, 980–990 (2002)
46. R. J. Bartlett, Int. J. Mol. Sci. **3**, 579–603 (2002)
47. R. F. Bishop, U. Kaldor, H. Kummel, D. Mukherjee, *The Coupled Cluster Approach to Quantum Many-Particle Systems* (Springer-Verlag, Berlin, 2003)
48. X. Li, J. Paldus, J. Chem. Phys. **119**, 5320–5333 (2003)
49. D. G. Fedorov, K. Kitaura, J. Chem. Phys. **123**, 134103 (2005) (1–11)
50. H. Hanrath, J. Chem. Phys. **123**, 084102 (2005) (1–12)
51. F. A. Evangelista, W. D. Allen, H. F. Schaefer III, J. Chem. Phys. **125**, 154113 (2006) (1–16)
52. W. Klopper, F. R. Manby, S. Ten-no, E. F. Valeev, Int. Rev. Phys. Chem. **25**, 427–468 (2006)
53. S. Hirata, Theor. Chem. Acc. **116**, 2–17 (2006)
54. F. A. Evangelista, W. D. Allen, H. F. Schaefer III, J. Chem. Phys. **127**, 024102 (2007) (1–17)
55. A. Takatsuka, S. Ten-no, W. Hackbusch, J. Chem. Phys. **129**, 044112 (2008) (1–4)
56. X. Li, J. Paldus, J. Chem. Phys. **129**, 174101 (2008) (1–15)
57. T. Shiozaki, M. Kamiya, S. Hirata, E. F. Valeev, J. Chem. Phys. **130**, 054101 (2009) (1–10) and references therein
58. K. Yamaguchi, F. Jensen, A. Dorigo, K. N. Houk, Chem. Phys. Lett. **149**, 537–554 (1988)
59. Y. Takahara, K. Yamaguchi, T. Fueno, Chem. Phys. Lett. **158**, 95–101 (1989)
60. K. Yamguchi et al., Chem. Phys. Lett. **210**, 201–210 (1993)
61. S. Yamanaka, T. Kawakami, H. Nagao, K. Yamaguchi, Chem. Phys. Lett. **231**, 25–33 (1994)
62. M. Shoji et al., Chem. Phys. Lett. **432**, 343–347 (2006)
63. S. Yamanaka et al., J. Magn. Magn. Mater. **310**, e492–e494 (2007)
64. Y. Kitagawa et al., Chem. Phys. Lett. **442**, 445–450 (2007)
65. R. Takeda, S. Yamanaka, K. Yamaguchi, Int. J. Quantum Chem. **106**, 3303–3311 (2006)
66. S. Nishihara et al., Int. J. Quantum Chem. **108**, 2966–2977 (2008)
67. S. Nishihara et al., J. Phys. Condens. Matter **21**, 064227 (2009) (1–5)
68. Practically, one exception is the orbital-dependent type of the exchange-correlation (XC) functional in Kohn-Sham DFT, by which the virtual excitation processes yielding the dispersion forces seem to be described correctly. For instance, see the special topic of orbital-dependent functional in J. Chem. Phys. **123**, 062101–062207 (2005). Also we should note that density and energy of strongly correlated systems can be exactly described by the DFT in principle, although an efficient XC functional has not been developed for such systems and nondynamical correlation effects might cause the diversity of the computational costs of such a XC functional even if it exists: see reference 77

69. K. Yamaguchi, T. Fueno, H. Fukutome, Chem. Phys. Lett. **22**, 461–465 (1973)
70. K. Yamaguchi, Chem. Phys. Lett. **33**, 330–335 (1975)
71. K. Yamaguchi, Chem. Phys. Lett. **35**, 230–235 (1975)
72. P. W. Anderson, Phys. Rev. **115**, 2–13 (1959)
73. K. Yoshida, *Theory of Magnetism* (Springer, Berlin, 1996)
74. S. Yamanaka, T. Ohsaku, D. Yamaki, K. Yamaguchi, Int. J. Quantum Chem. **91**, 376–383 (2003)
75. B. O. Roos, P. R. Taylor, P. E. M. Siegbahn, Chem. Phys. **48**, 157–173 (1980)
76. A. Kay, Phys. Rev. A **76**, 030307R (2007) (1–4)
77. V. A. Rassolov, S. Garashchuk, Chem. Phys. Lett. **464**, 262–264 (2008)
78. J. Finleya, P.-Å. Malmqvist, B. O. Roos, L. Serrano-Andrés, Chem. Phys. Lett. **288**, 299–306 (1998)
79. H. A. Witek, Y.-K. Choe, J. P. Finley, K. Hirao, J. Comput. Chem. **23**, 957–965 (2002)
80. K. Yamaguchi et al., Chem. Phys. Lett. **73**, 563–568 (1980)
81. M. Shoji et al., Int. J. Quantum Chem. **106**, 3288–3302 (2007)
82. S. Niu, J. A. Nichols, T. Ichiye, J. Chem. Theory Comput. (2009), doi:10.1021/ct800357c
83. D. Small et al., J. Am. Chem. Soc. **126**, 13850–13858 (2004)
84. P.-O. Löwdin, Phys. Rev. **97**, 1509–1520 (1955)
85. H. B. Schlegel, J. Phys. Chem. **92**, 3075–3078 (1988)
86. R. E. Peierls, J. Yoccoz, Proc. Phys. Soc. A **70**, 381–387 (1957)
87. A. Igawa, Int. J. Quantum Chem. **54**, 235–242 (1995)
88. S. Yamanaka, M. Okumura, K. Yamaguchi, K. Hirao, Chem. Phys. Lett. **225**, 213–220 (1994)
89. H. Fukutome, Prog. Theor. Phys. **80**, 417–432 (1988)
90. P. Y. Ayala, H. B. Schlegel, J. Chem. Phys. **108**, 7560–7567 (1998)
91. R. L. Martin, J. Chem. Phys. **74**, 1852–1854 (1981)
92. A. D. McLean, B. H. Lengsfield II, J. Pacansky, Y. Ellinger, J. Chem. Phys. **83**, 3567–3576 (1985)
93. C. F. Jackels, E. R. Davidson, J. Chem. Phys. **63**, 4672–4677 (1975).
94. D. Feller, E. S. Huyser, W. T. Borden, E. R. Davidson, J. Am. Chem. Soc. **105**, 1459–1466 (1983)
95. J. F. Stanton, J. Gauss, J. Chem. Phys. **101**, 8938–8944 (1994)
96. A. J. Cohen, P. Mori-Sánchez, W. Yang, J. Chem. Theory Comput. **5**, 786–792 (2009)
97. W. A. Goddard III, Phys. Rev. **157**, 81–91 (1967)
98. L. Pauling, J. Am. Chem. Soc. **53**, 1367–1400 (1931)
99. P. C. Hiberty, S. Shaik, J. Comp. Chem. **28**, 137–151 (2007) and references therein
100. S. Yamanaka, K. Yamaguchi, Bull. Chem. Soc. Jpn. **77**, 1269–1286 (2004)
101. A. T. Amos, G. C. Hall, Proc. R. Soc. Lond. A **263**, 483–493 (1961)
102. S. Nishiharå et al., unpublished.
103. M. J. Frisch et al., Gaussian 03, Revision C.02 (Gaussian Inc., Wallingford, CT, 2004)
104. J. F. Stanton et al., Aces II Mainz-Austin-Budapest version, http://www.aces2.de, accessed 1 May 2009
105. H. Lischka et al., COLUMBUS, an ab initio electronic structure program, release 5.9.1 (2006)
106. PSIMRCC, http://www.ccc.uga.edu/psimrcc/. This code is included in PSI3 package, http://www.psicode.org/
107. R. Takeda, S. Yamanaka, K. Yamaguchi, Int. J. Quantum Chem. **96**, 463–473 (2004)
108. C. Lee, W. Yang, R. G. Parr, Phys. Rev. B **37**, 785–789 (1988)
109. S. Yamamoto, H. Tatewaki, H. Moriyama, H. Nakano, J. Chem. Phys. **124**, 124302 (2006) (1–8) and references therein
110. S. Yamanaka et al., Int. J. Quantum Chem. **107**, 3178–3190 (2007) and references therein
111. A. J. Cohen, P. Mori-Sánchez, W. Yang, J. Chem. Phys. **126**, 191109 (2007) (1–5)

INDEX

P. Čársky et al. (eds.), Recent Progress in Coupled Cluster Methods, 649–657.
DOI 10.1007/978-90-481-2885-3, © Springer Science+Business Media B.V. 2010